



Francoz, Charlotte (2023) *Saltmarsh resilience in a changing climate: geomorphological and biological processes in natural and managed salt marshes in the North East of Scotland*. PhD thesis.

<https://theses.gla.ac.uk/83810/>

Copyright and moral rights for this work are retained by the author

A copy can be downloaded for personal non-commercial research or study, without prior permission or charge

This work cannot be reproduced or quoted extensively from without first obtaining permission from the author

The content must not be changed in any way or sold commercially in any format or medium without the formal permission of the author

When referring to this work, full bibliographic details including the author, title, awarding institution and date of the thesis must be given

Enlighten: Theses

<https://theses.gla.ac.uk/>  
[research-enlighten@glasgow.ac.uk](mailto:research-enlighten@glasgow.ac.uk)

# **Saltmarsh Resilience in a Changing Climate: Geomorphological and Biological Processes in Natural and Managed Salt Marshes in the North East of Scotland**

Charlotte Francoz

MSc



Submitted in fulfilment of the requirements for the  
Degree of Doctor of Philosophy

School of Geographical and Earth Sciences  
College of Science and Engineering  
University of Glasgow

August 2023



## Abstract

Salt marshes are regarded as one of the world's most productive ecosystems due to the unique habitat they provide, which is essential to our ecological structure, and their ability to act as sinks for organic and inorganic sediment. Salt marshes have long attracted human settlement and exploitation due to their location along the coast, on the sheltered shores typical of estuaries and tidal inlets. The permanent loss of saltmarsh ecosystems is between 25 and 50 percent of their global historical coverage, and the decline continues globally. This is exacerbated by rising temperatures, sea level rise, and increasing storm intensity, which erode salt marshes. Since 1945, roughly 15 percent of saltmarsh area in the United Kingdom has been lost due to human intervention, primarily agricultural and industrial reclamation, and is now being exacerbated by coastal erosion and sea level rise. Saltmarsh formation and development are influenced by the interdependence of physical and biological processes, whereas vertical growth and saltmarsh stability are highly dependent on sediment supply and tidal range. However, the cumulative impact of human disturbance and sea level rise on the fundamental saltmarsh dynamics remains obscure and must be better understood at both the local and global scales.

This thesis aims to improve understanding of the processes, mechanisms and patterns that 1) favour saltmarsh formation and development 2) enable saltmarsh capacity to recover from environment and anthropological disturbances 3) promote some of the regulating and supporting services salt marshes provide. My thesis has carried out a biogeomorphological appraisal of the first salt marsh managed realignment in Scotland since its breaching in 2003 in comparison with two adjacent natural salt marshes across different time scales. The study has employed a methodology to assess jointly managed/anthropogenically modified and natural salt marshes at different temporal scales. A set of managed and adjacent natural salt marshes within the same salt marsh system at Nigg Bay, NE Scotland provided a comparative case study of the links between sediment availability, vegetation presence and saltmarsh stability over time and space. Above ground changes in vegetation and sedimentation patterns were quantified over different timescales from short (annual) to longer (centennial) timescale using a combination of field measurements: sediment deposition, sedimentation plates and DEM time series in tandem with vegetation sampling. This multi-method approach has proven to be a powerful tool to analyse spatial distribution patterns of sediment accretion. Below ground physical and biological changes were explored using a combination of traditional sedimentary techniques and applying Luminescence to salt marsh for the first time, to gain knowledge on the possible mechanisms driving these changes. These results were used to assess the potential implications on the supporting and regulating benefits that salt marshes provide, as such contributing to saltmarsh blue carbon

inventories for natural and managed realignment salt marsh in Scotland; and, on capacity of marshes to keep up with rising sea levels.

The cumulative results of my thesis work highlight that natural salt marshes have limited space to respond to environmental changes, which reduces their long-term resiliency. In terms of sea level rise, the marsh is responding due to the accommodation space provided by the managed realignment.

Furthermore, the study has developed a new application of Optically Stimulated Luminescence (OSL) that challenges the results of conventional techniques and allows exploration of modern sediment material registering the impacts of recent climate change. This work thus adds an important dataset to the Scottish context and more broadly to the growing literature on the ability for managed realignment sites to replicate natural saltmarsh functions and thus ecosystem services.

# Table of Contents

Abstract	ii
Table of Contents	iv
List of Tables	xi
List of Figures	xv
Acknowledgements	xxxvi
Authors Declaration	xxxvii
<b>Chapter 1. Introduction</b>	<b>1-2</b>
1.1 Rationale	1-3
1.2 Aims and Scope	1-7
1.3 Thesis structure	1-7
<b>Chapter 2. Saltmarsh Importance</b>	<b>2-11</b>
2.1 Introduction	2-12
2.2 Saltmarsh function and spatial distribution	2-13
2.3 Interface of geomorphology and ecology/biology: a key interface	2-18
2.3.1 Physical controlling factors	2-21
2.3.1.1 Morphodynamics	2-21
2.3.1.2 Hydrodynamics	2-24
2.3.1.3 Environmental factors influencing saltmarsh development	2-28
2.3.2 Biological controlling factors	2-28
2.3.2.1 Vegetation influences hydrodynamics	2-29
2.3.2.2 Organic matter is important	2-29
2.3.2.3 Plant structure modulates saltmarsh erosion	2-30
2.3.3 The societal value of salt marsh	2-31
2.3.3.1 Supporting services	2-32
2.3.3.2 Regulatory Services	2-33
2.4 Salt marsh in a changing climate	2-37
2.4.1 Climate-driven changes in saltmarsh systems	2-37
2.4.1.1 Sea level rise	2-39
2.4.1.2 Storminess	2-41
2.4.1.3 Temperature change	2-42
2.4.2 Salt marsh in a human-driven environment	2-43
2.5 Saltmarsh resilience and management	2-44
2.6 Summary: still gaps to fill?	2-46
<b>Chapter 3. Research Framework and Methods</b>	<b>3-49</b>
3.1 Research framework and design	3-50
3.2 Choice of study location	3-53
3.2.1 Tides, waves and winds	3-55
3.2.2 Sediments sources, types and characteristics	3-57
3.3 Sampling strategy	3-61
3.3.1 Measuring saltmarsh sedimentation and vegetation through time	3-62
3.3.2 General sampling strategy	3-64
3.3.2.1 Fieldwork programme	3-64
3.3.2.2 Integrated design	3-65
3.3.2.3 Physical drivers	3-71
3.4 Material and methods	3-76

3.4.1	Aboveground short-term (annual) dynamics methods	3-76
3.4.1.1	Sediment deposition methods	3-77
3.4.1.2	Vegetation and aboveground biomass	3-80
3.4.2	Aboveground long-term (multi-annual to centennial) saltmarsh dynamics	3-84
3.4.2.1	Mapping erosion and accretion	3-84
3.4.2.2	Sedimentation rates (accretion and erosion) using sedimentation plates	3-91
3.4.2.3	Multi-annual vegetation monitoring	3-94
3.4.3	Belowground long-term saltmarsh bio-geomorphic properties: organic and inorganic content.	3-94
3.4.3.1	Coring sampling strategy	3-96
3.4.3.2	Analysis of belowground organic and inorganic content	3-99
3.4.3.3	Sediment physical characteristics: Particle size analysis	3-103
3.4.4	A new application of Optically Stimulated Luminescence - OSL techniques to explore saltmarsh dynamics	3-105
3.4.5	Statistics	3-107
3.4.6	Summary	3-107
<b>Chapter 4.</b>	<b>Short-Term Dynamics: Aboveground Short-Term (annual) Biological and Geomorphological Processes within Managed and Natural Salt Marshes</b>	<b>4-111</b>
4.1	Introduction	4-112
4.2	Short-term (annual) physical processes: sediment deposition and accretion rate estimates	4-115
4.2.1	Sediment deposition rates	4-115
4.2.1.1	Spatial variation in sediment deposition rates using filter discs	4-116
4.2.1.2	Temporal variation in sediment deposition rates using filter discs	4-119
4.2.1.3	Spatial variation in sediment deposition rates using AstroTurf mats	4-124
4.2.1.4	Temporal variation in sediment deposition rates using AstroTurf mats	4-125
4.2.2	Sediment accretion rate estimates	4-130
4.2.2.1	BDD	4-130
4.2.2.2	Accretion rates	4-133
4.2.3	Summary	4-136
4.3	Short-term (annual) biological controls to saltmarsh development: vegetation characteristics and biological processes	4-138
4.3.1	Vegetation characteristics	4-139
4.3.1.1	Vegetation height	4-139
4.3.1.2	Vegetation density	4-141
4.3.1.3	Vegetation cover	4-142
4.3.2	Aboveground living biomass and organic content	4-144
4.3.3	Relationships between vegetation characteristics and biological processes	4-145
4.3.4	Summary	4-147
4.4	Water levels over the short-term (annual) sediment collection period	4-148
4.4.1	Average hydroperiod, flood depth and flood frequency	4-150
4.4.1.1	Average flood depth	4-150
4.4.1.2	Average flood frequency	4-153
4.4.1.3	Average hydroperiod	4-157
4.4.1.4	Summary on water levels spatial variation	4-161
4.4.2	Hydroperiod and Flood depth variations over the short-term sediment collection	4-162
4.4.2.1	Monthly Flood depth variations	4-162
4.4.2.2	Monthly Hydroperiod variations	4-165

4.4.2.3	Summary on water levels temporal variation	4-168
4.5	Interplay and controls on geomorphological and biological processes	4-169
4.5.1	Physical controls on saltmarsh sediment deposition and accretion	4-170
4.5.1.1	Relationships between filter discs deposition rates, accretion rate estimates and physical drivers and controls to saltmarsh development	4-171
4.5.1.2	Relationships between monthly filter disc sediment deposition and physical controls to saltmarsh development	4-176
4.5.1.3	Summary	4-181
4.5.2	Physical controls on biological processes	4-182
4.5.2.1	Physical controls on vegetation characteristics	4-183
4.5.2.2	Water levels and vegetation assemblages	4-187
4.5.2.3	Summary	4-189
4.5.3	Relationships between vegetation and sediment deposition and accretion rate estimates	4-190
4.5.3.1	Overall influence of vegetation on sediment deposition and accretion rates	4-190
4.5.3.2	Seasonality and influence of vegetation on sediment deposition and accretion rates	4-192
4.5.3.3	Summary	4-195
4.6	Aboveground short-term (annual) biological and geomorphological processes: Significance of the Results	4-196
4.6.1	Performance of the sampling techniques	4-196
4.6.2	Aboveground short-term (annual) biological and geomorphological processes: results and interpretations	4-201
4.6.2.1	Spatial and temporal variability of the physical processes that form salt marshes - estimating sediment deposition and accretion rates and their influences.	4-202
4.6.2.2	The spatial variability of the biological processes that form salt marshes - estimating vegetation processes and their influences.	4-213
4.6.2.3	Spatial and temporal variability of water levels factor influencing saltmarsh development	4-219
4.6.3	Aboveground short-term (annual) biological and geomorphological processes: implications	4-223
<b>Chapter 5.</b>	<b>Long-Term Dynamics: Aboveground Long-Term (Multi-Annual to Centennial) Geomorphological Evolution of Scottish Managed and Natural Salt Marshes</b>	<b>5-232</b>
5.1	Introduction	5-233
5.2	Geomorphological changes across centennial to decadal timescales: scaling saltmarsh change.	5-235
5.2.1	Historical mapping from 1750's to 2012	5-236
5.2.2	Quantifying historical changes: Areal changes from 1872 to 2012	5-239
5.2.3	Quantifying historical changes: coastline and MHWS movement from 1872 to 2017	5-241
5.3	Geomorphological change on a multi-annual scale	5-245
5.3.1	Morphological characteristics of a cross-shore transect profiles using airborne and TLS DEM surfaces from 2011 to 2017	5-246
5.3.2	Surface elevation change using airborne and TLS DEM surfaces from 2011 to 2017	5-250
5.4	Surface elevation changes (representing accretion and erosion) and sedimentation rates by means of sedimentation plates from 2015 to 2017	5-252
5.4.1	Sedimentation rates derived from sedimentation plates	5-253
5.4.1.1	Spatial variation in sedimentation rates derived from sedimentation plates	5-253

5.4.1.2	Temporal variation in sedimentation rates derived from sedimentation plates	5-255
5.4.1.3	Spatial and temporal variation in sedimentation rates derived from sedimentation plates	5-256
5.4.2	Biological and geomorphological controls on sedimentation rates (using sedimentation plates)	5-261
5.5	Aboveground long-term (multi-annual to centennial) geomorphological processes: Significance of the results	5-266
5.5.1	Centennial saltmarsh extent and MHWS migration	5-266
5.5.2	Height, volume and saltmarsh extent changes from 2011 to 2017	5-268
5.5.3	Sedimentation rates derived from sedimentation plates from 2015-2017	5-271
5.6	Aboveground long-term (multi-annual to centennial) geomorphological processes: implications	5-275
<b>Chapter 6.</b>	<b>Sedimentary Record of Belowground Organic and Inorganic Processes in Managed and Natural Salt Marsh</b>	<b>6-280</b>
6.1	Introduction	6-281
6.2	Belowground inorganics: physical characteristics and properties of Nigg Bay saltmarsh sediments	6-285
6.2.1	Physical characteristics of the Nigg Bay saltmarsh sediments: grains legacy	6-285
6.2.1.1	Sediment characteristics: grain type and size variation	6-288
6.2.1.2	Sediment characteristics: grain type and size variation with depth per transects per cores	6-289
6.2.2	Physical properties of Nigg bays young and mature salt marshes - Bulk dry density (BDD) and Water Content	6-297
6.2.2.1	Bulk dry density – BDD – Soil autocompaction	6-298
6.2.2.2	Water content in saltmarsh sediments	6-300
6.2.3	Belowground inorganic carbon content (SIC)	6-303
6.3	Belowground organics: Soil biological properties of Nigg Bay saltmarshes sediments	6-306
6.3.1	Belowground organic matter - SOM	6-308
6.3.2	Belowground organic carbon density - SOC	6-312
6.4	Anthropogenic legacy in saltmarsh soils	6-315
6.5	Sedimentary legacy of belowground organic and inorganic processes: significance of the results	6-318
6.5.1	Saltmarsh physical and biological sediment properties of natural and managed salt marshes	6-318
6.5.1.1	Sediment characteristics of natural and managed salt marshes at Nigg	6-319
6.5.1.1.1	Linkages between surface zonation and sediments type and size controls saltmarsh topography	6-319
6.5.1.1.2	Sediments type and size through depth and time: settings for saltmarsh formation and development	6-321
6.5.1.2	Physical sediment properties: natural versus managed salt marshes	6-322
6.5.1.3	Summary of saltmarsh physical sediment properties influence on saltmarsh development	6-326
6.5.2	Belowground physical and biological interactions on natural and managed salt marshes	6-326
6.5.2.1	Biological sediment properties: natural versus managed salt marshes: implication	6-327
6.5.2.2	Linkages between surface zonation and carbon stores	6-328
6.5.2.3	Temporal variation: historical legacy impacts on carbon stores	6-330
6.5.3	Summary of saltmarsh biological sediment properties influence on saltmarsh development	6-331

<b>Chapter 7.</b>	<b>Exploring the Potential of Optically Stimulated Luminescence to Trace Sediment Processes in Modern Dynamic Saltmarsh Systems</b>	<b>7-334</b>
7.1	Introduction	7-335
7.1.1	Basic principles	7-335
7.1.2	Rationale	7-340
7.2	Exploratory core and evaluation of Nigg bay's saltmarsh sediments luminescence signal	7-343
7.2.1	Sample choice and preparation: laboratory targeting	7-343
7.2.1.1	STEP ONE: Is there quartz and/or feldspar in Nigg Bay's sediment?	7-344
7.2.1.2	STEP TWO: Which instruments best measure Nigg Bay's sediment sensitivity?	7-345
7.2.1.3	STEP THREE: Which fractions provide a high sensitivity luminescence signal?	7-347
7.2.1.4	STEP FOUR: How to measure signal sensitivity in young saltmarsh sediments?	7-348
7.2.2	Sampling strategy summary for preliminary core MR24	7-351
7.2.3	Exploratory core results and outcomes	7-352
7.2.3.1	Blue-OSL (B-OSL) signal	7-353
7.2.3.1.1	Natural Signal for 1 cm disc samples using portable reader – Step 4a	7-353
7.2.3.1.2	Bleaching for 1 cm disc samples using portable reader – Step 4b	7-355
7.2.3.1.3	Regenerated signal for 1 cm disc samples using portable reader – Step 4c	7-356
7.2.3.1.4	Comparing instruments: B-OSL signal using portable reader versus automatic reader Risø DA-20 for 1 cm disc samples regenerated at 200 mGy	7-357
7.2.4	IRSL signal	7-358
7.2.4.1.1	IRSL signal for 1 cm disc samples using Portable Reader	7-358
7.2.4.1.2	ISRL signal: comparing Portable Reader versus automatic reader Risø DA- versus PPSL instruments for 1 cm disc samples regenerated at 200 mGy	7-359
7.2.4.1.3	IRSL signal using PPSL signal for 1 cm disc samples	7-360
7.3	Summary: results from the exploratory core	7-361
7.4	Developing a new methodology: improving and exploring Nigg bay saltmarsh sediment luminescence signal sensitivity	7-362
7.4.1	Increasing signal sensitivity	7-362
7.4.2	Increasing the sample size: from 1 cm aluminium discs to 3cm aluminium discs	7-364
7.4.3	Calibrating procedure	7-365
7.4.4	New proxies	7-366
7.5	Direct implications of the new methodology: tracing geomorphic processes.	7-372
7.5.1	Luminescence residuals or signal sensitivity versus organic and inorganic variables	7-373
7.5.2	Synthesising saltmarsh processes: insights from one key core.	7-374
7.6	Summary and significance of the results	7-379
7.7	Acknowledgement	7-380
<b>Chapter 8.</b>	<b>Discussion and conclusion</b>	<b>8-384</b>
8.1	Introduction	8-385
8.2	Biotic and abiotic processes over different spatio-temporal scales	8-386
8.2.1	Short-term to longer-term patterns of saltmarsh development	8-386
8.2.2	Short-term and longer-term rates of saltmarsh development	8-392

8.2.3	Relationships between aboveground and belowground saltmarsh processes: belowground geomorphic and biological controls on saltmarsh development	8-395
8.2.3.1	Sedimentary characteristics: Topographic niches and heterogeneity	8-395
8.2.3.2	Hydrodynamic and geomorphic settings controls physical soil structure and biological soil content	8-396
8.2.3.2.1	Anthropogenic legacy affecting belowground physical soil structure and biological soil content	8-397
8.2.3.2.2	Zonation patterns favouring sedimentary stores	8-398
8.3	Carbon accumulation and sea level rise: Implications for saltmarsh response to climate change	8-399
8.3.1	Soft engineering approach (section 2.5) for new carbon stores	8-400
8.3.2	The vertical accretion rates at the Nigg Bay salt marshes: new adaptation to sea-level rise?	8-405
8.4	Recommendations for future research	8-407
8.5	Conclusions	8-408
<b>References</b>		<b>410</b>
<b>APPENDICES</b>		<b>442</b>
<b>Appendix.A Supplementary references for Chapter 2</b>		<b>443</b>
A.1.	Saltmarsh Legal frame for Scotland	444
A.2.	Saltmarsh vegetation classification based on NVC classification	449
A.3.	Extract from UKCP18 High Emission Scenario –RCP8.5 Summary	449
A.4.	Miscellaneous Cores: fieldwork and sampling adaptation	449
A.5.	Loss on Ignition - LOI methodology to measure Inorganic and Organic content in Nigg saltmarsh sediments	450
<b>Appendix.B Supplementary references for Chapter 3</b>		<b>452</b>
B.1.	Cromarty and Invergordon tides - Additional Notes & Definitions:	452
B.2.	Physical variables	452
B.3.	DEM survey accuracy and dataset selection	453
<b>Appendix.C Supplementary references for Chapter 4</b>		<b>459</b>
C.1.	Sediment	459
C.2.	Vegetation	463
C.3.	Relationships between sediment, vegetation and physical processes	468
<b>Appendix.D Supplementary references for Chapter 5</b>		<b>478</b>
D.1.	Areal historical changes	478
D.2.	Sedimentation rates derived from sedimentation plates supplementary tables and statistics	478
D.3.	Water levels (Flood depth, Flood frequency and Hydroperiod) over 2.14 years sedimentation plates monitoring period	484
<b>Appendix.E Supplementary reference for Chapter 6</b>		<b>486</b>



	Below ground organic and inorganic saltmarsh evolution: shallow coring programme	486
E.1.		
E.2.	Bulk Dry Density – BDD and Water content	486
E.3.	Below ground Organic matter - SOM	488
	Water content, BDD and Organic matter for cores collected along the fronting marsh (FM) and Managed realignment (MR) transects.	491
E.4.		
	Water content, BDD and Organic matter for cores collected along the natural saltmarsh (ANK) Transect.	492
E.5.		
E.6.	Carbon density SOC	493
<b>Appendix.F</b>	<b>Supplementary references for Chapter 7</b>	497
<b>Appendix.G</b>	<b>Supplementary references for Chapter 8</b>	502

## List of Tables

Table 2-1	Background themes reviewed in Chapter 2.	2-12
Table 2-2	Geomorphological classification of salt marshes in Europe, Great Britain and Scotland. Adapted from Allen (2000).	2-15
Table 2-3	combined table of ecosystem services as defined by MEA (2005) and (some of the) processes and functions that salt marshes provides along with examples of values for these services after: † Barbier et al., 2011 and ◇ Working with Nature protection WWNP (2018).	2-31
Table 2-4	Observed trends and future projections of climate change where the level of confidence (low, medium, or high) has been based on the amount of evidence and the level of agreement as reviewed by Robins et al. (2016) for the river-estuary-coast catchment systems	2-38
Table 3-1	Tide values for Invergordon and Cromarty are in meter above Newlyn Ordnance Datum (Chart Datum is below 2.1m Newlyn Ordnance Datum. See additional notes & definitions in Appendix B). Data supplied by UK Hydrographic Office ©Crown Copyright*. Tidal ranges for both locations are 3.6 m during spring tide and 1.7 m during neap tides.	3-56
Table 3-2	Intertidal sediment characteristics and distribution from Rendall and Hunter (1986) fauna study (see sample location on Figure 3-6).	3-60
Table 3-3	Summary of the field campaigns. * not used in the statistical analysis; **See 3.4.2.3.	3-64
Table 3-4	presents sampling points that have changed NVC community/ sub-community type between 2011 SNH SSS and 2015 research survey. The table also presents TABLEFIT results using 2015 vegetation survey (1m2 quadrat) specifying the vegetation composition (species name and cover value as a percentage as defined in Hill 2015). The interpretation of the Mean Goodness-of-Fit values for TABLEFIT is 80-100 for Very good, 70-79 for Good, 60-69 for Fair, 50-59 for Poor and 0-49 for Very poor (Hill, 2015). *The TABLEFIT results also provides habitat types according to the European Environment Agency's EUNIS system. This system was not used in this thesis. EUNIS habitats are defined primarily by their ecosystem (woodland, dune, swamp, etc.), though the definitions may contain elements of vegetation composition and land use (Hill, 2015). ** Pla mar- stand for <i>Plantago maritima</i> Arm mar - <i>Armeria maritima</i> .	3-68
Table 3-5	NVC vegetation assemblages and corresponding saltmarsh zone (details in Haynes, T.A. (2016) and Appendix A2) present studied sampling points at Nigg Bay.	3-70
Table 3-6	Summary of the physical variables for the 60 sampling points used in the project by sites for each saltmarsh zones where HM is high marsh, MM is mid-marsh, LM low marsh and PM is pioneer marsh:	3-73
Table 3-7	Summary of the dataset available to analyse topographical changes on the saltmarsh sites.	3-86
Table 3-8	Extent of the survey data used to map erosion and accretion (Units are in meters. * Raw data from Glasgow University MSc projects design C. Francoz with survey MSc Geomatics students. ** Raw data from Glasgow University MSc projects design J.D. Hansom & RSPB).	3-87
Table 3-9	Summary of the dataset available to analyse topographical changes (small-scale mapping) on the saltmarsh sites (* in ArcGIS).	3-90

Table 3-10	Overall compaction ratio for the different coring devices used during the project.	3-98
Table 3-11	Summary of number of cores and samples retrieved across the sites and saltmarsh zones. * see section 3.4.3.1.	3-100
Table 3-12	Summary of calculation used for Organic and Inorganic Carbon content estimations.	3-101
Table 3-13	Combining Carbon Pool to estimates Blue Carbon stocks (Howard et al., 2014).	3-102
Table 3-14	Calculations for total Blue Carbon Stock. Aboveground allometric equation is based in Howard et al.(2014) and belowground allometric equation is based on Craft et al. (1991).	3-102
Table 3-15	Summary of sampling design carried out in three salt marshes studied in Nigg Bay	3-108
Table 4-1	Chapter 4 research questions and experimental hypotheses	4-114
Table 4-2	Filter disc sediment deposition rates (in g.m-2day-1) per sites and saltmarsh zones.	4-118
Table 4-3	Filter disc sediment deposition rates (in g.m-2day-1) per collection month.	4-119
Table 4-4	Filter disc sediment deposition (in g.m-2 day-1) in winter and summer by sites.	4-123
Table 4-5	AstroTurf Mat Sediment deposition rates (in g.m-2day-1) per sites per saltmarsh zones.	4-124
Table 4-6	AstroTurf mats sediment deposition rates in g.m-2day-1per collection month.	4-126
Table 4-7	Average AstroTurf mats deposition rates (in g.m-2day-1) in winter and summer by sites.	4-130
Table 4-8	Average BDD (g.cm-3) per sites by saltmarsh zones for the first 30 cm (depth corrected for compaction) of the cores used to calculate accretion rates. * No cores were collected in pioneer, so the overall average BDD was used for FM.	4-132
Table 4-9	Filter disc and AstroTurf mat accretion rate estimates	4-137
Table 4-10	Two-way feedbacks between biological and physical processes (ref Chapter 2 -2.2.1 and 2.3.2.2. citing (Möller, 2006; Mudd et al., 2009; Friess et al., 2011; Wang and Temmerman, 2013; Belliard et al., 2017; Leonardi et al., 2018; Reef et al., 2018)	4-138
Table 4-11	Overall vegetation height (cm) between saltmarsh zones (top) and between sites and saltmarsh zones (bottom) as surveyed in July 2016 (n=34).	4-140
Table 4-12	Vegetation density per m2 by site	4-142
Table 4-13	Average vegetation cover (%) per sites and saltmarsh zones There is significant differences of vegetation cover between saltmarsh zones (F=10.14, p<0.001) with highest percentage of bare cover found on PM zones. The same pattern is observed on ANK (F=4.6, p=0.03) and MR (F=3.54, p=0.04).	4-144
Table 4-14	Calculated average flood depth (m) between saltmarsh sites for the period of the sediment deposition campaign (filters and AstroTurf mats) from 09th March 2016 to 01st March 2017. Note that n corresponds to a 1m2 cell size.	4-150
Table 4-15	Calculated average flood depth (m) between sites' saltmarsh zones for the sediment deposition campaign (filters and AstroTurf mats) from 09th March 2016 to 01st March 2017. Note1 that n corresponds to a 1m2 cell size; * Note2 FM-HM marsh surface include sampling points that display mid-marsh vegetation assemblages (SM13d), therefore	4-153

	statistics also tested differences between FM's HM and ANK's MM and MR'S MM.	
Table 4-16	Calculated average flood frequency (%) between saltmarsh sites for the sediment deposition campaign (filters and AstroTurf mats) from 09th March 2016 to 01st March 2017. Note that n corresponds to a 1*1 m cell size.	4-154
Table 4-17	Calculated average flood frequency (%) between sites' saltmarsh zones for the sediment deposition campaign (filters and AstroTurf mats) from 09th March 2016 to 01st March 2017. See Table 4-15 Note1 & 2.	4-157
Table 4-18	Calculated average hydroperiod (m) between saltmarsh sites for the sediment deposition campaign (filters and AstroTurf mats) from 09th March 2016 to 01st March 2017. Note that n correspond to a 1*1 m cell size.	4-159
Table 4-19	Calculated average hydroperiod (m) between sites' saltmarsh zones for the sediment deposition campaign (filters and AstroTurf mats) from 09th March 2016 to 01st March 2017. See Table 4-15 Note1 & 2.	4-160
Table 4-20	Flood depth levels (m) between sediment deposition campaign (filters and AstroTurf mats) from 09th March 2016 to 01st March 2017. The last rows present the flood depth levels (m) during summer and winter season.	4-162
Table 4-21	Hydroperiod levels (m) between sediment deposition campaign (filters and AstroTurf mats) from 09th March 2016 to 01st March 2017. The last rows present the hydroperiod levels during summer and winter season.	4-165
Table 4-22	Average differences (%) between the collection/deployment levels of flood depth (m) and hydroperiod (m) and the monthly average, i.e. each day HW and LW depths (also calculated for 1 m <sup>2</sup> cell).	4-168
Table 5-1:	research questions tested in this chapter.	5-234
Table 5-2:	MHWS rate of changes in m per year. Positive values correspond to a landward migration (erosion) and negative values to seaward movement (accretion). The overall rates are averaged using FM and ANK marsh results.	5-242
Table 5-3:	Summary of the surface elevation height change (in m) using airborne and TLS DEMs from 2011 to 2017 surveys (table 3-9) on the three sites (n= a cell of 0.1*0.1 m).	5-250
Table 5-4:	Volumetric and areal changes on three studied salt marsh ANK, FM, and MR (sum total of 23.84±0.58 ha) over a period of 6 years (2011-17). SE has been calculated here on each cell where precision depends on the accuracy of survey measures of the mass points	5-251
Table 5-5:	Average sedimentation rates derived from sedimentation plates (cm per year) across the three salt marshes.	5-255
Table 6-1:	research questions tested in this chapter.	6-284
Table 6-2:	Summary of cores number and number of samples retrieved across the sites and saltmarsh surface zones as depicted in Figure 6-2 and used for sediment particle analysis. * Cores collected on saltmarsh edge.	6-286
Table 6-3:	Sediment distribution (clay, sand and silt %) for the nine cores presented in this section: A10, A11, A13, A15, FM6, MR16, MR24, MR36 and MR8.	6-296
Table 6-4:	BDD (g m <sup>-3</sup> ) per sites and saltmarsh surface zones .	6-299
Table 6-5:	Water content (%) per sites and saltmarsh surface zones . Top row provides one-way ANOVA results for each salt marsh of the variance of water content (loge%) versus saltmarsh surface zones between at	6-302

	using p-value<0.001=***, p-value<0.01=** and p-value<0.05=* (details in Table E-2)	
Table 6-6:	Averaged percentage of inorganic material using LOI at 800°C per site and saltmarsh surface zones .	6-305
Table 6-7:	Averaged percentage of organic matter loss using LOI at 450°C per site and saltmarsh surface zones. (Variance is established on median SOM % between saltmarsh surface zones using K-W test for ANK: H=102.34; p<0.001***; for FM: H=47.5 ; p<0.001***; for MR: H=24.38; p<0.001***).	6-310
Table 6-8:	Carbon density g.Ccm-3 by saltmarsh sites and zones (top row present results of ANOVA between saltmarsh surface zones per site and statistical significance using *<0.05, **<0.01** and <0.001***).	6-313
Table 7-1:	Schematic example of the single aliquot regenerative dose (SAR) procedure. The method consists in a series of measurements' cycles. The first cycle measures directly the natural grains (aliquot) luminescence signal until it fades completely (labelled L in graph) . By giving a controlled (known) radiation dose to the grains, labelled T in the graph, it allows to measure the luminescence or brightness' sensitivity and to correct any sensitivity changes. This is done by calculating the ratio between L and T. The same protocol is repeated in a second cycle of measurements after exposing the grains in the laboratory to an artificial radiation dose (known as regenerated dose), this regenerated OSL signal is then given the same test dose as during the first cycle to correct effect in sensitivity changes and their ratio is calculated providing a second corrected OSL. Successive cycles can measure different regenerated signal. Finally, plotting each cycle 's OSL corrected signal as a function of the laboratory dose (last row of the table) is used to calculate the sample or aliquot ED by projecting the natural OSL (corrected) to the response curve created by the regenerated OSL signal (redrawn from Duller ,2008, p.10)	7-339
Table 7-2:	Questions and experimental hypotheses tested under the thesis aims	7-342
Table 7-3:	Preliminary core MR24 sampling strategy. Note1: * sample number of 22. Note2: year 2016.	7-352
Table 7-4:	Correlation (Spearman's rho and significance values as <0.001***, <0.01** and <0.05*) between IRSL and OSL signal using three proxy methods, ED1, FED1 and ED2 for 3 cm discs aliquots.	7-369
Table 8-1:	Accretion and sedimentation rates in Scotland, the UK and Europe. Note 1: the method used determines Short-term or Long-term results. Note 2: MR managed realignment or RSM restored salt marsh.	8-389
Table 8-2:	Accretion rates Filter disc in cm yr-1 and Total Soil Carbon Store Soil in tC.ha-1	8-402

## List of Figures

Figure 1-1:	Biological and geomorphological interactions of marsh development through time. Adapted from Allen (2000), Cahoon et al.(2009); Davidson-Arnott et al.(2002).	1-8
Figure 2-1:	conceptualised diagram presenting the background themes discussed in this chapter framing the thesis overarching aims.	2-12
Figure 2-2:	Estimated global distribution of salt marshes and mangroves. Adapted from D’Odorico et al. (2013) and using Mcowen et al. (2017) data.	2-14
Figure 2-3:	Distribution of salt marshes in the UK (Taken from Boorman, 2003, p.13).	2-15
Figure 2-4:	Distribution of salt marshes across Scotland (5km grid). Data from Haynes, 2016.	2-15
Figure 2-5:	(a) & (b): Following D’Alpaos et al. (2016) and Wheaton et al. (2011) approach, the top chart (a) shows the number of publications (totalling to 14703) from 1990 to 2018 referring to Coastal wetland landscapes. Wheaton et al. (2011) argued that “scientists at the interface of physical and biological sciences have struggled with what to call their discipline” (Wheaton et al. 2011, p.266). The combinations of geo-, hydro-, eco-, bio- and morpho- represent different sub-disciplines that can be found in the literature and are presented here to show trends in the interdisciplinary research area. Bottom chart (b) presents the relative fractions (in %) of these publications containing the following terms in title, abstract or keywords: morphodynamic*; ecomorph*; biomorph*; ecohydr, hydrogeomorph*; ecogeomorph*; biogeomorph*.	2-19
Figure 2-6:	Biological and geomorphological interactions of saltmarsh development through time. Adapted from Allen, 2000; Davidson-Arnott et al., 2002; Cahoon et al., 2009.	2-20
Figure 2-7:	Processes that are affecting the supply and movement of the sediments across the coastal zone (Taken from Doody, 2008, p.2).	2-22
Figure 2-8:	World distribution of tidal range (taken from Davies 1972 in Eisma, 1998, p.12 )	2-24
Figure 2-9:	Tidal prediction values of Mean High Water Springs (MHWS), Mean Low Water Springs (MLWS), Mean High Water Neaps (MHWN) and Mean Low Water Neaps (MLWN) calculated over cycle of approximately 18.6 years for the UK National Tide Gauge Network station. Data source: National Tidal and Sea Level Facility). © Copyright 2016 The National Oceanography Centre (NOC) (NTSLF/NOC/NERC, n.d.).	2-25
Figure 2-10:	Frequency and average duration of tidal flooding of the principal zones in West European salt marshes in Eisma and Dijkema (1997), p.406.	2-26
Figure 2-11:	Flow diagram showing the main climatic drivers (blue) and primary (yellow) and secondary (orange) impacts of climate change to river-estuary-coast catchment in the UK (taken from Robins et al.,2016, p.131). Pathways in black lines are directed from the bottom/side to the top of a ‘driver/impact box’. Predominantly positive impacts are coloured green. Abbreviations: SST = sea surface temperature ; SPM = suspended particulate matter ; ETM = estuarine turbidity maxima.	2-38
Figure 2-12:	Scottish tide gauge trends plotted spatially to compare (a) longer-term average rates between 1957 and 2007 and (b) more recent rates between 1992 and 2007 (in Rennie and Hansom, 2011, p.199).	2-40
Figure 2-13:	main geomorphic impacts of storminess on saltmarsh ecosystems (taken from Leonardi et al., 2018, p.98).	2-42

Figure 2-14:	Source (Mieszkwoskaa et al., 2013, p.187) Overview of exposure of UK and Ireland coastal regions to erosion and coastal protection from 2004 Eurosion.	2-43
Figure 2-15:	Coastal squeeze showing how a marsh position in the tidal frame (top left) moves landward in response to SLR (bottom left). This scenario differs with the constraints of physical barriers such as seawalls (top right) where the marsh edge erodes (bottom right) (Taken from Foster et al., 2013, p.101).	2-44
Figure 2-16:	Examples of strength and weakness of possible built defences, natural defences and hybrid defences (taken from Leonardi et al. 2018, p. 103).	2-46
Figure 3-1:	Knowledge gaps addressed in this research.	3-52
Figure 3-2:	(left) Cromarty Firth river sediment catchment area (adapted from <a href="https://www.sepa.org.uk/data-visualisation/water-environment-hub/?riverbasindistrict=Scotland">https://www.sepa.org.uk/data-visualisation/water-environment-hub/?riverbasindistrict=Scotland</a> ).	3-55
Figure 3-3:	(right) Moray Firth saltmarsh extent and study area (red box).	3-55
Figure 3-4:	MR-Managed Realignment-, FM-Fronting Marsh- and ANK-Ankerville (river) salt marsh-: the three sites selected for this research.	3-55
Figure 3-5:	Sediment type and tidal dynamics in Cromarty Firth. This map has been redrawn from Stapleton and Pethick (1996) using 2014 OS Mastermap and 2016 HydroSpatial One Bathymetric data.	3-58
Figure 3-6:	Sediment type and Tidal dynamics in Nigg Bay. The research sites extent is shown in black. Sources: Stapleton and Pethick (1996), 2014 OS Mastermap and 2016 HydroSpatial One Bathymetric data.	3-59
Figure 3-7:	Nigg Bay post-realignment showing secondary defences (grey), blocked culverts (grey) constructed in advances of the two breaches (east and west in grey) through primary sea embankment (1950s in yellow) with the location of three research study sites.	3-61
Figure 3-8:	Methods to measure saltmarsh sedimentation adapted from Nolte et al., 2013.	3-63
Figure 3-9:	Research methods employed to simultaneously measure biological and physical patterns, processes and mechanisms of saltmarsh development. Dark captions make up the empiric dataset and grey captions comprise historic datasets used in analysis.	3-64
Figure 3-10:	RSPB - MR monitoring campaigns since 2001. Abbreviations: Cr = A. Crowther (2007) – PhD on restoration of intertidal habitats for non-breeding waterbirds; RSPB = RSPB internal report (Elliott, 2015); BSL = baseline Survey McHaffie (2002); Bab = Babtie Group (2002).	3-66
Figure 3-11:	RSPB’s 2002-14 baseline sampling design in MR & 2006-2007 Crowther’s sampling design in FM.	3-67
Figure 3-12:	image to the left shows the 2015 1m2 quadrats for sampling point FM3 where the sedimentation plate is located and provided TABLEFIT results as follows:	3-69
Figure 3-13:	Sample locations marked with a X correspond to the vegetation assemblage that had changed between 2011 SSS (SNH) and the start of the research in 2015. The map is overlaid on MHWS (2.1m OD) and 2011’s SSS (SNH) polygon data for the managed realignment (MR), Fronting Marsh (FM) and Natural Marsh (ANK).	3-69
Figure 3-14:	Saltmarsh zonation for MR, FM and ANK at the start of research study. MHWS (blue) as defined at the start of the research project used for the stratified random sampling integrated with NVC classification as presented in Table 3-5 and detailed in A-2.	3-70
Figure 3-15:	Overall research sampling strategy for MR, FM and ANK saltmarsh sites, short-term sampling plots (yellow, discs n=32 and mats=18), multi-annual sampling plots (black, n=60), shallow & narrow cores	3-71

- (orange, n=23), longer and wider cores along two transects (violet/heliotrope, n=8).
- Figure 3-16: This diagram taken from Buckley (2010) illustrates a combination of profile and plan curvatures which helps to understand the flow across a surface. The profile curvature influences the acceleration and deceleration of flow across the surface a) surface is upwardly convex at that cell, b) surface is upwardly concave at that cell, and c) indicates the surface is linear. Planform curvature relates to the convergence and divergence of flow across a surface d) surface is sideways convex at that cell, e) surface is sideways concave at that cell, f) indicates the surface is linear. 3-73
- Figure 3-17: Water channels (creeks), saltmarsh edge and MHWS across the three saltmarsh, ANK, FM and MR along with location of sampling points (in green) and transducer pressure logger (orange star). 3-74
- Figure 3-18: Location of pressure transducer symbolised with a yellow arrow at low (left) and high (right) tide. 3-75
- Figure 3-19: Conceptual diagram illustrating how the hydroperiod parameters have been calculated. Diagram adapted from Kefelegn (2019)) 3-75
- Figure 3-20: Filter disc and AstroTurf mat after spring tide sediment deposition. The enclosed image (bottom right) presents the DVD disc mounted with a metal weight at its base. 3-78
- Figure 3-21: Number of traps placed across the salt marsh between February 2016 to March 2017. Collection dates marked with \*\* (first and last) have not been used in the short-term deposition analysis. 3-78
- Figure 3-22: The spatial distribution of filter discs and AstroTurf mats sampling sites on the three studied salt marshes and MHWS (blue) derived from 2011 LIDAR. 3-79
- Figure 3-23: Number of traps retrieved and used in the short-term deposition analysis (except dates marked \*\*). 3-80
- Figure 3-24: 0.25m<sup>2</sup> quadrat layout 3-81
- Figure 3-25: Example of the photographic record from the 0.25m<sup>2</sup> quadrats (FM3) used for aboveground biomass survey. a) showing the sub-quadrats A1 & E5 used for density (stem counting); b) micro -detail in photographs and c) after harvesting. 3-82
- Figure 3-26: Estimation of vegetation cover where the image is first geo-rectified (a) and reclassified (b) in Arcgis to quantify Soil 21.29% - Vegetation 78.7%. Data quality was cross-checked using the two records (ArcGIS and field records) and where differences were found, the field record was chosen over the photography. 3-83
- Figure 3-27: Spatial distribution of vegetation cover sampling location (black circles) and vegetation height and biomass sampling plots (green squares). 3-83
- Figure 3-28: Example of the results of MHWS cumulative rate of change (m.yr<sup>-1</sup>), thus enabling to assess erosion (red gradients) and accretion (green gradients), at 10 m interval distance for each studied salt marsh depicted along a coloured scale baseline. 3-85
- Figure 3-29: Number of monitored sedimentation plates (y-axis) per sites for each survey campaigns between 30th July 2015 to 20th September 2017 and showing seasonal sampling for 2 winters (October to March) and 2 summers (April to September) season. 3-91
- Figure 3-30: Diagram of 20 X 20 cm sedimentation plates once inserted depicting the location of manual measurements in blue using a graduated metal rod from M1 to M5 and DGPS survey from GPS1 & GPS2 in black. These manual measurements formed the empirical data used to calculate 3-92



	surface elevation change representing accretion and erosion and sedimentation rates for the three salt marshes.	
Figure 3-31:	a) General view of the saltmarsh vegetation photography using 1 m2 quadrat prior the insertion of the sedimentation plates (photograph a) taken in July 2015 in high-marsh sampling plot MR2 b) c) & d) depict the three stages of the 20 X 20 cm sedimentation plate insertion (photograph b) on mid-marsh sampling plot MR22 and photograph c) & d) on low-marsh plot MR57).	3-93
Figure 3-32:	Spatial distribution of sedimentation plates on the three studied salt marshes showing MHWS (blue) derived from 2011 LIDAR.	3-93
Figure 3-33:	a) Corer tested in February 2016 to retrieve 30 cm deep and 11 cm of diameter cores proved to ease manual coring, provide wide cores to reduce soil compaction and allow multiple aliquot sampling and analysis	3-97
Figure 3-34:	a) In-house bespoke manual corer designed to insert a 1m long and 0.08m diameter PVC tube into sealed steel core barrel for easy assemblage, transportability and protection from light. b) The corer prior to coring c) coring on the FM salt marsh in April 2016.	3-97
Figure 3-35:	Cores sampling location addressing biogeomorphic properties of the three studied salt marshes overlaid on saltmarsh zones and 2011-MHWS (blue line).	3-98
Figure 3-36:	Box plot showing the overall coring compaction ratio (real depth/tube depth) from the different coring devices sizes.	3-98
Figure 3-37:	A stepped coring compaction approach where the error is removed at regular intervals through the core. The bar graph (right) shows real depth of core (black), recorded depth in the tube (red) and how overall compaction factor may not be the best option (eg at Depth 4 and Depth 6).	3-99
Figure 3-38:	Spatial distribution of cores sampling location addressing physical characteristics on the three studied salt marshes showing saltmarsh zones and MHWS derived from 2011LIDAR (blue line). Note that MR36 and MR24 are both located in PM zones, only MR24 was used for analysis. Red lines present the two transects running axis.	3-104
Figure 3-39:	Pebble retrieved 52cm deep in Core A13.	3-104
Figure 4-1:	Chapter 4 focusses on biological and geomorphological interactions of short-term (annual) saltmarsh development in light of environmental processes and extrinsic and intrinsic factors influencing its evolution (after (Allen (2000); Davidson-Arnott et al. (2002) and Cahoon et al.(2009)).	4-113
Figure 4-2:	a) Boxplot of the Filter disc sediment deposition rates (in g.m-2day-1) per the sites' saltmarsh zones. Boxplots represent median (middle line) interquartile range (box), 1.5 times interquartile range (bar) and outliers (black dots). b) same boxplots with significant differences between saltmarsh sites and zones (Kruskal-Wallis H test and significant pair-test comparison using Wilcoxon rank tests results by the p-value significance: ns, *,**,*** for > 0.05, ≤0.05, ≤0.01, ≤0.001).	4-118
Figure 4-3:	Spatial variation for the average filter disc sediment deposition rates showing sampling points with graduated symbol size estimated in g.m-2day-1 superimposed on the creek system and the extent of saltmarsh sites and saltmarsh zones (Basemap Source: OrdnanceSurvey@CrownCopyright Aerial photography(2011)).	4-118
Figure 4-4:	a) Bar graph of the Filter disc sediment deposition rates ( ( in g.m-2day-1) in g.m-2day-1) from 09th March 2016 to 31st January 2017 (top of bar is average deposition, error bars calculated from individual standard	4-120

- error). b) Boxplot of the Filter disc sediment deposition rates (g.m-2day-1) presenting the significant results of Games Howell pairwise comparison tests between collection dates (Mann-Whitney-Wilcoxon tests results are symbolised on the top rows by the p-value significance - ns, \*, \*\*, \*\*\* - for each pairwise tests. The statistical analysis was generated on transformed dataset to meet normality assumption and details are in Table C-2.
- Figure 4-5: Bar graph of filter disc sediment deposition mean ranks rates (g.m-2day-1) from 09th March 2016 to 31st January 2017 for ANK (a), FM (c) and MR (e). (Top of bar is mean rank average deposition, error bars calculated from individual standard error). Boxplot of filter discs deposition rates (g.m-2day-1) showing statistically significant differences between collection dates for ANK (b), FM (d) and MR (f) (The boxplots represent median and error bars are interquartile range; Mann-Whitney-Wilcoxon tests results are symbolised on the top rows by the p-value significance - ns, \*, \*\*, \*\*\* - for each pairwise tests) 4-122
- Figure 4-6: a) Average filter disc sediment deposition rates (g.m-2 day-1) between summer (n=153) and winter (n=151) (top of bar is average deposition, error bars calculated from individual standard error). The graph also present results and statistical significance of Games-Howell test between seasons (symbolised on the top rows by the p-value significance - ns, \*, \*\*, \*\*\*). 4-123
- Figure 4-7: Spatial variation for the AstroTurf mats sediment deposition rates showing sampling points with graduated symbol size calculated in g.m-2day-1 across sites and saltmarsh zones with depiction of creek system (Basemap Source: OrdnanceSurvey@CrownCopyright Aerial photography(2011)). 4-125
- Figure 4-8: a) Bar graph of the AstroTurf mats sediment deposition rates (in g.m-2day-1) from 09th March 2016 to 01st March 2017 (top of bar is average deposition, error bars calculated from individual standard error). b) Boxplot of the AstroTurf mats sediment deposition rates (in g.m-2day-1) highlighting the significant results of Games Howell pairwise comparison tests between each sediment collection's deposition (date of collection is shown in x-axis; Mann-Whitney-Wilcoxon tests results are symbolised on the top rows by the p-value significance - ns, \*, \*\*, \*\*\* - for each pairwise tests). Note that the statistical analysis was generated on transformed dataset to meet normality assumption and details are in Appendix C.1-Table C-5. 4-127
- Figure 4-9: Bar graph of ANK's (graph a), FM's (c) and MR's (e) AstroTurf mats sediment deposition mean ranks rates (in g.m-2day-1) from 09th March 2016 to 01st March 2017 (top of bar is mean rank's average deposition, error bars calculated from individual standard error). Boxplot of ANK's (graph b), FM's (d) and MR's (f) AstroTurf mats sediment deposition rates (in g.m-2day-1) showing statistically significant differences between rates during campaign (The boxplots represent median and error bars are interquartile range; Mann-Whitney-Wilcoxon tests results are symbolised on the top rows by the p-value significance - ns, \*, \*\*, \*\*\* - for each pairwise tests performed on ANK and MR and similarly Covoner's test results are presented for FM deposition rates). 4-129
- Figure 4-10: a) Average AstroTurf mats sediment deposition rates (in g.m-2day-1) between summer (n=93) and winter (n=103) (top of bar is average deposition, error bars calculated from individual standard error). The graph also present results and statistical significance of Games-Howell 4-130

- test between seasons (symbolised on the top rows by the p-value significance - ns, \*, \*\*, \*\*\*).
- Figure 4-11: Relationships between BDD (g cm<sup>-3</sup>) and corrected depth (cm) (corrected for compaction - see Chapter 3 – 3.4.3.2). The results of polynomial regressions are provided for the whole dataset (a), ANK's whole cores' depths (c), those of FM's (e) and of MR (f). Each graph also presents as an inset the same relationships for the upper 30 cm the whole dataset (b), ANK (d), FM (f) and MR (g). (Note the different scale of the y-axis in graphs c) and d) compared to graphs e) to h)). 4-132
- Figure 4-12: Upper 30cm Dry soil Bulk Density (BDD) calculated for each saltmarsh site and zone (as presented in Table 4-8 above) from the cores collected in 2016 on the salt marshes of Nigg Bay and used to convert deposition rates to accretion rates. 4-133
- Figure 4-13: Average accretion rate estimates (cm.yr<sup>-1</sup> and error bars calculated from individual SE) per sites per devices. The graph also present the statistical significance of Dunn Post-hoc test between sites (symbolised on the top rows by the p-value significance - ns, \*, \*\*, \*\*\* ; details in Table C-8). 4-134
- Figure 4-14: Average accretion rate estimates (cm.yr<sup>-1</sup> and error bars calculated from individual SE) (a) calculated from filter discs traps and (b) showing the statistical significance of Dunn Post-hoc test (using BH adjustments) between the sites' saltmarsh zones (symbolised on the top rows by the p-value significance - ns, \*, \*\*, \*\*\* ; details in Table C-9). Graph (c) and (d) are presenting the results from AstroTurf mat traps (pairwise comparisons are detailed in Table C-10). 4-136
- Figure 4-15: Boxplots of vegetation height (cm) mean ranks measured in July 2016 (a) between saltmarsh zones highlighting Welch Anova statistical results; and, (b) between sites and saltmarsh zones with Kruskal-Wallis statistical results. Both graphs highlight the statistical significance for Dunn test's pairwise comparison (using BH adjustments - symbolised on the top rows by the p-value significance - ns, \*, \*\*, \*\*\* ). Boxplots represent median (middle line) interquartile range (box), 1.5 times interquartile range (bar) and outliers (black dots). 4-140
- Figure 4-16: Boxplot of vegetation density (per m<sup>-2</sup>) mean ranks measured in July 2016 (a) between salt marshes highlighting Welch Anova statistical results; and, (b) between sites and saltmarsh zones with Kruskal-Wallis statistical results. Both graphs highlight the statistical significance for pairwise comparison tests ((a) Wilcoxon test; and, (b) Dunn test's (using BH adjustments) both symbolised on the top rows by the p-value significance - ns, \*, \*\*, \*\*\* ). Boxplots represent median (middle line) interquartile range (box), 1.5 times interquartile range (bar) and outliers (black dots). 4-141
- Figure 4-17 : Proportion of vegetation uniformity per sites showing FM having no variability in vegetation density whilst ANK display a wider display of vegetation characteristics across its zones and MR has predominantly clumped vegetation. 4-142
- Figure 4-18 : Stacked column graphs (to 100 %, error bars  $\pm$ SE) showing the average vegetation abundance cover (bare/vegetation in %) between sites and saltmarsh zones. Boxplot of average vegetation abundance cover (bare/vegetation in %) mean ranks measured in July 2016 (a) between saltmarsh sites; and, (b) between sites and saltmarsh zones. Both graphs highlight Kruskal-Wallis statistical results and the statistical significance for pairwise comparison tests (Dunn test's (using BH adjustments) both symbolised on the top rows by the p-value significance - ns, \*, \*\*, \*\*\* ). Boxplots represent median (middle line) 4-143

	interquartile range (box), 1.5 times interquartile range (bar) and outliers (black dots).	
Figure 4-19	: Trends between vegetation density and vegetation height per site along with regression results (p-value significance - ns, *, **, *** ).	4-145
Figure 4-20	: Scatter plot between aboveground carbon content (in OCg.m2 - y-axis) and vegetation height (in cm). Plots are showing linear regressions with their respective relationship equation (the regressions have been log transformed -dependent variable- to meet linear assumption), r2 values, p-value and p-value significance).	4-145
Figure 4-21	: Bar graphs showing mean ranks' vegetation height (a), density (b), cover (c) and aboveground organic content- OCg.m2 (d) for each NVC assemblages sampled on the three Nigg Bay salt marshes. The graphs also label Kruskal-Wallis results and the statistical significance of post-hoc pairwise comparison tests ((a and c) Wilcoxon test using Bonferroni adjustments; and, (b and d) Dunn test's using BH adjustments) both symbolised on the top rows by the p-value significance with p-value significance (ns, *, **, ***).	4-147
Figure 4-22	: High Water (HW) and Low Water (LW) levels from the 09th February 2016 to 01st March 2017 where the dates and green lines correspond to sediment data collection points. Note: The first -sediment collection (09/02/2016*) was a trial for equipment (filter discs and AstroTurf mats) and not included in the time series or sediment deposition analysis.	4-149
Figure 4-23	: Average (over 389days) flood depth (m) calculated at a 1m2 cell scale size for the three saltmarsh sites.	4-151
Figure 4-24	: Spatial variation of very high flood depth (outliers in yellow) and extremely high flood depth (red) values across the three studied salt marshes ranging from 0.42 m to 0.67 m.	4-151
Figure 4-25	: Boxplot of the flood depth mean ranks (m) for the sediment deposition campaign showing significant differences between saltmarsh sites (Kruskal-Wallis H test and Mann-Whitney-Wilcoxon tests results are symbolised on the top row by the p-value significance - ns, *, **, *** - for each pairwise test). Boxplots represent median (middle line) interquartile range (box), 1.5 times interquartile range (bar) and outliers (black dots).	4-152
Figure 4-26	: Plot of the flood depth mean ranks (m) for the sediment deposition campaign showing significant differences between sites' saltmarsh zones (The plots represent median and error bars are interquartile range. Kruskal-Wallis H test and Mann-Whitney-Wilcoxon tests results are symbolised on the top row by the p-value significance - ns, *, **, *** - for each pairwise tests -For full pair-test comparison boxplot see in Appendix C.3 Figure C-8).	4-153
Figure 4-27	: Average flood frequency (% - over 389days) calculated at a 1m2 cell scale size for the three saltmarsh sites.	4-154
Figure 4-28	: Boxplot of the flood frequency mean ranks (%) for the sediment deposition campaign showing significant differences between saltmarsh sites (The plots represent median (middle line) interquartile range (box), 1.5 times interquartile range (bar) and outliers (black dots. Kruskal-Wallis H test and Mann-Whitney-Wilcoxon tests results are symbolised on the top row by the p-value significance - ns, *, **, *** ).	4-155
Figure 4-29	: Plot of the flood frequency mean ranks (%) for the sediment deposition campaign showing significant differences between sites' saltmarsh zones (The plots represent median and error bars are interquartile range. Kruskal-Wallis H test and Mann-Whitney-Wilcoxon tests results are symbolised on the top row by the p-value significance - ns, *, **, *** -	4-156

	for each pairwise tests -For full pair-test comparison boxplot see in Appendix C.3 Figure C-9).	
Figure 4-30	: Spatial variation across the three salt marshes of very high flood frequency (outliers in yellow) and extremely high flood frequency (red) values across the three studied salt marshes ranging from 44 % to 97 %.	4-156
Figure 4-31	: Boxplot of the average hydroperiod mean ranks (m) for the sediment deposition campaign showing significant differences between saltmarsh sites (Kruskal-Wallis H test and Mann-Whitney-Wilcoxon tests results are symbolised on the top row by the p-value significance - ns, *, **, *** - for each pairwise tests). Boxplots represent median (middle line) interquartile range (box), 1.5 times interquartile range (bar) and outliers (black dots).	4-158
Figure 4-32	: Average hydroperiod (m - over 389days) calculated at a 1m2 cell scale size for the three saltmarsh sites.	4-158
Figure 4-33	: Spatial variation of very high hydroperiod (outliers in yellow) and extremely high hydroperiod (red) values across the three studied salt marshes ranging from 0.45 to 1.12 m.	4-159
Figure 4-34	: Plot of the average hydroperiod mean ranks (m) for the sediment deposition campaign showing significant differences between sites' saltmarsh zones (The plots represent median and error bars are interquartile range. Kruskal-Wallis H test and Mann-Whitney-Wilcoxon tests results are symbolised on the top row by the p-value significance - ns, *, **, *** - for each pairwise tests -For full pair-test comparison boxplot see in Appendix C.3 Figure C-10).	4-160
Figure 4-35	: Flood depth and extent across the three salt marshes (calculated for 1m2cell) for each sediment deposition collection (from 9th March to 03rd August 2016) during the campaign (Basemap Source: OrdnanceSurvey@CrownCopyright Aerial photography(2011)).	4-163
Figure 4-36	: Flood depth and extent across the three salt marshes (calculated for 1m2cell) for each sediment deposition collection (from 18th September 2016 to 01st March 2017) during the campaign (Basemap Source: OrdnanceSurvey@CrownCopyright Aerial photography(2011)).	4-164
Figure 4-37	: Bar graph of the flood depth level (m) for each sediment deposition campaign showing Welch's Anova F test results (for Games-Howell post hoc procedure results, see Appendix C.3 - Table C-16 for full details). Top of bar is mean levels and error bars their standard deviation.	4-164
Figure 4-38	: Bar graph of hydroperiod level (m) for each sediment deposition campaign showing Welch's Anova F test results (for Games-Howell post hoc procedure results, see Appendix C.3 - Table C-16 for full details). Top of bar is mean levels and error bars their standard deviation.	4-165
Figure 4-39	: Hydroperiod (in m) and extent (calculated for 1m2 cell) for each sediment deposition collection (from 9th March to 03rd August 2016) during the campaign (Basemap Source: OrdnanceSurvey@CrownCopyright Aerial photography(2011)).	4-166
Figure 4-40	: Hydroperiod and extent (calculated for 1m2cell) for each sediment deposition collection (from 18th September 2016 to 01st March 2017) during the campaign (Basemap Source: OrdnanceSurvey@CrownCopyright Aerial photography(2011)).	4-167
Figure 4-41	: Schematic research framework of this study's short-term physical and biological saltmarsh dynamics, in which the influence of physical drivers as defined in Chapter 3 - section 3.3.2.3 was used to qualify short-term characteristics and controls to sediment and vegetation results, as presented in the following sections.	4-169

Figure 4-42	: Diagram of the process variables and intrinsic factors known to influence short-term deposition and accumulation that have been measured on the three salt marshes of Nigg Bay.	4-170
Figure 4-43	: PCA biplot for sediment deposition rates and physical controls to saltmarsh development showing in x-axis and y-axis the principal components that contribute the most to the variance of the dataset (PC1 and PC2). Individual samples are symbolised with a point coloured by vegetation assemblage with a confidence ellipse plotted around group mean points and each variable represented by an arrow with its length informing on the PCA loading scores (longer arrows have higher contribution and vice versa Variables used are:	4-171
Figure 4-44	: Correlation matrix between variables showing correlation coefficients strength represented by a hue gradient (blanks have insignificant p-values) and p-value significance by * for <0.05,** for <0.01,*** for <0.001 (see Figure 4-43 for variables abbreviations).	4-172
Figure 4-45	: a) Scatter plot between filter disc sediment deposition rates (in g.m <sup>2</sup> .yr) and flood depth (in m). b) Scatter plot between filter disc sediment deposition rates (in g.m <sup>2</sup> .yr) and hydroperiod (in m). Both graphs show data coloured by vegetation assemblages (NVC) with linear regression. They also indicate the regression formulae (note that y values are normalised using Box-Cox transformation with a lambda value of 0.3), r <sup>2</sup> adj and p-value.	4-173
Figure 4-46	: a) PCA Dim1 (x-axis) and 2 (y-axis) biplot using accretion rate estimates and physical controls to saltmarsh development showing. Each variable is represented by an arrow with its length informing on the PCA loading scores, the samples are coloured using vegetation assemblages with a confidence ellipse plotted around group mean points. Variables used are:	4-174
Figure 4-47	: Correlation matrix between variables showing correlation coefficients strength represented by a hue gradient (blanks have insignificant p-values) and p-value significance by * for <0.05,** for <0.01,*** for <0.001 (see Figure 4-46 for variables abbreviations).	4-174
Figure 4-48	: a) Scatter plot between filter discs accretion rate estimates (in cm.yr <sup>-1</sup> ) and hydroperiod (in m); b) Scatter plot between filter disc sediment deposition rates (in g.m <sup>2</sup> .yr) and flood depth (in m). Both graphs show the second predictor variable as a gradient colour representing its distance to the saltmarsh edge. They also indicate the regression formulae (note that y values are normalised using Box-Cox transformation with a lambda value of 0.3), r <sup>2</sup> adj and p-value.	4-175
Figure 4-49	: PCA plots a) to k) for each sediment deposition campaign showing in x-axis and y-axis the principal components that contribute the most to the variance of the dataset (PC1 and PC2). Individual samples are symbolised with a point coloured by vegetation assemblage and each variable represented by an arrow with its length and gradient color informing on the PCA loading scores (dark longer arrows have higher contribution and vice versa). Graphs d and j have a ellipse plotted around vegetation assemblages highlighting clustering.	4-180
Figure 4-50	: PCA biplot for vegetation characteristics and physical controls to saltmarsh development showing in x-axis and y-axis the principal components that contribute the most to the variance of the dataset (PC1 and PC2). Each variable represented by an arrow with its length informing on the PCA loading scores. Variables used:	4-183
Figure 4-51	: Scatter plots between vegetation height (in cm - y-axis) and elevation (in m - plot a), distance to saltmarsh edge (m - plot b), soil bulk density (g.cm <sup>3</sup> - plot c), hydroperiod (in m - plot d), flood frequency (in % - plot	4-184

	e) and flood depth (in m - plot f) . Plots are showing linear regressions relationship, r2 values and p-value.	
Figure 4-52	: Scatter plots (with linear regressions relationship, r2 values and p-value) between vegetation density (n per m2 - y-axis) and elevation (in m - plot a), distance to saltmarsh edge (m - plot b), and hydroperiod (in m - plot c).	4-184
Figure 4-53	: Scatter plots (with linear regressions relationship, r2 values and p-value) between vegetation cover (in % - y-axis) and elevation (in m - plot b), hydroperiod ( in m - plot b), flood frequency (in % - plot c) and flood depth (in m - plot d).	4-185
Figure 4-54	: Scatter plots between aboveground organic content (in g.m2 - y-axis) and BDD (in g.cm3 - plot a) and distance to saltmarsh edge (in m - plot b). Plots are showing linear regressions with their respective relationship equation, r2 values and p-value	4-186
Figure 4-55	: PCA biplot for vegetation characteristics and tidal controls to saltmarsh development showing in x-axis and y-axis the principal components that contribute the most to the variance of the dataset (PC1 and PC2). Each variable represented by an arrow with its length informing on the PCA loading scores. Variables used:	4-186
Figure 4-56	: Average flood depth (m- top), flood frequency (%- middle) and average hydroperiod (m -bottom) levels for each vegetation assemblages (details in see Appendix C.3 Figure C-25 to 27). The top row (grey) represents Mann-Whitney-Wilcoxon tests results are symbolised on the top row by the p-value significance - ns, *, **,*** - for each pairwise tests. For full pair-test comparison see Appendix C.3 Figure C-4, C-5, C-6.) The plot represent median and error bars are interquartile range.	4-188
Figure 4-57	: Mean ranks' flood depth (m- top), flood frequency (%- middle) and hydroperiod (m -bottom) levels between vegetation assemblages present for each saltmarsh site. The bar graph represent median and error bars are interquartile range.	4-189
Figure 4-58	: PCA biplot for vegetation characteristics and short-term sediment deposition rates (deposition and accretion) showing in x-axis and y-axis the principal components that contribute the most to the variance of the dataset (PC1 and PC2). Each variable represented by an arrow with its length informing on the PCA loading scores. Variables used:	4-191
Figure 4-59	: Bar graphs showing Filter Discs a) Deposition rate (g.m-2.day-1) and b) accretion rate estimates (cm.yr-1 ) mean rank's for each NVC assemblages sampled on the three Nigg Bay salt marshes. The graphs also label Kruskal-Wallis results and the statistical significance of post-hoc pairwise comparison tests Wilcoxon test using Bonferroni adjustments symbolised on the top rows by the p-value significance with p-value significance (ns, *, **,***). The bar graph represent median and error bars are calculated using standard errors (SE).	4-192
Figure 4-60	: Bar graph of mean ranks' Filter Discs a) Deposition rates (g.m-2.day-1) and b) accretion rate estimates (cm.yr-1) between vegetation assemblages sampled on a saltmarsh site. The bar graph represent median and error bars are interquartile range.	4-194
Figure 4-61	: Bar graph and scatter plot (inset on right) of deposition rates (g.m-2.day-1) between filter discs and AstroTurf mats showing Welch's Anova F test and regression's results (r2, F-statistics and p-value in bold - the regressions have been box-cox transformed -dependent variable-to meet linear assumption). The bar graph represent mean and error bars are the standard error	4-197

Figure 4-62	: Bar graph (a) and scatter plots (b) of deposition rates (g.m <sup>-2</sup> .day <sup>-1</sup> ) between sites' filter discs and AstroTurf mats.	4-198
Figure 4-63	: Scatter plots of deposition rates (g.m <sup>-2</sup> .day <sup>-1</sup> ) between sites' filter discs and AstroTurf mats. The plots provide the correlation strength and significance (rho and p-value ) respective to each saltmarsh zones.	4-198
Figure 4-64	: Scatter plots of deposition rates (g.m <sup>-2</sup> .day <sup>-1</sup> ) between sites' filter discs and AstroTurf mats. The plots provide the correlation strength and significance (rho and p-value) respective to each sampling point.	4-199
Figure 4-65	: Sediment deposition samples with significant correlation between trap types. The graduated symbol size of the sample points represents the correlation strength and significance (rho and p-value) superimposed on the on creek/water channel system, and the orange circles highlight the location of the breaches.	4-200
Figure 4-66	: Scatter plots of deposition rates (g.m <sup>-2</sup> .day <sup>-1</sup> ) between sites' filter discs and AstroTurf mats. The plots provide the correlation strength and significance (rho and p-value) respective to each sampling campaign.	4-200
Figure 4-67	: a) to k): Filter disc sediment deposition rates (g.m <sup>2</sup> .day <sup>-1</sup> ) for the three studied salt marshes of Nigg Bay between 09th March 2016 to 31st January 2017.	4-208
Figure 4-68	:a) to l): AstroTurf mat sediment deposition rates (g.m <sup>2</sup> .day <sup>-1</sup> ) for the three studied salt marshes of Nigg Bay between 09th March 2016 to 01st March 2017.	4-210
Figure 4-69	: Hydroperiod parameters over the ANK, FM and MR elevation heights (m) : mean hydroperiod (m), flood depth (m), flood frequency (ratio of floods – number of floods per tidal period – for the study period – 778 tidal periods). MHWS and MLWS were calculated for the period of the sediment deposition collection from March 2016 to March 2017.	4-221
Figure 4-70	: Bar graph showing the aboveground organic carbon stock (t C ha <sup>-1</sup> ) in the pioneer, low-mid (low and mid-marsh zone values have been averaged for Nigg salt marshes to match Miller et al. (2023) results as there was no distinction made between mid and low marsh in their study) and high-marsh zones of ANK, FM, MR and Dornoch point and Morrich More saltmarshes (Error bars are standard deviation).	4-226
Figure 4-71	: Sampling points with graduated symbol calculated for the mean accretion rate (in cm yr <sup>-1</sup> for filter discs) across the three salt marshes at Nigg Bay. The symbols are superimposed on a surface model that represents the accretion rates at a constrained distance using the extent of each vegetation community (NVC-assemblage). To interpolate values from the accretion rates (filter discs), a geostatistical interpolation technique called Kriging, which uses the statistical properties of the measured points, was employed. As evidenced by the statistics presented in Chapter 4, vegetation assemblages significantly explain these rates, a diffusion interpolation model was run using the extent of vegetation communities (NVC assemblages - see Chapter 3 - section 3.3.2.2 - paragraph Research baseline NVC vegetation assemblages) as barriers (ESRI (1), n.d.). Where an area lacked sufficient samples, Empirical Bayesian Kriging (with values transformed to meet normal distribution requirements; (ESRI (2), n.d.)) was used to fill in the gaps (i.e. not enough sample points to accurately interpolate the full extent of the vegetation polygon - in all cases the gaps never exceeded more than 1% of the vegetation assemblage polygon).	4-228
Figure 5-1:	Chapter 5 focus on biological and geomorphological interactions of long-term saltmarsh development (decadal to centennial) in light of	5-233



environmental processes and extrinsic and intrinsic factors influencing its evolution (after (Allen, 2000; Davidson-Arnott et al., 2002; Cahoon et al., 2009)).

Figure 5-2:	Roy's map (1747-1753).	5-236
Figure 5-3:	Ainslie' 1785 chart of the Nigg's Sand	5-237
Figure 5-4	a) & b): 1872 OS 1st edition One-inch	5-237
Figure 5-5:	a) 1942 Admiralty Charts of Scotland b)1943-Bartholomew's map c) 1947 OS One-inch map.	5-237
Figure 5-6:	1958 OS One-inch map is the first cartographic evidence to provide a timestamp for the last reclamation (green) in the study site MR and the sea defence extension (red).	5-237
Figure 5-7:	1960 OS 1:10K- scale showing saltmarsh extent (blue) and embankment (red).	5-238
Figure 5-8:	Combined 1977(a) and 1980 (b) OS 1:10K- scale showing the increased extent of fronting marsh and	5-238
Figure 5-9:	Aerial view of the three research study sites (MR, FM and ANK) in October 2003 post-breach (red circle) at MHWS.	5-238
Figure 5-10:	Historical evolution of Nigg Bay saltmarsh areal extent (%).	5-240
Figure 5-11:	Areal changes between 1872 to 1977-81 representing the loss of salt marshes in red ( $38.1\pm 0.7$ ha), gain in green ( $24.4\pm 0.4$ ha) and no areal change in white ( $56.6\pm 1$ ha) and black outline depicting the extent of the research study sites (MR, FM and ANK).	5-240
Figure 5-12:	Areal changes between 1977-81 to 2012 with same symbology as above: Loss = $10.2\pm 0.2$ ha; Gain = $32.2\pm 0.6$ ha and No change = $70.8\pm 1.3$ ha.	5-241
Figure 5-13:	Overall Areal changes between 1872 to 2012 with same symbology as above: Loss = $19.8\pm 0.4$ ha; Gain = $27.5\pm 0.5$ ha and No change = $75.2\pm 1.3$ ha.	5-241
Figure 5-14:	The bar graphs (error bars calculated from individual standard errors SE) depicts the rate of change in m.yr <sup>-1</sup> of MHWS in the past 145 years providing slightly different scenarios if we are looking at the changes between 1872 and 2017 (grey bars) and the cumulative changes that occurred between these two dates (from 1872 to 2017) which include differences between MHWS of 1872, 1977, 2011, 2014, 2015, 2016 and 2017 (black bars).	5-242
Figure 5-15:	Rates of change in MHWS between 1872 to 1977-81 for the study sites are presented on a graduated colour baseline located in the foreshore. The results show an overall seaward migration of the MHWS of $-0.28\pm 0.03$ m.yr <sup>-1</sup> . The seawall construction separating MR and FM sites in 1950's impacted on the MHWS migration resulting in a seawards movement of $-81.3\pm 8.9$ m on MR, whereas the natural salt marsh benefited from accretion of $-4.8\pm 2.2$ m for FM fronting marsh and $-9.4\pm 1.8$ m on ANK.	5-243
Figure 5-16:	Between 1977-81 to 2011, a period that includes RSPB managed realignment of MR (2003) resulting in the MHWS moving $139.4\pm 10.6$ m landward. Similarly, the fronting marsh FM moved $3.1\pm 1.1$ m and ANK MHWS moved of $14.8\pm 1.4$ m landward. In 34 years, MHWS for the three salt marshes migrates landward 5 times faster than the previous 109 years at an overall rate of change $1.5\pm 0.2$ m.yr <sup>-1</sup> .	5-244
Figure 5-17:	Rates of change in MHWS migration between 2011 to 2017 for the study sites averaged at $-3\pm 0.4$ m.yr <sup>-1</sup> seawards. MR site expanded onto the lower marsh of $39\pm 6.6$ m, FM onto the intertidal $4.4\pm 0.5$ m and the natural salt marsh ANK MHWS also migrated towards the foreshore of $11.9\pm 1.6$ m.	5-244

Figure 5-18:	Cumulative rates of change in MHWS migration for the entire 145 years (1872 to 2017) with an overall MHWS seawards shift at $-0.02 \pm 0.01$ m.yr <sup>-1</sup> .	5-245
Figure 5-19:	d) A schematic overview of some morphological characteristics of a cross-shore profile for the natural salt marsh ANK showing the marsh surface height from 2011 to 2017 depicted as line coloured for different survey type used in this analysis. a) and b) are insets that provide an enlarged views of the eastern and western cross-shore profiles. Note1: vertical exaggeration 21.3X Note2: the major creek system on the eastern part of the marsh (right on graph) has not been captured during 2016 TLS campaign. Also a shallow depression is visible: the creek may have full during capture – however this feature has been removed from the height change analysis (see Figure 5-22).	5-248
Figure 5-20:	A schematic overview of some morphological characteristics of a cross-shore profile for the fronting marsh FM and managed realignment MR (transect location see Figure 5-22) showing the marsh surface height from 2011 to 2017 depicted as line coloured for different survey type used in this analysis. b) is an inset that provides an enlarged view of the south-west-south cross-shore profiles. Note1: vertical exaggeration 21.3X.	5-249
Figure 5-21:	Summary graph presenting the extent (as a percentage of its size) has gained and lost height from 2011 to 2017 airborne and TLS surveys (table 3-9) by salt marsh as depicted in Figure 5-22.	5-250
Figure 5-22:	Height change map (in m) from 2011 to 2017 airborne and TLS surveys (table 3-9) highlighting areas of accretion (light to dark green) primarily located on vegetated areas of the marsh and erosion tends to occur on the foreshore.	5-251
Figure 5-23:	Column graphs presenting the volume (left) and areal (right) change that occurred on the three salt marsh sites from 2011 to 2017 using TLS, Orthophotography and Lidar datasets showing in green gains, red losses and black line symbol representing average rate per year in m <sup>3</sup> per year.	5-252
Figure 5-24:	Boxplot of the average sedimentation rates per sites depicting high sedimentation on MR and ANK whilst FM exhibited a low sediment gain. (Kruskal-Wallis H test and significant pair-test comparison using Dun's tests results by the p-value significance: ns, *, **, *** for $> 0.05$ , $\leq 0.05$ , $\leq 0.01$ , $\leq 0.001$ . Boxplots represent median (middle line) interquartile range (box), 1.5 times interquartile range (bar) and outliers (stars)).	5-253
Figure 5-25:	Boxplot of the average sedimentation rates plates (cm per year) derived from sedimentation plates per sites' saltmarsh zones depicting high sedimentation. (Kruskal-Wallis H test and significant pair-test comparison using Dun's tests results by the p-value significance: ns, *, **, *** for $> 0.05$ , $\leq 0.05$ , $\leq 0.01$ , $\leq 0.001$ . Boxplots represent median (middle line) interquartile range (box), 1.5 times interquartile range (bar) and outliers (stars)).	5-254
Figure 5-26:	Interval plot of the overall sedimentation rates derived from sedimentation plates from 29th July 2015 to 19th September 2017 (Standard Deviation used to calculate errors bar intervals).	5-256
Figure 5-27:	Boxplot of the average sedimentation rates plates (cm per year) derived from sedimentation plates by monitoring period. (Kruskal-Wallis H test and significant pair-test comparison using Dun's tests results by the p-value significance: ns, *, **, *** for $> 0.05$ , $\leq 0.05$ , $\leq 0.01$ , $\leq 0.001$ . Boxplots represent median (middle line) interquartile range (box), 1.5 times interquartile range (bar) and outliers (stars)).	5-256

Figure 5-28:	Interval plots of ANK (top- in green), FM (middle - in blue) and MR (bottom- in yellow) compared to the average sedimentation average sedimentation rates derived from sedimentation plates (all- in back) from 29th July 2015 to 19th September 2017 (SD used to calculate errors bar intervals).	5-257
Figure 5-29:	Sedimentation rates (cm per years) using sedimentation plates for 3.2 months (July to November 2015). Note that FM and ANK were not in place yet.	5-259
Figure 5-30:	Sedimentation rates (cm per year) using sedimentation plates for 6.3 months (July 2015 to February 2016) for plates shown in Figure 5-29 & 3.1 months for the remaining plates.	5-259
Figure 5-31:	Sedimentation rates (cm per year) using sedimentation plates for 8.7 months (from July 2015 to April 2016) for plates shown in Figure 5-29 & 5.5 months for the remaining plates.	5-259
Figure 5-32:	Sedimentation rates (cm per year) using sedimentation plates for 11.6 months (July 2015 to July 2016) for plates shown in Figure 5-29 & 8.4 months for the remaining plates.	5-259
Figure 5-33:	Sedimentation rates (cm per year) using sedimentation plates for 1.2 year (July 2015 to October 2016) for plates shown in Figure 5-29 & 11.5 months for the remaining plates.	5-260
Figure 5-34:	Sedimentation rates (cm per year) using sedimentation plates for 1.7 year (July 2015 to March 2017) for plates shown in Figure 5-29 & 1.3 years for the remaining plates.	5-260
Figure 5-35:	Sedimentation rates (cm per year) using sedimentation plates for 2.15 year (July 2015 to September 2017) for plates shown in Figure 5-29 & 1.9 years for the remaining plates.	5-260
Figure 5-36:	PCA plot for sedimentation rates showing in x-axis and y-axis the principal components that contribute the most to the variance of the dataset (PC1 and PC2). Each variable represented by an arrow with its length and gradient color informing on the PCA loading scores (Red longer arrows have higher contribution and blue short the least).	5-262
Figure 5-37:	PCA plot for ANK sedimentation rates - see notes and details in Figure 5-36	5-263
Figure 5-38:	Plot matrix of the square cosine (cos <sup>2</sup> ) which is the quality of representation of the variables of the PCA on ANK sedimentation rates. Note1: Large and dark circles indicate a good representation of the variable on the principal component and viceversa. Note2: see notes and details in Figure 5-37	5-263
Figure 5-39:	PCA plot for FM sedimentation rates - see notes and details in Figure 5-36	5-264
Figure 5-40:	Plot matrix of the square cosine (cos <sup>2</sup> ) which is the quality of representation of the variables of the PCA on FM sedimentation rates. Note1: see notes and details in Figure 5-38	5-264
Figure 5-41:	PCA plot for MR sedimentation rates - see notes and details in Figure 5-36	5-265
Figure 5-42:	Plot matrix of the square cosine (cos <sup>2</sup> ) which is the quality of representation of the variables of the PCA on MR sedimentation rates. Note1: see notes and details in Figure 5-38	5-265
Figure 5-43:	Overall sedimentation rates (cm. yr-1) by vegetation assemblages showing highest sedimentation rates with SM13a ( <i>Puccinellia maritima</i> dominant and <i>Puccinellia maritima</i> sub-community) in the low-marsh. (Kruskal-Wallis H test and significant pair-test comparison using Dun's tests results by the p-value significance: ns, *, **, *** for > 0.05, ≤0.05, ≤0.01, ≤0.001. Boxplots represent median (middle line) interquartile range (box), 1.5 times interquartile range (bar) and outliers (stars)).	5-266

Figure 5-44:	a) saltmarsh surface collapse at the base of FM cliff edge and b) at the entrance of one of ANK's creek (November 2015).	5-270
Figure 5-45:	The DEM cut & fill highlights salt marsh gain and loss over 6 years (derived from both airborne and terrestrial laser scanning (TLS) datasets spanning from 2011 to 2017) with clear gain on the vegetated part of the marsh and also sediment input on the foreshore.	5-271
Figure 5-46:	a), b) and c) Seasonal Rainfall (y-axis in mm) for East Scotland	5-274
Figure 5-47:	Sampling points with graduated symbol calculated for the average surface elevation rates (in cm.yr-1 for 2.15 years period) across the three salt marshes at Nigg Bay. The symbols are superimposed on a surface model that represents the surface elevation rate at a constrained distance using the extent of each vegetation community (NVC-assemblage). See Figure 4-71 for details of the interpolation method (ESRI (1), n.d.; ESRI (2), n.d.).	5-277
Figure 6-1:	Chapter 6 focusses on Belowground organic and inorganic characteristics within the Nigg Bay marshes in light of environmental processes that have influenced past evolution (after (Allen, 2000; Davidson-Arnott et al., 2002; Cahoon et al., 2009)).	6-281
Figure 6-2:	Location of all the cores used this analysis: Red lines = Transects; Red dots = cores used for both particle analysis (this section 6.2.1) and organic matter analysis (6.3.1); Black dots = cores used for inorganic carbon content (6.2.3) organic matter analysis (6.3.1). Blue (thick) arrow represents the prevailing wave approach direction from the southwest of tidal. Orange (thin) arrow represents riverine flows (interpreted from Stapleton and Pethick, 1996); Abbreviations in legend: HM=High marsh, MM= Mid marsh, LM= Low marsh, and PM= pioneer marsh.	6-286
Figure 6-3:	Transect 1 across the saltmarsh surface zones of FM and FM and MR sites in a SW / NE alignment showing the location of the large cores (0.11 m and 0.08 diameter) used for organic and inorganic analysis. Note 1: (vertical exaggeration 21.3X).	6-287
Figure 6-4:	Transect 2 across the saltmarsh surface zones of ANK site in a SW / NE alignment showing the location of the large cores (0.08m diameter) used for organic and inorganic analysis. Note 1: (vertical exaggeration 21.3X). Note 2: Core A15 is located on cliff edge in HM zone.	6-287
Figure 6-5:	Bar plot showing the overall average sediment distribution (clays, silt and sand in percentage) at a 10 cm interval until 50 cm and from 50 to 87 cm through the core depth for the cores taken on ANK, FM and MR (see Figure .-4 for core location) (Note: error bar are made of sample mean and lower and upper Gaussian confidence limits based on the t-distribution).	6-289
Figure 6-6:	GSD of Core MR36 ( $\emptyset = 8\text{cm}$ ) is located behind remains of sea embankment on MR's PM of.	6-290
Figure 6-7:	GSD of Core MR24 ( $\emptyset = 11\text{cm}$ ) located at the limit of MR's PM and LM.	6-290
Figure 6-8:	GSD of Core MR16 ( $\emptyset = 8\text{cm}$ ) located at the limit of MR's LM and MM, east of the main creek.	6-290
Figure 6-9:	GSD of Core MR8 ( $\emptyset = 8\text{cm}$ ) is situated in MR's HM.	6-291
Figure 6-10	: Four major creeks (black) in the vicinity of Core A13	6-293
Figure 6-11	: Core A11 located to the north (c.1.8m deep at point) of biggest creek of ANK salt marsh	6-293
Figure 6-12	: GSD of core A13 is located on ANK's western edge PM. The red band corresponds to rounded pebble (21mm <sup>3</sup> ) lodged in the profile (see 3.4.3.3.)	6-293

Figure 6-13	:: GSD of Core A10 ( $\varnothing=8\text{cm}$ ) located on ANK's LM north of the major creek channel.	6-293
Figure 6-14	: GSD of Core A11 ( $\varnothing=8\text{cm}$ ) located on ANK's MM.	6-294
Figure 6-15	: GSD of Core FM6 (8cm diameter $\varnothing$ ) located on FM cliff edge.	6-295
Figure 6-16	: GSD of Core A15 ( $\varnothing=8\text{cm}$ ) located on ANK's cliff edge.	6-295
Figure 6-17	: Matrix plot showing the relations between silt (top), sand (middle) and clays (bottom) to depth in the core (black regression line is only intended to be informative).	6-295
Figure 6-18	: Boxplot of average BDD (g.cm-3) per saltmarsh surface zones . (Note1: Kruskal-Wallis H test and significant pair-test comparison using Dun's tests results by the p-value significance: ns, *, **, *** for $>0.05, \leq 0.05, \leq 0.01, \leq 0.001$ . Note1: Boxplots represent median (middle line) interquartile range (box), 1.5 times interquartile range (bar) and outliers (black dots)).	6-298
Figure 6-19	: Boxplot of BDD (g m-3) per Sites per saltmarsh zones. (Note: Kruskal-Wallis H test and significant pair-test comparison using Dun's tests results by the p-value significance - Results in table E-1.)	6-299
Figure 6-20	: BDD (g.m-3) versus depth (in cm and corrected for compaction) per sites and saltmarsh surface zones. Blank box: absence of core for this saltmarsh zone. Polynomial trends shown in blue and the results of polynomial regressions (correlation coefficients and statistical significances) are provided as bottom of each graphs.	6-300
Figure 6-21	: Boxplot of water loss percentage per sites. Boxplot of water loss percentage per Sites. (Note: Kruskal-Wallis H test and significant pair-test comparison using Dun's tests results by the p-value significance - Results in table E-2.)	6-301
Figure 6-22	: Boxplot of water loss percentage per saltmarsh zones. (Note: Kruskal-Wallis H test and significant pair-test comparison using Dun's tests results by the p-value significance - Results in table E-2.)	6-302
Figure 6-23	: Boxplot of water loss percentage per sites' saltmarsh zones. (Note: Kruskal-Wallis H test and significant pair-test comparison using Dun's tests results by the p-value significance - Results in table E-2.)	6-302
Figure 6-24	: Water loss (%) versus depth (in cm and corrected for compaction) per sites and saltmarsh surface zones with the cores represented by different colours. Blank box: absence of core for this saltmarsh zone.. Blank box: absence of core for this saltmarsh zone. Polynomial trends shown in blue and the results of polynomial regressions (correlation coefficients and statistical significances) are provided as bottom of each graphs.	6-303
Figure 6-25	: Relationship between loss of inorganic carbon content (%) and depth (cm) per sites and saltmarsh surface zones. Polynomial trends shown in blue and the results of polynomial regressions (correlation coefficients and statistical significances) are provided as bottom of each graphs.	6-306
Figure 6-26	: Inorganic carbon content (%Loge values on the y-axis) and depth (cm) for Core MR24 highlighting in red carbonate concretion at 36 cm in depth.	6-306
Figure 6-27	: a) : Boxplot of SOM (%) a) between saltmarsh sites and b) between sites' saltmarsh zones. (Note: Kruskal-Wallis H test and significant pair-test comparison using Dun's tests results by the p-value significance - Results in table E-4.)	6-309
Figure 6-28	: Relationship between SOM (%) and depth (cm) per sites. Polynomial trends shown in blue and the results of polynomial regressions (correlation coefficients and statistical significances) are provided as bottom of each graphs.	6-310

Figure 6-29	: SOM (% natural log) in y-axis versus depth in x-axis for core A13 and A5.	6-311
Figure 6-30	: Relationship between SOM (%) and depth (cm) per sites with the cores represented by different colours. Blank box: absence of core for this saltmarsh zone. Polynomial trends shown in blue and the results of polynomial regressions (correlation coefficients and statistical significances) are provided as bottom of each graphs.	6-312
Figure 6-31	: Boxplot of SOC in g.Ccm3 between sites' saltmarsh zones. (Note: Kruskal-Wallis H test and significant pair-test comparison using Dun's tests results by the p-value significance - Results in table E-9 .	6-313
Figure 6-32	: Carbon stock density in g.Ccm3 by saltmarsh vegetation community - NVC type (Vegetaion reference to Table 3.4 and App. A.2) and zones using individual SD to calculate error bars.	6-314
Figure 6-33	: Relationship between SOM (g.Ccm3) and depth (cm) per saltmarsh sites. Polynomial trends shown in blue and the results of polynomial regressions (correlation coefficients and statistical significances) are provided as bottom of each graphs.	6-315
Figure 6-34	: Relationship between SOM (g.Ccm3) and depth (cm) per sites. Polynomial trends shown in blue and the results of polynomial regressions (correlation coefficients and statistical significances) are provided as bottom of each graphs.	6-315
Figure 6-35:	Cores from Nigg Managed Realignment (MR) from left to right, from PM to HM in ascending elevation height order: MR24 (PM-1.57mOD), MR47(PM-1.82mOD), MR53(LM-1.86mOD), MR26(LM-2.04mOD), MR45 (LM-2.05mOD), MR38 (LM-2.06OD), MR55 (MM-2.08mOD), MR19 (HM-2.37mOD), and MR60 (HM-2.54mOD). Red arrow represents clear stratigraphic break associated with change in soil colour present in 8 out of 9 cores photographed and interpreted as reclamation years. Note: the cores in photographs have not been corrected from core compaction (see 3.4.3.1) unlike all core data used and presented so far.	6-316
Figure 6-36	: Water and Soil organic Content from four MR cores which presented soil discoloration in photographs 6-37. From left to right, from PM to HM, in ascending elevation height order: MR24 (PM-1.57mOD), MR26(LM-2.04mOD), MR38 (LM-2.06OD) and MR60 (HM-2.54mOD). Red lines represent the depth at which the colour shift is visible on the photograph (top a-: series with depth uncorrected for core compaction; and, b-: bottom corrected as explained in 3.4.3.1).	6-317
Figure 6-37	:PCA plot for grain size distribution including the physical variables of elevation (m), hydroperiod (m), flood depth (m), flood frequency, distance to MHWS, distance to water channels (m), distance to saltmarsh edge (m) , slope (percent) and curvature.	6-321
Figure 6-38	: Plot matrix of the square cosine (cos <sup>2</sup> ) which is the quality of representation of the variables of the PCA for Sediment size grain. Note1: Large and dark circles indicate a good representation of the variable on the principal component and vice-versa.	6-321
Figure 6-39	: BDD (g.m-3) versus depth (in cm and corrected for compaction) per saltmarsh sites, with intercepts in red on the y-axis at 8 cm in depth and on the x-axis at 0.2 and 1.5 g.cm <sup>3</sup> .	6-324
Figure 6-40	: water content (%Loge) versus sediment type per sites showing positive trends between water moisture and porous fine sediment grains such clayey and silty soil structure and negative trends for less porous soils such as sands (quadratic fits as red lines).	6-326
Figure 6-41	: Bar graph showing the belowground organic carbon stock (t C ha <sup>-1</sup> ) in the low-mid (mid-marsh and low-marsh zone values have been averaged for Nigg salt marshes to match Miller et al. (2023) results as	6-328

	there was no distinction made between mid and low marsh in their study) pioneers and high-marsh zones of ANK, FM, MR and Dornoch point and Morrich More saltmarshes (Error bars are standard deviation).	
Figure 6-42	: Scatter plots between SOM (in % - y-axis) and BDD (in g.cm <sup>3</sup> ) . Plots are showing r <sup>2</sup> values and p-value.	6-329
Figure 6-43	:PCA plot for SOC including the physical variables of elevation (m), hydroperiod (m), flood depth (m), flood frequency, distance to MHWS, distance to water channels (m), distance to saltmarsh edge (m) , slope (percent) and curvature.	6-330
Figure 6-44	: Plot matrix of the square cosine (cos <sup>2</sup> ) which is the quality of representation of the variables of the PCA for SOC.	6-330
Figure 7-1:	Reduction of Quartz and Feldspar luminescence signals during exposure to light for OSL techniques or heat using TL techniques (taken from Duller, 2008, p.8).	7-337
Figure 7-2:	A schematic view of the OSL (quartz) decay curve with hypothetical location of its several component: F- fast component, M, the medium component, and BG, the background (taken from Durcan and Duller (2011), p.1066)	7-337
Figure 7-3:	Location of all the cores used for Luminescence : Red lines = Transects; Red dots = cores. Abbreviations in legend: HM=High marsh, MM= Mid marsh, LM= Low marsh, and PM= pioneer marsh.	7-343
Figure 7-4:	a) General stratigraphy of core MR24 based on a simple visual assessment showing six major horizons (0-7 cm, 7-11cm, 11 to 17 cm, a very distinct layer at 17 to 18 cm, 18 to 24 and 24 to 31 cm) overlain by yellow boxes representing sample location. b) SEM imagery of sediment grains, at working distance by magnification (from top to bottom) 11.8mm *40; 11.8mm *40; 11.5mm*42; 11.6*37c) SEM results (%) for the fraction 250-150µm. SEM is used as a qualitative tool to detect the presence of additional minerals and debris, residues or contamination of the sample.	7-344
Figure 7-5:	SUERC portable reader	7-346
Figure 7-6:	PPSL system (top) developed for irradiated foods detection measure IRSL signal; and, diagram (bottom) showing how photons are counted when Infrared are stimulated for 30s.	7-346
Figure 7-7:	Risø DA-20 automatic reader at SUERC (top) with small diagram (bottom) showing how automation of the samples stimulation on the carousel by red and blue LEDs which is then detected through filter to allow photomultiplier to detect light emitted by the samples with in parallel an irradiator source (90Sr) permitting to regenerate luminescence signal.	7-346
Figure 7-8:	Field profiling proxies sequence developed by Prof. D. Sanderson (Ghilardi et al., 2015; Sanderson and Murphy, 2010) for SUERC portable reader and used to measure the luminescence (OSL and IRSL) signal from core MR24 saltmarsh sediments.	7-350
Figure 7-9:	Interval plots showing the natural B-OSL net signal between 1 cm disc aliquots per grain size fractions. Error bars are calculated using individual SD. Red dashed line represents the overall dark count limit (average of all screening – fraction and aliquots –) from which emitted luminescence (if any) signal cannot be counted	7-354
Figure 7-10	: Boxplot highlighting the spread of the net B-OSL natural signal between 1cm disc aliquots through the interval depth of the core for the investigated grain size fraction (in µm). Red dashed line represents the overall dark count limit.	7-354

- Figure 7-11 : B-OSL net signal (photon counts) after one hour (grey) and >21 hours (black) of artificial bleaching for the investigated grain size fractions through depth (cm) dispensed on 1 cm disc. Error bars are one standard error from individual mean. Red dashed line represents the overall dark count limit. 7-356
- Figure 7-12 : Overall regenerated B-OSL signal versus natural B-OSL signal through core depth (cm) per grain fraction for 1 cm disc samples. Association between natural and regenerated signal demonstrated linear regression fit for fractions 250-150  $\mu\text{m}$   $r^2 = 38.1\%$  (Reg. B-OSLLoge =  $3.56 + 0.55 \cdot \text{Natural B-OSLLoge}$ ); 150-90  $\mu\text{m}$   $r^2 = 91.6\%$  (Reg. B-OSLLoge =  $0.41 + 0.96 \cdot \text{Natural B-OSLLoge}$ ); 90-30  $\mu\text{m}$   $r^2 = 38.1\%$  (Reg. B-OSLLoge =  $2.42 + 0.68 \cdot \text{Natural B-OSLLoge}$ ); <30  $\mu\text{m}$   $r^2 = 8.6\%$  (Reg. B-OSLLoge =  $4.17 + 0.29 \cdot \text{Natural B-OSLLoge}$ ). 7-357
- Figure 7-13 : Overall regenerated B-OSL signal intensity measured with the portable reader and automated Risø for fractions 150-90  $\mu\text{m}$  and 90-30  $\mu\text{m}$ . Error bars are calculated using individual SD. Red dashed line represents the overall dark count limit. 7-357
- Figure 7-14 : 200 mGy regenerated B-OSL signal (in photon count) measured with the portable reader and automated Risø for fractions 150-90  $\mu\text{m}$  and 90-30  $\mu\text{m}$  dispensed on 1 cm disc. Error bars (very small) using individual SD and red dashed line represents the overall dark count limit. 7-358
- Figure 7-15 : Overall Portable Reader IRSL signal (in photon count and error bars using individual SD) for 1 cm disc samples per grain size fractions showing from left to right natural IRSL, bleached and 200 mGy regenerated IRSL signal (in photon counts). Red dashed line representing the dark count range for all measurements. 7-359
- Figure 7-16 : Overall signal intensity between Portable Reader (PR), PPSL and automated Risø instruments for fractions 150-90  $\mu\text{m}$  and 90-30  $\mu\text{m}$  dispensed on 1 cm discs. Error bars using individual SD and red dashed line represents the overall dark count limit. 7-360
- Figure 7-17 : Fractions 150-90  $\mu\text{m}$  and 90-30  $\mu\text{m}$  PPSL-IRSL signal (in photon count) normalised to weight through the core depth (cm) dispensed on 1 cm discs. Red dashed line represents the signal range achieved with portable reader for the two fractions. Error bars using individual SD and red dashed line represents the overall dark count limit. 7-360
- Figure 7-18 : a) super bright blue diode newly fitted for an exclusively B-OSL portable reader.; b) simultaneous working system to record samples aliquots on two IRSL (left) and B-OSL (right) portable reader. 7-363
- Figure 7-19 : a) exploratory core MR24 using 3 cm discs aliquots showing 200 mGy regenerated IRSL signal (photon count) with large SD (error bars) measured with original portable reader compared to b) 200 mGy regenerated IRSL signal for MR16 aliquots (also 3 cm discs) located c.30 m in NE direction from MR24 (see Figure 7-3) measured using the "special" double IR version of the portable OSL reader which we made (using thin BG39 filters and high power IR diode arrays. Note1: the two core depth differences & red line on y-axis of MR16 at approximate base of core MR24. 7-363
- Figure 7-20 : Net B-OSL natural signal for grains < 30  $\mu\text{m}$  (photon counts) dispensed on 1cm and 3 cm disc per aliquots A & B measured with same portable instrument (core MR24). Error bars are one standard error from individual mean. Red dashed line represents the overall dark count limit (average of all screening – fraction and aliquots –) from which emitted luminescence (if any) signal is considered unsatisfactory or/and insufficient or/and even false 7-364



Figure 7-21	: Custom made glass jars (left) by Robert McLeod and Calum Prentice in the SUERC glassblowing workshop for making these used to receive pipetted < 30 µm grain in acetone and dispense on 3cm aluminium planchettes.	7-365
Figure 7-22	: Diagram of new <sup>90</sup> Sr Source irradiator showing the fitting of the aluminium ring and stub (red arrow for assemblage) allowing to raise in height the source position and accommodate large irradiation geometry. Samples are placed in a drawer (right on figure) and then pushed in the irradiator ready to receive a beta dose.	7-366
Figure 7-23	: 30 seconds sequence for both IRSL and B-OSL stimulations using newly adapted portable readers. The figure highlight the fast component of OSL signal that is the most easily bleached (Wintle, 2008).	7-367
Figure 7-24	: Relationship between IRSL (x-axis) and B-OSL (y-axis) (in photon count Loge) for a) regenerated signal at 200 mGy and b) regenerated signal at 1 Gy. All sediments < 30 µm dispensed on 3 cm discs.	7-369
Figure 7-25	: (left) a) overall signal sensitivity using ED1 and (right) b) using FED1 for all cores collected along the two transects crossing the saltmarshes. Note: the drawing size is deliberately left quite small as to allow a simple visual assessment between the residuals (in Gy).	7-370
Figure 7-26	: Relationship between FE-IRSL and FE-B-OSL where only the fastest component of the signal is kept the front end photon count (stimulation 1 – stimulation 2 or the fastest component) signal of the same regenerated signal at 200 mGy. All sediments < 30 µm dispensed on 3 cm discs.	7-370
Figure 7-27	: Left graph: IRSL (red) and B-OSL (blue) ED1 through the core depth (y-axis) and apparent age value (Log10 for illustration on x-axis) with calculated apparent age value (in years) at each luminescence peak at a putative dose rate of 1 mGy a-1. Right graph: IRSL (red) and B-OSL (blue) FED1 through core depth depth (y-axis) and apparent age value (x-axis) with calculated apparent age value (in years) at each luminescence peak at a putative dose rate of 1 mGy a-1.	7-371
Figure 7-28	: Overall front-end equivalent dose for IRSL (red) and B-OSL (blue) signals for all cores collected along transects crossing FM/MR and ANK salt marshes as depicted on Figure 7-3.	7-372
Figure 7-29	: Overall B-OSL and IRSL signal sensitivity across the saltmarsh zones for the transects crossing ANK and crossing FM/MR salt marshes.	7-373
Figure 7-30	: IRSL signal sensitivity (/Gy Loge) versus Dry Bulk Density (g.cm-3Loge), Organic matter (%Loge), inorganic content (%Loge) and water content (%Loge) depicting with coloured symbols all saltmarsh zones of the three salt marshes.	7-374
Figure 7-31	: Core (red dots) location along the two transects (red lines) superimposed onto OS 2nd revision One-inch map (1907) showing in blue HWM derived from LIDAR dataset.	7-375
Figure 7-32	: Core MR8 FED1 B-OSL and IRSL (in Gy Log2 and error bars from individual standard errors) through core depth (in cm). Blue arrows (bold colour major shifts and pale colour minor shifts) present breaks or shifts in B-OSL signal trends and red arrows presents shifts in IRSL signal. The thick grey line is a significant change in the trend that can be linked to the 2003 breaching.	7-378
Figure 7-33	: FED1 IRSL/B-OSL ratio (in GyLoge) inferring on mineralogical variation with grey arrows indicating shifts (Bold grey = major shift and pale colour = minor shifts). The thick grey line is a significant change in the trend that can be linked to the 2003 breaching.	7-378
Figure 7-34	: Depletion index of the regenerated B-OSL (blue) and IRSL (red) signals indicating shifts on colour, mineralogy and residuals (inherited	7-378

from prior deposition). Values higher than 1 indicates rapid decays. The thick grey line is a significant change in the trend that can be linked to the 2003 breaching. (Arrows same as Figure 7-32).

Figure 7-35	: Profiles of water content (%), BDD (g.cm-3), Organic content (%Loge) and mean grain size ( $\mu$ m) from Core MR8 showing on right of mean grain size plot an extrapolated chronology using accretion rates of $0.417 \pm 0.24$ cm.yr-1 from filter discs MR8. Arrows indicating shifts in the trend (Bold grey = major shift and pale colour = minor shifts). The grey dash is a significant change in the trend that can be linked to the 2003 breaching.	7-378
Figure 8-1	Conceptualised framework for chapter 8	8-386
Figure 8-2	Scatterplot between (100+loge) accretion rate (x-axis) and (100+loge) SEC-plates (y-axis) per site with regression fit line (linear = light grey & lighth grey & quadratic = dotted blue)	8-393
Figure 8-3	Scatterplot between (100+loge) accretion rate (x-axis) and (100+loge) SEC-plates (y-axis) per site & saltmarsh zones with regression fit line	8-393
Figure 8-4	Historical saltmarsh extent from 1872 to 2012 as developed in Chapter 5.2.	8-395
Figure 8-5	Average Blue Carbon stock in tC.ha-1 for the three studied salt marshes demonstrating significance difference between the natural, ANK, and managed salt marsh, MR ( $F=3.3$ , $p<0.05^*$ ).	8-403
Figure 8-6	Average Blue Carbon stock in tC for each salt marsh at average soil depths of 40 cm (MR), 58 cm (FM) and 55 cm (ANK).	8-403
Figure 8-7	Possible new realignment in Nigg Bay accommodating space the natural salt marshes and new blue carbon stores.	8-404

## Acknowledgements

Maybe it's superstition, but I have put off writing these acknowledgments until the very end. As a result, they will be simple rather than original. I also apologise to the people who I will inevitably forget to thank.

I'd like to express my gratitude to my supervisors Prof. Larissa Naylor, Dr. Jim Hansom and Prof. David Sanderson, for providing me with the opportunity to complete this PhD, which has been an incredible journey. It has not been easy, but it would have been infinitely more difficult without their insight, advice, patience and encouragement.

I would also like to thank my funders, MASTS and the University of Glasgow, as well as MASTS Coastal Processes & Dynamics Forum, which funded the successful first phase of OSL dating in 2015. Thank you also to Stef at the RSPB, who the stewardess of both study sites. Thank you to Dr Alistair Rennie of Scottish Natural Heritage for the extremely useful metal clip pliers that I used to collect sediment from filter discs for a year.

I would like to thank the SUERC team, Lorna Carmichel, David Sanderson, Simon Murphy and Tim Kinnaird, for making me feel welcome and for always being willing to teach and share their knowledge. This has been an incredible and extremely valuable experience. Thank you, Sevi, for the spirit-lifting car ride to the luminescence lab.

I must thank Kenny Roberts for his invaluable assistance and advice in the field, in the lab, and on these three years of long drives. Thank you to my colleagues PhD student, who began in room 303 and ensured that I was included in the promotion.

I would like to express my biggest thanks to my mum for her unrelenting encouragement, trust, and love. I couldn't have done it without you. I'd also like to thank my brother for his spirit and being here no matter what. I'd like to thank those who have left but still believed there was an end to this thesis... an end to begin another adventure. I couldn't have done it without you too. Et puis, merci aux matins où le martin-pêcheur montrait ses couleurs!

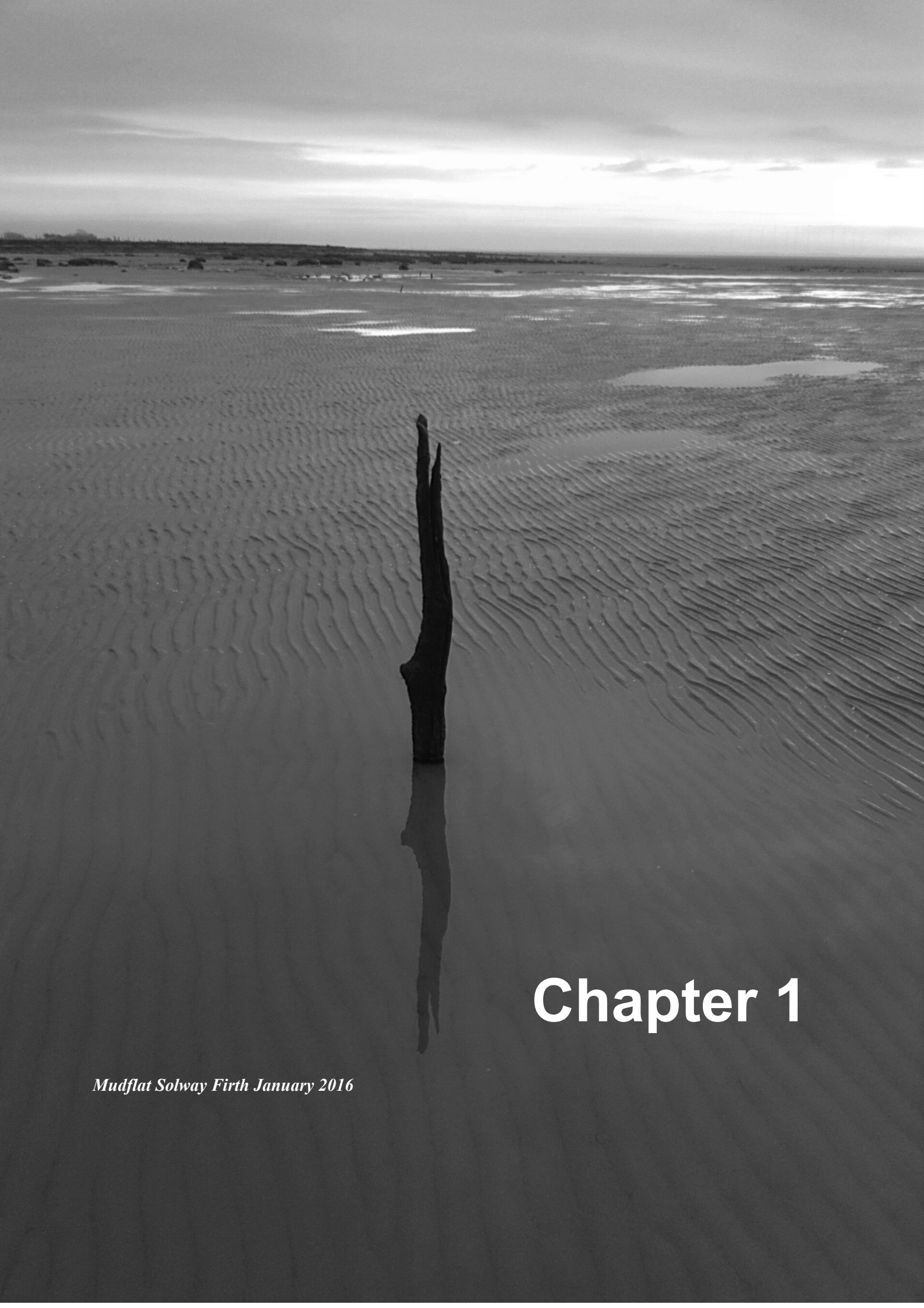
Finally, I would like to dedicate this PhD to Lonnie, my son.

Thank you all.

## **Authors Declaration**

I declare that except where explicit reference is made to the contribution of others, that this thesis is the result of my own work and has not been submitted for any other degree at the University of Glasgow or any other institution.

Charlotte Francoz



# Chapter 1

*Mudflat Solway Firth January 2016*

# Chapter 1. Introduction

## 1.1 Rationale

Salt marshes are at a critical interface between land and sea and are regarded as being one of the most productive ecosystems on earth on account of the unique habitat they offer, essential to our ecological structure (Zedler and Kercher, 2005; Gedan et al., 2009; Townend et al., 2011), and due to their capacity to act as sinks for organic and inorganic sediment (Long and Mason, 1983; Chmura et al., 2003; Mcleod et al., 2011; Hyndes et al., 2014). Because of their position along the coast, on sheltered shores typical of estuaries and tidal inlets, salt marshes have long attracted human settlement and exploitation (Gedan et al., 2009). However, coupled with the climate change threat of rising temperature, sea level rise and increasing storm severity producing saltmarsh erosion, the permanent loss of the saltmarsh ecosystems is estimated at between 25% and 50% of their global historical coverage and they continue to decline in area around the world (Mcowen et al., 2017). Since 1945 approximately 15% of UK saltmarsh area has been lost through human interference, chiefly agricultural and industrial reclamation (Beaumont et al., 2014), but now augmented by coastal erosion and sea level rise (Allen, 2000).

Because salt marshes are a key ecosystem where the physical, chemical and biological interactions between saltmarsh organisms (flora and fauna) and their environment generate functions and services of great value. These services provide food and fuel (Alongi, 2008); support biodiversity (Lefeuvre et al., 2003); attenuate coastal flooding (Pethick, 2002); attenuate wave and storm activity (Temmerman et al., 2013; Möller et al., 2014; Fagherazzi, 2014; Spencer et al., 2015); stabilise shorelines (Ford et al., 2016); filter pollution (Shepard et al., 2011) and act as a sink for 'Blue Carbon' (carbon sequestered and stored by marine and coastal habitats) (Mcleod et al., 2011; Hyndes et al., 2014). Because of better recognition of the resources and services salt marshes provide and how they contribute to coastal adaptation as a flood and coastal natural defence (Pethick, 2002; Möller, 2006; Leonardi et al., 2018), they have gained prominence over recent years with a rise of legislation to manage these losses.

The Intergovernmental Panel on Climate Change (Pachauri and Meyer, 2014) has highlighted the unequivocal human influence on recent climate change, with major concerns on the impact of global warming and enhanced greenhouse leading to rises in temperature, sea level and CO<sup>2</sup> and warnings on land degradation and water exploitation. The latest international agreement at Conference of the Parties - COP21 in Paris in December 2015 and the following IPCC sessions (with latest 47th Session of the IPCC took place in March 2018, but also IPCC 2014, 2007 & 2009) prompted the UK and Scotland to adapt their policies to promote a more sustainable approach to resource use, thus driving to local legislation change. Promulgated in December 2000, the EU Water Framework Directive (WFD) has strongly influenced Scottish water policy development

and implementation by setting targets & monitoring schemes for aquatic and wetland natural heritage (Aspinall et al., 2011). The legislative and policy responses have been important for societal reaction to the loss of intertidal mudflats and salt marshes. As a signatory to the Ramsar, Bern, Bonn and Biodiversity Conventions, the UK has the obligation to protect and stimulate actions to maintain or restore the ‘favourable’ status of intertidal mudflats and salt marshes (Foster et al., 2014). These have been transposed into European and UK policies reflected in increasing number of conservation actions with establishment of protected areas and measures. They have a direct effect on how Scotland’s coasts and coastal habitats are managed such as such Marine Protected Areas (MPAs) network including Nature Conservation MPAs (NCMPAs), Special Areas of Conservation (SACs), Special Protection Areas (SPAs), and Sites of Special Scientific Interest (SSSIs). Table A-1 (appendix A) shows the legal frame for Scotland salt marshes.

There is now greater legal protection for saltmarsh environments including action plans to adapt, realign, restore and create new habitats (Table A-1). Mitigation of storm surge flood risks and sea-level rise have led to an increased interest from the scientific community and society to ecosystem-based or nature-based flood defence programs such as Working with Natural processes WWNP (Burgess-Gamble et al., 2018) and Building with Nature (BwN, 2019). Historically, hard infrastructures such as groynes and sea walls have been put in place to provide coastal protection destroying natural habitat that could provide ecosystem-based coastal protection and enhance coastal resilience (Shepard et al., 2011). In the UK, there has been increasing interest in recreating salt marshes (termed managed realignment), motivated either by general concerns about past and future loss of salt marsh at a regional scale or by specific requirements to mitigate the loss of individual sites (Adam, 2002). However, there remain challenges in the identification of the best coastal protection measures to adopt (Leonardi et al., 2018) and concerns as to whether restoration schemes fulfil their intended purpose (Spencer and Harvey, 2012).

In Scotland, recent research (Teasdale et al., 2011) suggests that some Scottish salt marshes (in Argyll) have exhibited a significant accelerating trend in accretion since the 1970s, a period during which the rate of sea-level rise has out-paced the rate of isostatic adjustment everywhere in Scotland (Rennie and Hansom, 2011) with current rates about 2-3 times higher than the values observed for much of the 20<sup>th</sup> Century. Since the general tenor of saltmarsh research in the UK suggests losses of salt marsh rather than gains (Beaumont et al., 2014), the work of Teasdale et al., 2011 prompts a series of questions relating to how salt marshes respond to external change and forcing. For example, how do saltmarsh landforms respond to environmental forcing and keep pace with sea level rise? How much sediment reorganisation has already occurred in Scottish salt marshes? Might climate change increase the resilience of saltmarsh habitats? Can salt marshes increase their ability to sequester carbon and/or provide even greater ecosystems services?



The cumulative impact of human disturbance and sea level rise on fundamental saltmarsh dynamics remains far from clear and needs to be better understood at local and global scale. Three key ecological and geomorphological theories can help us frame, interpret and improve our understanding of salt marsh and managed realigned (MR) systems. These are briefly outlined to provide a context for the research aims of this thesis.

- The concept of resilience and stability of ecological systems has been introduced by Holling in the 1970s as the ability of to recover from or tolerate natural and human disturbances (Holling, 1973). However, experimental data is still sparse in showing mechanisms of the underlying shifts in ecosystems that is critical for conservation and restoration (Altieri et al., 2013). Still, salt marshes are good systems to examine this resilience since globally they are amongst the most valuable ecosystems per unit area despite have been heavily modified and exploited over millennia, although with high increases over the last century (Lotze et al., 2006; Gedan et al., 2009; Altieri et al., 2013). Moreover, resilience of the saltmarsh environment is closely related to positive feedbacks experienced between the different sedimentological, geomorphic and biological processes that interact within the system at different spatial and temporal scales (Friess et al., 2011).
- On a short timescale, saltmarsh plants develop resilient mechanisms to counteract stress induced in the system and are known to have evolved growth form and life history characteristics. Some of these traits are further described in Chapter 2 and are simply recalled here as examples: plant tolerance to high salinity, rapid stem growth and stem flexibility against drag force and current velocity and repeated tidal inundation, self-scouring may aid seed dispersal, rapid vegetative spread or propagation allows colonisation where diaspore has difficulty to settle and anchor (Friess et al., 2011; Spencer et al., 2012; Balke et al., 2014; van Wesenbeeck et al., 2017; Möller and Christie, 2019). Coastal vegetation may conform to the alternative stable state theory by surpassing seedling biomass or density thresholds to enhance seedlings survival and facilitate later ecosystem success (Friess et al., 2011). Plant stems also tends to flex during powerful storms (with a reduction in dissipation potential) making them more resilient to structural damage, and in turn their flexing helps to protect the marsh substrate against erosion (Pethick, 1984; Adam, 1990; Möller, 2006; Spencer et al., 2015). However, there is even in the short-term, dominance of sedimentological processes over ecological processes, that are responsible for saltmarsh formation where in many instances, resuspension on mudflats strongly controls sediment concentration that floods that saltmarsh platform (Gunnell et al., 2013; Mariotti and Carr, 2014). Furthermore, considered as the most important physical factor for saltmarsh restoration, surface elevation has a direct influence over plant colonization through controlling the hydroperiod (Howe et al., 2010; Spencer et al., 2017). High

inorganic sedimentation rates have been found to be associated with wind-driven waves allowing sediment to reach the marsh platform (Stumpf, 1983; Reed, 1989; Fagherazzi et al., 2013; Mariotti and Carr, 2014). The highly inorganic salt marsh of the Blyth (Suffolk, UK) has shown that vertical sedimentation can be governed by gross changes in estuary morphology and process regime rather than regional sea-level rise. (French and Burningham, 2003).

- On longer timescales (decadal to centennial), the capacity of temperate salt marshes to respond to environmental changes and anthropogenic alteration determine long-term resilience of these systems (Wolanski et al., 2009). As a landform salt marshes have been shown to counteract lateral erosion by rapid lateral expansion of their seaward edge driven through redeposition of large amounts of sediment (Gunnell et al., 2013; Fagherazzi, 2013). This fast time scale of migration indicates that salt marshes respond resiliently to coastal forcings. Moreover, if space is available and sediment supply plentiful, saltmarsh morphodynamics have the capacity to respond to flooding and sea level rise in the long term (J. French, 2006; Kirwan et al., 2016; Crosby et al., 2016; Schuerch et al., 2018). Cahoon et al. (2009) assessed the relationship between accretion, surface elevation change, and sea level rise across a sample of 78 coastal marshes in North America, Europe, and Australia and showed that average accretion and elevation rates were greater than corresponding rates of Relative Sea Level Rise. These demonstrated that salt marshes can ‘keep up’ with sea level rise (Cahoon et al., 2009) and would indicate a relatively high resilience for many saltmarsh sites (Kirwan et al., 2016), it is important to highlight that sediment supply has also been proven to be a key factor for marsh resilience to sea level rise (J. French, 2006; Kirwan and Guntenspergen, 2010; D’Alpaos et al., 2016). Still saltmarsh elevation that cannot keep pace with sea-level rise are endangered. Crosby et al. (2016) found that under the most optimistic IPCC emissions pathway (citing IPCC, 2013) 60% of the studied salt marsh could not maintain their elevation to match the sea level rate by 2100.

The interdependency of physical and biological processes has a major role on saltmarsh formation and development (Pethick, 1993; Allen, 2000; Fagherazzi et al., 2004; Corenblit et al., 2011) whilst vertical growth and saltmarsh stability is highly dependent on sediment supply and tidal range (Morris et al., 2002; P.W. French, 2006). To clarify what favour saltmarsh formation and development and to better understand saltmarsh capacity to recover from environmental and anthropogenic disturbances, this thesis examines adjacent but different salt marshes to establish changes over time in the sedimentation dynamics and vegetation characteristics of an artificially realigned salt marsh and two adjacent natural salt marshes.

## 1.2 Aims and Scope

The overarching theme of this research is to improve the understanding of the processes, mechanisms and patterns 1) that promote the formation and development of salt marsh; 2) that allow salt marsh to recover from environmental and anthropogenic disturbances; and, 3) that promote some of the regulating and supporting services provided by salt marsh. A set of managed and adjacent natural salt marshes within the same tidal system at Nigg Bay, NE Scotland provided a comparative case study of the links between sediment availability, vegetation presence and saltmarsh stability over time and space.

The specific aims that sit within this overarching theme are as follows:

- quantify aboveground changes in vegetation and sedimentation patterns on different timescales ranging from short (annual) to long (centennial);
- explore the possible mechanisms of these aboveground changes;
- establish belowground physical and biological changes that have occurred in the studied salt marshes;
- explore the possible mechanisms of these belowground changes using a combination of traditional sedimentary techniques and a dating technique not previously used on salt marshes;
- appraise the potential implications of the aboveground and belowground results:
  - on the supporting and regulating benefits that natural and restored salt marshes provide;
  - on the recent and past adaptative capacity to a rising sea level.

## 1.3 Thesis structure

Chapter 1 provides an introduction, rationale, aims and scope for the thesis.

Chapter 2 presents the theoretical background reflected in the published literature on saltmarsh processes and functioning, and the benefits and ecosystem services they provide. Chapter 2 also reviews the impacts that could threaten these intertidal habitats and how international and national policies are designed to protect, mitigate, enhance or manage them.

Chapter 3 outlines the (theoretical) framework of the research, the research design and sampling, and the choice and suitability of the experimental site.

Chapter 4 uses Figure 1-1 to summarise the annual biological and physical processes that occur during saltmarsh development and to highlight their constant interaction and feedback pathways.

This chapter presents the results of a short-term experiment focussing on a one-year cycle of water levels, sediment deposition and vegetation distribution at the three saltmarsh study sites.

Chapter 5 extends the short-term research to the longer-term (multi-annual to centennial) evolution of the marshes by assessing the aboveground patterns and rates of marsh elevation and sedimentation that contribute to the development of the three adjacent saltmarsh sites.

Chapter 6 presents long-term physical and biological processes that have taken place belowground from last recorded tide in 2016 up to 100-year timescales.

Chapter 7 presents the use of optically stimulated luminescence (OSL) techniques, and, for the first time in the global saltmarsh literature, a novel application to trace the dynamics and sedimentary processes of very young (less than 100 years) salt marsh to examine how they have varied over the short and long term.

Chapter 8 takes up the results of Chapters 4 to 7 into a broader framework to discuss and evaluate the research results in the national and international literature and context. It assesses the future of managed saltmarsh development in Scotland and the longer-term changes that may affect it. Chapter 8 also outlines the limitations of the study, presents areas for future research development and concludes.

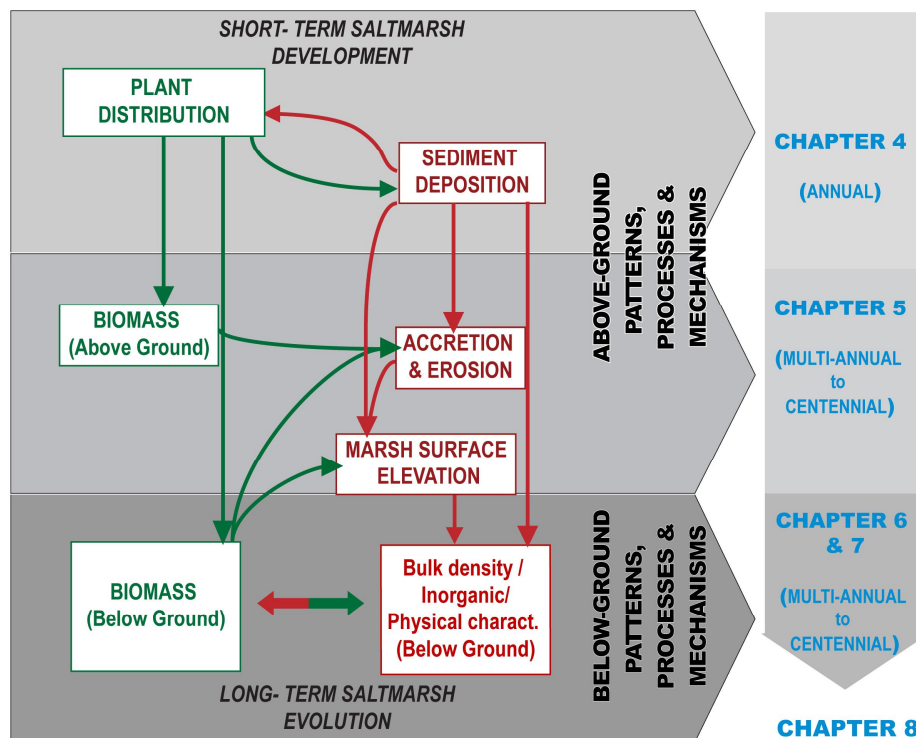
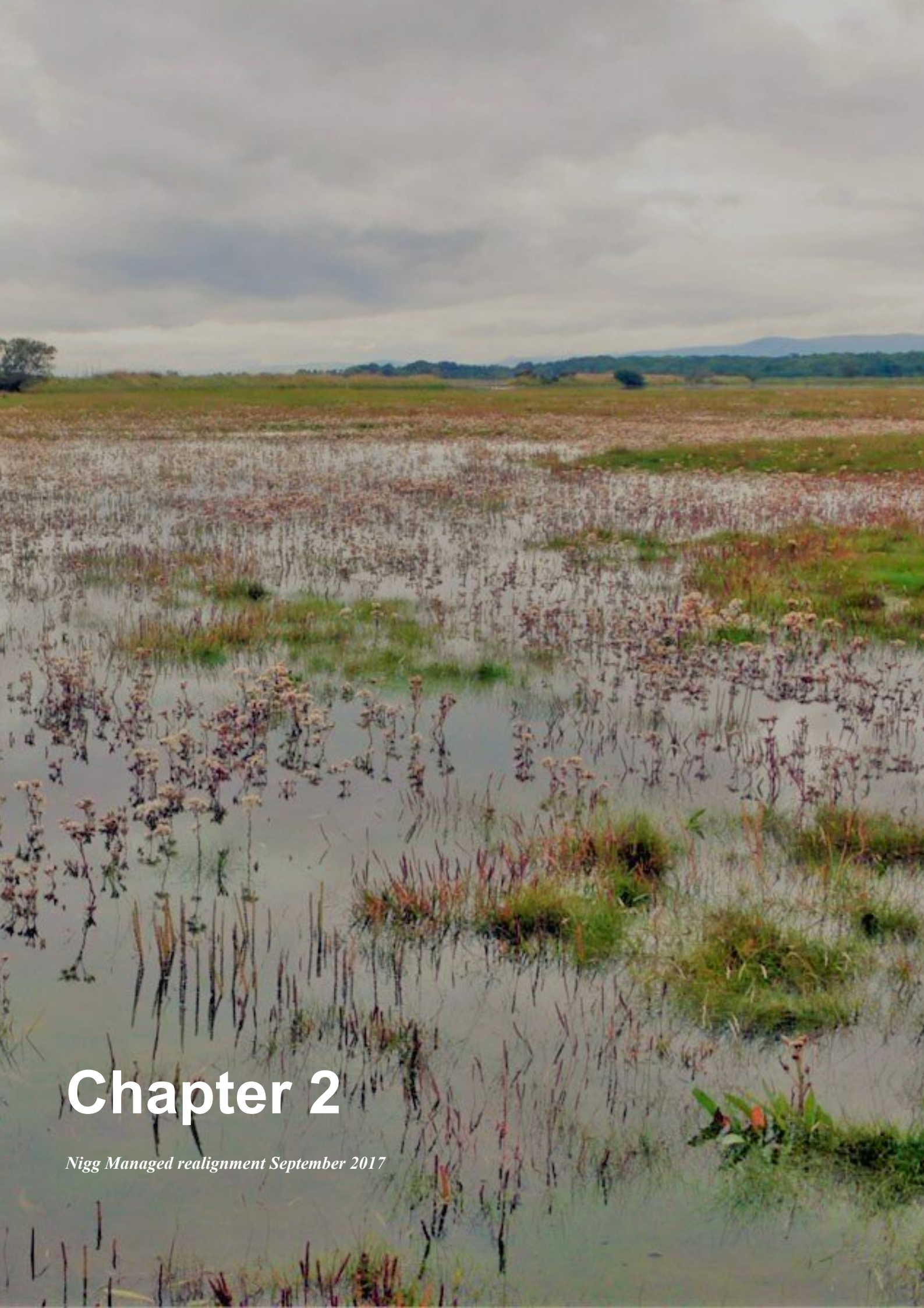


Figure 1-1: Biological and geomorphological interactions of marsh development through time. Adapted from Allen (2000), Cahoon et al.(2009); Davidson-Arnott et al.(2002).







# Chapter 2

*Nigg Managed realignment September 2017*

## **Chapter 2. Saltmarsh Importance**

## 2.1 Introduction

This chapter provides a contextual background outlining the motivation for the overall thesis aim by reviewing existing literature. The diagram below (Figure 2 1) presents the themes discussed in this review chapter which focus on the interdependency of physical (geomorphology) and ecological/biological processes: processes that are shaped by environmental and human interactions and play a key role to saltmarsh establishment, development, functioning and their derived value (societal).

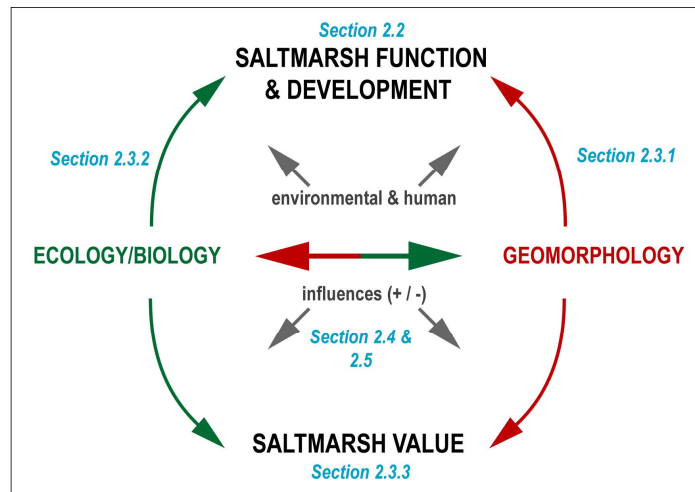


Figure 2-1: conceptualised diagram presenting the background themes discussed in this chapter framing the thesis overarching aims.

Table 2-1 below frames the contextual theme discussed in this chapter: (i) salt marshes at the interface between land and sea: their habitat function and distribution; (ii) salt marshes at the interface of geomorphology and ecology: controlling factors, interactions and benefits; (iii) salt marshes in a changing climate, and; (iv) salt marshes in a human-driven environment.

Table 2-1: Background themes reviewed in Chapter 2.

Chapter sections	Theme	Relevant thesis question
<b>Salt marshes at the interface between land and sea</b>		
2.1	Habitat function	How salt marshes have been functioning in the past and what has now? What are salt marshes and coastal wetlands purposes?
	Spatial distribution	How salt marshes and coastal wetlands are distributed across the world, the UK and Scotland?
<b>Salt marsh geomorphology and ecology/biology: a key interface</b>		
2.2	Physical influences on saltmarsh ecosystems	How and why geomorphology is significant to saltmarsh formation and development?
	Biological influences on saltmarsh ecosystems	How and why biology and ecology are significant to saltmarsh formation and development?
	Influences of saltmarsh ecosystem	How salt marshes physical and biological processes and functions provide valuable services?
2.3	<b>Salt marshes in a changing climate</b>	
	Salt marshes in a climate-driven environment	How salt marshes respond to environmental and climate pressures?
2.4	salt marshes in a human-driven environment	How salt marshes respond to anthropogenic disturbances?
	<b>Summary: Still Gaps to fill?</b>	



## 2.2 Saltmarsh function and spatial distribution

Salt marshes are part of a suite of coastal wetlands found throughout the world (Figure 2-2) including seagrasses, tidal flats, mud and sand flats, salt flats, mangroves, freshwater marshes (tidal) and forests (Wolanski et al., 2009). Mangroves develop in the tropics and subtropics whilst maritime and inland salt marshes are found in all regions from the Arctic to sub-tropics but are most commonly found in the upper intertidal zone of temperate areas (Chapman, 1977; Davidson-Arnott, 2009).

These coastal wetlands are formed dynamically and present similar general features. They are positioned along an hydrological gradient from bare sand or mud (mudflats or sandflats) through low growing vegetation zones in salt marshes or tree vegetation (Mangal) in mangroves, to merge with a transition zone through brackish or fresh water vegetation marsh in temperate areas or swamp forest in the tropics (Chapman, 1977). This transition point coincide landward where the sea passes its hydrologic influence to groundwater and atmospheric processes (Wolanski et al., 2009). Salt marsh and mangroves are both dissected by a network of tidal creeks allowing ingress and egress of water (and sediments) during the tidal cycle (Kesel and Smith, 1978).

Salt marshes form in low energy sheltered environments such as estuaries, behind barrier islands, spits, embayments and open shores exposed to low wave energy as well as fringing coastal lagoons where fine sediment accumulates, providing a suitable substrate for pioneer plant species (Adam, 1990; Allen, 2000; Boorman, 2003). This substrate is composed of allochthonous sediment and autochthonous organic material both subject to tidal (e.g. Atlantic Ocean or North Sea) or seasonal saline flooding (e.g. Baltic or Mediterranean Sea). Sediments that deposit on salt marsh have been transported by waves and currents from adjacent mudflats and open coastal waters, with relatively little sediment from river catchments, whilst the organic matter that accumulates on salt marshes is mainly composed of roots, leaves, stems from saltmarsh plant decomposition, that can then compact to form peat layers that themselves can be eroded and redeposited. Both sediments and organic matter contribute to the vertical and horizontal accretion of salt marshes (Eisma and Dijkema, 1997; Davidson-Arnott, 2009).

Although coastal ecosystems have been globally estimated to cover 33.7 to 115.2 Mha (Pendleton et al., 2012), the extent of salt marshes is more uncertain (Figure 2-2). Pendleton et al. 2012 estimate they extend over 2.2 to 40 Mha with central estimates of 5.1Mha and McOwen et al. in 2017 estimate c. 5.49 Mha . The large uncertainty in coastal ecosystems extents stems mainly from uncertainty in tidal marshes since mangrove and seagrass systems have been quantified more accurately (Pendleton et al., 2012). The reason lies with the lack of systematic global mapping

(Mcowen et al., 2017) and, in particular, an underestimation of the extent of tropical salt marsh resulting from a presumption that latitude dictates marsh and mangrove distribution (Friess et al., 2011). McOwen et al. 2017 estimated from remote sensing and field-based surveys that saltmarsh area in the United Kingdom (UK) stretched to c. 81842 ha. Burd (1989) in the first systematic inventory of salt marshes in Great Britain identified saltmarsh spatial extent to c. 44370 ha. Although the calculation excludes Northern Ireland, it is very unlikely that Northern Ireland accommodates the balance of 37472 ha of salt marsh (estimated by McOwen et al. (2017) at 9889 ha). These differences have also been noted by Allen in 2000 (after Dijkema's 1987 review) quoting a total saltmarsh area of the UK to 37100 ha. SNH noted in the most up-to-date Scottish Saltmarsh Survey (Haynes, 2016) that there was, on average, 28% of a difference between the latest Scottish saltmarsh extent (7704 ha) compared to Burd (1989) (6089 ha) and previous SNH surveys (5747ha 1998 and 6248ha in 2009). Surveying and quantifying methods and also a clear definition on which landforms (e.g. freshwater swamps) included in the surveys are in this case the main reason for the differences (Haynes, 2016).

Although present all along the U.K. coastline (Figure 2-3), salt marshes mainly occupy the major estuaries of low lying areas whilst in contrast salt marshes backed by upland hinterlands are more isolated and scattered and can be found sheltered from wave energy in minor estuaries, firths, heads of sea lochs and even on exposed salt-spray affected cliff tops well above high water mark (Boorman, 2003).

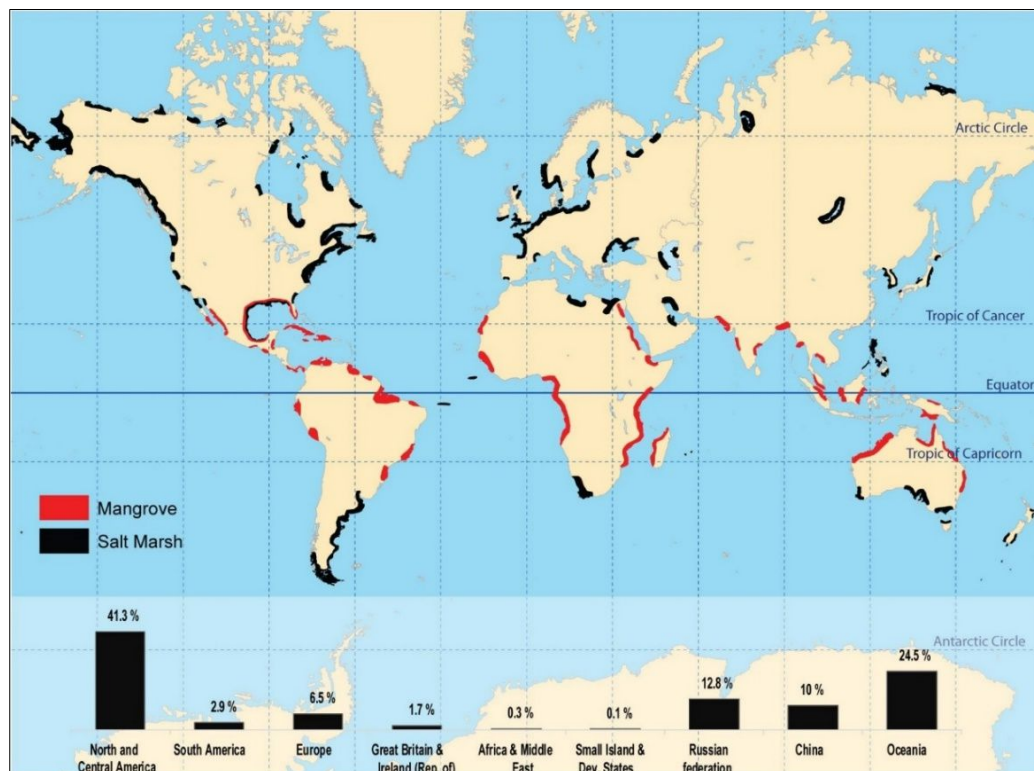
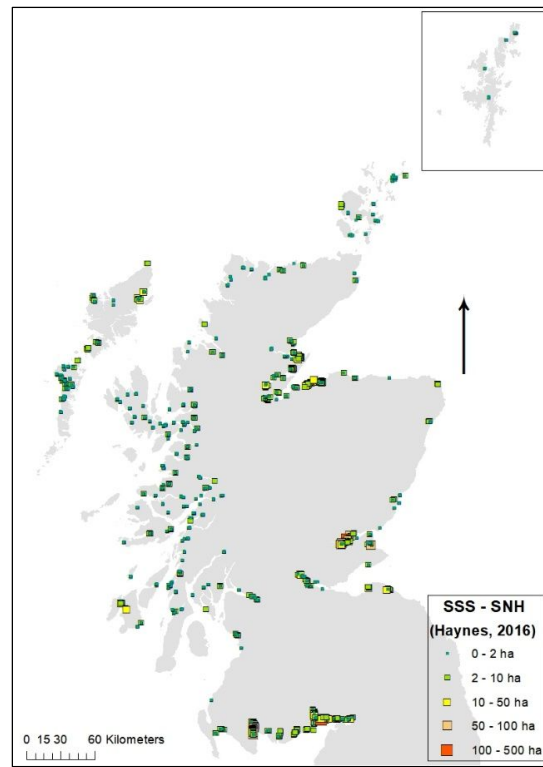


Figure 2-2: Estimated global distribution of salt marshes and mangroves. Adapted from D'Odorico et al. (2013) and using Mcowen et al. (2017) data.



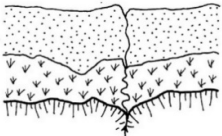
**Figure 2-3: Distribution of salt marshes in the UK**  
(Taken from Boorman, 2003, p.13).

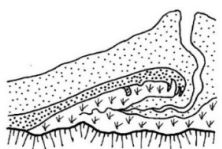
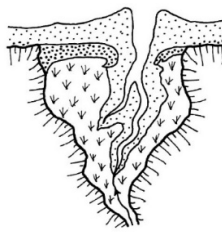
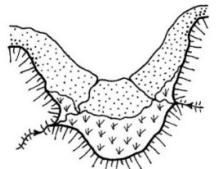
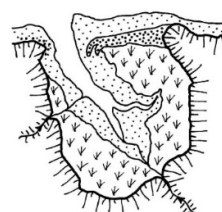
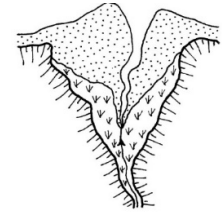


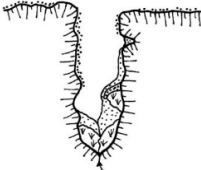
**Figure 2-4: Distribution of salt marshes across Scotland (5km grid).** Data from Haynes, 2016.

Following Eisma et al. (1998) description of geomorphology of the Dutch saltmarsh types, Allen and Pye (1992) classified U.K. active salt marshes into five groups based on their physical settings, a classification sub-categorised further by Allen in 2000 for all European marshes. Allen (2000) acknowledged that salt marshes may differ geomorphologically but are linked genetically as they are either made up of a ‘convex-up, planar, or concave-up vegetated platform high in the tidal frame that is regularly flooded by the tide’ as well as having ‘generally unconnected networks of tidal channels that branch and diminish inland toward the interior of the marsh from its seaward edge’ (Allen and Pye, 1992; Eisma et al., 1998; Allen, 2000).

**Table 2-2: Geomorphological classification of salt marshes in Europe, Great Britain and Scotland.** Adapted from Allen (2000).

Saltmarsh type (Allen and Pye, 1992)	(Allen, 2000)	Geomorphological classification of salt marshes (Allen, 2000)	European examples from both authors	Scottish Saltmarsh Survey (Haynes, 2016)
<b>Open coast</b> Poorly developed in UK due to the high wave energy found along the coast	Sandy systems coupled with relatively exposed sandflats.		<ul style="list-style-type: none"> <li>Essex coast (Dengie peninsula &amp; Foulness Islands)</li> <li>North Norfolk</li> <li>Schleswig-Holstein (Germany)</li> <li>Wadden sea (Man-made marshes)</li> </ul>	

<p><b>Back-barrier</b> In the shelter of spits or islands</p>	<p><b>Open coast Back-barrier</b> Sandy-muddy systems. Present on sheltered, landward sides of coastal barrier islands and spits.</p>		<ul style="list-style-type: none"> <li>· South Lincolnshire</li> <li>· Culbin (Moray)</li> <li>· Moricambe bay</li> <li>· North Norfolk</li> <li>· Frisian Islands (Netherlands, Germany, Denmark)</li> </ul>	<ul style="list-style-type: none"> <li>· Tynninghame Shore</li> <li>· Morrich More</li> <li>· Dornoch Point</li> <li>· Whiteness Head</li> <li>· Strathbeg</li> </ul>
	<p><b>Estuarine Back-barrier</b> Usually muddy with major riverine water and sediment input. Inner parts marshes is influenced by freshwater (lower salinity &amp; only seasonal flooding).</p>		<ul style="list-style-type: none"> <li>· Teifi, Dyfi, Mawddach (west Wales)</li> <li>· Gironde (France)</li> </ul>	<ul style="list-style-type: none"> <li>· Kirkconnell Merse &amp; Caerlaverock (Nith Estuary)</li> <li>· Lochar Water &amp; Wigtown (Cree esturay)</li> <li>· Forth firth</li> <li>· Beaully Firth</li> <li>· Cromarty Firth</li> <li>· Tay estuary (mostly brackish though)</li> <li>· Clyde</li> <li>· Part of Solway Firth</li> </ul>
<p><b>Embayment</b></p>	<p><b>Open Embayment</b>  Generally sandy. At the edges of large tidal open (no obstruction) embayments and can be drain by rivers.</p>		<ul style="list-style-type: none"> <li>· Portsmouth harbour</li> <li>· Langstone harbour</li> <li>· Chichester harbour</li> <li>· Pagham harbour</li> <li>· Poole harbour</li> <li>· The Wash (East Anglia)</li> </ul>	<p>Embayment marsh is often present in estuarine salt marshes and larger sea lochs</p> <ul style="list-style-type: none"> <li>· Findhorn Bay</li> <li>· East Coast</li> <li>· Solway Firth</li> <li>· Outer Hebrides (North Uist and Lewis)</li> <li>· Sandi Sand (Orkney)</li> <li>· Nigg Bay (Cromarty Firth)</li> <li>Abbott Hall , Salcott channel</li> </ul>
	<p><b>Restricted-entrance embayment</b> Sandy-muddy, restricted-entrance embayment with marshes is partly closed of at the mouth by one or more spits or promontories.</p>		<ul style="list-style-type: none"> <li>· Bassin d'Arcachon (France)</li> <li>· Anse de l'Aiguillon (France)</li> <li>· Dollard (Netherlands)</li> <li>· Jade bay (germany)</li> <li>· Shell Island and Y Foryd (wales)</li> </ul>	
<p><b>Estuarine-fringing</b></p>	<p>Sandy with an insignificant river discharge is with mainly a seaward sediment input.</p>		<ul style="list-style-type: none"> <li>· Shannon</li> <li>· Solway Firth</li> <li>· Severn Estuary</li> <li>· Thames Estuary</li> <li>· Westerschelde &amp; Oosterschelde (Netherlands)</li> </ul>	<ul style="list-style-type: none"> <li>· Inner Forth firth</li> <li>· Beaully Firth</li> <li>· Linne Mhuirich</li> <li>· Spey Bay</li> <li>· Solway: Wigtown, Kirkconnell Merse, Caerlaverock, Lochar Water (Estuarine marshes).</li> </ul>

<b>Loch or fjord-head marshes</b>	<b>Loch-head/ria</b> Generally muddy. Partly in sheltered spits in low salinity waters and on high platforms are botanically distinct from other marshes.		<ul style="list-style-type: none"> <li>· Brittany</li> <li>· west of Ireland (e.g. Dingle Bay)</li> <li>· western Scotland</li> </ul>	Main type found on the west and north coasts of Scotland: <ul style="list-style-type: none"> <li>· Loch Sunart Head</li> </ul>
<b>Perched salt marshes</b>	<b>Perched salt marshes</b> form on sea cliffs and in the shelter of raised rocky outcrops, where shallow sediment develops in the wave splash-zone		Occur mainly on rocky promontories in N and NW Scotland: <ul style="list-style-type: none"> <li>· Portskerra</li> <li>· Boddin Point (Angus)</li> <li>· Rubh' an Dunain (Stoer)Portskerra on the north coast</li> </ul>	

Biological traits of saltmarsh systems have been in general defined by comparing salt marsh to mangrove system (Friess et al., 2011), however the remarkable feature that salt marshes display is a zonation of vegetation communities caused by physical factors such as the marsh geomorphology and hydrodynamics (See also 2.3.1) defined by their elevation gradient affecting soil salinity which will determine and favour number of halophyte species to grow. In the UK, saltmarsh vegetation type classification started with A.G. Tansley in 1939 and extensively reviewed by Adam in 1990s until National Vegetation Classification (NVC) was established by the integration of Lancaster University survey and Rodwell (1999) synthesis (Boorman, 1999; Rodwell, 2006). J. Rodwell (2006) describes the 28 saltmarsh communities occurring in the UK (mainland, Isle of Man, Isles of Scilly and Scottish Isles) and covering vegetation communities, distribution and diversity using the percentage cover of species. NVC provides a standard classification for British saltmarsh communities recognised by most governmental agencies in England and Wales (e.g.: DEFRA/Environment Agency Flood and Coastal Erosion) and in Scotland (SNH). Four main general types of salt marsh are recognised: **pioneer marsh** (typically patchy cover of *Salicornia spp.*, *Suaeda maritima*, *Aster tripolium*); **low marsh** (continuous cover with *Puccinellia maritima* or *Atriplex portulacoides* often dominant) **mid and upper marsh** (*Festuca rubra*, *Limonium vulgare*, *Armeria maritima*, *Plantago maritima*) and **driftline or transitional marsh** (depending on the salt marsh include grassland/brackish swamp/sand dune communities). These NVC species assemblage's classification has been used in this thesis and an extract of SNH Scottish Saltmarsh Survey (SNH SSS) (Haynes, 2016) showing species present in Scottish salt marshes is provided in Appendix A.2.

Some limitations expressed by Boorman (1999) should be acknowledged that within any detailed saltmarsh vegetation classification, some features may reflect the past history of that particular

marsh and perhaps of less significance to the general vegetation classification. L. A Boorman pointed out that plant distribution pattern in a mature high marsh may still reflect its own original pioneer vegetation distribution patterns. Haynes (2016) also concluded that:

“It is important to note that most salt marshes in Scotland do include a lower, middle and upper marsh zone, but may have a variety of upper marsh vegetation integrated into each zone. When identifying saltmarsh zones, it may be more appropriate to use saltmarsh morphology, informed by the presence of saltmarsh vegetation types, rather than an NVC correspondence approach for zone definition. It is possible to create a zone map with the data [...] *and* would provide useful and simplified data compared to the NVC sub-community database “(Haynes, 2016, p. 189).

These precincts were considered and further developed in Chapter 3 – Research framework section 3.3.2.

### **2.3 Interface of geomorphology and ecology/biology: a key interface**

‘Salt marshes are areas of land covered chiefly halophytic vegetation which are regularly flooded by the sea’ (Allen, 2000, p.1157) and ‘represent a morphological response to waves, tides and sea level changes’ (Pethick, 1994, p.75).

The saltmarsh definitions above tend to vary depending on the discipline and which physical or biological controlling factors are described. For biological studies there is an emphasis on species and distribution whilst geomorphological studies lay stress on wave energy, tides and sediment interactions, sometimes with vegetation attenuating the processes. Mudge in 1858 first publish on relations between salt marsh and tidal levels, and later in 1886, Shaler focuses his studies on saltmarsh formation (Davis and Dalrymple, 2012). In the past decades, our understanding of the functioning of salt marsh has grown rapidly with a clear focus on saltmarsh ecosystem studies. As early as 1991, Mann & Lazier suggested that physical processes create the condition and structure in which biological processes occur and influences their functioning in many indirect ways (Mann and Lazier, 1991). They stressed the importance of limiting mechanisms and events that are studied to a strict spatial and temporal scale, a point also made by Allen (2000) as very short (days-years), short (decades), medium (centuries) and the long (millennia) terms. Friess et al. (2011) reinforce the concept of spatial and temporal scales stating that processes occurring at a smaller scale, such as sedimentation patterns and initial marsh colonisation, may be the research focus but at the larger spatial and temporal scales the hydrological regime, sediment supply, erosional processes, storm and sea level may be of more relevance (Friess et al., 2011). The authors validate this also in explaining that short-term processes (monthly to annual) such as drag force for vegetation establishment is important during early colonisation, but surface elevation change relative SLR



and feedbacks between vegetation hydrodynamic forces increase at ecosystem scale. And these factors do not act in isolation and the strength of interaction will vary across space. This is also true for coastal management concerns in order to determine the upper and lower limits of salt marsh relevant to a particular management scheme (Hough et al., 1999).

Although there is an increased number of studies in both biological and physical aspects of saltmarsh dynamics (Figure 2-5 (a)), this is only recently (Figure 2-5 (b)) that there is noticeable rise in literature on the crucial role of biogeomorphic feedbacks on saltmarsh dynamics. Interdisciplinary studies coupling the evolution of geomorphological and ecosystem structure (D’Alpaos et al., 2016) has stemmed from the work of Viles (1988) which does not consider biology as a by-product of physical processes but ‘rather highlights how biota feeds back on, directly modifies, and contributes to shape their physical environment’ (D’Alpaos et al., 2016, p.151). Many questions remain to be addressed and the difficulty resides in the fact that marsh vulnerability is mainly assessed by feedbacks between sedimentation, hydrodynamics and vegetation and is thus interdisciplinary in focus and application (Webb et al., 2013; Belliard et al., 2017).

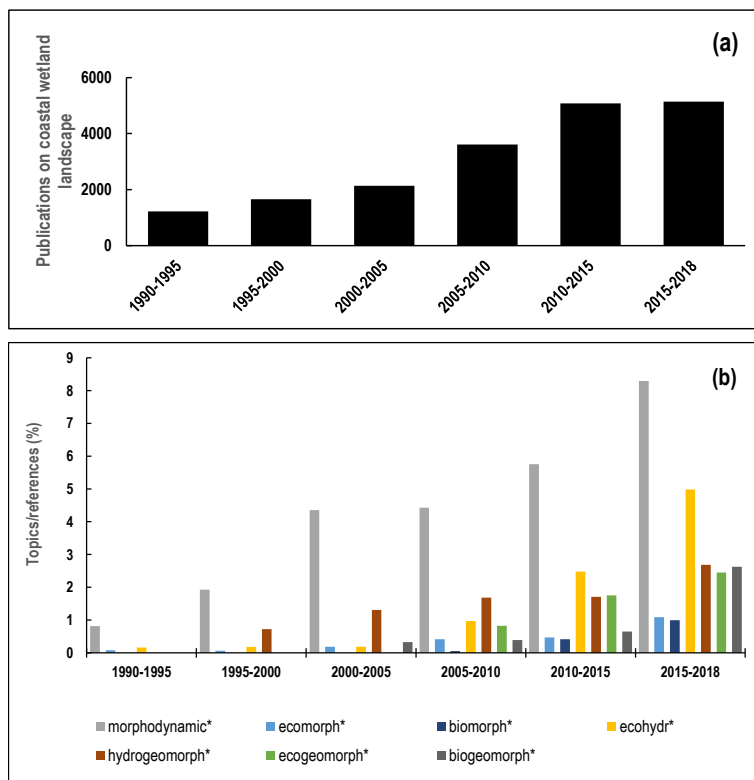


**Figure 2-5 (a) & (b):** Following D’Alpaos et al. (2016) and Wheaton et al. (2011) approach, the top chart (a) shows the number of publications (totalling to 14703) from 1990 to 2018 referring to Coastal wetland landscapes. Wheaton et al. (2011) argued that “scientists at the interface of physical and biological sciences have struggled with what to call their discipline” (Wheaton et al. 2011, p.266). The combinations of geo-, hydro-, eco-, bio- and morpho-represent different sub-disciplines that can be found in the literature and are presented here to show trends in the interdisciplinary research area. Bottom chart (b) presents the relative fractions (in %) of these publications containing the following terms in title, abstract or keywords: morphodynamic\*; ecomorph\*; biomorph\*; ecohydr, hydrogeomorph\*; ecogeomorph\*; biogeomorph\*.

Each salt marsh is subtly different, and variations occur as much worldwide as on a short distance (within a single intertidal area). Thus finding an appropriate methodology to assess saltmarsh vulnerability is not necessarily uniform and systematic (J. French, 2006). Saltmarsh characteristics depend on which processes are dominant: sediment or organic or both and how much human

interference is occurring or may have occurred (Allen, 2000; Baptist et al., 2016). There is no single controlling factor but a continuum of relationships that take place on different temporal and spatial scales (Pethick, 1984). Figure 2-6 presents a conceptual diagram of saltmarsh formation and development at different temporal scale that combines work from Allen (2000), Davidson-Arnott et al. (2002) and Cahoon et al. (2009). The figure illustrates phases of saltmarsh evolution at key time scale (labelled annual, decadal and longer timescale in figure 2-6) that are determined by a series of external processes such as wind, waves, tidal regime, salinity (labelled ‘process variables’ in figure 2-6) and controls such as shoreline morphology, seasons, sea level and glacial history, climate change (labelled ‘intrinsic and extrinsic factors’ in figure 2-6) interact positively and negatively (by use of arrows in figure 2-6) on saltmarsh development affecting biota (text in green in figure 2-6) and geomorphology (text in dark red in figure 2-6).

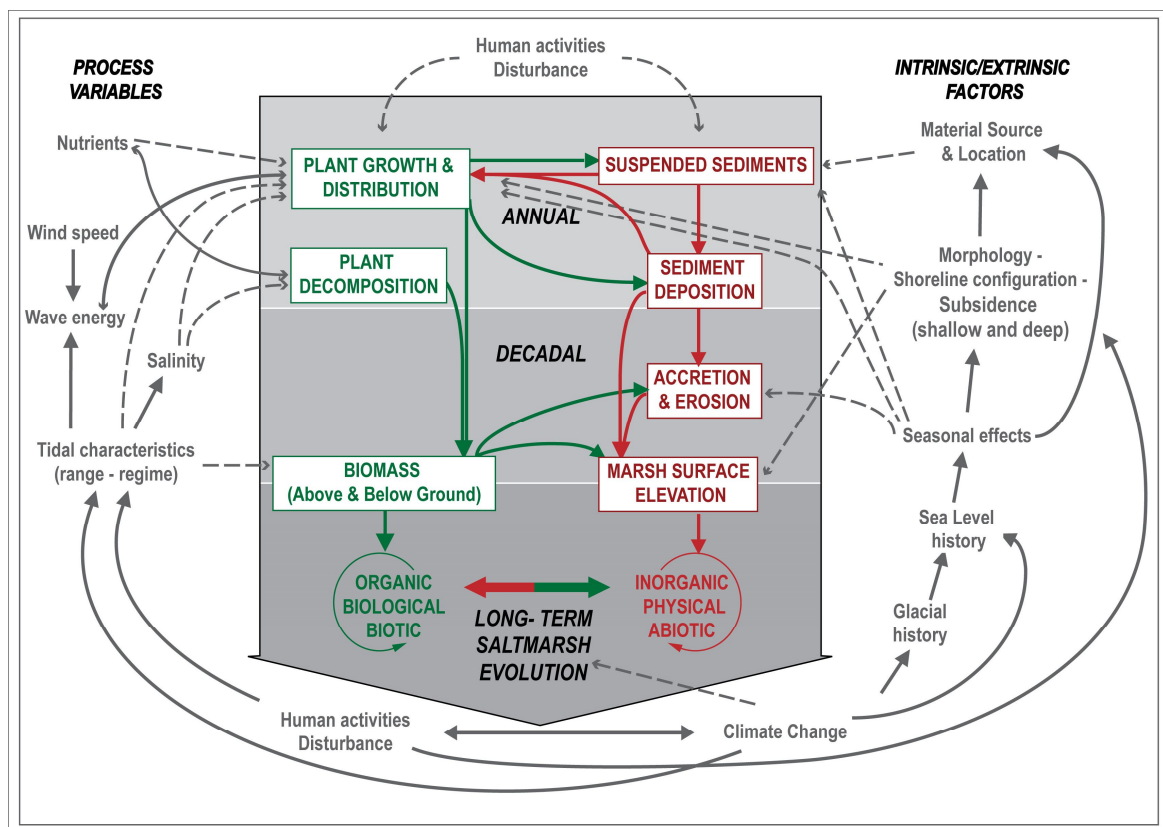


**Figure 2-6: Biological and geomorphological interactions of saltmarsh development through time.** Adapted from Allen, 2000; Davidson-Arnott et al., 2002; Cahoon et al., 2009.

These factors and processes that influence saltmarsh development are developed further in the following sections. Although these processes are discussed separately, it is important to reaffirm the assertion of Spencer, 1988 that no causality is implied, and the product of these biological and physical interactions create the landform as a whole.



### 2.3.1 Physical controlling factors

How do hydrodynamics, morphodynamics and climate influence, control and govern saltmarsh occurrence, type and development?

#### 2.3.1.1 Morphodynamics

Morphodynamics are the process by which morphology affects evolution of the morphology itself (Friedrichs, 2011). Geology and coastal physiography govern the occurrence of salt marsh (Chapman, 1977) and the physical space in which salt marsh can develop. This is also called accommodation space (J. French, 2006). Accommodation space is the volume available for sediment or water storage in an estuary and is a function of relative sea-level change, basin hypsometry and sediment supply. When accommodation space is limited, it is expected that the estuary channel will migrate laterally and may be associated with erosion. In contrast, during period when accommodation space is unrestricted, marsh vegetation can potentially develop on the extensive area available (Townend et al., 2011).

Shoreline configuration and nature of the substrate will influence local waves, nearshore slope, and gradient of the marsh surface. Salt marshes develop along protected coastlines (bays, lagoons, estuaries, shores behind spits and offshore islands) where the low energy waves favour the establishment and growth of saltmarsh vegetation seedlings and where shallow shores support greater extent of saltmarsh communities (Chapman, 1977). The substrate can originate from marine, coastal, fluvial or in-situ reworking (Pethick, 1984) and can vary widely in composition (sand, silt and clays). Soil composition, soil salinity which gradually increases with soil elevation and flooding regime will play a part in determining community composition such as presence of halophyte plants and plant performance (Ranwell, 1972; Chapman, 1977; Silvestri and Marani, 2004). Plant growth is depending on oxygen and oxygen availability is determined by the flood frequency which can affect root respiration, germination and early seedling growth (Silvestri et al., 2005). Soil type and tidal velocity will also influence surface erodibility and permeability, which can be in turn enhanced by biological activity. Micro-phytobenthos' action has been described as a bio-stabiliser, worms, snails and crabs as bioturbators as they can pelletise the surface muds, changing the sediment's physical characteristics and diatoms can stabilise the interfacial sediments through secretion of extracellular polymeric substances. (Black and Paterson, 1996; Eisma et al., 1998; Townend et al., 2011).

In Allen, the rate of soil autocompaction, dependent on the entire marsh history as defined by its particular stratigraphical characteristics (grain size distribution and Holocene basement depth) is

a significant factor influencing the marsh surface elevation change as it can provide accommodation space. When the systems are primarily minerogenic (such as NW Europe and Canada) autocompaction cause shallow subsidence (Allen, 2000). And this should be taken in account when measuring changes of surface elevation as it may contribute to overestimate results on accretion (Friess et al., 2011).

There is a clear effect of geological context on the distribution of salt marshes (and sand dunes) in the United Kingdom with a natural division between the hard rock formation of the Highlands and the soft rocks of the Lowlands and this is reflected in the predominance of coarse sediment deposits in the salt marshes of the north and west and the finer sediments in the south and east (Ranwell, 1972; Boorman, 2003).

Geology and geomorphology also affect the whole basin geometry in defining the volume of water exchanged between Mean Low Water Spring (MLWS) and Mean High Water Spring (MHWS) also referred to as the tidal prism. The nature of the substrate will govern the water drainage characteristics of the overall tidal area (mudflats and salt marsh) with shallow tidal channels for small marsh systems and deeper channels for larger systems some of which may have developed from relict morphologies (Eisma et al., 1998; Townend et al., 2011). The inherited marsh geomorphology may also lead to a tidal asymmetry (where the magnitude and duration between ebb and flood is different) will have significant impact on sediment delivery and salinity level across the marsh (Friedrichs, 2011).

Salt marsh as depositional landforms are mainly controlled by sediment availability, movement, deposition and redeposition. Doody (2008) enumerates three main sediment sources (Figure 2-7) in the coastal zone: 1) Fluvial and maritime transport of sediment originated from erosion of elevated land; 2) Tides, waves and storms transport sediment originated from erosion of adjacent shores and move it by longshore drift; 3) Coastal waters move sediment that has been reworked from subtidal offshore banks (Doody, 2008).

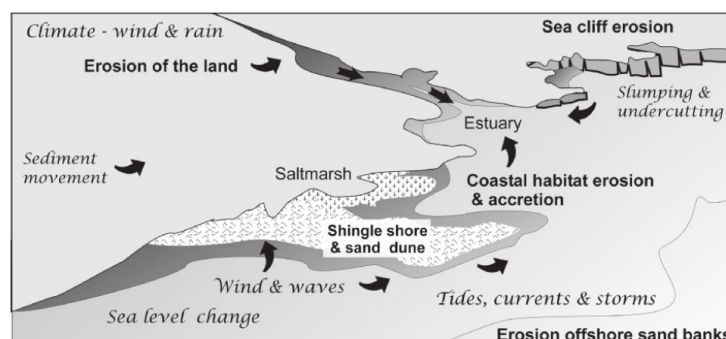


**Figure 2-7: Processes that are affecting the supply and movement of the sediments across the coastal zone** (Taken from Doody, 2008, p.2).

In the UK, most of the sediment originates from nearshore marine sources and coastal erosion) with little fluvial supply (Hansom, 1988). However, Ranwell (1972) also notes that in Scotland the high altitudes of catchments and high rainfall produces greater fluvial discharge (e.g. the Tay) reducing estuarine salinity and changing pioneer species distribution. Allen (2000) adds another important sediment source which is anthropogenic. Over the last few centuries sewage and industrial wastes and from mid-Holocene deforestation and agriculture have enhanced greatly the supply of natural fine-grained source material but due to the construction of coastal defences (1950s onwards) local supplies have been greatly reduced.

The sediment transported through the system is influenced by hydrodynamics and morphodynamics where the tides and waves initiate, transport and deposit sediments. Finer cohesive sediments are transported as suspended load and settle out at or near high water at the point when tidal velocities are at their slowest. Coarser and non-cohesive sediments are transported as bedload forming bedforms which in turn influence the fluid motion and sediment transport. The sediment is transported at a rate proportional to the flow velocity and becomes mobile once the critical entrainment velocity for that grade of sediment is exceeded. When tidal flow changes velocity and direction or when the water is completely unstressed (at slack tide), bedforms will change shape such as herring-bone cross-stratification or lenticular, wavy, and flaser bedding (Davis Jr. and Dalrymple, 2012). A further distinction can be made between tide-dominated estuaries where the sediment dynamics are dominated by tidal currents at the mouth, and wave-dominated estuaries where sediment transport and deposition is predominantly due to wave action (Davis Jr. and Dalrymple, 2012).

In the upper portion of the tidal prism and in shallowing waters the flow velocities become very low and decrease to zero at high water, thus allowing sediment deposition, accumulation and accretion (Pethick, 1984) so that the marsh surface becomes elevated. This rise in elevation reduces the hydroperiod and progressively allows longer periods and areas that are inundation-free and favours the colonisation of salt-tolerant plant species that form salt marsh (Allen, 2000; Doody, 2008; Davis and Dalrymple, 2012).

Fagherazzi et al. (2013) referring to Gunnell et al. (2013) highlights the dominance of sedimentological processes over ecological processes, showing that high sedimentation rates are promoted by sediment availability in sheltered areas (marsh area at the mouth of Newport river, USA) and are responsible for marsh formation, whilst the role of the vegetation became important only in the last phase of marsh emergence. This corresponds to French and Burningham (2003) who examined a reclaimed salt marsh in the Blyth estuary, Suffolk, and recognised that sediment supply enabled elevations of the marsh to be maintained and to drive sedimentary infilling of the

tidal frame. They suggested that the morphodynamic behaviour of the marsh appears to be governed by gross changes in estuary morphology and process regime (French and Burningham, 2003; Mudd et al., 2013; Gunnell et al., 2013).

### 2.3.1.2 Hydrodynamics

Coastal salt marshes are distinct from terrestrial landforms by dint of tidal submergence (Adam, 1990). Tidal currents crossing the marsh represent the basic circulatory system feeding the marsh with water but also sediments, organic matter and nutrients (Fagherazzi et al., 2004; Wolanski et al., 2009; Kearney and Fagherazzi, 2016) and regulate the flow through tidal creeks, the extent and duration of the inundation of the marsh surface and the horizontal and vertical extent of the salt marsh (Davidson-Arnott, 2009). Tides are periodic sea level changes generated by gravitational forces of the moon and sun on the waters of the oceans. The effects of sub-marine and coastal topography along with rotating earth forces alters further the tidal feature's resonance in bays and estuaries (Ippen, 1966). This is clearly demonstrated by variation of tidal range across the world coastlines classified by Davies (1972) (Figure 2-8) into microtidal (<2m), mesotidal (2-4m), low macro (4-8m) & high macro (>8m). At short distances, the variation can be as striking such as north and south of the English Channel such as Weymouth's mean high water springs (MHWS) for example is 1.4 m high and St. Helier's MHWS in Jersey is 11 m (Figure 2-9). Consequently, tidal range has repercussion on the coastal morphology and landforms and influences the direction of movement of sediments: the higher the range, the greater the tendency for the sediment to be driven landwards into coastal bays, to form estuarine, lagoon, barrier island, open coast or loch-head (Doody, 2008) and the strength of the currents allowing more sediments to be transported. Where the tidal range is great then there is more scope for the development of tidally produced landforms such as saltmarsh and mudflats in places where accommodation space is available (Hansom, 1988).

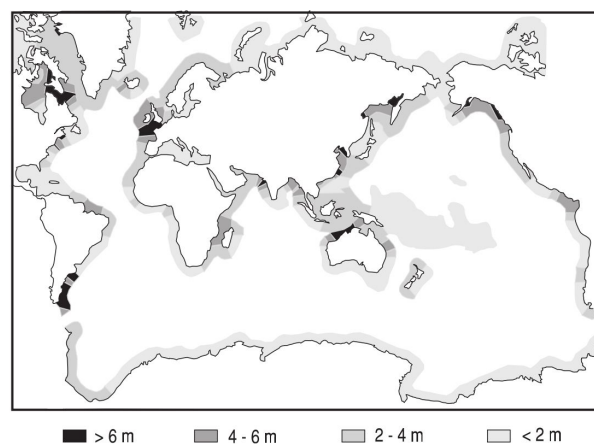
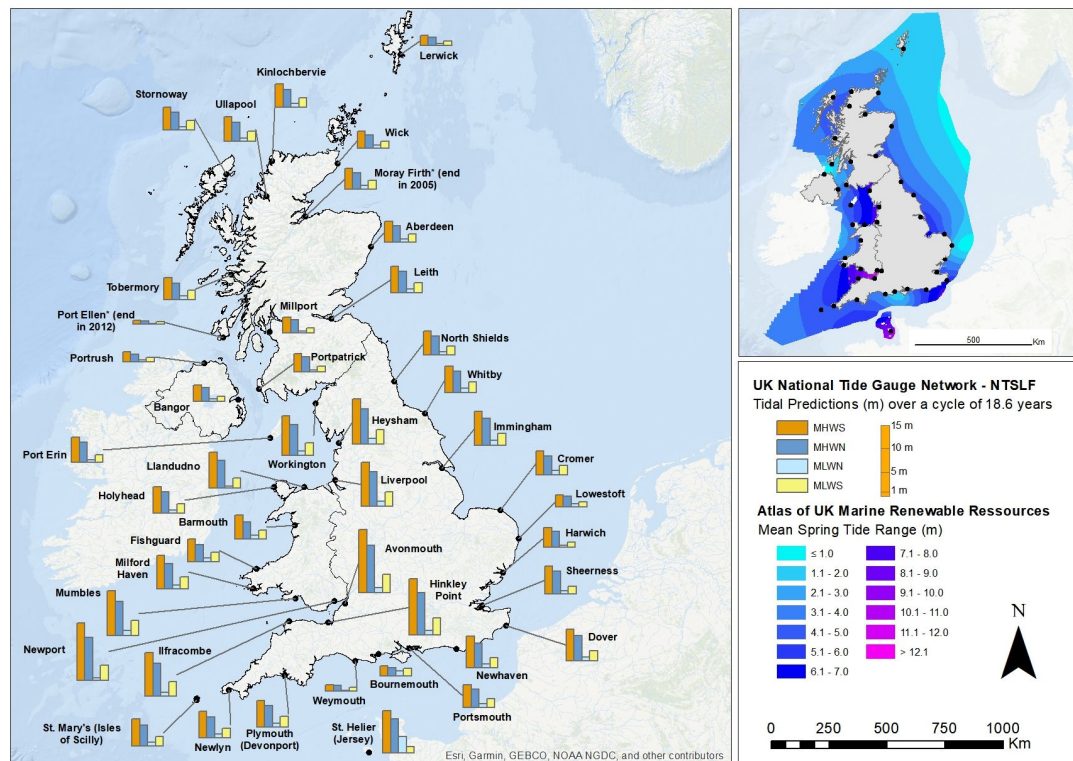


Figure 2-8 : World distribution of tidal range (taken from Davies 1972 in Eisma, 1998, p.12 )



**Figure 2-9: Tidal prediction values of Mean High Water Springs (MHWS), Mean Low Water Springs (MLWS), Mean High Water Neaps (MHW) and Mean Low Water Neaps (MLWN) calculated over cycle of approximately 18.6 years for the UK National Tide Gauge Network station. Data source: National Tidal and Sea Level Facility). © Copyright 2016 The National Oceanography Centre (NOC) (NTSLF/NOC/NERC, n.d.).**  
**Map inset: UK and Channel Islands territorial waters' Mean Spring Range (MSR). Data Source: Atlas of UK Marine Renewable Energy Resources. © Crown Copyright (ABPmer, 2008)**

Tides also control sediment transport across the tidal flat and subsequently determine sediment suspension, sedimentation and the vertical and horizontal extent of saltmarsh area. As seen above, higher in the tidal frame, the low velocity of the currents and salinity levels enables some salt tolerant species seedlings to germinate. This combined with an increase in light due to less turbidity and less flooding facilitates these halophytic plants to flourish (Pethick, 1984). Furthermore, tidal hydrodynamic such as repeated inundation or drag force can facilitate or prevent transport and dispersal of diaspore for short-distance events (except in extreme weather). The energy of tides coupled with wave actions (see below) impose multiple stresses on colonisation and seedlings of vegetation species. This is all relevant for identifying suitable site for restoration (Friess et al., 2011). Friess et al. (2011) highlight that further quantitative research is required to identify the impact of location and coastal regime on thresholds of hydrodynamics on vegetation establishment.

The traditional view is that an orderly succession of plant communities develops over time across the marsh between the Mean High Water Neap Tide (MHWNT) and the Highest Astronomical Tide (HAT) where the initial colonisation phase with pioneer vegetation will promote stabilising

and aeration of the substrate favouring plant growth and strongly influence sediment deposition and promote sedimentation. The increasing elevation will in turn reduce saline influences and enhance freshwater influences and so favour species competition allowing less salt tolerant species to colonise the higher grounds (Figure 2-10) (Odum, 1988; Eisma and Dijkema, 1997; Allen, 2000).

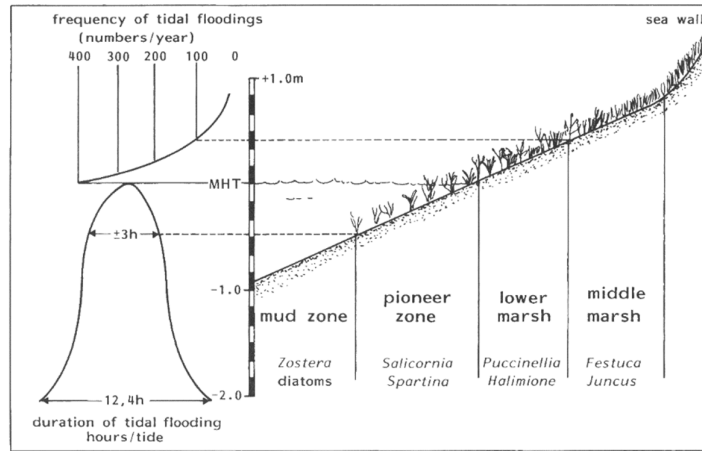


**Figure 2-10: Frequency and average duration of tidal flooding of the principal zones in West European salt marshes in Eisma and Dijkema (1997), p.406.**

However, saltmarsh establishment and development may not always follow this specific succession dynamic. While saltmarsh zones can be defined directly by tidal levels, they cannot form the basis for comparison of salt marshes, and, biological criteria has not been proven to be used to define universally comparable zones (Adam, 1990). Many environmental (e.g. soil salinity, submergences, duration of submergences) and physiochemical (e.g. sediment properties) factors correlated with elevation can influence species composition but not necessarily zonation patterns, or number of zones, neither determine *per se* zonation (Adam, 1990).

Silvestri and Marani (2004) studied saltmarsh halophyte species across different sites in the Venice lagoon, showing that halophytes were strongly correlated to marsh topography and morphology but were not necessarily associated with soil elevation, flooding duration or distance to the channel, soil salinity and soil topography. They suggest that if species distribution and zonation cannot be confirmed by general theories of soil salinity and tidal regime, the influence on zonation may be found in the dynamics of root oxygen availability. Subsurface flow may facilitate soil properties such as conductivity which will in turn alter aeration and marsh non-local topography. Spatial heterogeneities of soil properties and interplay between evapotranspiration patterns and sub- surface could explain different zonation patterns observed.

Soil salinity is closely related to the tidal flooding and opposing effects of evapotranspiration and precipitation which will affect the flux and level of salts through the marsh. Because of this



complex interplay the salinity is not increasing because of surface elevation and can be found relatively constant, rarely exceeding or different from that of the flooding water. This is true except during summer months where there is relatively high evapotranspiration and shorter tidal inundation, salinity levels can rise to high values until alteration points where salt crust forms on soil surface. There is also a zone below which flood frequency exceed evapotranspiration and leaching effects from rainfall causing high salinity levels. This influences plant species depending on their tolerant to salinity to establish themselves such as riparian species invading the higher marsh more prone to the dominant effect of rainfall leaching (Beefink in Chapman, 1977, Adam 1990).

Water salinity is defined by the magnitude of the tidal current relative to the river inflow creating a longitudinal gradient in most tidal basins/channel. When the currents are low the water is not well mixed and 'salt-wedge' occurs; the tidal basins are mixed to well mixed when the magnitude of the tidal currents is such that the intensity of the small-scale turbulence created by the bottom friction is high enough to keep the water column mixed most of time (Eisma et al., 1998).

As Townend et al (2011) remind us the physical role of waves on saltmarsh systems is either studied for its the impact on saltmarsh communities or how salt marshes influence and dissipate wave energy (see 2.3.2 p.2-28). Although tidal wave which propagates (from the entrance toward the end of the basin up until the rivers discharging into tidal basin) is determined by the overall length and depth in the main channel, meteorological forcing can also induce a large-scale circulation within an estuary. Wind waves can completely reverse the normal tidal flow pattern as reported for the Potomac River estuary (Chesapeake Bay, USA) where wind waves occur 20 % of the time compared to a normal circulation of 43 % of the time (same flow direction in the surface and bottom water is c.20 % of the time and complex flow 17 % of the time). These waves are due to either incoming waves from adjacent shelf or directly generated by wind forces and can have drastic effect on shallow tidal flats by bringing sediments from bottom surface into suspension (Eisma et al., 1998). Leonardi et al. (2016) have found from analysing data from eight different locations (United States, Australia, and Italy) that long-term (c.20 years) marsh deterioration is influenced by average wave conditions (i.e. variation in the mean wave energy) where extreme conditions, such as violent storms and hurricanes, play a role in less than 1% to long-term marsh erosion rates (see also 2.4.1.2 - Storminess).

### 2.3.1.3 Environmental factors influencing saltmarsh development

Salt marshes and coastal wetlands began to form when mean sea level (MSL) approached its present levels following the rapid rise from c.120 m below present MSL experienced during the last glacial maximum ~ 18 000 years ago (May and Hansom, 2003). MSL rose very rapidly from c. 20,000 years ago and largely resulted in coastal transgression rather than coastal modification and landform construction. However, about c.6000 years ago MSL approached close to its present level and this coincided with the development of extensive landforms including salt marshes. The changes in sea level history have controlled estuarine location (Adam, 2002; Wolanski et al., 2009), so that, on sea level rise, estuaries migrate landward, and vice versa, on sea level fall, a marine transgression process referred to as estuary rollover (Townend et al., 2011). For example, the Forth estuary in Scotland migrated landward during the Late glacial and mid Holocene periods before migrating seaward since then (Hansom and Evans, 2000), a process which has only recently been reversed as a result of modern sea level rise across Scotland (Rennie and Hansom, 2011).

Sea-level influence has an indirect link to accommodation space and marine transgression, but it has a direct impact on saltmarsh ability to adjust rapidly to such changes (Allen, 1990; Reed, 1995; Morris et al., 2002). Salt marsh must maintain their elevation relative position to tidal frame which changes due to SLR by vertical substratum adjustment through accretion and sediment accumulation. Micro-tidal salt marshes where SLR is proportionally larger than tidal frame are more susceptible to suffer from SLR (Friess et al., 2011).

Recent literature shows the growing concern in predict impact of SLR on salt marsh (Kirby, 1992; Cahoon et al., 2000; Mudd et al., 2009; Webb et al., 2013; Rogers et al., 2014; Kirwan et al., 2016). State shifts in ecosystems are common but our capacity to forecast them and understand what drives them is still limited. What are then the impacts on salt marsh when sea level changes? Answers are further developed in section 0.

### 2.3.2 Biological controlling factors

Biologic processes that influence sedimentation are visible at different temporal and spatial scale of saltmarsh development and will not operate in isolation. This section presents how saltmarsh plants can regulate saltmarsh systems by influencing hydrodynamics, reducing soil erosion and aiding accretion.

As seen above succinctly (2.3.1 and in more detail in 2.4.1.3) vegetation establishment and development have found various mechanical ways to counteract the physical stresses due to



prolonged and frequent inundation and drag force from current and waves; but vegetation can also attenuate and enhance sedimentation throughout marsh development. The surface elevation which is controlled by long-term sediment availability and accumulation which is partly determined by trapping efficiency. The velocity and height of tides and wave can be dampened by aboveground and stem vegetation morphologies to allow sediment particles to fall out of suspension (Allen, 2000; Morris et al., 2002), resuspension (Friess et al., 2011) and direct erosion of saltmarsh surfaces (Fagherazzi et al., 2012).

#### 2.3.2.1 Vegetation influences hydrodynamics

The increased presence of vegetation and when vegetation is finally established on the marsh, hydrodynamics of the entire system may be attenuated by the reduction the energy of incoming waves (Möller, 2006). Vegetation stems and leaves increasing surface roughness and frictional resistance reducing flow velocity of waves and currents but also the topographic variations over the marsh surface (Pethick, 1984; Eisma and Dijkema, 1997). Plant characteristics will affect wave attenuation where geometry, stem density, spatial coverage, and stiffness, but also the hydrodynamic conditions such as water depth (Fig. 4), wave period, and wave height are all relevant. Möller (2006) demonstrated that tall canopy can have significant control on wave attenuation ( $H_s/h$  threshold of 0.55 for *Spartina* beyond which the flow reduction is not significant). Cahoon et al. (2000) further propose that short-term (<10 years) sedimentation project should monitor tidal range, biological productivity and sediment supply. However, the authors make a distinction between marsh of different sedimentary fabric: organogenic and minerogenic marshes. Organogenic marshes which are formed by plant production's accumulation (belowground) owe their stability on the rate of carbon burial and are for this reason more susceptible to rapid sea level rise, thus increasing hydroperiod and reducing productivity (Allen, 1990; Cahoon et al., 2000). Conversely, in NW Europe, minerogenic marshes are predominantly formed by externally derived inorganic sediments. These marshes are consequently controlled by strong tidal processes exchanging water and materials onto the marsh surface and their elevational adjustment will be more susceptible to the feedbacks between elevation and rate of inorganic sedimentation (Allen, 1990; Cahoon et al., 2000).

#### 2.3.2.2 Organic matter is important

Accretion on salt marsh requires supply of inorganic as well as organic material which can be formed by fine plant detritus brought in by tides, waves or during storms (even ice rafting) and by the marsh productivity. The supply of organic material will be dependent on the marsh conditions for plant growth but also degree of preservation of both plants and roots that could otherwise be

easily removed by the tides or microbial degradation. However, role of vegetation in sedimentation is distinct between salt marshes which occupy macro- and mesotidal coasts with well-aerated marsh upper layer such as the ones in the west of Europe and salt marshes in USA on micro- and low mesotidal coasts which favour a high groundwater table permitting favourable anaerobic conditions to root and plant preservation (Eisma and Dijkema, 1997). In 2004, Christian and Blum found that the aboveground litter is not a significant factor to marsh sedimentation (in Fagherazzi et al., 2004), however through growth and decay, salt marsh plants play a crucial role in maintaining the ecosystem's biological richness and diversity (Allen, 2000).

### 2.3.2.3 Plant structure modulates saltmarsh erosion

Plant roots does offer resistance to erosion and species differences in root architecture and characteristics such as density and flexibility will affect erodibility (Adam, 1990). Beeftink (in Chapman, 1977) notes that most significant difference between *Salicornia* and *Spartina* is the root system where *Salicornia* makes the soil in which is growing more resistant (with channel banks undercut), firmer and promoting aeration which in turn enhance biomass production. Plant diversity has been found to increase soil stabilisation (and root biomass) notably in biogeographical contexts where soils are prone to erosion such as sandy soils and low in organic content (Ford et al., 2016). Allen (2000) draws attention to surface elevation change from soil expansion caused by belowground production due to organic matter accumulation. Belowground production is equal to or exceeds the aboveground production. When marshes are more dependent on organic production or when sediment supply is low, belowground productivity can be critical to the marsh survival under accelerated SLR (Allen, 2000; Yu and Chmura, 2009; Townend et al., 2011; Blum and Christian, 2013; Costanza et al., 2014). This is illustrated in Nova Scotia on the inner Scotian shelf where rapid sea level rise during the early Holocene exceeded the rate of saltmarsh elevation, and, in places of accretion deficit, soil was found submerged with substantial lateral erosion of the remaining wetlands releasing carbon stored from their deposits (Chmura et al., 2003).

In their Mont-St-Michel research Langlois et al. have quantified differences of accretion between bare flats and *Puccinella maritima* vegetated area on three study sites. The species have demonstrated to have pronounced effect on sediment stabilisation and once the micro-topography has been established, the rate of soil level rise and vegetation succession accelerates preventing erosion by waves and currents (Langlois et al., 2003). Reef et al. have found that during calm summer conditions vegetation height or biomass had little impact sediment trapping; but during periods of higher wind/wave energy and stronger vertical mixing of suspended sediments, the role of canopy structure could prove significant (Reef et al., 2018). A negative feedbacks may be also

acknowledged where self-scouring is often displayed by pioneer plants when waves and currents increase their movements and can enhance surface to erosion (Friess et al., 2011; Reef et al., 2018).

### 2.3.3 The societal value of salt marsh

In addition to its geomorphological and biological significance, salt marshes are particularly important from a human perspective. The UK National Ecosystem Assessment (UK National Ecosystem Assessment, 2011) define ecosystem services as ‘the outputs of ecosystems from which people derive benefits’ (Luisetti et al., 2013; Beaumont et al., 2014). The Millennium Ecosystem Assessment (MEA) classified in 2005 ecosystem services into four categories: Supporting, provisioning regulating, and cultural services presented in Table 2-3 (Millennium Ecosystem Assessment, 2005).

Lefeuvre et al. (2003) remind us that it took almost 20 years of research on the role of the Mont-St-Michel wetlands to highlight the ecological, social and economic interest of this ecotone. Barbier et al. (2011) stated that:

‘as long as nature makes a contribution to human well-being, either entirely on its own or through joint use with other human inputs, then we can designate this contribution as an ecosystem service’.

In his review study of ecosystem services provided by estuarine and coastal ecosystems (incl. coral reefs, seagrasses, salt marsh, mangroves and sand dunes and beaches) he provided a first attempt in ‘real’ estimation of these ecosystem services for salt marshes (used in Table 2-3).

My research aims to understand differences in short term vegetation dynamics, alongside medium to long-term sediment dynamics between natured and managed realignment salt marshes. These datasets are useful to help support improved understanding of the supporting habitat and regulatory services that salt marshes provide. These aspects are the focus in my review of ecosystem services provided by salt marshes

**Table 2-3: combined table of ecosystem services as defined by MEA (2005) and (some of the) processes and functions that salt marshes provides along with examples of values for these services after: † Barbier et al., 2011 and ◇ Working with Nature protection WWNP (2018).**

<b>Ecosystem services</b>	<b>Example of human benefits</b>	<b>Ecosystem service value examples after Barbier et al. (2011)</b>
<b>Provisioning</b>	Food and fuel	Livestock grazing- Turf cutting- Fine clay for brick cement - Salt and chemical production and industry - Aquaculture (animal and seaweed production) & maintenance of fisheries - Exploitation of macroalgae - Food from saltmarsh plants, wildfowl and fish and shellfish
		£15.27 ha <sup>-1</sup> .yr <sup>-1</sup> net income from livestock grazing, UK. † US\$6471/acre and \$981/ acre capitalized value for recreational fishing for the east and west coasts, respectively, of Florida, USA \$0.19–1.89/acre marginal value product in Gulf Coast blue crab fishery, USA . †

<b>Supporting</b>	Biodiversity Habitat	Habitat refuge - primary production - biodiversity	estimates unavailable †
	Coastal protection	Storm and waves protection Flood protection	US\$ 8236 ha <sup>-1</sup> .yr <sup>-1</sup> in reduced hurricane damages, USA. †  Salt marsh (80 m width) fronting a flood defence structure could save about £4,600 m <sup>-1</sup> in additional wall protection ◇
<b>Regulating</b>	Erosion control	Sediment stabilization and soil retention in vegetation root structure	estimates unavailable †
	Water purification	Nutrient cycling & water filtering (pollutant),	US\$ 785–15 000/acre capitalized cost savings over traditional waste treatment, USA. † £1,793 ha/year for water quality ◇
	Carbon sequestration	biogeochemical activity, sedimentation, biological productivity	US\$30.50 ha <sup>-1</sup> .yr <sup>-1</sup> † £34.56 –£118.26 ha <sup>-1</sup> .yr <sup>-1</sup> ◇
<b>Cultural</b>	Tourism, recreation, education and research	Unique and aesthetic landscape Birdwatching Recreational hunting, fishing,	£31.60/person for otter habitat creation and £1.20/person for protecting birds, UK. † Marginal value of £1394 ha <sup>-1</sup> .yr <sup>-1</sup> for Aesthetic and amenity ◇

### 2.3.3.1 Supporting services

Salt marshes facilitate biodiversity by providing sheltered living space assuring reproductive habitat, nursery grounds and refuge to living species (faunal and floral included).

#### **Biodiversity**

Salt marshes and intertidal mudflats significance has been internationally recognised by the adoption of the 1971 Ramsar convention (see also Appendix A.1) agreeing to support the conservation of biodiversity, the sustainable use of its components, and the fair and equitable sharing of benefits of wetlands. Biodiversity tends to be defined through the specific richness of the habitat, which in turn will define its patrimonial value. The recognition of intertidal mudflats and salt marshes is that they are hosting rare and vulnerable plant species, providing habitats for migratory birds, wildfowl and threatened bird species and nursing grounds for fish stocks (Foster et al., 2013). However, Lefeuvre et al (2003) in their Mont-St-Michel salt marsh case study demonstrate the difficulty to assess the biological diversity by considering only the specific richness: diversity of halophytic communities, time that the species spend on salt marshes through a whole cycle year, also the origin of the species, and lack of complete inventories. They would favour a mere holistic definition of biodiversity moving from the account conception towards an integrative approach of the global functioning of the ecosystem that would not only include the knowledge of species present but also the complexities of the system processes (Lefeuvre et al., 2003).

## **Habitat**

The shelter and protection from saltmarsh vegetation provide an essential refuge habitat for young fish and crustaceans but also feeding, roosting and nesting habitat for migratory waterfowl, shorebirds, waders passerines and bird of prey (Boorman, 2003; Gedan et al., 2009; Barbier et al., 2011). Agricultural intensification has caused the decline and loss of breeding habitats and forced bird population to find new habitats such as the Common Redshanks whose approximately 50% of its breeding population is found now in British salt marshes (Sharps et al., 2016). As seen above (biodiversity), this estimate is important as the numeric distribution of water birds is used as an assessment of the importance of wetlands for the 1971 Ramsar convention (see also Appendix-A1); thus making UK marshes both nationally and internationally important for the species. However recent surveys of British salt marshes found that a 52.8% reduction in nesting pairs between 1985 and 2011 emphasising the importance of adaptive conservation management (Sharps et al., 2015). By allowing the tide to inundate former pasture or agricultural land breaching or removing sea wall, managed coastal realignment (MR) is becoming the most widely applied strategy in creating new intertidal habitats such as Freiston shore (Mossman et al., 2012) and Tollesbury in SE England. or the first MR scheme in Scotland at Nigg Bay (Crowther, 2007; Elliott, 2015).

### **2.3.3.2 Regulatory Services**

Defining the regulatory services that saltmarsh ecosystems provide serves to highlight the important controlling and adjusting mechanisms that takes place through this landscape, such as water filtration, biological productivity, carbon storage and sequestration, coastal protection, thus reasserting the importance of measuring physical and biological processes which is the aim of the thesis study.

### **Salt marsh as sink or filter**

Salt marshes are one of the most productive ecosystems in the world, due to largely to their capacity to act as sinks for organic and fine-grained inorganic sediments (Long and Mason, 1983). Eutrophication of coastal waters due to excessive nutrient loading, also pollutants from agriculture and industries which all have long-term effects over long distance, is generally controlled by salt marshes through water movement (Wolanski et al., 2009). Cycling of nutrients results from activities from organisms, saltmarsh food web and geochemical processes (rock weathering, aeolian and tidal flow). Such cycles are generally self-maintained and largely closed using pathways from soil to plants and back again. Considerable quantity of nutrients from plant litter

are imported and exported on salt marsh through the tides. Inorganic nutrients absorbed from soil or water for benthic algae and incorporated by autotrophs as organic compounds. Nutrients are then released into soil from necromass, by leaching and mineralization processes (from organic to inorganic) (Packham and Willis, 1997). Nitrogen is a main nutrient cycled through salt marshes. They serve as sink (mainly young pioneer marsh) and source (mature marsh) of nitrogen, filtering runoff water and diminishing nitrogen input to estuaries via bacteria and algae. Left uncontrolled, excess nitrogen causes toxic algal blooms and marine dead zones (Gedan et al., 2009).

The suspended particulate matter that deposits on salt marshes is associated with nutrients and metals part of the natural geochemical weathering. Sediments and vegetation can absorb and transform 30-65% of deposited metals such zinc manganese or lead making the system as sink for metal contamination (this excludes erosion events). Deeper saltmarsh sediments are also considered as stable repositories for pollutants due to absence of oxygen in marine soils as long as there is no bioturbation or oxidation. Conversely, saltmarsh plants can be used as a bioindicator of pollution as halophytes have the capacity to tolerate heavy metal such Magnesium, Mercury or Chromium. However there are concerns that with the risk to re-introduce these contaminants into food web when bivalves, crabs and other marine fauna feed or graze on the contaminated plant litter (Gedan et al., 2009).

### **Primary Production**

Coastal wetlands including salt marshes are contributing to c.20% of the net total of primary production making it the most productive ecosystem of the world (Bouchard and Lefevre, 2000). The absence of oxygen in saltmarsh soils allows carbon sequestered by plants through photosynthesis to transfer a small fraction to the marine waters and in sediments via burial. This carbon is cycled over a short term (decennial) in biomass and slowly decaying biomass into peat and over longer (millennial) time scales in sediments.

Depending on the system only small fraction (<10%) of the produced biomass is buried within the marsh; however, the very high rate primary productivity in salt marshes still contribute significantly to carbon sequestration compared to other ecosystems such as terrestrial forests. Saltmarsh plants can produce 100 to 1000gC m<sup>-2</sup> annually (Sousa et al., 2010; Barbier et al., 2011; Artigas et al., 2015). Moreover, sediments in a 'healthy' salt marsh will continue to accumulate to maintain its elevation relative to sea level rise and potentially increasing the rate of sediment carbon sequestration and the size of sediment sink (Chmura et al., 2003; Mcleod et al., 2011). Saltmarsh roots systems (intertwined roots and rootlets) and dense vegetation (depending on plant architecture: upright stems, type of leaves) predispose their efficiency in trapping sediment and

organic material in the form of detritus from internal source (accumulation of organic litter containing mineral grains) and external sources (tidally introduced) but also from adjacent ecosystems, and, depending on tidal range the carbon burial, for example, can be dominantly allochthonous or autochthonous (Allen, 2000; Mcleod et al., 2011).

### **Carbon storage**

From Chmura (2003) and Duarte et al. (2005) work, salt marshes are estimated to sequester on average  $218 \pm 24 \text{ g C m}^{-2} \text{ yr}^{-1}$  (or  $2.1 \text{ Mg C ha}^{-1}$ ) (Mcleod et al., 2011). However, estimations of the long-term carbon sequestration are highly variable due to the hydroperiod, salinity or sediment supply, and also plant species, plants composition and decomposition and primary productivity. These variations are well illustrated in the recent studies carried out in the UK. Work from Andrews et al. in one of the largest estuary in the UK, the Humber have shown that management realignment has a the potential to significantly enhance or at least being an option for net carbon burial but also methane and storage of contaminants (Copper, lead and Zinc) in the estuary (Andrews et al., 2006). Burden et al. have similarly examined the potential for restored salt marshes 15 years after realignment, at Tollesbury, Essex, UK, to sequester carbon, and found that they can provide a modest, but sustained, sink for atmospheric CO<sub>2</sub> at a rate of  $0.92 \text{ t C ha}^{-1} \text{ yr}^{-1}$ . However, their results suggested that after 15 years the restored sites are not fully equivalent to the natural salt marsh in terms of biological and chemical function. They established that although aboveground biomass, extractable N and substrate mineralisation rates capacities of the restored site were similar to the natural site, the soil C stock, C/N ratio and belowground biomass capacities were slower to recover and this might take c.100 years (Burden et al., 2013). These differences were not observed by Adams et al. (2012) in the Blackwater estuary. The carbon density and nitrogen density of the restored (managed realignment and accidental retreat sites) saltmarsh sediments generally increased with the degree of vegetation development on the site and it was found that restored sites (4 years old) had a greater carbon density and nitrogen density than the natural marshes (11 years old). This study also shows that the rate of sediment accumulation will dominate all other controlling factors of carbon sequestration (Chmura et al., 2003; Adams et al., 2012).

### **Blue carbon in Scottish salt marshes**

To date, there is no publication using empirical datasets to quantify carbon sequestration capacity in a Scottish saltmarsh system. Given the average sequestration capacity from Chmura and the estimated extent of Scottish salt marshes to 7704 ha (Haynes, 2016) which is about 15% of the total extent of salt marshes in the UK, Scottish salt marshes may have an average sequestration



potential of c.1680 t C/yr (0.017 Mt C annually). A comprehensive assessment carried in 2015 on the potential extent of blue carbon stores in Scotland coastal and marine environment highlighted that ‘the primary source of organic carbon in sediments is phytoplankton estimated at 3.9MtC/yr and carbon fixed by marine seaweeds, primarily kelp, may contribute up to a further 1.8MtC/yr. Other Maerl, seagrasses and saltmarsh plants and other coastal marine plants contribute to a much smaller quantity (18 000 tC/yr)’ (Burrows et al., 2014). However, the results were limited (and shown some disagreement) due to the lack of data on sediment accumulation rates for Scotland.

Recent work on saltmarsh blue carbon potential in a restored tidal saltmarsh in Secaucus, New Jersey potential highlights that more studies are required to measure carbon accretion and sequestration rates. As stated by Artigas et al. (2015), this is critical for two reasons: ‘First, to determine if tidal wetlands provide an effective long-term carbon storage alternative to terrestrial vegetation and second, to determine if accretion rates are keeping up with sea level rise’.

### **Salt marsh as coastal protection**

Wave energy dissipation by salt marshes is a physical mechanism that has shown in the past decade great interest (Temmerman et al., 2013; Möller et al., 2014; Spencer et al., 2015) as it encompasses the many aspects and traits of saltmarsh dynamics: morphology, hydrodynamics, biological response to stress, resilience to climate change such storm surges and hurricanes but also flooding attenuation. Leonardi systematic review highlights that as an ecosystem service, saltmarsh systems have been demonstrated to effectively reduce storm surge height. Salt marshes value for buffering against the impact of storms has been estimated up to 5million USD per km<sup>2</sup> in the United States (from Costanza et al., 2008), and 786 million GBP per year for UK marshes (data from Foster et al., 2013; Möller et al., 2014). However, empirical studies have also shown that the effectiveness of the storm surge height reduction can greatly vary because waves and their transformation with distance are dependent on vegetation characteristics, water depth and incident wave conditions (Möller and Christie, 2019). Hydrodynamic and modelling studies based on geometries and on the specificities of landscape have highlighted two mechanisms taking place during storm surges on salt marshes: within marsh attenuation (wave attenuation is due to friction exerted by the marsh vegetation and soil on the landward propagating storm surge) and along-channel attenuation (wave attenuation is due to lateral flooding and water storage on marshes adjacent to that channel). These studies and model have shown that the effectiveness of the reduction of the storm surge height is increased during moderate storm surges (> 1day) on wide (<10km) elevated and continuous (as opposed as patchy) salt marshes comprising few or small channels and preferably located inland along funnel-shaped estuarine and deltaic channels (Leonardi et al., 2018).



Saltmarsh role in storing and slowing the flow of floodwater has been associated in USA with an increased interest in restoring wetlands in flood prone areas as floodplains are known to be critical in mitigating flood damage, as they store large quantities of water, effectively reducing the height of flood peaks and the risk of flooding downstream. It was estimated that 3% to 7% of the area of a watershed in temperate zones should be maintained as wetlands to provide both adequate flood control and water quality improvement functions (Zedler and Kercher, 2005) .

Salt marshes also contribute to the shoreline stabilisation by maintaining their elevation through sedimentation and organic matter accumulation processes which help to maintain the marsh edges and reduce erosion. Salt marshes moderate erosion through the vegetation structure which increases the surface roughness and frictional resistance but by increasing the soil stability. In 2016, through experiments on two different salt marshes in Essex and in the Morecambe bay, it was found that plant species richness had a strong association to erosion reduction and soil stabilization with stronger impact in salt marsh with sandy and low organic content (Ford et al., 2016).

## **2.4 Salt marsh in a changing climate**

### **2.4.1 Climate-driven changes in saltmarsh systems**

Sea-level rise, storm surge, sea surface temperature and river flow are the four main processes that are likely to affect the most salt marshes and coastal ecosystems. The projected trends of Robins et al. (2016) are summarised in Table 2-4 and the likely impacts of these on ecosystems and society are summarised in Figure 2-11. Robins et al. (2016) concluded that the key changes to physical and primary processes are likely to be increased flooding and coastal squeeze caused by SLR, storm and waves surges. SLR, Storm surge and temperature changes are most directly related to my thesis aims, as they impact on the short-term (seasons) and long-term (>decadal) sedimentation and vegetation processes that take place in saltmarsh lifecycle, and so will be reviewed in detail below.

Owing to the clear increase of SLR rate since 19<sup>th</sup> Century, tremendous attention has been held on the past c. 250 years (from c.1700 when first tide gauges started measurements in European ports) of global mean SLR (Church et al., 2013). Church et al. (2013) have shown that long-term global mean sea level rates were  $1.7 \pm 0.2 \text{ mm.yr}^{-1}$  between 1901 to 2010 and of  $0.19 \pm 0.2 \text{ mm.yr}^{-1}$  for a total sea level rise and that short-term rates from 1993 to 2012 (using satellite altimeter record) have increased even faster to  $3.2 \pm 0.2 \text{ mm.yr}^{-1}$  for the global means sea level. The overall observed recent acceleration in global estimates is attributed to the increase in global temperature thermal expansion of surface layer (ocean warming) and land-ice melting (Church et al., 2013).

**Table 2-4: Observed trends and future projections of climate change where the level of confidence (low, medium, or high) has been based on the amount of evidence and the level of agreement as reviewed by Robins et al. (2016) for the river-estuary-coast catchment systems**

Process	Observed trend for the UK	Confidence	Projected 21st century change for the UK	Confidence
Sea surface temperature	+0.7 °C (1971 - 2010)	High	+1.5 °C to +4 °C	High
Sea-level rise	+1 to +3 mm.yr <sup>-1</sup> during last century	High	+0.44 m to +0.74 m (Steric and eustatic processes)	High
		Medium	+1.9 m (Ice sheet melt) Centennial changes in extreme water levels are marginally significant (i.e., are of the same order as the natural climatological variability).	Low Low
Storm surge	Pole-ward shift of storm tracks.	High	Increased intensity/ decreased frequency extra- tropical cyclones. High variability in storm surges Clustering of extreme sea- levels	Medium
		Medium		
		Low		
River flow	1969 -2008: Increased flow during autumn and winter, decreased flow during spring, no trends during summer	High	Increase in winter mean flow by up to 25% Decrease in summer mean flow by 40 - 80%	Medium
	Rainfall (river flows) occurring in clustered events	Low		

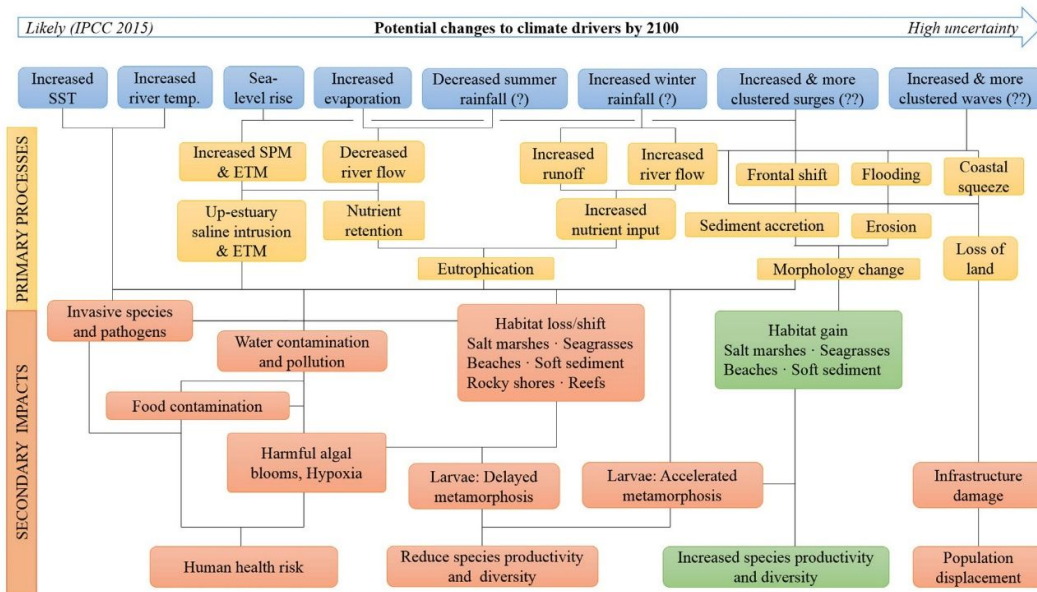


**Figure 2-11: Flow diagram showing the main climatic drivers (blue) and primary (yellow) and secondary (orange) impacts of climate change to river-estuary-coast catchment in the UK (taken from Robins et al.,2016, p.131). Pathways in black lines are directed from the bottom/side to the top of a 'driver/impact box'. Predominantly positive impacts are coloured green. Abbreviations: SST = sea surface temperature ; SPM = suspended particulate matter ; ETM = estuarine turbidity maxima.**

### 2.4.1.1 Sea level rise

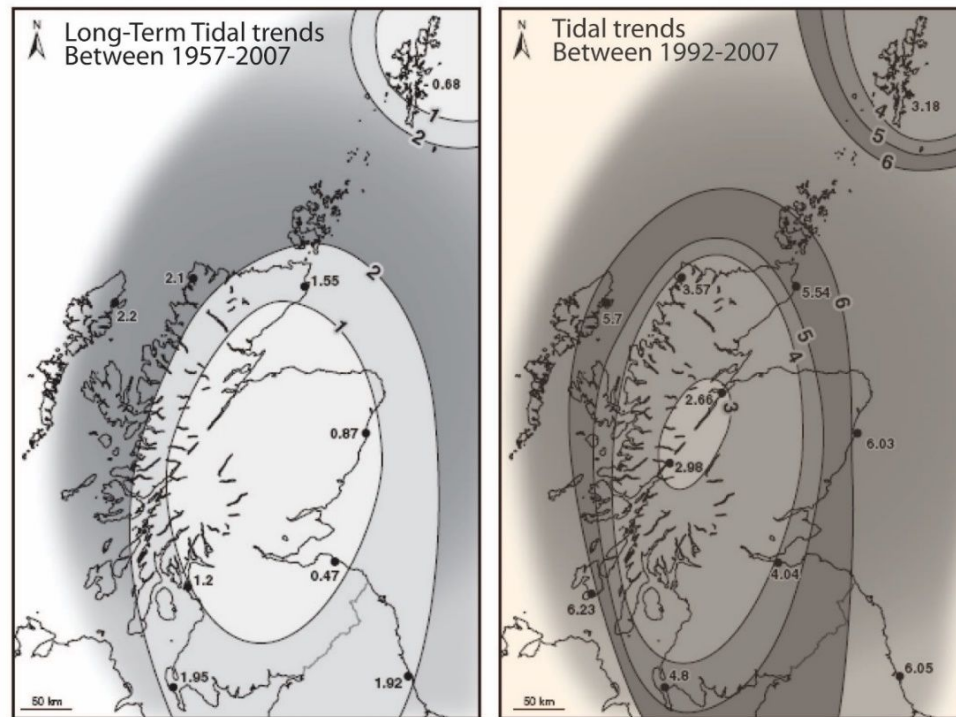
Because sea level is a combination between eustatic sea level and vertical land movement, where eustatic sea level is driven by thermal expansion, melting of glaciers and ice sheets and surface groundwater, and, land vertical movement is influenced by glacio- and hydro- isostatic loading, tectonic activity and sediment compaction (Dawson et al., 2001; Church et al., 2013), local sea level change will differ from global sea level average where local and regional processes driving height changes of the ocean surface and ocean floor will result in very distinct spatial patterns of sea level change.

In Scotland, vertical land movement is primarily driven by glacial isostatic recovery from the last deglaciation of the British Ice Sheet that occurred between 20 and 11 kyr BP (and to a lesser extent of the Scandinavian ice sheet) (Milne et al., 2006). Deglaciation led to the earth crust, deformed by ice mass load, to rebound and still in state of recovery over the Holocene uplifting rapidly where ice sheet was the thickest (with centre of the ice mass located at Rannoch Moor in the Highland) and subsiding where the ice was the thinnest (Stapleton and Pethick, 1996; Rennie and Hansom, 2011). Rapid rise in eustatic sea level following the final collapse of the Laurentide ice sheet in North America (Milne et al., 2006) led to have in Scotland a temporary reverse effect with sea level falling due to the isostatic uplift whilst sea level rose elsewhere. The consequence of this is that sea-level in northern UK and Scotland display a non-monotonic behaviour (Milne et al., 2006) and therefore difficult to model.

The recent higher rate of relative sea level (RSL) observed with satellite altimeter record (for the period 1993 – 2012), is also seen in the tide gauge data. Rennie and Hansom (2011) compared the rate of long-term relative land and sea level change derived from tide gauges in Scotland with the recent records (15 years). Their work shows that the RSL rates measured from tide gauges at Scottish ports range between 2.6 and 6.2 mm/year and now outpace glacio-isostatic uplift across Scotland and that all Scottish coastal landforms are now subject to rising sea levels (Figure 2-12).

Work in the northwest of Scotland by Barlow et al. (2013) present a 2000 year-long continuous saltmarsh-based reconstruction of relative sea-level (RSL) change based on sites characterised by slow RSL fall during the Late Holocene due to glacial isostatic adjustment rebound. Their observations show a general pattern of marsh progradation characterised by a long-term, gradual fall in RSL over the last 2000 years and that a switch in the rate of sea level data was dated to the AD 1940-1950s (not yet been associated to sea-level tendency recorded elsewhere in Scotland). They found no evidence for a significant acceleration in late 19<sup>th</sup> or early 20<sup>th</sup>C. sea level in the Scottish salt marshes studied (as suggested by the Aberdeen tide gauge). The results show that the rate of RSL rise from ~AD 200-1940 has not increased more than 0.4mm/yr. However, they

carefully state that a 20th century sea-level acceleration is not excluded, but it is not apparent in the western North Atlantic record (Barlow et al., 2013). In contrast, work by Teasdale et al. (2011) using geochemistry, radiometric dating, and diatom analysis on four coastal salt marshes in western Scotland has shown recent significant increases in the rate of sediment accretion (ranging from 5 to 10 mm yr<sup>-1</sup>) which are 2-3 times the average values for the last 20<sup>th</sup> C. Comparison between <sup>210</sup>Pb and <sup>137</sup>Cs suggests that this increase is due to sedimentation with Diatom analysis indicating recent sedimentation had a marine dominance. All sites presented evidence of active erosion accompanied by tidal scours; landward migration forced by tidal flooding occurred on one of the sites; and the furthest inland site (Loch Etive) has shown evidence of increased salinity of the near-shore ground water. These results suggest a very recent increase in the rate of regional relative sea-level rise is outpacing the estimated rates of glacio-isostatic adjustment (GIA) of the Scottish uplift dome.



From Rennie, A.F., Hansom, J.D. (2011)

**Figure 2-12: Scottish tide gauge trends plotted spatially to compare (a) longer-term average rates between 1957 and 2007 and (b) more recent rates between 1992 and 2007 (in Rennie and Hansom, 2011, p.199).**

Friess et al. (2011) summarise clearly the impact of SLR on salt marsh and mangroves. In a saltmarsh system where landward migration is limited, the long-term balance of the ecosystem is primarily governed by rates of Sea Level Rise (SLR) and positive vertical surface elevation change. The differences between these rates will determine the threshold between loss, stability or long-term expansion. They state that although SLR is a physical factor that occurs on regional-local level, the variables contributing to the intertidal surface elevation change are spatially

heterogeneous are affected by four main tectonic, geomorphological and biological processes (Friess et al., 2011, pp. 11-12):

- 1) Vertical movement changed by tectonic processes is due to a large-scale isostatic adjustment such as the overall UK coastline to the last glaciation or isolated tectonic events such as earthquakes over small spatial scale;
- 2) Vertical accretion is controlled by long-term sediment availability and accumulation determined by sediment supply and sediment trapping and consolidation by vegetation;
- 3) Although the review highlights a gap for saltmarsh study, but it demonstrates that Mangroves systems surface elevation change has different responses to SLR by belowground productivity from root biomass and organic production to adjust to the recent (100 years) sea level rise;
- 4) Surface elevation change involves negative processes in soil properties where autocompaction, dewatering, sediment settling, water table depth and organic matter oxidation can cause shallow subsidence.

Friess et al (2011) review shows how critical and important true surface elevation change data is required in order to assess salt marsh (and coastal wetlands) potential vulnerability or resilience to SLR. Furthermore, there is substantial spatial variation in secular sea level trends, and sediment consolidation effects and artificial modifications, such as embankment construction and dredging, have further complicated the apparent rate of relative sea-level rise such as recorded by tide-gauges (van der Wal and Pye, 2004). UKCP18 high emission scenario (Lowe et al., 2018) provides the anticipated mean sea level rise for a selection of Scottish location above 1980-2000 averages and referenced in Appendix 1 – Table A4.

My thesis aims to examine if natural and recreated salt marshes are potentially ecosystem in state of expansion and resilient or of degradation and vulnerable to SLR.

#### 2.4.1.2 Storminess

Leonardi et al. (2018) in her recent, comprehensive review of dynamics of coastal storms and salt marsh outlines the absolute certainties according to Pachauri and Meyer (2014) that the intensity of cyclone activity has increased in the North Atlantic since 1970 (99–100% probability) and that extreme sea levels such as the ones experienced during storm surges have increased since 1970 on a global average (66–100% probability). However, the evaluation and projections on long term changes are very complex. The take home message is that there will be an increase in peak wind intensities, and near storm precipitations in future cyclones, with an increased occurrence of

violent storms in spite of the likely decrease in the total number of storm (Solomon, S. et al., 2007). On a regional scale, model scenario between 1961-1990 & 2071-2100 shows a significant increase of storm surge extremes along most of the North Sea coast. Figure 2-13 outlines Leonardi et al. (2018) summary of the main geomorphic impacts of storms on saltmarsh ecosystems.

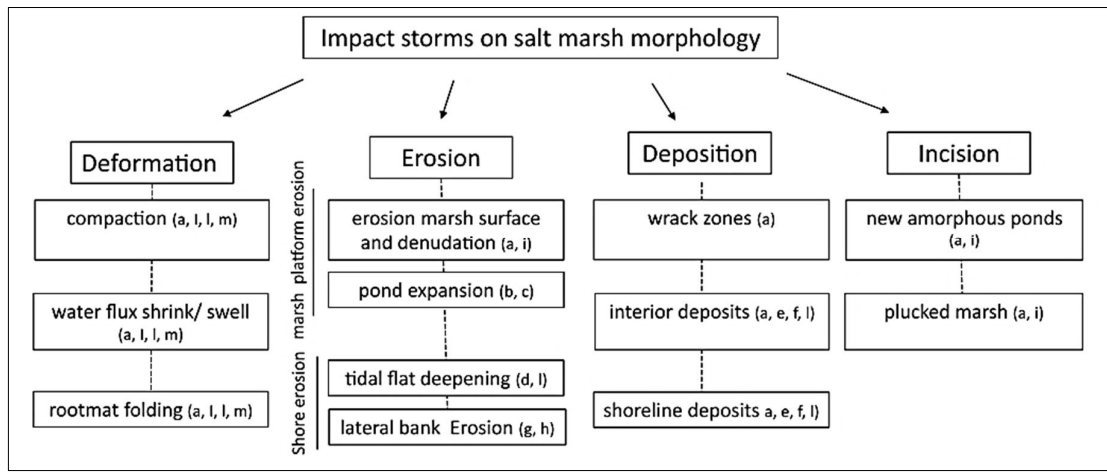


Figure 2-13: main geomorphic impacts of storminess on saltmarsh ecosystems (taken from Leonardi et al., 2018, p.98).

#### 2.4.1.3 Temperature change

The warming of the global climate system is unequivocal despite yearly and even decadal variations (Robins et al., 2016). A change in sea temperature may modify the geographical distribution of salt marshes, but is likely to modify saltmarsh plant species, distribution and productivity. Soil salinity may increase due evapotranspiration from temperature rising, but increase in rainfall may reduce considerably salinity level provoking a shift of saline to freshwater system (Chapman, 1977; Adam, 2002).

It is important to realise that many climate change scenarios and modelling predictions lack resolution and spatial cover and to highlight that long-term monitoring and increased research within coastal ecosystems is needed to support risk predicting and mitigatory strategies (Robins et al., 2016). Mudd and Kirwan developed in 2012 a numerical model to understand direct impact of warming on saltmarsh soil carbon accumulation rates. The model based on *Spartina alterniflora* (dominant in North American Marshes) showed that plant growth can be stimulated by inundation up to a threshold of water depth and that rate of productivity and decay increased by temperature rise. They concluded to say that a rise in temperature and sea level may increase carbon burial rates in the first half of the twenty-first century, but to slightly decrease carbon burial rates in the second half of the century. The observed switch in feedback direction appear to even occur when the marshes survived SLR and productivity rates increased in response to climate change.



However, a threshold of 1 m in SLR by 2100 would lead in all models submergence and loss of productivity (Kirwan and Mudd, 2012).

#### 2.4.2 Salt marsh in a human-driven environment

There is little doubt that anthropogenically-induced climate change such as eutrophication, biological invasions, increasing air and sea surface temperatures, increasing CO<sub>2</sub> concentrations, altered hydrologic regimes, pollution and sea level rise and its associated impacts to living species are regarded as the major threat facing saltmarsh and coastal wetlands (Reinhardt et al., 2010). Aside from anthropogenically-induced climate change which is not the focus of this research and not described in further details, reclamation of coastal land for agricultural or industrial use alone, here termed ‘land claim’, has accounted for an estimated 25% loss of intertidal land in estuaries worldwide (French, 1997; Temmerman, Govers, Meire, et al., 2003). Coastal margin habitats have been subject to considerable land use change over the last 100 years (French, 1997; Delbaere, 1998), with land claim through draining occurring on an industrial scale since the 1700s (Hansom et al., 2001) until 1979 (Doody, 2013) in the UK. The threat of SLR, flooding and coastal erosion has led to a construction of fixed defence structures along a significant proportion of the UK coastline (Figure 2-14) (Mieszkowska et al., 2013).

Region	Coast length (km)	Coast length that is eroding (km)	Coast length with defence works and artificial beaches (km)
Scotland	11,154	1,298 (11.6%)	733 (6.6%)
Wales	1,498	346 (23.1%)	415 (27.7%)
England	4,273	1,275 (29.8%)	1,947 (45.6%)
Northern Ireland	456	89 (19.5%)	90 (19.7%)
Ireland	4,577	912 (19.0%)	475 (10.0%)

**Figure 2-14: Source Mieszkowska et al. (2013, p.187) Overview of exposure of UK and Ireland coastal regions to erosion and coastal protection from 2004 EuroSION.**

Seawalls and other protective structures have prevented or limited the natural landward migration (‘roll-over’) of salt marshes to maintain their position within the tidal frame in response to SLR leading to system to drown. The physical constraint is termed coastal squeeze (see Figure 2-15). Moreover, defence structures by deflecting the wave energy can lead to erosion in particular noticeable on the marsh edge (Morris et al., 2002; Doody, 2013).

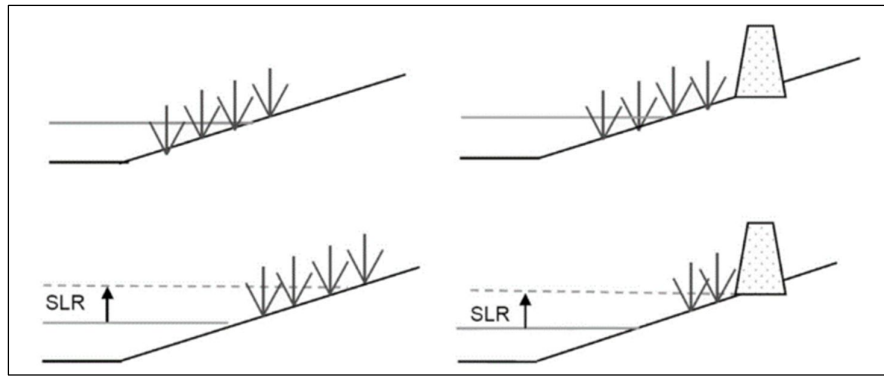


Figure 2-15: Coastal squeeze showing how a marsh position in the tidal frame (top left) moves landward in response to SLR (bottom left). This scenario differs with the constraints of physical barriers such as seawalls (top right) where the marsh edge erodes (bottom right) (Taken from Foster et al., 2013, p.101).

## 2.5 Saltmarsh resilience and management

As long as relative sea levels rise, ‘coastal squeeze’ will continue to put pressure on the intertidal and terrestrial coastal land and is considering as one of the main threats to already declining UK saltmarsh habitats, which in turn may reduce their species diversity and food webs.

New approaches on non-intrusive and sustainable forms of coastal protection have been increasingly developed in recent years. Soft engineering approaches are intended to move away from hard defence structures such as sea walls, embankments or groynes to prevent coastal erosion and defend land against flooding, and use softer techniques such as replenishment, or nourishment of eroding coastlines (Hanson, 2002; Fletemeyer et al., 2018) (e.g. in Scotland: 2006 – Aberdeen beach, 2016 – Arran beach) or allowing hard structures to be removed (deliberately or naturally) to work with natural processes such as sea and tides. Breach sea walls or embankments allows to recover, re-attain or restore coastal ecosystems such as saltmarsh or mudflats acting as natural buffers against storms, stabilising sediment, dissipating waves (2.3.3.2). Since the 1990s, in the United Kingdom, managed realignment (MR) schemes have been increasingly used to restore or create new saltmarsh sites by breaching existing sea defences to allow tidal inundation landwards (Adam, 2002; Garbutt et al., 2006; Leonardi et al., 2018). Since 1998, UK government (via DEFRA sixth report of Committee of Agriculture) has clearly stated that managed realignments must be given greater priority than unsustainable (in the long-term) flood or coastal defences (P.W. French, 2006). Similarly, Scottish Government in The Flood Risk Management (Scotland) Act (2011) favours MR and habitat creation as an alternative form of flood defence as it also provides an opportunity to compensate for loss habitat and supporting ecosystem services (2.3.3.1). Although, sciences and management (governmental policies here) agree on the principles of ecosystems restoration, Elliott et al. (2007) highlighted the need of an expanded knowledge base and good case studies and even on adaptive management schemes (also called “let’s try it and see



what happens”) which has to involve knowledge of physical, biological social and cultural sciences.

Leonardi et al. (2018) recognise that there are still large challenges in the identification of best coastal protection measures to adopt. The difficulty in choosing between hard, natural or hybrid defences (Figure 2-16) may be partly due to the benefit allocation at the start of the design: hard structures are efficiently engineered but cause habitat losses resulting in shorter lifespan; natural infrastructures may have many co-benefits but are slow to respond to immediate risk; and, hybrid measure have potentially best characteristics of both hard and natural but may never provide the same benefit than natural solutions. Back in 2002, Pethick raised similar concerns that wetlands restoration in the United Kingdom (as opposed to USA) draws less attention to ‘enhanced habitat than with sustainable defences against flooding and erosion’ (Pethick, 2002), as demonstrated by the restoration c. 200 ha of salt marsh as managed retreat in England with the primary goal to create a more natural coastal flood buffer. More emphasis has now been placed on the habitat provision and economic and societal value saltmarsh ecosystem provide and translated by adoption of EU directives such as driven by EU legislative requirements such the 2009 Habitats and Birds Directives and Act from the 2001 Committee on Mitigating Wetland Losses. Recent projects like 2018 Working with Natural Processes (Burgess-Gamble et al., 2018) have evolved to redefine strategies to reduce flood and coastal erosion risk by protecting, restoring and emulating ‘the natural functions of catchments, floodplains, rivers and the coast’ in putting the accent on the multiple benefits of coast and estuary management (as well as river, floodplain, woodland and run-off management in urban and rural areas) such as climate regulation, habitat, health, socio-economic, cultural services (Burgess-Gamble, 2017). More so, it has been highlighted that the public (and landowners) needed to be informed and convinced on the risks that coastal erosion and flooding and on the benefits and values provided by the habitats and ecosystems to be willing to pay towards MR and restoration scheme (P.W. French, 2006; Elliott et al., 2007; Simpson and Hanley, 2016).

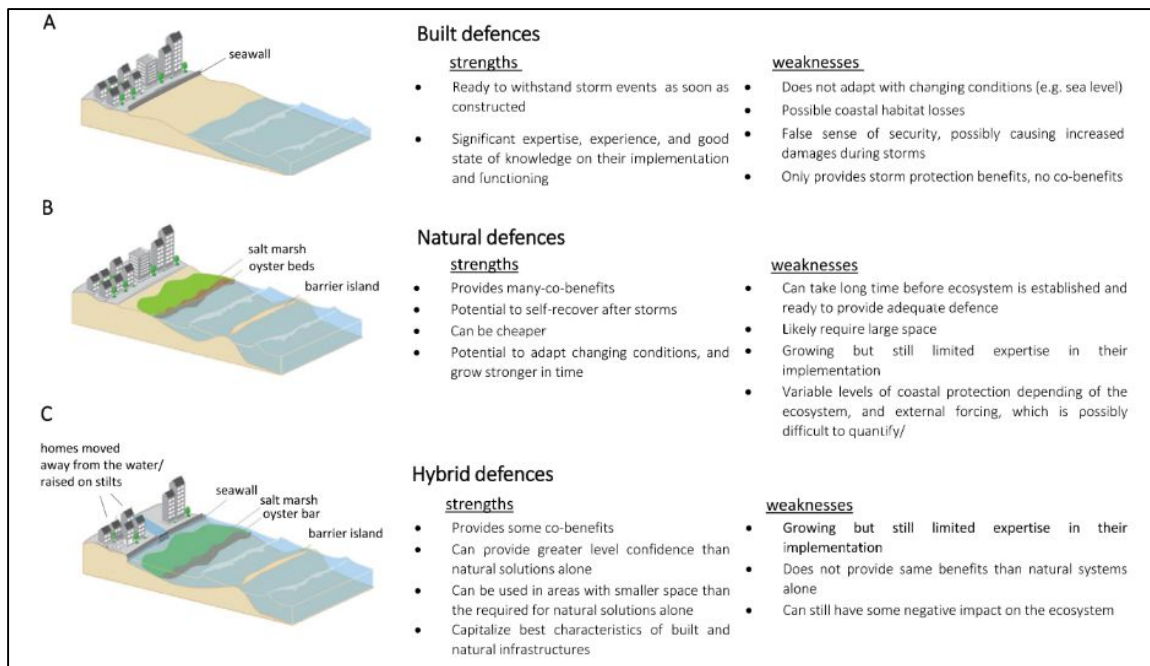


**Figure 2-16: Examples of strength and weakness of possible built defences, natural defences and hybrid defences (taken from Leonardi et al. 2018, p. 103).**

However, there is also a concern as to whether restoration schemes fulfil their intended purpose (Spencer and Harvey, 2012); and whether the benefit and disadvantage balance fully acknowledges the complex and dynamic interplay between geomorphology, biology and biochemistry that occurs on saltmarsh systems.

## 2.6 Summary: still gaps to fill?

Figure 2-1 highlighted the motivation's theme for the overall thesis aim. This literature review has established that physical and biological processes plays a major role on saltmarsh formation and development and the saltmarsh stability against environmental and anthropogenic disturbances is highly dependent to its vertical growth, to the sediment supply and tidal range (Pethick, 1993; Allen, 2000; Morris et al., 2002; Fagherazzi et al., 2004; P.W. French, 2006; Corenblit et al., 2011). However, Townend et al. (2011) reminded us that still some limitations to predict and model the development of salt marsh due to lack of measured data on soil organic matter and belowground productivity (Fagherazzi et al., 2004), on detailed relationships in different geographic locations (Morris et al., 2002) between biomass and marsh depth/elevation and hydrodynamics (inundation) and morphodynamics (distance to creeks) (Mudd et al., 2004).

By examining geomorphological and biological patterns, processes and mechanisms taking place aboveground and belowground on short (annual) to long (centennial) time scale between natural and managed salt marshes, my research aims to increase our understanding on the response of

Scottish saltmarsh landforms to environmental forcing (sea level rise), anthropogenic disturbance (land management); of the viability to recreate a  
“self-supporting and self-maintaining ecosystem which ultimately does not require further management” (Elliott et al., 2007)  
whilst contributing to the wider bio-geomorphology literature (Viles, 1988; Naylor et al., 2002; Reinhardt et al., 2010; Spencer and Harvey, 2012) .





# Chapter 3

*Nigg July 2016*

# Chapter 3. Research Framework and Methods

### 3.1 Research framework and design

Chapter 2 highlighted that, at the turn of the millennium, a general consensus was building across both science and society to recognise the importance and value of intertidal mudflat and salt marshes and acknowledge the adverse impacts of their loss (Barbier et al., 2011; Luisetti et al., 2013; Beaumont et al., 2014). Research and policies have highlighted benefits and shown saltmarsh resilience, but limitations and uncertainties remain in quantifying saltmarsh vulnerabilities and the success of rehabilitation and attempts at realignment (Ledoux et al., 2004; Wolters et al., 2005; Boorman and Hazelden, 2017).

‘Science-based research must continue to identify and to better understand the complex links within and between inter-tidal mudflats and salt marshes, their rate of change, the causes and consequences of their loss, and the methods for their reparation’ (Foster et al., 2014).

Alternative engineering measures that depart from the use of hard structures for coastal protection are increasingly used, such as managed realignment (MR) (see 2.4.2). This review also highlighted that in order to assess the pros and cons of such MR schemes, a better understanding of biotic and abiotic relationships is necessary, particularly in the context of climate change adaptation and mitigation (Viles, 1988; Naylor et al., 2002). Chapter 2 – 2.3 established that the interdependency of physical and biological processes has a major role on saltmarsh formation and development (Pethick, 1993; Allen, 2000; Fagherazzi et al., 2004; Corenblit et al., 2011) and that saltmarsh stability depends on vertical growth, sediment supply and tidal range (Morris et al., 2002; P.W. French, 2006; Balke et al., 2014). A set of young salt marshes and mature salt marsh set within the same saltmarsh system would provide an ideal comparative case study to establish saltmarsh formation and development and understand the capacity of salt marsh to recover from disturbance caused by managed realignment.

Figure 3-1 below summarises the knowledge gaps identified in Chapter 2 that this research aims to address which processes, mechanisms and patterns 1) that promote the formation and development of salt marsh; 2) that allow salt marsh to recover from environmental and anthropogenic disturbances; and, 3) that promote some of the regulating and supporting services provided by salt marsh. My research sets out to test the assumption that vegetation and sedimentation dynamics are the principal processes enabling saltmarsh formation and development. However, choosing a framework to address both biological and physical processes is difficult because the interactions occur at different time and spatial scales as presented in (**GAP 1** - section 2.3 & 2.5). It is also labour-intensive with sampling methods that are not necessarily complementary and so studies rarely investigate saltmarsh dynamics simultaneously. Webb et al., 2013 have also highlighted this data gap and proposed ways to solve this regionally by a coordinated expansion of monitoring efforts (e.g. regional networks). Often such studies span long periods, such as LOIS (Land Ocean Interaction Study - over 6-years) which aimed to monitor



water and sediment in the Humber estuary (Black and Paterson, 1996). Spencer et al., 2012 at Freiston shore, England, used an integrated remote sensing approach to quantify the biogeomorphological relationship between surface elevation and saltmarsh presence in response to a sudden change in surface elevation due to saltmarsh restoration. Spencer and Harvey, 2012 used Freiston shore and another MR site at Tollesbury Fleet, to quantify the temporal characteristics of processes contributing to the short-term and overall elevation change on salt marshes (~5.5yrs) related to sediment accretion. Work in Germany on the north Frisian marshlands (Schindler et al., 2014) compared short-term (multi-annual) deposition to long-term (centennial) using  $^{137}\text{Cs}$  and  $^{210}\text{Pb}$  core dating on the same spatial scale. The research reported here in chapters 4 and 5 aims to quantify the deposition and vegetation distribution on a short-time (from annual to multi-annual) scale (**GAP 2**) and investigate the resulting patterns on a longer-time (from multi-annual to centennial) scale (**GAP 3**). Due to recent successes in the application of Optically Stimulated Luminescence (OSL) to establish chronologies in intertidal deposits and reconstruct paleo-environmental landscape evolution in relation to sea-level changes (Mauz et al., 2010; Sander et al., 2015), Luminescence was identified here as a potential method (**GAP 4**) to act as a tracer of saltmarsh sediment dynamics that may also provide age profiling of saltmarsh sediment.

To address the gaps highlighted in Figure 3-1 and address the overarching aim of this thesis, which is to improve the understanding of the processes, mechanisms and patterns that promote the formation and development of salt marsh, that enable salt marsh to recover from environmental and anthropogenic disturbances and that promote some of the regulating and supporting services provided by salt marsh; this study focuses on a series of specific objectives to establish spatial and temporal links between sediment availability, vegetation presence and saltmarsh stability.

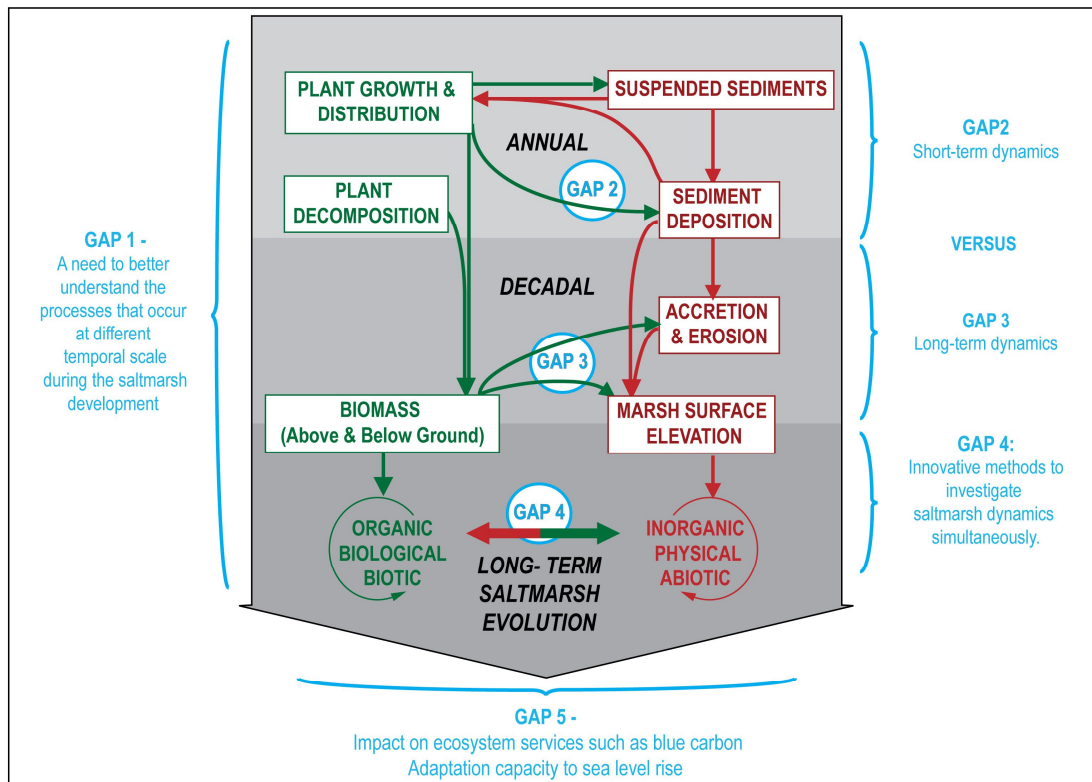


Figure 3-1: Knowledge gaps addressed in this research.

These objectives are:

- i. to identify short-term (annual) aboveground processes at natural and managed saltmarsh sites by quantifying an annual cycle of:
  - a) sediment deposition rates and accretion rates
  - b) vegetation distribution
  - c) water levels and physical controls on salt marsh development;
- ii. quantify long-term (multi-annual to centennial) aboveground geomorphological changes in natural and managed salt marsh sites by:
  - a) quantifying sedimentation (accretion and erosion) and surface elevation change
  - b) qualifying spatial variation (lateral and/or vertical changes)
  - c) qualifying the temporal fluctuations;
- iii. to examine whether long-term (multi-annual) patterns are reflected in the sediment cores:
  - a) using established techniques (such as water content, bulk density, organic and inorganic content and physical characteristics of the sediment)
  - b) using luminescence techniques as a potential tracer of past sediment dynamics and processes across the three saltmarsh sites;
- iv. to assess some of the supporting and regulating benefits that natural and restored salt marsh provide.



To implement the study objectives, the research design falls into four areas of study presented below and conceptualised in Figure 3-1:

The first area (methods in section 3.4.1 and results in Chapter 4) focuses on the short-term dynamics of both newly restored and managed saltmarsh sites employing a set of short-term (annual) measurements of sediment deposition together with biomass of different vegetation species across the saltmarsh sites. The results are aimed to quantify the short-term spatial variation of sediment and vegetation on natural and restored (i.e. realigned for Nigg Bay) saltmarsh sites.

The second area (methods in section 3.4.2) concentrates on the long-term aboveground saltmarsh dynamics between vegetation and sedimentation. The results of saltmarsh vegetation distribution and sedimentation pattern and rates (results in Chapter 5) aim to establish the spatial variation of sedimentation at different temporal scales. This uses a combination of topographical surveys to assess marsh stability over time: >100 years accretion and erosion using historical mapping; >100 years movement of MHWS using a combination of historical mapping and terrestrial laser scanning; <10 years surface elevation changes using airborne and terrestrial laser scanning; and <5 years sedimentation rates using a network of buried sedimentation plates. This network was also used to measure the vegetation distribution over same timescale of <5 years to allow quantification of the aboveground biomass per species assemblage for all sites. These results combine with the aboveground dataset to evaluate saltmarsh capacity to sea-level rise (chapter 8).

The third area (methods in section 3.4.3) investigates belowground saltmarsh development over the long-term (results in Chapter 6) using a series of shallow ( $0.5\pm 0.02$  m) and narrow (<5 cm) cores (n=21) across the saltmarshes and of longer ( $0.7\pm 0.04$ ) and wider (<8 cm) cores (n=8) along two transects crossing the sites. The aim is to quantify organic and inorganic belowground matter and evaluate change through time to compare with the observed aboveground results. These results help evaluate the potential carbon sequestration of the different saltmarsh systems (Chapter 7).

The fourth (briefly reviewed in 3.4.4 with results in Chapter 7) strand aims to evaluate if Optically Stimulated Luminescence (OSL) techniques can be used to measure young (<100 years) sediments and investigate the potential use of OSL as a tracer of modern dynamics on natural and restored salt marshes. This involved developing new protocols, methodology and calibration and assessing the novel application of OSL to the larger cores collected over two transects across the studied set of salt marshes.

### **3.2 Choice of study location**

A successful ecosystem restoration aims to establish communities that are similar in species composition, population density and size and biomass structure to that previously or present at a comparable (unimpacted, unaffected) site (Elliott et al., 2007). However, few restoration projects (10% worldwide) are monitored after they have been completed and there is still a lack of robust data to determine their success (Reinhardt et al., 2010). Ongoing restored salt marshes can also be used as large-scale field experiments where fundamental geomorphological and biological processes responding to environmental and human forcing, as well as service provision, can be evaluated (Allen, 2000; Reinhardt et al., 2010). Adjacent restored and natural salt marshes should offer a good platform to examine such effects. The first salt marsh to be restored in Scotland took place only 15 years ago (in 2003) at Nigg Bay in the Cromarty Firth. Nigg Bay is designated as a Ramsar site, Special Protection Area (SPA- European Union Directive on the Conservation of Wild Birds) and Sites of Special Scientific Interest (SSSI - statutory designation by Scottish Natural Heritage under Nature Conservation (Scotland) Act 2004 for areas of special interest for their flora or fauna, geology or geomorphology). 25.9 ha of former agricultural land at Nigg Bay was purchased by RSPB in 2001 and an enclosing sea wall was breached in 2003 allowing the site to revert to salt marsh. It was the first Managed Realignment (named thereafter MR) site in Scotland. The recovery monitoring of saltmarsh restoration is mostly focused on ecological goals (Reinhardt et al., 2010) and the Nigg MR site is no exception with vegetation, birds and benthic organisms assessed and no attempt to monitor the geomorphological features of the newly reformed salt marsh. For this reason, the MR site was selected for this research along with a) 4.1 ha of fronting marsh (named thereafter FM) that had naturally developed in front (seawards) of an adjacent 1950s sea-wall and b) 9.3 ha of adjoining mature natural salt marsh (named thereafter ANK), situated to the east of MR at the Ankerville river mouth (Figure 3-4). Both sites are fronted by approximately 8 km of the intertidal sand of Nigg Bay.

The Cromarty Firth (Figure 3-3) is an inlet of the Moray Firth whose 650km coastline extends from Duncansby Head to and Kinnaird Head comprising 43% cliffs, 9% low sandy coast, 11% of low rocky shore platform and 37% of intertidal flats (Stapleton and Pethick, 1996). The Cromarty Firth inlet accepts the waters and sediment of the larger Conon, Orrin and Black Water rivers whilst the much smaller Balnagowan and Ankerville (also marked as a canal) rivers flow into the northern shore of Nigg Bay close to the studied marshes (Figure 3-2).

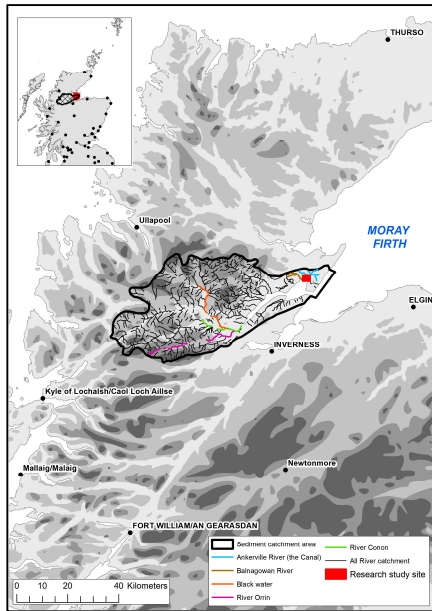


Figure 3-2 (left) Cromarty Firth river sediment catchment area (adapted from <https://www.sepa.org.uk/data-visualisation/water-environment-hub/?riverbasindistrict=Scotland>).

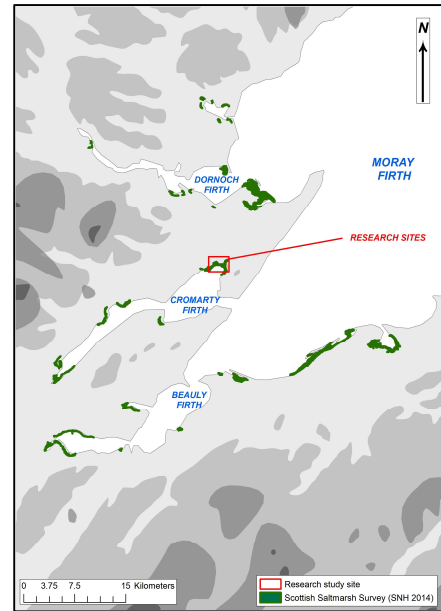


Figure 3-3 (right) Moray Firth saltmarsh extent and study area (red box).



Figure 3-4: MR-Managed Realignment-, FM-Fronting Marsh- and ANK-Ankerville (river) salt marsh-: the three sites selected for this research.

### 3.2.1 Tides, waves and winds

The Cromarty Firth is a sheltered tidal basin that is affected by ocean waves only to a limited extent. Walton (1967) notes that the deep and long channel at the firth entrance has allowed waves to create cliffs at the North and South Sutors. Nevertheless, the majority of waves are generated

by SW-NE wind (Stapleton and Pethick, 1996) and have very limited effect within Nigg Bay except when approaching from the south (3 kms) and south west (8kms) fetch lengths. In spite of the existence of a deep-water channel in the centre of the firth, the 4 kms of intertidal mud and sand flats at Nigg serve to attenuate wave impact at the saltmarsh edge even at high tide and with an onshore wind.

The Chart Datum for the Cromarty Firth is 2.1 m above Ordnance datum (see details in Table 3-1).

**Table 3-1: Tide values for Invergordon and Cromarty are in meter above Newlyn Ordnance Datum (Chart Datum is below 2.1m Newlyn Ordnance Datum. See additional notes & definitions in Appendix B). Data supplied by UK Hydrographic Office ©Crown Copyright\*. Tidal ranges for both locations are 3.6 m during spring tide and 1.7 m during neap tides.**

	Cromarty	Invergordon
LAT (Lowest astronomical tide)	2.9	2.9
MHWS (Mean High Water Springs)	2.2	2.2
MHWN (Mean High Water Neaps)	1.2	1.2
MSL (Mean tide levels)	0.36	0.38
MLWN (Mean Low Water Neaps)	-0.5	-0.5
MLWS (Mean Low Water Springs)	-1.4	-1.4
HAT (Highest astronomical tide)	-2.1	-2.1

*\*All rights reserved. Copyright material, its derivatives and outputs are prohibited from sale and distribution prior written permission of the UK Hydrographic Office.*

The Cromarty Firth is a mesotidal estuary with tide levels ranging from 3.5 m at Conon bridge to 3.7 m at Invergordon 8 kms to the west of Nigg. This limited range is also reflected in the inequality in semi-diurnal tides (0.18 m differences on the High-Water Spring Tides at Invergordon) and an ebb-tide dominance through the narrow outer channel at Cromarty. Tidal velocities vary north/south throughout the 18.5 km-long tidal basin with an ebb-current dominance on the south whilst the northern section of the channel is dominated by the flood current (Figure 3-5). Stapleton and Pethick (1996) note that as the result of Coriolis, the incoming tidal flows are forced to the right (north bank) creating an anticlockwise circulation movement. These forcings also affect the salinity gradient with freshwaters on the south bank and more saline tidal water to the north. Yet, this anticlockwise pattern is not evident in Nigg Bay as shown in Figure 3-5 and Figure 3-6. The flood fills the bay in a clockwise direction via the main drainage channels of Delney Dock, Big Audle and the Pot. The ebb currents use these channels to exit the bay. The flood has been recorded to last between 30 to 60 minutes less than at Invergordon and ebb commences 30 to 60 minutes earlier than at Invergordon (Barr et al., 1974). Influenced by the Firth currents and waves and constrained to its southern edge by the deep central fjord, tidal system of Nigg Bay is morphologically independent from the deep waters circulation of the Firth, making Nigg Bay an uncommon landform (Stapleton and Pethick, 1996).

### 3.2.2 Sediments sources, types and characteristics

The Cromarty Firth is a complex glacial landform where minor morphological change has occurred since the Holocene and is described as a fossil glacial landform consisting of a deep central glacial trough bounded to the North by Nigg Bay and South by Udale Bay (Stapleton and Pethick, 1996). A low level of suspended and bedload sediments has limited the sedimentation rates and restricted the development of Holocene landforms within the intertidal area of Nigg Bay mudflats and salt marshes. The physical separation from the deep glacial trough makes the Nigg salt marshes very sensitive to changes in sea level or sediment supply (Stapleton and Pethick, 1996).

However, any sediments preserved in the Bay may also provide a record of past sea level changes that should enable an assessment of supply change over time in comparison to the present sedimentological conditions. Using the Nigg Bay saltmarsh sediment may help address this thesis overarching aim to address which processes, mechanisms and patterns 1) that promote the formation and development of salt marshes, 2) that allow salt marshes to recover from environmental and anthropogenic disturbances, and, 3) that promote some of the regulating and supporting services provided by salt marshes.

Boreholes taken by Peacock et al. (1976 and 1980) near the A9 Bridge (between Arduillie and Findon) show rockhead to lie at 120m below sea level SL and is overlain by c.40m of cold marine clays deposited during the last glaciation, themselves then buried by c.60m of Flandrian marine silt and silty sands. Figure 3-5 shows large expanses of sand and mudflats at Nigg, Udale Bays and near Dingwall. Similar stratigraphy in Nigg Bay was reported by Babbie group (1969) where bedrock was exposed at 2.7m deep below the surface on eastern bank of the bay and at 4.2 m deep on the western bank, dipping towards the centre of the bay to >9 m below the surface. This is overlain by a succession of sands, gravel and silts which lie 2.4 to 4m deep within 1m of the surface. However, very little work has been carried to determine how sediment is transported in and out of the firth. Stapleton and Pethick (1996) suggest that the presence of beaches at Nigg and Cromarty indicates sediment movement and that lag deposits of gravel north of Cromarty imply erosion and transport of finer sediment deposits under the action of waves and currents into the firth.



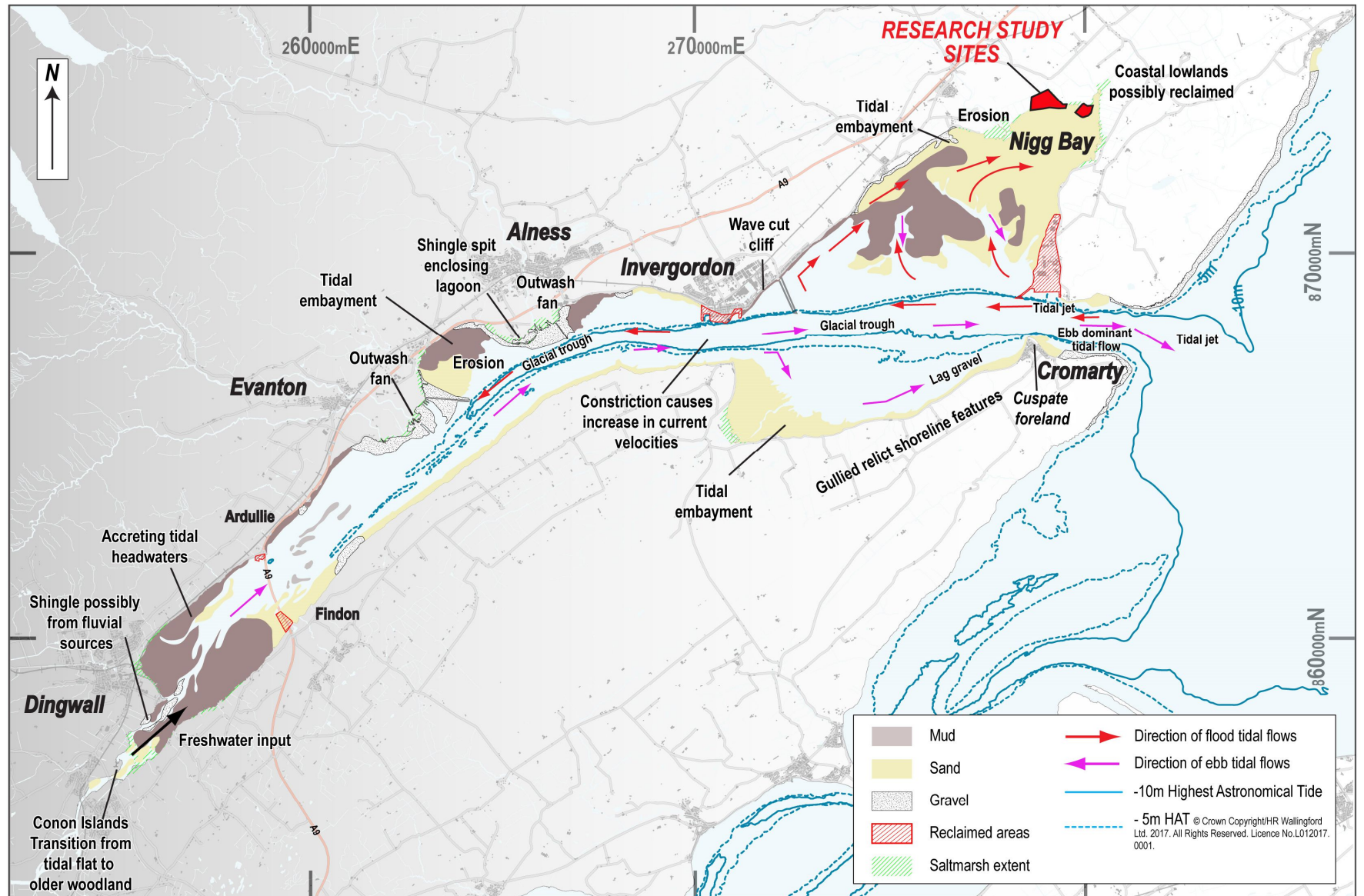
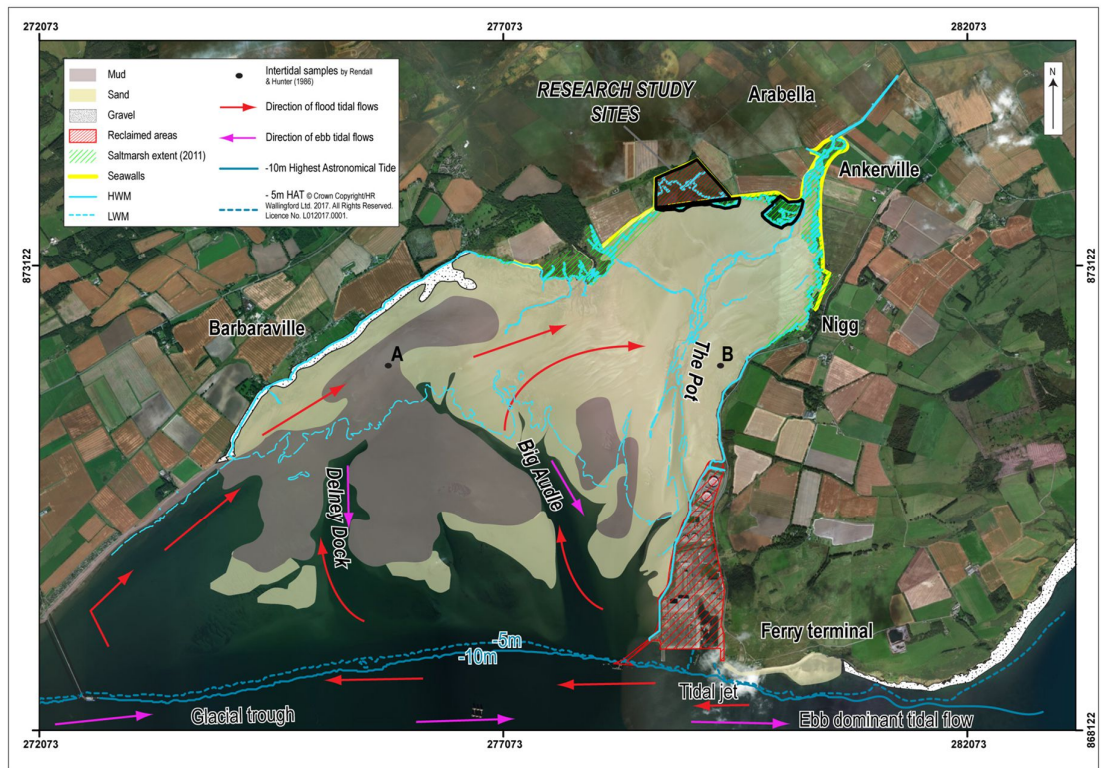


Figure 3-5: Sediment type and tidal dynamics in Cromarty Firth. This map has been redrawn from Stapleton and Pethick (1996) using 2014 OS Mastermap and 2016 HydroSpatial One Bathymetric data.

The summarised sediment characteristics and distribution for Nigg Bay referred to in several technical and governmental reports comes from two articles published in 1986 *the Proceedings of the Royal Society of Edinburgh, Section B: Biological Sciences* on the intertidal Microfauna (Raffaelli and Boyle, 1986) and the littoral Fauna of the Firth (Rendall and Hunter, 1986).



**Figure 3-6: Sediment type and Tidal dynamics in Nigg Bay.** The research sites extent is shown in black. Sources: Stapleton and Pethick (1996), 2014 OS Mastermap and 2016 HydroSpatial One Bathymetric data.

The eastern part of Nigg Bay contains mainly of fine sand (180-250 $\mu$ m) with coarser material (>500 $\mu$ m) and <5% of silts with some sandstone bedrock on the surface. The shore is interposed of gravel beach, rock outcrop and low vegetated sandy areas. The western part of the Bay comprises between 5-20% of silts with >20% of silts on the upper parts. Sandstone bedrock, shingle and gravelly sands are predominantly present at the river mouths with shingle beach and an outcrop of Old Red Sandstone on the foreshore (Raffaelli & Boyle, 1986). These sediment characteristics are reflected in the particle size distribution (Table 3-2) of two intertidal sands samples excavated east and west of the Bay (marked A & B in Figure 3-6) where low silt and clay amounts occur to the east and north.

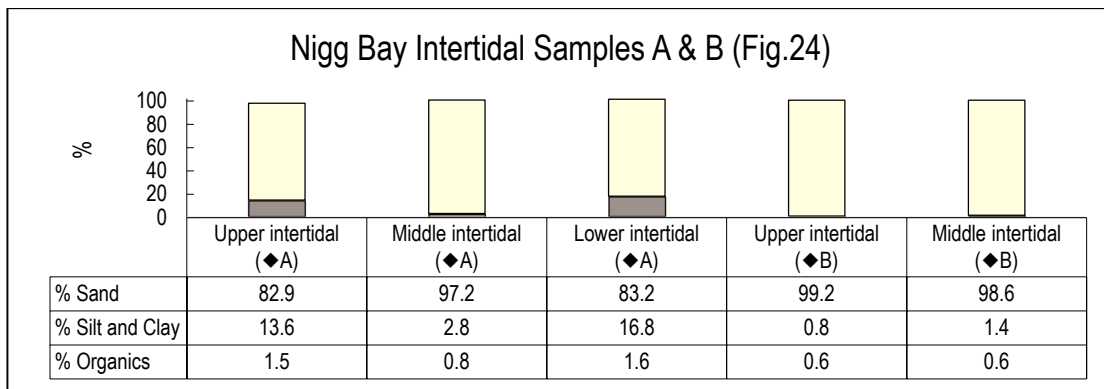


**Table 3-2: Intertidal sediment characteristics and distribution from Rendall and Hunter (1986) fauna study (see sample location on Figure 3-6).**

Nigg Bay is the largest stretch of intertidal flats in the Firth with a drying area of 21 km<sup>2</sup> and backed by 135ha of salt marsh that accounts for ca.52% of the Firth salt marshes. Unfortunately, large areas have been reclaimed for agricultural and industrial purposes in the past, resulting in fringing salt marsh on the northernmost shores that obstruct the important transition from tidal to freshwater marsh landforms. Sea walls and a major drainage scheme during the 1950s resulted in partial fragmentation and erosion of the saltmarsh seaward edge and an advancement of the salt marsh at the mouth of the Arabella and Ankerville river/canal exits (Stapleton and Pethick, 1996). The largest areas of sandflats and salt marshes were reclaimed on the east bank for the construction of a fabrication yard in 1970 (48ha) and an oil terminal (45ha) in 1979 (red hatch in

Figure 3-5 and Figure 3-6). This industrial reclamation may have also resulted in diverting the course of The Pot channel between the 1970s and 1990s as shown on OS maps. In 1978, Kesel and Smith estimated that the surface edge of salt marshes ‘micro-falaises’ at Ankerville can erode up to several centimetres per year, whilst Crowther assessed that Nigg Bay saltmarsh erosion rate between 1947 and 1997 was 0.068 ha yr<sup>-1</sup> (Kesel and Smith, 1978; Crowther, 2007).

In 2001, the RSPB purchased 26ha of reclaimed salt marsh in Nigg Bay that had been used for grazing since the 1950s, with an aim to recreate lost intertidal habitat for foraging, roosting and breeding of waterbirds. In February 2003, the RSPB reinforced an existing secondary sea dyke, blocked two culverts and breached of two 20m wide sections of the southern seawall (that had been eroding) allowing the 26ha to be open to tidal influx (Figure 3-7). Chapter 5 – section 2 explores historical cartography to quantify the impact that human intervention had on saltmarsh landscape of the Bay.





Figure 3-7: Nigg Bay post-realignment showing secondary defences (grey), blocked culverts (grey) constructed in advances of the two breaches (east and west in grey) through primary sea embankment (1950s in yellow) with the location of three research study sites.

### 3.3 Sampling strategy

Section 3.1 presented the rationale for the research framework, section 3.2 discussed the selection of study sites, and this section explains the rationale for the sampling strategy..

The response of saltmarsh systems to environmental and anthropogenic disturbances is expected to be reflected in sediment availability, its deposition patterns on the marsh surface and how it has accumulated through time (Pethick, 1993; Allen, 2000; Morris et al., 2002; Fagherazzi et al., 2004; French, 2006; Corenblit et al., 2011 in Chapter 2 2.3.1) and the presence of vegetation enhances the rates of short-term deposition in reducing flow velocities over the marsh surfaces (Pethick, 1984; Eisma and Dijkema, 1997 in Chapter 2 2.3.2). As such, measuring sedimentation in salt marshes can include:

- sediments dynamics (erosion - transport – deposition) and sediment budgets (over tidal cycles or over marsh surfaces) (Reed, 1989; Allen and Duffy, 1998; Temmerman, Govers, Wartel, et al., 2003);
- measuring sediment accumulation and rate of vertical growth (Cahoon et al., 2000; French and Burningham, 2003);
- changes in areal extent by dating sediment ( $^{137}\text{Cs}$ ,  $^{210}\text{Pb}$  - (Kearney et al., 1994; Harvey et al., 2007; De Groot et al., 2011; Schindler, Karius, Arns, et al., 2014; Schuerch et al., 2018))

or measuring rate growth (Optically Stimulated Luminescence - OSL (Madsen et al., 2005; Madsen and Murray, 2009)) ;

- developing simulation models to explore one (or more) aspects of the controls on saltmarsh evolution (French and Spencer, 1993; Davidson-Arnott, 2009; Callaway et al., 2012; Schile et al., 2014; Bouma et al., 2016; Morris et al., 2016).

Similarly, measuring aboveground biomass in salt marshes can include:

- at the macro scale: by qualitative survey to establish distribution, species percentage cover, height and density using quadrats or point survey transects (Leendertse et al., 1997; Bouchard and Lefeuvre, 2000; Langlois et al., 2003; Stagg and Mendelssohn, 2011) or using of digital photography to provide percentage of vegetation density and cover (Möller, 2006; Roner et al., 2016). These studies often lead to vegetation classifications at national or regional level estimating vegetation species assemblage such as National Vegetation Classification (NVC) in the UK.
- at the micro scale: using aerial photography and remote sensing (close-range using hyperspectral spectroradiometers; airborne multispectral scanners; or spaceborne satellite systems) to classify, delineate and digitise key vegetation boundaries (Van der Wal et al., 2008; Friess et al., 2012; Sghair and Goma, 2013; Balke et al., 2016).
- Paleo-environmental methods allow links historical vegetation and sedimentation rates over timescales from decades up to millennia (Kearney et al., 1994; Allen and Dark, 2007; Wright et al., 2017) and similarly  $^{14}\text{C}$  can date organic material in peaty saltmarsh environments (>300 years) and can be cross-calibrated with other dating methods (Marshall, 2015).

### **3.3.1 Measuring saltmarsh sedimentation and vegetation through time**

The choice of methods and sampling used in this study had to consider the timeframe limitations of a three-year PhD research project, requirements of the site owners (RSPB) as well as the logistics of sites distant from Glasgow. It was important to combine methods that could measure both short-term (annual across 12 high spring tidal cycles) and long-term sedimentation (~3 years) and to relate this to any existing datasets (i.e. vegetation data, such as that collected by the RSPB since the 2003 breach) and historical topographical maps of the Bay.

The fieldwork campaigns fell into two categories: those studying the short-term processes and those studying the longer-term processes. As sedimentation varies in space and time, it is important at this stage to recall the distinction used here between deposition and sedimentation which has defined the sampling strategy for this research. Deposition corresponds to the amount of

accumulated material whilst sedimentation is the differences in elevation, attributed to accretion and erosion, based on a reference height over a given time interval (Pye and French, 1993). Recent studies on salt marsh (Nolte et al., 2013; Schindler, Karius, Deicke, et al., 2014; Schindler, Karius, Arns, et al., 2014) and seagrass (Macreadie et al., 2014) systems have produced a comprehensive review of efficiency, costs and accuracy of sedimentation measurements summarised in Figure 3-8 below.

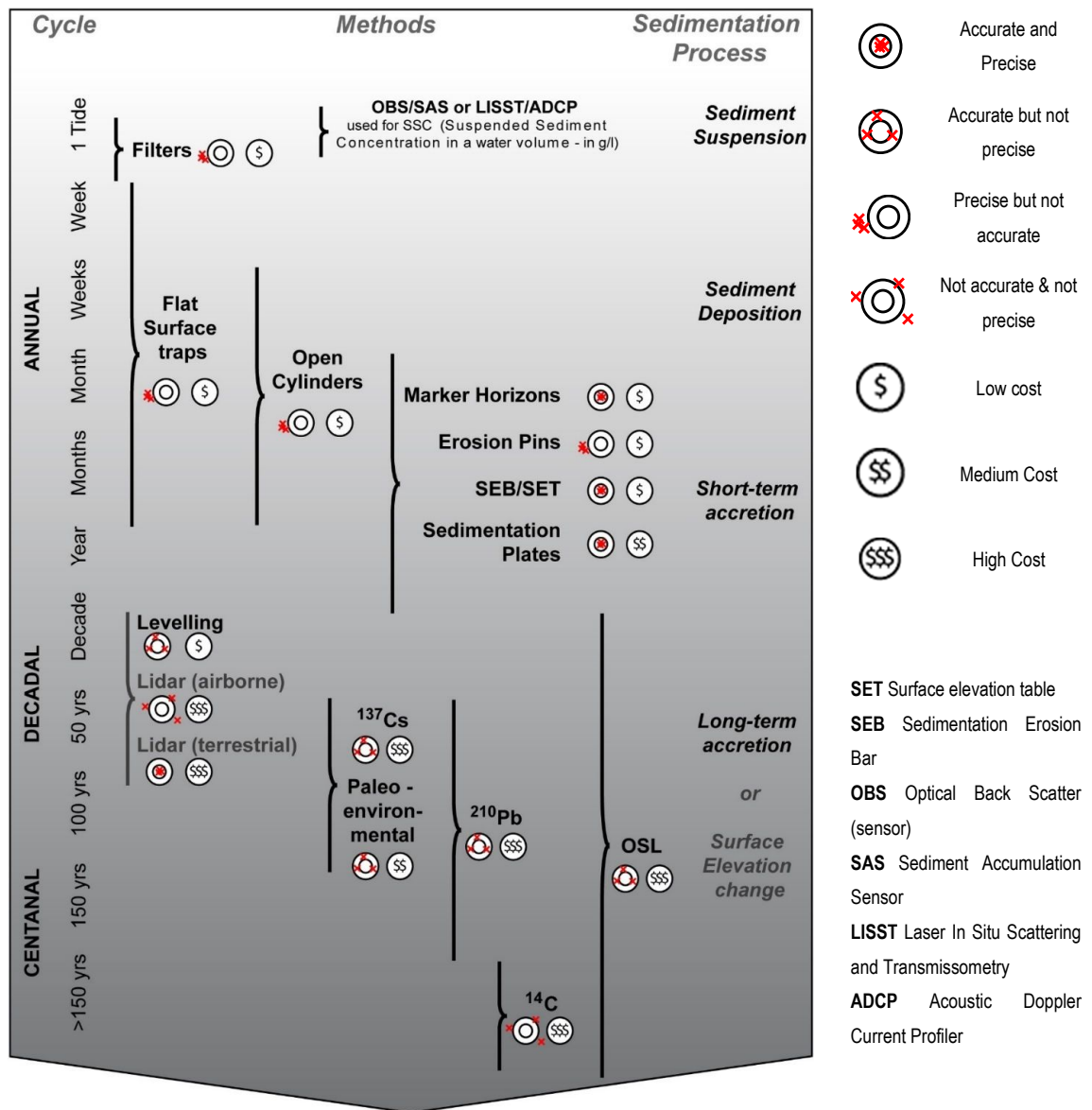


Figure 3-8: Methods to measure saltmarsh sedimentation adapted from Nolte et al., 2013.

The methods as presented in Figure 3-8 do not fully capture the biotic and abiotic components of saltmarsh processes through time. Figure 3-9 presents the methods used here to address both biotic and abiotic measurement techniques and enable appraisal of their interactions via saltmarsh development.

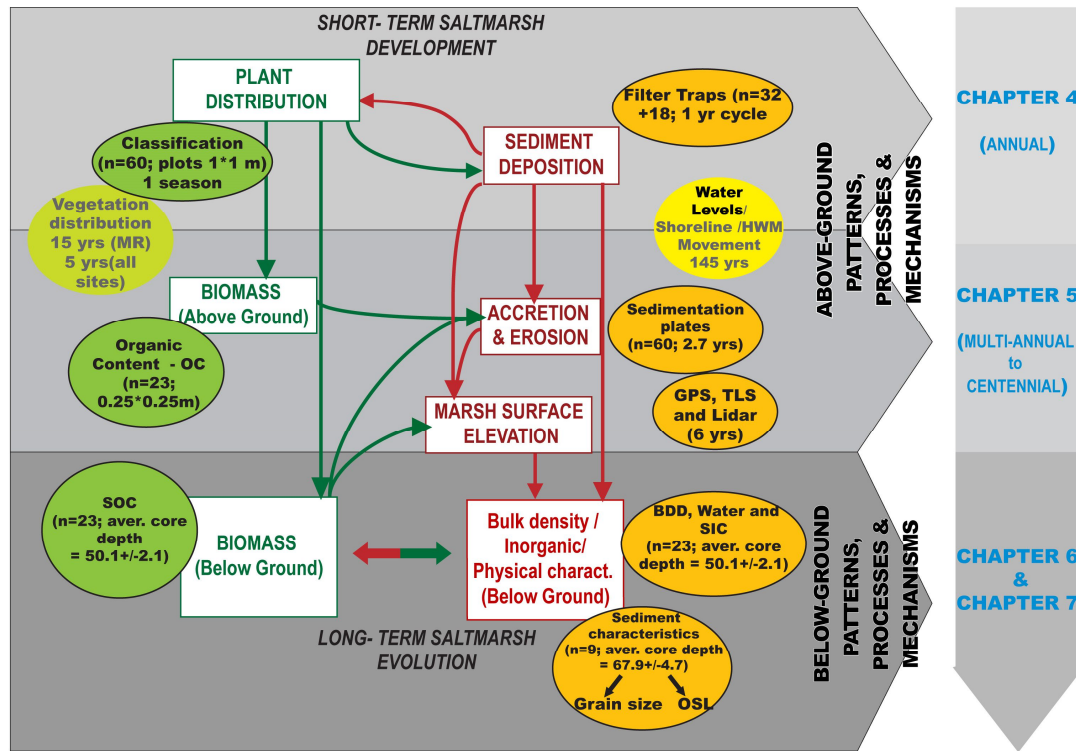


Figure 3-9: Research methods employed to simultaneously measure biological and physical patterns, processes and mechanisms of saltmarsh development. Dark captions make up the empiric dataset and grey captions comprise historic datasets used in analysis.

### 3.3.2 General sampling strategy

#### 3.3.2.1 Fieldwork programme

The fieldwork programme was conducted through a series of campaigns designed to address the research objectives as presented in Table 3-3 below:

Table 3-3: Summary of the field campaigns. \* not used in the statistical analysis; \*\*See 3.4.2.3.

	Time scale	Processes	Research Objectives	Fieldwork - Collection Date	Number of surveys	Methodology used
Short-term Aboveground dynamics	Annual	Sediment deposition	Accretion rate estimation	09/02/2016*	13 High Spring tides	See 3.4.1.1
				09/03/2016		
21/04/2016						
06/05/2016						
06/06/2016						
04/07/2016						
03/08/2016						
18/09/2016						
17/10/2016						
14/11/2016						
14/12/2016						
31/01/2017						
01/03/2017*						
				04 <sup>th</sup> July 2016	1	See 3.4.1.2

Long-term Aboveground dynamics	Multi-annual	Sedimentation	Sedimentation (Accretion and erosion) rates	July 2015 to September 2017	30&31/07/2015 05/11/2015 08&09/02/2016 18&19/04/2016 16&17/07/2016 16&17/10/2016 01&02/03/2017 18-20/09/2017	10	See 3.4.2.2
		Vegetation cover and distribution*	Vegetation distribution**	July 2015 to September 2017	16&17/07/2016**		**See 3.4.2.3
		Topographic changes	Shoreline movement Accretion and erosion	July 2014 to July 2016 July 2014 to July 2016	20/07/2014 30&31/07/2015 23-25/07/ 2016 18-20/06/2017 &19/09/2017	3	See 3.4.2.1
Long-term Belowground Dynamics	From one tide to over century	Organic changes through saltmarsh evolution	Organic matter and Soil Organic Carbon content (SOC)			1	See 3.4.3.2
		Physical changes through saltmarsh evolution	Inorganic (carbonates – BDD – water content and Soil Inorganic Carbon content (SIC)	19 <sup>th</sup> and 20 <sup>th</sup> April 2016			See 3.4.3.2
		Dynamic tracers through time	Physical Characteristics Optically Stimulated Luminescence (OSL) and Infra-Red Stimulated Luminescence (IRSL)			NA	See 3.4.4

### 3.3.2.2 Integrated design

The experimental design and sampling location to measure short-term and longer-term processes for vegetation and sedimentation via vegetation quadrats, sediment traps, sedimentation plates, shallow and longer cores aimed to consider: elevation, tidal dynamics (water levels, distance to MHWS and to the water channels/creeks) and vegetation community types, all of which are generally reflected in saltmarsh zones and their classification. Haynes (2016) calls for an informed redefinition of saltmarsh classification/zonation and this is supported by the recognition that zonation is fundamental to the ‘tidal landscape’ and the feedback of ecological and physiological processes on soil accretion and belowground organic soil content (Da Lio et al., 2013; Roner et al., 2016).



This section describes how the sampling was designed to accommodate the above-mentioned considerations and the use of existing data collected at Nigg before 2015 when this research started:

- The 2001-2014 RSPB monitoring scheme;
- The 2011-2 SNH Scottish Saltmarsh Survey (SNH SSS);
- The 2011-2 LIDAR (Light Detection and Ranging) data which offered the only systematic and uniform elevation dataset for the research sites.

To avoid ecosystem disturbances, RSPB requested that any sampling on the MR site should replicate as closely as possible to the original monitoring sampling design established at the time of seawall breach in 2003 to avoid vegetation disturbance. RSPB had set up a baseline monitoring scheme using permanent quadrats (1 m<sup>2</sup> - Figure 3-11) aimed to measure vegetation and sediment accumulation with the last monitoring results reviewed in 2015 (Elliott, 2015). However, and as reviewed in Figure 3-10, RSPB’s past surveys concentrated on the biological aspects of the managed realignment (MR) site. Additionally, further surveys were carried out in 2006-2007 on the fronting salt marsh (site FM in this research) that had developed naturally south of the sea wall (Crowther, 2007) and in 2014 survey work on geomorphology was only carried by Glasgow University (raw data from this work has been included in this research - see 3.4.2.1).

Geomorphology	Bab		Cr.		Cr.		Cr.		Cr.		RSPB		RSPB&SNH		GU
Vegetation	BSL		Cr.		Cr.		Cr.		Cr.		RSPB		RSPB		GU
Benthic invertebrates	RSPB		RSPB		Cr.		Cr.		Cr.		Cr.		Cr.		
Birds	RSPB	RSPB	Cr.	Cr.	Cr.	Cr.	RSPB	RSPB	RSPB	RSPB	RSPB	RSPB	RSPB	RSPB	
	2001	2002	2003	2004	2005	2006	2007	2008	2009	2010	2011	2012	2013	2014	

**Figure 3-10: RSPB - MR monitoring campaigns since 2001. Abbreviations: Cr = A. Crowther (2007) – PhD on restoration of intertidal habitats for non-breeding waterbirds; RSPB = RSPB internal report (Elliott, 2015); BSL = baseline Survey McHaffie (2002); Bab = Babbie Group (2002).**

### RSPB’s legacy - Quadrat’s selection

The RSPB vegetation quadrats (1 m<sup>2</sup>) used a random sampling pattern along two sets of five transects, each positioned parallel with the southern sea wall on an east-west alignment and covering a range of elevations and positions in the tidal frame (Figure 3-11). RSPB’s vegetation survey classification used the standard National Vegetation Classification (NVC) defined by J. Rodwell (2006) which describes the 28 saltmarsh communities occurring in the UK (mainland, Isle of Man, Isles of Scilly and Scottish Isles) and covering vegetation communities, distribution and diversity using the percentage cover of species. In 2006, in her PhD thesis, A. Crowther provided information for the fronting marsh (FM) site using 109 samples (10cm deep cores) located on 14 transects (running perpendicularly to sea wall on a north-south alignment) for

vegetation species, invertebrates and sediment characteristics as a foraging source for birds (Figure 3-11).

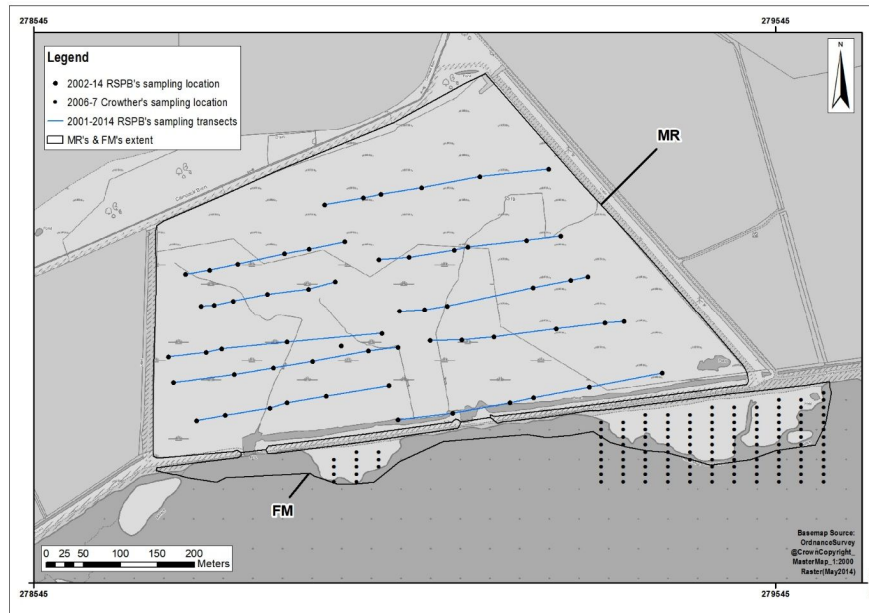


Figure 3-11: RSPB's 2002-14 baseline sampling design in MR & 2006-2007 Crowther's sampling design in FM.

To extend both the RSPB and Crowther sampling design to the adjoining Ankerville (ANK) saltmarsh site, a similar randomly stratified sampling design was adopted by subsampling along sets of transects across the sites in consideration of the vegetation community type present, tidal range and elevation across the sites.

To reproduce the RSPB sampling transects in ArcGIS for the MR, FM and ANK salt marshes a series of transects were produced (Figure 3-15), using an east-west alignment for the FM site (same angle of rotation as the MR site) and a SW-NE alignment for ANK in keeping with the tidal flow (Figure 3-6). To provide accurate estimates and high-precision population metrics (shape, position, elevation, edge density, class, type of landscape), NOAA Biogeography Branch's Sampling Design Tool in ArcGIS (Buja and Menza, 2013) was used to randomly subsample MR, FM and ANK saltmarsh transects following a stratification of saltmarsh zones (as described above, in consideration with elevation height and vegetation) and creeks in order to measure short and long-term processes on site. Probability-based grid design utilises software (i.e. ArcView in this study) to create grids that fit over and are proportional to each stratum. NOAA Software is used to generate random stratified points in each grid to be surveyed.

## Research baseline NVC vegetation assemblages

In August 2011, the SNH Saltmarsh Survey of Scotland (SNH SSS) (using NVC classification - see Chapter 2 - 2.2) had inspected the vegetation assemblages and zones of all the study sites including ANK, thus providing a recent vegetation survey baseline for the natural saltmarsh site.

Following the preliminary site visits in April (20<sup>th</sup>) and June (18<sup>th</sup>) 2015, it was noted that the research sites drift-line zone dominantly composed of *Elytrigia repens* (SM28) occurred primarily along and at the base of the boundary sea-wall, in line with Stapleton and Pethick (1996) remarks on the disappearance of tidal to freshwater transitional zone. The driftline zones (SM28 in Figure 3-13) were excluded from this study for two main reasons: i) it was anticipated that this substrate material would be difficult to sample, and, ii) the research aims focus on the initial and recent stages of saltmarsh colonisation and sedimentation of the newly formed salt marsh (by realignment) in relation to the adjacent natural salt marshes.

Preparatory site visits in 2015 (18<sup>th</sup> June, 30<sup>th</sup> & 31<sup>st</sup> July and 04<sup>th</sup> to 06<sup>th</sup> November 2015) had also revealed that since 2011's SNH SSS, vegetation type had changed on the managed realignment (see also Elliott, 2015, pp. 16-18, for vegetation changes from 2003 to 2011). Therefore, each sample quadrats on MR and FM were revisited at the start of the research project to assess vegetation assemblages following NVC. TABLEFIT program (version2) was used to identify community and sub-community type and name (Hill, 2015). Between 2011 (SNH SSS) and 2015 (start of the research project), nine quadrats out of the 60 sampled location were updated: two in FM and seven in MR (see). The changes are presented below in Table 3-4 and Figure 3-12 describes an example of a quadrat alongside TABLEFIT results.

**Table 3-4: presents sampling points that have changed NVC community/ sub-community type between 2011 SNH SSS and 2015 research survey. The table also presents TABLEFIT results using 2015 vegetation survey (1m2 quadrat) specifying the vegetation composition (species name and cover value as a percentage as defined in Hill 2015). The interpretation of the Mean Goodness-of-Fit values for TABLEFIT is 80-100 for Very good, 70-79 for Good, 60-69 for Fair, 50-59 for Poor and 0-49 for Very poor (Hill, 2015). \*The TABLEFIT results also provides habitat types according to the European Environment Agency's EUNIS system. This system was not used in this thesis. EUNIS habitats are defined primarily by their ecosystem (woodland, dune, swamp, etc.), though the definitions may contain elements of vegetation composition and land use (Hill, 2015). \*\* Pla mar- stand for *Plantago maritima* Arm mar - *Armeria maritima*.**

Sampling points	SNH SSS Date of Survey - Surveyors: T. Haynes + R. Haynes	SNH SSS - NVC Vegetation assemblage (community / sub-community type)	Research - Date of Survey	2015 NVC Vegetation assemblage (community / sub-community type)
FM3	03-04/08/2011	SM16c		SM13d
FM4	03-04/08/2011	SM16a		SM13d
MR10	03-04/08/2011	SM13a		SM13d
MR11	03-04/08/2011	SM13a	30-31 / 07 / 2015	SM13d
MR22	03-04/08/2011	SM13a		SM13d
MR25	03-04/08/2011	SM16d		SM13d
MR51	03-04/08/2011	SM13a		SM13b



TABLEFIT (vo2) results

	EUNIS* code	EUNIS habitat type	NVC community / sub community	Mean GoF	Four component GoF values	NVC community / sub-community name
FM3	A2.54	Low-mid salt marsh	SM13d	84	84 100 85 100	<i>Puccinellia salt-marsh</i> <i>Pla mar-Arm mar</i>
FM4	A2.54	Low-mid salt marsh	SM13d	72	68 100 75 96	<i>Puccinellia salt-marsh</i> <i>Pla mar-Arm mar</i>
MR10	A2.54	Low-mid salt marsh	SM13d	74	83 84 71 77	<i>Puccinellia salt-marsh</i> <i>Pla mar-Arm mar</i>
MR11	A2.54	Low-mid salt marsh	SM13d	69	73 100 66 94	<i>Puccinellia salt-marsh</i> <i>Pla mar-Arm mar</i>
MR22	A2.54	Low-mid salt marsh	SM13d	77	65 89 90 92	<i>Puccinellia salt-marsh</i> <i>Pla mar-Arm mar</i>
MR25	A2.54	Low-mid salt marsh	SM13d	64	70 80 63 79	<i>Puccinellia salt-marsh</i> <i>Pla mar-Arm mar</i>
MR51	A2.54	Low-mid salt marsh	SM13b	77	100 84 70 69	<i>Puccinellia salt-marsh</i> <i>Glaux maritima</i>
MR55	A2.54	Low-mid salt marsh	SM13b	74	100 83 65 69	<i>Puccinellia salt-marsh</i> <i>Glaux maritima</i>
MR9	A2.54	Low-mid salt marsh	SM13b	71	100 73 68 63	<i>Puccinellia salt-marsh</i> <i>Glaux maritima</i>



Figure 3-12: image to the left shows the 2015 1m<sup>2</sup> quadrats for sampling point FM3 where the sedimentation plate is located and provided TABLEFIT results as follows:

NVC type of FM3 is SM13 with goodness of fit 84 - very good NVC Community: *Puccinellia salt-marsh* - Subcommunity: *Pla mar* and *Arm mar* - EUNIS: Low-mid salt marsh EUNIS code: A2.54

Analysis of top 5 possibilities:

- A2.54 SM13d 84 | 84 100 85 100| *Puccinellia salt-marsh*- *Pla mar-Arm mar*
- A2.54 SM13b 81 |100 100 65 80| *Puccinellia salt-marsh* *Glaux mar*
- A2.54 SM13e 62 | 76 100 49 92| *Puccinellia salt-marsh* *Fuclid*
- A2.54 SM13 62 |100 90 36 55| *Puccinellia salt-marsh*
- A2.54 SM13a 58 | 88 91 38 53| *Puccinellia salt-marsh* Typical

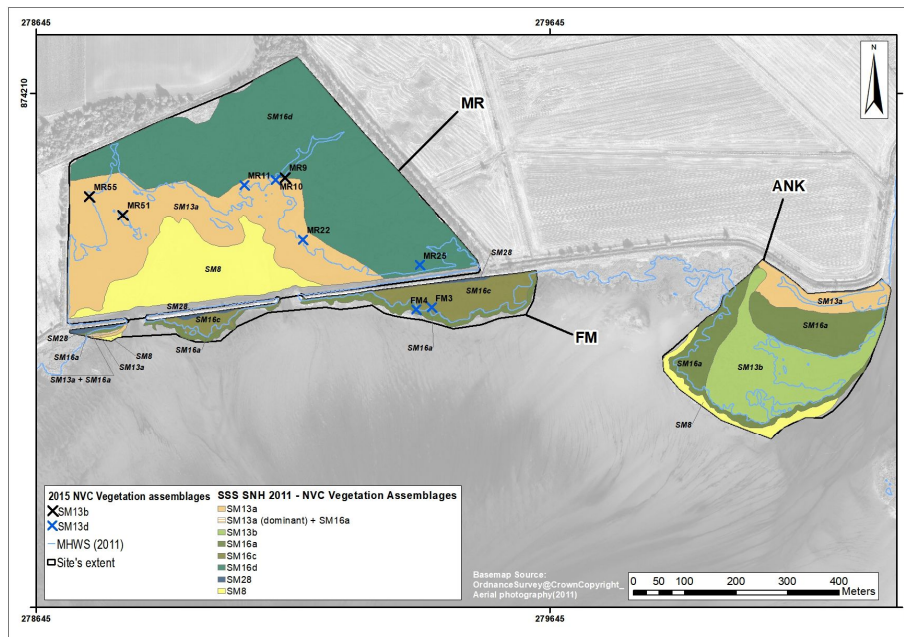


Figure 3-13: Sample locations marked with a X correspond to the vegetation assemblage that had changed between 2011 SSS (SNH) and the start of the research in 2015. The map is overlaid on MHWS (2.1m OD) and 2011's SSS (SNH) polygon data for the managed realignment (MR), Fronting Marsh (FM) and Natural Marsh (ANK).

## Research baseline zonation classification

These changes in vegetation between 2011 and 2015 on MR led to a mis-representation of the upper low marsh and lower high marsh tidal zones' limits (see Figure 3-13 above). So, in keeping with 2011 SNH SSS's polygon data, a transitional zone above 2.1 m OD (MHWS), that matched 2015 Mid-Marsh (MM) NVC - vegetation assemblages, was then defined in ArcGIS. FM's polygon data was unchanged, but vegetation classification updated for the research sampling design. This provided four saltmarsh sampling zones where vegetation classification was in keeping with NVC community/sub-community name as presented in Figure 3-14 and Table 3-5. It should be noted that in statistical analysis, the vegetation assemblages quadrat recorded at the sampling point is utilised. However, if the statistical analysis relates to an area of interest, such as water levels, all vegetation assemblages communities within that specific area are considered for the statistical calculations.

**Table 3-5: NVC vegetation assemblages and corresponding saltmarsh zone (details in Haynes, T.A. (2016) and Appendix A2) present studied sampling points at Nigg Bay.**

Saltmarsh zones	Thesis saltmarsh Code	Height range (in m OD)	NVC community/sub-community type & species name
Pioneer marsh	PM	≤1.76	SM8 (annual <i>Salicornia</i> );
Low Marsh	LM	≤ 1.9	SM13a ( <i>Puccinellia maritima</i> dominant, <i>Puccinellia m.</i> sub-community). SM13b ( <i>Puccinellia m.</i> dominant, <i>Glaux maritima</i> sub-community) ;
Mid-Marsh	MM	≤ 2.1	SM13d ( <i>Puccinellia m.</i> dominant, <i>Plantago maritima</i> - <i>Armeria maritima</i> sub-community). SM16a ( <i>Festuca rubra</i> dominant, <i>Puccinellia m.</i> sub-community);
High Marsh	HM	> 2.2	SM16c ( <i>Festuca rubra</i> dominant, <i>Festuca rubra</i> and <i>Glaux maritima</i> sub-community); SM16d ( <i>Festuca rubra</i> dominant, <i>Festuca rubra</i> sub-community).

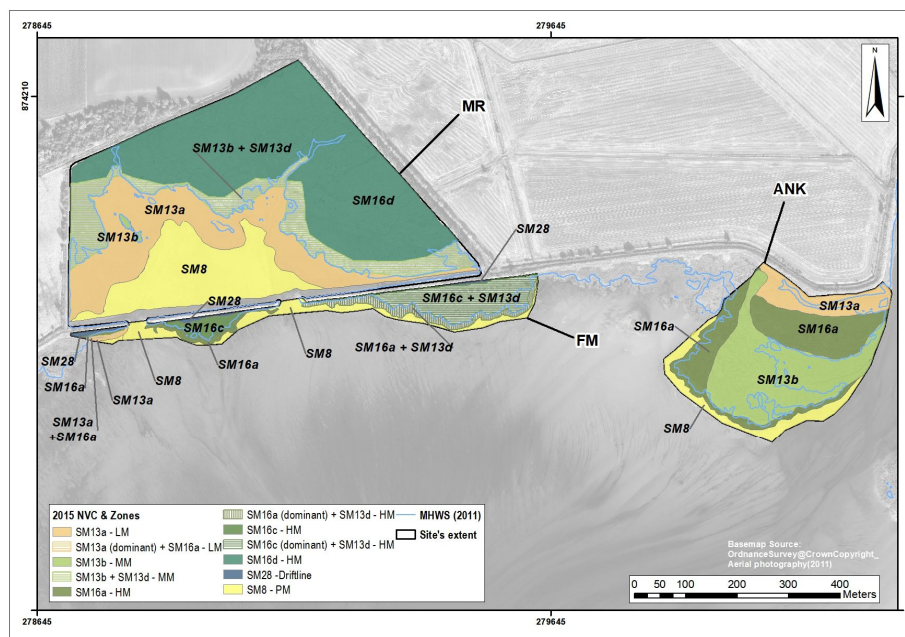


**Figure 3-14: Saltmarsh zonation for MR, FM and ANK at the start of research study. MHWS (blue) as defined at the start of the research project used for the stratified random sampling integrated with NVC classification as presented in Table 3-5 and detailed in A-2.**

Finally, Figure 3-15 presents the 60 sampling locations for all experiments carried out in the project: sediment traps, sedimentation plates, shallow and deeper cores.

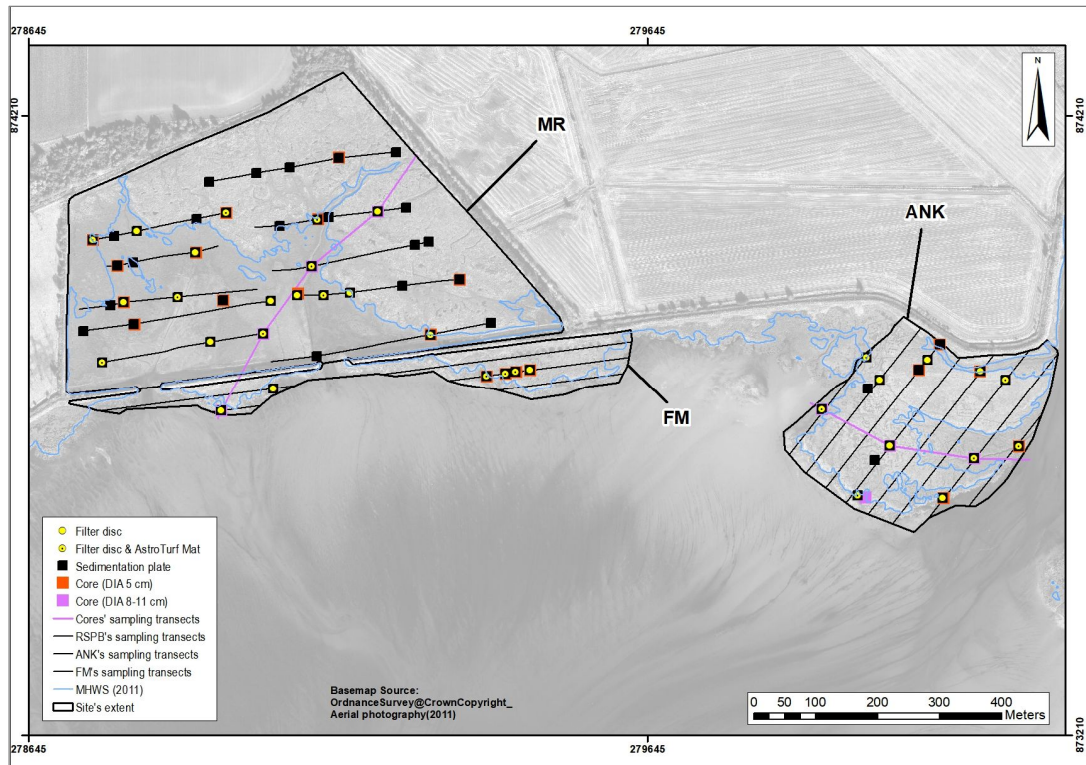


Figure 3-15: Overall research sampling strategy for MR, FM and ANK saltmarsh sites, short-term sampling plots (yellow, discs n=32 and mats=18), multi-annual sampling plots (black, n=60), shallow & narrow cores (orange, n=23), longer and wider cores along two transects (violet/heliotrope, n=8).

### 3.3.2.3 Physical drivers

As reviewed in Chapter 2, hydro- and morpho- dynamics are key to saltmarsh processes. Therefore, it was deemed important to include a baseline dataset for physical variables to better understand patterns, influences and processes that take place on the three salt marshes studied in Nigg Bay.

In this research, physical controls that may contribute to saltmarsh development include elevation (m), topographic or morphometric surface attributes such as slope and curvature, distance to MHWS, distance to water channels (m), distance to saltmarsh edge (i.e. vegetation edge between mudflat and pioneer zones; in m), soil bulk dry density (referring to autocompaction, thereafter BDD, in  $\text{g.cm}^3$ ) and tidal characteristics. These are summarised in Table 3-6 below and depicted in Figure 3-17. Qualitative output for these physical drivers has been generated by Principal Component Analysis (PCA) followed by multiple linear regression to test for significant relationships between combinations of environmental variables and measured variables during this research (see also 3.4.5). Problem of multicollinearity/autocorrelation in this study data was

assessed before performing multiple regression and presented in Appendix B.2. Multicollinearity/autocorrelation was addressed by performing principal component analysis (PCA), checking the Variance Inflation Factor (VIF) in regression models, and removing one or more highly correlated variables.

**Elevation height** has been measured using different equipment (Terrestrial Laser scanner, Differential-GPS or DGPS, manually, orthophotography) during the research project which are further discussed below in see 3.4.2.1 below (see also Appendix- B3). For clarity, elevation height using DGPS measured in 2015 (start of the research project) was used for sampling points data (Figure 3-17) and 2011 Lidar dataset was used when a full coverage of the three saltmarsh surfaces was required (each time referenced in text).

**Slope** - Slope influences drainage and sediment transport on salt marshes (Ranwell, 1972; Kirwan and Murray, 2007) and is calculated by applying each cell gradient (or rate of maximum change in z-value) of the LIDAR dataset. For this study, percentage rise was chosen using a range from 0 to infinity, where a flat surface is 0 percent and a 45 degree surface is 100 percent, and as the surface becomes more vertical, the percent rise becomes increasingly larger. This physical variable has been used for the multi-annual analysis that is presented in Chapter 5.

**Curvature** - Surface curvature impacts on the micro-topography (Langlois et al., 2003; Townend et al., 2011) and can be calculated from the curvature of the 2011 LIDAR surface where a positive curvature indicates the surface is upwardly convex at that cell and a negative curvature indicates the surface is upwardly concave at that cell. A value of 0 indicates the surface is flat. Units are one hundredth (1/100) of a z-unit (e.g. expected values a hilly area (moderate relief) can vary from -0.5 to 0.5; while for steep, rugged mountains (extreme relief) values can vary between -4 and 4. It is possible to exceed this range for certain raster surfaces). The use of variations in curvature across a surface offers the distinct advantage of enabling the identification of regions characterised by continuous and discernible geological attributes pertaining to the sedimentary strata. Curvature tool in ArcGIS toolbox can be used to make a set of curvature rasters: an output curvature raster, an optional profile curve raster, and an optional plan curve raster. Buckley (2010) explains how it is important to understand how plan and profile curvature work together (Figure 3-16). How fast you move downhill depends on how steep the slope is. The direction of flow is set by the aspect. Flow speeds up and slows down because of the shape of the profile, which also affects erosion and deposition. The shape of the plan affects how the flow comes together and goes apart. When we look at both plan and profile curvature together, we can get a better idea of how flow moves across a surface. These physical variables have been used for the multi-annual analysis that is presented in Chapter 5.



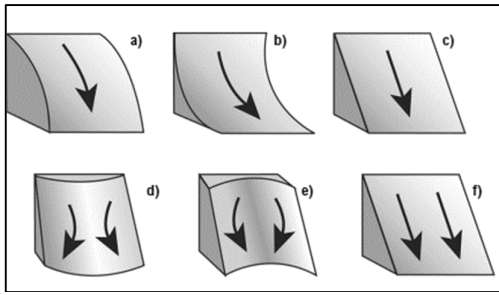


Figure 3-16: This diagram taken from Buckley (2010) illustrates a combination of profile and plan curvatures which helps to understand the flow across a surface. The profile curvature influences the acceleration and deceleration of flow across the surface: a) surface is upwardly convex at that cell, b) surface is upwardly concave at that cell, and c) indicates the surface is linear. Planform curvature relates to the convergence and divergence of flow across a surface: d) surface is sideways convex at that cell, e) surface is sideways concave at that cell, f) indicates the surface is linear.

**BDD (Dry Bulk Density)** measurements are further presented in section 3.4.3.2 below and processed results in chapter 4 - 4.2.2.1 and chapter 6 - 6.2.2.1.

**Distance to MHWS** for the saltmarsh zones (morphodynamic variable) as defined in 3.3.2.2. was used as a hydrodynamic variable, and, the distance was generated in ArcGIS for each sampling point (n=60, Table 3-6 and Figure 3-17).

**Distance to Water channels** - As seen in Chapter 2 – 2.3.1, tidal creeks or channel networks (in text simplified to water channels) mediate the exchange of water, nutrients and sediment between the estuary and tributary salt marshes (Fagherazzi et al., 2004; Kearney and Fagherazzi, 2016). A watershed was first constructed from the 2011 Lidar datasets and executed in ArcGIS (see Figure 3-17). The watershed is a stepped procedure that can be performed in spatial analysis in ArcGIS onto a DEM (digital elevation model) or DTM (digital terrain model) enabling the representation and digitisation of the general water flow of a defined area derived from its slope gradient. 2011 Ordnance Survey aerial photography and 2017 orthophotography (see 3.4.1.4) were further utilised to manually check and remove or digitised (when required) the extent of the water channels/creeks' extent. Each sampling points' distance to water channel was generated in ArcGIS and summarised in Table 3-6. Although not used in this research, it is of interest to highlight recent work (Chirol et al., 2018) that has developed tools to assist the monitoring of water channels/creeks characteristics (amplitude, length, sinuosity ratio, junction angle, width, depth, cross-sectional area, creek order, bifurcation ratio, drainage density, and drainage efficiency) designed to improve future managed realignment schemes.

Table 3-6: Summary of the physical variables for the 60 sampling points used in the project by sites for each saltmarsh zones where HM is high marsh, MM is mid-marsh, LM low marsh and PM is pioneer marsh:

	Overall Mean	SD	n
Elevation in meters (DGPS 2015)	2.1	0.3	60
Distance to saltmarsh edge in meters (DGPS 2015)	148.1	97.4	60
Distance to MHWS in meters (at 2.11m)	28.5	28.7	60
Distance to Water channels in meters	7.2	5.9	60
Curvature /Planform Curvature/Profile Curvature	0.0585 // -0.234 // -0.293	6.394 // 3.748 // 4.043	60
Slope (percent)	2.7	2.3	60

	ANK		FM		MR		ANK		FM		MR	
	Mean	SD	Mean	SD	Mean	SD	Mean	SD	Mean	SD	Mean	SD
Elevation in meters (DGPS 2015)						Distance to saltmarsh edge in meters (DGPS 2015)						
overall	2.1	0.2	1.9	0.4	2.1	0.4	88.1	64.1	31.2	32.3	189.0	88.2
HM	2.2	0.1	1.9	0.4	2.5	0.2	101.0	74.0	51.4	36.6	259.0	77.2
MM	2.1	0.2	2.0	0.1	2.1	0.1	72.9	36.6	12.4	8.8	207.0	68.5
LM	2.1	0.1			2.0	0.1	138.0	54.8			148.0	66.6
PM	1.6	0.2	1.4	NA	1.6	0.2	1.0	0.6	8.1	NA	105.0	47.2
Distance to MHWS in meters (at 2.11m)						Distance to Water channels in meters						
overall	16.7	12.6	11.8	9.3	35.6	32.6	5.4	5.6	6.8	4.5	8.0	6.1
HM	12.6	16.1	16.5	11.3	62.7	36.2	7.4	4.6	4.7	5.7	9.0	5.9
MM	28.5	6.3	4.8	2.8	3.5	4.4	7.1	8.4	9.8	2.1	8.7	5.9
LM	10.0	8.4			22.8	16.3	2.0	2.2			7.4	6.9
PM	8.5	0.3	11.9	NA	42.0	17.8	3.8	0.3	7.3	NA	6.0	6.3
	ANK		FM		MR		ANK		FM		MR	
	Mean	SD	Mean	SD	Mean	SD	Mean	SD	Mean	SD	Mean	SD
Curvature (1/100 of a z-unit)						Planform Curvature (1/100 of a z-unit)						
overall							0.7	4.1	-3.7	2.3	-0.1	3.6
HM	4.1	9.8	-7.6	4.2	-0.4	6.5	0.0	1.8	-5.0	1.8	-0.9	4.8
MM	2.0	6.4	-8.1	1.1	-0.7	6.1	-0.6	4.5	-3.5	1.3	-0.3	3.1
LM	1.8	8.3			2.6	5.1	2.2	5.2			1.4	2.8
PM	-0.6	8.0	0.7	NA	-1.2	4.5	2.7	6.1	-0.2	NA	-0.6	2.3
Profile Curvature (1/100 of a z-unit)						Slope in %						
overall	-1.4	5.5	2.7	2.6	-0.3	3.4	3.62	3.47	2	1.08	2.38	1.69
HM	-4.1	8.7	2.6	2.5	-0.4	3.4	2.70	3.48	2.17	0.66	2.99	1.96
MM	0.4	4.0	4.6	0.2	-1.2	3.8	5.82	4.55			2.43	1.55
LM	-2.6	3.4			0.4	3.6	2.78	1.91	2.42	1.64	2.22	1.81
PM	3.3	2.0	-0.9	NA	0.6	2.8	1.62	0.17	0.66	NA	1.45	0.54

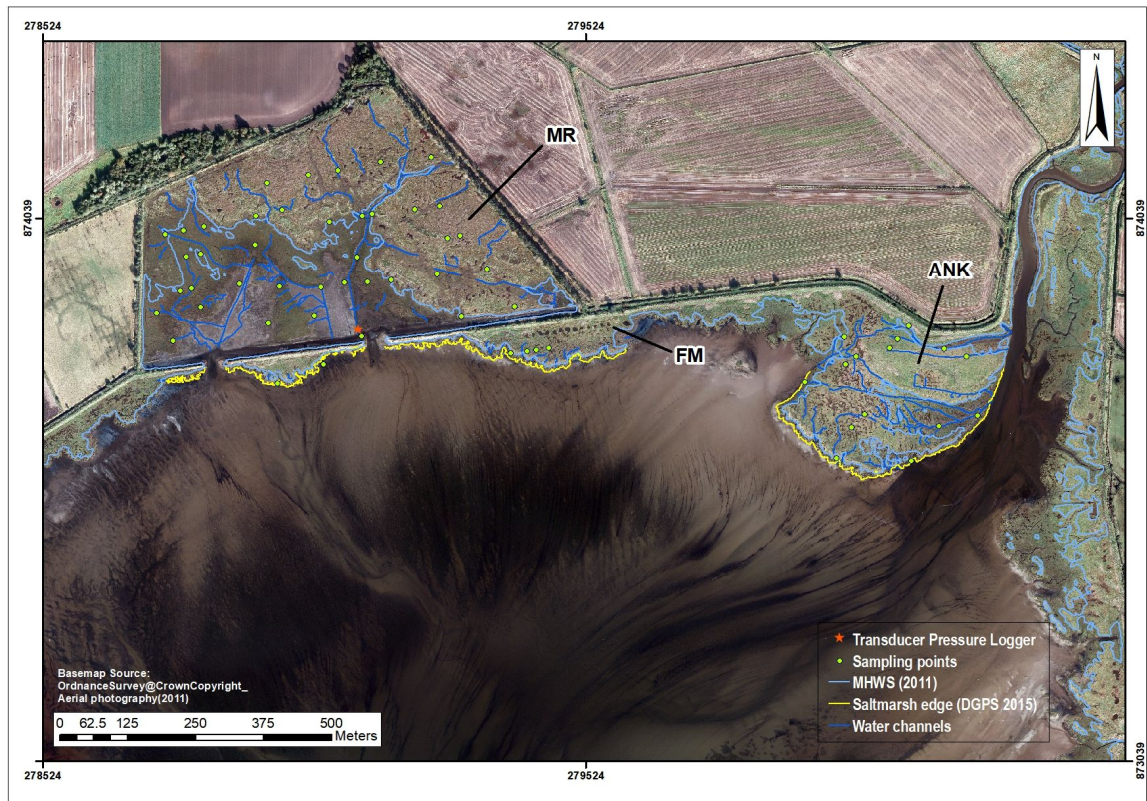


Figure 3-17: Water channels (creeks), saltmarsh edge and MHWS across the three saltmarsh, ANK, FM and MR along with location of sampling points (in green) and transducer pressure logger (orange star).

**Water levels** - As seen Chapter 2- 2.3.1.2, tides control sediment transport across the tidal flat, crucial for sediment suspension, sedimentation and the vertical and horizontal saltmarsh

development. Tides regulate the water flow across the marsh via tidal creeks, the extent and duration of the inundation of the marsh source of sediments, organic matter and nutrients (Fagherazzi et al., 2004; Wolanski et al., 2009; Davidson-Arnott, 2009; Kearney and Fagherazzi, 2016).

Using a pressure transducer (Rugged TROLL 100) installed by RSPB in the MR site following the realignment in 2003 (orange start in Figure 3-17 above and yellow arrows on Figure 3-18), data was selected for the duration of the sedimentation plates monitoring campaign (see 3.4.2.1) that took place between 30<sup>th</sup> July 2015 to 21<sup>st</sup> September March 2017 (i.e.: c.786 days or c. 1461 tidal periods - high and low tide where low tide last c.12h and high tide c12h55 - see 3.2.1) and the overlapping filter and AstroTurf mat sediment deposition monitoring period (8<sup>th</sup> February 2016 to 01<sup>st</sup> March 2017 i.e. 359 days or 778 tidal periods, see 3.4.1.1).



Figure 3-18: Location of pressure transducer symbolised with a yellow arrow at low (left) and high (right) tide.

Salt marshes are inundated when the tidal water height exceeds the land surface and flooding varies for each tidal period and differs across the marsh (Morris et al., 2002; Morris, 2006; Kefelegn, 2019). Therefore, the water height, high and low water, was extracted, analysed and processed in RStudio for the aforementioned time period (details Chapter 4 -4.4 for the aboveground short-term dynamics and results and in Appendix D-3 for the aboveground long-term dynamics). Three components of the hydroperiod were then calculated using time series pressure transducer data: a) flood depth, b) flood frequency and c) hydroperiod (conceptualised in Figure 3-19):

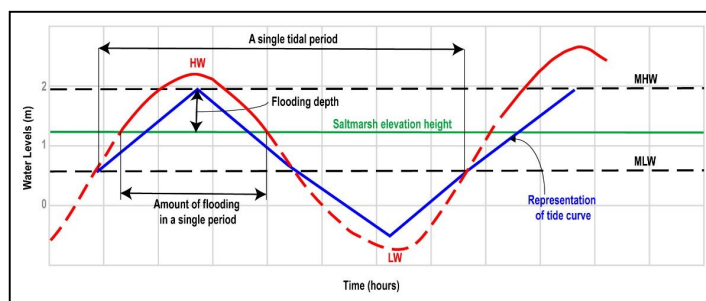


Figure 3-19: Conceptual diagram illustrating how the hydroperiod parameters have been calculated. Diagram adapted from Kefelegn (2019))

- a) **Flood depth** was estimated using the difference between the average of all high water (HW) heights and the saltmarsh surface elevation. The flood depth is calculated as follows:



$$\text{Flooding Depth (m)} = \text{HW} - \text{Elevation Height}$$

The average flood depth is defined for the number of tidal periods, which is analysed as follows:

$$\text{Average Flooding Depth (m)} = \frac{1}{n} \sum_{i=1}^n (\text{HW}(i) - \text{Elevation height})$$

Where  $n = 778$  tidal periods for the sediment deposition campaign (filter and AstroTurf mats) and  $n=1572$  tidal periods for the sedimentation plates survey campaign; and elevation height was averaged at a 1 m<sup>2</sup> cell size when using Lidar 2011 for the full coverage of the saltmarsh area.

b) **Flood frequency** corresponds to the number of times the saltmarsh area (1m<sup>2</sup> cell) is flooded during the survey period analysed and calculated as follows:

$$\text{Flooding Frequency} = \begin{cases} \text{if Flooding} = 1 \\ \text{if No Flooding} = 0 \end{cases} \quad \text{for 1 tidal period}$$

$$\begin{aligned} \text{Average Flooding Frequency (\%)} \\ = \left( \frac{\sum \text{Flood frequency for the survey period}}{n} \right) * 100 \end{aligned}$$

c) **Hydroperiod** corresponds to the ratio between the flood depth for each elevation height (1m<sup>2</sup> cell) for the total tidal period analysed and the tidal range (the difference between the average of all high water (HW) heights that have inundated and the average of all low water heights). Hydroperiod is calculated as follows:

$$\text{Average Hydroperiod (m)} = \frac{\text{Flood depth}}{\text{HW} - \text{LW}}$$

$$\text{Average Hydroperiod (m)} = \frac{\text{Average Flood depth}}{\frac{1}{n} \sum_{i=1}^n (\text{HW}(i)) - \frac{1}{n} \sum_{i=1}^n (\text{LW}(i))}$$

### 3.4 Material and methods

#### 3.4.1 Aboveground short-term (annual) dynamics methods

To address the thesis overarching aim which is to improve our understanding of processes, mechanisms and patterns: that promote the formation and development of salt marshes, that allow salt marshes to recover from environmental and anthropogenic disturbances, and that promote some of the regulating and supporting services provided by salt marshes, short-term (annual)

sediment and vegetation dynamics (linkages and possible interactions) are crucial to salt marsh stability. These were measured to address questions on:

- Spatial variation: how does deposition vary on the MR and natural marsh?
- What is the vegetation distribution across the saltmarsh sites and do sediment and vegetation distribution differ between saltmarsh zones?
- Temporal sediment variation: Does sediment deposition change seasonally and differ between the MR and natural salt marsh?
- Dynamic variation: Is sediment deposition on the study sites influenced by physical drivers or biological drivers? What are the implications for aboveground processes of the sites and can this inform a budget for accretion rate and aboveground biomass?

#### 3.4.1.1 Sediment deposition methods

**Sampling Techniques** - Recent studies (Butzeck, 2014) evaluated the performance of different sediment traps: ceramic tiles, AstroTurf mats and plain circular traps with and without lids. Carried out in a flume tank, Butzeck's study showed that circular traps were more efficient than flat traps (sediment deposited on circular traps were found up to 45% higher than tiles and 20% higher than mats) and found that 'remarkable' differences that could affect comparability between different studies (Butzeck, 2014). Schindler et al. 2014a evaluated the sampling and trapping efficiency of one litre LDPE bottles and PE-synthetic turf mats installed in the Hallingen tidal flats of the North Frisian Wadden Sea for a complete storm season (October to April 2013) and concluded that although traps may overestimate or underestimate the natural sediment deposition rates, there was a clear advantage in using both methods (Schindler, Karius, Arns, et al., 2014). With these studies in mind, it was decided to use paper filters – prevailing for sediment deposition collection (Reed, 1989; Boorman et al., 2002; Temmerman, Govers, Wartel, et al., 2003; Temmerman et al., 2005; Maynard et al., 2011; Nolte et al., 2013; Butzeck et al., 2014) – and Astroturf mats to collect tidal sediment across the site.

The filter paper traps measured 110 mm in diameter (category Whatman no.1001-110) with the filter edge protected by a rubber ring with a rim of <2mm high and clipped to a DVD disc fitted with a metal weight (Figure 3-20). Alongside the filter traps, a subset of AstroTurf mats (n=18) of similar surface area (95\*100mm) and c.12mm in height were directly anchored to the ground with pegs (Figure 3-20). It was hoped that the use of Astroturf mats would replicate more accurately the deposition mechanisms of the vegetated part of the salt marsh (i.e. where the sediment sits on the top of the grass (or fake grass) and then gradually falls to the ground surface before burial),

with the filter paper replicating direct surface deposition with no direct vegetation interception. To date there has been no attempt to co-examine filter and mats in field conditions.

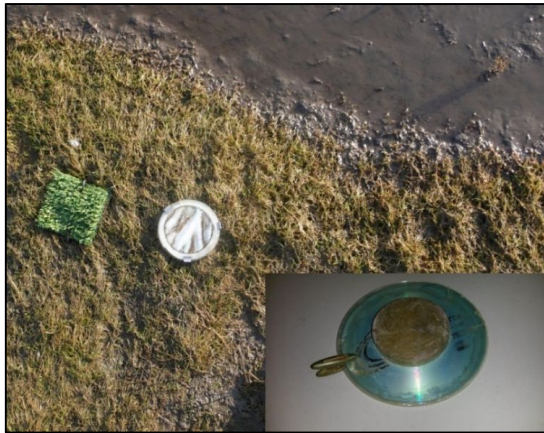


**Figure 3-20: Filter disc and AstroTurf mat after spring tide sediment deposition. The enclosed image (bottom right) presents the DVD disc mounted with a metal weight at its base.**

**Collection** - Surface sediment sampling (Table 3-3) was carried out from February 2015 to January 2016 using a network of pre-prepared filter traps (n=34) and AstroTurf mats (n=18) to gather sediment once a month (x12) at high spring tides carried. A total of 342 filters and 196 mats were placed between February 2016 and March 2017 (Figure 3-21 and Figure 3-22). Samplings from February 2016 allowed to test the sampling and materials and was not kept for the analysis. Similarly, Filter discs samples from the March 2017 was kept for Optical Luminescence Stimulation.

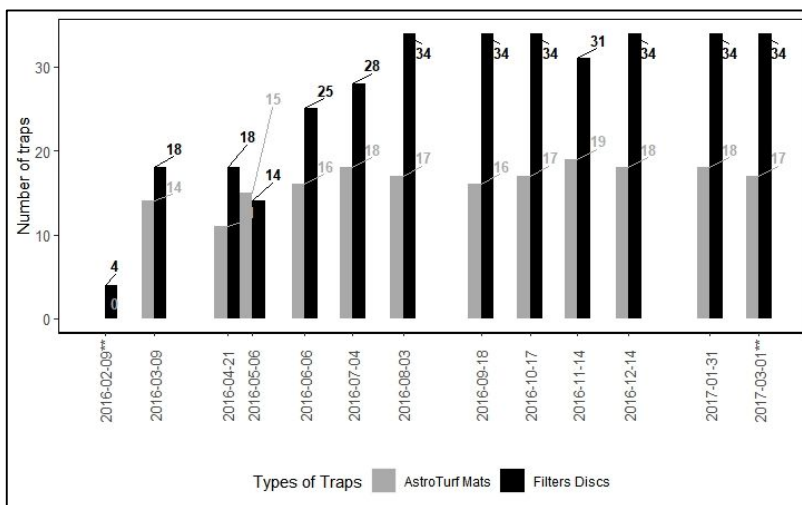


**Figure 3-21: Number of traps placed across the salt marsh between February 2016 to March 2017. Collection dates marked with \*\* (first and last) have not been used in the short-term deposition analysis.**

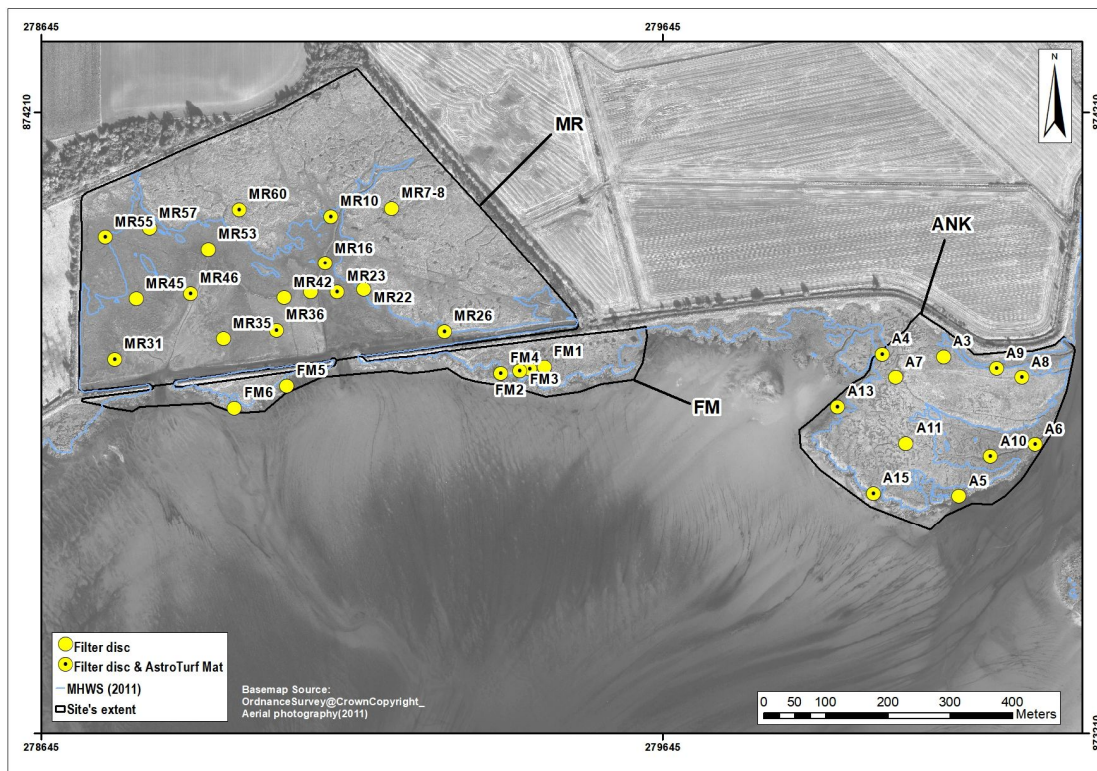


**Figure 3-22: The spatial distribution of filter discs and AstroTurf mats sampling sites on the three studied salt marshes and MHWs (blue) derived from 2011 LIDAR.**

Using baseline sampling as per described in 3.3.2, both traps were placed once a month in advance of the highest spring tide inundation when sediment deposition rates are likely to be highest. The traps were then retrieved after the tide had retreated (see Chapter 4. Section 4-4). To fulfil the dating requirement for Optically Stimulated Luminescence (OSL) dating (Chapter 7), the samples were kept in dark conditions until returned to the laboratory where under subdued light, the filter discs and AstroTurf mats were cleaned of small gastropods and vegetation detritus. Where the small *hydrobia ulvae* had eaten part of the filter, these samples had to be excluded from the datasets. To separate the grains from the mats, these were further washed with distilled water and left in individual beakers for c. 2 hours (to keep clays but exclude finer particles). All samples were individually dried until constant weight at a temperature not exceeding 50°C (higher temperatures can erode the OSL signal of sediment).

**Processing** - A total of 304 filters discs representing 11 high-spring tides (one cycle was kept for OSL experiments - see also results Chapter 4 section 4-4) and 196 mats were used for the short-term deposition analysis representing 12 high-spring tides from March 2016 to March 2017 (Figure 3-23).

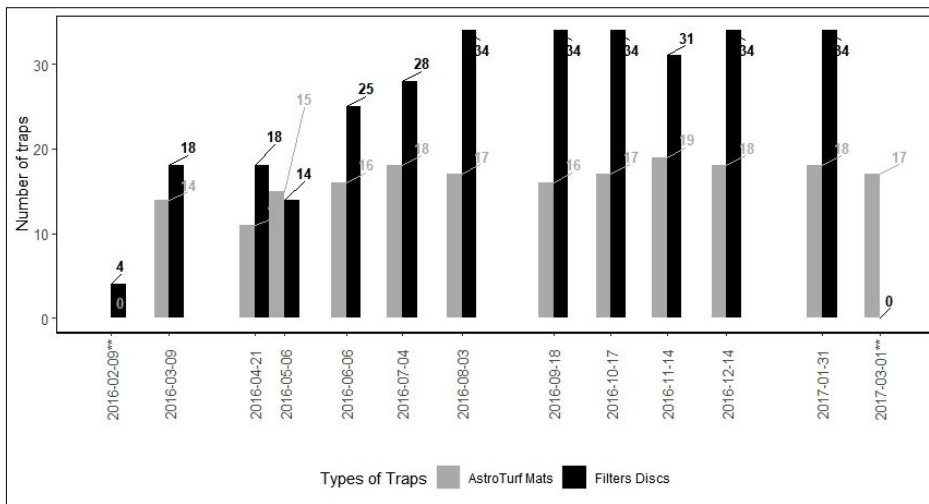


Figure 3-23: Number of traps retrieved and used in the short-term deposition analysis (except dates marked \*\*).

**Accretion rates** - Nolte et al. (2013) and Butzeck et al. (2014) describe the difference between accretion rates and sediment deposition rates, where deposition rates measure sedimentation of particle over time and accretion rates describe vertical adjustments to a specific soil layer during time (year or more) as a balance of deposition, erosion, and compaction processes of organic and mineral particles and interstitial water. Therefore, to translate the sediment deposition (expressed in  $\text{gm}^{-2}$ ) time series into a vertical accretion rate, Temmerman, Govers, Meire, et al. (2003), Nolte et al. (2013), Butzeck et al. (2014), Schindler, Karius, Arns, et al. (2014) and Morris et al. (2016) suggest using the average upper part of the core bulk dry density (BDD) per location (i.e. in this study per site per saltmarsh zone) and convert sediment deposition rate (expressed in  $\text{gm}^{-2}$  per year; this is calculated by averaging the sediment deposition measurements over the monitoring period) to an estimated accretion rate ( $\text{cm yr}^{-1}$ ) as follows:

$$\text{Accretion rate}_{\text{cm year}^{-1}} = \left( \frac{\text{sediment deposition rate}_{\text{g m}^{-2}\text{yr}^{-1}}}{\text{BDD}_{\text{g cm}^{-3}}} \right) / 10000$$

Details on BDD calculation in section 3.4.3 and chapter 4 - 4.2.2.1.

### 3.4.1.2 Vegetation and aboveground biomass

Using the same baseline sampling as described in 3.3.2, vegetation sampling was used to investigate short-term dynamics between sediment deposition and vegetation distribution (species assemblage using standard NVC), abundance, vegetation height, density, cover and finally aboveground biomass. This set of plots ( $n=21$ ) is smaller than the sediment deposition sampling point as there was not always vegetation to be measured at the location (within  $<1$  m radius of the sediment deposition sampling point - Figure 3-27). Because of a relatively small number of vegetation sampling points, bootstrapping was used to obtain reliable statistics. The measurements



were collected between 16<sup>th</sup> to 18<sup>th</sup> July 2016 and plots were revisited until September 2017 to ensure vegetation growth (see multi-annual survey dates in Table 3-3). The characteristics for vegetation and biomass were measured as follows:

**Vegetation distribution** - Preparatory site visits in 2015 (18<sup>th</sup> June, 30<sup>th</sup> & 31<sup>st</sup> July and 04<sup>th</sup> to 06<sup>th</sup> November 2015) allowed to revisit each sample quadrats on MR and FM at the start of the research project and assess new sampling on ANK to assess vegetation assemblages and vegetation distribution (see 3.3.2.2 and 0).

**Vegetation height** - Prior to harvesting, 25 measurements of vegetation height were taken in July 2016 from each 0.25m<sup>2</sup> quadrat (n=21) at the centre of the subplots sampled (A1, A2, etc.) (see Figure 3-24) by placing a horizontal ruler and measuring the vertical vegetation height. The observations were then averaged to provide a height per m<sup>2</sup> and the biomass volume (cm<sup>3</sup>) per plot across the zones of each salt marsh.

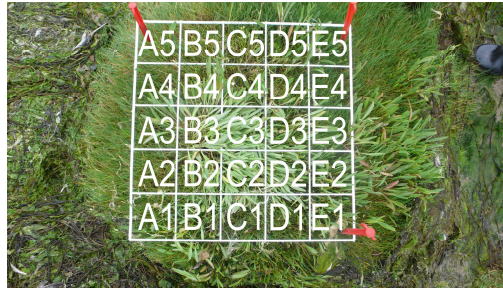


Figure 3-24: 0.25m<sup>2</sup> quadrat layout

**Vegetation density** - The dataset was further analysed for population density by stems counting two 0.1m<sup>2</sup> plot (A1& E5 in Figure 3-25) for each 0.25m<sup>2</sup> quadrats as follows:

$$Density_D = \left( \frac{A_{m^2}}{a_{m^2}} \right) * n$$

where A corresponds to entire area, a the area sampled and n the number of individuals

The density can then be scaled as a dispersion factor as follows:

$$Dispersion = \left( \frac{(n_{A1})^2 + (n_{E5})^2}{((n_{A1+E5}) - 1) * D} \right) * n$$

uniform ≤ 1  
clumped ≥ 1  
random ≈ 1

**Aboveground biomass** - To determine the aboveground biomass (mass of living material present), the vegetation from the 0.25m<sup>2</sup> quadrat plots (n=21) was harvested in July 2016 as illustrated in Figure 3-25. When present, dead biomass was bagged separately. The retrieved plants were counted (per stem), classified (per species) and photographed. Vegetation was then dried for 3 days at 80°C and dry weight determined in g.m<sup>-2</sup> per site and for each salt marsh. The aboveground

organic content (OC) of the harvested biomass was calculated using conversion factor (0.45) as detailed in Howard et al. (2014) relative to quadrat plot area calculated as follows:

Carbon in Aboveground Living  
Biomass in  $g\cdot m^{-2}$

$$Biomass_{g\cdot m^2} = \frac{\text{plant dry weight in } g. \text{ at } 80^{\circ}}{\text{plot area}_{m^2}}$$

$$OC_{g\cdot m^2} = Biomass_{g\cdot m^2} * 0.45$$

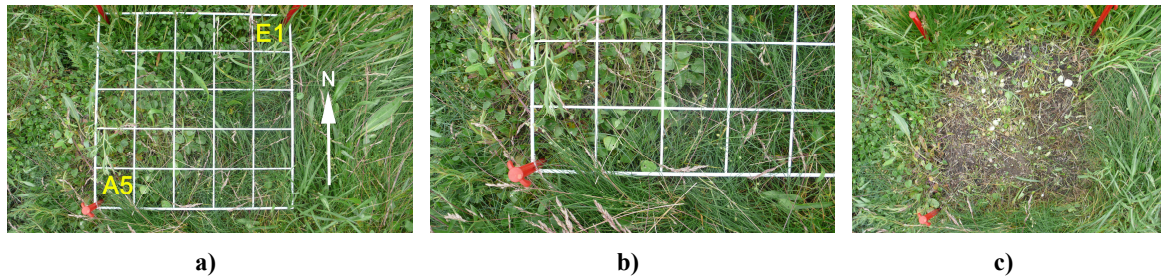


Figure 3-25: Example of the photographic record from the  $0.25m^2$  quadrats (FM3) used for aboveground biomass survey.: a) showing the sub-quadrats A1 & E5 used for density (stem counting); b) micro -detail in photographs and c) after harvesting.

**Vegetation cover** - The vegetation cover was assessed in the field by eye and recorded using digital photography prior to harvesting for aboveground biomass. Imagery was then rectified and georeferenced in the ArcGIS. To maximise the statistical analysis, the number of photographed sample plots was increased to match the number of sediment deposition traps ( $n=32$ ) by using the  $1 m^2$  quadrats. The photography was gathered as part of the multi-annual vegetation monitoring – see Figure 3-27 only 12 days after the biomass harvest. In order to quantify percentage vegetation cover to bare soil, the rectified raster image was spaced on a regular grid of  $25cm^2$ . This involved a two steps classification executed in ArcGIS with an ISO cluster unsupervised image classification for : **step-1**) image raster was first classified to principal component (to a max. value of 7: for pegs, quadrat frame, detritus, bare ground, plant dominant 1, plant subset 1, plant subset 2); then, **step-2**) reclassified to 3 values and provide a percentage quantification for 1) soil; 2) dominant vegetation community; and, 3) vegetation sub-community as demonstrated on Figure 3-26. Data quality was cross-checked using the two datasets (ArcGIS and field records) and where differences were found, the field record was chosen over the photography.



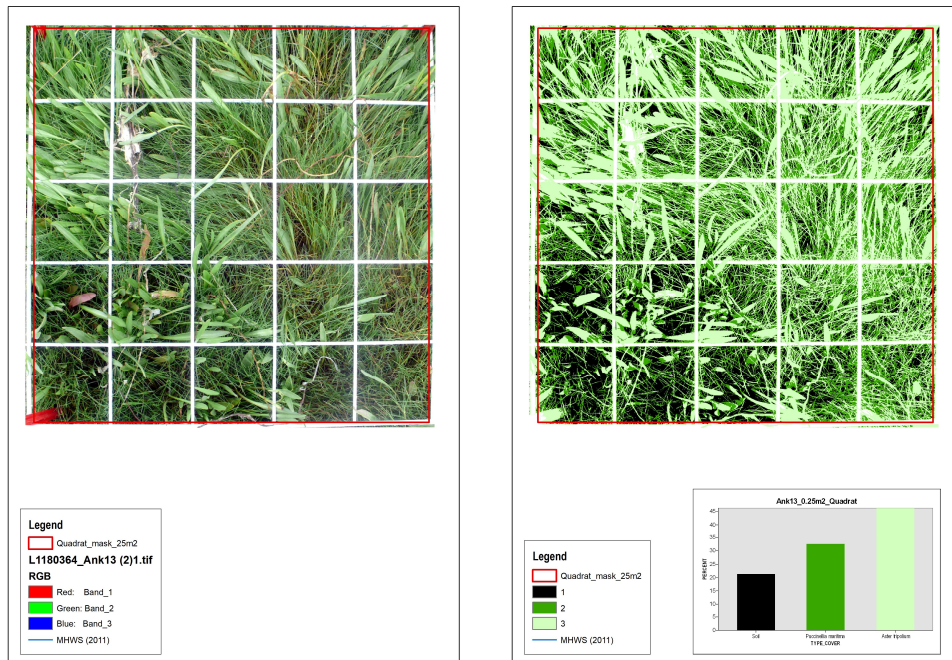


Figure 3-26: Estimation of vegetation cover where the image is first geo-rectified (a) and reclassified (b) in Arcgis to quantify Soil 21.29% - Vegetation: 78.7%. Data quality was cross-checked using the two records (ArcGIS and field records) and where differences were found, the field record was chosen over the photography.

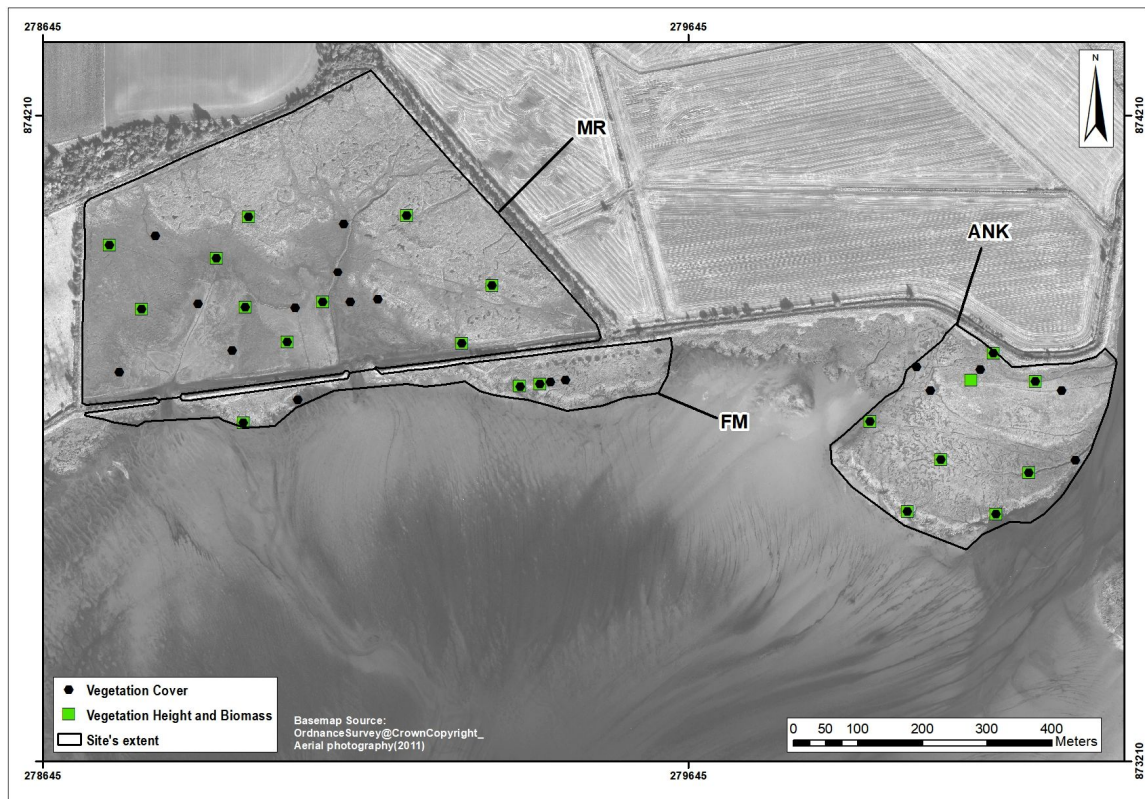


Figure 3-27: Spatial distribution of vegetation cover sampling location (black circles) and vegetation height and biomass sampling plots (green squares).

### 3.4.2 Aboveground long-term (multi-annual to centennial) saltmarsh dynamics

To address the overarching aim of this thesis, sediment availability and vegetation presence are crucial to saltmarsh stability and how it responds to anthropogenic and environmental disturbances. Thus, we need to understand long-term (multi-annual to centennial) saltmarsh dynamics. Long-term saltmarsh dynamics were investigated to address the following questions:

- Spatial variation: what are the patterns of saltmarsh erosion and surface accretion? what are the patterns and rates of sedimentation across saltmarsh sites and saltmarsh zones?
- How far has MHWS migrated in the past century and has movement been regular across time?
- Temporal sediment variation: Do sedimentation change seasonally? How does sedimentation (accumulation and loss) change (multi-annual to decadal to centennial) impact on sedimentation rates?
- Dynamic variation: Is sedimentation on the study sites mainly influenced by physical or biological drivers?

The empirical work was split in two strands of work (see Table 3-3):

- Geomorphological changes across centennial to decadal timescale (Chapter 5 – 5. 2) involved:
  - historical map analysis to show changes in Nigg Bay from 1750s to present;
  - quantifying areal changes to the saltmarsh extent in Nigg Bay from 1872 to 2012;
  - quantifying coastline and MHWS migration from 1872 to 2017 on the three studied salt marshes.
- Geomorphological changes on a multi-annual timescale (Chapter 5 – 5.3) involved:
  - monitoring vegetation distribution and cover across the three sites;
  - quantifying erosion and accretion on the three saltmarsh shore fronts and using two targeted transects across the three sites by calculating areal, volume and elevation height changes (2011-2017) using terrestrial and airborne DEM surface model;
  - quantifying sedimentation (accretion and erosion) using a network of sedimentation plates across the three salt marshes as described in 3.4.2.2 (timescale of 2.6 years).

#### 3.4.2.1 Mapping erosion and accretion

**Historical mapping** - 2011 LIDAR digital surface model (DSM) (Table 3-8) and geo-referenced historical maps from 1872 to 2017 were executed in ArcGIS to quantify:

i) **saltmarsh areal changes over 145 years in Nigg Bay; Results in Chapter 5.2.1 and 5.2.2.** The large-scale mapping was carried using OS One-inch first edition (1872), the OS 1:10K (1977-81) and the 1:4000K Scottish Saltmarsh Survey (SNH SSS) dataset surveyed by SNH in 2012 (Haynes, 2016). From this last dataset, pioneer marsh was excluded from the long-term analysis as it extends onto the sand/mudflat zone and, in any case, is not depicted on historical maps.

ii) **MHWS migration at the three studied salt marshes over 145 years. Results in Chapter 5.2.3.** The coastline migration was analysed for the three research sites MR, FM and ANK using the same cartographic dataset as for the areal changes ( (i) above) with the addition of 2011 Lidar to replace the 2012 SNH dataset (which only surveyed saltmarsh extent, whereas Lidar also includes the MHWS position) along with DGPS, TLS and ortho-photographic surveys carried out during this research project between 2014 and 2017 (Table 3-7). Identification of the ‘soft coast’ boundary between salt marsh and the intertidal presents challenges using early historical datasets (absence of imagery and no clear consensus on the edge of salt marsh) and since MHWS is one of the few features depicted on early maps, MHWS was extracted from all newly captured data (from 2011 to 2017) using the current MHWS height (2.1m OD – see 3.3.2). ArcGIS was used to quantify the rates of long-term (>60 years) and short-term (<30 years) MHWS changes using an end-point rate calculation where the distance differences between two MHW/shorelines are divided by the span of time elapsed between the MHW/shorelines. At 10 m interval, MHWS cumulative rate of change ( $\text{m.yr}^{-1}$ ) results are then depicted along an illustrative baseline representing the foreshore contour of each salt marsh as presented in Figure 3-28 below.

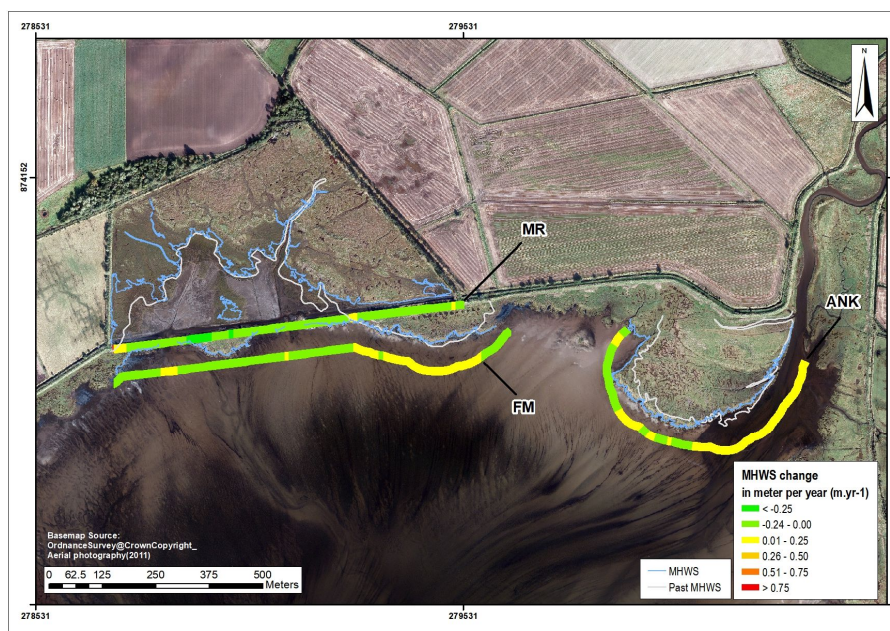


Figure 3-28: Example of the results of MHWS cumulative rate of change ( $\text{m.yr}^{-1}$ ), thus enabling to assess erosion (red gradients) and accretion (green gradients), at 10 m interval distance for each studied salt marsh depicted along a coloured scale baseline.



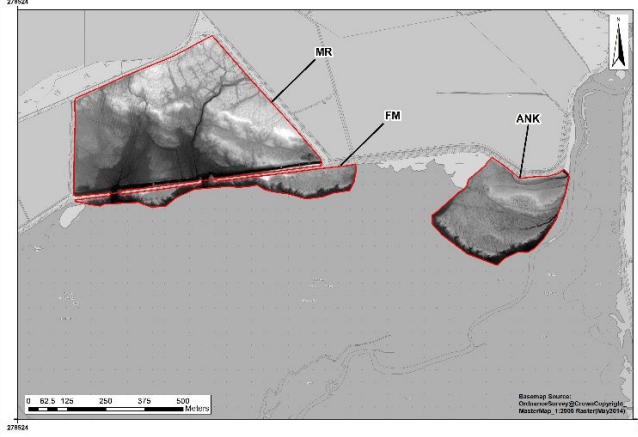
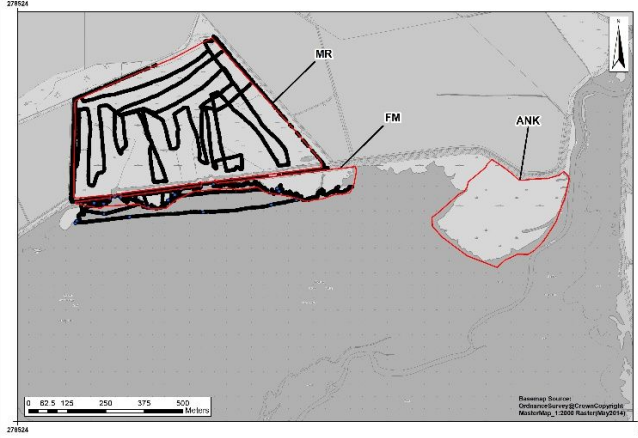
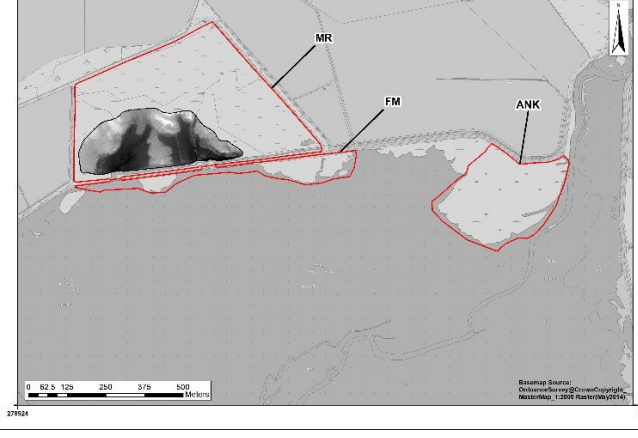
**Erosion and Accretion using Digital Elevation Models (DEM)** - Mapping erosion and accretion patterns over a time series of DEMs created from 2011 to 2017 (Table 3-7) including the 2011 airborne LIDAR; 2014 topographical surveys using a Total station; 2014 to 2016 Real-Time Kinematic (RTK) Differential-GPS(DGPS); 2014 to 2017 Terrestrial Laser Scanner (TLS); and, 2017 low-level aerial photography (accuracy and extent details of surveys in Table 3-8 below). The accuracy of this data is primarily determined by the point resolution of the topographical data when the survey was created. However, to monitor geomorphological changes geo-referencing is needed using common ground-controls, the accuracy of which determines dataset accuracy (i.e. if ground controls have Easting and Northing accuracy of  $\pm 0.15\text{m}$  and ortho-height accuracy of  $\pm 0.3\text{m}$ , the TLS data which may reached  $0.001\text{m}$  resolution will have the same accuracy as the ground controls).

**Table 3-7: Summary of the dataset available to analyse topographical changes on the saltmarsh sites.**

	<b>RMSE <math>\pm</math> (in m)</b>	<b>MR</b>	<b>FM</b>	<b>ANK</b>
2011 Lidar	0.054	✓	✓	✓
TLS 2014	0.032	✓	✓ (west breach only)	
TLS 2015		✓		
TLS 2016	0.009		✓	✓
TLS 2017	0.007		✓	✓
Orthophotography 2017	0.023	✓	✓	✓

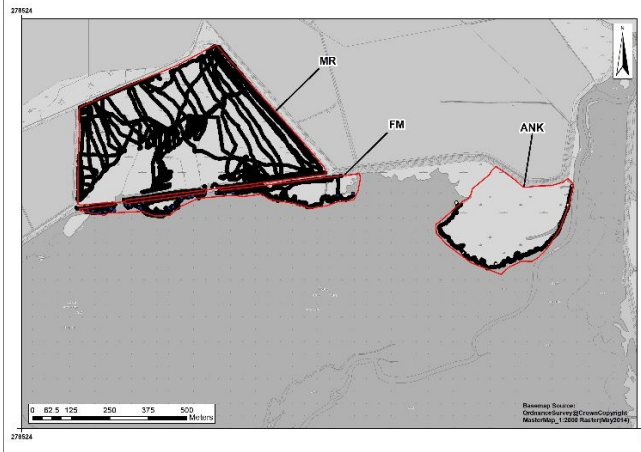
During the preliminary survey in June 2015, differential-GPS established ground control point as no accurate Ordnance Survey control points were available close to the site (closest one is NH54/T57 on the Meddat c.60 mE & c.220 mN with a logged accuracy of 8m in height), and the automatic correction for RTK-GNSS was unstable due to poor internet connection. Three base reference stations were established in July 2015 to provide a stable radio signal correction network and this was used for the remainder of the project. On 26<sup>th</sup> August 2016, Ordnance Survey GNSS control networks and geoid models were changed for Great Britain, Ireland and Northern Ireland to a new coordinate system (OSGB36(15)), but it was decided to persevere with the original OSGB36 system to ensure that all survey data collected on site (sedimentation plates, saltmarsh edges, control points for TLS, etc.) were under the same projection (UKTM) geoid (OSGM02) and CSCS (OSTN02) models.

Table 3-8: Extent of the survey data used to map erosion and accretion (Units are in meters. \* Raw data from Glasgow University MSc projects design C. Francoz with survey MSc Geomatics students. \*\* Raw data from Glasgow University MSc projects design J.D. Hansom & RSPB).

Year	Source & Survey Extent	Survey type and resolution (A-posteriori Uncertainty Evaluation)
2011-2	<p>SOURCE: SNH</p> 	<p>Lidar - DEM generated by SNH (info not provided on Flight data collection)</p> <p>DSM errors:</p> <p>ANK : Samples 92715 of 92715 - Mean 0.00084 - RMSE <math>\pm</math> 0.04736</p> <p>MR : Samples 41033 of 41033 - Mean 0.00015 - RMSE <math>\pm</math> 0.05524</p> <p>FM : Samples 259060 of 259060 - Mean -0.00038 - RMSE <math>\pm</math> 0.06020</p>
	<p>MR &amp; FM (MSc** -Peter Tawse)</p> 	<p>RTK-DGPS -</p> <p>DSM error: Samples 5205 of 5205 - Mean -0.009 - RMSE <math>\pm</math> 0.189</p>
2014		<p>MR</p> <p>TLS point cloud = 59545063 estimated points derived from 13-point clouds registered, geo-ref.&amp; unified in Cyclone 10.3.</p> <p>DSM error: samples 81246 of 81246 - Mean -5.861 - RMSE <math>\pm</math> 0.0322</p>

2015

MR, FM & ANK (marsh edge only) (MSc\* - Roza Zaminian & C. Francoz)



RTK-GNSS (MR & FM)

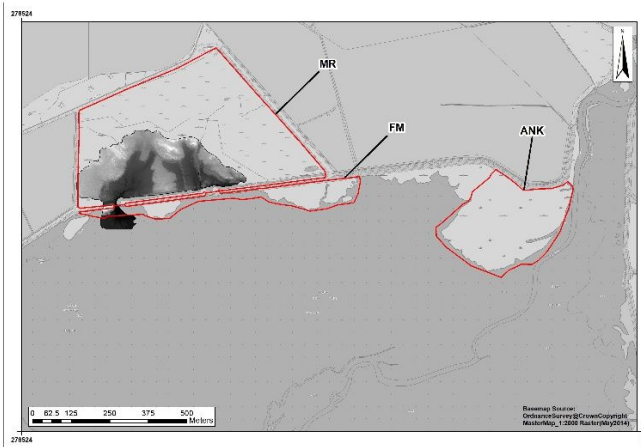
DSM error:

Samples 16126 of 16126

Mean -0.0058 –

RMSE ±0.1201

MR – part of FM (MSc\* - Roza Zaminian & C. Francoz)



TLS – point cloud = 67060945 estimated points derived from 23-point clouds registered, geo-ref. & unified in Cyclone 10.3.

DSM

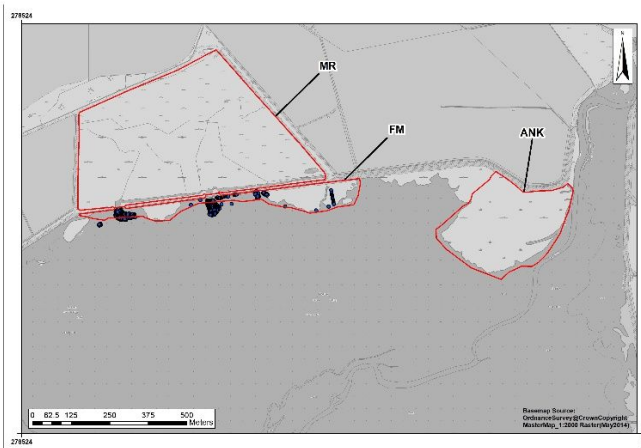
Samples 8710028 of 8710028

Mean -1.2020400113976278e-006

RMSE ± 0.006743

2016 (June)

FM marsh edge (MSc \* student - Calum McBride)



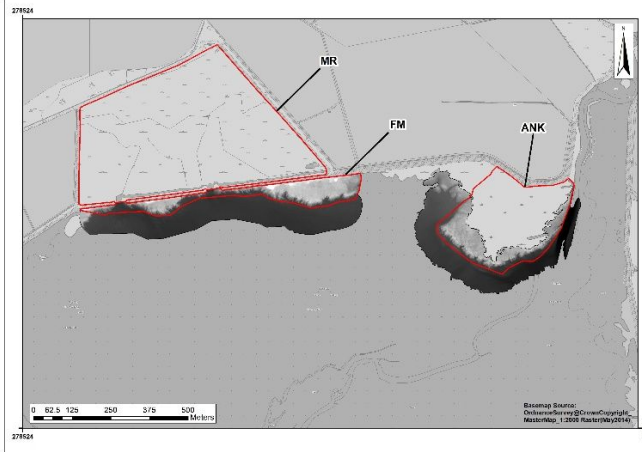
RTK-GNSS (FM)

DSM error: Samples 1398 of 1398 Mean 0.0018

RMSE ± 0.0469

2016 (June)

FM (MSc \* student - Calum McBride) and ANK (MSc \* student Luke Grant)

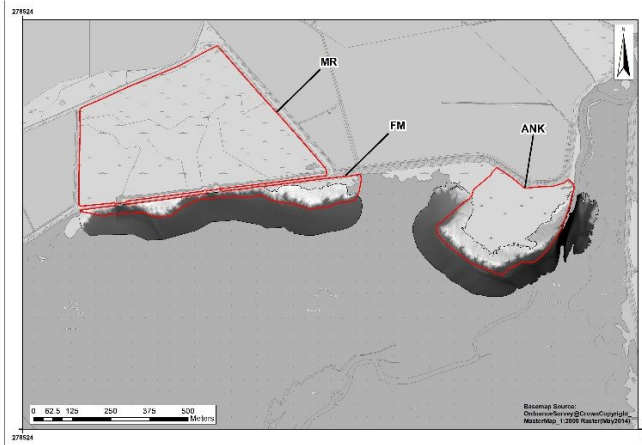


**TLS data FM**  
**DSM generated in ArcGIS 10.3**  
**DSM error:** Samples 11436903 of 11436903 – Mean -8.7367 - RMSE ± 0.0092

**TLS data ANK**  
**DSM error:** Samples 8668589 of 8668589 Mean -1.1032 RMSE ± 0.009.

2017 (June)

FM and ANK (MSc \* student - Ewan Mansley)

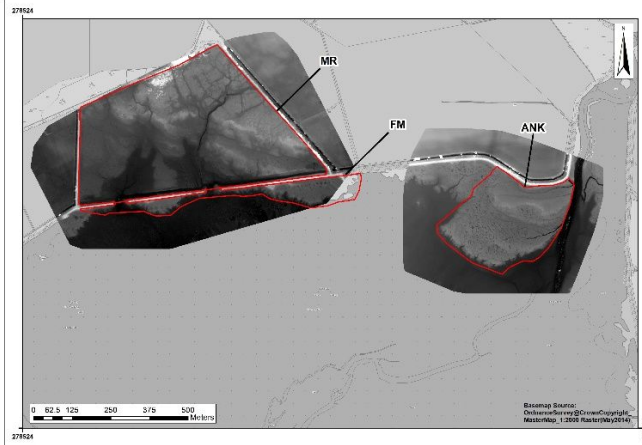


**TLS data FM and mudflat**  
 (50.1741 ha)  
**DSM error:** Samples 10572537 of 10572537  
 Mean -2.209  
 RMSE ±0.0075

**TLS data ANK:**  
**DSM error:** Samples 8668589 of 8668589  
 Mean - 1.103  
 RMSE ±0.008

2017 (July & Sept.)

MR & FM (July) – ANK (Sept.)\*\*\* (K. Roberts & C. Francoz).



**Orthomosaic and DSM**  
 Generated with Pix4Dmapper Pro (version 4.0.25) –

**MR & FM (50.17ha):**  
 138 Sampled images from CanonIXUS220HS\_4.3\_4000x3000 (RGB)  
 average ground sampling distance of 4.44 cm+ Average density 38 m<sup>3</sup>  
 sampled points 15577712  
 RSME ± 0.032m (x,y,z)

**ANK (29.74ha):**  
 793 Sampled images from FC330\_3.6\_4000x3000 (RGB)  
 average ground sampling distance of 3.12 cm+ Average density 106.25 m<sup>3</sup>  
 sampled points 52768113  
 RSME ± 0.015m (x,y,z)



All topographical survey dataset (Table 3-8) collected in this thesis was reprocessed to assess accuracy and assure uniformity. Further details on data assessment, precision and accuracy are discussed in Appendix B-3.

All data captured during this project provided a RMSE (x, y and z) ranging from 0.007m to 0.054m (Table 3-7), but there are large differences depending on the dataset or methods used (see details on data selection in Appendix B-3). It was decided to quantify accretion and erosion for three saltmarsh sites between 2011 to 2017 using dataset summarised in Table 3-9 below.

**Table 3-9: Summary of the dataset available to analyse topographical changes (small-scale mapping) on the saltmarsh sites (\* in ArcGIS).**

	<b>Resolution*</b> <b>(in m)</b>	<b>MR</b>	<b>FM</b>	<b>ANK</b>
2011 Lidar	1*1	✓	✓	✓
TLS 2014	0.1*0.1	✓		
TLS 2015	0.1*0.1	✓		
TLS 2016	0.1*0.1		✓	✓
TLS 2017	0.1*0.1		✓	✓
Orthophotography 2017	0.1*0.1	✓	✓	

Each survey dataset was post-processed (to assess uniformity and extent, noise removal, etc.) in CloudCompare (3D point cloud processing software *from* [www.danielgm.net/cc/](http://www.danielgm.net/cc/)) and time series DEM changes generated in ArcGIS using the GCD toolbox package. The analysis of the DEMs involved three steps of data analysis as presented by Wheaton et al., (2010) and Eamer and Walker (2013) (see further notes in Appendix B-3):

- statistical review of the survey accuracy and precision using Geostatistical analyst toolbox for ArcGIS;
- use of statistics to clusters of significant deposition and erosion relative to the mean to generate geomorphic changes maps (area and volume);
- generation of height differences maps based on cells subtraction from two DEM surfaces following Montané and Torres (2006), Chassereau et al. (2011) and McClure et al. (2016).

DEMs analysis results are presented in Chapter 5 – 5.3:

- section 5.3.1 reports on two cross-sections profiles generated from two targeted transects crossing 1) FM and MR and 2) ANK (as depicted in red lines on Figure 3-15) which were selected to represent spatial heterogeneity in saltmarsh zones, proximity and distance to the saltmarsh edge and high water mark, elevation, salinity and sediment depositional environment (marine and riverine). The transect profiles are aimed to provide details on the lateral and vertical evolution dynamics of the natural and managed salt marshes.

- section 5.3.2 reports on overall DEM surface changes that occurred from 2011 to 2017 using the same datasets as section 5.3.1.

### 3.4.2.2 Sedimentation rates (accretion and erosion) using sedimentation plates

Sedimentation plates data comes from 2.14 years of direct observations of sedimentation plates inserted beneath the saltmarsh surface from 30<sup>th</sup> July 2015 (for MR) and 05<sup>th</sup> November 2015 (on FM and ANK) until 20<sup>th</sup> September 2017 (see Table 3-3 and Figure 3-29).

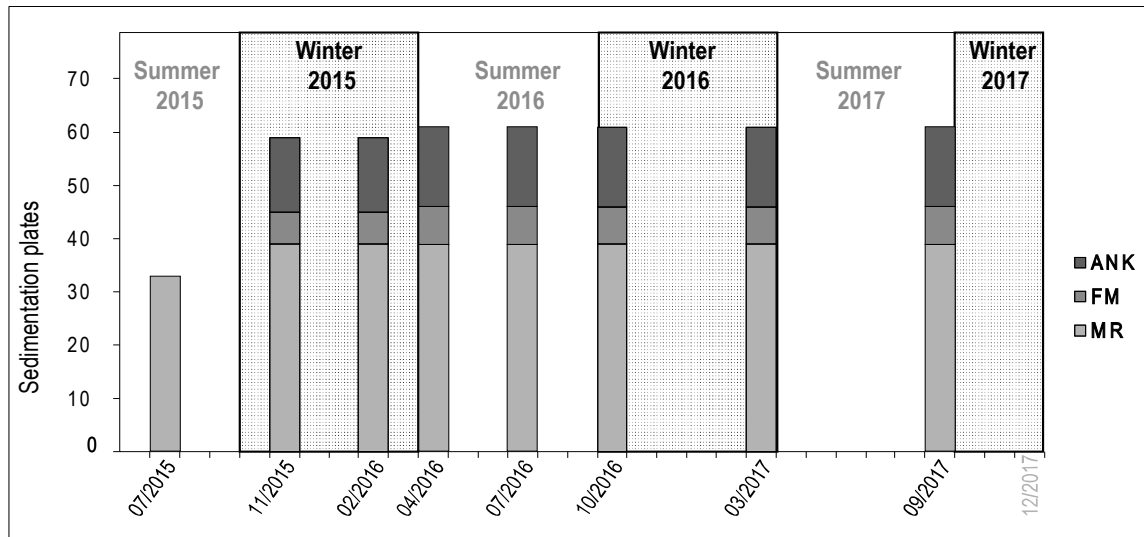


Figure 3-29: Number of monitored sedimentation plates (y-axis) per sites for each survey campaigns between 30<sup>th</sup> July 2015 to 20<sup>th</sup> September 2017 and showing seasonal sampling for 2 winters (October to March) and 2 summers (April to September) season.

The amount of vertical saltmarsh sedimentation (accretion and erosion) is measured using sedimentation plates (n=60) measure. They are made of a firm plate made of metal (Stokes et al., 2010) or plastic (French and Burningham, 2003) buried horizontally in the soil under the saltmarsh turf, or, inserted into and exposed vertical marsh edge such as a creek bank. The principal requirement is that the plate be horizontal and settled for at least a month before measurement starts (Stokes et al., 2010).

The 400 cm<sup>2</sup> (20x20 cm) plates used here were formed of a 3mm thick aluminium sheet with 64 (8x8) drilled holes to allow water movement and root development. Soil was excavated as a monobloc using a flat spade to a size slightly greater (10-20%) than the plate and to below root depth to the first soil horizon ( $\mu 12.9 \pm 0.21$ ) to minimise rooting disturbance. The soil and plants were carefully replaced (Figure 3-31.b to d). Each plate was pinned securely to the surface, one plate on the fronting marsh (FM4) had to be repositioned in February 2016 to a more stable position (0.2m east and 0.5 north). The exact geolocation of the plates prior burial used a DGPS1200 (Leica Viva) for the corners of each plate (Figure 3-32). Once reinstated, a bamboo cane was placed to

help relocation. Once buried, a further two points, in the plate centre and c.50 cm east of the centre, were surveyed then using DGPS and these exact points were revisited and recorded during each survey campaign (Figure 3-30).

Although three permanent base stations were set up on the sites, the DGPS vertical height accuracy averaged c.0.013 m (across 2.2 years) could not be used to quantify sedimentation rate alone. Thus, the plate depth of the four corners and centre of each plate was also measured using a graduated metal rod (graduated knitting needle). The aluminium plates were installed during filed campaign with a first set (n=39) on the MR in July 2015 and a second set was placed on FM (n=6) and ANK (n=15) in September 2016 (Figure 3-32). Based on research work demonstrating that sedimentation plates should settle first (Stokes et al., 2010; Nolte et al., 2013), a period of three months was given before measurements were taken on the three salt marshes. Thereafter measurements were taken 3-monthly until the end of 2016 and then 6-monthly during the year 2017– See also 3.3.2.3. Five measurement points (four corners and centre) per plate are averaged to produce one value per plate over 2.2 years.

Cumulative surface elevation changes with respect to an initial control observation were calculated for each plate providing and a sedimentation rate (calculated using the ratio of the average change in surface elevation, representing the accretion and erosion, to time lag). The sedimentation plates were spatially distributed across the study sites according to the sampling (details in 3.3.2.2) and to be evaluated in relation to the major physical variables (3.3.2.3). The results are presented in Chapter 5 – 5.4.

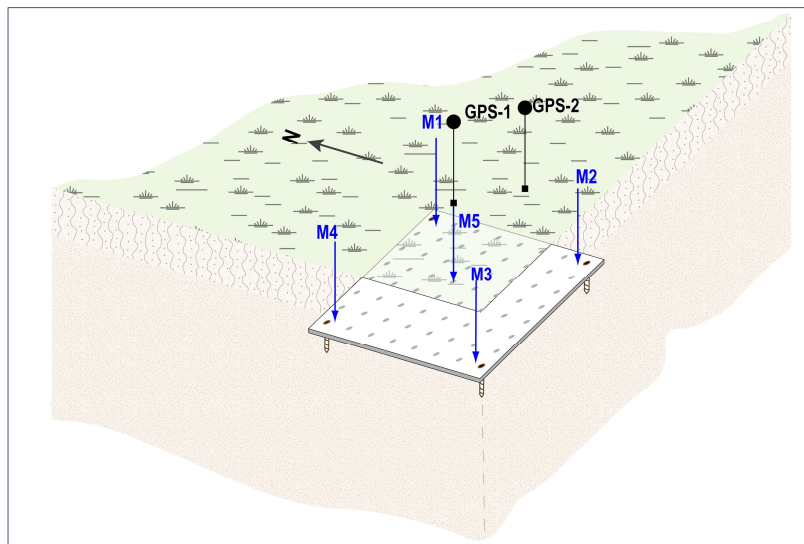


**Figure 3-30: Diagram of 20 X 20 cm sedimentation plates once inserted depicting the location of manual measurements in blue using a graduated metal rod from M1 to M5 and DGPS survey from GPS1 & GPS2 in black. These manual measurements formed the empirical data used to calculate surface elevation change representing accretion and erosion and sedimentation rates for the three salt marshes.**





a)



b)



c)



d)

Figure 3-31 a) General view of the saltmarsh vegetation photography using 1 m<sup>2</sup> quadrat prior the insertion of the sedimentation plates (photograph a) taken in July 2015 in high-marsh sampling plot MR2 b) c) & d) depict the three stages of the 20 X 20 cm sedimentation plate insertion (photograph b) on mid-marsh sampling plot MR22 and photograph c) & d) on low-marsh plot MR57).

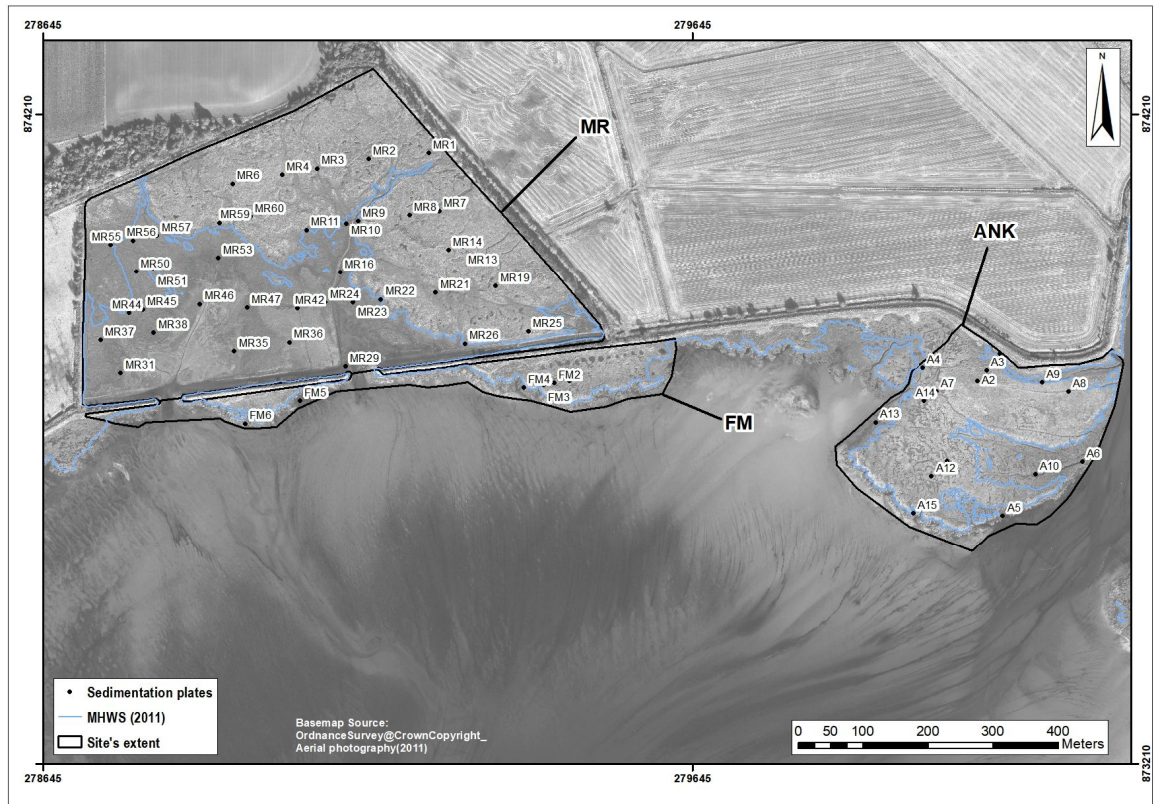


Figure 3-32: Spatial distribution of sedimentation plates on the three studied salt marshes showing MHWS (blue) derived from 2011 LIDAR.

### 3.4.2.3 Multi-annual vegetation monitoring

Vegetation monitoring occurred from July 2015 until September 2017 together with the sedimentation plate monitoring (Figure 3-29 and Table 3-3). 1 m<sup>2</sup> quadrats (n=60) were placed along a N/S axis 1m north of the central point of each sedimentation plate (general view of the quadrats placement on Figure 3-31a) allowing the frame to be exactly relocated to ease processing (and rectification of digital photography when necessary). It is important to note that the digital photography was first designed to:

- i) establish vegetation classification for all sampling plots (n=60) where sedimentation plates (Figure 3-32) had been inserted;
- ii) provide a multi-annual photographic record of the vegetation to assess the percentage changes of bare ground and vegetation cover as described in 3.4.1.2.

The vegetation distribution was first assessed in the field by eye and 1 m<sup>2</sup> quadrats recorded using digital photography. The dataset provided species identification and classification according the National Vegetation Classification (NVC) using TABLEFIT program (see details above in 3.3.2.2 - Research baseline NVC vegetation assemblages). However, the second aim (ii) using digital photography, detecting changes in vegetation cover over the timescale used here was problematic due to seasonal change in colour due to winter die-back, which were greater than the overall changes observed. It is possible that method may be better suited to only saltmarsh shore fronts and pioneer zones, e.g. Langlois et al. (2003) study of influence of *Puccinellia maritima* on sediment deposition. Therefore, the photographs from 16<sup>th</sup> & 17<sup>th</sup> July 2016 formed the only dataset used and presented in this thesis given that it closely coincides with the biomass harvesting (4<sup>th</sup> July 2016) used to quantify the saltmarsh short-term dynamics (3.4.2.1) and provided a baseline for vegetation distribution used for this research project.

### **3.4.3 Belowground long-term saltmarsh bio-geomorphic properties: organic and inorganic content.**

Saltmarsh belowground soil constitutes a repository of past saltmarsh processes that may be detectable in changes in physical and biological properties. Furthermore, it has been well established that organic matter (OM) storage in saltmarsh sediment is influenced by sediment physical characteristics (Dyer, 1989; Packham and Willis, 1997; Killops and Killops, 2004; Andrews et al., 2006; Hyndes et al., 2014; Roner et al., 2016), facilitates vertical soil accretion,

maintains relative elevation as sea level rises and is critical to saltmarsh sustainability (Chmura et al., 2003; Mudd et al., 2009; Yu and Chmura, 2009). As sediments form crucial links with tidal processes (Dyer, 1989), measurements of the past belowground inorganic and organic content provide a means to address the thesis aim to improving understanding of the sedimentary and biological development of natural and managed salt marshes. Specifically, evaluating the past biogeomorphic processes salt marshes of Nigg Bay allows an improved understanding of saltmarsh response to changes (anthropogenic or environmental) over time and any links to changes in belowground inorganic characteristics and organic storage. This informs saltmarsh function and how its evolution contributes as an ecosystem to provide regulating (ability to keep pace with relative sea-level rise (SLR)) and supporting services (blue carbon sequestration through saltmarsh sediments) as defined in Chapter 2 – 2.3.3.

Long-term saltmarsh evolution was investigated to address:

- Spatial variations: Are there identifiable patterns in the belowground processes? Do they differ between natural and managed salt marshes and between saltmarsh zones?
- Temporal sediment variations: are there changes in the belowground processes through depth? Can they inform on saltmarsh formation and response through time to anthropogenic disturbances (such as reclamation and/or breaching)?
- Dynamic variations: do belowground physical properties of the sediment influence biological characteristics and vice versa?

The empirical work was split in two strands of work:

- Measuring **organic** content changes (section 3.4.3.2.) through shallow coring (average depth  $50.1 \pm 2.1$  cm) programme spatially distributed across the sites by:
  - quantifying soil organic matter (SOM) using Loss-on-ignition (LOI);
  - quantifying carbon content derived from SOM.
- Measuring changes of **inorganic** content (section 3.4.3.2.) and sediment physical characteristics (section 3.4.3.3.) through shallow coring (average depth  $50.1 \pm 2.1$ ) spatially distributed across the sites by:
  - quantifying soil dry bulk density (BDD) and soil water content;
  - quantifying soil inorganic content (SIC) using Loss-on-ignition (LOI);
  - quantifying carbon content derived from SIC;
  - characterising physical properties of the saltmarsh sediments using a subset of cores (average depth  $67.9 \pm 4.3$ ).



Cores collection was executed across 2 days (19th and 20th April) and aimed to retrieve cores that could be used for traditional geomorphic analysis and Luminescence analysis (3.4.4). It was not known at the time of collection if the application luminescence techniques (a technique that is light sensitive) would be successful on Nigg saltmarsh sediments, therefore wider cores were collected protected from light exposure (3.4.3.1.). Belowground fieldwork and methodology are summarised in Table 3-3 and further developed in section 3.4.3.2 and 3.4.3.3.

#### 3.4.3.1 Coring sampling strategy

A series of four corers (see Figure 3-33) were tested in February 2016 to evaluate if coring compaction could be minimised, transportation eased across the salt marshes and if the corers could work on different soils including waterlogged, dry, sand and clay. A further condition was required to keep the cores protected from light exposure and so permit a subset to be used for Optically Stimulated Luminescence (OSL) (section 3.4.4). From a total of thirty-two cores collected (Figure 3-35):

- Nineteen cores were recovered using an adapted Russian corer fitted with a 1m long and 5 cm diameter PVC tube (Figure 3-33b), to core down to an average depth of  $0.5\pm 0.1$  m;
- Three cores were recovered using corer that allowed an 11cm diameter core to a maximum depth of 0.3 m (see Figure 3-33a). Although, this corer prevented compaction, but could not be fitted with protection tube of any sort to keep the core intact and shield it from light;
- Nine cores were recovered using a bespoke corer, designed for this project, to combine the advantages of the two above cores and allow sediment cores to be transported undisturbed and shielded from light. The new design (see Figure 3-33a) was created to fit a 1m long and 8 cm diameter PVC tube to allow easy changes on site and transport across the marsh. The maximum length of 1 m was based on random sediment probing of the saltmarsh zones to a depth beyond the organic matter horizon is replaced by coarse sand. Therefore, the cores were excavated down to refusal depth, in this study to a maximum depth of 0.87 m and averaging at  $0.7\text{m}\pm 0.4$  cores. However, fieldwork in water saturated zones such as pioneer zones proved difficult (see A.4) and using powered Vibrocorer that are often used when sampling sand/mud- flats may provide better results.

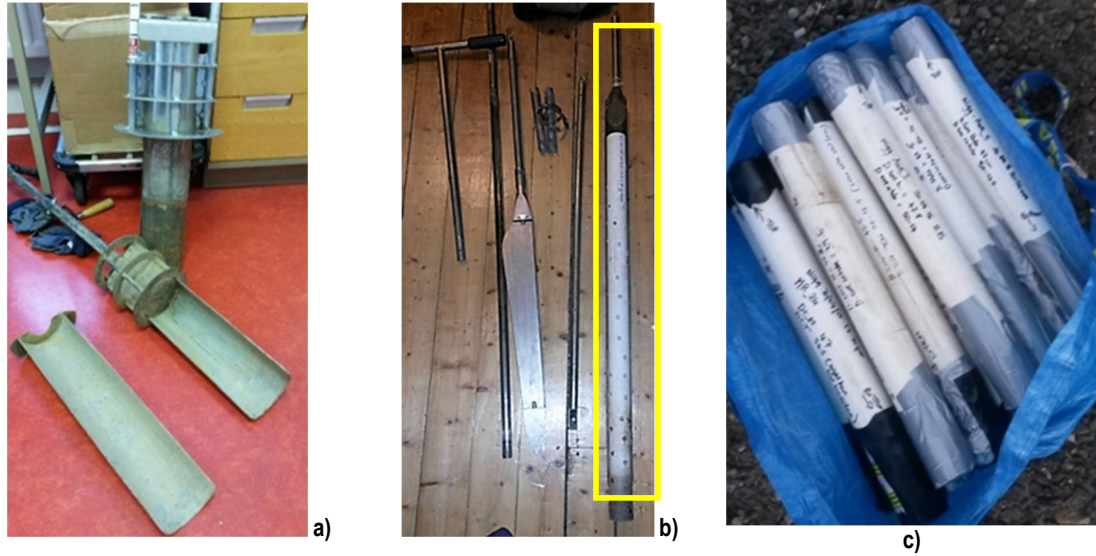


Figure 3-33: a) Corer tested in February 2016 to retrieve 30 cm deep and 11 cm of diameter cores proved to ease manual coring, provide wide cores to reduce soil compaction and allow multiple aliquot sampling and analysis

. b) Traditional manual gouge auger was also used (left on image) and an adapted version fitted with 1m long and 5cm diameter PVC tube (in yellow box) was finally chosen for Organic and Inorganic content measurements

c) 18 of the 23 ready to be analysed to provide long-term storage capacity of salt marshes.

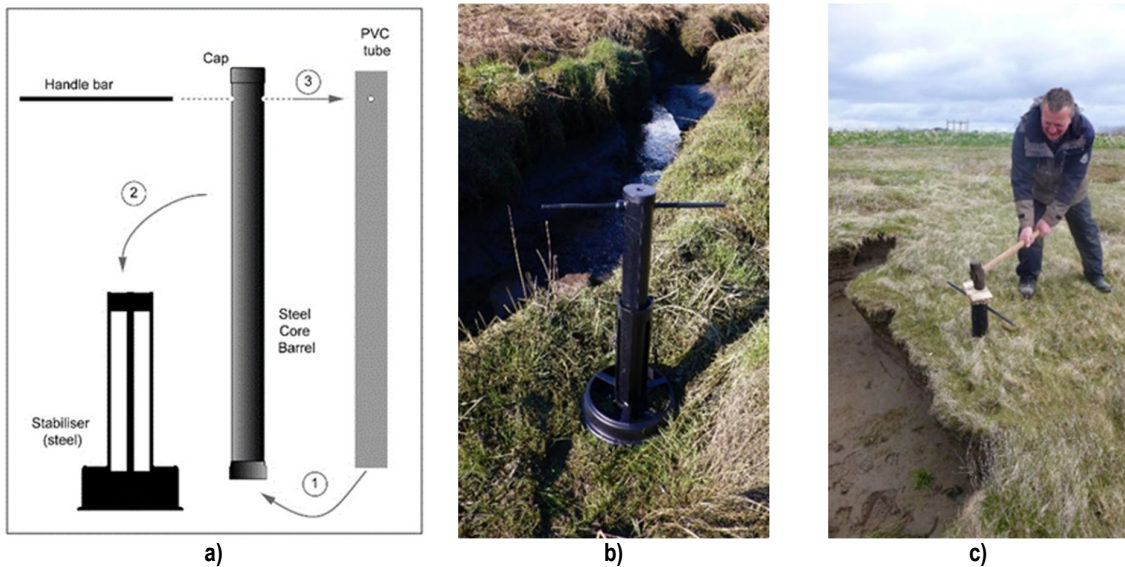


Figure 3-34: a) In-house bespoke manual corer designed to insert a 1m long and 0.08m diameter PVC tube into sealed steel core barrel for easy assemblage, transportability and protection from light. b) The corer prior to coring c) coring on the FM salt marsh in April 2016.

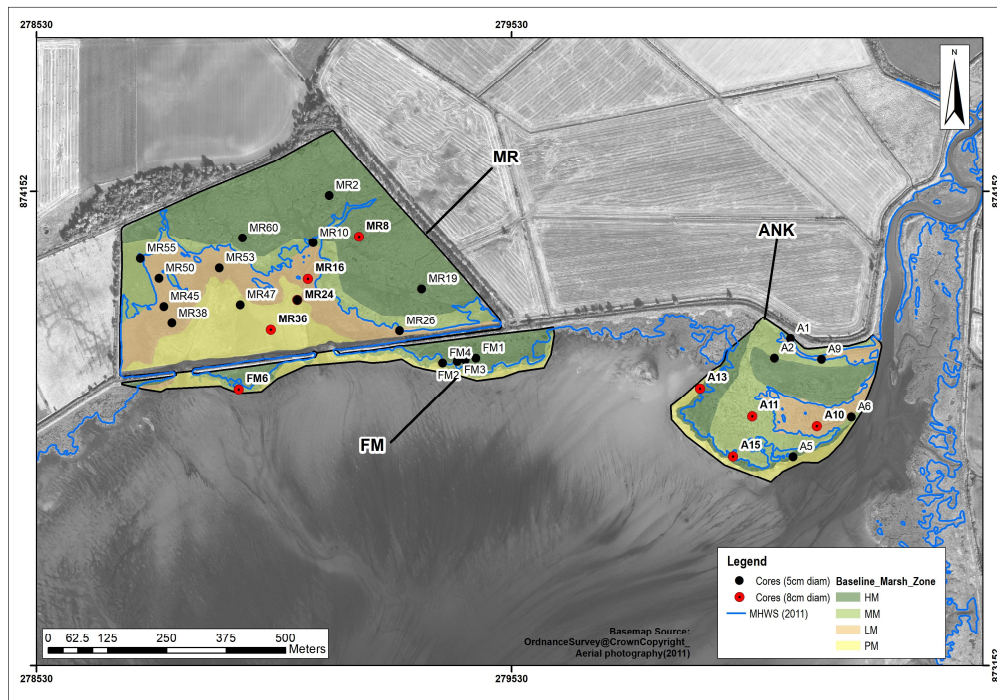


Figure 3-35: Cores sampling location addressing biogeomorphic properties of the three studied salt marshes overlaid on saltmarsh zones and 2011-MHWS (blue line).

Core compaction is an issue in saltmarsh sediment coring. When compiling a dataset of 5075 wetland samples, Morris et al (2016) have found that the coring operation was the most significant source of error when estimating bulk dry density and Loss-on-ignition (LOI) in sediments. In this research project (Table 3-3), there was no significant relationship between core compaction and the depth of the core (using One-way ANOVA of  $\log_e$  transformed data to ensure normality produced  $F=2.53$ ,  $p\text{-value}=0.08^*$ ) but the compaction differed significantly due to core diameter ( $F=15.6$ ,  $p<0.001^{***}$ ), demonstrated for ANK ( $F=27.1$ ,  $p<0.01^{**}$ ) and MR ( $F=15.6$ ,  $p<0.01^{**}$ ) sites but not found on FM ( $F=1.39$ ,  $p=0.35$ ) (Figure 3-36).

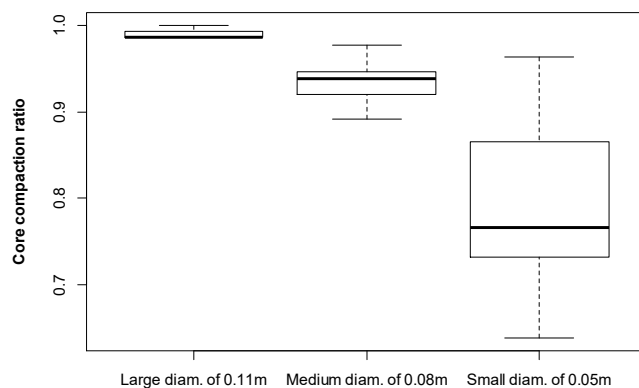


Figure 3-36: Box plot showing the overall coring compaction ratio (real depth/tube depth) from the different coring devices sizes.

Table 3-10: Overall compaction ratio for the different coring devices used during the project.

Core diameter	Mean	SD	Sample Size
0.11m	0.99	0.007	3
0.08m	0.93	0.026	8
0.05m	0.79	0.093	18

As it is not always possible to use a large diameter core to pre-empt coring compaction errors, an overall correction factor derived from the ratio between the length of the core tubing and soil column is generally applied (i.e. Schindler et al., 2014a). However, during the coring program, it became apparent that compaction was not homogenous across the cores, so compaction was measured at regular intervals (c.10cm) to spread the error more accurately and regularly across the core's stratigraphical units. As shown on Figure 3-37, applying an overall correction factor may adversely affect a part of the core with little or no compaction.

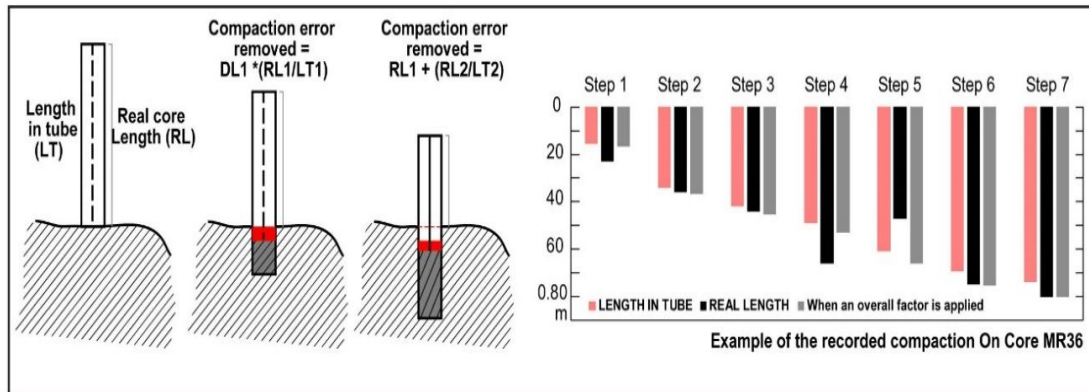


Figure 3-37: A stepped coring compaction approach where the error is removed at regular intervals through the core. The bar graph (right) shows real depth of core (black), recorded depth in the tube (red) and how overall compaction factor may not be the best option (eg at Depth 4 and Depth 6).

The compaction error was then removed as follows:

- . Step 1:  $Length\ 1\ of\ tube * \left(\frac{length\ 1\ of\ the\ core}{length\ 1\ of\ the\ tube}\right)$
- . Step 2:  $Length\ 1\ of\ the\ core + \left(\frac{length\ 2\ of\ the\ core}{length\ 2\ of\ the\ tube}\right)$
- . Step 3 :  $Length\ 2\ of\ the\ core + \left(\frac{length\ 3\ of\ the\ core}{length\ 3\ of\ the\ tube}\right)$  and so on.

Roner et al. (2016) show that all available methods to determine of soil organic and inorganic matter (SOM and SIM) have limitations. The samples can be treated using Hydrogen Peroxide (H<sub>2</sub>O<sub>2</sub>) only or using H<sub>2</sub>O<sub>2</sub> and sodium hypochlorite (NaClO) or LOI analyses which the most widely used procedure as it can be applied to a larger number of samples that can be re-used for particles size analysis (Roner et al., 2016). For this reason, LOI was preferred to other methods as it allowed measure both for the same sample organic (section 3.4.3.2) and inorganic (section 3.4.3.3) content.

### 3.4.3.2 Analysis of belowground organic and inorganic content

The bio-geomorphic (physical, organic and inorganic) and spatial soil properties of the three salt marshes:



- were defined by a subset of the sampling plots (n=23) used for aboveground sediment and vegetation dynamics (n=60) using ArcGIS spatial stratified random sampling as per described in section 3.3.2.2 (Figure 3-35).
- changes in sediment organic and inorganic content were assessed via 23 undisturbed shallow (<60cm) cores (Table 3-3).

In total, twenty-three cores were used for the measurement of organic matter and inorganic content (Table 3-11). The cores were sliced longitudinally in two halves in the laboratory and divided into 1cm (for n=5) and 2cm (n=18) intervals to reflect a putative sedimentation rate of 1 to 2 cm.yr<sup>-1</sup> and provided a total of 608 samples with depths corrected for compaction (see 3.4.3.1).

**Table 3-11: Summary of number of cores and samples retrieved across the sites and saltmarsh zones. \* see section 3.4.3.1.**

	Number of cores				No of samples
	HM	MM	LM	PM	
ANK	2	3	2	2	257
FM	2	1	*	*	103
MR	4	1	4	2	248

LOI is a simple and rapid method of assessing organic matter and inorganic (BDD, water and carbonate) content in soils using sequential heating of the samples in a muffle furnace. After sediment is dried to remove water content, the organic matter is burned to ash and carbon dioxide and the weight loss is proportional to the amount of organic carbon contained in the sample (Heiri et al., 2001). Carbon dioxide is evolved from carbonate (leaving oxide) when LOI procedure reaches higher temperatures from 800 to 1000°C (Santisteban et al., 2004). Standard protocol may be used, but it has been demonstrated that one-fits-all methodology may lead to unprecise and erroneous results (Plater et al., 2015) and an accepted standardised LOI procedure for wetland studies is still lacking (Roner et al., 2016).

The quantification of belowground soil properties addresses:

- changes in water content (INORGANIC). This reflects alteration in the sedimentary environment through time such as dewatering (as a result of reclamation for instance) and increases soil density and reduces porosity (Tempest et al., 2015); flooding (as a result of breaching the embankment and sea level rise) accelerates downwash of fine particles into the subsurface (Boorman, 2003);
- changes in dry bulk density (also referred as autocompaction) - BDD (INORGANIC) has a direct impact on the calculation of sediment accretion rates (3.4.1.2), sediment dating (Madsen et al., 2007; Madsen et al., 2011), surface elevation change (Allen, 2000)

representing sedimentation rates and estimation of belowground carbon densities. Autocompaction increases with depth, however soils with a high proportion of pore space to solids such as mud have lower bulk dry densities than those that are more compact and have less pore space such as sand (Allen, 2000; Davies, 2001; Davis and Dalrymple, 2012; Schindler, Karius, Arns, et al., 2014);

organic matter (ORGANIC) and carbonate content (INORGANIC) has a direct connection to quantification of saltmarsh carbon. The methodology chosen for LOI and duration of temperature of loss-on-ignition (LOI) methods was based on existing literature (Ball, 1964; Craft et al., 1991; Sutherland, 1998; Heiri et al., 2001; Santisteban et al., 2004; Roner et al., 2016; Aitkenhead and Coull, 2016), yet there are serious concerns using LOI to estimates organic matter (OM) and soil organic carbon (SOC).

LOI methodology to measure inorganic and organic content in Nigg saltmarsh sediments is further described in Appendix A. A-5.

Soil Organic Matter (SOM) was calculated using standard procedure (difference between dry and combusted soil weights) based on Ball (1964) work and expressed in percentage. Craft (1991) quadratic equation was used to translate SOM into soil organic carbon densities (SOC) using a conversion factor of  $0.40 \pm 0.01$  (Table 3-14). Finally, soil inorganic (carbonates) content (SIC) content used Heiri (2001) procedure for LOI and carbon content calculation followed the work of Santisteban (2012). This sequential LOI procedure calculation are presented in Table 3-12 as follows:

**Table 3-12: Summary of calculation used for Organic and Inorganic Carbon content estimations.**

	Steps	Equation
<b>Water</b>	1a	$\% \text{ Water Content}_{60^{\circ}\text{C}} = \left( \frac{\text{mass}_{\text{wet}} - \text{mass}_{60^{\circ}\text{C}}}{\text{mass}_{\text{wet}}} \right) * 100$
<b>BDD</b>	1b	$\text{BDD}_{\text{g/cm}^{-3}} = \frac{\text{mass}_{105^{\circ}\text{C}}}{\text{volume}_{\text{cm}^{-3}}}$
<b>SOM</b>	2a	$\% \text{ LOI}_{375^{\circ}\text{C}} = \left( \frac{\text{mass}_{60^{\circ}\text{C}} - \text{mass}_{375^{\circ}\text{C}}}{\text{mass}_{375^{\circ}\text{C}}} \right) * 100$
	2b	$\% \text{ LOI}_{450^{\circ}\text{C}} = \left( \frac{\text{mass}_{60^{\circ}\text{C}} - \text{mass}_{375^{\circ}\text{C}}}{\text{mass}_{375^{\circ}\text{C}}} \right) * 100$
<b>SIC</b>	3	$\% \text{ LOI}_{800^{\circ}\text{C}} = \left( \frac{\text{mass}_{450^{\circ}\text{C}} - \text{mass}_{800^{\circ}\text{C}}}{\text{mass}_{60^{\circ}\text{C}}} \right) * 100$

These calculations have therefore direction implications in the results proposed in this thesis:



- 1) BDD (or autocompaction) is an important factor to consider as it may introduce large error into the calculation of vertical sediment accretion rates (Allen, 2000; Davies, 2001; Davis and Dalrymple, 2012; Schindler, Karius, Arns, et al., 2014);
- 2) Blue carbon stocks/budget by combining aboveground OC (3.4.1.2) and belowground SOC and SIC and provide estimates of carbon sequestration rates using accretion rates.

Recent work on assessing Blue Carbon stocks not only for salt marsh but also mangroves, salt marshes, and seagrass meadows across the world (Howard et al., 2014) proposes to calculate Blue Carbon budget by estimating each different carbon pool that exists within the system as presented in Table 3-13.

**Table 3-13: Combining Carbon Pool to estimates Blue Carbon stocks (Howard et al., 2014).**

			Thesis research
<b>Carbon Pool 1</b>	Aboveground living biomass (shrubs, grasses, herbs, etc).	Most dead aboveground biomass is taken by tides and is excluded without compromising accuracy (Howard et al., 2014)	Aboveground Biomass Carbon (OC)
<b>Carbon Pool 2a</b>	Belowground living biomass where primary productivity is generated by roots and rhizomes	Most carbon in tidal salt marsh is stored belowground which includes the living belowground biomass and the sedimentary pool, and as the two pools are difficult to separate, it has been established that they can be calculated as one single pool without altering accuracy (Chmura et al., 2003; Howard et al., 2014).	Soil Organic Carbon (SOC) +
<b>Carbon Pool 2b</b>	Belowground sediment		Soil Inorganic Carbon (SIC)

To provide blue carbon storage estimates for the salt marshes of Nigg Bay, the mineral and organic mass needs to be converted to a volume (density) of sediment, using a similar method for studies of vertical sediment accretion (Howard et al., 2014; Morris et al., 2016). This conversion is calculated using bulk dry density (BDD) values for each sample. Details on regression and resulting dataset adjustments between LOI at 375°C & 450°C Versus BDD are detailed in Appendix E – E3. The calculation steps used in this thesis to provide a Blue Carbon budget is presented in Table 3-14.

**Table 3-14: Calculations for total Blue Carbon Stock. Aboveground allometric equation is based in Howard et al.(2014) and belowground allometric equation is based on Craft et al. (1991).**

<b>Carbon Pool 1</b>	<b>OC</b>	Carbon in Aboveground Living Biomass in gm <sup>-2</sup> (in 3.4.1.2)	$\text{Biomass}_{\text{g.m}^2} = \frac{\text{plant dry weight}_{\text{in g. at } 80^\circ}}{\text{plot area}_{\text{m}^2}}$
			$\text{OC}_{\text{g.m}^2} = \text{Biomass}_{\text{g.m}^2} * 0.45$
	<b>Vegetative Total carbon</b>	Total carbon in tC.ha <sup>-1</sup>	$\text{tC.ha}^{-1} = \text{OC}_{\text{g.m}^2} * ((1\text{t}/1000000\text{g}) * (10000\text{m}^2/1\text{ha}))$

<b>Carbon Pool 2a+b</b>	<b>SIC</b>	Soil Inorganic Carbon	$SIC_{\%} = (LOI_{800^{\circ}C}) * 0.273$
	<b>SOC</b>	Soil Organic Carbon Content	$SOC_{\%} = ((0.40 \pm 0.01) * (LOI_{450^{\circ}C}) + (0.0025 \pm 0.003) * (LOI_{450^{\circ}C})^2) - SIC_{\%}$
		Soil Carbon density	$SOC_{g.cm^3} = BDD * (\frac{SOC_{\%}}{100})$
	<b>Soil Total carbon</b>	Total carbon per core in tonneC.ha <sup>-1</sup>	$Core\ Carbon_{g.cm^3} = \sum_{n=1}^{Core\ depth} SOC_{g.cm^3} * interval\ thickness_{cm}$ $Core_{tC.ha^{-1}} = (Core\ Carbon_{g.cm^3}) * (\frac{1t}{100000g}) * (\frac{100000000\ cm^2}{1ha})$

### 3.4.3.3 Sediment physical characteristics: Particle size analysis

Chapter 2 showed how physical characteristics stored belowground may reflect past sediment input and sources (tidal and estuarine influences) (Reed, 1989; Temmerman, Govers, Wartel, et al., 2003; De Groot et al., 2011) as well as the long-term sediment availability necessary to maintain saltmarsh elevation on sea level rise (Allen and Duffy, 1998; Allen, 2000). Sediment type differs across the marsh and is important to understand retention capacity where fine grains reduce soil porosity and influence vegetation growth (Yang et al., 2008; Mudd et al., 2010)

The spatial physical properties of the three saltmarshes sediments were defined and assessed by a subset of cores (n=9). Because both the MR36 and MR24 cores are located in PM zones, only the MR24 core was used, resulting in a total of 8 cores studied. Organic and inorganic content (cores n=23, section 3.4.3.2) was analysed along two transects crossing FM, MR and ANK as depicted Figure 3-38. These transects were selected to represent spatial heterogeneity in saltmarsh zones, proximity and distance to the saltmarsh edge, elevation, high water mark and sediment depositional environment (marine and riverine).

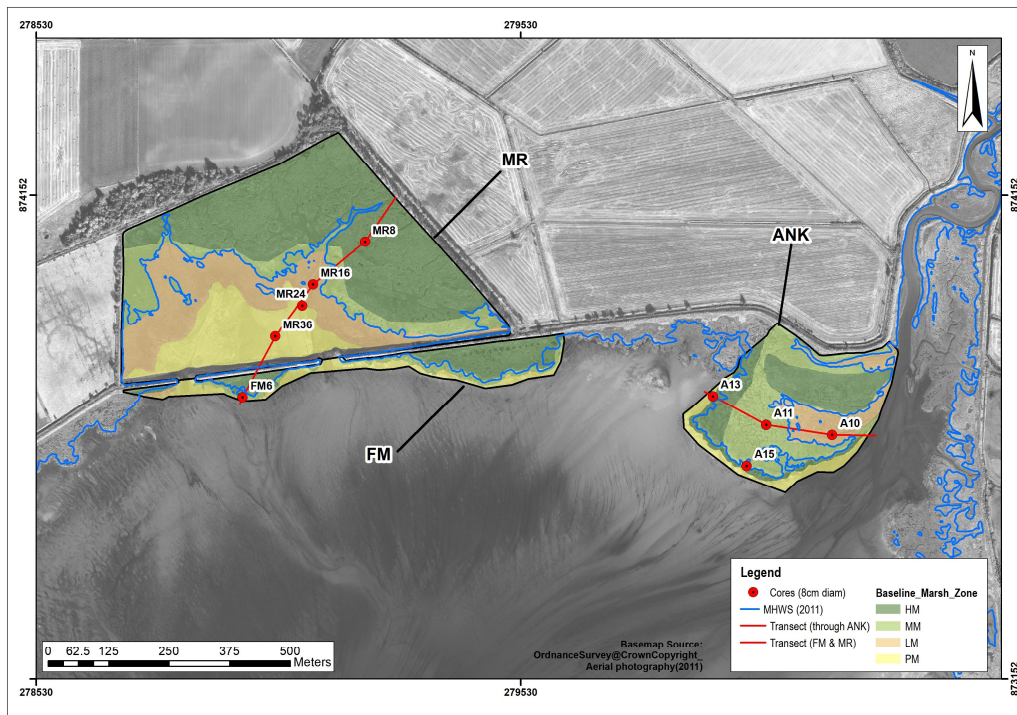


Figure 3-38: Spatial distribution of cores sampling location addressing physical characteristics on the three studied salt marshes showing saltmarsh zones and MHWs derived from 2011LIDAR (blue line). Note that MR36 and MR24 are both located in PM zones, only MR24 was used for analysis. Red lines present the two transects running axis.

These subsets of the cores used for organic and inorganic (3.4.3.2) were sliced longitudinally in two halves in the laboratory and divided 2cm (n=18) intervals. All depths were corrected for compaction (see 3.4.3.1). Each sample was dry sieved up to 2 mm, ready for fine-fraction size distributions analysis using laser diffraction spectroscopy with a Coulter LS230 Variable Speed Fluid Module.

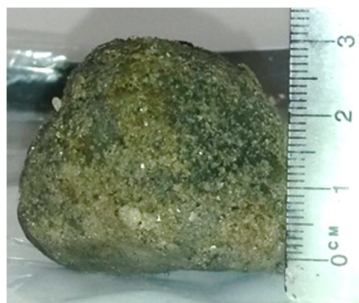


Figure 3-39: Pebble retrieved 52cm deep in Core A13.

Only one core presented material larger <2 mm, located in PM of ANK, core A13 contained a pebble retrieved 45 cm in depth (Figure 3-39). Geomorphologically relevant and informs intertidal composition pre-dating saltmarsh formation, the sample was removed from the analysis to avoid bias.

The laser diffraction technique is based on the theory of light scattering where a laser beam is scattered by particles and the angle of the light scattering is inversely proportional to particle size. For instance, small particles size will be associated with a large angle of light scattering. Similarly, the intensity of the light diffraction varies depending the particle sizes where high intensity is linked to large particles sizes. Because the samples vary widely in size and shape, the instrument is equipped with 127 detectors placed on lenses to permit detection of particles sizes ranging from

0.40 $\mu\text{m}$  to 2mm. The Coulter LS230 data was interpreted using the Fraunhofer model and does not require knowledge of the optical properties of the sample to provide accurate results for particles larger than 10 $\mu\text{m}$ .

Physical characteristics were statistically analysed to present the mean, median, D(p,q), SD, variance, Skewness, Kurtosis and percentiles of the 0-3.9  $\mu\text{m}$  (**clays**), 3.9-63  $\mu\text{m}$  (**silts**), 63-156  $\mu\text{m}$  (**very fine sand**), 156-312  $\mu\text{m}$  (**fine sand**), 312-625  $\mu\text{m}$  (**medium sand**), 625-1250  $\mu\text{m}$  (**coarse sand**), and 1250-2000  $\mu\text{m}$  present in the cores.

Although the use of the Coulter laser diffractor is faster than the pipette method analysis of fine-fraction size distributions, the accuracy and precision can only be achieved with a rigorous and consistent protocol. This was ensured at different stage through the analysis:

- Sample preparation. The finer material (<2mm) was split and placed a beaker to soak in water with 3-5% solution of sodium hexametaphosphate (Calgon) to prevent flocculation. The wet fraction was placed in an ultrasonic bath for a 15minutes and then kept in suspension using a magnetic stirrer until pipetted in the instrument water column compartment.
- Density of the sample. Obscuration index (PIDS) allows to keep the suspended sample density within a range no to clog and block the system. This level although determined by the machine is generally around 40-50% when there is high clay content.
- Instrument reproducibility. Every hour, an automatic background check was run to check and readjust the laser detectors offsets and to check the detector array alignment. Before each sample measurement, the machine is rinsed, and the instrument calculates a background scatter pattern of the water column that can be accounted by the software.
- Operator Settings. Depending on the type of samples (sand, silt or clay) the fluid pump settings had to be set to the appropriate speed (between 62 to 40). For five of these cores, 3 sample runs were evaluated, and upon these results it was deemed sufficient to use 2 runs per sample to ensure reproducibility of the model analysis.

#### **3.4.4 A new application of Optically Stimulated Luminescence - OSL techniques to explore saltmarsh dynamics**

Several geo-chronology dating tools are available, but only some of these are suitable for application to the research questions in this specific study area. As seen in section 3.3.1, there are few techniques that enable the measurement of longer-term properties of saltmarsh sedimentation directly. Radiocarbon dating requires autochthonous organic material present in sediments not younger than c.450 years (due to past atmospheric production of  $^{14}\text{C}$ ). Techniques using natural

fallout radionuclides  $^{210}\text{Pb}$  or artificial radionuclides such  $^{241}\text{Am}$  and  $^{137}\text{Cs}$  are, on the other hand, used to date directly deposited sediment of an approximate age of 150 year old. Recent progress in radiometric studies has shown that burial age of younger coastal sands (c.100 years) can be accurately determined using Optically Stimulated Luminescence - OSL techniques (Madsen et al., 2005). Application of luminescence dating of intertidal deposits has been successful to establish a chronology and reconstruct paleo-environmental landscape evolution in relation to sea-level changes (Fruegaard et al., 2015; Mauz et al., 2010) and to get a high-resolution chronological reconstruction (Cordier, 2010; Sanderson and Murphy, 2010). Further progress in OSL has also shown the potential to date young sediments but few fully explored the bleaching of modern sediments empirically (Sommerville et al., 2001; Cunningham et al. 2015; King et al. 2014). Key to successful luminescence dating is that the energy been trapped through time in sediment minerals (quartz and feldspars) and subject to natural radioactive decay is released as luminescence (light) when exposed to visible light (bleached) thus resetting (bleaching) the luminescence signal to zero. However depositional and biogeomorphic processes will influence wavelength and bleaching intensity. This is particularly relevant in tidal dominated environments where individual sediment components may have diverse transport and bleaching histories and different sensitivities to luminescence. In some case, only partial bleaching will occur with potential for overestimation of OSL ages.

This project aimed to investigate the potential of Luminescence for saltmarsh sediments and designed and developed a reproducible method to date young (<100yrs) saltmarsh sediment by improving its signal and increasing its sensitivity. The novel technique aimed to track the changes that occur in signal intensity, sensitivity and bleaching and help address questions on sediment processes and dynamics in the hope that Luminescence could be used as a potential process tracer in modern dynamic systems.

The methods and results are discussed in Chapter 7 in three steps:

- 1) A general introduction to luminescence dating and reasonings behind to the research study;
- 2) The methodology is presented through the results of the exploratory work based on one small core (0.3m in depth) collected in the managed realignment MR to evaluate the sediment quality for luminescence, which grain size (from 500 to <30 $\mu\text{m}$ ) and which instruments may be capable to measure the young saltmarsh sediment sensitivity.
- 3) Based on this work, the experimental work aimed to develop a reproducible method to investigate luminescence as a dating or tracer tool by improving the sediment signal and increasing its sensitivity by the use of a new sediment preparation protocol; by modifying the portable instruments used for screening the sediments to a high

power and bright Blue-light (B-OSL) and Infra-Red light (IRSL) stimulations; and, finally by calibrating the procedure using a bespoke manual <sup>90</sup>Sr source providing a small regenerative dose (200mGy as opposed as a minimum of 1Gy in the standard instruments).

- 4) From the pioneer to high marsh zones, 4 cores collected along a transect running through the fronting and managed realignment marshes (SW/NE) and 4 cores along a transect (WSW/ENE) running through the natural salt marsh ANK (see Figure 3-38) provided 326 samples used in this experiment to investigate saltmarsh sediment signals as a potential tracer of modern dynamics of Nigg Bay salt marshes.

The upper 30 cm of Core MR24 was used to explore the use of stimulated Luminescence (section 7.2.2) and all cores' sediments are presented to highlight the new methodology development (7.4) and finally core MR8 results are presented in more details (7.5).

### **3.4.5 Statistics**

Statistical data presented from chapter 3 to 7 were performed using principally Minitab and R packages some limited analysis carried out using Matlab (Chapter 6 and 7) and Sigmaplot (Chapter 5 and 7). Statistics are at 95% confidence level and datasets have been checked for normality. If not normally distributed, the data were transformed (root squared, logarithmically or Box-Cox; as indicated in the text) to allow for linear statistical analysis (One-way ANOVA, Welch's ANOVA, followed by post-hoc Holm-Sidak, Tukey's HSD or Games-Howell t-test - as indicated in the text) and linear regression. When normality could not be resolved or group size was too small, non-parametric statistical tests were performed (Kruskal-Wallis Test (K-W test) followed by post-hoc pairwise tests: Mann-Whitney-Wilcoxon adjusted with Bonferroni correction or Conover-Iman using BH (Benjamini-Hochberg) adjustments. Problem of multicollinearity/autocorrelation in this study data was assessed before performing multiple regression and presented in Appendix B.2. Multicollinearity/autocorrelation was addressed by performing principal component analysis (PCA), checking the Variance Inflation Factor (VIF) in regression models, and removing one or more highly correlated variables.

### **3.4.6 Summary**

The research framework is summarised in Figure 3-9 and below, the sampling design is summarised in Figure 3-15 and Table 3-3.



Table 3-15: Summary of sampling design carried out in three salt marshes studied in Nigg Bay

			Short-term Dynamics					Long-term Dynamics										
			Sed.		Veg.			Aboveground			Sed.		Belowground					
Sites	Zones	Area (ha)	Dep°	Dep°	Veg. height	Veg. Density	Veg. Cover	Cover	Distribu tion	Biomass	Acc° and Erosion		Bulk Density	Water content	Organic content	Charact eristics	Luminesc ence	
			g.m <sup>2</sup>		cm	pop <sup>0</sup> /m <sup>2</sup>	%	%	NVC	g.m2	m.yr <sup>-1</sup>		g/cm <sup>3</sup>	%	%	Gray		
			Filter traps	Astroturf Mats	Quadrat s 0.25m <sup>2</sup>	Quadrat s 0.25m <sup>2</sup>	Quadrat s 1m <sup>2</sup>	Quadrat s 1m <sup>4</sup>	Quadrat s 1m2	Quadrat s 0.25m <sup>2</sup>	Plates	Mapping	Cores (Ø. 5&8cm)	Cores (Ø. 5&8cm)	Cores (Ø. 5&8cm)	Cores (Ø. 8&11 cm)	Cores (Ø. 8&11cm)	
MR	PM	4.1	5	2	3	3	3	7	7	3	7	2001	2	2	2	2	2	
	LM	5.5	7	5	4	3	3	12	12	3	12	2006	4	4	4	1	1	
	MM	3.2	3	1	1	1	1	7	7	1	7	2014	1	1	1	0	0	
	HM	11.9	2	1	3	3	3	13	13	3	13	2015	4	4	4	1	1	
	Total MR	24.7	17	9	11	10	10	39	39	10	39		11	11	11	4	4	
FM	PM	1.1	1	0	0	0	0	1	1	0	1	2001	0	0	0	0	0	
	LM	0.1										2006						
	MM	0.8	2	2	2	2	2	2	2	2	2	2014-15-	1	1	1	0	0	
	HM	2.2	3	1	1	1	1	3	3	1	3	16-17	2	2	2	1	1	
	Total FM	4.1	6	3	3	3	3	6	6	3	6		3	3	3	1	1	
ANK	PM	0.9	2	1	1	2	1	2	2	2	2	2001	2	2	2	1	1	
	LM	1.2	3	1	2	2	2	4	4	2	4	2015	2	2	2	0	0	
	MM	4.0	4	2	2	2	0	5	5	2	5	2016	3	3	3	2	2	
	HM	3.2	2	2	2	2	2	4	4	2	4	2017	2	2	2	1	1	
	Total ANK	9.3	11	6	7	8	5	15	15	8	15		9	9	9	4	4	
<b>Overall total</b>		<b>38.1</b>	<b>34</b>	<b>18</b>	<b>21</b>	<b>21</b>	<b>18</b>	<b>60</b>	<b>60</b>	<b>21</b>	<b>60</b>	<b>N/A</b>	<b>23</b>	<b>23</b>	<b>23</b>	<b>9</b>	<b>9</b>	

Sed. Sediments Veg. Vegetation Dep° Deposition Acc° Accretion Pop° Population (individuals) Ø diameter





# Chapter 4

*Nigg (MR46) July 2016*

# **Chapter 4. Short-Term Dynamics: Aboveground Short-Term (annual) Biological and Geomorphological Processes within Managed and Natural Salt Marshes**



*“Tidal landforms in lagoons and estuaries exist in a constant pursuit of sea-level rise, offset by an interplay of inorganic and organic sediment deposition. An outcome of such pursuit is the generation of some striking biological and morphological patterns at different scales. [...] many aspects of tidal bio-geomorphodynamics and of the associated patterns have been seen to be tightly linked to interactions between biotic and abiotic processes”* (D’Alpaos et al., 2016, p.2).

## **4.1 Introduction**

In order to better understand the increasing loss of coastal salt marshes, Chapter 2 reviewed the biological and physical processes that contribute to the vertical and lateral expansion of salt marshes, as well as the many regulatory, supporting, provisioning, and cultural services that salt marshes provide (Barbier et al., 2011; Costanza et al., 2014; Beaumont et al., 2014; Robins et al., 2016). However, these studies tend to focus on either specifics of hydrodynamics and morphodynamics that influence sediment transport (Chapter 2- 2.3.1.1), saltmarsh vertical or horizontal development (Chapter 2- 2.3.1.1), or on specific biological effects such as plant species, plant traits or root traits that may control sediment deposition and attenuate wave energy (Eisma and Dijkema, 1997; van der Wal and Pye, 2004; Möller, 2006; Friess et al., 2011; Fagherazzi et al., 2012; Vannoppen et al., 2017). However, these mechanisms have not necessarily been well-coupled together (Fagherazzi et al., 2013; Silinski et al., 2016) since they may not occur over the same time scales (Friess et al., 2011). For this reason, there are few studies that measure both biological and physical properties within an entire saltmarsh system that may have different processes and timescales operating across both mature and young saltmarsh zones. Belliard et al. (2017) further highlighted that despite significant advances in understanding the implications of marsh surface elevation for ecology, few field studies have addressed biomass – surface elevation relationships through direct measurements in European salt marshes compared to American salt marshes (work in South Carolina and Chesapeake Bay salt marshes).

This chapter addresses part of this knowledge gap by reporting data collected in the relation to the overarching research questions: which processes, mechanisms and patterns 1) favour saltmarsh formation and development; 2) enable saltmarsh capacity to recover from environmental and anthropogenic disturbances; 3) promote some of the regulating and supporting services salt marsh provide? Integral to these questions are an assumption that vegetation and sedimentation dynamics are the principal processes enabling saltmarsh formation and development. A subsidiary concept recognised that biological and geomorphological dynamics vary temporally and spatially (see Figure 4-1, the concept of spatial and temporal scales in section Chapter 2 – section 2.3 and 2.5 referring to Friess et al. (2011)). Long-term (multi-annual to centennial) aboveground processes in the Nigg Bay salt marshes are addressed

in Chapter 5, long-term (multi-annual to centennial) belowground changes are examined in Chapter 6 with Chapter 4 addressing the short-term (annual) biological and geomorphological processes that take place aboveground on the paired natural saltmarsh sites and managed realignment of Nigg Bay focussing on:

- the aboveground short-term (annual) sediment deposition rates and accretion rate estimates on the paired salt marshes and managed realignment sites over one year of tidal cycle measurements using two types of sediment traps: Filter discs and AstroTurf mats at the same sampling plots;
- the aboveground vegetation distribution, characteristics and biomass at the same sampling plots;
- the relationships between the measured aboveground processes and known physical controls (intrinsic factors and processes variables).

Chapter 3 discussed the sampling strategy (3.3.2.2 and 3.3.2.3) and methods (3.4.1.1) that were selected to empirically investigate in this chapter the questions addressed and detailed in Table 4-1.

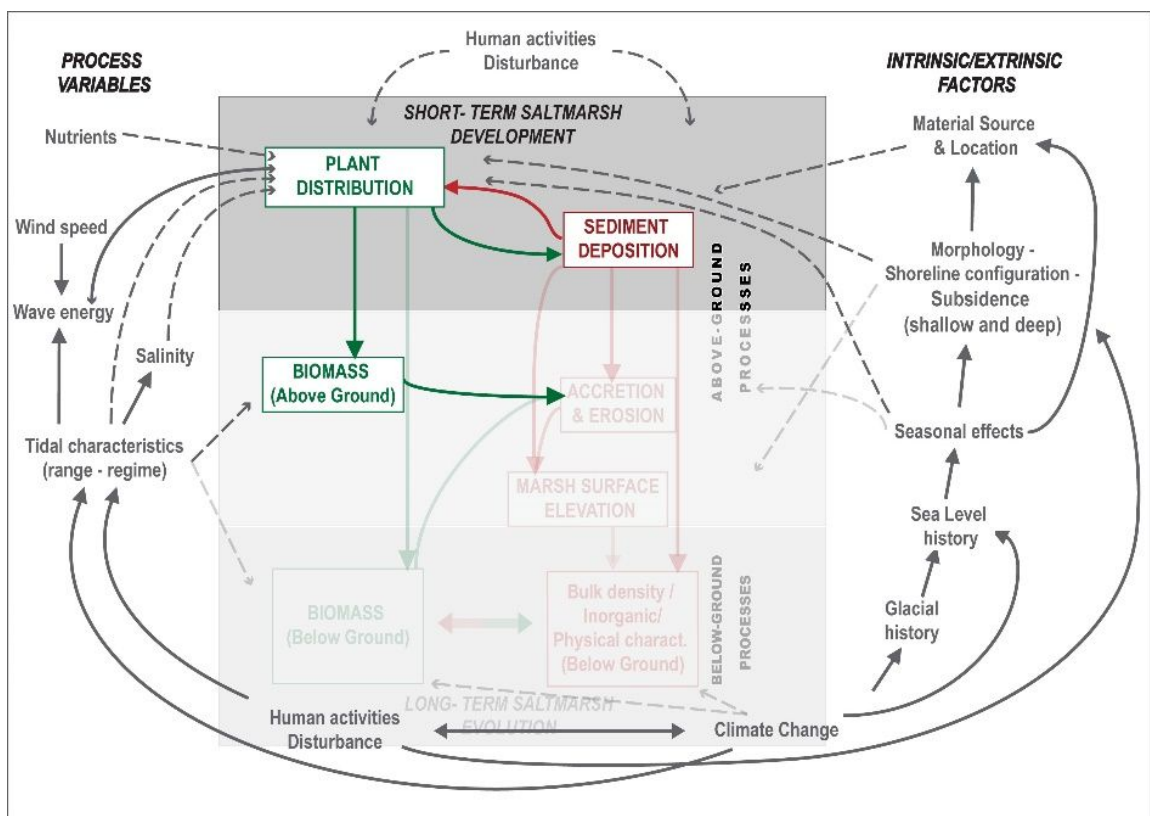


Figure 4-1: Chapter 4 focusses on biological and geomorphological interactions of short-term (annual) saltmarsh development in light of environmental processes and extrinsic and intrinsic factors influencing its evolution (after (Allen (2000); Davidson-Arnott et al. (2002) and Cahoon et al.(2009)).



**Table 4-1: Chapter 4 research questions and experimental hypotheses**

Thesis aims	Specific research questions	Experimental hypotheses	Methods	Chapter sections
<p><b>To improve the understanding of saltmarsh physical development by quantifying aboveground sedimentation changes on a short-term (annual) timescale.</b></p>	<p>How much sediment is deposited in Nigg Bay? Does this amount differ between natural and managed salt marshes? Between saltmarsh zones?</p>	<p>- It is expected that one-year sediment deposition will differ between the salt marshes as the sites do not share same topographical characteristics (elevation and remnants of sea embankment may favour or reduce deposition).                      - It is expected that sediment deposition will differ between saltmarsh zones as tidal inundations regime changes across the zones.                      It is expected that sediment deposition will vary seasonally, and each salt marsh may be impacted by this differently.</p>	<p>Filter traps AstroTurf mats sediment deposition</p>	<p>4.2</p>
	<p>Can these results provide information on the development of salt marsh?</p>	<p>- It is expected sediment availability provide means to qualify patterns and rates of aboveground sedimentation (accretion) across the sites.</p>	<p>Estimated sediment accretion rates</p>	
<p><b>To improve understanding of saltmarsh biological development by quantifying aboveground vegetation patterns on a short-term (annual) timescale.</b></p>	<p>How do vegetation characteristics differ between natural and managed salt marshes? Between saltmarsh zones?</p>	<p>The vegetation characteristics are expected to reflect the zonation of the salt marsh (as defined in Chapter 3 – 3.3.2.2).</p>	<p>Vegetation height, density and cover</p>	<p>4.3</p>
	<p>How does aboveground biomass compare between sites, saltmarsh zones and plant species?</p>	<p>It is expected that different part of the salt marshes, high, mid, and low will have different levels of aboveground biomass and carbon (as defined in Chapter 3 – 3.4.1.2.).</p>	<p>Aboveground biomass</p>	
<p><b>To improve understanding of saltmarsh physical development by quantifying water levels on a short-term (annual) timescale.</b></p>	<p>How water levels compare between natural and managed salt marshes? Do they differ between saltmarsh zones?</p>	<p>Water levels are not expected to differ across the site but between saltmarsh zones (which defines the distribution of vegetation -see section 4.5)</p>	<p>Calculation of flood depth, flood frequency and Hydroperiod</p>	<p>4.4</p>
	<p>Are there seasonal variations during short-term monitoring of saltmarsh development?</p>	<p>It is expected that water levels will vary from one monitoring campaign to the next and show seasonal trends.</p>		
<p><b>Improve understanding of physical and biological saltmarsh development on a short-term (annual) timescale</b></p>	<p>What influences sediment deposition and biological processes on short (annual) time scales? Do these relationships show trends?                      Are there relationships between aboveground biomass and sediment deposition on short (annual) time scales? Do these relationships show trends?</p>	<p>- Vegetation is expected to influence sediment deposition and this influence is expected to differ between the sites' saltmarsh zones                      - Where vegetation has less influence, physical factors have a stronger impact.                      - It is expected that water levels, elevation and distance to saltmarsh edge are the principal factors influencing deposition and vegetation patterns.</p>		<p>4.5</p>

---

<b>Significance and implication of the results</b>	<p>How did the different sediment sampling techniques perform?</p> <p>What can these results tell us about the development of Nigg Bay salt marshes?</p> <p>Can these results help predict the stability and future development of Nigg Bay salt marshes?</p>	<p>- Spatial and temporal variations in sediment deposition and biomass will identify saltmarsh areas that are or are not at risk.</p> <p>- Short-term (annual) accretion rate estimates will provide the information necessary to assess the condition of Nigg Bay salt marshes in relation to the sediment supply required to cope with the SLR.</p> <p>- The short-term (annual) biomass results will inform on aboveground blue carbon stock for Nigg Bay salt marshes.</p>	4.6
--	---	---	-----

---

## Data Analysis

Details of the statistics used can be found in Chapter 3 – 3.4.5. For the sake of brevity, a list of abbreviations and acronyms used in this Chapter is provided in Appendix A.

### **4.2 Short-term (annual) physical processes: sediment deposition and accretion rate estimates**

Results of short-term (annual) sedimentary processes are now examined aiming to address:

- i. How much sediment is deposited in Nigg Bay salt marshes?
- ii. Does deposition differ between salt marshes or/and between saltmarsh zones?
- iii. Is deposition regular across time?
- iv. How sediment deposition patterns translate into accretion rates?

Results of sediment deposition measured over one annual high-spring tides cycle and across the three saltmarsh sites at Nigg Bay are presented in 4.2.1 and the resulting consequences to saltmarsh development is provided by determining and analysing the accretion rate estimates for each site in section 4.2.2.

#### **4.2.1 Sediment deposition rates**

It has been found that spring-neap tides was best to characterise saltmarsh inundation, such as highest levels of deposition in winter and the lowest in the summer, as cumulative inundation time reflects both the magnitude and frequency of inundations during a spring–neap cycle (Cahoon and Reed, 1995; Temmerman, Govers, Wartel, et al., 2003; Temmerman, Govers, Meire, et al., 2003). Furthermore, S. Temmerman et al. observed a positive linear relationship between inundation suspended sediment concentration (ISSC) and maximum inundation height with the increase of ISSC being much greater during the winter (October to March) as the inundation height is at its maximum than during the summer period (April to September). This

section presents results of sediment deposition over an annual cycle of high-spring tides across the saltmarsh zones of the three studied sites using a network of filter discs (section 4.2.1.1) together with AstroTurf mats (section 4.2.1.2) covering the marsh elevation gradients and vegetation assemblage types on the salt marshes. Figure 3-21 and 22 in Chapter 3 reviewed the location and number of traps (34 filter discs and 19 AstroTurf mats) deployed across the three studied salt marshes. A total of 342 filters and 196 mats were placed between February 2016 and March 2017 (Figure 3-23). The filter discs dataset for sediment deposition represents 11 high-spring tides (12 recorded plus one cycle of filter discs kept for Stimulated Luminescence (OSL and IRSL) experiments – see Chapter 3 – 3.4.1.1) spanning from 09<sup>th</sup> March 2016 to 31<sup>st</sup> January 2017 (one sampling on 01<sup>st</sup> March 2017 was kept for Optical Luminescence Stimulation see Chapter 3 – 3.4.1.1). The 12 high-spring tides, from March 2016 to March 2017, were kept for the AstroTurf mats over the sampling period, however when comparisons between the two methods have been made, they are based on the same sampling period. Consequently, the objective of this study is to quantify sediment deposition for spring tides events and not the neap-spring sequence; as a result, the study does not cover the full range of low to high inundation events and seeks to estimate accretion rates for the high-spring cycle. In their mesotidal marsh study, Carrasco et al. (2023) found no significant differences in deposition rates between neap and spring tides. Sediment deposition spatial and temporal variability is addressed for both trapping methods within sections 4.2.1.1 and 4.2.1.2.

#### 4.2.1.1 Spatial variation in sediment deposition rates using filter discs

Overall sediment deposition rates from the filter discs were derived from 304 filter traps retrieved across the three salt marshes from March 2016 to end of January 2017 (some traps could not be used - see section 3.4.1.1 for methods and Figure 3-23 for collection dates).

##### **Filter disc sediment deposition rates between saltmarsh sites**

Sediment deposition averaged at  $23.4 \pm 2.3 \text{ g.m}^{-2}\text{day}^{-1}$  and ranged from 0 to  $343.16 \text{ g.m}^{-2}\text{day}^{-1}$ . The data for every filter disc retrieved during the campaign has been arranged according to which of the three salt marshes the sampling point is located in (as shown in Figure 3-22). Analysis of the data demonstrated that overall, the sites are not statistically different (Table 4-2).

##### **Filter disc sediment deposition between the sites' saltmarsh zones**

As the number of filter discs varies between saltmarsh zones, they cannot be summed up, and an analysis of filter disc sediment deposition rates between the sites' saltmarsh zones has been performed and is summarised in Table 4-2. Analysis across the deployment period has shown statistically significant differences between sites and zones deposition rates means (*Welch's Anova*:

$F_{(DFn=10, DFd=83.4)} = 4.8^{***}$ ) and means' ranks ( $H_{(df=10)} = 41.352^{***}$ ) (Figure 4-2a). Performing Wilcoxon pairwise tests (adjusted with Bonferroni correction; Figure 4-2b) demonstrated that on ANK, the mid-marsh (MM) hold the highest sediment deposition mean rank compared to the and pioneer zones (PM), high-marsh (HM) and low-marsh (LM) zones. The low-marsh (LM) is also found significantly lower than PM and HM. This spatial variability between the overall sediment deposition is further depicted in Figure 4-3. It shows the highest deposition located within the marsh, at distance from the saltmarsh edge also along the major creeks (sampling point A10 and A6). On the pioneer zone, deposition is spatially variable with highest rates on the eastern parts of the marsh (sampling point A5) where tidal energy is attenuated due to the sheltered position (Figures 3-5 and 3-6) and highest wind frequency occurs WSW and SSW (Stapleton and Pethick 1996, p.40).

On FM, sediment deposition rates present significantly higher mean ranks levels on the PM zone compared to MM. It is worth noticing the exceptionally large variability of sediment deposition rates on the PM zone which had experienced lowest ( $0 \text{ g.m}^{-2}\text{day}^{-1}$  in October 2016) and highest deposition ( $343 \text{ g.m}^{-2}\text{day}^{-1}$  in November 2016) across the campaign. This variation can be explained by the fact that sampling site FM5, situated at the edge of the marsh, has consistently recorded the highest levels of deposition. This could suggest that the location is either profiting from direct tidal input or from erosion on FM's cliff edge.

On MR, overall sediment deposition rates experienced on MM zone is found significantly lower compared than LM and HM. Figure 4-3 shows higher rates experienced on the westernmost low and pioneer zones of the managed realignment site at sampling points MR31, 45 and 46 all benefitting of tidal input from the west breach (see figure 3-7) and of shelter behind the sea wall embankment remnants reducing the tidal flow dragging force.

Of relevance, across all sites and saltmarsh zones, ANK's sediment deposition rates on MM zone are found considerably higher than MR's and FM's MM zones. Conversely, ANK's rates on LM zone are statistically lower than MR's LM (Figure 4-2). These differences can be attributed to a better shelter on ANK's LM and MR's LM preventing dragging force of the retreating tides. These relationships when further examined using a simple linear model demonstrates that differences between saltmarsh sites and zones can explain 10 % ( $r^2_{\text{adj}}$ ) of the sediment deposition variation ( $F_{(10, 273)} = 4.27, p < 0.001^{***}$ ) where mostly ANK's pioneer, low and mid-marsh contribute significantly to the model (Appendix C-1 Table C-1).

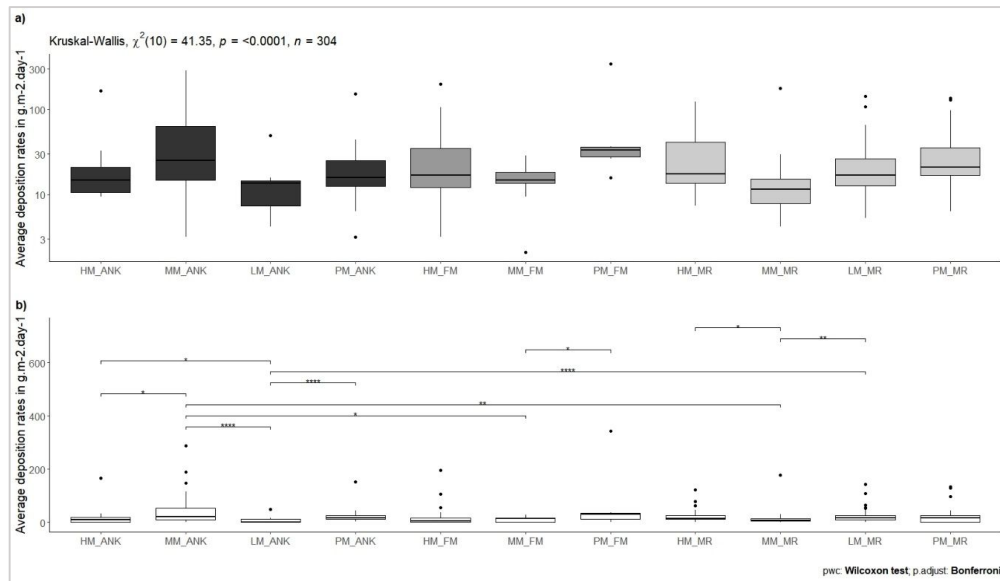


Figure 4-2: a) Boxplot of the Filter disc sediment deposition rates (in g.m<sup>-2</sup>day<sup>-1</sup>) per the sites' saltmarsh zones. Boxplots represent median (middle line) interquartile range (box), 1.5 times interquartile range (bar) and outliers (black dots). b) same boxplots with significant differences between saltmarsh sites and zones (Kruskal-Wallis H test and significant pair-test comparison using Wilcoxon rank tests results by the p-value significance: ns, \*, \*\*, \*\*\* for > 0.05, ≤ 0.05, ≤ 0.01, ≤ 0.001).

Table 4-2: Filter disc sediment deposition rates (in g.m<sup>-2</sup>day<sup>-1</sup>) per sites and saltmarsh zones.

	ANK				FM				MR			
	Mean	SD	Median	n	Mean	SD	Median	n	Mean	SD	Median	n
Overall	26.2	44.3	14.2	102	22.6	52.6	12.6	57	21.7	29.1	14.74	145
HM	19.6	37	10.5	19	20	41.4	6.32	28	27.3	32.6	14.7	17
MM	42.9	58.5	21.1	39	11.4	9.24	14.7	21	15	31.9	8.42	29
LM	5.98	10.8	0	25					22.3	24.8	15.8	61
PM	25.2	32.6	15.8	19	61.1	115	29.5	8	23.3	32	16.8	38

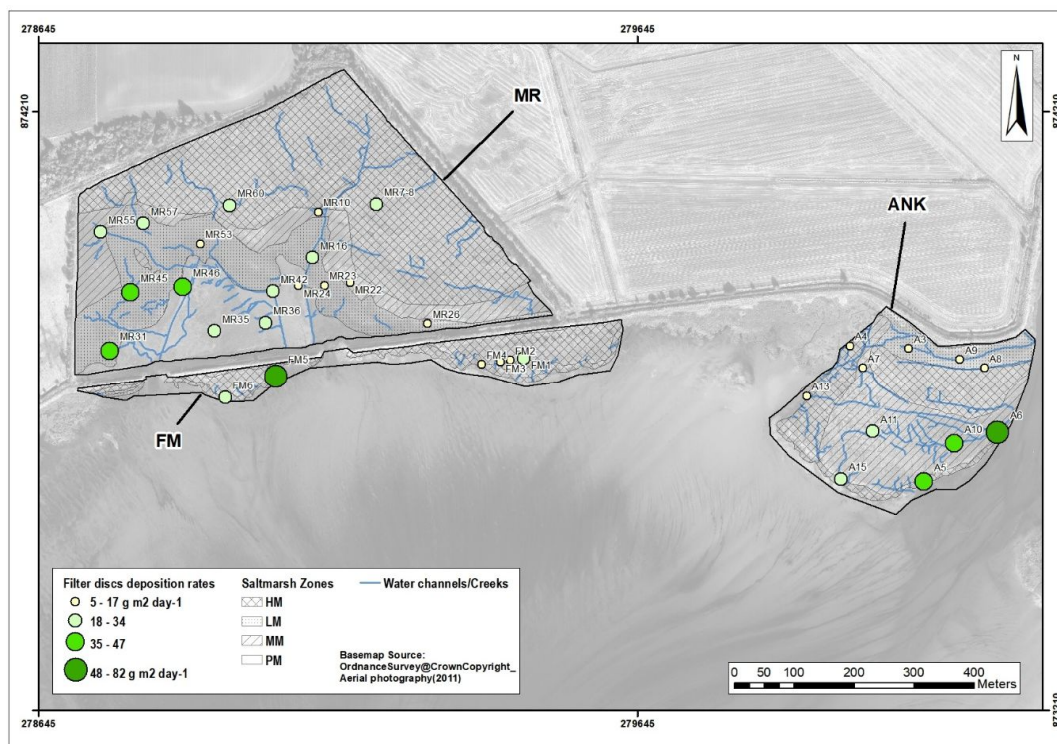


Figure 4-3: Spatial variation for the average filter disc sediment deposition rates showing sampling points with graduated symbol size estimated in g.m<sup>-2</sup>day<sup>-1</sup> superimposed on the creek system and the extent of saltmarsh sites and saltmarsh zones (Basemap Source: OrdnanceSurvey@CrownCopyright Aerial photography(2011)).

#### 4.2.1.2 Temporal variation in sediment deposition rates using filter discs

##### **Filter disc sediment deposition rates variation over the sediment collection period**

From March 2016 to the end of January 2017, filter disc sediment deposition rates (Table 4-3) is found to be significantly different between each monthly collection campaign (*Welch's Anova*:  $F_{(DFn=10, DFd=103.3)} = 9.89^{***}$ ). Figure 4-4 shows a clear increase in deposition rates from September 2016 to November 2016 with large variation between samples which can be attributed to the differences that occur between saltmarsh sites and zones as per described in the above section 4.2.1.1. Games-Howell post-hoc comparisons were conducted to determine which sediment deposition collection differed from each other. The statistical analysis indicates that sediment deposition rates for March 2016, August 2016 and January 2017 are substantially lower than the previous months of November (March diff.= 43.2 g.m<sup>-2</sup>day<sup>-1\*\*</sup>, August diff.= 49.8 g.m<sup>-2</sup>day<sup>-1\*\*\*</sup> & January diff.= 53 g.m<sup>-2</sup>day<sup>-1\*\*\*</sup>), October (March diff.= 34.2 g.m<sup>-2</sup>day<sup>-1\*\*</sup>, August diff.= 40.8 g.m<sup>-2</sup>day<sup>-1\*\*\*</sup> & January diff.= 44 g.m<sup>-2</sup>day<sup>-1\*\*\*</sup>) and December 2016 (March diff.= 6.90 g m<sup>-2</sup>day<sup>-1\*</sup>, August diff.= 13.5 g.m<sup>-2</sup>day<sup>-1\*\*\*</sup> & January diff.= 16.7 g.m<sup>-2</sup>day<sup>-1\*\*\*</sup>). Deposition rates that occurred in April, June, and July 2016 are also found significantly lower than the winter months of November (April diff.= 47.6 g.m<sup>-2</sup>day<sup>-1\*\*</sup>, June diff.= 41 g.m<sup>-2</sup>day<sup>-1\*</sup> & July diff.= 43.6 g.m<sup>-2</sup>day<sup>-1\*</sup>) and April 2016's is also significantly lower than October 2016 (diff.= 38.6 g.m<sup>-2</sup>day<sup>-1\*</sup>). The summer month of June, July and September 2016 had seen on contrary deposition rates significantly higher than the winter month of January 2017 (June diff.= 12 g.m<sup>-2</sup>day<sup>-1\*</sup>, July diff.= 9.4 g.m<sup>-2</sup>day<sup>-1\*</sup> & September diff.= 25.9 g.m<sup>-2</sup>day<sup>-1\*\*</sup>). The statistical results are presented in Figure 4-4b and details are provided in Appendix C.1-Table C-2.

**Table 4-3: Filter disc sediment deposition rates (in g.m<sup>-2</sup>day<sup>-1</sup>) per collection month.**

	Min	Max	Mean	SD	Median	n
March 2016 (09.03.2016)	0	153	14.6	36.1	0	18
April 2016 (21.04.2016)	0	36.8	10.2	10.4	8.95	18
May 2016 (06.05.2016)	0	38.9	13.5	9.94	13.2	14
June 2016 (06.06.2016)	0	89.5	16.8	19.2	14.7	25
July 2016 (04.07.2016)	0	36.8	14.2	10.3	13.7	28
August 2016 (03.08.2016)	0	32.6	7.99	9.54	5.79	34
Sept. 2016 (18.09.2016)	0	287.6	30.7	50.7	14.7	34
October 2016 (17.10.2016)	0	176.8	48.8	50.6	26.8	34
Nov. 2016 (14.11.2016)	0	343.2	57.8	75.5	20	31
Dec. 2016 (14.12.2016)	0	52.6	21.5	13	16.8	34
Jan. 2017 (31.01.2017)	0	26.3	4.8	6.73	1.58	34



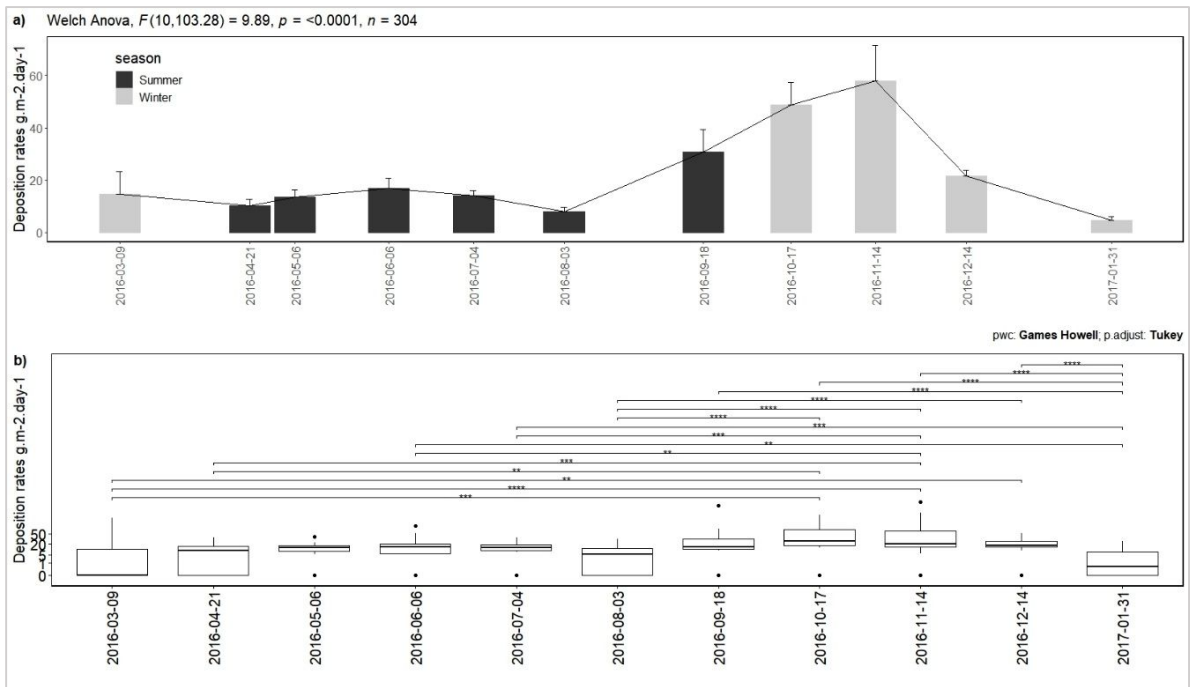


**Figure 4-4: a) Bar graph of the Filter disc sediment deposition rates ( (in  $\text{g.m}^2\text{day}^{-1}$ ) in  $\text{g.m}^2\text{day}^{-1}$ ) from 09<sup>th</sup> March 2016 to 31<sup>st</sup> January 2017 (top of bar is average deposition, error bars calculated from individual standard error). b) Boxplot of the Filter disc sediment deposition rates ( $\text{g.m}^2\text{day}^{-1}$ ) presenting the significant results of Games Howell pairwise comparison tests between collection dates (Mann-Whitney-Wilcoxon tests results are symbolised on the top rows by the p-value significance - ns, \*, \*\*, \*\*\* - for each pairwise tests. The statistical analysis was generated on transformed dataset to meet normality assumption and details are in Table C-2.**

The temporal variation in deposition between each collection is further confirmed in a linear regression model (details in Appendix C.1-Table C-3) which indicates that, overall, variation between collections can explain 23 % ( $r^2_{\text{adj}}$ ) of sediment deposition variability with most months contributing to the model apart for the months of April, August 2016 and January 2017. The model's residuals are found to be normally distributed, however quantile-quantile plot (plot to compare the quantiles of the data set against theoretical quantiles) suggests a possible bimodal distribution. This is further explored by using sites' category which have been found to have a significant influence in sediment deposition rates. Although this slightly improves the model strength ( $r^2_{\text{adj}}=0.23.5$ ;  $F_{(12, 291)} = 8.78, p < 0.001$  \*\*\*), the sites are not found to contribute significantly to the model. Therefore, variation between collection months in sediment deposition rates for each site is analysed in the next section.

Using collection dates, sites and saltmarsh zones can support 30.2 % ( $r^2_{\text{adj}}$ ) of sediment deposition rates variation ( $F_{(20, 23)} = 7.55, p < 0.001$  \*\*\*, standardised residuals met the normality assumption) where most factors contribute significantly to the model with interaction effect (details in Appendix C.1-Table C-3).

### **Filter disc sediment deposition rates variation per saltmarsh sites over the sediment collection period**

The filter disc sediment deposition across the three salt marshes display significant monthly variations with **ANK** showing the highest mean rank sediment deposition rates in June and October 2016 ( $\eta = 21.1 \text{ g.m}^{-2} \text{ day}^{-1}$  and  $20 \text{ g.m}^{-2} \text{ day}^{-1}$  respectively) and lowest in January 2017 and April 2016 ( $\eta = 0 \text{ g.m}^{-2} \text{ day}^{-1}$  both) (Figure 4-5 a & b). Collection dates can explain 21 % ( $r^2_{\text{adj}}$ ) of sediment deposition rates variation on ANK ( $F_{(10, 91)} = 3.7, p < 0.001$  \*\*\* standardised residuals met the normality assumption), however collection months do not contribute significantly to the model (regression model details are in Appendix C.1-Table C-4).

**FM** experiences its highest sediment deposition rates during winter, in November and October 2016 ( $\eta = 37.4 \text{ g.m}^{-2} \text{ day}^{-1}$  and  $15.8 \text{ g.m}^{-2} \text{ day}^{-1}$  respectively) and lowest in summer June 2016 ( $0 \text{ g.m}^{-2} \text{ day}^{-1}$ ) (Figure 4-5 c & d). Collection dates can explain 35.4 % ( $r^2_{\text{adj}}$ ) of sediment deposition rates variation on FM ( $F_{(10, 46)} = 4.06, p < 0.001$  \*\*\* standardised residuals met the normality assumption with tendency to light tailed distribution) with April, September, October, November and December 2016 contributing the most to the model (regression model details are in Appendix C.1-Table C-4 including note 2 in caption).

**MR**'s highest and lowest rates were also measured during winter months (Figure 4-5 e & f). The managed realignment displays its highest mean rank sediment deposition rates in October and November 2016 ( $\eta = 29.5 \text{ g.m}^{-2} \text{ day}^{-1}$  and  $23.7 \text{ g.m}^{-2} \text{ day}^{-1}$  respectively) and lowest in March 2016 and at the end of January 2017 ( $\eta = 0 \text{ g.m}^{-2} \text{ day}^{-1}$  and  $\eta = 4.2 \text{ g.m}^{-2} \text{ day}^{-1}$  respectively). Changes between collection dates are found to explain 33.6 % ( $r^2_{\text{adj}}$ ) of sediment deposition rates variation on MR ( $F_{(10, 134)} = 7.7, p < 0.001$  \*\*\* standardised residuals met the normality assumption), and, all months apart August 2016 and January 2017 contribute significantly to the model (regression model details are in Appendix C.1-Table C-4).

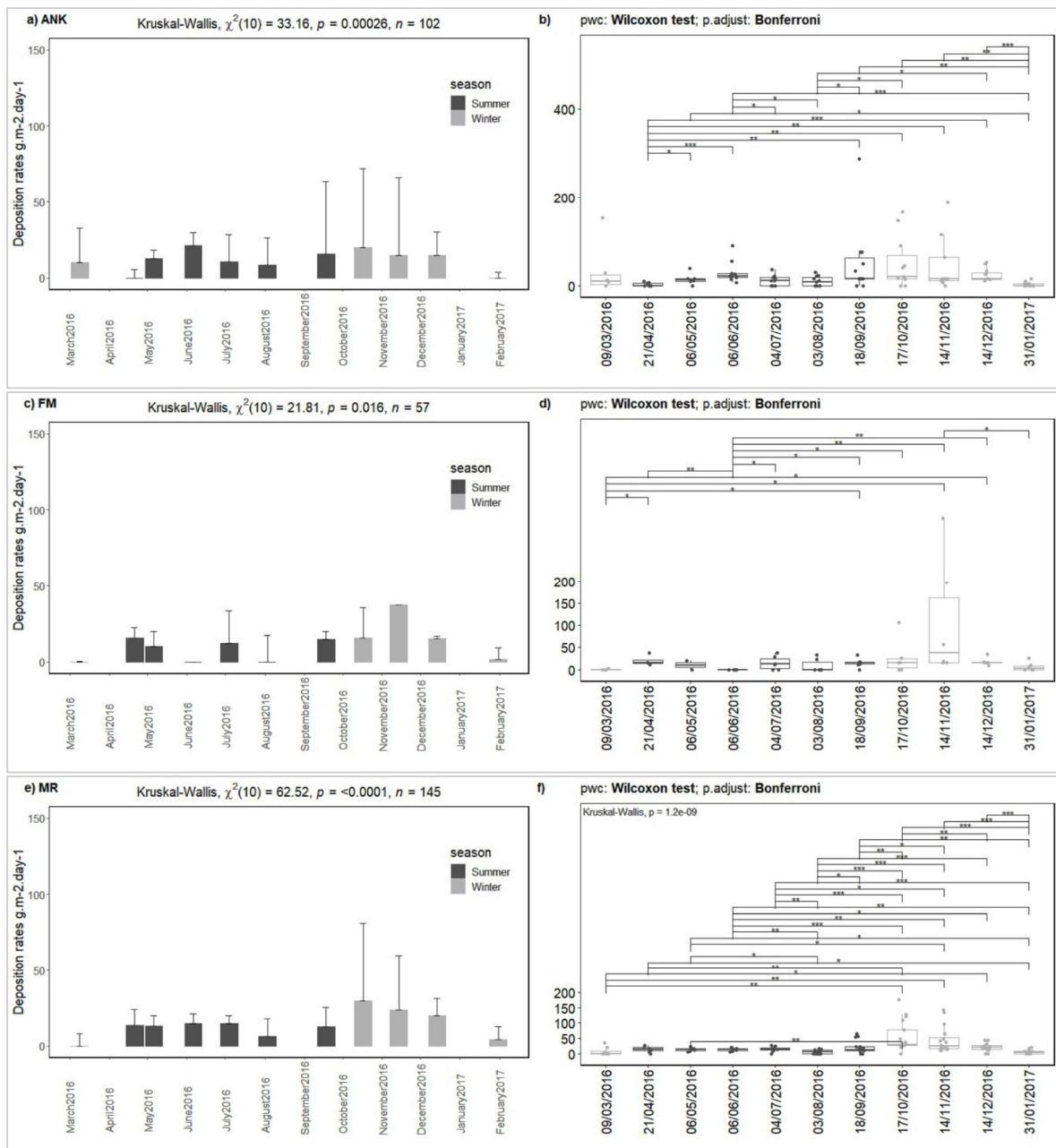


Figure 4-5: Bar graph of filter disc sediment deposition mean ranks rates ( $\text{g.m}^{-2}\text{day}^{-1}$ ) from 09<sup>th</sup> March 2016 to 31<sup>st</sup> January 2017 for ANK (a), FM (c) and MR (e). (Top of bar is mean rank average deposition, error bars calculated from individual standard error). Boxplot of filter discs deposition rates ( $\text{g.m}^{-2}\text{day}^{-1}$ ) showing statistically significant differences between collection dates for ANK (b), FM (d) and MR (f) (The boxplots represent median and error bars are interquartile range; Mann-Whitney-Wilcoxon tests results are symbolised on the top rows by the p-value significance - ns, \*, \*\*, \*\*\* - for each pairwise tests)

### Filter disc sediment deposition rates variation between summer and winter

Overall, the results presented in the above section suggest also that sediment deposition rates can be higher during the winter months and lower during summer months. Using a seasonal definition of summer (April to September) and winter (October to March), Games Howell comparisons test (non-parametric test used to deal with unequal sample size between the season: 153 summer samples and 151 winter samples) finds that sediment deposition rates are significantly different between seasons ( $F_{(df=236)} = 3.14^{**}$ ) with an increase of 86% from summer

( $16.4 \pm 2.2 \text{ g.m}^{-2}\text{day}^{-1}$ ) to winter ( $30.5 \pm 3.9 \text{ g.m}^{-2}\text{day}^{-1}$ ). Figure 4-6a further highlights outliers with sampling point A6 presenting highest deposition rate in Summer and FM6 in winter. Although statistically significant, seasons are found to only explain 1.7% ( $r^2$ ) of deposition rates variation between summer and winter ( $F_{(1, 302)} = 5.401, p < 0.03^*$ ).

Differences between sediment deposition rates, seasons and sites were further analysed using Kruskal-Wallis test. As the test was rejected (Figure 4-6b), a non-parametric pairwise multiple-comparison procedure was performed by using Dunn's test (BH - Benjamini-Hochberg - adjustments). It indicates that there is strong evidence that filter disc sediment deposition rates differ significantly ( $p = 0.02^*$ ) on MR salt marsh with a median decrease of 37 % between summer and winter (Table 4-4, Figure 4-6b). There was no evidence of differences between summer and winter deposition rates for ANK and FM. The results further show that deposition rates are fairly uniform across the three salt marshes during winter ranging between  $34.1 \pm 13.8$  to  $28.9 \pm 4.3 \text{ g.m}^{-2}\text{day}^{-1}$  and during summer  $22 \pm 5.7$  to  $11.5 \pm 2.4 \text{ g.m}^{-2}\text{day}^{-1}$ .

Similarly, differences between summer and winter filter discs deposition rates are not found statistically significant between the sites' saltmarsh zones and were found to explain 9.5 % ( $r^2_{\text{adj}}$ ) of deposition rates variation ( $F_{(21, 282)} = 2.52, p < 0.001^{***}$ ) where only ANK's low-marsh (LM) deposition rates are significantly contributing to the model.

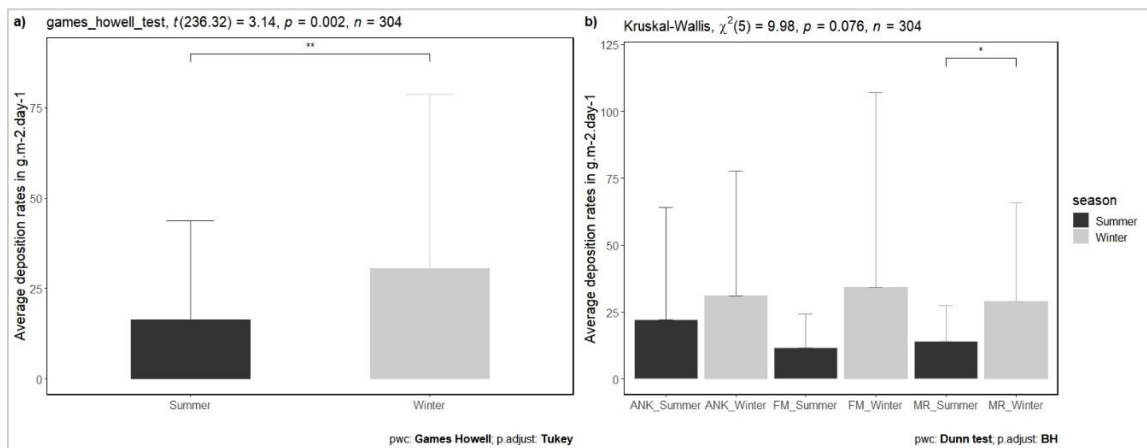


**Figure 4-6: a) Average filter disc sediment deposition rates ( $\text{g.m}^{-2}\text{day}^{-1}$ ) between summer ( $n=153$ ) and winter ( $n=151$ ) (top of bar is average deposition, error bars calculated from individual standard error). The graph also present results and statistical significance of Games-Howell test between seasons (symbolised on the top rows by the p-value significance - ns, \*, \*\*, \*\*\*).**

**b) Average summer and winter filter disc sediment deposition rates ( $\text{g.m}^{-2}\text{day}^{-1}$ ) between sites (top of bar is average deposition, error bars calculated from individual standard error). The graph also highlights results and statistical significance of Dunn's Test pairwise comparison test (symbolised on the top rows by the p-value significance - ns, \*, \*\*, \*\*\*)** between seasonal filter discs deposition mean ranks rates and saltmarsh sites.

**Table 4-4: Filter disc sediment deposition (in g.m<sup>-2</sup> day<sup>-1</sup>) in winter and summer by sites.**

FILTER DISC SEDIMENT DEPOSITION RATES					
		Mean	SD	Median	n
ANK	Summer	22	42	14.2	54
	Winter	30.9	46.8	14.2	48
FM	Summer	11.5	12.7	11.6	29
	Winter	34.1	72.9	14.7	28
MR	Summer	14	13.4	12.6	70
	Winter	28.9	37.1	20	75

#### 4.2.1.3 Spatial variation in sediment deposition rates using AstroTurf mats

The sediment deposition rates derived from AstroTurf mats were calculated using 196 traps retrieved across the three salt marshes from March 2016 to February 2017 (see section 3.4.1.1 for methods and Figure 3-23 for collection dates and Figure 3-22 for location). Sediment deposition rates average at  $20.7 \pm 3.6 \text{ g.m}^{-2} \text{ day}^{-1}$  ranging from 0 to  $397.89 \text{ g.m}^{-2} \text{ day}^{-1}$ .

#### **AstroTurf mats sediment deposition rates between saltmarsh sites**

The overall amount of AstroTurf mat sediment deposition rates averages at  $35.1 \pm 0.1 \text{ gm}^{-2} \text{ day}^{-1}$  on ANK, at  $19.6 \pm 0.1 \text{ g.m}^{-2} \text{ day}^{-1}$  on FM and at  $11.2 \pm 0.02 \text{ g.m}^{-2} \text{ day}^{-1}$  on MR, the overall sediment deposition rates' mean ranks are not statistically different between sites which may be attributed to the large deviation between the collection campaign (Table 4-5 and further explored below in section 4.2.1.4). Similarly, overall sediment deposition rates don't differ statistically between the sites' saltmarsh zones. This 'lack' of statistical difference is emphasised in Figure 4-7. It shows that ANK's sediment deposition rates were comparatively uniform across the salt marsh, and this is true for the saltmarsh edge (points A15, A13 and A4) or landwards (points A9 and A8). Only two sampling points (A10 and A6) along the major creeks have experienced higher rates, comparable to the same filter discs deposition rates sampling points (Figure 4-3). On FM, AstroTurf mats trapped more sediment on the saltmarsh edge (point FM4) compared to all other sampling points located in the mid-marsh reversing the trend observed for the filter discs deposition rates. On MR, again the overall sediment deposition rates for the year looks fairly uniform, only two sampling points stand out with slightly higher rates and are located on the low-marsh (MR16) and pioneer-marsh (MR46).

It is worth noticing the exceptionally large variability of sediment deposition rates on all saltmarsh site (Table 4-5) which may be attributed to the temporal variability experienced during the collection campaign. This is further explored in the section 4.2.1.4 below.

**Table 4-5: AstroTurf Mat Sediment deposition rates (in g.m<sup>-2</sup>.day<sup>-1</sup>) per sites per saltmarsh zones.**

	ANK				FM				MR			
	Mean	SD	Median	n	Mean	SD	Median	n	Mean	SD	Median	n
overall	35.1	77.5	7.89	66	19.6	38.6	4.74	34	11.2	16.3	6.32	96
<b>HM</b>	9.91	10	9.47	17	9.19	16.3	2.11	11	9.47	9.54	7.37	11
<b>MM</b>	82.8	115	13.2	24	24.6	45.2	6.32	23	4.94	4.77	3.16	23
<b>LM</b>	2.83	3.23	2.11	13					12	17.4	6.32	40
<b>PM</b>	10.4	10.3	7.89	12					17.1	22.3	9.47	22

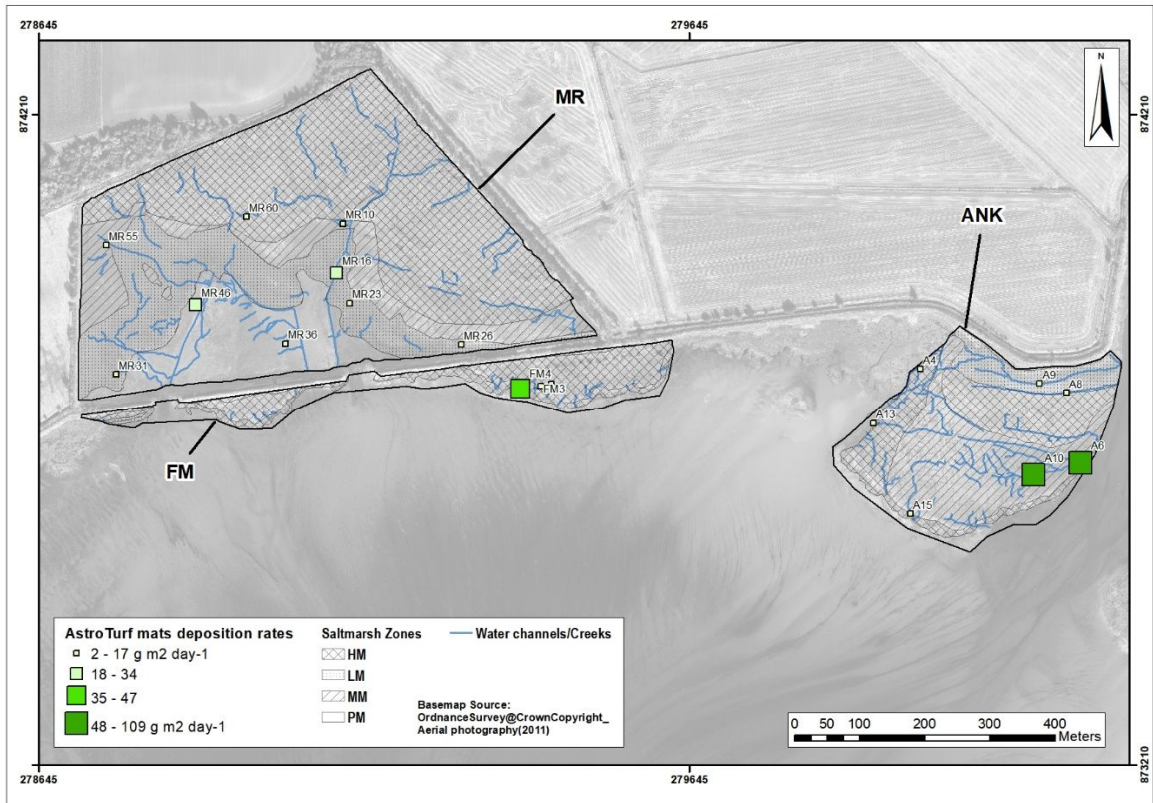


**Figure 4-7: Spatial variation for the AstroTurf mats sediment deposition rates showing sampling points with graduated symbol size calculated in g.m<sup>-2</sup>.day<sup>-1</sup> across sites and saltmarsh zones with depiction of creek system (Basemap Source: OrdnanceSurvey@CrownCopyright Aerial photography(2011)).**

#### 4.2.1.4 Temporal variation in sediment deposition rates using AstroTurf mats

##### **AstroTurf mats sediment deposition rates variation over the sediment collection period**

From March 2016 to the end of January 2017, AstroTurf sediment deposition (Table 4-6) are significantly different between each monthly collection (*Welch's Anova*:  $F_{(DFn=11, DFd=68.98)} = 8.65^{***}$ ). Like the results obtained with the filter discs (4.2.1.2), Figure 4-8a depicts a clear increase in deposition rates from September 2016 to November 2016. Games-Howell post-hoc comparisons were conducted to determine which sediment deposition collection differed from each other (Figure 4-8b). The statistical analysis indicates that sediment deposition rates for March 2016 were substantially lower than all other months (details of differences are compiled in Appendix C.1-Table C-5). Deposition rates that occurred in the summer months of July and August 2016 are significantly lower than the winter months of October (July diff.=  $43.3 \pm 22.7$  g.m<sup>-2</sup>.day<sup>-1\*\*</sup> &



August diff.= 39.3±22 g.m<sup>-2</sup>day<sup>-1</sup>\*\*\*), of November which had seen the highest deposition rate record (July diff.= 61.6±19.5 g.m<sup>-2</sup>day<sup>-1</sup>\*\* & August diff.= 57.6±18.8 g.m<sup>-2</sup>day<sup>-1</sup>\*\*\*) and of December (July diff.= 27±9.1 g.m<sup>-2</sup>day<sup>-1</sup>\*\* & August diff.= 23±8.4 g.m<sup>-2</sup>day<sup>-1</sup>\*\*\*) 2016. Linear regression confirms that temporal variation between AstroTurf mats collection can explain 33 % (r<sup>2</sup>adj) of sediment deposition rates variability with all months contributing to model (F<sub>(11, 184)</sub> = 9.757, p < 0.001 \*\*\*; standardised residuals met the normality assumption - see details in Appendix C.1-Table C-6). The model's residuals are normally distributed, however quantile-quantile plot suggests that the model under and overestimates extreme values (and that the model should not be used to make a prediction for a point that is outside the range of this dataset because the relationship between the variables might change). These relationships between deposition rates and temporal variation are further explored by saltmarsh sites.

Saltmarsh sites and time of collection can explain 34.6 % (r<sup>2</sup>adj; F<sub>(13, 182)</sub> = 9.737, p < 0.001 \*\*\*; standardised residuals met the normality assumption) of the overall sediment deposition rates variation where all months and MR contribute significantly to the model. Sediment deposition rates temporal variation for each site is further developed below. Collection dates, sites and saltmarsh zones can support 48.3 % (r<sup>2</sup>adj) of sediment deposition rates variation (F<sub>(20, 175)</sub> = 10.12, p < 0.001 \*\*\*; standardised residuals met the normality assumption) where all months and ANK's low-marsh and mid-marsh contribute significantly to the model (details in Appendix C.1-Table C-6).

**Table 4-6: AstroTurf mats sediment deposition rates in g.m<sup>-2</sup>day<sup>-1</sup>per collection month.**

	Min	Max	Mean	SD	Median	n
March 2016 (09.03.2016)	0	10.5	1.5	3.82	0	14
April 2016 (21.04.2016)	0	54.7	12.5	19.2	2.11	11
May 2016 (06.05.2016)	0	198.9	17.8	50.3	3.16	15
June 2016 (06.06.2016)	0	90.5	10.8	23.8	3.16	16
July 2016 (04.07.2016)	0	17.9	5.15	5	4.21	18
August 2016 (03.08.2016)	0	29.5	5.51	7.06	3.16	17
Sept. 2016 (18.09.2016)	1.05	195.8	21.5	49.3	5.26	16
October 2016 (17.10.2016)	7.37	397.9	44.8	97.7	11.6	17
Nov. 2016 (14.11.2016)	0	311.6	63.1	89.4	35.8	19
Dec. 2016 (14.12.2016)	3.16	155.8	28.5	43.1	14.2	18
Jan. 2017 (31.01.2017)	2.11	21.1	5.96	5.19	4.74	18
March 2017 (01.03.2017)	0	94.7	20.4	23.7	10.5	17

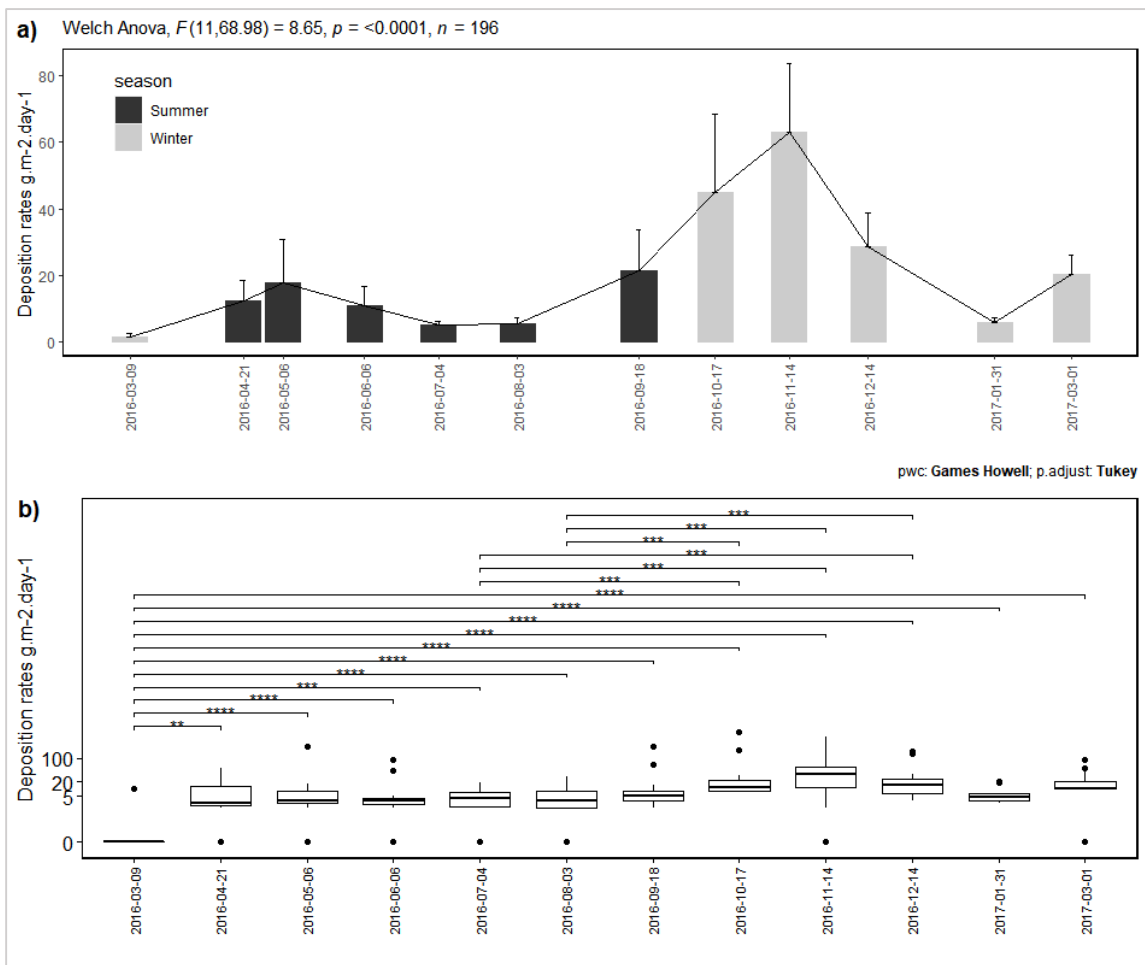


**Figure 4-8: a)** Bar graph of the AstroTurf mats sediment deposition rates (in  $\text{g.m}^{-2}.\text{day}^{-1}$ ) from 09<sup>th</sup> March 2016 to 01<sup>st</sup> March 2017 (top of bar is average deposition, error bars calculated from individual standard error). **b)** Boxplot of the AstroTurf mats sediment deposition rates (in  $\text{g.m}^{-2}.\text{day}^{-1}$ ) highlighting the significant results of Games Howell pairwise comparison tests between each sediment collection's deposition (date of collection is shown in x-axis; Mann-Whitney-Wilcoxon tests results are symbolised on the top rows by the p-value significance - ns, \*, \*\*, \*\*\* - for each pairwise tests). Note that the statistical analysis was generated on transformed dataset to meet normality assumption and details are in Appendix C.1-Table C-5.

### AstroTurf mats sediment deposition rates variation per saltmarsh sites over the sediment collection period

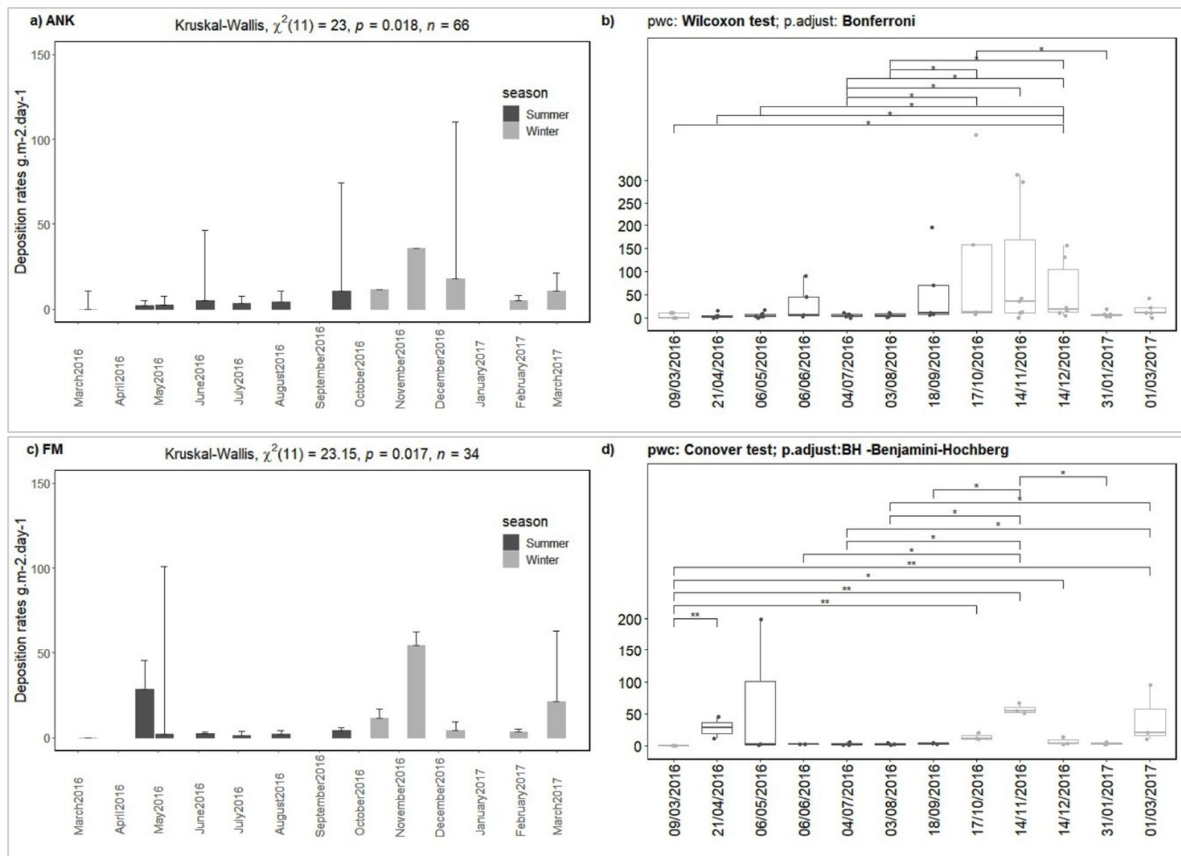
AstroTurf mats sediment deposition rates across the three salt marshes display significant monthly variations. Figure 4-9a for ANK, Figure 4-9c for FM and Figure 4-9e for MR highlight the changes that occurred during the yearly collection along with their respective statistical significance.

AstroTurf mats deployment and collection on ANK exhibit the highest mean rank sediment deposition rates occurring in winter during November and December 2016 ( $\eta = 35.8 \text{ g.m}^{-2} \text{ day}^{-1}$  and  $17.9 \text{ g.m}^{-2} \text{ day}^{-1}$  respectively) and the lowest in March and April 2016 ( $\eta = 0 \text{ g.m}^{-2} \text{ day}^{-1}$  and  $2.11 \text{ g.m}^{-2} \text{ day}^{-1}$  respectively) (Figure 4-9b). Collection dates were found to explain 19.2 % ( $r^2_{\text{adj}}$ ) of sediment deposition rates variation on ANK ( $F(11,54) = 2.41^*$  standardised residuals met the normality assumption), where both summer months of June and September 2016 and winter months

of October, November and December 2016 contribute the most to the model (regression model details are in Appendix C.1-Table C-7).

**FM's** AstroTurf mats collection includes fewer samples per month for inner-marsh statistical comparison, yet multiple pairwise comparisons (using post-hoc Conover's statistical test - Figure 4-9d) demonstrate that mean rank deposition rates are significantly higher during the winter months of November 2016 and early March 2017 ( $\eta = 54.7 \text{ g.m}^{-2} \text{ day}^{-1}$  and  $21.1 \text{ g.m}^{-2} \text{ day}^{-1}$  respectively) compared to August, July and May 2016 ( $\eta = 2.11 \text{ g.m}^{-2} \text{ day}^{-1}$ ,  $1.05 \text{ g.m}^{-2} \text{ day}^{-1}$  and  $2.11 \text{ g.m}^{-2} \text{ day}^{-1}$  respectively). Furthermore, deposition rates for March 2016 are found significantly lower than October, November, December 2016 and March 2017. This is confirmed in a regression model where all AstroTurf mats collection contributes significantly to the variation of sediment deposition rates on FM explaining 65.3 % ( $r^2_{\text{adj}}$ ) of the variance of the dataset ( $F_{(11,22)} = 6.65^{***}$ , details are in Appendix C.1-Table C-7).

**MR's** AstroTurf mats collection (Figure 4-9 e) also displays highest sediment deposition rates in winter months of November and December 2016 ( $\eta = 35.8 \text{ g.m}^{-2} \text{ day}^{-1}$  and  $17.9 \text{ g.m}^{-2} \text{ day}^{-1}$  respectively) and in March and April 2016 ( $\eta = 0 \text{ g.m}^{-2} \text{ day}^{-1}$  and  $2.11 \text{ g.m}^{-2} \text{ day}^{-1}$  respectively) (Figure 4-9 f). 39.3 % ( $r^2_{\text{adj}}$ ) of the variance of MR's deposition rates is explained by all collection dates collectively ( $F_{(11,84)} = 6.603^{***}$ , details are in Appendix C.1-Table C-7).



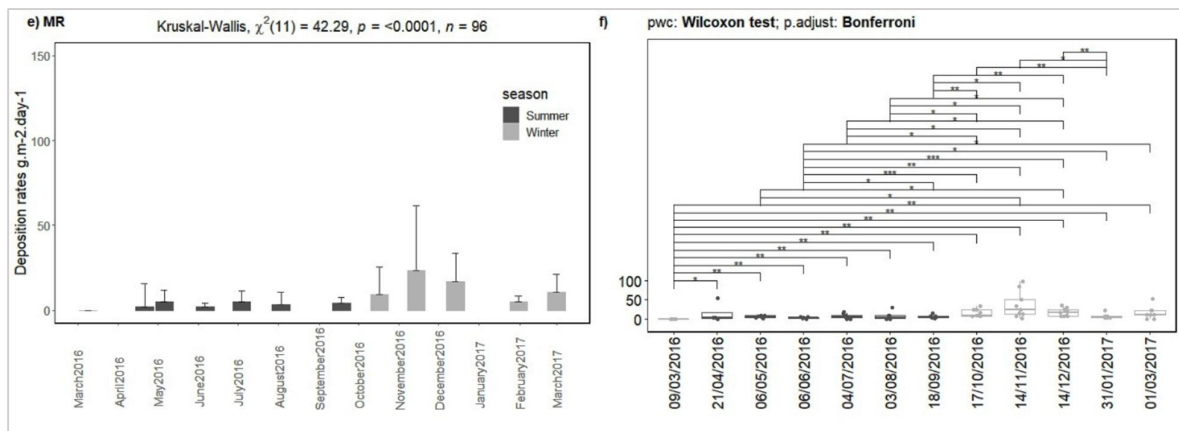


**Figure 4-9: Bar graph of ANK's (graph a), FM's (c) and MR's (e) AstroTurf mats sediment deposition mean ranks rates (in  $\text{g.m}^{-2}\text{day}^{-1}$ ) from 09<sup>th</sup> March 2016 to 01<sup>st</sup> March 2017 (top of bar is mean rank's average deposition, error bars calculated from individual standard error). Boxplot of ANK's (graph b), FM's (d) and MR's (f) AstroTurf mats sediment deposition rates (in  $\text{g.m}^{-2}\text{day}^{-1}$ ) showing statistically significant differences between rates during campaign (The boxplots represent median and error bars are interquartile range; Mann-Whitney-Wilcoxon tests results are symbolised on the top rows by the p-value significance - ns, \*, \*\*, \*\*\* - for each pairwise tests performed on ANK and MR and similarly Covover's test results are presented for FM deposition rates).**

#### **AstroTurf mats sediment deposition rates variation between summer and winter**

Comparably to the filter discs deposition rates, the results presented in the above section suggest that sediment deposition rates can be higher during the winter months and lower during summer months (as defined above in 4.2.1.2). Although the overall AstroTurf mats sediment deposition rates are slightly lower than the overall filter disc sediment deposition, it showed a similar trend with an increase of 58.4 % from summer ( $11.9 \pm 3.2 \text{ g.m}^{-2} \text{ day}^{-1}$ ) to winter ( $28.6 \pm 6.1 \text{ g.m}^{-2} \text{ day}^{-1}$ ) (Table 4-7) and pairwise comparisons test confirms that sediment deposition rates are significantly different between seasons ( $F_{(df= 186)} = 2.19^*$ ). However, seasons are found to only explain 2.3 % ( $r^2$ ) of AstroTurf mats deposition rates variation ( $F_{(1, 194)} = 4.65, p= 0.03^*$ ) (Figure 4-10a).

Using pairwise comparison tests (Figure 4-10b) show that sediment trapped on ANK's mats rose of 208.8% from summer ( $16.9 \pm 6.8 \text{ g.m}^{-2}\text{day}^{-1}$ ) to winter ( $52.2 \pm 17 \text{ g.m}^{-2}\text{day}^{-1}$ ) and MR experienced an increase of 158.2% from summer ( $6.1 \pm 1.4 \text{ g.m}^{-2}\text{day}^{-1}$ ) to winter ( $15.7 \pm 2.8 \text{ g.m}^{-2}\text{day}^{-1}$ ), whereas no statistical differences could be established on FM. Similarly, no statistical significant variation is found between winter and summer sediment deposition rates were observed between the sites' saltmarsh zones.

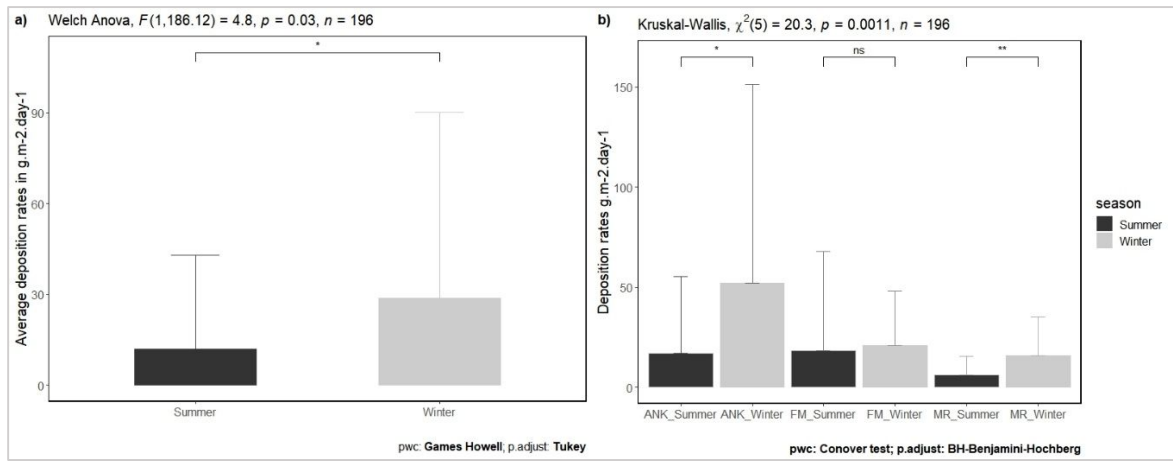


Figure 4-10: a) Average AstroTurf mats sediment deposition rates (in g.m<sup>-2</sup>.day<sup>-1</sup>) between summer (n=93) and winter (n=103) (top of bar is average deposition, error bars calculated from individual standard error). The graph also present results and statistical significance of Games-Howell test between seasons (symbolised on the top rows by the p-value significance - ns, \*, \*\*, \*\*\*).

b) Average summer and winter AstroTurf mats sediment deposition rates (in g.m<sup>-2</sup>.day<sup>-1</sup>) between sites (top of bar is average deposition, error bars calculated from individual standard error). The graph also highlights results and statistical significance of Conover-Iman pairwise comparison test (symbolised on the top rows by the p-value significance - ns, \*, \*\*, \*\*\*) between seasonal AstroTurf mats deposition mean ranks rates and saltmarsh sites.

Table 4-7: Average AstroTurf mats deposition rates (in g.m<sup>-2</sup>.day<sup>-1</sup>) in winter and summer by sites.

ASTROTURF MATS SEDIMENT DEPOSITION RATES					
		Mean	SD	Median	n
ANK	SUMMER	16.9	38.3	4.21	32
	WINTER	52.2	99.2	10.5	34
FM	SUMMER	18.3	49.4	2.63	16
	WINTER	20.8	27.3	10.5	18
MR	SUMMER	6.08	9.28	3.16	45
	WINTER	15.7	19.7	9.47	51

## 4.2.2 Sediment accretion rate estimates

An assessment of the vertical accretion rates is essential to understand saltmarsh stability and is critical to its sustainability if it is to maintain its relative elevation as sea level rises. The vertical accretion rate estimates for the three salt marshes are presented in this section based on the methodology described in Chapter 3 section 3.4.1.1 which requires to use soil bulk dry density (BDD here, also referred as autocompaction) to convert sediment deposition rates (section 4.2.1 above) into accretion rate estimates. This is because accretion rates describe vertical adjustments to a specific soil layer per year as a balance of deposition, erosion and compaction processes (Kearney et al., 1994; Nolte et al., 2013; Butzeck et al., 2014; Schindler, Karius, Arns, et al., 2014; Morris et al., 2016). Therefore, BDD used in this conversion is presented succinctly in 4.2.2.1 (results on the cores' results for bulk density/autocompaction are further in Chapter 6 as belowground soil processes) followed by the accretion rate estimates obtained from the filter discs and AstroTurf mats sediment deposition for 2016-2017 high-spring cycles (4.2.2.2).

### 4.2.2.1 BDD

BDD in Nigg Bay sediments were measured using a total of 608 samples across 23 depth-corrected sediment cores (see BDD calculation described in Chapter 3 -section 3.4.3.2 and Table 3-12). As the measurements were made across the three salt marshes using cores of depth varying from 33cm to 87 cm, BDD results were found to be highly variable, ranging from 0.09 to 2.2 g.cm<sup>-3</sup> (F=57.71, *p*<0.001\*\*\*). Recent saltmarsh literature shows that using BDD to estimate recent accretion rates is subject to assumptions as reflected in Kearney et al. (1994); Nolte et al., 2013; Butzeck et al. (2014); Thorne et al. (2014); Schindler, Karius, Deicke, et al. (2014); Spencer et al. (2017), and that there is no relationship between depth and the volume of organic matter of the upper part (10cm) of the cores (Nyman, 1990; Callaway et al., 2012). To test this, non-parametric regressions were conducted for the whole dataset (three salt marshes), then on a per site per saltmarsh zone basis. The overall values demonstrate a moderate correlation between BDD and core depth, a moderate correlation for MR's BDD and weak correlations were found on ANK and FM (see Figure 4-11 a, c, e and g). However, by using a cut-off depth at 0.3m (displayed with red lines on Figure 4-11 a, c, e and g), BDD show less variation with depth (Figure 4-11 b, d, f and h), it was then decided that this depth was acceptable to represent BDD's upper layer horizon for the studied salt marshes in Nigg Bay. Furthermore, the average topsoil bulk density reported by Countryside survey for Nigg Bay is between 0.8±0.02 to 1±0.02 g.cm<sup>3</sup> comparable to the overall BDD calculated for the studied salt marshes producing an overall mean is 0.89±0.02 and overall mean for upper 30cm is 0.76±0.02 g.cm<sup>3</sup> (CountrysideSurvey, 2007). The average BDD's upper soil layer is summarised per site and saltmarsh zone (Table 4-8 and Figure 4-12) and then used to translate sediment deposition into an accretion rate estimates as described in Chapter 3.4.1.1 (overall soil bulk density results are further discussed in Chapter 6 - 6.2.2.1 relating to the saltmarsh belowground processes).



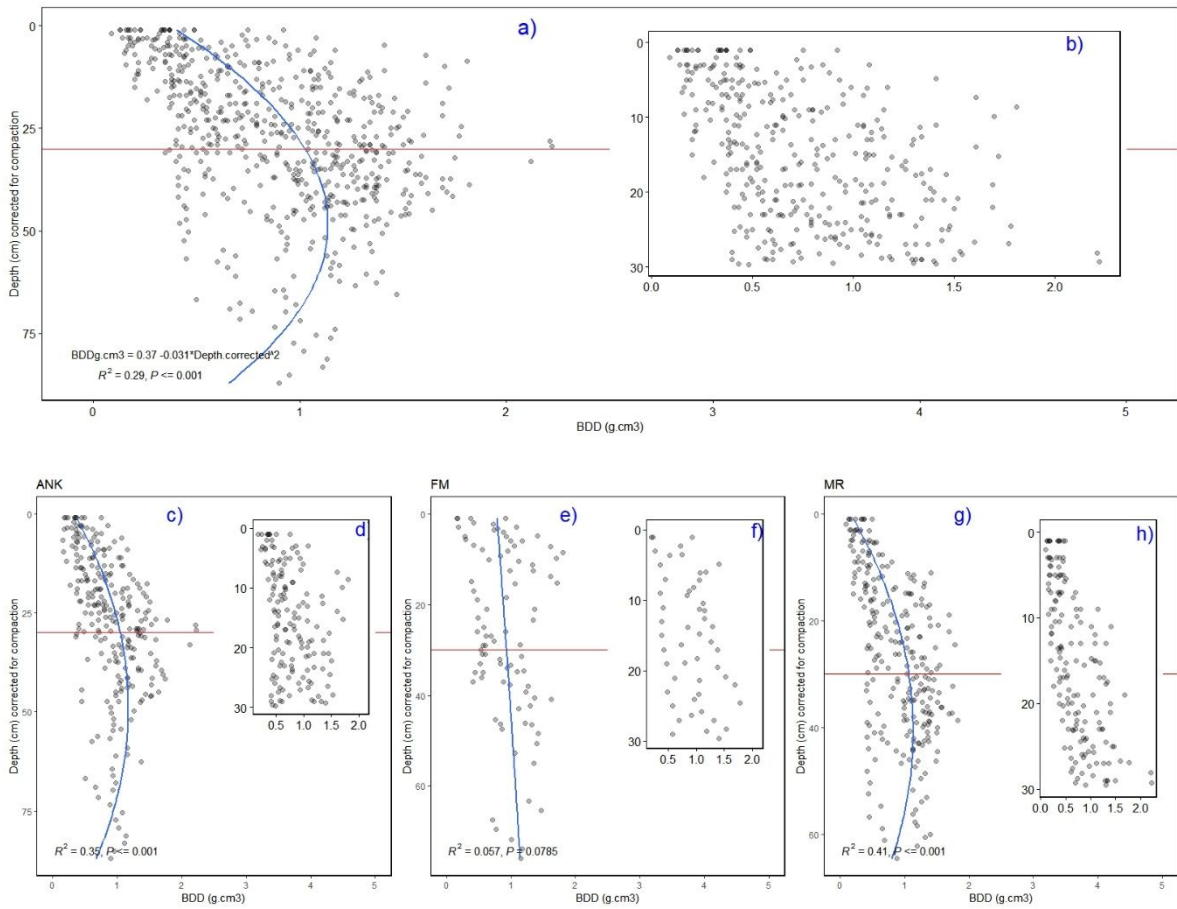


Figure 4-11: Relationships between BDD (g cm<sup>-3</sup>) and corrected depth (cm) (corrected for compaction - see Chapter 3 – 3.4.3.2). The results of polynomial regressions are provided for the whole dataset (a), ANK's whole cores' depths (c), those of FM's (e) and of MR (f). Each graph also presents as an inset the same relationships for the upper 30 cm: the whole dataset (b), ANK (d), FM (f) and MR (g). (Note the different scale of the y-axis in graphs c) and d) compared to graphs e) to h)).

Table 4-8: Average BDD (g.cm<sup>-3</sup>) per sites by saltmarsh zones for the first 30 cm (depth corrected for compaction) of the cores used to calculate accretion rates. \* No cores were collected in pioneer, so the overall average BDD was used for FM.

	ANK			FM			MR		
	Mean	SD	n	Mean	SD	n	Mean	SD	n
<b>Overall</b>	<b>0.77</b>	<b>0.37</b>	<b>147</b>	<b>0.90</b>	<b>0.40</b>	<b>52</b>	<b>0.69</b>	<b>0.44</b>	<b>160</b>
HM	0.88	0.28	27	0.62	0.29	27	0.71	0.47	69
MM	0.59	0.16	57	1.20	0.275	25	0.40	0.24	12
LM	0.61	0.36	25	N/A	N/A	N/A	0.74	0.33	48
PM	1.07	0.44	38	*	*	*	0.70	0.52	31

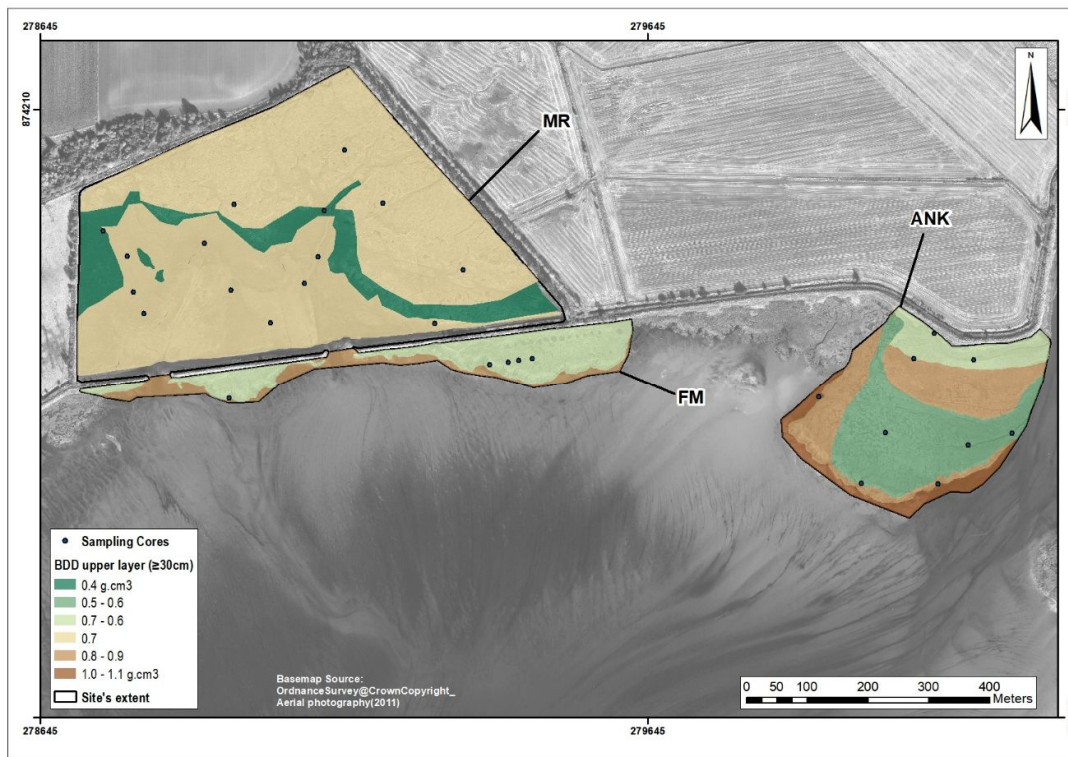


Figure 4-12: Upper 30cm Dry soil Bulk Density (BDD) calculated for each saltmarsh site and zone (as presented in Table 4-8 above) from the cores collected in 2016 on the salt marshes of Nigg Bay and used to convert deposition rates to accretion rates.

#### 4.2.2.2 Accretion rates

Total accretion rate estimates using filter discs range from 0 to 17.8 cm yr<sup>-1</sup> with an average accretion rate estimates 1.34±0.14 cm yr<sup>-1</sup>. Accretion rate estimates using Astroturf mats range from 0 to 24.6 and average at 1.1±0.21 cm yr<sup>-1</sup>.

Overall accretion rates' mean ranks derived from filter disc traps are found to be significantly different (K-W test  $H_{adj}=17.08$ ,  $p<0.001$  \*\*\*). A pairwise multiple-comparison Dunn's test (with BH adjustments) shows that the mean rank for the accretion rate estimates from filter disc traps is the highest on ANK (median difference with FM= 0.18 cm.yr\*\* & MR = 0.25cm.yr\*) and lowest on FM (median diff. with MR = 0.43 cm.yr\*\*\*) (Figure 4-13 and Table C-8). These relationships were further examined using a simple linear model demonstrates that differences between saltmarsh sites can only explain 4 % ( $r^2_{adj}$ ) of the filter discs accretion rate variation ( $F_{(2, 281)} = 6.99$ ,  $p=0.001$  \*\*\*) where mostly FM contributes significantly to the model (details in Table C-11). No statistical difference is found between the sites' accretion rate estimates using AstroTurf mats (Figure 4-13 and Table C-8).

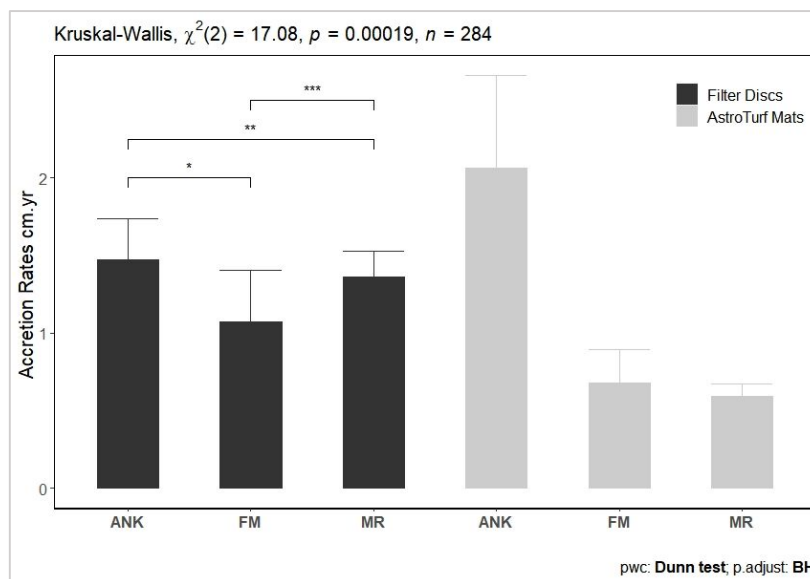


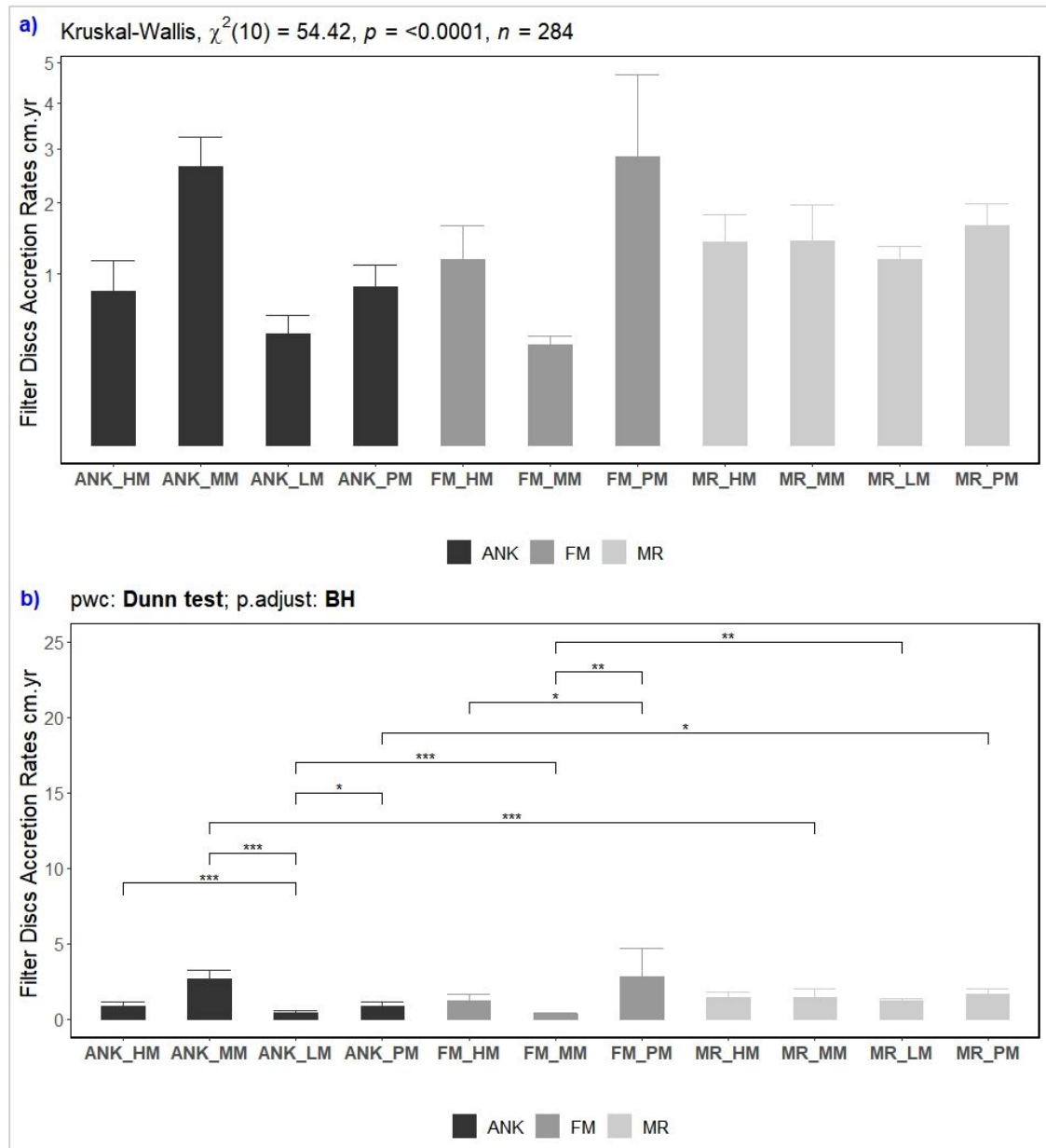
Figure 4-13: Average accretion rate estimates(cm.yr<sup>-1</sup> and error bars calculated from individual SE) per sites per devices. The graph also present the statistical significance of Dunn Post-hoc test between sites (symbolised on the top rows by the p-value significance - ns, \*, \*\*, \*\*\* ; details in Table C-8).

From the three saltmarsh sites, the mean ranks accretion rate estimates derived from both traps, filters and mats, are found to differ significantly between the sites' saltmarsh zones (Figure 4-14 a and c).

The mean rank of accretion rate estimates generated from filter discs on ANK's MM was the highest compared to the HM (median diff. = 0.9 cm.yr<sup>\*\*\*</sup>), LM (median diff. = 1.3 cm.yr<sup>\*\*\*</sup>) and PM (median diff. = 0.8 cm.yr<sup>\*</sup>) zones (Figure 4-14b). Conversely on FM, The mean rank of accretion rate estimates (filter discs) on PM zone is the highest on the salt marsh (median difference with MM= 0.9 cm.yr<sup>\*\*</sup> & HM = 0.9 cm.yr<sup>\*</sup>) (Figure 4-14b and Table C-9). Across the salt marshes, ANK's LM and PM accretion rates' mean ranks from filter discs were significantly lower than MR's LM (median diff. = 0.8 cm.yr<sup>\*\*\*</sup>) and MR's PM (median diff. = 0.5 cm.yr<sup>\*</sup>) respectively (Figure 4-14b). Accretion rates' mean rank was significantly lower on FM's MM compared to ANK's MM (median diff. = 0.9 cm.yr<sup>\*\*\*</sup>) and MR's MM (median diff. = 0.37cm.yr<sup>\*\*</sup>) (Table C-9).

These relationships are confirmed using a simple linear model demonstrating that differences between saltmarsh sites and zones can explain 12.5 % ( $r^2_{adj}$ ) of the filter discs accretion rate estimates variation ( $F_{(10, 273)} = 5.04, p < 0.001$  <sup>\*\*\*</sup>) where ANK's MM, FM's PM and MR's LM and PM rates contribute significantly to the model (details in table C-11 model 2). Combining temporal and spatial variation to the model improves the results and residuals where 34.2 % of the changes in accretion rate estimates can be explained by sites' saltmarsh zones and monthly variables (table C-11 model 4). In this scenario, all saltmarsh zones except FM's HM and MM along with all winter months and September contribute significantly to the model.

AstroTurf mats results presented similar pattern on ANK than the filter discs' where the highest accretion rates' mean rank was found on MM compared to PM (median diff. = 0.55 cm.yr\*\*), LM (median diff. = 0.69 cm.yr\*\*\*) and HM (median diff. = 0.42 cm.yr\*\*) (Figure 4-14d). ANK's MM mean rank accretion rate estimates was also significantly higher than FM's MM (median diff. = 0.62 cm.yr\*\*\*) and MR's MM (median diff. = 0.53 cm.yr\*\*) (details in table C-10). A simple linear model using the sites' saltmarsh zones confirms that ANK's MM and LM are solely contributing significantly to the AstroTurf mats accretion rate estimates variation ( $r^2_{adj} = 18.7\%$  with variability of  $F_{(10, 273)} = 5.04, p < 0.001$  \*\*\*- details in table C-11 model 3). When linking temporal (monthly variation) and spatial patterns, the model shows that 47.5 % of the changes that occur in accretion rate estimates in year can be explained by zonation and time where ANK's MM and LM and winter months of March, October, November and December influence considerably the model (table C-11 model 5).



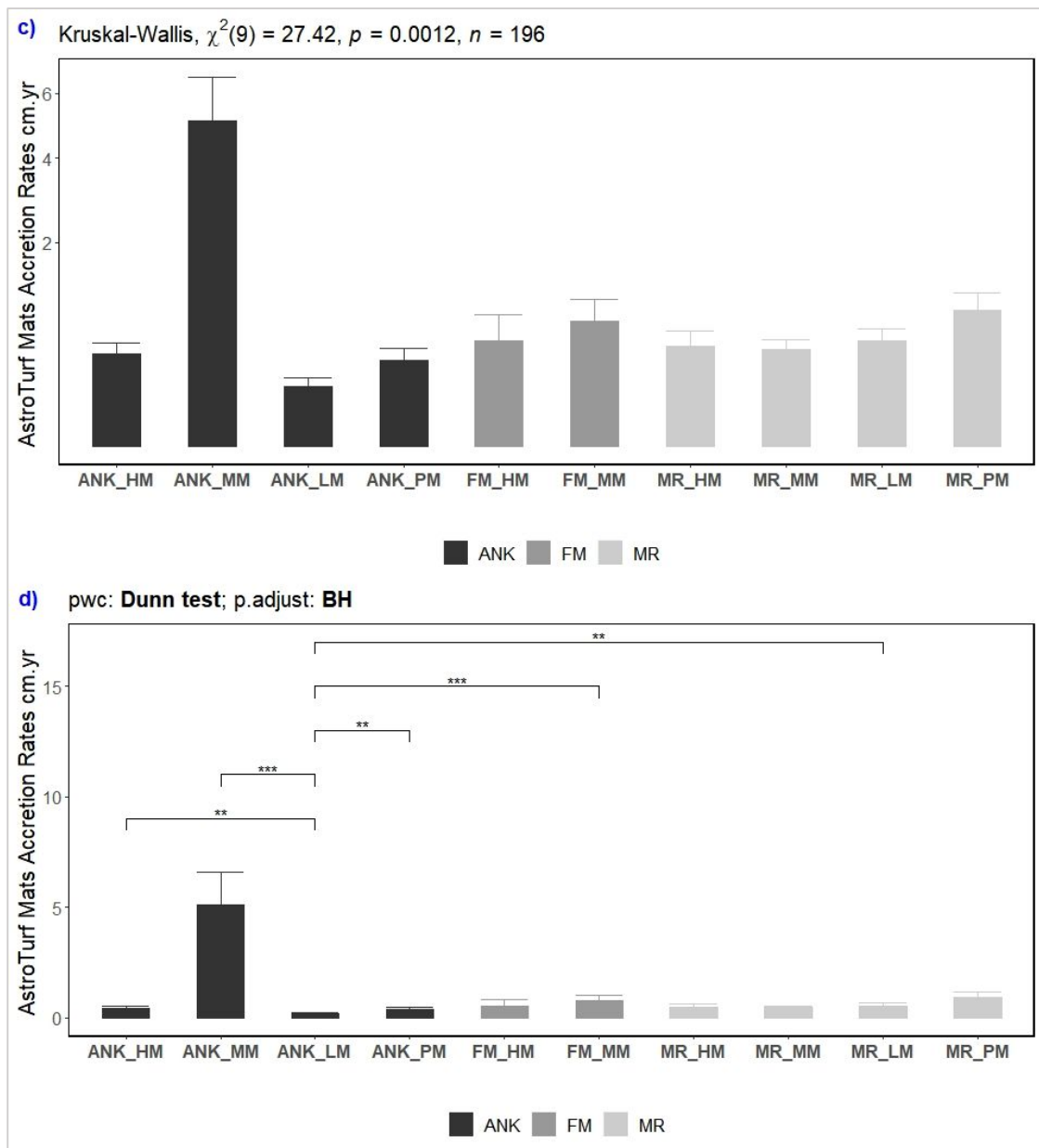


Figure 4-14: Average accretion rate estimates ( $\text{cm.yr}^{-1}$  and error bars calculated from individual SE): (a) calculated from filter discs traps and (b) showing the statistical significance of Dunn Post-hoc test (using BH adjustments) between the sites' saltmarsh zones (symbolised on the top rows by the p-value significance - *ns*, \*, \*\*, \*\*\*; details in Table C-9). Graph (c) and (d) are presenting the results from AstroTurf mat traps (pairwise comparisons are detailed in Table C-10).

### 4.2.3 Summary

This chapter section (4.2) aimed to improve our understanding of short-term saltmarsh development by assessing spatially and temporally sediment availability which was measured through sediment deposition across three salt marshes of Nigg Bay (4.2.1) using two different types of traps, filter discs and AstroTurf mats. Patterns and rates of accretion across the saltmarsh sites were assessed by quantifying short-term (annual) accretion rate estimates (4.2.2) across the three sites for each saltmarsh zone (Table 4-9).

The results presented show that, over the short-term (annual) intensive monitoring period, aboveground deposition rates (averaging  $23.4 \pm 2.3 \text{ g m}^{-2} \text{ day}^{-1}$  for filter discs and  $20.7 \pm 3.6 \text{ g m}^{-2} \text{ day}^{-1}$  for AstroTurf mats) are highly variable in space and time. Although overall deposition rates are uniform between managed and natural salt marshes, they differ significantly between the sites' saltmarsh zones (Filter discs: Table 4-2; AstroTurf mats: Table 4-5) and between the monthly collection (Filter discs: Table 4-3; AstroTurf mats: Table 4-6) suggesting seasonal (winter and summer seasons) variation (Filter discs: Table 4-4; AstroTurf mats: Table 4-7). The study further shows a strong seasonal variability where overall deposition rates (using Filter discs - Figure 4-4 - and AstroTurf Mats - Figure 4-8 -) are at highest during the months of September, October, November and December. This trend, in which winter months coincide with the highest deposition rates, is confirmed at each site, with the exception of filter disc deposition at ANK, where both June and October have high deposition rates, whilst the lowest deposition varies between trap types and sites (Figure 4-5 & Figure 4-9). The findings establish that collection dates, sites and saltmarsh zones can support between c.30% (filter discs) to c.48% (AstroTurf mats) of the variation in sediment deposition rates. These results suggested a seasonal pattern (summer/winter) which was confirmed for both traps, for MR with filter discs and MR and ANK with AstroTurf mats (Figure 4-6 & Figure 4-10).

Sediment deposition has been successfully transferred into vertical accretion rate estimates using the bulk dry density (details in section 3.4.1.1) from cores collected across the three salt marshes, thus providing means to qualify patterns and rates of accretion across the sites. The results presented show that the sediment deposition trend (that inferred uniformity between saltmarsh sites) holds true for accretion rate estimates derived from AstroTurf mats (averaging at  $1.1 \pm 0.21 \text{ cm yr}^{-1}$ ), however, filter disc accretion rate estimates (averaging at  $1.34 \pm 0.14 \text{ cm yr}^{-1}$ ) demonstrate significant differences between sites (Figure 4-13). Spatial variation between sites' saltmarsh zones presented by the filter discs deposition rates is mirrored for ANK's and FM's accretion rate estimates but are not reflected on MR (Figure 4-14a&b). In the same way than AstroTurf mats deposition rates, accretion rate estimates demonstrate less significant variation between the sites' saltmarsh zones (Figure 4-14c&d). Relationships between sediment, vegetation and physical drivers are further examined in section 4.5 and discussed in section 4.6.

**Table 4-9: Filter disc and AstroTurf mat accretion rate estimates**

Filter Discs accretion rate estimates in $\text{cm yr}^{-1}$									
	ANK			FM			MR		
	Mean	SD	n	Mean	SD	n	Mean	SD	n
overall	1.47	2.62	98	1.07	2.49	56	1.36	1.87	130
HM	0.81	1.53	19	1.18	2.44	28	1.40	1.68	17
MM	2.65	3.62	39	0.35	0.28	21	1.42	2.95	28
LM	0.43	0.69	21				1.18	1.23	57
PM	0.86	1.11	19	2.83	4.92	7	1.65	1.75	28

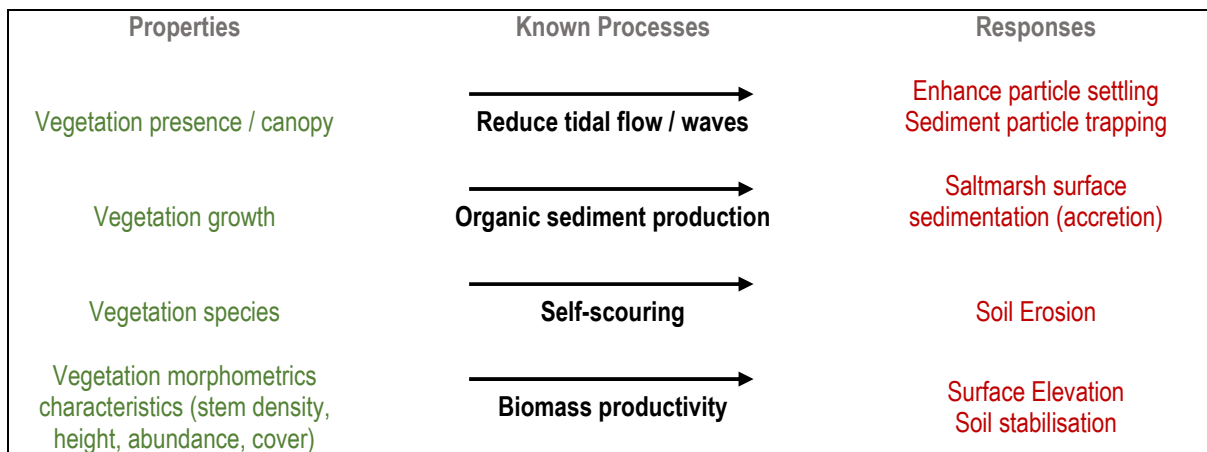


AstroTurf mats accretion rate estimates in cm yr <sup>-1</sup>									
	ANK			FM			MR		
	Mean	SD	n	Mean	SD	n	Mean	SD	n
overall	2.07	4.82	66	0.68	1.24	34	0.59	0.81	96
HM	0.41	0.42	17	0.54	0.96	11	0.49	0.49	11
MM	5.12	7.09	24	0.75	1.37	23	0.45	0.44	23
LM	0.17	0.19	13				0.54	0.79	40
PM	0.36	0.35	12				0.89	1.16	22

#### 4.3 Short-term (annual) biological controls to saltmarsh development: vegetation characteristics and biological processes

To maintain their elevation relative to sea-level rise, tidal landforms rely on the interplay of inorganic and organic sediment deposition displayed by striking biological and morphological patterns at different scales (Da Lio et al., 2013, p.2). This concept is reflected by the recognition that vegetation can regulate saltmarsh systems and can attenuate (e.g. surface scouring - Friess et al., 2011) or enhance (e.g. slowing water flows - Möller, 2006; Möller et al., 2014 – Soil stabilisation - Ford et al., 2016) sedimentation through saltmarsh life-cycles. Chapter 2 -2.2.1 and 2.3.2.2 has introduced some of the influences, controls and feedbacks between biological and geomorphological processes and highlighted below in Table 4-10 some of them:

**Table 4-10: Two-way feedbacks between biological and physical processes** (ref Chapter 2 -2.2.1 and 2.3.2.2. citing (Möller, 2006; Mudd et al., 2009; Friess et al., 2011; Wang and Temmerman, 2013; Belliard et al., 2017; Leonardi et al., 2018; Reef et al., 2018)



Vegetation characteristics and distribution across salt marshes are traditionally seen as fixed biological features with little morphological variations but increasingly recent contributions in the field of bio-geomorphology have shown that vegetation traits and zonation are integral part of biogeomorphic feedbacks taking places in saltmarsh landscapes (Da Lio et al., 2013; D'Alpaos et al., 2016; Belliard et al., 2017). At the size-scale of the three salt marshes of Nigg

Bay, and at short annual timescale, it is hypothesised that vegetation characteristics such as height, density, cover and biomass productivity:

- i. are indicators of biogeomorphic feedbacks between sedimentation (deposition rates and accretion rate estimates measured here) and vegetation; and,
- ii. demonstrate strong spatial relationships with physical processes results.

This chapter section presents results of vegetation characteristics measured during the summer 2016 (same year of sediment deposition measurements) across the saltmarsh zones of the three studied sites (section 4.3.1). Vegetation was assessed in terms of abundance (height and density) and the resulting implications of this variability for saltmarsh biological development is presented in relation to biomass (section 4.3.2.1) and organic content (4.3.2.2). Investigations into the possible physical controls of the vegetation processes are addressed in section 4.5.2, physical controls on sediment deposition rates and accretion rate estimates results are examined in section 4.5.1, and the final implications of the vegetation and biomass results for the aboveground blue carbon storage in Scottish salt marshes are reviewed in section 4.6.3 as this aspect is relevant to of the supporting ecosystem services saltmarsh systems provide: carbon storage and sequestration (Blue Carbon). These results also constitute Blue Carbon Pool 1 (biomass productivity is used in this study to inform on the aboveground organic carbon stock following Howard et al. (2014) conversion - see Chapter 3- 3.4.1.2 and Table 3-13 and 3-14).

### **4.3.1 Vegetation characteristics**

Vegetation height, density and cover (methodology in 3.4.1.2) are the vegetation characteristics studied and presented in the following sections for the three salt marshes. Because each area doesn't comprise same number of sampling plot, the statistics used below are principally non-parametric or the data has been normalised (as percentage).

#### **4.3.1.1 Vegetation height**

Overall vegetation height between the three salt marshes does not differ. However, vegetation height is significantly different between saltmarsh zones (Figure 4-15a and Table 4-11). It demonstrates a large range of height in each zone (e.g. 12.64 to 54.84 cm on MM zone) and presents an overall trend that decreases closer to the shore (Figure 4-15a) confirmed by Dunn's test (using BH - adjustments) pairwise comparison test where vegetation on PM is found to be statistically significantly lower than all other zones.

Dunn's test was also performed to test differences between vegetation height and sites and saltmarsh zones. The results show that only significant difference is found between MR's HM and PM zones ( $p < 0.01$ \* Figure 4-15b).

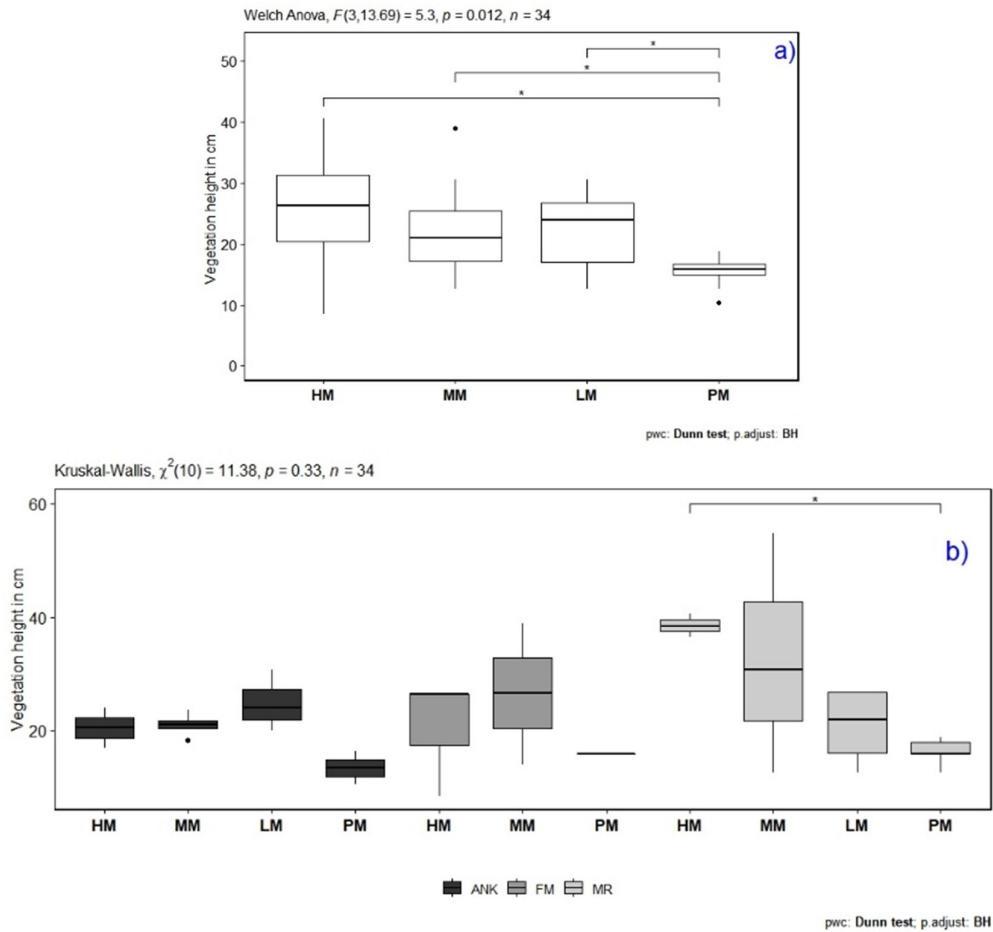


Figure 4-15: Boxplots of vegetation height (cm) mean ranks measured in July 2016 (a) between saltmarsh zones highlighting Welch Anova statistical results; and, (b) between sites and saltmarsh zones with Kruskal-Wallis statistical results. Both graphs highlight the statistical significance for Dunn test's pairwise comparison (using BH adjustments - symbolised on the top rows by the p-value significance - ns, \*, \*\*, \*\*\* ). Boxplots represent median (middle line) interquartile range (box), 1.5 times interquartile range (bar) and outliers (black dots).

Table 4-11: Overall vegetation height (cm) between saltmarsh zones (top) and between sites and saltmarsh zones (bottom) as surveyed in July 2016 (n=34).

ALL Site		Vegetation height (cm) July 2016										
	Mean	SD	Median	Sample size								
HM	25.6	10.9	26.3	7								
MM	26.1	13.5	21	9								
LM	22.2	6.14	23.9	10								
PM	15.4	2.7	15.8	8								
Vegetation Height (cm) July 2016												
ANK				FM				MR				
	Mean	SD	Median	Sampling	Mean	SD	Median	Sampling	Mean	SD	Median	Sampling
HM	20.4	4.95	20.4	2	20.4	10.3	26.3	3	38.5	2.97	38.5	2
MM	21	2.22	21	3	26.5	17.7	26.5	2	32.7	21.2	30.6	7
LM	24.8	5.4	23.9	4					20.9	6.53	21.9	3
PM	13.4	4.12	13.4	2	15.8	NA	15.8	1	16.2	2.39	15.8	5

### 4.3.1.2 Vegetation density

Figure 4-16a displays the significant difference of vegetation density between the saltmarsh sites (F=6.37,  $p=0.01^{**}$ ). MR average vegetation population per  $m^2$  ( $\eta=13300\pm 2547$ ) is approximately half as dense than on ANK natural saltmarsh ( $\eta=34450\pm 2878$ ) (Table 4-12).

Across sites and saltmarsh zones, vegetation density is statistically different ( $H=18.7$ ,  $p<0.05^*$ ) and pairwise comparison test shows that vegetation is denser on ANK's HM and MM compared to MR's HM and MM (Figure 4-16b).

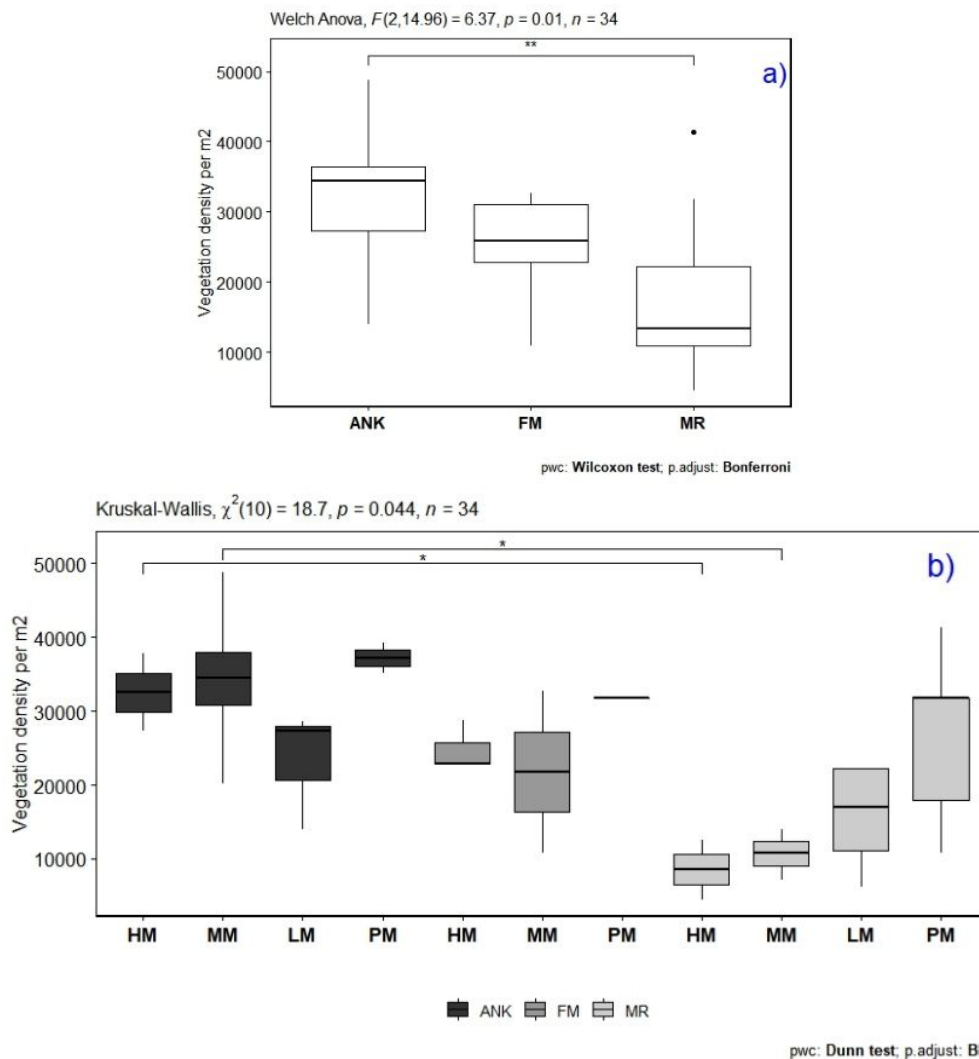


Figure 4-16 Boxplot of vegetation density (per  $m^2$ ) mean ranks measured in July 2016 (a) between salt marshes highlighting Welch Anova statistical results; and, (b) between sites and saltmarsh zones with Kruskal-Wallis statistical results. Both graphs highlight the statistical significance for pairwise comparison tests ((a) Wilcoxon test; and, (b) Dunn test's (using BH adjustments) both symbolised on the top rows by the p-value significance - ns, \*, \*\*, \*\*\* ). Boxplots represent median (middle line) interquartile range (box), 1.5 times interquartile range (bar) and outliers (black dots).

Vegetation density was scaled to provide a dispersion factor resulting in grouping vegetation dataset in three categories: uniform, clumped or random (3.4.1.2). Overall, 83.3% of the

vegetation cover is found to be clumped against 16.6% uniform. These proportions are of similar proportion on the natural and managed salt marshes, ANK and MR, but not on FM a higher proportion of the vegetation was uniform (Figure 4-17).

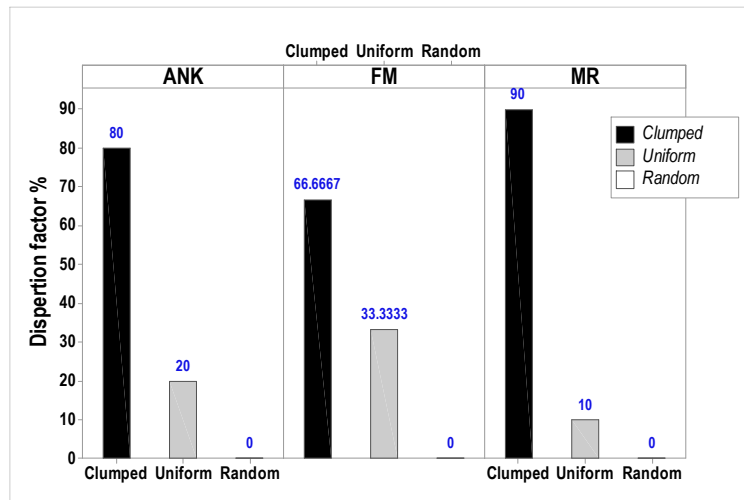


Figure 4-17: Proportion of vegetation uniformity per sites showing FM having no variability in vegetation density whilst ANK display a wider display of vegetation characteristics across its zones and MR has predominantly clumped vegetation.

Table 4-12: Vegetation density per m<sup>2</sup> by site

	Vegetation Density (per m <sup>2</sup> )											
	ANK				FM				MR			
	Mean	SD	Median	Sample	Mean	SD	Median	Sample	Mean	SD	Median	Sample
overall	31564	9546	34450	11	24965	8122	25788	6	17395	10501	13300	17
HM	32550	7495	32550	2	24800	3421	22825	3	8550	5728	8550	2
MM	34450	11717	34450	4	21775	15450	21775	2	10667	3429	10850	3
LM	23300	8084	27250	3					15890	7143	16965	7
PM	37200	2970	37200	2	31840	NA	31840	1	26776	12214	31840	5

#### 4.3.1.3 Vegetation cover

Vegetation distribution methodology and monitoring is addressed in Chapter 3 in sections 3.3.2.2, 3.4.1.2 and 3.4.2.3 and presented in tables 3-5 and 3-4, figures 3-13 and 3-14, constituting this research baseline NVC vegetation assemblages.

In ANK, the mature natural marsh is mainly composed with NVC community **SM8** in the pioneer-marsh (PM) zone; with **SM13a** on the low-marsh (LM); **SM13b** on the mid-marsh (MM); and, **SM16a** on the high-marsh (HM). In FM, the natural fronting marsh comprises NVC community **SM8** on the PM; **SM16a** and **SM16c** on the HM where community **SM13d** was also recorded and sampled (belonging to MM zone). FM also includes areas, not sampled, of NVC community **SM13a** (LM) location on westernmost part of the site and driftline vegetation (**SM28**) along the embankment wall. The managed realignment salt marsh (MR) is composed with NVC community **SM8** and bare mud on the PM; NVC community **SM13a** on the LM;

NVC community **SM13b and SM13d** on the MM; the HM characterised by NVC community **SM16d**.

Although vegetation height and density are relatively homogenous between sites (4.3.1.1 and 4.3.1.2), significant differences in percentage vegetation cover are demonstrated between saltmarsh zones (K-W test  $H_{adj}=7.93$ ,  $p<0.05^*$ ) with the pioneer zones exhibiting highest percentage of bare surface compared to the HM, MM and LM (Dunn test results in Figure 4-18b). Although this trend is not confirmed statistically (possibly due to the low number of samples), overall, vegetation cover is also seen to be lower on PM zones across ANK and MR salt marshes. Between saltmarsh sites and zones, pairwise comparison tests find ANK's MM has significantly more cover than ANK's PM and FM's HM significantly more than MR's HM zone (Table 4-13 and Figure 4-18b).

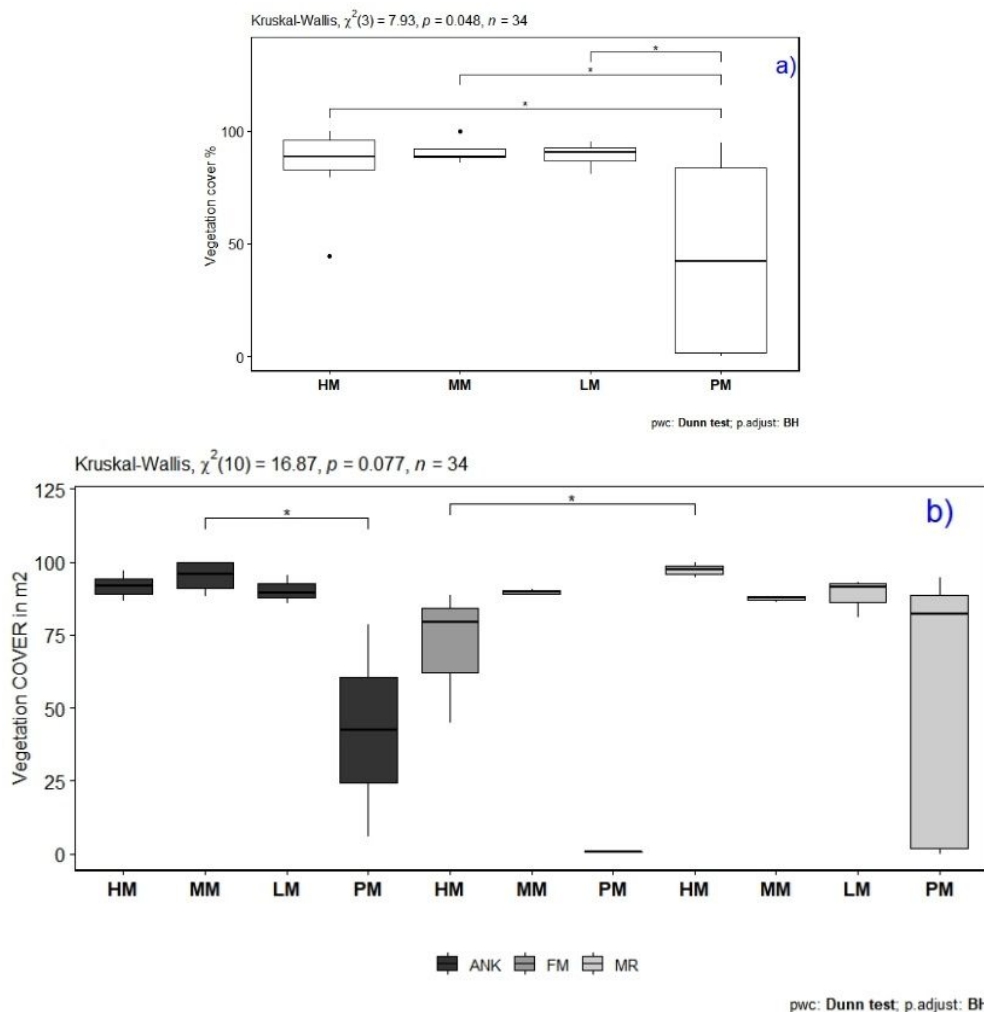


Figure 4-18: Stacked column graphs (to 100 %, error bars  $\pm$ SE) showing the average vegetation abundance cover (bare/vegetation in %) between sites and saltmarsh zones. Boxplot of average vegetation abundance cover (bare/vegetation in %) mean ranks measured in July 2016 (a) between saltmarsh sites; and, (b) between sites and saltmarsh zones. Both graphs highlight Kruskal-Wallis statistical results and the statistical significance for pairwise comparison tests (Dunn test's (using BH adjustments) both symbolised on the top rows by the p-value significance - ns, \*, \*\*, \*\*\* ). Boxplots represent median (middle line) interquartile range (box), 1.5 times interquartile range (bar) and outliers (black dots).



**Table 4-13: Average vegetation cover (%) per sites and saltmarsh zones** There is significant differences of vegetation cover between saltmarsh zones ( $F=10.14$ ,  $p<0.001^{***}$ ) with highest percentage of bare cover found on PM zones. The same pattern is observed on ANK ( $F=4.6$ ,  $p=0.03^*$ ) and MR ( $F=3.54$ ,  $p=0.04^*$ ).

	Vegetation cover (%)											
	ANK				FM				MR			
	Mean	SD	Median	Sampling	Mean	SD	Median	Sampling	Mean	SD	Median	Sampling
HM	91.8	7.52	91.8	2	70.9	23.2	79.4	3	97.4	3.74	97.4	2
MM	95.1	5.9	96	4	89.7	1.59	89.7	2	87.5	1.23	88	3
LM	90.3	4.72	89.6	3					88.9	5.01	91.4	7
PM	42.4	51.4	42.4	2	0.65	NA	0.649	1	53.5	48.2	82.1	5

### 4.3.2 Aboveground living biomass and organic content

Potentially important mechanism for climate mitigation, saltmarsh vegetation can play an significant role as carbon sinks counteracting rapid increase atmospheric carbon dioxide concentration owing to close feedbacks, that takes place on salt marsh, between vegetation, sedimentation and anoxic conditions, promoting carbon storage (Andrews et al., 2006; Kirwan and Mudd, 2012; Fagherazzi, 2013; Duarte et al., 2013). Aboveground biomass and subsequent organic content constituting the aboveground short-term saltmarsh feedbacks between biological (plant type, density and organisms) and physical processes (inundations and temperatures) and the response to belowground circumstances affecting the net change in organic matter. Living plants productivity generates biomass of the saltmarsh ecosystem supporting services of carbon storage, and constitutes Carbon Pool 1 of a Blue Carbon budget estimates which is used in this study to inform on the aboveground organic carbon stock following Howard et al. (2014) conversion (see Chapter 3- 3.4.1.2 and Table 3-14).

Overall biomass (averaging  $422.9 \pm 23.2$  g.m<sup>2</sup> ranging from 202.4 to 667.7 g.m<sup>2</sup>) or aboveground organic content (averaging  $190.3 \pm 10.4$  OC<sub>g.m2</sub> ranging from 91.1 to 300.5 OC<sub>g.m2</sub>) do not demonstrate statistical variability between sites suggesting that managed salt marsh and natural salt marshes present similar properties in 2016, when the data was collected. Overall aboveground biomass and OC are not statistically different between saltmarsh zones or sites and saltmarsh zones.

The summary statistics for both biomass and aboveground organic content are presented in Appendix C-2 - Table C-12). Since a conversion equation (Howard et al., 2014) is used to convert biomass to OC<sub>g.m2</sub>, only OC<sub>g.m2</sub> will be presented in the following section.

### 4.3.3 Relationships between vegetation characteristics and biological processes

In Nigg Bay, trends for vegetation height and density can be depicted despite the small dataset, indeed there is a modest relationship between vegetation height and density ( $r^2_{adj} = 18.7\%$  with variability of  $F_{(1, 31)} = 8.432, p < 0.01^{**}$ ). The relationships are significantly clearer between sites as depicted in Figure 4-19. The results of regression analysis show that vegetation height is a significant predictor for vegetation density on ANK (55 % of the variation can be explained by vegetation height) and FM (85 % of the variation can be explained by vegetation height) but not MR. Therefore, the analysis shows that the taller is the vegetation, the less dense it is and vice versa.

From vegetation morphometric characteristics measured on the three salt marshes of Nigg Bay, only vegetation height is found to be strongly correlated to aboveground organic carbon content (OC) and can explain 40 % of its variation (Figure 4-20 and LM1 in Appendix C2- Table C-13). Notably, Nigg Bay vegetation density or cover are not found significant predictors for aboveground OC.

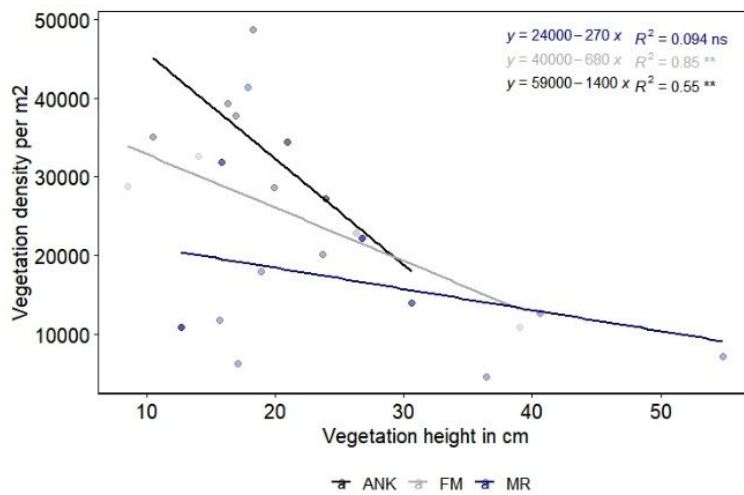


Figure 4-19: Trends between vegetation density and vegetation height per site along with regression results (p-value significance - ns, \*\*, \*\*\*).

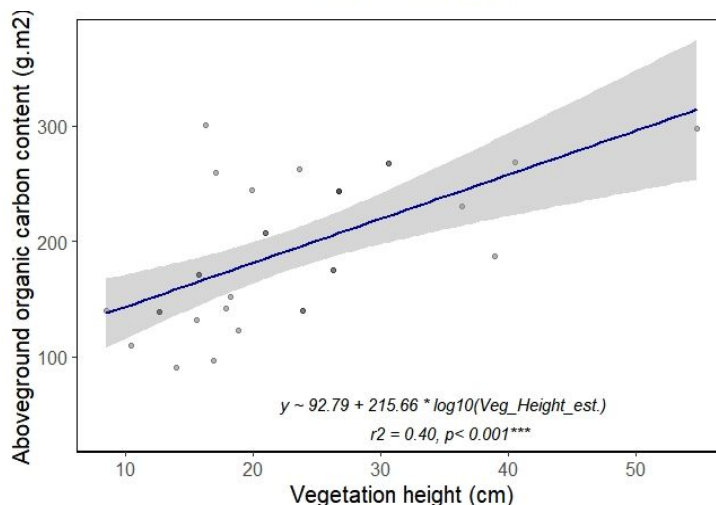


Figure 4-20: Scatter plot between aboveground carbon content (in  $OC_{g.m2}$  - y-axis) and vegetation height (in cm). Plots are showing linear regressions with their respective relationship equation (the regressions have been log transformed - dependent variable- to meet linear assumption),  $r^2$  values, p-value and p-value significance).

As salt marshes and saltmarsh zones are for the most part defined by their vegetation assemblages and elevation within tidal frame (chapter 3- 3.3.2.2), relationships between NVC vegetation assemblages and vegetation characteristics and processes (aboveground organic content) are further analysed.

As expected, vegetation height in SM8 assemblage (pioneer zone) is found to be significantly lower than in SM13a (low-marsh), SM13b (mid-marsh) and SM16c (high-marsh) (Figure 4-21a). Similarly, SM8 vegetation cover means ranks are found significantly lower than SM13a and SM13b (Figure 4-21c). Overall, vegetation density or aboveground organic content mean ranks are not found significantly different between NVC assemblages. Pairwise comparison tests identify surprisingly SM8 mean ranks density higher than SM13a's (Figure 4-21b) and mean ranks OC for SM16a lower than SM13b, and understandably lower than SM16d (high-marsh) (Figure 4-21d).

To test for significant relationships between the combinations of biological variables and NVC assemblages, a regression model has shown that NVC can explain 24 % ( $r^{2adj}$ ) of the variance in vegetation height (LM4 in Appendix C2- Table C-13). By adding vegetation density as an independent variable to NVC assemblages, 31% ( $r^{2adj}$ ) of the variability in vegetation height can be accounted for, with mid and high-marsh vegetation (SM13b and SM16a) and vegetation density contributing the most to the model (LM5 in Appendix C2- Table C-13). NVC assemblages are found to support 22 % ( $r^{2adj}$ ) of the variance in vegetation density with a significant contribution from SM8 and SM16d to the model (LM6 in Appendix C2- Table C-13). The vegetation assemblages can support 34 % ( $r^{2adj}$ ) of the variance in vegetation cover with pioneer-marsh vegetation have the most impact in the model (LM7 in Appendix C2- Table C-13). NVC assemblages and vegetation height are also significantly influencing aboveground OC and can explain 38 % ( $r^{2adj}$ ) of its variance with SM16a contributing significantly to the model (LM2 in Appendix C2- Table C-13).

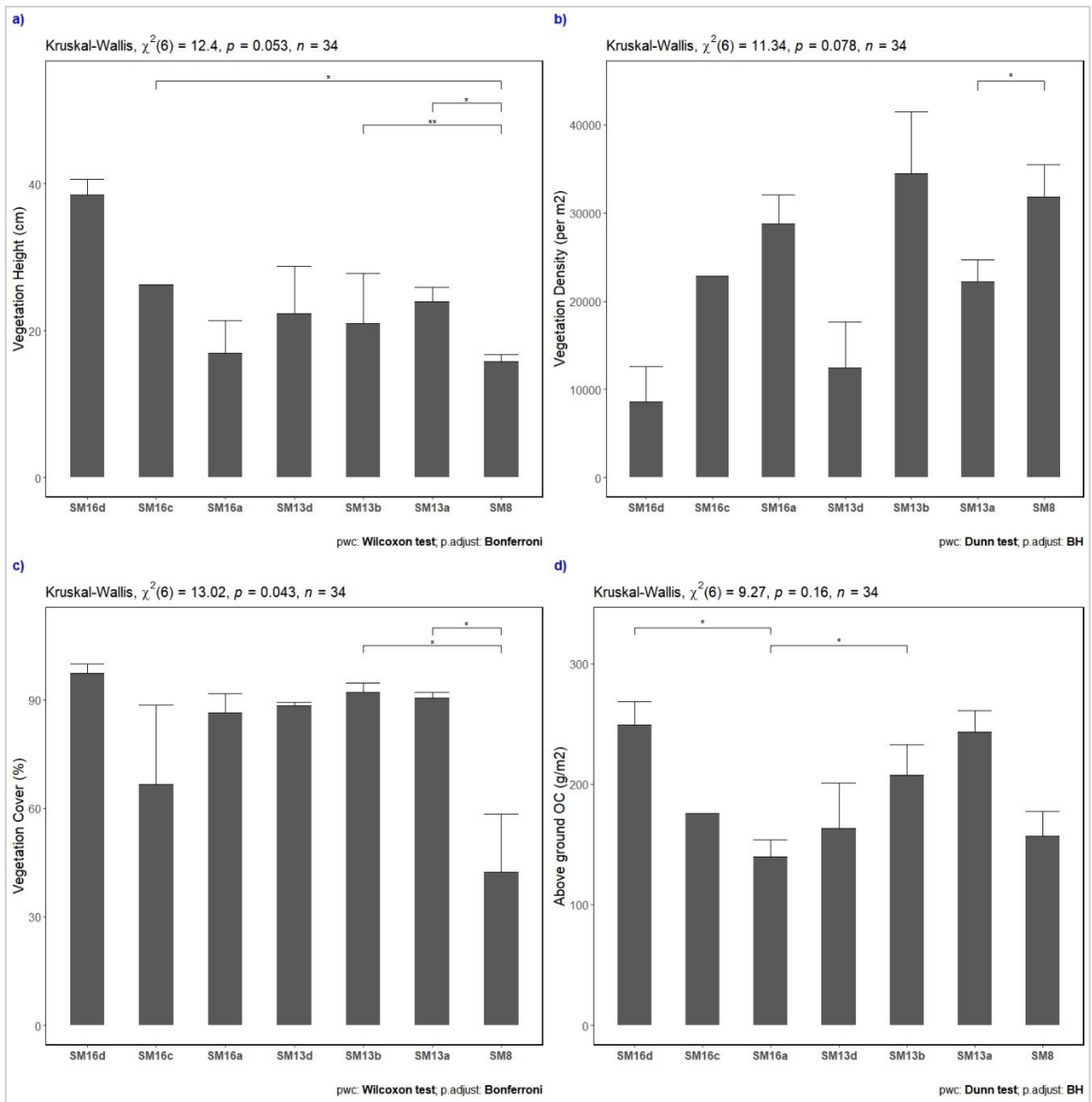


Figure 4-21: Bar graphs showing mean ranks' vegetation height (a), density (b), cover (c) and aboveground organic content-  $OC_{g,m^2}$  (d) for each NVC assemblages sampled on the three Nigg Bay salt marshes. The graphs also label Kruskal-Wallis results and the statistical significance of post-hoc pairwise comparison tests ((a and c) Wilcoxon test using Bonferroni adjustments; and, (b and d) Dunn test's using BH adjustments) both symbolised on the top rows by the p-value significance with p-value significance ( $ns, *, **, ***$ ).

#### 4.3.4 Summary

This chapter section (4.3) aimed to improve our understanding of short-term (annual) saltmarsh development by quantifying spatially and temporally the vegetation characteristics and processes which were measured during the sediment deposition collection (09<sup>th</sup> March 2016 to 31<sup>st</sup> January 2017) across three salt marshes and saltmarsh zones in Nigg Bay (methods in 3.4.1.2) and by assessing spatial patterns and relationships between these predictors.

Overall, this analysis indicates that the height and coverage of vegetation at natural and managed sites were comparable. All PM zones (across all sites) had significantly shorter vegetation than

all other zones. The MM zone at ANK is more vegetated (as percentage cover) than the PM zone, while the HM zones at MR and FM are more vegetated than the HM zone at FM. This performance can be explained by the difference in vegetation assemblages present on these salt marshes (SM16d on MR and SM16a and SM16c on FM). On the other hand, the analysis shows that vegetation density differs between the natural saltmarsh and managed realignment, ANK and MR, and between these sites' higher saltmarsh zones (HM and MM).

The study also shows that the aboveground organic carbon estimated for Nigg Bay saltmarsh vegetation does not differ between natural and managed salt marshes or between saltmarsh zones but is predominantly enhanced by some vegetation assemblages (SM13b, SM16a and SM16d), and, that biological predictors of these assemblages are associated with vegetation height. In section 4.5 and 4.6, the relationships between sediment, vegetation and physical drivers are explored further.

#### **4.4 Water levels over the short-term (annual) sediment collection period**

As seen in Chapter 2 - 2.3.1.2 and Chapter 3 - 3.3.2.3, tides are one of the principal controls on sedimentary processes by way of sediment transport across the tidal flat, sediment suspension, deposition, accretion, sedimentation and vertical and horizontal marsh extension. By regulating the water flow across the marsh surface via tidal creeks, the tides define the extent and duration of the inundation, principal source of sediments, organic matter and nutrients (Fagherazzi et al., 2004; Wolanski et al., 2009; Davidson-Arnott, 2009; Kearney and Fagherazzi, 2016).

Using the time series data from the transducer pressure logger in the MR site (see figure 3-17 and 3-18), flood depth, flood frequency and hydroperiod (as defined in chapter 3 - 3.3.2.3) were determined across the three saltmarsh sites' area (see figure 3-14) for the filter and AstroTurf mat sediment deposition monitoring period (8<sup>th</sup> February 2016 to 01<sup>st</sup> March 2017 i.e. 359 days or 778 tidal periods) following Kefelegn (2019) methodology. Figure 4-22 presents the water levels for this period at each sediment collection date. Relationships between water levels and physical and biological processes that take place on the three salt marshes is further discussed in section 4.5.

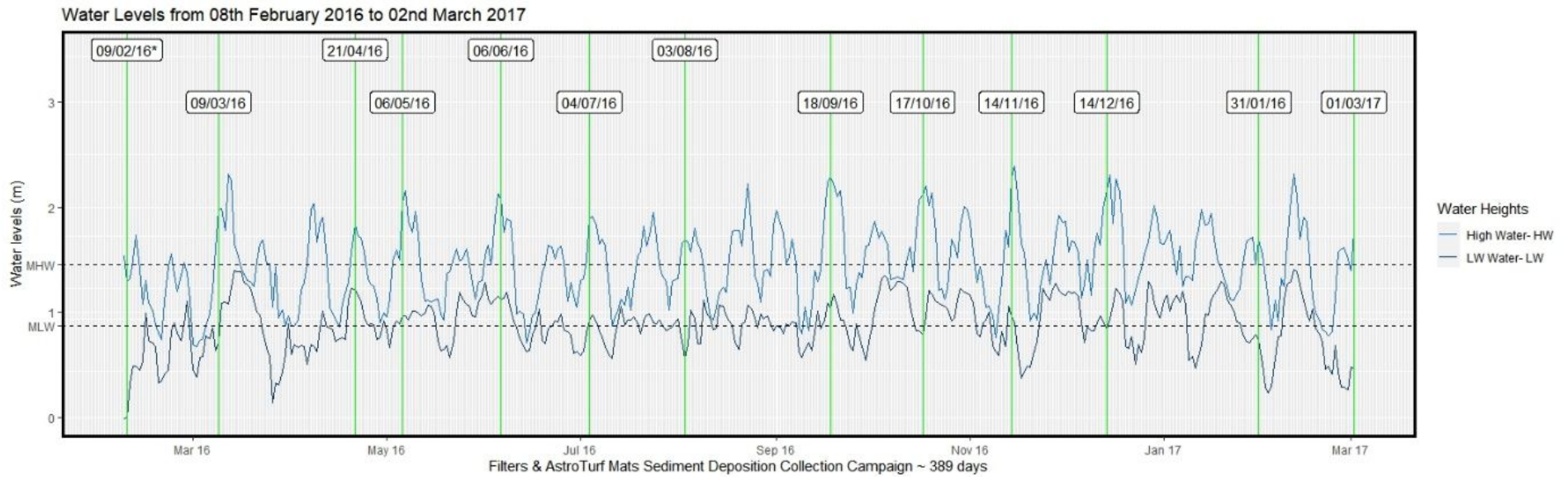


Figure 4-22: High Water (HW) and Low Water (LW) levels from the 09<sup>th</sup> February 2016 to 01<sup>st</sup> March 2017 where the dates and green lines correspond to sediment data collection points. Note: The first -sediment collection (09/02/2016\*) was a trial for equipment (filter discs and AstroTurf mats) and not included in the time series or sediment deposition analysis.



#### 4.4.1 Average hydroperiod, flood depth and flood frequency

##### 4.4.1.1 Average flood depth

###### Average flood depth between saltmarsh sites

The average flood depth which is the difference between the average of all high water (HW) heights for the period analysed (Figure 4-22) and the saltmarsh surface elevation (Figure 4-25 and Table 4-14) demonstrates statistically significant differences between the saltmarsh sites' mean ranks ( $H = 9726.6$ ,  $p < 0.001^{***}$ , Table 1) and strong variations between the sites with a mean rank flood depth of 0.16 m for MR, 0.15 m for FM and 0.11 m for ANK ( $p < 0.001^{***}$ , Mann-Whitney-Wilcoxon pairwise tests adjusted with Bonferroni correction) between March 2016 and March 2017 (Figure 4-25). These levels impact the amount of each saltmarsh area that can be flooded each day: 94 % for ANK, 93% for FM, whereas only 65 % of MR is concerned (Figure 4-23). Figure 4-25 further depicts quantity of observations that have a significantly higher flood depth on ANK compared to FM and MR. ANK's flood depth ranges up to 0.67 m compared to 0.51 m for FM and 0.47 m for MR. These significantly higher flood depth corresponds to areas of the salt marsh that have a flood depth higher or equal to 0.43 m and extremely high flood depth is equal or higher than 0.63 m. On ANK, these very high flood equates to 0.5 % of ANK's surface and extreme flood 0.01 % of the marsh surface. They are fronting the easternmost saltmarsh

platform and the mouth of the largest creeks also located on the east (Figure 4-23 and Figure 4-24). On FM, outliers' values are minimal (0.15 % of FM surface) with no extreme flood depth and are located south of the western breach (Figure 4-24). Only 0.01 % of MR surface experiences a flood depth higher or equal to 0.42 m and principally affect areas are north of the western and eastern breaches (Figure 4-24), whereas no extreme flood depth can be observed. These high and extreme flood depth are in the shallowest part of the marsh that experiences most drag from tidal flow and ebb, also the effect of the river outlet may contribute to a greater scouring on ANK's eastern marsh edge.

A linear regression model tested the influence of the sites on the flood depth ( $F_{(2, 285282)} = 3738$ ,  $p < 0.001^{***}$ ) which explained 2.5 % of the variance (details in Appendix C.3: Table C-14).

**Table 4-14: Calculated average flood depth (m) between saltmarsh sites for the period of the sediment deposition campaign (filters and AstroTurf mats) from 09<sup>th</sup> March 2016 to 01<sup>st</sup> March 2017. Note that n corresponds to a 1m<sup>2</sup> cell size.**

Site	Variable	n	mean	SD	median	IQR	Flooded Area (%)
ANK	Flood depth	87167	0.13	0.09	0.11	0.10	94
FM	Flood depth	38206	0.17	0.11	0.15	0.20	93
MR	Flood depth	159912	0.15	0.08	0.16	0.13	65

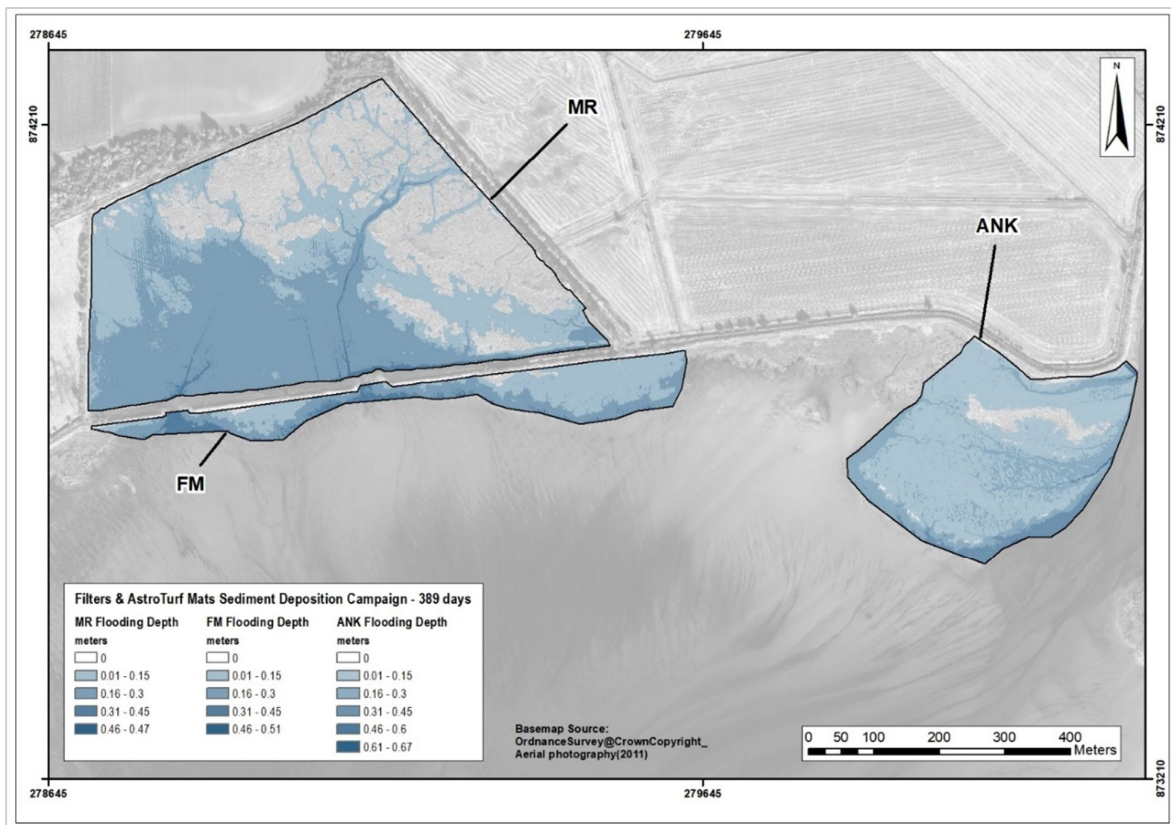


Figure 4-23: Average (over 389days) flood depth (m) calculated at a 1m<sup>2</sup> cell scale size for the three saltmarsh sites.

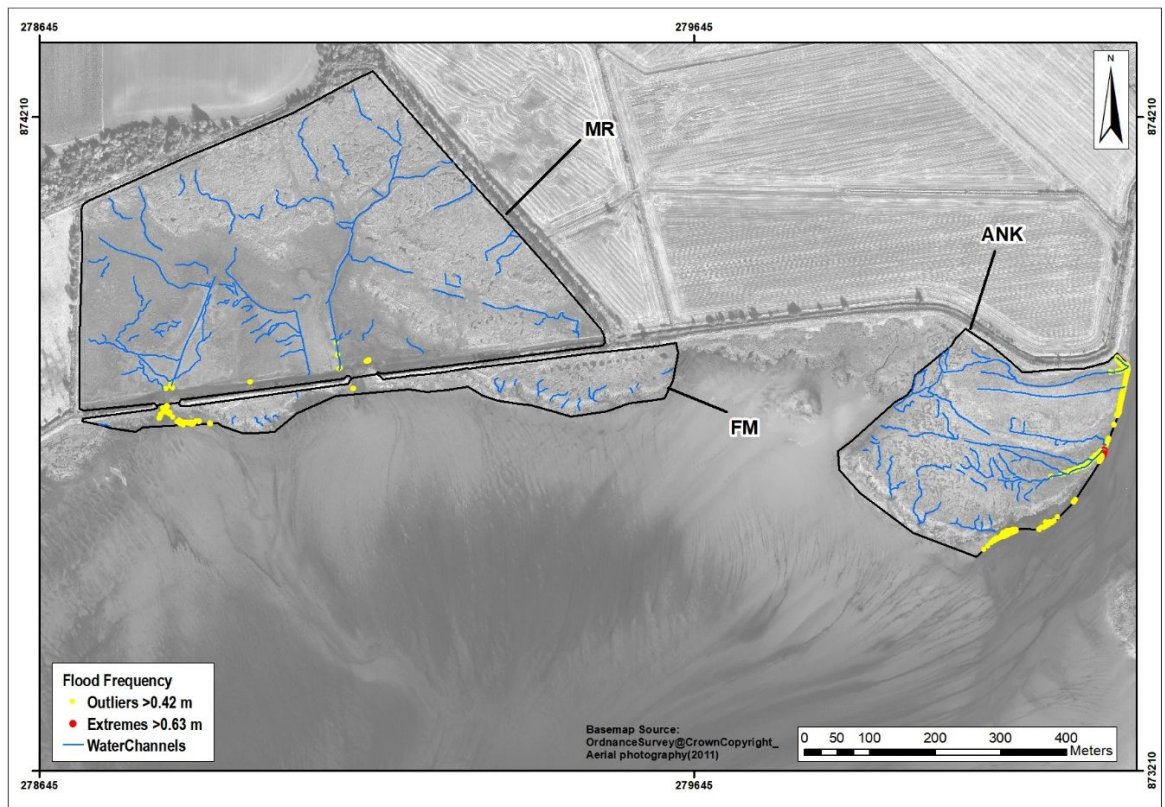


Figure 4-24: Spatial variation of very high flood depth (outliers in yellow) and extremely high flood depth (red) values across the three studied salt marshes ranging from 0.42 m to 0.67 m.

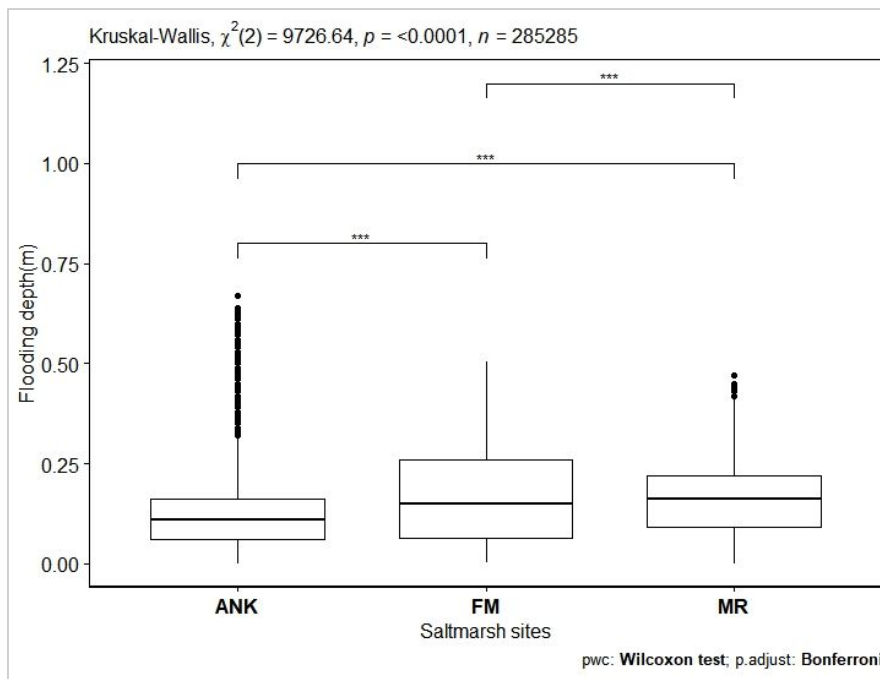


Figure 4-25: Boxplot of the flood depth mean ranks (m) for the sediment deposition campaign showing significant differences between saltmarsh sites (Kruskal-Wallis H test and Mann-Whitney-Wilcoxon tests results are symbolised on the top row by the p-value significance - ns, \*\*, \*\*\* - for each pairwise test). Boxplots represent median (middle line) interquartile range (box), 1.5 times interquartile range (bar) and outliers (black dots).

#### Average flood depth between sites and saltmarsh zones

Differences between sites' saltmarsh zones (using all marsh surfaces as illustrated in Figure 3-14) were tested and were found statistically significant ( $H = 183715, p < 0.001^{***}$ ). Pairwise comparisons (Mann-Whitney-Wilcoxon pairwise tests adjusted using Bonferroni) further demonstrated that all sites' saltmarsh zones differ significantly from each other (Table 4-15, Figure 4-26 and Appendix C.3 Figure C-1). On the three salt marshes, flood depth followed the elevational gradients: highest flood depth is found on pioneer zones and lowest on high-marsh zones. In addition, the comparison showed that flood depth mean ranks are significantly higher on the HM of FM compared to the ANK and MR which has the lowest rank, thus having an impact on the flood depth which can reach over 90% of the surface of ANK and FM whilst only c. 31% of the MR marsh is affected. These results can be explained by FM's HM having a shorter distance from the saltmarsh edge compared to MR (an average difference of  $71.02 \pm 2.33$  m). This explanation is sustained for the pioneer zones where the flood depth mean ranks are the highest on ANK, slightly lower on FM, whilst MR is having the lowest rank (on average MR's PM is 20.9 m farther from the edge of the salt marsh compared to ANK or FM). Flood depth mean ranks are the highest on FM's LM, then on MR's and lowest on ANK's. The flood depth on MM is fairly homogeneous in height between the salt marshes (0.11 to 0.09 m - Table 4-15), but the analysis shows that on ANK and FM tidal flooding can cover over 99.8 % of ANK, 90.4 % of FM whereas 85 % of MR is affected. Outliers and extreme values coincide with

above-mentioned observations, however only ANK's MM display extreme flood depth, higher or equal to 0.63 m (Appendix C-3 - Figure C-1).

A linear regression model assessed the influence of the sites and zones on flood depth ( $F_{(10, 285274)} = 43650, p < 0.001^{***}$ ) and is found to explain 60.5% ( $r^2_{adj}$ ) of the variance where all sites' zones are positively influencing the model except MR's HM (details in Appendix C.3: Table C-15).

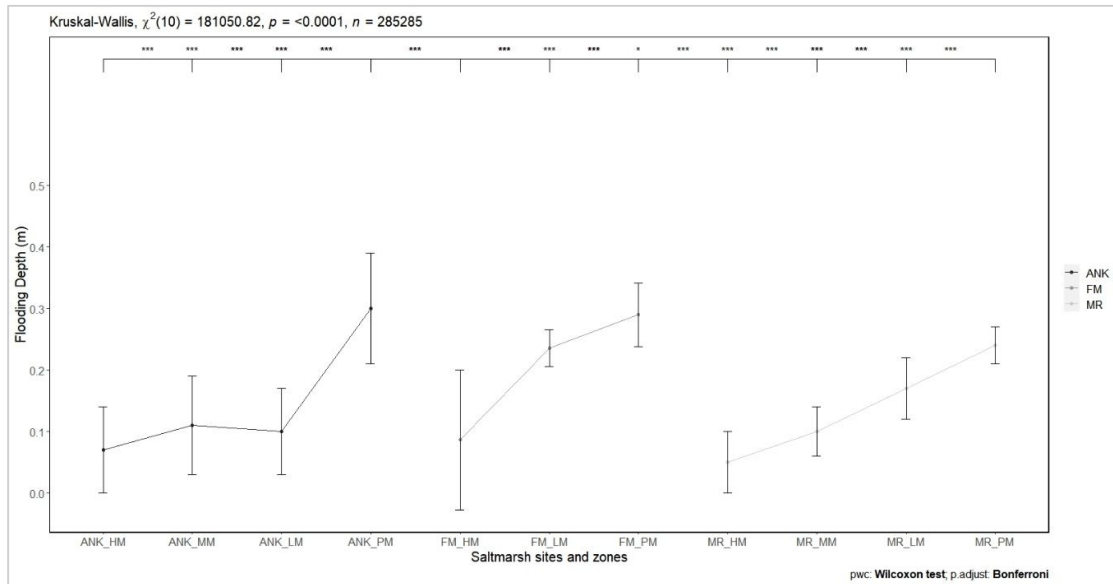


**Figure 4-26: Plot of the flood depth mean ranks (m) for the sediment deposition campaign showing significant differences between sites' saltmarsh zones** (The plots represent median and error bars are interquartile range. Kruskal-Wallis H test and Mann-Whitney-Wilcoxon tests results are symbolised on the top row by the p-value significance - ns, \*, \*\*, \*\*\* - for each pairwise tests -For full pair-test comparison boxplot see in Appendix C.3 Figure C-8).

**Table 4-15: Calculated average flood depth (m) between sites' saltmarsh zones for the sediment deposition campaign (filters and AstroTurf mats) from 09<sup>th</sup> March 2016 to 01<sup>st</sup> March 2017.** Note1: that n corresponds to a 1m<sup>2</sup> cell size; \* Note2: FM-HM marsh surface include sampling points that display mid-marsh vegetation assemblages (SM13d), therefore statistics also tested differences between FM's HM and ANK's MM and MR'S MM.

Site	Variable	n	Mean	SD	median	IQR	Flooded Area (%)
ANK_HM	Flood depth	27280	0.0958	0.07	0.07	0.07	100
ANK_MM	Flood depth	11002	0.113	0.06	0.11	0.08	99.9
ANK_LM	Flood depth	39917	0.108	0.07	0.1	0.07	31.3
ANK_PM	Flood depth	8968	0.308	0.06	0.3	0.09	85.0
FM_HM*	Flood depth	26380	0.109	0.07	0.09	0.11	99.7
FM_LM	Flood depth	672	0.228	0.03	0.24	0.03	100
FM_PM	Flood depth	11154	0.292	0.05	0.29	0.05	100
MR_HM	Flood depth	37320	0.0615	0.04	0.05	0.05	99.9
MR_MM	Flood depth	27635	0.0989	0.04	0.1	0.04	31.3
MR_LM	Flood depth	54443	0.179	0.05	0.17	0.05	85.0
MR_PM	Flood depth	40514	0.241	0.03	0.24	0.03	99.7

#### 4.4.1.2 Average flood frequency

##### Average flood frequency between saltmarsh sites



The average flood frequency which corresponds to the number of times the saltmarsh area (1m<sup>2</sup> cell) is flooded during the survey period analysed (expressed in percentage), shows statistically significant differences between the saltmarsh sites' mean ranks (H= 9450.5,  $p < 0.001^{***}$ , Table 4-16) and pairwise tests confirmed a very strong evidence of differences between each site ( $p < 0.001^{***}$ , Mann-Whitney-Wilcoxon tests adjusted with Bonferroni) showing that flood frequency for MR is ranging from 0.3 to 80.5 % with a mean rank of 7.5 %, for FM from 0.3 to 84.6 % with a mean rank of 6.7 % and for ANK from 0.3 to 97.2 % with a mean rank of 4.4 % during March 2016 and March 2017 (Figure 4-28). These large variations are highlighted in Figure 4-28 and Figure 4-27 where very high number of flooding relates to flooding that occurred at least or more than 44 % on ANK (up to 97.2 %), FM (up to 84.6 %) and MR (up to 80.5 %) surface area (Figure 4-30). However, a linear regression model assessed the influence of the sites on flood frequency ( $F_{(2,285282)} = 4806$ ,  $p < 0.001^{***}$ ) and demonstrates to only explain 3.3% of the variance (details in Appendix C.3: Table C-14).

**Table 4-16: Calculated average flood frequency (%) between saltmarsh sites for the sediment deposition campaign (filters and AstroTurf mats) from 09<sup>th</sup> March 2016 to 01<sup>st</sup> March 2017. Note that n corresponds to a 1\*1 m cell size.**

Site	Variable	n	mean	SD	median	IQR	Flooded Area (%)
ANK	Flood frequency	87167	9.96	15.5	4.37	5.15	94
FM	Flood frequency	38206	18.9	20.2	6.68	37.5	93
MR	Flood frequency	159912	13.7	13.8	7.46	20.6	65

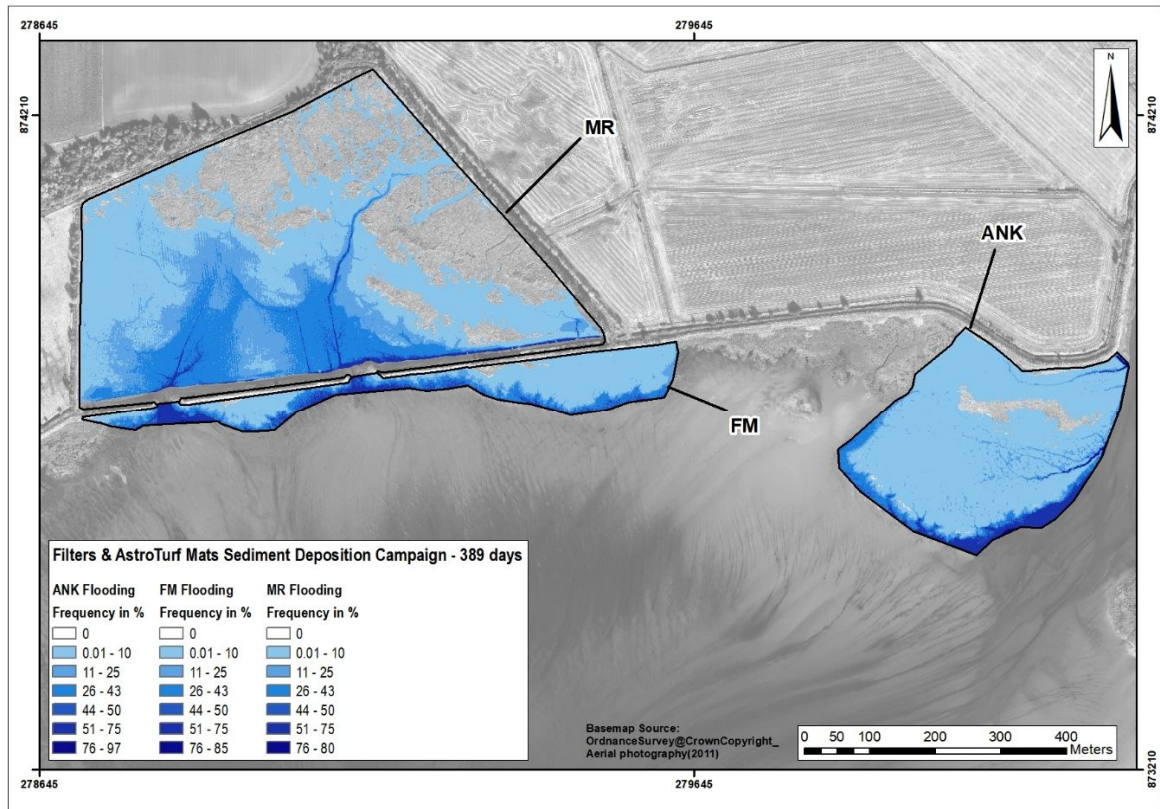


**Figure 4-27: Average flood frequency (% - over 389days) calculated at a 1m<sup>2</sup> cell scale size for the three saltmarsh sites.**

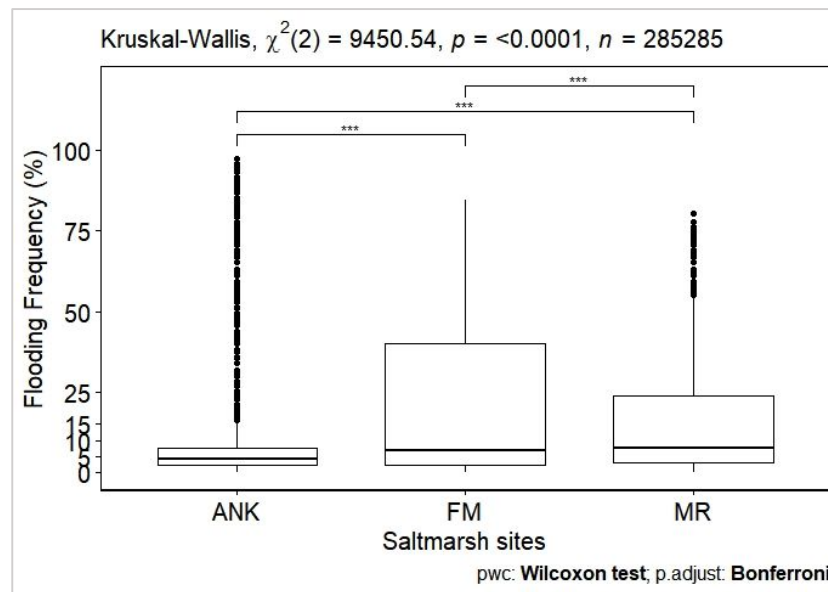


**Figure 4-28: Boxplot of the flood frequency mean ranks (%) for the sediment deposition campaign showing significant differences between saltmarsh sites** (The plots represent median (middle line) interquartile range (box), 1.5 times interquartile range (bar) and outliers (black dots). Kruskal-Wallis H test and Mann-Whitney-Wilcoxon tests results are symbolised on the top row by the p-value significance - *ns*, \*, \*\*, \*\*\*).

#### Average flood frequency between sites and saltmarsh zones

Average flood frequency is also statistically different between sites' saltmarsh zones mean ranks ( $H = 184718, p < 0.001^{***}$ ). Using Mann-Whitney-Wilcoxon pairwise tests (with Bonferroni adjustments), every sites' saltmarsh zones demonstrate very strong differences from each others (Table 4-17, Figure 4-29 and in Appendix C-3: Figure C-2). Similar remarks observed for the flood depth spatial variation are seen for flood frequency, such as the number of tides that decreases with elevational gradient. However, we can witness (Figure 4-29) on ANK a sharp drop from PM to LM reducing its average frequency to 93.3 % whereas on FM and MR it is more gradual (-38.2 % and -67.5 % respectively) which can be explained by differences in topography and vegetation between the sites (analysis is further developed in 4.5). The pairwise comparison tests (Appendix C-3: Figure C-2) show that very high flood frequency ( $\geq 44\%$ ) covers 62.8 % of ANK's PM surface and extremely high flood frequency (69 % to 87 %) is experienced on 5.1 % of the zone. Similarly, 58.6 % of FM's PM has flood frequency higher or equal to 44 % and 3.6% of the zone experience extremely high number of flooding (69 to 85 %). Whereas only 7.8 % of ANK's PM undergo very high flood frequency ( $\geq 44\%$ ) and 0.2 % of the zone has a flood frequency higher than 69 % up to 81 %. Very high flood frequency ( $\geq 44\%$ ) is encountered on the LM zone of the three salt marshes, however it is only observed on 2% of ANK surface, 1.3 % of FM and 2.4 % of MR. Extreme flood frequency (69 to 94 %) is just observed on ANK for 1.1 %. On all the studied sites, less than 1 % of MM's and HM's surfaces experience very high flood frequency (and only ANK present extreme flood frequency covering  $< 0.5\%$  of its surface). Figure 4-30 depicts the spatial variation of very high and extreme flood frequency located closest to the saltmarsh edge and following the tributary creeks on MR



flowing from west and east breach. A linear regression model assessed the influence of the sites and zones on flood frequency ( $F_{(10, 285274)} = 59780, p < 0.001^{***}$ ) which explained 67.7% ( $r^2_{adj}$ ) of flood frequency variance with standardised residuals meeting normality assumption (Details in Appendix C-3: Table C-15).

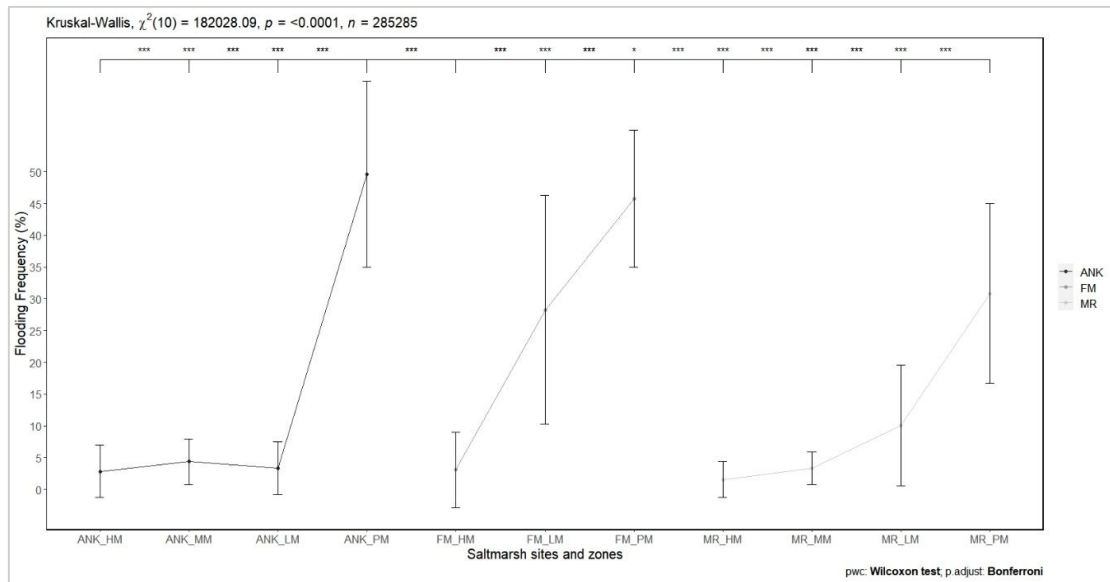


**Figure 4-29: Plot of the flood frequency mean ranks (%) for the sediment deposition campaign showing significant differences between sites' saltmarsh zones** (The plots represent median and error bars are interquartile range. Kruskal-Wallis H test and Mann-Whitney-Wilcoxon tests results are symbolised on the top row by the p-value significance - ns, \*, \*\*, \*\*\* - for each pairwise tests -For full pair-test comparison boxplot see in Appendix C.3 Figure C-9).

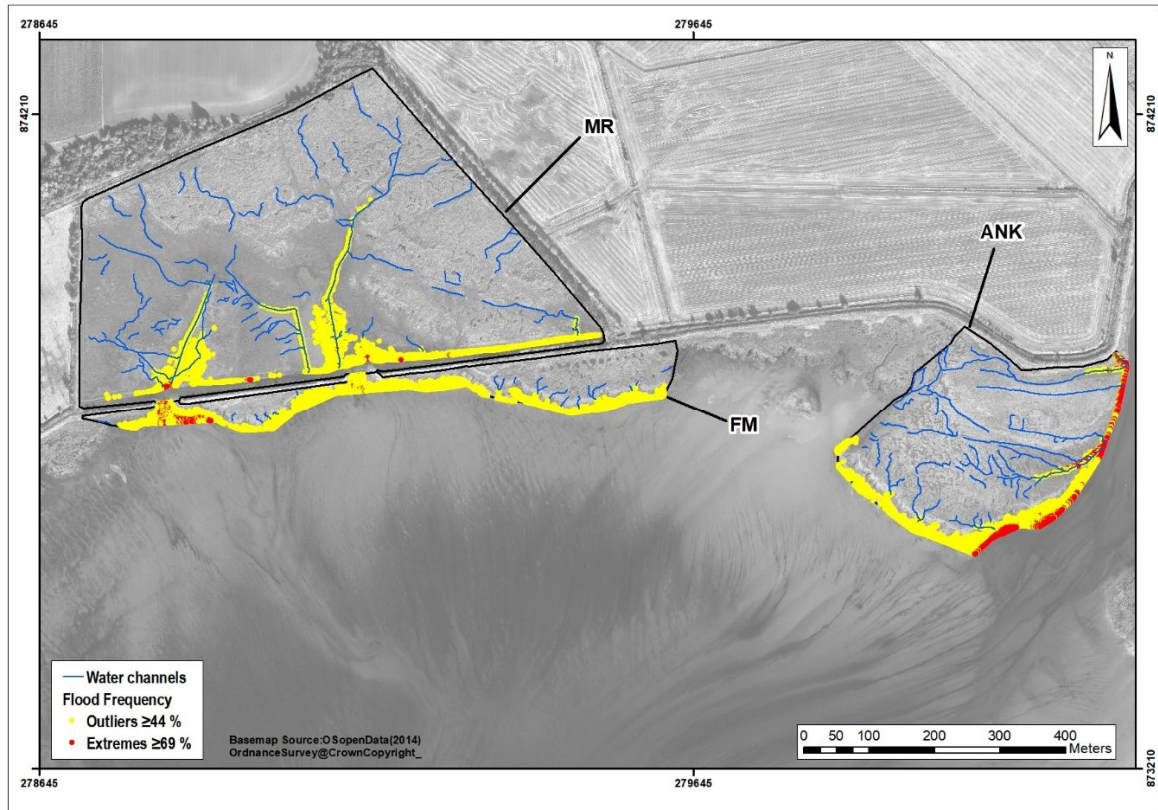


Figure 4-30: Spatial variation across the three salt marshes of very high flood frequency (outliers in yellow) and extremely high flood frequency (red) values across the three studied salt marshes ranging from 44 % to 97 %.

Table 4-17: Calculated average flood frequency (%) between sites' saltmarsh zones for the sediment deposition campaign (filters and AstroTurf mats) from 09<sup>th</sup> March 2016 to 01<sup>st</sup> March 2017. See Table 4-15 Note 1 & 2.

Site	Variable	n	Mean	SD	median	IQR	Flooded Area (%)
ANK_HM	Flood frequency	28414	6.1	10.1	2.8	4.1	86
ANK_LM	Flood frequency	38931	6.0	8.1	4.4	3.6	100
ANK_MM	Flood frequency	11589	6.0	10.5	3.3	4.1	94
ANK_PM	Flood frequency	8233	47.7	12.4	49.6	14.6	100
FM_HM*	Flood frequency	26380	7.6	10.3	3.1	5.9	90
FM_LM	Flood frequency	672	27.4	10.6	28.3	18.0	100
FM_PM	Flood frequency	11154	45.1	12.1	45.8	10.8	100
MR_HM	Flood frequency	37322	2.1	2.1	1.5	2.8	31
MR_LM	Flood frequency	27633	4.5	4.4	3.3	2.6	85
MR_MM	Flood frequency	54443	13.4	10.3	10.0	9.5	100
MR_PM	Flood frequency	40514	31.0	10.5	30.8	14.1	100

#### 4.4.1.3 Average hydroperiod

##### Average hydroperiod between saltmarsh sites

The average hydroperiod being the ratio between the flood depth for each elevation height (1m<sup>2</sup> cell) for the total tidal period analysed and the tidal range presents statistically significant differences between the saltmarsh sites' mean ranks ( $H = 9442.9, p < 0.001^{***}$ , Figure 4-31). Mann-Whitney-Wilcoxon pairwise tests (adjusted using the Bonferroni correction) were carried out for

the three pairs of saltmarsh sites and shows very strong evidence of all the differences between the sites with a mean rank hydroperiod of 0.14 m for MR, 0.13 m for FM and 0.09 m for ANK (Table 4-18 and Figure 4-31). Alike flood depth, hydroperiod values higher than 0.45 m significantly differ from the average, they cover a larger surface area of the marshes: 2.2 % of ANK, 3.1 % of FM and 0.2 % of MR. Extreme hydroperiod are significantly different when reaching 0.7 m covering 0.27 % of ANK marsh surface, only 0.01 % of FM but does not reach this height on MR (Figure 4-31, Figure 4-32 and Figure 4-33). They are located in same areas that experience very high and extreme flood depth (Figure 4-24 and Figure 4-33): on the eastern part of ANK, they expand to both western and eastern breaches of the sea-wall separating FM and MR and can now be observed on MR along and north of the sea-wall in the former field drain and now filled (Figure 3-7). A linear regression model assessed the influence of the sites on hydroperiod ( $F_{(2, 285285)} = 3877, p < 0.001^{***}$ ) which only explained 2.6% ( $r^2_{adj}$ ) of the variance (details in Appendix C.3: Table C-14).

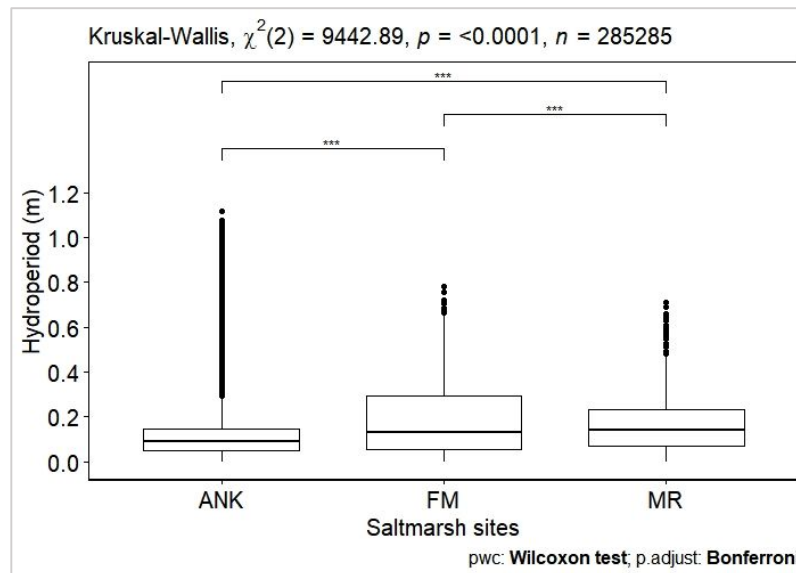


Figure 4-31: Boxplot of the average hydroperiod mean ranks (m) for the sediment deposition campaign showing significant differences between saltmarsh sites (Kruskal-Wallis H test and Mann-Whitney-Wilcoxon tests results are symbolised on the top row by the p-value significance - ns, \*, \*\*, \*\*\* - for each pairwise tests). Boxplots represent median (middle line) interquartile range (box), 1.5 times interquartile range (bar) and outliers (black dots).

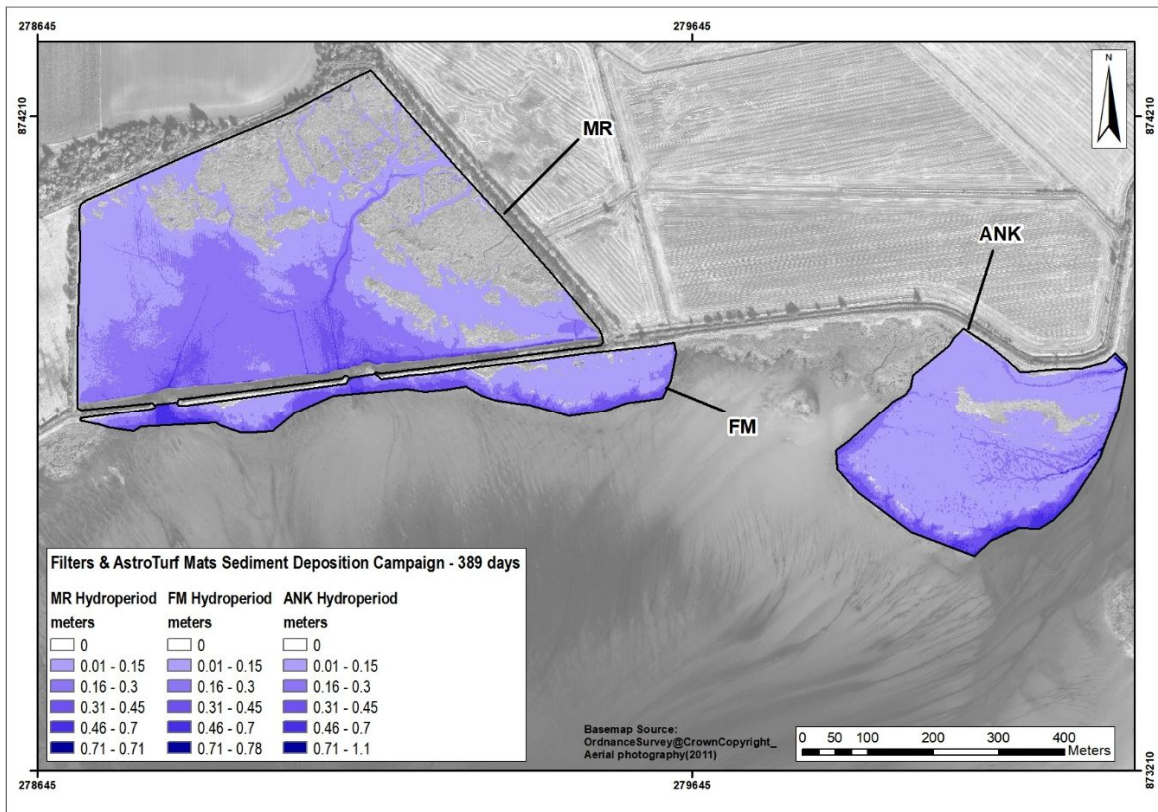


Figure 4-32: Average hydroperiod (m - over 389days) calculated at a 1m<sup>2</sup> cell scale size for the three saltmarsh sites.

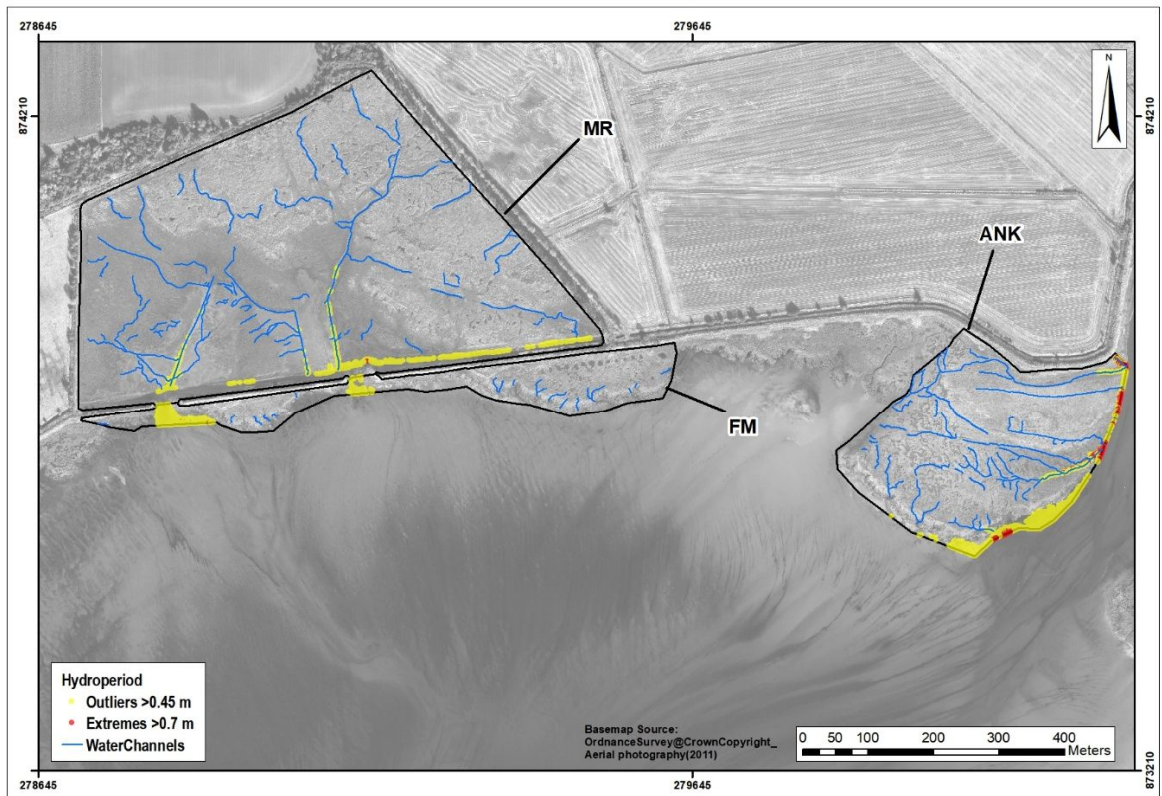


Figure 4-33: Spatial variation of very high hydroperiod (outliers in yellow) and extremely high hydroperiod (red) values across the three studied salt marshes ranging from 0.45 to 1.12 m.



**Table 4-18: Calculated average hydroperiod (m) between saltmarsh sites for the sediment deposition campaign (filters and AstroTurf mats) from 09<sup>th</sup> March 2016 to 01<sup>st</sup> March 2017. Note that n correspond to a 1\*1 m cell size.**

Site	Variable	n	mean	SD	median	IQR	Flooded Area (%)
ANK	Hydroperiod	87167	0.12	0.11	0.09	0.10	94
FM	Hydroperiod	38206	0.18	0.14	0.13	0.24	93
MR	Hydroperiod	159912	0.15	0.10	0.14	0.16	65

### Average hydroperiod between sites and saltmarsh zones

Average hydroperiod mean ranks are as well statistically significantly different between sites' saltmarsh zones ( $H= 183616$ ,  $p<0.001^{***}$ , Table 4-19). Using Mann-Whitney-Wilcoxon pairwise tests (adjusted with Bonferroni method), every sites' saltmarsh zones demonstrate strong differences from the others and follow similar spatial variation trend than flood depth where the lower parts of the marsh exhibit the near permanent hydroperiod (highest) and (Figure 4-34 and boxplot showing full pair-test comparison see Appendix C-3: Figure C-3). The analysis shows that MR PM has the lowest hydroperiod compared to ANK (the highest from pioneer zones) and FM. Hydroperiod on ANK's LM is 200% lower than FM's LM (the highest) and 86 % than MR's LM. Having the shortest distance to saltmarsh edge, it is not surprising that FM's HM displays the highest hydroperiod compared to ANK and MR which is having the lowest.

**Table 4-19: Calculated average hydroperiod (m) between sites' saltmarsh zones for the sediment deposition campaign (filters and AstroTurf mats) from 09<sup>th</sup> March 2016 to 01<sup>st</sup> March 2017. See Table 4-15 Note1 & 2.**

Site	Variable	n	Mean	SD	median	IQR	Flooded Area (%)
ANK_HM	Hydroperiod	28414	0.09	0.08	0.06	0.06	85.7
ANK_MM	Hydroperiod	38931	0.10	0.07	0.09	0.07	99.8
ANK_LM	Hydroperiod	11589	0.10	0.09	0.09	0.06	94.2
ANK_PM	Hydroperiod	8233	0.38	0.10	0.37	0.13	100
FM_HM*	Hydroperiod	26380	0.10	0.08	0.07	0.10	90.4
FM_LM	Hydroperiod	672	0.25	0.05	0.26	0.06	100
FM_PM	Hydroperiod	11154	0.35	0.09	0.34	0.08	99.9
MR_HM	Hydroperiod	37322	0.05	0.03	0.04	0.03	31.3
MR_MM	Hydroperiod	27633	0.08	0.04	0.09	0.03	85.0
MR_LM	Hydroperiod	54443	0.17	0.06	0.16	0.06	99.7
MR_PM	Hydroperiod	40514	0.27	0.06	0.26	0.05	100

Very high hydroperiod (outliers) and extreme hydroperiod concur with aforementioned observations (differences between sites). They can be categorised across the sites' saltmarsh zones with extremes values ( $\geq 0.71$  m) only observed on all ANK's zones but principally on ANK's LM and PM covering 0.6 % and 0.5 % of its surface. Extreme hydroperiod is only seen sporadically ( $<0.1\%$ ) on FM's PM and MR's PM (Figure 4-33 and Appendix C-3 - Figure C-1).

A linear regression model assessed the influence of the sites and zones on hydroperiod ( $F_{(10, 285274)} = 51790$ ,  $p < 0.001^{***}$ ) which explained 64.5% ( $r^2_{adj}$ ) of the variance with standardised residuals normally distributed (Details in Appendix C-3: Table C-15).

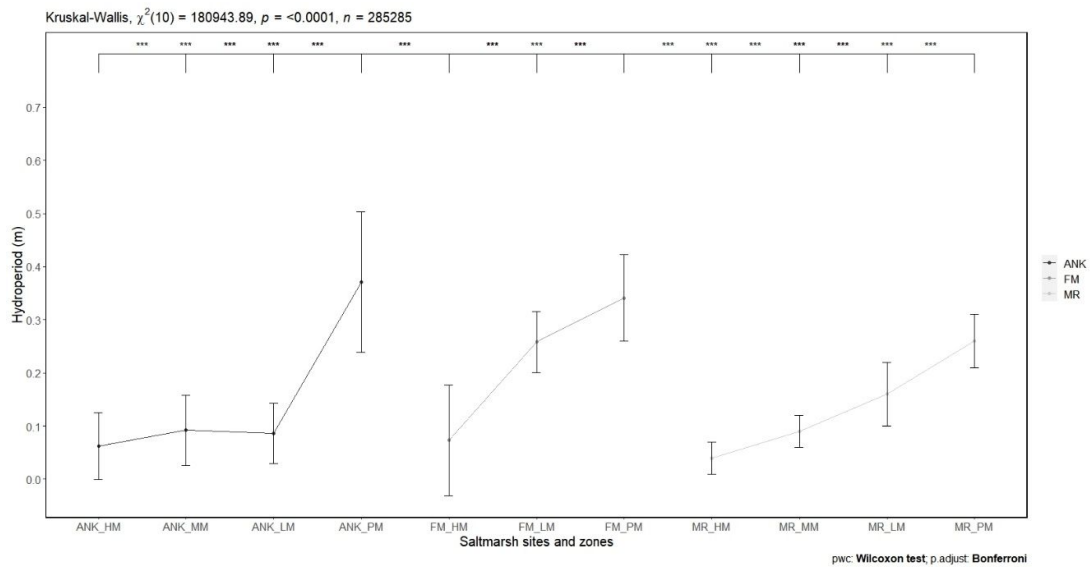


**Figure 4-34: Plot of the average hydroperiod mean ranks (m) for the sediment deposition campaign showing significant differences between sites' saltmarsh zones** (The plots represent median and error bars are interquartile range. Kruskal-Wallis H test and Mann-Whitney-Wilcoxon tests results are symbolised on the top row by the p-value significance - ns, \*, \*\*, \*\*\* - for each pairwise tests -For full pair-test comparison boxplot see in Appendix C.3 Figure C-10).

#### 4.4.1.4 Summary on water levels spatial variation

This chapter section (4.4.1) aimed to improve our understanding of short-term saltmarsh development by quantifying the spatial variations of water levels that occurred across the three studied salt marshes during the sediment deposition monitoring period (8<sup>th</sup> February 2016 to 01<sup>st</sup> March 2017, i.e. 359 days or 778 tidal periods).

The results show that by using Kefelegn's (2019) mathematical formulation of different hydroperiod parameters are suitable to Nigg Bay water levels and allow us to differentiate spatial pattern on each salt marsh. Overall, higher hydroperiod, inundation frequencies and flood depths are, as expected, experienced on all sites' lower marsh zones (pioneer and low) whereas the zones higher elevation all have lower values.

Figure 4-23, Figure 4-27 and Figure 4-32 also demonstrate that overall flooding covers a greater area on the natural salt marshes with 94 % of ANK and 93.1% of FM inundated at least once during the year against 64.8 % of MR (Table 4-14, Table 4-16 and Table 4-18). ANK and FM, natural salt marshes, experience a greater hydroperiod, flood depth and flood frequency compared to MR.

Flooding across all sites and saltmarsh zones is shown to cover the least the high-marsh zones and much of the pioneer zones (Table 4-15, Table 4-17 and Table 4-19); however, there is a clear spatial variability between the high-marsh zones of each site (31% of MR extent is flooded against 85 % of ANK and 90 % of FM 85 %), and, this is confirmed by a strong and significant



variation of hydroperiod parameters between sites' saltmarsh zones (Figure 4-26, Figure 4-29 and Figure 4-34). ANK displays greatest range of water levels parameters on all its zones: PM, LM, MM and HM; and, all displaying significantly high (flood depth  $\geq 0.42$  m, flood frequency  $\geq 44$  % , hydroperiod  $\geq 0.47$  m) and extreme values (flood frequency  $\geq 68$  % , hydroperiod  $\geq 0.70$  m) expect for extreme flood depth which is only witnessed on MM (flood depth  $\geq 0.63$  m). MR and FM only experience very high and extreme flood depth on PM zones. All zones of FM can experience very high flood frequency, but PM has extreme flood frequency. All MR zones except HM demonstrate very high flood frequency but only LM and PM are exposed to extreme flood frequency. Finally, MR and FM present very high hydroperiod on PM zone with no extreme value.

Relationships between water levels and sediment deposition and accretion are examined in in section 4.5.1 and relationships between water levels and vegetation types and vegetation production are further explored in further explored in 4.5.2.

#### **4.4.2 Hydroperiod and Flood depth variations over the short-term sediment collection**

This section presents a summary of the tidal flood depth and hydroperiod levels for the deployment's day of each sediment collection (i.e. the tide that brought the sediments collected, Figure 4-22). Note that flood frequency is not used as the flood depth results enable to assess which area cell ( $1\text{m}^2$ ) has or has not been flooded that particular day. These results are aimed to further understand if the hydroperiod parameters at each collection may have an influence on the amount of sediment collected and is further presented and discussed in section 4.5.1).

##### **4.4.2.1 Monthly Flood depth variations**

One-way Analysis of Variance was used to examine whether flood depth (m) differs between each sediment collection/deployment date (Table 4-20, Figure 4-35 and Figure 4-36). Although residuals met normality assumption, Levene's F test revealed that the homogeneity of variance was not met for this data. As such, the Welch's F test was used and reported significant differences between the flood depth and the deployment dates ( $F_{(DFn=11, DFd=472571)} = 14354^{***}$ ). The estimated adjusted omega squared ( $\omega^2 = 0.034$ ) indicated that approximately 3.4% of the total variance in the flood depth is accounted for by the sediment collection dates.

Post hoc comparisons, using the Games-Howell post hoc procedure, were conducted to determine which flood depth's date differed significantly. The results are given in Appendix C.3

- Table C-16 and indicate that most flood depths differ significantly at each sediment collection apart between 3<sup>rd</sup> August 2016 and 31<sup>st</sup> January 2017 where no significance was found. Flood depth was found to be considerably lower in August compared to the months of May, June, September, October, November (being the highest) and December (Figure 4-37, Figure 4-35 and Figure 4-36). A linear regression model was performed and has shown that although the differences are statistically significant, they do not contribute greatly ( $r^2_{adj} = 5.5\%$  ,  $F_{(11, 1570737)} = 8351, p < 0.001^{***}$ ) to the change in flood depth.

The flood depth differences between summer (April-September) and winter (October-March) season illustrated on Figure 4-37 (also Figure 4-35 and Figure 4-36) were assessed in paired t-tests. There was statistical significant evidence ( $t_{(1570748)} = 2833.8, p < 0.001^{***}$ ) of a change between summer's and winter's flood depth with a relatively small increase of 0.4% on average in winter. However, using Cohen (1988) guidelines for interpretation, the magnitude of this change in flood depth is considered large (eta squared = 0.836).

**Table 4-20: Flood depth levels (m) between sediment deposition campaign (filters and AstroTurf mats) from 09<sup>th</sup> March 2016 to 01<sup>st</sup> March 2017. The last rows present the flood depth levels (m) during summer and winter season.**

Collection Date	Variable	n	mean	sd	median	Welch's ANOVA	p
09.03.16	Flood depth	376261	0.28	0.17	0.29		
21.04.16	Flood depth	376261	0.23	0.13	0.22		
06.05.16	Flood depth	376261	0.29	0.20	0.30		
06.06.16	Flood depth	376261	0.30	0.21	0.28		
04.07.16	Flood depth	376261	0.25	0.15	0.25	F=183616, DFn	
03.08.16	Flood depth	376261	<b>0.13</b>	0.10	0.11	=11,	$<2e-16^{***}$
18.09.16	Flood depth	376261	0.33	0.26	0.26	DFd=472571,	
17.10.16	Flood depth	376261	0.30	0.22	0.26	$\omega^2 = 0.034$	
14.11.16	Flood depth	376261	<b>0.34</b>	0.26	0.26		
14.12.16	Flood depth	376261	0.31	0.23	0.25		
31.01.17	Flood depth	376261	0.14	0.10	0.12		
01.03.17	Flood depth	376261	0.18	0.11	0.16		
Collection Date	Variable	N	mean	sd	median		
Summer	Flood depth	2257566	0.285	0.22	0.24		
Winter	Flood depth	2257566	0.29	0.23	0.23		

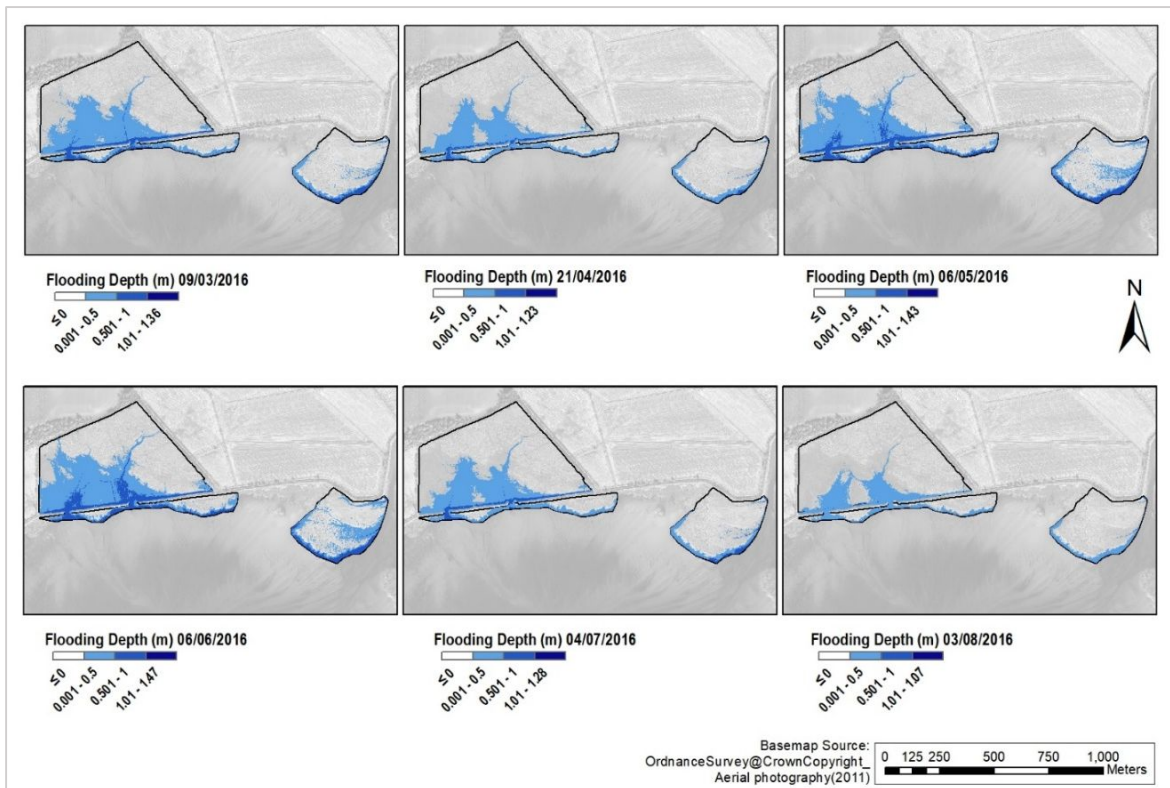


Figure 4-35: Flood depth and extent across the three salt marshes (calculated for 1m<sup>2</sup>/cell) for each sediment deposition collection (from 9<sup>th</sup> March to 03<sup>rd</sup> August 2016) during the campaign (Basemap Source: OrdnanceSurvey@CrownCopyright Aerial photography(2011)).

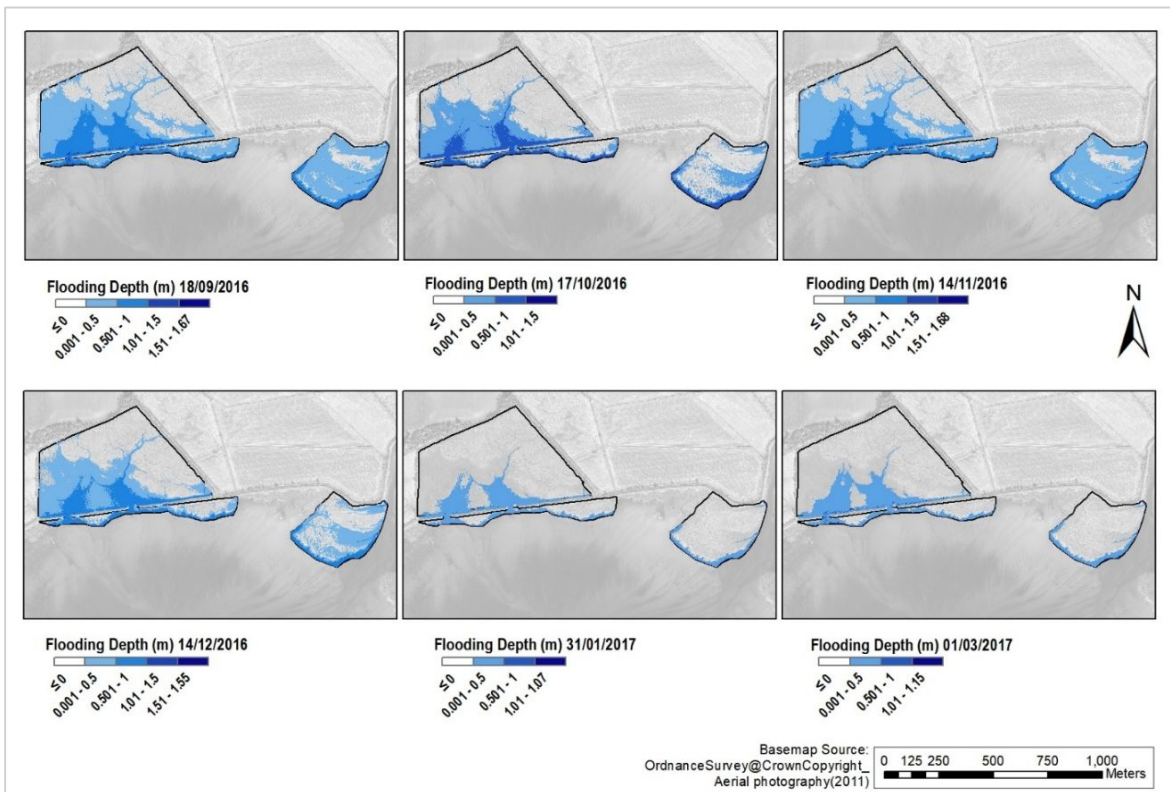
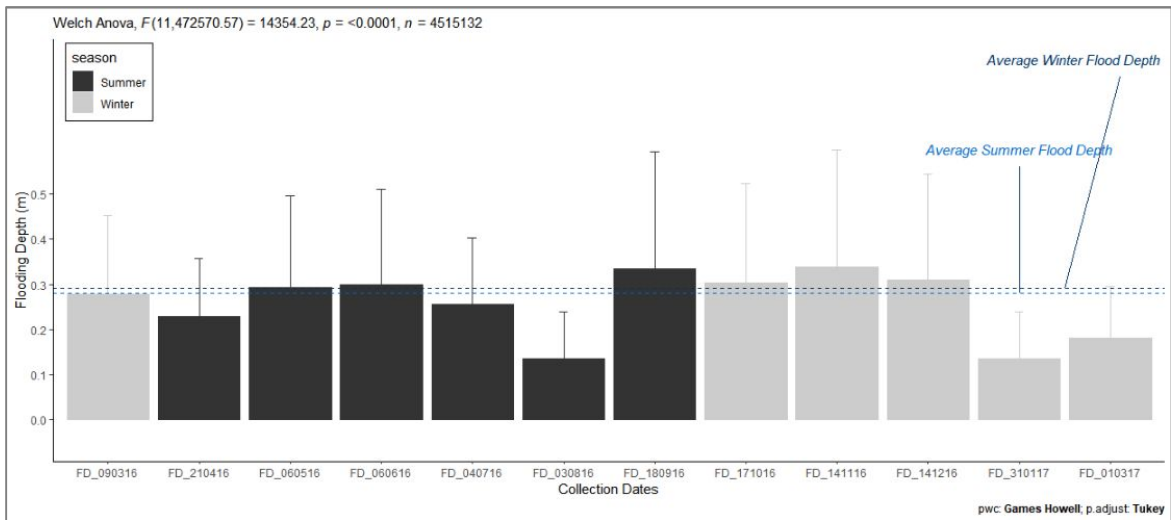


Figure 4-36: Flood depth and extent across the three salt marshes (calculated for 1m<sup>2</sup>/cell) for each sediment deposition collection (from 18<sup>th</sup> September 2016 to 01<sup>st</sup> March 2017) during the campaign (Basemap Source: OrdnanceSurvey@CrownCopyright Aerial photography(2011)).



**Figure 4-37: Bar graph of the flood depth level (m) for each sediment deposition campaign showing Welch's Anova F test results (for Games-Howell post hoc procedure results, see Appendix C.3 - Table C-16 for full details). Top of bar is mean levels and error bars their standard deviation.**

#### 4.4.2.2 Monthly Hydroperiod variations

Statistical analysis to examine whether hydroperiod (m) differs between each sediment collection date has produced comparable results than for the flood depth (Table 4-21, Figure 4-39 and Figure 4-40). As such, the Welch's F test reported significant differences between the hydroperiod and showed that approximately 3.6% of the total variance in the hydroperiod is accounted for by the collection dates.

Post hoc comparisons (Games-Howell post hoc procedure) were conducted to determine which hydroperiod's date differed significantly. The results are given in Appendix C.3 - Table C-16 and indicate that most hydroperiod differ significantly at each sediment collection apart between 31<sup>st</sup> January 2017 and 01<sup>st</sup> March 2017 and between 06<sup>th</sup> May 2016 and 18<sup>th</sup> September 2016 where no significance was found. This differs from flood depth comparison tests. Hydroperiod was found to be the lowest in August compared to April (being the highest) and March 2016 and January 2017 (Figure 4-38, Figure 4-39 and Figure 4-40). A linear regression model was also performed and has shown that although the differences are statistically significant, they do not contribute greatly ( $r^2_{adj}$  6.6 %,  $F_{(11, 1572577)} = 10170, p < 0.001$  \*\*\*) to the change in hydroperiod.

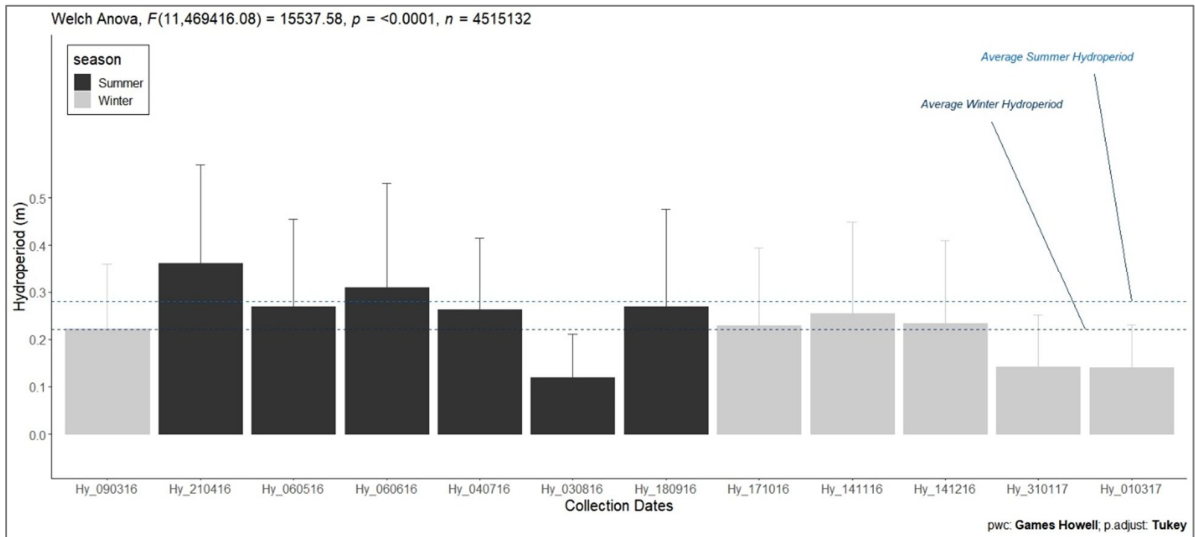


**Figure 4-38: Bar graph of hydroperiod level (m) for each sediment deposition campaign showing Welch's Anova F test results** (for Games-Howell post hoc procedure results, see Appendix C.3 - Table C-16 for full details). Top of bar is mean levels and error bars their standard deviation.

**Table 4-21: Hydroperiod levels (m) between sediment deposition campaign (filters and AstroTurf mats) from 09<sup>th</sup> March 2016 to 01<sup>st</sup> March 2017. The last rows present the hydroperiod levels during summer and winter season.**

Collection Date	Variable	n	mean	sd	median	Welch's ANOVA	p	
09.03.16	Hydroperiod	376261	0.22	0.14	0.23			
21.04.16	Hydroperiod	376261	<b>0.36</b>	0.21	0.35			
06.05.16	Hydroperiod	376261	0.27	0.19	0.27			
06.06.16	Hydroperiod	376261	0.31	0.22	0.29			
04.07.16	Hydroperiod	376261	0.26	0.15	0.26			
03.08.16	Hydroperiod	376261	<b>0.12</b>	0.09	0.10	F= 15538 , DFn =11,	<2e-16 ***	
18.09.16	Hydroperiod	376261	0.27	0.21	0.21	DFd=469416,		
17.10.16	Hydroperiod	376261	0.23	0.17	0.20	ω2 = 0.036		
14.11.16	Hydroperiod	376261	0.25	0.20	0.20			
14.12.16	Hydroperiod	376261	0.23	0.18	0.19			
31.01.17	Hydroperiod	376261	0.14	0.11	0.12			
01.03.17	Hydroperiod	376261	0.14	0.09	0.13			
Collection Date	Variable	n	mean	sd	median			
Summer	Flood depth	2257566	0.28	0.20	0.24			
Winter	Flood depth	2257566	0.22	0.17	0.18			



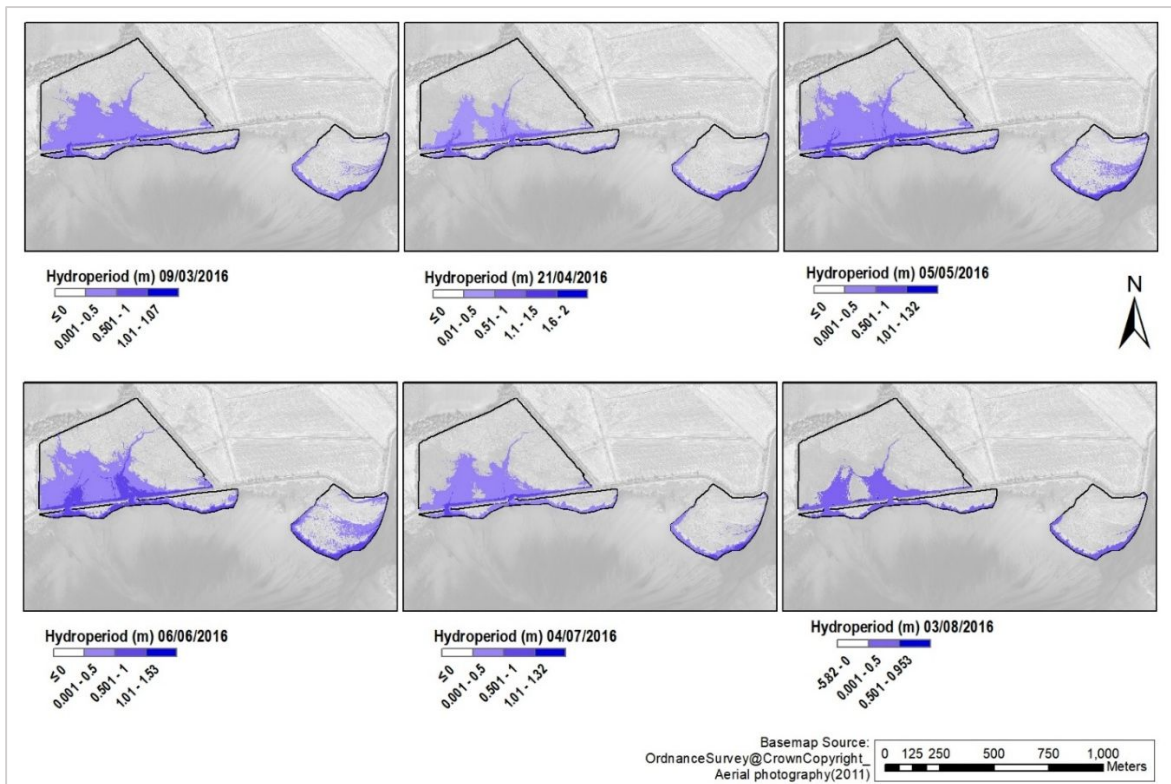


Figure 4-39: Hydroperiod (in m) and extent (calculated for 1m<sup>2</sup> cell) for each sediment deposition collection (from 9<sup>th</sup> March to 03<sup>rd</sup> August 2016) during the campaign (Basemap Source: OrdnanceSurvey@CrownCopyright Aerial photography(2011)).

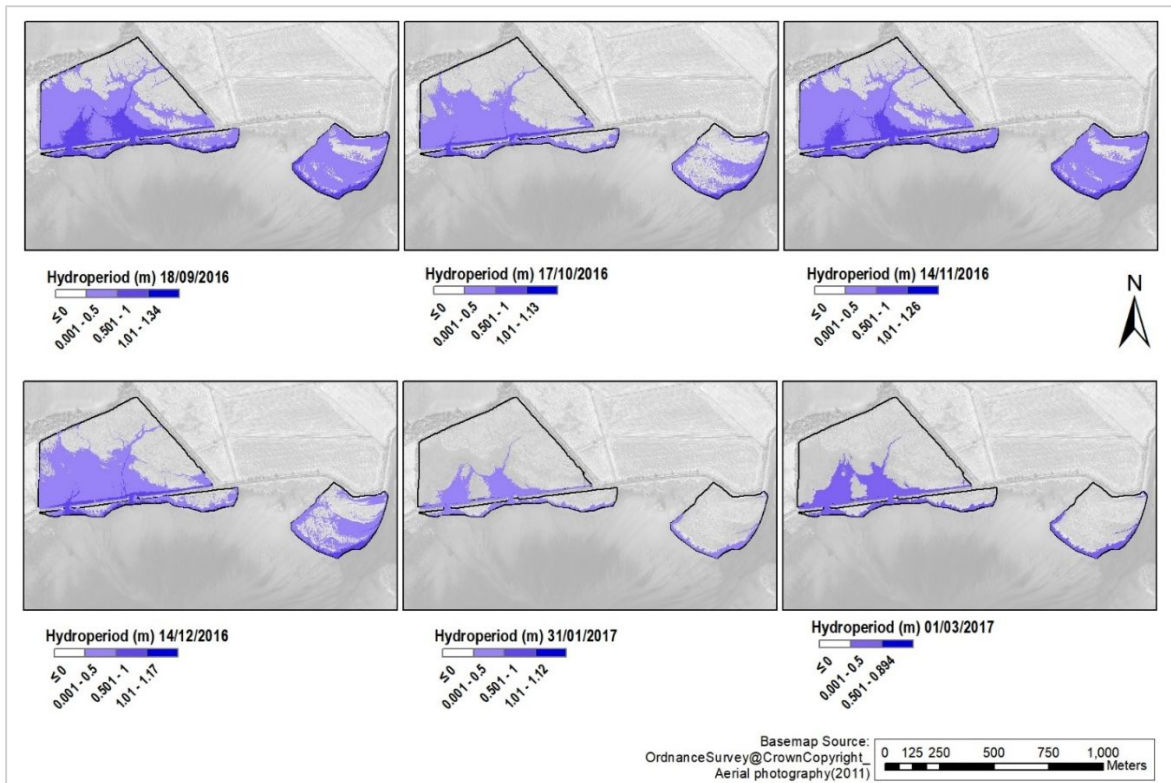


Figure 4-40: Hydroperiod and extent (calculated for 1m<sup>2</sup> cell) for each sediment deposition collection (from 18<sup>th</sup> September 2016 to 01<sup>st</sup> March 2017) during the campaign (Basemap Source: OrdnanceSurvey@CrownCopyright Aerial photography(2011)).



The hydroperiod differences between summer (April-September) and winter (October-March) seasons (Figure 4-38, also Figure 4-39 and Figure 4-40) were assessed in a paired t-test. There was statistical significant evidence ( $t_{(748889)} = 2002.2, p < 0.001^{***}$ ) of a change between winter's and summer's hydroperiod with a decrease of 10.2 % on average in winter. The magnitude of the change in hydroperiod level is considered large (eta squared = 0.842) (Cohen, 1988).

#### 4.4.2.3 Summary on water levels temporal variation

This chapter section (4.4.2) aimed to improve our understanding of short-term saltmarsh development by quantifying the temporal variations of water levels (flood depth and hydroperiod) that occurred during the sediment deposition monitoring period (8<sup>th</sup> February 2016 to 01<sup>st</sup> March 2017 i.e. 359 days or 778 tidal periods).

The statistical analysis establishes that each sediment collection experiences significantly different flood depth and hydroperiod levels, this impacting on the inundation extent across the three salt marshes during the campaign (Figure 4-35, Figure 4-36, Figure 4-39 and Figure 4-40) and ultimately the sediment deposition extent over areas of the marsh. The results also show that flood depth and hydroperiod was the lowest in August, highest flood depth in November and the highest hydroperiod in April. However, although statistically significant, the tidal levels recorded on the collection day do not reflect strong seasonality, with a departure from the expected winter/summer pattern. There is 0.4% increase in flood depth between the winter and summer sediment collection's tides, however hydroperiod decreases by 10.2 % during winter. Therefore, it seems noteworthy to compare these results with the overall water level time series (i.e. using all water levels values per months from March 2016 to March 2017, not just levels on collection dates) as it can highlight differences between the overall tidal flooding and the monitoring period that coincide with sediment trap deployment. The analysis (t-test) reveals that, for an uninterrupted period from March 2016 to March 2017, there is an increase between winter and summer of  $5.3 \pm 0.3$  % in flood depth ( $t_{(249106)} = 1400, p < 0.001^{***}$  - compared to 0.4 % for sediment collection/deployment date) and the hydroperiod increases of  $4.8 \pm 0.4$  % ( $t_{(249106)} = 1215.8, p < 0.001^{***}$  - compared to a decrease of 10.2 % for sediment collection/deployment date). These differences manifest themselves for each collection date where there is a  $30.8 \pm 0.1$  % mean decrease (and  $-24 \pm 0.1$  % median) with the monthly flood depth and  $15.6 \pm 0.1$  % mean decrease (and  $-16.4 \pm 0.1$  % median) with the monthly hydroperiod (Table 4-22).

**Table 4-22: Average differences (%) between the collection/deployment levels of flood depth (m) and hydroperiod (m) and the monthly average, i.e. each day HW and LW depths (also calculated for 1 m<sup>2</sup> cell).**

Comparing Month and collection date		Variable	Mean difference	Median difference	Variable	Mean difference	Median Difference
Mar-16	09.03.16	Flood depth	-65%	-66%	Hydroperiod	-8%	-16%
Apr-16	21.04.16	Flood depth	-12%	-5%	Hydroperiod	-52%	-49%
May-16	06.05.16	Flood depth	-45%	-44%	Hydroperiod	-36%	-48%
Jun-16	06.06.16	Flood depth	-46%	-47%	Hydroperiod	-36%	-38%
Jul-16	04.07.16	Flood depth	-36%	-31%	Hydroperiod	-36%	-38%
Aug-16	03.08.16	Flood depth	11%	34%	Hydroperiod	26%	56%
Sep-16	18.09.16	Flood depth	-52%	-38%	Hydroperiod	-33%	-25%
Oct-16	17.10.16	Flood depth	-36%	-30%	Hydroperiod	-22%	-44%
Nov-16	14.11.16	Flood depth	-54%	-56%	Hydroperiod	-28%	-26%
Dec-16	14.12.16	Flood depth	-32%	-16%	Hydroperiod	-21%	-21%
Jan-17	31.01.17	Flood depth	24%	41%	Hydroperiod	11%	2%
Feb/Mar-17	01.03.17	Flood depth	-26%	-30%	Hydroperiod	47%	50%

#### 4.5 Interplay and controls on geomorphological and biological processes

As it is widely accepted that ‘vertical accretionary adjustments to sea level rise [are] the primary factor in determining long-term marsh stability’ (Kearney et al., 1994), section 4.2 provided dataset necessary to evaluate the relationships between sediment deposition, as an indicator of sediment input into the Nigg Bay, and, accretion rates recognised as essential for saltmarsh sustainability to keep pace with rising sea level. In addition, previous studies highlights that suspended sediment concentrations and the deposition rate can be modulated by plants (through the effects of bed shear stress and turbulence of flow within the canopy although being dependent on local ecology and hydro-geomorphology) (Davidson-Arnott et al., 2002; Marion et al., 2009; Carrasco et al., 2023). It has also been found that factors such as vegetation height and composition, microtopography, and elevation can influence the relationship between vegetation (including height, thickness, and stiffness) and sediment accumulation (Boorman et al., 1998; Tempest et al., 2015). Section 4.3 and 4.4 also provided the necessary dataset to evaluate the relationships between sediment, vegetation and physical drivers which are further examined here.

Figure 4-41 schematises this concept further tested here by evaluating influences on short-term ( $\leq 1$  year) accretion in Nigg Bay salt marshes with physical drivers as defined in Chapter 3-3.3.2.3, and vegetation processes measured and presented in section 4.3.

As the dataset covers a smaller spatial dataset (see Chapter 3 - Section 3.4.1.1 for methods and Figure 3-21, 22 and 23) and dataset size will sway results overall AstroTurf mats results are not used in this section. The performance between trap types is further discussed in section 4.6.1.

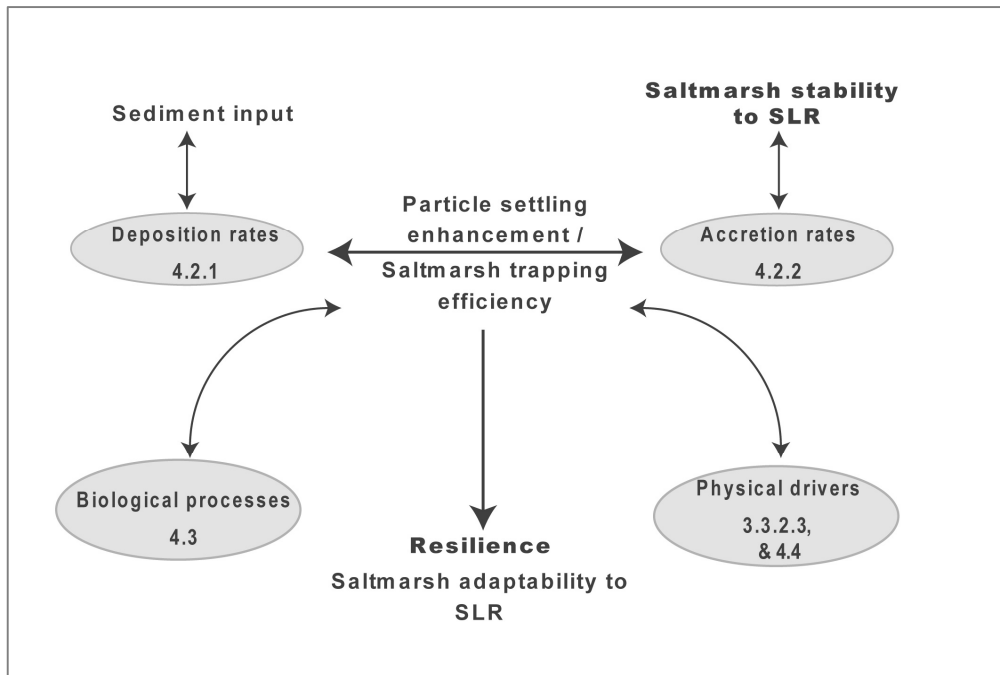


Figure 4-41: Schematic research framework of this study's short-term physical and biological saltmarsh dynamics, in which the influence of physical drivers as defined in Chapter 3 - section 3.3.2.3 was used to qualify short-term characteristics and controls to sediment and vegetation results, as presented in the following sections.

#### 4.5.1 Physical controls on saltmarsh sediment deposition and accretion

Relationships between sediment deposition and saltmarsh accretion intrinsic factors (i.e. shoreline configuration, morphology, seasonal effects) and process variables (i.e. tidal characteristics) (Figure 4-1 and Chapter 3- 3.3.2.3) are presented in this section to assess which factor or processes may influence the short-term (< 1 year) saltmarsh development of Nigg Bay and enhance surface accretion, as schematised in Figure 4-42 below.

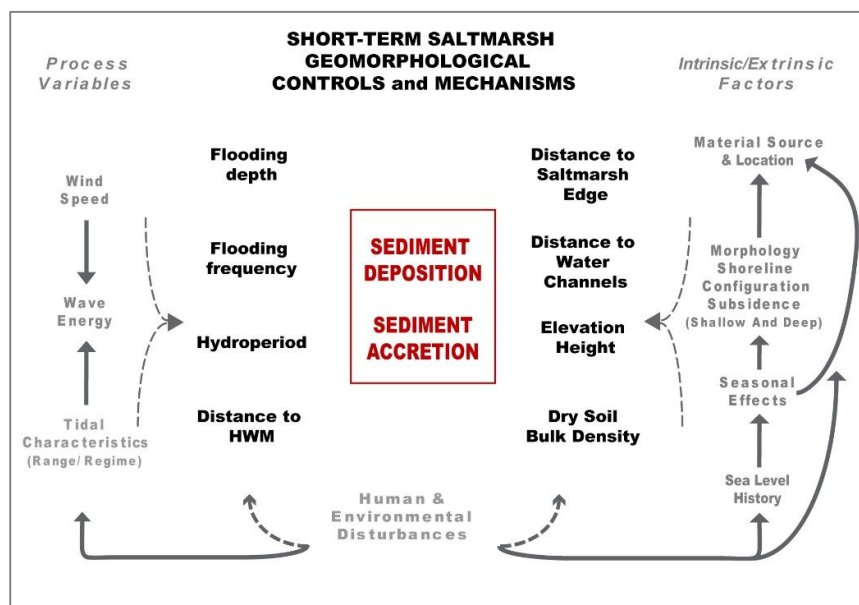


Figure 4-42: Diagram of the process variables and intrinsic factors known to influence short-term deposition and accumulation that have been measured on the three salt marshes of Nigg Bay.

#### 4.5.1.1 Relationships between filter discs deposition rates, accretion rate estimates and physical drivers and controls to saltmarsh development

Principal component analysis (PCA) were performed to explore how physical controls to saltmarsh development (elevation (m), hydroperiod (m), flood depth (m), flood frequency, distance to MHWS, distance to water channels (m), distance to saltmarsh edge (m), soil bulk density ( $\text{g.cm}^3$ ) may contribute the overall sediment deposition rates and accretion rate estimates at Nigg. The 4.2.1 results clearly indicated that there was no statistically significant difference between the three salt marshes, so site-specific statistical analysis was not conducted.

##### **Sediment deposition rates (filter discs)**

PCA first and second dimensions (also called here principal components) explains 59.23 % of the variation in the dataset (Figure 4-43) and suggests that elevation, flood depth, hydroperiod, flood frequency, BDD, distance to the saltmarsh edge and water channels (in decreasing order of influence) are associated to filter disc sediment deposition rates. Figure 4-44 further shows that hydroperiod and flood depth have significant correlations to filter disc sediment deposition rates. Regression models (Appendix C.4 - Table C-19- model 1 and 2) confirm that both flood depth and hydroperiod control significantly sediment deposition rates variance ( $r^2 = 15.1\%$   $p < 0.001$  and  $16.1\%$   $p < 0.001$  respectively).

Additionally, PCA biplot indicates clusters of NVC vegetation assemblages where SM16d is found where elevation is high, SM13b and SM13d at distance to water channel and HMW saltmarsh edge, SM8 associated to high water levels. Vegetation communities were therefore added to each regression model. The results show that vegetation along with flood depth can support 26 % ( $r^2$  adj., Figure 4-45a) of the variation in sediment deposition rates or 28 % ( $r^2$  adj., Figure 4-45b) if using vegetation along with hydroperiod. Both models show the significant contribution of samples taken in SM8 (pioneer-marsh), SM13b (mid-marsh) and SM16d (high-marsh) (Appendix C.4 - Table C-19- model 3 and 4).

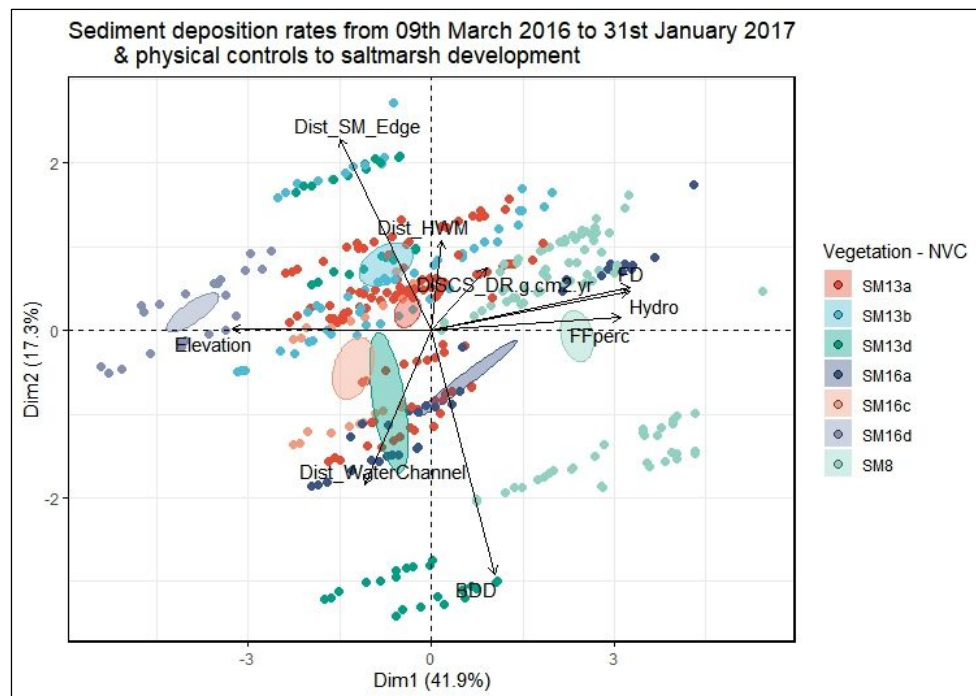


Figure 4-43: PCA biplot for sediment deposition rates and physical controls to saltmarsh development showing in x-axis and y-axis the principal components that contribute the most to the variance of the dataset (PC1 and PC2). Individual samples are symbolised with a point coloured by vegetation assemblage with a confidence ellipse plotted around group mean points and each variable represented by an arrow with its length informing on the PCA loading scores (longer arrows have higher contribution and vice versa). Variables used are:

DISCS_DR.g.cm2.yr	Filter disc sediment deposition rate in in g.cm <sup>2</sup> .yr <sup>-1</sup>	FFperc	Flood Frequency in %
Dist_HWM	Distance to MHWS in m	Hydro	Hydroperiod in m
Dist_WaterChannel	Distance to water channels in m	FD	Flood depth in m
Dist_SM_Edge	Distance to saltmarsh edge in m	Elevation	Elevation height in m
BDD	Soil Bulk density in g.cm <sup>3</sup>		

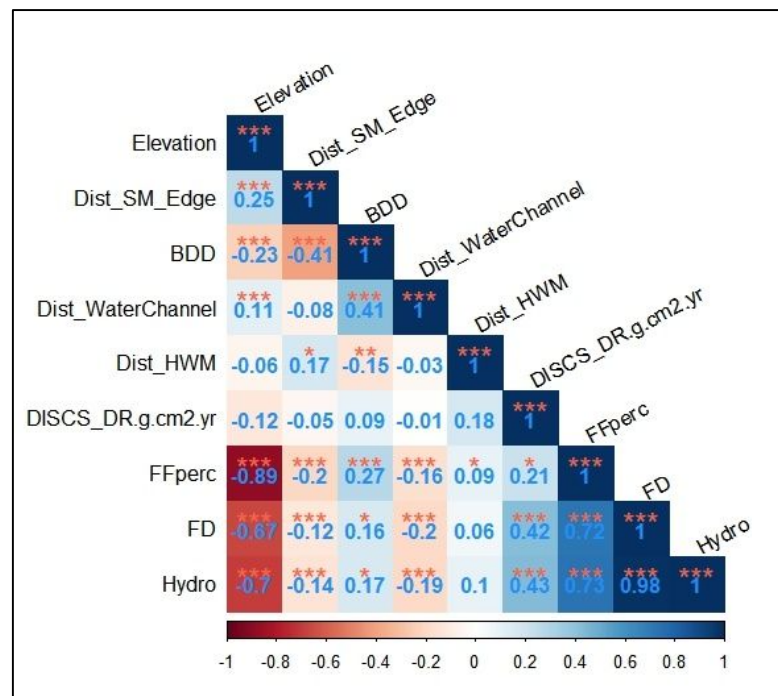


Figure 4-44: Correlation matrix between variables showing correlation coefficients strength represented by a hue gradient (blanks have insignificant p-values) and p-value significance by \* for <math>p < 0.05</math>, \*\* for <math>p < 0.01</math>, \*\*\* for <math>p < 0.001</math> (see Figure 4-43 for variables abbreviations).

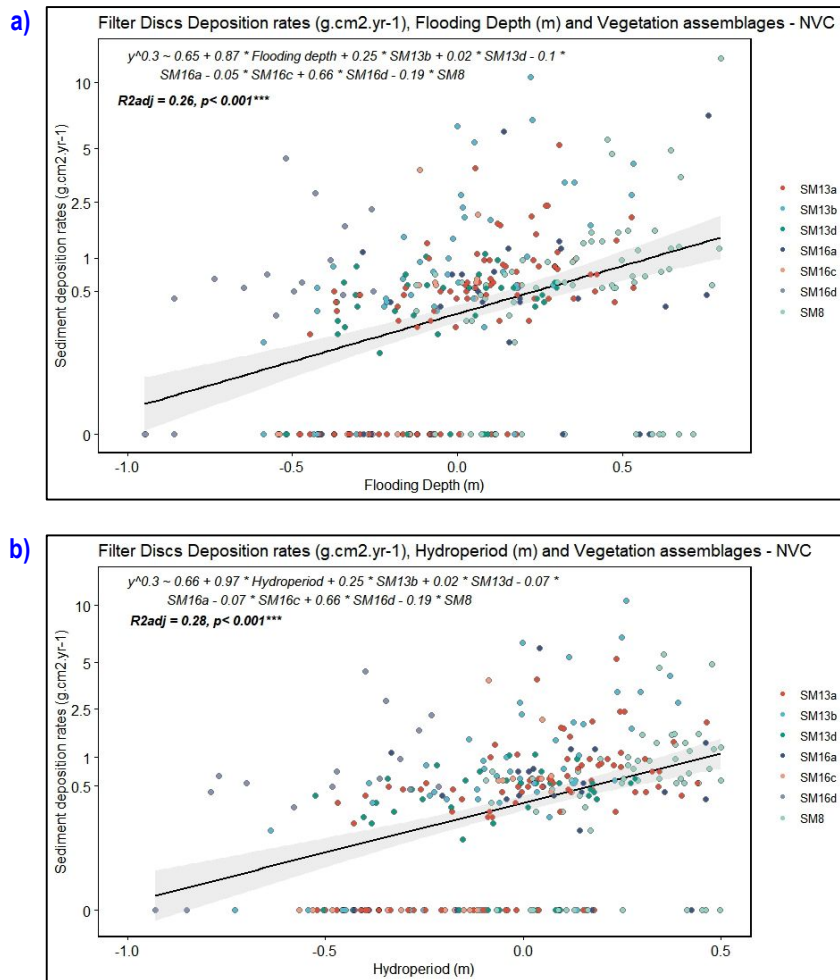


Figure 4-45: **a)** Scatter plot between filter disc sediment deposition rates (in g.m<sup>2</sup>.yr) and flood depth (in m). **b)** Scatter plot between filter disc sediment deposition rates (in g.m<sup>2</sup>.yr) and hydroperiod (in m). Both graphs show data coloured by vegetation assemblages (NVC) with linear regression. They also indicate the regression formulae (note that y values are normalised using Box-Cox transformation with a lambda value of 0.3),  $r^2_{adj}$  and p-value.

### Sediment accretion rate estimates (filter discs)

Using PCA to explore the relationships between accretion rate estimates and the abovementioned physical controls (apart BDD as it is used to translate deposition rates into accretion rates) to saltmarsh development indicates that 60.9 % of the dataset variance can be explained where the hydrodynamic parameters contribute the most to the dataset and where accretion is associated positively to distance to saltmarsh edge, to MHWS and to water channels (Figure 4-46). Correlation matrix plot (Figure 4-47) confirms that hydroperiod, flood depth and distance to water channels are significantly correlated to accretion rates.



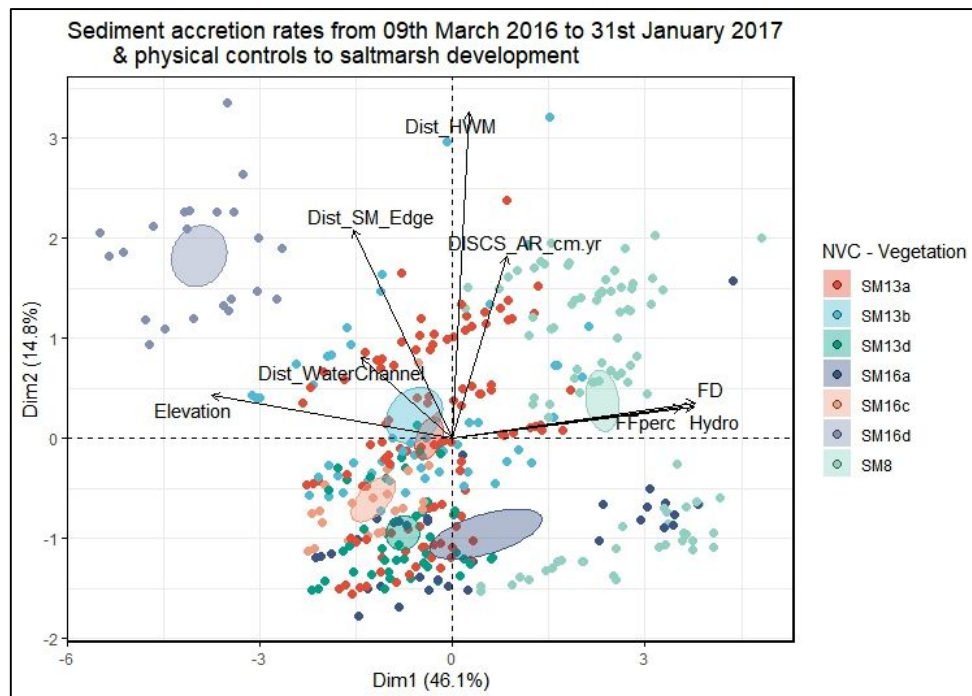


Figure 4-46: a) PCA Dim1 (x-axis) and 2 (y-axis) biplot using accretion rate estimates and physical controls to saltmarsh development showing. Each variable is represented by an arrow with its length informing on the PCA loading scores, the samples are coloured using vegetation assemblages with a confidence ellipse plotted around group mean points. Variables used are:

DISCS_AR_cm_yr	Filter discs accretion rate estimates in cm.yr <sup>-1</sup>	FFperc	Flood Frequency in m
Dist_HWM	Distance to MHWS in m	Hydro	Hydroperiod in m
Dist_WaterChannel	Distance to water channels in m	FD	Flood depth in m
Dist_SM_Edge	Distance to saltmarsh edge in m	Elevation	Elevation height in m

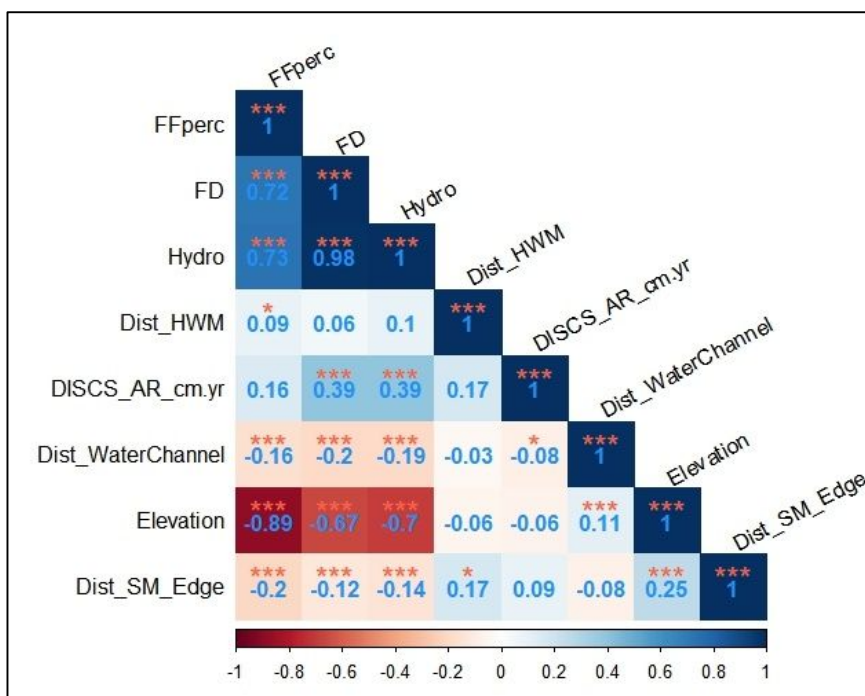


Figure 4-47: Correlation matrix between variables showing correlation coefficients strength represented by a hue gradient (blanks have insignificant p-values) and p-value significance by \* for <0.05, \*\* for <0.01, \*\*\* for <0.001 (see Figure 4-46 for variables abbreviations).

Hydroperiod is significantly predicting 14 % ( $r^2$ ) of accretion rate estimates variance ( $F_{(1, 302)} = 50.56^{***}$ ) with a relationship defined as *accretion rate estimates in cm.yr<sup>-1</sup>*<sup>0.3</sup> = 0.77 + 0.65 \* *Hydroperiod in m* (Appendix C.4 - Table C-20- model 1). As suggested by PCA results, hydroperiod along with distance to saltmarsh edge improve the model explaining 16% ( $r^2$ adj) of accretion rate estimates variance ( $F_{(1, 301)} = 30.46^{***}$ ) (Figure 4-48a, Table C-20- model 2). Similarly, flood depth can explain 14 % ( $r^2$ ) of accretion rate estimates variance ( $F_{(1, 302)} = 47.24^{***}$ ) with a relationship defined as *accretion rate estimates in cm.yr<sup>-1</sup>*<sup>0.3</sup> = 0.76 + 0.58 \* *Flood depth in m* (Table C-20- model 3). Flood depth combined with distance to saltmarsh edge can influence accretion rate estimates 15 % ( $r^2$ adj,  $p < 0.001$ ) (Figure 4-48b, Table C-20- model 4).

The PCA biplot (Figure 4-46) further suggests clustering of NVC vegetation assemblages, and these were added as a categorical predictor to the models mentioned above (Table C-20- model 1 and 3). The results (Table C-20- models 5 and 6) show that NVC vegetation and hydroperiod can explain 29% ( $r^2$ adj,  $p < 0.001$ ) of accretion rate estimates variance and NVC and flood depth can support 29% ( $r^2$ adj,  $p < 0.001$ ) of accretion rate estimates variance where samples taken from SM8, SM13b and SM16d contribute significantly to both models.

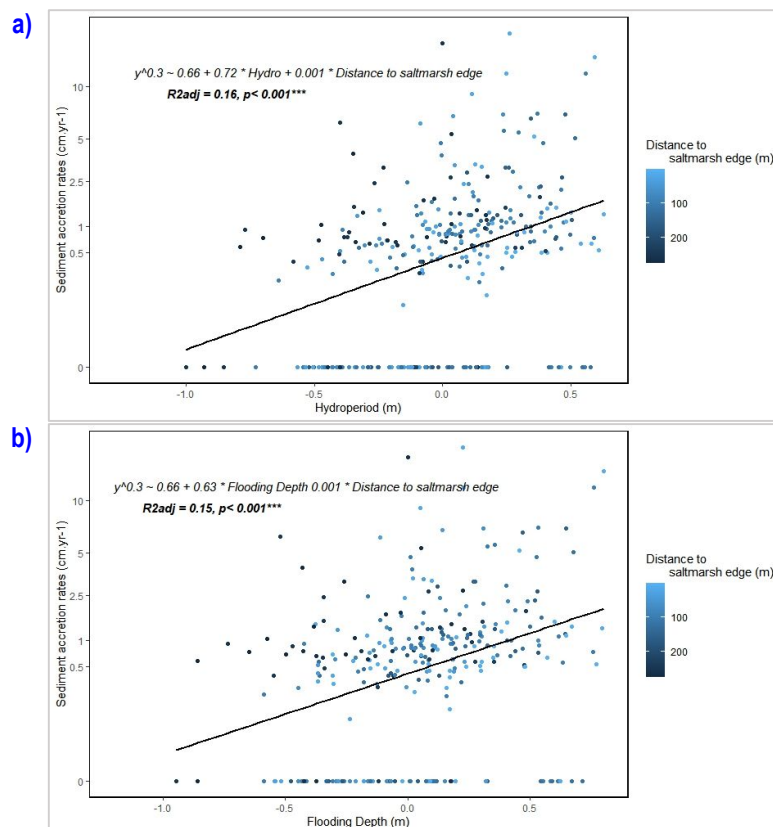


Figure 4-48: Scatter plots between filter discs accretion rate estimates (in  $\text{cm.yr}^{-1}$ ) and **a)** hydroperiod (in m); **b)** and flood depth (in m). Both graphs show the second predictor variable as a gradient colour representing its distance to the saltmarsh edge. They also indicate the regression formulae (note that y values are normalised using Box-Cox transformation with a lambda value of 0.3),  $r^2$ adj and p-value.

#### 4.5.1.2 Relationships between monthly filter disc sediment deposition and physical controls to saltmarsh development

Sections 4.2.1.2 (and 4.2.1.4 for AstroTurf mats) has demonstrated that there is a significant variation in sediment deposition between each collection campaign (see also Appendix C-1 table C-3 and C-4) . Furthermore, section 4.4.2 has shown that overall there is significant spatial and temporal variation in hydroperiod parameters between each sediment collection campaign. To test for statistically significant differences in environmental characteristics between different areas of the marshes including sites, sites and zones and vegetation assemblages, a quantitative output has been generated by Principal Component Analysis (PCA) followed by multiple linear regression to test for significant relationships between combinations of environmental variables and sediment deposition.

PCAs were first run to explore how physical controls to saltmarsh development which include elevation (m), hydroperiod (m), flood depth (m), flood frequency, distance to MHWS, distance to water channels (m), distance to saltmarsh edge (i.e. vegetation edge between mudflat and pioneer zones; in m), soil bulk density ( $\text{g.cm}^3$ ) may contribute to the monthly sediment deposition. For all physical variables and monthly sediment deposition, section 4.5.1.1 has shown that the first two dimensions of the PCA account for 59.23 % of the dataset variance (Figure 4-43) and the first three dimensions account for 72.1 % of the variance. Multiple linear regression analyses were then performed on each sediment collection to further elucidate the relationships between deposition rates and the environmental variables (the models are only presented below if it has met statistical tolerance level).

March 2016 PCA (Figure 4-49a) shows that the first two components ('Dim1' and 'Dim2' in Figure 18a) explain 62.6 % where elevation, hydroperiod and flood depth contribute the most to the dataset whilst deposition, distance to the saltmarsh edge and distance to the MHWS have the least influence.

Figure 4-49b indicates that the first two components account for 64 % of the total variance for April's dataset. Here the plot shows similar but stronger relationships than March where hydroperiod, flood depth, elevation, BDD and deposition contribute to the total variance. April's PCA biplot also shows that pioneer vegetation assemblages (SM8 - symbolised in the plots with coloured points) receive more sediment and high-marsh plants (SM16d) the least. April's sediment deposition was found to be significantly influenced by elevation with the relationship  $\sqrt{\text{deposited sediment } \text{g.m}^2\text{day}^{-1}} = \text{appr. } 22.79 - 14.77 * \sqrt{\text{Elevation in m}}$  which explained

56.3% ( $r^2$ ) of the variance in deposition ( $F_{(1,16)} = 20.66, p < 0.001^{***}$  - Appendix C.4: Table C-17 model 1).

In May 2016, PCA plot (Figure 4-49c) indicates that the first two components make up 60.8 % of the dataset variance where hydroperiod, flood depth and elevation contribute the most to the model whilst other variables are relatively negligible. May's sediment deposition is seen concomitant to distance to MHWS and mid-marsh plant assemblage (SM13a and SM13b) however the relationship was not found statistically significant.

June 2016 PCA (Figure 4-49d) found that 62.6 % of the variance is explained by the first two components where hydroperiod, flood depth and elevation contribute the most to the model. The plot suggests that deposition is higher when close to the water channels and that mid-marsh plants (SM13a and SM13b) receive most sediment. The relationship is partially confirmed in a multiple linear regression between sediment deposition and all vegetation assemblages ( $F_{(6, 18)} = 5.92, p < 0.01^{**}$ ) where 53.4% ( $r^2_{adj}$ ) of the variance in deposition is explained with a significant interaction in the model from SM13b ( $p < 0.01^{**}$ ) and SM16c ( $p < 0.05^*$ ) vegetation assemblage. (Appendix C.4: Table C-18).

July 2016 PCA first and second components explain 65.8 % of the variance with most variables contributing to the model apart distance to MHWS (Figure 4-49e). The plot shows that July's high sediment deposition is related to soil BDD, hydroperiod and flood depth in areas where pioneer (SM8) and low-marsh (SM13a) plant grows with one mid-marsh sample (SM13d). Linear regression ( $F_{(1, 26)} = 5.85, p < 0.05^*$ ) demonstrates that a significant relationship between July's sediment deposition and BDD, saltmarsh elevation and distance to saltmarsh edge with the relationship  $\sqrt{\text{deposited sediment } g.m^{-2}.day^{-1}} = 6.26 - 8.37 * \sqrt{\text{Elevation height in m}} + 8.59 * \sqrt{\text{BDD in } g.cm^{-3}} + 0.16 * \sqrt{\text{Distance to SM Edge in m}}$  contributing to 30.5 % ( $r^2_{adj}, F_{(3, 24)} = 4.93, p < 0.01^{**}$ ) of the variance in deposition (Appendix C.4: Table C-17 model 2).

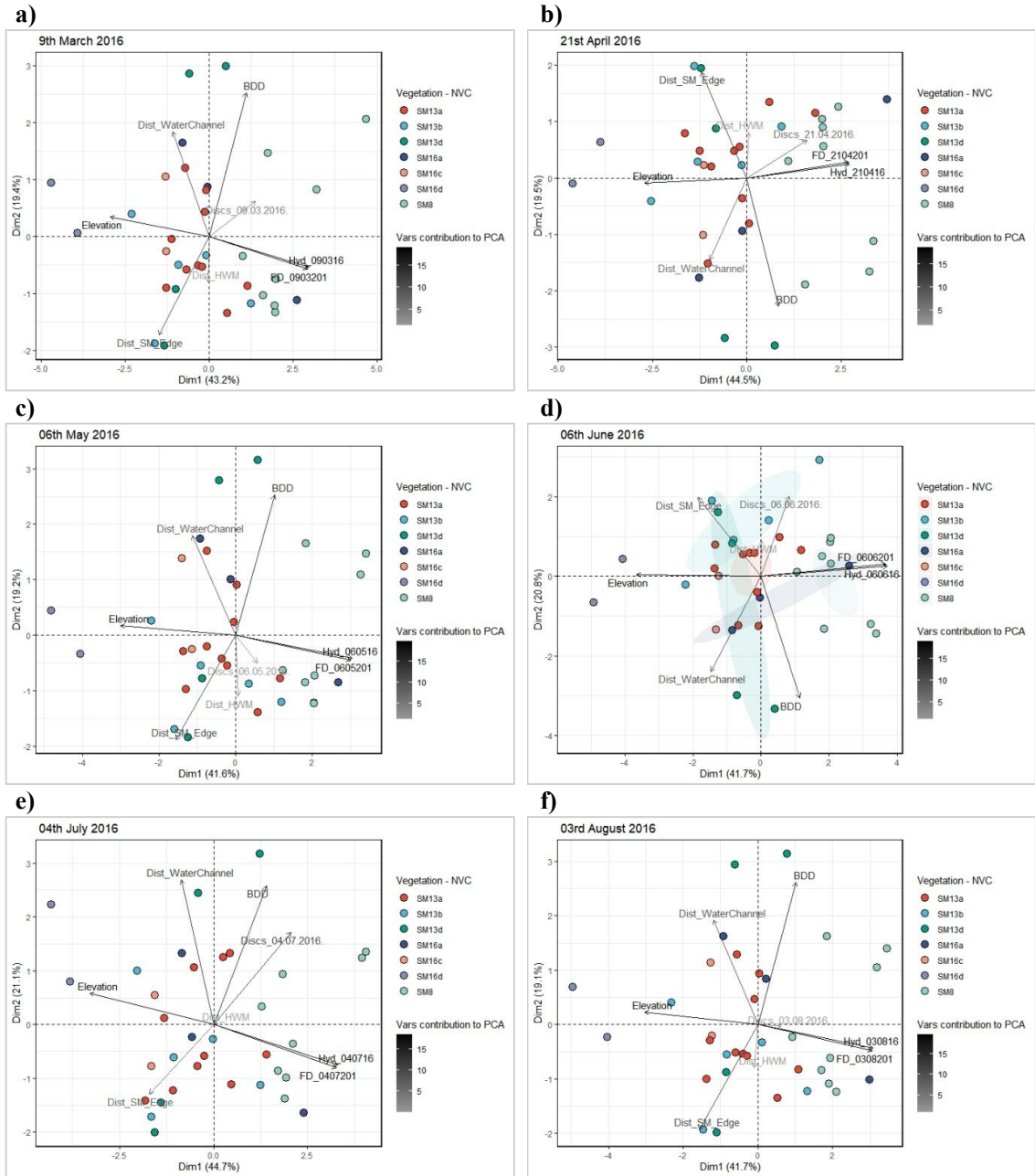
The first and second dimensions of August PCA explain 60.8 % of the variance where hydroperiod (28.3 %), flood depth (28 %), elevation (27.7 %) contributes the most pioneer and low-marsh assemblages are associated to higher sediment deposition's samples and high-marsh plants to low deposition samples (Figure 4-49f). However, the relationships were not found statistically significant, which may be explained by the fact that August had one of the lowest sediment deposition rates of the campaign (i.e. empty filter discs were collected - section 4.2.1.2).

September (Figure 4-49g) and October 2016 (Figure 4-49h) PCAs are explaining 60.8 % and 62.7 % respectively of the dataset variance with their first two components. Hydroperiod, flood depth and elevation contribute the most to the model and where sediment deposition seems associated to distance to MHWS and to the saltmarsh edge and is highest with pioneer and low-marsh plants, but PCA demonstrates that deposition a weak loading score (Figure 4-49g).

November 2016 PCA first and second components resume 63.3 % of the dataset inertia and are a measure of the quality of hydroperiod (26.2 % in first dimension), flood depth (25.8 % in first dimension), elevation (26.1 % in first dimension), and to a lesser extent BDD (45.7 % in second dimension) (Figure 4-49i). This was confirmed by linear regression ( $F_{(1, 29)} = 9.45, p < 0.001^{***}$ ) where 24.6 % ( $r^2$ ) of the sediment deposition is explained by elevation with a relationship defined as  $\sqrt{\text{deposited sediment } g.m^{-2}day^{-1}} = 34.33 - 19.89 * \sqrt{\text{elevation height in m}}$  (Appendix C.4: Table C-17 model 3).

December 2016 PCA first and second dimensions summarise 62.3 % of the dataset variance with contribution of hydroperiod (27.2 % in first dimension), flood depth (26.7 % in first dimension) and elevation (26.7 % in first dimension) (Figure 4-49j). It was also found that distance to MHWS can be a significant predictor for 19 % ( $r^2$ ) of December's sediment deposition variance ( $F_{(1, 34)} = 7.45, p < 0.01^{**}$ ) with a relationship defined as  $\text{deposited sediment } g.m^{-2}day^{-1} = 10.62 + 2.69 * \sqrt{\text{distance to MHWS in m}}$  (Appendix C.4: Table C-17 model 4). The biplot highlights clusters of pioneer (SM8) and mid-marsh plants (SM13b) associated to higher deposition and high-marsh plants (SM16a and SM16c) to lower deposition. This is confirmed in a linear regression ( $F_{(1, 27)} = 3.04, p < 0.05^*$ ) showing vegetation assemblages are found to explain 27.1 % ( $r^2_{adj}$ ) were pioneer plants (SM8) and mid-marsh NVC community (SM13b) contribute the most to the model (Appendix C.4: Table C-18). Both regressions met the assumptions of homogeneity of variance and linearity, and the residuals are approximately normally distributed with minor underestimation using distance to MHWS and overestimation when using vegetation assemblages.

January PCA biplot (Figure 4-49k) shows that hydroperiod, flood depth, elevation, distance to the water channel contribute the most to the PCA first and second dimensions corresponding to 64.9 % of the dataset variance. The biplot also depicts cluster of pioneer and low-marsh plant assemblages associated to higher sediment deposition. Elevation is found a significant predictor for 27.3 % ( $r^2$ ) of January's sediment deposition variance ( $F_{(1, 32)} = 12.03, p < 0.01^{**}$ ) with a relationship defined as  $\sqrt{\text{deposited sediment } g.m^{-2}day^{-1}} = 7.15 - 2.91 * \text{elevation in m}$ , however the regression tends to under- and overestimate deposition (Appendix C.4: Table C-17 model 5).





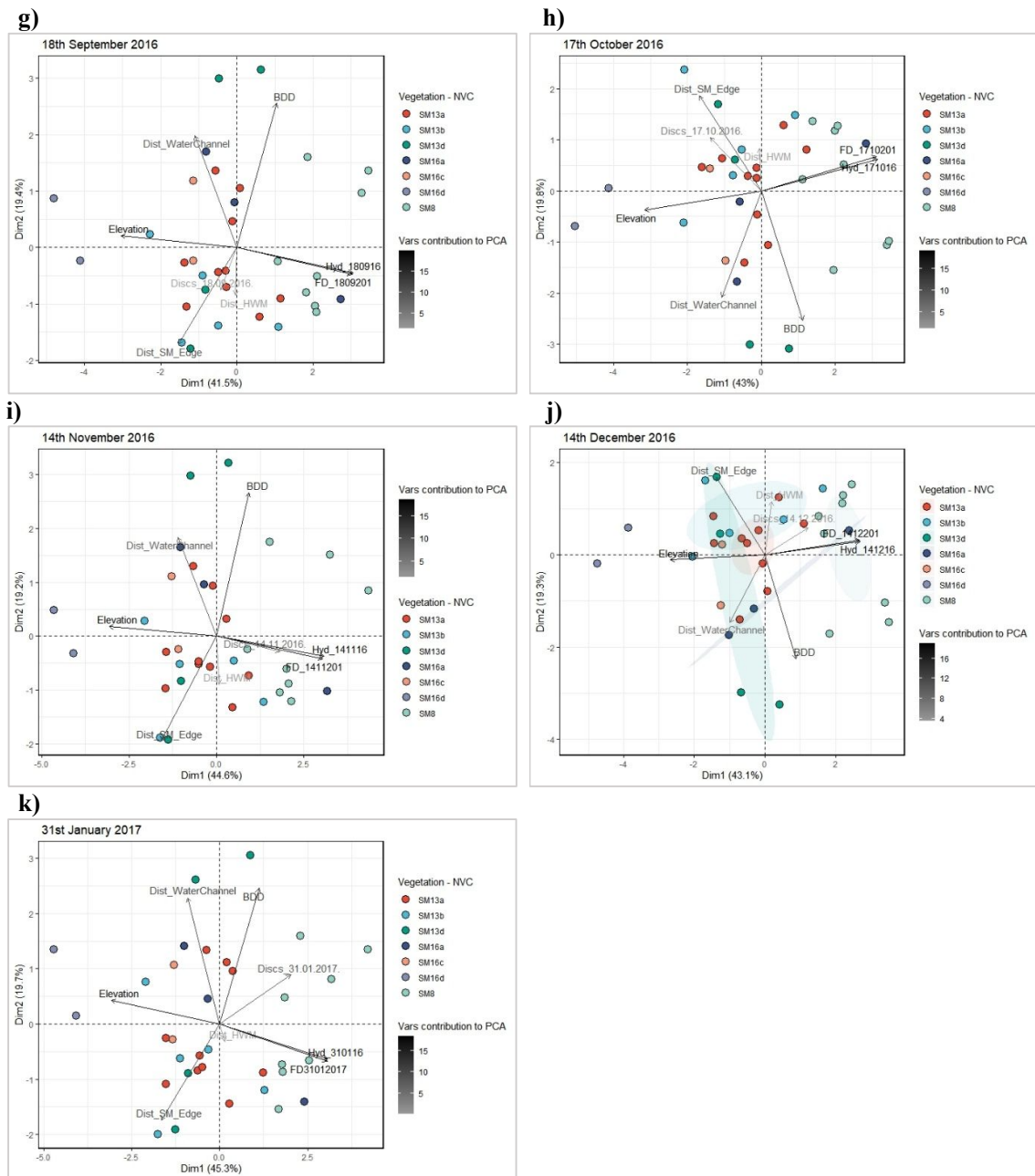


Figure 4-49: PCA plots a) to k) for each sediment deposition campaign showing in x-axis and y-axis the principal components that contribute the most to the variance of the dataset (PC1 and PC2). Individual samples are symbolised with a point coloured by vegetation assemblage and each variable represented by an arrow with its length and gradient color informing on the PCA loading scores (dark longer arrows have higher contribution and vice versa). Graphs d and j have a ellipse plotted around vegetation assemblages highlighting clustering.

DISCS_DDMMYY	Monthly sediment deposition in g standardised to a 1 m <sup>2</sup> area
Dist_HWM	Distance to MHWS in m
Dist_WaterChannel	Distance to water channels in m
Dist_SM_Edge	Distance to saltmarsh edge in m
BDD	Soil Bulk density in g.cm <sup>3</sup>
Hyd_DDMMYY	Hydroperiod in m
FD_DDMMYY	Flood depth in m
Elevation	Elevation height in m

### 4.5.1.3 Summary

Section 4.5.1.1 aimed to investigate the relationships between the measured filter discs deposition rates, accretion rate estimates and physical drivers and controls to saltmarsh development across the three salt marshes studied in Nigg Bay. The results show that distance to the saltmarsh edge and tidal parameters (flood depth and hydroperiod) constitute a major control on the overall short-term deposition and accretion rate estimates of Nigg Bay salt marshes and are significantly and positively influenced by maximum water levels. Running PCA enabled the visualisation of vegetation assemblages' clusters. The analyses confirm that modelling sediment deposition and accretion rate estimates and hydroperiod or flood depth can be significantly improved by vegetation assemblages. They show that rates are higher at high water levels and enhanced where annual *Salicornia* (SM8) grows, and rates are lower at low water levels and suppressed by assemblages such as *Puccinellia mar.* and *Glaux mar.* subcommunity (SM13b) and *Festuca Rubra* (SM16d).

The objective of Section 4.5.1.2 was to investigate which physical factors and controls related to saltmarsh development could influence the monthly filter disc deposition rates measured across the three salt marshes studied in Nigg Bay. The results of the PCA confirm that hydroperiod, inundation depth, and elevation height are co-linear. PCA biplots enable the visualisation of clusters of pioneer and low-marsh vegetation assemblages (SM8 and SM13a) when hydroperiod and flood depth are at their highest levels (see section 4.5.2) and clusters of high-marsh plants (SM16d) on the elevated ground surface of the marsh. April (56.3% of the variance explained), November (24.6%), and January 2017 (27% of the variance explained) are identified as months in which monthly sediment deposition had a positive and significant relationship with elevation height. For these months, the vegetation groupings of the biplots corroborate that overall sediment deposition is highest in the pioneer zones where SM8 vegetation assemblage grows and lowest in the high-marsh zones comprised of SM16d vegetation assemblage, as hypothesised. In most cases, vegetation assemblages enhanced the prediction models. The sediment deposition rates in July and December of 2016 have been linked to other physical drivers. In July, BDD, distance to saltmarsh edge, and elevation were found to explain 30.5% of the variability in sediment deposition rates, whilst in December, sediment deposition was related to the distance to the MHWS and the model was improved by pioneer and low-marsh vegetation assemblages (SM8 and SM13a). The vegetation assemblages were found to be a good predictor for more than half of the variability in sediment deposition rates in June 2016, where low deposition was primarily found in mid and high-marsh plants (SM13b and SM16).

The analysis also concurs with results presented in section 4.2.1.2 which highlights the months of September, October and November 2016 having the highest flood depth and hydroperiod and in turn coinciding with the months with the highest sediment deposition rates and conversely August 2016, April 2016 and January 2017 as having the lowest flood depth consistent with lower deposition rates. Although, water levels in summer and winter at Nigg Bay do not display distinct difference, section 4.4.2 demonstrates that during Spring (March, April, May) and Autumn (September, October, November), both hydroperiod and flood depth exhibit highest levels. These results confirm the importance of physical and hydrodynamic drivers of sediment deposition in Nigg Bay.

#### **4.5.2 Physical controls on biological processes**

In this research study, biological dynamics (e.g. plant succession on short - multi-annual- and long -decadal- timescale) have not been studied specifically (e.g. plant succession on short - multi-annual- and long -decadal- timescale), but, within one same framework, under the recognised assumption that saltmarsh systems are by nature biogeomorphic systems (Stallins, 2006; Belliard et al., 2017), whereby vegetation biomass and its physical properties (morphometrics such as vegetation height, density and cover) and saltmarsh surface elevation are sustaining saltmarsh development, biological processes have been measured to investigate interactions and influences between geomorphic, physical and ecological components in order to quantify and validate these empirical relationships across the three salt marshes studied in Nigg Bay. These relationships are first presented in this section and relationships between vegetation and sediment deposition and accretion are presented in 4.5.3.

PCA allows exploration of relationships between vegetation and physical controls that governs the three salt marshes studied at Nigg Bay. The biplot of the PCA first and second components (Figure 4-50) illustrates that 60.7 % of the dataset variance with three clusters of interpretation that can inform on the relationships of (i) vegetation cover; (ii) vegetation height, biomass and aboveground organic carbon (OC); (iii) vegetation density. The biplot further shows that the further away from saltmarsh edge, higher the vegetation is, which in turn can be associated to higher biomass and aboveground OC levels. The biplot shows that there is a negative relationship between vegetation density and height (as established in section 4.3.3) and that in turn density is associated with BDD. Finally, the biplot implies that the more there is vegetation cover, the higher is the elevation and lower are the hydroperiod, flood frequency and flood depth. These relationships are further examined in the following sections.

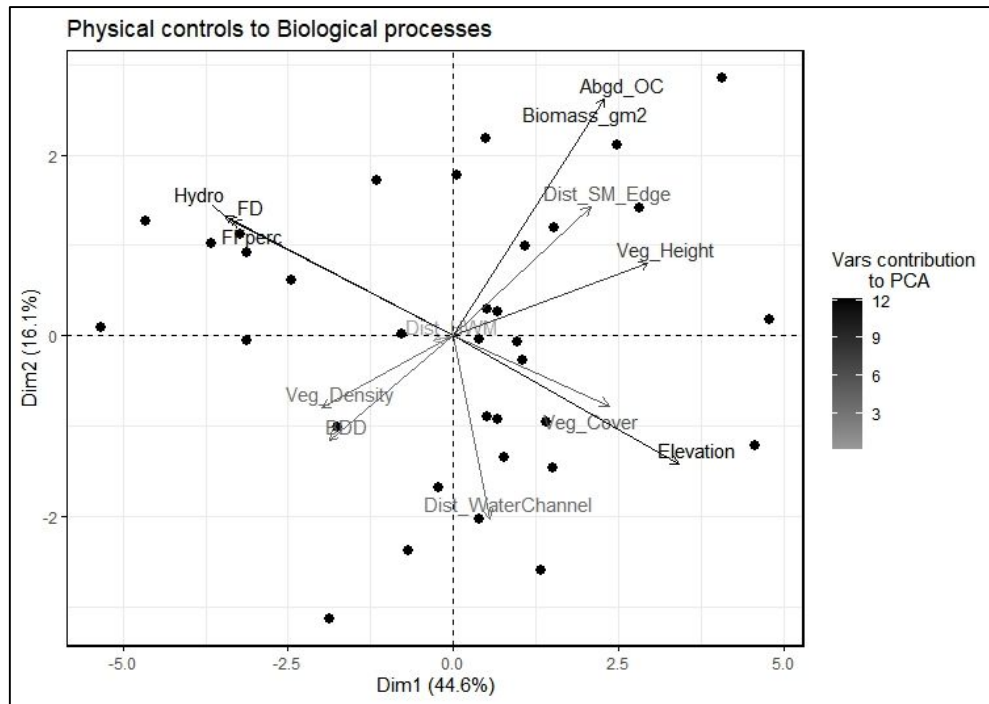


Figure 4-50: PCA biplot for vegetation characteristics and physical controls to saltmarsh development showing in x-axis and y-axis the principal components that contribute the most to the variance of the dataset (PC1 and PC2). Each variable represented by an arrow with its length informing on the PCA loading scores. Variables used:

<b>Elevation</b>	Elevation height (m)	<b>Veg_Density</b>	Vegetation density number of individual per m <sup>2</sup>
<b>BDD</b>	Soil Bulk density (g.cm <sup>3</sup> )	<b>Abgd_OC</b>	Aboveground Organic Carbon Content (g per m <sup>2</sup> )
<b>FD</b>	Flood depth (m)	<b>Veg_Cover</b>	Vegetation cover in percentage
<b>FFperc</b>	Flood Frequency in m	<b>Dist_SM_Edge</b>	Distance to saltmarsh edge (m)
<b>Hydro</b>	Hydroperiod (m)	<b>Dist_HWM</b>	Distance to MHWS (m)
<b>Veg_Height</b>	Vegetation height (cm)	<b>Dist_WaterChannel</b>	Distance to water channels (m)
<b>Biomass_gm2</b>	Biomass in g per m <sup>2</sup>		

#### 4.5.2.1 Physical controls on vegetation characteristics

##### Vegetation height

Vegetation height was found to have statistically significant relationships with most morphological controls to saltmarsh development (Figure 4-51a to c): soil density (BDD) and distance to the saltmarsh edge were weak relationships ( $r^2 = 17\%$   $F_{(1, 31)} = 6.48$ ,  $p < 0.01^{**}$  and  $r^2 = 17\%$   $F_{(1, 31)} = 6.34$ ,  $p < 0.01^{**}$  respectively) whereas elevation explained 40% of the vegetation height variance ( $F_{(1, 31)} = 20.98$ ,  $p < 0.001^{***}$ ). Tidal controls were also found to be significant predictors to vegetation height (Figure 4-51d to c) with positive relationships where flood depth explained 40 % of vegetation height variance, flood frequency 42 % and hydroperiod 44% (Appendix C.4 - Table C-22).

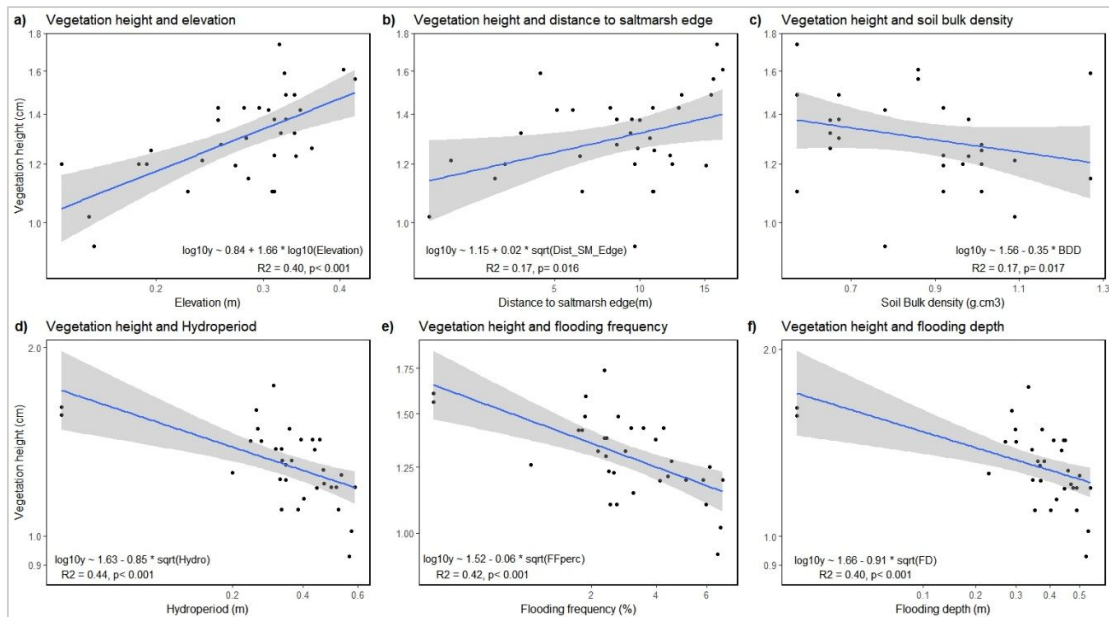


**Figure 4-51: Scatter plots between vegetation height (in cm - y-axis) and elevation (in m - plot a), distance to saltmarsh edge (m - plot b), soil bulk density (g.cm<sup>3</sup>- plot c), hydroperiod (in m - plot d), flood frequency (in % - plot e) and flood depth (in m - plot f) . Plots are showing linear regressions relationship, r<sup>2</sup> values and p-value.**

### Vegetation density

The PCA biplot (Figure 4-50) suggests that vegetation density does not contribute greatly to the overall dataset variance. This is confirmed when trying to model vegetation density (Appendix C.4 - Table C-23) which is found to be negatively and weakly (13 %) associated with elevation (Figure 4-52a,  $F_{(1, 31)} = 4.7$   $p < 0.05^*$ ) and positively and weakly (12 %) associated with hydroperiod (Figure 4-52c,  $F_{(1, 31)} = 4.7$   $p < 0.05^*$ ). Morphological controls were also found to be significant predictors to vegetation density with a stronger negative relationship where distance to the saltmarsh edge explains where 27 % of the vegetation density variance (Figure 4-52b,  $F_{(1, 31)} = 11.57$ ,  $p < 0.01^{**}$ ).

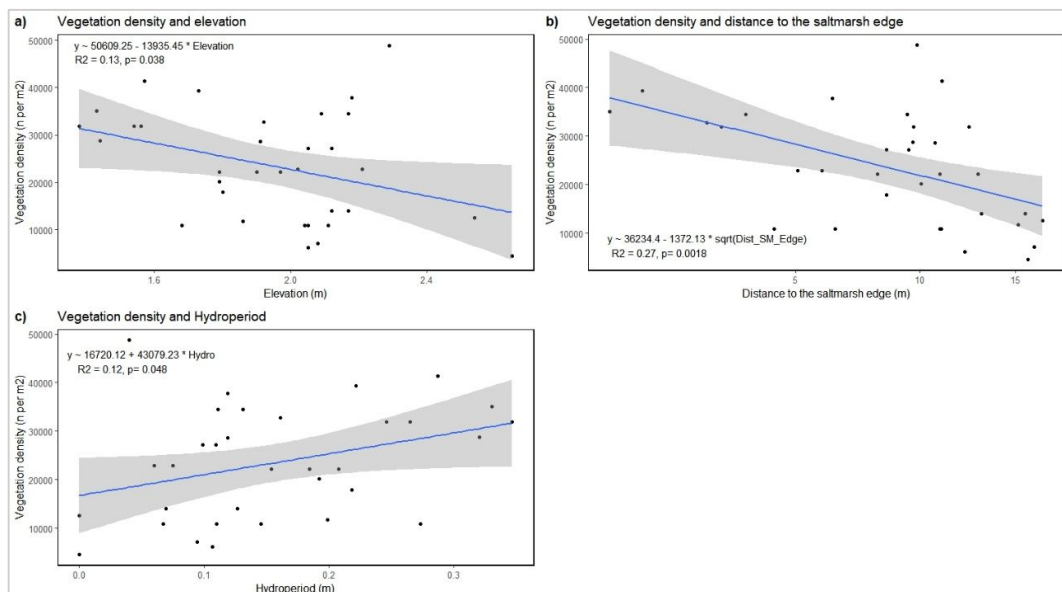


**Figure 4-52: Scatter plots (with linear regressions relationship, r<sup>2</sup> values and p-value) between vegetation density (n per m<sup>2</sup> - y-axis) and elevation (in m - plot a), distance to saltmarsh edge (m - plot b), and hydroperiod (in m - plot c).**

## Vegetation cover

These aforementioned interpretations and illustrated by the above biplot (Figure 4-50) were further tested using linear regressions. Results indicate a significant relationship between vegetation cover and elevation ( $F_{(1, 32)} = 16.24, p < 0.001^{***}$ ) where 34 % of the vegetation cover variance is explained by elevation. Similarly, each water levels parameter (hydroperiod, flood frequency and flood depth) has been found to explain approximately a quarter of the vegetation cover variance (Figure 4-53 and Appendix C.4 - Table C-21).

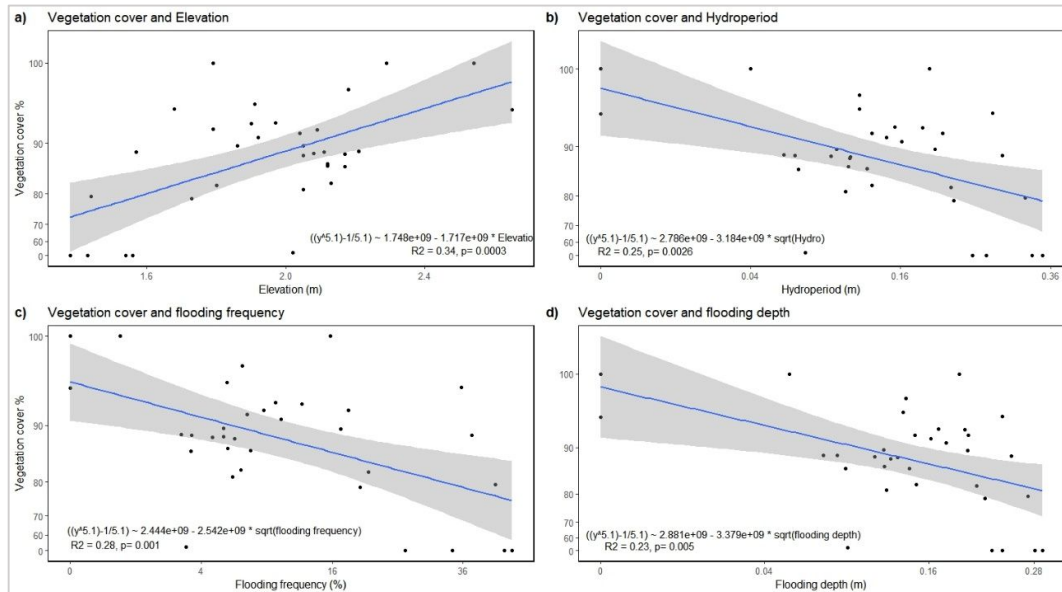


**Figure 4-53: Scatter plots** (with linear regressions relationship,  $r^2$  values and p-value) **between vegetation cover (in % - y-axis) and elevation (in m - plot a), hydroperiod (in m - plot b), flood frequency (in % - plot c) and flood depth (in m - plot d).**

**Aboveground biomass and aboveground organic carbon content.** PCA biplot (Figure 4-50 above) illustrates the strong relationships between biomass and aboveground organic carbon (OC) content and vegetation height as per described in section 4.3.3 and it was expected that both variables would be associated to same physical controls to saltmarsh development. However, linear regressions suggest that elevation and tidal controls does not appear to predict biomass aboveground OC content for the salt marshes of Nigg Bay. Regression analyses confirm that distance to the saltmarsh edge ( $r^2 = 15\%, F_{(1, 31)} = 5.54, p < 0.05^*$ ) and BDD ( $r^2 = 14\%, F_{(1, 31)} = 5.06, p < 0.05^*$ ) have a statistically significant but weak relationship to aboveground biomass (Appendix C.4 - Table C-24 ; Figure 4-54). Regression results show the same results using the aboveground biomass or aboveground OC (see 3.4.1.2 - aboveground biomass is only distinguished from aboveground OC by the conversion factor as defined in Howard et al. (2014)).



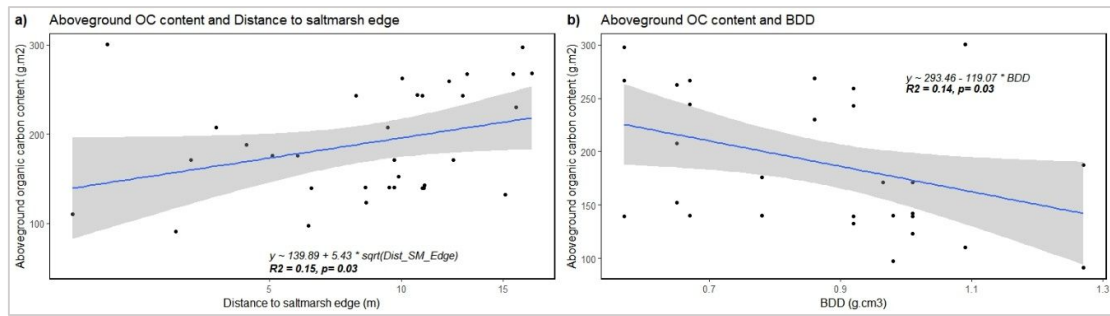


Figure 4-54: Scatter plots between aboveground organic content (in g.m2 - y-axis) and distance to saltmarsh edge (in m - plot a). Plots are showing linear regressions with their respective relationship equation, r<sup>2</sup> values and p-value

Running PCA with all vegetation characteristics as presented above and tidal processes solely (hydroperiod, flood frequency and flood depth) has demonstrated that 77.1 % of the dataset variance can be explained with the first two dimensions with alongside distinct cluster of vegetation assemblages (Figure 4-55). Therefore, the saltmarsh vegetation assemblages of Nigg Bay may now be evaluated against water levels parameters and results are presented in the next section.

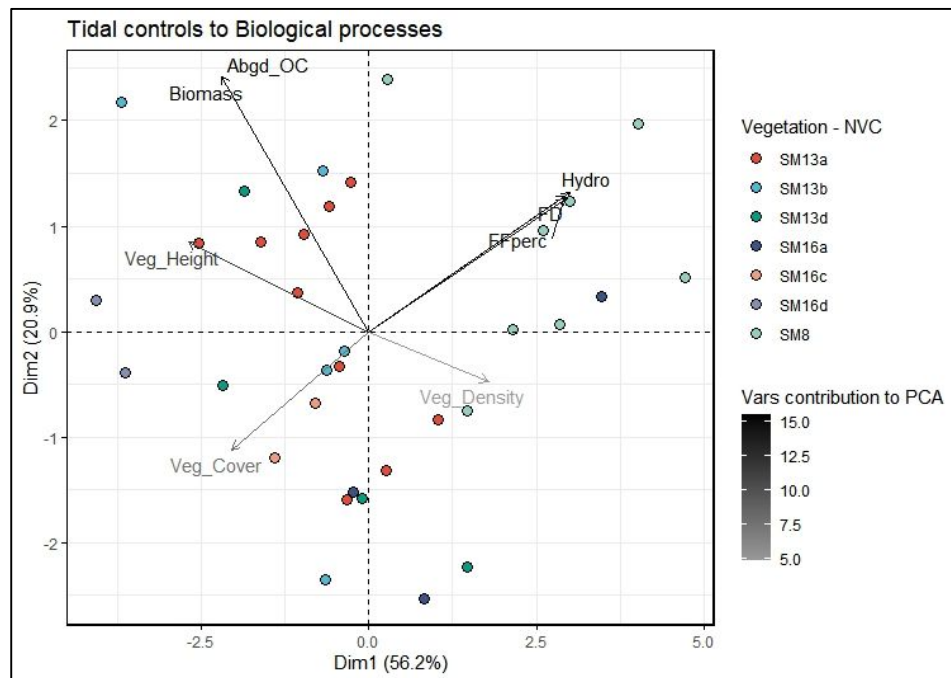


Figure 4-55: PCA biplot for vegetation characteristics and tidal controls to saltmarsh development showing in x-axis and y-axis the principal components that contribute the most to the variance of the dataset (PC1 and PC2). Each variable represented by an arrow with its length informing on the PCA loading scores. Variables used:

FD	Flood depth (m)	Veg_Density	Vegetation density number of individual per m <sup>2</sup>
FFperc	Flood Frequency in m	Abgd_OC	Aboveground Organic Carbon Content (g per m <sup>2</sup> )
Hydro	Hydroperiod (m)	Veg_Cover	Vegetation cover in percentage
Veg_Height	Vegetation height (cm)	Biomass_gm2	Biomass in g per m <sup>2</sup>

#### 4.5.2.2 Water levels and vegetation assemblages

Flood depth, flood frequency and hydroperiod for monitoring period (8<sup>th</sup> February 2016 to 01<sup>st</sup> March 2017 i.e. 359 days or 778 tidal periods - as defined in chapter 3 - 3.3.2.3) are used in this section to assess relationships between water levels and vegetation assemblages across the three saltmarsh sites' area (referring to figure 3-14).

The analysis conducted in this section utilises all vegetation assemblages-NVC community present within the areal extent, as presented in section 3.2.2.2 (paragraph "Research baseline zonation classification") as depicted in figure 3-14 (for example, high-marsh zones which are predominantly characterised by the SM16a vegetation community. However, in certain quadrats, SM13d assemblages have been recorded). This enhances the comprehension of the factors influencing the distribution of vegetation assemblages across the three salt marshes in Nigg.

Overall, all hydroperiod parameters demonstrate statistically significant differences between the vegetation assemblages' mean ranks (Figure 4-56): flood depth ( $H = 179804, p < 0.001^{***}$ , Appendix C-3: Table C-25), flood frequency ( $H = 181133, p < 0.001^{***}$ , Table C-26) and hydroperiod ( $H = 180485, p < 0.001^{***}$ , Table C-27). Mann-Whitney-Wilcoxon pairwise comparison tests adjusted with Bonferroni correction show that most vegetation assemblages change significantly per hydroperiod parameters levels (for the period between March 2016 and March 2017). Few exceptions suggest that flood depth, frequency and hydroperiod are uniform where SM16c and SM16a are present; similarly, no significant difference is found for flood depth on SM16d and SM28 (Appendix C-3: Figure C-4, C-5, C-6). This can be explained by SM28 being only present on FM and SM16d only on MR (Figure 4-57). Figure 4-56 highlights that the three water levels parameters follow gradient profiles associated with vegetation assemblages where pioneer plants (SM8) are present when flood depth, frequency and hydroperiod mean's ranks are the highest ( $\eta \pm \text{IQR} = 0.24 \pm 0.06$  m,  $17 \pm 35.9$  %,  $0.27 \pm 0.09$  m respectively) and high-marsh plant's assemblages (SM28, SM16d, SM16c, SM16a) when the levels are the lowest ( $\eta \pm \text{IQR}$  are for SM28 =  $0 \pm 0.03$  m,  $2.57 \pm 1.99$  %,  $0.04 \pm 0.03$  m respectively; SM16d =  $0 \pm 0.03$  m,  $2.82 \pm 2.1$  %,  $0.04 \pm 0.04$  respectively; SM16c =  $0.07 \pm 0.07$  m,  $4.4 \pm 4.9$  %,  $0.06 \pm 0.07$  respectively ; SM16a =  $0.07 \pm 0.09$  m,  $5.14 \pm 6.93$  %,  $0.06 \pm 0.07$  respectively). Standing out from the trend are water levels averaged on areas that have been identified with mixed assemblages during sampling collection (i.e. sampling points have been identified as belonging to another assemblages than originally surveyed by Haynes (2016) - see 3.3.2.2 & Figure 3-14): SM13a+SM16a (only on FM;  $\eta \pm \text{IQR}$  for flood depth, frequency and hydroperiod are  $0.23 \pm 0.03$  m,  $14.1 \pm 24.8$  %,  $0.25 \pm 0.05$  respectively), SM13b+SM13d (only on MR;  $\eta \pm \text{IQR}$  for flood depth, frequency and hydroperiod are  $0.1 \pm 0.06$  m,  $2.57 \pm 4.45$  %,  $0.09 \pm 0.04$  respectively), SM16a+SM13d (only on FM;  $\eta \pm \text{IQR}$  for

flood depth, frequency and hydroperiod are  $0.2 \pm 0.07$  m,  $20.8 \pm 18.4$  %,  $0.19 \pm 0.1$  respectively), and SM16c+SM13d (only on FM;  $\eta \pm \text{IQR}$  for flood depth, frequency and hydroperiod are  $0.06 \pm 0.06$  m,  $2.06 \pm 2.66$  %,  $0.05 \pm 0.05$  respectively); thus suggesting that these areas may be transitioning to low-marsh vegetation assemblages (wetter more often and longer requiring vegetation to have higher threshold of salinity tolerance).

Linear regression models to assess how much flood depth, hydroperiod and flood frequency may influence the change of vegetation assemblages (details in Appendix C.3: Table C-28) confirm that 63% ( $r^2_{\text{adj}}$ ,  $F_{(10, 285274)} = 47952.52^{***}$ ) of the flood depth variance is explained by vegetation assemblages. Regression models for flood frequency and hydroperiod demonstrate that 62 % ( $r^2_{\text{adj}}$ ) of both water parameters variance ( $F_{(10, 285274)} = 46767.02^{***}$  and  $F_{(10, 285274)} = 47190.63^{***}$  respectively) are explained by plant assemblages.

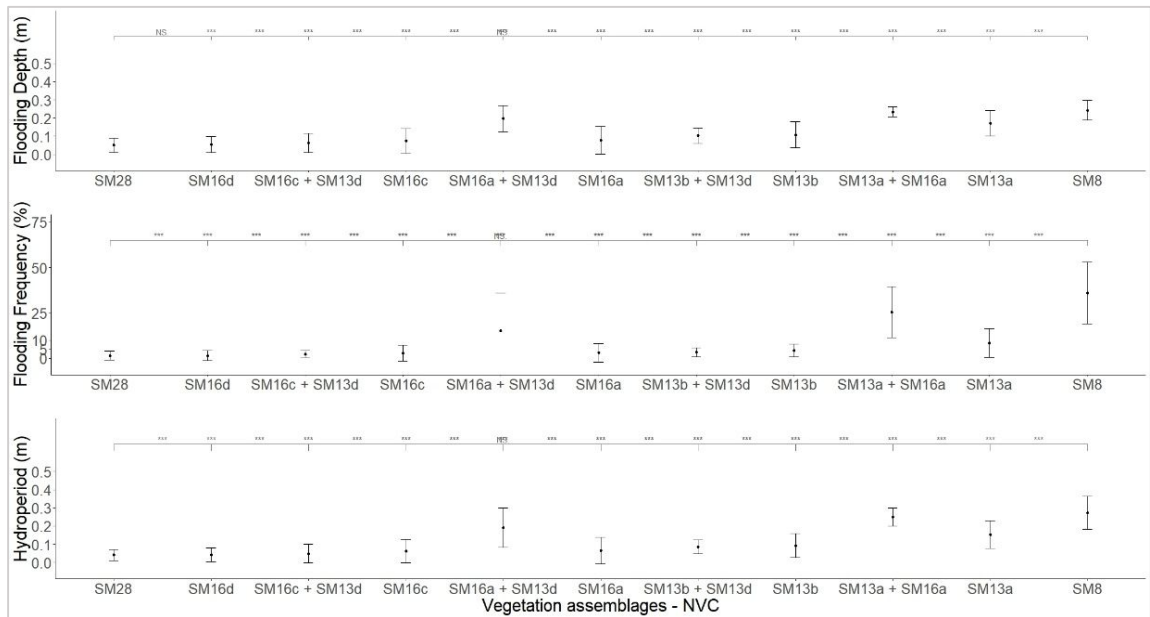


**Figure 4-56: Average flood depth (m- top), flood frequency (%- middle) and average hydroperiod (m -bottom) levels for each vegetation assemblages (details in see Appendix C.3 Figure C-25 to 27). The top row (grey) represents Mann-Whitney-Wilcoxon tests results are symbolised on the top row by the p-value significance - ns, \*, \*\*,\*\*\* - for each pairwise tests. For full pair-test comparison see Appendix C.3 Figure C-4, C-5, C-6.) The plot represent median and error bars are interquartile range.**

These differences and patterns between assemblages were further explored using Kruskal-Wallis and Mann-Whitney-Wilcoxon pairwise comparison tests performed between vegetation assemblages present on each saltmarsh site and all mean's ranks have demonstrated the same strong significant differences and patterns between vegetation assemblages under all flooding parameters with no exception (Figure 4-57). The most striking results is how most vegetation assemblages on the MR site experience less flood frequency with lower hydroperiod and flood depth than on the natural salt marsh. However flood frequency for ANK's SM13a departs slightly from this trend which is significantly lower than on MR or FM. This can be explained by

the tidal fetch (for this assemblage) which distinctively greater on ANK's SM13a compared to FM and MR.

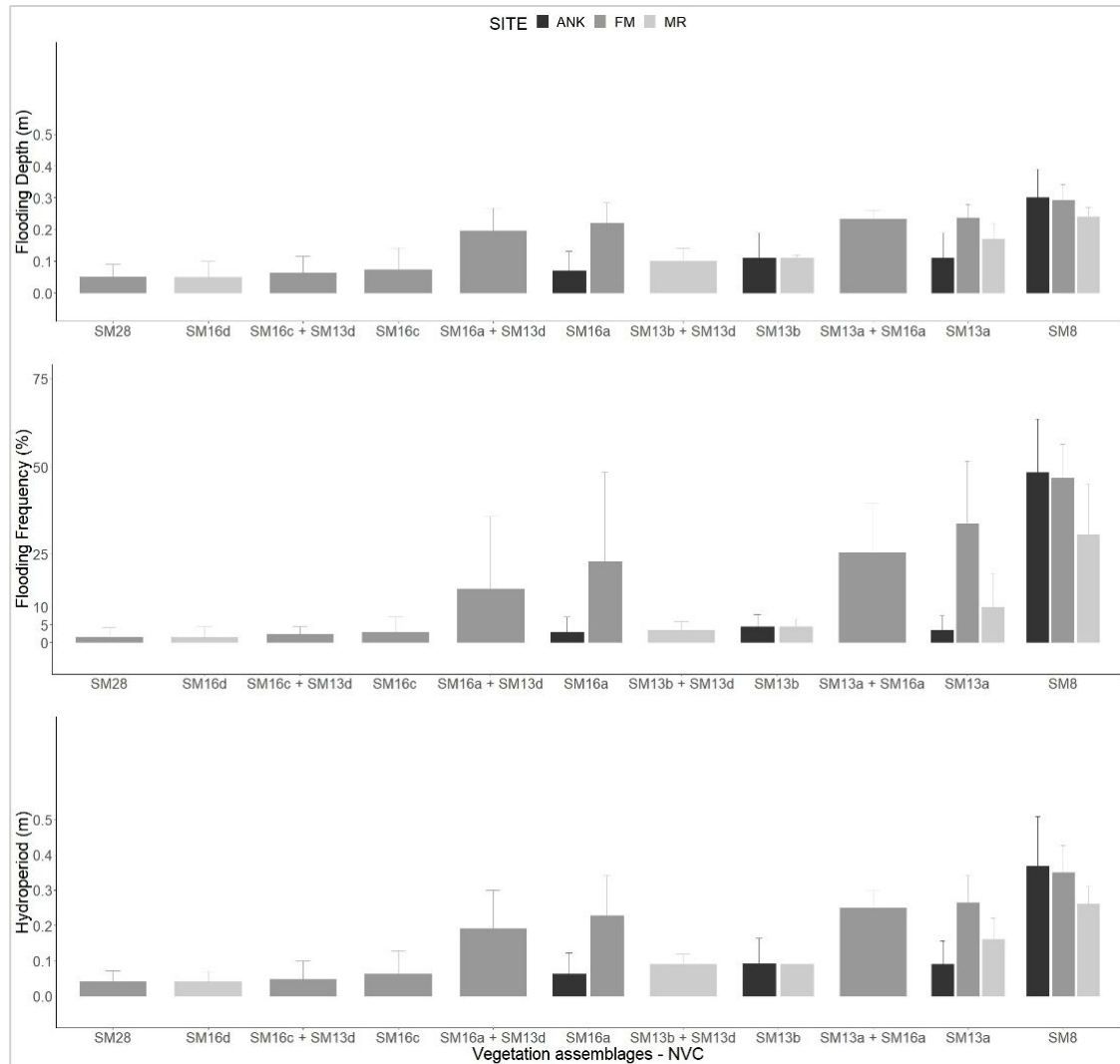


Figure 4-57: Mean ranks' flood depth (m- top), flood frequency (%- middle) and hydroperiod (m -bottom) levels between vegetation assemblages present for each saltmarsh site. The bar graph represent median and error bars are interquartile range.

#### 4.5.2.3 Summary

Section 4.5.2.1 addressed relationships between the measured vegetation characteristics (height, cover, density) and physical drivers and controls to saltmarsh development such as elevation, tidal parameters, distance to saltmarsh edge, to MHWS, to water channels and BDD measured across the three salt marshes studied in Nigg Bay. The analysis shows that elevation and tidal parameters constitute a major control on the overall salt marsh vegetation characteristics of Nigg Bay, principally vegetation cover and height, allowing the identification of vegetation assemblage groups.

Section 4.5.2.2 addressed relationships between the saltmarsh vegetation assemblages and water levels parameters of Nigg Bay, specifically, it aimed to answer questions such as: do vegetation assemblages favour distinct levels of inundation? Does the relationship exist on every studied marsh? Do all marsh's assemblages respond in the same way?

The results show that the water level variations occurring across the marshes have a significant control on vegetation assemblages by altering the wetting-drying regime and the depth of inundation. The recognised pattern that pioneer and low-marsh (SM8 and SM13a) vegetation would support a wetter regime and high-marsh plants (SM16a, c and d) a drier regime along the elevational gradient is broadly apparent across the three salt marshes of Nigg Bay. However, assessment of the vegetation assemblages using hydroperiod and flood depth shows an irregular profile in the plant sequence (not fully following the sloping profile with elevation), suggesting a change in plant succession (Figure 4-57). These areas may be in transition to a wetter regime, this being intrinsically linked to the elevation of the marsh.

### **4.5.3 Relationships between vegetation and sediment deposition and accretion rate estimates**

Essential to assessing coastal saltmarsh vulnerability are the relationships between sedimentation and the living biomass both regulated by tidal hydrodynamics (Fagherazzi et al., 2012; D'Alpaos et al., 2016; Belliard et al., 2017). Furthermore, it has been established that this has direct implications on saltmarsh restoration and rehabilitation projects aiming to reinstate a similar habitat to natural salt marsh (Montalto et al., 2006; Howe et al., 2010). This section aims to test relationships between vegetation characteristics, the sampled NVC vegetation assemblages and sediment deposition and accretion rate estimates for the three salt marshes of Nigg Bay.

#### **4.5.3.1 Overall influence of vegetation on sediment deposition and accretion rates**

Sections 4.5.1.1 and 4.5.1.1 have shown that models testing the relationships between physical controls and sediment deposition rates (Figure 4-49d & j and Figure 4-43) and accretions rates (Figure 4-46) can be improved by using vegetation assemblages. This section briefly presents relationships between short-term deposition rates and accretion rates, vegetation characteristics and vegetation assemblages which were explored using PCA and regression analysis.

PCA's first and second dimensions explains 71.2 % of PCA of the variation in the dataset. The biplot (Figure 4-58) suggests that vegetation cover is associated to the overall filter disc sediment deposition rates and accretion rates, however, cover and density have the lowest contribution to

the PCA whilst aboveground biomass has the highest but not related to short-term deposition rates. This pattern is confirm in a linear regression model where vegetation cover is a significant predictor for 13.7 % ( $r^2$ ) of filter disc sediment deposition rates variance ( $F_{(1, 32)} = 5.093, p < 0.03^*$ ) with a relationship defined as  $\sqrt{\text{sediment deposition (g.m}^2\text{day}^{-1})} = 7.5 - 1.19 \text{ vegetation cover}^{0.2}(\%)$ . This pattern was not confirmed for filter discs accretion rate estimates or using other vegetation characteristics, aboveground biomass and organic carbon content (OC).

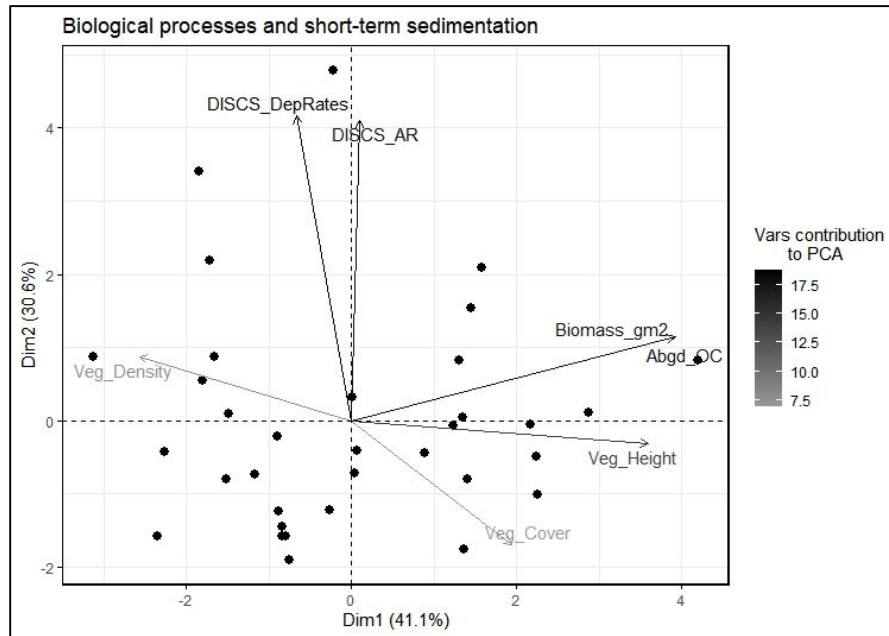


**Figure 4-58: PCA biplot for vegetation characteristics and short-term sediment deposition rates (deposition and accretion) showing in x-axis and y-axis the principal components that contribute the most to the variance of the dataset (PC1 and PC2). Each variable represented by an arrow with its length informing on the PCA loading scores. Variables used:**

<b>DISCS_AR</b>	Filter discs accretion rate estimates cm.yr <sup>-1</sup>	<b>Biomass_gm2</b>	Biomass in g per m <sup>2</sup>
<b>DISCS_DepRates</b>	Filter disc sediment deposition rate in g.cm <sup>2</sup> .yr <sup>-1</sup>	<b>Abgd_OC</b>	Aboveground Biomass/Organic Carbon Content in g per m <sup>2</sup>
<b>Veg_Height</b>	Vegetation height in cm	<b>Veg_Cover</b>	Vegetation cover in percentage
<b>Veg_Density</b>	Vegetation density n# per m <sup>2</sup>		

So far, overall associations between sediment deposition and accretion are too weak to suggest any biological enhancement and contribution to deposition or sediment settlement and accretion. Although, vegetation assemblages have not improved here modelling, it seems pertinent in this chapter on short-term biological and geomorphological processes of the three salt marshes of Nigg Bay to evaluate how deposition rates and accretion rate estimates have been performing between the sampled NVC assemblages.

The results from pairwise comparison tests (Mann-Whitney-Wilcoxon) indicate that deposition rates and accretion rate estimates mean ranks from SM8 are significantly higher than SM16a (Figure 4-59a and Figure 4-59b). SM8 assemblage has been associated with low height, density and cover (see 4.3.3 and Figure 4-21) in areas where plants experienced high inundation (depth



and frequency - see 4.5.1.1- Table C-20- models 5 and 6), suggesting that these characteristics can promote deposition and sediment settling. SM16c was found to promote deposition and accretion rates relative to SM16a and SM16d in high marsh plant communities (accretion rate estimates only).

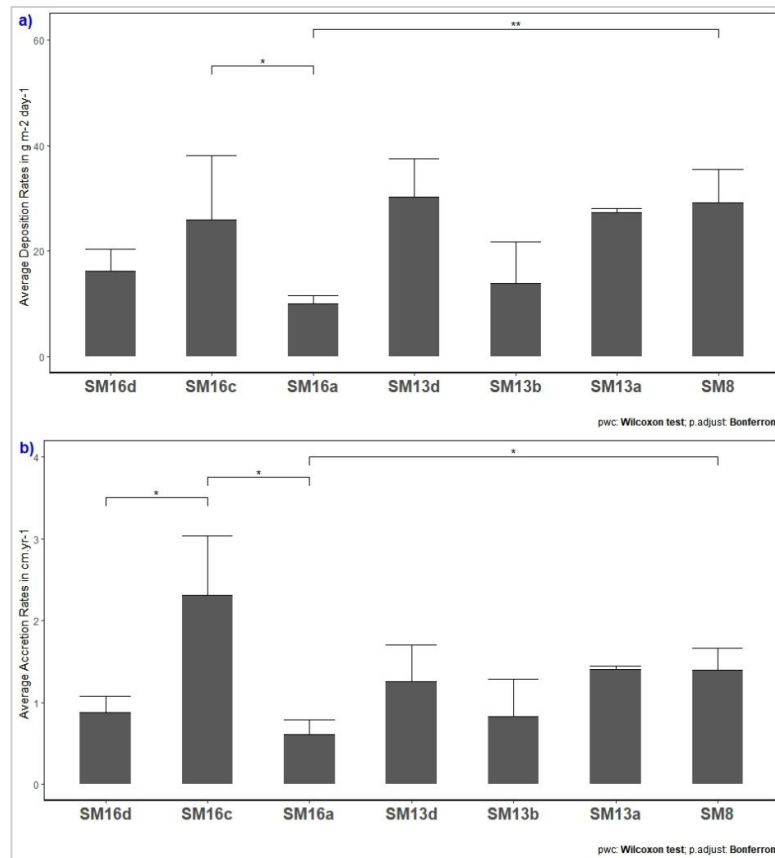


**Figure 4-59: Bar graphs showing Filter Discs a) Deposition rate (g.m<sup>-2</sup>.day<sup>-1</sup>) and b) accretion rate estimates (cm.yr<sup>-1</sup>) mean rank's for each NVC assemblages sampled on the three Nigg Bay salt marshes. The graphs also label Kruskal-Wallis results and the statistical significance of post-hoc pairwise comparison tests Wilcoxon test using Bonferroni adjustments symbolised on the top rows by the p-value significance with p-value significance (ns, \*, \*\*, \*\*\*). The bar graph represent median and error bars are calculated using standard errors (SE).**

#### 4.5.3.2 Seasonality and influence of vegetation on sediment deposition and accretion rates

In sections 4.5.1.1 and 4.5.1.1, modelling results (tables C-18, C-19 and C-20) have shown that vegetation assemblages (NVC) categorisation can improve the understanding of relationships between deposition and accretion rate estimates and hydroperiod and flood depth. Furthermore, sections 4.2.1.1 and 4.2.1.2 (for AstroTurf mats 4.2.1.3 and 4.2.1.4) have shown that during a year cycle, deposition rates have strong spatial and temporal variation. As vegetation characteristics were not measured monthly and cannot be used to assess the relationships between monthly deposition and vegetation characteristics, this section will only address

relationships between vegetation assemblages and the measured short-term deposition rates and accretion rates.

**Sediment deposition rates (filter discs).** Using monthly seasonal filter disc dataset categorised by seasons (summer/winter as defined in 4.2.1.2 - for AstroTurf mats 4.2.1.4), pairwise comparison tests (Mann-Whitney-Wilcoxon) demonstrate that, overall, deposition rates rankings differ significantly between vegetation assemblage during winter and summer, but do not follow the same patterns during the two seasons (Figure 4-60a) or do not follow the expected sequence of succession the species composition which changes with elevation (Doody, 2008). Across all assemblages, only SM8 deposition rates mean ranks is significantly higher in winter compared to summer. Comparing all assemblages during winter shows that SM8 deposition rates mean ranks are also found higher than deposition rates that took place on SM13d (mid-marsh plant assemblages). Comparing all assemblages during summer SM8 deposition rates mean ranks are significantly higher than deposition rates on SM16c (high-marsh plant assemblages). Moreover, during summer, SM16c deposition rates mean ranks are consistently lower than all other rates on the sampled vegetation assemblages (Figure 4-60a and Figure C-7). Although statistically significant, regression modelling relationship between deposition rates and vegetation assemblages is weak ( $r^{2\text{adj}} = 0.037$ ,  $F_{(df=6,297)} = 2.95$ ,  $p < 0.01$  \*\*). These results are slightly lower than those presented by regression models using sites' saltmarsh zones (in section 4.2.1.1, table C-1), suggesting that zonation categorisation may be more appropriate to explain the short-term deposition rates in Nigg.

As seen in sections 4.2.1.1 (also for AstroTurf mats 4.2.1.3), the variability can be better explained on each salt marsh. Therefore, the same model (i.e. average deposition rates and vegetation assemblages) applied to each saltmarsh site demonstrates that on MR and on FM the relationships are not significant, whilst on ANK vegetation assemblages can explain 22.15% ( $r^{2\text{adj}}$ ,  $F_{(df=3,98)} = 10.98$ ,  $p < 0.001$  \*\*\*) of sediment deposition rates variability. This suggests that overall that vegetation assemblages are not representative of the short-term sediment deposition that take place on these two young salt marshes and be an indication that vegetation is not established yet and shifting.

Seasonality has been proven to be a strong component in this short-term assessment of sediment deposition (sections 4.2.1.2 and also for AstroTurf mats 4.2.1.4), this is confirmed in regression models, where 27.49 % ( $r^{2\text{adj}}$ ,  $p < 0.001$  \*\*\*) of sediment deposition rates can be explained by monthly variation and vegetation assemblages. The analysis shows that all months (except April and August) along with SM8, SM13b and SM16c contribute the most to sediment deposition (table C-29, model 1). These results are comparable to sediment deposition rates between sites'

saltmarsh zones (4.2.1.1 and table C-3-model 3). Looking at each saltmarsh site, on ANK, monthly variation and vegetation assemblages can explain 47.53 % ( $r^{2adj}$ ,  $p < 0.001$ \*\*\*) of the deposition rates variability; where SM8 (pioneer) and SM13b (mid-marsh) and SM16a (high-marsh) plants along with all months except May, July and August contribute the most to the model. On FM 37.23 % ( $r^{2adj}$ ,  $p < 0.001$ \*\*\*) and MR 31.17 % ( $r^{2adj}$ ,  $p < 0.001$ \*\*\*) (table C-29, model 2-3-4). However, on FM and MR, ANOVA (type II - testing the factor of the regression model) results show that vegetation assemblages sum of squared residuals are not significant confirming that on these young salt marshes, vegetation assemblages are not as representative as on the mature natural salt marsh. Although not presented in the section 4.2, modelling same relationships between monthly deposition rates and sites' saltmarsh zones displays relationships of similar strengths for the three salt marshes (on ANK,  $r^{2adj} = 47.5$  %\*\*\* of the deposition rates variability is explained by the monthly collection and zonation, on FM  $r^{2adj} = 34.9$  %\*\*\* and MR  $r^{2adj} = 32.7$  %\*\*\*), and similarly to modelling sediment deposition and vegetation assemblages, saltmarsh zones are not significantly influencing deposition. This suggest that seasonality, temporality is a stronger factor than spatial variation pattern related to vegetation or zonation.

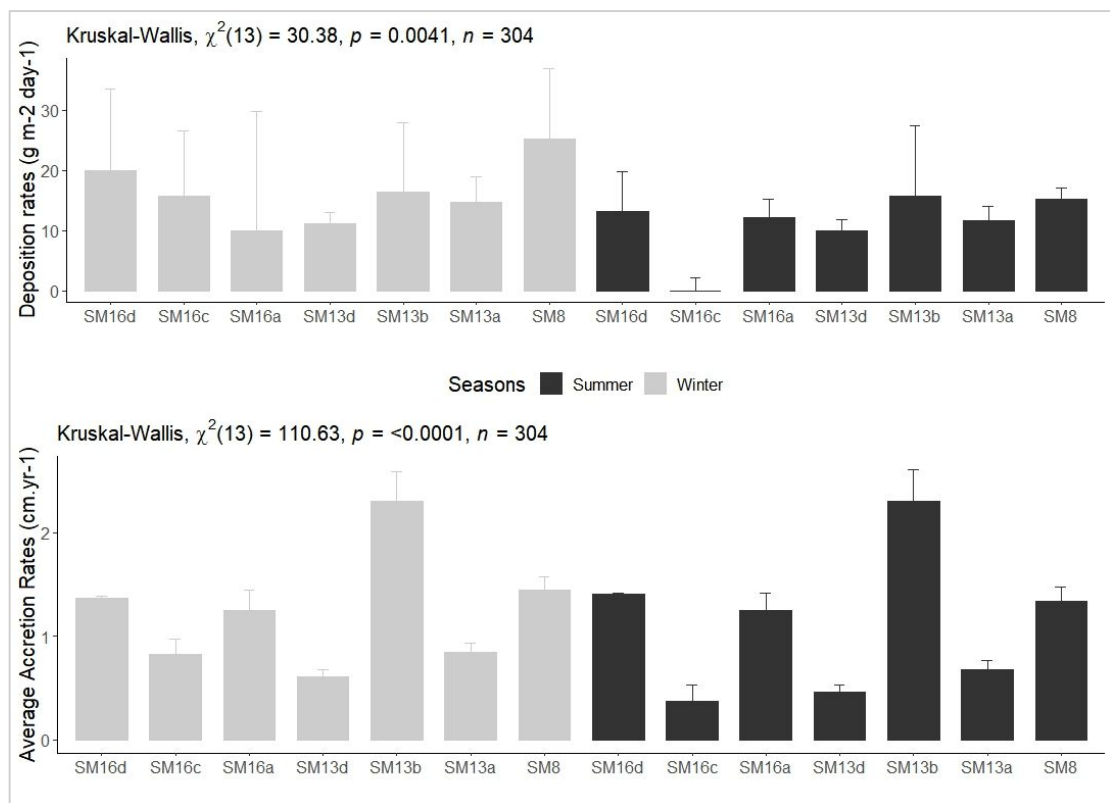


Figure 4-60: Bar graph of mean ranks' Filter Discs a) Deposition rates (g.m<sup>-2</sup>.day<sup>-1</sup>) and b) accretion rate estimates (cm.yr<sup>-1</sup>) between vegetation assemblages sampled on a saltmarsh site. The bar graph represent median and error bars are interquartile range.

**Accretion rate estimates (filter discs).** Comparison tests show that accretion rate estimates (filter discs) follow similar patterns between vegetation assemblages in winter and in summer (Figure 4-60b). Accretion rate estimates occurring on SM13b rank the highest in winter and

summer (Figure C-8). Similarly, accretion rate estimates on SM13d are significantly different to all other assemblages (except to SM16c during summer and during winter), ranking the lowest during winter; whilst rates on SM16c rank the lowest during summer. Like deposition rates, modelling vegetation assemblages influence on accretion rate estimates is statistically significant but weak ( $r^{2\text{adj}} = 6.8\%^{***}$ ). However, factoring monthly changes and vegetation assemblages shows that 26.04 % of accretion rate estimates variation is explained where September and all winter months (March, October, November, December and January), SM8 and SM16c are significant predictors (Table C-30 - model 1). Like deposition rates, only accretion rate estimates measured on ANK are significantly influence by both monthly variation and vegetation assemblages where pioneer and low-marsh plants (SM8 and SM13b) and SM16c (high-marsh) along with all winter months and September contribute the most to the model (Table C-30 - model 2).

#### 4.5.3.3 Summary

This section addressed relationships between vegetation assemblages, seasonality and the measured short-term (annual) deposition rates and accretion rates, specifically it aimed to answer questions such as: can some vegetation characteristics and/or assemblages favour sediment deposition rates and accretion rates? Are these patterns comparable or different during summer and winter? Do these relationships exist every month? Do all studied salt marshes and saltmarsh zones behave in the same manner?

The results of this section show that vegetation cover can be a significant predictor of filter disc sediment deposition rates, but relationships with vegetation characteristics such as height, density or aboveground biomass and organic carbon content are not confirmed. On the other hand, this section identifies that deposition rates (mean ranks) and accretion rate estimates (mean ranks) where pioneer-marsh (SM8) assemblage prevails are significantly higher compared to high-marsh vegetation assemblages (and SM16d).

The analysis shows that overall only winter deposition rates, which occur within SM8 plant assemblages, are significantly higher than summer deposition rates. During the winter, sediment deposition rates do not show significant differences between vegetation assemblages, except for pioneer plants (SM8), which have accumulated more sediment than middle marsh assemblages (SM13d). During summer, the analysis shows that sediment deposition rates follow a different pattern, with rates significantly lower on high-marsh plants (SM16c) compared to all assemblages. In contrast to deposition rates, accretion rate estimates show similar spatial patterns between winter and summer vegetation assemblages, with mid-marsh plants (SM13b)

experiencing the highest accretion in both seasons. In winter, mid-marsh areas dominated by SM13d plants also experience the lowest rates, whereas in summer, high-marsh SM16c plants experience the lowest accretion.

The section further demonstrates that vegetation assemblages do not only characterise the spatial variation in overall sediment deposition rates but that seasonality is an important factor in the variation of sediment deposition rates. The results show a significant relationship between monthly sediment deposition rates (which occurred from May to July and September to December) and vegetation assemblages (with a substantial contribution from pioneer (SM8), middle (SM13b) and high-marsh (SM16c) plants). Interpreting these relationships further, the results in this section identify that only on ANK do vegetation assemblages (SM8, SM13b and SM16a) have a strong influence on average sediment deposition rates (appr.27 %) or monthly sediment rates (appr.48 %). These results also infer that vegetation assemblages do not characterise sediment deposition rates on the two young salt marshes, FM and MR. This pattern is also confirmed by the observation of relationships between monthly deposition rates and sites' saltmarsh zones where these associations could only be verified on ANK.

#### **4.6 Aboveground short-term (annual) biological and geomorphological processes: Significance of the Results**

In Chapter 1 and 3, the key research aims of this research were outlined: to increase knowledge of the processes, mechanisms and patterns that promote the formation and development of salt marshes, that enable salt marshes to recover from environmental and anthropogenic disturbances, and that promote some of the regulating and supporting services provided by salt marshes. This chapter examined the spatial and temporal variability of aboveground physical and biological processes that occurred on short (annual) timescale in Nigg Bay, as summarised in Table 4-1. This section first evaluates the sediment sampling strategy before summarising and interpreting the significant results discovered during the research.

##### **4.6.1 Performance of the sampling techniques**

We have seen in section 4.4.2.3 that water depths during the sediment collection campaign can differ from 2 to 66 % from the monthly average (Table 4-22) and this can impact on the amount of sediment used to calculate sediment deposition rate and accretion rates. Although the decision to sample at spring tides was made because spring-neap tides are best suited to characterise saltmarsh inundation and there is no significant difference between sediment deposition at spring and neap tides (4.2.1 and 4.4.2.3), assessing the suspended sediment concentration (water

column) in Nigg Bay, which varies greatly on a daily basis, may also be a way of evaluating the performance of the traps and the results obtained. Importantly, AstroTurf mats were not deployed at all filter disc sampling locations (i.e., when the ground was bare, no mats were used), which makes it difficult to interpret the similarities and differences between the trap types. In this section, we are assessing the performance of filter discs and AstroTurf mats using the results obtained during this research.

Overall sediment deposition rates differ significantly between filter discs (n=342) and AstroTurf mats (n= 196) ( $F_{(1, 748)} = 5.34^*$ ) and on average AstroTurf mats retained c.17 % less ( $4.3 \pm 0.6 \text{ g.m}^{-2}\text{day}^{-1}$ ) than filter discs (Figure 4-61). However, only 40.7% of the deposition rates variation can be explained by the different traps ( $r^2 = 0.407$ ,  $F_{(1, 164)} = 112.5^{***}$ ). Although, only MR's deposition rates display significant differences between trap types (Figure 4-62a), regression models shows that there are positive relationships on all saltmarsh deposition rates between trap types where AstroTurf mats consistently retain less sediment than filter discs with approximately half of the sediment deposition rates variance explained by the differences between traps (Figure 4-62b).

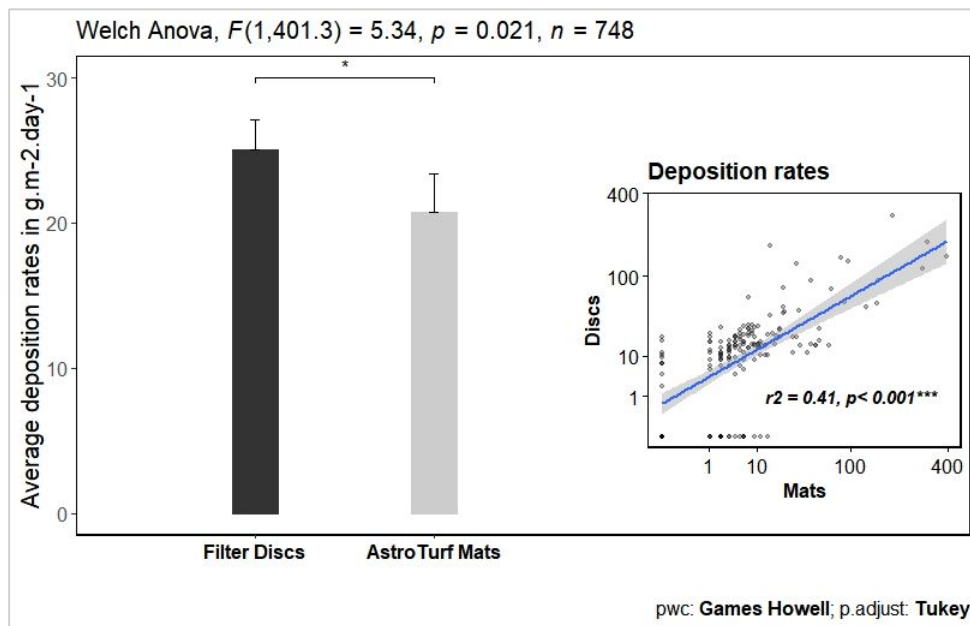


Figure 4-61: Bar graph and scatter plot (inset on right) of deposition rates ( $\text{g.m}^{-2}\text{.day}^{-1}$ ) between filter discs and AstroTurf mats showing Welch's Anova F test and regression's results ( $r^2$ , F-statistics and p-value in bold - the regressions have been box-cox transformed -dependent variable- to meet linear assumption). The bar graph represent mean and error bars are the standard error

This trend, showing consistently higher sediment deposition rates on Filter discs compared to AstroTurf mats, was partially confirmed when examining the saltmarsh zones per sites. As depicted in Figure 4-63, all saltmarsh zones deposition rates except HM zones are very well associated on ANK and MR, and, inversely on FM's HM zone is strongly correlated (Figure 4-63). This suggests, on natural and managed re-alignment, the sediment deposited at higher elevation, when flood depth, flood frequency and hydroperiod (Figure 4-26, Figure 4-29, Figure



4-34) is the lowest, is inconsistent depending on which trap type is used. There is not enough evidence to explain why this differs on FM, however this may be explained by the number of samples to be compared, and, or a large disparity for those measured up with other factors explaining the differences.

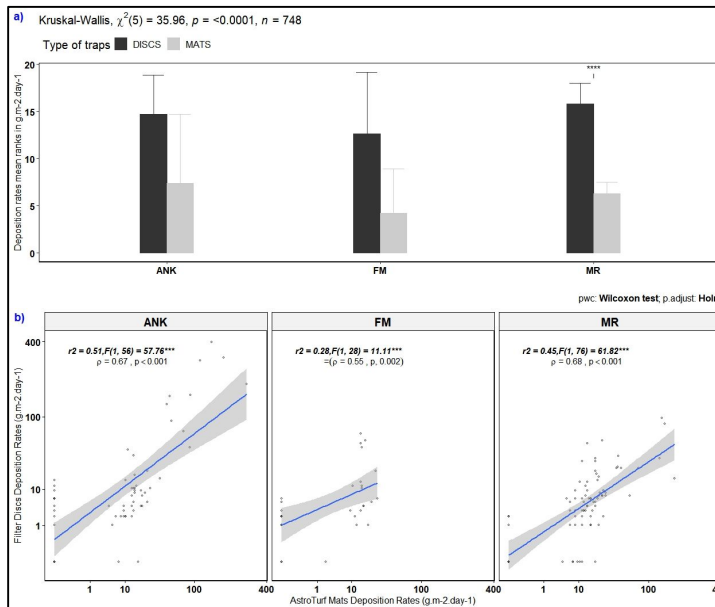


Figure 4-62: Bar graph (a) and scatter plots (b) of deposition rates ( $g \cdot m^{-2} \cdot day^{-1}$ ) between sites' filter discs and AstroTurf mats. (a) The bar graph labels Kruskal-Wallis results and the statistical significance of post-hoc pairwise comparison tests Wilcoxon test using Bonferroni-Holm adjustments symbolised on the top rows by the p-value significance with p-value significance (ns, \*, \*\*, \*\*\*); The bar graph represent median and error bars are the standard error. (b) Regression result ( $r^2$ , F-statistics and p-value in bold - the regressions have been box-cox transformed -dependent variable- to meet linear assumption) and correlation ( $\rho$  and p-value) summaries and significance are provided above each plot.

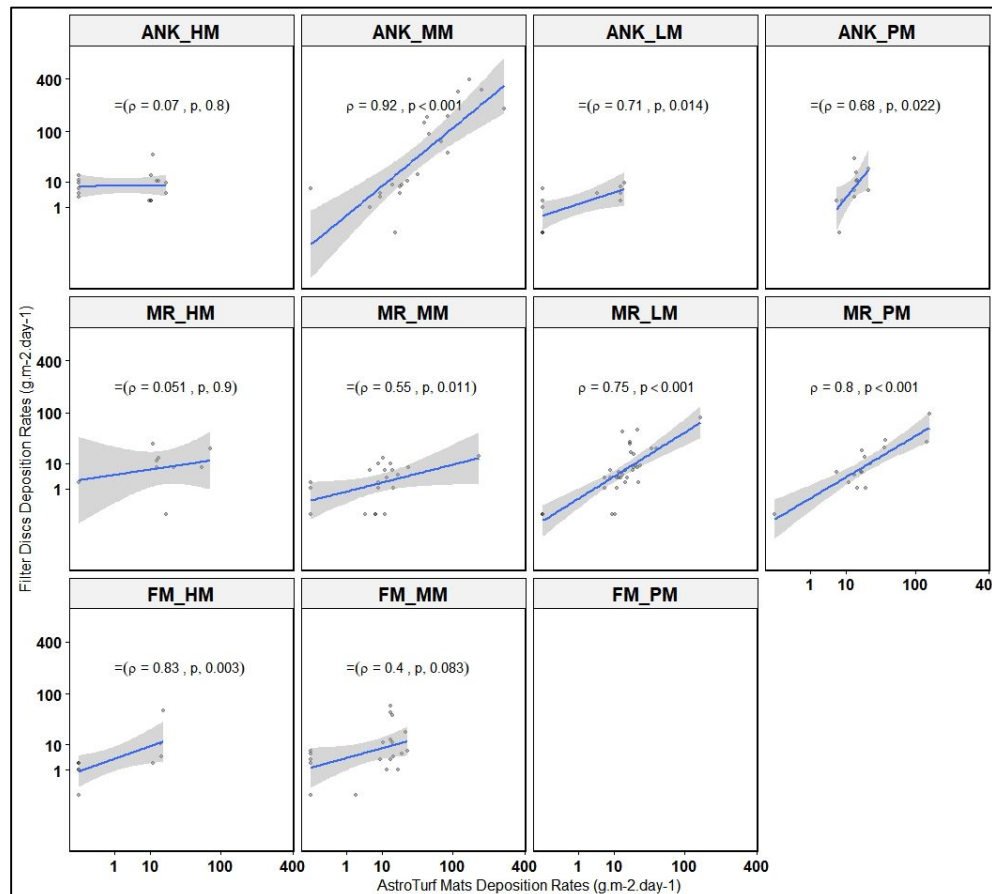


Figure 4-63: Scatter plots of deposition rates ( $g \cdot m^{-2} \cdot day^{-1}$ ) between sites' filter discs and AstroTurf mats. The plots provide the correlation strength and significance ( $\rho$  and p-value) respective to each saltmarsh zones.

Across the three salt marshes and 19 sample locations (that can be used for comparison), only seven (36.8 %) samples have demonstrated a positive correlation between the trap types during the year collection (Figure 4-64). They are all found to close proximity to water source (Figure 4-65) where the highest hydroperiod and flood depth are experienced (see Figure 4-33) such as along largest creeks (samples A10 and A6), at the creek’s mouthpiece (samples FM2 and A13), directly north of the western and eastern breach (samples MR46 and MR 23 respectively) or on the edge (samples MR26) of the former drainage ditch (now filled).

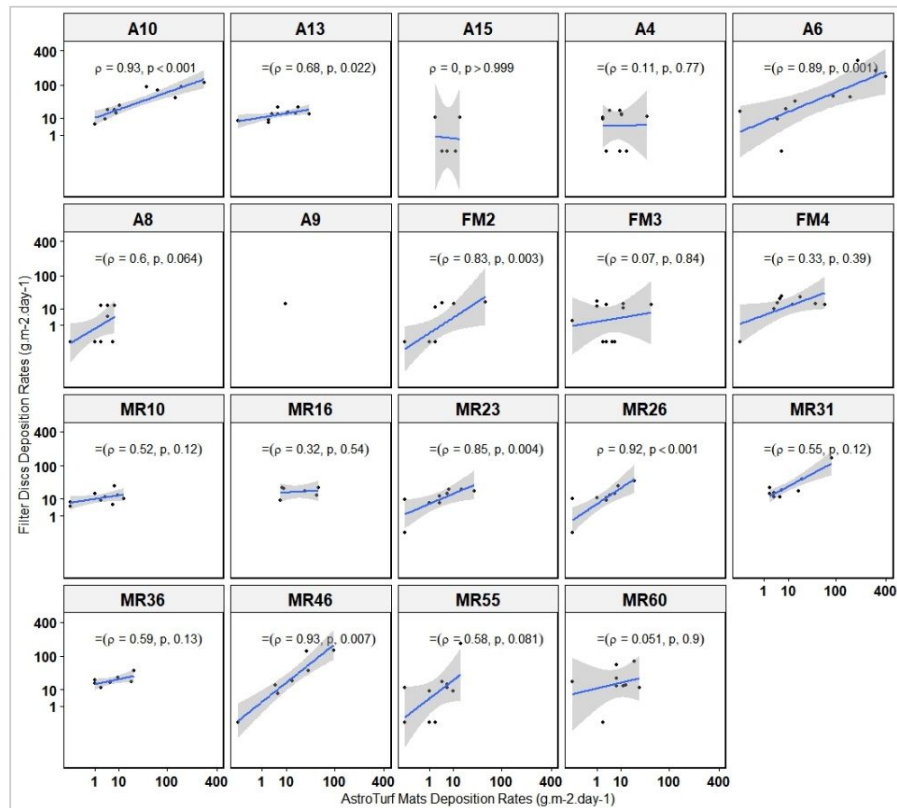


Figure 4-64: Scatter plots of deposition rates (g.m<sup>-2</sup>.day<sup>-1</sup>) between sites’ filter discs and AstroTurf mats. The plots provide the correlation strength and significance (rho and p-value) respective to each sampling point.

Across the collection campaign, months of April, June, September, October, November and December 2016 have shown a significant correlation between the trap types with AstroTurf mats showing lower deposition rates (Figure 4-66). However, the remaining sediment deposition campaigns have displayed insignificant correlations between the trap types. It may be explained by the extremely low deposit on mats in March 2016, and on filter discs at the end of January 2017. As for May, July and August 2016, the disparities between traps may be explained by the inconsistent deposition across the three salt marshes during summer.

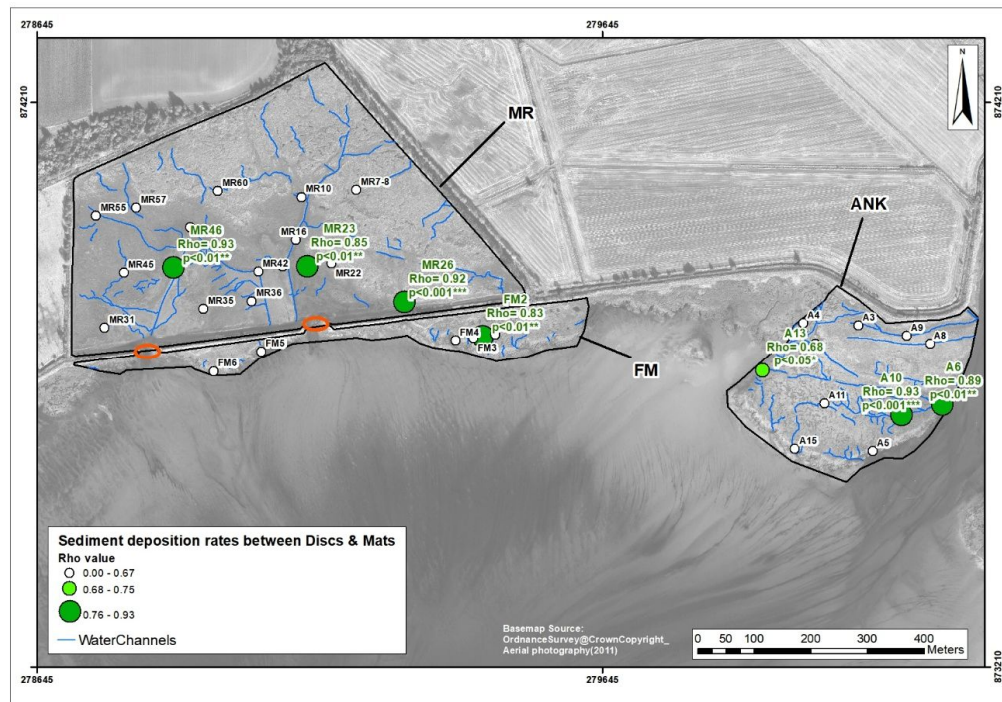


Figure 4-65: Sediment deposition samples with significant correlation between trap types. The graduated symbol size of the sample points represents the correlation strength and significance (rho and p-value) superimposed on the creek/water channel system, and the orange circles highlight the location of the breaches.

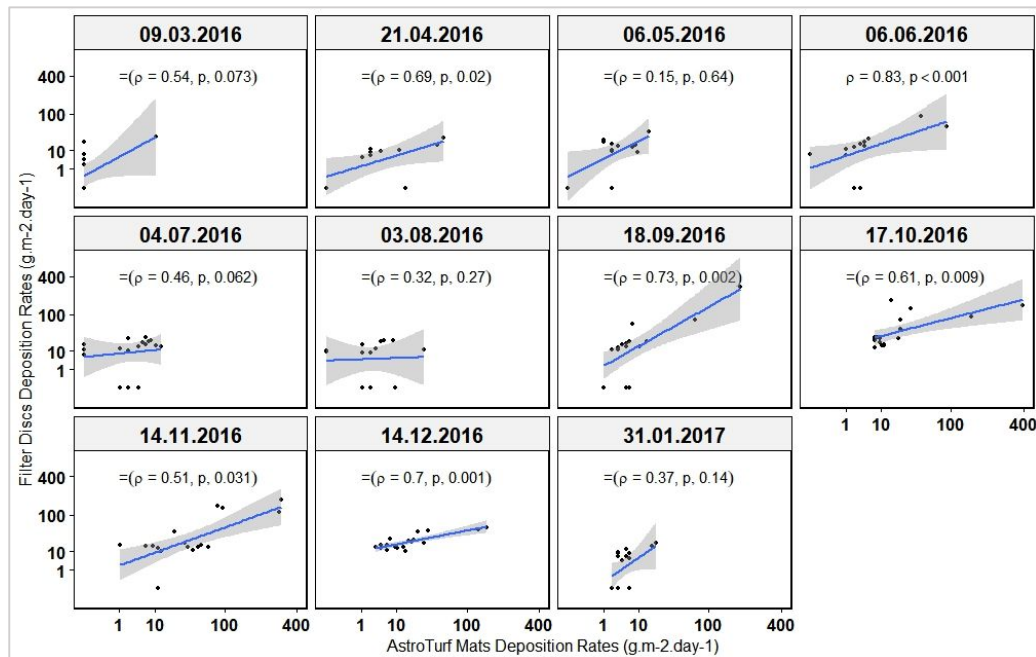


Figure 4-66: Scatter plots of deposition rates ( $\text{g.m}^{-2}\text{.day}^{-1}$ ) between sites' filter discs and AstroTurf mats. The plots provide the correlation strength and significance (rho and p-value) respective to each sampling campaign.

In line with Nolte et al. (2019), trapping efficiency was found to differ significantly between sediment trap types. The review of traps placed on the salt marshes of Nigg Bay suggests that AstroTurf mat traps are less efficient as filter discs when there is minimal tidal input and when the distance to the saltmarsh edge or water channels (i.e. sediment source) increases, such as in the higher part of the marsh. As it is generally accepted that deposition decreases with elevation

and distance from the saltmarsh edge, it is difficult to interpret the comparison between traps across the entire tidal range. In addition, the results of the filter discs suggest that there are more complex interactions occurring in the marsh that are not captured by the AstroTurf mats and that the design of the AstroTurf mats is not effective across the entire saltmarsh elevation gradient. Depending on the type of sediment trap, Nolte et al. (2019) suggest that higher sediment deposition rates on circular sediment traps (e.g., circular trap plain or with lid) and flat-surface sediment traps (e.g., floor mat or ceramic tile) may indicate resuspension, lateral sediment transport, or both processes, and may occur at different scales. This observation consistent with and supports the opinion that AstroTurf mats are not designed to detect specific sediment dynamics. The authors also observe that the rim of the circular sediment trap can prevent lateral dispersion to the surrounding surface and resuspension of trapped sediment. This may have occurred in the Nigg Bay study, but it wasn't intentional, unlike in the Nolte et al. study, the filter discs in this study were fixed with a rim, but do not have a lid (see section 3.4.1.1).

During the research, filter discs were preferred over AstroTurf mats for practical reasons: i) sediment retained on mats was difficult to remove for analysis when washing sediment grains with distilled water, and therefore underestimated the amount of sediment that had been deposited; and, ii) mats cannot be reused (and are difficult to recycle). In agreement with Schindler, Karius, Deicke, et al. (2014) who also combined different types of sediment traps (LDPE bottles and AstroTurf mats), it was found that the two methods allowed for internal inconsistencies, detection of outliers and estimation of the effect of extreme events (post-storm remobilisation) on sediment deposition rates. This was found to be the case for some sample locations, such as A6 and A10 along ANK's main creek, which deposited significantly more sediment than other location, even during the 'drier' summer months (excluding June).

#### **4.6.2 Aboveground short-term (annual) biological and geomorphological processes: results and interpretations**

The results of this chapter have fulfilled one of the aims of this research, which is to inform and better understand some of the patterns, processes and mechanisms that drive saltmarsh formation and development, by answering specific questions (Table 4-1), about the short-term (annual) physical and biological processes that take place in the three salt marshes of Nigg Bay:

- 1) How much sediment has been deposited and accumulated in the salt marshes of Nigg Bay? Has it varied spatially? Has it changed over time?
- 2) What were the plant characteristics and biological processes existed in Nigg Bay? Was there a difference between the three salt marshes?

- 3) Is it possible to identify particular variables that may promote sediment and biological processes in Nigg Bay?
- 4) Finally, can this study provide information on the stability of natural and managed salt marshes and some of the protective services they provide?

#### 4.6.2.1 Spatial and temporal variability of the physical processes that form salt marshes - estimating sediment deposition and accretion rates and their influences.

This thesis research aimed to improve the understanding of the short-term (annual) patterns, processes, and mechanisms that drive the formation and development of salt marsh by estimating aboveground sediment deposition rates and accretion rates on the paired natural salt marsh and managed realignment site in Scotland over the course of one year of tidal cycle measurements.

**How did short-term (annual) sediment deposition and accretion rate estimates compare between natural and managed salt marshes?** The results presented showed that for both trap types, the overall sediment deposition rates ( $23.4 \pm 2.3 \text{ g.m}^{-2}\text{day}^{-1}$  for filter discs and  $20.7 \pm 3.6 \text{ g.m}^{-2}\text{day}^{-1}$  for AstroTurf mats) over a full year's sedimentary cycle were not significantly different between the managed and natural salt marshes. This first suggests that sediment availability is uniform across the three salt marshes, despite anthropogenic disturbances such as the breaching of seawall defences and despite the significant differences in inundation depth and hydroperiod between the sites (see 4.4.1). This finding contradicts the general trend that restored coastal wetlands trap more sediment than natural coastal wetlands, but unlike most restored salt marshes, MR is not located lower in the tidal range, a position that benefits from higher tidal sediment inputs (Liu et al., 2021). This is not the case for MR.

Sediment deposition has been successfully converted to provide vertical accretion rate estimates using the bulk dry density of cores collected from the three salt marshes (details in section 3.4.1.1), providing a means for qualifying patterns and rates of accretion across the sites. The results have shown that the trend in sediment deposition holds true for accretion rate estimates derived from AstroTurf mats (averaging at  $1.1 \pm 0.21 \text{ cm yr}^{-1}$ ), however, filter disc accretion rate estimates (averaging at  $1.34 \pm 0.14 \text{ cm.yr}^{-1}$ ) show significant differences between sites. FM has the lowest accretion rate estimates ( $1.07 \pm 0.33 \text{ cm.yr}^{-1}$  filter discs) compared to ANK ( $1.47 \pm 0.26 \text{ cm.yr}^{-1}$  filter discs) and MR ( $1.36 \pm 0.16 \text{ cm.yr}^{-1}$  filter discs). These results disagree with the prevalent notion that a decrease in elevation increases the tidal prism and, consequently, the volume of water and sediments transported to wetlands (Liu et al., 2021) as FM has the lowest position in the tidal frame compared to ANK and MR. Although we have seen that flood depth, frequency and hydroperiod were indeed highest on FM (4.4.1), and the results suggest that this



may also result in greater exposure to higher tidal energy, thus preventing sediment to settle and sediment deposition. This further suggests that the sediment fluxes in the three salt marshes at consistent are driven by geomorphological processes, which are known to alter the tidal prism, tidal asymmetry and residual tidal flow which determine the amount of sediment that can accumulate, consistent with studies by van der Wal and Pye (2004) and Li et al. (2019). The results from the salt marshes of Nigg Bay are similar to the study by Davidson-Arnott et al. (2002), which, although conducted in a macro-tidal marsh, found that in Allen Creek Marsh (Bay of Fundy), the greatest amounts of deposition did not occur in the low-marshes (and low-marsh region), and that deposition may be primarily controlled by wave activity which must be low for deposition to occur even in the presence of a high concentrations of suspended sediment in the water column. A second explanation may contribute to FM having the lowest accretion overall and may lie in the type and texture of the sediments, where coarser grains are generally found at the pioneer part of the marsh, based on physics alone and due to the wave energy and flow velocity required to transport heavier grains (Rahman and Plater, 2014). Larger and coarser grains increase autocompaction/BDD rates, as on FM, and consequently reduce net accretion (as BDD is used to calculate AR) and can lead to erosion and scouring, which can be avoided in densely vegetated areas but exacerbated in the pioneer zone (Allen, 2000; Yang et al., 2008; Schwarz et al., 2015).

**How do short-term (annual) sediment deposition and accretion rate estimates compare between the saltmarsh zones of the sites (high-marsh HM, mid-marsh MM, low-marsh LM, pioneer-marsh PM)?** The one-year sediment campaign has revealed that the deposition rates vary significantly between sites' saltmarsh zones (Filter discs: Table 4-2; AstroTurf mats: Table 4-5). The study demonstrated that the highest level of deposition rates was found on the PM of FM and MR, supporting the relationship between tidal height and sediment deposition. This is consistent with the findings of Marion et al. (2009), Temmerman et al. (2003) and Pethick (1993), who found that mineralogical deposition rates are highest in low elevation salt marshes that are inundated for long periods of time and lowest in high elevation salt marshes that are inundated only intermittently. Section 4.5.1.1 also highlighted that at Nigg, very high flood depths especially near the saltmarsh edge such as on FM, were associated with high deposition and accretion rates. Therefore, higher sediment deposition near the saltmarsh edge of FM can certainly be explained by proximity to higher and more frequent tidal inputs, but the sediment may also be coming from the eroding saltmarsh cliff edge (lateral movement of the saltmarsh edge is further explored in Chapter 5 - 5.3.1).

However, the clear-cut vision of higher deposition in the lower part of the salt marsh does not hold true in the natural marsh ANK and the realigned marsh MR, where the highest level of



deposition is found on the MM of ANK, whilst the MM of MR as lower deposition rates than both HM and LM. As seen in 4.2.1.1 and Figure 4-3, the location of sampling points near large creeks on ANK may justify these high deposition rates on the MM. In their study of sediment dynamics in the Hut marsh (Norfolk coast), French and Spencer (1993) have observed that traps deployed during single tidal cycles showed remarkably high sedimentation close to the creek system. They attribute this to resuspension (under peak flood velocities) of poorly consolidated muddy sediments deposited within the creeks during preceding neap tides. Reed et al.(1999) have also shown a significant trend of decreasing sediment deposition away from the creek and an increased sediment supply to the marsh surface associated with an increased creek velocities at higher tides, providing more potential for resuspension within the creek. Tsujimoto and Shimizu (1994) show that floodplain vegetation is highly effective at reducing the flow velocity on the floodplain relative to that in the main channel, and their observations indicate strong circulation perpendicular to the main flow direction in the channel. Davidson-Arnott et al. (2002) further suggest that the presence of pronounced levees along the creek banks will prevent water (and sediment) from flowing across the marsh favouring sediment deposition near tidal creeks. The authors point out that in the absence of such levees, material that settles during the tidal event may remain in the viscous sublayer of the plant canopy, thus preventing resuspension. In their study of short-term sedimentation dynamics in a meso-tidal marsh, Carrasco et al. (2023) have also found higher values of deposition rates (deposition and resuspension rates) in the mid-upper marsh, where the hydroperiod is lower, as observed in the three salt marshes of Nigg , and attribute this trend to the presence of higher stem density (height and branching level), which increases the trapping of sediment particles and enhances mineral deposition, as described in studies by Leonard and Luther (1995); Temmerman, Govers, Meire, et al. (2003) and Bouma et al. (2014). Carrasco et al (2023) further highlight that although the canopy and physical structure of saltmarsh plants can attenuate the flow velocity, it can consequently reduce the supply of sediment downdrift. This scenario may indeed explain the low deposition rates found on the MM of MR (Figure 4-2), as it is located where the plant assemblages on HM are higher (c. 89%) compared to ANK and FM, possibly because they are still in transition from grazing plants to saltmarsh plants (Elliott, 2015). Plant communities on managed realignment sites have been found to differ from surrounding natural salt marsh and intertidal habitats in that they lack the full range of biodiversity even 100 years after inundation (Mossman et al., 2012). Results have further highlighted those areas of MR (Figure 4-3) that benefited from higher sediment deposition can be attributed to a sheltered position (such as for sampling points MR31, MR45 and MR46). As noted above, deposition is sensitive to tidal energy and sediment is retained in more sheltered areas of the salt marsh, consistent with the findings of Langlois et al. (2003) findings in the Mont-Saint-Michel salt marshes. Previous studies (van der Wal and Pye, 2004; Fagherazzi, 2013; Silinski et al., 2016) have reported similar findings, indicating the deposition

of substantial sediment or a decrease in the extent of expansion or erosion in the wave-sheltered region of a saltmarsh.

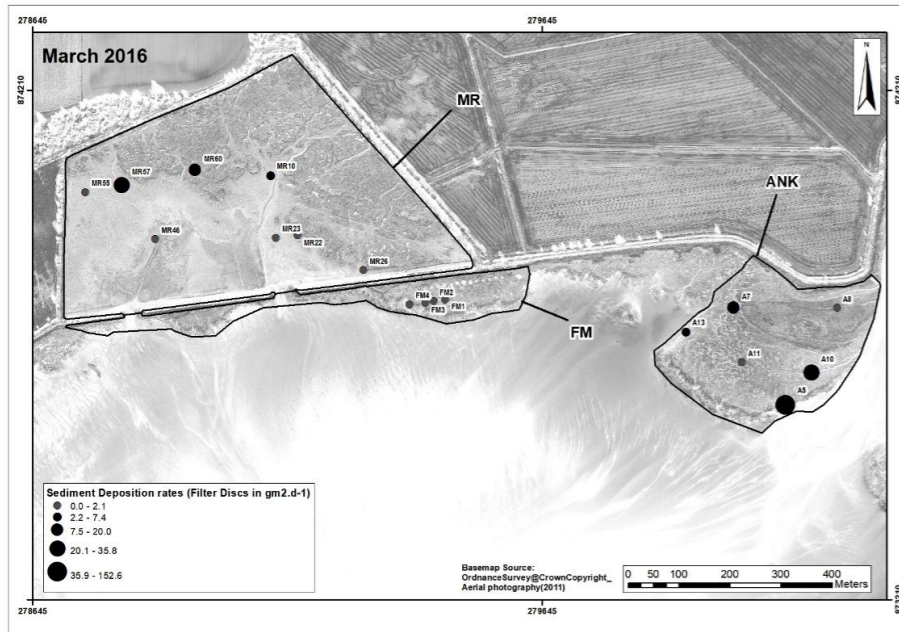
The spatial variation demonstrated by the filter discs deposition rates is reflected in accretion rate estimates on ANK and FM salt marshes (same variation between sites and saltmarsh zones than deposition rates), but not on MR salt marsh (Table 4-9), which exhibited no variation in accretion rate estimates between its saltmarsh zones. This may be explained by the accretion rate estimates calculation which requires to use the values of the upper layer's BDD. These values have been found on MR to lack of variability (Table 4-8 and Figure 4-12), which can be indicative of the effect of land reclamation (Friess et al. (2014) (further developed in Chapter 6), and, consequently impact on accretion rate estimates results. Lawrence et al. (2018) further found that topographic variation differs with age maturity and absent on restored and managed realignment salt marshes displaying more similarities to agricultural landscape they originate from. In agreement with these findings, MR's accretion is principally enhanced by water flow and water accumulation suggesting that increased topography may act as a driver (Lawrence et al., 2018) to increase sedimentation on young managed salt marshes, still, this also indicates that MR lack of such topographical features 15 years since breaching.

**Were seasonal variations in short-term (annual) sediment deposition rates observed? And did they differ between the saltmarsh sites and zones? (high-marsh HM, mid-marsh MM, low-marsh LM, pioneer-marsh PM)?** The short-term (annual) study also revealed a significant seasonal pattern with higher sediment deposition rates in the winter (October to March) than in summer (April to September), with an increase 86 % for filter discs and 58.4% for AstroTurf mats (Figure 4-6 & Figure 4-10). When filter discs were utilised, the pattern was statistically confirmed only at MR; when Astro-Turf mats were utilised, the pattern was statistically confirmed at MR and ANK, but not FM. Variations in particle size have been identified as the cause of seasonal variations in sediment deposition. Allen and Dark (2007) found that on the Severn Estuary coarsest sediments in the Severn estuary are found in the winter (January to October) and the finest sediments are found in the summer (August to September), suggesting that heavier grain in winter may increase deposition calculations. Davidson-Arnott et al. (2002) found that reduced vegetation cover due to winter dieback reduces deposition or increases remobilisation by currents and wave action on the saltmarsh surface.

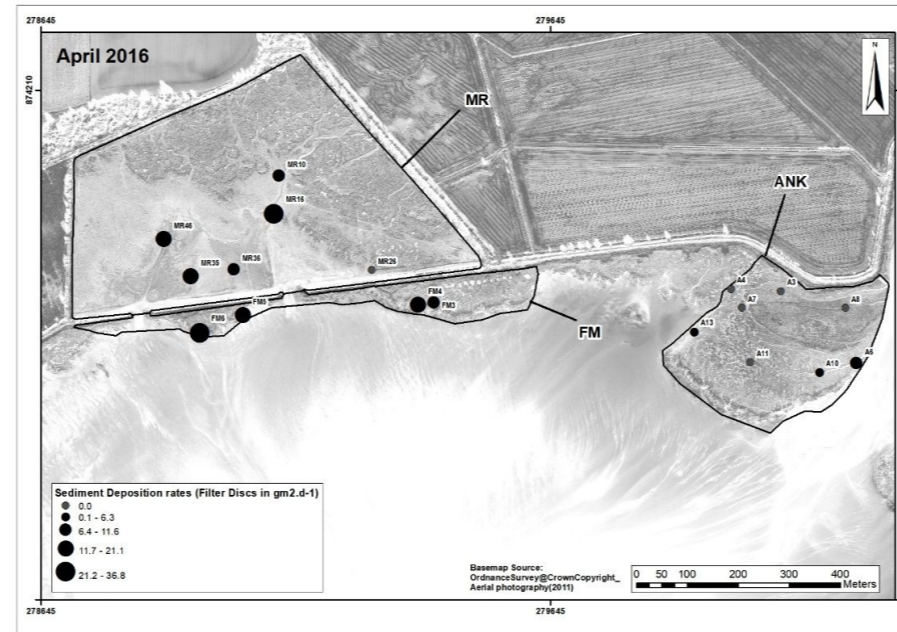
This research also demonstrated a significant seasonal variation (Figure 4-67 and Figure 4-68), with the highest overall deposition rates (measured with Filter discs and AstroTurf Mats) occurring in September, October, November, and December. Each site confirmed the trend that the maximum deposition rates occurred during the winter months, but the lowest deposition rates

varied depending on the type of trap and the site. However, filter disc deposition at ANK was distinct, with high deposition rates in June and October, coinciding with months of very high flood depth (Figure 4-35 and Figure 4-36) and high rainfall, particularly in June, July and August 2016 compared to other years (Figure 5-46 in Chapter 5).

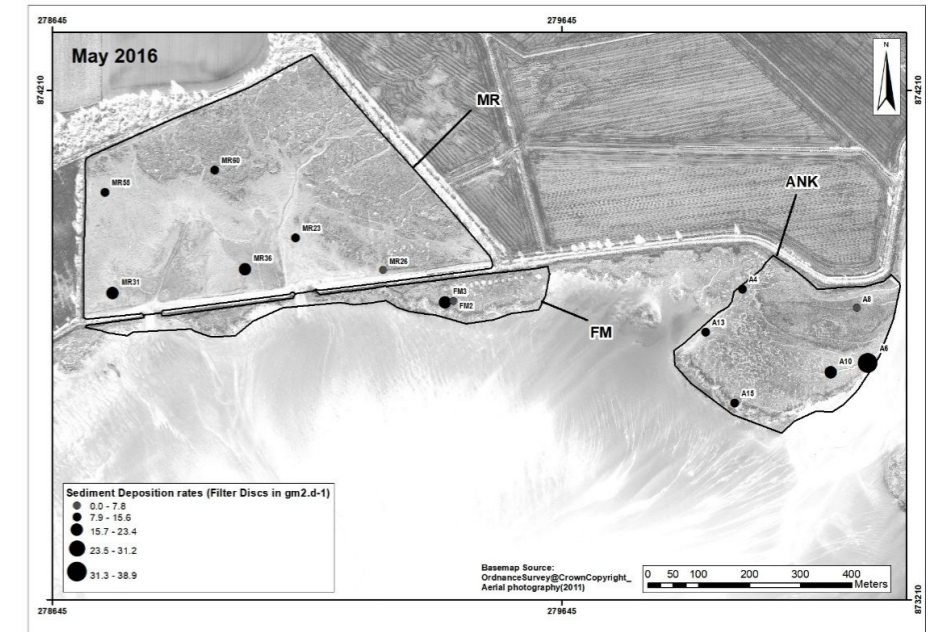
Several saltmarsh studies (Reed, 1989; Pethick, 2002; Temmerman, Govers, Meire, et al., 2003; Butzeck et al., 2014) have shown that variations in sediment concentration of tidal waters can be caused by higher rainfall and riverine or intense wind and wave activity. Figure 4-22 would support this explanation, where the highest water levels were found on the day of the sediment collection campaign in September, October, November and December 2016. Marion et al. (2009) observed in a short-term research (2 years) that sedimentation of mudflats and salt marshes in Portugal was extremely rapid during the months of March and April (2003 in their study using three types of measurements: ultrasonic altimeter, Rod Surface-Elevation Table, and filter traps). The authors explained that this may be the result of the combined effect of the increased sediment input from winter storms and equinoctial tides, resulting in elevated (recorded) water levels during a time when a longer hydroperiod favours sedimentation. Therefore, the authors warn that point sampling stations can affect the analysis of temporal and spatial sedimentation patterns in salt marshes, so interpretations should be made with caution. This may provide an explanation for Nigg results that established that collection dates, sites and saltmarsh zones can support between c.30% (filter discs) to c.48 % (AstroTurf mats) of the variation in sediment deposition rates.



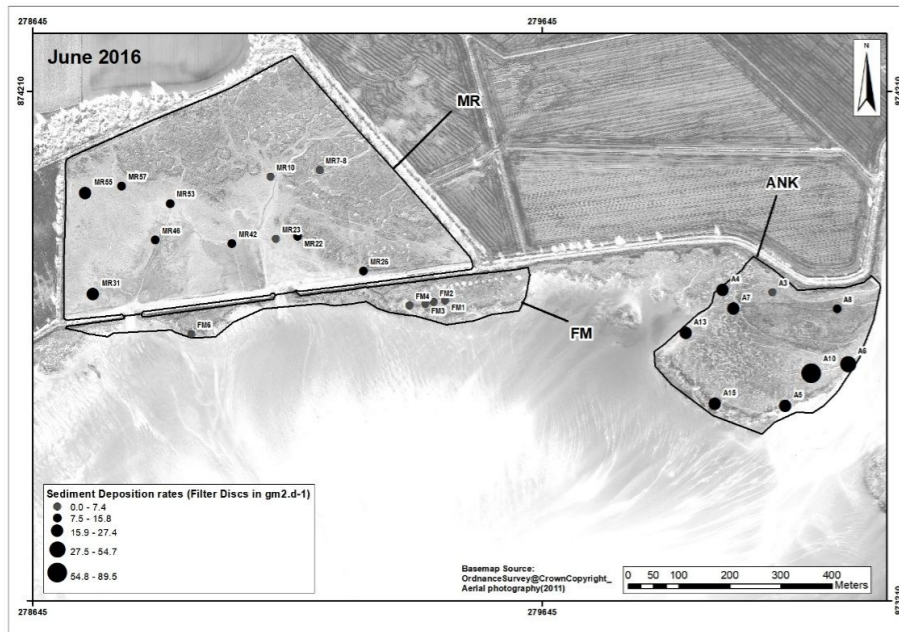
a) March 2016 filter disc sediment deposition rates (g.m<sup>2</sup>.day<sup>-1</sup>) for the three salt marshes studied in Nigg Bay



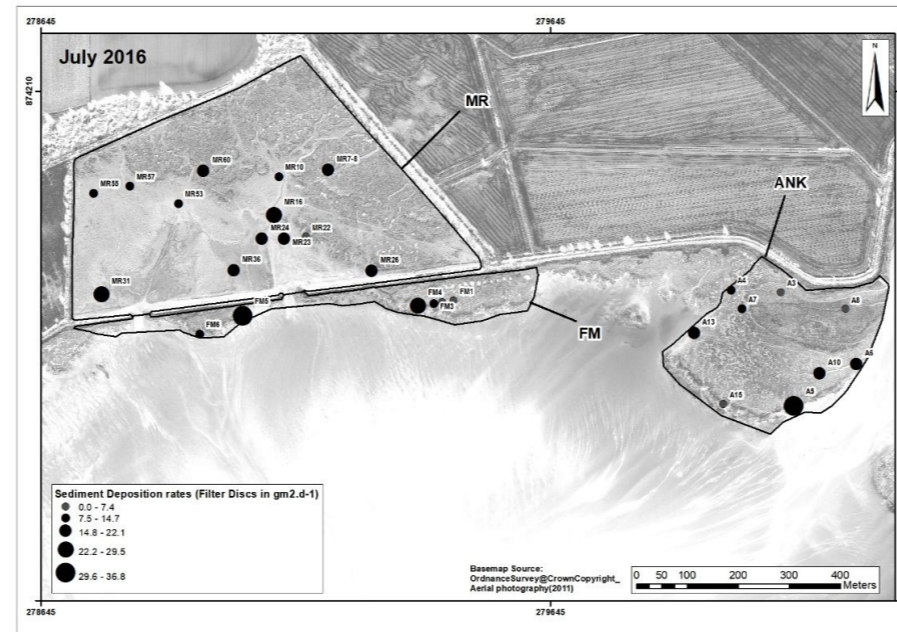
b) April 2016 filter disc sediment deposition rates (g.m<sup>2</sup>.day<sup>-1</sup>) for the three salt marshes studied in Nigg Bay



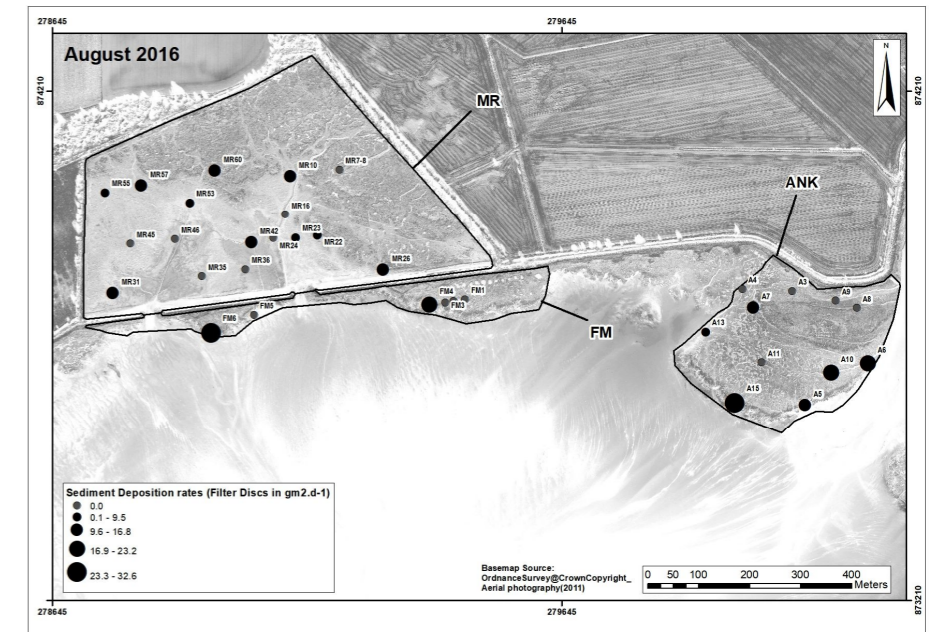
c) May 2016 filter disc sediment deposition rates (g.m<sup>2</sup>.day<sup>-1</sup>) for the three salt marshes studied in Nigg Bay



d) June 2016 filter disc sediment deposition rates (g.m<sup>2</sup>.day<sup>-1</sup>) for the three salt marshes studied in Nigg Bay

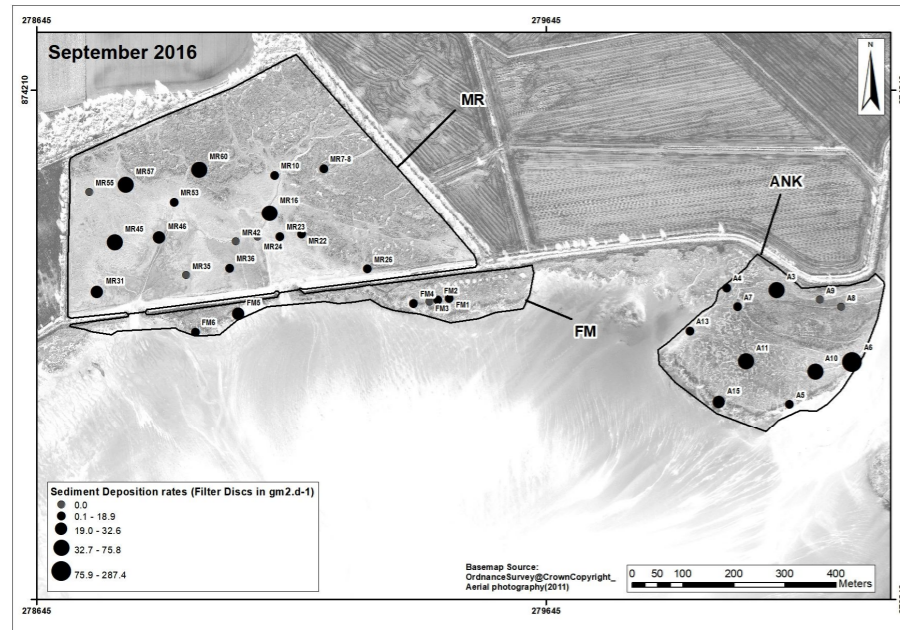


e) July 2016 filter disc sediment deposition rates (g.m<sup>2</sup>.day<sup>-1</sup>) for the three salt marshes studied in Nigg Bay

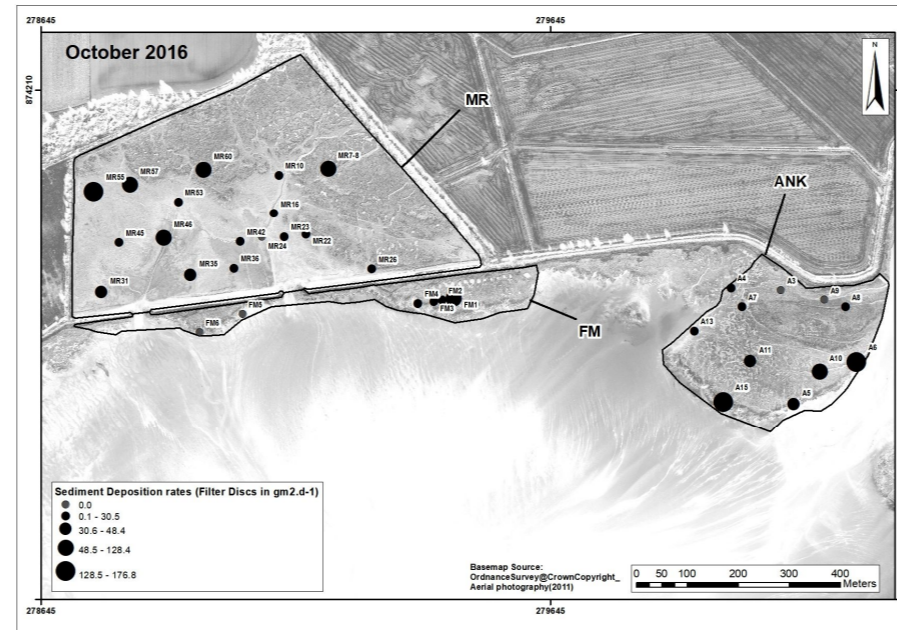


f) August 2016 filter disc sediment deposition rates (g.m<sup>2</sup>.day<sup>-1</sup>) for the three salt marshes studied in Nigg Bay

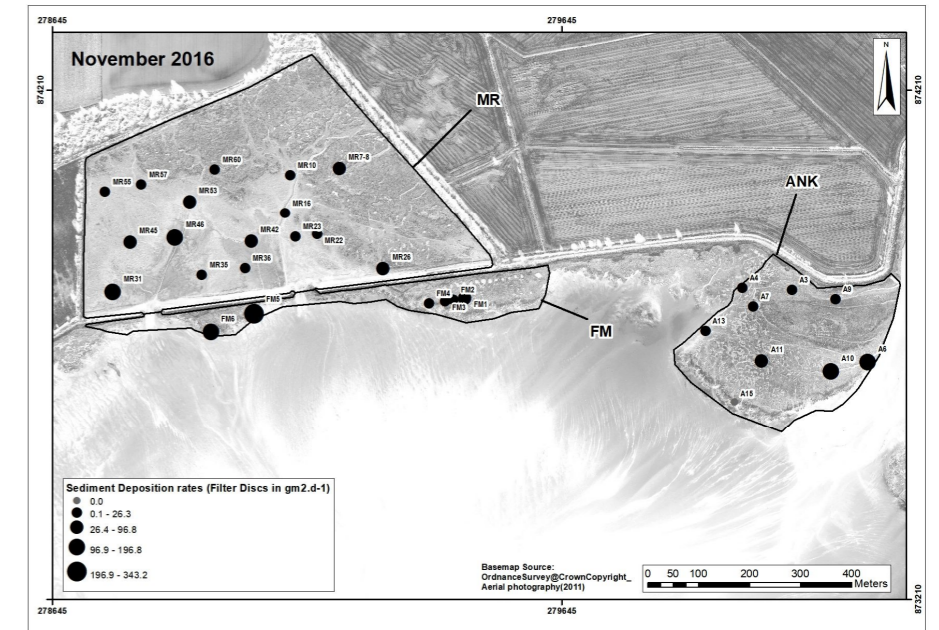




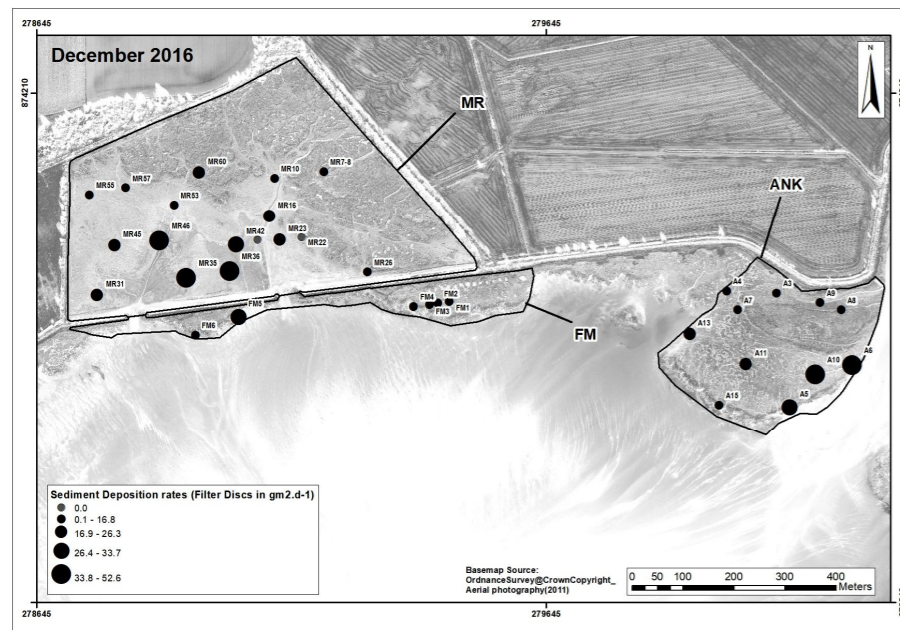
g) September 2016 filter disc sediment deposition rates (g.m<sup>2</sup>.day<sup>-1</sup>) for the three salt marshes studied in Nigg Bay



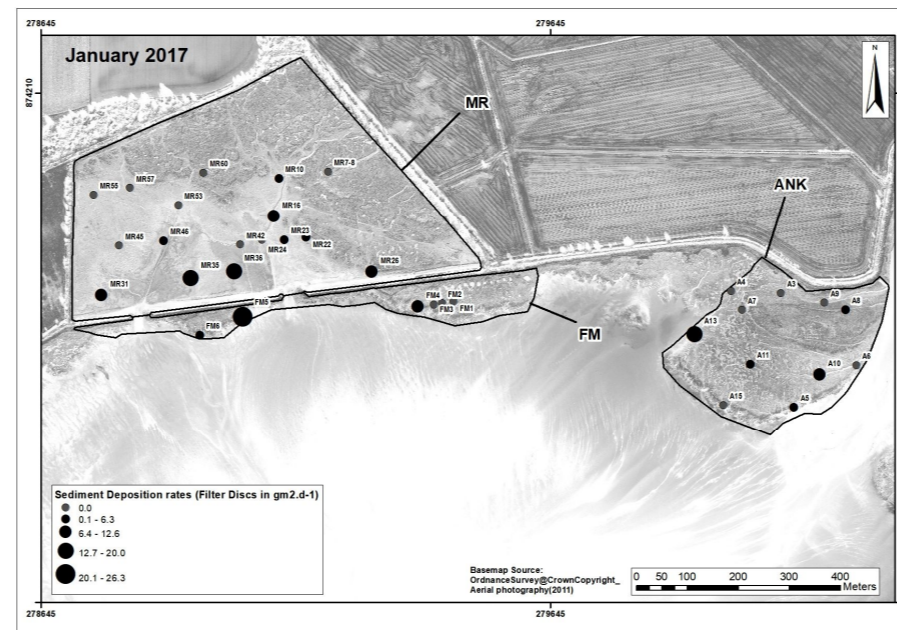
h) October 2016 filter disc sediment deposition rates (g.m<sup>2</sup>.day<sup>-1</sup>) for the three salt marshes studied in Nigg Bay



i) November 2016 filter disc sediment deposition rates (g.m<sup>2</sup>.day<sup>-1</sup>) for the three salt marshes studied in Nigg Bay

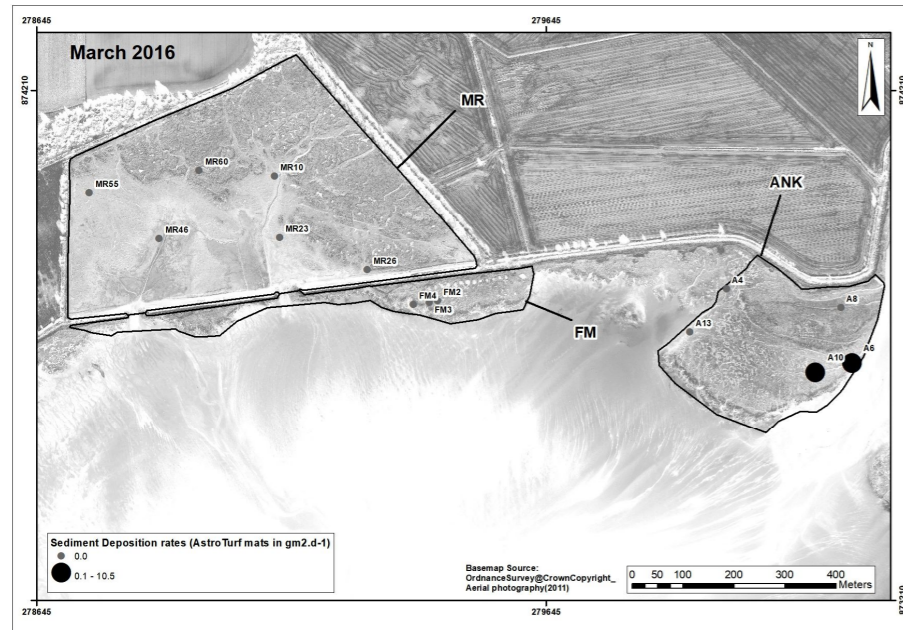


j) December 2016 filter disc sediment deposition rates (g.m<sup>2</sup>.day<sup>-1</sup>) for the three salt marshes studied in Nigg Bay

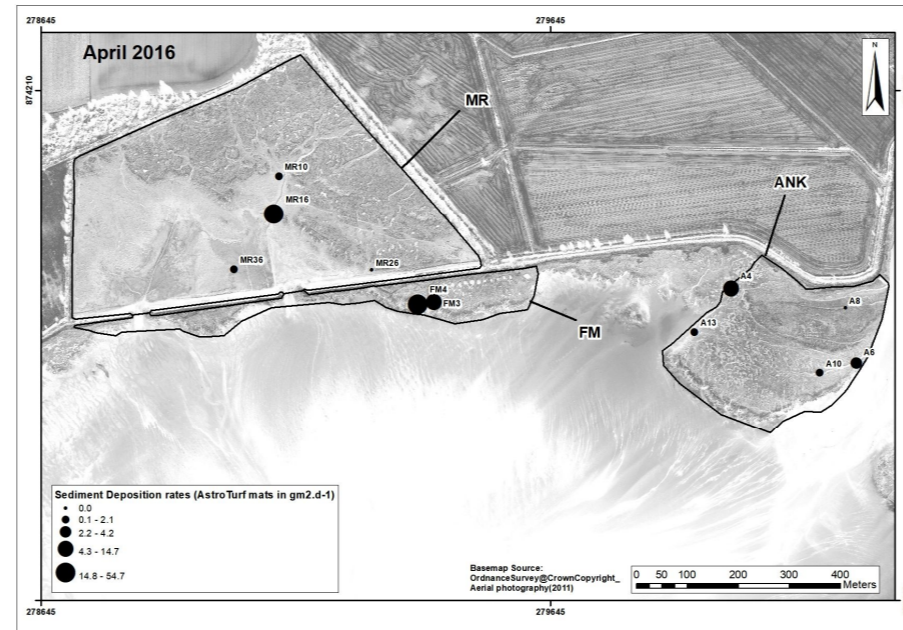


k) January 2017 filter disc sediment deposition rates (g.m<sup>2</sup>.day<sup>-1</sup>) for the three salt marshes studied in Nigg Bay

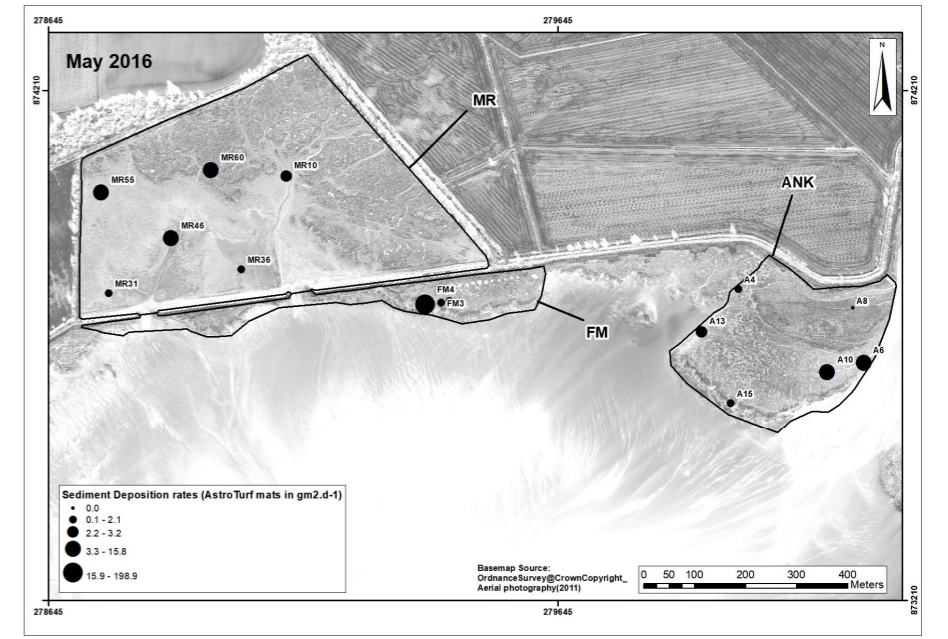
Figure 4-67 a) to k): Filter disc sediment deposition rates (g.m<sup>2</sup>.day<sup>-1</sup>) for the three studied salt marshes of Nigg Bay between 09<sup>th</sup> March 2016 to 31<sup>st</sup> January 2017.



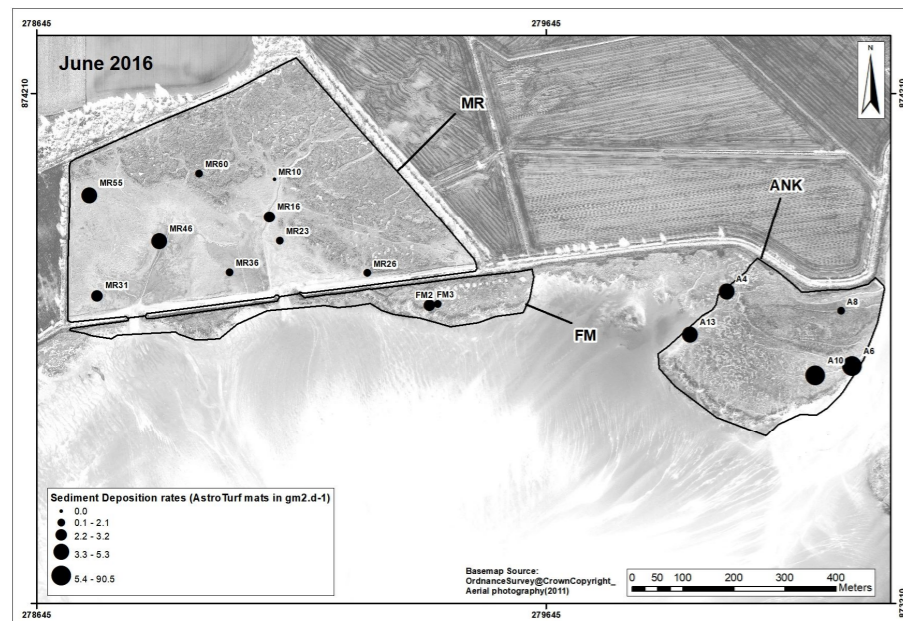
a) March 2016 AstroTurf mats sediment deposition rates (g.m2.day-1) for the three salt marshes studied in Nigg Bay



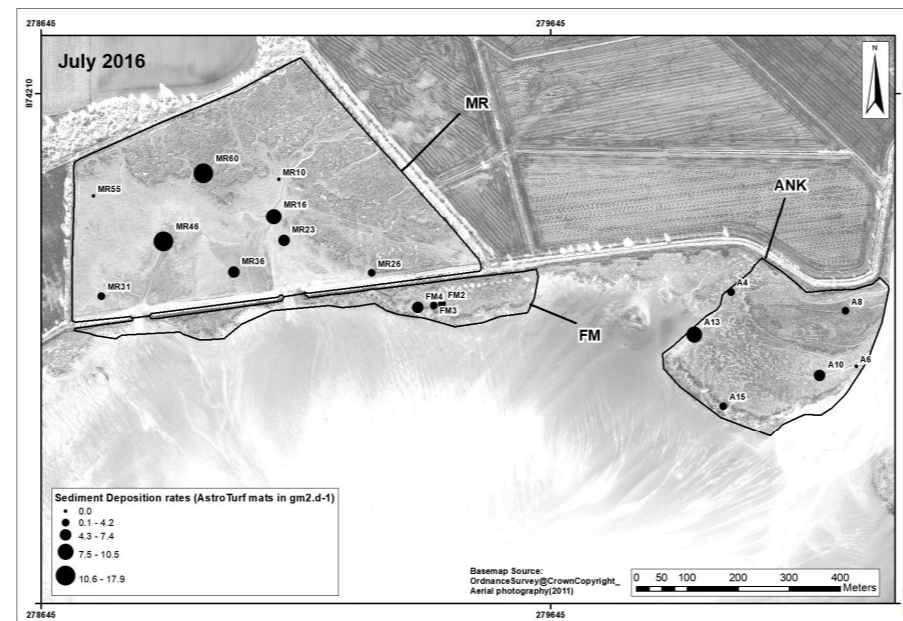
b) April 2016 AstroTurf mats sediment deposition rates (g.m2.day-1) for the three salt marshes studied in Nigg Bay



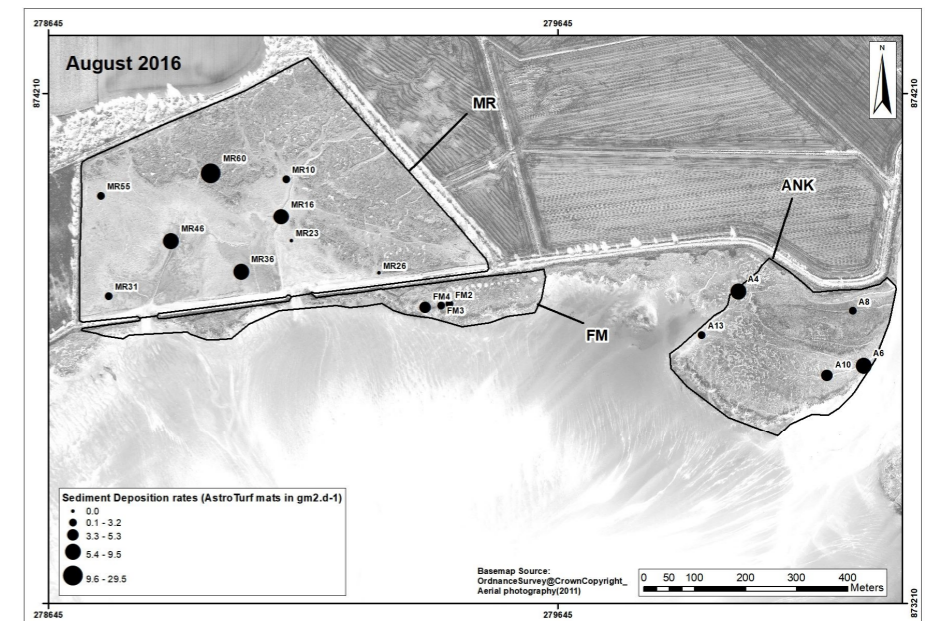
c) May 2016 AstroTurf mat sediment deposition rates (g.m2.day-1) for the three salt marshes studied in Nigg Bay



d) June 2016 AstroTurf mat sediment deposition rates (g.m2.day-1) for the three salt marshes studied in Nigg Bay

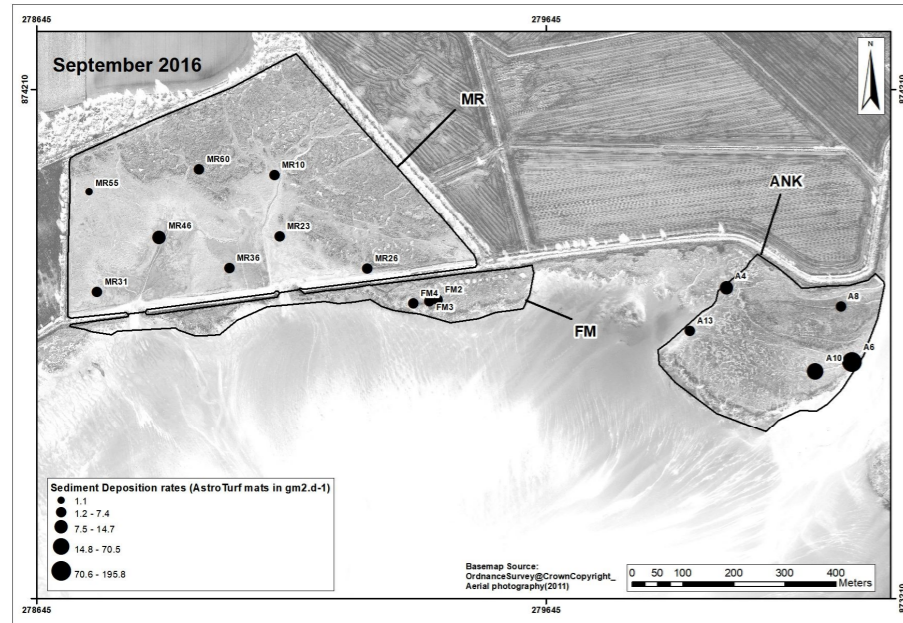


e) July 2016 AstroTurf mat sediment deposition rates (g.m2.day-1) for the three salt marshes studied in Nigg Bay

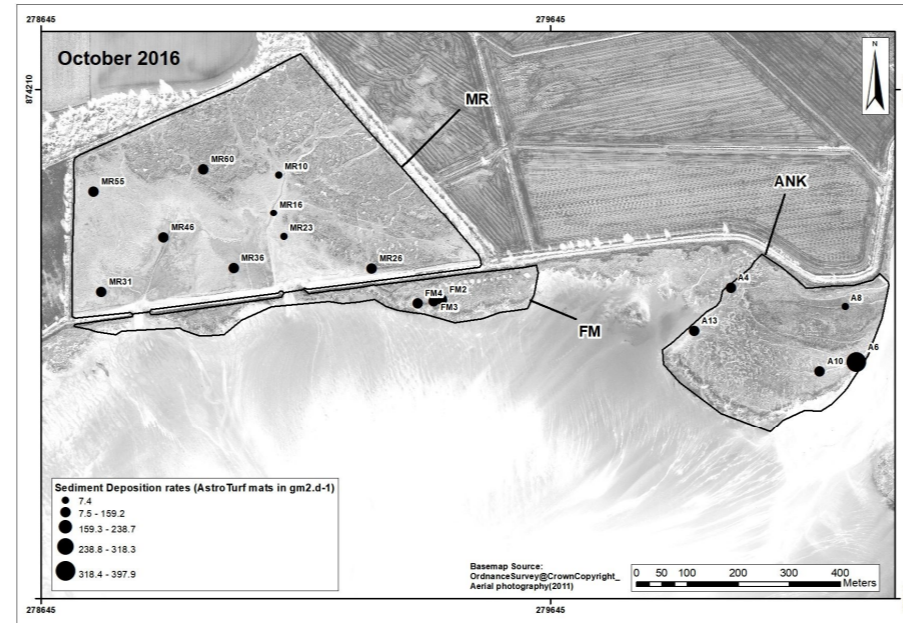


f) August 2016 AstroTurf mat sediment deposition rates (g.m2.day-1) for the three salt marshes studied in Nigg Bay

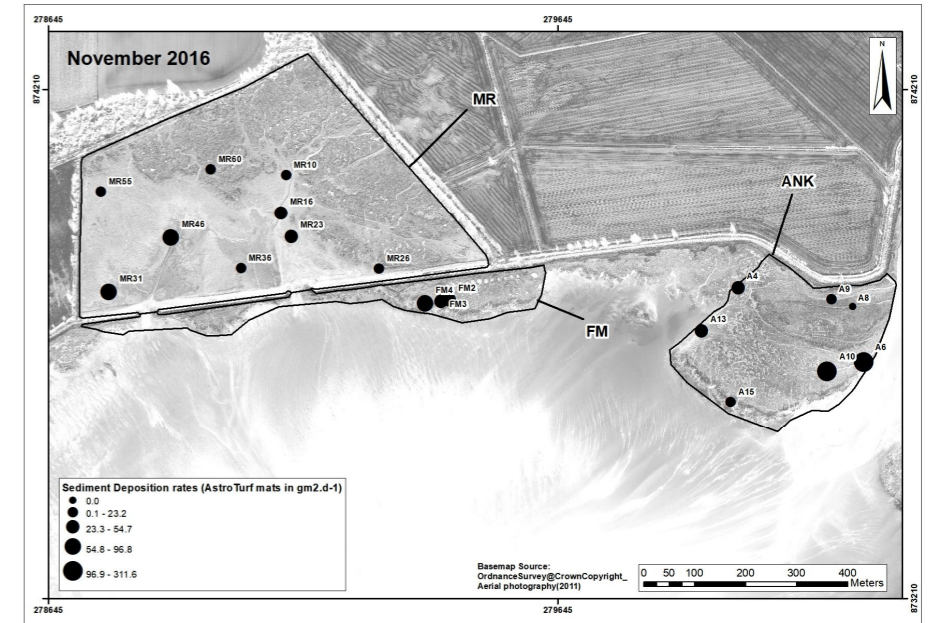




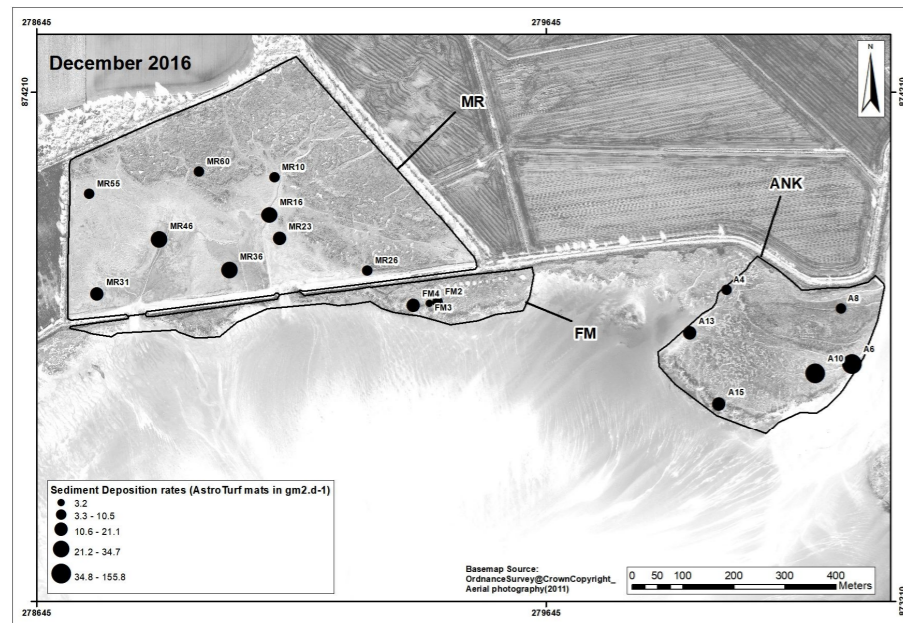
g) September 2016 AstroTurf mat sediment deposition rates (g.m2.day-1) for the three salt marshes studied in Nigg Bay



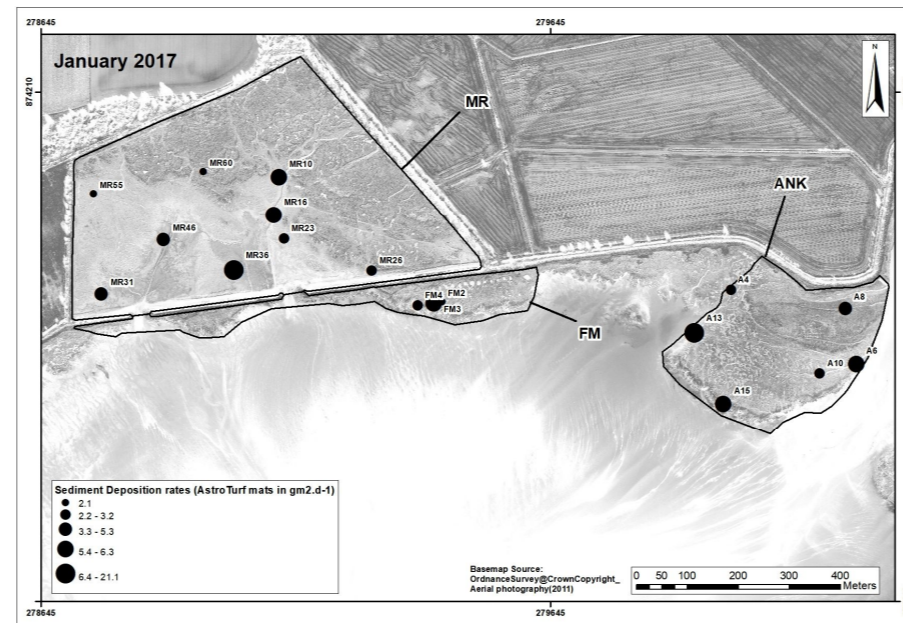
h) October 2016 AstroTurf mat sediment deposition rates (g.m2.day-1) for the three salt marshes studied in Nigg Bay



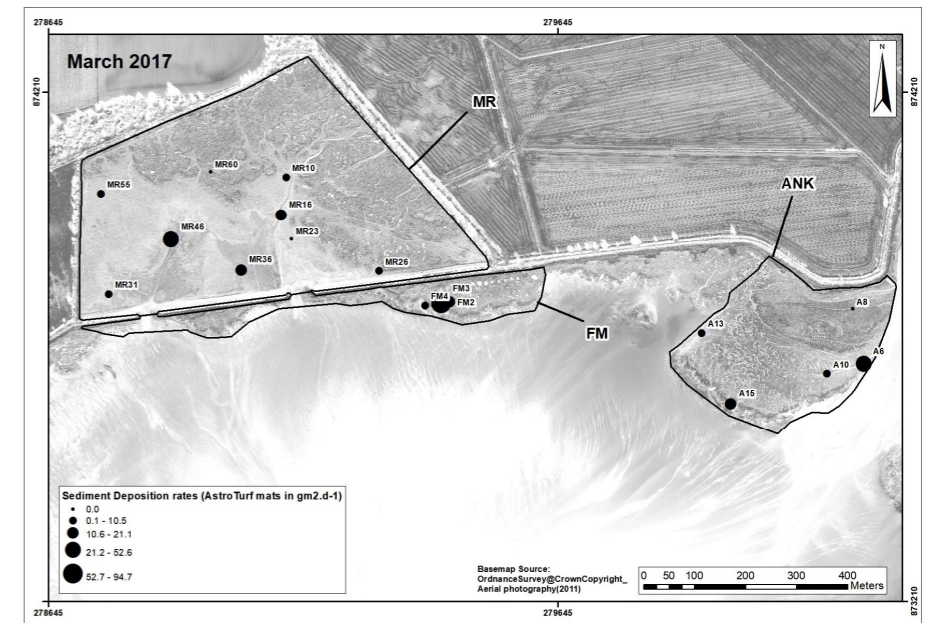
i) November 2016 AstroTurf mat sediment deposition rates (g.m2.day-1) for the three salt marshes studied in Nigg Bay



j) December 2016 AstroTurf mat sediment deposition rates (g.m2.day-1) for the three salt marshes studied in Nigg Bay



k) January 2017 AstroTurf mat sediment deposition rates (g.m2.day-1) for the three salt marshes studied in Nigg Bay



l) March 2017 AstroTurf mat sediment deposition rates (g.m2.day-1) for the three salt marshes studied in Nigg Bay

Figure 4-68 a) l): AstroTurf mat sediment deposition rates (g.m2.day-1) for the three studied salt marshes of Nigg Bay between 09<sup>th</sup> March 2016 to 01<sup>st</sup> March 2017.

**What drivers influence the average deposition and accretion rate estimates, what does this tell us about the short-term (annual) saltmarsh development at Nigg Bay?** The key message is that the deposition rates of natural, young, mature, and managed salt marshes do not differ substantially. The mature natural salt marsh ANK had the highest estimated accretion rate, while the newly formed natural fronting salt marsh FM had the lowest. Estimates of the maximum rates of deposition and accretion were found in the mid-marsh zones of ANK, the pioneer zones of FM, and the low-marsh zone of MR. This indicates that re-suspension of deposited sediment is more sensitive to tidal and wave erosion in exposed areas such as pioneer zones, whereas sediment retention is favoured in sheltered areas higher in the tidal frame, consistent with the findings of Langlois et al. (2003) findings in the Mont-Saint-Michel salt marshes. Accretion rates can be enhanced landwards by the presence of vegetation for smaller particles (Stumpf, 1983), tend to be the most stable in interior marshes and are reduced in the less vegetated areas such as pioneer zones (Kearney et al., 1994). This interpretation is conceptualised further by (Friedrichs, 2011), who demonstrates that, during typical spring tides (that is, excluding storm events), sediment moves away from areas of higher energy and towards areas of lower energy. The fronting marsh FM, which is closest to the saltmarsh edge and has most of its surface below MHWS, demonstrates that hydrodynamics has a negative effect on accretion as a whole. The section 4.5.1.1 regression analyses further reveal that hydroperiod and inundation depth are the primary drivers of the short-term (annual) average deposition and accretion rates and that maximum water levels have a significant and positive effect. In their field flume study, Reef et al. (2018) demonstrated that sediment budgets (deposition minus erosion of sediment) exhibit a similar pattern (higher sediment concentration at high water levels) during the flood and ebb periods. At Nigg, hydroperiod and distance to the saltmarsh edge or distance to the water channels have been found to improve the prediction of accretion rates; the further away from a marsh edge or a creek/water channel, the lower the accretion rates. This is due to the topography's significant influence on the frequency and duration of marsh surface flooding. Cahoon and Reed (1995) discovered on the Louisiana salt marshes that accumulation of both organic and mineral matter was significantly related to duration of flooding and was primarily delivered during the marsh flooding, thereby affecting marsh sustainability if insufficient (i.e. maintaining equilibrium level relative to tidal frame). Factors and processes associated to the salt marshes of Nigg Bay controlling deposition and accumulation on the saltmarsh surface itself such distance to saltmarsh edge and distance to the water channels, tidal inundation (Friedrichs, 2011; Townend et al., 2011) are geomorphological and hydromorphological variation owing to saltmarsh specificity and maturity (Stallins, 2006; Lawrence et al., 2018). These results further relate to (Schindler, Karius, Arns, et al., 2014) findings who measured accretion rates for three years to inform long-term saltmarsh evolution demonstrating a more consistent spatial pattern typically emerges identifying the importance in flux and water exchange permitting sediment to

arrive on the salt marshes (tidal characteristics) and in suitable morphology (slope, curvature and elevation) allowing sediment to remain on the salt marsh. This interpretation in line with this study findings suggests therefore that a key determinant to sedimentation the inundation/hydroperiod (Reed, 1995) and that morphology is mostly inherited from tidal flow and visible through water channels networks (Townend et al., 2011).

Modelling sediment deposition and accretion rate estimates (filter discs) and hydroperiod or flood depth can be significantly improved by vegetation assemblage, as higher rates are observed at high water levels and enhanced by annual *Salicornia* (SM8), whilst lower rates at low water levels are suppressed by assemblages such as *Festuca Rubra* (SM16d). This is supported by the findings of Baaij et al. (2021), who discovered that the presence of vegetation increased sedimentation by an average of 42%. Sedimentation was highest where pioneer plants (*Salicornia*) grew and increased with stem height and branching level. Li and Yang, (2009) discovered that the amount of sediment captured by vegetation per unit land area in the low-marsh margin decreased at a rate of 1% to 3% per metre distance from the water source where sediment suspended concentrations were greater, such as the outer marsh edge (bordering mudflat) or the tidal creek. The conclusion of their study was that the quantity of sediment captured by tidal marsh vegetation was related to plant properties, sediment concentrations in suspension, and the bed level, which determines tidal submergence. They found that non-native plants (*S. alterniflora*) were substantially more effective than native plant species (*Scirpus and Phragmites*) at capturing suspended sediment. On the other hand, Reef et al. (2018) found no significant relationship between sediment trapping efficiency and canopy morphology in a novel field flume study, whilst maximum inundation depth was positively correlated with deposition (and erosion) rates.

The results confirm the section 4.4.1 hypothesis that tides are one of the primary controls on sedimentary processes through sediment transport across the tidal flat, sediment suspension, sedimentation, and vertical and horizontal marsh expansion. By regulating the water flow across the marsh surface through tidal creeks, tides determine the extent and duration of the inundation, which is the primary source of sediments, organic matter, and nutrients (Fagherazzi et al., 2004; Wolanski et al., 2009; Davidson-Arnott, 2009; Kearney and Fagherazzi, 2016).

**Are the same drivers influence monthly deposition rates?** Exploration of the influence of physical drivers and controls on saltmarsh development on monthly filter disc deposition rates (4.5.1.2) have confirmed, as with the analysis of average deposition and accretion rates, that clusters of pioneer and low-marsh vegetation assemblages (SM8 and SM13a) occurred when hydroperiod and inundation depth were at their peak, and clusters of high-marsh plants (SM16d)

occurred on the elevated ground surface of the marsh. In April, November 2016, and January 2017, the relationship between filter disc sediment deposition rates and elevation height was significant and positive. The analysis revealed that overall filter disc sediment deposition was greatest in pioneer zones, where the SM8 vegetation assemblage is present, and lowest in high-marsh zones, where the SM16d vegetation assemblage is found. Plant communities significantly improved prediction models. In July 2016, filter disc sediment deposition rates were correlated with BDD, distance to the saltmarsh edge, and elevation. In December 2016, filter disc sediment deposition was correlated with distance from the MHWS, and the model was improved by pioneer and low-marsh plant communities. The results found in Nigg Bay were consistent with those of the aforementioned studies by Reed (1995) and Townend et al. (2011). In contrast to (Reef et al., 2018), the vegetation assemblages were found to be a good predictor for more than half of the variability in filter disc sediment deposition rates in June 2016 and December 2016, with low deposition predominantly occurring in mid- and high-marsh plants (SM13b and SM16).

Furthermore, the analysis showed that September, October, and November 2016 had the greatest inundation depth and hydroperiod, which coincided with the highest sediment deposition rates. However, August, April 2016, and January 2017 have had the shallowest inundation, resulting in a decrease in deposition rates. Butzeck et al. (2014) also found that seasonal differences in Elbe estuarine wetlands can be explained by higher water levels during these periods. Both hydroperiod and inundation depth are greatest in Nigg Bay during the spring (March, April, and May) and autumn (September, October, and November), highlighting the significance and importance of physical and hydrodynamic factors in sediment deposition.

The key outcome of this study, which examined the short-term (annual) assessment of physical processes governing the development of Nigg Bay salt marshes, was that monthly seasonal deposition was primarily influenced by geomorphological factors such as elevation, distance to high water mark (MHWS), and distance to saltmarsh edge. On the other hand, overall average deposition and accretion rates were primarily driven by tidal parameters and were further enhanced by vegetation assemblages.

#### 4.6.2.2 The spatial variability of the biological processes that form salt marshes - estimating vegetation processes and their influences.

As emphasised by Belliard et al. (2017) that despite significant advances in understanding the implications of marsh surface elevation for ecology, few field studies have addressed biomass – surface elevation relationships through direct measurements in European salt marshes. This thesis research aimed to improve understanding of these relationships in this short-term (annual)

study of Scottish salt marshes, by characterising the vegetation on the three salt marshes studied in Nigg Bay and quantifying their association with physical and environmental factors, thus providing information (better understanding) on what may favour saltmarsh development.

**How did short-term (annual) sediment monitoring campaign estimates of vegetation characteristics and related processes, biomass and aboveground organic carbon, compare between paired natural and managed salt marshes and saltmarsh zones?** Da Lio et al. (2013) explained that the time evolution of topographic elevation (relative to mean sea level) at any position on the marsh surface is jointly determined by the rate of inorganic sediment deposition, the rate of organic soil production, the erosion rate (due to wind waves and, possibly, to tidal flows), and the rate of relative sea-level rise. And in turn, vegetation development is strongly linked to marsh elevation (summarising the effects of sediment salinity and aeration, the stress factors that act more directly on marsh vegetation), so that there is strong feedback between geomorphic characteristics and biomass production. Moreover, characterisation of local reference marsh hydraulic conditions, which are interlinked with marsh surface topography and experienced by the various species of saltmarsh vegetation, has been identified as a critical factor for successful saltmarsh restoration and rehabilitation (Montalto et al., 2006; Howe et al., 2010). However, due to uncertainty and a lack of data on physical drivers of saltmarsh development, the effectiveness and success of these rehabilitation efforts have often been questioned (Millennium Ecosystem Assessment, 2005; Howe et al., 2010).

Overall, this present study reveals that the height and cover of vegetation at natural and managed sites were comparable. On the PM, vegetation (SM8 assemblages) was substantially shorter than in all other zones. The MM zone at ANK was more vegetated (as percentage cover) than the PM zone, whilst the HM zones at MR were more vegetated than the HM zone at FM. SM16d on MR and SM16a and SM16c on FM have different vegetation assemblages on these salt marshes, which can explain this performance. This first highlighted that all saltmarsh species are present on the MR site, but this is rarely going to be a fully 'natural' functioning ecosystem because of the nature of the original disturbed site (French, 2006). In their comparative study of 18 paired sites, Garbutt and Wolters (2008) discovered that overall vegetation was taller on de-embanked sites (less than 50 years old) compared to natural salt marshes; however, for certain assemblages, such as SM8, this was not always the case. Although their study did not examine high-marsh plants (such as *Festuca rubra*), it revealed that the percentage cover of dominant plant species in the pioneer and low-marsh zones of Nigg (e.g., *Puccinellia maritima*, *Plantago maritima*, *Salicornia europaea* agg.) was not significantly different between realigned and natural salt marshes. This trend was confirmed by comparing the mid-marsh MM and high-marsh HM zones at Nigg. Although little is known about the effect of plant structure and properties on the



adhesion of sediment to plants, density and aboveground biomass have been linked to a plant's ability to trap sediment (Morris et al., 2002).

Overall aboveground organic carbon estimated for Nigg Bay saltmarsh vegetation did not differ between natural and managed salt marshes or between saltmarsh zones, but was primarily enhanced by vegetation assemblages, and biological predictors of these assemblages were found to be associated with vegetation height. These findings concur with Burden et al. (2013) study on carbon sequestration in the Tollesbury, Southeast England, in which it was discovered that the aboveground biomass on arable land (on former high-shore salt marsh) and a managed realignment restoration site were quite comparable to the natural site. Their study further demonstrated that there was approximately twice as much aboveground organic content on managed realignment compared to the natural salt marsh. Due to the vegetation dominance of *Puccinellia mar.* (monoculture) and the absence of dynamic ecosystem properties, their study revealed that the managed realignment had approximately double the amount of aboveground organic matter compared to the natural salt marsh. Similar observations can be made for the MR of Nigg Bay (Figure 3-14), where SM13a covers 22.1 % of the marsh surface, compared to 1.6 % on FM and 13 % on ANK. Meirland et al. (2015) have also found that plant species richness increases with vegetation age in the Bay of Somme and predicted that richness increases in conjunction with higher sedimentation rates to counteract sea-level rise until the latter reaches a critical rate that drowns the saltmarsh vegetation.

**What factors influence vegetation characteristics and their related processes?** The physical, biogeochemical, hydrodynamical, and biological factors of a salt marsh, including sediment supply, soil type, grain size, soil salinity, pH, nutrient availability, oxygen levels, decomposition rates, drainage, hydroperiod, water velocity, grazing, bioturbation, and plant species, have been identified as the primary determinants of the carbon retention capacity of salt marshes (Sousa et al., 2010; Callaway et al., 2012; Kelleway et al., 2016; Kelleway et al., 2017; Thompson et al., 2021). The present study has examined the associations between various vegetation characteristics (specifically, height, cover, and density) and key physical factors that influence the development of saltmarshes. These factors include elevation, tidal parameters, distance to the saltmarsh edge, distance to the highest water mark (MHWS), proximity to water channels, and soil density (as measured by bulk density, or BDD) across three saltmarshes of Nigg Bay. The findings of the analysis indicate that elevation plays a significant role in shaping the overall vegetation characteristics of Nigg Bay. Specifically, it has been observed that higher elevations within the marsh exhibit greater vegetation cover, taller plant growth, and higher biomass. Conversely, lower elevations are associated with lower plant density. As the distance from the salt marsh edge increases, there is a corresponding increase in vegetation height, decrease in



vegetation density, and elevation of aboveground carbon content. The study revealed that there is a positive correlation between BDD and vegetation height, while a negative correlation exists between BDD and biomass. The analysis revealed that there is a significant negative correlation between water level parameters (flood depth and frequency and hydroperiod) and vegetation height, as well as vegetation cover. Additionally, there is a relatively weaker negative relationship between hydroperiod and vegetation density.

It has been acknowledged by researchers that the vertical distribution of biomass within the canopy is influenced by variations in morphology and vegetation density. These variations have implications for the velocities of flow at the local level, the losses in momentum, and the formation of skimming flow (Tempest et al., 2015; Thompson et al., 2021). In addition, there is a growing body of experimental and field evidence that quantifies flow dissipation across, suggesting that the complete saltmarsh vegetation communities or saltmarsh ecosystems could be an integral part of coastal flood and erosion protection (Möller et al., 1999; Möller et al., 2014; Thompson et al., 2021).

The results of the analysis of the relationship between the vegetation assemblages found in Nigg Bay and tidal levels (4.5.2.2) indicated that changes in water level across marshes exerted a significant influence on vegetation assemblages by changing the pattern of wetting and drying and the depth of flooding. This is consistent with Da Lio et al. (2013), who stated that vegetation zonation is likely the most recognisable characteristic of tidal marshes and that this is true at multiple spatial scales (from a few centimetres to approximately 100 metres). In addition, the authors demonstrated that spatial vegetation patterns and zonation are not just biological patterns but also biogeomorphological patterns exhibited by key feedbacks between biomass productivity and soil accretion. Across the three salt marshes of Nigg Bay, the pattern where pioneer and low-marsh (SM8 and SM13a) vegetation would endure a wetter regime and high-marsh (SM16a, c, and d) plants would endure a drier one according to the elevational gradient was evident. Assessment of vegetation assemblages using hydroperiod and flood depth levels, on the other hand, has shown an irregular profile in the vegetation succession (not following a sloping profile with elevation). This suggests a change in plant succession (irregular sequence with elevation; Figure 4-57), as sampling points on the fronting marsh FM were identified as belonging to other assemblages such as SM13a and SM13d but were originally surveyed by (Haynes, 2016) as SM16a (high-marsh). Changes in species colonisation can be indicators of a transition to a wetter (tidal) regime, the result of an abiotic stress intrinsically linked to hydrodynamics and sign of sea level rise, which increases salinity and soil salinity, forcing plants to increase their tolerance to it (Fagherazzi et al., 2019).

**Can this long-term (annual) study identify any relationships or influences between the studied salt marshes vegetation traits and processes and sediment deposition?** The analysis demonstrated that vegetation cover is a significant predictor of the variance in sediment deposition rates on filter discs. At Nigg Bay, the SM8 assemblage has been linked to low height, density, and cover in areas where plants experienced high inundation (depth and frequency), indicating that these characteristics may promote deposition and sediment settling. Compared to SM16a and SM16d (for accretion rate estimates only), SM16c, which is also associated with low height, density, and cover, was found to promote deposition and accretion rates. Experiments conducted on two distinct salt marshes in Essex and Morecambe Bay revealed in 2016 that plant species richness has a strong correlation with erosion reduction and soil stabilisation, with a greater impact in salt marshes with sandy soil and low organic content (Ford et al., 2016). However, the overall associations at Nigg Bay were insufficient to infer a biological role to sediment deposition, sediment settlement, or accretion. On the other hand, these findings confirmed the mineralogenic characteristics of the salt marshes of Nigg Bay, and, further suggested that the geomorphological characteristics of the salt marsh (elevation gradients; water levels; subsurface environment - BDD-; distance to marsh edge and sediment source such as tidal creeks) have a greater influence on the vertical accretion of the salt marsh than the physical characteristics of the saltmarsh vegetation (Schuerch et al., 2018). Also observed by Reef et al. (2018), and contrary to theoretical predictions, vegetation (i.e. canopy morphology) played a minor role in sediment accumulation in situ. Their study only monitored summer deposition under calm conditions, suggesting that vegetation structure and canopy may have a greater impact during the winter season.

**The research investigated whether vegetation assemblages could influence sediment deposition and accumulation rates. Did this relationship hold month after month? Did all the salt marshes studied behave in the same manner?** Empirical studies on salt marsh display mixed findings on direct relationships between biomass and sediment deposition which have been found either not to affect deposition rates (Boorman et al., 1998; Temmerman, Govers, Wartel, et al., 2003), or, to positively influence accretion on salt marsh (Da Lio et al., 2013; Belliard et al., 2017). In addition, research examining the impact of sedimentation and vegetation commonly concentrates on a specific plant species, such as *Spartina alter*. (Mudd et al., 2010), *Spartina mar*. (Sousa et al., 2010) or a single saltmarsh zone with two plant types (Houwing et al., 1999; Langlois et al., 2003; Maynard et al., 2011; Silinski et al., 2016).

This thesis research revealed that, when considering the entire season, only the winter deposition rates within SM8 plant assemblages exhibited a statistically significant increase compared to the summer deposition rates. In the winter season, there were no significant variations observed in

sediment deposition rates among different vegetation assemblages, with the exception of pioneer plants (SM8) which exhibited a higher accumulation of sediment compared to mid-marsh assemblages SM13d. During the summer season, the analysis revealed that there was a distinct variation in sediment deposition rates. Specifically, the rates of sediment deposition on high-marsh plants SM16c were significantly lower in comparison to all other assemblages. This partially contradicts Reef et al. (2018) observations that plant structure and canopy may have a greater impact in winter. The analysis at Nigg Bay has revealed, however, that summer vegetation at its peak - at its densest, tallest and most extensive - will influence where sediment is deposited. This is consistent with the findings of Temmerman et al. (2012), who have found that a significant decline in vegetation, it would not only reduce the rate at which sediment accumulates on the platform, but also reduce the amount of sediment filling the channels. In contrast to deposition rates, estimates of accretion rates at Nigg Bay exhibited comparable spatial patterns between winter and summer vegetation assemblages. Specifically, it was observed that mid-marsh plants (SM13b) demonstrated the highest levels of accretion during both seasons. During the winter season, the mid-marsh areas characterised by SM13d plants had the lowest rates of accretion. Conversely, in the summer season, the high-marsh areas dominated by SM16c plants demonstrated the lowest levels of accretion. Although, the analysis implied that there is a degree of seasonal variation in how sediment is deposited between vegetation assemblages, the results also suggest that there is no clear pattern distinguishing a succession the species whose composition varies with elevation (Doody, 2008), and, that vegetation assemblages do not solely characterise the spatial variation in sediment deposition rates. On the other hand, the results demonstrated that the presence of vegetation communities consisting of pioneer- (SM8), mid- (SM13b), and high- (SM16c) marsh plants can have a substantial impact (approximately 25%) on the fluctuations in sediment deposition rates observed during the periods of May to July and September to December.

Based on the interpretation of the relationships observed in each salt marsh, the analysis revealed that only on the ANK vegetation assemblages, pioneer (SM8), mid- (SM13b), and high- (SM16a) marsh plants demonstrated significant relationships on the average sediment deposition rates (approximately 27%) or monthly sediment rates (approximately 48%) observed during the months of April, June, and from September to December. The findings of this study also indicated that the presence of vegetation did not significantly influence sediment deposition rates on the two young salt marshes (FM and MR). This pattern was confirmed by examining the relationship between monthly deposition rates and salt marsh zones at each site. The study showed that the associations were of comparable strength. When analysing each salt marsh, only ANK, the natural salt marsh, showed significant correlations between monthly sediment deposition rates and salt marsh zones. In contrast, the young salt marshes, FM and MR, did not

show such relationships. The observed results suggest that the influence of seasonality or temporal variation on sediment deposition rates was a stronger contributor to sediment deposition rates than spatial variation related to vegetation or zonation. Differences between the natural salt marsh ANK and managed realignment MR could be also interpreted as MR forming a semi-enclosed tidal cell adjusting differently to tidal processes than natural salt marshes as Pethick warned in 1993.

The primary outcome obtained from this short-term (annual) study of the biological mechanisms governing the development of the Nigg Bay salt marshes revealed spatial patterns that implied a correlation between the succession of vegetation assemblages and the deposition and accretion of sediment. However, the study also suggested that this observed succession was not influenced by short-term deposition and accretion rates on an annual scale, irrespective of seasonal fluctuations (e.g., summer/winter). Another key outcome from this analysis of vegetation and its physical drivers in Nigg Bay salt marsh was that vegetation characteristics were predominantly influenced by geomorphological factors, including elevation and proximity to the saltmarsh edge. Conversely, tidal parameters had a substantial influence on the formation of vegetation communities.

#### 4.6.2.3 Spatial and temporal variability of water levels factor influencing saltmarsh development

Tides play a key role in controlling sedimentary processes, mainly through the transport of sediment across the tidal flats, the suspension of sediment, the deposition and accumulation of sediment, the process of sedimentation, and the expansion of marshes in both vertical and horizontal directions. The extent and duration of flooding in marshes, as well as the main sources of sediment, organic matter, and nutrients, are determined by the tides through their regulation of the flow of water across the marsh surface via tidal creeks. The frequency and duration of floods, which in turn influence sediment transport patterns and transitional zones (ecotones), are determined by the local elevation and tidal range. These factors are important because they shape the preferences, competition, and adaptations of the flora and fauna that inhabit the salt marsh (Fagherazzi et al., 2004; Wolanski et al., 2009; Davidson-Arnott, 2009; Friess et al., 2014; Kearney and Fagherazzi, 2016; Wilson et al., 2021).

#### **How did the water levels in the paired natural marsh and managed salt marshes and saltmarsh zones perform during the short-term (annual) sediment monitoring campaign?**

During the sediment deposition monitoring period (8<sup>th</sup> February 2016 to 01<sup>st</sup> March 2017 i.e. 359 days or 778 tidal periods), the low-marsh zones (both pioneer and low) of Nigg Bay exhibited

higher hydroperiods, more frequent inundation events, and greater flood depths compared to the zones at higher elevations. This observation aligns with existing literature on tidal and freshwater marshes. (Chmura et al., 2001; Temmerman, Govers, Wartel, et al., 2003; Butzeck et al., 2014).

An examination of the mean water levels at Nigg Bay, encompassing flood depth, flood frequency, and hydroperiod, provided additional evidence that the extent of flooding was more pronounced on the natural salt marshes. Specifically, 94% of the ANK area and 93.1% of the FM area experienced inundation at least once during the year, compared to 64.8% of the MR area. The natural salt marshes, ANK and FM, exhibited higher levels of hydroperiod, flood depth, and flood frequency in comparison to MR. Figure 4-69 below further suggests that this may not be related to the area of the marsh surface, but rather to the elevation of the marsh: ANK elevation ranges from 0.81 to 3.07 m, FM from 1.05 to 6.43 m and MR from 1.11 to 8.57 m. This is unusual for embanked salt marshes which have in general lower elevation than in the adjacent tidal marshes. According to Temmerman, Govers, Meire, et al. (2003) and Beauchard et al. (2011), embanked salt marshes typically have lower elevation than the adjacent tidal marshes due to subsidence (by compaction and mineralization of the sediments) and reduced tidal sedimentation. While the seawall may have prevented or limited the natural landward migration (or "roll-over") of ANK and FM salt marshes to maintain their position within the tidal frame in response to SLR, which caused system to drown, the higher MR elevation height in comparison to the natural marshes may be a reflection of absence of erosion during its land reclamation. Additionally, it has been demonstrated by Morris et al. (2002), Doody (2013) (Leonardi et al., 2018) that defence structures that deflect wave energy can cause erosion (Figure 2-16).

Figure 4-69 also demonstrates that the relationship between overall flood depth and the variables of hydroperiod and flood frequency is more linear. The graphs presented below illustrate that there is a close correspondence between the flood depth and hydroperiod levels for high elevations of the marshes, while a significant divergence is observed at lower elevations (in particular, the flood depth in the three saltmarsh sites is approximately half that observed in other marshes.). The flood depth (represented by the green line) and hydroperiod (represented by the red line) exhibit a rapid and linear decline until they reach a marsh surface elevation of approximately 1.60 m, as indicated by the y-axis intercept. Subsequently, the inundation follows a more gradual and consistent pattern. Nevertheless, it can be observed that the frequency of floods (represented by the blue lines) in the upper marsh regions decrease rapidly at around 1.80 m, as indicated by the intercept on the y-axis. Subsequently, there is a gradual decrease in flood frequency for the remaining elevation of the marsh.

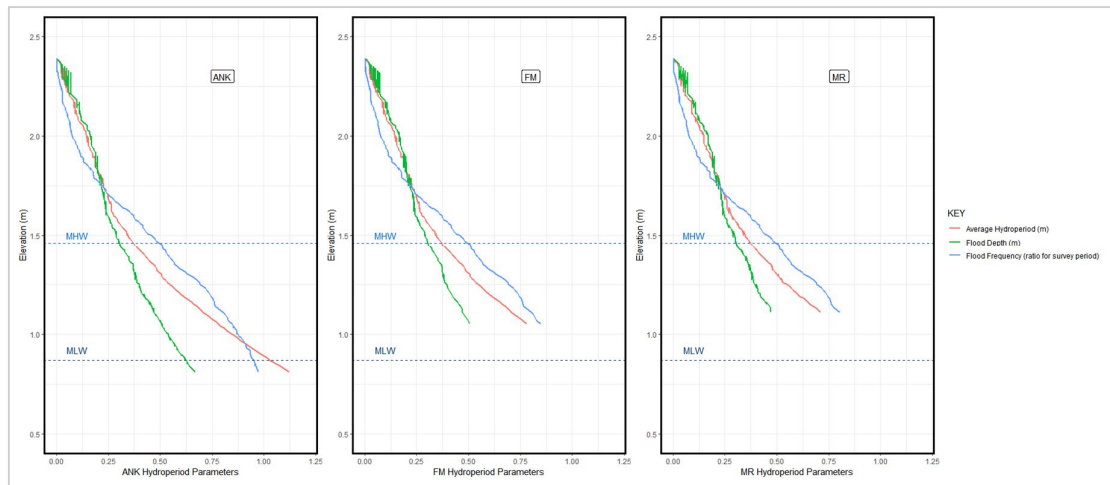


**Figure 4-69: Hydroperiod parameters over the ANK, FM and MR elevation heights (m) : mean hydroperiod (m), flood depth (m), flood frequency (ratio of floods – number of floods per tidal period – for the study period – 778 tidal periods). MHS and MLS were calculated for the period of the sediment deposition collection from March 2016 to March 2017.**

The occurrence of floods is observed in all sites and saltmarsh zones, primarily affecting the high-marsh zones and a significant part of the pioneer zones. Nevertheless, the analysis has clearly shown that there exists a distinct spatial variability between the high-marsh zones of three salt marshes. This is supported by the contrasting percentages of floods observed, with 31% of the MR extent being flooded compared to 85% of ANK and 90% of FM 85%. Furthermore, the hydroperiod parameters of the saltmarsh zones across the sites exhibit a substantial and statistically significant variation (Figure 4-26, Figure 4-29 and Figure 4-34).

The findings of the analysis confirmed that the geomorphic characteristics of each salt marsh were significantly influenced by water levels. The salt marsh zones of ANK demonstrated the most extensive variation in water level parameters. Its pioneer, low, middle and high marsh zones showed high values for flood depth ( $\geq 0.42$  m), flood frequency ( $\geq 44\%$ ) and hydroperiod ( $\geq 0.47$  m). Additionally, these zones exhibited extreme values for flood frequency ( $\geq 68\%$ ) and hydroperiod ( $\geq 0.70$  m), with the exception of extreme flood depth, which was observed solely in the middle marsh zone ( $\geq 0.63$  m). The pioneer marsh zones of MR and FM salt marshes were the only areas where very high and extreme flood depths were observed. The frequency of flooding was very high on all salt marsh zones in FM and MR, with the exception of the high marsh of MR. Extreme flooding frequency occurred mainly in FM and MR pioneer zone and in the low marsh of MR. The pioneer zones of both MR and FM exhibited very high hydroperiods, which were distinguished by the absence of extreme values. On MR, high hydroperiod is located along and north of the sea-wall in the former field drain. This is consistent with research on saltmarsh restoration schemes, which were found to contribute significantly to water surface slopes (during the ebb of the tidal cycle) by holding back water near breached embankments and causing high flow velocities through constrained channel connections between restored and



existing marsh, which lead to significant bank erosion (Friess et al., 2014; Möller and Christie, 2019). In this study at Nigg Bay, it is hypothesised that (i) high and extreme flood depth occur in the shallowest part of the marsh that experience the most drag from tidal flow and ebb, the effect of the river outlet which may contribute to greater scour on the eastern marsh edge of ANK marsh; (ii) high and extreme flood frequency in certain parts of the marshes is related to their distance to saltmarsh edge and to the principal tidal routes that feed the marsh; and (iii) high and extreme hydroperiod can be a combination of both.

**Were there seasonal variations in water levels observed during short-term (annual) sediment monitoring campaign?** The statistical analysis shows that each sediment collection has a different flood depth and hydroperiod level, which affects the inundation extent across the three salt marshes during the campaign (Figure 4-35, Figure 4-36, Figure 4-39 and Figure 4-40) and sediment deposition over marsh areas. Flood depth and hydroperiod were lowest in August, highest in November, and highest in April. Although statistically significant, the collection day tidal levels show no strong seasonality, deviating from the expected winter/summer pattern. Winter hydroperiod decreases by 10.2%, but flood depth increases by 0.4%. This may be explained by the higher levels of flooding experienced during storm surges and wind-wave activity (Reed, 1989; Pugh, 1996; Temmerman, Govers, Wartel, et al., 2003). These events are more frequent during winter but have not occur during the deployment days when the tide levels were recorded and used for the statistical analysis (Figure 5-46 in Chapter 5). Considering all water level values per month rather than just the levels on the collection dates, the comparison reveals that, for an uninterrupted period from March 2016 to March 2017, there is a 5% increase in tidal depth and hydroperiod between winter and summer. In contrast, for the specific sediment collection/deployment date, there is a smaller increase of 0.4 % in tidal depth and a decrease of 5% in hydroperiod. This corresponds to a monthly decrease of 31 % in tidal depth and 16 % in hydroperiod (Table 4-22). There exist significant disparities that have the potential to influence the quantity of sediment campaign. However, it should be noted that the concentration of suspended sediment can exhibit considerable daily variations. Aforementioned, previous studies have demonstrated that the utilisation of spring-neap tides is most effective in characterising saltmarsh inundation. These studies have identified an increase of ISSC being much greater during the winter (October to March) as the inundation height is at its maximum than during the summer period (April to September) (Cahoon and Reed, 1995; Temmerman, Govers, Wartel, et al., 2003; Temmerman, Govers, Meire, et al., 2003). Hence, the evaluation of suspended sediment concentration at Nigg Bay could serve as a means to assess the efficacy and outcomes of sediment deposition and accretion rates. Moreover, the findings presented in this study demonstrate the importance and reliability of incorporating the flood depth and hydroperiod levels on the deployment days, rather than relying solely on averages. This approach allows for a

more accurate assessment of the potential impact of tidal water levels on the sediment accumulation in the marsh.

The results align with existing literature that has established the significance of hydroperiod in the formation of a "hydrologic signature" within salt marshes, wherein distinct areas of the marsh experience varying hydroperiods (Kefelegn, 2019). Hydroperiod has been observed to exhibit a correlation with alterations in vegetation assemblages (presented in 4.5.2 and discussed in 4.6.2.2). Additionally, it has been determined that hydroperiod directly impacts the productivity of saltmarsh vegetation, as evidenced by studies conducted by (Morris et al., 2002; D'Alpaos et al., 2007; Friedrichs, 2011; Belliard et al., 2017). This finding is pertinent to one of the objectives of this thesis research, which aims to provide estimations of protective services, including the aboveground carbon content.

#### **4.6.3 Aboveground short-term (annual) biological and geomorphological processes: implications**

So far, the findings have examined the relationships among aboveground biomass, sediment deposition and accretion rate estimates over short time scale (i.e., annually). These results have provided insight into the patterns in these associations and identified the potential physical factors that influence sediment deposition and vegetation distribution in the three salt marshes of Nigg Bay. Consequently, one of the objectives of this study has been successfully met by contributing to the knowledge of the immediate physical and biological dynamics of salt marsh environments.

##### **What can we learn from these findings about short-term (annual) saltmarsh development?**

This study clearly showed that sediment deposition ( $23.4 \pm 2.3 \text{ g.m}^{-2}\text{day}^{-1}$  for filter discs and  $20.7 \pm 3.6 \text{ g.m}^{-2}\text{day}^{-1}$  for AstroTurf mats) was not significantly different between the natural and managed salt marshes. The findings presented in this study align with those reported by Taylor et al. (2019), who similarly observed no statistically significant differences in deposition rates between restored, characterised by the presence of *Bolboschoenus maritimus* plants, and natural salt marshes. They interpreted this similarity in deposition rates, despite variations in tidal inundation between the restored and natural areas, as evidence of functional equivalence in terms of deposition rates and organic content of deposits. The deposition rates observed in the Eden Estuary, Scotland, were significantly greater than those observed in Nigg Bay. In the natural salt marsh, the deposition rate was measured at  $47.64 \text{ g.m}^{-2}\text{day}^{-1}$  (equivalent to  $17.39 \text{ kg.m}^{-2}$  over the

course of a year). In the restored marsh, the deposition rate was measured at  $79.92 \text{ g.m}^{-2}\text{day}^{-1}$  (equivalent to  $29.17 \text{ kg.m}^{-2}$  over the course of a year).

However, in Nigg Bay, accretion rate estimates using filter discs (with a mean rate estimated at  $1.3 \pm 0.1 \text{ cm.yr}^{-1}$ ) were found to be different between the three salt marshes. Overall, the young and natural fronting salt marsh FM had the lowest accretion rates ( $1.1 \pm 0.3 \text{ cm.yr}^{-1}$ ) compared to the natural salt marsh ANK ( $1.5 \pm 0.3 \text{ cm.yr}^{-1}$ ) and the managed realignment MR ( $1.4 \pm 0.2 \text{ cm.yr}^{-1}$ ). The rates observed in this study exceed those reported by Miller et al. (2023) in their analysis of carbon accumulation and storage in Scotland using sedimentation rates from  $^{210}\text{Pb}$  and  $^{137}\text{Cs}$  chronologies. Specifically, Miller et al. found that the Dornoch Point marsh exhibited an average increase of  $0.18 \pm 0.01 \text{ cm.yr}^{-1}$  over the long term.

In Nigg Bay, distinctions between individual saltmarsh zones could be identified with higher estimated deposition and accretion rates in lower part (pioneer and low marsh zones) of the two young salt marshes, FM and ANK, compared to the high part of the marsh (trend highlighted by Pethick (1993); Temmerman, Govers, Wartel, et al. (2003); Marion et al. (2009)). The mature and natural saltmarsh ANK had higher rates in the mid-marsh zone, which differs from general findings in salt marsh studies. Sediment retention was interpreted to be enhanced by geomorphology, hydromorphology and the presence of vegetation, most stable in the interior of the marshes and reduced in the less vegetated areas such as pioneer zones (in with Stumpf (1983); Kearney et al. (1994); Allen (2000); Langlois et al. (2003); Rahman and Plater (2014); Schwarz et al. (2014); Schwarz et al. (2015)). Consistent with Butzeck et al. (2014) in their Elbe estuarine marsh study, physical predictor variables known to influence accretion rates (as schematised in Figure 4-1) differed significantly within the same saltmarsh. This was found true at Nigg Bay, between natural and managed salt marshes, and between seasons. Overall, the study at Nigg Bay showed that tidal parameters had the greatest influence on the estimated deposition and accretion rates, and that the presence of vegetation assemblages improved the accuracy of assumptions made about these rates. In contrast, the elevation, proximity to the high water mark (MHWS) and distance to the saltmarsh edge were geomorphological factors that significantly influenced monthly seasonal deposition.

The short-term (annual) study of the biological processes that control the development of the salt marshes at Nigg Bay has revealed spatial patterns that suggest an interaction between the succession of plant communities and the deposition and accretion rates. The findings of this study are consistent with the research conducted by Kelleway et al. (2017), which suggests that surface accretion differs among various vegetation assemblages. Specifically, the medium-term (19 month) bulk accretion rates observed in the upper marsh rush (*Juncus*) assemblage were consistently higher ( $1.74 \pm 0.13 \text{ mm y}^{-1}$ ) than the estimated local sea level rise ( $1.15 \text{ mm y}^{-1}$ ). The rate of accretion was found to be comparatively lower and less uniform in the succulent

(*Sarcocornia*) ( $0.78 \pm 0.18$  mm y<sup>-1</sup>) and grass (*Sporobolus*) ( $0.88 \pm 0.22$  mm y<sup>-1</sup>) communities situated at lower positions within the tidal zone. The short-term study at Nigg Bay also demonstrated that annual variations in seasonal conditions (summer/winter, for example) had no effect on the observed succession. Vegetation traits (characteristics) in Nigg Bay salt marsh were found to be primarily influenced by elevation and proximity to the saltmarsh edge. However, tidal parameters shaped vegetation communities.

Seasonal and spatial variations in deposition and accretion on the three salt marshes of Nigg Bay suggest that the amount of sediment retained on the saltmarsh surface, thereby allowing it to expand in height, is influenced by saltmarsh-specific physical variables in response to the forcings each salt marsh faces due to its position within the bay and its topographical development maturity. This confirms the importance of variability in time and space and should be considered when modelling and predicting future accretion rates in tidal salt marsh. But, in a broader perspective, can these short-term (annual) results quantify aboveground appraise: i) some of the regulating and supporting services salt marsh provide; ii) Capacity of Nigg Bay salt marshes to persist under sea-level rise (SLR)?

#### **Aboveground (blue) carbon stock (aboveground biomass)**

Coastal blue carbon habitats (mangrove forests, saltmarshes, seagrass meadows, and macroalgal forests) are strong candidates for nature-based solutions to address climate change and sequester carbon (Santos et al., 2022). This is because they can promote biodiversity and other important functions while also limiting global temperature increases to less than 1.5C above preindustrial levels (Andersen, 2021). The findings of this short-term (annual) study contribute to the estimation of saltmarsh blue carbon stock, which is recognised as a key regulatory services (Artigas et al., 2015). Aboveground plant biomass provides the information and values required to calculate the aboveground Blue Carbon (**Pool 1**) as defined in Chapter 3 – 3.4.3.2 (tables 3-12 to 3-14; the methodology employed in this thesis, as documented by (Howard et al., 2014), serves as a reference for the quantification of blue carbon stocks in coastal ecosystems, specifically mangroves, tidal salt marshes, and seagrass meadows.). Across the three salt marshes, aboveground organic carbon is not found to differ significantly with an average estimate of  $2.1 \pm 0.2$  tC.ha<sup>-1</sup> for MR,  $1.9 \pm 0.3$  tC.ha<sup>-1</sup> for FM and  $1.4 \pm 0.3$  tC.ha<sup>-1</sup> for ANK (Figure 4-70). These results differ slightly from Burden et al (2013) findings in the Tollesbury salt marsh where both low and high zones of restored salt marsh had approximately twice more aboveground biomass than natural ones. In a recent study conducted by Miller et al. (2023) on Scottish salt marshes has produced detailed information on two salt marshes in Moray Firth, where Cromarty Firth and Nigg Bay are situated, at Dornoch point and Morrich More.

Compared to the Moray Firth dataset, the aboveground carbon storage of Nigg Bay salt marshes is greater for the pioneer zones (approximately 49 % more), for ANK and MR low- and mid-marsh zones (approximately 26 % more), and for FM low- and mid-marsh zones (approximately 130 % less). The high marsh zones of Nigg Bay have, on average, 58 % lower values than Morrich more and Dornoch point. This direct comparison proves to be valuable as it showcases that, on the whole, the values exhibit minimal variation, yet there is observable diversity within specific zones and ultimately among plant species. Furthermore, it was observed in section 4.3.3 that the presence of biomass and, as a result, aboveground organic carbon exhibited distinct characteristics specific to various vegetation communities. In the ecological context of Nigg Bay, it is observed that SM16a exhibits the lowest aboveground carbon stock, measuring at 1.26 tC.ha<sup>-1</sup>. This value is notably lower when compared to SM16d, which records a higher aboveground carbon stock of 2.49 tC.ha<sup>-1</sup>, representing an increase of 49.4%. Similarly, SM13b also demonstrates a higher aboveground carbon stock of 2.25 tC.ha<sup>-1</sup>, indicating a relative increase of 44 % in comparison to SM16a.

However, aboveground total blue carbon is considerably higher on the managed salt marsh, being the biggest site of the three, with 50.6±5.4 tC compared to ANK with 17.7±2.4 tC or FM with 5.7±1.1 tC.

As a stock, managed realignment has positive impact on the aboveground carbon storage ecosystem services, especially has it provides the largest extent

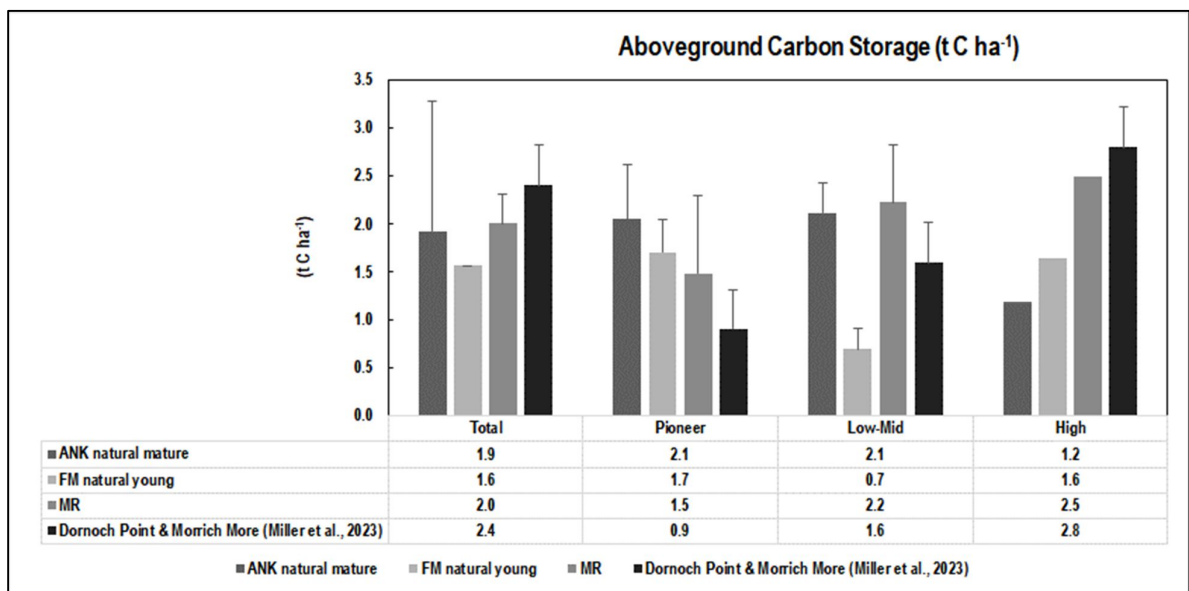


Figure 4-70: Bar graph showing the aboveground organic carbon stock (t C ha<sup>-1</sup>) in the pioneer, low-mid (low and mid-marsh zone values have been averaged for Nigg salt marshes to match Miller et al. (2023) results as there was no distinction made between mid and low marsh in their study) and high-marsh zones of ANK, FM, MR and Dornoch point and Morrich More saltmarshes (Error bars are standard deviation).

### **Accretion rates and sediment supply**

Short-term (annual) accretion results demonstrate that each salt marsh adapt rapidly through various mechanisms to the prevailing conditions, “and the prevailing state at any given time often represents a relatively short-term dynamic balance. Thus, it is this short-term adaptability that serves to maintain a longer-term stability within marsh systems“ (Townend et al., 2011, p.481), critical for the marsh to maintain its elevation in the tidal frame in light of recent relative sea-level rise (RSLR is sea level rise coupled with subsidence rates) observed in Scotland is now outpacing estimated rates of glacio-isostatic adjustment (Teasdale et al., 2011) and from Scottish local tide gauges (Rennie and Hansom, 2011). Recent publications clearly identify sediment supply and space availability as fundamental to saltmarsh survival against sea-level rise (SLR) and drowning. According to Liu et al. (2021), moderate rates of SLR have the potential to enhance hydroperiod (both the frequency and duration of tidal inundation). Additionally, these moderate rates of SLR may also serve as a stimulus for vegetation growth, thereby expediting the process of accretion. Can the short-term (annual) dataset inform on the capacity of Nigg Bay salt marshes to this recent sea level rise?

Overall short-term (annual) accretion rates using filter discs of  $1.34 \pm 0.14$  cm.yr<sup>-1</sup> ranging  $1.47 \pm 0.26$  on ANK,  $1.07 \pm 0.33$  on FM and  $1.36 \pm 0.16$  cm.yr<sup>-1</sup> on MR. These results from one year sediment deposition suggest that at an observed rate of  $0.3$  cm.yr<sup>-1</sup> in relation to past understanding of RSLR history in Cromarty Firth from long-term tide gauge trends (Rennie and Hansom, 2011; Lowe et al., 2018) across the three salt marshes and all saltmarsh zones (Table 4-9), there is, for now, enough sediment to supply the marsh to compensate this moderate rate of sea level rise.

However, more recent tide gauge trends in Scotland suggest that the short-term (15 years) rates of RSL show that present rates match those predicted at the 95% upper limit of a High Emissions Scenario, observed RSL rise rates of between 2.6 and 6.2 mm.yr<sup>-1</sup> (Rennie and Hansom, 2011), highlighting the vulnerability of the three salt marshes studied due to inadequate sediment input. Interpolation of the accretion rates across the salt marshes as shown in Figure 4-71, clearly depicts an alarming picture, with most of the eastern part of the fronting marsh FM, the western part of the natural marsh ANK, and the south-eastern part of the managed realignment MR and its high marsh (ENE part) are at threat. According to the findings Butzeck et al. (2014), sediment deposition rates in the tidal low marshes of the Elbe estuary they studied, appeared to be sufficient to compensate for moderate rates of sea-level rise. In contrast, they found that high salt marshes may be vulnerable due to insufficient sediment input and may (partially) revert to low marshes. The mapping (Figure 4-71) also shows an asymmetric delivery of flood-derived



sediment in the managed realignment on the ESE part of the MR marsh, possibly due to backwater in the remnants of reclamation drainage ditches (see Figure 3-7 showing remnants of reclamation features after the 2003-realignment).

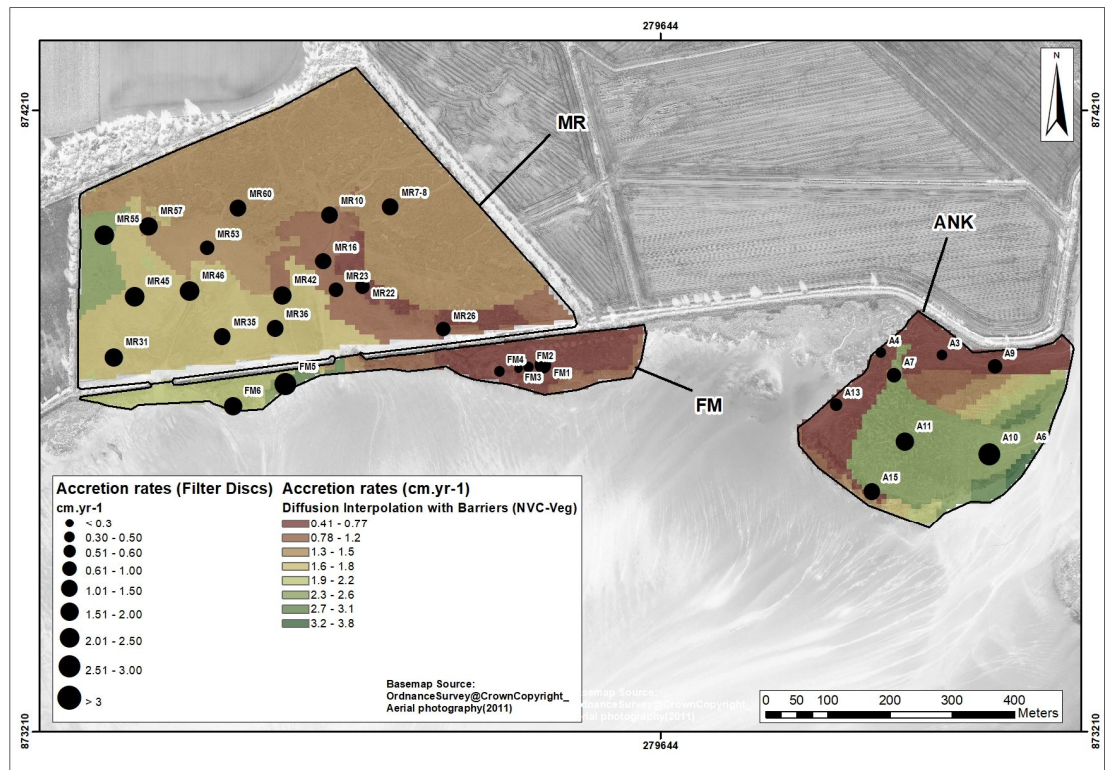
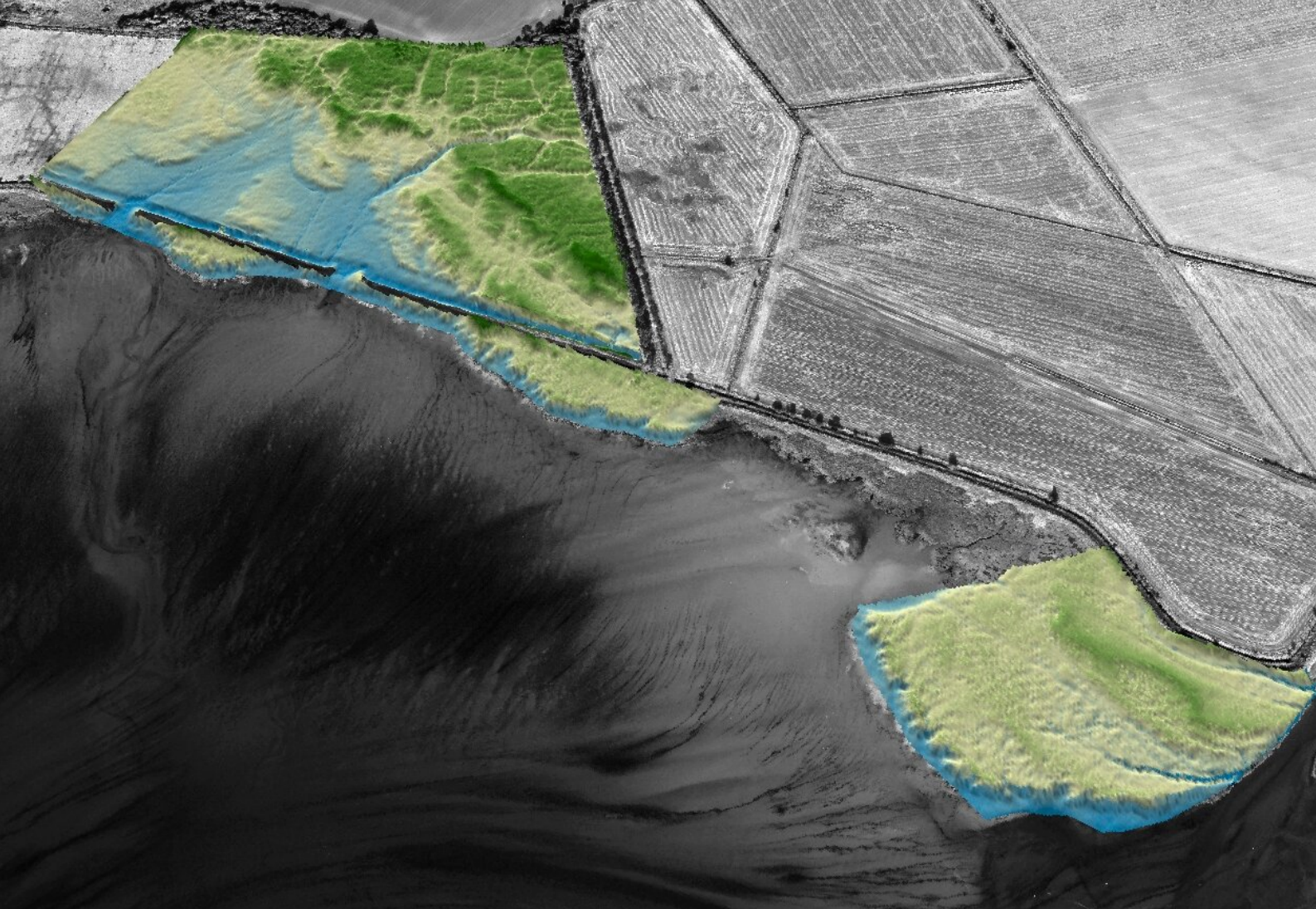


Figure 4-71: Sampling points with graduated symbol calculated for the mean accretion rate (in cm yr-1 for filter discs) across the three salt marshes at Nigg Bay. The symbols are superimposed on a surface model that represents the accretion rates at a constrained distance using the extent of each vegetation community (NVC-assemblage). To interpolate values from the accretion rates (filter discs), a geostatistical interpolation technique called Kriging, which uses the statistical properties of the measured points, was employed. As evidenced by the statistics presented in Chapter 4, vegetation assemblages significantly explain these rates, a diffusion interpolation model was run using the extent of vegetation communities (NVC assemblages - see Chapter 3 - section 3.3.2.2 - paragraph Research baseline NVC vegetation assemblages) as barriers (ESRI (1), n.d.). Where an area lacked sufficient samples, Empirical Bayesian Kriging (with values transformed to meet normal distribution requirements; (ESRI (2), n.d.)) was used to fill in the gaps (i.e. not enough sample points to accurately interpolate the full extent of the vegetation polygon - in all cases the gaps never exceeded more than 1% of the vegetation assemblage polygon).

However, subsurface processes such as shallow subsidence (vertical accretion greater than elevation change) can have a strong influence on elevation change and sedimentation rates (Cahoon et al., 2000) and therefore salt marsh capacity to adapt to SLR. This concept is further developed in Chapter 8, together with the findings presented in the following Chapters 5 to 7, to provide a comprehensive appraisal of the stability of the Nigg Bay salt marshes in the face of present and future sea-level rise.







# Chapter 5

*South view of the three salt marshes studied at Nigg Bay.*





**Chapter 5. Long-Term Dynamics:  
Aboveground Long-Term (Multi-Annual to  
Centennial) Geomorphological Evolution  
of Scottish Managed and Natural Salt  
Marshes**

## 5.1 Introduction

Chapter 2 (2.3) showed how saltmarsh sedimentation varies in space and time, driven by external factors such as sea level, tidal regime and wave energy and internal factors such as morphological adjustment (Figure 5-1). Vertical adjustments of salt marshes at specific locations is a subtle balance of sediment accretion and erosion rates and organic and inorganic compaction processes which may vary in time according to localised drivers such as micro-hydrodynamics as well as above and belowground biomass (Cahoon et al., 2000; Allen, 2000; Temmerman, Govers, Meire, et al., 2003; Langlois et al., 2003; French, 2006; Baptist et al., 2016). These adjustments over time reflect variation in saltmarsh location, sediment supply and rate of organic matter accumulation and also within marsh variations due to tidal range (low-marsh versus high-marsh). They also reflect marsh response to the impact of fluctuation in SLR and SLR rates on the number of flooding cycles and marsh elevation (Allen, 2000; Madsen et al., 2007).

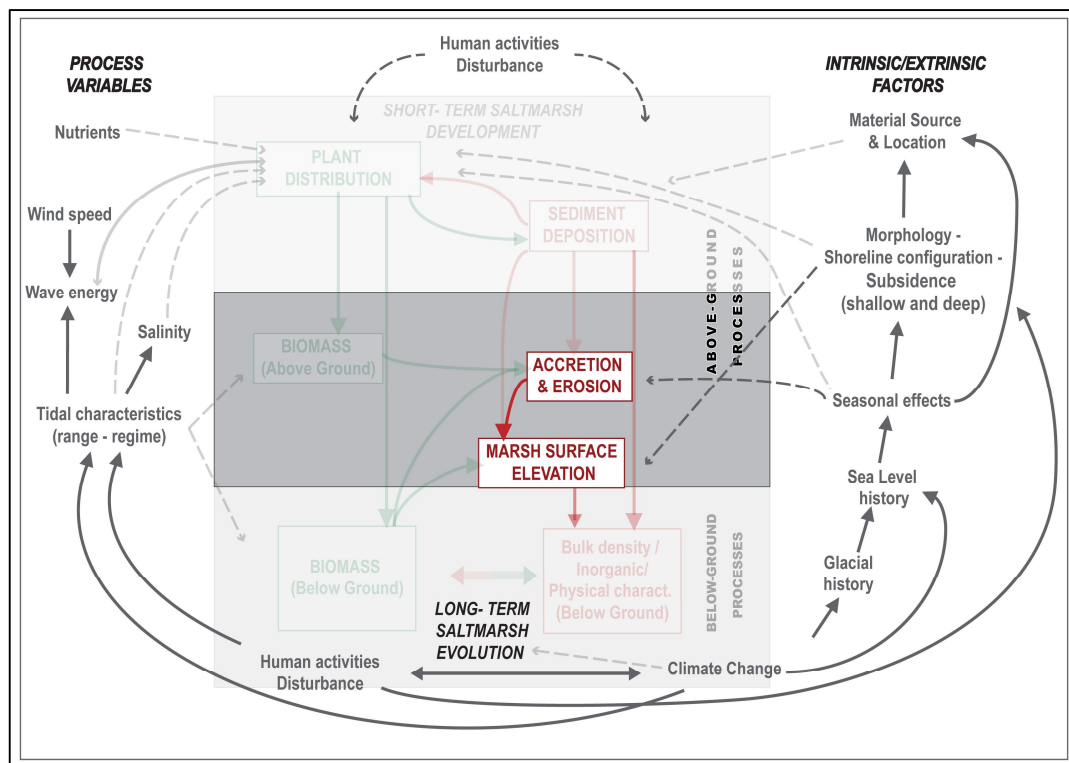


Figure 5-1: Chapter 5 focus on biological and geomorphological interactions of long-term saltmarsh development (decadal to centennial) in light of environmental processes and extrinsic and intrinsic factors influencing its evolution (after (Allen, 2000; Davidson-Arnott et al., 2002; Cahoon et al., 2009)).

To address the overarching aim of this thesis – which is to improve our understanding of: *which processes, mechanisms and patterns favour saltmarsh formation and development and enable saltmarsh capacity to recover from environmental and anthropological disturbances* – provides insights into the spatial and temporal development of saltmarsh sedimentation and the ability of salt marshes to keep pace with sea level rise. To answer this, aboveground changes in Nigg



saltmarsh geomorphological dynamics are quantified from multi-annual to centennial scale, focussing on:

- **Spatial variation:** what are the patterns of saltmarsh erosion and surface accretion? How much change has occurred in Nigg Bay salt marshes in the light of major anthropogenic disturbances: land reclamation/seawall breaching? Have these changes occurred laterally or vertically?
- **Temporal variation:** Are these changes regular across time?
- **Dynamic variation:** Is sedimentation on the study sites influenced by physical drivers or biological drivers?

Chapter 3-3.4.2 identified the research strategy to address these objectives. Table 5-1 presents specific questions and hypothesis tested in this Chapter to contribute to the understanding of sedimentation patterns and rates of natural and managed salt marsh in light of their capacity to keep pace with sea-level rise.

**Table 5-1: research questions tested in this chapter.**

Thesis aims	Specific research questions	Experimental hypotheses	Methods	Timescale	Chapter section
Improve understanding of aboveground saltmarsh long-term dynamics.	How much has the salt marshes in Nigg Bay changed?	- Land reclamation is the major anthropogenic disturbance in Nigg Bay and has resulted in significant saltmarsh loss. - Managed breaching of the seawall has not compensated for the loss of salt marsh from reclamation.	Historical mapping from 1747 to 2012 Details in 3.4.2	CENTENNIAL	5.2.1
	Spatial variation in shoreline migration between natural and managed salt marshes? Were these changes have been regular between the salt marshes?	- MHWS migration is not uniform - Rate of changes varies amongst the salt marshes	Combined dataset from 1872 to 2017 Details in 3.4.2		5.2.2
	How much has changed in terms of height, area and volume occurred in recent years? Are geomorphological responses differ between natural and managed salt marshes?	Erosion is expected to be higher near sea defence, with cliff edge formation as a response. Accretion varies between salt marshes and areas of salt marshes (i.e. pioneer-marsh development)	Two transects across the saltmarsh sites Digital Elevation Models for sediment budgets focussed on lower salt marsh (the shore front).	DECADAL	5.3

	Spatial variation: What are the changes in saltmarsh surface elevation (representing accretion and erosion) and sedimentation rates? Do they differ between natural and managed salt marshes? Do they differ between saltmarsh zones? Temporal Variation: do surface elevation changes (representing accretion and erosion) and sedimentation rates vary seasonally?	Surface elevation change (representing accretion and erosion) and sedimentation rates vary between salt marshes and saltmarsh zones reflecting external forcing and process variable.	Using a comprehensive network of sedimentation plates to improve our understanding on spatiality and temporality of the sedimentation saltmarsh dynamics	<b>MULTI-ANNUAL</b>	<b>5.4.1 &amp; 5.4.2</b>
	Can we relate differences in sedimentation rates between salt marshes and saltmarsh zones to physical and biological variables?	Changes in growth and abundance are closely related to the tidal range and the greater the distance from the saltmarsh edge, the less erosive are the tidal forces, providing settlement areas with higher sedimentation rates.	Statistical analysis		<b>5.4.3</b>
<b>Significance and implication of the results</b>	Can these results help predict the stability and future development of the Nigg Bay salt marshes?	The capacity of salt marshes to adapt to SLR varies between the sites studied due to historical anthropogenic disturbance.	Sedimentation rates Vs SLR		<b>5.5</b>

Data specifics on statistical results presented in this chapter are the same as in Chapter 4 and 6. A list of abbreviations used in this Chapter is provided in Appendix A.

## 5.2 Geomorphological changes across centennial to decadal timescales: scaling saltmarsh change.

Major shifts of state in ecosystems are common, but our capacity to understand what drives them is limited. Salt marshes sit at a dynamic interface between land and sea and are subject to constant change driven by variables that include flood, storm, coastal erosion and accretion and vegetation dynamics. Shoreline positions can change between seasons, years and decades. Salt marshes can be used as indicator of environmental change (for example Morton (1996); Coast Dynamic, (2019)). The analysis and information provided by such change in space and time provide important insights into the potential losses and gains of these systems and the services they provide. Time-series plots enable tracking of the changes and functioning of both geomorphology and ecosystems and the following section presents the aboveground geomorphological and ecological changes across centennial to decadal, and multi-annual time scales via historical mapping, airborne and Terrestrial Laser Scanner (TLS) Digital Elevation Models (DEM) analysis and analysis of sedimentation plates monitoring as per described in Chapter 3.4.2.

The reliability of historical maps to assess changes of saltmarsh extent has been questioned on many occasions (Bromberg and Bertness, 2005; Rennie, 2006; Baily and Pearson, 2007; Van der

Wal et al., 2008; Baily, 2011; Hansom et al., 2011; Baily and Inkpen, 2013; Godet and Thomas, 2013), aided by aerial photography (from about the 1940's). Therefore, it is important to understand the limitations and potential errors of such data (Baily and Inkpen, 2013). For this research, a combination of ground control points (GCPs) and visual comparison was followed to avoid large spatial differences between different data sources which may have used several geo-referencing systems (i.e. map tiles surveyed at different times). In terms of mapping errors, we can estimate for 1:10k map  $\pm 8.8$  m per 500 m (99% confidence) equating to 1.79% of error per map which was used for the historic cartographic analysis here (even though smaller-scale maps were used).

### **5.2.1 Historical mapping from 1750's to 2012**

Long-term changes in the Nigg Bay salt marsh is summarised through a map regression with the first detailed maps from the 1750's being the Roy Military Survey of Scotland (Figure 5-2) and John Ainslie 1785 chart (Figure 5-3), both of which depict the original extent of salt marsh prior land reclamation Nigg (Roy did not survey arable land in the site's vicinity). We have to wait for the Ordnance Survey (OS) One-inch first edition surveyed between 1843-1878 (Nigg Bay was surveyed in 1872) to locate detailed changes that took place in the Bay including first land reclamation west of the existing MR site and behind the newly built coastal embankment to the east of Ankerville River (Figure 5-4). A series of maps including the 1942 Admiralty Charts of Scotland, 1943 Bartholomew's map and OS One-inch maps of 1926-7 and 1947 do not show apparent changes (Figure 5-5). The OS One-Inch 7<sup>th</sup> series surveyed in 1956 (Figure 5-6) show the MR site fully enclosed by a new reinforced coastal embankment/seawall from Tarbat House and the remains of medieval Milntown Castle gardens and woodland (E277992, N873579) to Bayfield House (E280662, N873031), south-east of the ANK research site. From 1960 to 1980, OS maps are patchy as the digital content is incomplete, mainly due to the map tiles extent causing geo-referencing errors. However, some notable changes are visible south of the embankment where the front Marsh FM expands against the structure (Figure 5-6 Figure 5-7 Figure 5-8). In 2003, the primary coastal defence was artificially breached as part of the MR works, and secondary coastal defences placed around the boundary of the MR site (Figure 5-9).

Figure 5-2: Roy's map (1747-1753). No arable fields are depicted near sites.



NB: Roy's map cartographic style uses **Yellow** for cultivated ground; **Dark green** for woodland and **blue-green** for water parallel with **hatching** for tilled land and **stipple** for sands or shoals) (from NLS, <https://maps.nls.uk/roy/style.html>)

Figure 5-3: Ainslie's 1785 chart of the Nigg's Sand



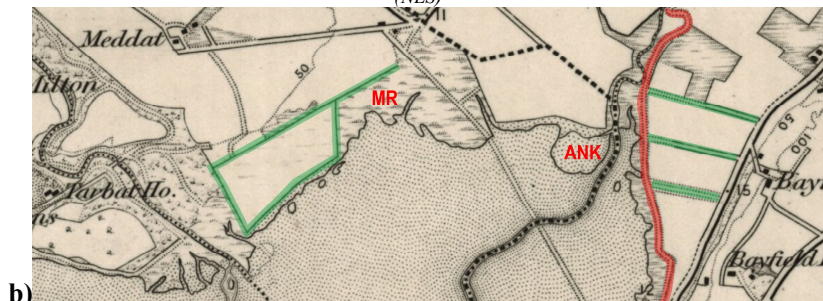
(NLS)

19th Century

Figure 5-4 a) & b): 1872 OS 1st edition One-inch showing coastal embankment (in red) and early reclamations of salt marsh to cultivation (green) except study sites areas (noted as MR and ANK).

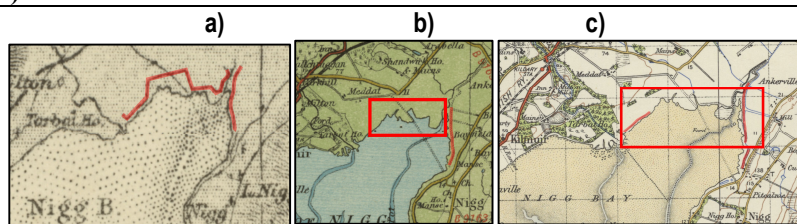


(NLS)



b)

Figure 5-5: a) 1942 Admiralty Charts of Scotland  
b) 1943- Bartholomew's map  
c) 1947 OS One-inch map.



(NLS)



Figure 5-6: 1958 OS One-inch map is the first cartographic evidence to provide a timestamp for the last reclamation (green) in the study site MR and the sea defence extension (red).



Figure 5-7: 1960 OS 1:10K- scale showing saltmarsh extent (blue) and embankment (red).

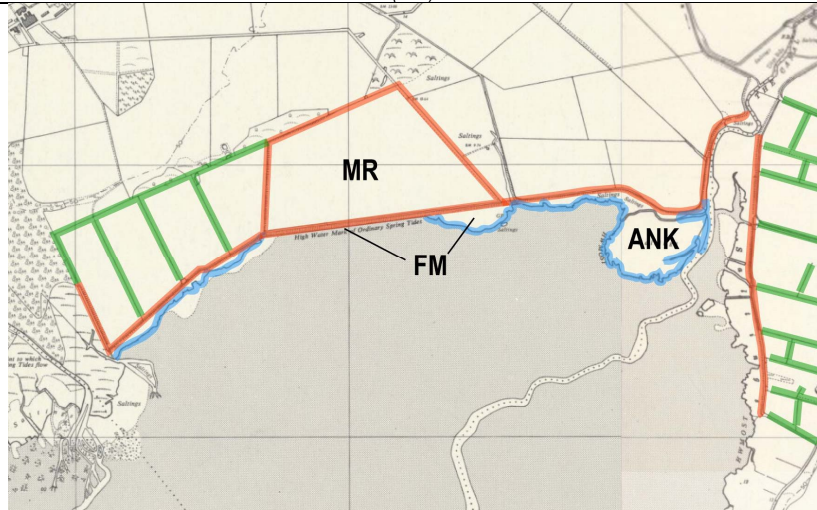
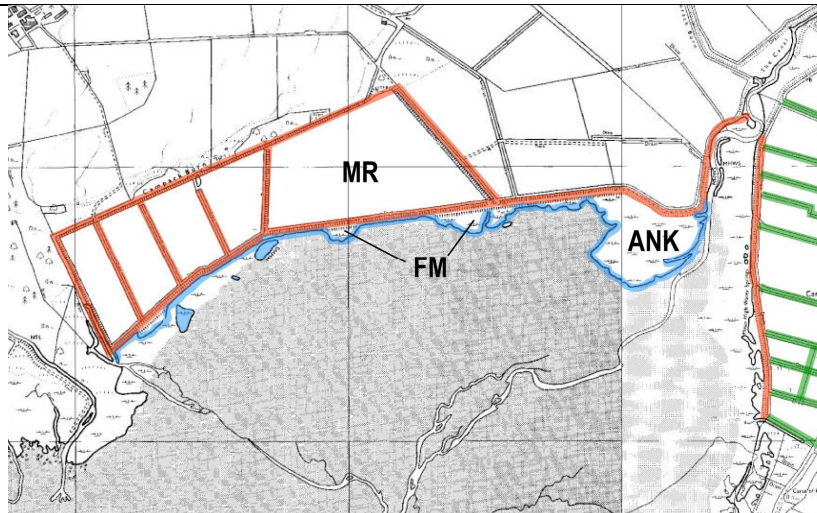
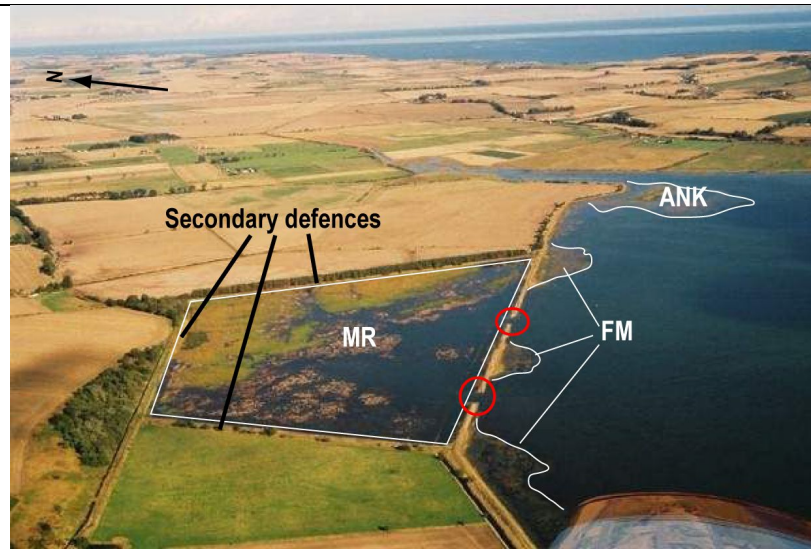


Figure 5-8 Combined 1977(a) and 1980 (b) OS 1:10K- scale showing the increased extent of fronting marsh



**Figure 5-9: Aerial view of the three research study sites (MR, FM and ANK) in October 2003 post-breach (red circle) at MHWS.**



**Cartographic sources**

- Roy Military Survey of Scotland, 1747-55 – *Highlands* – (British library maps C.9.b 27/5d).
- John Ainslie – *A chart of part of the North of Scotland, from Banff to Duncansby Head* printed in 1785 (South West section).
- OS One-inch first edition – *Ross-shire & Cromartyshire (Mainland)*, **Sheet LV** (includes: Fearn; Logie Easter; Nigg), Survey date: 1872, Publication date: 1881; and, **Sheet LIV** (includes: Kilmuir Easter; Logie Easter), Survey date: 1872, Publication date: 1880.
- OS One-inch popular – *Nairn & Cromarty*, **Sheet 28**; Survey date: 1926-7 Publication date: 1929.
- Bartholomew’s revised Half-Inch Map – *Sutherland, Great Britain*, **Sheet 59**; Printed in 1943.
- Admiralty Charts of Scotland, **115** - *Peterhead to Pentland Firth, incl. Moray Firth*; revised in Aug. 1942.
- OS One-inch popular – *Nairn & Cromarty*, **Sheet 28**; Publication date: 1947.
- OS One-inch popular 7<sup>th</sup> series (1952-1961) – *Dornoch*, **Sheet 22**; Publication date: 1958.
- OS 1:10560 scale map – NH77SE NH87SW & part of NH87SE - A (includes: Fearn; Kilmuir Easter; Logie Easter; Nigg) survey date:1930 & revisited in 1959; publication date: 1960.
- OS 1:10000 scale map – NH77SE - Surveyed / Revised: 1972 to 1976; publication date: 1977 –&– NH87SW & part of NH87SE – A - Survey date: 1971-79; publ. date: 1980

The physical coastal and saltmarsh changes over the past 200 years have been closely linked to land management and reclamation and so identifying whether changes are the result of land reclamation or natural erosion/accretion and gain presents problems. However, for the study sites here, land management and areal changes can be quantified within a GIS to identify areas and changes prior to and post reclamation, breaching, etc using OS One-inch first edition (1872 - Figure 5-4), the OS 1:10K (1977-81 - Figure 5-8) and the 1:4000K Scottish Saltmarsh Survey (SSS) dataset surveyed by SNH in 2012 (Haynes, 2016).



## 5.2.2 Quantifying historical changes: Areal changes from 1872 to 2012

Methods, choice of dataset and details of scale and precision were presented in Chapter 3 - Section 3.4.2.1. The results presented relate to the area highlighted in red box in Figure 5-10 to Figure 5-13, which is between 4.3% and 5.4% of Nigg Bay. For the past c.140 years, the cumulative average saltmarsh edge erosion rate is  $-0.03 \pm 0.001$  ha.yr<sup>-1</sup>, this equating to  $6.33 \pm 0.1$  % loss of salt marsh in Nigg Bay (Figure 5-10 and Figure 5-13) and a non-cumulative areal gain for same period of  $0.06 \pm 0.001$  ha.yr<sup>-1</sup> equating to a total of  $8.7 \pm 0.2$  % saltmarsh loss (Appendix D – Table D1).

Between 1872 until the late 1970's, an estimated overall  $11.5 \pm 0.2$  % of salt marsh was lost at a rate of  $-0.13 \pm 0.001$  ha.yr<sup>-1</sup>. During this period, the mapping analysis shows despite an overall loss of  $38.1 \pm 0.7$  ha ( $32 \pm 0.6$ %) chiefly through land reclamation, saltmarsh areas along the new sea defence structures expanded by up to  $24.4 \pm 0.4$  ha ( $20.5 \pm 0.4$  %) whilst  $56.6 \pm 1$  ha ( $47.5 \pm 0.9$  %) of salt marsh remain unchanged (Figure 5-11). Since the 1980's, the extent of the salt marsh of Nigg Bay has increased by  $32.2 \pm 0.6$  ha ( $28.5 \pm 0.6$  %) mainly attributed to the breaching of sea wall defence at the MR site to add  $26.7$  ha. This increase also coincided with a loss of  $10.2 \pm 0.2$  ha ( $9 \pm 0.2$  %) of salt marsh, to the east and south-east of ANK site (Figure 5-12), whilst the  $70.8 \pm 1.3$  ha ( $62.6 \pm 1.1$  %) marsh extent remains unchanged on ANK. These results provide an overall positive accretion rate of  $0.71 \pm 0.007$  ha. yr<sup>-1</sup> (overall extent accretion of  $19.5 \pm 0.3$  %) for the past c.30 years for Nigg bay (Figure 5-10).

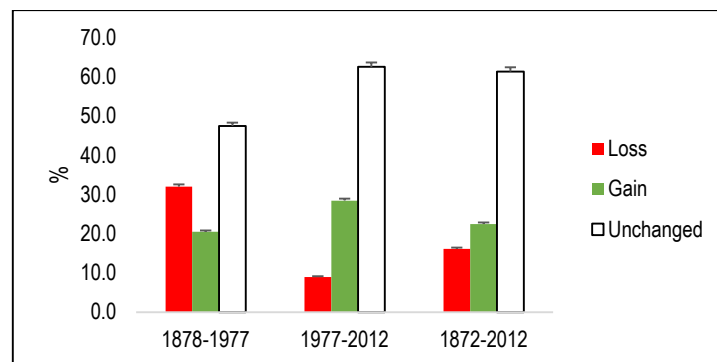


Figure 5-10: Historical evolution of Nigg Bay saltmarsh areal extent (%).

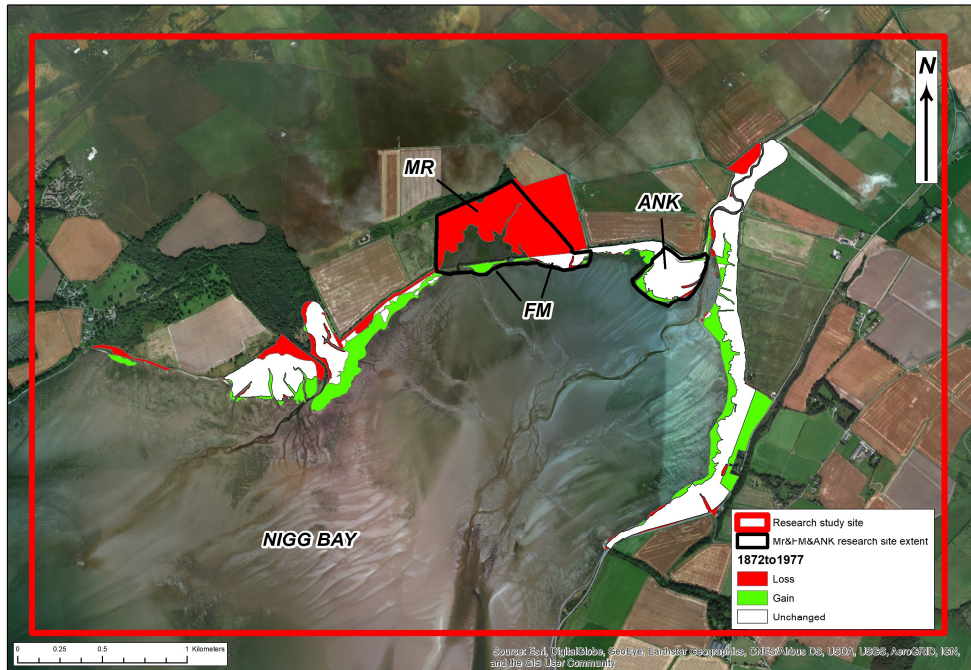


Figure 5-11: Areal changes between 1872 to 1977-81 representing the loss of salt marshes in red ( $38.1 \pm 0.7$  ha), gain in green ( $24.4 \pm 0.4$  ha) and no areal change in white ( $56.6 \pm 1$  ha) and black outline depicting the extent of the research study sites (MR, FM and ANK).

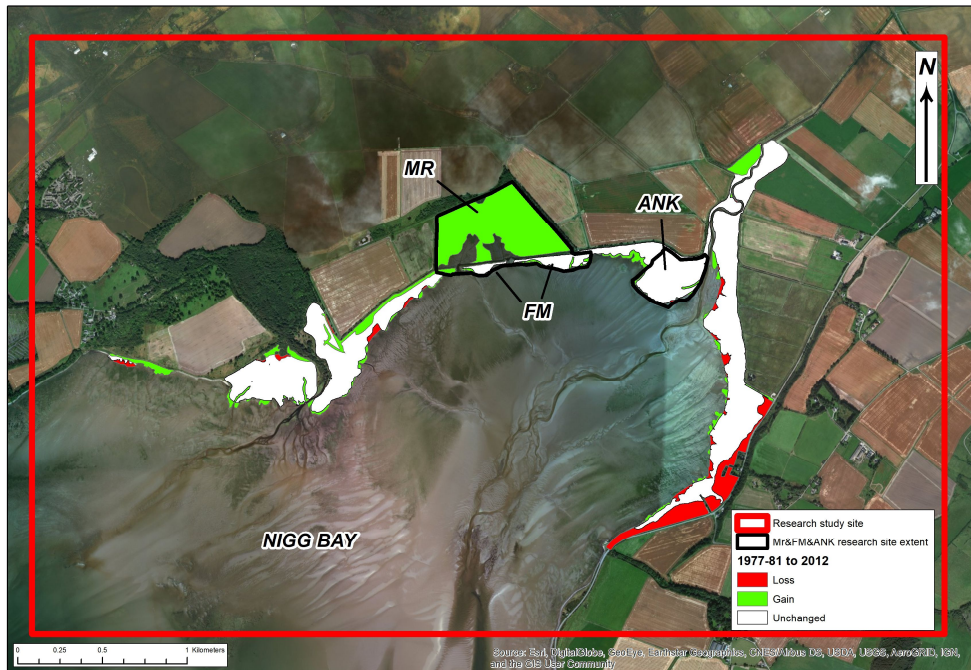


Figure 5-12: Areal changes between 1977-81 to 2012 with same symbology as above: Loss =  $10.2 \pm 0.2$  ha; Gain =  $32.2 \pm 0.6$  ha and No change =  $70.8 \pm 1.3$  ha.

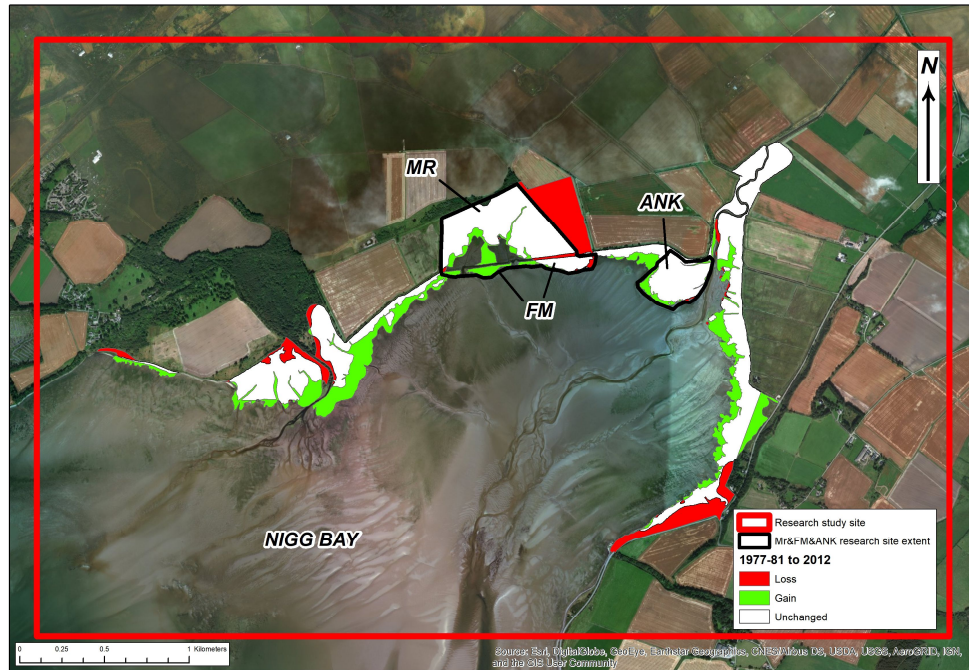


Figure 5-13: Overall Areal changes between 1872 to 2012 with same symbology as above: Loss =  $19.8 \pm 0.4$  ha; Gain =  $27.5 \pm 0.5$  ha and No change =  $75.2 \pm 1.3$  ha.

### 5.2.3 Quantifying historical changes: coastline and MHWS movement from 1872 to 2017

MHWS migration between 1872 and 2017 was landwards at  $0.01 \pm 0.01$  m.yr<sup>-1</sup>, but with a wide variation in amount and direction ( $-124.2$  to  $+128.9$  m). MHWS rate of changes (non-cumulative – grey bars in Figure 5-14) varied significantly between the sites ( $F = 25.57$ ,  $p < 0.001$ \*\*\*) with both FM and ANK migrating seawards at  $-0.07 \pm 0.01$  m.yr<sup>-1</sup> and  $-0.01 \pm 0.02$  m.yr<sup>-1</sup> respectively. On the other hand, the MHWS in the MR site moved landward over 145 years at a rate  $0.14 \pm 0.03$  m.yr<sup>-1</sup>.

However, overall rates of change of position of MHWS (cumulative – black bars in Figure 5-14 and Figure 5-18) show that MHWS has generally been moving seawards and gaining in height at a rate of  $-0.02 \pm 0.01$  m.yr<sup>-1</sup>. Significant differences were observed between sites ( $F = 14.37$ ,  $p < 0.001$ \*\*\*) and also between each site (MR & ANK  $p < 0.001$ \*\*\*; FM & ANK  $p < 0.05$ \*; MR & FM  $p < 0.01$ \*\*\*) showing that both FM and MR have been moving seawards (respectively  $-0.01 \pm 0.004$  m.yr<sup>-1</sup> and  $-0.07 \pm 0.02$  m.yr<sup>-1</sup>) whilst ANK MHWS has been moving landwards at a rate of  $0.01 \pm 0.01$  m.yr<sup>-1</sup> (Figure 5-14).



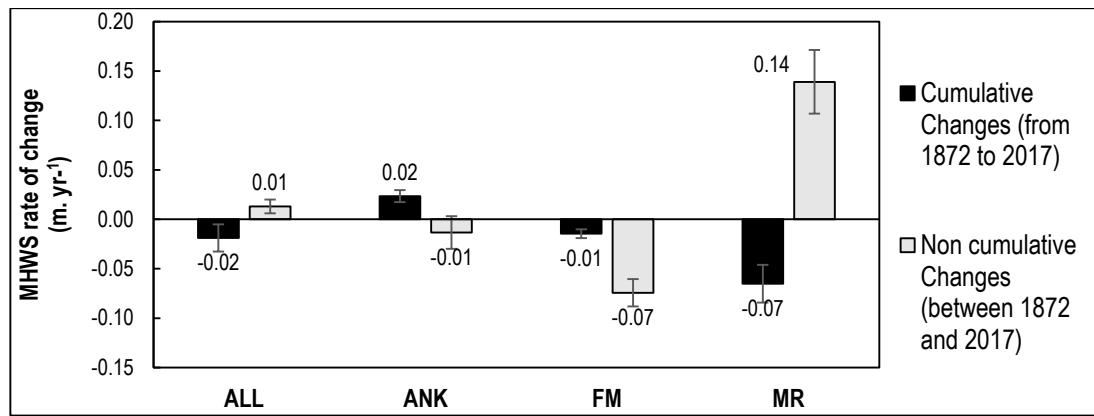


**Figure 5-14:** The bar graphs (error bars calculated from individual standard errors SE) depicts the rate of change in  $m.yr^{-1}$  of MHWS in the past 145 years providing slightly different scenarios if we are looking at the changes between 1872 and 2017 (grey bars) and the cumulative changes that occurred between these two dates (from 1872 to 2017) which include differences between MHWS of 1872, 1977, 2011, 2014, 2015, 2016 and 2017 (black bars).

During the period of land reclamation, the natural salt marshes likely benefitted from higher sediment availability, reflected in a seaward migration of MHWS. Between 1872 and 1977, when Nigg Bay experienced an overall  $14.3 \pm 0.3$  % loss of salt marsh (see above), MHWS migrated seaward at an overall rate of  $-0.28 \pm 0.03 m.yr^{-1}$  (Figure 5-15). This trend is reversed over the next 34 years, a period that includes the managed realignment of MR (2003). Consequently, between 1977-81 to 2011, overall MHWS migrates landward at an rate of  $1.48 \pm 0.15 m.yr^{-1}$  which is about 5 times faster than in the past 109 years (Figure 5-16). Between 2011 and 2017, the last six years of monitoring using Lidar, terrestrial laser scanning and photogrammetry, shows MHWS to have moved rapidly seawards at  $-2.97 \pm 0.39 m.yr^{-1}$ , albeit with significant variations between the MR and the two natural sites FM and ANK (Figure 5-17).

**Table 5-2: MHWS rate of changes in m per year. Positive values correspond to a landward migration (erosion) and negative values to seaward movement (accretion). The overall rates are averaged using FM and ANK marsh results.**  
**Note\*1:** In 2014 and 2015, the top and bottom saltmarsh edges/coastlines on the fronting marsh FM and natural marsh ANK were recorded using DGPS. In one year, the marsh edge moved landward by  $0.29 \pm 0.13 m$ . From these datasets, it was not possible to generate an accurate surface model to extract MHWS at 2.1m OD; consequently, these results were not integrated in the cumulative rate of migration change.  
**Note\*2:** In 2016, there was no Terrestrial laser scanner (TLS) survey on the managed realignment MR.

From 1872 (OS map)																		
to 1977-81 (OS map)				to 2011 (lidar)				to 2014 *1		to 2015 *1		to 2016 <sup>2</sup>			to 2017			
MHWS rate of changes in m per year																		
ANK	FM	MR	Overall	ANK	FM	MR	Overall	MR	Overall	MR	Overall	ANK	FM	Overall	ANK	FM	MR	Overall
minu s0.0 4	minu s0.0 9	minu s0.7 5	minu s0.2 8	0.07	minu s0.0 5	0.43	0.14	0.1	0.1	0.15	0.15	minu s0.0 2	minu s0.0 8	minu s0.0 5	0.01	minu s0.0 7	minu s0.1 4	0.01
±	±	±	±	±	±	±	±	±	±	±	±	±	±	±	±	±	±	±
0.02	0.02	0.08	0.03	0.02	0.01	0.04	0.02	0.02	0.02	0.02	0.02	0.02	0.01	0.01	0.02	0.01	0.03	0.01
Seawards	Seawards	Seawards	Seawards	Landwards	Seawards	Landwards	Landwards	Landwards	Landwards	Landwards	Landwards	Seawards	Seawards	Seawards	Landwards	Seawards	Seawards	Landwards

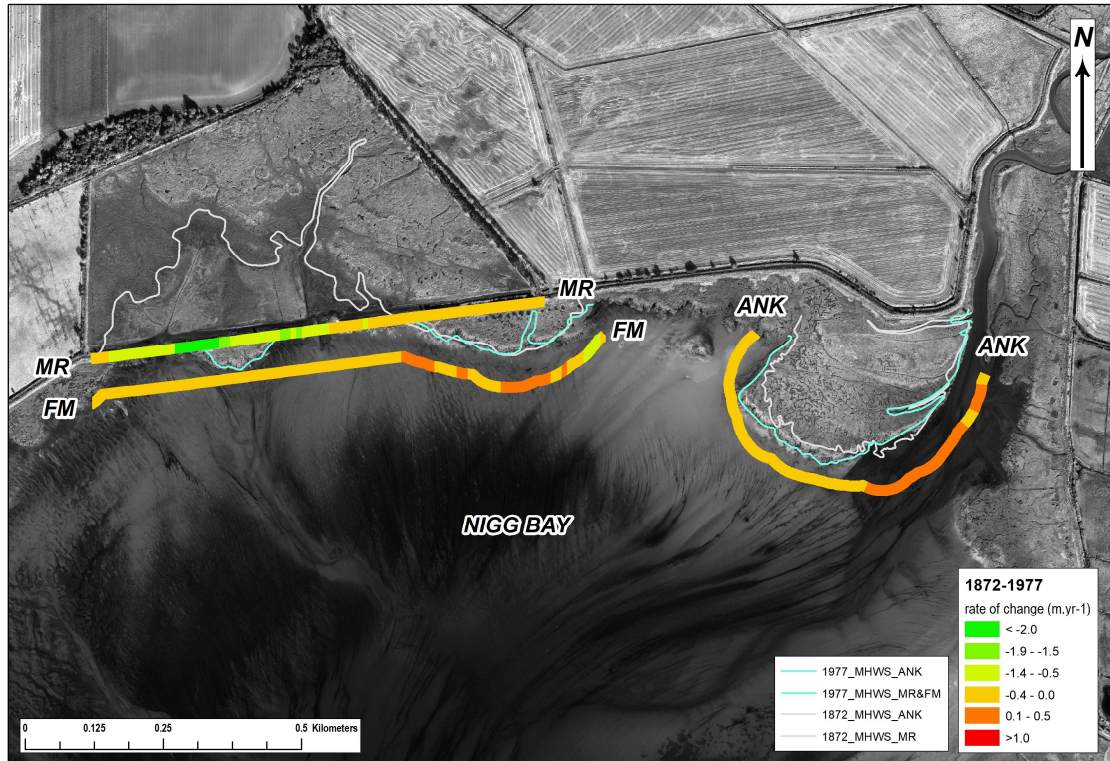


Figure 5-15: Rates of change in MHWS between 1872 to 1977-81 for the study sites are presented on a graduated colour baseline located in the foreshore. The results show an overall seaward migration of the MHWS of  $-0.28 \pm 0.03 \text{ m.yr}^{-1}$ . The seawall construction separating MR and FM sites in 1950's impacted on the MHWS migration resulting in a seawards movement of  $-81.3 \pm 8.9 \text{ m}$  on MR, whereas the natural salt marsh benefited from accretion of  $-4.8 \pm 2.2 \text{ m}$  for FM fronting marsh and  $-9.4 \pm 1.8 \text{ m}$  on ANK.

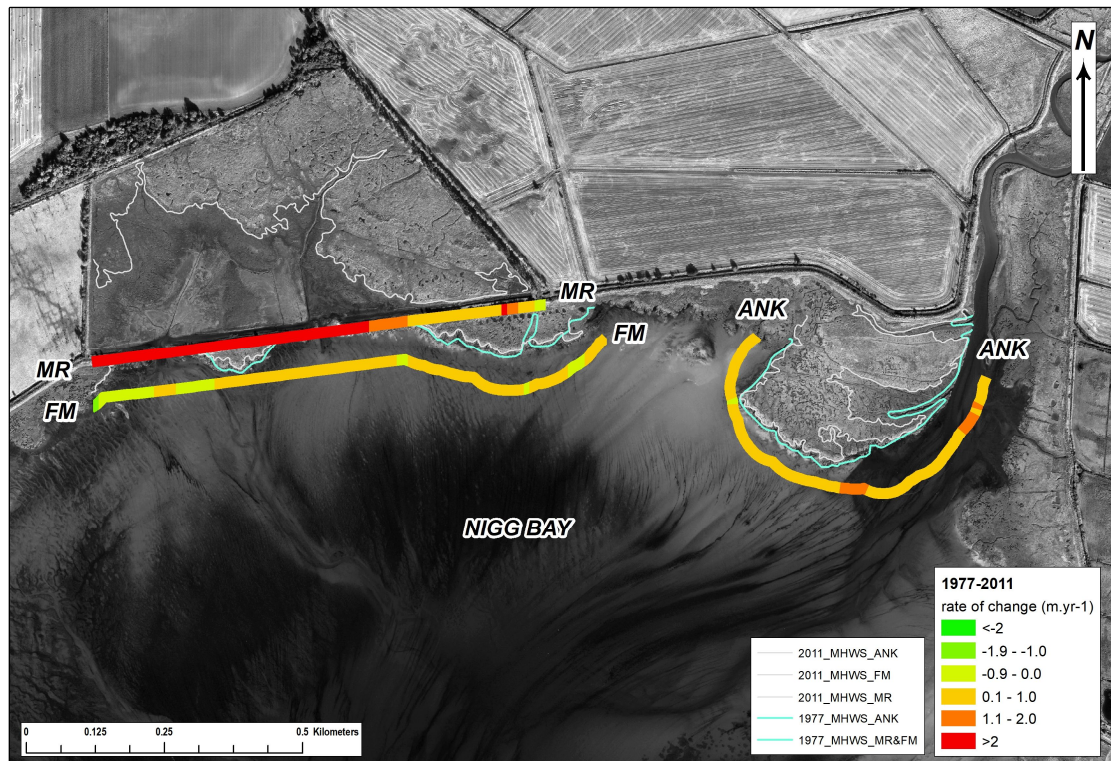


Figure 5-16: Between 1977-81 to 2011, a period that includes RSPB managed realignment of MR (2003) resulting in the



MHWS moving  $139.4 \pm 10.6$  m landward. Similarly, the fronting marsh FM moved  $3.1 \pm 1.1$  m and ANK MHWS moved of  $14.8 \pm 1.4$  m landward. In 34 years, MHWS for the three salt marshes migrates landward 5 times faster than the previous 109 years at an overall rate of change  $1.5 \pm 0.2$  m.yr<sup>-1</sup>.

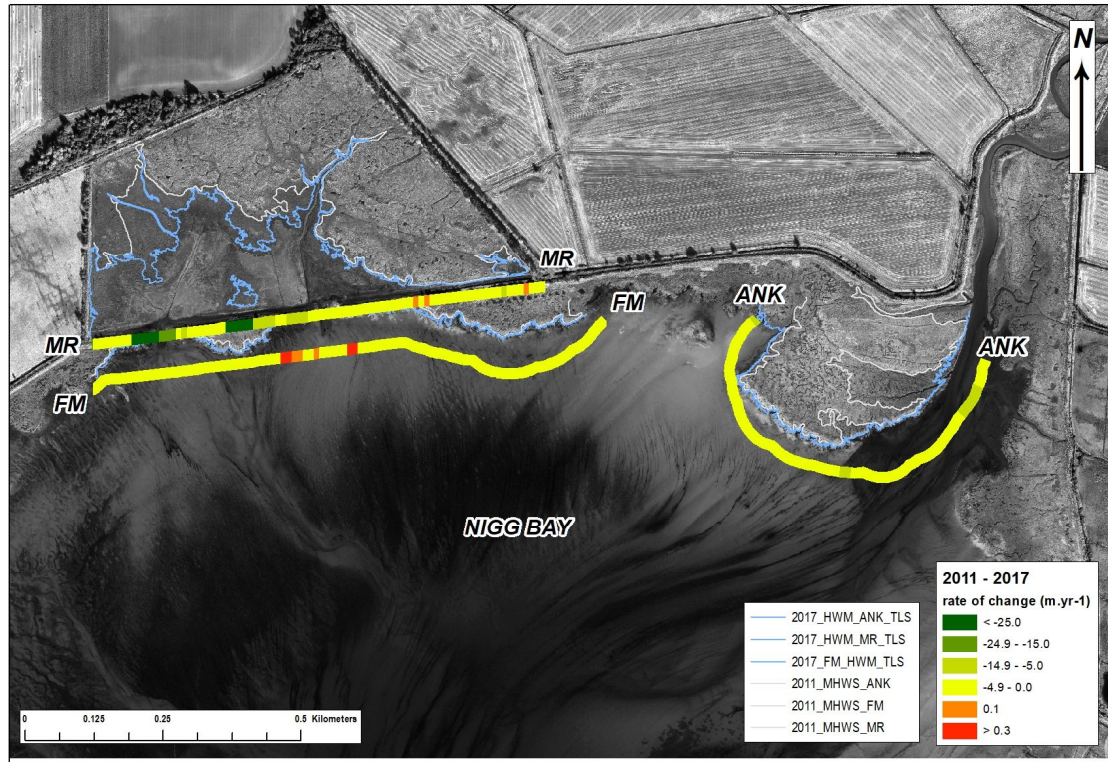


Figure 5-17: Rates of change in MHWS migration between 2011 to 2017 for the study sites averaged at  $-3 \pm 0.4$  m.yr<sup>-1</sup> seawards. MR site expanded onto the lower marsh of  $39 \pm 6.6$  m, FM onto the intertidal  $4.4 \pm 0.5$  m and the natural salt marsh ANK MHWS also migrated towards the foreshore of  $11.9 \pm 1.6$  m.

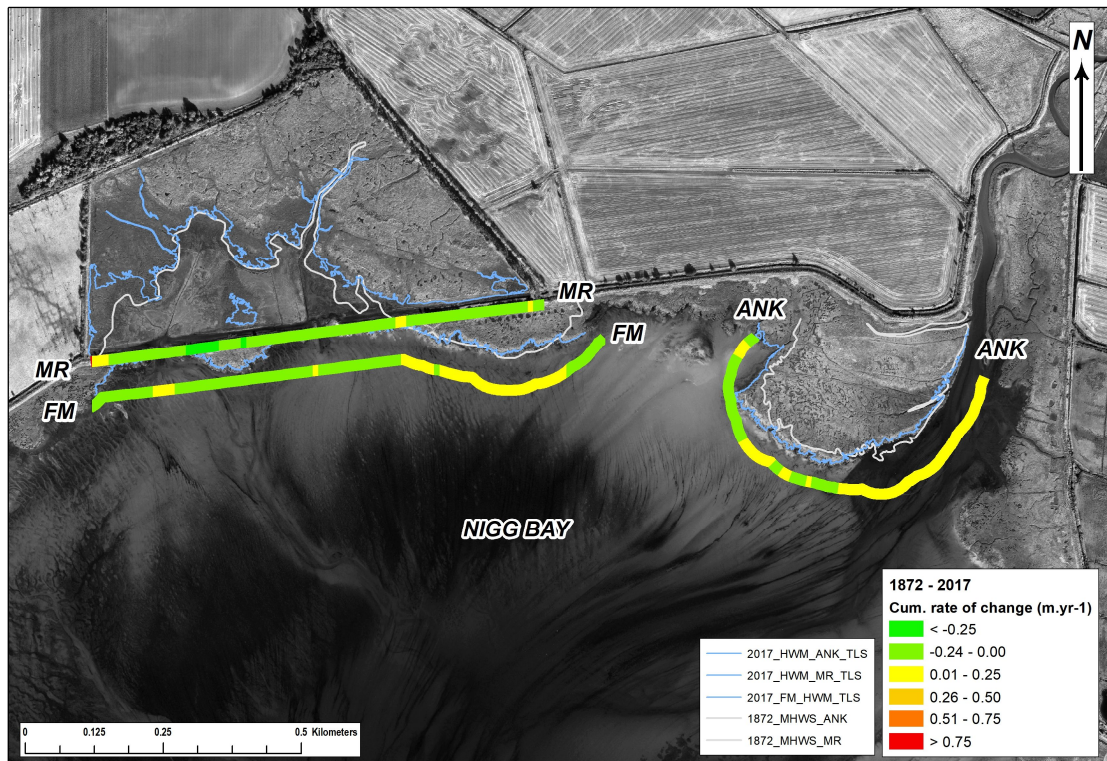


Figure 5-18: Cumulative rates of change in MHWS migration for the entire 145 years (1872 to 2017) with an overall MHWS seawards shift at  $-0.02 \pm 0.01$  m.yr<sup>-1</sup>.



Therefore, for 145 years spanning from 1872 to 2017, an overall MHWS seawards shift at  $-0.02 \pm 0.01$  m.yr<sup>-1</sup>. However, this migration was not uniform across the sites. Although the managed realignment MR MHWS appears higher in 2017 than it was in 1872, there is still a cumulative difference of  $-9.4 \pm 2.7$  m between the two MHWS due to the sea embankment on SE end of the site. Similarly, the fronting marsh FM demonstrated an overall gain on the foreshore of  $-2.1 \pm 0.6$  m. The natural marsh ANK, on the other hand, retreats landwards by  $3.4 \pm 0.9$  m in 145 years. The overall trend shows that the easternmost part of the pioneer-marsh on both FM and ANK are prone to erosion. Post-breaching phase demonstrate rates of change in MHWS migration between 2011 to 2017 for the study sites averaged at  $-3 \pm 0.4$  m.yr<sup>-1</sup> seawards. MR site expanded onto the lower marsh of  $39 \pm 6.6$  m, FM onto the intertidal  $4.4 \pm 0.5$  m and the natural salt marsh ANK MHWS also migrated towards the foreshore of  $11.9 \pm 1.6$  m.

### **5.3 Geomorphological change on a multi-annual scale**

This section presents the results of elevational and volumetric changes on the three sites at Nigg using Digital Elevational Models (DEM) generated from the 2011 Lidar data, 2015, 2016, 2017 Terrestrial Laser Scanning (TLS) and orthophotography from July and September 2017. The DEM time series aims to:

- i. characterise and quantify accretion and erosion on the most dynamic part of the marsh systems (foreshore and low part of the salt marshes)
- ii. investigate differences in micro-topography between the three saltmarsh sites
- iii. establish if these differences are related to accretion and/or erosion.

Details on data assessment, accuracy and precision and selection are treated in Chapter 3 - 3.4.2.1 (tables 3-7 and 3-8) and comprehensive details in Appendix B – B3. Based on these results the selection of the dataset used to quantify accretion and erosion for our three sites between 2011 to 2017 is summarised in Table 3-9.

#### **5.3.1 Morphological characteristics of a cross-shore transect profiles using airborne and TLS DEM surfaces from 2011 to 2017**

Chapter 3 - section 3.4.2.1 provide the rationale behind the two cross-shore transect profiles selection as depicted on Figure 5-19 and Figure 5-20 (location shown as black lines on Figure 5-22). These were selected to capture the key morphological and vegetation characteristics of the saltmarsh zonation as seen on adjacent sections of marsh and foreshore. Both cross-sections display the general topographic variation of the study sites and exposed a lack of intermediate plant succession stages between the mudflat/pioneer zone and the upper marsh on FM and ANK,

a phenomenon which explains the complex and irregular marsh edge of Nigg Bay already reported by Kessel (1978) in his work on salt pans and creek formation in the bay.

The transect cross-shore profile through ANK (Figure 5-19) demonstrates an overall increase in elevation of  $c.0.045 \pm 0.0008$  m (for vegetated marsh, pioneer and fronting mudflat surfaces) with a clear gain from 2011 to 2016 and loss from 2016 to 2017. The pioneer zones and cliff edges displayed an overall landward migration of  $c.5.65 \pm 0.1$  m, with differences between the western and eastern edges. The western edge retreated  $c.11.83 \pm 0.21$  m landwards and gained  $c.0.11 \pm 0.002$  m in height (gain of  $c.0.25 \pm 0.004$  m between 2011 to 2016 and loss of  $c.-0.03 \pm 0.001$  m between 2016-2017), giving rise to the formation of a sloping terrace edge angled at  $4.74^\circ$  to  $15.79^\circ$  between 2011 to 2016 and  $13.76^\circ$  from 2016 to 2017. The eastern edge formed a steeper terrace of  $11.7^\circ$  in 2011,  $58.66^\circ$  in 2016 and  $52.94^\circ$  in 2017) and had migrated  $c.1.37 \pm 0.02$  m seawards, gaining  $c.0.04 \pm 0.001$  m in height ( $0.014 \pm 0.0002$  m from 2011 to 2016 and  $-0.07 \pm 0.001$  m for 2016-17). The mudflat section for this transect showed an overall erosion of  $c.-0.03 \pm 0.001$  m for the same time period.

The second transect cross-shore profile (Figure 5-20) crosses the two sites, FM and MR, on a SWS/NEN axis and reveals topographic differences between these two salt marshes. FM shows an overall increase in elevation  $c.0.019 \pm 0.001$  m (for vegetated marsh, pioneer and fronting mudflat surfaces) with a clear gain from 2011 to 2016 and a small loss from 2016 to 2017. The pioneer zones and cliff edges running along the southern edge of the site showed an overall landwards migration of  $c.0.87 \pm 0.02$  m and slight expansion of  $c.0.2 \pm 0.004$  m of the marsh surface along the sea wall. Similar to the eastern edge of ANK, the cliff top is slightly higher than the marsh surface which may be the result of sediment overtopping at high tide. During the six years of monitoring, the vegetated surface gained in height of  $c.0.16 \pm 0.003$  m (2011-16=  $\uparrow c.0.37 \pm 0.007$  m and 2016-17=  $\downarrow c.-0.05 \pm 0.001$  m) and the cliff edge became steeper from  $8.1^\circ$  in 2011,  $32.88^\circ$  in 2016 and  $32.52^\circ$  in 2017. At its base, blocks of eroded material are mixed with established patches of *Salicornia* and hummocks of *Puccinellia mar.* forming the pioneer zone of this site. Its height has barely changed during the monitoring period, showing an overall loss of  $c.-0.075 \pm 0.001$  m in height, comparable to the loss of  $c.0.03 \pm 0.001$  m in height of fronting mudflat. At MR, there is an overall accretion of  $c.0.05 \pm 0.001$  m in height from 2011 to 2017, with an increase of  $c.0.15 \pm 0.002$  m in height on the high and mid-marsh zones, whilst the pioneer and low-marsh zones exhibit an overall rise of  $c.0.02 \pm 0.0003$  m. Although the low zones of the site increased by  $c.0.12 \pm 0.002$  m between 2011 and 2014, it has demonstrated a continuous loss in height since 2014: from 2014 to 2015  $\downarrow c.-0.04 \pm 0.001$  m and 2015 to 2017  $\downarrow c.-0.02 \pm 0.0003$  m.



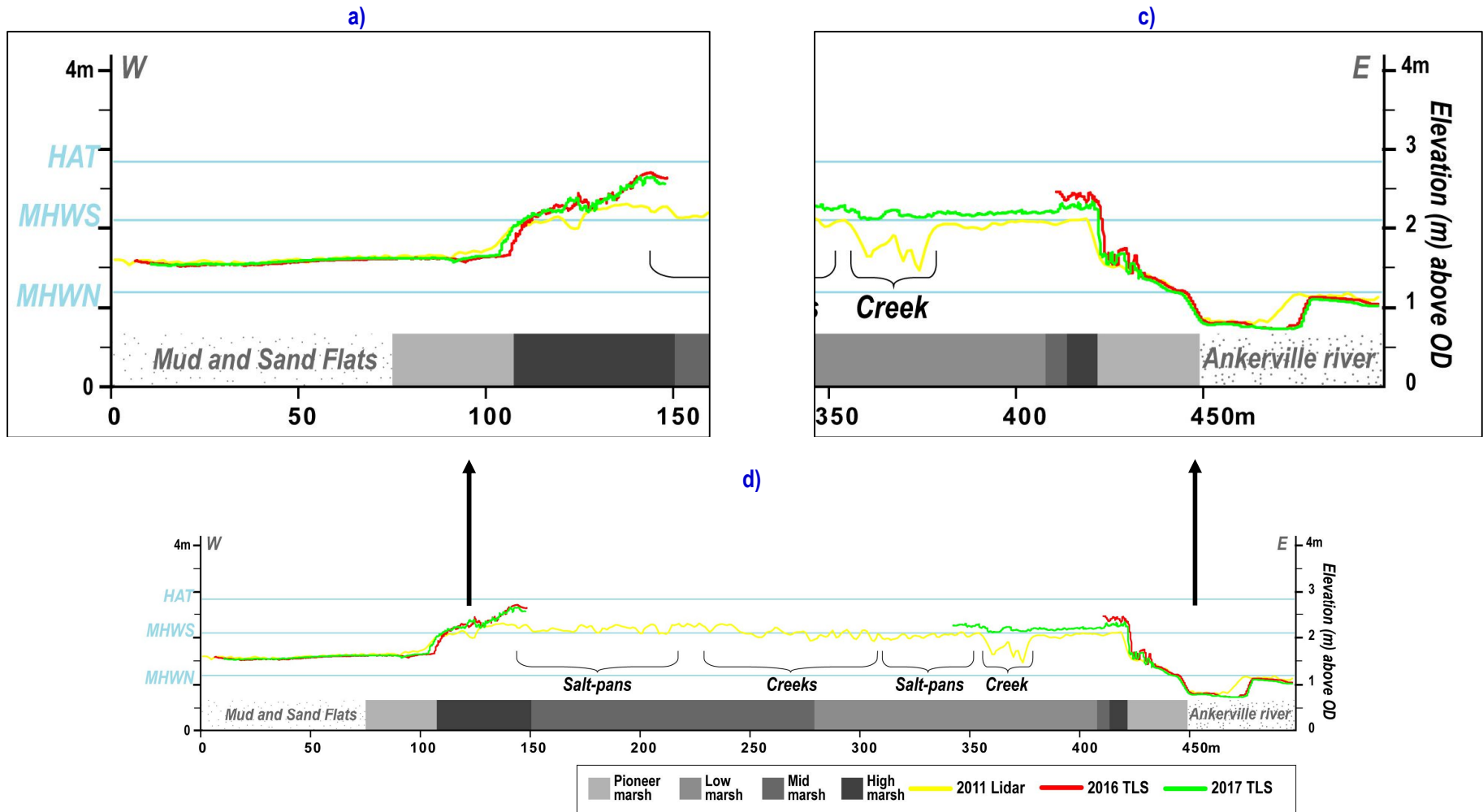
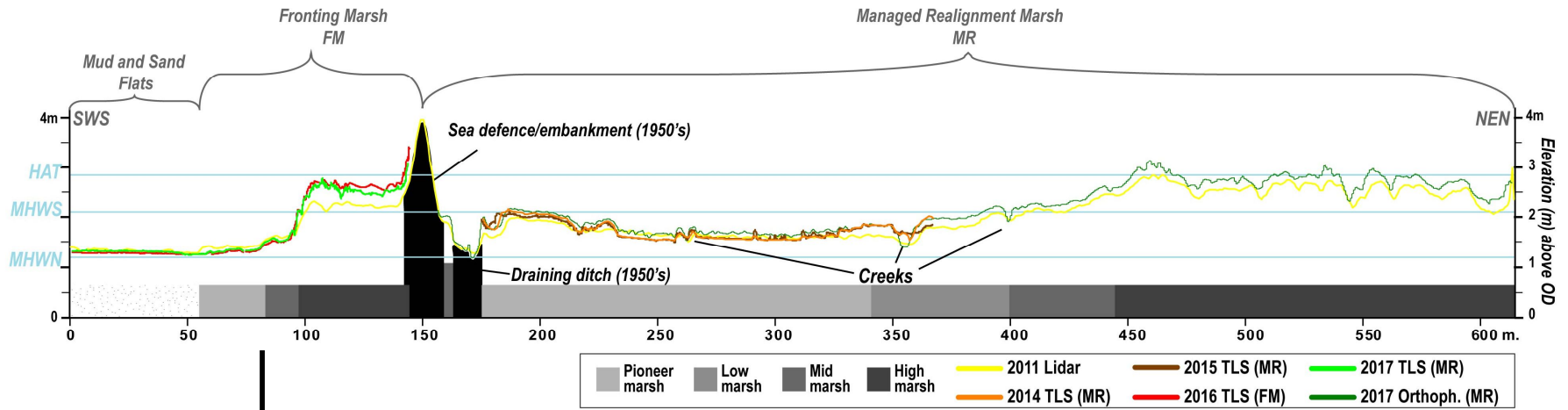


Figure 5-19: **d)** A schematic overview of some morphological characteristics of a cross-shore profile for the natural salt marsh ANK showing the marsh surface height from 2011 to 2017 depicted as line coloured for different survey type used in this analysis. **a)** and **b)** are insets that provide an enlarged views of the eastern and western cross-shore profiles. **Note1:** vertical exaggeration 21.3X **Note2:** the major creek system on the eastern part of the marsh (right on graph) has not been captured during 2016 TLS campaign. Also a shallow depression is visible: the creek may have full during capture – however this feature has been removed from the height change analysis (see Figure 5-22).

a)



b)

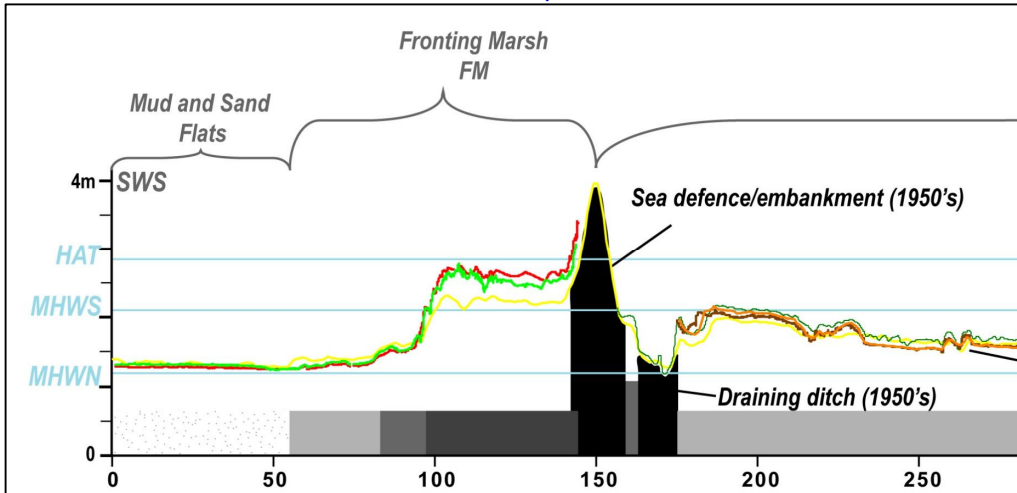


Figure 5-20: A schematic overview of some morphological characteristics of a cross-shore profile for the fronting marsh FM and managed realignment MR (transect location see Figure 5-22) showing the marsh surface height from 2011 to 2017 depicted as line coloured for different survey type used in this analysis. **b)** is an inset that provides an enlarged view of the south-west-south cross-shore profiles. Note1Note1: vertical exaggeration 21.3X.



### 5.3.2 Surface elevation change using airborne and TLS DEM surfaces from 2011 to 2017

The previous section 5.3.1 provided 2D analysis of airborne and TLS DEM (Digital Elevation Model) surfaces from 2011 to 2017 by means of cross-sections allowing a detail snapshot of changes in the saltmarsh cross-shore profiles; using the same surfaces, a 2.5D analysis (2.5 Dimensions is a pseudo-dimensional construct that refers to a functional surface, represented by a planar 2D object with Z (height) attributes as opposed as 3D describes a space with three parametric directions of movement - height, width, and depth-) is presented in this section accounting for changes that occurred in height, area and volume on the low parts (fronting mudflat, pioneer and low-marsh zones) of the three salt marshes (Table 5-3 and Figure 5-21). Overall changes in elevation height display loss primarily located on mudflats and pioneer zones whilst overall gain is situated on the vegetated areas of the salt marshes (Figure 5-22).

On ANK 2.2±0.8 ha (26.5% of the marsh) primarily located on the vegetated areas increase of 0.05 to 0.15 m in height whilst 4.1±1.4 ha (48.7% of the marsh) concentrated on the pioneer and mudflat areas demonstrate an elevation loss of -0.05 to 0 m associated with further loss (-0.6±0.2 ha) on the mudflats reaching up to 0.24 m in height where tidal current cause deep scouring. On FM, 5.3±1.9 ha (65.8 % of its extent) is in height deficit of -0.05 to 0 m also accompanied by deep scouring on FM mudflats especially south of westernmost breach. 1±0.4 ha of FM (12.9 % of the marsh) gain height of 0.05 to 0.15 m and 0.9±0.3 ha (10.7 % of the marsh) rise of 0.15 to 0.25 m. In parallel, MR does not present signs of tidal forcings like FM and ANK allowing 6±0.1 ha (80.6 % of the marsh) to benefit of the sediment input of which 3.7±1.4 ha (50.1 % of the marsh) increased of in 0 to 0.05 m height and 2.3± 0.8 (30.4% of the marsh) rise of 0.05 to 0.15m in height.

**Table 5-3: Summary of the surface elevation height change (in m) using airborne and TLS DEMs from 2011 to 2017 surveys (table 3-9) on the three sites (n= a cell of 0.1\*0.1 m).**

ANK					FM					MR				
Min	Max	Mean	SD	n	Min	Max	Mean	SD	n	Min	Max	Mean	SD	n
-0.46	+0.52	+0.021	0.07	195657	-0.21	+0.46	+0.022	0.08	169275	-0.24	+0.21	+0.021	0.03	116289

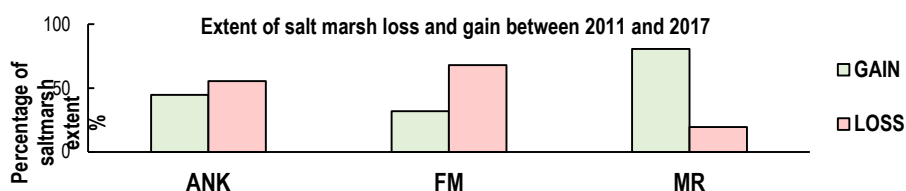


**Figure 5-21: Summary graph presenting the extent (as a percentage of its size) has gained and lost height from 2011 to 2017 airborne and TLS surveys (table 3-9) by salt marsh as depicted in Figure 5-22.**

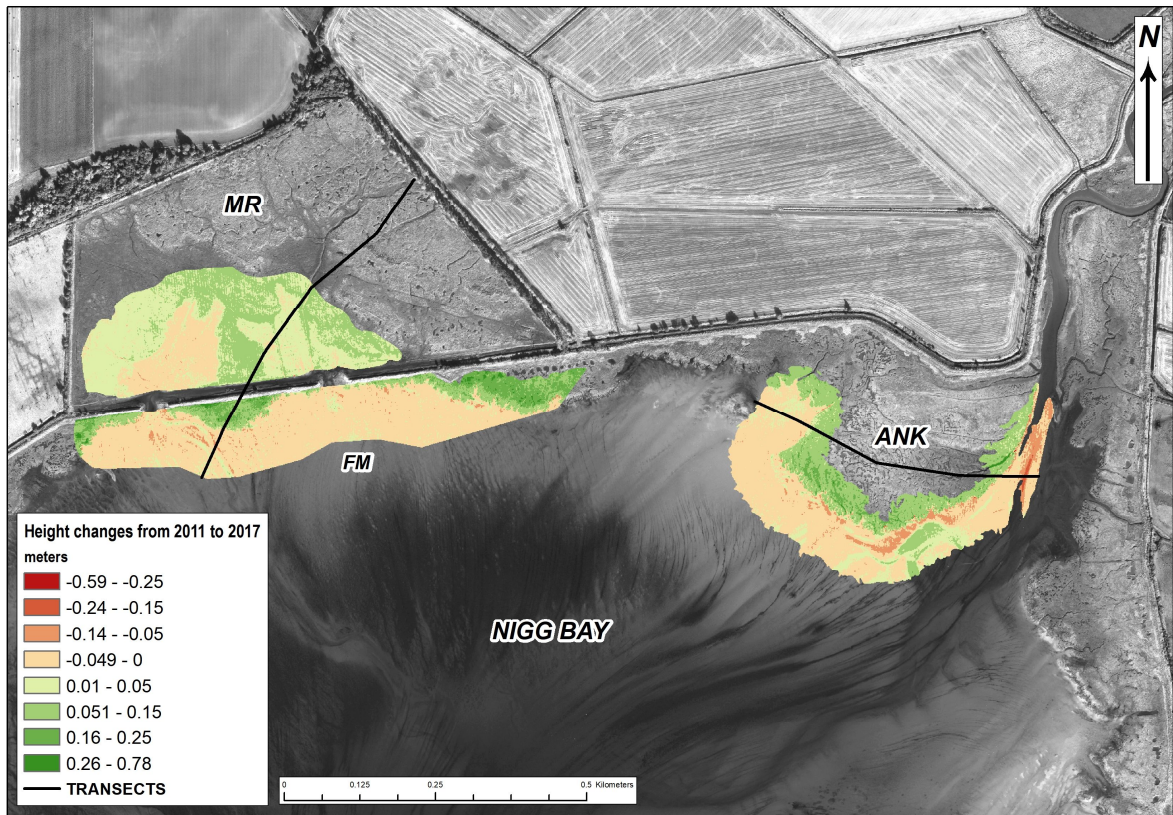


Figure 5-22: Height change map (in m) from 2011 to 2017 airborne and TLS surveys (table 3-9) highlighting areas of accretion (light to dark green) primarily located on vegetated areas of the marsh and erosion tends to occur on the foreshore.

The results display for the total area of salt marsh surveyed from 2011 to 2017 an overall areal increase of  $1.28 \pm 0.12\%$  at a rate of  $0.002 \pm 0.0001 \text{ ha} \cdot \text{yr}^{-1}$  (or  $21.29 \pm 3.55 \text{ m}^2 \cdot \text{yr}^{-1}$ ). The natural saltmarsh sites ANK and FM have lost  $-5.8 \pm 0.01\%$  and  $-18.8 \pm 0.04\%$  respectively. In contrast, the managed realignment expanded by  $30.76 \pm 0.4\%$  (Table 5-4). These areal changes were accompanied on the three salt marshes, an overall volumetric gain of  $25.61 \pm 0.34\%$  is at a rate of  $0.04 \pm 0.0004 \text{ m}^3 \cdot \text{yr}^{-1}$ . Across 6 years there is a striking uniformity in the volumetric results (loss and gain of volume of marsh (vegetation + sediment)) on the two-natural salt marshes ANK and FM which both gain c.20% in volume whilst MR gain  $42.15 \pm 0.55\%$  in volume (Figure 5-23); yet there is an elevational loss in all but MR (Figure 5-21 and Figure 5-22) suggesting a release of sediments from surface of ANK and FM or better interception of sediments by MR as it is now acting as a sink.

Table 5-4: Volumetric and areal changes on three studied salt marsh ANK, FM, and MR (sum total of  $23.84 \pm 0.58 \text{ ha}$ ) over a period of 6 years (2011-17). SE has been calculated here on each cell where precision depends on the accuracy of survey measures of the mass points

	% changes (ANK)			% changes (FM)			% changes (MR)		
	Loss	Gain	Overall	Loss	Gain	Overall	Loss	Gain	Overall
<b>Volum</b> <b>e</b>	$29.91 \pm 0.4$ 2	$70.09 \pm 0.4$ 2	$20.09 \pm 0.05$	$29.25 \pm 0.3$ 0	$70.75 \pm 0.3$ 0	$20.75 \pm 0.04$	$7.85 \pm 0.32$	$92.15 \pm 0.3$ 2	$42.15 \pm 0.5$ 5
<b>Area</b>	$55.79 \pm 0.4$ 2	$44.21 \pm 0.3$ 3	$-5.79 \pm 0.0$ 1	$68.79 \pm 0.3$ 0	$31.21 \pm 0.4$ 4	$-18.79 \pm 0.0$ 4	$19.24 \pm 0.3$ 2	$80.76 \pm 0.3$ 6	$30.76 \pm 0.4$

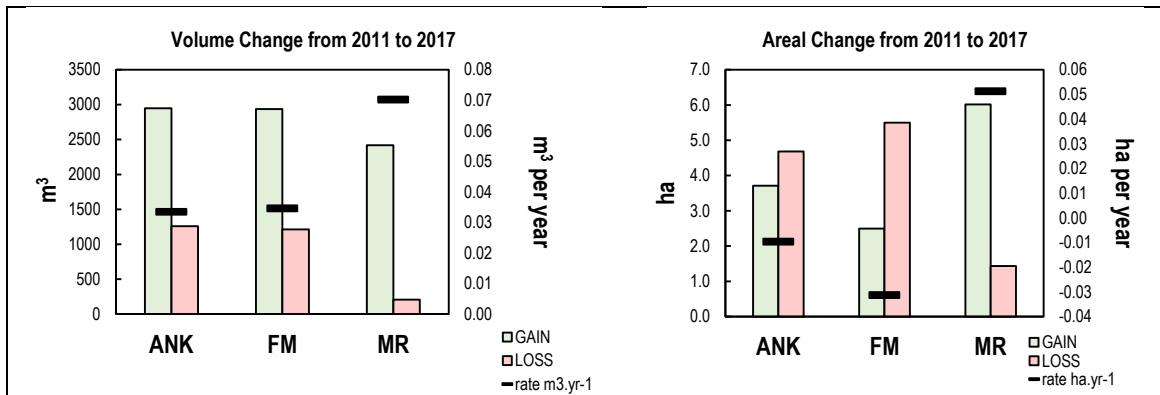


Figure 5-23: Column graphs presenting the volume (left) and areal (right) change that occurred on the three salt marsh sites from 2011 to 2017 using TLS, Orthophotography and Lidar datasets showing in green gains, red losses and black line symbol representing average rate per year in m<sup>3</sup> per year.

#### 5.4 Surface elevation changes (representing accretion and erosion) and sedimentation rates by means of sedimentation plates from 2015 to 2017

We have seen in Chapter 3 – 3.3.1 that deposition corresponds to the amount of accumulated material, whilst sedimentation is the difference in elevation due to accretion and erosion, based on a reference height over a given time interval (Pye and French, 1993). The analysis of the digital elevation model (DEM) in section 5.3.2 provides information on the changes in elevation, area, and volume of the salt marsh surface during the overflight or survey. Nevertheless, there are certain limitations associated with the ability of this method to accurately determine the variation in sedimentation rates over a long-term period, particularly if it spans multiple years or decades, as well as the ability to establish the underlying driving mechanisms. To address this, a network of 60 sedimentation plates (see Chapter 3 – 3.4.2.2 and Figure 3-32) was deployed between the months of July and November 2015 with measurements taken until September 2017 (Chapter 3 – 3.4.2.2.). The primary aim of this deployment was to establish:

- i. spatial variation of surface elevation change across all saltmarsh zones in the three salt marshes relative to a 0 cm benchmark to provide a measure of accretion and erosion rates known as sedimentation rates;
- ii. seasonal variation in sedimentation rates over 2 summers (September/October) and 2 winters (March/April). (Chapter 3 - Figure 3-29);
- iii. dynamic variation: are sedimentation rates calculated from sedimentation plates influenced by physical and/or biological factors?

Details on fieldwork, spatial and temporal sampling, measurements and calculations are treated in Chapter 3 – 3.4.2.2. Details of the statistics used can be found in Chapter 3 – 3.4.5.

### 5.4.1 Sedimentation rates derived from sedimentation plates

The average sedimentation rates between each survey campaign, site and saltmarsh zone, ranging between  $-1.01$  and  $1.92 \text{ cm.yr}^{-1}$ , are estimated to  $0.21 \pm 0.07 \text{ cm.yr}^{-1}$  over 2.15 years (22 lunar cycles).

#### 5.4.1.1 Spatial variation in sedimentation rates derived from sedimentation plates

Sedimentation rates as measured by sedimentation plates are found to be significantly different between the sites ( $H_{(df=2)} = 18.1^{***}$ ). The managed realignment salt marsh exhibits a positive sedimentation rates at  $0.33 \pm 0.03 \text{ cm.yr}^{-1}$ , whereas ANK maintains its height at  $0.01 \pm 0.04 \text{ cm.yr}^{-1}$  and FM show a negative rate of  $-0.09 \pm 0.16 \text{ cm.yr}^{-1}$  (Table 5-5) with MR showing the highest rank compared to ANK and FM, whilst no difference is detected between ANK and FM, but no difference between ANK and FM (Figure 5-24 and Table D-2).

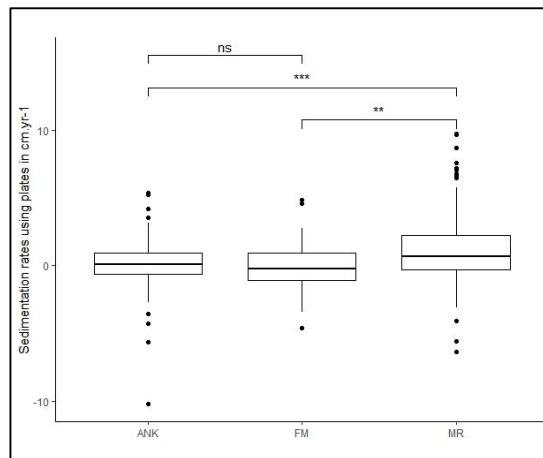


**Figure 5-24: Boxplot of the average sedimentation rates per sites depicting high sedimentation on MR and ANK whilst FM exhibited a low sediment gain.** (Kruskal-Wallis H test and significant pair-test comparison using Dun's tests results by the p-value significance: *ns*, \*, \*\*, \*\*\* for  $> 0.05$ ,  $\leq 0.05$ ,  $\leq 0.01$ ,  $\leq 0.001$ ). Boxplots represent median (middle line) interquartile range (box), 1.5 times interquartile range (bar) and outliers (stars)).

Sedimentation rates as measured by sedimentation plates are found to be significantly different between the sites' saltmarsh zones ( $H_{(df=10)} = 53.46^{***}$ ); with MR's low-marsh, LM, showing the highest rank compared to its mid-marsh, MM, and high-marsh, HM, zones and compared to ANK's low-marsh (Figure 5-25 and Table D-3).

Despite the impact of the high standard deviation and wide confidence intervals on the statistical significance of the pairwise comparisons, it is evident from Figure 5-25 that discernible distinctions exist between saltmarsh zones at each site. In the study, it was observed that the LM zones of MR and ANK exhibited the highest rates when compared to all other zones, as indicated

in Table 5-5. The elevation of ANK's high marsh (HM) exhibited a greater increase compared to its pioneer-marsh, PM (Table 5-5). Conversely, ANK's PM zones witnessed the highest erosion rates during the project, in contrast to the MR and FM salt marshes, especially on the ESE shore edge where sampling point A5 constantly lost height confirming trends observed between 2011 to 2017. In contrast to the MR and FM salt marshes, the PM zones of ANK experienced the highest erosion rates throughout the project, particularly along the ESE shoreline where sampling point A5 consistently lost height (Figure 5-29 to Figure 5-35). This pattern validates the trends observed from 2011 to 2017 (Figure 5-22). Based on the observed sedimentation rate on the MR salt marsh mentioned above, it can be inferred that the increase in MR comes at the cost of a decrease in FM (and potentially ANK) in a manner consistent with the broader conclusions discussed in section 5.3.

In this study, the variation between sites and saltmarsh zones was examined using a general linear model. The results of this analysis are presented in Table D-6. The analysis reveals that a mere 5 % ( $r^2_{adj}$ ) of the observed variation in sedimentation can be accounted for by the sites alone, while 12% ( $r^2_{adj}$ ) of the variability can be explained by incorporating the saltmarsh zones of the sites as predictors. Specifically, the ANK's PM zone, FM's HM and MM zones, and MR's LM zone make the most significant contributions to the predictive model.

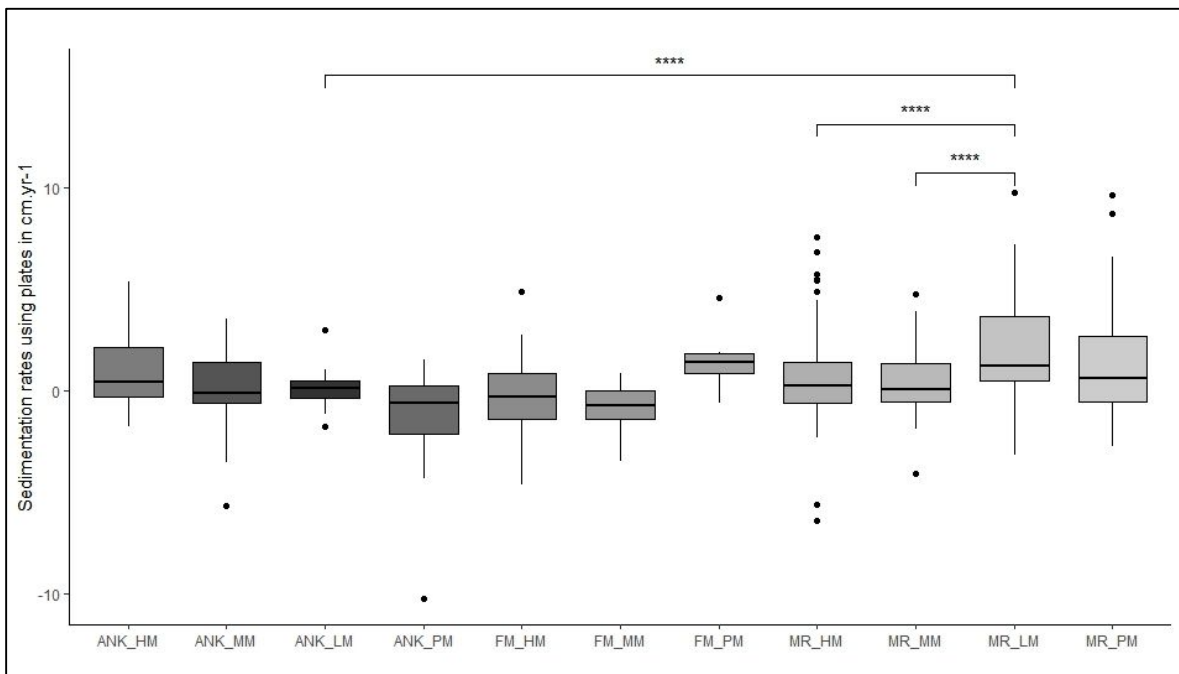


**Figure 5-25: Boxplot of the average sedimentation rates plates (cm per year) derived from sedimentation plates per sites' saltmarsh zones depicting high sedimentation.** (Kruskal-Wallis H test and significant pair-test comparison using Dun's tests results by the p-value significance: *ns*, \*, \*\*, \*\*\*\* for  $> 0.05$ ,  $\leq 0.05$ ,  $\leq 0.01$ ,  $\leq 0.001$ ). Boxplots represent median (middle line) interquartile range (box), 1.5 times interquartile range (bar) and outliers (stars).

**Table 5-5: Average sedimentation rates derived from sedimentation plates (cm per year) across the three salt marshes.**

	ANK					FM					MR				
	Min	Max	Mean	SD	n	Min	Max	Mean	SD	n	Min	Max	Mean	SD	n
HM	-0.12	0.75	<b>0.19</b>	0.36	-0.12	-0.74	0.29	<b>-0.12</b>	0.46	21	-0.45	0.64	<b>0.12</b>	0.38	91
MM	-0.07	0.63	<b>0.10</b>	0.27	-0.07	-0.43	-0.16	<b>-0.30</b>	0.14	14	-0.58	0.69	<b>0.09</b>	0.37	84
LM	-0.15	0.30	<b>-0.01</b>	0.19	-0.15						-0.63	1.40	<b>0.63</b>	0.55	49
PM	-1.07	0.11	<b>-0.48</b>	0.61	-1.07	0.41	0.41	<b>0.41</b>	0.00	7	-0.36	1.92	<b>0.42</b>	0.74	49
<b>Overall</b>	<b>-1.1</b>	<b>0.8</b>	<b>0.01</b>	<b>0.4</b>	<b>105</b>	<b>-0.7</b>	<b>0.4</b>	<b>-0.09</b>	<b>0.4</b>	<b>42</b>	<b>-0.6</b>	<b>1.9</b>	<b>0.33</b>	<b>0.6</b>	<b>273</b>

#### 5.4.1.2 Temporal variation in sedimentation rates derived from sedimentation plates

The sedimentation rates derived from sedimentation plates exhibit a lack of a discernible linear trend, as evidenced by the low  $r^2$  value ( $r^2_{adj}=0.18\%$  - Figure 5-26). However, there are significant variations in these changes based on the time of the collection ( $H_{df=6} = 45.782$ ;  $p < 0.001$ \*\*\*). Sediment accumulation occurred between the burial dates of the plates (July 2015 for MR and September 2015 for ANK and FM) until November 2015, with an average accumulation rate of 2.77 cm per year. The aforementioned trend was subsequently succeeded by a reduction in rate, reaching 0.94 cm per year, during the period spanning from November 2015 to February 2016. During a three-month period from February to April 2016, which marked the conclusion of the winter season, there was an observed increase in sediment accumulation at a rate of 2 cm per year in the overall surface elevation. The obtained results exhibited a statistically significant increase compared to all other measurements conducted throughout the duration of the project (Figure 5-27). The combined results from July and October 2016 indicate a decrease in sedimentation rate of 0.55 cm per year. Furthermore, there was an additional decrease from October to April 2016, with a low rate of 0.06 cm per year. During the period spanning the four winter months of 2016/17, the Nigg Bay salt marshes exhibited a sedimentation rate of 0.11  $\text{cm.yr}^{-1}$ . Subsequently, following the conclusion of summer in 2017, the three salt marshes observed an augmentation in their sedimentation rate, amounting to 0.192  $\text{cm.yr}^{-1}$  over a duration of six months. The sedimentation rates obtained from sedimentation plates indicate a general increase of  $0.21 \pm 0.07$  cm per year over the duration of the survey, which spanned a period of 2.15 years. Although, there is a significant variation in sedimentation rates between each collection campaign, time lag appears not to account for the ability to predict sedimentation rates (Table D-6 (3);  $r^2_{adj} = 5\%$ \*\*\*).



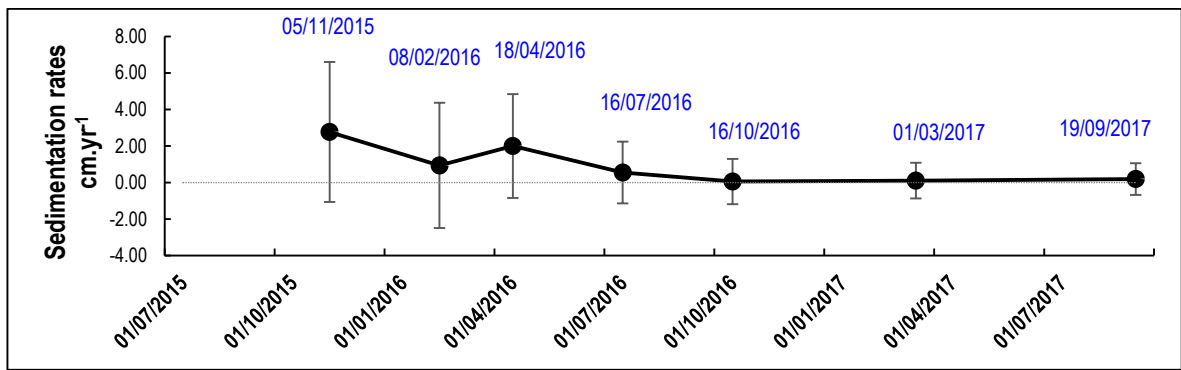


Figure 5-26: Interval plot of the overall sedimentation rates derived from sedimentation plates from 29<sup>th</sup> July 2015 to 19<sup>th</sup> September 2017 (Standard Deviation used to calculate errors bar intervals).

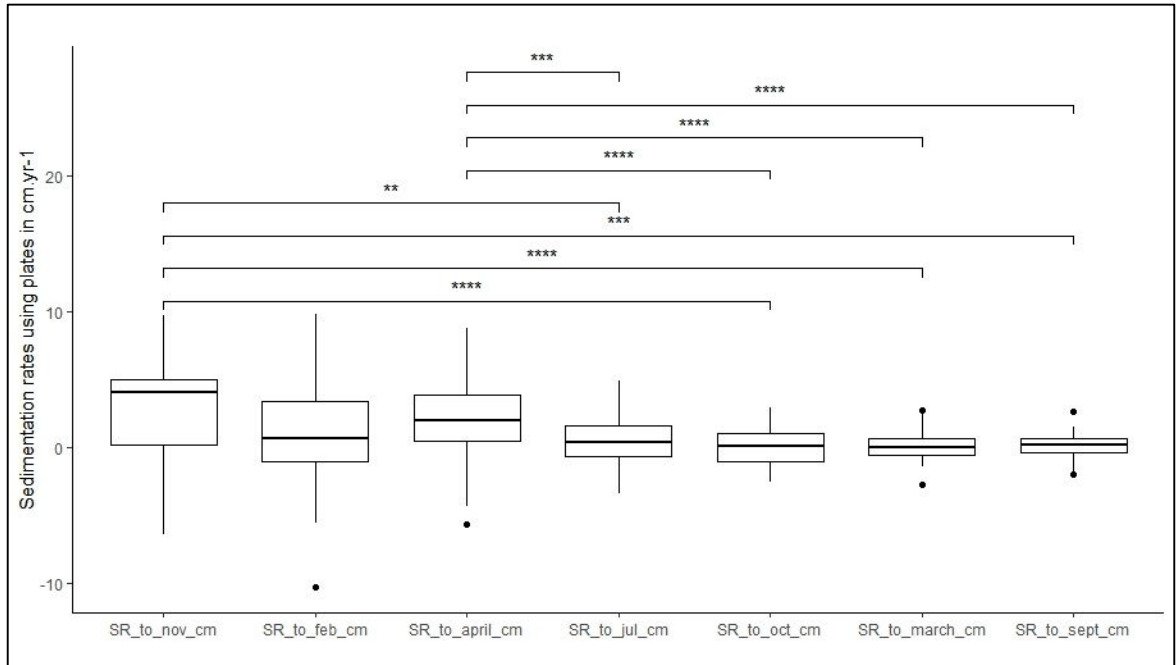


Figure 5-27: Boxplot of the average sedimentation rates plates (cm per year) derived from sedimentation plates by monitoring period. (Kruskal-Wallis H test and significant pair-test comparison using Dun's tests results by the p-value significance: ns, \*, \*\*, \*\*\* for  $> 0.05$ ,  $\leq 0.05$ ,  $\leq 0.01$ ,  $\leq 0.001$ . Boxplots represent median (middle line) interquartile range (box), 1.5 times interquartile range (bar) and outliers (stars)).

#### 5.4.1.3 Spatial and temporal variation in sedimentation rates derived from sedimentation plates

Caution should be exercised when contemplating the observed temporal variation in the previous section 5.4.1.2. The results also suggest that, following a duration of 2.15 years, the sedimentation plates have achieved a state of equilibrium, as demonstrated by the decline in standard deviation values starting from October 2016 (Figure 5-26). This assertion is substantiated when examining the outcomes for each salt marsh (Figure 5-28). This also implies that the plates have attained the ability to produce dependable and meaningful measurements.

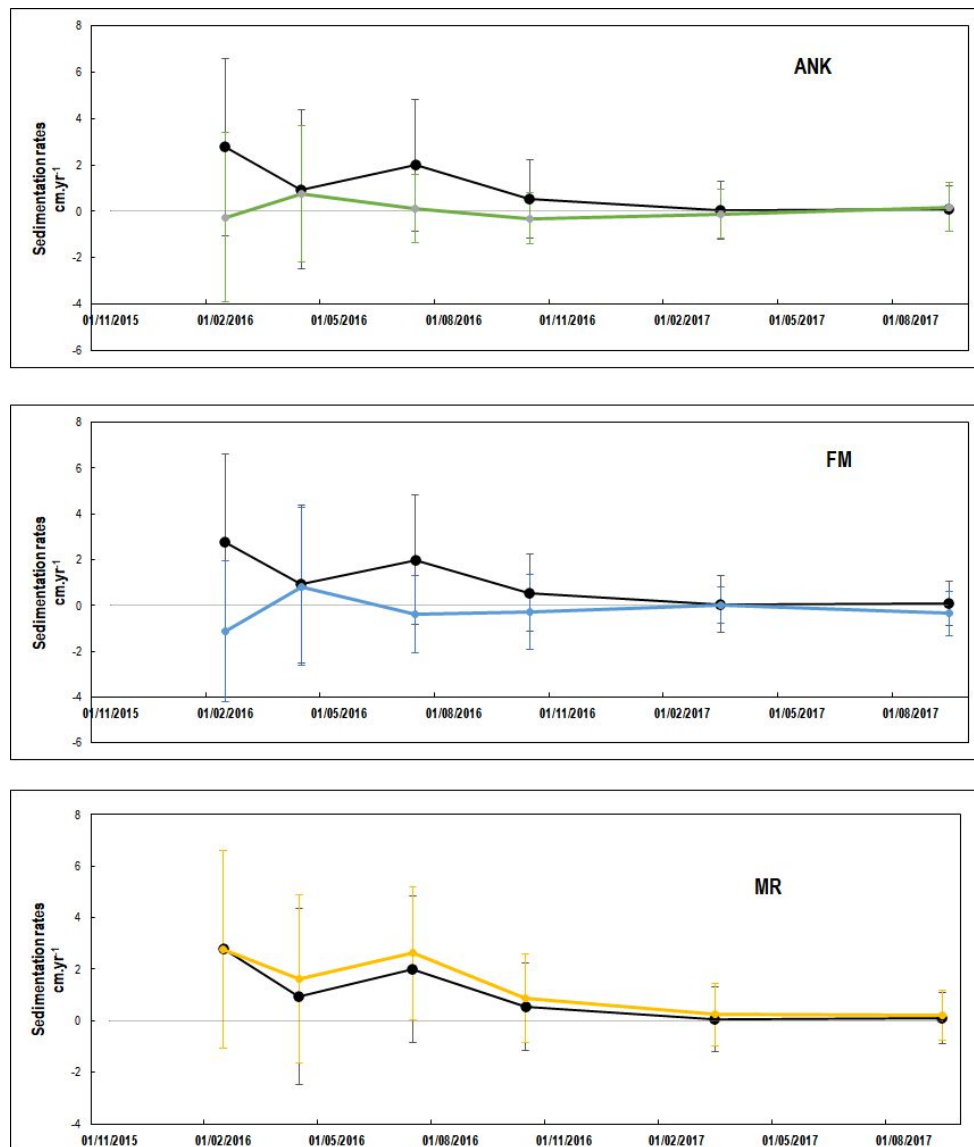


Figure 5-28: Interval plots of ANK (top- in green), FM (middle - in blue) and MR (bottom- in yellow) compared to the average sedimentation average sedimentation rates derived from sedimentation plates (all- in back) from 29<sup>th</sup> July 2015 to 19<sup>th</sup> September 2017 (SD used to calculate errors bar intervals).

The time series mapping, as depicted in Figure 5-29 to Figure 5-35, serves to emphasise the variations in sedimentation rates obtained from sedimentation plates over the project study, encompassing all sites and saltmarsh zones. The maps demonstrate that the MR's HM and MM zones exhibit greater variability in sedimentation compared to the lower zones (LM and PM). This variability may be potentially ascribed to seasonal fluctuations arising from vegetation dieback (Baaij et al., 2021). Furthermore, it is evident that there is a distinct trend of erosion in the east-southeast (ESE) and deposition in the west-southwest (WSW) parts of the MR marsh (observation is supported by the data presented in Figure 5-30, Figure 5-34 and Figure 5-35). This finding also confirms the previously discussed asymmetry in sediment distribution as shown in the spatial variation of short-term accretion rates presented in Chapter 4 (Figure 4-3 and Figure 4-71). This asymmetry is thought to be due to the presence of backwater in the remaining reclamation ditches, as shown in Figure 3-7, which shows the remnants of the

reclamation features after the 2003 realignment. In addition, it is possible that the vegetation present in the MM and HM zones of MR, which are still undergoing transition since their breach, may not effectively contribute to sediment retention compared to the vegetation assemblages observed in the western section of MR marsh. This western area is primarily characterised by LM vegetation, including *Puccinellia maritima* and *Aster Tripolium*.

The time series mapping analysis also indicates that the easternmost coastal edges of the natural salt marshes FM and ANK consistently exhibit vulnerability to erosion. This is true of location A15, FM3 and FM4 (Figure 5-29 to Figure 5-35). The phenomenon of reduced sedimentation rates has been analysed and interpreted by multiple researchers (Deegan et al., 2012; Lowe et al., 2018; Fung et al., 2018) as a potential causative factor in the decline and submergence of the marsh.



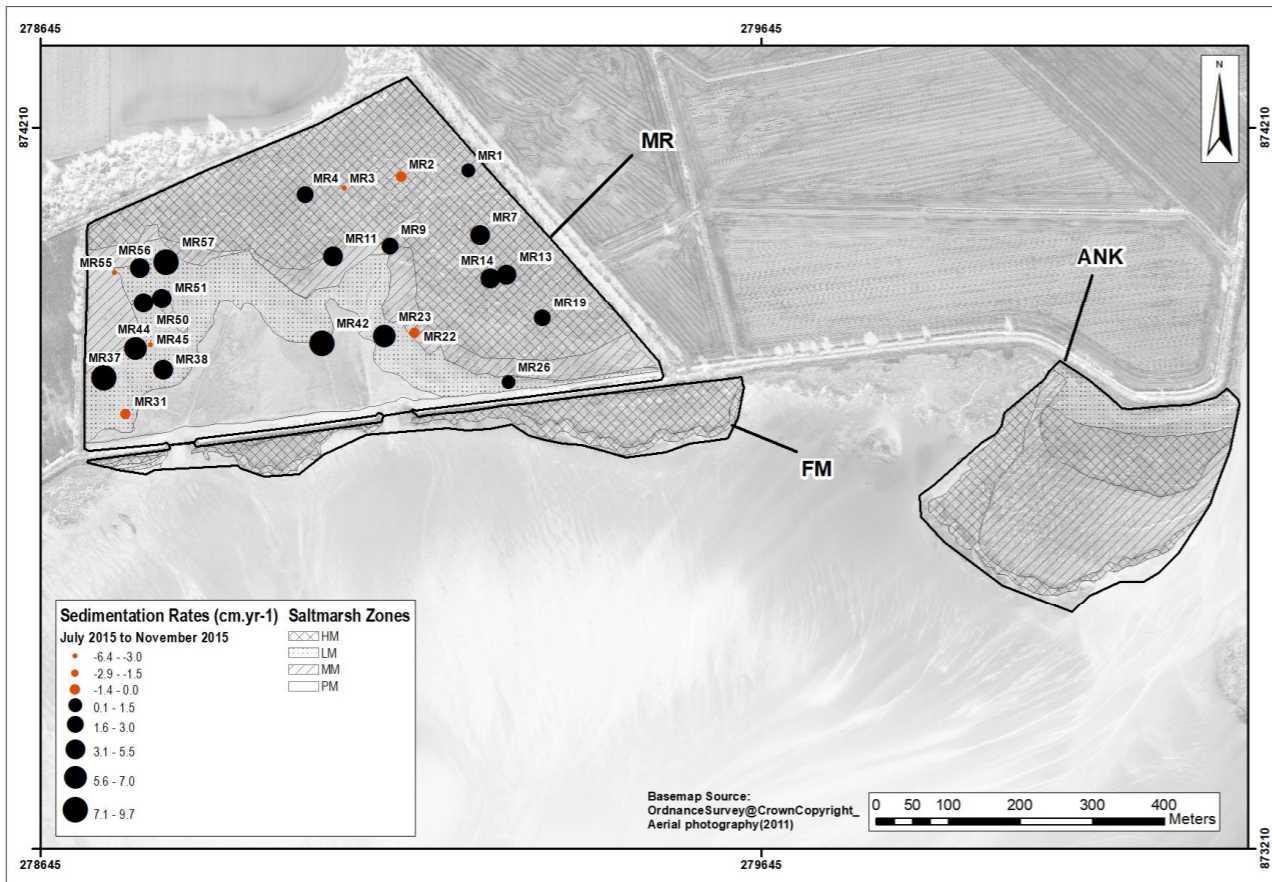


Figure 5-29: Sedimentation rates (cm per years) using sedimentation plates for 3.2 months (July to November 2015). Note that FM and ANK were not in place yet.

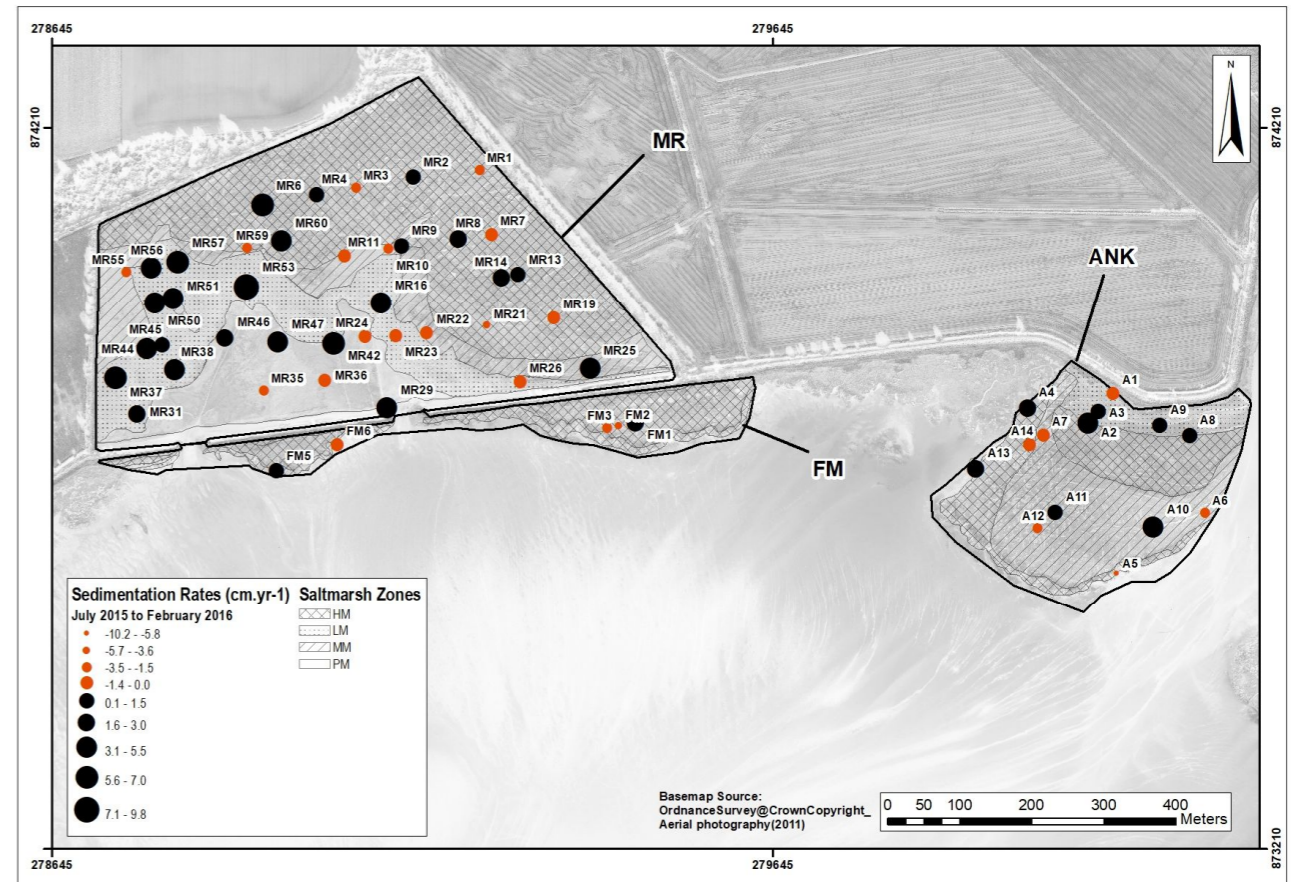


Figure 5-30: Sedimentation rates (cm per year) using sedimentation plates for 6.3 months (July 2015 to February 2016) for plates shown in Figure 5-29 & 3.1 months for the remaining plates.

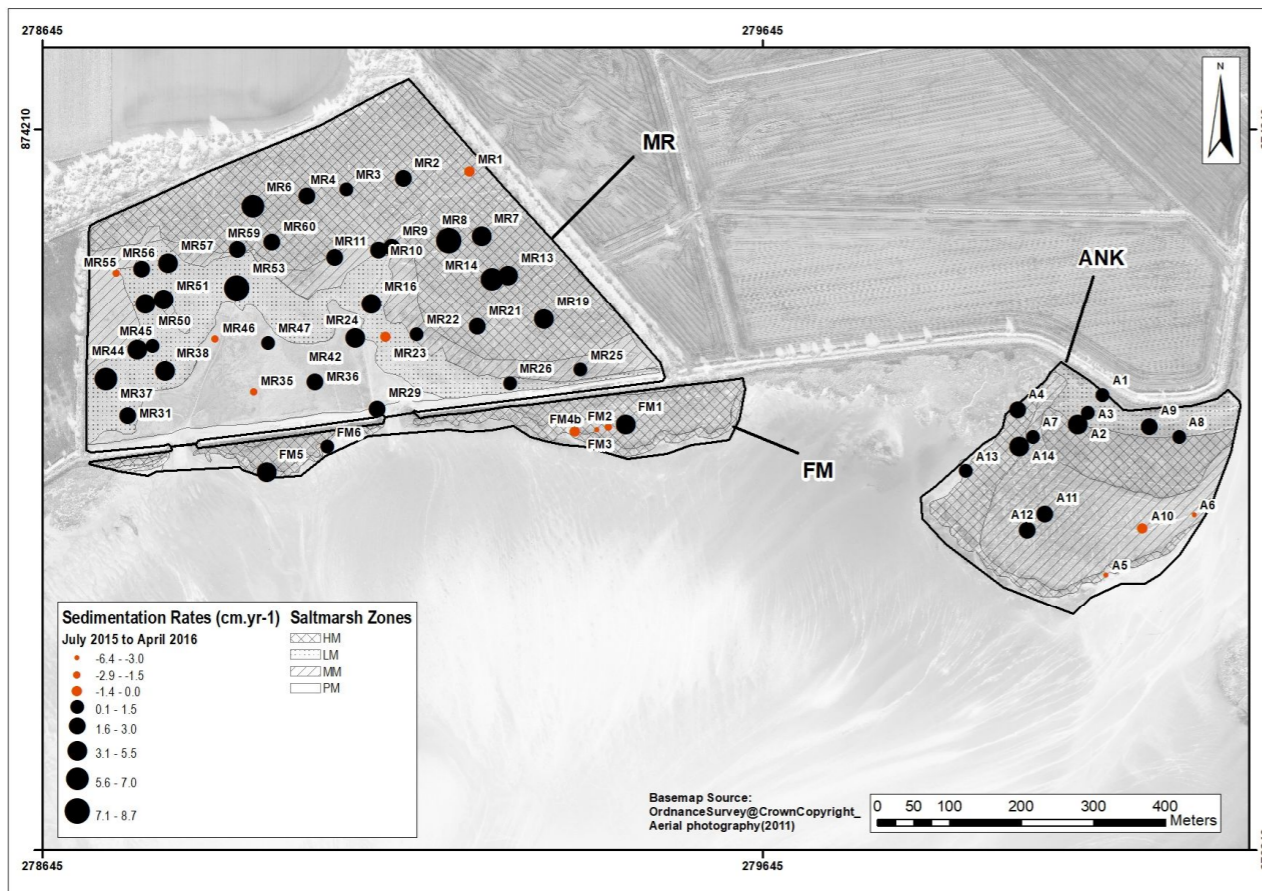


Figure 5-31: Sedimentation rates (cm per year) using sedimentation plates for 8.7 months (from July 2015 to April 2016) for plates shown in Figure 5-29 & 5.5 months for the remaining plates.

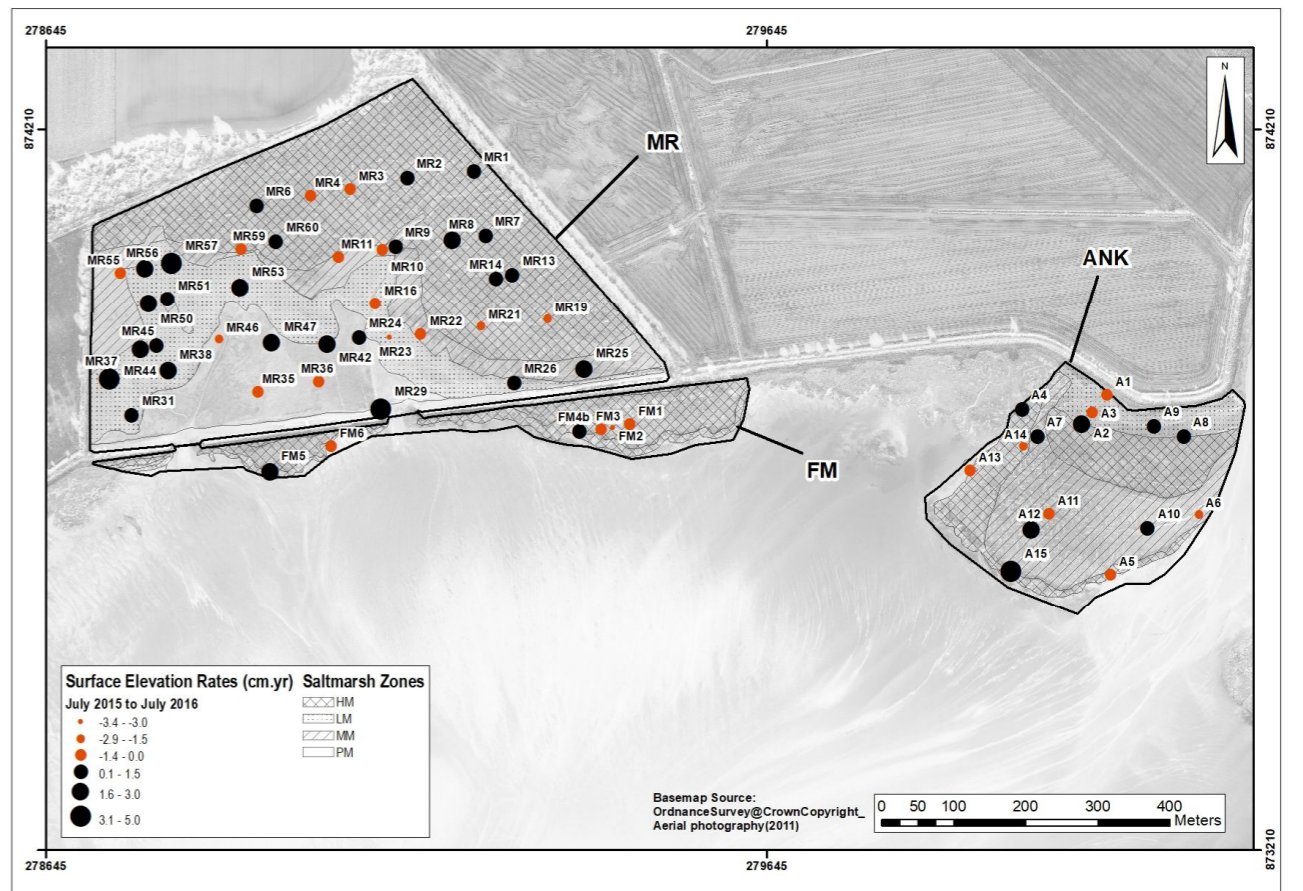


Figure 5-32: Sedimentation rates (cm per year) using sedimentation plates for 11.6 months (July 2015 to July 2016) for plates shown in Figure 5-29 & 8.4 months for the remaining plates.



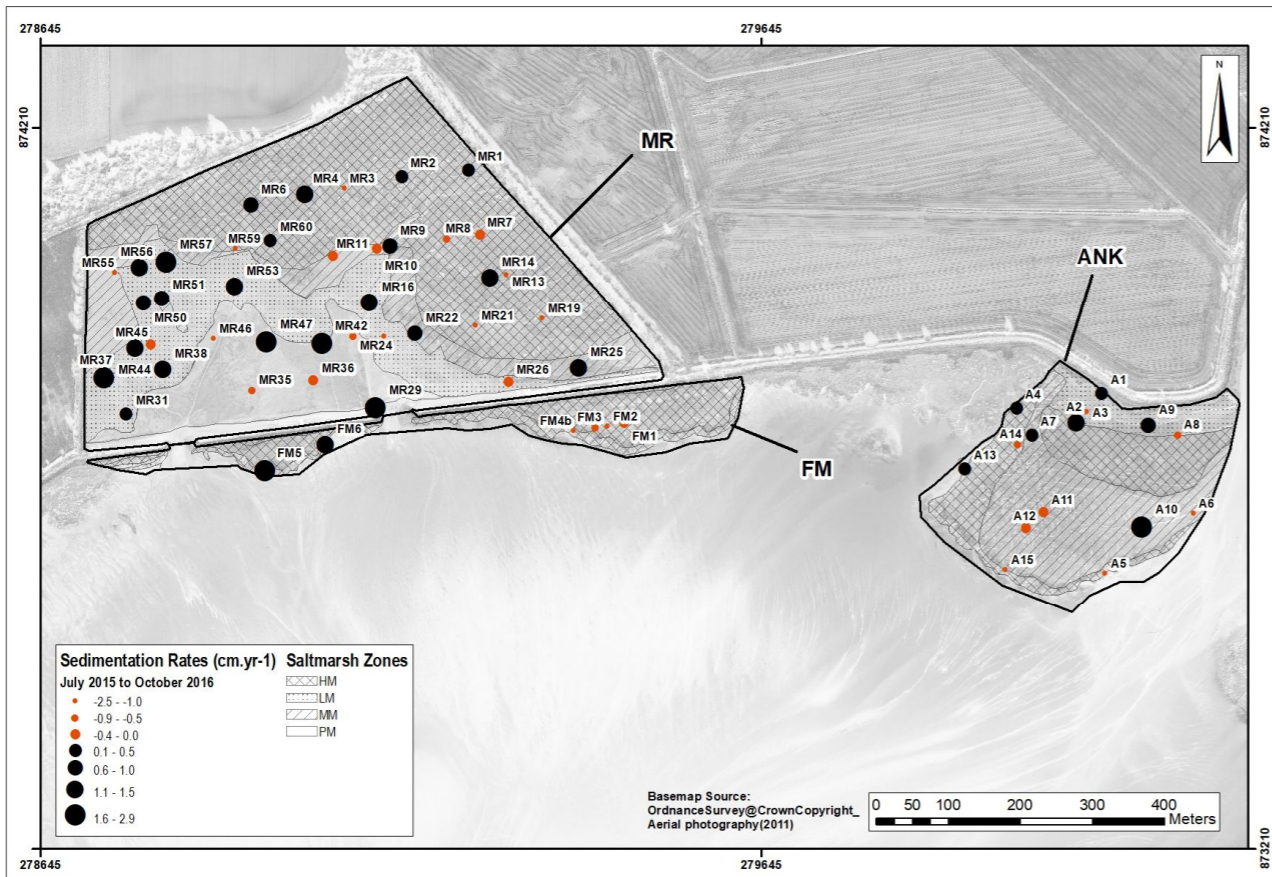


Figure 5-33: Sedimentation rates (cm per year) using sedimentation plates for 1.2 year (July 2015 to October 2016) for plates shown in Figure 5-29 & 11.5 months for the remaining plates.

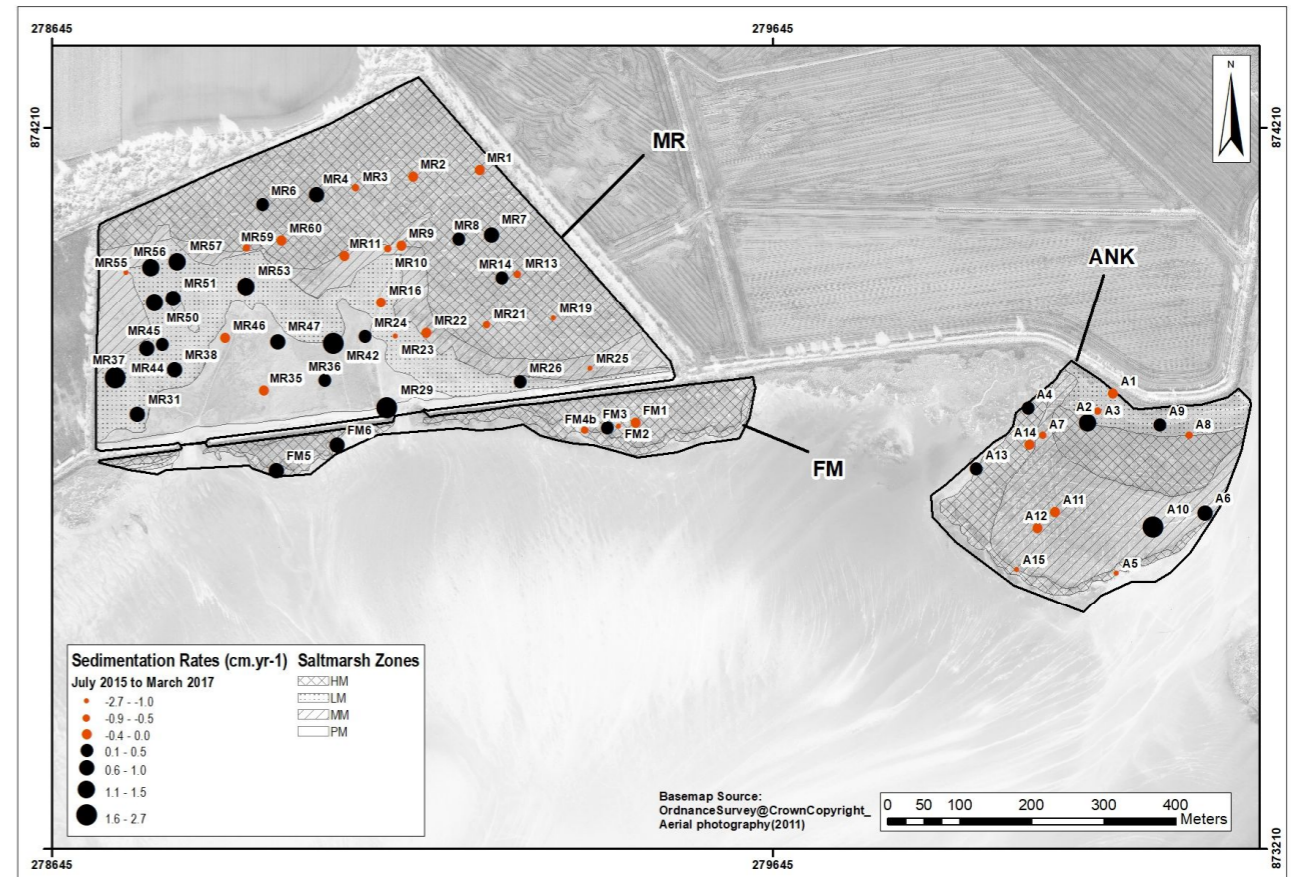


Figure 5-34: Sedimentation rates (cm per year) using sedimentation plates for 1.7 year (July 2015 to March 2017) for plates shown in Figure 5-29 & 1.3 years for the remaining plates.

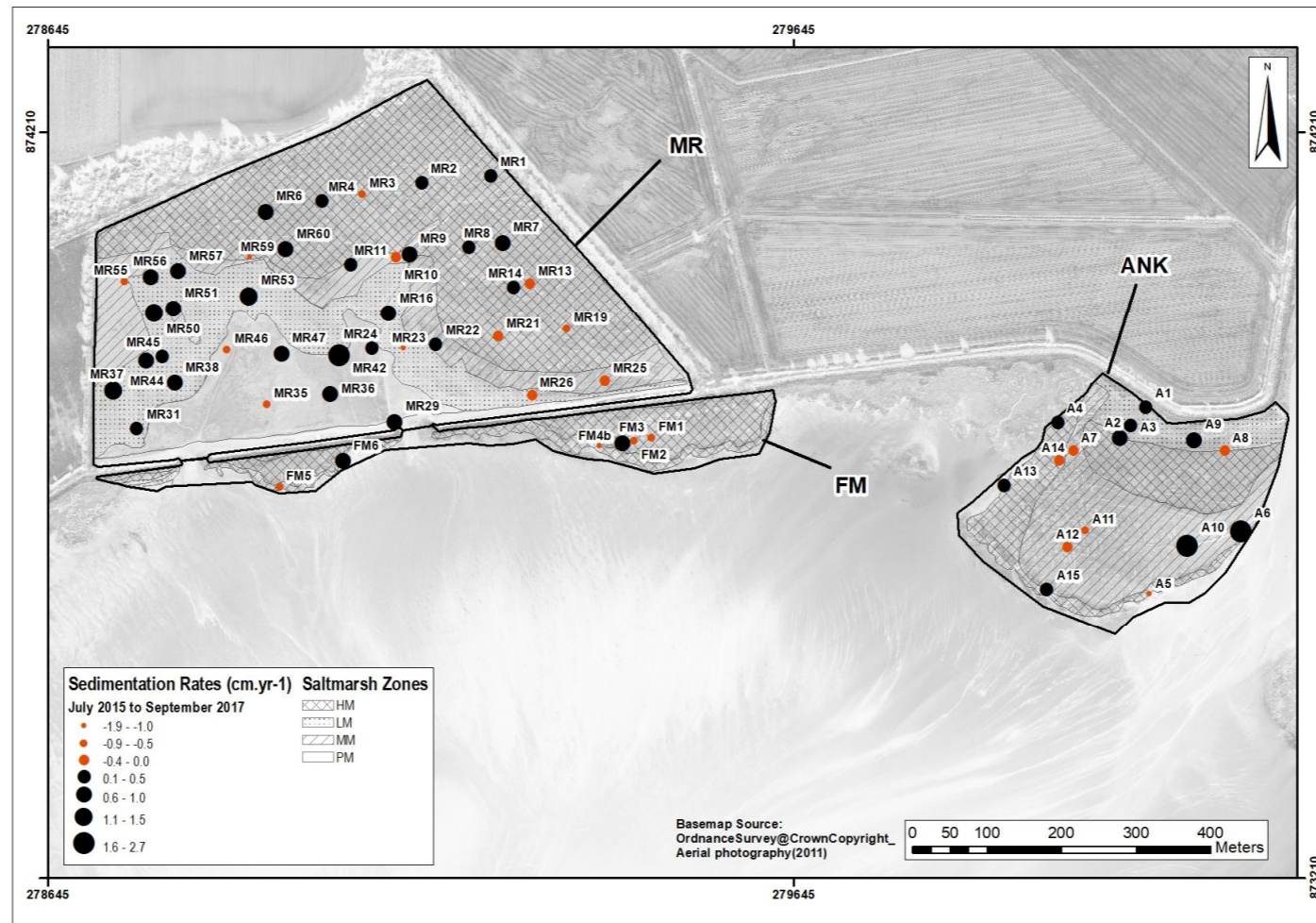


Figure 5-35: Sedimentation rates (cm per year) using sedimentation plates for 2.15 year (July 2015 to September 2017) for plates shown in Figure 5-29 & 1.9 years for the remaining plates.

#### **5.4.2 Biological and geomorphological controls on sedimentation rates (using sedimentation plates)**

The examination of sedimentation patterns involved the identification of associations between physical drivers, in Chapter 3 – section 3.3.2.3, Appendix B.2 and D.3, and biological variables represented by saltmarsh vegetation assemblages, as described in sections 3.3.2.3, 3.4.1.3, and Appendix A -Table A-2. The 5.4.1.2 results clearly indicated that time lag between the monitoring surveys did not predict the sedimentation rates variability, so month-specific statistical analysis was not conducted.

The study initially employed principal component analyses (PCA) to examine the influence of various physical factors on saltmarsh development in relation to sedimentation rates (derived from sedimentation plates). These factors encompassed elevation (m), hydroperiod (m), flood depth (m), flood frequency, distance to mean high water spring (MHWS), distance to water channels (m), distance to saltmarsh edge (i.e., the vegetation edge between mudflat and pioneer zones; in m), soil bulk density (g.cm<sup>3</sup>), slope (percent), and curvature. Additionally, the study investigated the potential contribution of biological factors, such as vegetation height, density, distribution, cover, and biomass, to sedimentation rates. The results of the Principal Component Analysis (PCA) indicate that the initial two dimensions explain 46.04% of the variance in the dataset (Figure 5-36). Furthermore, the first three dimensions account for 55.03% of the variance. Notably, elevation, hydroperiod, flood depth and frequency exhibit multicollinearity, indicating a high correlation among these four independent variables. Among all the variables, elevation, hydroperiod, flood depth and frequency, distance to salt marsh edge, vegetation cover, and above ground organic content have the most significant contributions to the dataset. Conversely, sedimentation rates, curvature, slope, distance to Mean High Water Springs (MHWS), vegetation height, and density have the least influence.

Subsequently, best subsets regression was employed to provide additional clarification on the associations between sedimentation rates and the physical and biological variables. The findings suggest that factors such as vegetation height, density, cover, distance to saltmarsh edge, curvature, and slope play a significant role in predicting the dataset of sedimentation rates.



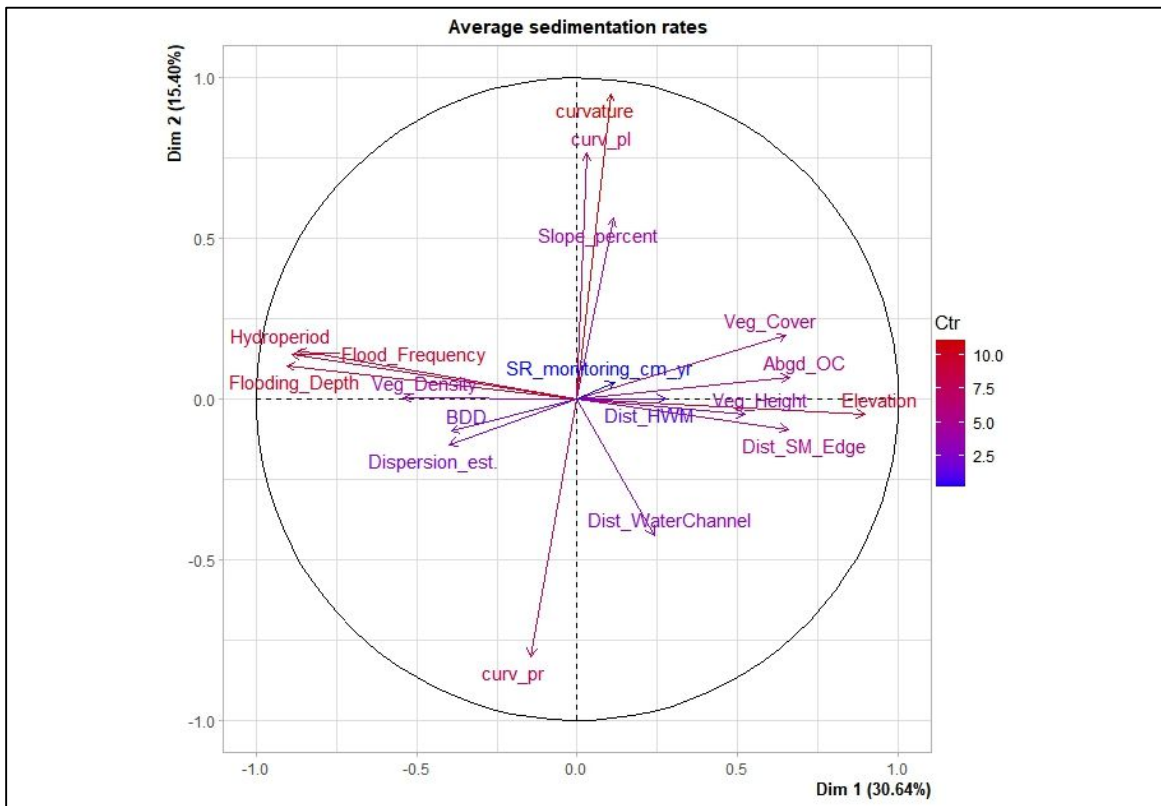


Figure 5-36: PCA plot for sedimentation rates showing in x-axis and y-axis the principal components that contribute the most to the variance of the dataset (PC1 and PC2). Each variable represented by an arrow with its length and gradient color informing on the PCA loading scores (Red longer arrows have higher contribution and blue short the least).

SR.cm.year	Sedimentation rates derived from sedimentation plates over 2.15 years		
Elevation	Elevation height in m	Curvature	Curvature (1/100 of a z-unit)
Dist_HWM	Distance to MHWS in m	Curv_pr	Profile Curvature
Dist_WaterChannel	Distance to water channels in m	Curv_pl	Planform Curvature
Dist_SM_Edge	Distance to saltmarsh edge in m	Veg_Density	Vegetation density number of individual per m <sup>2</sup>
BDD	Soil Bulk density in g.cm <sup>3</sup>	Abgd_OC	Aboveground Organic Carbon Content (g per m <sup>2</sup> )
Hydroperiod	Hydroperiod in m	Veg_Cover	Vegetation cover in percentage
Flooding depth	Flood depth in m	Veg_Height	Vegetation height (cm)
Flood Frequency	Flood Frequency in %	Dispersion_est	Dispersion factor
Slope_percent	Slope in percent		

The study observed that sedimentation rates had a significant impact on vegetation height, density, cover, planform curvature, and slope. However, it is important to note that these variables only accounted for 15.2% ( $r^{2adj}$  ;  $p < 0.05^*$ ) of the variability in sedimentation rates (see Appendix D.2: Table D-7). Nevertheless, the current model is inadequate in elucidating the occurrence of highly negative values, specifically related to erosion phenomena. Principal component analyses (PCA) were conducted on each salt marsh to determine the physical or biological factors that influence sedimentation rates.

The application of Principal Component Analysis (PCA) to ANK sedimentation rates revealed that several factors, including elevation, water levels (specifically flood depth, frequency, and

hydroperiod), soil bulk density (BDD), distance to the saltmarsh edge, and vegetation cover and height, made substantial contributions to the dataset. These findings are illustrated in Figure 5-37 and Figure 5-38. The hypothesis was examined using a multiple regression model, which revealed that vegetation cover and bulk dry density (BDD) exhibited a significant and positive predictor of sedimentation rates. These variables accounted for 28.1% ( $r^{2adj}$  ;  $p < 0.05^*$ ) of the variability observed in sedimentation rates occurring on ANK (Table D-8).

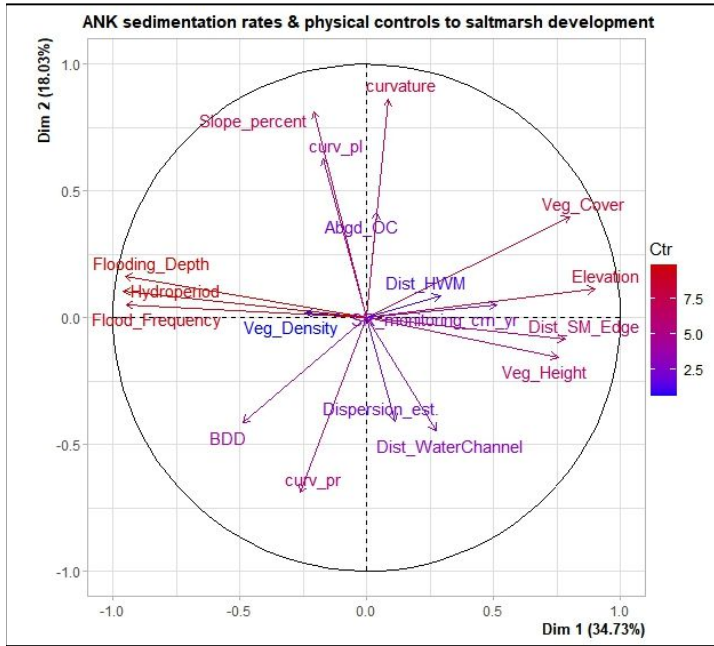


Figure 5-37: PCA plot for ANK sedimentation rates - see notes and details in Figure 5-36

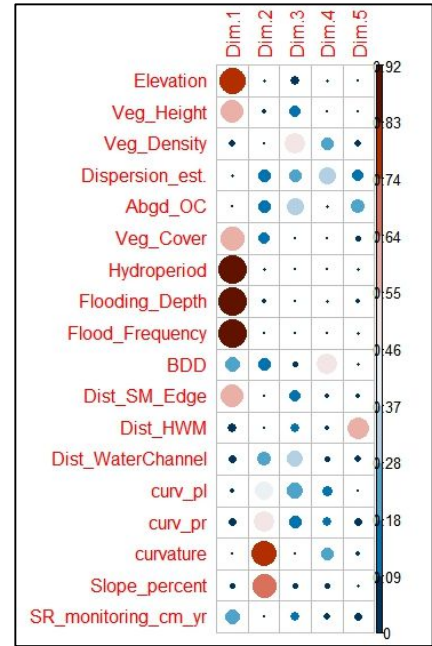


Figure 5-38: Plot matrix of the square cosine (cos2) which is the quality of representation of the variables of the PCA on ANK sedimentation rates. Note1: Large and dark circles indicate a good representation of the variable on the principal component and viceversa. Note2: see notes and details in Figure 5-37

PCA was performed on the sedimentation rates of FM. The analysis revealed significant influences from various physical factors, including elevation, water levels (such as flood depth, frequency, and hydroperiod), soil bulk density (BDD), and distance to the saltmarsh. Additionally, biological factors such as vegetation height and cover were found to contribute significantly to the sedimentation rates (Figure 5-39 and Figure 5-40). The hypothesis was tested using a linear regression model, which indicated that hydroperiod was a significant predictor of 14.7% ( $r^{2adj}$  ;  $p < 0.05^*$ ) of the variability in sedimentation rates in the fronting marsh FM (Table D-9).

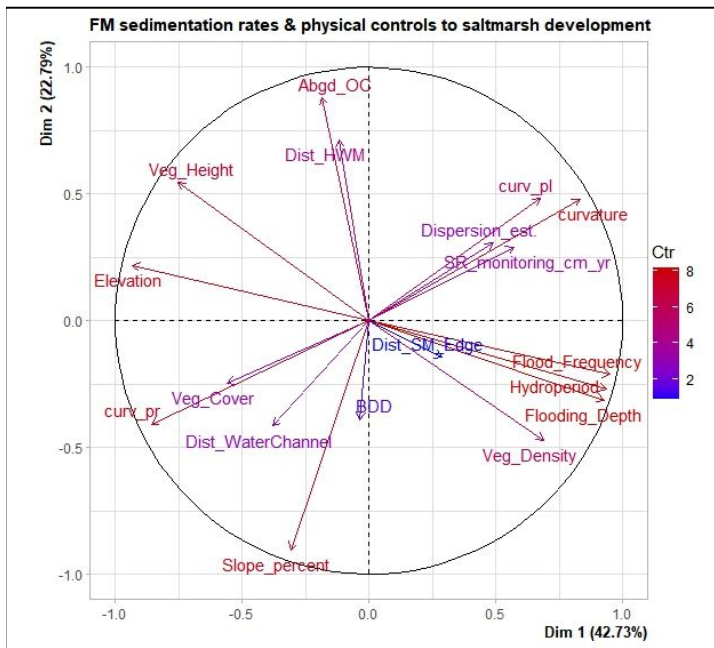


Figure 5-39: PCA plot for FM sedimentation rates - see notes and details in Figure 5-36

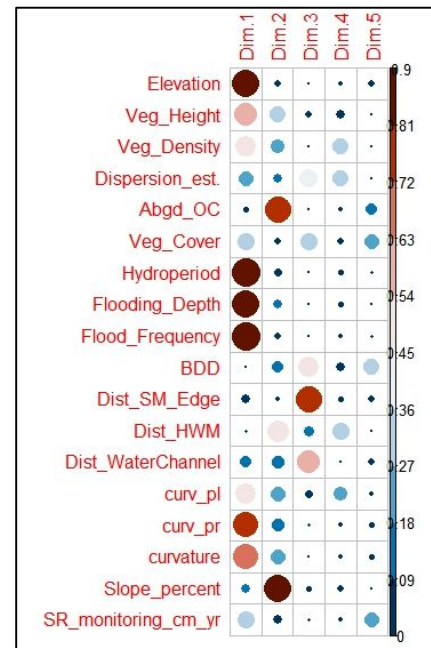


Figure 5-40: Plot matrix of the square cosine (cos2) which is the quality of representation of the variables of the PCA on FM sedimentation rates. Note1: see notes and details in Figure 5-38

As depicted in Figure 5-41 and Figure 5-42, the PCA conducted on the MR sedimentation rates revealed significant contributions from slope, soil bulk density (BDD), and vegetation cover within the dataset. These variables collectively explain 9.5% ( $r^{2adj}$ ;  $p < 0.05^*$ ) of the observed variability in sedimentation rates within managed realignment sites (refer to Table D - 10). The influence observed in this context is relatively limited in its strength. The absence of significant relationships between the managed realignment saltmarsh sedimentation and expected physical drivers such as elevation, curvature, or water levels could be interpreted as a lack of topographical variation. This suggests that, although these factors may play a role if present, the absence of such relationships also indicates that the managed realignment saltmarsh differs topographically from natural salt marshes.

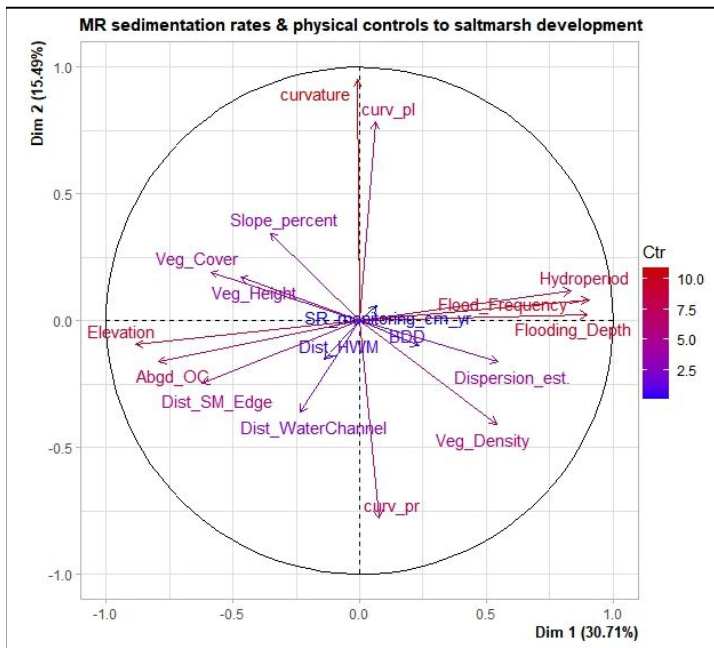


Figure 5-41: PCA plot for MR sedimentation rates - see notes and details in Figure 5-36

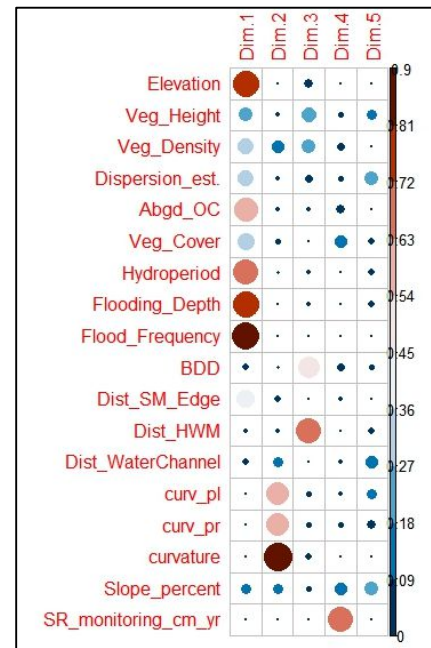
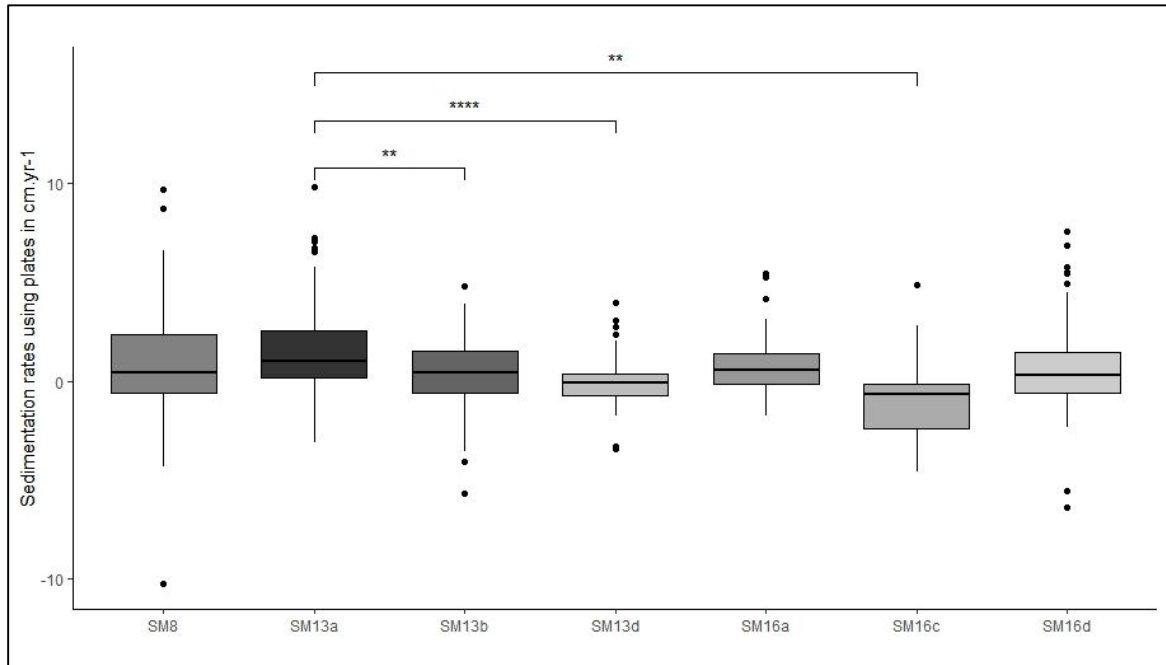


Figure 5-42: Plot matrix of the square cosine (cos2) which is the quality of representation of the variables of the PCA on MR sedimentation rates. Note1: see notes and details in Figure 5-38

**Sedimentation rates and vegetation assemblages - NVC communities.** The analysis reveals that just 5% ( $r^2_{adj}$  ;  $p < 0.001^{***}$ ) of the observed variability in sedimentation rates can be attributed to the composition of vegetation assemblages-NVC communities (refer to Table D-6 (3)). Nevertheless, the mean rank differences observed among the vegetation assemblages exceed what would be anticipated by random chance. Furthermore, a statistically significant overall difference was detected among these communities ( $H_{(df=6)} = 27.84$ ,  $p < 0.001^{***}$  ; Table D-5). The application of pairwise comparison using Dunn's Method revealed a significant difference in sedimentation rates among various plant communities within the marsh ecosystem. Specifically, the sedimentation rates were found to be significantly higher in the presence of low-marsh plant community SM13a, characterised by the dominance of *Puccinellia maritima* and as a sub-community composition. In contrast, mid-marsh communities SM13b (*Puccinellia maritima* dominant with *Glaux maritima* sub-community) and SM13d (*Puccinellia maritima* dominant with *Plantago sub-community*), as well as high-marsh plant community SM16d (dominated by *Festuca rubra* with a sub-community), exhibited lower sedimentation rates. These findings are illustrated in Figure 5-43. However, there is a difference between the results of sedimentation rates and short-term accretion rates. It was observed that high-marsh plants (SM16c) and pioneer plants (SM8) exhibited higher rates of accretion compared to other assemblages (see Chapter 4 section 4.5.3.1). The findings of this study are stimulating as they

suggest that plant assemblage SM13a exhibits a potentially higher ability to facilitate long-term sediment settling compared to other plant assemblages. The observed phenomenon for sedimentation rates can be attributed to the persistence of *Puccinellia mar.*, which remains green throughout winter, with its foliage and stem remain intact, but ceases to grow. This characteristic enables the trapping of sediment during the period of maximum sediment deposition, as discussed in Chapter 4, sections 4.2.1 and 4.5.3.2.



**Figure 5-43: Overall sedimentation rates (cm. yr<sup>-1</sup>) by vegetation assemblages showing highest sedimentation rates with SM13a (*Puccinellia maritima* dominant and *Puccinellia maritima* sub-community) in the low-marsh.** (Kruskal-Wallis H test and significant pair-test comparison using Dun's tests results by the p-value significance: ns, \*, \*\*, \*\*\* for  $> 0.05$ ,  $\leq 0.05$ ,  $\leq 0.01$ ,  $\leq 0.001$ ). Boxplots represent median (middle line) interquartile range (box), 1.5 times interquartile range (bar) and outliers (stars).

## 5.5 Aboveground long-term (multi-annual to centennial) geomorphological processes: Significance of the results

This chapter focuses on the examination of the spatial and temporal aspects of aboveground sedimentation over centennial to pluri-annual timescales as outlined in Table 5-1. This section provides a concise overview and analysis of the key findings from the research study:

- 1) How much has occurred in Nigg Bay salt marshes in the light of major anthropogenic disturbances: land reclamation/seawall breaching?
- 2) Have these changes occurred both laterally and vertically
- 3) Are these changes regular across time?



### 5.5.1 Centennial saltmarsh extent and MHWS migration

In a typical RSLR (relative sea level rise) scenario, it is expected that salt marshes will undergo a gradual landward and upward migration along the shoreface. According to Spencer et al., (2012), in the context of managed realignment, there is a sudden shift in the progressive migration when the defence line is breached. Research on managed realignment primarily focuses on examining the internal dynamics of these land management projects in order to assess their feasibility. However, it is widely acknowledged that there is a need to investigate the broader impact of realignment on a larger scale, such as across a bay or estuary Spencer et al., (2012). Moreover, empirical studies have demonstrated that realignment schemes can yield unintended consequences, potentially resulting in the opposite outcome of their intended purpose. Additionally, the creation of new habitats through such schemes may come at the cost of adjacent natural habitats (Rotman et al., 2008).

In order to assess the extent and migration of saltmarshes over a long-term period, specifically prior to the land reclamation activities in the 1950s or prior to the breaching and managed realignment creation of Nigg Bay in 2003, sections 5.2.1 and 5.2.2 of the study have demonstrated that between the years 1872 and 1977, the management and reclamation of coastal salt marshes in the Bay resulted in a loss of approximately  $32 \pm 0.6\%$  of the saltmarsh area. This loss is more than twice the estimated saltmarsh loss observed in the United Kingdom as a whole (Beaumont et al., 2014). Yet, during this time it was observed that salt marshes in Nigg Bay experienced a significant expansion of approximately  $20.5 \pm 0.4\%$  into the intertidal zone and in proximity to newly constructed sea defence structures. The data presented in Figure 5-11 supports the observation that there has been a consistent movement of Mean High Water Springs (MHWS) towards the sea, with an average migration distance of  $30.78 \pm 3.67\text{m}$  between the years 1872 and 1977. This finding indicates that despite the decrease in available space due to land reclamation (accommodation space), the saltmarsh systems have shown resilience and have been able to take advantage on the increased sediment supply in the bay. While not specifically examined in the context of realignment, this phenomenon aligns with the mechanisms investigated by Wang and Temmerman (2013). Their study revealed that the transition from low-lying bare flats to a vegetated state occurs at a relatively rapid pace, approximately 2 to 8 times faster than in an equilibrium state. Furthermore, these shifts may be linked to catastrophic transitions between alternative stable states. The expansion of saltmarsh vegetation onto the bare mudflats towards the sea provides a prominent example of positive biogeomorphic feedback mechanisms. The process of expansion is facilitated by the establishment of plants through lateral clonal propagation or seed dispersal. The phenomenon is subject to a range of factors, including the abundant availability of sediment, patterns of elevation, and the hydrodynamic

characteristics specific to the local environment. The Mean High Water Springs (MHWS) is a significant factor in determining the duration of periods of inundation and exerting an impact on sediment deposition on the mudflat (Fagherazzi et al., 2012; Wang and Temmerman, 2013; Silinski et al., 2016). Furthermore, the expansion of the fronting marsh FM towards the sea, following the land reclamation activities in Nigg Bay, can be compared to the pre-breaching of the Wash in 2001 (Friess et al., 2012). Intertidal vegetation communities in the Wash region responded to local relative sea-level rise (RSLR), which ranged from rates ranging from 0.54 to 2.54 mm per year between 1956 and 2006, by an expansion seaward of the algal and pioneer saltmarsh zones.

The analysis of MHWS migration at Nigg (5.2.3) reveals that over a span of 145 years, the cumulative rate of MHWS has exhibited a seaward movement at a rate of  $-0.02 \pm 0.01 \text{ m.yr}^{-1}$ , and this despite the significant land management changes that occurred (Figure 5-18). Nevertheless, the examination of the migration of the MHWS and the extent of saltmarsh has indicated that both FM and ANK are experiencing landward retreat. Additionally, it has been observed that the pioneer zones of these areas located on the easternmost part of the shorefront are susceptible to erosion (Figure 5-11).

These combined findings provide:

- 1) signs of local sea level rise, albeit on a short-term scale. This finding aligns with previous data collected from tide gauges in Scotland (Rennie and Hansom, 2011);
- 2) that the salt marshes in Nigg Bay have demonstrated the ability to adapt to human-induced disturbances, highlighting their high resilience as an ecosystem;
- 3) an emphasis on the need for further research into the recent response of the saltmarsh to changes in the shoreline, which will be discussed in the following section.

### 5.5.2 Height, volume and saltmarsh extent changes from 2011 to 2017

Thesis aims	Specific research questions	Experimental hypotheses	Methods	Timescale
Improve understanding of aboveground saltmarsh long-term dynamics.	Spatial variation in shoreline migration between natural and managed salt marshes? Were these changes have been regular between the salt marshes?	- MHWS migration is not uniform - Rate of changes varies amongst the salt marshes	Combined dataset from 1872 to 2017 Details in 3.4.2	CENTENNIAL
	How much has changed in terms of height, area and volume occurred in recent years? Are geomorphological responses differ between natural and managed salt marshes?	Erosion is expected to be higher near sea defence, with cliff edge formation as a response. Accretion varies between salt marshes and areas of salt marshes (i.e. pioneer-marsh development)	Two transects across the saltmarsh site DEMs sediment budgets focussed on low part of the saltmarshes	DECADAL

Using DEM surface from 2011 to 2017, two cross-shore transect profiles (5.3.1) across the three saltmarsh sites show an overall salt marsh gain of c.0.33m in surface height, but this has been slowing since 2014. On MR, although there is overall accretion of c.0.05±0.001 m in height, since 2014, the LM zone demonstrates a continuous loss in height. Both natural salt marshes, ANK and FM, gained in elevation height on their vegetated, pioneer and fronting mudflat surfaces (c.0.045±0.0008 m and c.0.019±0.001 m respectively) with a clear gain from 2011 to 2016 and loss from 2016 to 2017.

The cross-shore transect profiles (Figure 5-20) highlight a striking difference in elevation height between MR and FM salt marshes. Behind the sea wall (north), MR surface is c.0.65 m lower than FM marsh surface elevation. The height difference ranges between c.0.4 to c.0.69 m for most of MR pioneer zone compared to FM whereas both sites high-marsh zones are of comparable height.

The natural (FM and ANK) saltmarsh edges and pioneer zones all exhibited a general landward migration but performed differently, possibly a function of age, maturity and their stage of development (Allen, 2000). The monitoring results from 2011 to 2017 also show that the response is not uniform between or within the salt marshes:

- i. The western saltmarsh edge of ANK extended laterally but gradually led to the formation of a small cliff margin. As reported by (Allen, 2000) and (Yapp et al., 1917) on a Welsh marsh (Dovey estuary), this cycle may result from intrinsic factors reflecting feedbacks between vertical growth and the establishment of a steep outer edge. Thanks to its sheltered position away from the river exit, the flow velocity at ANK is reduced and favours sediment accretion, vegetation growth and seaward expansion of the shallow gradient pioneer zone (Figure 5-22). This is similar to Silinski et al. (2016) in the Scheldt Estuary who found twice more vegetation expansion on the sheltered site. However, in Nigg, this expansion served to reduce the extent of mud/sand flats and increase its steepness which in turn may strengthen wave activity at the cliff-edge boundary (Leonardi and Fagherazzi, 2014). If this negative feedback scenario progresses then it will develop a cliff, as seen in the rest of the ANK frontal marsh. This suggests that more understanding of lateral dynamics in salt marshes is needed, in particular how the gradient of elevation change close to saltmarsh edge develops and over what timescale this might occur (Callaghan et al., 2010; Silinski et al., 2016) .
- ii. the southern edge of FM and eastern edge of ANK are formed by cliffs that have steepened over the monitoring period. The profiles may not all have signs of present

erosion, however remnants of the former saltmarsh surface are present at their base (Figure 5-44) that result from past erosion and/or undercutting by wave and tide processes. These lateral cyclic processes can be explained by the saltmarsh slope becoming more sensitive to wave attacks as the slope steepens during the saltmarsh vegetation expansion onto the tidal flat (Yapp et al., 1917; Callaghan et al., 2010).

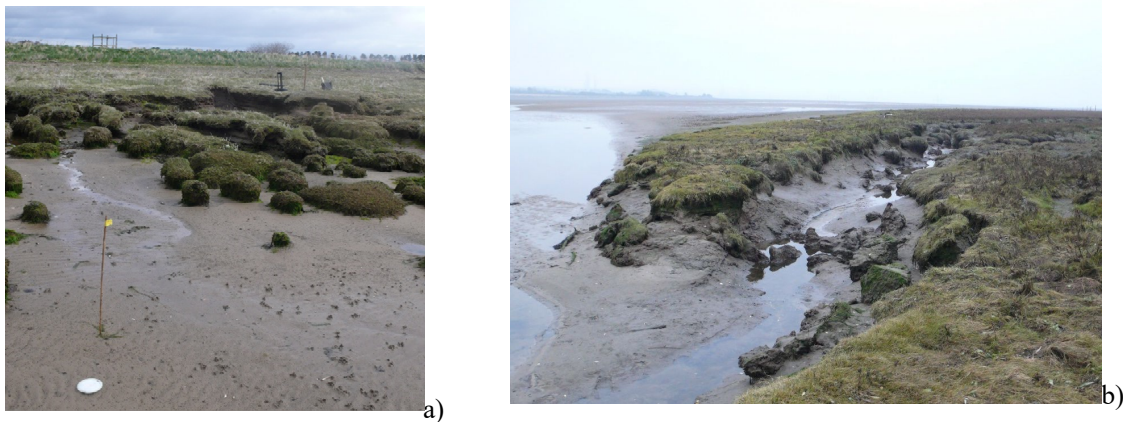


Figure 5-44: a) saltmarsh surface collapse at the base of FM cliff edge and b) at the entrance of one of ANK's creek (November 2015).

The cross-shore transect profiles present a useful tool to assess the dynamics of the marsh. However, it introduces a complication in the calculation of the overall balance or budget of saltmarsh changes. Using the same digital elevation model (DEM) series derived from both airborne and terrestrial laser scanning (TLS) datasets spanning from 2011 to 2017, the analysis of surface elevation change (5.3.2) also found:

- i. for the total area of salt marsh surveyed ( $23.84 \pm 0.58$  ha) from 2011 to 2017, an areal increase of  $1.28 \pm 0.12\%$  at an overall rate of  $0.002 \pm 0.0001 \text{ ha.yr}^{-1}$  (or  $21.29 \pm 3.55 \text{ m}^2 \cdot \text{yr}^{-1}$ ). The natural saltmarsh sites ANK and FM lost  $-5.8 \pm 0.01\%$  and  $-18.8 \pm 0.04\%$  of area respectively whilst the MR area expanded by  $30.76 \pm 0.4\%$  (Table 5-4).
- ii. These areal changes were accompanied by an overall volumetric gain  $25.61 \pm 0.34\%$  at a rate of  $0.04 \pm 0.0004 \text{ m}^3 \cdot \text{yr}^{-1}$ . For 6 years, there is a striking uniformity in the volumetric results (loss and gain of volume of marsh (vegetation + sediment)) on the two-natural salt marshes ANK and FM which both gain c.20% in volume (Figure 5-23). This may imply either that there is little variability on the amount of sediment input or that the marshes have similar capability in sediment retention. The managed realignment has gained  $42.15 \pm 0.55\%$  in volume demonstrating the advantages of a sheltered position behind the sea embankment that favours sediment retention and vegetation growth fuelled by sediment derived from adjacent salt marshes and mudflats located seawards.



Figure 5-45 and highlight areas where tidal energy is low enough to allow sedimentation such as at the Ankerville river mouth or in front of the west breach of MR, areas where sediment supply may be enhanced by inflow/outflow. However, overall the mudflat surface during the six years study has largely lost height suggesting that the salt marshes are fed by sediment lost from the mudflat. Rotman et al. (2008) explored sediment provenance within managed realignment and identified that the primary source (~54%) originated from sediment seaward of the breaches, 27% sourced from the breached seawall, and 19% from intertidal and subtidal mudflats/sandflats seaward of the established marsh.

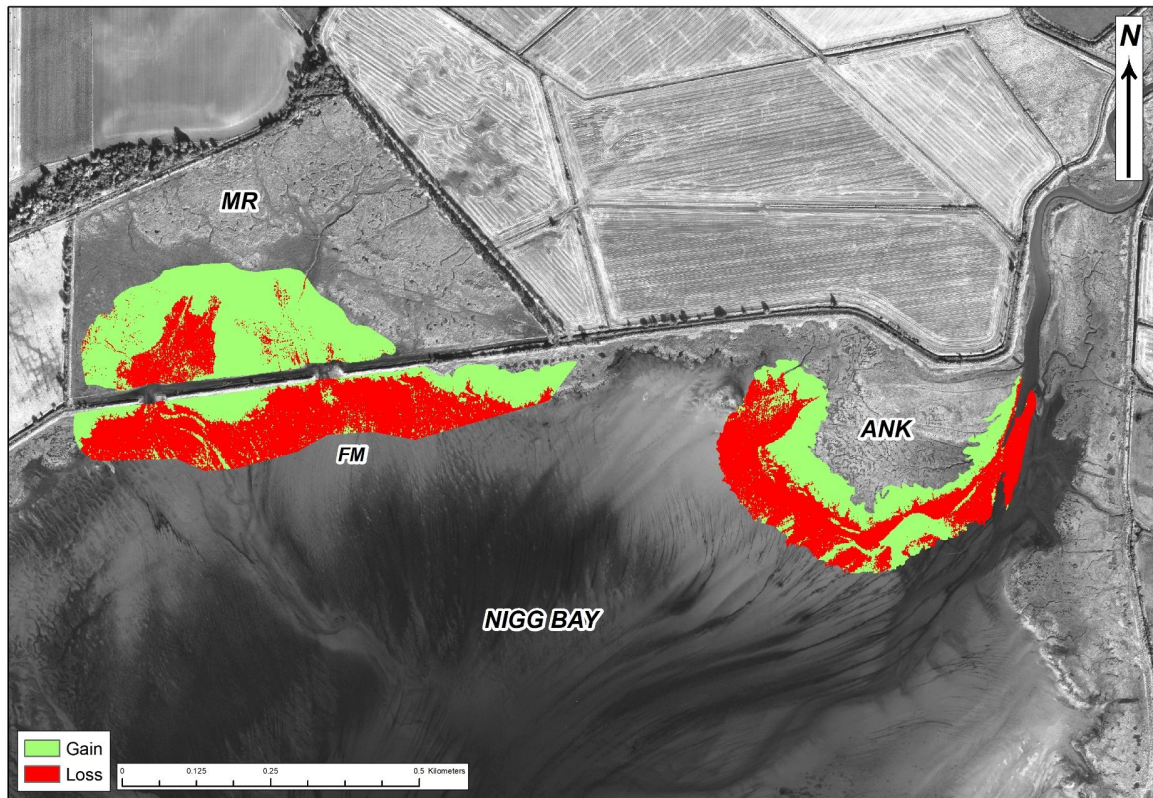


Figure 5-45: The DEM cut & fill highlights salt marsh gain and loss over 6 years (derived from both airborne and terrestrial laser scanning (TLS) datasets spanning from 2011 to 2017) with clear gain on the vegetated part of the marsh and also sediment input on the foreshore.

### 5.5.3 Sedimentation rates derived from sedimentation plates from 2015-2017

The sedimentation rates derived from sedimentation plates work aimed to provide a comprehensive network of sedimentation to improve our understanding on spatiality and temporality of the sedimentation saltmarsh dynamics as described in Table 5-1.

A key result is in the 2.15 years of monitoring, the sedimentation plates showed an overall positive sedimentation rate amount of  $0.21 \pm 0.03 \text{ cm.yr}^{-1}$  from July 2015 to September 2017. These rates are approximately 6 times lower than the accretion rates estimated from 2016/2017 filter disc sediment deposition averaging  $1.34 \pm 0.14 \text{ cm.yr}^{-1}$ . Work in the muds of the Solway by



Harvey et al. (2007) produced much higher rates of 2.5/2.8 cm. yr<sup>-1</sup>, however work on the east coast of Scotland have produced sedimentation rates closer to Nigg ranging between 0.34 to 0.38 cm. yr<sup>-1</sup> in the Eden estuary, Scotland (Maynard et al., 2011) and 0.5 to 0.9 cm. yr<sup>-1</sup> at Bettyhill, at the mouth of the River Naver on the north coast of Scotland (Teasdale et al., 2007). However, the rates observed in this study of Nigg Bay salt marsh align with the findings of (Miller et al., 2023) who utilised <sup>210</sup>Pb and <sup>137</sup>Cs chronologies to estimate long-term sedimentation rates. Specifically, the Dornoch Point marsh exhibited an average increase of 0.18 ± 0.01 cm.yr<sup>-1</sup>.

### **Spatial variation**

The analysis demonstrated that both physical and biological factors play a substantial role in determining the location of sedimentation in Nigg Bay. The study revealed that the distribution of sedimentation is influenced by various factors related to marsh topography, such as curvature and slope. Additionally, biological factors including vegetation height, density, and cover were found to play a significant role in this process. The analysis reveals that the majority of the pioneer-zones are subject to the effects of tidal and wave forces, which can transport sediment but impede its settling and accumulation. Additionally, there is a consistent pattern of increased sedimentation observed in relation to the level of protection afforded to each site, which aligns with previous studies conducted by Langlois et al. (2003), Doody (2008) and Silinski et al. (2016). In contrast, the analysis that sedimentation occurring at greater distances from the saltmarsh edge is influenced by localised topography. The rates of sedimentation were found to show significant differences between natural and managed saltmarshes, indicating that the underlying factors driving these rates also differ.

The average sedimentation rates for **FM and ANK** are -0.09 cm.yr<sup>-1</sup> and 0.01 cm.yr<sup>-1</sup>, respectively. The plot maps depicted in Figure 5-29 to Figure 5-35 indicate that sedimentation rates, as determined from sedimentation plates, may not align with the anticipated erosion-prone frontal regions. After a duration of 2.15 years, it has been observed that erosion has occurred in the easternmost region of the pioneer zones on both FM and ANK. This erosion may be attributed to the influence of the clockwise tidal gyre at Nigg, which is particularly pronounced during low tide (Chapter 3 - section 3.2.1). Additionally, wave erosion resulting from the prevailing south-westerly winds could also be a contributing factor, particularly on ANK close to the stream exit. In the context of ANK, it has been observed that pioneer-marsh and low-marsh areas exhibit the lowest rates of sedimentation, which stands to concur with the observed trend in short-term accretion rates. The drivers for these processes have been observed to vary between the two marshes. In the case of FM sedimentation rates, hydrodynamics play a primary role, particularly in the shallowest part of the marsh where high and extreme water levels result in significant drag from tidal flow and ebb. This prevents sediment accumulation, despite the

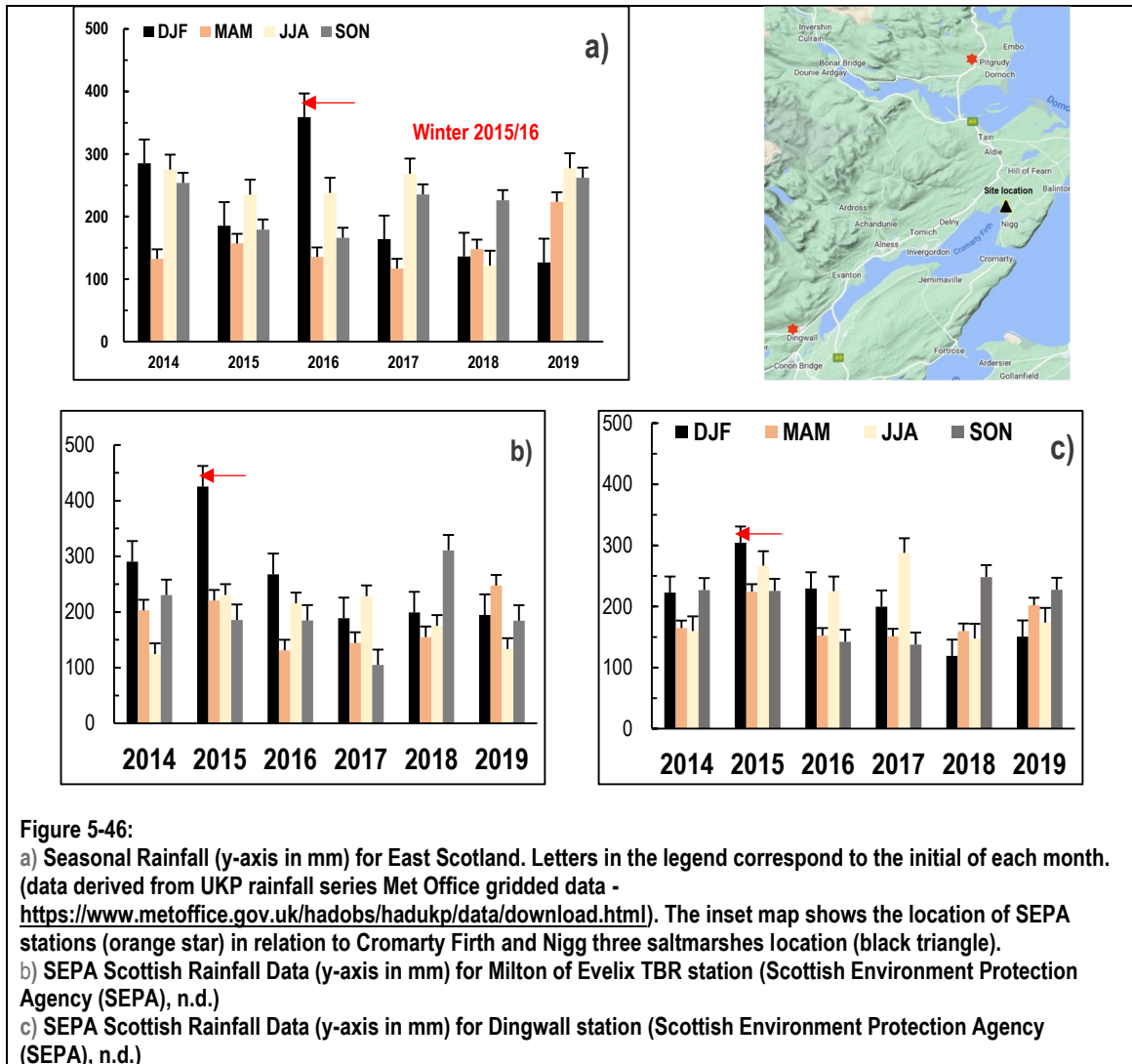
presence of areas with high deposition. Furthermore, the overall negative sedimentation rates may simply due to the restricted spatial extent of the site due to the presence of the seawall and not much scope for movement. Although, the FM pioneer-marsh experiences high sedimentation rates with localised erosion on the easternmost region, the lack of ability to move may lead to the FM high-marsh regressing into low marsh on sea level rise (Butzeck et al., 2014). On the other hand, the lowest sedimentation rates in ANK are associated with areas of high BDD (soil dry bulk density). Additionally, low vegetation cover (as depicted in Figure 4-18) is also linked to these low sedimentation rates. The sedimentation rate plots (Figure 5-29 to Figure 5-35) illustrate that the areas located south-east of FM and mid-marsh of ANK are consistently at risk of erosion. This implies that these zones may be susceptible to submergence as relative sea levels rise, as suggested by previous studies (Fagherazzi et al., 2012; Baptist et al., 2016).

The average sedimentation rates for **FM and MR** are  $-0.09 \text{ cm.yr}^{-1}$  and  $0.33 \text{ cm.yr}^{-1}$ , respectively. The data obtained from the sedimentation plates (Table 5-5) show that FM is experiencing a decrease in elevation height, while MR is showing an increase, although both benefit from the same sediment supply (and, as seen in Chapter 4 - 4.2, indicate that there is a uniform sediment availability, at least for the year 2016-2017). The variability observed in this phenomenon may be attributed to the high tidal energy experienced at the shorefront of the marsh, in contrast to the relatively sheltered conditions found in the MR area. The presence of a seawall provides protection, resulting in increased sedimentation in the MR (marshland) with limited erosion. It is also not uncommon to see such changes in newly restored marshes, and several recent studies have demonstrated that newly restored marshes gain sediment that is directly derived from adjacent established salt marshes (Rotman et al., 2008; Friess et al., 2014; Esteves and Williams, 2015). The interpretation is supported by the results and analysis of the cross-shore transect profiles conducted at Nigg (5.2.3).

**On MR**, the analysis of sedimentation rates (depicted in Figure 5-29 to Figure 5-30) provides further evidence that overall high-marsh (HM) and low-marsh (LM) zones of MR are susceptible to greater erosion, with a discernible pattern of erosion in the east-southeast (ESE) and deposition in the west-southwest (WSW) areas of the MR site. This suggests an asymmetry in the distribution of sediment. In Chapter 4, the examination of short-term (annual) accretion rates indicated that this phenomenon may be linked to the presence of reclamation drainage ditches, as illustrated in Figure 3-7 of the post-2003-realignment reclamation features (see Figure 3-7 post-2003-realignment reclamation features). Moreover, the analysis has revealed that high sedimentation rates on MR are linked to the slope gradient, which facilitates wave dissipation and promotes the accumulation of sediment. Additionally, these rates are influenced by low BDD (soil dry bulk density) and insufficient vegetation coverage.

## Temporal variation

Sedimentation rates equated to  $0.21 \pm 0.07 \text{ cm.yr}^{-1}$  over the survey period (2.15 years) with significant differences between survey collections occurred with largest increase during winter 2015-16 but likely reflect the high levels of rainfall and surface saturation, as depicted in Figure 5-46. Higher sediment delivery in estuaries and coasts and higher deposition rates often links to periods of higher rainfall and fluvial runoff or strong wind and wave activity mobilising sediments on the nearshore and intertidal flats (Reed, 1995; Stapleton and Pethick, 1996; Temmerman, Govers, Wartel, et al., 2003; Davidson-Arnott, 2009). Indeed, the storms of 2013-14 in NE Scotland were the most severe in the last 20 years with 2008-9 the most severe in 30 years (Met Office, n.d.). During 2015-16, 11 storms hit UK and Ireland including 4 (Abigail, Frank, Gertrude and Henry) with maximum wind gusts located in Scotland against five storms over 2016/17 and 8 in 2017/2018 (Met Office, 2019).



Despite the considerable variability in sedimentation rates observed during each collection campaign, it seems that time lag does not contribute to the predictability of sedimentation rates. Care should be exercised when considering the temporal variation observed in this time series. The findings also indicate that, after a period of 2.15 years, the sedimentation plates have reached a state of equilibrium. This also suggests that the plates have acquired the capability to generate reliable and significant measurements.

## **5.6 Aboveground long-term (multi-annual to centennial) geomorphological processes: implications**

The results presented here aim to improve our understanding of *processes, mechanisms and patterns that favour saltmarsh formation and development; enable saltmarsh capacity to recover from environment and anthropological disturbances; and, inform the regulating and supporting services salt marsh provide*. Chapter 4 addressed relationships between aboveground biomass, sediment deposition and accretion over short timescales (annual) and highlighted patterns in these relationships and what may influence sediment deposition and vegetation cover. The spatial and temporal development of salt marsh was examined in this chapter by quantifying the geomorphological changes taking place aboveground in a multi-annual to centennial time scale. The results clearly demonstrated that:

During a span of approximately 100 years, from 1877 to 1977, Nigg Bay experienced significant changes in land management and land reclaim of parts of coastal salt marshes. This occurred before the realignment of the MR saltmarsh site (2003) and the reclamation efforts that took place after the 1950s. These activities led to an overall loss of  $32\pm 0.6\%$  of the salt marsh, which is twice the estimated loss observed in the broader context of salt marshes in the United Kingdom (Beaumont et al., 2014). Yet, during this same period, there was a  $20.5\pm 0.4\%$  saltmarsh expansion into the intertidal zone. This trend is supported by a collective movement of the MHWS towards the sea, with an average migration distance of  $30.78\pm 3.67$  metres observed between the years 1872 and 1977. Over a period of 145 years, from 1872 to 2017, during which land reclamation and realignment of MR salt marsh took place, the overall rate of seaward (accretion) MHWS migration for the three salt marshes studied was  $-0.02\pm 0.01\text{m.yr}^{-1}$ .

The temporal changes that occur within the Nigg Bay saltmarsh systems over shorter timescales (decadal to multi-annual) reflect the vulnerability of the saltmarsh systems. This study has shown that the migration of the MHWS has not been consistent across the three saltmarsh sites over a period of 145 years. However, it has also shown that in the last 30 years (1977 to 2017), the analysis of combined MHWS and saltmarsh extent data signals a risk of erosion of the pioneer-

marsh zones, particularly in the easternmost regions. This affects both the young fronting saltmarsh FM and the mature saltmarsh ANK.

The study has also highlighted that low sedimentation rates that place the Nigg Bay salt marshes at threat to recent and future RSLR:

- Over a period of six years, the analysis of the Digital Elevation Model (DEM) surface using airborne and Terrestrial Laser Scanning (TLS) data between 2011 and 2017 showed a net increase of approximately 0.33 m in surface elevation, accompanied by a spatial expansion of approximately 1.28%. However, the overall rate of increase of salt marshes has decelerated since 2014 across all three salt marshes studied. On MR, although there is an overall increase in height by approximately  $0.05 \pm 0.001$ , since 2014, low-marsh zone has experienced a consistent decline in height. Both natural salt marshes, ANK and FM, experienced an increase in elevation on their vegetated pioneer-marsh zone and fronting mudflat surfaces (approximately  $0.045 \pm 0.0008$  m and approximately  $0.019 \pm 0.001$  m respectively) with a clear gain from 2011 to 2016 and a loss from 2016 to 2017. In the natural salt marsh at ANK, there has been a landward migration of the western marsh edge towards the east. In addition, small cliffs have formed in the sheltered areas of the bay towards the west. Furthermore, the existing cliffs in the most exposed areas, particularly to the south and east, have undergone erosional steepening. During this period, there has been evidence of erosion of the foreshore in the natural salt marshes ANK and FM, both in terms of (areal) extent and height, accompanied by a decrease in the height of the adjacent mudflats.
- Between 2015-2017, sedimentation rates (derived from sedimentation metal plates) have shown a strong spatial variability between the three salt marshes. On ANK, the mid and high-marsh zones tended to gain the most whilst the low and pioneer zones eroded the most. This phenomenon was also observed in the easternmost part of FM pioneer marsh. These low sedimentation rates were despite high rates of sediment deposition (shown by the short-term sediment deposition and accretion analysis in Chapter 4), suggesting strong erosive hydrodynamics in these zones leading to sediment scouring. Overall mid and high marsh zones on FM are eroding. On MR, the pioneer and low-marsh zones tended to gain the most, with a clear pattern of loss in the east and gain in the west of the realigned site MR was also recorded demonstrating an asymmetric sediment delivery via the breaches and that the transitional vegetation does not yet favour sedimentation. The sedimentation rates results have further shown that the fronting marsh FM may have lost at the expense of managed realignment MR which has more space to accommodate the same sediment supply. Although, a strong temporal variability was identified, this variability is difficult to assess as



the analysis also suggested that the sedimentation plates, over a duration of 2.15 years, have achieved a state of equilibrium, thus implying that the plates have attained the ability to produce dependable and meaningful measurements.

- A key result from the 2.15 years sedimentation plates record showed an overall positive sedimentation rates of  $0.21 \pm 0.03 \text{ cm.yr}^{-1}$  from July 2015 to September 2017.
- However, these sedimentation rates are not uniform across Nigg Bay salt marshes and have further implications for the stability and adaptation capacity of the Nigg Bay salt marshes to current and future sea level rise. With sedimentation rates as low as those measured at the three saltmarshes sites (ANK:  $0.01 \pm 0.04 \text{ cm.yr}^{-1}$ , FM:  $-0.09 \pm 0.16 \text{ cm.yr}^{-1}$ , and MR:  $0.33 \pm 0.03 \text{ cm.yr}^{-1}$ ) and RSLR moving at  $3 \text{ mm.yr}^{-1}$ , but rising to  $6 \text{ mm.yr}^{-1}$  and beyond in the future (Lowe et al., 2018; Fung et al., 2018), the Nigg Bay salt marshes may be just keeping pace now but are at high risk in the future. These current RSLR rates would be destructive to approximately 68 % marshes as depicted on Figure 5-47, but the detailed projections for five Scottish locations (with the Dornoch Firth ; Appendix A-3) estimate an increase to  $6 \text{ mm.yr}^{-1}$  and beyond in the future, suggesting that approximately 82 % of the marsh may be at serious risk in the future.

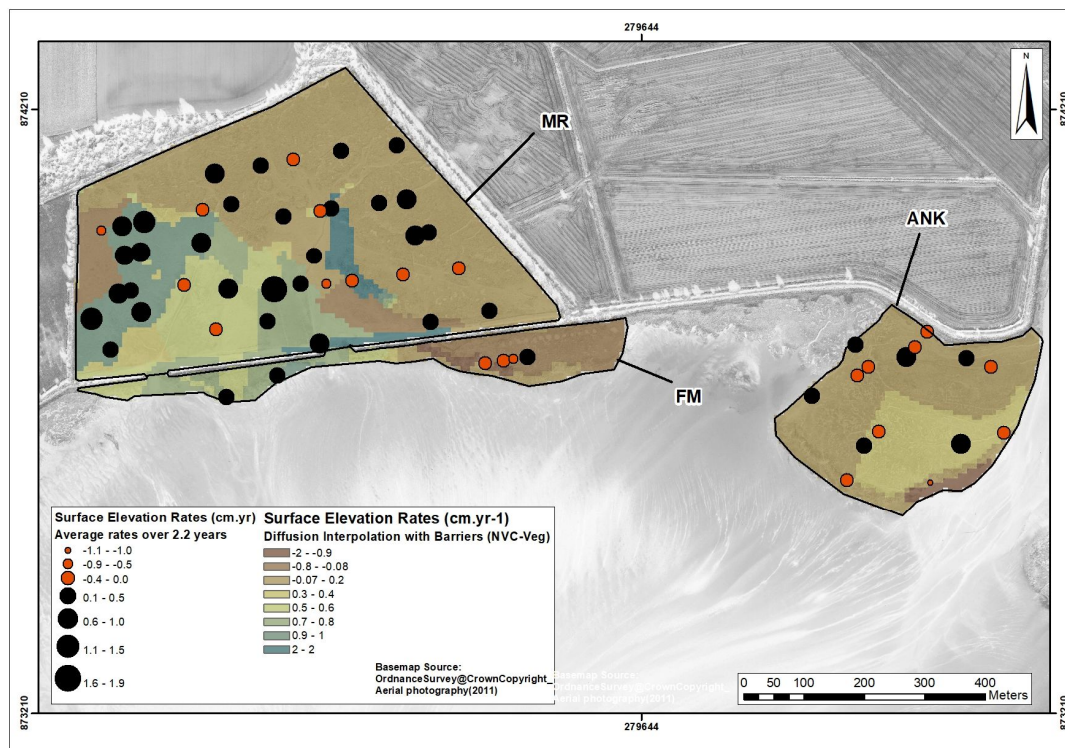
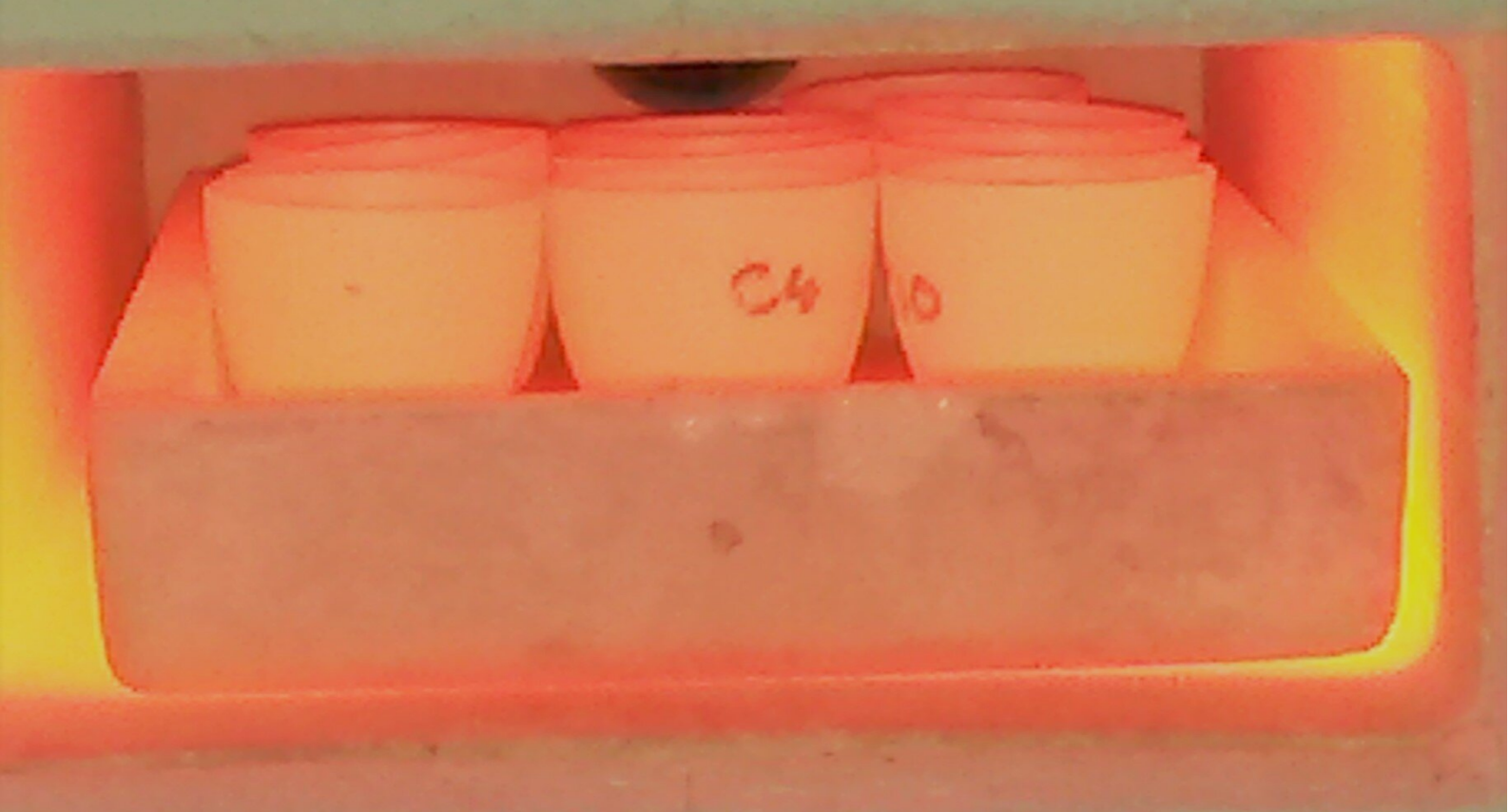


Figure 5-47: Sampling points with graduated symbol calculated for the average surface elevation rates (in  $\text{cm.yr}^{-1}$  for 2.15 years period) across the three salt marshes at Nigg Bay. The symbols are superimposed on a surface model that represents the surface elevation rate at a constrained distance using the extent of each vegetation community (NVC-assemblage). See Figure 4-71 for details of the interpolation method (ESRI (1), n.d.; ESRI (2), n.d.).



# Chapter 6



# **Chapter 6. Sedimentary Record of Belowground Organic and Inorganic Processes in Managed and Natural Salt Marsh**



“There is no other case in nature, save in the coral reefs, where the adjustment of organic relations to physical conditions is seen in such a beautiful way as the balance between the growing marshes and the tidal streams by which they are at once nourished and worn away.”  
 (Shaler, 1886 in Turner et al., 2000)

## 6.1 Introduction

The feedback between geomorphological and ecological dynamics are fundamental to understanding saltmarsh development, sustainability and response to environmental and anthropogenic forcings. However, the feedback between soil organics and inorganics remain relatively unexplored (Roner et al., 2016). This chapter aims to address this by investigating Belowground inorganics (sediment characteristics and properties) and organics (soil organic matter – SOM) processes in the Nigg Bay salt marshes (Figure 6-1).

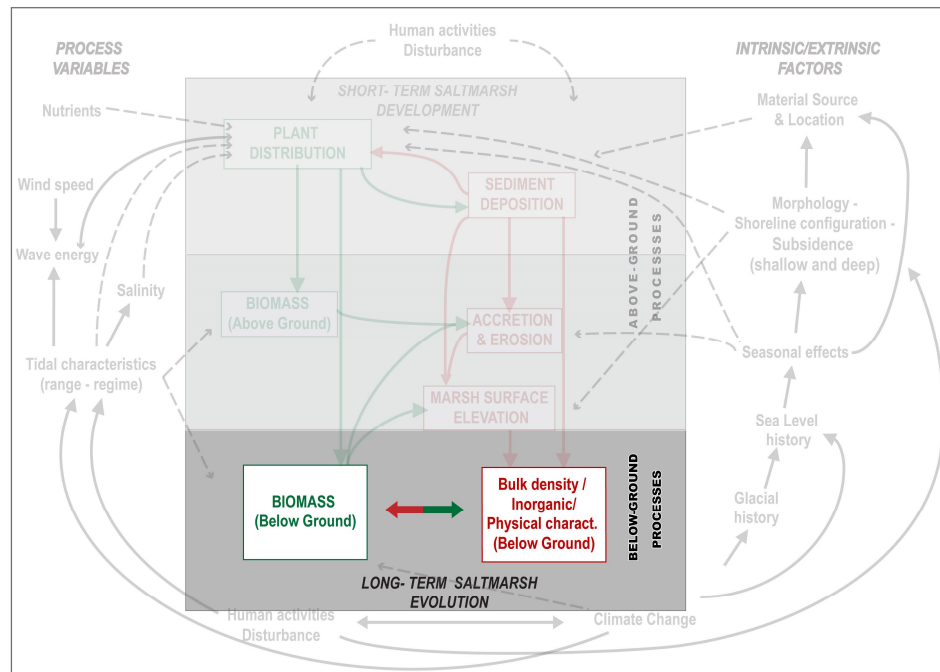


**Figure 6-1: Chapter 6 focusses on belowground organic and inorganic characteristics within the Nigg Bay marshes in light of environmental processes that have influenced past evolution (after (Allen, 2000; Davidson-Arnott et al., 2002; Cahoon et al., 2009)).**

Chapter 2-2.3 and Chapter 3-3.4.3 have identified belowground soil organic matter and inorganic content to be critical to saltmarsh sustainability via its role in vertical soil accretion which in turn helps saltmarsh maintain its relative elevation as sea levels rise (Chmura et al., 2003; Yu and Chmura, 2009; Mudd et al., 2009; Schindler, Karius, Arns, et al., 2014; Van de Broek et al., 2016; Schuerch et al., 2018). Since the accumulation and preservation of SOM in sediments is a geochemical process that is not continuous through time, the study of past processes can provide better understanding to present-day dynamics.



The formation of organic-rich sediments requires delivery of organic material from high producers such as terrestrial saltmarsh plants, saltmarsh macrophytes, benthic microalgae, phytoplankton. It also requires water velocities low enough to allow fine-grained organic rich material to accumulate in situ. Finally the SOM has to be preserved within sediments rather than degraded by detritivores or decomposers (Stumpf, 1983; Odum, 1988; Sousa et al., 2010). Anoxic conditions also favour burial of SOM and fine-grained sediment such as clays and silts result in rapid reduction of water circulation within sediment and with increased depth (Killops and Killops, 2004; Andrews et al., 2006; Hyndes et al., 2014). The availability of fine-grained particles due to flocculation controls the mechanisms by which sediments are entrained and transported and in turn impacts on the texture of the resulting sediment by influencing soil aeration and drainage (Dyer, 1989; Packham and Willis, 1997; Roner et al., 2016). So saltmarsh feedbacks will influence inorganic sediment deposition and organic accretion (Roner et al., 2016). So, fundamentally, salt marshes preserve in soil the legacy of the past feedbacks and relationships.

Environmental and anthropogenic disturbances can alter or disrupt the natural accumulation of organics and inorganics and can be reflected in the sedimentary records including sediment particle characteristics (i.e. grain size and type), water content (i.e. dewatering or flooding), autocompaction or bulk density (BDD) and organic matter (Allen, 2000; Davies, 2001; Boorman, 2003; Madsen et al., 2011; Davis Jr. and Dalrymple, 2012; Schindler, Karius, Arns, et al., 2014; Tempest et al., 2015).

Measurement of belowground organics and inorganics is also relevant to the carbon storage with the saltmarsh system. Estimating the amount of organic and inorganic carbon stored in salt marshes is subject to large uncertainties that can be attributed to: poor estimates of the total area of global salt marshes (in Chapter 2 - 2.1; Pendleton et al., 2012; Mcowen et al., 2017); limited data on geographical variation (Esteves and Williams, 2015; Kelleway et al., 2016) and investigations reporting only averaged carbon densities or accumulation rates (Connor et al., 2001); analysis confined to topsoil samples with limited data on deeper carbon storage (Van de Broek et al., 2016); lack of understanding of sedimentary processes (Esteves and Williams, 2015) and lack of studies on subsurface sediment properties and structures especially in recreated salt marsh (Tempest et al., 2015; Spencer et al., 2017); and poor representation of the geomorphic settings of carbon pools (Kelleway et al., 2016) as noted in Van de Broek et al. (2016).

As sediments are linked to tidal processes (Dyer, 1989), measurements of the past belowground inorganic and organic content allow these relationships to be examined. To address the overarching aim of this thesis – which is to improve our understanding of *processes, mechanisms and patterns that favour saltmarsh formation and development; enable saltmarsh capacity to recover from environment and anthropological disturbances; and, promote some of the*

*regulating and supporting services saltmarsh provide* – the spatial and temporal development of salt marsh was examined by quantifying above-ground short-term (annual) change in Chapter 4 and multi-annual to centennial changes in Chapter 5. Chapter 6 now addresses the past physical and biological changes that have been stored belowground within the Nigg saltmarsh sediments. The belowground soil of saltmarshes serves as a reservoir of historical saltmarsh processes, which can potentially be identified through alterations in physical and biological characteristics. In natural systems, there is often a correlation between sediment bulk density, soil water content, particle size, and organic matter content. However, it is important to note that each of these variables provides unique information about sediment characteristics. By considering these variables within a geographical context, a more comprehensive understanding of sediment properties can be obtained. The examination of the closely interconnected yet distinguishable attributes of saltmarsh sediments enables the assessment of their potential impact on physical and ecological processes as well as historical and contemporary dynamics of the ecosystem. This, in turn, contributes to the advancement of our comprehension regarding the effects of sediment characteristics on both the ecosystem and its habitats. Examining the individual effects of soil bulk density, water content, and organic matter enables a comprehensive understanding of their respective impacts on sediment stability, water retention, nutrient cycling, and the overall health of ecosystems. This approach helps identify the dominant factor in specific locations and under different conditions, as well as predict the unique responses of saltmarsh ecosystems to alterations in these parameters, including sea-level rise, climate change, and human activities.

Chapter 3- section 3.4.3 outlined the method adopted to investigate the past sedimentary evolution of Nigg Bay salt marshes focussing on:

- Spatial variation: Are there identifiable patterns in the belowground processes? Do they differ between natural and managed salt marshes and between surface zones of salt marshes?
- Temporal sediment variation: do changes in the belowground processes occur with depth? Can they provide information on saltmarsh formation and response over time to anthropogenic disturbances (such as reclamation and/or breaching)?
- Dynamic variation: do belowground physical properties of the sediment influence biological characteristics, and vice versa?

Table 6-1 below presents specific questions and hypothesis tested in this chapter to answer the aims posed in Chapter 3 -section 3.4.3.

**Table 6-1: research questions tested in this chapter.**

Thesis aims		Specific research questions	Experimental hypotheses	Methods	Chapter section
Improve understanding of spatial and temporal variation of saltmarsh evolution through depth/time.	Belowground Inorganic	Are there identifiable patterns in space and time in the sediment characterisation? How does belowground inorganics compare between a paired natural and managed salt marsh?	It is expected that the changes induced by land management in the Nigg Bay salt marsh have affected the characteristics of the sediment, creating different depositional and environmental gradients.	Particle characteristics (grain size) results of 8 cores along two transects traversing each saltmarsh surface zones of the managed and natural salt marshes of Nigg Bay ( Figure 6-2, Figure 6-3 and Figure 6-4).	6.2.1
			It is anticipated that mineral matter, such as the supply of fine-grained sediment, will vary over time. As such, it may enable the identification of source of sediment supply.		
	Belowground Organic	Are there identifiable patterns in the belowground organic content?  How these patterns compare on a paired natural and managed salt marsh?	Spatial characteristics of the sediment are expected to differ between natural and managed saltmarshes, affecting soil stability and topography (affecting water storage and wave attenuation).	BDD (Autocompaction) and Water content of 23 boreholes cores across the three study sites MR, FM and ANK (Figure 6 2).	6.2.2
			It is hypothesised that the changes that have occurred to the salt marshes of Nigg Bay over time (such as reclamation, managed realignment and natural salt marsh development from intertidal) will affect the characteristics of the sediments and may be detectable in the subsurface cores.		
			Environmental gradients may affect the cycling of the organic matter.		
SOM may differ between natural and managed. it is anticipated that there will be significant changes between the core results (i.e. newly managed salt marshes to increase organic matter production over time and so differ from natural salt marshes).	6.3.2				
				Photographic record of MR cores	6.4
Can these results inform on saltmarsh ecosystem services?			The measurement of SOM is relevant to the determination of the organic carbon (SOC) stored in the system. Environmental differences between the salt marshes studied are expected to affect carbon cycling and sequestration.	Carbon densities of 23 boreholes cores across the three study sites (Figure 6 2).	6.5.3

Data specifics on statistical results presented in this chapter are the same as in Chapter 4 and 6.

A list of abbreviations used in this chapter is provided in Appendix A.

## **6.2 Belowground inorganics: physical characteristics and properties of Nigg Bay saltmarsh sediments**

Sediment characteristics (presented in 6.2.1) and properties (presented in 6.2.2) have been recognised to be of primary importance to saltmarsh structure and function across many geomorphic zones (Esteves and Williams, 2015; Kelleway et al., 2016) as they influence consolidation of the saltmarsh sediment. They contribute to resistance to saltmarsh erosion, are a key predictor of system health and are relevant to ecosystem service delivery and carbon densities within the inorganics (presented in 6.2.3) and organics of the three saltmarsh sites studied here (presented in 6.3.2).

Section 6.2.1 below presents the physical characteristics from height cores collected across the three salt marshes in Nigg Bay; Section 6.2.2 covers the sediment properties (BDD and Water Content) of these cores augmented by a further 15 shallow cores; and section 6.2.3 presents the inorganic characteristics of all 23 cores.

### **6.2.1 Physical characteristics of the Nigg Bay saltmarsh sediments: grains legacy**

The sediment particle analysis below aims to identify:

- 1) any belowground patterns/sequences of sediment characteristics that can inform saltmarsh evolution through time and space.
- 2) whether belowground inorganics differ between the salt marshes studied (between paired natural and managed) or between saltmarsh surface zones to inform saltmarsh development through space?

This chapter section tests the hypotheses that:

- i. The accumulation of sediments belowground over time is expected to be similar between the natural salt marsh ANK and FM as they benefit of the same tidal input. However the influence of fluvial input (from Ankerville river) to the eastern/northeastern area of ANK is currently unknown;
- ii. The accumulation of sediments belowground over time is expected to differ between MR, ANK and FM owing to:
  - a. MR is situated in a sheltered position further inland and is protected by the remains of an embankment, resulting in reduced wave and tidal energies. This may lead to a decrease in the transport of coarse and heavy particles, favouring the settling of smaller particles such as silts and clays;
  - b. Disturbances caused by reclamation and de-embankment activities can also impact sediment accumulation;

- iii. The higher zones of the saltmarsh are primarily composed of fine grains, such as silts and clays. The size of sediment particles is expected to decrease as distance from the coast increases;
- iv. The processes of reclamation, realignment, and extreme events (such as storms) can have an impact on sediment delivery and burial. These processes can be reflected in the properties of subsurface soils at different depths. These changes are expected to be identifiable as indicators within subsurface cores.

Two transects presented in Chapter 3 – 3.4.3.3 were selected to test spatial heterogeneity within saltmarsh surface zones, proximity and distance to the saltmarsh edge, elevation, salinity and sediment depositional environment (marine and riverine). Cores extracted along these two transect are summarised in Table 6-3 and displayed as red lines on Figure 6-2. Figure 6-3 and Figure 6-4 cross-section profiles of each transect provide a position through the salt marsh and saltmarsh surface zones for each of the cores used in sediment particle analysis. Sediment treatment, methodology and analysis of the eight cores used for particle analysis are described in 3.4.3.3.

**Table 6-2: Summary of cores number and number of samples retrieved across the sites and saltmarsh surface zones as depicted in Figure 6-2 and used for sediment particle analysis. \* Cores collected on saltmarsh edge.**

Sites	Number of cores				No of samples
	HM	MM	LM	PM	
ANK	2	3	2	2	257
FM	2	1	*	*	103
MR	4	1	4	2	248

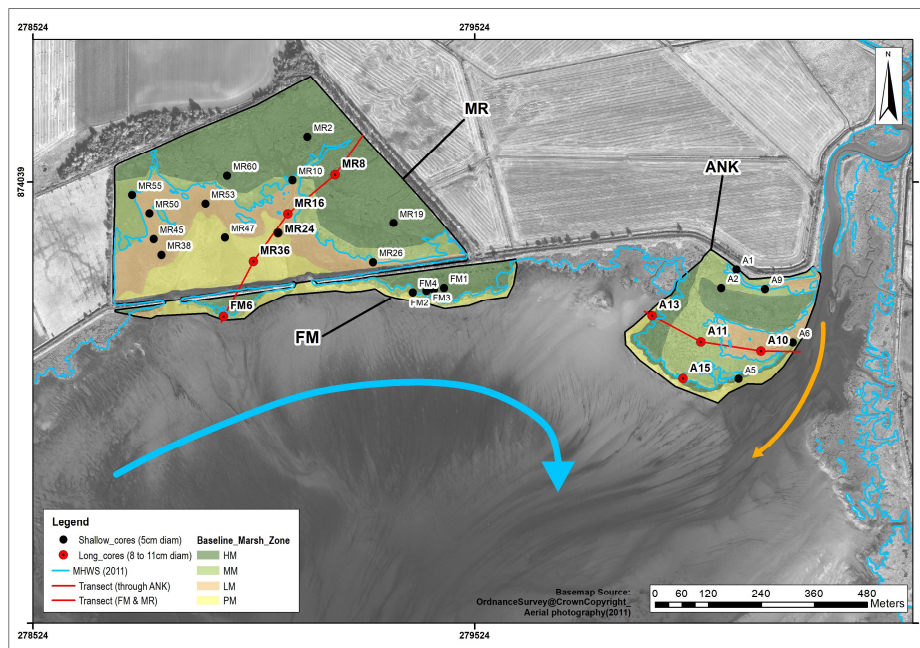


**Figure 6-2: Location of all the cores used this analysis: Red lines = Transects; Red dots = cores used for both particle analysis (this section 6.2.1) and organic matter analysis (6.3.1); Black dots = cores used for inorganic carbon content (6.2.3) organic matter analysis (6.3.1). Blue (thick) arrow represents the prevailing wave approach direction from the southwest of tidal. Orange (thin) arrow represents riverine flows (interpreted from Stapleton and Pethick, 1996); Abbreviations in legend: HM=High marsh, MM= Mid marsh, LM= Low marsh, and PM= pioneer marsh.**



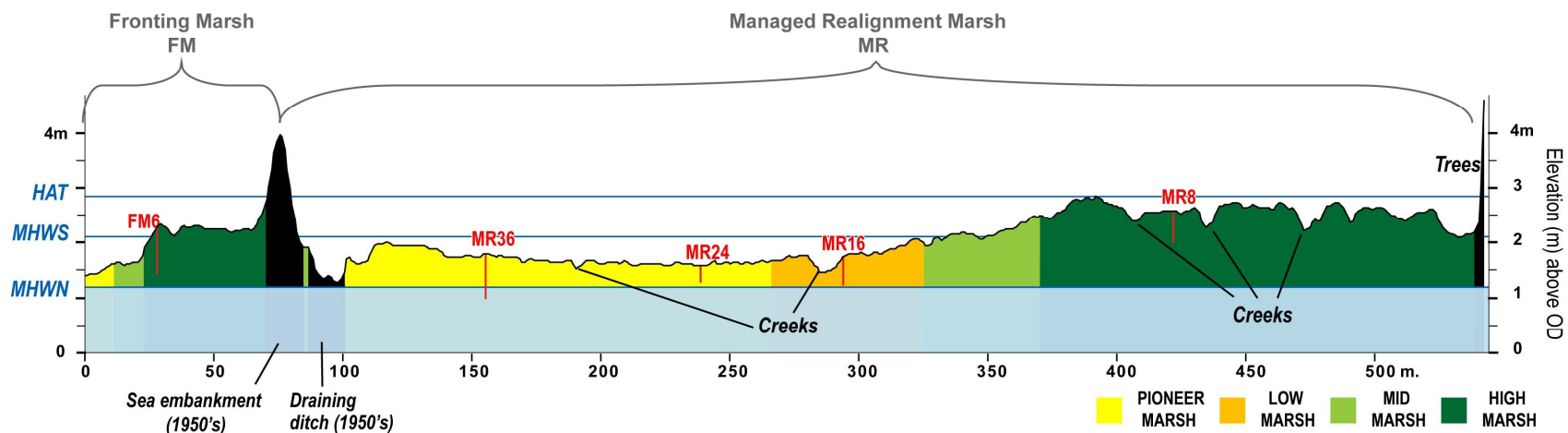


Figure 6-3: Transect 1 across the saltmarsh surface zones of FM and MR sites in a SW / NE alignment showing the location of the large cores (0.11m and 0.08 diameter) used for organic and inorganic analysis. Note 1: (vertical exaggeration 21.3X).

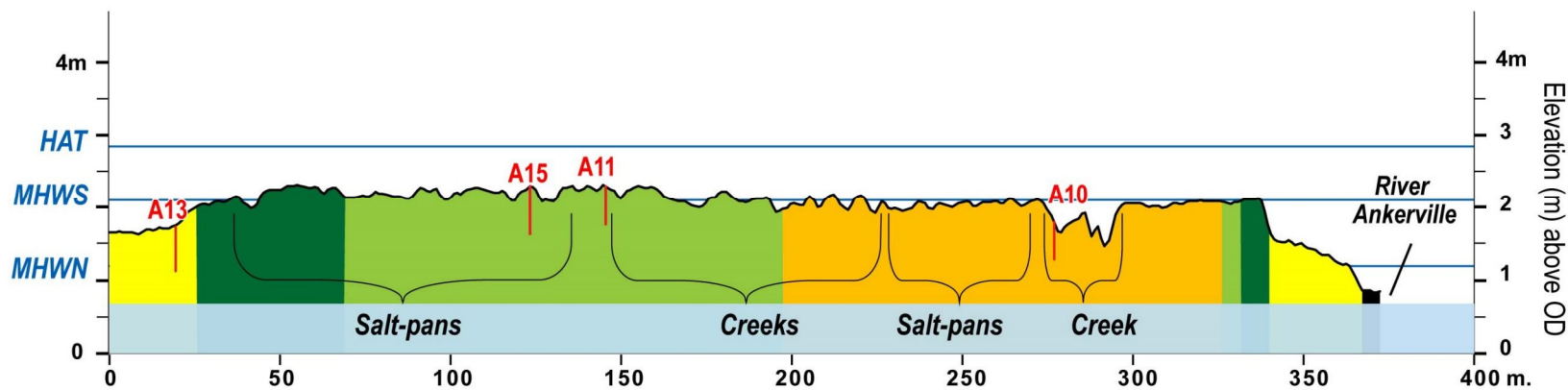


Figure 6-4: Transect 2 across the saltmarsh surface zones of ANK site in a SW / NE alignment showing the location of the large cores (0.08m diameter) used for organic and inorganic analysis. Note 1: (vertical exaggeration 21.3X). Note 2: Core A15 is located on cliff edge in HM zone.

### 6.2.1.1 Sediment characteristics: grain type and size variation

Across the two transects, sediment exhibits an overall mean grain size of  $91 \pm 2.95 \mu\text{m}$  (very fine sands) but comprising only  $8 \pm 0.3 \%$  of clays, and  $43 \pm 1.5 \%$  and  $48.7 \pm 1.3 \%$  of sand and silt respectively. Clays and silts are seen to moderately decrease with depth (spearman's  $\rho = -0.39$  and  $-0.43$  respectively, *p-value*\*\*\*) whereas sands are increasing with depth ( $\rho = 0.41$ , *p-value*\*\*\*). The majority of sediment retrieved across the three salt marshes is composed of fine sands (with skewness ranging 1.5 to 2.5).

The results indicate that there are notable variations in the average grain size among the three saltmarsh sites, namely ANK, FM, and MR ( $F=3.8272$ , *p-value* $<0.05^*$ ), as demonstrated in (Table 6-3). The analysis reveals that the clay distribution on MR is significantly greater compared to the natural salt marshes ANK and FM ( $F = 16.81$ , *p-value*  $<0.001$  \*\*\*). The sand proportion on ANK was significantly higher ( $45.9 \%$ ) compared to MR ( $38.2 \%$ ) ( $F = 3.13$ , *p-value* $<0.05^*$ ), the sand proportion on FM was comparable to the other sites. The silt content was observed to be relatively consistent across the three marshes.

To ensure a balanced distribution of samples for the purpose of statistical analysis, a total of six depth intervals were chosen. The first five intervals were chosen at 10 cm increments, spanning from the uppermost section of the core to a depth of 50 cm. Additionally, a sixth interval was chosen, encompassing the range from 50 cm to 87 cm. Specifically, for the sediment retrieved on ANK and FM, Figure 6-5 shows that across these intervals, there is a consistent decrease in the quantity of silt as depth increases, while the trend for sand reverses, showing an increase with depth. The distribution of clay, on the other hand, remains relatively consistent throughout the depth profile. However, in the context of MR, there is a notable alteration in the sediment composition at a depth ranging from 30 to 40 cm (as depicted in Figure 6-5). Specifically, the proportion of sands increases significantly to approximately  $56.47 \pm 3.8 \%$  until 50 cm in depth, with a visible increase in sand proportion towards the base of the cores (more than  $75 \%$ , at a maximum depth of 87 cm). Conversely, silts exhibit the highest sediment concentration (approximately  $58.7 \%$ ) in the upper portion of the cores (at a depth of 30-40 cm), and experience a substantial decline to approximately  $38.6 \pm 3.2 \%$ . The clay content exhibits a gradual decrease to approximately  $3.2 \%$  within a depth range of 30 to 40 cm, after which it remains relatively constant.

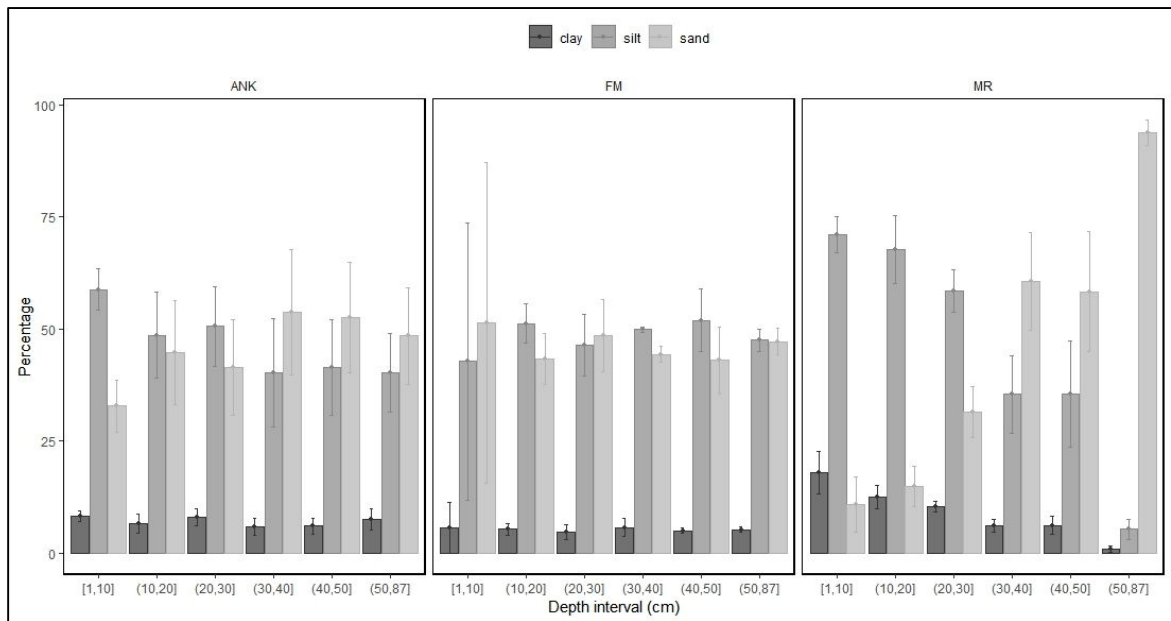


**Figure 6-5:** Bar plot showing the overall average sediment distribution (clays, silt and sand in percentage) at a 10 cm interval until 50 cm and from 50 to 87 cm through the core depth for the cores taken on ANK, FM and MR (see Figure -4 for core location) (Note: error bar are made of sample mean and lower and upper Gaussian confidence limits based on the t-distribution).

#### 6.2.1.2 Sediment characteristics: grain type and size variation with depth per transects per cores

Association of sand, silt and clay proportion with depth for each core is summarised in Figure 6-17. Details of the cores that demonstrate homogeneous, gradual and discernible shifts through stratigraphy/depth are presented per transect on a seaward/ landward axis from Figure 6-6 to Figure 6-9 and from Figure 6-12 to Figure 6-16.

#### **SW/NE Transect through MR (see Figure 6-2 and Figure 6-3 for core locations)**

The overall mean grain size of the cores extracted from the MR site demonstrates a strong positive correlation to depth ( $\rho=0.71$ ,  $p$ -value\*\*\*) with the proportion of sands increasing from 10.9 % (1-10 cm deep) to 93.72 % at 50- 87cm depth.

This clear and gradual increase in the sand proportion is exhibited through the three cores MR36, MR24 and MR16 (Figure 6-6 to Figure 6-8), all associated with peaks in Skewness and Kurtosis suggesting shifts in mineralogy (Table 6-3).The upper cores of MR36 and MR24 present discernible shifts in grain size at respective depth of 5 cm and 11 cm. Further down, peaks take place on cores MR36, MR24 and MR16 at the respective depth of 31, 33 and 36cm, suggesting that depth increases with elevation and distance to the saltmarsh edge with cores spanning the PM to LM zones on a SW/NE landward axis. However, MR24 and MR16 display further discernible shifts lower in the core at the respective depth of 37 and 41 cm where coarser grains decrease until a steady-state has been reached at 43cm deep in both cores. Although MR36 sand proportion

increases to the base of the core ( $\rho=0.97$ ,  $p\text{-value}^{***}$ ), a small mineralogical shift is also displayed at a depth of 41 cm like MR24. The observed changes in the core records indicate a transition in the salt marsh ecosystem, specifically at the specified locations, from a sand/mudflat to an pioneer salt marsh. This phenomenon can be associated with the expansion of saltmarshes.

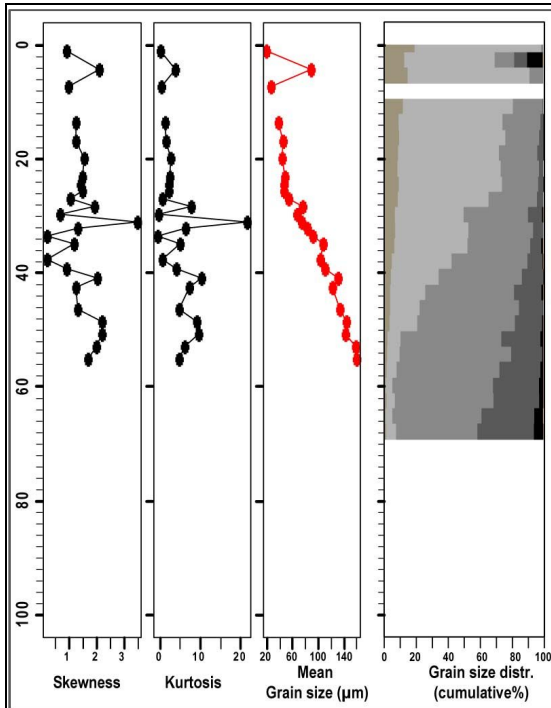


Figure 6-6: GSD of Core MR36 ( $\varnothing = 8\text{cm}$ ) is located behind remains of sea embankment on MR's PM of.

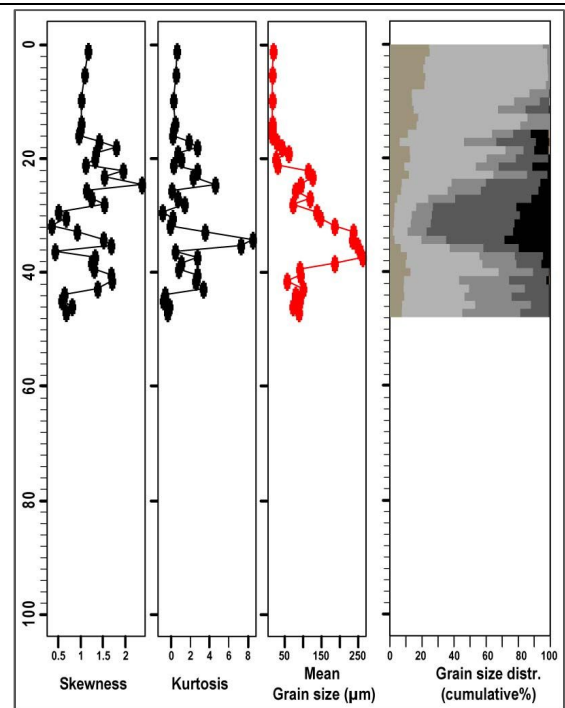


Figure 6-7: GSD of Core MR24 ( $\varnothing = 11\text{cm}$ ) located at the limit of MR's PM and LM.

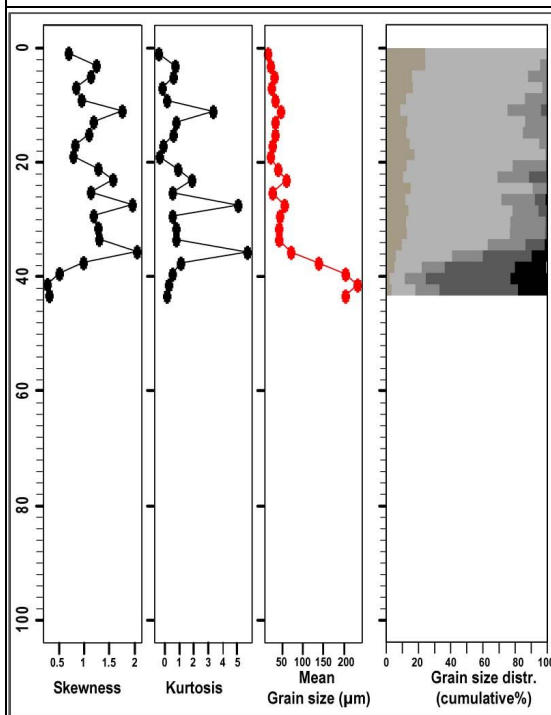
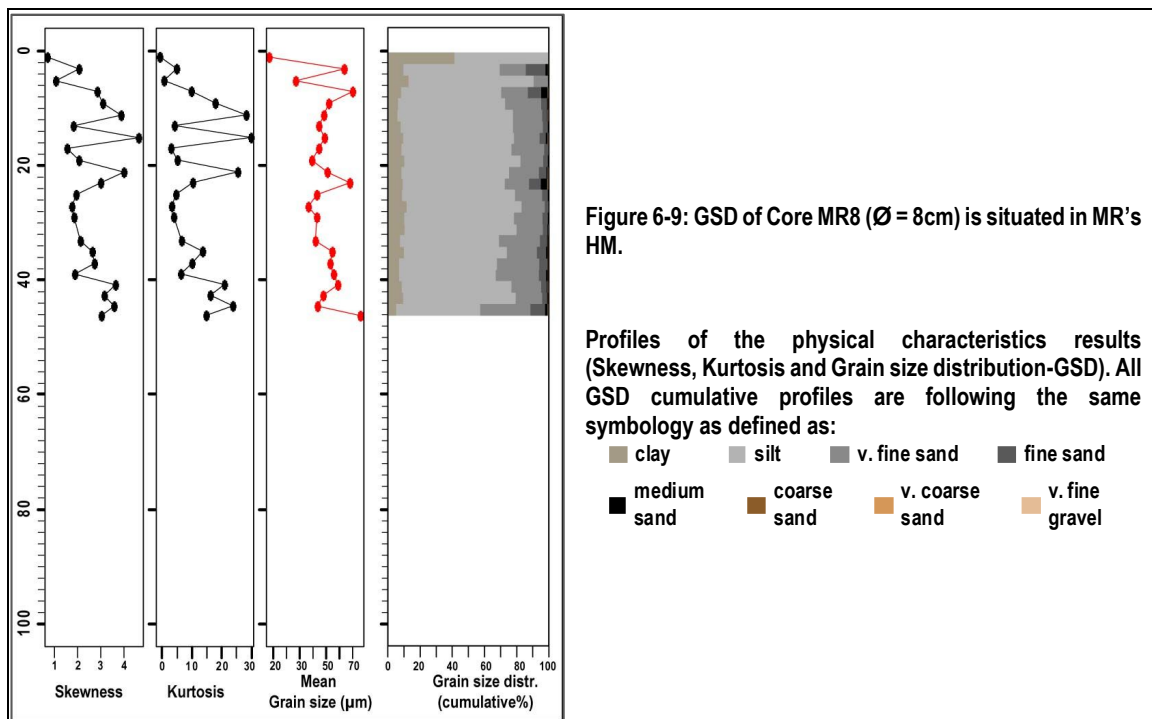


Figure 6-8: GSD of Core MR16 ( $\varnothing = 8\text{cm}$ ) located at the limit of MR's LM and MM, east of the main creek.

Profiles of the physical characteristics results (Skewness, Kurtosis and Grain size distribution-GSD). All GSD cumulative profiles are following the same symbology as defined as:

- clay      ■ silt      ■ v. fine sand      ■ fine sand
- medium sand      ■ coarse sand      ■ v. coarse sand      ■ v. fine gravel

Higher in the salt marsh, core MR8 sediment content is dominated by silts and displays numerous peaks which are difficult to clarify. The core is located in the high marsh and is the furthest away from saltmarsh edge and creek network and only inundated during spring tide where sedimentation will be slower. Each fraction (clays, sands and silts) exhibits up-down patterns at a 1 to 2 cm scale across the core (Figure 6-9). This pattern is accompanied by series of sharp peaks in sediment type, skewness and kurtosis at the top of the core to 9 cm in depth. These peaks may be caused by several events, but it is likely that bioturbation (plant rootlets, burrowing, trampling and grazing by animals - French and Burningham, 2003; van der Wal and Pye, 2004; Doody, 2008; Tempest et al., 2015) have all affected the upper thin horizons, the sudden change in grain size when coarse grains can only be brought in this high marsh zone irregularly with high spring tides and storm and extreme events influencing shifts lower in the core. From 9 to 23 cm in depth, a much more stable phase is observed. A step up at 35 cm is associated with shift in autocompaction (BDD) and in organic content (SOC) as depicted in Figure E- 8 profiles (and Chapter 7 Figure 7-35 for core MR 8). This stratigraphical horizon was preceded by small sediment coarsening associated with increase in organic content and finally, underlain (from 43 cm deep) by a core base containing 75.5 % more sands that extended down to at least 74 cm in depth (see details in Chapter 3 -3.4.3.1) and coincide with absence of organic matter and high soil compaction (BDD) inferring another depositional sequence such presence as pioneer marsh or mud/sand flat.



W/E Transect through ANK (see Figure 6-2 and Figure 6-4 for core locations)



Overall grain size for the cores excavated on the natural salt marsh ANK was strongly correlated with depth (Table 6-3). On the pioneer marsh, Core A13 skewness and kurtosis profiles alongside with the mean grain size displays five principal horizons through the core (Figure 6-12). An upper unit exhibiting an uneven trend on grain size up to c.15cm comprising c.61.9±1.8 % of silts, 28.8±2.3 % of sands and 8.9±0.4 % of clays. From c.15cm up to 32cm a regular increase is visible and demonstrated by a rise of sands (60.2±5.5 %) and clays (10.3±0.7 %) and loss of silts (35±4.9 %). From 32 to 40cm deep, the proportion of coarser sediment continues to increase further where sands make up 90.5±1 % of the unit with 11±0.9 % of clays, and, overall this sediment is symmetric and rounded (Skewness & Kurtosis  $\leq 0.5$ ). From 40 to 60cm depth, the proportion of coarse and very coarse sand steadily increases to 80.2±10.1 % whilst clay content reaches 14.8±1.3 % but in an irregular pattern. The base of A13 core presents a highly variable sediment distribution comprising a wide range of material, from fine sand to very fine gravel, suggesting that another stratigraphical unit has been reached. This basal sediment is very similar to that visible in the creek beds located close to the core (Figure 6-10) (unlike the creek beds of the eastern edge). The changes and variations observed in the core produce a moderate correlation between grain size to depth (Spearman's rho  $\rho = 0.47$ , *p-value*\*\*\*) (Figure 6-17), however, from c.15 cm to almost the core base, a strong correlation between grain size and depth is evident ( $\rho = 0.71$ , *p-value*\*\*\*).

Further east, on the mid-marsh transect, core A11 presents clear peaks and changes through its sedimentary development but still displays strong negative correlations for clays and silts with depth ( $\rho = -0.74$ , and  $-0.76$  respectively, both *p-value*\*\*\*) and a very strong positive association between sand content and depth ( $\rho = -0.8$ ), *p-value*\*\*\*. Five horizons are also discernible at the depth of 21, 27, 40, 45 and 53 cm; they display comparable trends to the A13 core stratigraphy where the upper unit is highly variable with series of up-and-down peaks, followed by a decrease of sediment size and skewness until a stable phase is reached (27 to 40cm) where the sediment size increases and minerology is fairly uniform (skewness and kurtosis profiles in Figure 6-14). As in core A13, this unit was preceded by strong and irregular changes (high peaks) in minerology with a clear input of coarser sediments in the marsh. From 45 to 53cm deep, the horizon displays a gradual increase of medium and coarse sand content (from c.66 % at 53cm to 33 % at 45cm) in favour of clay and silts. The last two samples of the core exhibit the highest sand content of the core averaged at 63.2±2.8 % suggesting a new horizon.

Contrastingly, core A10 located in the low marsh and in the proximity of one of the biggest creek of ANK salt marsh (Figure 6-11), behaves in the opposite manner to the previous cores where overall clays and silts contents were strongly and positively correlated to depth ( $\rho = 0.72$ , and  $0.72$  respectively, both *p-value*\*\*\*) and sands proportion was negatively correlated to depth ( $\rho = -0.80$ ,

*p-value*\*\*\*). However, the profile, shows a decreasing trend of mean grain size slits punctuated by high peaks of coarse sand at 18 and 27cm. These peaks may be residual from storm or extreme events that took place during this phase, but they are at similar depth to horizons displayed in core A11. Two phases from 31 cm to 39 cm and then from 39 to 45 cm display a loss of coarse sediment in favour of finer grains. From 45 to 59cm, there is steady decrease of coarse sediment meaning that sands content has indeed in time accrued from 2 % to 17.5 % whilst silts declined from 77.7 % to 67.8 % and clays fell from 20.4 % to 14.8 %. The last sample at 57-58 cm depth exhibit a reverse trend.

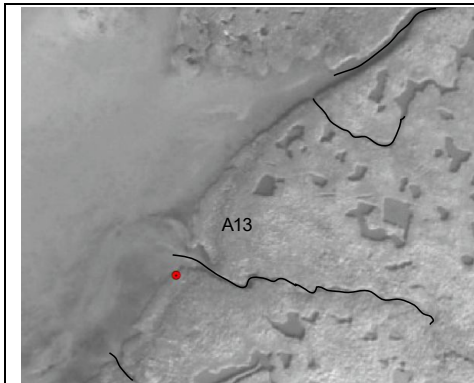


Figure 6-10: Four major creeks (black) in the vicinity of Core A13

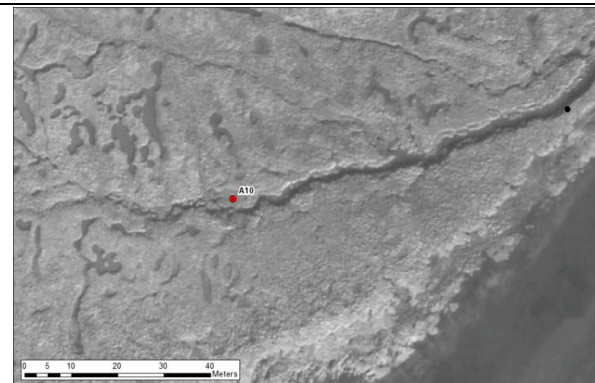


Figure 6-11: Core A11 located to the north (c.1.8m deep at point) of biggest creek of ANK salt marsh

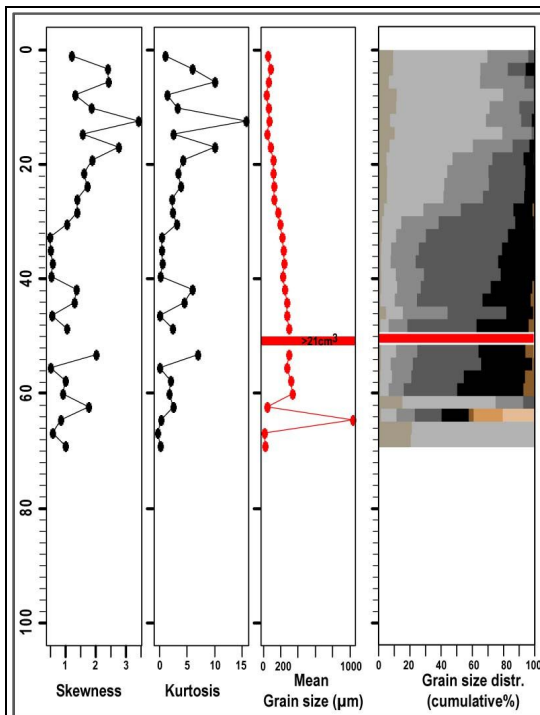


Figure 6-12: GSD of core A13 is located on ANK's western edge PM. The red band corresponds to rounded pebble (21mm<sup>3</sup>) lodged in the profile (see 3.4.3.3.)

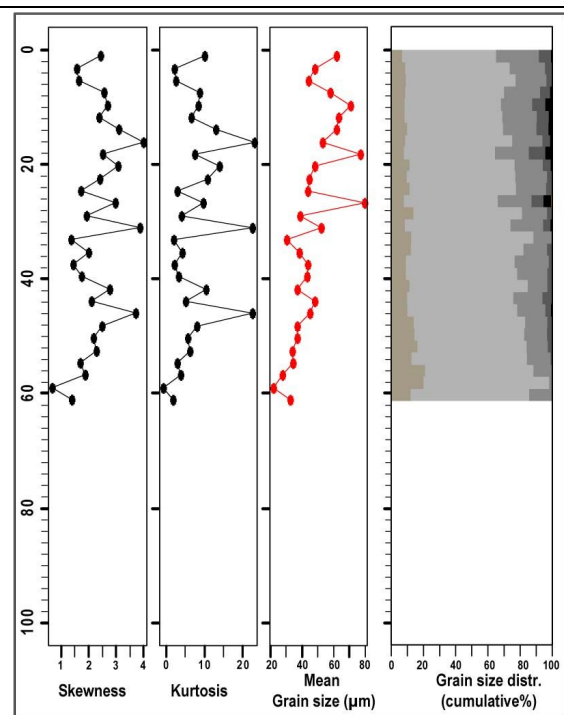
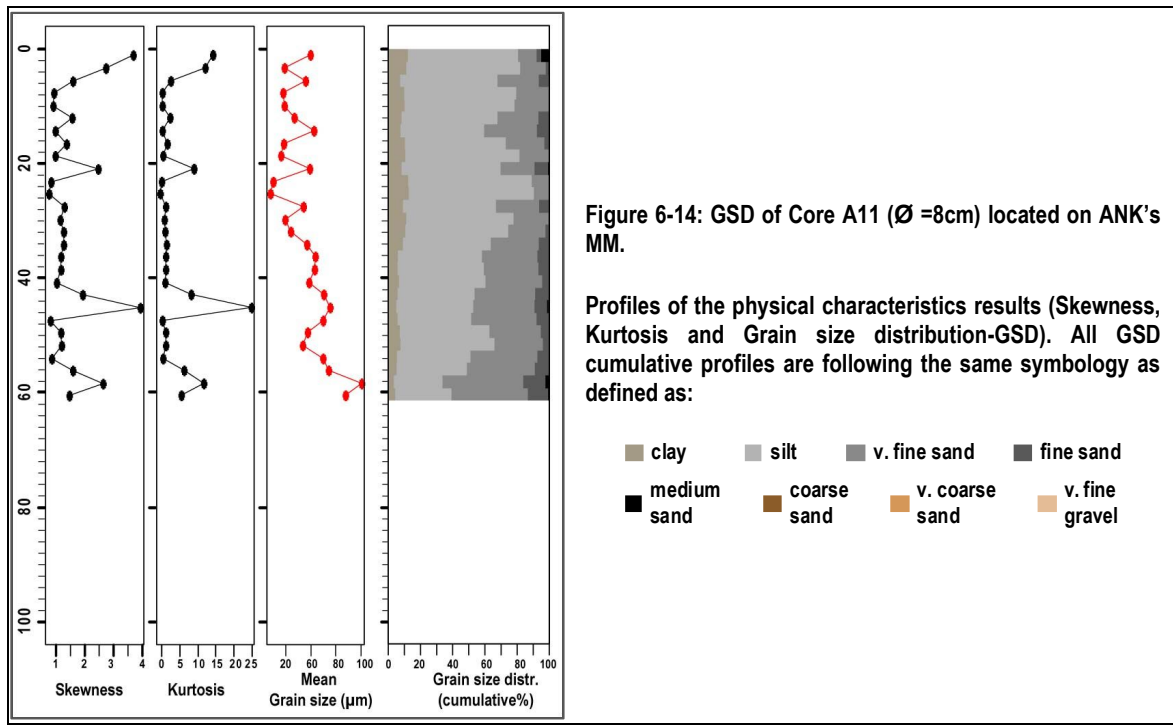


Figure 6-13: GSD of Core A10 (Ø =8cm) located on ANK's LM north of the major creek channel.



**Cores collected at the saltmarsh edge (see Figure 6-2, Figure 6-3 and Figure 6-4 for core locations)**

The two cores FM6 (Figure 6-15) and A15 (Figure 6-16) taken few meters from the cliff edge of the fronting marsh FM and natural salt marsh ANK are fundamentally different than the other cores as the grain size, mineralogy and sediment distribution do not demonstrate any association with depth (Table 6-3). Therefore, accumulation and sedimentation analysis are more complex as the cliff can be formed, at top and/or bottom, from previously dislodged portions of the marsh surface. The profiles show laminated facies that reflect marsh response to tide, seasonal growth and die back, winter and summer sediment input and, possibly, extreme events. As the two cores have been exposed to similar events, it is tempting to assume the profile peaks at the depth 8cm, 21cm, 51cm and 61 cm, displayed on the two cores are correlated; however, their maturity and their response to extrinsic and intrinsic factors will differ. In this respect, the overall clays, sands and silts proportion have been found significantly different between the two cores (respectively  $F=16.48$ ;  $F=48.95$ ;  $F=52.78$ ; all  $p\text{-value}^{***}$ ) but these differences were not demonstrated statistically at a 10cm interval depth suggesting the sediment content response is comparable on the two marsh edges.

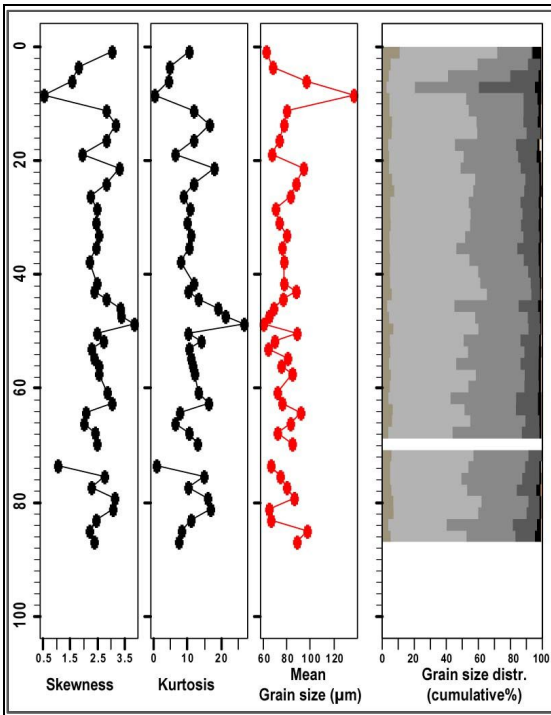


Figure 6-15: GSD of Core FM6 (8cm diameter Ø) located on FM cliff edge.

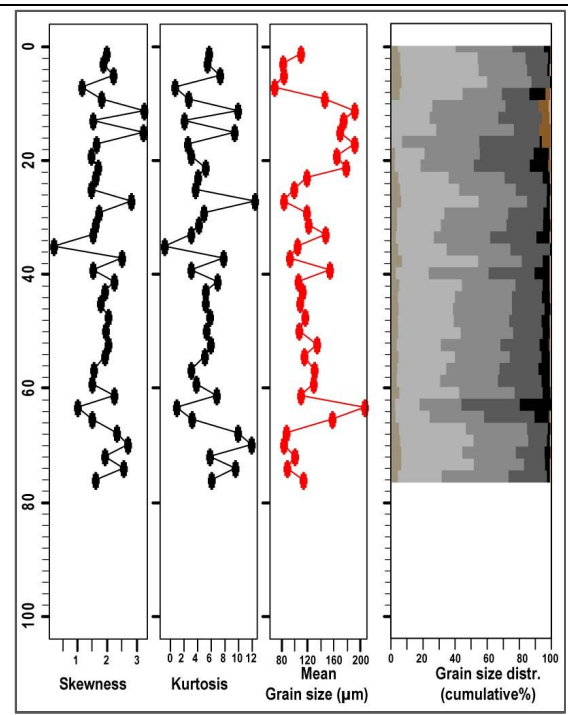


Figure 6-16: GSD of Core A15 (Ø =8cm) located on ANK's cliff edge.

Profiles of the physical characteristics results (Skewness, Kurtosis and Grain size distribution-GSD). All GSD cumulative profiles are following the same symbology as defined as:

- 
 clay
- 
 silt
- 
 v. fine sand
- 
 fine sand
- 
 medium sand
- 
 coarse sand
- 
 v. coarse sand
- 
 v. fine gravel

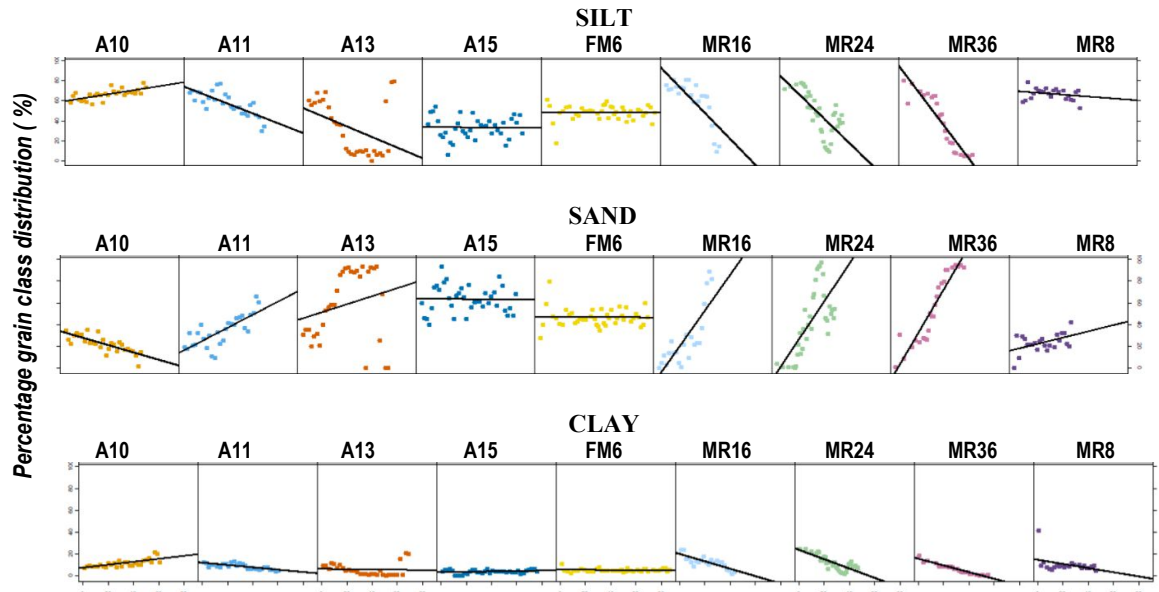


Figure 6-17: Matrix plot showing the relations between silt (top), sand (middle) and clays (bottom) to depth in the core (black regression line is only intended to be informative).

**Table 6-3: Sediment distribution (clay, sand and silt %) for the nine cores presented in this section: A10, A11, A13, A15, FM6, MR16, MR24, MR36 and MR8.**

Depth intervals	Core	CLAY (%)		SAND (%)		SILT (%)		n
		Mean	SD	Mean	SD	Mean	SD	
[1,10]	A10	8.72	0.86	29.14	4.76	62.20	4.00	5
[10,20]		9.10	0.93	30.35	4.31	60.55	4.08	4
[20,30]		11.16	2.23	24.30	5.60	64.54	3.75	5
[30,40]		10.60	1.89	20.10	5.54	69.36	3.89	5
[40,50]		11.73	1.91	19.40	4.23	68.88	3.14	4
[50,87]		16.42	3.81	12.85	5.66	70.75	4.22	6
[1,10]	A11	10.62	1.82	22.32	5.57	67.08	3.97	5
[10,20]		9.65	1.48	29.38	9.16	61.00	7.79	4
[20,30]		11.20	2.02	21.12	10.79	67.68	8.88	5
[30,40]		8.25	2.33	35.95	7.42	55.80	5.37	4
[40,50]		6.54	0.80	43.62	5.04	49.84	4.34	5
[50,87]		5.64	1.51	51.96	12.29	42.40	10.80	5
[1,10]	A13	9.18	2.04	30.18	6.93	60.70	5.33	4
[10,20]		8.18	2.57	34.68	12.12	57.22	9.95	5
[20,30]		4.85	0.90	60.95	6.97	34.23	6.10	4
[30,40]		1.74	0.34	89.54	2.80	8.74	2.49	5
[40,50]		2.13	1.79	88.95	3.77	8.90	2.44	4
[50,87]		7.03	9.10	51.03	43.76	28.53	33.65	9
[1,10]	A15	5.24	0.92	49.12	8.14	45.66	7.26	5
[10,20]		0.46	1.03	78.96	8.54	20.60	8.63	5
[20,30]		4.16	1.63	63.00	13.39	32.82	11.81	5
[30,40]		3.92	1.66	65.90	12.24	30.16	10.55	5
[40,50]		4.24	0.40	58.90	2.60	36.86	2.43	5
[50,87]		4.23	1.30	62.88	11.12	33.08	9.61	12
[1,10]	FM6	5.75	3.57	51.38	22.51	42.85	19.43	4
[10,20]		5.35	0.87	43.40	3.60	51.25	2.76	4
[20,30]		4.73	1.01	48.58	5.06	46.50	4.33	4
[30,40]		5.78	1.22	44.40	1.15	49.90	0.42	4
[40,50]		5.03	0.55	43.00	7.02	51.97	6.63	6
[50,87]		5.27	1.19	47.21	6.23	47.56	5.35	21
[1,10]	MR16	18.66	5.35	6.62	5.98	74.74	3.71	5
[10,20]		13.20	3.30	11.88	9.19	74.90	6.07	5
[20,30]		12.78	1.79	22.28	8.52	64.98	6.81	5
[30,40]		9.12	3.51	44.02	24.01	46.84	20.57	5
[40,50]		2.70	0.85	85.15	4.60	12.15	3.75	2
[1,10]		MR24	24.00	1.49	2.03	1.62	74.00	2.56
[10,20]	18.04		3.75	11.69	12.02	70.27	9.14	7
[20,30]	11.18		3.35	40.46	14.93	49.48	10.82	8
[30,40]	4.82		2.93	80.43	16.98	20.70	12.18	9
[40,50]	9.33		1.87	48.03	8.54	43.06	7.28	8
[1,10]	MR36		15.17	3.32	13.50	15.25	71.33	12.41
[10,20]		7.38	5.07	17.18	11.77	50.50	33.70	4
[20,30]		7.83	0.95	35.45	10.78	56.73	9.83	6
[30,40]		4.13	1.07	67.22	12.51	28.65	11.49	6
[40,50]		1.35	0.48	91.98	2.27	6.70	1.79	4
[50,87]		0.97	0.32	93.73	1.17	5.33	0.90	3
[1,10]	MR8	15.62	14.66	19.00	13.67	65.40	7.90	5
[10,20]		8.34	1.67	20.98	2.19	70.72	1.78	5
[20,30]		9.60	1.27	21.92	3.97	68.50	3.09	5
[30,40]		8.63	1.73	26.95	5.58	64.43	4.00	4
[40,50]		7.48	2.00	29.40	10.19	63.08	8.22	4



## **6.2.2 Physical properties of Nigg bays young and mature salt marshes - Bulk dry density (BDD) and Water Content**

Physical sediment characteristics and properties are rarely examined in restoration schemes even though recognised as being crucial to plant establishment, succession, diversity and abundance as poor sediment structure and moisture can lead to high soil toxicity, high salinity and anoxia (Spencer et al., 2017). Inversely this can contribute to the long-term survival of the salt marsh by consolidation and compaction of the new marsh sediments which will in turn determines soil strength resistance to erosion (Zhang et al., 2001; Boorman et al., 2002). The changes in bulk density are influenced by the relative proportion and porosity of solid organic and inorganic particles that then impacts on drainage. Bulk density has also a central and pivotal role in this thesis research as it is used to determine accretion rates from sediment deposition (presented in Chapter 4 - section 4.2.2.1) and is also used to quantify soil blue carbon stocks (methodology is presented in Chapter 3 - section 3.4.3.2). Changes in water content through the marsh stratigraphy relates to the past exchange of water through sub-surface abiotic conditions and soil aeration (Zhang et al., 2001; Fearnley, 2008; Spencer et al., 2017). Water content is of particular importance for sediments at land-ocean interface where water-table fluctuations are common, furthermore, the water present within the sediment matrix contains itself radiation dose which has to be accounted to date sediments using radionuclides or isotopes (Clarke and Rendell, 2000; Mellett, 2013). Variations in water content have the potential to affect the concentration of salts in the sediment pore water and consequently the overall salinity of the marsh ecosystem. The influence of salinity on the composition of saltmarsh species and vegetation communities is of paramount importance. The water content of salt marshes can be significantly influenced by various meteorological factors, such as rainfall, as well as hydrological variations, including tidal flooding or water and sediment regulation schemes (dredging, dams). Consequently, these factors can lead to changes in the composition of surface soils and other physicochemical properties of the soil (Bai et al., 2016).

The coring programme aimed to:

- 1) determine whether the sediment properties in managed salt marsh are similar to those found in natural marsh sediments;
- 2) provide insights into soil properties (BDD and water content) feedbacks by examining variations over time (i.e. depth);

This section aims to test whether sediment properties such as belowground BDD and water content will:

- i. differ between natural and managed saltmarsh sites as a result of reclamation and de-embankment;
- ii. differ between saltmarsh surface zones and distance from saltmarsh edge as consequence of a reduced tidal sediment input;
- iii. differ through the stratigraphic depth, reflecting impact of disturbances (reclamation and realignment, prolonged inundations and extreme events such as storms), possibly visible as sudden shifts within the core profiles.

The sediment treatment, methodology, and analysis of the 23 cores are detailed in Chapter 3, specifically in section 3.4.3.2, corresponding to step 1a and 1b in Table 3.12. Additionally, the profile results for a subset of cores, which are equivalent to sediment grain profiles, are provided in Appendix E, specifically in section E4, spanning from Figure E-4 to E-12.

#### 6.2.2.1 Bulk dry density – BDD – Soil autocompaction

Soil dry bulk density (BDD) quantifies the mass of dry soil that occupies a specific volume of space. Soil compaction, porosity, and structure are fundamental components of soil that merit substantial consideration owing to their significance and influence.

##### **BDD variation between saltmarsh sites and variation between saltmarsh surface zones**

Overall BDD ( $\mu=0.89\pm 0.02 \text{ g.cm}^{-3}$ ) was not found to differ significantly between the three saltmarsh sites but greater difference was found between saltmarsh surface zones ( $H_{df=3}= 24.5$ ,  $p<0.001^{***}$ ). Pioneer zones (Figure 6-18) are found to have highest bulk density compared to significantly to all other saltmarsh zones.

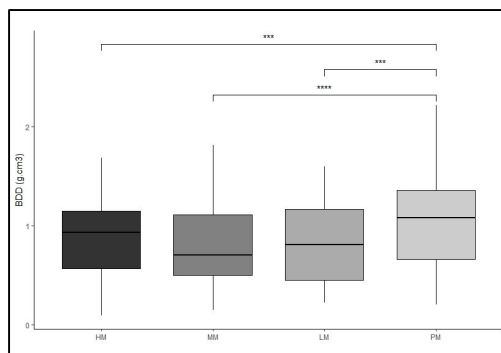


**Figure 6-18: Boxplot of average BDD ( $\text{g.cm}^{-3}$ ) per saltmarsh surface zones. (Note1: Kruskal-Wallis H test and significant pair-test comparison using Dun's tests results by the p-value significance: *ns*, \*, \*\*, \*\*\* for  $> 0.05$ ,  $\leq 0.05$ ,  $\leq 0.01$ ,  $\leq 0.001$ . Note1: Boxplots represent median (middle line) interquartile range (box), 1.5 times interquartile range (bar) and outliers (black dots)).**



Correlating BDD and depth between sites and saltmarsh surface zones demonstrates variability enabling an appreciation of any external changes or disturbances impacting the sediment structure. The expected trends of increasing BDD with depth (Callaway et al., 2012) is only demonstrated in varying degrees across all of ANK's saltmarsh zones: the correlation between HM and LM with depth is moderate, whereas the correlation between MM and PM zones with depth is weak (Figure 6-20 illustrates the linear regression with polynomial terms and the caption provides the regression results). ANK's BDD on HM and PM zones only increases to about 40 cm in depth, then decreases to the base of the cores, indicating a drastic change in the saltmarsh evolution. On FM, the HM and MM zones (corresponding to FM's cliff edge) are moderately correlated to depth (Figure 6-20). In contrast to the observed monotonic relationships between BDD and depth on ANK and FM, MR's BDD exhibits moderate to very strong positive linear correlations with depth on all saltmarsh surface zones (Figure 6-20). Similarly to ANK, the BDD of MR on HM and PM decreases at depths of approximately 25 cm and 35 cm. This analysis is covered in more depth in Chapter 4 - section 4.2.2.1 and figure 4-11.

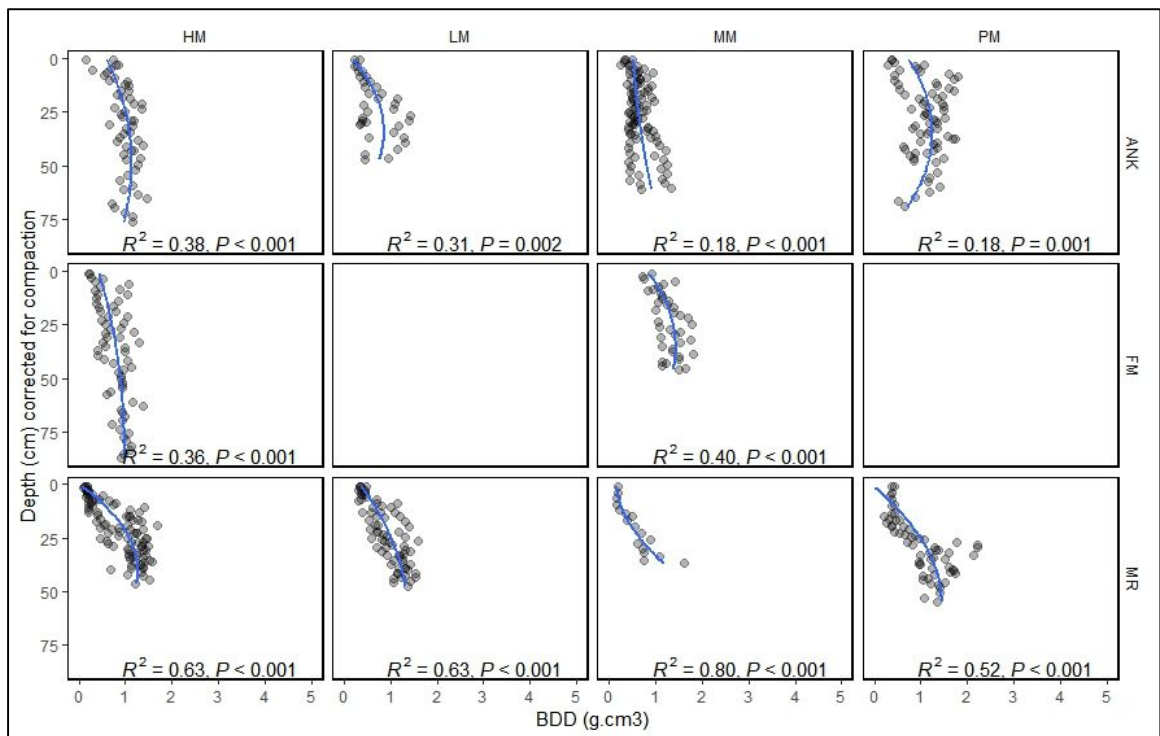


Figure 6-20: BDD ( $\text{g}\cdot\text{m}^{-3}$ ) versus depth (in cm and corrected for compaction) per sites and saltmarsh surface zones. Blank box: absence of core for this saltmarsh zone. Polynomial trends shown in blue and the results of polynomial regressions (correlation coefficients and statistical significances) are provided as bottom of each graphs.

### 6.2.2.2 Water content in saltmarsh sediments

As previously discussed in section 2.2, marsh stratigraphy reflects past water exchange through subsurface abiotic conditions and soil aeration (Zhang et al., 2001; Fearnley, 2008; Spencer et al., 2017). Water content is especially important for sediments at the land-ocean interface, where water-table fluctuations are common, and the water in the sediment matrix contains radiation dose that must be accounted for when dating sediments with radionuclides or isotopes (Clarke and Rendell, 2000; Mellett, 2013). Water content can affect sediment porewater salt concentration and marsh ecosystem salinity. Salinity affects saltmarsh species and vegetation communities. Rainfall, tidal flooding, and water-sediment regulation schemes (dredging, dams) can also significantly affect saltmarsh water content. These factors can alter surface soil composition and other physicochemical properties (Bai et al., 2016).

**Water content variations between saltmarsh sites and variation between saltmarsh surface zones** (Figure 6-21 and Figure 6-22)

Different overall results show that water content ( $\mu 39.12 \pm 0.8$  %) differ significantly between the three saltmarsh sites with sediments moisture ranging between 35.74 % to 40.65 % (Figure 6-21;  $H_{df=2} = 13.5, p < 0.001$  \*\*\*). Pairwise comparison demonstrates that ANK's sediment moisture is significantly higher than MR.

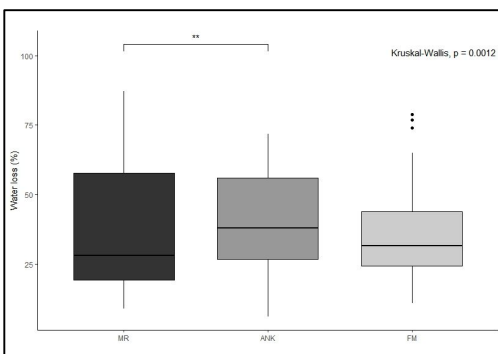


**Figure 6-21: Boxplot of water loss percentage per sites. Boxplot of water loss percentage per Sites. (Note: Kruskal-Wallis H test and significant pair-test comparison using Dun's tests results by the p-value significance - Results in table E-2.)**

In general, the analysis reveals a consistent pattern of water loss based on elevation, following the tidal gradient across the salt marsh from the pioneer-zone to mid-marsh with significant differences observed among the various surface zones within the salt marshes ( $H_{df=3} = 28.4, p < 0.001$  \*\*\*). PM has the least amount of water loss when compared to LM and MM. Figure 6-22 and table E-2 demonstrate that the HM zone has significantly higher water loss than the MM zone, but not when compared to the other zones.



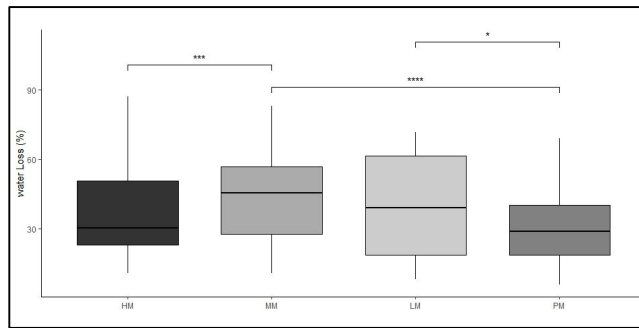


**Figure 6-22: Boxplot of water loss percentage per saltmarsh zones. (Note: Kruskal-Wallis H test and significant pair-test comparison using Dun's tests results by the p-value significance - Results in table E-2.)**

**Water content variation between saltmarsh surface zones per saltmarsh sites (Figure 6-23)**

Analysis of variance confirms that water loss of LM zone on natural salt marsh ANK is significantly higher than PM zone, not what we would expect. This would be containing the most water and HM the least. FM's MM zone has consistently less water loss than ANK's MM and MR's MM. It also shows the lowest amount of water loss. Similarly, MR is not following expected elevation gradient, MR's MM zone is consistently ranked having the most water loss the HM, MM and PM zones (Table 6-5 , Figure 6-23 and table E-2).

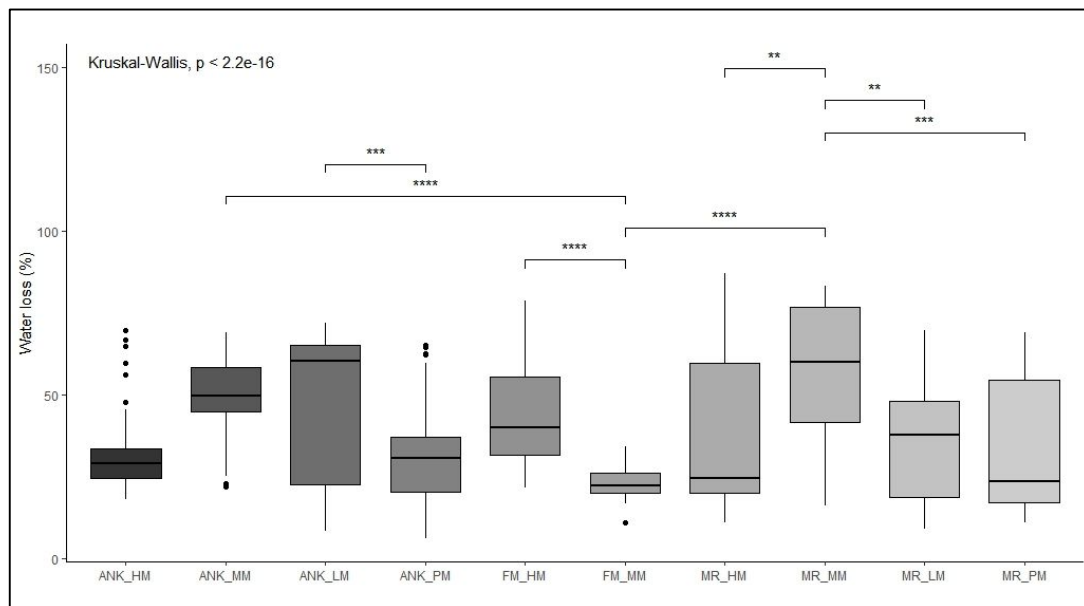


**Figure 6-23: Boxplot of water loss percentage per sites' saltmarsh zones. (Note: Kruskal-Wallis H test and significant pair-test comparison using Dun's tests results by the p-value significance - Results in table E-2.)**

**Table 6-5: Water content (%) per sites and saltmarsh surface zones . Top row provides one-way ANOVA results for each salt marsh of the variance of water content (log<sub>e</sub> %) versus saltmarsh surface zones between at using p-value<0.001=\*\*\*, p-value<0.01=\*\* and p-value<0.05=\* (details in Table E-2)**

	ANK (F=75.43***)			FM (F=179.47***)			MR (F=4.63**)		
	Mean	SD	n	Mean	SD	n	Mean	SD	n
<b>Overall</b>	40.65	16.45	257	35.74	15.13	103	37.35	21.89	248
<b>HM</b>	31.9	11.8	55	43.3	14.1	64	37.23	24.86	95
<b>MM</b>	49.9	10.7	94	23.2	5.16	39	55.51	20.35	17
<b>LM</b>	47.7	22.5	36				35.95	18.1	74
<b>PM</b>	31.5	13.7	72				34.17	19.52	61

### Water content variation with depth (Figure 6-24)

As with BDD, correlating water content and depth between sites and saltmarsh surface zones allows an assessment of whether or not external changes and/or disturbances may have impacted soil moisture over time. Overall water content is seen to moderately decrease with depths on ANK's MM and LM zones of whilst the values collected on HM and PM only decrease up to c. 40cm to rise again to the base of the cores signalling change in soil structure. On FM, water content presents a moderate decrease with depth for HM zone whilst water content on MM zone displays a weak increase with depth departing from all other saltmarsh sites and zones trends. Water content on MR displays strong to very strong relationships with depth for all saltmarsh surface zones with same reversal trend observed on BDD plots for HM and PM demonstrating a rise at c.30 cm on HM and c.40 cm on PM.

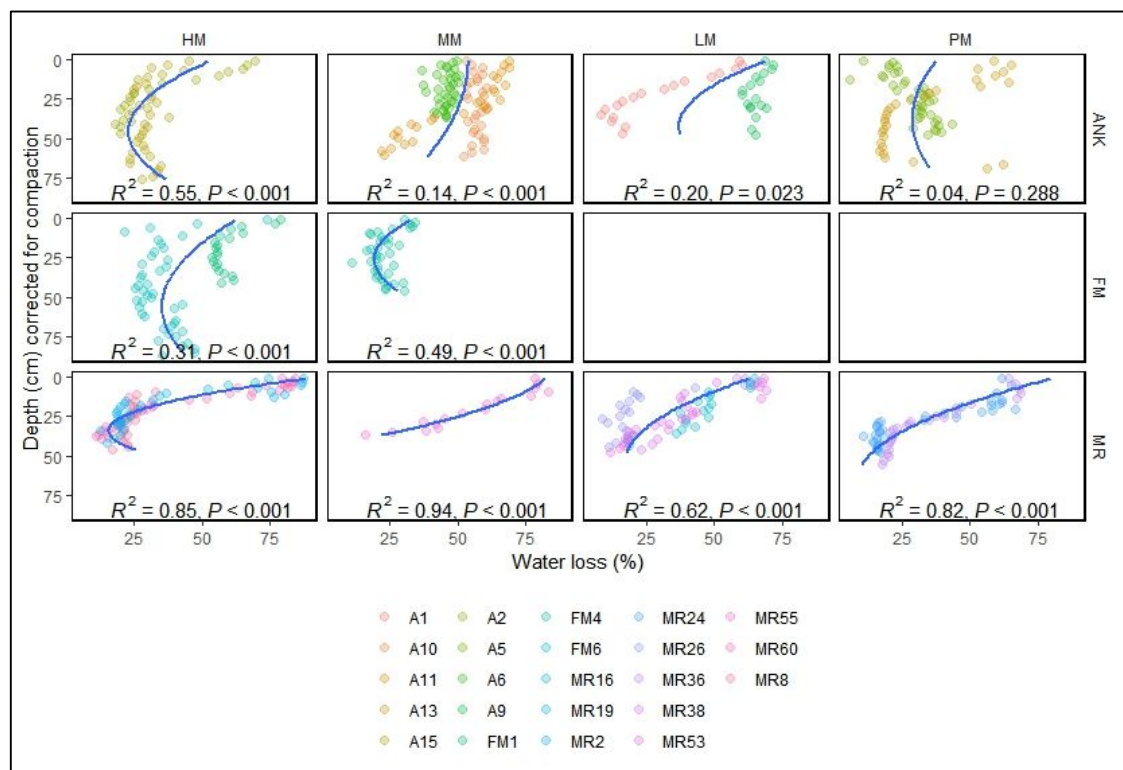


Figure 6-24: Water loss (%) versus depth (in cm and corrected for compaction) per sites and saltmarsh surface zones with the cores represented by different colours. Blank box: absence of core for this saltmarsh zone.. Blank box: absence of core for this saltmarsh zone. Polynomial trends shown in blue and the results of polynomial regressions (correlation coefficients and statistical significances) are provided as bottom of each graphs.

### 6.2.3 Belowground inorganic carbon content (SIC)

Inorganic content of saltmarsh sediments is found strongly and directly related to bulk density and soil moisture. Due to its high density and inherent stability, the inorganic matter present in

saltmarshes exhibits limited compression within the soil top layer. The presence of inorganic matter plays a crucial role in maintaining the volumetric stability of saltmarsh soils and is a fundamental factor in the formation of saltmarshes. Inorganic matter serves as the framework that enables the accumulation of organic material (Turner et al., 2000; Morris et al., 2016). In a state of equilibrium, where the marsh is experiencing a constant rate of sea level rise (SLR), the rate of vertical accretion is determined by the final mass of a cohort and its bulk density (Yu and Chmura, 2009; Morris et al., 2016). Section 6.2.1 and 6.2.2 addressed the spatial and temporal variability of physical characteristics – grain size and type-and properties - BDD and water content - for the three natural and managed salt marshes. Soil physical structure following reclamation is generally found to be immature and associated with processes such as acidification, leaching of carbonates and oxidization due to changes in water levels (Pye et al., 1997; Fernández et al., 2010). Inorganics buried in saltmarsh soils also reflect past and present biogeochemical processes, exchanges and fluxes associated over long timescale (centuries to millennia) related to their position at the marine-terrestrial interface (Wang et al., 2016), and, over shorter timescales (decadal to centuries) to land management disturbances. Inorganic material in saltmarsh sediments also has a direct impact on the carbon cycle (Hyndes et al., 2014) where carbon is found in three forms: organic, inorganic and elemental (used in isotopic dating). As such, this thesis does not aim specifically to examine the implications of inorganic concentrations in saltmarsh soil as a potential source and sink within the carbon cycle, but to obtain accurate belowground inorganic estimates (carbonates mainly) required in the quantification of carbon stocks in a blue carbon budget. The results are not further discussed beyond the details presented in this section other than being directly integrated in the carbon stock calculation. Therefore, the section focusses on the presentation of a quantification of the:

- 1) spatial variability of belowground SIC between a paired natural and managed salt marsh and saltmarsh surface zones;
- 2) identification of temporal variability of belowground SIC through core-depth/time to inform differences between saltmarsh evolution.

Detailed in Chapter 3 – 3.4.3.2, the quantification of belowground inorganic matter for 603 samples taken at interval depths of 1 cm for 5 cores and 2 cm for 18 cores was carried out using LOI at 800°C (step 3 in Table 3.14 and Table 3.16) where choice and duration of temperature was based on existing literature (Ball, 1964; Craft et al., 1991; Sutherland, 1998; Heiri et al., 2001; Santisteban et al., 2004; Roner et al., 2016).

#### **Inorganic variation between saltmarsh sites and variation between saltmarsh surface zones**

Average inorganic carbon content is not significantly different between sites , however an overall

difference is demonstrated between saltmarsh surface zones ( $H_{df=3} = 74.16, p < 0.001^{***}$ ) with highest content on the mid-marsh zones (ranging between 1.4 to 2.2 %) and lowest on the low-marsh zones (ranging between 0.7 to 1 %). These differences are also demonstrated by saltmarsh surface zones for each site (Table 6-6, ( $H_{df=8} = 90.6, p < 0.001^{***}$ ) presenting a similar pattern on all sites.

**Table 6-6: Averaged percentage of inorganic material using LOI at 800°C per site and saltmarsh surface zones .**

	ANK			FM			MR		
	Mean	SD	n	Mean	SD	n	Mean	SD	n
<b>Overall</b>	<b>0.99</b>	<b>0.66</b>	<b>257</b>	<b>0.91</b>	<b>0.53</b>	<b>64</b>	<b>1.21</b>	<b>1.24</b>	<b>248</b>
<b>HM</b>	<b>0.75</b>	<b>0.52</b>	<b>55</b>	<b>0.91</b>	<b>0.53</b>	<b>64</b>	<b>1.18</b>	<b>1.28</b>	<b>96</b>
<b>MM</b>	<b>1.39</b>	<b>0.50</b>	<b>94</b>				<b>2.18</b>	<b>0.83</b>	<b>17</b>
<b>LM</b>	<b>0.67</b>	<b>0.64</b>	<b>36</b>				<b>1.03</b>	<b>0.72</b>	<b>74</b>
<b>PM</b>	<b>0.79</b>	<b>0.82</b>	<b>72</b>				<b>1.20</b>	<b>1.61</b>	<b>61</b>

### **Inorganic variation with depth (Figure 6-25)**

For all cores collected, the correlation between inorganic carbon content and organic matter and organic content through depth is very strong ( $r^2_{adj.} 82.56\%$ ). Overall, SIC accounts for  $9.75 \pm 0.05\%$  of SOM, which is consistent with the findings of Morris et al. (2016), who used 10 % of organic production as a conservative constant for inorganic carbon content in soil. As the trends of organic matter through depth/time are discussed in detail in 6.3.1, it is unnecessary to discuss the trends of inorganic matter through depth in this section; only Figure 6-25 is presented as reminder of the differences between the sites' saltmarsh zones.

The combustion at 800 °C of sediments in one core, MR24, revealed peaks of carbonate lower in the core (Figure 6-26), an exception to the relative similarities between the trends through depth of organic and inorganic content. This is described here as it presents some characteristics of the hydrologic changes in saltmarsh soil. For the first 20 cm in depth, inorganic carbon content remains approximately constant ( $2.6 \pm 0.4\%$ ) and seen to decrease gradually with depth until 36 cm to a level of 0.27 %. From then to 42.7 cm, carbonate sharply increases with a peak at 38.4 cm to 10.2 %. For the rest of core to the base, at 49 cm, carbonates levels average at  $0.2 \pm 0.1\%$ . This sudden change has been related to carbonate concretions which are widespread in sediment close to a permanent groundwater table (Pye et al., 1997). In their work on the Lower Warham young (< 50 years) salt marsh, Pye et al. (1997) found that these concretions, mainly composed of cemented siderite, occurred in super-saline conditions due to. As a reclaimed area, the location of Core MR24 would have been close to the drainage ditch located behind sea-wall embankment (see Figure 3-8 in Chapter 3) which may explain the presence of such concretion.

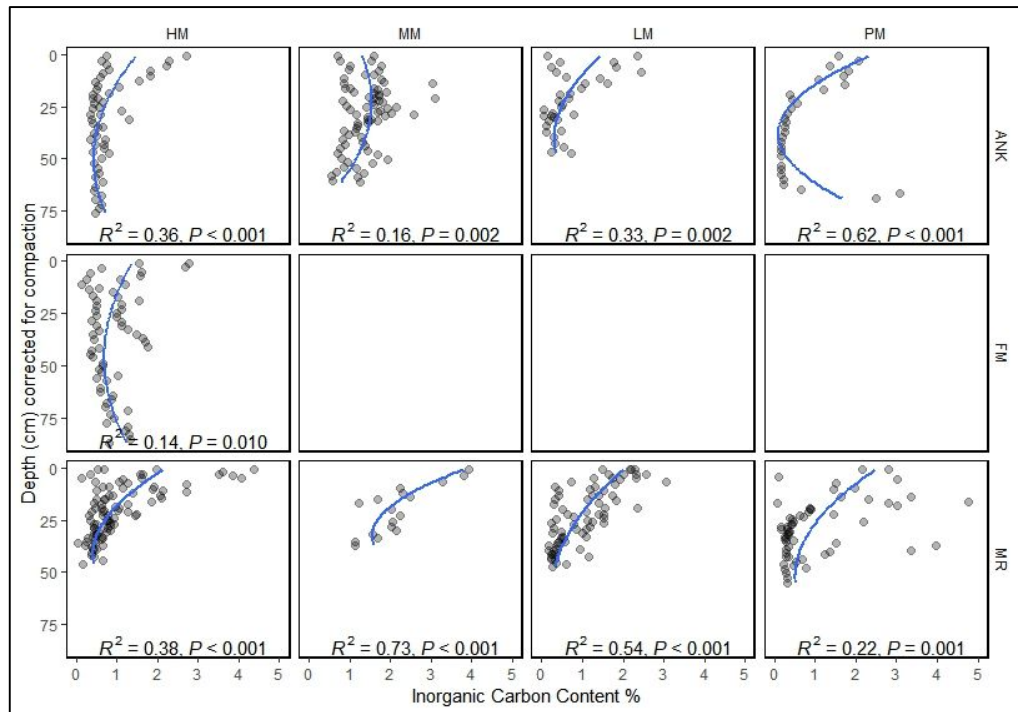


**Figure 6-25: Relationship between loss of inorganic carbon content (%) and depth (cm) per sites and saltmarsh surface zones. Polynomial trends shown in blue and the results of polynomial regressions (correlation coefficients and statistical significances) are provided as bottom of each graphs.**

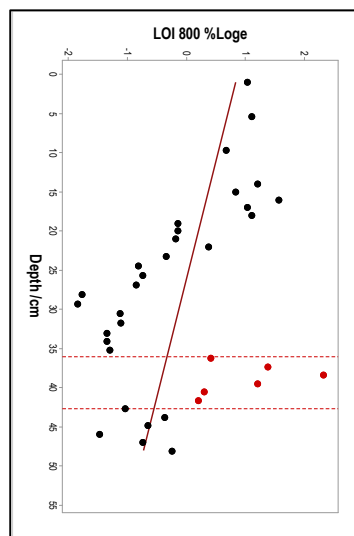


**Figure 6-26: Inorganic carbon content (%Log<sub>e</sub> values on the y-axis) and depth (cm) for Core MR24 highlighting in red carbonate concretion at 36 cm in depth.**

### 6.3 Belowground organics: soil biological properties of Nigg Bay saltmarshes sediments

Despite relatively modest surface areas, salt marshes play an important role in biogeochemical cycles due to the massive inputs of terrestrial organic matter (and nutrients) together with exchanges of large amount of marine matter and energy (Gattuso et al., 1998; Hyndes et al., 2014). They also display great variability in the accumulation of soil organic matter SOM due to depositional environments and events. Environmental and anthropogenic disturbances can further alter or even disrupt the natural accumulation of sediment processes. To achieve an equilibrium



state, the production of belowground organic matter is critical to saltmarsh sustainability (Yu and Chmura, 2009) by contributing to accretion and elevation. It has been demonstrated that accretion rates can be more influenced by organic belowground biomass than inorganic accumulation (Turner et al., 2004). However, this scenario is reliant on whether organic or minerogenic processes dominate and whether organic or inorganic material is the most influential contributor (Allen, 2000; Morris et al., 2016). Nevertheless, there is always an organic component that is incorporated into the salt marsh (Baptist et al., 2016), and this aspect is relevant to the supporting ecosystem services saltmarsh systems provide, such as carbon storage and sequestration (Blue Carbon).

Organic matter is generated at various soil depths through the processes of root growth and the decomposition of vegetation material. This occurs when the rate of productivity surpasses the rate of decay. Additionally, alterations in soil volume or elevation can disrupt the accumulation of mineral and organic components (Kirwan and Mudd, 2012). Chapter 4 - 4.3.2 presented the results on Aboveground biomass and subsequent organic content constituting the aboveground short-term saltmarsh feedbacks between biological (plant type, density and organisms) and physical processes (inundations and temperatures) and the response to belowground circumstances affecting the net change in organic matter. Organic matter contained in saltmarsh soils may come from different sources within and outside the bay as traces of upland, riverine, estuarine and marine environment, and, more importantly, their concentrations reflecting both organic matter losses and inputs can only be interpreted as a 'net' result (Van de Broek et al., 2016).

In the section below, the spatial variability in carbon density and carbon accumulation of surface soils is examined on the three salt marshes at Nigg Bay and the factors controlling this variability discussed. The sampling design combined biological and physical factors with vegetation assemblage and geomorphic settings and represented a gradient across each saltmarsh zone to reflect hydroperiod and its effect on sedimentation across the salt marshes (such as distance to saltmarsh edge, elevation, slope, curvature, etc. - see 3.3.2.3). The analysis focusses on exploring patterns in carbon density and its storage through depths (i.e. over timescales of years to centuries). This is relevant to estimating the magnitude of carbon sequestration in the system - Blue Carbon - and to identify areas of potentially high carbon sequestration within natural and restored or reclaimed salt marshes (Connor et al., 2001; Owers and Rogers, 2016). Dyked and drained in the 1950's for reclamation and breached in 2003, the MR Nigg site offers the opportunity to compare how the carbon stock may have been altered by land management disturbances.

Belowground organics are characterised by presenting the results of organic matter content and its primary component organic carbon across the three salt marshes in Nigg Bay and through depth/time for the 23 cores (also used for inorganics characteristics (section 6.2. and in Figure 6-2 cores represented by black and red dots)). Very much like belowground inorganics (6.2.3), belowground organic matter (SOM) aims to find out if:

- 1) there are identifiable belowground organic patterns in space and depth/time informing on saltmarsh evolution through time.
- 2) If belowground organics differ between a paired natural and managed salt marsh informing on the ‘natural’ status of managed salt marsh or differ between saltmarsh surface zones informing on saltmarsh development through space.

This chapter section tests the hypotheses that:

- i. natural and mature salt marshes display a higher belowground organic matter compared to young or managed realignment site sediment;
- ii. differences in organic content between sites reflect different land use patterns/changes.
- iii. changes in organic content through depth/time can be traced in core profiles as markers of anthropogenic (reclamation and managed breaching) and environmental (storms, SLR) disturbances;
- iv. the proportion of carbon in organic matter (SOC) increases with increasing soil organic matter (SOM) content and both content increase with distance to saltmarsh edges and water channels;

Detailed in Chapter 3 – 3.4.3.2, the quantification of belowground organic matter for 603 samples taken at interval depth of 1 cm for 5 cores and 2 cm for 18 cores was carried out using loss-on-ignition (LOI - step 2a and 2b in Table 3.12 and Table 3-14) and the choice and duration of temperature of LOI methods was based on existing literature (Ball, 1964; Craft et al., 1991; Sutherland, 1998; Heiri et al., 2001; Santisteban et al., 2004; Roner et al., 2016).

### **6.3.1 Belowground organic matter - SOM**

#### **Biased Results adjustments**

Selection As discussed in Chapter 3 – 3.4.3.2, the appropriate choice of ignition temperatures is closely linked to sediment characteristics and reproducibility is not always reached (Craft et al., 1991; Plater et al., 2015). This hypothesis may not answer this thesis aims but impacts on its results and quantification carbon content. In Appendix E, Section E-3, the hypothesis is examined through the comparison of differences in LOI (Loss on Ignition) values at temperatures of 375 °C

and 450 °C, along with the subsequent adjustments made to the dataset (see appendix E- section E-3).

### Organic matter variation between saltmarsh sites and variation between saltmarsh surface zones

Overall SOM ranged between 0.4 to 97.3 % averaging at  $10.84 \pm 0.6$  % for the three saltmarsh sites (Table E.4.). SOM measured from ANK's sample was found to rank significantly higher than FM (Figure 6-27a, Appendix E- Table E-4.). Overall average SOM varied between saltmarsh surface zones where the highest SOM was found in PM zone compared to LM, MM and HM, and SOM from HM zones is significantly lower than MM (Figure 6-27b, Table 6-7 and Table E-4.).

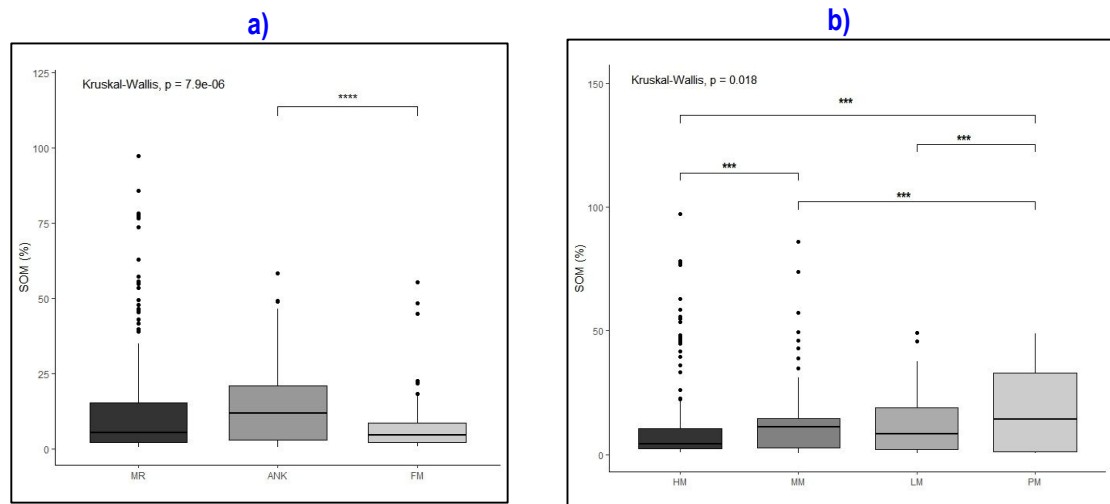


Figure 6-27: a) : Boxplot of SOM (%) a) between saltmarsh sites and b) between sites' saltmarsh zones. (Note: Kruskal-Wallis H test and significant pair-test comparison using Dun's tests results by the p-value significance - Results in table E-4.)

### Organic matter variation between saltmarsh sites and saltmarsh surface zones

The analysis of SOM reveals notable variations within each site when comparing the marsh zones, as indicated by the significant differences observed in Table 6-7 and table E-5. Dunn's test revealed a significant difference in the rankings between MR's MM and HM, LM, and PM zones. Specifically, ANK's saltmarsh surface zones display the highest SOM content in the PM zone and the lowest in the HM zone (Table E-5). Unexpectedly, the saltmarsh surface zones of ANK exhibit a greater quantity of organic matter in the upper portion of the marsh and a lesser quantity in the lower portion of the marsh. The saltmarsh surface zones of ANK exhibit varying concentrations of SOM, and interestingly, they demonstrate contrasting behaviour compared to other sites which shows higher quantity of organic matter in the upper part of the marsh and lower quantity in the lower part of the marsh. Additionally, FM's MM was found to have a lower ranking compared to FM's HM.

Table 6-7: Averaged percentage of organic matter loss using LOI at 450°C per site and saltmarsh surface zones. (Variance is established on median SOM % between saltmarsh surface zones using K-W test for ANK:  $H=102.34$ ;  $p<0.001^{***}$ ; for FM:  $H=47.5$ ;  $p<0.001^{***}$ ; for MR:  $H=24.38$ ;  $p<0.001^{***}$ ).

	ANK			FM			MR		
	Mean	SD	n	Mean	SD	n	Mean	SD	n
<b>Overall</b>	14.2	12.5	257	7.4	9.1	103	13.4	19.0	248
<b>HM</b>	6.4	11.0	55	10.4	10.4	64	16.7	25.2	96
<b>MM</b>	12.0	5.0	94	2.3	1.5	39	32.2	24.7	17
<b>LM</b>	17.5	12.4	36				8.6	8.7	74
<b>PM</b>	21.2	15.8	72				7.3	8.2	61

**Organic matter variation with depth** (Figure 6-28 and Figure 6-30 and Appendix E.4 & E.5)

SOM demonstrates a moderate overall decrease with depth ( $r^2 = -0.21^{***}$ ). Simple linear model between SOM and depth are found negatively weak on ANK and FM and negatively moderate on MR (Figure 6-28)

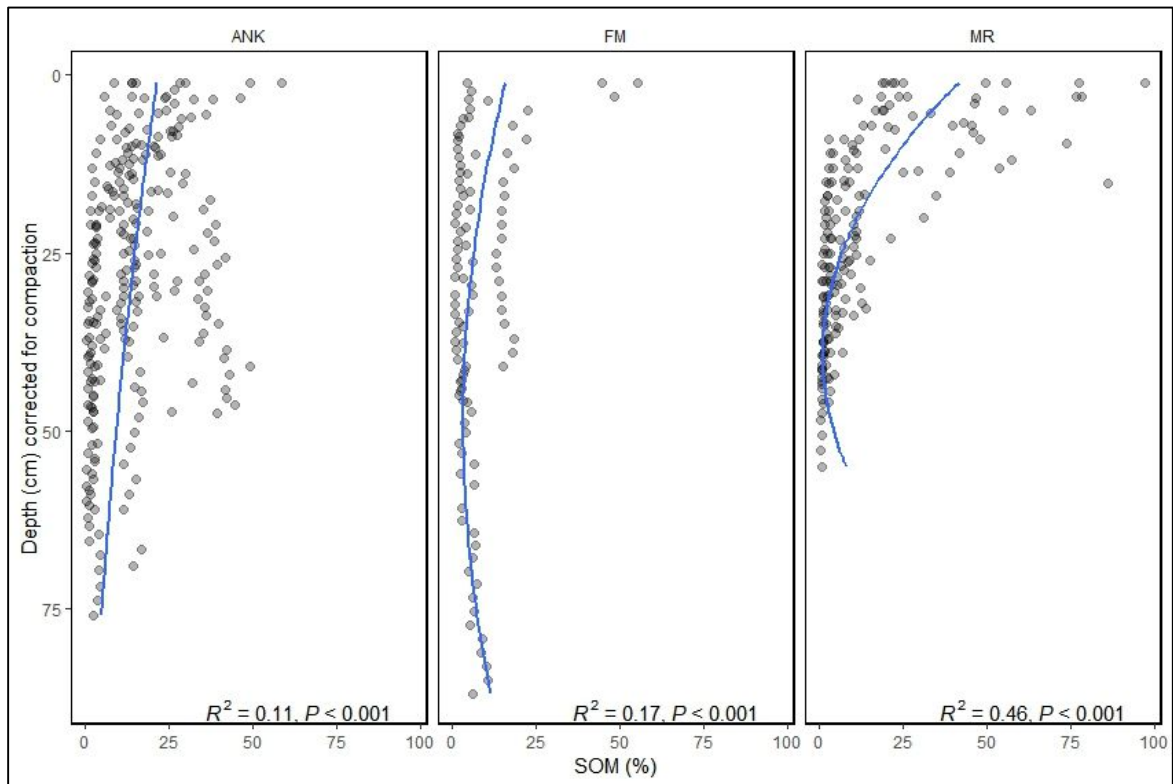


Figure 6-28: Relationship between SOM (%) and depth (cm) per sites. Polynomial trends shown in blue and the results of polynomial regressions (correlation coefficients and statistical significances) are provided as bottom of each graphs.

Figure 6-30 and Table E-5 illustrate SOM results variability demonstrating that linear regression with polynomial terms have different strength (on MR’s LM and PM and ANK’s LM) for each saltmarsh zone. On the natural salt marsh ANK, organic content differs significantly with depth between each saltmarsh zone. On the HM zone, SOM decreases rapidly for the first 10 cm averaging at  $25.96 \pm 5.2\%$  and a further  $7.64 \pm 5.2\%$  until 20 cm and appear to maintain its level  $c.2.4\%$  to the base of the cores. ANK’s MM zone shows also rapid decreasing trend ( $c.14.4\%$ )

until c.35 cm in depth to sustain similar level of SOM (c.4.8 %). In contrast, ANK's SOM on LM zones averages around  $21.35 \pm 2.8$  % of its upper 10cm of soil and is not seen to decrease with depth but maintains its level to c.16.8 %. The SOM values for ANK's pioneer marsh clearly differ between the two collected cores. On one hand, Core A5 no trend is visible for with depth, On the other, core A13 collected in the western pioneer marsh displays a rapid decrease of SOM with depth up to approximately 18cm in depth (from  $16.5 \pm 5.2$  % to  $2.5 \pm 0.5$  %), then SOM is less than 1 % up to 65cm and seen to abruptly rise at 66cm up 16.5 % of organic matter suggesting that the presence of organic matter in the past that has collapsed and eroded since (Figure 6-29).

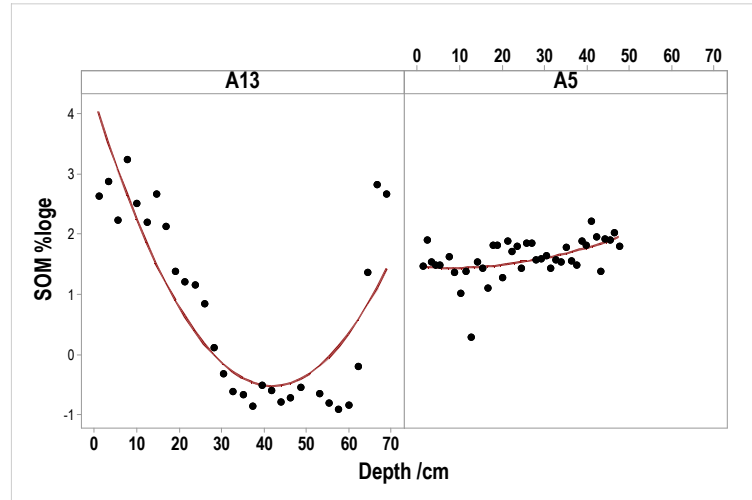


Figure 6-29: SOM ( % natural log) in y-axis versus depth in x-axis for core A13 and A5.

Both saltmarsh surface zones, HM and MM, on FM demonstrate a sharp decrease in SOM until 10cm depth; however, the proportion of SOM in HM zones ( $33.2 \pm 3.5$  %) is significantly higher than in MM zones ( $7.5 \pm 3.5$  %). Both zones, maintain their SOM content to the base of the cores averaging at c.15.2 % for the high marsh and c.3.4 % on the pioneer marsh.

On MR, SOM values for all saltmarsh surface zones decrease with depth with a steep trend up to c.10cm depth on the high ( $50.3 \pm 6.7$  % organic loss) and low ( $19.7 \pm 2.2$  % organic loss) marsh zones and up to c.20cm deep on the mid (c.53.7 %) and pioneer (19.1 %) marsh zones.



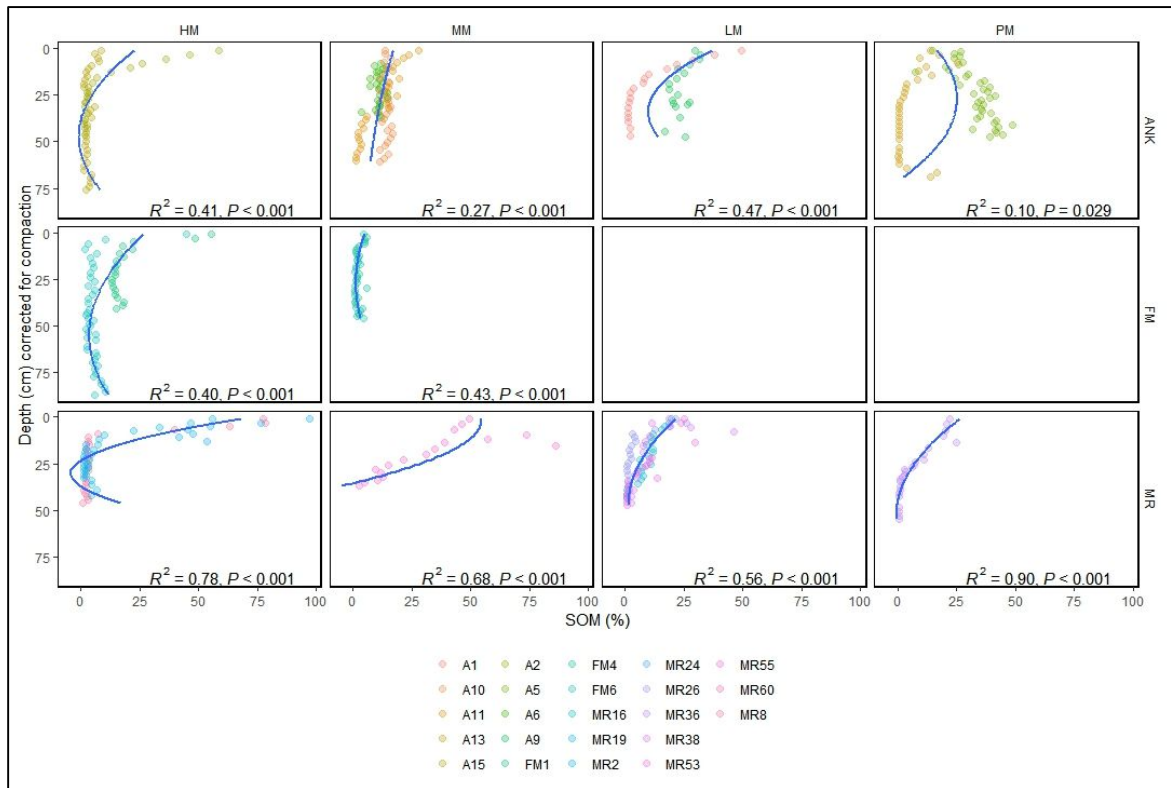


Figure 6-30: Relationship between SOM (%) and depth (cm) per sites with the cores represented by different colours. Blank box: absence of core for this saltmarsh zone. Polynomial trends shown in blue and the results of polynomial regressions (correlation coefficients and statistical significances) are provided as bottom of each graphs.

### 6.3.2 Belowground organic carbon density - SOC

To provide blue carbon estimates for Nigg Bay salt marshes, mineral and organic mass needs to be converted to a volume (density) of sediment, using a similar method for studies of vertical sediment accretion (Howard et al., 2014; Schindler, Karius, Deicke, et al., 2014; Morris et al., 2016). This conversion is calculated using bulk dry density (BDD) values for each sample. The methodology is further justified by a strong association between LOI at 450°C and BDD ( $r^2_{adj} = 71\%$  \*\*\*  $\rho = -0.86$ , Table E-7). This section presents the results of our 23 cores carbon density necessary to calculate the Pool 2 Blue Carbon stock pool (Table 3-13 and 3-14).

#### Soil Carbon Density variation between saltmarsh sites and variation between saltmarsh surface zones

Overall organic carbon density ranged 0.000 to 0.26 g.Ccm<sup>-3</sup> and averaging at 0.025±0.001 g.Ccm<sup>-3</sup>. The overall mean carbon density was found to differ significantly between the saltmarsh sites ( $H_{df=2} = 8.22$ ,  $p = 0.016^*$ ). However, the pairwise multiple comparison procedures (Dunn's method) did not indicate any distinct ranking among the three salt marshes.

The analysis reveals a significant difference in overall SOC variability among the saltmarsh surface zones ( $H_{df=3} = 26.4$ ,  $p < 0.001^{***}$ ). Specifically, the PM zones exhibit the lowest SOC

levels compared to the LM and MM zones, while the MM zones display the highest SOC levels compared to the LM zones (Table E-8). In the context of the natural salt marsh ANK, it is observed that the LM zones exhibit significantly higher rankings compared to the MM and PM zones, as well as the LM zones of MR. In the context of MR, it has been observed that the MM zones within the MR areas exhibit notably higher rankings compared to the HM, LM, and PM zones. Furthermore, the MM zones within the MR areas also demonstrate higher rankings when compared to the MM zones within the FM areas. In conclusion, within FM, HM exhibits the highest ranking in comparison to the MM zones, displaying the lowest overall carbon density at  $0.012 \pm 0.002 \text{ g.Ccm}^{-3}$  (Figure 6-31, Table 6-8 and Table E-9).

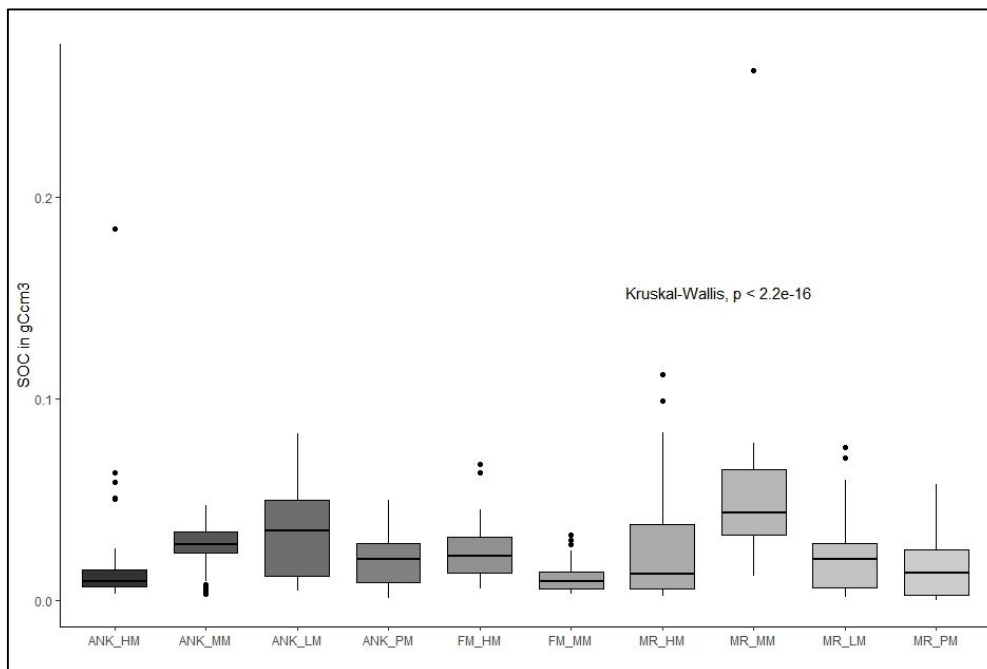


Figure 6-31: Boxplot of SOC in  $\text{g.Ccm}^3$  between sites' saltmarsh zones. (Note: Kruskal-Wallis H test and significant pair-test comparison using Dun's tests results by the p-value significance - Results in table E-9 .

Table 6-8: Carbon density  $\text{g.Ccm}^{-3}$  by saltmarsh sites and zones (top row present results of ANOVA between saltmarsh surface zones per site and statistical significance using  $* < 0.05$ ,  $** < 0.01$  and  $< 0.001$ \*\*\*).

	ANK $F=11.73^{***}$			FM $F=73.78^{***}$			MR $F=12.492^{***}$		
	Mean	SD	n	Mean	SD	n	Mean	SD	n
Overall	0.024	0.018	257	0.019	0.013	103	0.024	0.027	248
HM	0.018	0.027	55	0.024	0.013	64	0.026	0.026	96
MM	0.028	0.010	94	0.012	0.007	39	0.059	0.056	17
LM	0.034	0.020	36				0.021	0.016	74
PM	0.019	0.012	72				0.016	0.015	61

### Soil Carbon Density variation versus vegetation type (Figure 6-32 and Table E-10)

Kruskal-Wallis and One Way Analysis of Variance on Ranks test were conducted to examine the soil carbon density (SOC) and determine if there is a significant difference in carbon density among various vegetation types. Despite the limited impact of vegetation types on soil carbon density ( $r^2_{\text{adj}} = 8.7\%$ ,  $p < 0.001^{***}$ ), all vegetation assemblages make significant contributions to the regression model. The highest levels of SOC are observed in the SM16d community

(*Festuca rubra* dominant and dominant sub community) located on the high marsh (HM) zone. This is followed by the SM13b community (*Puccinellia mar.* dominant, *Glaux maritima* sub-community) found on the mid-marsh (MM) zone. The SM13a community (*Puccinellia maritima* dominant and dominant sub community) is found on the low marsh (LM) zone and exhibits lower SOC levels compared to SM16d. The lowest SOC levels are found in the SM13d community (*Puccinellia mar.* dominant, *Plantago maritima -Armeria mar.* sub-community) located on the MM zone. Additionally, the SM8 community, consisting of Annual *Salicornia*, found on the pioneer marsh (PM) zone, also exhibits relatively low SOC levels (details in Table E-10).

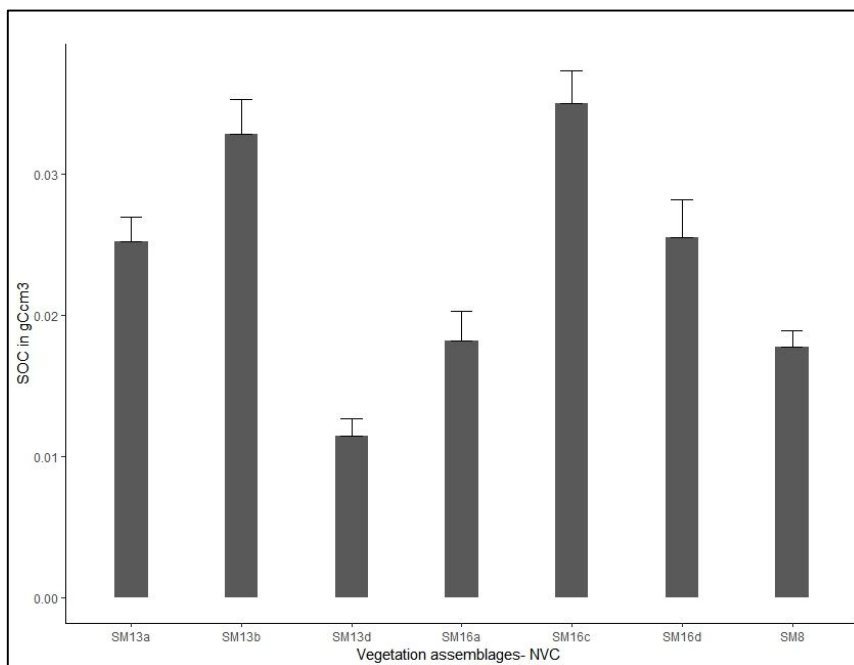


Figure 6-32: Carbon stock density in g.Ccm<sup>3</sup> by saltmarsh vegetation community - NVC type (Vegetaion reference to Table 3.4 and App. A.2) and zones using individual SD to calculate error bars.

### Soil Carbon Density variation with depth (Figure 6-33 and Figure 6-34)

The study reveals that there are negative correlations between carbon stock density and depth, and these correlations vary among the three saltmarsh sites. The organic carbon content in the natural salt marsh ANK and the fronting marsh FM exhibits a weak decrease of carbon content with depth ( $r^2= 0.2^{***}$  and  $r^2= 0.1^{***}$ ). The carbon densities for MR exhibit a sharp decrease starting at a depth of approximately 15 cm. Subsequently, there is a moderate decreasing trend ( $r^2= 0.3^{***}$ ) observed until the end of the core depth.

The carbon density trends through depth/time do not differ from organic matter versus depth by saltmarsh sites and zones (Figure 6-34), it was therefore not found necessary to describe them here. However, it seems pertinent to highlight again the differences between the managed realignment MR results which display very rapid decrease carbon density compared to the natural salt marshes (especially in the lower saltmarsh surface zones).

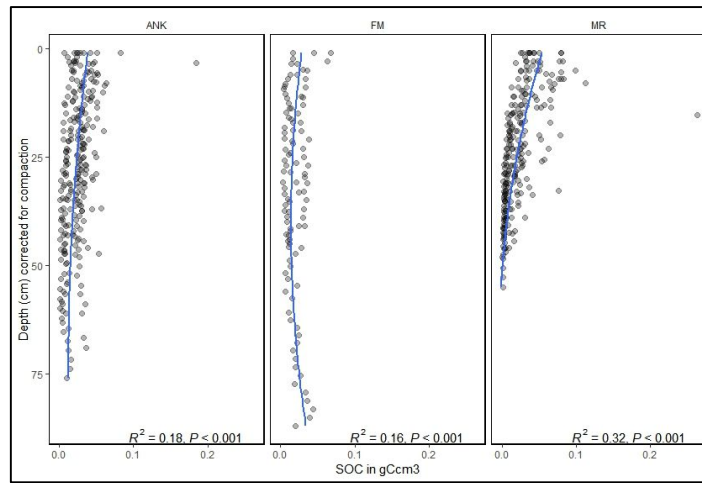


Figure 6-33: Relationship between SOC (g.Ccm<sup>3</sup>) and depth (cm) per saltmarsh sites. Polynomial trends shown in blue and the results of polynomial regressions (correlation coefficients and statistical significances) are provided as bottom of each graphs.

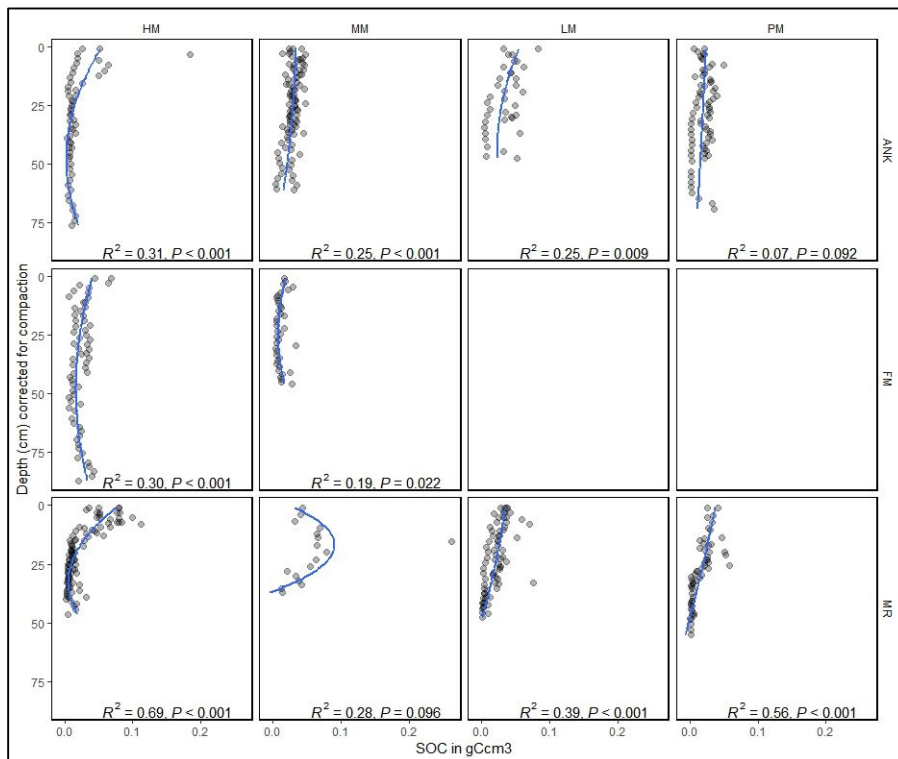


Figure 6-34: Relationship between SOM (g.Ccm<sup>3</sup>) and depth (cm) per sites. Polynomial trends shown in blue and the results of polynomial regressions (correlation coefficients and statistical significances) are provided as bottom of each graphs.

#### 6.4 Anthropogenic legacy in saltmarsh soils

Rectified photographs were taken for 17 of 32 cores collected on the MR, FM and ANK salt marshes by Nigg. Nine of these cores collected on the managed realignment salt marsh MR are presented below in Figure 6-35. The photographs reveal a clear discontinuity and soil discoloration in the upper layers of MR cores, not present on the ANK cores (App. E-1- Fig. E-1b) and located at different depths. This discoloration can be traced at an increasing depth with elevation height demonstrating, first, that a single event disturbed MR salt marsh soil zones in the

recent past; and, second that sedimentation on MR is directly linked to elevation height and distance from saltmarsh edge. This discolouration is interpreted as a stratigraphic sequence corresponding to the years of land reclamation that occurred since the 1950's until the 2003 breach of MR and so acts as a chronometric tracer. Profiles of SOC and Water content of the four cores presented below in Figure 6-36 (top row a - top four profiles are uncorrected for core compaction as in the photographs and bottom row b- are the profiles corrected core depth – see 3.4.3.1 for details) show shifts at the same depth as discussed in the inorganic (6.2) and organic (6.3) belowground soil records but were difficult to characterise and identify with certainty.

On average, the discoloration for PM cores occurs at depth of 8 to 15 cm (uncorrected for core compaction, and, between 18 and 25 cm at corrected depth), for LM cores at 6 to 9 cm deep (7 to 10 cm corrected), for MM at 5.5 to 9.5 cm deep (5.5 to 10 corrected) and HM 5.5 to 8 - 11 cm in depth (6 to 8 -12 cm corrected).

Tempest et al. (2015) and Boorman et al. (2002) have discussed impact of reclamation on soil due to dewatering and known to increase soil density and compaction (by decreasing porosity), when tidal flooding is reintroduced, like on the managed realignment MR of Nigg Bay, water drainage is altered by the old soil density and permeability and intensified by plant roots and algae.

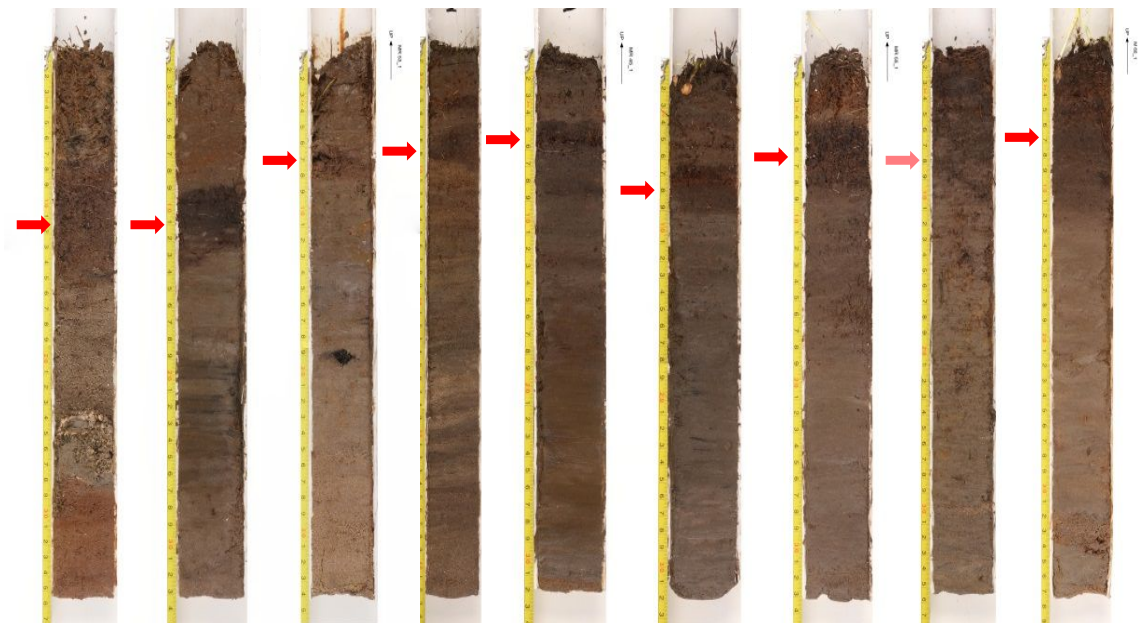


**Figure 6-35: Cores from Nigg Managed Realignment (MR) from left to right, from PM to HM in ascending elevation height order: MR24 (PM-1.57mOD), MR47(PM-1.82mOD), MR53(LM-1.86mOD), MR26(LM-2.04mOD), MR45 (LM-2.05mOD), MR38 (LM-2.06OD), MR55 (MM-2.08mOD), MR19 (HM-2.37mOD), and MR60 (HM-2.54mOD). Red arrow → represents clear stratigraphic break associated with change in soil colour present in 8 out of 9 cores photographed (lighter red arrow indicates more subtle shift) and interpreted as reclamation years. Note: the cores in photographs have not been corrected from core compaction (see 3.4.3.1) unlike all core data used and presented so far.**



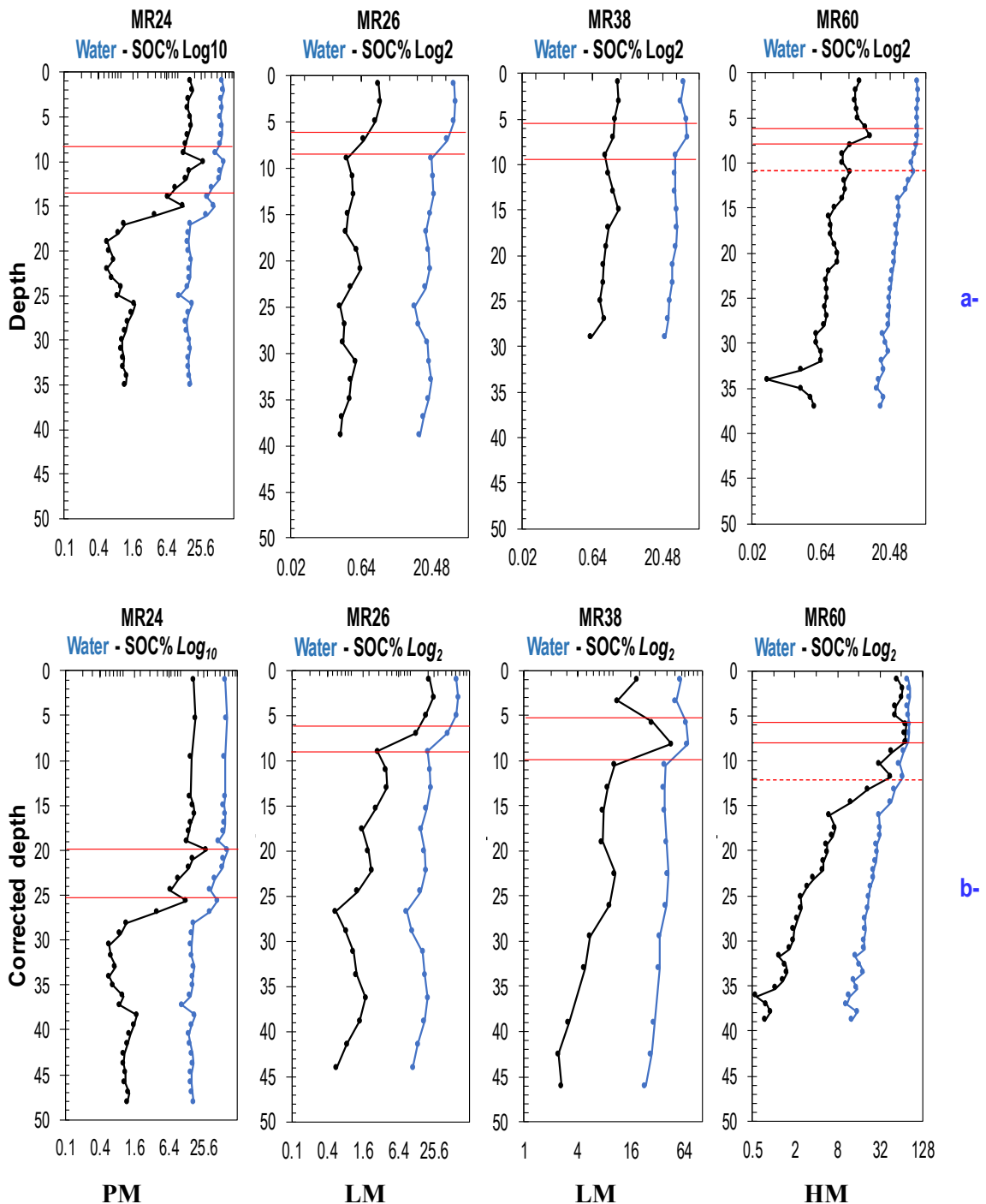


Figure 6-36: Water and Soil organic Content from four MR cores which presented soil discoloration in photographs 6-37. From left to right, from PM to HM, in ascending elevation height order: **MR24** (PM-1.57mOD), **MR26** (LM-2.04mOD), **MR38** (LM-2.06OD) and **MR60** (HM-2.54mOD). Red lines represent the depth at which the colour shift is visible on the photograph (top row **a**:- series with depth uncorrected for core compaction; and, bottom row **b**:- series with depth corrected as explained in 3.4.3.1).

## **6.5 Sedimentary legacy of belowground organic and inorganic processes: significance of the results**

Turner et al (2007) describes coastal saltmarsh sediments as being primarily composed “of inorganic matter, organic matter, water, and pore space. The soil volume is reduced as organic matter decomposes, pore spaces are compressed, as water is squeezed out when these soils are overlain by newer material, and as they age. Plants add to the volume of the deposited soils by way of their root and rhizome production” (Turner et al., 2007, pp1231). As such, belowground sediment and soil are critical to saltmarsh sustainability by enhancing vertical growth enabling saltmarsh surface to maintain its relative elevation as sea levels rise (Chmura et al., 2003; Yu and Chmura, 2009; Mudd et al., 2009; Schindler, Karius, Arns, et al., 2014; Van de Broek et al., 2016). Soil and sediments properties govern the strength, consolidation and cohesion required for the long-term stability of the aboveground surface. This balance when altered by environmental -i.e. erosion, storm, tidal waves-, and anthropogenic disturbances -i.e. embankment-, can be irreversible and prevent a return to the normal functioning of the saltmarsh system (Boorman et al., 2002; Kadiri et al., 2011; Tempest et al., 2015; Spencer et al., 2017). Per se, linkages between belowground soil and sediment are addressing two aims of this thesis research: *which processes, mechanisms and patterns favour saltmarsh formation and development, how salt marsh can recover from anthropogenic disturbances*. Their results can then inform on *saltmarsh ecosystem service capacity* via carbon sequestration addressing third aim of this study.

### **6.5.1 Saltmarsh physical and biological sediment properties of natural and managed salt marshes**

Salt marshes, when in an healthy state, tends to be in equilibrium. This equilibrium is characterised by a simultaneous decrease in inorganic accretion rates and the rate of elevation increase as one moves inland and away from the main channels. At the same time, there is an increase in organic accretion. This observation has been supported by studies conducted by Christiansen et al. (2000); Kirwan and Mudd (2012); Roner et al. (2016). Section 6.2 discussed the significance of sediment characteristics and properties in relation to saltmarsh surface elevation. It emphasised the importance of evaluating these factors in order to assess the condition of surface ground-water interaction, which is influenced by sediment texture (porosity) and structure (stratigraphy) (Spencer et al., 2017). The level of organic density can be increased by sediment characteristics, specifically the type and size of grains. For instance, clays have the ability to bind higher levels of soil organic matter (SOM) (Kadiri et al., 2011). The study conducted by Kelleway et al. (2016) provided evidence indicating that the size and composition of grains play a significant role in determining carbon density. This finding highlights the significance of considering these variations when identifying areas with high carbon storage

potential, known as blue carbon hotspots, and when making decisions regarding the conservation and management of saltmarsh ecosystems.

#### 6.5.1.1 Sediment characteristics of natural and managed salt marshes at Nigg

Through a series of 9 cores along two transects crossing the natural salt marsh ANK (Figure 6-3) and another crossing FM and MR (Figure 6-4), the aim was to identify if:

- 1) sediment characteristics were spatially similar between natural and managed realignment and/or saltmarsh surface zones;
- 2) sediment characteristics were similar through time/depth where a gradual increasing/decreasing trend might suggest steady evolution and sudden/abrupt changes might suggest abrupt shifts within the system;

##### 6.5.1.1.1 Linkages between surface zonation and sediments type and size controls saltmarsh topography

The cores collected on the three Nigg salt marshes showed the overall mean grain size to differ significantly between the natural and managed salt marshes with finer silty grains dominating the managed salt marsh MR whilst coarser sands were found on ANK and FM. This first pattern suggests tidal flow to be lower on MR (see figure 4-23, 4-27 and 4-32 and appendix D-3) and allow smaller sediment particles to settle in a sheltered environment. This sediment accumulation process has been found to be influenced by micro-topography (Langlois et al., 2003). The overall mean grain size for the marsh sediments were found highly variable between zones ( $F=33.9$ ,  $p$ -value<sup>\*\*\*</sup>) with concentration of coarser grains ( $>125\mu\text{m}$ ) on PM zones, silts were principally found on LM and very fine sand ( $>63\mu\text{m}$ ) on MM and HM. This pattern does not completely agree with the sediment fining trend in a landward direction (Kadiri et al., 2011), and appear to be more typical of siliciclastic systems where the lithofacies zonation will depend on the hydrodynamics of tidal energy (Eisma and Dijkema, 1997; French, 2018). On areas of coastal salt marshes, where there is strong wave activity and tides, sands are found in higher concentration and sheltered parts will retain more silts and clays, whilst the higher plants of the high marsh zones will play an important role in the sediment retention (Eisma and Dijkema, 1997).

Comparing the cores from the natural and managed saltmarsh surface zones has shown that overall the natural salt marsh offered a much wider range of grain type per zones and more heterogeneity whereas sediment from the managed salt marsh are more homogeneous. This pattern suggests a lack topographic variability enabling different grain size to settle. This concept of topographic niche is well described by Stallins (2006) in coastal sand dune system. On the PM

zone, fine sands ( $187.4 \pm 19.6 \mu\text{m}$ ) were most common on ANK whilst the MR site is principally very fine sands ( $95.6 \pm 4.8 \mu\text{m}$ ) ( $F=34.6$ ,  $p\text{-value}^{***}$ ). ANK's LM preserves mainly coarse silts ( $46.7 \pm 1.5 \mu\text{m}$ ), whilst MR LM zone sediment structure is mostly made of very fine sand grains ( $64.0 \pm 8 \mu\text{m}$ ) ( $F=5.9$ ,  $p\text{-value}^*$ ). Although MM zones are compared between two natural sites ANK and FM (A11 and MR16), they differ in age and maturity as the fronting marsh only developed recently along the sea wall embankment (see Chapter 5 – section 5.2). The overall sediment content of these MM cores is also significantly different with coarse silts ( $56 \pm 1.9 \mu\text{m}$ ) on ANK and very fine sands ( $78.7 \pm 1.2 \mu\text{m}$ ) on FM ( $F=118.35$ ,  $p\text{-value}^{***}$ ). Finally, the most striking difference is in the HM zone, where ANK's core consists primarily of fine sands ( $123.8 \pm 3.3 \mu\text{m}$ ) and MR's core consists of far fewer coarse silts ( $48.4 \pm 1.7 \mu\text{m}$ ) ( $F=291.4$ ,  $p\text{-value}^{***}$ ). The comparison highlights the hydrodynamic dissimilarities of the two systems as presented in Chapter 4 - section 4-4 and Appendix D-3.

Therefore, a principal component analysis (PCA) was conducted to investigate the potential influence of various physical factors, including elevation (m), hydroperiod (m), flood depth (m), flood frequency, distance to mean high water springs (MHWS), distance to water channels (m), and distance to saltmarsh edge (m), on the distribution of grain size within the salt marshes studied in Nigg Bay. PCA first and second dimensions (also called here principal components) account for 60.72 % of the variability observed in the dataset (Figure 6-37). These dimensions indicate a strong correlation between grain size distribution and factors such as slope and curvature, distance to the saltmarsh edge, and to the MHWS. Figure 6-37 demonstrates that the parameters of water levels and elevation make a substantial contribution to the dataset. The correlation plot depicted in Figure 6-38 reveals a limited representation of grain size distribution in the first and second dimensions (only in the fourth dimension), potentially indicating a connection to topographical factors such as curvature and slope. Following that, the method of best subsets regression was utilised to offer further elucidation on the relationships between the average distribution of grain size across all cores and the physical variables. The results obtained at this level, encompassing all cores, indicate that none of the variables examined can sufficiently explain the predictive capability of mean grain size. Therefore, future research should focus on elucidating these parameters for each core and various depth levels.

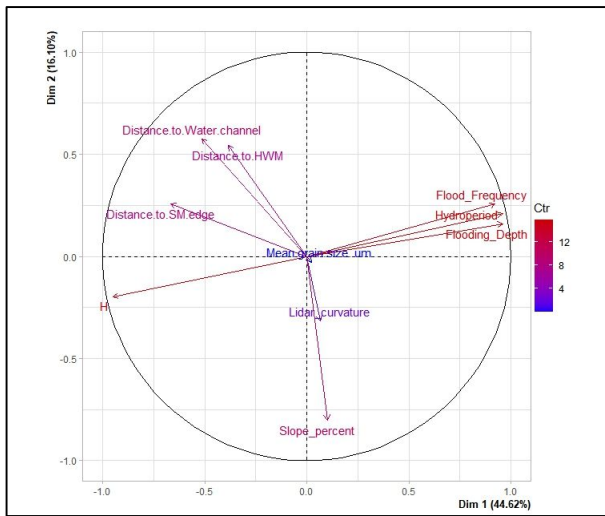


**Figure 6-37: PCA plot for grain size distribution including the physical variables of elevation (m), hydroperiod (m), flood depth (m), flood frequency, distance to MHWS, distance to water channels (m), distance to saltmarsh edge (m), slope (percent) and curvature.**

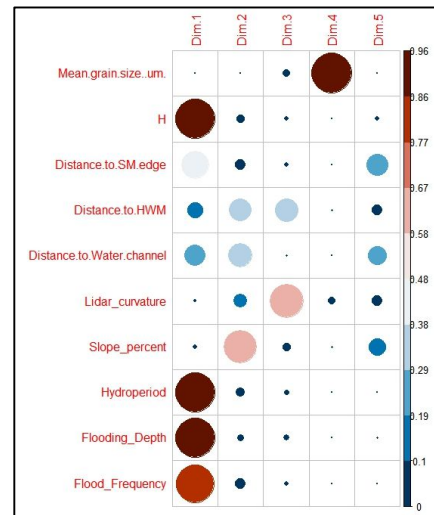


**Figure 6-38: Plot matrix of the square cosine (cos<sup>2</sup>) which is the quality of representation of the variables of the PCA for sediment size grain. Note1: Large and dark circles indicate a good representation of the variable on the principal component and vice-versa.**

#### 6.5.1.1.2 Sediments type and size through depth and time: settings for saltmarsh formation and development

Sediment differences at depth between natural and managed salt marshes were further examined through the core profiles. The sedimentary analysis of each core at Nigg Bay (6.2.1.2) shows that smaller fractions, especially clays, to be the least prone to variation through depth/time whereas the peaks in silts and sands may be a good indicator of changes in saltmarsh dynamics, at least for the sandy salt marshes of Nigg Bay. Variability analysis through depth has further shown that sands within the marsh stratigraphy enable interpretation of shifts within the system itself. The analysis of the four cores excavated on MR (MR36, MR24, MR16 and MR8) presents mineralogic shifts at depths of 32 to 43 cm (depending on the surface elevation) from silts to fine and medium sands and reflect the onset of saltmarsh vegetation colonisation and mud accumulation. Similar patterns have been observed in the young Warham Lower Marshes (1950's) sediment stratigraphy (Pye et al., 1997). On ANK, core A13, located in the pioneer zone, indicates a system change between sand/mudflat to vegetative salt marsh at depth of 17-18 cm whilst the remainder of the core comprises the highest sand proportions collected across the three marshes. Located in the middle of ANK, Core A11 stratigraphy shows two evolution phases interpreted at 54 cm deep as a shift from pioneer marsh to low marsh and at 26-28 cm deep as a shift from low marsh to mid-marsh.



Nigg Bay findings on sediment size and type agree with Fearnley (2008) and Kadiri et al. (2011) comparisons of sediment properties between natural and restored salt marshes which all displayed significant differences between sediment characteristics, however their studies focussed on salt marsh recreated by dredging material which found that sediment characteristics were largely dependent on the source of the dredged sediment. This is not the case for the Nigg Bay salt marshes. Nevertheless, the results point to a clear difference between natural and managed salt marshes, with the legacy of reclamation on sediment characteristics remaining even after 16 years of de-embankment, in agreement with Spencer et al. (2017) and Boorman et al. (2002).

#### 6.5.1.2 Physical sediment properties: natural versus managed salt marshes

Recent work, for the most part on restored and natural salt marshes of SE England, has shown that changes in soil properties, such as porosity and bulk density as a consequence of original marsh enclosure, embankment, drainage and subsequent agriculture compaction, can be irreversible once the reclaimed land is de-embanked (Kadiri et al., 2011; Tempest et al., 2015; Spencer et al., 2017). This is principally due to the dewatering of soil during reclamation which increases soil density and compaction (by decreasing porosity), then, when tidal flooding is reintroduced, water drainage is hindered by the dense and impermeable underlying old soil, a phenomenon that can be aggravated by clayey sediment or reinforced by plant roots and algae (Boorman et al., 2002). Cohesion of the new saltmarsh sediment, soil consolidation and soil shear strength is needed for long-term survival of the salt marsh (Zhang et al., 2001; Boorman et al., 2002). Recent research by Evans et al. (2022) assessing the effect of vegetation on salt marsh erodibility revealed that vegetation and sedimentology interact to control shear strength (the resistance to forces that cause the material's internal structure to slide against itself) and erodibility of sediment. In addition, they discovered a consistent relative pattern of shear strengths by cover type at each site, with bare ground having the lowest shear strength and *Puccinellia* having the highest.

As such, the results in this section address one of the aims of this research: *how salt marsh can recover from anthropogenic disturbances*. Belowground soil properties have also been recognised to influence carbon density impacting on saltmarsh ecosystem service capacities (Kelleway et al., 2016) a further concern of this thesis. By using a collection of subsurface cores obtained from the ANK and FM natural salt marshes, as well as the MR managed salt marsh (Figure 6-2), the study aimed to:

- 1) determine if the properties in managed salt marsh develop to conditions resembling to natural marsh sediments;

- 2) provide insights into sediment properties (BDD and water content) feedbacks by looking at variations through time/depth;

### **Autocompaction/BDD controls on saltmarsh surface structure and Hydrodynamics controls soil structure via sediment delivery**

It was hypothesised (Table 6-1) that MR's BDD would exhibit the greatest differences compared to the other salt marshes. The findings from section 6.2.2.1 and Chapter 4 - section 4.2.2.1 indicate that there is no significant difference in BDD among the three salt marshes. The findings presented in section 6.2.2.1 and Figure 6-39 are in disagreement with the results reported by Tempest et al. (2015), who observed a notably higher BDD on de-embanked salt marshes. This phenomenon can potentially be explained by the fact that Nigg Bay managed realignment site (MR) has experienced limited grazing activities rather than being actively cultivated until it was breached in 2003.

The analysis of BDD variability between saltmarsh surface zones which demonstrated the highest compactions on PM zones. This can be due to the different geomorphic settings of pioneer marsh compared to all other zones which is the closest to saltmarsh edge and having the shortest distance to MHWS (Chapter 3 – Table 3-6), thus causing most of its surface to be entirely submerged twice a day (see Chapter 4 - section 4.4 and Appendix D- Section D-3) and affecting its soil structure. These results are in agreement with Zhang et al. (2001) who identify that high amounts of water movement increases the shear strength of suspended sediments leading to intensive local soil deformation leading to a surface layer with higher bulk density, lower porosity, lower hydraulic conductivity and increased soil shear strength. Soil shear strength is linked to soil erosion whilst tensile strength of soils has been found to decrease with low BDD and high-water content.

BDD's variability between the sites' saltmarsh surface zones shows that the natural saltmarsh surface zones on both natural sites, ANK and FM, display more heterogeneity in that MR soil structure was more homogenous across the saltmarsh surface zones. The MM zones closest to MHWS display the lowest BDD compared. This lack of soil structure heterogeneity on MR was further confirmed within each of the 10 cm interval depth steps analysed. Section 6.2.2.1 brings attention to additional disparities, specifically in relation to ANK's HM, which exhibits the highest BDD. Conversely, MR demonstrates an opposite trend, as its pioneer zones display the highest BDD.

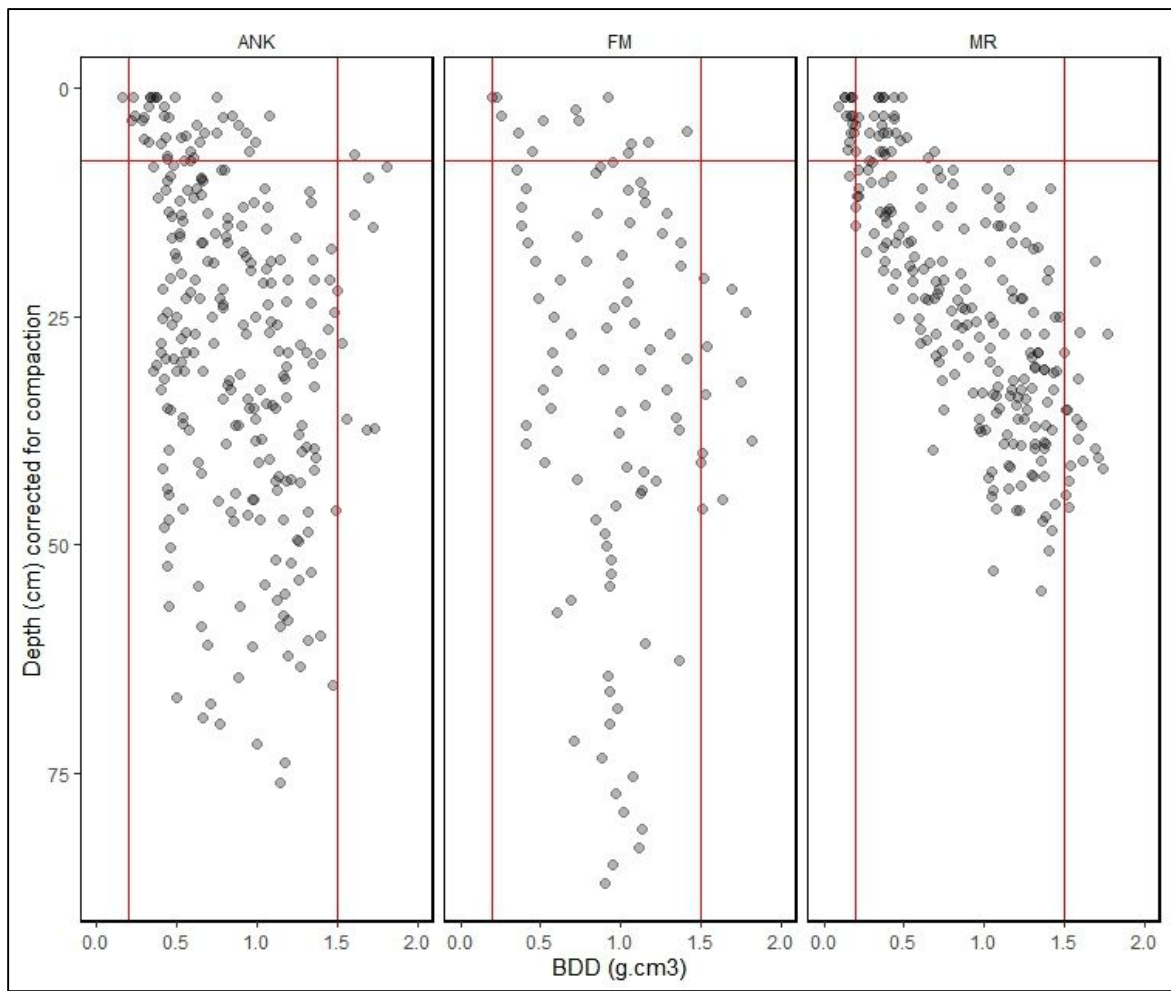


Figure 6-39: BDD ( $\text{g}\cdot\text{m}^{-3}$ ) versus depth (in cm and corrected for compaction) per saltmarsh sites, with intercepts in red on the y-axis at 8 cm in depth and on the x-axis at 0.2 and 1.5  $\text{g}\cdot\text{cm}^3$ .

### Impact on soil compaction from anthropogenic disturbances: Natural versus managed realignment

This study set out to test the assumption that BDD would change through depth/time reflecting external and anthropogenic disturbances. The expected trend of increasing BDD with depth (Callaway et al., 2012) was not clearly demonstrated on all saltmarsh sites and zones. Analysis of BDD at a 10 cm interval depth showed that overall MR's BDD was significantly lower than the natural salt marshes down to 20 cm (compared to ANK) 30 cm (compared to FM) depth, beyond which BDD was significantly higher.

Sequential shifts were confirmed in upper soil profile using photographic record where a change in soil discoloration was present in most of the cores Figure 6-35 between depths of 18 and 25 cm (corrected) on PM cores, at 7 to 10 cm deep for LM cores, at 5.5 to 10 cm deep for MM (5.5 to 10 corrected) and HM 6 to 12 cm in depth. This discoloration could be traced through the core profiles at an increasing depth landward direction suggesting, first, that a single event disturbed MR saltmarsh soil zones in the recent past; and second that sedimentation on MR is directly linked

to elevation height and distance from saltmarsh edge. These results agree with Tempest et al. (2015), Spencer and Harvey (2012) and Spencer et al. (2017) who report lower BDD on MR sites for shallow cores.

The analysis has further shown lower in core profiles that on ANK at approximately 40 cm in depth, BDD changes drastically. This shift was also reflected on MR's HM and PM zones at c.25 cm and c.35 cm deep (Figure 6-20, Figure 6-39 and Appendix E - section E-4). These profiles are not uncommon on longer/older cores such as the 2 m deep cores in the Wadden Sea presented by Madsen et al. (2007) which display increasing and decreasing compaction sequences. The two signals on ANK and MR reflect a clear change in sediment structure inferring a change in the system. On MR, as the depths differ, 2003 MR breaching may be excluded to explain this change, just as 1950's reclamation (as sedimentation is slower on HM, the shifts would be at higher depths in the cores and confirmed by shift). These changes may signify geomorphologic changes that occurred within the system regime, a change from mud/sand flat to pioneer salt marsh which was also reflected in the grain size analysis.

#### **Impact on soil moisture from anthropogenic disturbances: Natural versus managed realignment**

Water content variability per saltmarsh sites, saltmarsh surface zones or through depth as profiles shown strong relationship where an increase in bulk density (BDD) coincided with decrease in water content and vice versa. Therefore, variability in sediment moisture does not differ from the BDD results. However, at Nigg clear linkages between grain type and water content were made suggesting that the water moves the most through porous soil structures where grains are the smallest (Figure 6-40) .

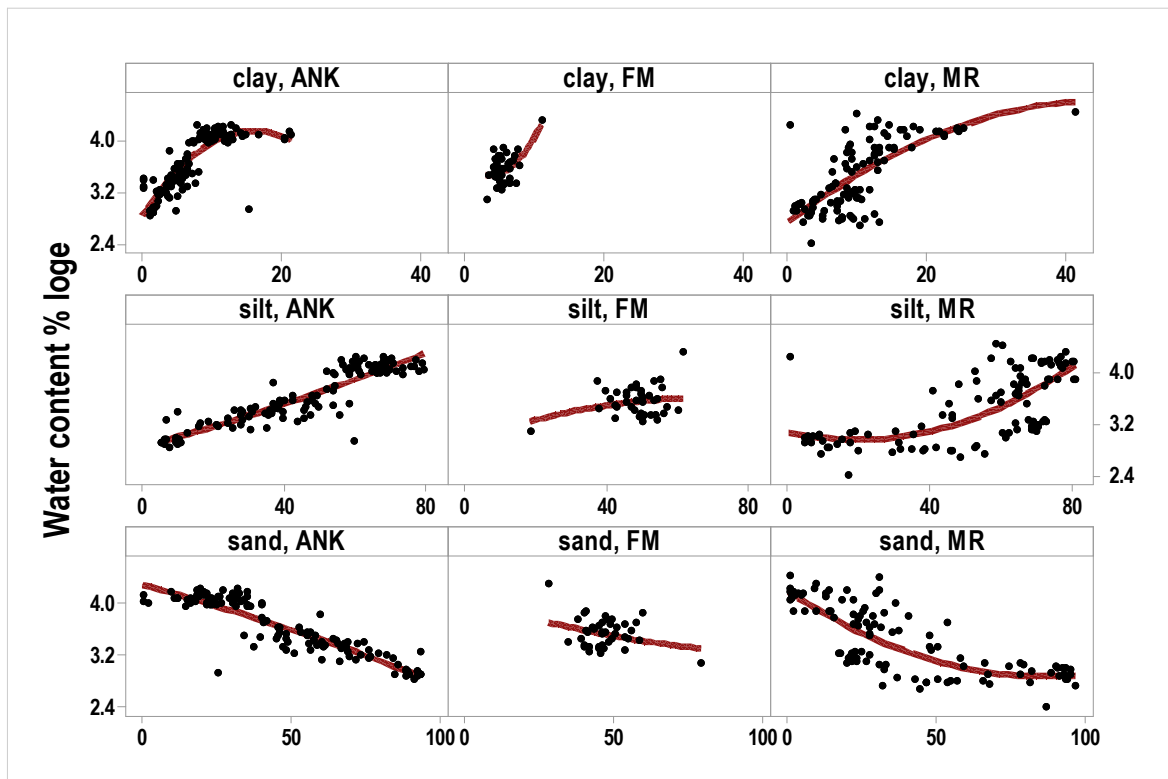


Figure 6-40: water content ( $\%Log_e$ ) versus sediment type per sites showing positive trends between water moisture and porous fine sediment grains such clayey and silty soil structure and negative trends for less porous soils such as sands (quadratic fits as red lines).

### 6.5.1.3 Summary of saltmarsh physical sediment properties influence on saltmarsh development

While not demonstrated in this particular study, it is possible that factors such as distance to the saltmarsh edge, slope, and hydroperiod could influence sediment grain size and type, soil bulk density, and water variation. This aligns with the findings of Roner et al. (2016) in their research on the salt marshes of San Felice and Rigà. The study further highlights the importance of the sediment grain size influence on soil moisture in Nigg Bay and confirm that soil moisture can be used to interpret changes, such as autocompaction (Turner et al., 2007) within the saltmarsh system, hence its importance in radionuclides studies. Finally, natural salt marshes demonstrate more heterogeneity in grain type and soil structure compared to the managed realigned marsh, agreeing with Spencer et al.'s (2017) conclusions drawn from eight salt marshes in SE England.

## 6.5.2 Belowground physical and biological interactions on natural and managed salt marshes

(Howard et al., 2014) highlight that belowground soil carbon pools are the least studied despite the fact that they constitute between 50 to 90 % of the total ecosystem carbon stock of tidal salt marshes. The Nigg research aimed to fill this gap by exploring patterns in carbon density across three salt marshes and its storage through depths, over timescales of years to centuries, in order

to estimate the magnitude of carbon sequestration in the system -referred as Blue Carbon - and to identify areas of high carbon sequestration in restored or reclaimed salt marshes (Connor et al., 2001; Owers and Rogers, 2016). It was hypothesised that land management disturbances such as sea-embankment, dyking and drainage in the 1950's for reclamation and the sea-wall breach in 2003, would have altered the carbon stock on the managed realignment MR salt marsh compared to the natural salt marshes FM and ANK.

#### 6.5.2.1 Biological sediment properties: natural versus managed salt marshes: implication

Although there was a statistically significant difference in mean carbon density between saltmarsh sites, no clear ranking was observed. The soil carbon density (SOC), representing carbon concentrations stored in the organic matter of the compacted saltmarsh sediments, is the lowest on the youngest salt marsh, FM which emerged since the 1950's displays when compared to the managed (MR) and natural (ANK) salt marshes. These results confirm that overall carbon density increases with maturity, in agreement with Elschot et al. (2015) work on tidal marsh carbon stocks in Schiermonnikoog back-barrier (Netherlands). The thesis results also identify that overall the managed saltmarsh carbon storage was significantly impacted by 50 years of reclamation and agreeing with most findings on de-embankment and restored salt marsh in England (Burden et al., 2013; Tempest et al., 2015). Carbon densities levels also concur with findings such as Connor et al. (2001) in the Bay of Fundy where similar carbon densities to the Nigg salt marshes and found: Outer Bay of Fundy averaged (low and high marsh zones combined) at  $0.0247 \text{ g.Ccm}^{-3}$  and compared to an overall average of  $0.025 \pm 0.001 \text{ g.Ccm}^{-3}$  at Nigg. These findings suggest that northern latitude salt marshes share similarities despite a completely different geomorphic settings. They also suggests that shorter growing seasons may impede the high carbon level and carbon sequestration capacity of these saltmarsh sediments, only high sedimentation rate would enhance this carbon storage capacity (Chmura and Hung, 2004). In a recent study conducted by Miller et al. (2023), presented in Chapter 4 - section 4.6. 3, has produced detailed information on two salt marshes at Dornoch point and Morrich More, both located in the Morray Firth, as is Cromarty Firth where is located Nigg Bay. There is no direct comparison for the pioneer zone, however the belowground carbon storage for the low- and mid-marsh zones, ANK and MR carbon storage is greater than the Morray Firth marshes (approximately 48 % and 40 % more respectively) and lower on FM (approximately 33 % less). The high marsh zones of Nigg Bay have, on average, 24 % lower values than Morrich more and Dornoch point with ANK and FM having 56 % and 17 % less carbon stored in their soil, whilst MR is having 108 % more carbon in its soil compared to the Dornoch. Despite these differences, the total belowground carbon storage the natural salt marsh ANK and managed realignment MR of Nigg Bay is similar to the Dornoch and Morrich More at  $2.4 \text{ tCha}^{-1}$  (Figure 6-41).



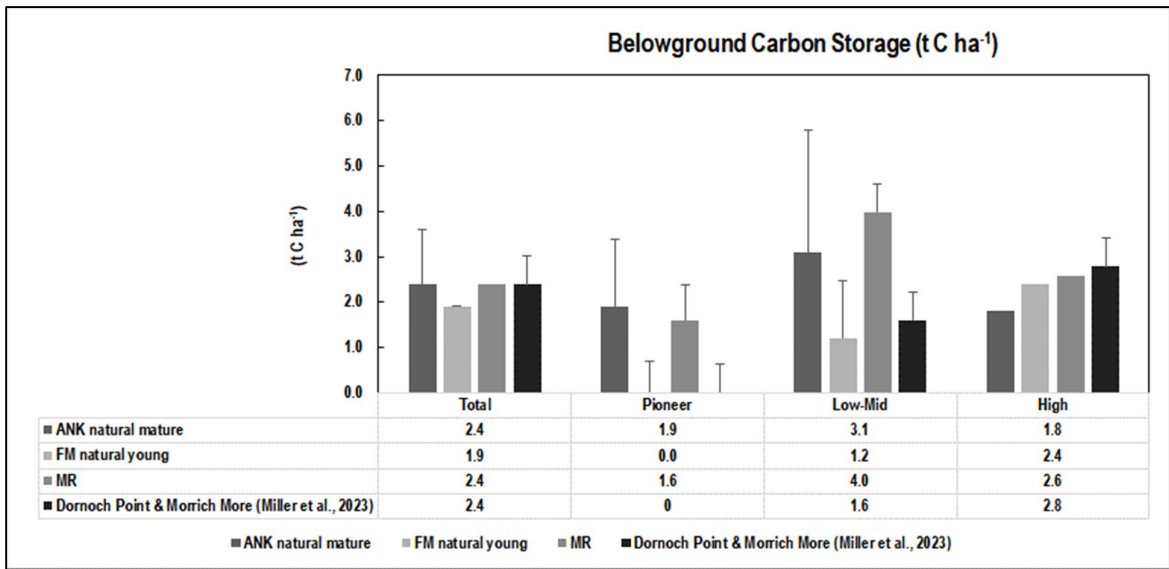


Figure 6-41: Bar graph showing the belowground organic carbon stock ( $t C ha^{-1}$ ) in the low-mid (mid-marsh and low-marsh zone values have been averaged for Nigg salt marshes to match Miller et al. (2023) results as there was no distinction made between mid and low marsh in their study) pioneers and high-marsh zones of ANK, FM, MR and Dornoch point and Morrich More saltmarshes (Error bars are standard deviation).

#### 6.5.2.2 Linkages between surface zonation and carbon stores

This thesis research also suggests that saltmarsh zonation leads to spatial heterogeneity in the distribution of organic carbon density. Overall carbon storage was found to be significantly lower in the most exposed part of the marsh, PM zones, and higher in LM zones decreasing in carbon content landwards and with elevation. This pattern was exhibited in the mature natural salt marsh ANK. Connor et al (2001) have also found such variability where carbon densities increased seawards from HM to LM for saltmarsh sites in the upper Bay of Fundy whilst salt marshes in the outer bay decreased seawards from HM to LM. However, the study in Nigg Bay showed a reverse trend in the FM, where the highest SOC was found in the HM and the lowest in the LM, and in the MR, where the highest SOC was found in the MM.

Unlike Schindler, Karius, Arns, et al. (2014) findings in the Wadden sea salt marshes who found that decomposition of organic matter to be the main driving factor for carbon densities, vegetation type was not found to explain this carbon densities variability (approximately 8.9 %  $r^2_{adj}$ ) in the saltmarsh surface zones, it appears that geomorphological drivers control carbon densities variability in Nigg Bay. To illustrate this interpretation, it was seen in section 6.5.1.1.1, that overall mean grain size was found highly variable between saltmarsh surface zones with concentrations of coarser grains ( $>125\mu m$ ) on the pioneer zones, silts on the low marsh and very fine sand ( $>63\mu m$ ) on the mid and high marsh. These patterns suggest that, by controlling overall sediment input, tidal flooding and frequency (highly correlated with monthly sediment deposition rates as seen in Chapter 4 - section 4.5.1) have created geomorphic settings favouring carbon storage on areas with fine sediments, low compacted and moist soils. Furthermore, running a linear regression shows that 48 % ( $r^2$ ;  $p < 0.001^{***}$ ) soil organic matter variability can be

explained by soil dry bulk density ( $F_{(1, 604)} = 556.8^{***}$ ) with a relationship defined as  $SOM = 32.046 - (23.912 * BDD \text{ in } g.cm3)$  (see Figure 6-42). These findings are in agreement with Kelleway et al. (2016) who identify sedimentary factors as key predictors of carbon storage and further establish that sediment grain size is a key predictor of carbon density attributed to the enhanced carbon preservation capacity of fine sediments.

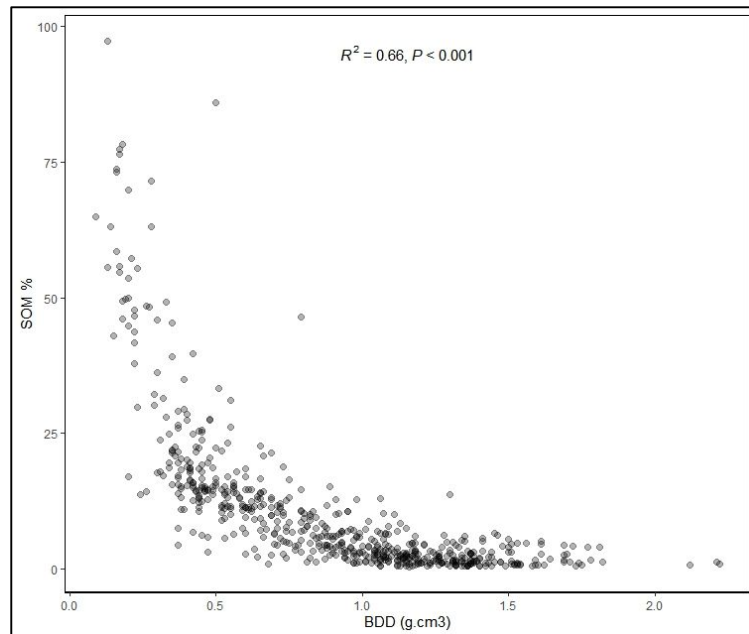


**Figure 6-42: Scatter plots between SOM (in % - y-axis) and BDD (in g.cm3) . Plots are showing  $r^2$  values and p-value.**

A principal component analysis (PCA) was conducted to investigate the potential influence of various physical factors, including elevation (m), hydroperiod (m), flood depth (m), flood frequency, distance to mean high water springs (MHWS), distance to water channels (m), and distance to saltmarsh edge (m), on the variation of carbon density within the salt marshes studied in Nigg Bay. Although, PCA first and second dimensions (also called here principal components) account for 60.92 % of the variability observed in the dataset (Figure 6-43), the correlation plot depicted in Figure 6-44 reveals a limited representation of carbon density in the first and second dimensions, and it is present only in the fourth dimension. This correlation plot indicates a correlation between soil carbon density to distance to the saltmarsh edge and distance to water channels. Subsequently, best subsets regression was employed to provide additional clarification on any potential associations between SOC across all cores and the physical variables. The results obtained at this level, encompassing all cores, indicate that only distance to saltmarsh edge can contribute to predict approximately 3 % ( $r^2, p < 0.001^{***}$ ) of soil carbon density, but homogeneity of variances is not met. Connor et al. (2001) found that overall flooding regimes, tidal frequencies and elevation, which differed on the studied areas, explain carbon densities variability and that overall soil formed at lower elevation under higher-frequency flooding regimes benefits of a greater input of mineral sediment. The thesis results can only agree in part with these

interpretations because i) tidal frequency has been altered twice on MR salt marsh in past c.70 years; and ii) the studied sites in the Bay of Fundy had minor bulk density variability between high and low marshes which is not the case at Nigg. However, further work with Nigg Bay dataset should aim on interpreting carbon density for each core and at different depth levels.

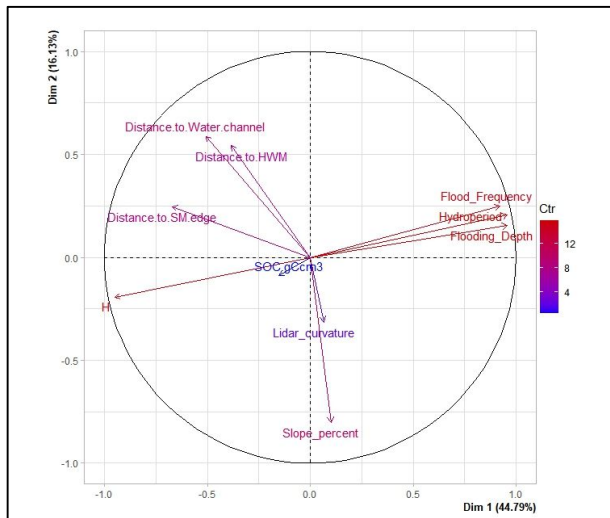


**Figure 6-43: PCA plot for SOC including the physical variables of elevation (m), hydroperiod (m), flood depth (m), flood frequency, distance to MHWS, distance to water channels (m), distance to saltmarsh edge (m), slope (percent) and curvature.**

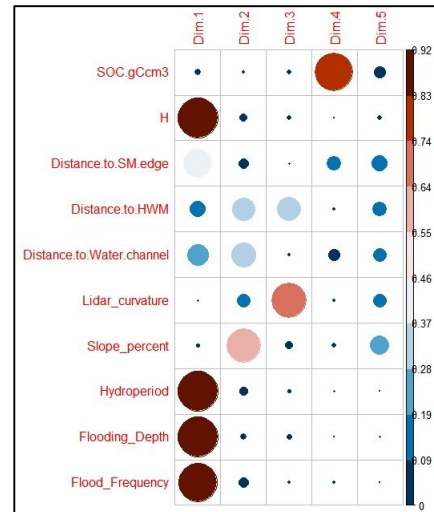


**Figure 6-44: Plot matrix of the square cosine (cos2) which is the quality of representation of the variables of the PCA for SOC.**

### 6.5.2.3 Temporal variation: historical legacy impacts on carbon stores

This thesis research also hypothesised that soil carbon densities would differ through depth between natural and managed salt marshes. This was confirmed by demonstrating that SOC on the two natural salt marshes, FM and ANK, maintains higher level through soil depth (Figure 6-33) whilst MR's SOC is only found at its highest level at depths of 0-10 and 10-20 cm and is seen to rapidly decrease with depth. These findings suggest that the higher SOC level on MR are recent and, as suggest photographic record presented in section 6.4, this vertical increase in carbon density is clearly associated with new tidal sediment input since the de-embankment in 2003 allowing the marsh to accrete, unlike reclaimed agricultural soil which may have similar carbon density but unable to increase its carbon storage. These results are consistent with Tempest et al. (2015) who found a pronounced increase in the top 5 cm of the de-embankment salt marshes in SE England and with Connor et al. (2001) findings in the Bay of Fundy which further found that salt marshes with high amounts of suspended sediment may dilute soil carbon concentrations. However, high amounts of suspended sediment may also serve to increase carbon storage capacity by forcing high rates of saltmarsh accumulation.

### **6.5.3 Summary of saltmarsh biological sediment properties influence on saltmarsh development**

This chapter established that sedimentary properties such as grain size are key predictor of carbon storage. This is an important consideration for saltmarsh restoration and realigned management in Scotland whose marsh sediments are typically much coarser than English and Welsh saltmarshes sediments (May & Hansom, 2003). Furthermore, 73 % of the published literature (worldwide: Belgium, Germany, Spain, USA and Canada) relevant to de-embankment and saltmarsh restoration relates to English and Welsh salt marshes (Esteves and Williams, 2015). The results of these chapter have also a wider impact in the context of 2015 Paris Climate Agreement which has set a clear target for all nations to shift to a low carbon economy where carbon storage is one potential mechanism for meeting these targets. Reverting to salt marshes is a way to accelerate the transition to a low carbon economy by developing and integrating nature-based solutions into land-use planning to meet Scottish Government climate mitigation and adaptation targets. There has been no direct evaluation of coastal saltmarsh carbon storage in Scotland and the results reported here provide preliminary estimates of organic carbon density using the three sites at Nigg: a mature natural salt marsh ANK, a young natural salt marsh FM and the managed realignment salt marsh MR.

Chapter 8 aims to bring together the results provided in this chapter for Soil Blue Carbon and from Chapter 4 for Vegetative Blue Carbon for the three salt marshes studied over short (monthly) and longer timescales (century).

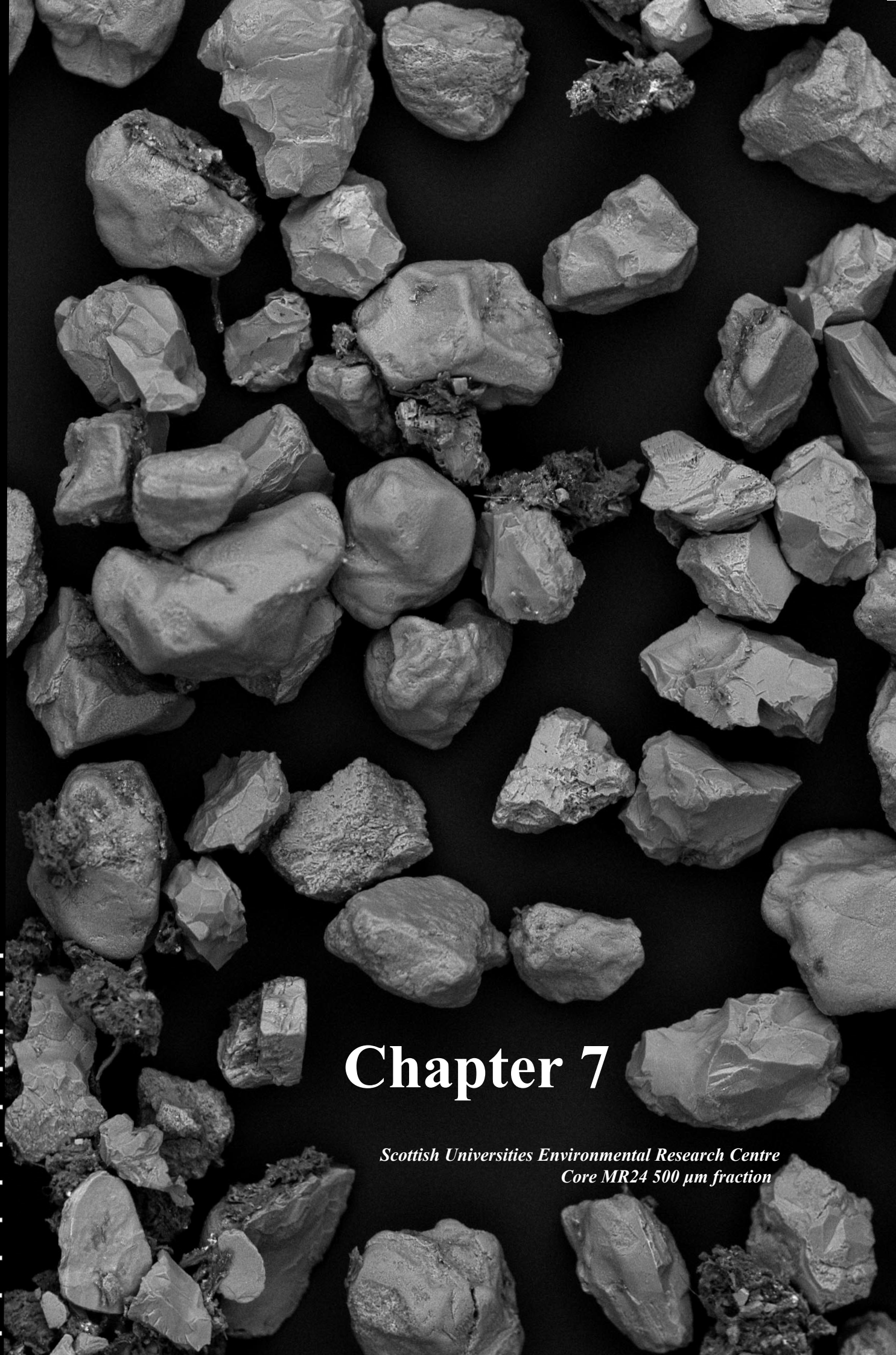


S3400 20.0kV 11.6mm X70 BSE3D 30Pa 6/21/2016 11:47

500um

# Chapter 7

*Scottish Universities Environmental Research Centre  
Core MR24 500  $\mu$ m fraction*





**Chapter 7. Exploring the Potential of Optically  
Stimulated Luminescence to Trace Sediment  
Processes in Modern Dynamic Saltmarsh Systems**

## 7.1 Introduction

Chapter 4 presented short-term (annual) processes between biomass and sediments taking place **aboveground** on the three saltmarshes at Nigg Bay, Chapter 5 long-term (multi-annual to centennial) **aboveground** sedimentary processes and Chapter 6 focussed on long-term **belowground** processes between organics and inorganics through a series of cores. The results show high spatial and temporal variability between sedimentation and vegetation processes which may inform the health, sustainability and vulnerability of the saltmarsh system. However, these results have also demonstrated difficulties faced when using traditional geomorphological techniques to contextualise depositional sequences or events that took place during saltmarsh development. This chapter hypothesises that each sediment grain holds the story of its transport, settlement and burial stability. By using the same sediments as for organics and inorganics analysis (Chapter 6), it aims to develop new way of using Optically Stimulated Luminescence (OSL) to trace the narrative of sediment grains sealed in the past sedimentary record of the natural and managed realignment saltmarsh sites. As such, within this thesis framework as conceptualised in Table 7-2, this chapter focusses on the results obtained through the application of OSL to trace sedimentary processes that took place during saltmarsh past and recent development.

### 7.1.1 Basic principles

Luminescence is the phenomenon where material exposed to some of energy of radiation is absorbed and re-emitted as electromagnetic radiation. Luminescence dating methods, including thermoluminescence (TL - stimulation by heat), Optically Stimulated Luminescence (OSL - using beam of light) and Infrared stimulated Luminescence (IRSL) estimate the impact of ionising radiation on the crystal lattice of minerals which can store energy through trapping charge carriers (electrons and holes) at defect sites. Subsequent stimulation using heat or light releases the trapped charge, resulting in observable luminescence which can be quantified and related to the magnitude of the preceding exposure to ionising radiation since an early “zeroing” process or event (Aitken, 1998; Wintle, 2008; Duller, 2008; Cordier, 2010). Almost exclusively, luminescence from quartz and feldspar grains is used in dating and these minerals can be found in almost all sedimentary environments. A low level of ionizing radiation comes from radionuclides which are present in the mineral and its natural environment, mainly uranium (U), thorium (Th) and potassium (K) (and  $^{40}\text{K}$ ,  $^{238}\text{U}$ ,  $^{235}\text{U}$ ,  $^{232}\text{Th}$  and daughter products,  $^{87}\text{Rb}$ ) and cosmic rays.

Energy from radiation is stored by electrons which can be trapped in the defects of the crystal lattice of a mineral (defects due to a missing atom, or atom out of position or impurity atom). Some of the traps are ‘shallow’ or ‘unstable’ because the electrons inside are easily evicted and will not

remain trapped for the whole duration of burial. In contrast, deep or stable traps inside the lattice are associated with high energy levels and there is negligible leakage over millions of years (Aitken, 1989). The depth of the trap is defined by the energy necessary to detach its electron and allow it to diffuse briefly. The total amount of trapped electrons within a crystal is proportional to the total energy absorbed and retained by the crystal (or dose), hence the time it was exposed to radiation (Aitken, 1989; Cordier, 2010).

When the mineral is eroded, transported and deposited, it is exposed to daylight and the energy previously acquired is released from the traps. This release of trapped electrons (“bleaching”) results in the emission of a luminescence signal and associated with a resetting (“zeroing”) of the dosimetric clock; resetting the signal to zero (bleaching), and when buried again, the luminescence signal builds once more.

When collected, the mineral can be stimulated by photo-stimulated luminescence (PSL) using either visible light for quartz (OSL typically performed with blue, green and more recently violet Light Emitting Diodes - LED), or infrared light for feldspars (Infrared) or thermal luminescence (TL) uses heat. OSL dating focuses on the light-sensitive part of the signal (which is faster and more completely bleached) while TL also measures the non-bleachable signal; hence OSL dating makes it possible to date younger sediments, and to reduce the occurrence of partial bleaching (Aitken, 1989; Wintle, 2008; Cordier, 2010).

The stimulation empties progressively the traps from the electrons, the stored energy is released, mainly in the form of heat, but some fraction of the recombination events release energy in the form of light photons, known as thermoluminescence. The number of UV photons will decrease with exposure time (Figure 7-1) as the trapped charge is released, and the total amount of emitted light will be related to the total amount of radiation absorbed by the mineral throughout its burial since formation or last resetting (or zeroing). Figure 7-1 shows that that OSL signals from quartz and feldspars are reset by exposure to sunlight much more rapidly than is the TL signal (for 100s exposure, the quartz OSL signal is reduced to <0.1 % compared to 85 % for TL), process known as bleaching (Duller, 2008) . The figure also shows that under the laboratory conditions used the quartz signal depletes more rapidly than those from feldspars. Indeed, the OSL signal is made up of several exponentials as schematised in Figure 7-2 and relates to different levels of traps reflecting the existence of a fast component (associated with the emptying of the most light-sensitive traps) (Madsen et al., 2009; Durcan and Duller, 2011; Mellett, 2013).

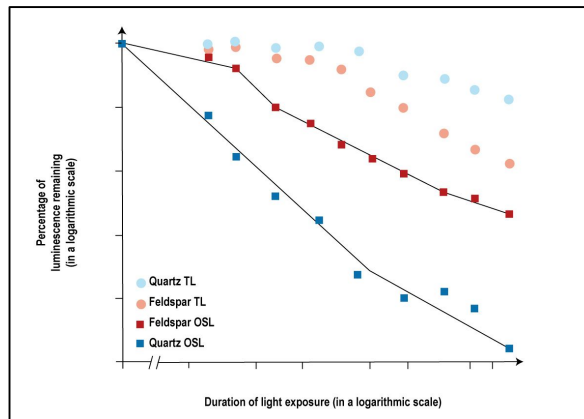


Figure 7-1: Reduction of Quartz and Feldspar luminescence signals during exposure to light for OSL techniques or heat using TL techniques (taken from Duller, 2008, p.8).

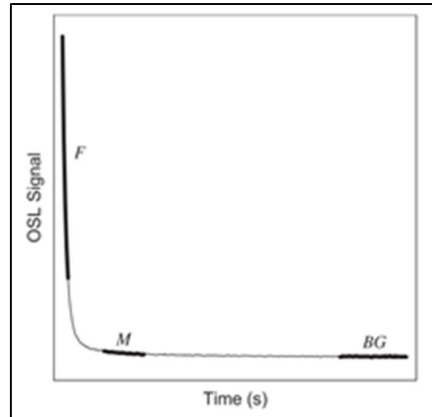


Figure 7-2: A schematic view of the OSL (quartz) decay curve with hypothetical location of its several component: F- fast component, M, the medium component, and BG, the background (taken from Durcan and Duller (2011), p.1066)

The analysis of the OSL signal allows to calculate the time elapsed since burial, i.e., the age of the sediment. This age is derived using the following equation:

$$\text{Age (year)} = \frac{\text{ED (in Gray)}}{\text{DR (in Gray/year)}}$$

The Equivalent Dose (ED) is the radiation dose delivered to the mineral grains in the laboratory to stimulate luminescence, equating to the total amount of radiation absorbed by the mineral throughout its burial since formation or last resetting (or zeroing). The mineral is used as a natural dosimeter. ED is measured in Gray (Gy or J/kg) representing absorbed radiation energy per unit mass. Dose Rate (DR) is the rate at which the sediment is exposed to natural radiation. It can be obtained via measurements of the concentration of radioactive elements in the sediment (K, U, Th, Rb and cosmic rays) using conversion factors, or direct measurements of the radioactivity by counting the emissions of alpha, beta and gamma using field or laboratory spectrometers (this method requires to correct the amount of radiation in the water present in the sediment pores)

(Duller, 2008; Mellett, 2013). DR as dose per unit time or Gy/year and computed in laboratory following several literature sources (Sanderson, 1988b; Aitken, 1989).

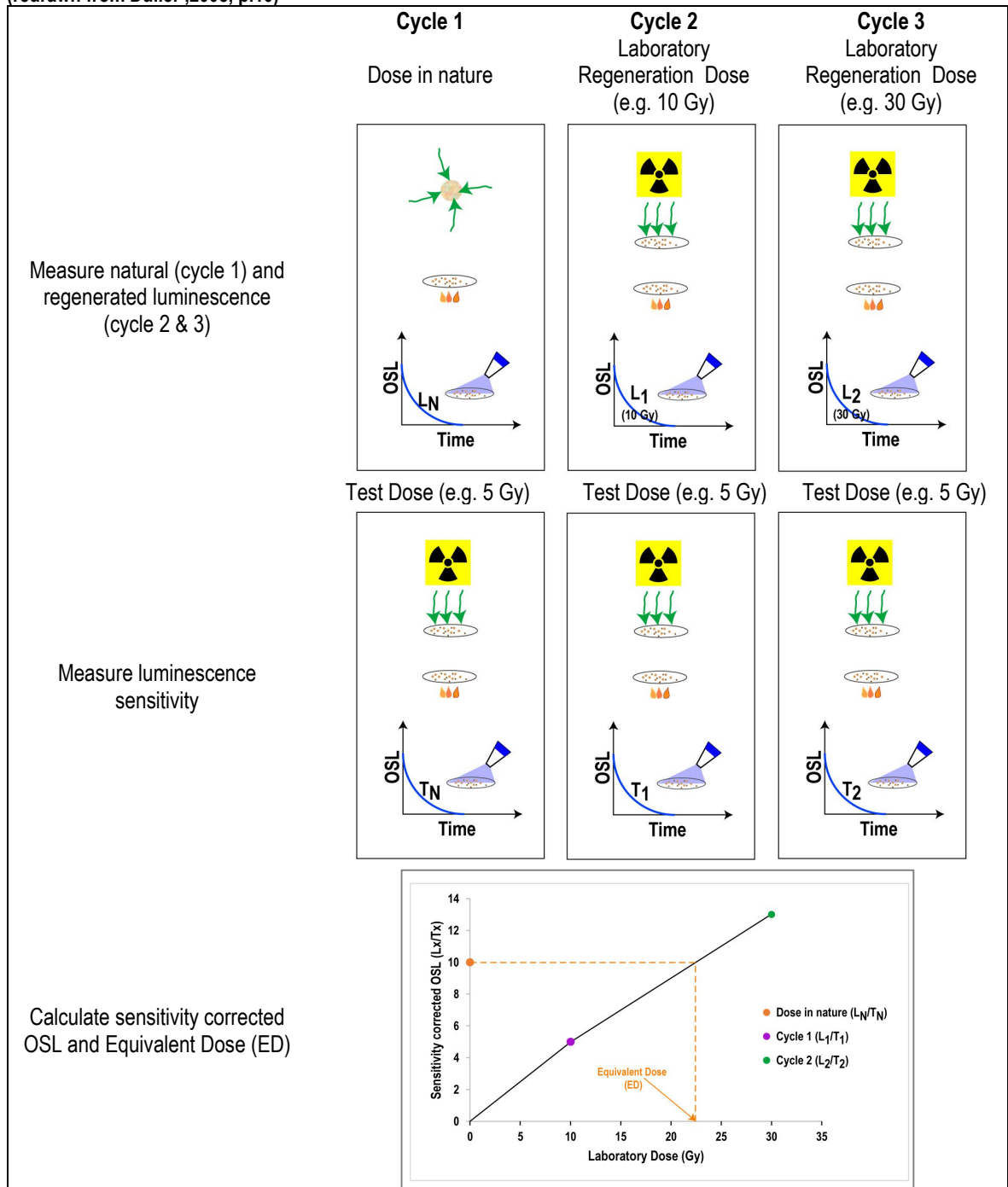
Consequently, determining the equivalent dose (ED) is considered the most time-consuming step of the luminescence dating and techniques and protocols will differ depending on:

- . the grain type: quartz or feldspars guiding the procedures;
- . mineral depositional settings (aeolian, fluvial or coastal) affecting the resetting/zeroing of the signal;
- . additive and regenerative procedures:
  - additive procedure consists to use several aliquots to obtain only one equivalent dose (ED). The principle is to give laboratory radiation doses on top of the signal acquired during burial, causing the luminescence signal to increase, to which a mathematical function can be applied (extrapolation of the natural signal on a curve derived from various laboratory doses). The procedures were derived from TL studies and principally used in the 1990's with the most notable Multiple Aliquot Additive Dose or MAAD procedure (Duller, 2008; Cordier, 2010);
  - the most notable regenerative procedure, which has now become the standard protocol in luminescence dating is the Single Aliquot Regenerative (SAR) protocol was developed for quartz grains (Murray and Wintle, 2003; Wintle and Murray, 2006; Madsen et al., 2010) and applied also to feldspars (Wallinga et al., 2000). The SAR procedure is now a standard protocol used in luminescence dating (Wintle and Murray, 2006) (see Table 7-1).
- . single aliquot versus single grain protocols. Most laboratories would dispense aliquots on 1 cm diameter discs for measurement, however the number of grains on these discs can vary depending on the covered area and the grain size of the subsample. The ED being the sum of the luminescence emitted by all grains present on the disc, the measurements between multiple single aliquots will not be uniform (due to different degree of bleaching or post-depositional mixing). There is therefore in some occasion justifications to measure the OSL signal from single grains (Duller, 2008; Mellett, 2013).

Wintle reviews in 2008 the major advancements in luminescence dating, Madsen and Murray (2009) luminescence dating for young sediments and Jacobs (2008) the coastal and marine sediments. Relevant to this research is the recent advances and applications of the use of OSL portable readers that reduce considerably the time and labour of luminescence

dating (that can take up to 6 months to obtain an age). Although the technique does not provide an absolute age, it allows to determine if samples can be dated by providing luminescence characteristics and sensitivity range.

**Table 7-1: Schematic example of the single aliquot regenerative dose (SAR) procedure. The method consists in a series of measurements' cycles. The first cycle measures directly the natural (aliquot) luminescence signal until it fades completely (labelled L in graph) . By giving a controlled (known) radiation dose to the grains, labelled T in the graph, it allows to measure the luminescence or brightness' sensitivity and to correct any sensitivity changes. This is done by calculating the ratio between L and T. The same protocol is repeated in a second cycle of measurements after exposing the grains in the laboratory to an artificial radiation dose (known as regenerated dose), this regenerated OSL signal is then given the same test dose as during the first cycle to correct effect in sensitivity changes and their ratio is calculated providing a second corrected OSL. Successive cycles can measure different regenerated signal. Finally, plotting each cycle 's OSL corrected signal as a function of the laboratory dose (last row of the table) is used to calculate the sample or aliquot ED by projecting the natural OSL (corrected) to the response curve created by the regenerated OSL signal (redrawn from Duller ,2008, p.10)**





### 7.1.2 Rationale

Absorption and emission of light by a material is a powerful tool to identify how it behaves and the processes it has been subject to over different timescale and environmental conditions (Ballarini et al., 2007). Application of Optically Stimulated luminescence OSL relies on the energy trapped through time in minerals (quartz and feldspars) within sediment during natural radioactive decay is released as luminescence (light) when exposed to visible light (bleached), thus resetting the luminescence signal. However depositional and bio-geomorphic processes influence wavelength and bleaching intensity and this is relevant in tidal dominated environments where individual sediment components may have diverse transport and bleaching histories and different sensitivities to luminescence. Richardson (2000) demonstrated that for samples collected on marsh clays, the selection of water content used in Stimulated Luminescence dating (in his study feldspar based method with use of Infra-Red Stimulated Luminescence – IRSL) dating could add over two thousand years to the maximum age and influence dose rate. The finding also suggests that residual luminescence signals will differ from naturally high and variable water contents. Richardson's work within the NERC funded LOIS programme is relevant for this research thesis as her research explored the use of polymineral IRSL measurements to date young coastal sediments. With the available laboratory procedures at that time both sensitivity and initial zeroing conditions were limitations, and it was also noted that uncertain water contents were also important. When dating young sediments, early work from Aitken (1988) on quartz found that the repeated cycles of bleaching and burial prior to the ultimate deposition could substantially reduce the importance of recuperation (as after bleaching, the signal has been found to increase during subsequent storage or preheating), and in some cases, partial bleaching leads to potential overestimation of OSL ages. But the study also suggests that sediments that received prolonged light exposure may be suitable to recent sedimentation (Madsen and Murray, 2009). Subsequent studies (on quartz principally) investigated the complete zeroing or resetting of modern aeolian, fluvial and coastal sediments and highlighted the importance of sample pre-treatment and working protocol (e.g. low preheating temperature, improvement of the signal-to-background ratio by using different signal-pass filters). Madsen and Murray (2009) (quartz based method) identified specific problems with dating young sediments in tidal systems: (1) insufficient luminescence sensitivity to allow measurement at the very low doses involved (~tens of mGy) resulting in a low signal to noise ratio and imprecise doses, (2) significant thermal transfer during the thermal pre-treatment (preheating) that takes place prior to OSL measurement, leading to overestimates in dose, (3) incomplete resetting of the sediment, giving rise to overestimation of the OSL age, and (4) alteration of the sedimentary environment (e.g. changes in water content, sediment matrix or sample depth) that result in a time-dependent dose rate. In many situations (e.g. sediment de-watering and compression), this results

in an increase in dose rate with time, and so a tendency to underestimate age if the dose rate at the time of sampling is employed without correction.

Much of this work on tidal and modern sediments has been to establish absolute chronologies using OSL by improving the selection of datable sediment determined by the sample sensitivity (response of a sample to irradiation). However, changes in sensitivity can also inform on the provenance of a sample. Bleaching susceptibility may vary with mineral type, grain size, sediment transparency as much as environmental history. Bleaching is key to luminescence and is key to the story contained within each mineral. The degree of bleaching may inform on the dynamics of the system or landscape depending on the speed of sediment accumulation. These issues are close to the aims of this thesis than solely determining the age of saltmarsh sediment.

OSL dating necessitates full laboratory based OSL dating protocols laborious due to sample preparation and relatively expensive due to specialised analytical equipment. In 2010, Sanderson & Murphy proposed a novel way to assess the luminescence of their samples by the use of the pulsed photon-stimulated luminescence (PPSL) unit, also known as Scottish Universities Environmental Research Centre (SUERC) portable OSL reader. The portable reader unit contains a photo-multiplier allowing to measure directly the luminescence signals of bulk samples when placed in its chamber (through a Petri dish) by stimulating the sample owing to an array of diodes for the optical stimulation in blue (B-OSL) and infrared (IRSL) wavelengths. Parallel to this instrumental innovation, from the late 1990s through early 2000s, methodological development such as core profiling started to be used in laboratory conditions where samples are collected in dark condition at each stratigraphic level of a core. From 2005, portable readers allowed taking the techniques directly in the field. The reliability and reproducibility pulsed photon-stimulated luminescence (PPSL) unit used for core profiling is a fast and accurate way to inform complex depositional sequences, directly estimate relative age of deposits, identify heterogenous and incomplete bleaching which can be then used for full OSL dating (Sanderson and Murphy, 2010; Muñoz-Salinas et al., 2011; Munyikwa et al., 2012; Stone et al., 2015; Portenga and Bishop, 2016). Work at SUERC in 1996 and 1997 at Caerlaverock salt marsh in the Solway, have shown that PPSL systems have sufficient sensitivity to resolve natural luminescence signals within cores covering <30 years (Meldrum, 1996; McKeown, 1997). It therefore appears that while traditional OSL dating of young sediments may encounter difficulties relating to sensitivity, bleaching, and luminescence behaviour, that luminescence profiling techniques and systems may have potential to add new information to studies of young salt marshes. The Nigg Bay's systems offer a well characterised environment to appraise this potential. This chapter presents the outline of new methodology in OSL techniques (7.2) and the applied to the Nigg saltmarsh sediments to address:

- Is there a measurable luminescence signal?
- Does this signal increase with depth?
- Can it be enhanced and calibrated?
- Can the results inform the sediment history to complement the short-term and long-term results from previous chapters?

More specifically, questions and experimental hypotheses tested under the thesis aims are synthesised in the Table 7-2 below.

**Table 7-2: Questions and experimental hypotheses tested in this chapter under the thesis aims**

Research Aims	Specific research questions	Experimental hypotheses
Develop new reproducible techniques and applications to trace saltmarsh processes	Can we develop a reproducible and fast method to trace saltmarsh processes using young (<100 years) sediment grains?	<ul style="list-style-type: none"> <li>• A requisite of the viability of Luminescence (OSL and IRSL) is the presence of a signal, that is big enough to be recorded. It is hypothesised that an exploratory core can provide this answer and allow the appreciation of the technique for the young saltmarsh sediments of Nigg.</li> <li>• Based on these results, technique to be improved to increase the signal sensitivity and reproducibility and calibrate it in order to make geomorphological assessment. As transport and deposition variability may impede on the 'bleaching rule' (Mauz et al., 2010) and sediment reworking and resuspension prevent traditional protocols to be applied or turbulent conditions favour sediment bleaching as suggested by Berger (1990). This bleachability can be rapid or slow depending on its transport (sub-areal -wind or storms- or subaquatic), mineral type but also settling location such as on salt marshes where high vegetation may prevent grains to fully bleach prior burial. It is therefore important to improve a rapid technique that can quantify and differentiate between the bleachability of the sediment.</li> </ul>
	<p>Can new application of luminescence techniques inform on mineralogic variation and sources during the saltmarsh evolution?</p> <p>Can we trace depositional events through time in order to better understand saltmarsh formation and development?</p> <p>Can new application of luminescence techniques be a reliable process tracer for saltmarsh development history?</p>	<p>It is hypothesised that intensity and sensitivity of the luminescence signal will reflect:</p> <ul style="list-style-type: none"> <li>• Deposition history differs between the natural salt marshes ANK and FM due to their maturity and will differ from the young managed realignment salt marshes;</li> <li>• Depositional processes also vary significantly between saltmarsh zones reflected in the intensity and sensitivity of the signal;</li> </ul> <p>It is hypothesised that:</p> <ul style="list-style-type: none"> <li>• Deposition sequences are traceable through core depth reflected in the signal sensitivity and mineralogical variations (depletion indices) with depth. Through time/depth sediment's grains luminescence signal changes as it reflects the energy and duration of bleaching of the sediments prior to their deposition.</li> </ul>

Data Analysis: Details of the statistics used can be found in Chapter 3 – 3.4.5. For the sake of brevity, a list of abbreviations and acronyms used in this Chapter is provided in Appendix A.

## 7.2 Exploratory core and evaluation of Nigg bay's saltmarsh sediments luminescence signal

The cores collected for overall Luminescence analysis are presented as red dots in Figure 7-3 along the two transects (red lines in maps), previously described in Chapter 3 – 3.4.3.3 and Chapter 6 - 6.2.1 to test spatial heterogeneity within salt marshes. Cores extracted along these two transects are summarised in Table 6-3. Sediment treatment, methodology and analysis of the eight cores used for particle analysis are described in 3.4.3.3.

The exploratory work presented in this section is based on one small core (0.3m in depth) collected in the managed realignment MR, MR24, to evaluate the sediment quality for luminescence, which grain size (from 500 to <30 $\mu$ m) and which instruments may be capable to measure the young saltmarsh sediment sensitivity.

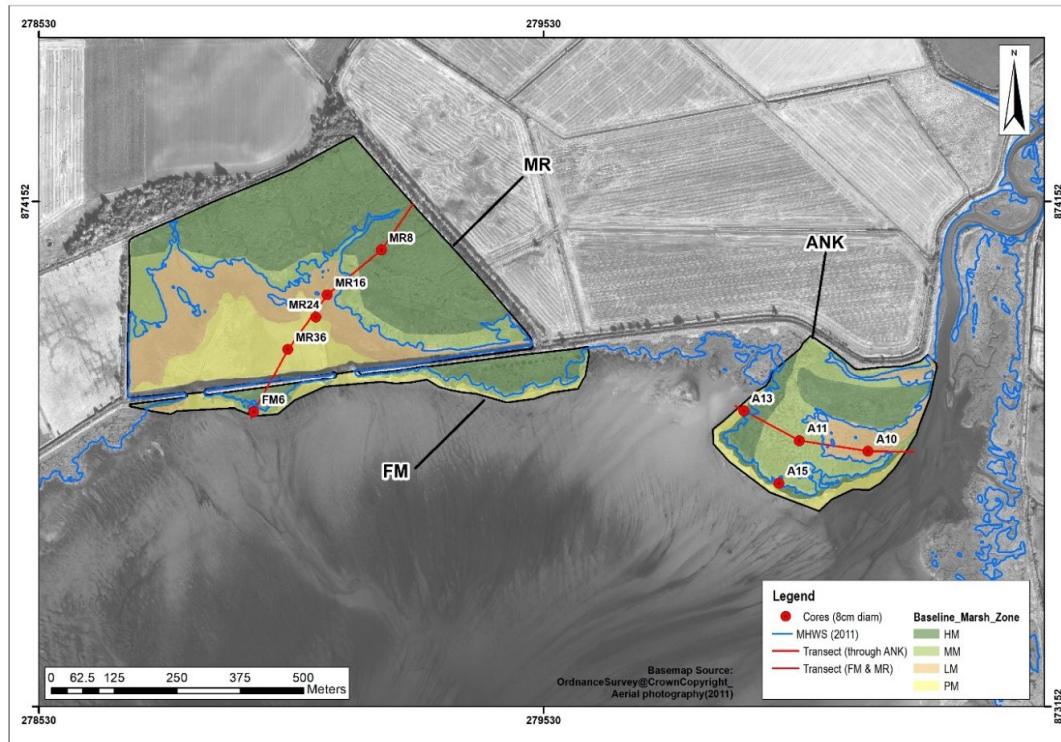


Figure 7-3: Location of all the cores used for Luminescence : Red lines = Transects; Red dots = cores. Abbreviations in legend: HM=High marsh, MM= Mid marsh, LM= Low marsh, and PM= pioneer marsh.

### 7.2.1 Sample choice and preparation: laboratory targeting

To evaluate if young saltmarsh sediments can emit a blue OSL and/or red IRSL luminescence signal and measure the luminescence quality and sensitivity, exploratory work focused firstly on one short core (id=MR24; 0.11m in diameter and 0.30m in depth) using different mineral fractions (from 500 to <30  $\mu$ m) on three different systems including SUERC portable readers, SURRC

PPSL (pulsed photo stimulated luminescence) and traditional Risø DA15/DA20 readers. This exploratory core was chosen from Nigg Bay managed realignment salt marsh which had a recognised recent history of 1950's reclamation and enclosure and then managed sea-wall breaching in 2003 which provide potential chrono markers in the core stratigraphy. The sediment core MR24 was split in two with one half used for organic and inorganic content analysis (see 3.4.2.3). The core length was divided at 20 cm intervals and half of the samples was kept in the dark for further analysis.

To measure if there is a luminescence signal from Nigg Bay young saltmarsh sediments, a series of prerequisite steps were needed in the laboratory programme.

### 7.2.1.1 Step One: Is there quartz and/or feldspar in Nigg Bay's sediment?

**Step one** focuses on the exploration of the mineral composition of two large fractions (500-250  $\mu\text{m}$  and 250-150  $\mu\text{m}$ ) using elemental mapping system (Scanning Electron Microscopy - SEM *Hitachi S3400 SEM*) and quantify the amount of quartz and feldspar present in the sampled core. The sample choice was small to best represent a quick visual assessment of the overall core stratigraphy. The results were satisfactory for both infrared and blue light stimulation (IRSL and OSL) with an overall higher quantity of quartz (Figure 7-4). The results demonstrate also for grains of the same fraction 250-150  $\mu\text{m}$  quartz/feldspar ratio is highly variable through the core depth.

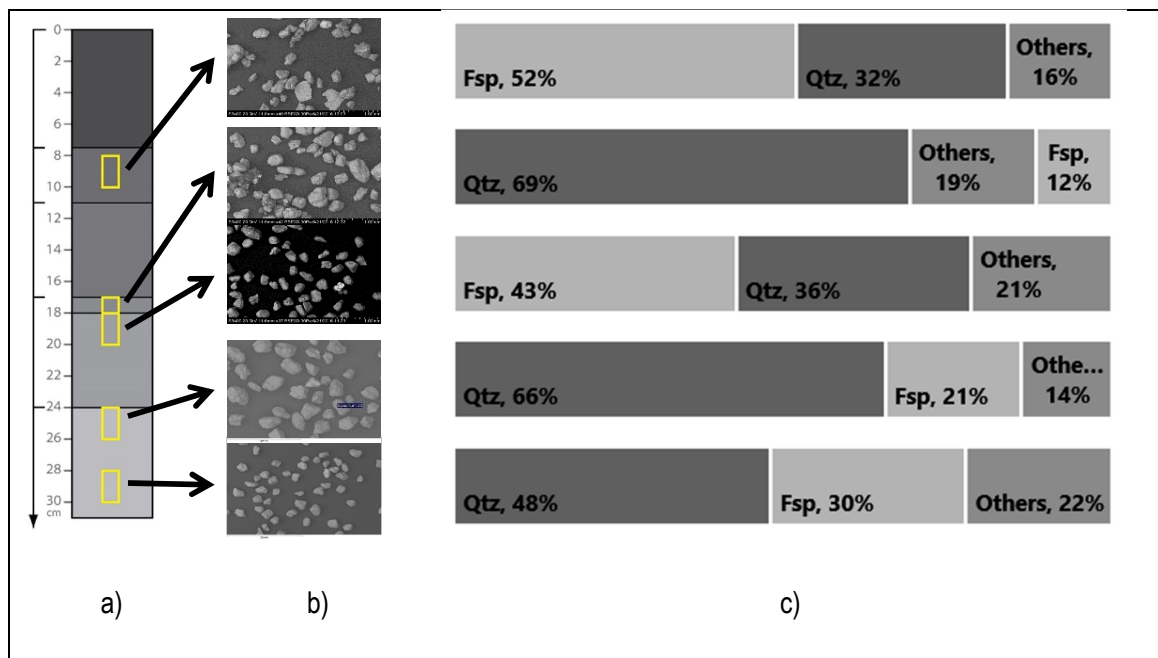


Figure 7-4: a) General stratigraphy of core MR24 based on a simple visual assessment showing six major horizons (0-7 cm, 7-11cm, 11 to 17 cm, a very distinct layer at 17 to 18 cm, 18 to 24 and 24 to 31 cm) overlain by yellow boxes representing sample location. b) SEM imagery of sediment grains, at working distance by magnification (from top to bottom) 11.8mm \*40; 11.8mm \*40; 11.5mm\*42; 11.6\*37c) SEM results (%) for the fraction 250-150 $\mu\text{m}$ . SEM is used as a qualitative tool to detect the presence of additional minerals and debris, residues or contamination of the sample.

### 7.2.1.2 Step Two: Which instruments best measure Nigg Bay's sediment sensitivity?

Three instruments were tested to assess the luminescence signal quantity and quality of the sediment samples.

**SUERC portable reader** (Figure 7-5) stimulates the poly-mineral grain sample discs with an infrared (880 nm) and a blue (470 nm) light emitted from small diodes, 9 in total for each of the stimulation sources. The luminescence is detected through filters (RG780 filters for the IR diodes and CG420 filters for the 470 nm blue diodes) then counted by a single photon counting photomultiplier with the data logged parallelly to a laptop computer. The portable reader can operate in CW mode or pulse mode according to a programmed sequence. CW proxy sequence (see detail in Figure 7-8) which implements the measurements of IRSL and OSL intensity, depletion indices and IRSL/OSL ratios as described in Sanderson & Murphy (2010) was chosen to allow 10 seconds dark count measurements, two IRSL two IRSL measurements of 30 s duration, a second 10 seconds dark count before, two OSL measurements of 30s allowing the monitoring of post-stimulation phosphorescence (PSP) from the sample and a final 10s dark count as depicted in Figure 7-8.

IR signals were evaluated further using a subset of paired aliquots using **PPSL** (pulsed photo stimulated luminescence, Figure 7-6) system, an instrument designed and developed SURRC (Scottish Universities Research and Reactor Centre) to enable effective detection of irradiated foods. The innovative system stimulates sample with an array of Infra-Red (IR) pulsed symmetrically on and off for equal periods and measures Ultraviolet-visible Anti-Stokes Luminescence UV-VIS Anti Stokes luminescence with phase locked photon counting which automatically suppresses background signal (such as dark count). This instrument is used in the international standards method EN13751 for Pulsed PSL Screening of Irradiated Foods and has been adopted commercially in more than 300 laboratories. As shown in the exploratory work of Medlrum (1996) and McKeown (1997) it has exceptional sensitivity for measuring young natural sediments. This suppression of background measurements allows to record luminescence signal with exceptional sensitivity.





Figure 7-5: SUERC portable reader

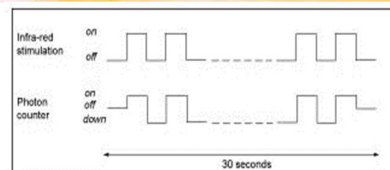


Figure 7-6: PPSL system (top) developed for irradiated foods detection measure IRSL signal; and, diagram (bottom) showing how photons are counted when Infrared are stimulated for 30s.

**Automated Risø TL/OSL system** (TL-DA-20, Figure 7-7) equipped with a  $^{90}\text{Sr}/^{90}\text{Y}$   $\beta$ -source for irradiation, using blue light-emitting diodes with a wavelength of 470nm for stimulation. The Risø sequence procedure aimed to replicate previous stimulations analysis as followed: (1) OSL with red LED diodes for 30 seconds at low temperature of 50 °C (no stimulation for 10s before and after); (2) OSL with blue LED diode for 30s at 125°C (no stimulation for 10s before and after); (3) Thermo Luminescence -TL at standard of 500 °C; (4) Background subtraction; (5) Regenerative dose (BETA  $^{90}\text{Sr}$ ) of the equivalent of 1Gy; (6) Preheat 220 °C for 30s ; (7) repeat 1 ; (8) repeat 2; (9) repeat 3; (10) Background subtraction. A fast decay curve was chosen to calculate net signal (background subtracted).

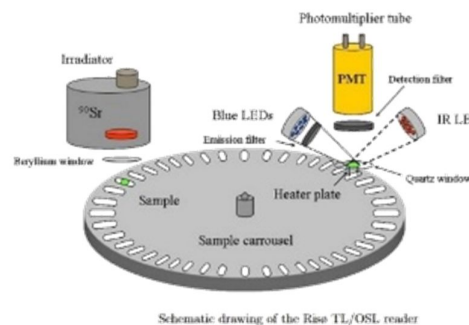
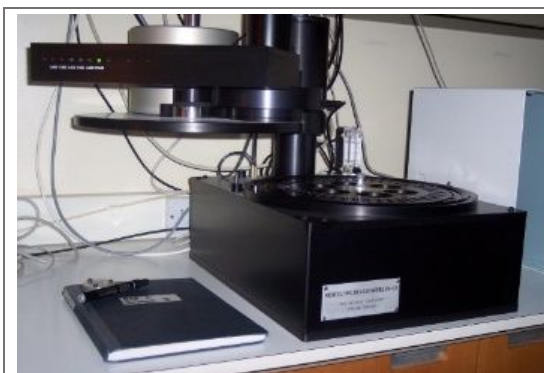


Figure 7-7: Risø DA-20 automatic reader at SUERC (top) with small diagram (bottom) showing how automation of the samples stimulation on the carousel by red and blue LEDs which is then detected through filter to allow photomultiplier to detect light emitted by the samples with in parallel an irradiator source ( $^{90}\text{Sr}$ ) permitting to regenerate luminescence signal.

### 7.2.1.3 Step Three: Which fractions provide a high sensitivity luminescence signal?

**Step three** hypothesises that the evaluation of small calibrated sub-samples on 1 cm discs would alleviate large uncertainties (such as is absence or low signal due to salt, dark organic material covering minerals, etc.) that unprepared and untreated bulk samples commonly used (Sanderson et al., 2007; Sanderson and Murphy, 2010; Muñoz-Salinas et al., 2011; Munyikwa et al., 2011; Munyikwa et al., 2012; King et al., 2014; Bateman et al., 2015; Ghilardi et al., 2015; Stone et al., 2015; Muñoz-Salinas et al., 2017) when profiling with portable OSL measurements can produce. Furthermore, several studies have investigated the influence of grain sizes on radiation dose (the regenerative dose given in laboratory used to reconstruct the environmental dose of the sample) indicating that there is no dependence between the dose rate with 55–250  $\mu\text{m}$  grains unlike smaller fractions ( $<40 \mu\text{m}$ ) which demonstrate clear dependence. This dependency has been attributed to source geometry and mounting support (aluminium or stainless-steel SS discs reported to produce higher backscattering and enhancing the beta dose rate – SS disc itself account from 14 to 16.6% dose rate of the  $\beta$ -source). Finally, fine grains  $< 4 \mu\text{m}$  mounted on aluminium discs have demonstrated little to no dependence (c.2 %) of dose rate to sample mass (Truelsen and Wallinga, 2003; Armitage and Bailey, 2005; Mauz et al., 2005). However, earlier work from P. A. Clark (1994) on Isochron methods for luminescence dating in archaeology investigated the effect of variation of sample mass on radiation ( $\alpha$ ,  $\beta$  and  $\gamma$ ) efficiency of feldspar and quartz, showing a suitable sample mass of fine grains to be dispensed (for 1cm disc  $\sim 2.5 \text{ mg}$  corresponding to  $\sim 12 \text{ mg}$  sample thickness) and if exceeded, the light output of the sample would attenuate as the top layer of the sample emits light (Clark, 1994).

Based on this work, under safe light conditions, core MR24 sediment samples were extracted at 2cm intervals and wet sieved to separate fractions of 500 -250, 250 -150, 150 -90  $\mu\text{m}$  using nylon mesh and settling times. Smaller fraction sizes 90-30  $\mu\text{m}$  and  $<30 \mu\text{m}$  were separated in a static column of deionised water following Stoke's Law and density values following standard scientific data textbooks (CRC Handbook of Chemistry and Physics); and, sediment remained in suspension for more than 40 minutes were labelled and stored in dark. The grains retained by the meshes were decanted in labelled beakers then resuspended in acetone (to reduce settling times compared to water) and check under microscope to assess if the grain sorting was successful. Each grain size fractions were washed using 1M HCl and neutralise using  $\text{NH}_3$  treatment to remove organic and carbonates. As carbonates were low to absent in the samples, each fraction was then washed up to four times in deionised water and up to four times in acetone ( $(\text{CH}_3)_2\text{CO}$ ) to accelerate the drying of the grains. They were dispensed in settling tubes to calculate settling density per fractions. Two aliquots per fractions were chosen to allow an evaluation on the scatter of the signal between samples which were dispensed on 1 cm aluminium discs.

Here it is important to remind that all work presented in this chapter is on polymineral sediment fractions where quartz and feldspars have not been separated as we are first evaluating the potential application of luminescence techniques to Nigg Bay sediment. On average quartz luminescence (stimulated by blue light only) is typically 100 times dimmer than feldspar luminescence (stimulated by infra-red light only) and it is very likely that blue luminescence signal may be emitted by feldspars from alumino-silicates framework which have a wide compositional range (and classed according their main element -calcium, sodium and potassium-). This process has implications when calculating equivalent dose and therefore dating feldspar grains which tend to be difficult due to a phenomenon called anomalous fading (not observed on quartz) characterised by the loss of charge from thermally stable traps (Wintle, 2008; Reimann et al., 2015). Feldspar signal once irradiated is not fading continuously but present thermal instability resulting in an underestimation of feldspar luminescence ages (Clark and Sanderson, 1994; Wintle, 2008). Although not all feldspars exhibit anomalous fading and the rate of fading and luminescence signal may vary from one sample to another (Aitken, 1989; Duller, 2008). However, as explained by Wintle (2008), feldspars may play a role in future dating of young sediments once anomalous fading is overcome as they carry a much greater luminescence signal and higher internal dose. The question of anomalous fading is a huge subject and very contentious. In this research study, anomalous fading was not characterised and no correction applied, but, the procedure has deliberately used low pre-heat temperatures and low- irradiation dose pre-empting such phenomenon. Furthermore, if there is a signal and if it progresses stratigraphically, then clearly what ever part of the system is capable to storing information is managing to do so.

#### 7.2.1.4 Step Four: How to measure signal sensitivity in young saltmarsh sediments?

##### **Step 4 a)** Natural signal

When dispensed, paired aliquots natural luminescence IRSL and OSL signal was measured under safe light conditions and net signal intensities being calculated as followed:

$$\mathbf{Net\ Signal} = \mathbf{Stimulation1} + \mathbf{Stimulation2} - 2 * (\mathbf{Dark\ count1}) - 2 * (\mathbf{Dark\ count2})$$

$$\pm$$

##### **Net Signal error**

$$= \sqrt{\mathbf{Stim.1}^2 + \mathbf{Stim.2}^2 - \mathbf{Dk.cnt.1}^2 - \mathbf{Dk.cnt.2}^2 + \mathbf{Dk.cnt.2}^2 + \mathbf{Dk.cnt.2}^2}$$

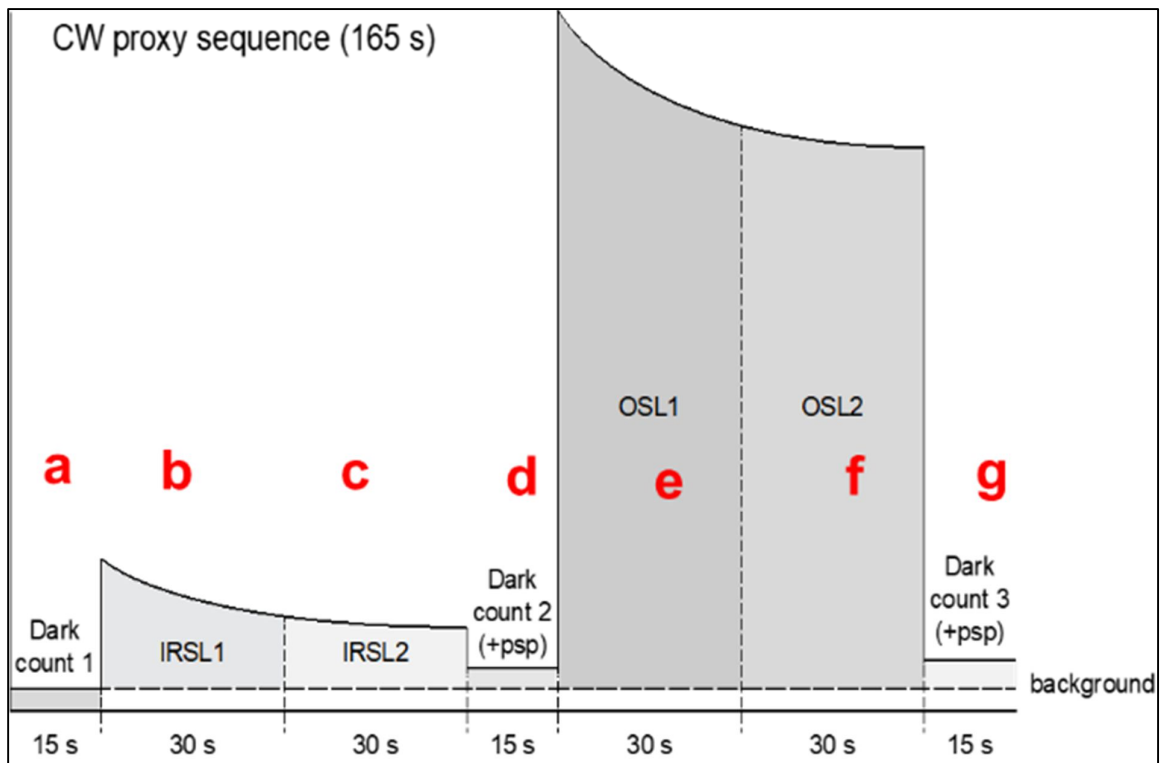
Following Ghilardi et al. (2015) further indices have been deduced from the signal intensity measured with portable reader as described in further detail in Figure 7-8. This methodology allows to deduce reasons of luminescence shifts in core profiling by variation in mineralogy, residuality, photon fluence or diagnosis.

#### **Step 4 a) Bleached signal**

The samples were then bleached (or zeroing, resetting removing all luminescence signal) using a 2\*50\*50 m lightbox built at SUERC laboratory containing four 40W artificial daylight fluorescent tubes coated internally with TiO<sub>2</sub> reflector paint with a measured energy fluences of 7.3 and 7.7 mW.cm<sup>2</sup>. Different length times of bleaching were evaluated between aliquots of the same grain size fraction from 1 h to 24h. The artificial bleached discs were screened and quantified any leftover signal.

#### **Step 4 b) Regenerated signal**

The decision was made to adapt the standard “Single Aliquot Regenerative” (SAR) procedure (for quartz (Murray and Wintle, 2000; Wintle and Murray, 2006) and for feldspar (Wallinga et al., 2000)) which allows to compare the natural signal (NS) with the artificial-regenerated luminescence signals (RS) called equivalent dose (ED) aimed to directly interpolate the palaeodose (which is the total amount of dose absorbed by the mineral since its burial). To avoid overestimating of the signal as artificial irradiation can lead to the trapping of electrons in unstable traps of the mineral crystal lattice which in turn can be released during the optical stimulation. Preheating the samples permits to empty unstable traps. It was chosen to preheat the sample at a low temperature 120±2 °C following suggestions of Sanderson (1988) which is also in line with the more recent work on the dating of young sediment ((Ward et al., 2003; Truelsen and Wallinga, 2003; Madsen and Murray, 2009)). A regenerative dose was then applied by irradiating the 1 cm discs samples with a small dose of 200 mGy (may correspond to an OSL age of approximately 200 years) using an automated ELSEC irradiator equipped with a 1.85 GBq <sup>90</sup>Sr source (dose rate 1.66 Gy.min<sup>-1</sup> at time of the experiment).



IRSL and OSL signal intensities	Signal Depletion indices	IRSL/OSL ratio
$IRSL = b+c-2a-2d \pm \sqrt{(b+c+2a+2d)}$	$IRdep = (b-a-d)/(c-a-d) \pm IRdep * \sqrt{((b+a+d)/(b-a-d))^2 + (c+a+d)/(c-a-d)}$	$IRSL/OSL = (b+c-2a-2d)/(e+f-2d-2g) \pm IRSL/OSL * \sqrt{((b+c+2a+2d)/(b+c-2a-2d))^2 + (e+f+2d+2g)/(e+f-2d-2g)}$
$OSL = e+f-2d-2g \pm \sqrt{e+f+2d+2g}$	$OSLdep = (e-d-g)/(f-d-g) \pm OSLdep * \sqrt{((e+d+g)/(e-d-g))^2 + (f+d+g)/(f-d-g)}$	
<b>Proxy for age, sensitivity, dose rate</b>		<b>May indicate mineralogical variations</b>
	<b>May indicate residuality, colour (photon fluence) or diagenesis variations</b>	

Figure 7-8: Field profiling proxies sequence developed by Prof. D. Sanderson (Ghilardi et al., 2015; Sanderson and Murphy, 2010) for SUERC portable reader and used to measure the luminescence (OSL and IRSL) signal from core MR24 saltmarsh sediments.

#### Step 4 c) Equivalent dose

The equivalent dose ED (in Gy) is the ratio between natural signal and artificially regenerated dose by the radiation dose delivered to the mineral grains in the laboratory can be calculated as follows:

$$ED = \left( \frac{\text{natural signal } NS}{\text{regenerative signal } RS} \right) * \text{Laboratory Dose}$$

Dose-rate (DR in Gy.yr<sup>-1</sup>) is the rate at which ionising energy is delivered from background radiation or more simply the rate at which sediment is exposed to natural radiation which is considered to remain constant during the whole burial span (Aitken, 1998). Dose rate can be determined directly in the field (using radiation dosimeter or a field gamma spectrometer) but the alpha and beta contribution (to radioactivity) coming from the internal content of U, Th and K and the surrounding material. The effective dose rates are evaluated in laboratory by microdosimetric modelling using the measurements and taking account of the water content (using representative sediment samples by spectrum of energy (in keV) of gamma emissions; or thick source alpha counting – TSAC; or GM-beta counting – INAA; or combination of High Resolution Gamma Spectrometry (HRGS) and Thick Source Beta Counting (TSBC; (Sanderson, 1988b)).

Dose rate has not been measured for Nigg Bay saltmarsh site, therefore nominal rates (e.g. 0.5 and 1 Gy.ka<sup>-1</sup>) was applied to evaluate of the signals apparent age following equation:

$$\textit{Apparent Age} = \frac{DE}{DR}$$

## 7.2.2 Sampling strategy summary for preliminary core MR24

Table 7-4 below presents the methodology as described above in section 7.2.1.1 to 7.2.1.4 applied to core MR24 samples.

**Statistics:** All data were logarithmically normalised to enable statistical analysis (comparison testing, statistical significance and relationships). All errors quoted at 1σ. Johnson Transformations (at best fit *p-value* of 0.1) were performed for natural and regenerated signal results as the data contained negative values (Figure F- 1 and Figure F- 2). However, a best fit transformation could not be established for the artificially bleached samples, and so a standard constant for all fraction was added - as it may affect the means but not the variance - following standard formula  $\log_e(Y + a)$  where *a* was found averaging at 600 for this core.



Table 7-3: Preliminary core MR24 sampling strategy. Note1: \* sample number of 22. Note2: year 2016.

			500-250	250-150	150-90	90-30	<30	<30	<30	
<b>Grain size (microns)</b>										
<b>Dispensing Discs (size - cm)</b>			1	1	1	1	1	3	3	<b>Step 1</b>
<b>Aliquots no.</b>			A & B	A & B	A & B	A & B	A & B	C		
<b>Number of Sample no.</b>			30	30	30	28	30	30	15	
<b>Date Dispensed</b>			22 to 23/06	22 to 23/06	12/09	12/09	23 to 25/11	23 to 25/11	30/11	<b>Step 3</b>
<b>Natural signal</b>	Portable reader	OSL & IRSL	23/06	12 to 13/09	13/09	28/11	29/11			<b>Step 4a</b>
	PPSL	IRSL only						30/11		
<b>Bleaching - Light Box</b>			2hrs	1+21hrs	1 + 24hrs	24hrs	24hrs	24hrs		<b>Step 4b</b>
<b>Bleached signal</b>	Portable reader	OSL & IRSL	23/06	13 & 14/09	13 & 15/09	06/12	05/12	05/12		
	PPSL	IRSL only						06/12		
<b>Regenerated signal</b>	Regenerative Dose automated ELSEC 1	200 mGy	23/06	14/09	15/09	06/12			Challenge1: Need of a new irradiation source for sample discs as large as 3 cm. See section 7.4	<b>Step 4c</b>
	Preheat Portable reader	120±2oC OSL & IRSL	17hrs 24/06	17hrs 15/09	17hrs 16/09	17hrs 07/12				
	Regenerative Dose automated ELSEC 1	200 mGy		29/09 *	29/09 *				Large 3 cm sample discs/planchettes cannot be screened in Risø readers.	<b>Step 2</b>
Preheat PPSL	120±2oC IRSL only		17hrs * 30/09*	17hrs 30/09*						
	Regenerative Dose automated ELSEC 1	200 mGy		29/09 *	29/09 *					
	Preheat Automated Risø TL/OSL system	120±2oC 200 mGy & 1 Gy		17hrs* 29/09 *	17hrs* 29/09 *					

### 7.2.3 Exploratory core results and outcomes

The results are presented following the aims of evaluation of this preliminary core:

- Is there a measurable luminescence signal?
- Does this signal increase with depth?

- Can it be enhanced and calibrated?
- Can the results inform the sediment history to complement the short-term and long-term results from previous chapters?

### 7.2.3.1 Blue-OSL (B-OSL) signal

Overall, B-OSL signals for core MR24 samples are presented in table F-1.

#### 7.2.3.1.1 Natural Signal for 1 cm disc samples using portable reader – Step 4a

##### **Signal versus weight**

No significant association was found between sample weights and B-OSL signal per grain fractions (Table F-1 and Figure F-3), except for the grain size 250-150  $\mu\text{m}$  exhibiting a strong positive dependence between sample weight and depth ( $\rho=0.75$ ,  $p < 0.001$ \*\*\*) suggesting a poor aliquot dispensing or presence of brighter and heavier mineral in the lower part of core. This was later confirmed by results (unknown at the time of experiment) from inorganics results presented in Chapter 6 – 6.2.3 showing presence of a carbonate concretion lower in the core (c. 42 cm depth). As described in step four (7.1.1.4), samples have been washed from carbonates, still remain the possibility of different mineral type (of possible different origin) present in this core deposit layer. As all other fractions did not show weight dependence, it was therefore considered unnecessary to adjust photon counts results to their respective weight for this preliminary core.

##### **Signal versus grain size**

Overall B-OSL natural signal for silts ( $<30 \mu\text{m}$ ) is found to be significantly lower ( $F=44.45$ ,  $p < 0.001$ \*\*\*) than all other grain size fractions exhibiting an overall negative photon count signal ( $-91.2 \pm 68.7$ ) suggesting that there is no signal emitted from the quartz or no quartz present in the samples or the instrument is not sensitive enough to measure the signal favouring the latter. Very fine sands (150-90  $\mu\text{m}$ ) and coarse silts (90-30  $\mu\text{m}$ ) demonstrate the highest photon counts at  $1949 \pm 252$  and  $1489 \pm 212$  respectively (Figure 7-9). These results support the hypothesis that different grain size and composition (as presented in 7.1.1.1) change luminescence intensity and in the case of core MR24 bigger quartz and felspar don't have brighter signals.

##### **Signal versus aliquots**

The overall variability between aliquots by grain size is significantly different ( $F=6.94$ ,  $p < 0.001$ \*\*\*) where the greatest disparities are exhibited by the coarser fraction (250-150  $\mu\text{m}$ ) averaging at  $125 \pm 32\%$  difference between aliquots and by the fine silts and clays ( $<30 \mu\text{m}$ ) partly due to the low luminescence sensitivity of the samples. The least disparities were found in the very fine sand (150-90  $\mu\text{m}$ ) with  $23 \pm 6\%$  of overall difference between aliquots and coarse silts (90-30

$\mu\text{m}$ ) with  $25\pm 7\%$  (Figure 7-8). The aliquot differences were not statistically associated with the sample weight differences between aliquots (Table F-3).

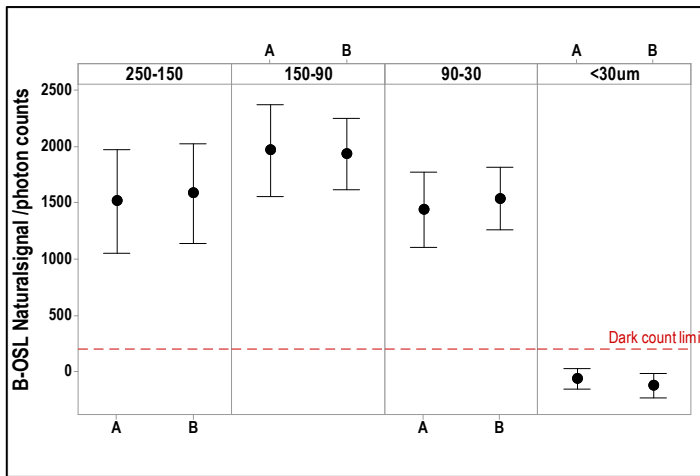


Figure 7-9: Interval plots showing the natural B-OSL net signal between 1 cm disc aliquots per grain size fractions. Error bars are calculated using individual SD. Red dashed line represents the overall dark count limit (average of all screening – fraction and aliquots –) from which emitted luminescence (if any) signal cannot be counted

### Signal versus grain size through core depths

Overall natural B-OSL signal for 90-30  $\mu\text{m}$  fraction exhibited a strong increase with depth ( $\rho=0.61^{***}$ ). A moderately positive correlation with depth can be observed for the coarser grains 250-150  $\mu\text{m}$  ( $\rho=0.55^{***}$ ) whilst very fine sand 150-90  $\mu\text{m}$  and grains  $< 30 \mu\text{m}$  display no correlation with depth (Figure 7-10). Spread of error between aliquots contributes partly to the clear signal increase with depth and its variation demonstrates different depositional sequences even for a shallow depth of 30 cm.

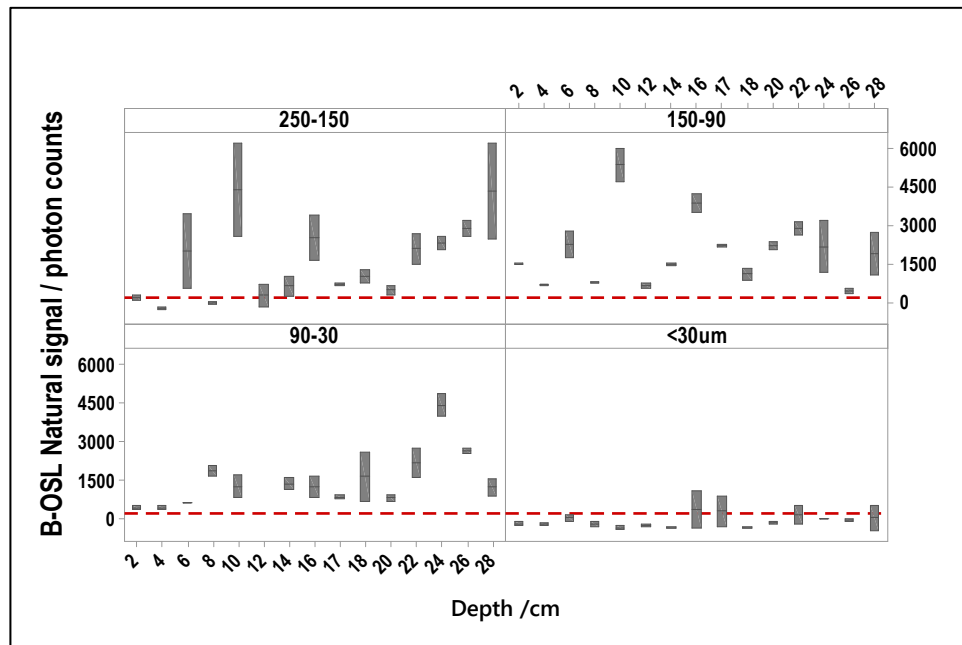


Figure 7-10: Boxplot highlighting the spread of the net B-OSL natural signal between 1cm disc aliquots through the interval depth of the core for the investigated grain size fraction (in  $\mu\text{m}$ ). Red dashed line represents the overall dark count limit.

#### 7.2.3.1.2 Bleaching for 1 cm disc samples using portable reader – Step 4b

After one hour of artificial bleaching, there is an overall  $52 \pm 8$  % decrease of signal which differ between grain size ( $\rho = -0.45^{***}$ ). The rapid artificial bleaching of the B-OSL signal is found to be more efficient for coarser grains (250-150  $\mu\text{m}$ ) where 26 samples out of the 30 decrease sufficiently B-OSL signal ( $118 \pm 13$  %) and four samples increased signal after one hour of artificial with average signal increase of  $99.9 \pm 33$  % (Figure 7-11). The 150-90  $\mu\text{m}$  samples display a more uniform response to the artificial bleaching where most samples (29 out of 30) decreased B-OSL signal of  $50 \pm 5$  % except for one sample which had increased of  $47 \pm 10$  %. However, most (29) samples still emitted a luminescence signal averaging at  $916.3 \pm 162$  photon count. Finally, 22 samples of 90-30  $\mu\text{m}$  grain size decreases their signal of  $45 \pm 4$  % and 6 increased it of  $73 \pm 5$  %. Overall, 27 samples of 90-30  $\mu\text{m}$  grain size still emitted a luminescence signal ( $911.4 \pm 96$  photon count) higher than the instrument dark count (Figure 7-11). The 150-90  $\mu\text{m}$  and 90-30  $\mu\text{m}$  grain size fractions were placed for further 20 and 23 hours respectively, and, both demonstrating a strong positive relationship between the two screenings (150-90  $\mu\text{m}$  displayed  $\rho = 0.72^{***}$  and 90-30  $\mu\text{m}$   $\rho = 0.79^{***}$ ). Overall, the very fine sands fraction (150-90  $\mu\text{m}$ ) bleached a further  $14 \pm 7$  % decreasing the overall signal to  $57 \pm 4$  % with a more uniform response between aliquots ( $F = 0.68$ ,  $p = 0.41$ ) and through depth except for the upper part of the core at depths of 2, 6 and 10 cm (one-ANOVA filtered from these depths provides a non-significant signal result with  $F = 1.68$ ,  $p = 0.19$ ). However, there is still left an overall net B-OSL signal of  $679.2 \pm 104.1$  photon count, higher than the dark count (191.5 photon count). The coarse silts (90-30  $\mu\text{m}$ ) which did not respond well to one-hour bleaching have displayed a further  $33 \pm 5$  % decrease in 23 hours of artificial bleaching. This is an overall reduction of  $50 \pm 6$  % from the natural signal count with a net leftover B-OSL signal of  $530.9 \pm 50.1$  photon count which is still higher than dark count (234.2 photon count). Here, also, there was no significant difference between aliquots ( $F = 1.81$ ,  $p = 0.19$ ) nor depth interval ( $F = 1.56$ ,  $p = 0.21$ ). Although silts ( $< 30$   $\mu\text{m}$ ) presented a negative natural net B-OSL signal ( $-91.2 \pm 68.2$ ) have decreased further their counts to 47 % with very little variability between aliquots ( $F = 2.38$ ,  $p = 0.13$ ) or per depth interval through the core ( $F = 1.18$ ,  $p = 0.38$ ) except at depth of 14 cm.

The experimental work carried out on the four grain size fractions demonstrates the difficulty to bleach the samples to zero using artificial light but also how difficult sediment bleaching is in environment with little light such as tidal salt marshes in northern latitudes. Thermal bleaching (300-350 °C) is known to be far more effective (Aitken and Smith, 1988), however it can also erode and alter luminescence performance such as systematic age over-estimation for young ( $\sim 300$  a) sediment (Truelsen and Wallinga, 2003; Reimann et al., 2015).

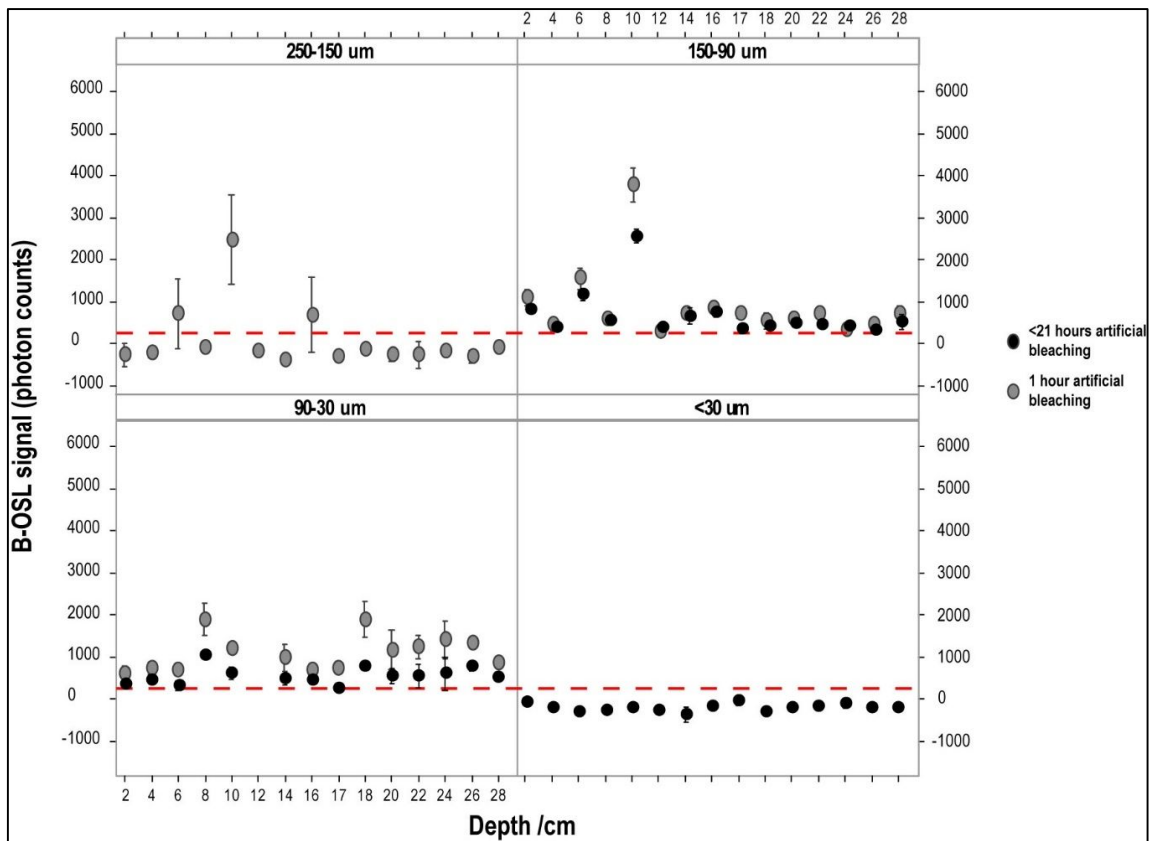


Figure 7-11: B-OSL net signal (photon counts) after one hour (grey) and >21 hours (black) of artificial bleaching for the investigated grain size fractions through depth (cm) dispensed on 1 cm disc. Error bars are one standard error from individual mean. Red dashed line represents the overall dark count limit.

#### 7.2.3.1.3 Regenerated signal for 1 cm disc samples using portable reader – Step 4c

A regenerative dose of 200 mGy (may correspond to an OSL age of approximately 200 years) was applied using the automated ELSEC irradiator (see 7.2.1). For this preliminary core, this allowed to assess: i) if the artificial regenerated signal was equivalent to the natural dose; ii) the signal sensitivity (the more intense signal equating to more sensitive sample signal) and its variability through depth;

Automated signal regeneration (ELSEC) using a low dose of 200 mGy demonstrated an overall 71.7% association to the natural signal ( $r^2$  using that has been logarithmically transformed photon count,  $p < 0.001$  \*\*\*). The natural signal increases by  $2.27 \pm 1.04$  for each regenerated signal increase. However, this linear modelled relationship tends to underestimate the natural dose (Table F-4). Adding fraction size as a predictor does improve slightly the relationship (76.31%  $r^2$  adj.,  $p < 0.001$  \*\*\*) but the residual's homoscedasticity (homogeneity of variances) is still not met. Using fraction size and depth, the overall regression improves to 77.9% ( $r^2$  adj.,  $p < 0.001$  \*\*\*) but the response is not uniform for all fractions across depths and where mainly grain size fraction 150-90  $\mu\text{m}$  has the best fit. Visual assessment of the samples which demonstrated a poor association to

irradiation are the samples which were not completely bleached using artificial light such as depths of 6, 10 and 16 cm for both 250-150 and 150-90  $\mu\text{m}$  fractions (Figure 7-11).

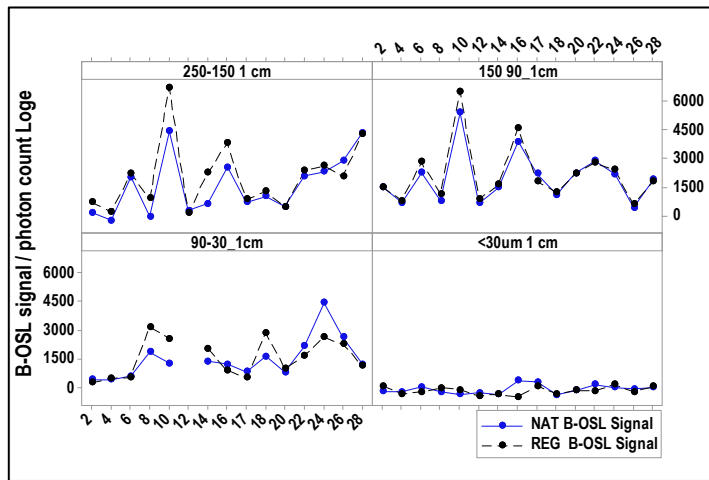


Figure 7-12: Overall regenerated B-OSL signal versus natural B-OSL signal through core depth (cm) per grain fraction for 1 cm disc samples. Association between natural and regenerated signal demonstrated linear regression fit for fractions 250-150  $\mu\text{m}$   $r^2 = 38.1\%$  (Reg.  $B-OSL_{Loge} = 3.56 + 0.55 * \text{Natural } B-OSL_{Loge}$ ); 150-90  $\mu\text{m}$   $r^2 = 91.6\%$  (Reg.  $B-OSL_{Loge} = 0.41 + 0.96 * \text{Natural } B-OSL_{Loge}$ ); 90-30  $\mu\text{m}$   $r^2 = 38.1\%$  (Reg.  $B-OSL_{Loge} = 2.42 + 0.68 * \text{Natural } B-OSL_{Loge}$ ); <30  $\mu\text{m}$   $r^2 = 8.6\%$  (Reg.  $B-OSL_{Loge} = 4.17 + 0.29 * \text{Natural } B-OSL_{Loge}$ ).

#### 7.2.3.1.4 Comparing instruments: B-OSL signal using portable reader versus automatic reader Risø DA-20 for 1 cm disc samples regenerated at 200 mGy

Fractions 150-90 and 90-30  $\mu\text{m}$  samples used in the portable reader had their signal bleached and regenerated following step four procedure (in 7.1.1.4) were measured using Risø automatic reader as per described in step two (in 7.1.1.2). For the same aliquots, the Risø reader demonstrated a  $73 \pm 66\%$  decrease of signal intensity for the 150-90  $\mu\text{m}$  and  $75 \pm 87\%$  decrease for the 90-30  $\mu\text{m}$  (Figure 7-13 and Table 7-3). Large standard deviations further highlight the large variations between signal intensity measurements.

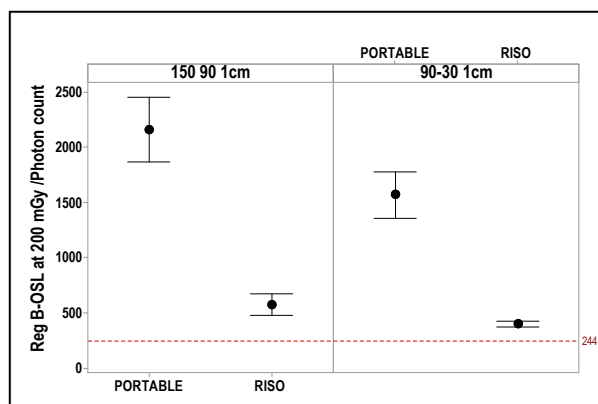


Figure 7-13: Overall regenerated B-OSL signal intensity measured with the portable reader and automated Risø for fractions 150-90  $\mu\text{m}$  and 90-30  $\mu\text{m}$ . Error bars are calculated using individual SD. Red dashed line represents the overall dark count limit.

Comparing Portable Reader and Automated Risø results through depths that for fraction 150-90  $\mu\text{m}$ , two aliquots were measured with a higher (<50%) signal intensity whilst over the half of the samples signals (6) decrease of at least 80%. Ten out of 11 samples with 90-30  $\mu\text{m}$  sediment



decrease signal intensity of at least 50 % using Automated Risø. These differences are therefore not associated with dim signal on top core layers as they are spread across the core depth, but as more instrument differences.

From this exploratory work, the 200 mGy regenerated signals are of 1.2 times greater using the portable reader than Risø for 150-90  $\mu\text{m}$  samples (dispensed on 1 cm discs) and 4.65 times greater for the 90-30  $\mu\text{m}$  samples (1 cm discs) (Figure 7-14).

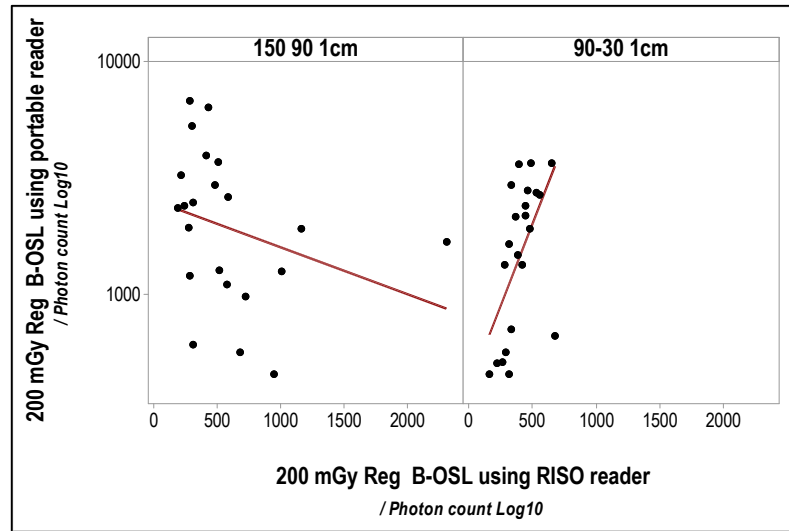


Figure 7-14: 200 mGy regenerated B-OSL signal (in photon count) measured with the portable reader and automated Risø for fractions 150-90  $\mu\text{m}$  and 90-30  $\mu\text{m}$  dispensed on 1 cm disc. Error bars (very small) using individual SD and red dashed line represents the overall dark count limit.

#### 7.2.4 IRSL signal

Overall, IRSL signals for core MR24 samples are presented in table F-5.

##### 7.2.4.1.1 IRSL signal for 1 cm disc samples using Portable Reader

As displayed in Figure 7-15, portable reader IRSL signal was very dim with a photon count lower or within dark count range except for the regenerated signal at 200 mGy for the fraction 90-30  $\mu\text{m}$ . As seen in 7.1.1.1, feldspars are present within the core, which is not explaining this low intensity, therefore, sample subsets were selected to be measured using two other instruments PPSL and automated Risø (7.1.1.2).

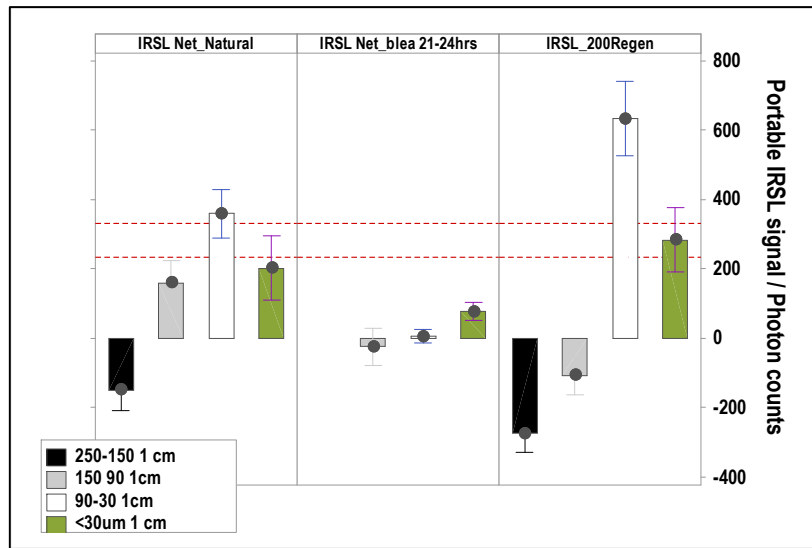


Figure 7-15: Overall Portable Reader IRSL signal (in photon count and error bars using individual SD) for 1 cm disc samples per grain size fractions showing from left to right natural IRSL, bleached and 200 mGy regenerated IRSL signal (in photon counts). Red dashed line representing the dark count range for all measurements.

#### 7.2.4.1.2 ISRL signal: comparing Portable Reader versus automatic reader Risø DA- versus PPSL instruments for 1 cm disc samples regenerated at 200 mGy

Overall significant differences were found between IRSL signal intensity recorded from the three instruments, Portable Reader (PR), PPSL and automated Risø ( $F=23.66, p<0.001$  \*\*\*) demonstrated that the PPSL-IRSL signal was  $6.4\pm 1.7$  times higher than the Risø reader and  $2.4\pm 3.4$  than the portable reader. The large variations in the overall PR-IRSL comes from the different signal intensities between sediment size fractions (150-90 & 90-30  $\mu\text{m}$ ) where 150-90  $\mu\text{m}$  grains had overall a signal lower than dark count compared to 90-30  $\mu\text{m}$  grains which contradict PPSL-IRSL measurements showing nearly twice as much signal intensity for sediment of 150-90  $\mu\text{m}$  than for 90-30  $\mu\text{m}$  grains. Again, these differences display instrument capacity more than sediment signal intensity.

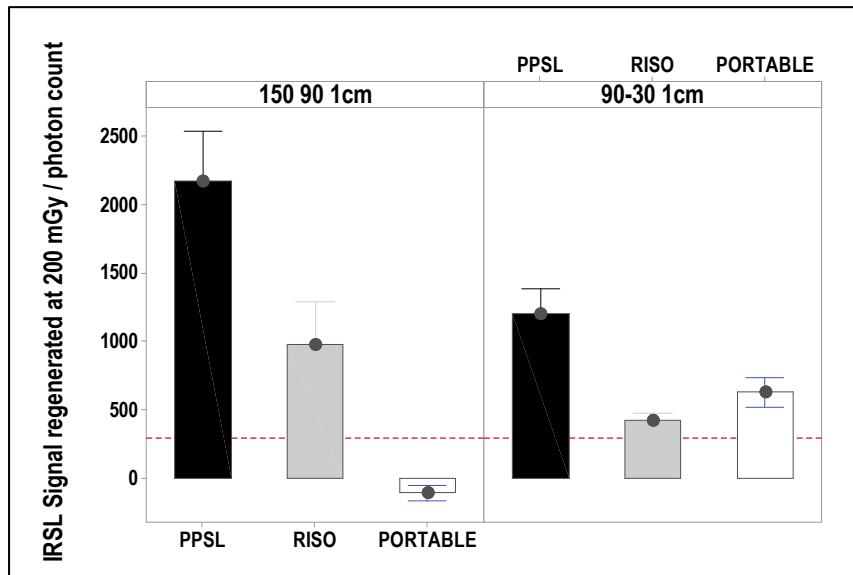


Figure 7-16: Overall signal intensity between Portable Reader (PR), PPSL and automated Risø instruments for fractions 150-90  $\mu\text{m}$  and 90-30  $\mu\text{m}$  dispensed on 1 cm discs. Error bars using individual SD and red dashed line represents the overall dark count limit.

#### 7.2.4.1.3 IRSL signal using PPSL signal for 1 cm disc samples

As PPSL signal versus weight demonstrated for both fractions investigated (and 90-30  $\mu\text{m}$ ) a moderate association with weight ( $\rho=0.53^{**}$  for 150-90  $\mu\text{m}$  and  $\rho=0.49^*$  for 90-30  $\mu\text{m}$ ), it was decided to normalise the signal. Overall the normalised signal is seen to increase significantly with depth for 150-90  $\mu\text{m}$  fractions ( $\rho=0.67^{***}$ ) and moderately for 90-30  $\mu\text{m}$  fractions ( $\rho=0.58^{**}$ ). For both fractions, two intensity peaks are discernible at 14 cm in depth followed by a reversible trend to rise again lower in the core from 24 cm (Figure 7-17).

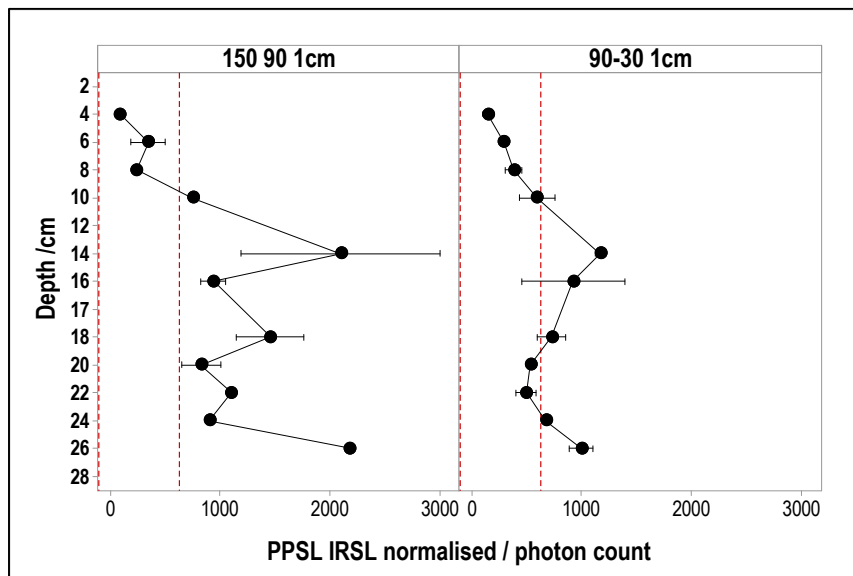


Figure 7-17: Fractions 150-90  $\mu\text{m}$  and 90-30  $\mu\text{m}$  PPSL-IRSL signal (in photon count) normalised to weight through the core depth (cm) dispensed on 1 cm discs. Red dashed line represents the signal range achieved with portable reader for the two fractions. Error bars using individual SD and red dashed line represents the overall dark count limit.

Overall signals up to 3000 photon counts from the very fine sand profiles (using 1 cm samples) and up to 10000 counts from the silt fractions is a clear improvement with PPSL food system compared to portable reader.

### **7.3 Summary: results from the exploratory core**

We asked:

- Is there a measurable luminescence signal?
- Does this signal increase with depth?
- Can it be enhanced and calibrated?
- Can the results inform the sediment history to complement the short-term and long-term results from previous chapters?

Luminescence signal was successfully measured for all fractions except grain size  $< 30 \mu\text{m}$ , suggesting that the amount of very small grains may be too small to emit enough detectable luminescence. The signal also varied in intensity with grain size hinting that different grain sizes held different mineral composition that influenced signal intensity. The experiment highlighted real disparities between the instruments when it came to measure B-OSL and IRSL signal and where one reader was not sufficient: the different portable reader had different sensitivities to IRSL and OSL compared with each other, which would need to be taken into account if results were merged for absolute results or their ratios across data sets gathered on multiple instruments. Therefore, merging the data sets would require a cross calibration or standardisation procedure to account for both instrument to instrument difference and samples to sample differences.

However, relative measurements of profiles using consistent individual instruments across sample series still reflect an overall B-OSL and IRSL signals increase with depth with sequential shifts and distinguished peaks through the 30 cm core inferring that luminescence can be used to trace recent geomorphological processes.

Overall artificial bleaching using light-box was not complete for most of the samples impacting then on the standardisation of signal sensitivity measurement when the luminescence signal is regenerated by irradiation. This is an important result which was also revealed in Meldrum (1996) study and decided to switch thermal zeroing/resetting before calibration (or regeneration). New work from Stone (2019 in preparation) which follows up on study on Namib sand sea (Stone et al., 2015) took account of the very long sequences of bleaching and measurements carried in this study and decided also to use thermal bleaching. However, potential effect on sensitivity change

following thermal bleaching on young (< 50 years old) saltmarsh sediments should be further investigated.

#### **7.4 Developing a new methodology: improving and exploring Nigg bay saltmarsh sediment luminescence signal sensitivity**

Building from this work, to develop and improve a reproducible method to measure B-OSL and IRSL signal for the young (<100yrs) saltmarsh sediment, a new protocol was tested and calibrated on multi-polymineral grain sediment samples for the 8 cores collected at Nigg Bay aiming to:

- 1) design portable instrument to measure simultaneously or at least in tandem with both IRSL and B-OSL signals;
- 2) Increase the size and mass of the sample for the small grain fraction <30 µm;
- 3) A new sample geometry required to upgrade irradiation source and calibrate it;
- 4) Develop new proxies to isolate the newly increased signal sensitivity.

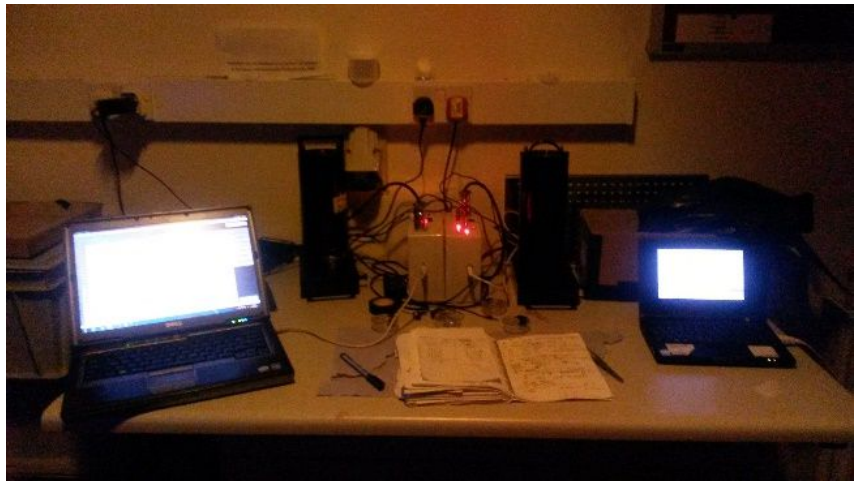
This chapter section will highlight this extension of the exploratory work and present the most relevant results addressing the aims of the study.

##### **7.4.1 Increasing signal sensitivity**

The OSL Portable reader used to explore the luminescence signal is fitted with an infrared (880 nm) and a blue (470 nm) light emitted from small diodes (9 in total). The luminescence is detected through UG11 filters (RG780 filters protecting the IR diodes or RG830 long pass filters, CG420 filters protecting the 470 nm diodes) and synchronically stimulated and counted by the board with data logged to a laptop (Section 7.1.1.3). However, this means that the strong detection band filters needed to protect the standard photomultipliers from the blue-stimulation wavelengths (12 mm UG11 band pass filters) confine the detection band to the near UV luminescence emissions. Whereas the IR stimulation system also emits IRSL within the visible band, which is not detected in the combined IRSL/OSL configuration of the standard portable OSL reader. But if the IR stimulation system is separated, it is possible to configure the instrument with broader detection band filters, which allow the visible components of the IRSL also to be detected (D. Sanderson, personal comments). Therefore, to increase the signal, the instrument was split in two machines that can be operated at the same location by one person, from two laptops simultaneously (Figure 7-18). Thus, permitting to modify to high power for very bright OSL with 3 ports of 890 nm and an IR fitted with a combination of BG39 filters and higher diode powers on 6 ports.



a)



b)

Figure 7-18: a) super bright blue diode newly fitted for an exclusively B-OSL portable reader.; b) simultaneous working system to record samples aliquots on two IRSL (left) and B-OSL (right) portable reader.

IRSL measurements were successfully increased as depicted in Figure 7-19. Two cores collected within the managed realignment MR salt marsh, MR24 (as described in exploratory core) and MR16 c.30 m NE in landward direction are presented here for comparison. It highlights the decrease of variability between aliquots (error bars) and clear increase in photon count from an average  $116 \pm 94$  for MR24 to  $49479 \pm 11580$  for MR16 (c.430 times higher!).

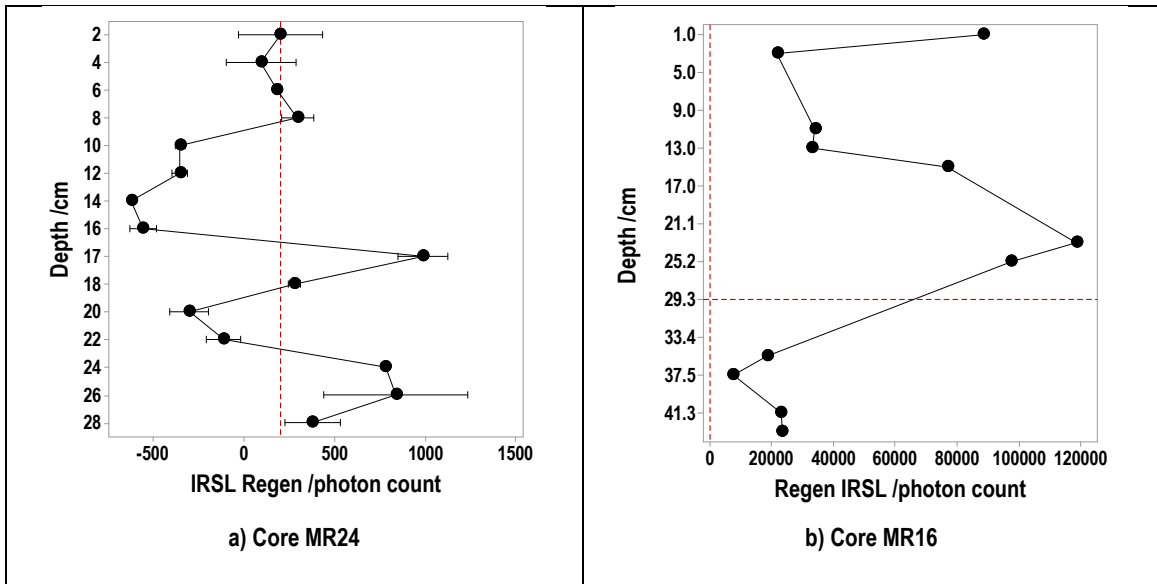


Figure 7-19: a) exploratory core MR24 using 3 cm discs aliquots showing 200 mGy regenerated IRSL signal (photon count) with large SD (error bars) measured with original portable reader compared to b) 200 mGy regenerated IRSL signal for MR16 aliquots (also 3 cm discs) located c.30 m in NE direction from MR24 (see Figure 7-3) measured using the "special" double IR version of the portable OSL reader which we made (using thin BG39 filters and high power IR diode arrays). Note1: the two core depth differences & red line on y-axis of MR16 at approximate base of core MR24.

Note2: the extremely high signal intensity showing dark count at 200 photon count. Note3: red dashed line on x-axis represents the overall dark count limit at 200 photon count calculated for core MR24.



## 7.4.2 Increasing the sample size: from 1 cm aluminium discs to 3cm aluminium discs

### Expanding work from preliminary core MR 24

Considering the dim B-OSL results from 1 cm disc <30  $\mu\text{m}$  fraction, it was decided to take the experiment further and dispense the same silt fraction on 3 cm discs. Overall, the observed natural signal was  $40.6 \pm 6.2$  times higher on the 3 cm aliquots than the 1 cm aliquots ( $T=6.38$ ,  $DF=58$ ,  $p < 0.001^{***}$ ) with no statistically significant difference between aliquots ( $T=0.17$ ,  $DF=28$ ,  $p=0.87$ ) (Figure 7-20). The natural signal is seen to increase moderately with depth ( $\rho=0.42^*$ ), however, the B-OSL signal results clearly displayed three clusters of signal level from 2 to 8 cm, 10 to 16 and 17 to 28, thus exhibiting with mixed trends (Appendix F -Figure F-5).

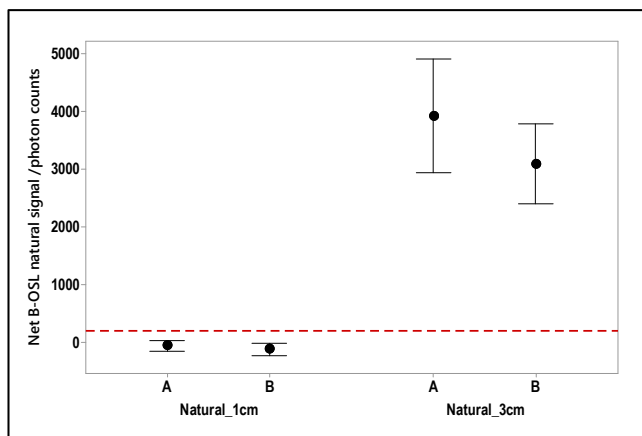


Figure 7-20: Net B-OSL natural signal for grains < 30  $\mu\text{m}$  (photon counts) dispensed on 1cm and 3 cm disc per aliquots A & B measured with same portable instrument (core MR24). Error bars are one standard error from individual mean. Red dashed line represents the overall dark count limit (average of all screening - fraction and aliquots -) from which emitted luminescence (if any) signal is considered unsatisfactory or/and insufficient or/and even false

### New Protocol and new lab system: How to deal with eight sedimentary cores?

All working procedures were executed in subdued light, 362 samples were taken at 2 cm intervals for 6 cores and at 5 cm interval for 2 cores (A13 and MR36) out of the 8 cores presented in Figure 7-31 (also in Chapter 6 - Figure 6-3 and 6-4). The samples were separated to a <30 $\mu\text{m}$  sandy-silt fraction using nylon mesh, washed in 1M HCl and N4H3 and settling density calculates as per described in step four (7.1.1.4). Under the fume cupboard, beakers were then placed in trays that fitted in a matrix of 5\*10 allowing a large number of samples to be dealt with the same amount of time. Two aliquots per fractions were then dispensed on 3cm aluminium planchettes instead of the traditional 1cm aluminium disc allowing to increase the area for more sensitivity. This require further adjustments to the traditional methods to allow the sediment to be uniformly deposited on the planchette in custom made glass jars using a volumetric pipette (Figure 7-21). Developing a standardised and reproducible methodology allowed to reduce error and bias between samples.



Figure 7-21: Custom made glass jars (left) by Robert McLeod and Calum Prentice in the SUERC glassblowing workshop for making these used to receive pipetted  $< 30 \mu\text{m}$  grain in acetone and dispense on 3cm aluminium planchettes.

### 7.4.3 Calibrating procedure

A calibrated procedure was then established to allow the screening of B-OSL & IRSL signals for the natural, artificially bleached (between 16 - 24hrs) and regenerated signal. As the regenerative dose of 200 mGy given to the preliminary core samples was overall satisfactory, it was decided to irradiate samples with the same dose and, for a limited number ( $n=169$ ) of samples, a further 1 Gy (beta) dose and this followed by 16 hours pre-heated at  $120^\circ\text{C}$  before signal measurements.

As automated irradiation is not possible on 3 cm planchettes, a manual Strontium-90 source was adapted by fitting 9 mm aluminium ring with  $5 \mu$  polyester metallic film in the irradiator; thus, increasing the height of  $^{90}\text{Sr}$  source to a total distance of 75.7 mm and subsequently enabling irradiation of a larger 3 cm sample size as presented in scaled drawing - Figure 7-22.

The calibration of the new manual source was carried out using a sample of Oligocene coastal dune quartz sand from the Fontainebleau sand formation (France) (used in Luminescence calibration work in several studies such as Schmidt et al., 2018) on aluminium and stainless steel discs for fine and coarse grains using Risø I and II and ELSEC I and II instruments (results in Table F-4). The calibration provided a dose rate of  $0.206 \pm 0.003 \text{ Gy} \cdot \text{min}^{-1}$  for aluminium discs (corrected for decay factor for 7<sup>th</sup> July 2018 – last consulted). This meant that each 3 cm planchette was manually placed in the irradiator for 59.03 seconds to receive a beta dose of 200 mGy.

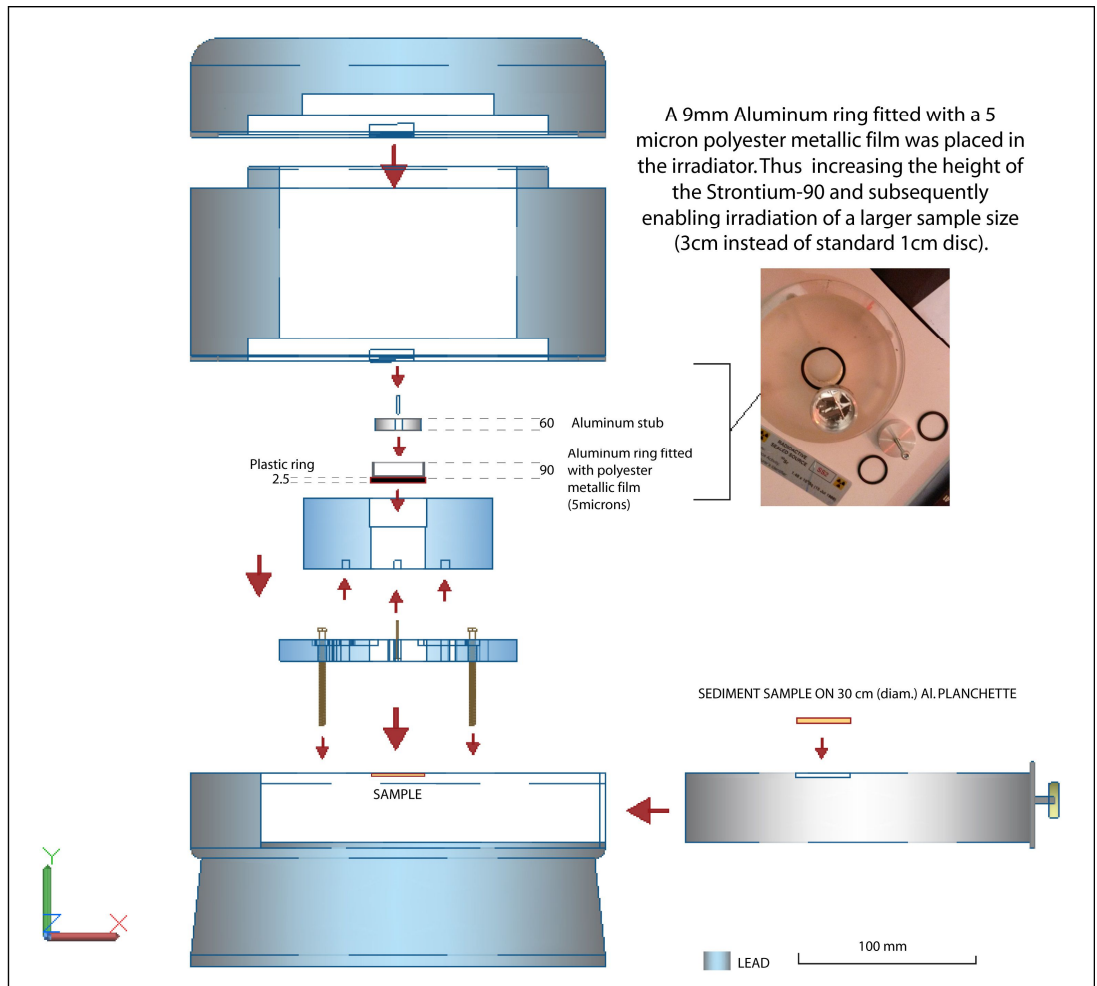


Figure 7-22: Diagram of new  $^{90}\text{Sr}$  Source irradiator showing the fitting of the aluminium ring and stub (red arrow for assemblage) allowing to raise in height the source position and accommodate large irradiation geometry. Samples are placed in a drawer (right on figure) and then pushed in the irradiator ready to receive a beta dose.

#### 7.4.4 New proxies

Light levels of suspended grains in estuarine environment have been found to be reduced by three orders of magnitude in the upper 80cm of the water column (Richardson, 2001) and at 1.5 m water depth wavelength shorter than 500 nm and longer than 750 nm are reduced to a negligible level (Sanderson et al., 2007). Therefore to improve the quality of the signal screening, new proxies have been investigated to isolate the strongest, fastest and brightest part of the signal as schematised in Figure 7-23 and were incorporated for each sediment sample calculation.

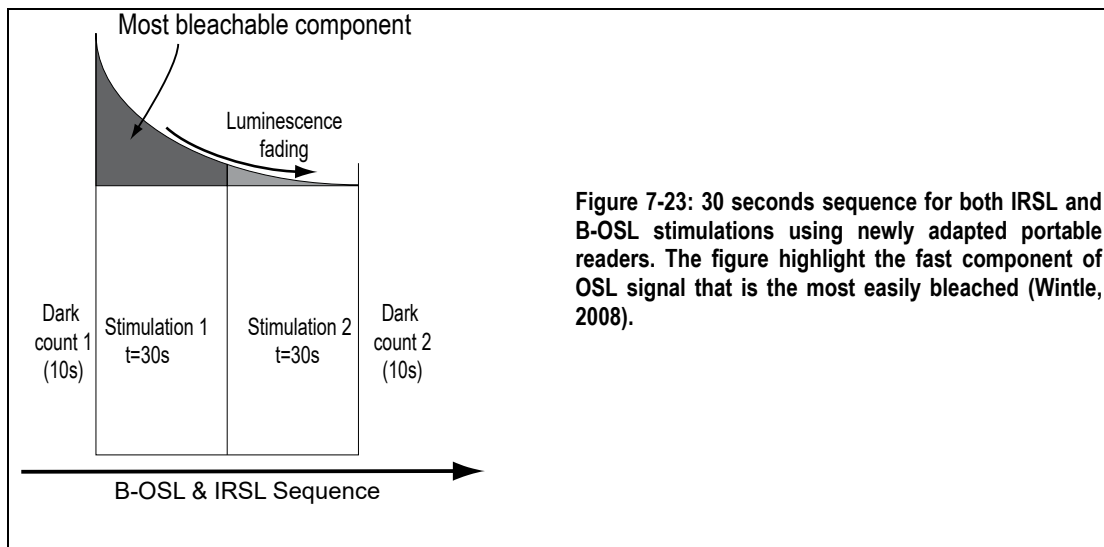


Figure 7-23: 30 seconds sequence for both IRSL and B-OSL stimulations using newly adapted portable readers. The figure highlight the fast component of OSL signal that is the most easily bleached (Wintle, 2008).

Proxies were then set up to address questions improving signal sensitivity and its implication as a process tracer:

- How much & fast do signals deplete?

One proxy presented in step four (7.1.1.4 - Figure 7-8) and used for exploratory core MR24, depletion indices has been kept in this methodology deemed important to investigate sediment/sample mineralogical variation and diagenesis . It is defined as:

$$\text{Depletion indices} = \frac{\text{stimulation1}}{\text{stimulation2}}$$

- How luminescent are the grains?

By deducting the signal background, net signal (see also 7.1.1.4 - Figure 7-8) as defined in equation below provides a net signal (photon count) representing the amount of luminescence detected :

$$\text{Net signal} = \sum \frac{\text{stimulation1} + \text{stimulation2} - \text{scaled background}((\text{darkcount1} + \text{darkcount2})/2)}$$

- How sensitive are the grains?

The sensitivity is the amount of luminescence generated per unit of radiation dose. So, the response to radiation (200 mGy and 1 Gy) allows looking at the variation sensitivity from sample to sample through the core depth. This sensitivity signal (Photon counts per Gy) will depend on how well

bleached the grains were. Therefore, proxies have been defined to consider each sample degree of bleaching when calculating the sensitivity signal.

- How easily bleached are the grains?

To target and isolate the signal sensitivity Section 7.2.1 and 7.2.2 presented the two treatments given to all samples (artificial bleaching of the grains in light box and a known dose was given), therefore the residuals (equivalent dose) from the natural and regenerated signal (bleached + dose) enable us to quantify the bleachability of the samples which can be formulated as such:

$$\mathbf{Equivalent\ Dose\ 1} = \left( \frac{\text{Net natural signal}}{\text{Net Regenerative signal}} \right) * \text{Dose given (in Gy)}$$

However, results on the artificial bleaching presented in 7.1.2.2 have shown that grains did not bleach well and this despite changing the exposure time. Two methods were then experimented with to counteract this difficulty:

$$\mathbf{ED2} = \left( \frac{\text{Net signal}}{\text{Net Regenerative signal} - \text{Net Bleached signal}} \right) * \text{Dose given (in Gy)}$$

By using the most bleachable component of the signal (the first 30s of light stimulation see Figure 7-22), it was assumed that only the OSL contribution from the fast component should be included in the integrated signal. This methodology has been used for OSL dating using quartz as a way to measure the light-sensitive traps by optical stimulation in which the power is increased from zero to the maximum value of the device (continuous wave -CW- OSL) instead of constant power (linear modulated -LM- OSL) resulting in the characterisation of fast and medium OSL components in quartz which can be mathematically separated (Wintle, 2008). By using a portable reader, it is possible to apply a similar calculation using the first and second optical stimulation. The front end (stimulation 1 is the fast component, the first 30s of light stimulation, as depicted Figure 7-23) can be calculated by subtracting the first stimulation from the second as such:

$$\begin{aligned} \mathbf{FrontEnd\ Equivalent\ Dose - FED\ 1} \\ = \left( \frac{\text{Natural signal stimulation1} - \text{Natural signal stimulation2}}{\text{Regenerative Stim. 1} - \text{Net Bleached signal Stim. 2}} \right) \\ * \text{Dose given (in Gy)} \end{aligned}$$

## Proxies results

Relationships between OSL/IRSL for each method (ED1, FED1 and ED2) are summarised in table 7-5 demonstrating poor association between IRSL and OSL using ED2 method.

**Table 7-4: Correlation (Spearman's rho and significance values as <math><0.001^{\*\*\*}</math>, <math><0.01^{\*\*}</math> and <math><0.05^{\*}</math>) between IRSL and OSL signal using three proxy methods, ED1, FED1 and ED2 for 3 cm discs aliquots.**

	IRSL ED1	IRSL ED2	IRSL FED1
OSL ED1	$\rho = 0.841^{***}$		
OSL ED2		$\rho = -0.05$	
OSL FED1			$\rho = 0.84^{***}$

It was first thought that these relationship variations may be explained by differences between natural IRSL and B-OSL signals, or artificial signals or regenerated signal at 200 mGy; however they all demonstrated very strong correlations (respectively  $\rho = 0.93^{***}$ ;  $\rho = 0.90^{***}$ ;  $\rho = 0.93^{***}$ ). By plotting these relationships, the results draw attention to clear differences between the cores where core A15 signals (purple triangles) are clearly underestimated when regenerated at 200 mGy as depicted on Figure 7-24 which was further confirmed by plotting all stepped OSL measurements (natural, bleached, regenerated at 200 mGy and at 1 Gy see in Appendix F: Figures F-6 and F-7) showing that a 1 Gy regenerative dose was a better fit reducing the large scatter between IRSL and B-OSL signals (Figure 7-24b) suggesting that core A15 contain old sediment material or unbleached residuals.

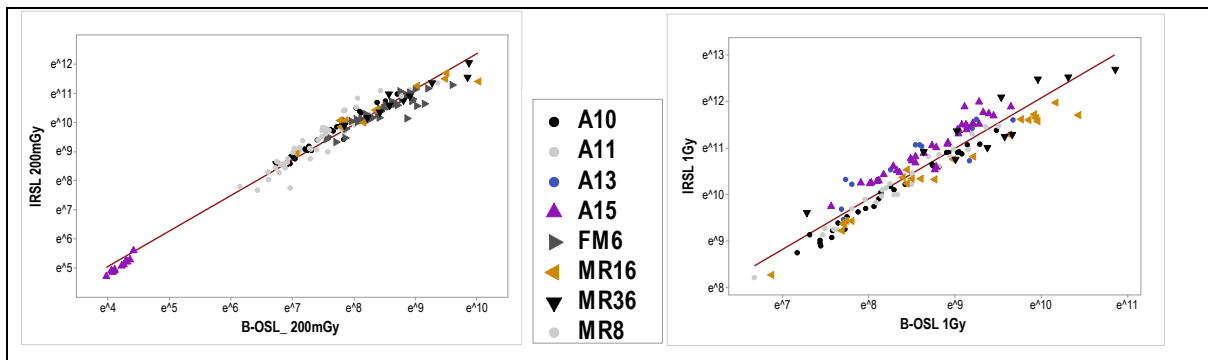


**Figure 7-24: Relationship between IRSL (x-axis) and B-OSL (y-axis) (in photon count logarithmically transformed) for a) regenerated signal at 200 mGy and b) regenerated signal at 1 Gy. All sediments <math><30\ \mu\text{m}</math> dispensed on 3 cm discs.**

Overall standard equivalent dose (ED1) did not provide the expected variation in sensitivity between results for this young saltmarsh sediments compared to the results provided by front-end equivalent dose (FED1) as clearly depicted in Figure 7-25. The results draw attention once more to the extremely high signal sensitivity of core A15, located on the SW cliff edge of ANK salt marsh. This may be explained by its close proximity to the sea front and experiencing strongest tidal forcings where sediment arrives rapidly twice per day and not allowing the material to be



bleached sufficiently and still carrying residuals signal. This is confirmed when applying FED1 proxy to the 200 mGy regenerated signal enabling to remove the slow component of the signal that is not bleached rapidly and clear the inherited luminescence signal as shown in Figure 7-26 where there is less scatter from sediment samples.

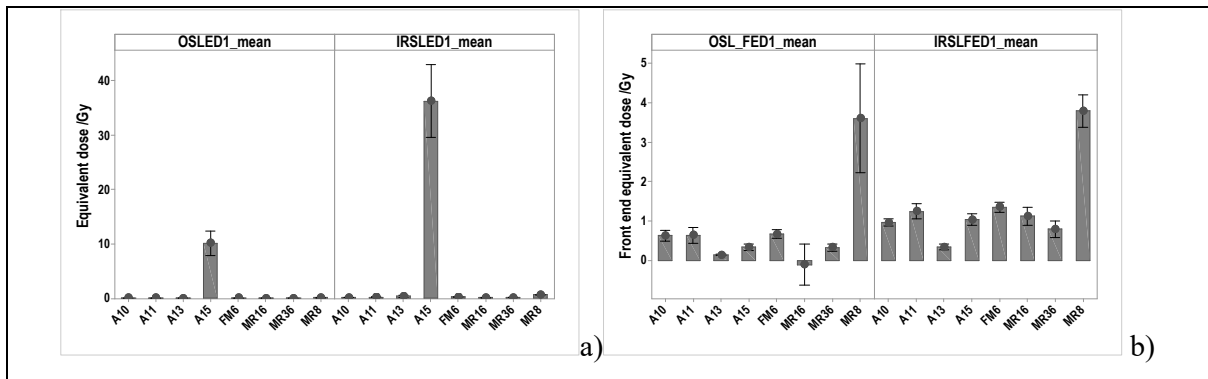


Figure 7-25: (left) a) overall signal sensitivity using ED1 and (right) b) using FED1 for all cores collected along the two transects crossing the saltmarshes. Note: the drawing size is deliberately left quite small as to allow a simple visual assessment between the residuals (in Gy).

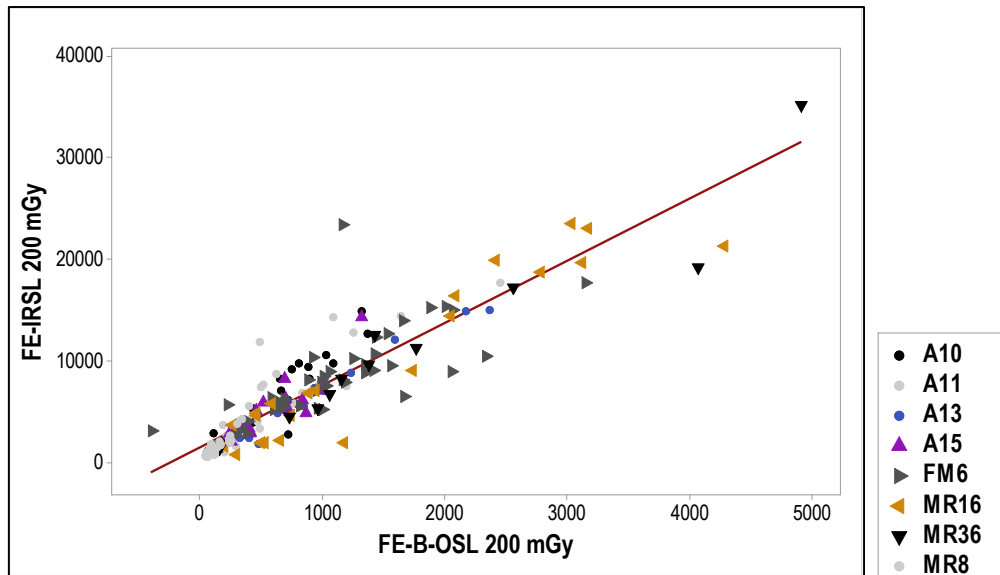


Figure 7-26: Relationship between FE-IRSL and FE-B-OSL where only the fastest component of the signal is kept the front end photon count (stimulation 1 – stimulation 2 or the fastest component) signal of the same regenerated signal at 200 mGy. All sediments < 30  $\mu$ m dispensed on 3 cm discs.

The findings of this study provide strong support for the use of OSL techniques as a process tracer in saltmarsh systems. The results demonstrate that the effectiveness of sediment bleaching can vary within a single saltmarsh system, as well as across different tidal settings (pioneer to high marsh). The technique enables to trace valuable environmental information such as sediment settling on the marsh surface. Furthermore, the application of proxy such as FED1 and ED1 allows to evaluate an approximate age more accurately for the sediments within the core. As it was noted in 7.2.1.3, samples are from mixed minerals (quartz and feldspars) and most of the luminescence signal may come from the alumino-silicate framework of feldspars having some implications to

luminescence dating. Although dose rates have not been explicitly determined at Nigg Bay, we could assume a  $1 \text{ mGy.yr}^{-1}$  to appreciate the differences between the procedures. If we would use B-OSL ED1 for Core A15, sediment at just 2 cm below the surface would have an apparent age of c.160 years, and, at the base of the core (73 cm depth) c.1098 years. This overestimation of the equivalent dose is demonstrated when using ED1 with IRSL signal showing that the upper core sediment at 2 cm would be of an age of c.345 years old and base of the core at 73 cm of c.5121 years. However, FED1 provide more sensible ages and where IRSL signal may be closer to the expected time range for this core A15 sedimentation on this particularly dynamic area of the marsh. B-OSL FED1 at top of core (2 cm) provides an age of c.4 years and c.12 years if using IRSL FED1, and, at the base of the core (50 cm on signal peak through depth) present an age of 47 years for B-OSL FED1 and 98 years old with IRSL FED1 (see graph Figure 7-27 that compares the two methodologies).

Therefore, ED1 as illustrated with core A15 clearly provides dates much older than the expected time range, and thus indicating that the signals are carrying residuals, whose magnitudes carry geomorphological process rather than chronometric signals as it was hypothesised in the introduction. On the other hand, the far smaller FED1 proxy provides dates closer to the range implying a combination of process and chronometric information.

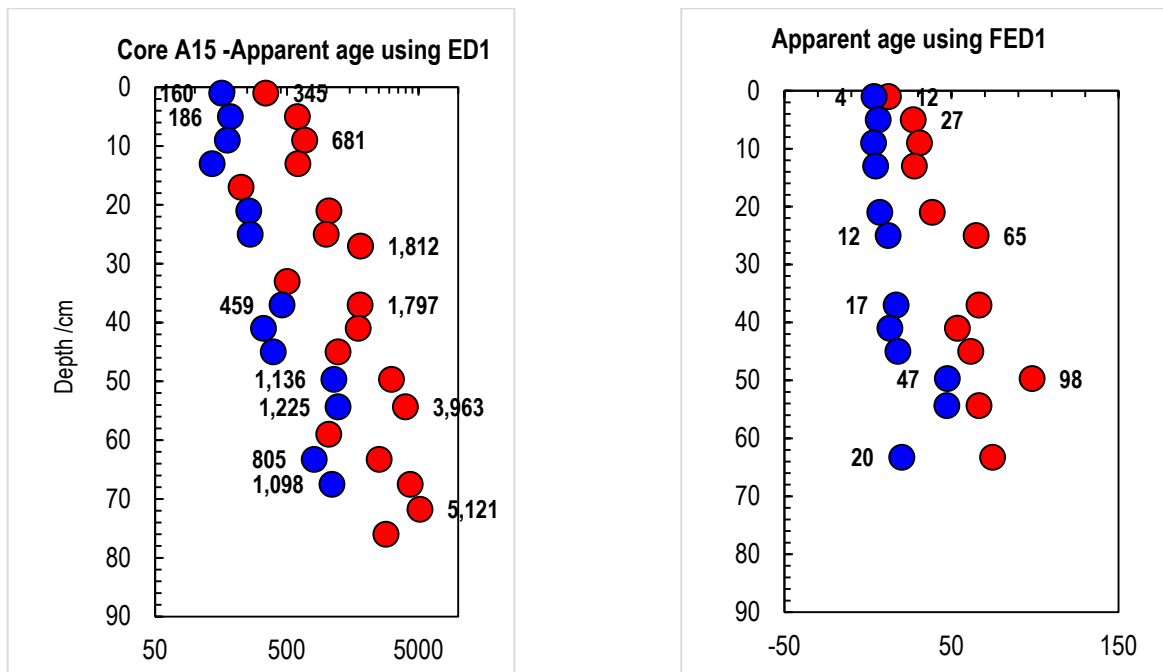


Figure 7-27: Left graph: IRSL (red) and B-OSL (blue) ED1 through the core depth (y-axis) and apparent age value ( $\text{Log}_{10}$  for illustration on x-axis) with calculated apparent age value (in years) at each luminescence peak at a putative dose rate of  $1 \text{ mGy.yr}^{-1}$ . Right graph: IRSL (red) and B-OSL (blue) FED1 through core depth depth (y-axis) and apparent age value (x-axis) with calculated apparent age value (in years) at each luminescence peak at a putative dose rate of  $1 \text{ mGy.yr}^{-1}$ .

The implications of these results clearly show that:

- The slower decaying parts of the signal have not been zeroed at the time of deposition;
- The B-OSL signal is better bleached than the IRSL signal, or is unstable; and,
- There is no sign that the IRSL signal show a pattern dominated by anomalous fading (otherwise signals would not progress with depth).

Front-end proxy was then favoured and kept for analysis providing an overall good agreement ( $\rho=0.84^{***}$ ) between front-end B-OSL equivalent dose and front-end IRSL equivalent dose for all core recorded (Figure 7-28). This association was stronger on the cores collected on the natural salt marsh ANK ( $\rho=0.78^{***}$ ) than on the core collected along the transect crossing MR and FM ( $\rho=0.86^{***}$ ). These results also highlight the successful standardisation of the new methodology.

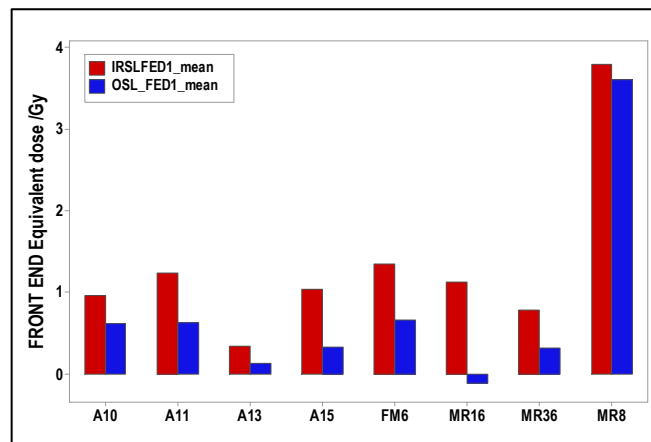


Figure 7-28: Overall front-end equivalent dose for IRSL (red) and B-OSL (blue) signals for all cores collected along transects crossing FM/MR and ANK salt marshes as depicted on Figure 7-3.

## 7.5 Direct implications of the new methodology: tracing geomorphic processes.

The new methodology's development has already demonstrated the ability to infer both geomorphological processes and chronometric information from luminescence signals. In what ways can Optically Stimulated Luminescence (OSL) contribute to the investigation of salt marshes? Can Optically Stimulated Luminescence (OSL) provide insights into the sedimentation processes discussed in previous chapters, which exhibit significant spatial and temporal variability? Specifically, can OSL help identify relationships between sedimentation and factors such as aboveground zonation and hydrodynamics (e.g., distance to High Water Mark and slope)? Additionally, can OSL be used to infer the potential influences of belowground soil and sediment properties (e.g., dry bulk density, organic matter, sediment size) on overall sediment accumulation, leading to the elevation rise of saltmarsh surfaces?

## 7.5.1 Luminescence residuals or signal sensitivity versus organic and inorganic variables

### Aboveground processes

Overall luminescence signal (B-OSL and IRSL) sensitivity was significantly different per saltmarsh zones ( $F=4.4$ ,  $p<0.01^{**}$ ) displaying a strong signal increase in landward direction certainly more pronounced from cores collected on FM and MR ( $F=17.29$ ,  $p<0.001^{**}$ ) compared to ANK partly due to core A15 as discussed above (ANOVA without A15:  $F=7.52$ ,  $p<0.001^{***}$ ).

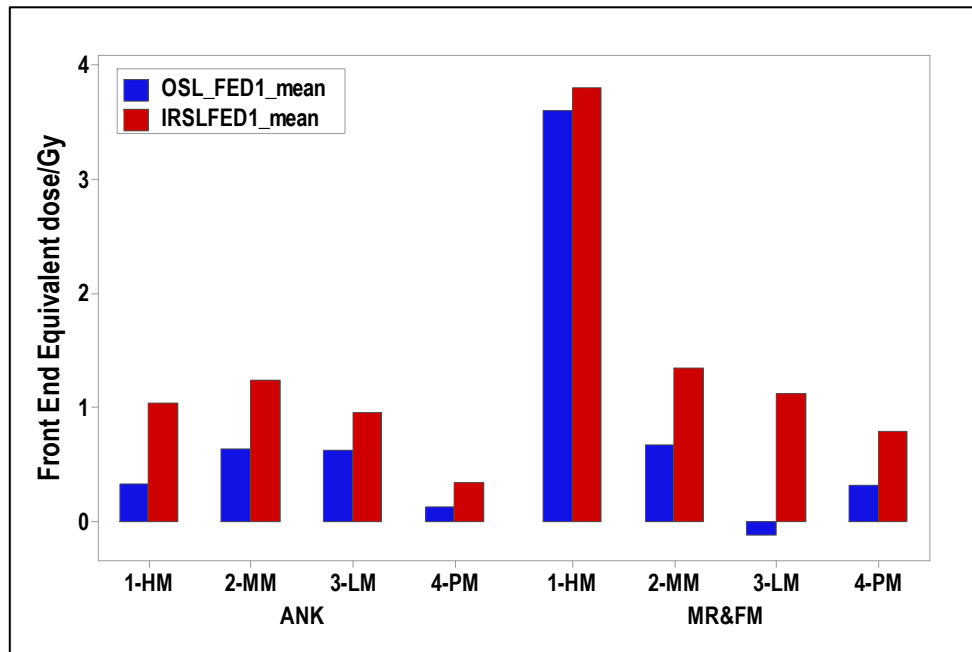


Figure 7-29: Overall B-OSL and IRSL signal sensitivity across the saltmarsh zones for the transects crossing ANK and crossing FM/MR salt marshes.

This association with zonation is in good agreement with McKeown (1997) final year project at Strathclyde university which followed work from David Meldrum (1996) on sediment dating of samples from Sellafield using PPSL instrument. McKeown used three cores located at back (1-HM), middle (2-MM) and front (3-LM) of Caerlaverock salt marsh to measure luminescence alongside gamma spectrometry and identify the  $^{137}\text{Cs}$  and  $^{241}\text{Am}$  activity profiles. Activity peaks of  $^{137}\text{Cs}$  and  $^{241}\text{Am}$  found at depths reflected the sedimentation rates of the three positions on the Caerlaverock salt marsh.

### Belowground processes

Overall luminescence (IRSL and B-OSL) residuals for the cores collected on the modern MR and FM salt marshes were significantly correlated to the organic and inorganic content measured in the same cores and presented in chapter 6 (see plots in E-4 and E-5). Compared to OSL signal, IRSL was more sensitive to organic matter ( $\rho=-0.33$ ,  $p<0.001^{***}$ ), inorganic content ( $\rho=-0.30$ ,

$p < 0.001$ \*\*\*), water content ( $\rho = -0.56$ ,  $p < 0.001$ \*\*\*), and with bulk density ( $\rho = 0.59$ ,  $p < 0.001$ \*\*\*) measurements suggesting that when autocompaction (natural dry bulk density) increase luminescence signal increases too as depicted in Figure 7-30. The IRSL sensitivity is also clearly clustered in saltmarsh zones.

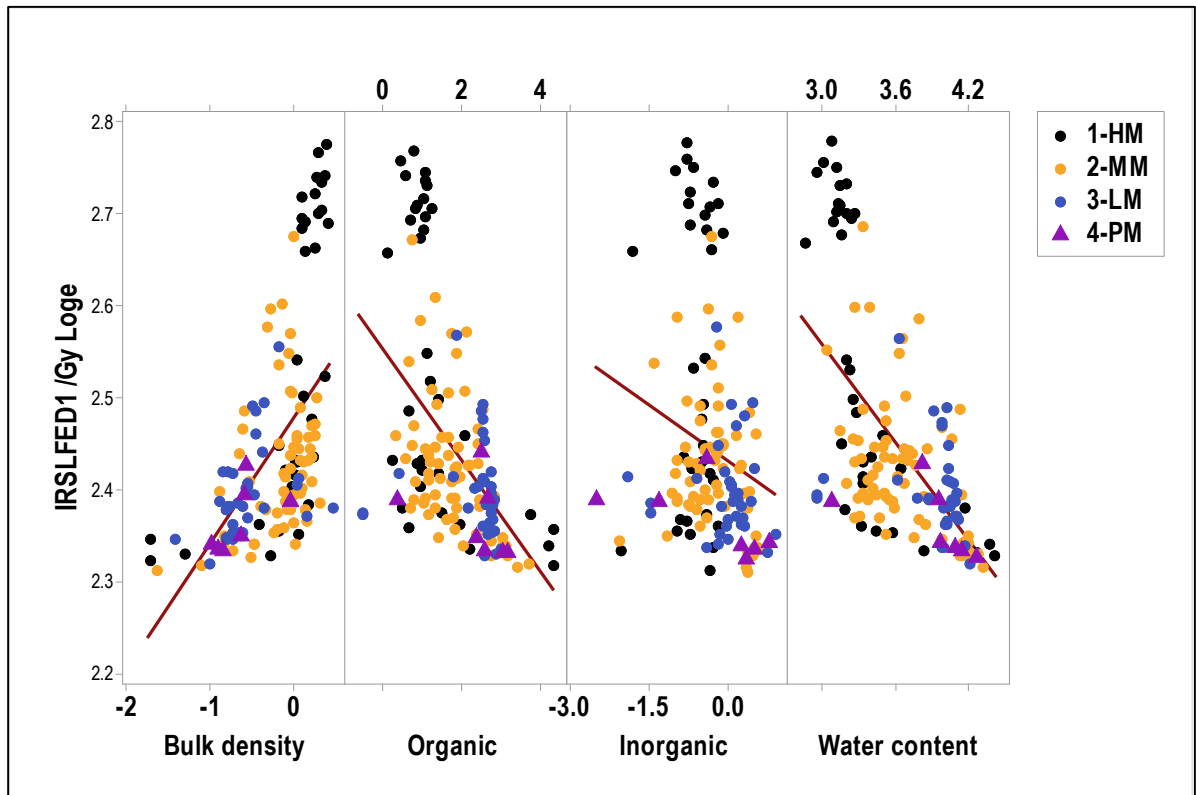


Figure 7-30: IRSL signal sensitivity ( $/\text{Gy } \text{Loge}$ ) versus Dry Bulk Density ( $\text{g}\cdot\text{cm}^{-3}\text{Loge}$ ), Organic matter ( $\%\text{Loge}$ ), inorganic content ( $\%\text{Loge}$ ) and water content ( $\%\text{Loge}$ ) depicting with coloured symbols all saltmarsh zones of the three salt marshes.

## 7.5.2 Synthesising saltmarsh processes: insights from one key core.

Using a core within the MR area where salt marsh had existed prior to the 1950's land reclamation and then reverted to salt marsh again after 2003, enables the luminescence results to potentially inform the changes in saltmarsh evolution, the aboveground accretion (chapter 4) and sedimentation patterns (chapter 5) superimposed on the belowground changes in water content, dry bulk density, organic matter and mean grain size (chapter 6). Core MR8 is a good exemplar of these interactions.

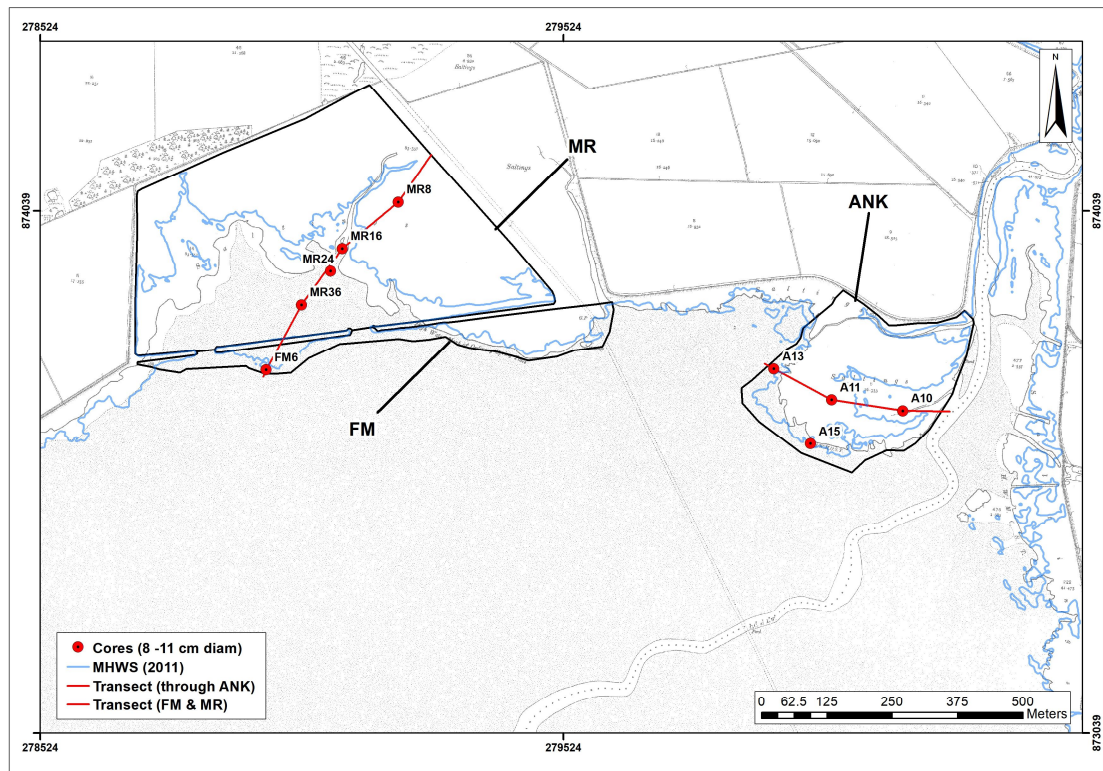


Figure 7-31: Core (red dots) location along the two transects (red lines; see also in Chapter 6 - Figure 6-3 and 6-4) superimposed onto OS 2<sup>nd</sup> revision One-inch map (1907) showing in blue HWM derived from LIDAR dataset.

The data collected for the full yearly cycle (2016-2017) from the Nigg salt marshes (Chapter 4) yielded results indicating overall accretion rates of  $1.34 \pm 0.1 \text{ cm} \cdot \text{year}^{-1}$  and  $1.4 \pm 0.1 \text{ cm} \cdot \text{year}^{-1}$  for the managed realignment salt marsh. The accretion rates observed at the specific location situated in the high-marsh area of MR where the core MR8 was extracted yielded a value of  $1.44 \text{ cm} \cdot \text{year}^{-1}$ . The sedimentation plate data spanning a period of 2.15 years (2015-2017, as documented in Chapter 5, Section 5.5.3) revealed average sedimentation rates of  $0.21 \pm 0.03 \text{ cm} \cdot \text{yr}^{-1}$  and  $0.38 \pm 0.07 \text{ cm} \cdot \text{yr}^{-1}$  for the MR8 plate. Geomorphic information (grain size distribution, water content, bulk density, organic matter and photographic record – Chapter 6) was evaluated using the same core (Figure 7-35). Photographs of cores collected on MR's high marsh (Figure 6-37), but not in vicinity of MR8 core (figure 6-2), highlight a soil discoloration forming a stratigraphical layer at 6 to 12 cm in depth (corrected depth from compaction). The utilisation of either accretion rates derived from filter discs or sedimentation plates rates would encompass a wide span of years, thereby compromising the accuracy of the measurements. Additionally, it is important to note that sedimentation rates are not consistent across a marsh system. As reported by Miller et al. (2023), the cores collected at Dornoch Point and Morrich More in the Morray Firth were analysed using  $^{210}\text{Pb}$  and  $^{137}\text{Cs}$  chronologies. The researchers determined that the material found at a depth of 11.5 cm in the cores began to accumulate in the years  $1872 \pm 24$  and  $1830 \pm 22$ , respectively. Furthermore, they observed that the high marsh at Dornoch Point increased at an average rate of  $0.09 \pm 0.02 \text{ cm} \cdot \text{yr}^{-1}$ , while at Morrich More, it increased at a rate of  $0.06 \pm 0.03 \text{ cm} \cdot \text{yr}^{-1}$ . By



employing either of the sedimentation rates techniques, it is evident that the core possesses sufficient depth to unveil the progression and transformation of salt marsh, encompassing alterations resulting from land reclamation and the breach that took place in 2003.

Luminescence signal sensitivity profile of core MR8 presents a good overall correlation between both B-OSL and IRSL signals (Figure 7-32) with major depositional trends and further minor variations which can be in part elucidated in taking in account results from IRSL/B-OSL (Figure 7-33) and Depletion Index (Figure 7-34) and geomorphic information. Results show four main shifts through the profiles indicated with bold coloured arrows on Figure 7-32 to Figure 7-34 as interpreted at 3 cm, 9 cm, at 15 cm and 44.5 to the base of core (46.2 cm) and minor sequences within the core are identified with pale coloured arrows in graphs. Excluding the thin upper soil layer ( to 3 cm) where bioturbation from roots will affect signal sensitivity (Madsen et al., 2007).

Based on B-OSL and IRSL signal sensitivity (FED1 - Figure 7-32), the upper **3 - 9 cm** of the core contains very young material providing an apparent age ranging from 9 to 23 a. (for B-OSL FED1) and 9 to 34 a. (for IRSL FED1) using a putative dose rate of 1 mGy.yr<sup>-1</sup>. These estimates are pointing to sea wall breaching of 2003 which are corroborated by clear signal peaks on the three profiles, FED1, IRSL/OSL (Figure 7-33) and Depletion index at 3 cm (Figure 7-34). **At 9 cm** a step-up indicated on FED1, IRSL/OSL and Depletion index profiles corresponds to clear discontinuities in water content, soil organic carbon content (SOC), BDD and mean grain size plots (Figure 7-35). These changes in rapid decrease of organic carbon content (SOC) and compaction through depth are associated with luminescence signal lowering and interpreted as a system shift such as reclamation. This shift is associated with a sudden change in grain size and photograph of a core collected on high marsh (Figure 6-37) depicts soil discoloration between 6-8 cm in depth and traced until 12 cm. Grain colours have importance for OSL signal sensitivity (see 7.2.1.4 -Figure 7-8) and can be located in the depletion index profile at same depth. **From 9 to 13 cm**, depletion index of B-OSL and IRSL are following same trend implying underlying changes in environmental condition which may be associated with land reclamation work in Nigg Bay where both vegetation and sediment are shifting between systems (from reclaimed land to post-reclamation salt marsh restrained from tidal input).

**At 15 cm**, B-OSL and IRSL signals diverge showing B-OSL signal depleting whilst IRSL does not increase but exhibits modulation pattern. Depletion index further indicates that IRSL signal is not changing (either in decay or growth, i.e. accretion or erosion) for approximately 18-20 cm whilst B-OSL presents a modulation pattern at same depths demonstrating little changes either. The observed depositional sequence exhibits a high degree of concordance with respect to the stratigraphic profile of bulk density, mean grain size, and organic matter at the corresponding depth

as depicted in Figure 7-35, wherein minimal variations in their overall composition are observed. This sequence is interpreted as corresponding to the former saltmarsh soil where sediment can only be brought in the high marsh zone irregularly as the tidal inundation is less frequent (see 6.2.1.4). To the base of the core, there is an overall increase in signal sensitivity suggesting sediment accretion but is at slow pace. There is also little evidence to suggest erosion or increased accretion as demonstrated by the slow rate of accumulation in organic carbon content (SOC). Overall, IRSL/OSL profile provides a good correlation with grain size, from 9 cm to the base of the core, where feldspar content weather rapidly (25-29 cm corresponds to a decreasing trend in feldspar signal) is inversely correlated with grain size coarsening ( showing medium silt to very fine sand). The trend reflects changes in mineralogy which could be further explored using quantitative X-Ray diffraction analysis (XRD) or Scanning Electron Microscopy (SEM) up and down the core to evaluate influence of mineralogical composition on this sediment and further inform on past hydrodynamics and tidal regime. These peaks are present at **25 cm** deep is visible on FED1, IRSL/OSL and **27 cm** depletion index, and, are only associated with minor changes in BDD and SOC whereas the major change in grain size is depicted with a steep grain coarsening is visible at **24 cm** and could relate to strong environmental disturbances such as strong tidal waves or storminess depositing coarse grains in the system.

This stratigraphic sequence is preceded by an abrupt shift in the system at **44.5 cm** visible in all plots showing similar increasing trends with in the depletion index between IRSL and B-OSL (Figure 7-32), feldspars weathering in IRSL/OSL profile (Figure 7-33), decrease signal intensity associated with highest increase level in grain size, distinct decrease in SOC and increase of BDD. This layer of coarser grains extended down to at least 74 cm in depth (see details in Chapter 3 - 3.4.3.1) which certainly suggests the presence of pioneer marsh or mud/sand flat at this depth.

Using a putative dose rate of  $1 \text{ mGy.yr}^{-1}$ , depth at the base of the core, 46.2 cm suggests an apparent age ranging between 82 a. (for B-OSL FED1) and 219 a. (for IRSL FED1).

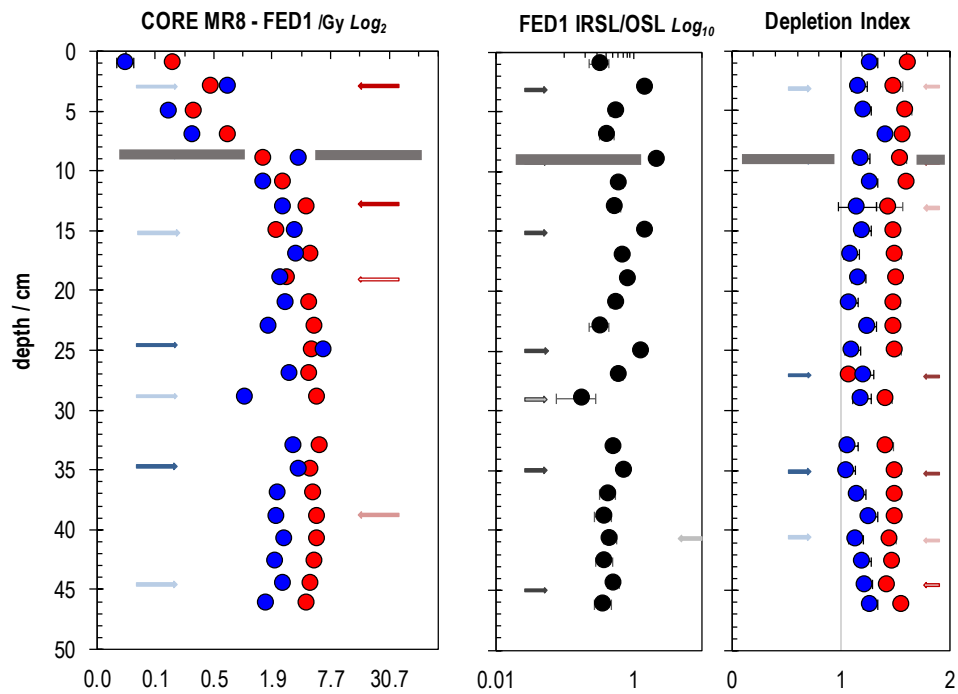


Figure 7-32: Core MR8 FED1 B-OSL and IRSL (in Gy  $Log_2$  and error bars from individual standard errors) through core depth (in cm). Blue arrows (bold colour major shifts and pale colour minor shifts) present breaks or shifts in B-OSL signal trends and red arrows presents shifts in IRSL signal. The thick grey line is a significant change in the trend that can be linked to the 2003 breaching.

Figure 7-33: FED1 IRSL/B-OSL ratio (in  $Gy_{Loge}$ ) inferring on mineralogical variation with grey arrows indicating shifts (Bold grey = major shift and pale colour = minor shifts). The thick grey line is a significant change in the trend that can be linked to the 2003 breaching.

Figure 7-34: Depletion index of the regenerated B-OSL (blue) and IRSL (red) signals indicating shifts on colour, mineralogy and residuals (inherited from prior deposition). Values higher than 1 indicates rapid decays. The thick grey line is a significant change in the trend that can be linked to the 2003 breaching. (Arrows same as Figure 7-32).

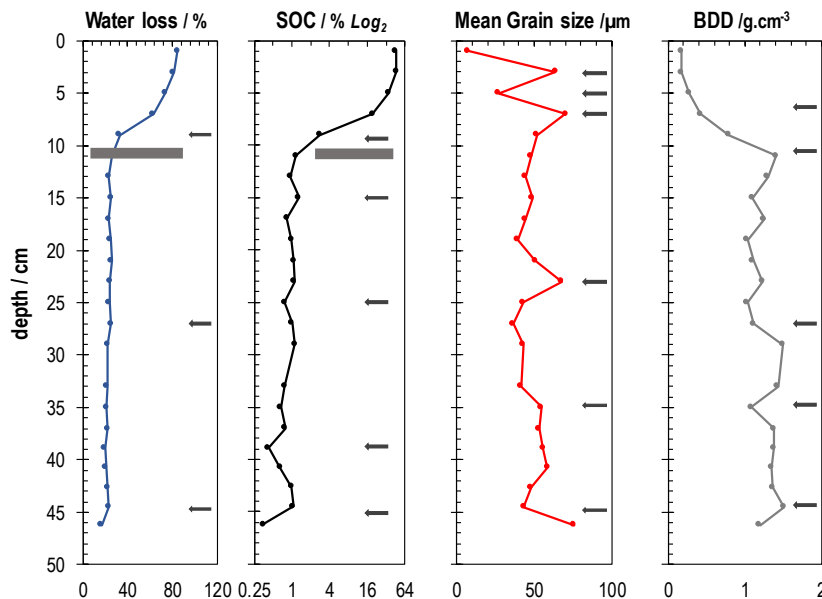


Figure 7-35: Profiles of water content (%), BDD ( $g.cm^{-3}$ ), Organic content ( $\%_{Loge}$ ) and mean grain size ( $\mu m$ ) from Core MR8 showing on right of mean grain size plot an extrapolated chronology using accretion rates of  $0.417 \pm 0.24 \text{ cm.yr}^{-1}$  from filter discs MR8. Arrows indicating shifts in the trend (Bold grey = major shift and pale colour = minor shifts). The grey dash is a significant change in the trend that can be linked to the 2003 breaching.

## 7.6 Summary and significance of the results

- 1) Is there a measurable luminescence signal? Can it be enhanced and calibrated? Does this signal increase with depth?

This research work has answered the aims of the study by developing new instrumentation, protocols and calibration, starting from very poor signal levels, luminescence signals, B-OSL and IRSL, have been increased permitting to read the luminescence profiles with this kind of sensitivity and coherence is a truly significant achievement in light of all difficulties reported in the prior literature.

- 2) Can the results inform the sediment history to complement the short-term and long-term results from previous chapters?

IRSL/B-OSL ratios infer on the state of weathering of sedimentary minerals showing feldspar weathering more rapidly than quartz (in core MR8, at depth 7, 13, 23 and 29 cm) and undergoing dissolution and transformation into clay minerals (Clarke and Rendell, 2000). This has potential effects on luminescence age determination, but more-so, it suggests that mineralogical changes and compositions can influence saltmarsh sedimentary processes such as increases in clay contents. Future work might look in more detail at the impact of chemical weathering influences on these types of sediment.

Depletion index revealed, in core MR8, modulation patterns inferring on depositional trends or where both B-OSL and IRSL depletion followed similar trends (e.g. at 3 cm between 9 and 13 cm and 44.5 and 46.5 cm) suggesting underlying changes in environmental conditions or anthropogenic disturbances (e.g. 2003 sea-wall breach and reclamation). Again, more information is needed to confirm or interpret these trends but could be further tested in future work.

Luminescence signal residuals have been greatly improved by calibrating and dose estimates (e.g. FED1) has confirmed that there enough sensitivity to read small luminescence within young and well-characterised (e.g. core A15 and MR8 ~ 10 years old sediment) saltmarsh cores further showing a good association with geomorphological features as reported in this study in previous chapters such as organic aboveground processes with zonation (Chapter 4 – 4.3 ) and belowground processes with Soil Organic Carbon content (Chapter 6 – 6.3) and such as sedimentary belowground properties with grain size and bulk density (Chapter 6 – 6.2). This is compelling evidence that variable residual signal levels are reflective of the sedimentary regime and the associated geomorphological processes of both the sedimentary sources and their depositional

settings. The combination of these new techniques allows us to track the changes that occur on signal intensity, sensitivity and bleaching to answer questions on sediment processes and dynamics and how the saltmarsh sediment deposition regime might work. To study these further, it would be valuable to extend the work in the future to include light-protected samples of freshly deposited material associated with the periodic flooding events. This will of necessity entail studying small samples from suspended sediments and filter mats for which the enhanced sensitivities developed in the work reported here will be critical. A unique training set of samples covering all the spring tides between February 2016 and February 2017 was gathered in association with this research programme. Now that the measurement systems have been developed to record stimulated luminescence from very young material with high sensitivity a future research project to explore the temporal and spatial variations in freshly deposited material would be possible.

This work lies with wider implications since Intergovernmental Panel on Climate Change (IPCC 2014 and 2018) predicts increasing severity and frequency of extreme events and weather systems in a climate altered world - pursuing the future investigation of freshly deposited material from the 2016 sampling period in comparison with resampling (for example at a 5 year interval) has the potential for registering future changes of system.

In order to enhance the comprehensiveness of the findings derived from this study, it is important to incorporate two additional statements that contribute to the significance of the obtained results. This project aims to develop an ultra-sensitive portable OSL (Optically Stimulated Luminescence) reader equipped with two infrared (IR) sources operating at wavelengths of 890 nm and 940 nm. These sources will be filtered to optimise the signal recovery from recently formed polymineral samples. This thesis work presents a novel appraisal and evaluation of the potential benefits of enhancing sensitivity in the study of young coastal sediments. The topic under consideration pertains to the utilisation of sample preparation techniques, thermal treatments, and calibration methods in conjunction with portable optically stimulated luminescence (OSL) readers. This research project has successfully devised a practical calibration procedure for 3 cm diameter samples of juvenile saltmarsh sediments. This novel approach expands the existing methodology for both portable optically stimulated luminescence (OSL) readers and laboratory profiling methods.

## **7.7 Acknowledgement**

All luminescence research was conducted at SUERC, East Kilbride, with the invaluable assistance and advice of Professor David Sanderson. Lorna Carmichael and Simon Murphy were extraordinarily helpful in facilitating the fine-tuning of all laboratory protocols and equipment.









# Chapter 8

*31st January 2017 - Managed realignment, Nigg Bay*

## **Chapter 8. Discussion and conclusion**



## 8.1 Introduction

Chapter 1 introduced a set of questions that have arisen in response to recent research conducted in Scottish salt marshes (Teasdale et al., 2011), examining how salt marshes can respond to external change and forcings. For example, how do saltmarsh landforms respond to environmental forcing and keep pace with sea level rise? How much sediment reorganisation has already occurred in Scottish salt marshes? Might climate change increase the resilience of saltmarsh habitats? Can salt marshes increase their ability to sequester carbon and/or provide even greater ecosystems services? In order to address some of these issues, the objective of this thesis was to improve understanding of the temporal and spatial relationships between sediment supply, vegetation presence, and saltmarsh stability. The following relationships were examined:

1. Aim 1: quantify the aboveground changes in vegetation and sedimentation patterns over different timescales, ranging from short (annual) to longer (centennial) timescales.
  - This has been presented in **Chapters 4 and 5**.
2. Aim 2: establish belowground physical and biological changes that have occurred on the studied salt marshes.
  - This topic is presented within **Chapter 6**.
3. Aim 3: explore the possible mechanisms driving these changes using a combination of traditional sedimentary techniques and using a dating technique not previously used on salt marshes.
  - This is the focus of **Chapter 6 and Chapter 7**.
4. Aim 4: appraise the potential implications of the aboveground and belowground results particularly in relation to the ecological services offered by natural and restored salt marshes, as well as the ability of these ecosystems to adapt to rising sea levels.
  - These implications have been discussed in the concluding sections of each chapter, specifically **Section 4.6.3, 5.6, 6.5.1 and 6.5.1 and 7.6**.

aims to integrate the findings from Chapters 4 through 7 with the existing body of literature on saltmarsh studies. It does so by examining the research questions that were specifically formulated for this study:

- 1) What are the biotic and abiotic processes, mechanisms, and patterns that contribute to the formation and development of salt marshes? This is presented in **section 8.2**.
- 2) What are the implications of climate change and anthropogenic disturbances on saltmarsh ecosystems? This is presented in **section 8.3**.

Chapter 8 is conceptualised in Figure 8-1 where section 8.2 integrates the short-term to long-term results, section 8.3 appraises saltmarsh resilience site to sea level rise and section 8.3 highlights the study implications for blue carbon ecosystem services.

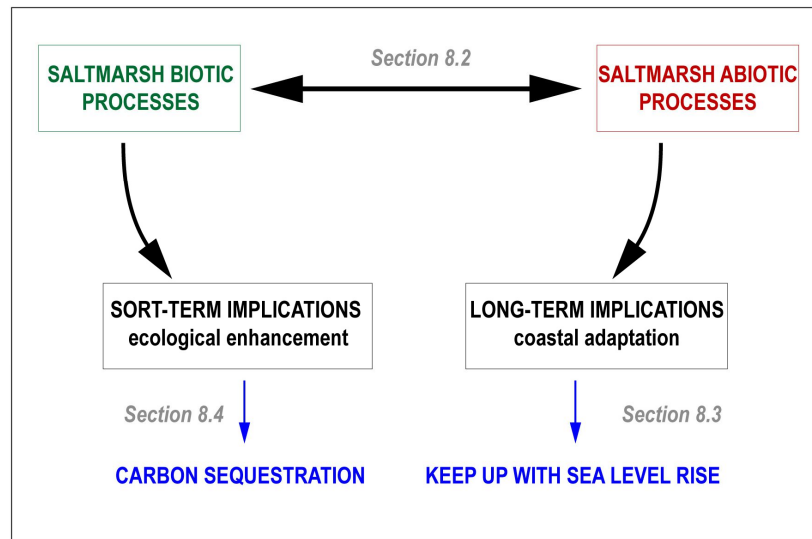


Figure 8-1: Conceptualised framework for chapter 8

For the sake of brevity, a list of abbreviations and acronyms used in this Chapter is provided in Appendix A.

## 8.2 Biotic and abiotic processes over different spatio-temporal scales

Which processes, mechanisms and patterns promote saltmarsh formation and development? Can the recent and past-trends of ecological and physical changes on the natural and managed salt marshes help to predict Nigg Bay saltmarsh stability and future development?

### 8.2.1 Short-term to longer-term patterns of saltmarsh development

Only a few studies have investigated sedimentary processes on salt marsh across different timescales (Marion et al., 2009; Schindler, Karius, Deicke, et al., 2014; Schindler, Karius, Arns, et al., 2014). The findings presented here, at annual, multi-annual, decadal and centennial timescales, aim to determine improving our understanding both sedimentary and biological processes operating across space and time at the MR and natural paired saltmarsh sites at Nigg.

Each salt marsh at Nigg Bay is characterised by a physiographic location that is affected by tidal conditions and this in turn determines the sedimentary regime. The variability among estuaries makes it challenging to conduct direct comparison of salt marshes. Factors such as sediment supply, hydrological parameters, and biological conditions will each have distinct effects on the system. Nevertheless, it is possible to utilise broader controls on saltmarsh development to

establish comparisons between different marshes and facilitate the analysis of the primary factors that govern sedimentation. Continued sedimentation is critical to keep saltmarsh elevation in pace with any changes in water level (hydroperiod) such as may be forced by relative sea level rise, provided that there is sufficient space landward for the salt marsh to migrate (Wolters et al., 2005). Hydroperiod influences saltmarsh sedimentation with areas in proximity to tidal waters such as tidal creeks (Adam, 1990; Pye and French, 1993; Cahoon et al., 2000) or seaward edge (Pethick, 1984) expected to have higher volumes of sediment deposited. The longer the hydroperiod and length of inundation, the higher sediment supply which will in turn controls the pace of saltmarsh surface elevation (Cahoon et al., 2000). For the MR site at Nigg, sediment enters the marsh via the two artificial breaches whilst sediment supply to the natural salt marshes FM and ANK, is directly delivered by creeks and saltmarsh edge overtopping, with some delivery via the Ankerville river to the east of ANK. The short-term variation of the water levels (hydroperiod, flood depth and flood frequency) have summarised in sections 4.4.1.4, 4.4.2.3 and in appendix D.3 and discussed in section 4.6.2.3. The variability of sedimentation is influenced by water levels, wind, storminess and vegetation abundance (Reed, 1989; Allen and Duffy, 1998). These variables can be attributed to a common seasonal denominator and have been studied in estuarine marshes which experience substantial freshwater input and are more sensitive to rainfall (Allen, 2000; Temmerman et al., 2003; Allen and Dark, 2007) rather than marine and tidal influences where seasonality takes form in increased winter storminess and windiness.

Chapter 4 key results is the determination of short-term accretion rates estimates using filter discs (with a mean rate estimated at  $1.3 \pm 0.1 \text{ cm.yr}^{-1}$ ). These rates were found to be different between the three salt marshes. Overall, the young and natural fronting salt marsh FM had the lowest accretion rates ( $1.1 \pm 0.3 \text{ cm.yr}^{-1}$ ) compared to the natural salt marsh ANK ( $1.5 \pm 0.3 \text{ cm.yr}^{-1}$ ) and the managed realignment MR ( $1.4 \pm 0.2 \text{ cm.yr}^{-1}$ ). These results disagree with the general findings on managed realignment in the UK. At this point it is useful to note that 73 % of the published literature (worldwide) relevant to de-embankment and saltmarsh restoration relates to English and Welsh salt marshes (Esteves and Williams, 2015), salt marshes that are principally composed of mud and silt. Scottish salt marshes and Nigg Bay, in particular, is mainly sandy requiring more tidal velocity to entrain than cohesive silts or muds and so will tend to have generally lower accretion rates (Davis and Dalrymple, 2012). Results from saltmarsh systems in England have shown that once sites are breached, relatively high accretion rates are recorded (e.g. up to 5 cm in the first two years of inundation at Orplands) as they rapidly undergo height increases to compensate for years of dewatering and compaction which may have left them below the levels of adjacent natural salt marshes (Burd, 1992; P.W. French, 2006). Examples of this include Freiston shore (Spencer et al., 2012), at Tollesbury and at Orplands (P.W. French, 2006) which show higher accretion rates in managed realigned marsh compared to the adjacent salt marsh. Similarly, van



der Wal and Pye (2004) found mature salt marshes in the Greater Thames area had accreted less ( $2\text{-}3\text{ mm.yr}^{-1}$ ) than younger marsh ( $3\text{-}5\text{ mm.yr}^{-1}$ ) to maintain their height in the tidal frame. Once established, managed salt marshes must sustain high accretion rates and continue to accrete vertically to keep pace with accelerating sea level rise.

Chapter 4 - section 4.5.3 examines the zonation and seasonality patterns observed in the three salt marshes studied at Nigg Bay, emphasising their vulnerability in the short-term (annual). The relationship between short-term sediment deposition and biogeomorphic controls is summarised in sections 4.5.1.3, 4.5.2.3, and 4.5.3.3. The significance of these findings is discussed in section 4.6.2.

The main result of Chapter 5 key result is the determination of multi-annual sedimentation rates using sedimentation plates with an overall positive sedimentation rate amount of  $0.21\pm 0.03\text{ cm.yr}^{-1}$  from July 2015 to September 2017. These rates were found to be significantly different between sites. The managed realignment salt marsh showed a positive sedimentation rate of  $0.33\pm 0.03\text{ cm.yr}^{-1}$ , whilst ANK maintains its height at  $0.01\pm 0.04\text{ cm.yr}^{-1}$  and FM shows a negative rate of  $-0.09\pm 0.16\text{ cm.yr}^{-1}$ . Chapter 5 - section 5.5 examines the patterns and rates of geomorphological change and discusses the relationships between these rates and the forcing factors that occurred in Nigg Bay on a centennial scale in section 5.5.1, on a decadal scale in section 5.5.2 and on multi-annual scale in section 5.5.3. The relationship between sedimentation rates and biogeomorphic controls is summarised in sections 4.5.1.3, 4.5.2.3, and 4.5.3.3. The significance of these results is discussed in section 4.6.2.

Table 8-1 gives accretion and sedimentation rates in Scotland, the UK and Europe, providing a context for the results obtained at Nigg Bay.

**Table 8-1: Accretion and sedimentation rates in Scotland, the UK and Europe. Note 1: the method used determines Short-term or Long-term results. Note 2: MR managed realignment or RSM restored salt marsh.**

	Location	Accretion rate (cm.yr.1)	Methods Used	Reference
	<b>Nigg Bay, Cromarty Firth</b>	<b>1.34±0.14</b> <b>0.21±0.03</b>	<b>Sediment trap (filter discs 1 year)</b> <b>Sedimentation plates (2.14 yrs)</b>	THIS RESEARCH 2016-2017
<b>NE Scotland</b>	Eden Estuary RSM	0.34 to 0.38	Sediment trap (filter discs)	(Maynard et al., 2011)
	Dornoch Point and Morrich More ( high marsh)	0.09 ± 0.02 to 0.06 ± 0.03	Radionuclides ( <sup>210</sup> Pb & <sup>137</sup> Cs)	(Miller et al., 2023)
	Stear marshes MR Somerset, UK	7.5 ± 2.8	LiDAR DTMs (2015 to 2018)	(Mossman et al., 2022)
<b>N Scotland</b>	Bettyhill, Farr, Highlands	0.5 to 0.9	Surface but no methods cited-	(Teasdale et al., 2007)
<b>SW Scotland</b>	Solway Firth - Orchardton	2.5 / 2.8	Plates vs Radionuclides ( <sup>137</sup> Cs/ <sup>241</sup> Am)	(Harvey et al., 2007)
	Loch Scridian	1.8	Radionuclides ( <sup>210</sup> Pb & <sup>137</sup> Cs)	(Teasdale et al., 2011)
<b>Western Scotland</b>	Loch Don	2.3 to 2.5	Radionuclides ( <sup>210</sup> Pb & <sup>137</sup> Cs)	(Teasdale et al., 2011)
	Loch Creran	2.7	Radionuclides ( <sup>210</sup> Pb & <sup>137</sup> Cs)	(Teasdale et al., 2011)
	Loch Etive	2.5	Radionuclides ( <sup>210</sup> Pb & <sup>137</sup> Cs)	(Teasdale et al., 2011)
	East Anglia - Scott Head Island	0.39 (0.1 to 0.8)	Marker layers & microcores	(Cahoon et al., 2000) French & Spencer (1993)
	East Anglia -Stiffkey	0.39	Sedimentation Plates	(Cahoon et al., 2000) using Möller (1997)
<b>SE England</b>	East Anglia - The wash	0.5	Sediment poles	(Cahoon et al., 2000) using Reed (1988)
	Thames estuary - mature marsh	0.25		
	Thames estuary - young marsh	0.4	Historical Mapping	van der Wal and Pye (2004)
	The Wash - Freiston shore MR	0.39	Sedimentation Plates & SET	Rotman et al., 2008; Friess et al., 2012
	Essex – Tollesbury – MR	0.43	Marker layers & SET	(Boorman et al., 1998)
	Suffolk – Blyth estuary	0.24	Sedimentation Plates	(French and Burningham, 2003)
<b>S England</b>	The Solent - Hampshire	0.45	Isotopes	Cundy and Croudace (1996)
<b>SW England</b>	Dorset	2.6 to 10.2	Marker layers & bamboo canes	(Brown et al., 1999)
	Severn Estuary	4.65		Allen and Duffy (1998)
		0.5	Historical Mapping	van der Wal et al. (2004)
<b>W &amp; NW England &amp; Wales</b>	Ribble Estuary	0.61 to 0.79	Radionuclides ( <sup>210</sup> Pb & <sup>137</sup> Cs)	(Brown et al., 1999)
	Mersey	0.45	Isotopes	Fox et al. 1999
	Dyfi Estuary	0.1	X-ray laminae counts	(Shi et al., 1995)
	NW (Sligo and Galway) - Ireland	0.5	Radionuclides ( <sup>210</sup> Pb & <sup>137</sup> Cs)	(Wheeler et al., 1999)
	Cotentin Peninsula - France	0.4 to 0.8	Radionuclides ( <sup>210</sup> Pb & <sup>137</sup> Cs)	(Haslett et al., 2003)
	Elbe estuary - Germany	2.03	Traps (plastic pots)	Butzeck 2016
<b>Europe</b>	Sylt - Germany	0.1 to 1.6	Historical Mapping Radionuclides ( <sup>210</sup> Pb & <sup>137</sup> Cs)	Schuerch 2016
	Halligen, North Frisian – Germany	0.15 ± 0.09; 0.12 ± 0.08; 0.26 ± 0.09	Filter traps	(Schindler, Karius, Arns, et al., 2014)
	Hooge Langeness N.Moor	0.10 ± 0.3 ; 0.12 ± 0.3; 0.26 ± 0.9	Radionuclides ( <sup>210</sup> Pb)	

## Pattern of vulnerability at a multi-annual timescale

Patterns of erosion on a multi-annual scale (Chapter 5 - section 5.3 and 5.5.2) were observed in the easternmost frontal areas of FM and ANK. Erosion to the east and gain to the west of the realigned site MR were also recorded, demonstrating an asymmetric sediment delivery via the breaches resulting from the remnants of reclamation drainage channels preventing deposition in the vicinity and with a vegetation presence that is still transitional and does not favour sedimentation in the way that mature saltmarsh vegetation would. This phenomenon has been observed by Spencer et al. (2012) where insufficient vegetation biomass in the algal-pioneer *Salicornia* zone (the same species as Nigg Bay saltmarsh pioneer-marsh PM zone) limited resuspension and encouraged deposition especially in the mudflats fronting the breach gap. However, within the MR, they also observed dramatic sediment erosion of the drainage channel located behind former defence.

DEM times series (2011-2017; Chapter 5 - section 5.3.2 and 5.5.2) from airborne surveys terrestrial laser scanning of the mudflats, pioneer and low-marsh zones of the three Nigg Bay salt marshes, further established that the overall gain on the managed realignment salt marsh, MR, occurred at the expense of the eroding fronting salt marsh FM. MR showed surface elevation change of  $0.3 \text{ cm.yr}^{-1}$  and area gains of 30.8% and volume gain of 42.2%. Whereas the eroding fronting salt marsh FM showed  $-0.1 \text{ cm.yr}^{-1}$  elevation loss, 18.8 % areal loss and 20.8 % in volume gain, and ANK with -5.8 % area loss and 20.1 % in volume gain. Rotman et al. (2008) explored sediment provenance within managed realignment and identified that the primary source (~54%) originated from sediment seaward of the breaches, 27% sourced from the breached seawall, and 19% from intertidal and subtidal mudflats/sandflats seaward of the established marsh. On the natural salt marsh at ANK, the marsh edge has migrated landward but small cliffs have developed in the sheltered areas of the bay (west), together with an erosional steepening of the existing cliffs in the most exposed areas (south and east). Although FM cliffs may not have signs of present erosion, the presence of former salt marsh vegetated surfaces are present at their base that result from past erosion and/or undercutting by wave and tide processes. This phenomenon may occur even when salt marshes are in elevational equilibrium with sea level rise, but they are inherently unstable in the horizontal direction as illustrated by marsh lateral retreat in a continuous cycle of erosion and collapse induced by the action of the impinging waves (P.W. French, 2006; Kirwan et al., 2010; Fagherazzi et al., 2013; Bondoni et al., 2016). Bondoni et al. (2016) review recent marsh retreat due to anthropogenic pressure and SLR and estimates this horizontal retreat in the order of  $0.12\text{-}0.22 \text{ cm. yr}^{-1}$  in the lagoon of Venice,  $0.04\text{-}300 \text{ cm. yr}^{-1}$  in the Netherlands,  $0.05\text{-}200 \text{ cm. yr}^{-1}$  in Virginia (USA) and  $230 \text{ cm. yr}^{-1}$  along the Savannah River (USA). In their study, they found a clear correlation between wave energy flux and erosion rate, at short (monthly) temporal scales,

without marsh collapse or very frequent mass collapse and that slumping of unstable blocks is not necessarily correlated to the instantaneous wave forcing but from wave attack destabilising the cliff or bank which may subsequently lead to collapse even during calm periods.

### **Pattern of resilience over short and long-term timescales**

The visible expansion of pioneer vegetation (Chapter 5 - section 5.3.1) in front of the cliffs at ANK and FM may be signs of a rapid and short-term biological response linked to a reduction in lateral retreat of the saltmarsh edge and, in case of severe erosion. Additionally, in instances of significant erosion, this response may also be associated with an elevation increase in the mudflat (van der Wal and Pye, 2004). At the macro-scale, plants exert a strong influence on the hydrodynamics, and, consequently temper and dissipate the effect of bed shear stress and flow turbulences (Marion et al., 2009). These signs of short-term resilience have been highlighted in the short-term vegetation study in Chapter 4 - section 4.5.3.1, where there are direct relationships between deposition and accretion, counteract the intense flooding the fronting marsh FM experiences due to its close proximity to the sea shore and small surface area mostly under MHWS (c. 78 %). Vegetation appears to propagate rapidly in response to intense flooding in conditions where seeds have difficulty to settle and anchor such as self-scouring allowing seed dispersal (Balke et al., 2014; Bouma et al., 2016).

Over longer timescales (decadal to centennial), the capacity of salt marshes to respond to environmental changes and anthropogenic alteration determines the long-term resilience of the system (Wolanski et al., 2009). Long-term (centennial) resilience of saltmarsh system may be reflected in an overall areal expansion and MHWS moving seaward. Over c.100 years (1877-1977; Chapter 5 - section 5.2.3 and 5.5.1), prior MR realignment and post 1950's reclamation, management and land claim of coastal salt marsh in Nigg Bay, as a whole, resulted in a 32 % loss of salt marsh (double the estimated UK salt marsh loss (Beaumont et al., 2014)), yet, during this time, there was a 20.5 % saltmarsh expansion into the intertidal zone. This trend is confirmed by an overall MHWS migration seawards of 30.78 m over the same period 1872-1977. Over the 145 years between 1872 and 2017 during which land reclamation and realignment of MR salt marsh took place the overall rate of seaward migration of MHWS for the three studied salt marshes was  $-0.02 \text{ m.yr}^{-1}$ . This pattern is consistent with salt marshes elsewhere that have been shown to offset lateral erosion by rapid frontal expansion of their seaward edge driven by deposition of large amounts of sediment (Gunnell et al., 2013; Fagherazzi, 2013). Balke et al. (2016) compared salt marshes and bare-flats and established that the seaward extents of salt marsh vegetation on tidal flats as defined by inundation frequency (and not duration) dictated the lower elevation limit of the salt marsh on the Dutch and German tidal flats in the North Sea. Möller et al (2014) showed

the presence of vegetation enabled saltmarsh stability and resilience in places exposed to large waves, undercutting and collapse of the cliff profiles and/or creek widening. They further predicted that the long-term balance between vertical and lateral marsh dynamics are key to future coastal protection schemes (Möller et al., 2014; Bouma et al., 2014).

Over the short-term annual analysis, the agreement of overall deposition rates between the sites (Chapter 4 - section 4.2.1 and 4.5) suggests a fairly uniform sediment supply which has also been shown to be a key factor for marsh resilience to sea level rise (J. French, 2006; Kirwan and Guntenspergen, 2010; D'Alpaos et al., 2016).

### **8.2.2 Short-term and longer-term rates of saltmarsh development**

Chapter 3 recalled the distinction used here between deposition and sedimentation which has defined the sampling strategy for this research. Deposition corresponds to the amount of accumulated material whilst sedimentation is the difference in elevation, attributed to accretion and erosion, based on a reference height over a given time interval (Pye and French, 1993). These distinctions are not always clearly followed in saltmarsh literature, however, they have been recognised of importance as the mean accretion rates exceed rates of positive sedimentation rates, indicating the importance of near-surface processes (termed 'shallow subsidence') (Spencer et al., 2012). Shallow subsidence is critical 'problem occurring on a global scale, and that may in many parts of the world strongly exceed the rate of sea level rise (Temmerman et al., 2013).

The differences between accretion rates using sediment deposition and sedimentation measured using sedimentation plates (Chapter 5 - section 5.4 and 5.5.3) have twofold implications: first, to maintain their surface elevation, salt marshes accumulate mineral and organic material which must be equal to the rate of crustal motion, occurring below the saltmarsh substrate in bedrock, as measured at a tide gauge, plus the rate of autocompaction or also called shallow subsidence of the marsh substrate, and, in a sea level rise scenario, this rate must equal to the rate of total subsidence plus local sea level trend (Cahoon, 2015). Second, autocompaction indicates that accretion rates are likely to have been overestimated (ibid).

Fieldwork campaigns at Nigg Bay on the three salt marshes allow an assessment of the influence of the shallow submergence, critical to understand local changes in sea level and saltmarsh elevation. Comparing results produced between the short-term accretion rates from filter discs presented in chapter 4 (section 4.2.2.2) and longer-term sedimentation rate using sedimentation plates in chapter 5 (section 5.4), there was positive relationship between sedimentation rate and accretion rate on ANK suggesting that overall sediment deposition drives sedimentation ( $\rho=0.8$ ,

<0.001), although the association is weak ( $r^2= 5.2\%$  Figure 8-2). However, this varies by site and saltmarsh zones as on the mid-marsh MM and low-marsh LM, whilst the negative fit of the regression on PM and high-marsh HM suggests that subsurface processes result in shallow surface subsidence (Figure 8-3). On FM, there is an overall positive influence of deposition on elevation ( $r^2= 24.5\%$  -Figure 8-2), for both HM and MM zones. On MR, the overall difference is minimal ( $r^2= 0.2\%$  -Figure 8-2) but pioneer and mid-marsh both depict shallow subsidence whilst LM is positively influence by sediment deposition, showing within site variability in trends.

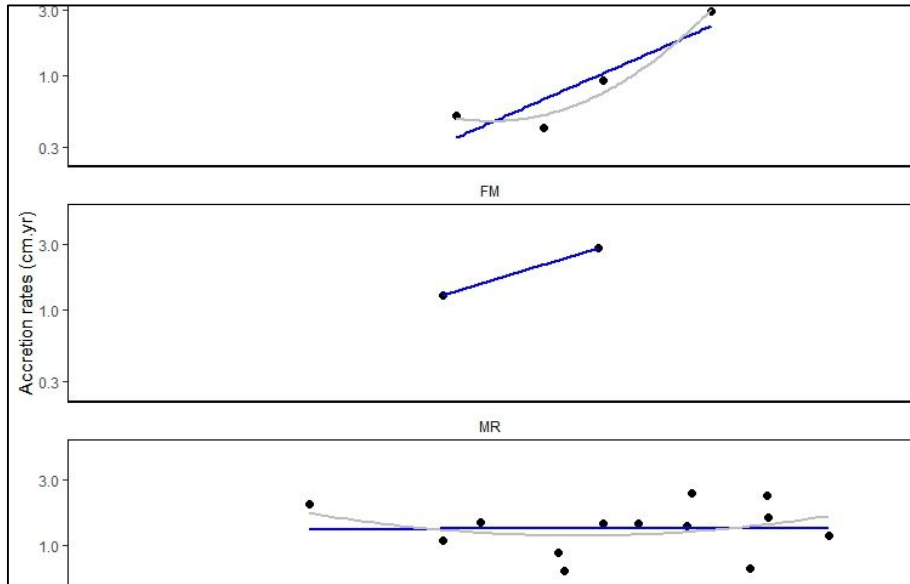


Figure 8-2 Scatterplot between accretion rates (x-axis) sedimentation rates (y-axis) with regression fit line for each saltmarsh site (linear regression is shown in light grey and quadratic with a dotted blue line).

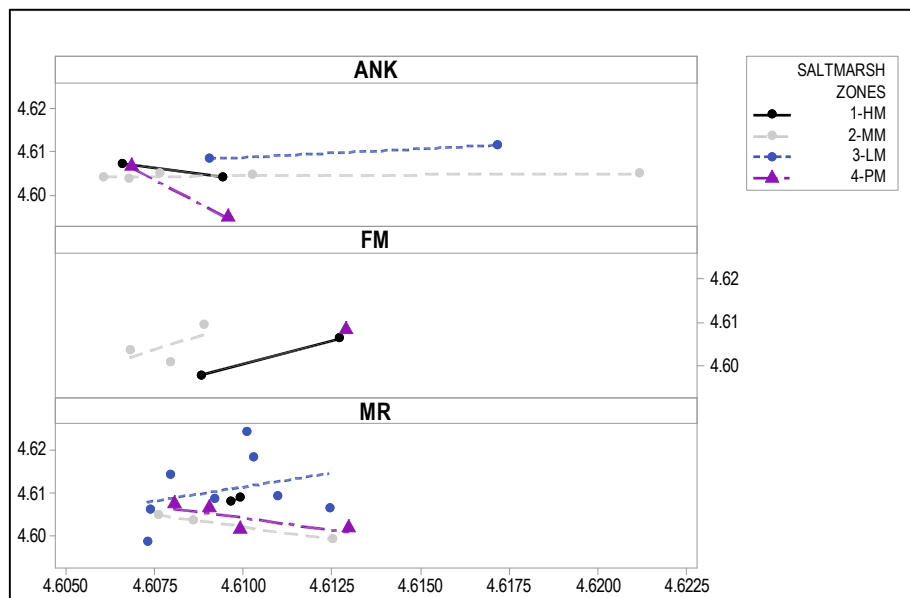


Figure 8-3 Scatterplot between accretion rates (x-axis; logarithmically transformed) sedimentation rates (y-axis; logarithmically transformed) on each site. The scatterplot also includes a regression fit line, which is colour-coded based on the saltmarsh symbol.

Shallow subsidence also suggests further implication, that the natural salt marshes, ANK and FM of Nigg Bay may be gradually submerged. This suggestion is supported by the long-term results presented in Chapter 5. The centennial time-series map recession from 1872 to 2012 (Figure 8-4)



show signs of erosion on the easternmost part of the pioneer zones on both FM and ANK. This is in line with Bouma et al (2014) who found that saltmarsh ecosystems affected by submergence are especially threatened by SLR unless they can migrate landwards and that the ‘drowning’ salt marsh may accrete vertically at same pace as SLR but will get narrower. However, the last 30 years of MHWS movement (1977-2017) observed on ANK and FM salt marshes also imply that there is simply not enough space to move landwards. Migration has been possible by realignment in 2003 for MR salt marsh, but erosion and loss of elevation shown by the DEM (2011-2017). Bouma et al. (2014) and Webb et al. (2013) note that when determining if a marsh will in the future be drowning or not, it is important to account both for sea-level rise and the often ignored shallow subsidence processes. Implications further recognised as critical as by Wolters et al. (2005) and Temmerman et al., (2013).

Subsurface processes that lead to the ‘shallow subsidence’ of deposited material thus play an important role on natural salt marshes and as has been widely reported elsewhere by Kearney et al. 1994 (Chesapeake Bay, USA); Cahoon et al. 1995 (Louisiana, USA); Cahoon et al (2000) (East Anglia) and Spencer et al. (2012). Cahoon et al. (2000) found that the differences of determination of accretion rate and elevation surface change of tidal salt marsh in East Anglia varied among marsh settings of different age and heights but the study also allowed them to assess which of the surface or subsurface processes controls the accretion on the sites. Whereas (Spencer 2012) concluded this is not the case inside the realignment site of Tollesbury and Freiston shore the differences between accretion rate and sedimentation rates were attributable to seasonal variation and that subsurface processes are likely to be less important inside the realignment site, due to the consolidated nature of the underlying substrate. At Nigg Bay, natural salt marshes appears to suffer from shallow subsistence, and, that the managed realignment accretion rate and sedimentation rates differences answers to its topography still in transition from reclaimed agriculture.

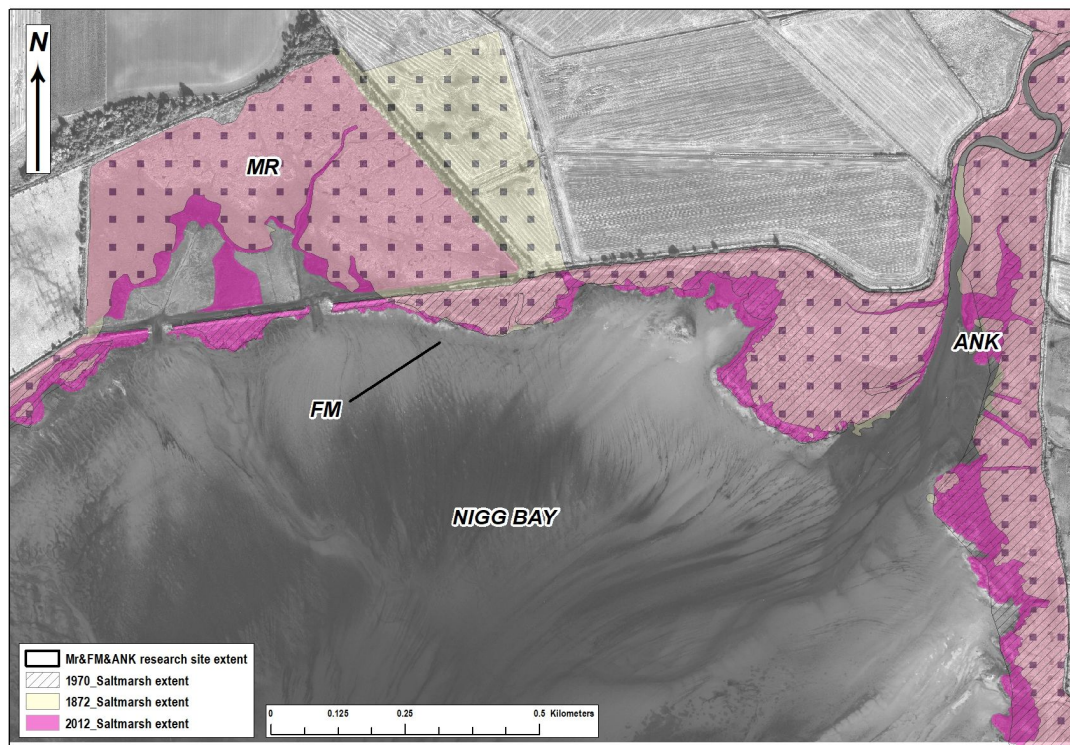


Figure 8-4: Historical saltmarsh extent from 1872 to 2012 as developed in Chapter 5.2.

### 8.2.3 Relationships between aboveground and belowground saltmarsh processes: belowground geomorphic and biological controls on saltmarsh development

Belowground soil organic matter is critical to saltmarsh sustainability via its role in vertical soil accretion which in turn helps salt marsh maintain its relative elevation as sea levels rise (Chmura et al., 2003; Yu and Chmura, 2009; Mudd et al., 2009; Schindler, Karius, Arns, et al., 2014; Van de Broek et al., 2016). Soil and sediments properties govern the strength, consolidation and cohesion required for the long-term stability of the aboveground surface and anthropogenic disturbances on this soil and sediment alter irreversibly the normal functioning of the saltmarsh system (Boorman et al., 2002; Kadiri et al., 2011; Tempest et al., 2015; Spencer et al., 2017). Per se, linkages between belowground, presented in Chapter 6 and 7, and aboveground processes, in Chapter 4 and 5, are addressing three aims of this thesis research: *which mechanism, patterns and processes favour saltmarsh formation and development, how salt marsh can recover from anthropogenic disturbances and how the results can influence saltmarsh ecosystem service capacity* via carbon sequestration.

#### 8.2.3.1 Sedimentary characteristics: Topographic niches and heterogeneity

There was no statistically significant difference observed in grain size and type between natural and managed salt marshes. However, the analysis conducted on a per core basis revealed that finer

silty grains dominating the managed salt marsh MR whilst coarser sands were found on ANK and FM (Chapter 6 - sections 6.2.1.1 and 6.5.1.1). This contrast can be explained by their different position in the tidal frame where tidal flow is tampered in the managed salt marshes with greater distance to the saltmarsh edge and the protection of the sea wall remains. This pattern agrees with Kadiri et al. (2011) results on the Wallasea Island managed realignment scheme showing sediment fining increasing with distance from sea.

Further differences were identified between natural and managed salt marshes at Nigg. While there was no significant difference between natural and managed salt marshes overall, variations were observed within specific zone of the salt marsh. The study revealed that autocompaction/BDD in the natural marshes exhibited higher rates in the upper section of the marsh (ANK's HM and FM's MM) in comparison to the managed realignment area. In the managed realignment area, increased compaction was observed in the PM zones, which receive "new" tidal sediments following the breach of the sea wall in 2003 (chapter 6 - section 6.2.2.1 and 6.5.1.1). Furthermore, the natural salt marshes, ANK and FM, offered a much wider range of grain type and more heterogeneity between their saltmarsh zones than the managed salt marsh. Structure of soil (i.e. BDD and water content) was more homogenous on the managed salt marsh MR (Chapter 6 - sections 6.2.2 and 6.5.1.2 ). These disparities highlight first hydrodynamic dissimilarities of the two saltmarsh systems, and, they also suggest that there are less topographical variations on the managed salt marsh to facilitate a range of sediment to settle. This concept is further developed by Stallins (2006) who outlines that abundance and diversity reflect the local disturbance regime by constructing and reinforcing topographic niches in light of the historic frequency at which disturbance forcings have occurred. As a result of their increased vulnerability exposure to the tidal forcings, ANK and FM salt marsh present more topographic niches having further consequences on sedimentation and vegetation. (Fearnley, 2008) and (Kadiri et al., 2011) comparisons of sediment characteristics between natural and restored salt marshes finding not becoming similar to those in the natural salt marsh.

### 8.2.3.2 Hydrodynamic and geomorphic settings controls physical soil structure and biological soil content

Moreover, the comparative analysis of soil autocompaction (BDD) and water content across the three salt marshes revealed that the realignment of the MR site had a relatively minor impact on soil compaction and drainage (Chapter 5 - 6.5.2.1) compared to typical managed realignments (Boorman, 2003; Tempest et al., 2015). Additionally, the study demonstrated that the pioneer marsh zones displayed a notably greater degree of autocompaction compared to the other marsh zones. This finding was interpreted as a consequence of its proximity to the saltmarsh edge and its

shorter distance to the mean high water springs (MHWS), resulting in frequent submergence of its surface twice daily and affecting its soil structure. Zhang et al. (2001) who identify that high amounts of water movement increases the shear stresses of suspended sediments leading to intensive local soil deformation leading to a surface layer with higher bulk density, lower porosity, lower hydraulic conductivity and increased soil strength. Soil strength is affected by erosion, and tensile strength decreases with low BDD and high-water content. Soil density is crucial for saltmarsh studies.

#### 8.2.3.2.1 Anthropogenic legacy affecting belowground physical soil structure and biological soil content

SOC represents the concentration of carbon stored in the organic matter of the compacted saltmarsh sediments. The findings of the thesis indicate that although there are differences in soil carbon density (SOC) between natural and managed saltmarsh sites, no clear ranking was observed between these sites (Chapter 6 - section 6.3.2 and 6.5.2). Carbon density (SOC) at Nigg Bay indicated instead that the youngest salt marsh, FM which emerged since the 1950's displays the lowest SOC when compared to the managed (MR) and natural (ANK) salt marshes. These results deviate from the majority of research on de-embankment and restored salt marsh in England (Burden et al., 2013; Tempest et al., 2015). These results may confirm that overall carbon density increases with maturity, in agreement with Elschot et al. (2015) work on tidal marsh carbon stocks in Schiermonnikoog back-barrier (Netherlands).

However, differences between the natural and managed salt marshes at Nigg Bay were observed at depth, in water and soil organic carbon density levels. At specific depths through the cores collected on the managed realignment MR and not from FM or ANK, clear depositional sequences were consistently depicted on the profiles. For instance, SOC on the two natural salt marshes, FM and ANK, maintains higher level through soil depth whilst MR's SOC is only found at its highest level at depths of 0-10 and 10-20 cm and is seen to rapidly decrease with depth (Chapter 6 -section 6.3.2). These results are consistent with Tempest et al. (2015) who found a pronounced increase in the top 5 cm of the de-embankment salt marshes in SE England. Furthermore, photographic record confirmed a change in soil discoloration for most of the cores (Chapter 6 -section 6.4 and Figure 6.37). This discoloration could be traced at an increasing depth with elevation height demonstrating, first, that a single event disturbed MR saltmarsh soil zones in the recent past; and, second that sedimentation on MR is directly linked to elevation height and distance from saltmarsh edge. Optically Stimulated Luminescence - OSL (chapter 7 - section 7.5) identified the shift at same depth (e.g. between 9-11 and 13 cm) especially in both B-OSL and Infrared stimulated Luminescence (IRSL) depletion index profiles of core MR8, located in the high marsh, suggesting

underlying changes in environmental conditions or anthropogenic disturbances which can be interpreted as the breaching of the reclaimed land. These layers were not thick enough to impact on the overall content levels, but, were consistent enough to interpret as the legacy of 1950's reclamation on physical and biological processes showing clearly on cores collected on PM and HM a decrease in water content and carbon density. Using 3D-computed X-ray, Spencer et. (2017) have clearly demonstrated the impact of pre-restoration land-use has on sediment structure, hydrology and the sediment geochemical environment in restored salt marshes. This affects plant establishment, nutrient cycling, wild species diversity and hydrodynamics such as flood regulation, ecosystems services restoration scheme are striving to reach. This work completes a series of studies on restored and natural salt marshes, for the most part in SE England, showing that changes in soil properties, such as porosity and bulk density as a consequence of original marsh enclosure, embankment, drainage and subsequent agriculture compaction, is principally due to the dewatering of soil during reclamation which increases soil density and compaction (by decreasing porosity) (Boorman et al., 2002; Kadiri et al., 2011; Tempest et al., 2015; Spencer et al., 2017). This is, then, when tidal flooding is reintroduced, water drainage is hindered by the dense and impermeable underlying old soil, a phenomenon that can be aggravated by clayey sediment or reinforced by plant roots and algae (Boorman et al., 2002). There is, therefore, compelling evidence that a return to tidal inundation on the realigned marsh post breach has not yet resulted in the development of soil characteristics equivalent to that of a natural salt marsh.

#### 8.2.3.2.2 Zonation patterns favouring sedimentary stores

Grain size and type were found significantly different between site and saltmarsh zones where overall coarser grains ( $>125\mu\text{m}$ ) were present on PM zones, silts were principally found on LM and very fine sand ( $>63\mu\text{m}$ ) on MM and HM (Chapter 6 - section 6.2.1 and 6.5.1). This pattern can be further explained by strong association between lithofacies zonation and hydrodynamics of tidal energy found to be typical of siliciclastic systems (Eisma and Dijkema, 1997; French, 2018).

This association between sediments with zonation is further corroborated by strong association between IRSL and distance to the saltmarsh edge and moderate to elevation height and where hydrodynamics present also strong influence with luminescence signal demonstrated by strong correlations to the water flow channels and distance to the water channels (Chapter 7 -7.5.1).

Although aboveground Organic Carbon (OC) found strongly associated with vegetation assemblages (Chapter 4 - section 4.3.3 and 4.5.2), and Soil Organic Carbon density (SOC) varied significantly amongst vegetation assemblages, plant communities were found to explain little of the belowground carbon densities variability (Chapter 6 - section 6.3.2). These findings disagree with Chmura et al. (2003) who found higher SOC with *S. alterniflora* than *S. patens* but accretion



rates. However, the results are based on salt marsh from the Mississippi delta which overall have little similarities with Scottish saltmarsh vegetation. But the Nigg Bay findings also disagree with Schindler, Karius, Deicke, et al. (2014) who found that decomposition of organic matter to be the main driving factor for carbon densities in the Wadden sea. It emerges that geomorphological drivers may control variability in carbon densities in Nigg Bay such as distance to the saltmarsh edge (Chapter 6 - section 6.5.2.2).

Overall, belowground carbon storage was found to be significantly lower in the most exposed part of the marsh, PM zones, and higher in LM zones decreasing in carbon content landwards and with elevation. This pattern is presented by Chmura et al. (2001) who found that distinct sequestration rates on different elevational zones was due to rapid sediment deposition on lower elevation the sequestration rates were higher. This pattern was exhibited in the mature natural salt marsh ANK but a reverse trend was observed on FM and MR with highest SOC found on the HM and lowest on LM. Van de Broek et al. (2016) found high SOC in HM and low SOC in LM in the Scheldt estuary (Belgium and Netherlands) attributing carbon concentration to salinity gradient. Connor et al (2001) have also found such variability where carbon densities increased seawards from HM to LM for saltmarsh sites in the upper Bay of Fundy whilst salt marshes in the outer bay decreased seawards from HM to LM. Schindler, Karius, Deicke, et al. (2014) further attribute higher rates of organic matter accumulation within the upper soil to be related to less organic litter which is removed of the marsh surface due to an irregular flooding. The observed variations in organic matter and organic carbon density at Nigg Bay can be primarily attributed to the distinct physical characteristics exhibited by each salt marsh, as evidenced by sedimentary properties like grain size. Notably, grain size has been identified as a key predictor of carbon storage.

The discussion has dissected the importance of variability in time and space and should be considered when modelling and predicting future accretion rates in tidal salt marsh. But, in a broader perspective, can these short-term results quantified aboveground appraise: i) some of the regulating and supporting services salt marsh provide; ii) Nigg Bay saltmarsh capacity to SLR?

### **8.3 Carbon accumulation and sea level rise: Implications for saltmarsh response to climate change**

Which processes, mechanisms and patterns promote saltmarsh formation and development? Can the recent and past-trends of ecological and physical changes on the natural and managed salt marshes help to predict Nigg Bay saltmarsh stability and future development?

The carbon that is stored in salt marshes and other coastal ecosystems, commonly referred to as "Blue Carbon," is among the various ecosystem services that are examined in Chapter 2, Section



2-2.3. This section also highlights the risks associated with a significant rise in sea levels, climate change, and the escalating severity and frequency of extreme events. It also addresses the challenges posed by erosion, drowning, and the depletion of sediment, as well as the direct and indirect impacts of structures such as embankments, ditches, and barriers (Doody, 2008; Stahl, 2012; Beaumont et al., 2014). Furthermore, it acknowledges that salt marshes and coastal ecosystems are currently experiencing challenges on the services they can offer (Spencer et al., 2017). The objective of my thesis research was to enhance comprehension of the expanding body of literature concerning saltmarsh Blue carbon, a crucial regulatory ecosystem service. Specifically, I focused on three salt marshes located at Nigg Bay in order to evaluate the sustainability of the saltmarsh carbon sink in light of the recent sea level rise observed in Scotland.

### **8.3.1 Soft engineering approach (section 2.5) for new carbon stores**

Recognised only very recently as significant carbon sinks (Connor et al., 2001; Chmura, 2013), tidal salt marshes are the most productive ecosystem of the world contribution to c. 20 % of the net total of primary productivity (Bouchard and Lefevre, 2000). The absence of oxygen in saltmarsh soils allows carbon sequestered by plants to transfer a small fraction to the marine waters and in sediments via burial. This carbon is cycled over a short term (decennial) in biomass and slowing decaying biomass into peat and over longer (millennial) time scales in sediments. Scottish salt marshes are estimated to have an average sequestration potential of 14200 t.C.yr<sup>-1</sup> (0.014 Mt C yr<sup>-1</sup>) (Burrows et al., 2014), estimates based on Chmura, 2003 and Duarte *et al.*, 2005 work who estimated an average sequestration capacity of 218±24 g C m<sup>-2</sup> yr<sup>-1</sup> (or 2.1 Mg C ha<sup>-1</sup>) (McLeod et al., 2011). However, estimations of the long-term carbon sequestration are highly variable due to the hydroperiod, salinity or sediment supply, and, also plant species, plants composition and decomposition and primary productivity (Chmura, 2013). According to the research conducted by Mossman et al. (2022), a significant increase in carbon accumulation was observed following the breach of the flood defence embankment at the Steart marshes managed realignment site in Somerset, UK. The researchers discovered that the accumulation of carbon was 50 times higher than the estimated direct carbon expenses that were incurred during the construction of the site. The total organic carbon contents were measured to be 19.4 t.C.yr<sup>-1</sup>.

#### **Aboveground Carbon stocks**

Potentially important mechanism for climate mitigation, salt marsh can play an important role as carbon sinks counteracting rapid increase atmospheric carbon dioxide concentration owing to close feedbacks, that takes place on salt marsh, between vegetation, sedimentation and anoxic conditions, promoting carbon storage (Andrews et al., 2006; Kirwan and Mudd, 2012; Fagherazzi, 2013).

Overall aboveground organic carbon retained in saltmarsh vegetation was not different between natural and managed salt marshes. NVC assemblages and vegetation height are also significantly influencing aboveground organic content. SM16a (*Festuca rubra* dominant and *Puccinellia mar.* sub community) and SM13a type (*Puccinellia mar.* as main and dominant sub community) in the low marsh were found to have the highest level of aboveground carbon content (Chapter 4- section 4.3.3). Biological predictors of these assemblages were found to be associated to vegetation height. These findings concur with Burden et al. (2013) study on carbon sequestration in the Tollesbury, SE England, which found aboveground biomass on arable land (on former high-shore salt marsh) and a managed realignment restoration site were similar to the natural site but demonstrated approximately twice as much plant biomass compared to the natural due to its dominant *Puccinellia mar.* vegetation, and therefore lacking dynamic ecosystem properties. Meirland et al. (2015) have also found that plant species richness increases with vegetation age in the Bay of Somme and predicted that richness increases in association with higher sedimentation rates to counteract sea-level rise until the latter reaches a critical rate that drowns the saltmarsh vegetation.

### **Belowground Carbon Stocks**

In general, the quantity of belowground organic carbon stored in saltmarsh vegetation was found to be similar between natural and managed salt marshes. However, there was a notable disparity in soil organic carbon (SOC) levels among the different vegetation communities. The SM16d (*Festuca rubra* dominant and *Puccinellia mar.* sub community) community exhibits the highest levels of soil organic carbon (SOC), while the SM13b community, characterised by the dominance of *Puccinellia maritima* and the presence of the *Glaux maritima* sub-community, is found in the mid-marsh (MM) zone (Chapter 4- section 4.3.3). Overall carbon densities were found to increase with distance from the saltmarsh edge in soil with low autocompaction and finer grain size.

A study conducted by Miller et al. (2023) on Scottish salt marshes has produced detailed information on two salt marshes in Moray Firth, where Cromarty Firth and Nigg Bay are situated, at Dornoch point and Morrich More. The aboveground carbon storage of Nigg Bay salt marshes has lower carbon content  $1.8 \text{ t.C.yr}^{-1}$  compared to the Moray Firth dataset with  $2.4 \text{ t.C.yr}^{-1}$  (Chapter 4 - Figure 4-70). Belowground carbon density were found comparable for MR and ANK at  $2.4 \text{ t.C.yr}^{-1}$  to Dornoch point and Morrich More salt marsh (Chapter 6- Figure 6-41). Nigg Bay carbon densities results have been found to be close to carbon densities found in the Outer Bay of Fundy with an average (low and high marsh zones combined) of  $0.0247 \text{ g.Ccm}^{-3}$  (Connor et al., 2001) and compared to an overall average of  $0.025 \pm 0.001 \text{ g.Ccm}^{-3}$  at Nigg. These findings are lower from Chmura et al. (2003) synthesis work on 154 mangrove and saltmarsh sites providing an

average soil carbon density of  $0.039 \pm 0.003 \text{ g.Ccm}^{-3}$ . This further suggests that northern latitude and shorter growing seasons may impede the carbon capacity of saltmarsh sediments.

the findings from the study conducted in Nigg Bay indicate a comprehensive blue carbon stock estimate of  $4.37 \pm 0.12 \text{ tC.ha}^{-1}$  across the three salt marshes examined. Additionally, the analysis reveals a sequestration capacity of  $5.86 \pm 0.17 \text{ tC.ha}^{-1}\text{.yr}^{-1}$ , based on the accretion rates obtained from the filter discs dataset. The findings of Mossman et al. (2022) indicate a significantly greater value than the Nigg Bay salt marsh observation. The aboveground carbon content in Nigg Bay accounts for approximately  $43.1 \pm 1.09\%$  of the total Blue Carbon budget, which has an average value of  $1.9 \pm 0.07 \text{ tC.ha}^{-1}$ . In comparison, the Soil Blue Carbon has an average value of  $2.5 \pm 0.1 \text{ tC.ha}^{-1}$ , considering an average depth of  $49.9 \pm 2.7 \text{ cm}$ . The estimates for aboveground carbon content align closely with the findings of Burden et al. (2013) in their study on natural and managed realignment salt marshes in Tollesbury, Essex. Additionally, the belowground soil carbon pool exceeds the estimates provided by Chmura et al. (2003) of  $2.1 \text{ tC.ha}^{-1}$ . Furthermore, the burial rate capacity falls within the range of 4.8 to  $87.2 \text{ tC.ha}^{-1}\text{.yr}^{-1}$ .

The highest stock per hectare is on the natural salt marshes, ANK and MR, averaging respectively at  $4.3 \pm 0.25 \text{ tC.ha}^{-1}$  (55 cm in depth) and  $4.4 \pm 0.294 \text{ tC.ha}^{-1}$  (40cm in depth) and lowest on the managed salt marsh MR with a stock average of  $3.5 \pm 0.23 \text{ tC.ha}^{-1}$  (58 cm in depth) (Figure 8-5). The highest carbon stores were found on MR's mid-marsh ( $8.3 \text{ tC.ha}^{-1}$ ), then ANK's low marsh ( $5.6 \text{ tC.ha}^{-1}$ ) and FM's HM ( $4 \text{ tC.ha}^{-1}$ ). These results depart slightly from Burden et al. (2013) who found at Tollesbury the lowest pool on the natural and restored low shore sites ( $1.3$  and  $1.1 \text{ tC.ha}^{-1}$  respectively) and highest on natural high marsh  $3.1 \text{ tC.ha}^{-1}$ .

**Table 8-2: Accretion rates Filter disc in cm yr-1 and Total Soil Carbon Store Soil in tC.ha-1**

<b>Total Soil Carbon Store in tC.ha-1</b>						
	<b>ANK</b>		<b>FM</b>		<b>MR</b>	
	<b>Mean</b>	<b>SD</b>	<b>Mean</b>	<b>SD</b>	<b>Mean</b>	<b>SD</b>
overall	<b>4.33</b>	2.49	<b>3.47</b>	1.66	<b>4.41</b>	3.31
<b>HM</b>	<b>2.99</b>	3.00	<b>4.04</b>	1.51	<b>5.09</b>	2.87
<b>MM</b>	<b>4.87</b>	1.45	<b>2.59</b>	1.38	<b>8.25</b>	6.44
<b>LM</b>	<b>5.57</b>	2.68			<b>4.20</b>	2.18
<b>PM</b>	<b>3.95</b>	2.55			<b>3.09</b>	1.71

<b>Filter Discs Accretion Rates in cm yr<sup>-1</sup></b>						
	<b>Mean</b>	<b>SD</b>	<b>Mean</b>	<b>SD</b>	<b>Mean</b>	<b>SD</b>
overall	<b>1.47</b>	2.62	<b>1.07</b>	2.49	<b>1.36</b>	1.87
<b>HM</b>	<b>0.81</b>	1.53	<b>1.18</b>	2.44	<b>1.40</b>	1.68
<b>MM</b>	<b>2.65</b>	3.62	<b>0.35</b>	0.28	<b>1.42</b>	2.95
<b>LM</b>	<b>0.43</b>	0.69			<b>1.18</b>	1.23
<b>PM</b>	<b>0.86</b>	1.11			<b>1.65</b>	1.75

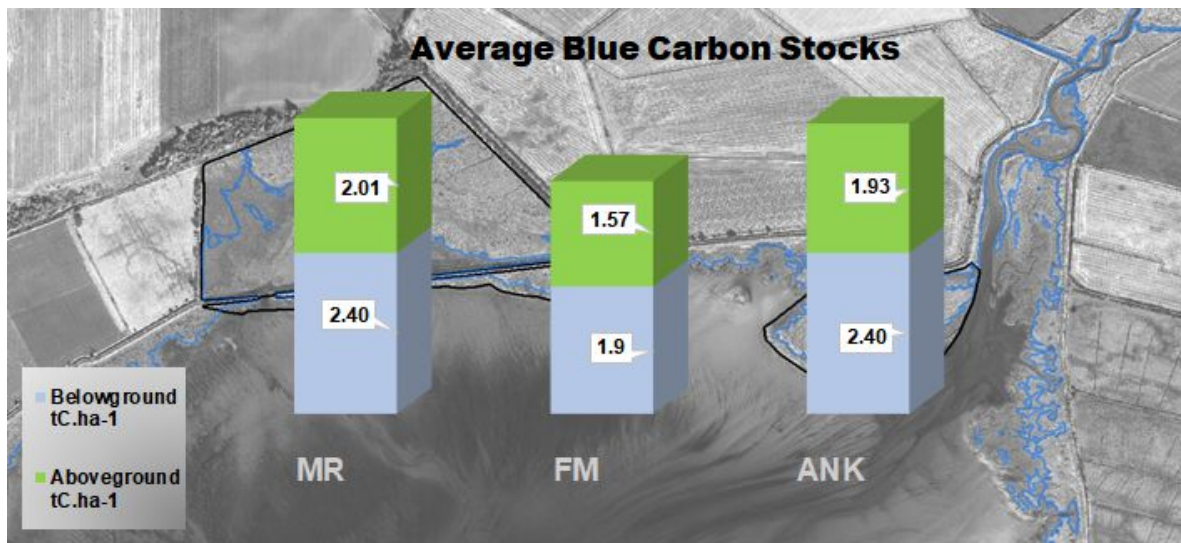


Figure 8-5: Average Blue Carbon stock in tC.ha<sup>-1</sup> for the three studied salt marshes demonstrating significance difference between the natural, ANK, and managed salt marsh, MR ( $F=3.3, p<0.05^*$ ).

Owing to their size, MR holds the highest Carbon stock ( $59\pm 5.3$  tC) followed by ANK ( $22.3\pm 2.4$  tC.ha<sup>-1</sup>) and FM ( $7.8\pm 1.1$  tC) exhibiting an overall potential of  $94.9\pm 0.2$  tC for the three studied salt marshes at Nigg Bay for the upper 50 cm of soil depth (Figure 8-6). Kirwan and Mudd (2012) suggest that in the first half of the twenty-first century, climate change, i.e. increase temperature and SLR, would increase carbon burial rates in a scenario where high temperature increases biomass and therefore organic matter through decomposition and eventually carbon stock densities, but that carbon–climate feedbacks will diminish over time up to a threshold the system cannot sustain.

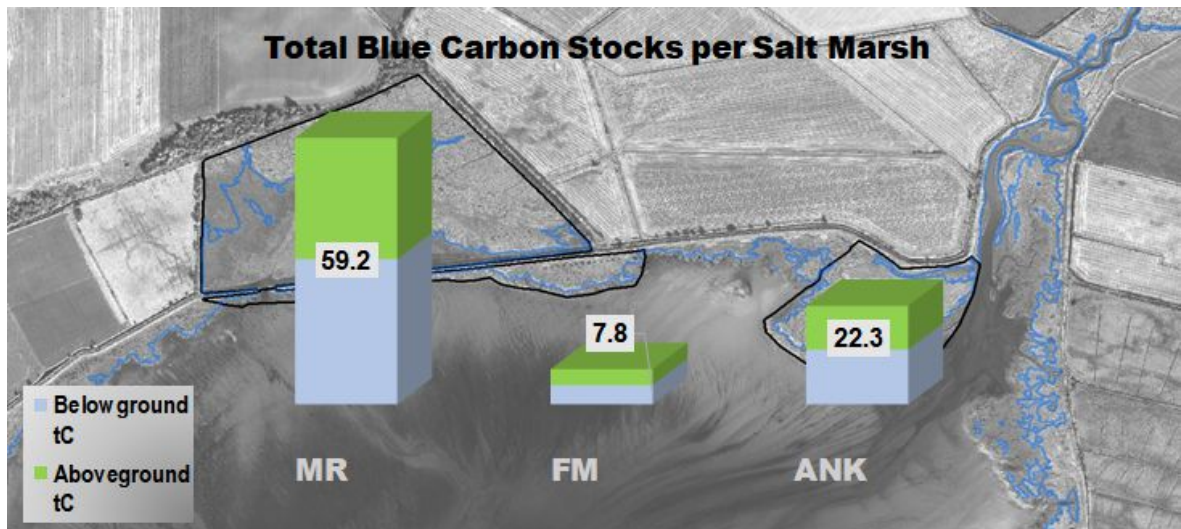


Figure 8-6: Average Blue Carbon stock in tC for each salt marsh at average soil depths of 40 cm (MR), 58 cm (FM) and 55 cm (ANK).

Because of the impossibility for Nigg Bay natural salt marshes to move landwards due to the existing sea wall, further realignments along the north coast of Nigg Bay may prevent irremediable consequences due increasing RSLR (see next). While this study indicates that the MR site at Nigg



Bay does not exhibit all the features typically found in a natural salt marsh, it does serve as a habitat refuge and has the potential to contribute to the formation of new blue carbon stores. Figure 8-7 shows three areas which could store c. 272.4 tC for c.60 cm in depth using carbon sequestration rates from this study for the managed realignment MR ( $3.47 \pm 0.294 \text{ tC} \cdot \text{ha}^{-1}$ ). Managed realignment of the Humber estuary was found to significantly enhance the carbon sequestration (150%) and reduce concentrations of nutrients (83-50%) and contaminant metals in the estuary (Andrews et al., 2006). Adam et al. 2002 conclude that, despite being net sources of CH<sub>4</sub> and N<sub>2</sub>O, MR sites provide regulatory service as sustainable coastal defence options with significant biogeochemical value and can sequester carbon and reduce estuarine nutrient loads (Adams et al., 2012). According to Robins et al. (2016), it has been observed that the United Kingdom exhibits a tendency to prioritise the protection of urban areas. In light of this, the authors suggest the implementation of local adaptation strategies that emphasise the utilisation of soft engineering techniques and the enhancement of community awareness.

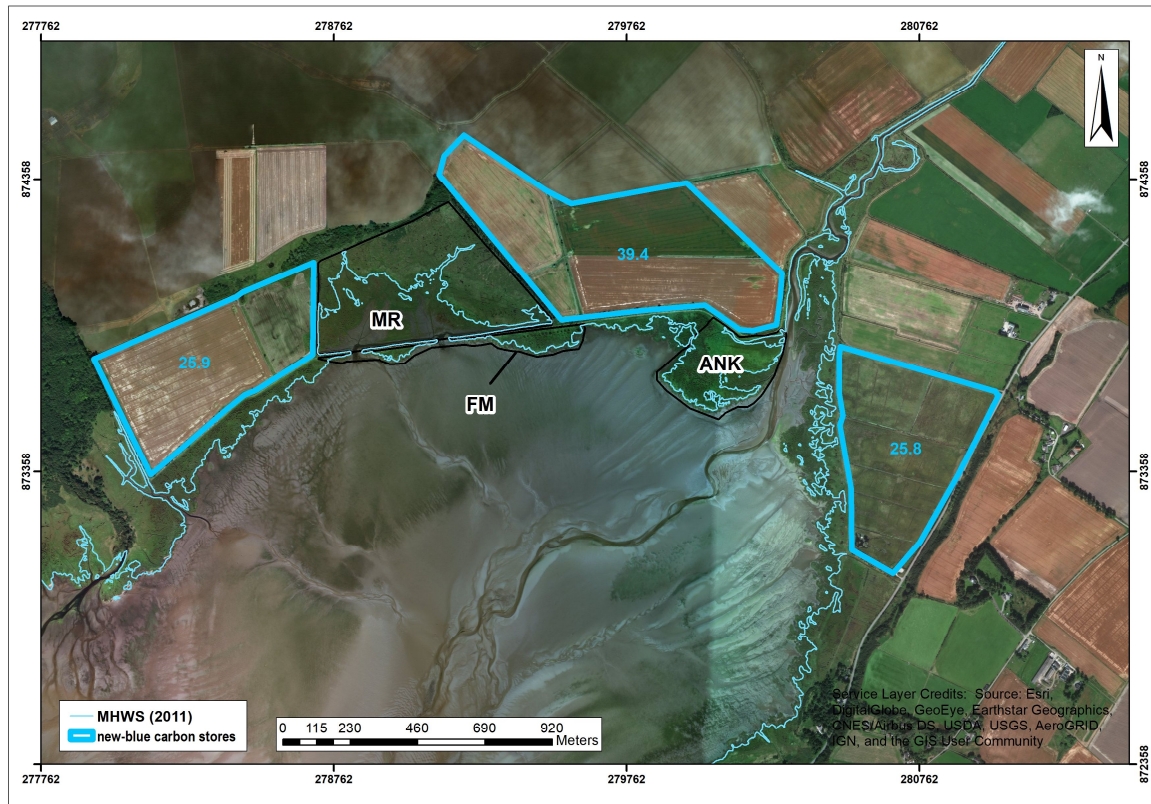


Figure 8-7: Possible new realignment in Nigg Bay accommodating space the natural salt marshes and new blue carbon stores.

However, these results are only estimates and consideration should be given to the rate of change and flux of a carbon stock as the saltmarsh carbon, similarly to sea grasses and mangroves, accumulates, stabilise, or erode. Net Ecosystem Production (NEP) is calculated as the difference between gross primary production (GPP; photosynthetic CO<sub>2</sub> uptake) and ecosystem respiration

(ER; production of CO<sub>2</sub> by plants and microbial decomposition of organic matter). (Howard et al., 2014; Macreadie et al., 2014).

### **8.3.2 The vertical accretion rates at the Nigg Bay salt marshes: new adaptation to sea-level rise?**

Saltmarsh adaptability and resilience have been recognised to be influenced by tidal range, inundation frequency, sediment availability and its transport (Allen 2000, D'Alpaos et al. 2007, Kirwan et al. 2010, Andersen et al. 2011, D'Alpaos et al. 2011) as well as on rates of subsidence (Vink et al. 2007) and autocompaction (Cahoon et al. 2006). These processes are linked to the balance between relative sea level and vertical accretion of the marsh via sedimentation. Salt marshes will retreat if relative sea level rise (RSLR) exceeds the ability of marsh vertical accretion to keep pace with the rise (Horton et al., 2018). In a saltmarsh system where landward migration is limited, perhaps by a wall or embankment, the long-term balance of the system is primarily constrained by rates of Sea Level Rise (SLR) and positive vertical sedimentation rate (Friess et al., 2011).

#### **The vertical accretion rates at the Nigg Bay salt marshes**

The most recent assessment of salt marsh and UK Relative Sea Level Rate (RSLR) predictions for 2020, 2040 and 2090 was compiled using Holocene relative sea level data to explore the limits to marsh vulnerability (Horton et al. 2018). They estimated a greater than 80% probability of marsh retreat for all Great Britain under Representative Concentration Pathway (RCP) 8.5 by 2100, with areas of southern and eastern England (areas of Glacial Isostatic Adjustment - GIA subsidence) achieving this by 2040. It should be noted that these predictions are based on long term Holocene rates derived from core data and with relatively limited modern salt marsh accretion data, particularly for Scotland. Nevertheless, the data shows that with Holocene RSLR of between -7.7 to 15.2mm/yr., UK salt marshes were 9 times more likely to retreat when RSLR rates were greater than or equal to 7.1mm/yr. Given that the world is on track for RCP 8.5, predictions that rely on lower RCP's are likely proven to be gross underestimates (RCP8.5 was intended to be a "very high baseline emission scenario" representing the 90th percentile of no-policy baseline scenarios available at the time). In any case, accretion rates are likely to accelerate or at least increase with the increased hydroperiod as a result of RSLR.

In Chapter 2, a recent analysis of Scottish tide gauge records compared the rate of long-term rate of relative land and sea level change derived from tide gauges up to 2007 with the rate of short-term trend rate spanning over 15 years of data from 1992-2007. This work strongly suggested that the current relative sea level rise (RSL) rates of between 2.6 and 6.2 mm/year now outpaces glacio-



isostatic uplift across Scotland and that all Scottish coastal landforms are now subject to rising sea levels (Rennie and Hansom, 2011). So, the current maximum tide gauge rates now approach those of the Holocene core rates and suggest salt marshes may already be in or approaching an erosional state. Between 1992-2007, the RLSR in the Cromarty Firth area lay between 3 and 4mm yr<sup>-1</sup> (Rennie and Hansom, 2011). UKCP 18 (Appendix A-3) provides for Dornoch Firth, within Moray Firth like Cromarty Firth, a RSLR anticipated to be reached by 2050 under RCP8.5 (95% probability) which is 30 cm or 6 mm.yr<sup>-1</sup>. For Nigg Bay salt marshes to keep pace with current RSLR then they need to be averaging 3-4 mm.yr<sup>-1</sup> and this needs to rise to 6 mm yr<sup>-1</sup> by 2050 to keep pace. The vertical accretion rates of the salt marshes in Nigg Bay, as determined by the mean rate of sediment deposition over one year, were observed to vary among the three salt marshes. The estimated mean rate of vertical accretion was 1.3±0.1 cm.yr<sup>-1</sup>. The young and natural fronting salt marsh FM had the lowest accretion rates (1.1±0.3 cm.yr<sup>-1</sup>) compared to the natural salt marsh ANK (1.5±0.3 cm.yr<sup>-1</sup>) and the managed realignment MR (1.4±0.2 cm.yr<sup>-1</sup>). The observed rates of accretion are sufficiently high to match the rates of relative sea level rise (RSLR). Nevertheless, the observed variations in sedimentation rates across different saltmarsh zones indicate inadequate sediment retention in specific areas. Specifically, the western portion of the middle and high marshes on the natural salt marsh ANK, the eastern portion of the fronting salt marsh FM, and the eastern portion of the high and low marshes on MR exhibit insufficient sediment retention. The depiction of higher sea-level rise scenarios in Chapter 4 - Figure 4-70 reveals a concerning situation, wherein the accretion rates across the salt marshes indicate a significant threat to these areas of FM, MR, and ANK.

Sedimentation plates record from the 2.2 years of monitoring showed an overall positive sedimentation from July 2015 to September 2017 at a rate of 0.21±0.03 cm.yr<sup>-1</sup>. However, these sedimentation rates are not uniform across the salt marshes of Nigg Bay ranging 0.01±0.04cm.yr<sup>-1</sup> on ANK, -0.09±0.16 on FM and 0.33±0.03 cm.yr<sup>-1</sup> on MR and current RSLR rates of currently 3 mm.yr<sup>-1</sup> would be destructive to c.68 % marshes as depicted on Chapter 5- Figure 5-47, but predictions estimate a rise to 6mm.yr<sup>-1</sup> and beyond in the future, suggesting that approximately 82 % of the marsh may be under serious threat in the future.

However, section 8.2.2 above has shown that subsurface processes can strongly influence elevation change and therefore saltmarsh capacity to adapt to SLR (Cahoon et al., 2000). Furthermore, increased inundations by RSLR, if sediment supply is plenty, will prompt accelerated accretion. This was observed by Teasdale et al. (2011) in the west-north-west coast of Scotland, where since the 1970's have exhibited a significant accelerating trend. However, if the marsh cannot migrate landward then it may well elevate rapidly but get eroded along its front. According to Esteves (2014) the transformation of mudflats into salt marshes serves as an indication that

coastal squeeze is unsustainable. Schuerch et al. (2018) suggest that resilience of salt marshes globally is primarily driven by the availability of accommodation space, which is strongly influenced by the building of anthropogenic infrastructure in the coastal zone and which has been demonstrated in this research study.

#### **8.4 Recommendations for future research**

This research has raised a number of issues which can only be resolved through further study.

1. The research would benefit from incorporating wind and wave datasets in conjunction with water level data as additional physical factors influencing accretion and sedimentation rates.
2. According to a recent study conducted by Schuerch et al. (2019), a logical progression in enhancing the accuracy of salt marsh resilience prediction would involve extending the scope of measurements to encompass the morphology and long-term evolution of the neighbouring mudflats.
3. Results of the short-term sediment deposition and lateral movement of saltmarsh edge in this research prompt to further investigation of biogeomorphological resilience of the pioneer zones. Such research should aim to quantify the rate at which plant species, such as Annual *Salicornia* (which has been observed in Nigg Bay) and *Salicornia* microspecies (which is currently absent in Scotland), develop, shift, or erode along the margins of mudflats and saltmarsh edges over a period of multiple years (e.g., every 2 years). This investigation should also consider seasonal variations, such as differences between winter and summer, as well as the influence of sediment deposition and lateral movement of the saltmarsh edge.
4. The monitoring of sedimentation rates typically occurs over timescales of less than a decade. According to Spencer et al. (2012), there is a significant benefit in expanding the observation of sedimentation rate to timeframes spanning multiple decades. Therefore, to utilise the findings of this study as a foundation for further investigation, ensuring ongoing monitoring of sedimentation rates in subsequent years across both natural and MR (man-made and restored) sites.
5. Further examination of the influential factors contributing to the variations observed in sediment, soil bulk density, and water content is warranted. This analysis should be conducted for each core and at various depths.
6. The findings from the analysis of short-term sediment deposition indicate a significant fluctuation in sediment accumulation patterns throughout different seasons. Additional examination utilising X-ray analysis and laminae counting of sediment cores has the potential to shed light on the historical patterns of seasonality in the marsh ecosystem. Moreover, it may serve as a means to identify extreme events that can be indicative of climate change.

7. In order to validate certain interpretations presented in Chapter 7, it would be advantageous to conduct parallel analyses and comparisons of the findings with  $^{137}\text{Cs}$  and  $^{210}\text{Pb}$  chronologies.
8. Finally, building on the work carried out in luminescence studies and development of new OSL application, my study has confirmed that there is enough sensitivity to read luminescence within young and well-characterised sediments. To study this further, it would be valuable to extend the work to include light-protected samples of freshly deposited material associated with periodic flooding events. This will, of necessity, entail studying small samples from suspended sediments and filter mats for which the enhanced sensitivities developed in the work reported here will be critical. A unique training set of samples covering all the spring tides between February 2016 and February 2017 was gathered in association with this research programme. Now that the measurement systems have been developed to record stimulated luminescence from very young material with high sensitivity a future research project to explore the temporal and spatial variations in freshly deposited material would be possible. This work would enable tracking of real-time system dynamics, which has been forecast to increase in severity and extreme event frequency (Intergovernmental Panel on Climate Change (IPCC 2014 and 2018)).

## 8.5 Conclusions

Overall, my thesis has conducted a comprehensive biogeomorphological evaluation of the first managed realignment in Scotland subsequent to its breach in 2003, with a comparative analysis of two neighbouring natural salt marshes over varying temporal scales. The study utilised a methodology to evaluate salt marshes that are at managed and anthropogenically modified, as well as those that are in their natural state, across various time periods. The findings from my thesis research indicate that natural salt marshes possess limited capacity to adapt to environmental changes, thereby impacting their long-term resilience. The ability of this marsh to adapt to relative sea level rise is facilitated by the accommodation space created through managed realignment.

The initial analysis utilising physical elevation data lies in the comprehensive collection of precise and accurate laser scanned primary data. This data was gathered repeatedly over a span of three years, with monthly measurements taken for twelve of these months. Furthermore, the data was obtained using a spatially distributed sampling design that covered all three sites. The short-term data, spanning from monthly to interannual intervals, presented in this study offer a distinctive dataset at this specific location. Furthermore, the methodology provide a well-defined and replicable methodology that can be employed in other research settings. The short-term data from Chapters 4 and 5 were subsequently compared to historical time series data, which consisted of 29 sediment cores (as discussed in Chapters 6). Additionally, a novel approach involving high

sensitivity luminescence profiling methods was developed in Chapter 7 to trace processes in recent sedimentary deposits. Through the integration of high-resolution repeat field monitoring of sedimentation with luminescence data, it becomes possible to ascertain the occurrence of sediment bleaching during low tide or when the sediment is submerged. This is unprecedented in luminescence analysis. The study also encompassed the introduction and characterization of a novel hypersensitive system designed for the measurement of signals in recently deposited sediments, utilising portable equipment developed at SUERC. Additionally, a thorough assessment of calibration methods for samples presented on planchettes was conducted. This study has provided evidence that recent coastal beach sediments, with an age of approximately 50 years, can serve as a reliable indicator of coastal processes occurring within shorter timeframes ranging from months to years, as opposed to longer timescales spanning decades. This represents a ground breaking advancement in the field of luminescence analysis. This study showcases the potential utilisation of luminescence process tracing in areas where conventional tracers like  $^{137}\text{Cs}$  and  $^{210}\text{Pb}$  are not accessible. This facilitates the expansion of regional analyses within the saltmarsh science community and the development of a novel tool for tracking short-term sediment deposition. This advancement enables a more comprehensive examination of contemporary sediment materials, thereby facilitating the assessment of forthcoming alterations within saltmarsh ecosystems.

This investigation is particularly significant in light of recent forecasts indicating a rise in the intensity and frequency of extreme events and weather patterns. This study contributes a significant Scottish perspective to the expanding body of literature on the challenges of MR sites in reproducing the natural salt marsh function and providing the anticipated ecosystem services.



# References

ABPmer 2008. Atlas of UK Marine Renewable Energy Resources. Available from: <http://www.renewables-atlas.info/>.

Adam, P. 1990. *Saltmarsh ecology* (Cambridge University Press, ed.).

Adam, P. 2002. Saltmarshes in a time of change. *Environmental Conservation*. **29**(01), pp.39–61.

Adams, C.A., Andrews, J.E. and Jickells, T. 2012. Nitrous oxide and methane fluxes vs. carbon, nitrogen and phosphorous burial in new intertidal and saltmarsh sediments. *Science of the Total Environment*. **434**, pp.240–251.

Aitken, M.J. 1989. Luminescence Dating: a Guide for Non-Specialists. *Archaeometry*. **31**, pp.147–159.

Aitken, M.J. 1998. *An introduction to Optical Dating. The dating of Quaternary sediments by the use of Photon-Stimulated Luminescence*. Oxford University Press.

Aitken, M.J. and Smith, B.W. 1988. Optical dating: Recuperation after bleaching. *Quaternary Science Reviews*. **7**(3–4), pp.387–393.

Allen, J.R.L. 1990. Salt-marsh growth and stratification: A numerical model with special reference to the Severn Estuary, southwest Britain. *Marine Geology*. **95**(2), pp.77–96.

Allen, J.R.L. 2000. Morphodynamics of Holocene salt marshes: A review sketch from the Atlantic and Southern North Sea coasts of Europe. *Quaternary Science Reviews*. **19**(12), pp.1155–1231.

Allen, J.R.L. and Dark, P. 2007. Seasonality of modern pollen and sediment deposition in an estuarine context: the Severn Estuary Levels, southwest England. *Journal of Quaternary Science*. **23**(3), pp.213–228.

Allen, J.R.L. and Duffy, M.J. 1998. Medium-term sedimentation on high intertidal mudflats and salt marshes in the Severn Estuary, SW Britain: The role of wind and tide. *Marine Geology*. **150**(1–4), pp.1–27.

Allen, J.R.L. and Pye, K. 1992. *Saltmarshes: Morphodynamics, Conservation and Engineering Significance*.



Alongi, D.M. 2008. Mangrove forests: Resilience, protection from tsunamis, and responses to global climate change. *Estuarine, Coastal and Shelf Science*. **76**(1), pp.1–13.

Altieri, A.H., Bertness, M.D., Coverdale, T.C., Axelman, E.E., Herrmann, N.C. and Lauren Szathmary, P. 2013. Feedbacks underlie the resilience of salt marshes and rapid reversal of consumer-driven die-off. *Ecology*. **94**(7), pp.1647–1657.

Andersen, I. 2021. UNEP Annual report. *Unep.*, pp.1–13.

Andrews, J.E., Burgess, D., Cave, R.R., Coombes, E.G., Jickells, T.D., Parkes, D.J. and Turner, R.K. 2006. Biogeochemical value of managed realignment, Humber estuary, UK. *Science of the Total Environment*. **371**(1–3), pp.19–30.

Anon 2013. *AR5 - Citations for IPCC 2013*.

Armitage, S.J. and Bailey, R.M. 2005. The measured dependence of laboratory beta dose rates on sample grain size. *Radiation Measurements*. **39**(2), pp.123–127.

Artigas, F., Shin, J.Y., Hobble, C., Marti-Donati, A., Schafer, K.V.R. and Pechmann, I. 2015. Long term carbon storage potential and CO<sub>2</sub> sink strength of a restored salt marsh in New Jersey. *Agricultural and Forest Meteorology*. **200**, pp.313–321.

Aspinall, R., Green, D., Spray, C., Shimmield, T. and Wilson, J. 2011. *Status and Changes in the UK Ecosystems and their Services to Society: Scotland. The UK National Ecosystem Assessment Technical Report - Chapter 19*. [Online]. Available from: [papers2://publication/uuid/A50F33AC-CDEA-4BD9-BA5F-0D1585C3CBF9](https://publications.ec.europa.eu/publication/uuid/A50F33AC-CDEA-4BD9-BA5F-0D1585C3CBF9).

Baaij, B.M., Kooijman, J., Limpens, J., Marijnissen, R.J.C. and van Loon-Steensma, J.M. 2021. Monitoring Impact of Salt-Marsh Vegetation Characteristics on Sedimentation: an Outlook for Nature-Based Flood Protection. *Wetlands*. **41**(6).

Bai, J., Zhang, G., Zhao, Q., Lu, Q., Jia, J., Cui, B. and Liu, X. 2016. Depth-distribution patterns and control of soil organic carbon in coastal salt marshes with different plant covers. *Scientific Reports*. **6**(October), p.34835.

Baily, B. 2011. Ordnance Survey data collection and the mapping of tidal features - a review of policy, methods and potential analysis. *Sheetlines*. (90), pp.4–17.

Baily, B. and Inkpen, R. 2013. Assessing historical saltmarsh change; an investigation into the reliability of historical saltmarsh mapping using contemporaneous aerial photography and cartographic data. *Journal of Coastal Conservation*. **17**(3), pp.503–514.

- Baily, B. and Pearson, A.W. 2007. Change Detection Mapping and Analysis of Salt Marsh Areas of Central Southern England from Hurst Castle Spit to Pagham Harbour. *Journal of Coastal Research*. **236(6)**, pp.1549–1564.
- Balke, T., Herman, P.M.J. and Bouma, T.J. 2014. Critical transitions in disturbance-driven ecosystems: Identifying windows of opportunity for recovery. *Journal of Ecology*. **102(3)**, pp.700–708.
- Balke, T., Stock, M., Jensen, K., Bouma, T.J. and Kleyer, M. 2016. A global analysis of the seaward salt marsh extent : the importance of tidal range. *Water Resources Research*. **52(5)**, pp.3775–3786.
- Ball, D.F. 1964. Loss-on-ignition as an estimate of organic matter and organic carbon in non-calcareous soils. *Journal of Soil Science*. **15(1)**, pp.84–92.
- Ballarini, M., Wallinga, J., Wintle, A.G. and Bos, A.J.J. 2007. Analysis of equivalent-dose distributions for single grains of quartz from modern deposits. *Quaternary Geochronology*. **2(1–4)**, pp.77–82.
- Baptist, M.J., de Groot, A. V. and van Duin, W.E. 2016. Contrasting biogeomorphic processes affecting salt-marsh development of the Mokbaai, Texel, The Netherlands. *Earth Surface Processes and Landforms*. **41(9)**, pp.1241–1249.
- Barbier, E.B., Hacker, S.D., Kennedy, C., Kock, E.W., Stier, A.C. and Sillman, B.R. 2011. The value of estuarine and coastal ecosystem services. *Ecological Monographs*. **81(2)**, pp.169–193.
- Barlow, N.L.M., Shennan, I., Long, A.J., Gehrels, W.R., Saher, M.H., Woodroffe, S. a. and Hillier, C. 2013. Salt marshes as late holocene tide gauges. *Global and Planetary Change*. **106**, pp.90–110.
- Bateman, M.D., Stein, S., Ashurst, R.A. and Selby, K. 2015. Instant luminescence chronologies? High resolution luminescence profiles using a portable luminescence reader. *Quaternary Geochronology*. **30**, pp.141–146.
- Beauchard, O., Jacobs, S., Cox, T.J.S., Maris, T., Vrebos, D., Van Braeckel, A. and Meire, P. 2011. A new technique for tidal habitat restoration: Evaluation of its hydrological potentials. *Ecological Engineering*. **37(11)**, pp.1849–1858.
- Beaumont, N.J., Jones, L., Garbutt, A., Hansom, J.D. and Toberman, M. 2014. The value of carbon sequestration and storage in coastal habitats. *Estuarine, Coastal and Shelf Science*. **137**, pp.32–40.
- Belliard, J.P., Temmerman, S. and Toffolon, M. 2017. Ecogeomorphic relations between marsh surface elevation and vegetation properties in a temperate multi-species salt marsh. *Earth Surface Processes and Landforms*. **42(6)**, pp.855–865.

- Bondoni, M., Mel, R., Solari, L., Lanzoni, S., Francalanci, S. and Oumeraci, H. 2016. Insights into lateral marsh retreat mechanism through localized field measurements. *Water Resources Research*. **52**, pp.1446–1464.
- Black, K.S. and Paterson, D.M. 1996. LISP-UK : an holistic approach to the interdisciplinary study of tidal flat sedimentation. *Terra Nova*. **8**(4), pp.304–308.
- Blum, L.K. and Christian, R.R. 2013. Belowground Production and Decomposition Along a Tidal Gradient in a Virginia Salt Marsh *In: The Ecogeomorphology of Tidal Marshes* [Online]. American Geophysical Union, pp.47–73. Available from: <http://dx.doi.org/10.1029/CE059p0047>.
- Boorman, L.A. 1999. Salt marshes - present functioning and future change. *Mangroves and Salt Marshes*. **3**(4), pp.227–241.
- Boorman, L., Hazelden, J. and Boorman, M. 2002. New Salt Marshes for Old - Salt Marsh Creation and Management. *Littoral 2002, The Changing Coast, EUROCOAST/EUCC.*, pp.35–45.
- Boorman, L.A. 2003. Salt marsh review. An overview of coastal salt marshes, their dynamic and sensitivity characteristics for conservation and management. *Environment*. (334), p.114.
- Boorman, L.A. and Hazelden, J. 2017. Managed re-alignment; a salt marsh dilemma? *Wetlands Ecology and Management*. **25**(4), pp.387–403.
- Bouchard, V. and Lefeuvre, J.C. 2000. Primary production and macro-detritus dynamics in a European salt marsh: Carbon and nitrogen budgets. *Aquatic Botany*. **67**(1), pp.23–42.
- Bouma, T.J., van Belzen, J., Balke, T., Zhu, Z., Airolidi, L., Blight, A.J., Davies, A.J., Galvan, C., Hawkins, S.J., Hoggart, S.P.G., Lara, J.L., Losada, I.J., Maza, M., Ondiviela, B., Skov, M.W., Strain, E.M., Thompson, R.C., Yang, S., Zanuttigh, B., Zhang, L. and Herman, P.M.J. 2014. Identifying knowledge gaps hampering application of intertidal habitats in coastal protection: Opportunities & steps to take. *Coastal Engineering*. **87**, pp.147–157.
- Bromberg, K.D. and Bertness, M.D. 2005. Reconstructing New England Salt Marsh Losses Using Historical Maps. *Estuaries*. **28**(6), pp.823–832.
- Brown, J.E., McDonald, P., Parker, A. and Rae, J.E. 1999. The vertical distribution of radionuclides in a Ribble Estuary saltmarsh: Transport and deposition of radionuclides. *Journal of Environmental Radioactivity*. **43**(3), pp.259–275.
- Buckley, A. 2010. Understanding curvature rasters. *ArcGIS Resources - Imagery & Remote Sensing*. [Online], pp.1–5. Available from: <https://blogs.esri.com/esri/arcgis/2010/10/27/understanding-curvature-rasters/>.

Buja, K. and Menza, C. 2013. *Sampling Design Tool for ArcGIS - Instruction Manual*. NOAA's Biogeography Branch. [Online]. NOAA's Biogeography Branch. Available from: <http://www.arcgis.com/home/item.html?id=ecbe1fc44f35465f9dea42ef9b63e785>.

Burd, F. 1989. *No.17: The saltmarsh survey of Great Britain An inventory of British saltmarshes*. Peterborough: Nature Conservancy Council.

Burd, F. 1992. *Erosion and vegetation changes on the Saltmarshes of Essex and North Kent between 1973 and 1988*. Nature Conservancy Council report No. 42. Nature Conservancy Council.

Burden, A., Garbutt, R.A., Evans, C.D., Jones, D.L. and Cooper, D.M. 2013. Carbon sequestration and biogeochemical cycling in a saltmarsh subject to coastal managed realignment. *Estuarine, Coastal and Shelf Science*. **120**, pp.12–20.

Burgess-Gamble, L. 2017. *Working with natural processes - the evidence base (SC150005 Technical Report)* [Online]. Available from: <https://www.gov.uk/government/publications/working->

Burgess-Gamble, L., Ngai, R., Wilkinson, M., Nisbet, T., Pontee, N., Harvey, R., Kipling, K., Addy, S., Rose, S., Maslen, S., Jay, H., Nicholson, A., Page, T., Jonczyk, J. and Quinn, P. 2018. *Working With Natural Processes – Evidence Directory*. Environment Agency. Project Number SC150005.

Burrows, M., Kamenos, N. and Hughes, D. 2014. *Assessment of carbon budgets and potential blue carbon stores in Scotland's coastal and marine environment*. Scottish Natural Heritage Commissioned Report No. 761. [Online]. Available from: <http://eprints.gla.ac.uk/96572/>.

Butzeck, C., Eschenbach, A., Gröngröft, A., Hansen, K., Nolte, S. and Jensen, K. 2014. Sediment Deposition and Accretion Rates in Tidal Marshes Are Highly Variable Along Estuarine Salinity and Flooding Gradients. *Estuaries and Coasts*., pp.434–450.

Butzeck, C.E.G. 2014. *Tidal marshes of the Elbe Estuary – spatial and temporal dynamics of sedimentation and vegetation*.

BwN 2019. Building with Nature, Interreg VB North Sea Region Programme. webpage <https://northsearegion.eu/building-with-nature/>. [Online]. Available from: <https://northsearegion.eu/building-with-nature/>.

Cahoon, D.R. 2015. Estimating Relative Sea-Level Rise and Submergence Potential at a Coastal Wetland. *Estuaries and Coasts*. (38), pp.1077–1084.

Cahoon, D.R. and Reed, D.J. 1995. Relationships among marsh surface topography, hydroperiod, and soil accretion in a deteriorating Louisiana salt marsh. *Journal of Coastal Research*. **11**(2), pp.357–369.

Cahoon, D.R., French, J.R., Spencer, T., Reed, D. and Moller, I. 2000. Vertical accretion versus elevational adjustment in UK saltmarshes: an evaluation of alternative methodologies. *Geological Society, London, Special Publications*. **175**(1), pp.223–238.

Cahoon, D.R., Reed, D.J., Kolker, A.S., Brinson, M.M., Stevenson, J.C., Riggs, S.R., Reyes, E., Voss, C.M. and Kunz, D. 2009. Coastal Wetland Sustainability. *Coastal Sensitivity to Sea-Level Rise: A Focus on the Mid-Atlantic Region SAP 4.1*. (February), pp.57–72.

Callaghan, D.P., Bouma, T.J., Klaassen, P., van der Wal, D., Stive, M.J.F. and Herman, P.M.J. 2010. Hydrodynamic forcing on salt-marsh development: Distinguishing the relative importance of waves and tidal flows. *Estuarine, Coastal and Shelf Science*. **89**(1), pp.73–88.

Callaway, J.C., Borgnis, E.L., Turner, R.E. and Milan, C.S. 2012. Carbon Sequestration and Sediment Accretion in San Francisco Bay Tidal Wetlands. *Estuaries and Coasts*. **35**, pp.1163–1181.

Carrasco, A.R., Kombiadou, K. and Matias, A. 2023. Short-term sedimentation dynamics in mesotidal marshes. *Scientific Reports*. **13**(1).

Chapman, V.J. 1977. *Ecosystems of the world: Volume 1, Wet Coastal Ecosystems*. (V. J. Chapman, ed.). Amsterdam: Elsevier Scientific Publishing Company.

Chassereau, J.E., Bell, J.M. and Torres, R. 2011. A comparison of GPS and lidar salt marsh DEMs. *Earth Surface Processes and Landforms*. **36**(13), pp.1770–1775.

Chirol, C., Haigh, I.D., Pontee, N., Thompson, C.E. and Gallop, S.L. 2018. Parametrizing tidal creek morphology in mature saltmarshes using semi-automated extraction from lidar. *Remote Sensing of Environment*. **209**(October 2017), pp.291–311.

Chmura, G.L. 2013. What do we need to assess the sustainability of the tidal salt marsh carbon sink? *Ocean and Coastal Management*. **83**, pp.25–31.

Chmura, G.L. and Hung, G. a. 2004. Controls on salt marsh accretion: A test in salt marshes of Eastern Canada. *Estuaries*. **27**(1), pp.70–81.

Chmura, G.L., Anisfeld, S.C., Cahoon, D.R. and Lynch, J.C. 2003. Global carbon sequestration in tidal, saline wetland soils. *Global Biogeochemical Cycles*. **17**(4).

Chmura, G.L., Coffey, A., Crago, R. and Winter, F. 2001. Variation in Surface Sediment Deposition on Salt Marshes in the Bay of Fundy. *Journal of Coastal Research*. **17**(1), pp.221–227.

Christiansen, T., Wiberg, P.L. and Milligan, T.G. 2000. Flow and Sediment Transport on a Tidal Salt Marsh. *Estuaries and Coasts*. **50**, pp.315–331.

Church, J.A., Clark, P.U., Cazenave, A., Gregory, J.M., Jevrejeva, S., Levermann, A., Merrifield, M.A., Milne, G.A., Nerem, R.S., Nunn, P.D., Payne, A.J., Pfeffer, W.T., Stammer, D. and Unnikrishnan, A.S. 2013. 2013: Sea Level Change. In: *Climate Change 2013: The Physical Science Basis. Contribution of Working Group I to the Fifth Assessment Report of the Intergovernmental Panel on Climate Change* [Stocker, T.F., D. Qin, G.-K. Plattner, M. Tignor, S.K. Allen, J. Boschung, A. Nauels, Y. Xia, [Online]. Cambridge University Press, Cambridge, United Kingdom and New York, NY, USA, pp.1137–1216. Available from: [https://www.ipcc.ch/pdf/assessment-report/ar5/wg1/WG1AR5\\_Chapter13\\_FINAL.pdf](https://www.ipcc.ch/pdf/assessment-report/ar5/wg1/WG1AR5_Chapter13_FINAL.pdf).

Clark, P.A. 1994. *Isochron methods for Luminescence dating in Archaeology*. PhD Thesis. University of Glasgow - Scottish Universities Research and Reactor Centre.

Clark, R.J. and Sanderson, D.C.W. 1994. Photostimulated luminescence excitation spectroscopy of feldspars and micas. *Radiation Measurements*. **23**(2/3), pp.641–646.

Clarke, M.L. and Rendell, H.M. 2000. The development of a methodology for luminescence dating of Holocene sediments at the land-ocean interface. *Geological Society Special Publication*. **166**, pp.69–86.

Coast Dynamic 2019. Dynamic Coast. Available from: <https://www.dynamiccoast.com/>.

Cohen, J. 1988. *Statistical Power Analysis for the Behavioral Sciences (2nd ed.)*. New York: Hillsdale, N.J.: Lawrence Erlbaum.

Connor, R.F., Chmura, G.L. and Beecher, C.B. 2001. Carbon acculmulation in Bay of Fundy saltmarshes: Implications for restoration of reclaimed mearshes. *Global Biogeochemical Cycles*. **15**(4), pp.943–954.

Cordier, S. 2010. Optically stimulated luminescence dating : procedures and applications to geomorphological research in France. *Géomorphologie : relief , processus, environnement*. **16**(1), pp.21–40.

Corenblit, D., Baas, A.C.W., Bornette, G., Darrozes, J., Delmotte, S., Francis, R.A., Gurnell, A.M., Julien, F., Naiman, R.J. and Steiger, J. 2011. Feedbacks between geomorphology and biota controlling Earth surface processes and landforms: A review of foundation concepts and current understandings. *Earth-Science Reviews*. **106**(3–4), pp.307–331.

Costanza, R., de Groot, R., Sutton, P., van der Ploeg, S., Anderson, S.J., Kubiszewski, I., Farber, S. and Turner, R.K. 2014. Changes in the global value of ecosystem services. *Global Environmental Change*. **26**(1), pp.152–158.

CountrysideSurvey 2007. UK Soil Observatory. *UKSO Website -BGS*. [Online]. Available from: <https://catalogue.ceh.ac.uk/maps/6372b558-ba64-4fbe-8766-019e01535b37?>



- Craft, C.B., Seneca, E.D. and Broome, S.W. 1991. Loss on ignition and kjeldahl digestion for estimating organic carbon and total nitrogen in estuarine marsh soils: Calibration with dry combustion. *Estuaries*. **14**(2), pp.175–179.
- Crosby, S.C., Sax, D.F., Palmer, M.E., Booth, H.S., Deegan, L.A., Bertness, M.D. and Leslie, H.M. 2016. Salt marsh persistence is threatened by predicted sea-level rise. *Estuarine, Coastal and Shelf Science*. **181**, pp.93–99.
- Crowther, A.E. 2007. *The restoration of intertidal habitats for non-breeding waterbirds through breached managed realignment*. University of Stirling.
- D’Alpaos, A., Lanzoni, S., Marani, M. and Rinaldo, A. 2007. Landscape evolution in tidal embayments: Modeling the interplay of erosion, sedimentation, and vegetation dynamics. *Journal of Geophysical Research: Earth Surface*. **112**(1), pp.1–17.
- D’Alpaos, A., Toffolon, M. and Camporeale, C. 2016. Ecogeomorphological feedbacks of water fluxes, sediment transport and vegetation dynamics in rivers and estuaries. *Advances in Water Resources*. **93**, pp.151–155.
- D’Odorico, P., He, Y., Collins, S., De Wekker, S.F.J., Engel, V. and Fuentes, J.D. 2013. Vegetation-microclimate feedbacks in woodland-grassland ecotones. *Global Ecology and Biogeography*. **22**(4), pp.364–379.
- Da Lio, C., D’Alpaos, A. and Marani, M. 2013. The secret gardener: Vegetation and the emergence of biogeomorphic patterns in tidal environments. *Philosophical Transactions of the Royal Society A: Mathematical, Physical and Engineering Sciences*. **371**(2004).
- Davidson-Arnott, R.G.D. 2009. *Introduction to Coastal Processes and Geomorphology*. Cambridge: Cambridge University Press.
- Davidson-Arnott, R.G.D., Van Proosdij, D., Ollerhead, J. and Schostak, L. 2002. Hydrodynamics and sedimentation in salt marshes: Examples from a macrotidal marsh, Bay of Fundy. *Geomorphology*. **48**(1–3), pp.209–231.
- Davies, J. 2001. Establishing monitoring programmes for marine features. *Marine Monitoring Handbook*. (March).
- Davis, R.A.J. and Dalrymple, R.W. 2012. *Principles of Tidal Sedimentology* (A. R. J. Davis & Robert W. Dalrymple, eds.). Springer Science+Business Media.
- Dawson, a. G., Smith, D.E. and Dawson, S. 2001. *Potential impacts of climate change on sea levels around Scotland*.

De Groot, A. V., Veeneklaas, R.M. and Bakker, J.P. 2011. Sand in the salt marsh: Contribution of high-energy conditions to salt-marsh accretion. *Marine Geology*. **282**(3–4), pp.240–254.

Deegan, L.A., Johnson, D.S., Warren, R.S., Peterson, B.J., Fleeger, J.W., Fagherazzi, S. and Wollheim, W.M. 2012. Coastal eutrophication as a driver of salt marsh loss. *Nature*. **490**(7420), pp.388–392.

Delbaere, B.C.W. 1998. Facts and figures on European biodiversity; state and trends 1998–1999. *European Centre for Nature Conservation*. (Tilburg, the Netherlands.), p.115.

Doody, J.P. 2008. Saltmarsh Conservation, Management and Restoration *In: Coastal Systems and Continental Margins, Volume 12*. Dordrecht: Springer, p.214.

Doody, J.P. 2013. Coastal squeeze and managed realignment in southeast England, does it tell us anything about the future? *Ocean and Coastal Management*. **79**, pp.34–41.

Duarte, C.M., Losada, I.J., Hendriks, I.E., Mazarrasa, I. and Marbà, N. 2013. The role of coastal plant communities for climate change mitigation and adaptation. *Nature Climate Change*. **3**(11), pp.961–968.

Duller, G.A.T. 2008. *Luminescence Dating: guidelines on using luminescence dating in archaeology*. Swindon: English Heritage.

Durcan, J.A. and Duller, G.A.T. 2011. The fast ratio: A rapid measure for testing the dominance of the fast component in the initial OSL signal from quartz. *Radiation Measurements*. **46**(10), pp.1065–1072.

Dyer, K.R. 1989. Sediment processes in estuaries: Future research requirements. *Journal of Geophysical Research*. **94**(C10), p.14327.

Eamer, J.B.R. and Walker, I.J. 2013. Quantifying spatial and temporal trends in beach-dune volumetric changes using spatial statistics. *Geomorphology*. **191**, pp.94–108.

Eisma, D. and Dijkema, K.S. 1997. The influence of salt marsh vegetation on sedimentation. *In: D. Eisma, ed. Intertidal Deposits: River Mouths, Tidal Flats and Coastal Lagoons*. Boca Raton, FL, USA., pp.403–414.

Eisma, D., de Boer, P.L., Cadee, G.C., Dijkema, K., Ridderinkhof, H. and Philippart, C. 1998. *Intertidal Deposits: River Mouths, Tidal Flats and Coastal Lagoons*. CRC Press. Boca Raton, FL, USA.

Elliott, M., Burdon, D., Hemingway, K.L. and Apitz, S.E. 2007. Estuarine, coastal and marine ecosystem restoration: Confusing management and science - A revision of concepts. *Estuarine, Coastal and Shelf Science*. **74**(3), pp.349–366.

Elliott, S. 2015. *Coastal Realignment at RSPB Nigg Bay Nature Reserve. RSPB Internal Report.*

ESRI (1) n.d. How Diffusion Interpolation With Barriers works. *ArcMap | Documentation.*

ESRI (2) n.d. Empirical Bayesian Kriging (Geostatistical Analyst). *ArcGIS Pro | Documentation.* [Online]. Available from: <https://pro.arcgis.com/en/pro-app/latest/tool-reference/geostatistical-analyst/empirical-bayesian-kriging.htm>.

Esteves, L.S. 2014. Managed Realignment: A Viable Long-Term Coastal Management Strategy? . (June).

Esteves, L.S. and Williams, J.J. 2015. Changes in coastal sediment dynamics due to managed realignment *In: Coastal Sediments 2015, 11-15 May 2015, San Diego, California, United States of America.* [Online]., p.14. Available from: [http://www.worldscientific.com/doi/abs/10.1142/9789814689977\\_0165](http://www.worldscientific.com/doi/abs/10.1142/9789814689977_0165).

Evans, B.R., Brooks, H., Chirol, C., Kirkham, M.K., Möller, I., Royse, K., Spencer, K. and Spencer, T. 2022. Vegetation interactions with geotechnical properties and erodibility of salt marsh sediments. *Estuarine, Coastal and Shelf Science.* **265**(December 2021).

Fagherazzi, S. 2013. The ephemeral life of a salt marsh. *Geology.* **41**(8), pp.943–944.

Fagherazzi, S. 2014. Coastal Processes: Storm-proofing with marshes. *Nature Geoscience.* **7**, pp.701–702.

Fagherazzi, S., Anisfeld, S.C., Blum, L.K., Long, E. V., Feagin, R.A., Fernandes, A., Kearney, W.S. and Williams, K. 2019. Sea level rise and the dynamics of the marsh-upland boundary. *Frontiers in Environmental Science.* **7**(FEB), pp.1–18.

Fagherazzi, S., Kirwan, M.L., Mudd, S.M., Guntenspergen, G.R., Temmerman, S., Rybczyk, J.M., Reyes, E., Craft, C. and Clough, J. 2012. Numerical models of salt marsh evolution: Ecological, geomorphic, and climatic factors. *Reviews of Geophysics.* **50**(RG1002), pp.1–28.

Fagherazzi, S., Marani, M. and Blum, L.K. 2004. *The ecogeomorphology of tidal marshes* Coastal an. (S. Fagherazzi, M. Marani, & L. K. Blum, eds.). American Geophysical Union.

Fagherazzi, S., Mariotti, G., Wiberg, P.L. and McGlathery, K.J. 2013. Marsh collapse does not require sea level rise. *Oceanography.* **26**(3), pp.70–77.

Fagherazzi, S., Wiberg, P.L., Temmerman, S., Struyf, E., Zhao, Y. and Raymond, P. a 2013. Fluxes of water, sediments, and biogeochemical compounds in salt marshes. *Ecological Processes.* **2**(3), p.3.

- Fearnley, S. 2008. The Soil Physical and Chemical Properties of Restored and Natural Back-Barrier Salt Marsh on Isles Dernieres, Louisiana. *Journal of Coastal Research*. **241**(241), pp.84–94.
- Fernández, S., Santín, C., Marquínez, J. and Álvarez, M.A. 2010. Saltmarsh soil evolution after land reclamation in Atlantic estuaries (Bay of Biscay, North coast of Spain). *Geomorphology*. **114**(4), pp.497–507.
- Fletemeyer, J., Hearin, J., Haus, B. and Sullivan, A. 2018. The Impact of Sand Nourishment on Beach Safety. *Journal of Coastal Research*. **341**(1), pp.1–5.
- Ford, H., Garbutt, A., Ladd, C., Malarkey, J. and Skov, M.W. 2016. Erosion stabilisation linked to plant diversity and environmental context in coastal grasslands. *Journal of Vegetation Science*., pp.1–10.
- Foster, N.M., Hudson, M.D., Bray, S. and Nicholls, R.J. 2013. Intertidal mudflat and saltmarsh conservation and sustainable use in the UK: A review. *Journal of Environmental Management*. **126**, pp.96–104.
- Foster, N.M., Hudson, M.D., Bray, S. and Nicholls, R.J. 2014. Research, policy and practice for the conservation and sustainable use of intertidal mudflats and saltmarshes in the Solent from 1800 to 2016. *Environmental Science and Policy*. **38**, pp.59–71.
- French, J. 2006. Tidal marsh sedimentation and resilience to environmental change: Exploratory modelling of tidal, sea-level and sediment supply forcing in predominantly allochthonous systems. *Marine Geology*. **235**(1-4 SPEC. ISS.), pp.119–136.
- French, J. 2018. *Tidal Salt Marshes*. Elsevier B.V.
- French, J.R. and Burningham, H. 2003. Tidal marsh sedimentation versus sea-level rise: a southeast England estuarine perspective. *Proceedings Coastal Sediments*. **3**(1992), p.14.
- French, J.R. and Spencer, T. 1993. Dynamics of sedimentation in a tide-dominated backbarrier salt marsh, Norfolk, UK. *Marine Geology*. **110**(3–4), pp.315–331.
- French, P. 1997. *Coastal and Estuarine Management* 1st Ed. London: Routledge.
- French, P.W. 2006. Managed realignment - The developing story of a comparatively new approach to soft engineering. *Estuarine, Coastal and Shelf Science*. **67**(3), pp.409–423.
- Friedrichs, C.T. 2011. Tidal Flat Morphodynamics: A Synthesis *In*: E. Wolanski and D. McLusky, eds. *Treatise on Estuarine and Coastal Science* [Online]. Elsevier Inc., pp.137–170. Available from: <http://dx.doi.org/10.1016/B978-0-12-374711-2.00307-7>.

- Friess, D. a., Krauss, K.W., Horstman, E.M., Balke, T., Bouma, T.J., Galli, D. and Webb, E.L. 2011. Are all intertidal wetlands naturally created equal? Bottlenecks, thresholds and knowledge gaps to mangrove and saltmarsh ecosystems. *Biological Reviews*. **87**(2), pp.346–366.
- Friess, D. a., Möller, I., Spencer, T., Smith, G.M., Thomson, A.G. and Hill, R. a. 2014. Coastal saltmarsh managed realignment drives rapid breach inlet and external creek evolution, Freiston Shore (UK). *Geomorphology*. **208**, pp.22–33.
- Friess, D. a., Spencer, T., Smith, G.M., Möller, I., Brooks, S.M. and Thomson, a. G. 2012. Remote sensing of geomorphological and ecological change in response to saltmarsh managed realignment, The Wash, UK. *International Journal of Applied Earth Observation and Geoinformation*. **18**(1), pp.57–68.
- Fung, F., Palmer, M., Howard, T., Lowe, J., Maisey, P. and Mitchell, J. 2018. UKCP18 Factsheet : Sea level rise and storm surge. *Met Office Hadley Centre, Exeter*. [Online], pp.1–8. Available from: <https://www.metoffice.gov.uk/binaries/content/assets/metofficegovuk/pdf/research/ukcp/ukcp18-fact-sheet-sea-level-rise-and-storm-surge.pdf>.
- Garbutt, A. and Wolters, M. 2008. The natural regeneration of salt marsh on formerly reclaimed land. *Applied Vegetation Science*.
- Garbutt, R.A., Reading, C.J., Wolters, M., Gray, A.J. and Rothery, P. 2006. Monitoring the development of intertidal habitats on former agricultural land after the managed realignment of coastal defences at Tollesbury, Essex, UK. *Marine Pollution Bulletin*. **53**(1), pp.155–164.
- Gattuso, J.-P., Frankignoulle, M. and Wollast, R. 1998. Carbon and Carbonate Metabolism in Coastal Aquatic Ecosystems. *Annual Review of Ecology and Systematics*. **29**(1), pp.405–434.
- Gedan, K.B., Silliman, B.R. and Bertness, M.D. 2009. Centuries of Human-Driven Change in Salt Marsh Ecosystems. *Annual Review of Marine Science*. **1**(1), pp.117–141.
- Ghilardi, M., Sanderson, D., Kinnaird, T., Bicket, A., Balossino, S., Parisot, J.C., Hermitte, D., Guibal, F. and Fleury, J.T. 2015. Dating the bridge at Avignon (south France) and reconstructing the Rhone River fluvial palaeo-landscape in Provence from medieval to modern times. *Journal of Archaeological Science: Reports*. **4**, pp.336–354.
- Godet, L. and Thomas, A. 2013. Three centuries of land cover changes in the largest French Atlantic wetland provide new insights for wetland conservation. *Applied Geography*. **42**, pp.133–139.
- Gunnell, J.R., Rodriguez, A.B. and McKee, B.A. 2013. How a marsh is built from the bottom up. *Geology*. **41**(8), pp.859–862.
- Hansom, J.D. 1988. *Coasts* Cambridge. Cambridge University Press.

Hansom, J.D. and Evans, D.J.A. 2000. The curse of Stirling. *Scottish Geographical Journal*. **116**(1), pp.71–78.

Hansom, J.D., Lees, R.G., Maslen, J., Tilbrook, C. and McManus, J. 2001. Coastal dynamics and sustainable management: the potential for managed realignment in the Forth estuary. In: J. E. Gordon and K. F. Lees, eds. *Earth Science and the Natural Heritage. Series: Natural heritage of Scotland*. The Stationery Office: Edinburgh, pp.148–160.

Hansom, J.D., Rennie, A.F., Drummond, J. and Dunlop, A. 2011. *A methodology to assess the causes and rates of change to Scotland's beaches and sand dunes – Phase 1. Scottish Natural Heritage Commissioned Report No. 364*.

Hanson, H. e. al. 2002. Beach nourishment projects, practices and objectives – a European overview. *Journal of coastal engineering*, 47 (2002) 81–111. Accessed: 21 April 2016. *Journal of coastal engineering*. **47**(0378), pp.81–111.

Harvey, M.M., Hansom, J.D. and MacKenzie, A.B. 2007. Constraints on the use of anthropogenic radionuclide-derived chronologies for saltmarsh sediments. *Journal of Environmental Radioactivity*. **95**(2–3), pp.126–148.

Haslett, S.K., Cundy, A.B., Davies, C.F.C., Powell, E.S. and Croudace, I.W. 2003. Salt marsh, sedimentation over the past c. 120 years along the West Cotentin Coast of Normandy (France): Relationship to sea-level rise and sediment supply. *Journal of Coastal Research*. **19**(3), pp.609–620.

Haynes, T.A. 2016. Scottish saltmarsh survey national report. *Scottish Natural Heritage Commissioned Report No. 786*. (786).

Haynes, T.A. 2016. *Scottish saltmarsh survey national report. Scottish Natural Heritage Commissioned Report No. 786*. [Online]. Available from: [https://www.nature.scot/sites/default/files/2017-05/Publication 2016 - SNH Commissioned Report 786 - Scottish saltmarsh survey national report %28A2215730%29.pdf](https://www.nature.scot/sites/default/files/2017-05/Publication%202016%20-%20SNH%20Commissioned%20Report%20786%20-%20Scottish%20saltmarsh%20survey%20national%20report%20-%20A2215730.pdf).

Heiri, O., Lotter, A.F. and Lemcke, G. 2001. Loss on ignition as a method for estimating organic and carbonate content in sediments: reproducibility and comparability of results. *Journal of Paleolimnology*. **25**, pp.101–110.

Hill, M. (CEH) 2015. *TABLEFIT version 2.0 for identification of vegetation types*. Wallingford: Centre for Ecology and Hydrology.

Holling, C.S. 1973. Resilience and Stability of Ecological Systems. *Annual Review of Ecology and Systematics*. **4**, pp.1–23.



- Horton, B.P., Shennan, I., Bradley, S.L., Cahill, N., Kirwan, M., Kopp, R.E. and Shaw, T.A. 2018. Predicting marsh vulnerability to sea-level rise using Holocene relative sea-level data. *Nature Communications*. **9**(1), pp.1–7.
- Hough, A., Spencer, C., Lowther, S. and Muddiman, S. 1999. *Technical report W153 - Definition of the Extent and Vertical Saltmarsh Range of Research and Development*.
- Houwing, E.J., van Duin, W.E., Smit-van der Waaij, Y., Dijkema, K.S. and Terwindt, J.H.J. 1999. Biological and abiotic factors influencing the settlement and survival of *Salicornia dolichostachya* in the intertidal pioneer zone. *Mangroves and Salt Marshes*. **3**(4), pp.197–206.
- Howard, J., Hoyt, S., Isensee, K., Pidgeon, E. and Telszewski, M. (eds. . 2014. Coastal blue carbon: methods for assessing carbon stocks and emissions factors in mangroves, tidal salt marshes, and seagrass meadows. *Conservation International, Intergovernmental Oceanographic Commission of UNESCO, International Union for Conservation of Nature. Arlington, Virginia, USA*.
- Howe, A.J., Rodriguez, J.F., Spencer, J., MacFarlane, G.R. and Saintilan, N. 2010. Response of estuarine wetlands to reinstatement of tidal flows. *Marine and Freshwater Research*. **61**(6), pp.702–713.
- Hyndes, G. a., Nagelkerken, I., Mcleod, R.J., Connolly, R.M., Lavery, P.S. and Vanderklift, M. a. 2014. Mechanisms and ecological role of carbon transfer within coastal seascapes. *Biological Reviews*. **89**(1), pp.232–254.
- Ippen, A.T. 1966. *Estuary and Coastline Hydrodynamics* Engineerin. McGraw-Hill, New York.
- Jacobs, Z. 2008. Luminescence chronologies for coastal and marine sediments. *Boreas*. **37**(4), pp.508–535.
- Kadiri, M., Spencer, K.L., Heppell, C.M. and Fletcher, P. 2011. Sediment characteristics of a restored saltmarsh and mudflat in a managed realignment scheme in Southeast England. *Hydrobiologia*. **672**(1), pp.79–89.
- Kearney, M., Stevenson, J. and Ward, L. 1994. Spatial and temporal changes in marsh vertical accretion rates at Monie Bay: Implications for sea-level rise. *Journal of Coastal Research*. **10**(4), pp.1010–1020.
- Kearney, W.S. and Fagherazzi, S. 2016. Salt marsh vegetation promotes efficient tidal channel networks. *Nature Communications*. **7**, p.12287.
- Kefelegn, H. 2019. Mathematical Formulations for Three Components of Hydroperiod in Tidal Wetlands. *Wetlands*. **39**(2), pp.349–360.

Kelleway, J.J., Saintilan, N., Macreadie, P.I. and Ralph, P.J. 2016. Sedimentary Factors are Key Predictors of Carbon Storage in SE Australian Saltmarshes. *Ecosystems*. **19**(5), pp.865–880.

Kelleway, J.J., Saintilan, N., Macreadie, P.I., Baldock, J.A. and Ralph, P.J. 2017. Sediment and carbon deposition vary among vegetation assemblages in a coastal salt marsh. *Biogeosciences*. **14**(16), pp.3763–3779.

Kesel, R.H. and Smith, J.S. 1978. Tidal creek and pan formation in intertidal salt marshes, Nigg Bay, Scotland. *Scottish Geographical Magazine*. **94**(3), pp.159–168.

Killops, S. and Killops, V. 2004. *Introduction to Organic Geochemistry*. Blackwell Publishing Ltd.

King, G.E., Sanderson, D.C.W., Robinson, R.A.J. and Finch, A.A. 2014. Understanding processes of sediment bleaching in glacial settings using a portable OSL reader. *Boreas*. **43**(4), pp.955–972.

Kirby, R. 1992. Effects of sea-level rise on muddy coastal margins *In: D. Prandle, ed. Dynamics and Exchanges in Estuaries and the Coastal Zone* [Online]., pp.313–334. Available from: <https://doi.org/10.1029/CE040p0313>.

Kirwan, M.L. and Guntenspergen, G.R. 2010. Influence of tidal range on the stability of coastal marshland. *Journal of Geophysical Research*. **115**(F2), pp.1–11.

Kirwan, M.L. and Mudd, S.M. 2012. Response of salt-marsh carbon accumulation to climate change. *Nature*. **489**(7417), pp.550–553.

Kirwan, M.L. and Murray, A.B. 2007. A coupled geomorphic and ecological model of tidal marsh evolution. *In: Proceedings of the National Academy of Sciences Apr 2007, 104 (15)*., pp.6118–6122.

Kirwan, M.L., Guntenspergen, G.R., D'Alpaos, A., Morris, J.T., Mudd, S.M. and Temmerman, S. 2010. Limits on the adaptability of coastal marshes to rising sea level. *Geophysical Research Letters*. **37**(23), pp.1–5.

Kirwan, M.L., Temmerman, S., Skeeahan, E.E., Guntenspergen, G.R. and Fagherazzi, S. 2016. Overestimation of marsh vulnerability to sea level rise. *Nature Climate Change*. **6**(3), pp.253–260.

Langlois, E., Bonis, a. and Bouzillé, J.B. 2003. Sediment and plant dynamics in saltmarshes pioneer zone: *Puccinellia maritima* as a key species? *Estuarine, Coastal and Shelf Science*. **56**(2), pp.239–249.

- Lawrence, P.J., Smith, G.R., Sullivan, M.J.P. and Mossman, H.L. 2018. Restored saltmarshes lack the topographic diversity found in natural habitat. *Ecological Engineering*. **115**(January), pp.58–66.
- Ledoux, L., Cornell, S., O’Riordan, T., Harvey, R. and Banyard, L. 2004. Towards sustainable flood and coastal management: Identifying drivers of, and obstacles to, managed realignment. *Working Paper - Centre for Social and Economic Research on the Global Environment*. **22**(1), pp.1–32.
- Leendertse, P.C., Roozen, a. J.M. and Rozema, J. 1997. Long-term changes (1953-1990) in the salt marsh vegetation at the Boschplaat on Terschelling in relation to sedimentation and flooding. *Plant Ecology*. **132**(1), pp.49–58.
- Lefevre, J.-C., Laffaille, P., Feunteun, E., Bouchard, V. and Radureau, A. 2003. Biodiversity in salt marshes: from patrimonial value to ecosystem functioning. The case study of the Mont-Saint-Michel bay. *C. R. Biologies*. **326 Suppl**, pp.S125–S131.
- Leonard, L.A. and Luther, M.E. 1995. Flow hydrodynamics in tidal marsh canopies. *Limnology and Oceanography*. **40**(8), pp.1474–1484.
- Leonardi, N. and Fagherazzi, S. 2014. How waves shape salt marshes. *Geology*. **42**(10), pp.887–890.
- Leonardi, N., Carnacina, I., Donatelli, C., Ganju, N.K., Plater, A.J., Schuerch, M. and Temmerman, S. 2018. Dynamic interactions between coastal storms and salt marshes: A review. *Geomorphology*. **301**, pp.92–107.
- Leonardi, N., Ganju, N.K. and Fagherazzi, S. 2016. A linear relationship between wave power and erosion determines salt-marsh resilience to violent storms and hurricanes. *Proceedings of the National Academy of Sciences*. **113**(1).
- Li, H. and Yang, S.L. 2009. Trapping effect of tidal marsh vegetation on suspended sediment, Yangtze Delta. *Journal of Coastal Research*. **25**(4), pp.915–936.
- Li, X., Leonardi, N. and Plater, A.J. 2019. Wave-driven sediment resuspension and salt marsh frontal erosion alter the export of sediments from macro-tidal estuaries. *Geomorphology*. **325**, pp.17–28.
- Liu, Z., Fagherazzi, S. and Cui, B. 2021. Success of coastal wetlands restoration is driven by sediment availability. *Nature Communications*. **2**(44), pp.1–9.
- Long, S.P. and Mason, C.F. 1983. *Saltmarsh ecology*. Blackie.

- Lotze, H.K., Lenihan, H.S., Bourque, B.J., Bradbury, R.H., Cooke, R.G., Kay, M.C., Kidwell, S.M., Kirby, M.X., Peterson, C.H. and Jackson, J.B.C. 2006. Depletion, Degradation, and Recovery Potential of Estuaries and Coastal Seas. *Science*. **312**(5781), pp.1806–1809.
- Lowe, J.A., Bernie, D., Bett, P., Bricheno, L., Brown, S., Calvert, D., Clark, R., Edwards, T., Fosser, G., Fung, F., Gohar, L., Good, P., Gregory, J., Harris, G., Howard, T., Kaye, N., Kendon, E., Krijnen, J., Maisey, P., McDonald, R., McInnes, R., McSweeney, C., Mitchell, J.F.B., Murphy, J., Palmer, M., Roberts, C., Rostron, J., Thornton, H., Tinker, J., Tucker, S., Yamazaki, K. and Belcher, S. 2018. UKCP18 Science Overview Report. *Met Office Hadley Centre: Exeter, UK*. [Online], pp.1–73. Available from: <https://www.metoffice.gov.uk/pub/data/weather/uk/ukcp18/science-reports/UKCP18-Overview-report.pdf>.
- Luisetti, T., Jackson, E.L. and Turner, R.K. 2013. Valuing the European ‘coastal blue carbon’ storage benefit. *Marine pollution bulletin*. **71**(1–2), pp.101–6.
- Macreadie, P.I., Baird, M.E., Trevathan-Tackett, S.M., Larkum, a. W.D. and Ralph, P.J. 2014. Quantifying and modelling the carbon sequestration capacity of seagrass meadows - A critical assessment. *Marine Pollution Bulletin*. **83**(2), pp.430–439.
- Madsen, a. T. and Murray, a. S. 2009. Optically stimulated luminescence dating of young sediments: A review. *Geomorphology*. **109**(1–2), pp.3–16.
- Madsen, a. T., Murray, a. S., Andersen, T.J., Pejrup, M. and Breuning-Madsen, H. 2005. Optically stimulated luminescence dating of young estuarine sediments: A comparison with <sup>210</sup>Pb and <sup>137</sup>Cs dating. *Marine Geology*. **214**(1–3), pp.251–268.
- Madsen, A.T., Buylaert, J.P. and Murray, A.S. 2011. Luminescence dating of young coastal deposits from New Zealand using feldspar. *Geochronometria*. **38**(4), pp.379–390.
- Madsen, A.T., Duller, G.A.T., Donnelly, J.P., Roberts, H.M. and Wintle, A.G. 2009. A chronology of hurricane landfalls at Little Sippewissett Marsh, Massachusetts, USA, using optical dating. *Geomorphology*. **109**(1–2), pp.36–45.
- Madsen, A.T., Murray, A.S., Andersen, T.J. and Pejrup, M. 2007. Temporal changes of accretion rates on an estuarine salt marsh during the late Holocene - Reflection of local sea level changes? The Wadden Sea, Denmark. *Marine Geology*. **242**(4), pp.221–233.
- Madsen, A.T., Murray, A.S., Andersen, T.J. and Pejrup, M. 2010. Spatial and temporal variability of sediment accumulation rates on two tidal flats in Lister Dyb tidal basin, Wadden Sea, Denmark. *Earth Surface Processes and Landforms*. **35**(13), pp.1556–1572.
- Mann, K.H. and Lazier, J.R.N. 1991. *Dynamics of marine ecosystems: biological-physical interactions in the oceans*. 1st ed. Blackwell Publishing Ltd.

- Marion, C., Anthony, E.J. and Trentesaux, A. 2009. Short-term ( $\leq 2$  yrs) estuarine mudflat and saltmarsh sedimentation: High-resolution data from ultrasonic altimetry, rod surface-elevation table, and filter traps. *Estuarine, Coastal and Shelf Science*. **83**(4), pp.475–484.
- Mariotti, G. and Carr, J. 2014. Dual role of salt marsh retreat: Long-term loss and short-term resilience. *Water Resources Research*. **50**, pp.2963–2974.
- Marshall, W.I.L. 2015. Chapter 25 Chronohorizons : indirect and unique event dating methods for sea-level reconstructions *In*: B. P. ; eds Shennan, I. ; Long, A.J.; Horton, ed. *Handbook of Sea-Level Research*. John Wiley & Sons, Ltd.
- Mauz, B., Baeteman, C., Bungenstock, F. and Plater, a. J. 2010. Optical dating of tidal sediments: Potentials and limits inferred from the North Sea coast. *Quaternary Geochronology*. **5**(6), pp.667–678.
- Mauz, B., Lang, A. and Kingdom, U. 2005. The dose rate of beta sources for optical dating applications: A comparison between fine silt and fine sand quartz. *Ancient TL*. **22**(2), pp.45–48.
- May, V.J. and Hansom, J.D. 2003. *Extract - Coastal Geomorphology of Great Britain* Geological. Joint Nature Conservation Committee (Geological Conservation Review).
- Maynard, C., McManus, J., Crawford, R.M.M. and Paterson, D. 2011. A comparison of short-term sediment deposition between natural and transplanted saltmarsh after saltmarsh restoration in the Eden Estuary (Scotland). *Plant Ecology & Diversity*. **4**(1), pp.103–113.
- McClure, A., Liu, X., Hines, E. and Ferner, M.C. 2016. Evaluation of Error Reduction Techniques on a LIDAR-Derived Salt Marsh Digital Elevation Model. *Journal of Coastal Research*. **318**(2), pp.424–433.
- McKeown, A. 1997. *Photostimulated luminescence of Marine Sediments, Final Year BSc Project Report*. Department of Physics, University of Strathclyde conducted at SURRC.
- McLeod, E., Chmura, G.L., Bouillon, S., Salm, R., Björk, M., Duarte, C.M., Lovelock, C.E., Schlesinger, W.H. and Silliman, B.R. 2011. A blueprint for blue carbon: toward an improved understanding of the role of vegetated coastal habitats in sequestering CO<sub>2</sub>. *Frontiers in Ecology and the Environment*. **9**(10), pp.552–560.
- Mcowen, C.J., Weatherdon, L. V., Van Bochove, J.W., Sullivan, E., Blyth, S., Zockler, C., Stanwell-Smith, D., Kingston, N., Martin, C.S., Spalding, M., Fletcher, S., Bochove, J.-W., Sullivan, E., Blyth, S., Zockler, C., Stanwell-Smith, D., Kingston, N., Martin, C.S., Spalding, M. and Fletcher, S. 2017. A global map of saltmarshes. *Biodiversity Data Journal*. **5**(1), p.e11764.
- Meirland, A., Gallet-moron, E., Rybarczyk, H., Dubois, F., Chabrierie, O., Picardie, U. De, Verne, J., Anthropisés, S., Cnrs, F.R.E. and Biodiversity, P. 2015. Predicting the effects of sea

level rise on salt marsh plant communities : does vegetation age matter more than sea level ? *Plant Ecology and Evolution*. **148**(1), pp.5–18.

Meldrum, D. 1996. *Sediment Dating of Samples from Sellafield using PSL, Industrial Project Report*.

Mellett, C.L. 2013. Luminescence Dating *In: Geomorphological Techniques (Chap. 4, Sec. 2.6)* [Online]. British Society for Geomorphology, pp.1–11. Available from: [http://www.geomorphology.org.uk/assets/publications/subsections/pdfs/OnsitePublicationSubsection/90/4.2.6\\_luminescencedating.pdf](http://www.geomorphology.org.uk/assets/publications/subsections/pdfs/OnsitePublicationSubsection/90/4.2.6_luminescencedating.pdf).

Met Office 2019. UK storm centre. [Accessed 12 June 2019]. Available from: <https://www.metoffice.gov.uk/weather/warnings-and-advice/uk-storm-centre/index/>.

Mieszkowska, N., Firth, L. and Bentley, M. 2013. Impacts of climate change on intertidal habitats. *MCCIP Science Review 2013*. xxx(November), xxx.

Millennium Ecosystem Assessment 2005. *Ecosystems and human well-being: Synthesis*. [Online]. Island Press, Washington, DC. Available from: <http://www.who.int/entity/globalchange/ecosystems/ecosys.pdf%5Chttp://www.loc.gov/catdir/toc/ecip0512/2005013229.html>.

Miller, L.C., Smeaton, C., Yang, H. and Austin, W.E.N. 2023. Carbon accumulation and storage across contrasting saltmarshes of Scotland. *Estuarine, Coastal and Shelf Science*. **282**(December 2022), p.108223.

Milne, G. a, Shennan, I., Youngs, B. a R., Waugh, a I., Teferle, F.N., Bingley, R.M., Bassett, S.E., Cuthbert-Brown, C. and Bradley, S.L. 2006. Modelling the glacial isostatic adjustment of the UK region. *Phil. Trans. R. Soc. A*. **364**(1841), pp.931–948.

Möller, I. 2006. Quantifying saltmarsh vegetation and its effect on wave height dissipation: Results from a UK East coast saltmarsh. *Estuarine, Coastal and Shelf Science*. **69**(3–4), pp.337–351.

Möller, I. and Christie, E. 2019. Hydrodynamics and modeling of water flow in coastal wetlands *In: G. M. E. Perillo, E. Wolanski, D. R. Cahoon and C. S. Hopkinson, eds. Coastal Wetlands: An Integrated Ecosystem Approach (Second Ed.)* [Online]. Elsevier B.V., pp.289–323. Available from: <http://dx.doi.org/10.1016/B978-0-444-63893-9.00008-3>.

Möller, I., Kudella, M., Rupprecht, F., Spencer, T., Paul, M., van Wesenbeeck, B.K., Wolters, G., Jensen, K., Bouma, T.J., Miranda-Lange, M. and Schimmels, S. 2014. Wave attenuation over coastal salt marshes under storm surge conditions. *Nature Geoscience*. **7**(10), pp.727–731.



- Möller, I., Spencer, T., French, J.R., Leggett, D.J. and Dixon, M. 1999. Wave transformation over salt marshes: A field and numerical modelling study from north Norfolk, England. *Estuarine, Coastal and Shelf Science*. **49**(3), pp.411–426.
- Montalto, F.A., Steenhuis, T.S. and Parlange, J.Y. 2006. The hydrology of Piermont Marsh, a reference for tidal marsh restoration in the Hudson river estuary, New York. *Journal of Hydrology*. **316**(1–4), pp.108–128.
- Montané, J.M. and Torres, R. 2006. Accuracy Assessment of Lidar Saltmarsh Topographic Data Using RTK GPS. *Photogrammetric Engineering & Remote Sensing*. (August), pp.961–967.
- Morris, J.T., Barber, D.C., Callaway, J.C., Chambers, R., Hagen, S.C., Hopkinson, C.S., Johnson, B.J., Megonigal, P., Neubauer, S.C., Troxler, T. and Wigand, C. 2016. Contributions of organic and inorganic matter to sediment volume and accretion in tidal wetlands at steady state. *Earth's Future*. **4**(4), pp.110–121.
- Morris, J.T., Sundareshwar, P. V, Nietch, C.T., Kjerfve, B. and Cahoon, D.R. 2002. Responses of coastal wetlands to rising sea level. *Ecology*. **83**(10), pp.2869–2877.
- Morton, R.A. 1996. Geoindicators of coastal wetlands and shorelines. In: Berger AR, Iams WJ (eds) *Geoindicators: assessing rapid environmental changes in Earth systems*. Balkema, Rotterdam., pp.207–230.
- Mossman, H.L., Davy, A.J. and Grant, A. 2012. Does managed coastal realignment create saltmarshes with ‘equivalent biological characteristics’ to natural reference sites? *Journal of Applied Ecology*. **49**(6), pp.1446–1456.
- Mossman, H.L., Pontee, N., Born, K., Hill, C., Lawrence, P.J., Rae, S., Scott, J., Serato, B., Sparkes, R.B., Sullivan, M.J.P. and Dunk, R.M. 2022. Rapid carbon accumulation at a saltmarsh restored by managed realignment exceeded carbon emitted in direct site construction. *PLoS ONE*. **17**(11 November), pp.1–24.
- Mudd, S.M., D’Alpaos, A. and Morris, J.T. 2010. How does vegetation affect sedimentation on tidal marshes? Investigating particle capture and hydrodynamic controls on biologically mediated sedimentation. *Journal of Geophysical Research: Earth Surface*. **115**(3), pp.1–14.
- Mudd, S.M., Fagherazzi, S., Morris, J.T. and Furbish, D.J. 2004. Flow, sedimentation, and biomass production on a vegetated salt marsh in South Carolina: toward a predictive model of marsh morphologic and ecologic evolution. *American Geophysical Union*., pp.165–187.
- Mudd, S.M., Fagherazzi, S., Morris, J.T. and Furbish, D.J. 2013. Flow, Sedimentation, and Biomass Production on a Vegetated Salt Marsh in South Carolina: Toward a Predictive Model of Marsh Morphologic and Ecologic Evolution In: *The Ecogeomorphology of Tidal Marshes*. American Geophysical Union, pp.165–188.

- Mudd, S.M., Howell, S.M. and Morris, J.T. 2009. Impact of dynamic feedbacks between sedimentation, sea-level rise, and biomass production on near-surface marsh stratigraphy and carbon accumulation. *Estuarine, Coastal and Shelf Science*. **82**(3), pp.377–389.
- Mudge, B.F. 1858. The salt marsh formations of Lynn In: *Proceedings of the Essex Institute, II (1856-1860)*., pp.117–119.
- Muñoz-Salinas, E., Bishop, P., Sanderson, D.C. and Zamorano, J.J. 2011. Interpreting luminescence data from a portable OSL reader: Three case studies in fluvial settings. *Earth Surface Processes and Landforms*. **36**(5), pp.651–660.
- Muñoz-Salinas, E., Castillo, M. and Arce, J.L. 2017. OSL signal resetting in young deposits determined with a pulsed photon-stimulated luminescence (PPSL) unit. *Boreas*. **46**(2), pp.325–337.
- Munykwa, K., Brown, S. and Kitabwalla, Z. 2012. Delineating stratigraphic breaks at the bases of postglacial eolian dunes in central Alberta, Canada using a portable OSL reader. *Earth Surface Processes and Landforms*. **37**(15), pp.1603–1614.
- Munykwa, K., Telfer, M., Baker, I. and Knight, C. 2011. Core drilling of Quaternary sediments for luminescence dating using the Dormer Drillmite(TM). *Ancient TL*. **29**(1), pp.15–24.
- Murray, A.S. and Wintle, A.G. 2000. Luminescence dating of quartz using an improved single-aliquot regenerative-dose protocol. *Radiation Measurements*. **32**(1), pp.57–73.
- Murray, A.S. and Wintle, A.G. 2003. The single aliquot regenerative dose protocol: Potential for improvements in reliability. *Radiation Measurements*. **37**(4–5), pp.377–381.
- Naylor, L.A., Viles, H.A. and Carter, N.E.A. 2002. Biogeomorphology revisited: Looking towards the future. *Geomorphology*. **47**(1), pp.3–14.
- Nolte, S., Butzeck, C., Baldwin, A.H., Felton, G.K. and Jensen, K. 2019. Efficiency of varying sediment traps under experimental conditions simulating tidal inundations. *Journal of Coastal Research*. **35**(4), pp.920–924.
- Nolte, S., Koppenaal, E.C., Esselink, P., Dijkema, K.S., Schuerch, M., De Groot, a. V., Bakker, J.P. and Temmerman, S. 2013. Measuring sedimentation in tidal marshes: A review on methods and their applicability in biogeomorphological studies. *Journal of Coastal Conservation*. **17**(3), pp.301–325.
- NTSLF/NOC/NERC n.d. National Tidal and Sea Level Facility (NTSLF). Available from: <https://www.ntsrf.org>.

- Nyman, J.A. 1990. Wetland Soil Formation in the Rapidly Subsiding Mississippi River Deltaic Plain : Mineral and Organic Matter Relationships. *Estuarine, Coastal and Shelf Science*. **31**, pp.57–69.
- Odum, W.E. 1988. Comparative Ecology of Tidal Freshwater and Salt Marshes. *Annual Review of Ecology and Systematics*. **19**, pp.147–176.
- Owers, C.J. and Rogers, K. 2016. Spatial Variation in Carbon Storage : A Case Study for Currumbene, NSW, Australia. *Journal of Coastal Research*. **75**, pp.1297–1301.
- Pachauri, R.K. and Meyer, L.A. 2014. IPCC, 2014: Climate Change 2014: Synthesis Report. Summary for Policymakers. *Contribution of Working Groups I, II and III to the Fifth Assessment Report of the Intergovernmental Panel on Climate Change*. (IPCC, Geneva, Switzerland), pp.1–32.
- Packham, J.R. and Willis, A.J. 1997. *Ecology of dunes, salt marsh and shingle*. London: Chapman & Hall.
- Pendleton, L., Donato, D.C., Murray, B.C., Crooks, S., Jenkins, W.A., Sifleet, S., Craft, C., Fourqurean, J.W., Kauffman, J.B., Marbà, N., Megonigal, P., Pidgeon, E., Herr, D., Gordon, D. and Baldera, A. 2012. Estimating Global ‘Blue Carbon’ Emissions from Conversion and Degradation of Vegetated Coastal Ecosystems. *PLoS ONE*. **7**(9).
- Pethick, J. 1984. *An introduction to coastal geomorphology*. London: Edward Arnold (Publishers) Ltd. Copublished in the U.S Central and South America by John Wiley & Sons.
- Pethick, J. 1993. Shoreline Adjustments and Coastal Management : Physical and Biological Processes under Accelerated Sea-Level Rise. *the Geographical Journal*. **159**(2), pp.162–168.
- Pethick, J., Falconer, R.A. and Goodwin, P. 1994. *Estuaries and wetlands: function and form* [Online]. Thomas Telford Publishing. Available from: <https://www.icevirtuallibrary.com/doi/abs/10.1680/wm.19942.0006>.
- Plater, A.J., Kirby, J.R., Boyle, J.F., Shaw, T. and Mills, H. 2015. Chapter 21 Loss on ignition and organic content *In*: B. P. ; eds Shennan, I. ; Long, A.J.; Horton, ed. *Handbook of Sea-Level Research*. John Wiley & Sons, Ltd, pp.312–330.
- Portenga, E.W. and Bishop, P. 2016. Confirming geomorphological interpretations based on portable OSL reader data. *Earth Surface Processes and Landforms*. **41**(3), pp.427–432.
- Pugh, D.T. 1996. Tides, surges and mean sea-level (reprinted with corrections). *Marine and Petroleum Geology*. **5**(3), p.301.

- Pye, K. and French, P. 1993. *Erosion & Accretion Processes on British Salt Marshes. Volume Five: Management of Salt Marshes in the Context of Flood Defence and Coastal Protection*. Cambridge: Cambridge Environmental Research Consultants.
- Pye, K., Coleman, M.L. and Duan, W.M. 1997. Microbial activity and diagenesis in saltmarsh sediments, North Norfolk, England In: T. D. Jickells and J. E. E. Rae, eds. *Biogeochemistry of Intertidal Sediments*. Cambridge Environmental Chemistry Series. Cambridge University Press, pp.119–151.
- Raffaelli, D. and Boyle, P.R. 1986. The intertidal macrofauna of Nigg Bay. *Proceedings of the Royal Society of Edinburgh. Section B. Biological Sciences*. **91**, pp.113–141.
- Rahman, R. and Plater, A.J. 2014. Particle-size evidence of estuary evolution: A rapid and diagnostic tool for determining the nature of recent saltmarsh accretion. *Geomorphology*. **213**, pp.139–152.
- Ranwell, D.S. 1972. *Ecology of salt marshes and sand dunes*. London : Chapman and Hall, 1972.
- Reed, D.J. 1989. Patterns of Sediment Deposition in Subsiding Coastal Salt Marshes , Terrebonne Bay, Louisiana : The Role of Winter Storms. *Estuaries*. **12**(4), pp.222–227.
- Reed, D.J. 1995. The response of coastal marshes to sea-level rise: Survival or submergence? *Earth Surface Processes and Landforms*. **20**(1), pp.39–48.
- Reed, D.J., Spencer, T., Murray, A.L., French, J.R. and Leonard, L. 1999. Marsh surface sediment deposition and the role of tidal creeks: Implications for created and managed coastal marshes. *Journal of Coastal Conservation*. **5**(1), pp.81–90.
- Reef, R., Schuerch, M., Christie, E.K., Möller, I. and Spencer, T. 2018. The effect of vegetation height and biomass on the sediment budget of a European saltmarsh. *Estuarine, Coastal and Shelf Science*. **202**, pp.125–133.
- Reimann, T., Ankjaergaard, C. and Wallinga, J. 2015. Testing the potential of a transferred IRSL (T-IRSL) feldspar signal for luminescence dating. *Radiation Measurements*. **81**, pp.275–281.
- Reinhardt, L., Jerolmack, D., Cardinale, B.J., Vanacker, V. and Wright, J. 2010. Dynamic interactions of life and its landscape: feedbacks at the interface of geomorphology and ecology. *Earth Surface Processes and Landforms*. **35**(1), pp.78–101.
- Rendall, D. and Hunter, J. 1986. A study of the littoral fauna of some soft shores of the Inverness, Cromarty and Dornoch Firths. *Proceedings of the Royal Society of Edinburgh. Section B. Biological Sciences*. **91**, pp.193–212.

Rennie, A.F. 2006. *Of The role of sediment supply and sea-level changes on a submerging coast , past changes and future management implications . PhD thesis.* University of Glasgow.

Rennie, A.F. and Hansom, J.D. 2011. Sea level trend reversal: Land uplift outpaced by sea level rise on Scotland's coast. *Geomorphology*. **125**(1), pp.193–202.

Richardson, C.A. 2001. Residual luminescence signals in modern coastal sediments. *Quaternary Science Reviews*. **20**(5–9), pp.887–892.

Robins, P.E., Skov, M.W., Lewis, M.J., Giménez, L., Davies, A.G., Malham, S.K., Neill, S.P., McDonald, J.E., Whitton, T.A., Jackson, S.E. and Jago, C.F. 2016. Impact of climate change on UK estuaries: A review of past trends and potential projections. *Estuarine, Coastal and Shelf Science*. **169**, pp.119–135.

Rodwell, J.S. 2006. *National Vegetation Classification : Users ' handbook, JNCC.* Peterborough.

Rogers, K., Saintilan, N. and Woodroffe, C.D. 2014. Surface elevation change and vegetation distribution dynamics in a subtropical coastal wetland: Implications for coastal wetland response to climate change. *Estuarine, Coastal and Shelf Science*. **149**, pp.46–56.

Roner, M., D'Alpaos, A., Ghinassi, M., Marani, M., Silvestri, S., Franceschinis, E. and Realdon, N. 2016. Spatial variation of salt-marsh organic and inorganic deposition and organic carbon accumulation: Inferences from the Venice lagoon, Italy. *Advances in Water Resources*. **93**(November), pp.276–287.

Rotman, R., Naylor, L., McDonnell, R. and MacNiocaill, C. 2008. Sediment transport on the Freiston Shore managed realignment site: An investigation using environmental magnetism. *Geomorphology*. **100**(3–4), pp.241–255.

Sander, L., Fruergaard, M., Koch, J., Johannessen, P.N. and Pejrup, M. 2015. Sedimentary indications and absolute chronology of Holocene relative sea-level changes retrieved from coastal lagoon deposits on Samsø, Denmark. *Boreas*. **44**(4), pp.706–720.

Sanderson, D.C.W. 1988a. Fading of thermoluminescence in feldspars: characteristics and corrections. *International Journal of Radiation Applications and Instrumentation. Part. 14*(1–2), pp.155–161.

Sanderson, D.C.W. 1988b. Thick source beta counting (TSBC): A rapid method for measuring beta dose-rates. *International Journal of Radiation Applications and Instrumentation. Part. 14*(1–2), pp.203–207.

Sanderson, D.C.W. and Murphy, S. 2010. Using simple portable OSL measurements and laboratory characterisation to help understand complex and heterogeneous sediment sequences for luminescence dating. *Quaternary Geochronology*. **5**(2–3), pp.299–305.

- Sanderson, D.C.W., Bishop, P., Stark, M., Alexander, S. and Penny, D. 2007. Luminescence dating of canal sediments from Angkor Borei, Mekong Delta, Southern Cambodia. *Quaternary Geochronology*. **2**(1–4), pp.322–329.
- Santisteban, J.I., Mediavilla, R., López-Pamo, E., Dabrio, C.J., Blanca Ruiz Zapata, M., José Gil García, M., Castaño, S. and Martínez-Alfaro, P.E. 2004. Loss on ignition: a qualitative or quantitative method for organic matter and carbonate mineral content in sediments? *Journal of Paleolimnology*. **32**(3), pp.287–299.
- Santos, I.R., Hatje, V., Serrano, O., Bastviken, D. and Krause-Jensen, D. 2022. Carbon sequestration in aquatic ecosystems: Recent advances and challenges. *Limnology and Oceanography*. **67**(S2), pp.S1–S5.
- Schile, L.M., Callaway, J.C., Morris, J.T., Stralberg, D., Thomas Parker, V. and Kelly, M. 2014. Modeling tidal marsh distribution with sea-level rise: Evaluating the role of vegetation, sediment, and upland habitat in marsh resiliency. *PLoS ONE*. **9**(2).
- Schindler, M., Karius, V., Arns, A., Deicke, M. and von Eynatten, H. 2014. Measuring sediment deposition and accretion on anthropogenic marshland – Part II: The adaptation capacity of the North Frisian Halligen to sea level rise. *Estuarine, Coastal and Shelf Science*. **151**, pp.246–255.
- Schindler, M., Karius, V., Deicke, M. and von Eynatten, H. 2014. Measuring sediment deposition and accretion on anthropogenic marshland – Part I: Methodical evaluation and development. *Estuarine, Coastal and Shelf Science*. **151**, pp.236–245.
- Schmidt, C., Friedrich, J., Adamiec, G., Chruścińska, A., Fasoli, M., Kreutzer, S., Martini, M., Panzeri, L., Polymeris, G.S., Przegiętka, K., Valla, P.G., King, G.E. and Sanderson, D.C.W. 2018. How reproducible are kinetic parameter constraints of quartz luminescence? An interlaboratory comparison for the 110 °C TL peak. *Radiation Measurements*. **110**(January), pp.14–24.
- Schuerch, M., Dolch, T., Bisgwa, J. and Vafeidis, A.T. 2018. Changing Sediment Dynamics of a Mature Backbarrier Salt Marsh in Response to Sea-Level Rise and Storm Events. *Frontiers in Marine Science*. **5**(May), pp.1–14.
- Schuerch, M., Spencer, T. and Evans, B. 2019. Coupling between tidal mudflats and salt marshes affects marsh morphology. *Marine Geology*. **412**(November 2018), pp.95–106.
- Schuerch, M., Spencer, T., Temmerman, S., Kirwan, M.L., Wolff, C., Lincke, D., McOwen, C.J., Pickering, M.D., Reef, R., Vafeidis, A.T., Hinkel, J., Nicholls, R.J. and Brown, S. 2018. Future response of global coastal wetlands to sea-level rise. *Nature*. **561**(7722), pp.231–234.
- Schwarz, C., Bouma, T.J., Zhang, L.Q., Temmerman, S., Ysebaert, T. and Herman, P.M.J.J. 2015. Interactions between plant traits and sediment characteristics influencing species establishment and scale-dependent feedbacks in salt marsh ecosystems. *Geomorphology*. **250**, pp.298–307.



- Schwarz, C., Ye, Q., Wal, D., Zhang, L., Bouma, T., Ysebaert, T. and Herman, P. 2014. Impacts of salt marsh plants on tidal channels initiation and inheritance. *Journal of Geophysical Research: Earth Surface.*, pp.385–400.
- Scottish Environment Protection Agency (SEPA) n.d. Scottish Rainfall Data for Milton Of Evelix TBR and Dingwall - provided by Scottish Environment Protection Agency (SEPA). [Accessed 22 February 2021]. Available from: <https://www2.sepa.org.uk/rainfall/data/index/>.
- Sghair, a and Goma, F. 2013. *Remote sensing and GIS for wetland vegetation study*. *Phd Thesis*. [Online] University of Glasgow. Available from: <http://theses.gla.ac.uk/id/eprint/4581>.
- Shaler, N.S. 1886. Sea-coast swamps of the Eastern United States. *U.S. Geological Survey, 6th Annual Report.*, pp.359–368.
- Sharps, E., Garbutt, A., Hiddink, J.G., Smart, J. and Skov, M.W. 2016. Light grazing of saltmarshes increases the availability of nest sites for Common Redshank *Tringa totanus*, but reduces their quality. *Agriculture, Ecosystems and Environment*. **221**, pp.71–78.
- Sharps, E., Smart, J., Skov, M.W., Garbutt, A. and Hiddink, J.G. 2015. Light grazing of saltmarshes is a direct and indirect cause of nest failure in Common Redshank *Tringa totanus*. *Ibis*. **157**(2), pp.239–249.
- Shepard, C.C., Crain, C.M. and Beck, M.W. 2011. The protective role of coastal marshes: A systematic review and meta-analysis. *PLoS ONE*. **6**(11).
- Shi, Z., Lamb, H.F. and Collin, R.L. 1995. Geomorphic change of saltmarsh tidal creek networks in the Dyfi Estuary, Wales. *Marine Geology*. **128**(1–2), pp.73–83.
- Silinski, A., Fransen, E., Bouma, T.J., Meire, P. and Temmerman, S. 2016. Unravelling the controls of lateral expansion and elevation change of pioneer tidal marshes. *Geomorphology*. **274**, pp.106–115.
- Silvestri, S. and Marani, M. 2004. Salt-Marsh Vegetation and Morphology: Basic Physiology, Modelling and Remote Sensing Observations *In: The Ecogeomorphology of Tidal Marshes* [Online]. American Geophysical Union (AGU), pp.5–25. Available from: <https://agupubs.onlinelibrary.wiley.com/doi/abs/10.1029/CE059p0005>.
- Silvestri, S., Defina, A. and Marani, M. 2005. Tidal regime, salinity and salt marsh plant zonation. *Estuarine, Coastal and Shelf Science*. **62**(1–2), pp.119–130.
- Simpson, K. and Hanley, N. 2016. Managed Realignment for Flood Risk Reductions : What are the Drivers of Public Willingness to Pay ? *In: Discussion papers in Environmental Economics - Paper 2016-6.*, p.26.

Solomon, S., D., Qin, M., Manning, Z., Chen, M., Marquis, K.B., Averyt, M.T., Miller HL, Solomon, S., Qin, D., Manning, M., Chen, Z., Marquis, M., Averyt, K.B., Tignor, M. and Miller, H.L. 2007. Summary for Policymakers. In: *Climate Change 2007: The Physical Science Basis. Contribution of Working Group I to the Fourth Assessment Report of the Intergovernmental Panel on Climate Change. D Qin M Manning Z Chen M Marquis K Averyt M Tignor and HL Miller New York Cambridge University Press pp. Geneva*, p.996.

Sousa, A.I., Lillebø, A.I., Pardal, M. a. and Caçador, I. 2010. The influence of *Spartina maritima* on carbon retention capacity in salt marshes from warm-temperate estuaries. *Marine Pollution Bulletin*. **61**(4–6), pp.215–223.

Spencer, K.L. and Harvey, G.L. 2012. Understanding system disturbance and ecosystem services in restored saltmarshes: Integrating physical and biogeochemical processes. *Estuarine, Coastal and Shelf Science*. **106**, pp.23–32.

Spencer, K.L., Carr, S.J., Diggins, L.M., Tempest, J.A., Morris, M.A. and Harvey, G.L. 2017. The impact of pre-restoration land-use and disturbance on sediment structure, hydrology and the sediment geochemical environment in restored saltmarshes. *Science of the Total Environment*. **587–588**, pp.47–58.

Spencer, T. 1988. Coastal biogeomorphology *In: H. A. Viles, ed. Biogeomorphology*. Basil Blackwell, Oxford & New York, pp.255-318.

Spencer, T., Friess, D. a., Möller, I., Brown, S.L., Garbutt, R. a. and French, J.R. 2012. Surface elevation change in natural and re-created intertidal habitats, eastern England, UK, with particular reference to Freiston Shore. *Wetlands Ecology and Management*. **20**(1), pp.9–33.

Spencer, T., Möller, I., Rupprecht, F., Bouma, T.J., van Wesenbeeck, B.K., Kudella, M., Paul, M., Jensen, K., Wolters, G., Miranda-Lange, M. and Schimmels, S. 2015. Salt marsh surface survives true-to-scale simulated storm surges. *Earth Surface Processes and Landforms*. **552**(December 2015), pp.543–552.

Stagg, C.L. and Mendelsohn, I.A. 2011. Controls on resilience and stability in a sediment-subsidized salt marsh. *Ecological Applications by Ecological Society of America*. **21**(5), pp.1731–1744.

Stahl, H. 2012. *Current status & knowledge about potential sequestration capacity for ‘ blue carbon ’ sinks in Scotland. Scottish Association for Marine Science Report. Sniffer - ClimateXChange*.

Stallins, J.A. 2006. Geomorphology and ecology: Unifying themes for complex systems in biogeomorphology. *Geomorphology*. **77**(3–4), pp.207–216.

Stapleton, C. and Pethick, J. 1996. *Coastal processes and management of Scottish estuaries I: The Dornoch, Cromarty and Beaulay/Inverness Firths. Scottish Natural Heritage Review No. 50*.

- Stokes, D.J., Healy, T.R. and Cooke, P.J. 2010. Expansion Dynamics of Monospecific, Temperate Mangroves and Sedimentation in Two Embayments of a Barrier-Enclosed Lagoon, Tauranga Harbour, New Zealand. *Journal of Coastal Research*. **26**(261), pp.113–122.
- Stone, A.E.C., Bateman, M.D. and Thomas, D.S.G. 2015. Rapid age assessment in the Namib Sand Sea using a portable luminescence reader. *Quaternary Geochronology*. **30**, pp.134–140.
- Stumpf, R.P. 1983. The process of sedimentation on the surface of a salt marsh. *Estuarine, Coastal and Shelf Science*. **17**(5), pp.495–508.
- Sutherland, R.A. 1998. Loss-on-ignition estimates of organic matter and relationships to organic carbon in fluvial bed sediments. *Hydrobiologia*. **389**, pp.153–167.
- Taylor, B.W., Paterson, D.M. and Baxter, J.M. 2019. Sediment dynamics of natural and restored Bolboschoenus maritimus saltmarsh. *Frontiers in Ecology and Evolution*. **7**(JUN), pp.1–10.
- Teasdale, P. a., Collins, P.E.F., Firth, C.R. and Cundy, A.B. 2011. Recent estuarine sedimentation rates from shallow inter-tidal environments in western Scotland: Implications for future sea-level trends and coastal wetland development. *Quaternary Science Reviews*. **30**(1–2), pp.109–129.
- Temmerman, S., Bouma, T.J., Govers, G. and Lauwaet, D. 2005. Flow paths of water and sediment in a tidal marsh: Relations with marsh developmental stage and tidal inundation height. *Estuaries*. **28**(3), pp.338–352.
- Temmerman, S., Govers, G., Wartel, S. and Meire, P. 2003. Spatial and temporal factors controlling short-term sedimentation in a salt and freshwater tidal marsh, scheldt estuary, Belgium, SW Netherlands. *Earth Surface Processes and Landforms*. **28**(7), pp.739–755.
- Temmerman, S., Meire, P., Bouma, T.J., Herman, P.M.J.J., Ysebaert, T. and De Vriend, H.J. 2013. Ecosystem-based coastal defence in the face of global change. *Nature*. **504**(7478), pp.79–83.
- Temmerman, S., Moonen, P., Schoelynck, J., Govers, G. and Bouma, T.J. 2012. Impact of vegetation die-off on spatial flow patterns over a tidal marsh. *Geophysical Research Letters*. **39**(3), pp.1–5.
- Tempest, J.A., Harvey, G.L. and Spencer, K.L. 2015. Modified sediments and subsurface hydrology in natural and recreated salt marshes and implications for delivery of ecosystem services. *Hydrological Processes*. **29**(10), pp.2346–2357.
- Tempest, J.A., Möller, I. and Spencer, T. 2015. A review of plant-flow interactions on salt marshes: the importance of vegetation structure and plant mechanical characteristics. *WIREs Water*. **2**(6), pp.669–681.

- Thompson, C.E.L., Farron, S., Tempest, J., Möller, I., Solan, M. and Godbold, J. 2021. Understanding Marsh Dynamics:: Laboratory Approaches *In*: D. Hughes and Z. FitzGerald, eds. *Salt Marshes: Function, Dynamics, and Stresses. Part II - Marsh Dynamics*. Cambridge, pp.300–334.
- Thorne, K.M., Elliott-Fisk, D.L., Wylie, G.D., Perry, W.M. and Takekawa, J.Y. 2014. Importance of Biogeomorphic and Spatial Properties in Assessing a Tidal Salt Marsh Vulnerability to Sea-level Rise. *Estuaries and Coasts*. **37**(4), pp.941–951.
- Townend, I., Fletcher, C., Knappen, M. and Rossington, K. 2011. A review of salt marsh dynamics. *Water and Environment Journal*. **25**(4), pp.477–488.
- Truelsen, J.L. and Wallinga, J. 2003. Zeroing of the OSL signal as a function of grain size: investigating bleaching and thermal transfer for a young fluvial sample. *Geochronometria Journal on Methods and Applications of Absolute Chronology*. **22**, pp.1–8.
- Tsujimoto, T. and Shimizu, Y. 1994. Flow and suspended sediment in a compound channel vegetation. *Proceedings 1st international symposium on habitat hydraulics, Trent, Norway.*, pp.357–370.
- Turner, R.E., Swenson, E.M. and Milan, C.S. 2000. Organic And Inorganic Contributions To Vertical Accretion In Salt Marsh Sediments *In*: D. Weinstein, MP; Kreeger, ed. *Concepts And Controversies In Tidal Marsh Ecology; at Meeting on Concepts and Controversies in Tidal Marsh Ecology in April, 1998*. Vineland, NJ, pp.583–595.
- Turner, R.E., Swenson, E.M., Milan, C.S. and Lee, J.M. 2007. Hurricane signals in salt marsh sediments: Inorganic sources and soil volume. *Limnology and Oceanography*. **52**(3), pp.1231–1238.
- Turner, R.E., Swenson, E.M., Milan, C.S., Lee, J.M. and Oswald, T. a. 2004. Below-ground biomass in healthy and impaired salt marshes. *Ecological Research*. **19**(1), pp.29–35.
- UK National Ecosystem Assessment 2011. *The UK National Ecosystem Assessment: Technical Report*. UNEP-WCMC, Cambridge.
- Van de Broek, M., Temmerman, S., Merckx, R. and Govers, G. 2016. The importance of an estuarine salinity gradient on soil organic carbon stocks of tidal marshes. *Biogeosciences Discussions*. (August), pp.1–30.
- van der Wal, D. and Pye, K. 2004. Patterns, rates and possible causes of saltmarsh erosion in the Greater Thames area (UK). *Geomorphology*. **61**(3–4), pp.373–391.
- Van der Wal, D., Wielemaker-Van den Dool, A. and Herman, P.M.J. 2008. Spatial patterns, rates and mechanisms of saltmarsh cycles (Westerschelde, The Netherlands). *Estuarine, Coastal and Shelf Science*. **76**(2), pp.357–368.

- van Wesenbeeck, B.K., de Boer, W., Narayan, S., van der Star, W.R.L. and de Vries, M.B. 2017. Coastal and riverine ecosystems as adaptive flood defenses under a changing climate. *Mitig Adapt Strateg Glob Change*. **22**, pp.1087–1094.
- Vannoppen, W., De Baets, S., Keeble, J., Dong, Y. and Poesen, J. 2017. How do root and soil characteristics affect the erosion-reducing potential of plant species? *Ecological Engineering*. **109**(January), pp.186–195.
- Viles, H.A. 1988. *Biogeomorphology* Viles, H.A. (H. A. Viles, ed.). Basil Blackwell, Oxford & New York.
- Wallinga, J., Murray, A. and Wintle, A. 2000. Single-aliquot regenerative-dose (SAR) protocol applied to coarse-grain feldspar. *Radiation Measurements*. **32**(5), pp.529–533.
- Wang, C. and Temmerman, S. 2013. Does biogeomorphic feedback lead to abrupt shifts between alternative landscape states?: An empirical study on intertidal flats and marshes. *Journal of Geophysical Research: Earth Surface*. **118**(1), pp.229–240.
- Wang, Z.A., Kroeger, K.D., Ganju, N.K., Gonneea, M.E. and Chu, S.N. 2016. Intertidal salt marshes as an important source of inorganic carbon to the coastal ocean. *Limnology and Oceanography*. **61**(5), pp.1916–1931.
- Ward, S., Stokes, S., Bailey, R., Singarayer, J., Goudie, A. and Bray, H. 2003. Optical dating of quartz from young samples and the effects of pre-heat temperature. *Radiation Measurements*. **37**(4–5), pp.401–407.
- Webb, E.L., Friess, D. a, Krauss, K.W., Cahoon, D.R., Guntenspergen, G.R. and Phelps, J. 2013. A global standard for monitoring coastal wetland vulnerability to accelerated sea-level rise. *Nature Climate Change*. **3**(5), pp.458–465.
- Wheaton, J.M., Brasington, J., Darby, S.E. and Sear, D.A. 2010. Accounting for uncertainty in DEMs from repeat topographic surveys: Improved sediment budgets. *Earth Surface Processes and Landforms*. **35**(2), pp.136–156.
- Wheaton, J.M., Gibbins, C., Wainwright, J., Larsen, L. and McElroy, B. 2011. Preface: Multiscale Feedbacks in Ecogeomorphology. *Geomorphology*. **126**(3–4), pp.265–268.
- Wheeler, A.J., Orford, J.D. and Dardis, O. 1999. Saltmarsh deposition and its relationship to coastal forcing over the last century on the north-west coast of Ireland. *Geologie en Mijnbouw*. **77**, pp.295–310.
- Wilson, C.A., Perillo, G.M.E. and Hughes, Z.J. 2021. Salt Marsh Ecogeomorphic Processes and Dynamics In: D. Hughes and Z. FitzGerald, eds. *Salt Marshes: Function, Dynamics, and Stresses. Part II - Marsh Dynamics*. Cambridge, pp.178–224.

- Wintle, A.G. 2008. Luminescence dating: Where it has been and where it is going. *Boreas*. **37**(4), pp.471–482.
- Wintle, A.G. and Murray, A.S. 2006. A review of quartz optically stimulated luminescence characteristics and their relevance in single-aliquot regeneration dating protocols. *Radiation Measurements*. **41**(4), pp.369–391.
- Wolanski, E, Brinson, M M, Cahoon, D R and Perillo, G M E 2009. Coastal wetlands: A synthesis *In: Gerardo M E Perillo, Eric Wolanski, Donald R Cahoon and Mark M Brinson, eds. Coastal Wetlands: An Integrated Ecosystem Approach (First Ed.)* [Online]. New York: Elsevier, pp.1–62. Available from: <http://pubs.er.usgs.gov/publication/5211463>.
- Wolters, M., Garbutt, A. and Bakker, J.P. 2005. Salt-marsh restoration: Evaluating the success of de-embankments in north-west Europe. *Biological Conservation*. **123**(2), pp.249–268.
- Wright, A.J., Edwards, R.J., van de Plassche, O., Blaauw, M., Parnell, A.C., van der Borg, K., de Jong, A.F.M., Roe, H.M., Selby, K. and Black, S. 2017. Reconstructing the accumulation history of a saltmarsh sediment core: Which age-depth model is best? *Quaternary Geochronology*. **39**, pp.35–67.
- Yang, S.L., Li, H., Ysebaert, T., Bouma, T.J., Zhang, W.X., Wang, Y.Y., Li, P., Li, M. and Ding, P.X. 2008. Spatial and temporal variations in sediment grain size in tidal wetlands, Yangtze Delta: On the role of physical and biotic controls. *Estuarine, Coastal and Shelf Science*. **77**(4).
- Yapp, R.H., Johns, D. and Jones, O.T. 1917. The Salt Marshes of the Dovey Estuary. *Journal of Ecology*. **5**(2), pp.65–103.
- Yu, O.T. and Chmura, G.L. 2009. Soil carbon may be maintained under grazing in a St Lawrence Estuary tidal marsh. *Environmental Conservation*. **36**(04), pp.312–320
- Yu, O.T. and Chmura, G.L. 2009. Soil carbon may be maintained under grazing in a St Lawrence Estuary tidal marsh. *Environmental Conservation*. **36**(04), pp.312–320.
- Zedler, J.B. and Kercher, S. 2005. Status, Trends, Ecosystem Services, and Restorability. *Review Literature And Arts Of The Americas.*, pp.39–74.
- Zhang, B., Zhao, Q.G., Horn, R. and Baumgartl, T. 2001. Shear strength of surface soil as affected by soil bulk density and soil water content. *Soil and Tillage Research*. **59**(3–4), pp.97–106.





# APPENDICES

<b>Abbreviations</b>	
$\lambda_x$	lambda value used for Box-Cox transformation
$\sqrt{\quad}$	square root transform of the value
$\mu$	mean
adj.	adjusted ( e.g. $r^2$ adj.)
ANK	Site name for mature natural salt marsh - west of Ankerville river
AR	Accretion rates ( $\text{cm.yr}^{-1}$ )
BDD	Bulk dry density – Autocompaction in $\text{g.cm}^{-3}$
B-OSL	Blue light Optically Stimulated Luminescence
DEM	Digital elevation model
diff.	difference
DR	Dose-rate in $\text{Gy.yr}^{-1}$
ED	Equivalent dose in Gy
F	F-value for Welch's Anova test
FM	young (<70 years old) natural saltmarsh fronting (seawards) MR
Gy	Gray
$\eta$	Means ranks /median
H	H-value ( $H_{\text{adj.}}$ = H value adjusted for ties) for Kruskal-Wallis chi-squared test
$\eta \pm I\text{OP}$	mean ranks (median) with interquartile range
HM	high-marsh - see also 3.3.2.2
HWM	High Water Mark
IRSL	Infra-Red Stimulated Luminescence
Ka	thousand years
K-W test, H	Kruskal-Wallis test, H-value ( $H_{\text{adj.}}$ = H value adjusted for ties)
LM	low-marsh - 3.3.2.2
Loge	logarithmic transform of the value
LOI	Loss-on-Ignition
MHWS	Mean High Water Springs tide
MM	mid-marsh - 3.3.2.2
MR	young managed realignment saltmarsh (breached in 2003)
M-W test, W	Mann-Whitney test, W-value
OC	Organic Content (derived from Aboveground Biomass) $\text{g.Cm}^{-2}$
OSL	Optically Stimulated Luminescence
$p <^*$	$p$ -value significant level $<0.05$ *; $<0.01$ **; $<0.001$ ***
PM	pioneer-marsh - 3.3.2.2
RSLR	Relative Sea Level rise
SD	standard deviation
SE	standard error
SEM	elemental mapping system
SIC	Soil Inorganic Content %
SLR	Sea level rise
SOC	Carbon Soil Organic Content % or $\text{g.cm}^{-3}$ (specified in text)
SOM	Soil Organic Matter - %
SR	Sedimentation rates
TLS	Terrestrial Laser Scanner
tonneC.ha-1	Total carbon content per tonne per hectare
W	W-value for Mann-Whitney-Wilcoxon test
XRD	X-ray diffractometry
$\rho$	Rho value from Spearman's ranking correlation

## **APPENDIX.A    Supplementary references for Chapter 2**

## A.1. Saltmarsh Legal frame for Scotland

Table A- 1: Legal framework surrounding Saltmarsh systems in Scotland

Scope	Legislation	Designation & Remit	Scotland
<b>International</b>	2002 <b>Johannesburg Declaration</b> - (Biological Diversity)	<b>Declaration</b> on Sustainable Development	
	1972 <b>OSPAR</b> Convention (followed in 1974-1992-1998)- (Biological Diversity)	<b>Convention</b> for the Protection of the marine Environment of the North-East Atlantic	Mapped on National Biodiversity Network - Identifying <b>MPAs</b>
		The UNFCCC is a “Rio Convention”, one of three adopted at the “” in 1992	
	1992 <b>Rio Conventions</b> - (Biological Diversity) <b>at the</b> Rio Earth Summit	1992 three Rio Conventions were adopted at the Rio earth summit: on Biodiversity, Climate change and Desertification	
	1982 United Nations Convention on the Law of the Sea (UNCLOS)	Rights and responsibilities of nations with respect to their use of the world's oceans, establishing guidelines for businesses, the environment, and the management of marine natural resources.	
	1979 Bern Convention on the Conservation of European Wildlife and Natural Habitats (ratified by UK 1982)	International legal instrument in the field of nature conservation. It aims to conserve wild flora and fauna and their natural habitats, as well as to promote European co-operation in this field.  Transposed into European obligations with: <ul style="list-style-type: none"> <li>· Council Directive <b>79/409/EEC</b> on the Conservation of Wild Birds (the Birds Directive)</li> <li>· the Council Directive <b>92/43/EEC</b> on the Conservation of Natural Habitats and of Wild Fauna and Flora (the Habitats Directive)</li> </ul> Into national law:	Place Coastal saltmarshes (Eunis code A2.5)as endangered natural habitat types

	<ul style="list-style-type: none"> <li>· Wildlife and Countryside Act (1981 as amended),</li> <li>· Nature Conservation (Scotland) Act 2004 (as amended),</li> <li>· Wildlife (Northern Ireland) Order 1985</li> <li>· Nature Conservation and Amenity Lands (Northern Ireland) Order 1985.</li> </ul>		
	1971 <b>Ramsar</b> Convention (ratified by UK 1976)	Wetland of International Importance (Ramsar site) - Conservation and wise use of wetlands	51 Ramsar sites designated in Scotland( 313,000 hectares).
	1972 United Nations Education, Science and Culture Organisation (UNESCO) Convention on <b>World Cultural and Natural Heritage</b> (ratified by UK 1984).	Protection of the World Cultural and Natural Heritage	1 natural world heritage site in Scotland (the islands of St Kilda)
	UNESCO Man and the Biosphere ecological programme 1970	<b>Biosphere reserve</b> is a non-statutory designation	2 biosphere reserves in Scotland (Beinn Eighe, in Wester Ross & the Galloway and Southern Ayrshire)
<b>European</b>	<b>2008/56/EC Marine Strategy Framework Directive</b> with adoption of a Maritime Spatial Planning and Integrated Coastal Management in 2013	to achieve or maintain good environmental status in the marine environment by the year 2020	
	<b>2009/147/EC</b> Directive of the European Parliament and of the Council on the conservation of wild birds (commonly known as the Birds Directive)	Directives was transposed into law in Scotland largely through the Wildlife and Countryside Act 1981 (as amended by the Nature Conservation (Scotland) Act 2004) Protection for bird species wholly dependent on the marine environment (agreed at a European level) to contribute to ensuring their survival and reproduction in their area of distribution within Europe.	<b>SPA</b> led by Marine Scotland – how many in Scotland ?
	2007/60/EC Floods Directive	Assessment and management of flood risks. Transposed in Scotland into Flood Risk Management National (Scotland) Act 2009	

	2002 EU Recommendation on Integrated Coastal Zone Management	Commission adopted on the 12th of March 2013 a draft proposal for a Directive establishing a framework for maritime spatial planning and integrated coastal management.	
	2001 Clean Water Act	Committee on Mitigating Wetland Losses – Habitat (re) creation for either conservation or compensation purposes	
	2000/60/EC EU Water Framework Directive	Reports published in 2007 and 2009 as well as the 3rd implementation report published in 2012	
	1992/43/EC Habitat directives	<b>SAC Special Areas of Conservation</b> – Areas best representing the range and variety within the European Union of habitats and (non-bird) species Article 3 of the Habitats Directive requires the establishment of a European network of important high-quality conservation sites that will make a significant contribution to conserving designated habitat types (189) and identified species (788). <b>Natura 2000 site (SPA &amp; SAC)</b> Assure the long-term survival of Europe's most valuable and threatened species and habitats.	<b>SAC</b> led by Marine Scotland - Protection of marine species and habitats agreed at a European level to contribute to the conservation of Europe's biodiversity
	<b>79/409/EEC</b> EC Directive on the conservation of wild birds	<b>SPA Special Protection Areas</b> are areas of the most important habitat for rare and migratory birds within the European Union.	153 SPAs in Scotland (over a million hectares)
<b>National</b>	Climate Change (Scotland) Act 2009	The Act is to create a statutory framework for greenhouse gas emissions reductions in Scotland (42% reduction by 2020 and 80% by 2050). It requires that Scottish ministers report regularly to the Scottish Parliament on Scotland's emissions and on the progress made to reduce emissions (i.e.: 2013 Low Carbon Scotland: Meeting our Emissions Reduction Targets 2013-202 ).	
	Planning etc. (Scotland) Act 2006 Town and Country Planning (Scotland) Act 1997	Planning etc. (Scotland) Act 2006 gives a statutory basis to National Scenic Areas <b>NSAs</b> by adding a new section to the Town and Country Planning (Scotland) Act 1997 – Areas of outstanding scenery & finest landscapes	40 National Scenic Areas (NSAs)



Marine and Coastal Act 2009 (offshore waters) Marine (Scotland) Act 2010 (territorial waters)	These 2 acts were followed in 2014 by the designation of a suite of Nature Conservation Marine Protected Areas ( <b>NCMPA</b> ) completing Scotland's MPA network (in complement of other protection such as SACs, SPAs and SSSIs). They aim to conserve Scotland's most important marine wildlife, habitats and geodiversity.	17 Nature Conservation MPAs in Scotland's territorial waters <b>NCMPA</b> led by Marine Scotland -
Flood Risk Management National (Scotland) Act 2009	Specific measures include: A coordination and cooperation framework between all organisations to assess flood risk and prepare flood risk management plans and (single authority) for the safe operation of Scotland's reservoirs.	Led by SEPA, Scottish Water and local authorities
2008 Marine and Coastal Access Bill	The Bill establishes the designation and protection of a new type of Marine Protected Areas ( <b>MPAs</b> ), to be known as Marine Conservation Zones ( <b>MCZs</b> ). MPAs are identified through a Scottish Marine Protected Area Projects. Non-Natura MPAs are established in Scottish Territorial Waters through a Scottish Marine Bill	Scotland's existing MPA network consists of over 180 designated areas incl. SAC, SPA, NCMPA, SSSI & Ramsar
Wildlife and Countryside Act 1981 Nature Conservation (Scotland) Act 2004	Scottish Natural Heritage holds the responsibility for identifying and protecting Sites of special scientific interest ( <b>SSSIs</b> ) give legal protection to the best sites for wildlife and geology.	over 1,425 SSSIs in Scotland- SSSIs led by SNH
Wildlife and Natural Environment (Scotland) Act 2011	Act was repealed in Scotland on 1 January 2012 Areas of special protection ASP – . First established as 'sanctuaries' under the Protection of Birds Act, then under the Wildlife and Countryside Act 1981 and finally Wildlife and Natural Environment (Scotland) Act 2011	
The Food and Environment Protection Act 1985 (FEPA)	It regulates activities involving construction or deposition of materials upon the seabed	
Coast Protection Act 1949	“An act to amend the law relating to the protection of the coast of Great Britain against erosion and encroachment by the sea; to provide for the restriction and removal of works detrimental to navigation; to transfer the management of Crown foreshore from the Minister	

---

of Transport to the Commissioners of Crown Lands; and for purposes connected with the matters aforesaid". It empowers Local Authorities with coastlines to carry out coast protection work inside and outside their area as necessary, subject to the approval of the Scottish Executive.

---

1949 National Parks and Access to the Countryside Act	Area of Outstanding Natural Beauty (AONB) - Conserve natural beauty including wildlife, physiographic features, cultural heritage, landscape and scenery. National Nature Reserves <b>NNR</b> are designated under the National Parks and Access to the Countryside Act 1949 or the Wildlife and Countryside Act 1981.	47 promoted NNRs in Scotland (May 2015).
---	---	--

---

## A.2. Saltmarsh vegetation classification based on NVC classification

Haynes, T.A. 2016. Scottish saltmarsh survey national report. Scottish Natural Heritage Commissioned Report No. 786, 204pp..

Saltmarsh zones and corresponding NVC classifications including types not present in Scotland (SNH 2010).

NVC community	Community name
<b>Pioneer marsh zone</b>	
SM3	<i>Eleocharis parvula</i> saltmarsh
SM4	<i>Spartina maritima</i>
SM5	<i>Spartina alterniflora</i>
SM6	<i>Spartina anglica</i> saltmarsh
SM7	<i>Sarcocornia perennis</i>
SM8	Annual <i>Salicornia</i> saltmarsh
SM9	<i>Suaeda maritima</i> saltmarsh
SM11	<i>Aster tripolium</i> var. <i>discooides</i> saltmarsh
SM12	Rayed <i>Aster tripolium</i> on saltmarsh
<b>Lower marsh zone</b>	
SM10	Transitional low marsh vegetation with <i>Puccinellia maritima</i> , annual <i>Salicornia</i> species and <i>Suaeda maritima</i> .
SM13a	<i>Puccinellia maritima</i> saltmarsh, <i>Puccinellia maritima</i> dominant sub-community
<b>Middle marsh zone</b>	
SM14	<i>Atriplex portulacoides</i> saltmarsh
SM13b	<i>Puccinellia maritima</i> saltmarsh, <i>Glaux maritima</i> sub-community
SM13c	<i>Puccinellia maritima</i> saltmarsh, <i>Limonium vulgare</i> - <i>Armeria maritima</i> sub-community
SM13d	<i>Puccinellia maritima</i> saltmarsh, <i>Plantago maritima</i> - <i>Armeria maritima</i> sub-community
SM13e	<i>Puccinellia maritima</i> saltmarsh, turf fuoid sub-community
SM13f	<i>Puccinellia maritima</i> – <i>Spartina maritima</i> sub-community
SM15	<i>Juncus maritimus</i> – <i>Triglochin maritima</i> saltmarsh
<b>Upper marsh zone</b>	
SM16a	<i>Festuca rubra</i> saltmarsh <i>Puccinellia maritima</i> sub-community
SM16b	<i>Festuca rubra</i> saltmarsh <i>Juncus gerardii</i> sub-community
SM16c	<i>Festuca rubra</i> saltmarsh <i>Festuca rubra</i> - <i>Glaux maritima</i> sub-community
SM16d	<i>Festuca rubra</i> saltmarsh tall <i>Festuca rubra</i> sub-community
SM16e	<i>Festuca rubra</i> saltmarsh <i>Leontodon autumnalis</i> sub-community
SM16f	<i>Festuca rubra</i> saltmarsh <i>Carex flacca</i> sub-community
SM17	<i>Artemisia maritima</i> saltmarsh
SM18	<i>Juncus maritimus</i> saltmarsh
SM19	<i>Blysmus rufus</i> saltmarsh
SM20	<i>Eleocharis uniglumis</i> saltmarsh
SM21	<i>Suaeda vera</i> - <i>Limonium binervosum</i> saltmarsh
SM22	<i>Atriplex portulacoides</i> - <i>Frankenia laevis</i> saltmarsh
SM23	<i>Spergularia marina</i> – <i>Puccinellia distans</i> saltmarsh
SM26	<i>Inula crithmoides</i> stands
SM27	Ephemeral saltmarsh vegetation with <i>Sagina maritima</i>
<b>Driftline zone</b>	
SM24	<i>Elytrigia atherica</i> saltmarsh
SM25	<i>Suaeda vera</i> drift-line
SM28	<i>Elytrigia repens</i> saltmarsh

## A.3. Extract from UKCP18 High Emission Scenario –RCP8.5 Summary

Table A- 3: Extract from UKCP18 High Emission Scenario –RCP8.5 Summary (Lowe et al., 2018; Fung et al., 2018). These tables provide the anticipated mean sea level rise for a selection of Scottish locations, above 1980-2000 averages. The anticipated level is 'extremely likely to be between the 5% and 95% figures (below)'. The top table gives anticipated sea level rise in meters for 2040, 2050 to 2099. The bottom table gives anticipated precipitation increase in mm per yr. Dornoch Firth part of the Moray is highlighted with a blue box.

Name	Lerwick			Hermaness			Wick			Dornoch			Fortrose			Peterhead			Aberdeen				
RCP	8.5			8.5			8.5			8.5			8.5			8.5			8.5				
2040	0.19	0.26	0.18	0.24	0.31	0.2	0.26	0.33	0.11	0.17	0.24	0.09	0.15	0.22	0.09	0.15	0.22	0.09	0.15	0.22	0.08	0.14	0.21
2050	0.26	0.36	0.23	0.32	0.42	0.26	0.34	0.44	0.14	0.23	0.33	0.12	0.2	0.3	0.12	0.2	0.3	0.12	0.21	0.31	0.11	0.2	0.3
2060	0.33	0.47	0.29	0.4	0.54	0.32	0.43	0.57	0.18	0.29	0.43	0.16	0.27	0.41	0.16	0.27	0.41	0.16	0.27	0.41	0.15	0.26	0.4
2070	0.41	0.6	0.35	0.49	0.67	0.38	0.52	0.7	0.23	0.37	0.55	0.2	0.34	0.52	0.2	0.34	0.52	0.21	0.35	0.53	0.19	0.33	0.52
2080	0.5	0.73	0.41	0.58	0.82	0.45	0.62	0.85	0.28	0.45	0.69	0.24	0.41	0.65	0.24	0.41	0.65	0.25	0.42	0.66	0.24	0.41	0.65
2090	0.58	0.88	0.47	0.68	0.97	0.51	0.72	1.01	0.33	0.53	0.83	0.29	0.49	0.79	0.29	0.49	0.79	0.3	0.51	0.8	0.28	0.49	0.79
2099	0.67	1.02	0.53	0.77	1.12	0.57	0.81	1.16	0.37	0.61	0.97	0.33	0.57	0.92	0.33	0.57	0.92	0.34	0.59	0.94	0.32	0.57	0.92

Yr	(mm/yr)			(mm/yr)			(mm/yr)			(mm/yr)			(mm/yr)			(mm/yr)							
	50%	95%		5%	50%	95%	5%	50%	95%	5%	50%	95%	5%	50%	95%	5%	50%	95%					
2010	7	3	3	3	7	3	3	7	3	3	3	0	3	3	0	3	3	0	3	3			
2020	4	6	4	6	7	4	6	7	2	4	5	2	3	5	2	3	5	2	4	5			
2030	5	6	4	5	7	5	6	8	3	4	6	3	4	6	3	4	6	2	3	5			
2040	5	8	5	7	9	5	7	9	4	6	8	3	5	7	3	5	7	3	5	7			
2050	7	10	5	8	11	6	8	11	3	6	9	3	5	8	3	5	8	3	6	9			
2060	7	11	6	8	12	6	9	13	4	6	10	4	7	11	4	7	11	4	6	10	4	6	10
2070	8	13	6	9	13	6	9	13	5	8	12	4	7	11	4	7	11	5	8	12	4	7	12
2080	9	13	6	9	15	7	10	15	5	8	14	4	7	13	4	7	13	4	7	13	5	8	13
2090	8	15	6	10	15	6	10	16	5	8	14	5	8	14	5	8	14	5	9	14	4	8	14
2099	10	16	7	10	17	7	10	17	4	9	16	4	9	14	4	9	14	4	9	16	4	9	14

## A.4. Miscellaneous Cores: fieldwork and sampling adaptation

Three cores (5 cm diameter: MR60, MR24; and; 8 cm diameter: MR36; Figure 3-35) retrieved from MR saltmarsh site had lost their base during retrieval. A 1 m long profiler was used to investigate the reason of the loss. When inserted at sampling plot MR8, it revealed that a sand unit could be traced up at least 74 cm in depth (Figure A- 2) but this drastic change of sediment type compared to the upper part of the core resulted in damaging the core base (Figure A- 1). This situation was similar for the other three cores where water saturation made the whole stratigraphical unit/ layer of coarse sand slip away whilst pulling the core. Therefore, the maximum depth was not reached but using manual corer, it was just not possible to keep the sediment. This further impacted the sampling design and limited the core retrieval on the fore-shore pioneer zone of FM as it is formed a cliff edge backing coarse sands with only strands of *Salicornia* (resulting in very little matter cohesion). It is perhaps possible to prevent such limitations by using powered Vibrocorer that are often used when sampling sand/mud- flats.



**Figure A- 1:** Sandy base of MR8 core (5cm) that got damaged from the rest of the core



**Figure A- 2:** Sandy base (from 39.5cm deep) of the core retrieve from 1m long profiler showing light grey sand unit of sand up to 62cm followed by a reddish layer of coarse sand.

#### **A.5. Loss on Ignition - LOI methodology to measure Inorganic and Organic content in Nigg saltmarsh sediments**

The methodology chosen for LOI and duration of temperature of loss-on-ignition (LOI) methods was based on existing literature (Ball, 1964; Craft et al., 1991; Sutherland, 1998; Heiri et al., 2001; Santisteban et al., 2004; Roner et al., 2016; Aitkenhead and Coull, 2016), yet there are serious concerns using LOI to estimates organic matter (OM) and soil organic carbon (SOC):

- i. standard procedures varies to remove the water content by drying the samples from 60 °C for 24 hours (longer if required until constant weight) to 105 °C overnight (Howard et al., 2014); these differences are firstly based on speed as the final weight has to remain constant no matter the method; secondly difference occur on type research studies such as sediment dating using sediment isotopes and radionuclides (water removal of temperature higher than 50-60 °C can erode grains (Aitken, 1989));
- ii. choice of the appropriate ignition temperatures is closely linked to the sediment characteristics. Ball (1964) suggests that structural water loss is not complete at temperature <105°C for clay minerals (when > 11%) and these samples require ignition at lower temperature of 375°C;

- iii. reproducibility is not always reached, as all SOM is not always combusted at 375 °C (Plater et al., 2015) and organic carbon oxidation may not be complete by using standard LOI temperature;
- iv. choice of ignition between 425 to 520°C minerals in soil can lose some CO<sub>2</sub> from minerals and inorganic carbon (in soil SIC) such as siderite, magnesite, rhodochrosite and dolomite leading to large overestimation of loss of organic matter (Sutherland and Walton, 1990; Santisteban et al., 2004; Wang et al., 2011);
- v. application of conversion factors such as conventional 1.724 ('Von Bemmelen' factor) to OM values derived from LOI to estimate SOC is not appropriate because the nature of OM differs significantly

It is unlikely that structural water loss (ii) may be affect the estimation of Nigg bay's sediments because clays form a very small percentage (<8%) of the overall soil sediments. This led to choose stepped procedure :

- 1) two sets of samples (same core) were dried to measure:
  - a. water content by ignition at 60°C for 24hours (n=603), cooling (in desiccator) and weighting;
  - b. dry bulk density by ignition at 105°C for 12hours (n=595) ), cooling (in desiccator) and weighting;
- 2) OM measured by:
  - a. igniting samples 1)a. at 375°C for 24hours, cooling (in desiccator) and weighting;
  - b. igniting samples 2)a. at 450°C, cooling (in desiccator), reweighting;
- 3) Carbonate content measured by igniting samples 2)b. at 800°C for 2 hours, cooling (in desiccator) and weighting;



## **APPENDIX.B      Supplementary references for Chapter 3**

### **B.1.    Cromarty and Invergordon tides - Additional Notes & Definitions:**

#### **Cromarty and Invergordon tides - Additional Notes & Definitions:**

MHWS (Mean High Water Springs); MLWS (Mean Low Water Springs). The height of mean high water springs is the average, throughout a year when the average maximum declination of the moon is  $23\frac{1}{2}^{\circ}$ , of the heights of two successive high waters during those periods of 24 hrs (approximately once a fortnight) when the range of the tide is greatest. The height of mean low water springs is the average height obtained by the two successive low waters during the same periods.

MHWN (Mean High Water Neaps) MLWN (Mean Low Water Neaps). The height of mean high water neaps is the average, throughout a year as defined above, of the heights of two successive high waters during those periods (approximately once a fortnight) when the range of the tide is least. The height of mean low water neaps is the average height obtained from the two successive low waters during the same periods.

The mean tidal levels were established empirically during a year when the average maximum declination of the moon was  $23.5^{\circ}$ . During such a year, the tidal observations were investigated, and the above-mentioned criteria followed in order to derive the appropriate levels, which would not necessarily result in the same levels as those derived from separate analyses of discrete sets of tidal observations that pre- or post-date those 'accepted' observations. Therefore, due to the method in which these levels were derived, they were effectively 'set-in-stone' and are unlikely to have been amended in many years.

HAT (Highest Astronomical Tide); LAT (Lowest Astronomical Tide) - The highest and lowest predicted tides that can occur are deemed Highest Astronomical Tide (HAT) and Lowest Astronomical Tide (LAT) respectively. These levels are the highest and lowest levels which can be predicted to occur under average meteorological conditions, and under any combination of astronomical conditions; these levels will not be reached every year. HAT and LAT are not the extreme levels which can be reached, as Storm Surges (wind-induced long period waves causing higher and lower-than-predicted levels to occur) and pressure effects can significantly alter the times and / or heights of the observed tide. HAT and LAT are obtained via the investigation of daily predictions for ports over a significantly long period of time (ideally the full Metonic cycle of 18.6 years).

### **B.2.    Physical variables**



One of the assumptions of the simple linear regression and multiple regression is that there is no **perfect** multi-collinearity between predictor/explanatory variables to avoid regression estimates to be unstable and have high standard errors. Although principal component analysis (PCA) were performed, VIF (Variance inflation factors) were measured when modelling, and one or more highly correlated variables were removed, the table below presents the correlation matrix of the physical drivers (Elevation, BDD in g.cm3, Distance to HWMS, distance to Water Channels (creeks) and distance to saltmarsh edge, Curvature and Slope) measured for 60 sampling points across the three saltmarsh. Water levels (flood depth, flood frequency and hydroperiod) are presented in chapter 4 - section 4-4 and in Appendix D.3.

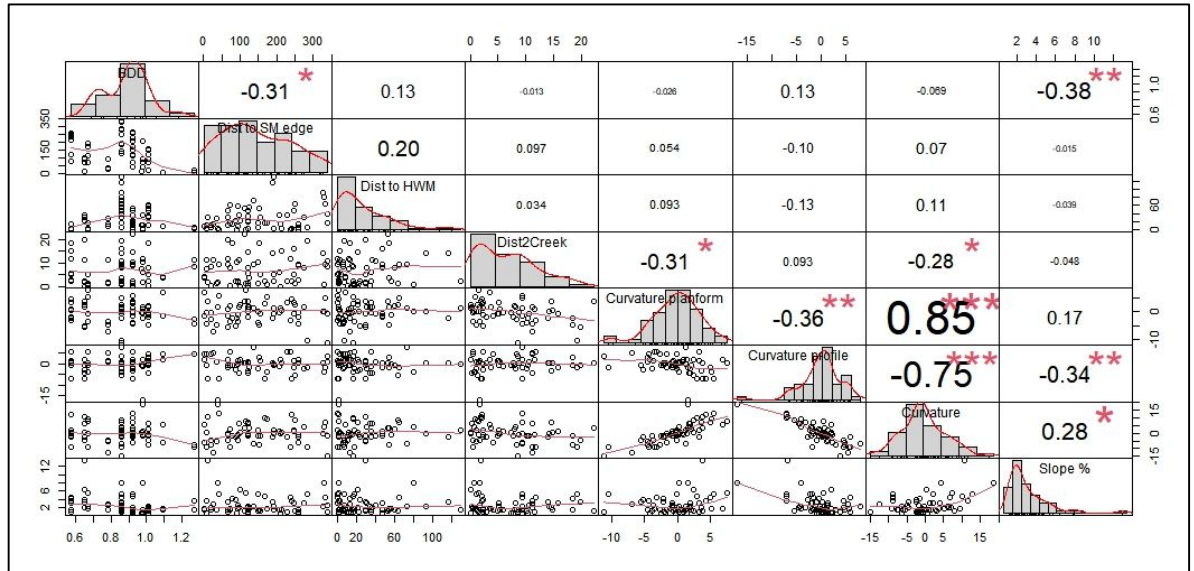


Figure B - 1: Correlation Matrix (lower = Scatter plot from untransformed data; upper = correlation value and p-significance; diagonal = data distribution histogram) between the physical variables (Elevation, BDD in g.cm3, Distance to HWMS, distance to Water Channels (creeks) and distance to saltmarsh edge) using spearman's Rho coefficient and p-values:  $p < 0.001$ \*\*\*,  $p < 0.01$ \*\* ,  $p < 0.05$ \*.

### B.3. DEM survey accuracy and dataset selection

#### Data assessment

DEMs derived from LIDAR (Light Detection and Ranging), Ortho-photogrammetry or terrestrial laser scanning are known to produce elevation errors on coastal marshes which can be different from errors on other ground surfaces, and this can result in misuse of the data and/or erroneous conclusions (Schmid et al., 2011). It is important to mention that the dataset has been carefully cleaned from noise, but it is not possible to fully differentiate between the changes in elevation height of the ground surface resulting from sediment supply and vegetation growth. Although, all terrestrial Laser Scanning (TLS) and orthophotography were carried at low tide and during the summer season to reduce the differences derive from seasonal vegetation variations, it is also possible that the starting point of the time series (2011 Lidar) may have been carried out during wetter conditions or at high tide (water leads to refraction of the LIDAR and TLS laser signal) and may affect the analysis. In order to justify which dataset should be used to

address the aims of this study, it seems pertinent to quantify first the precision and comparability of the methods for the three sites, then present the results of topographical changes on this pluri-annual scale. All terrestrial laser survey data was cleaned from noise where possible (see Figure B - 2 below), exported as .pts format file (Leica proprietary) and converted into .las format file and finally interpolated to create a Digital Elevation Model (DEM) in ArcGIS to allow geomorphological analysis and compare dataset. A-posteriori uncertainty evaluations of the models are presented in Chapter 3 - Table 3.9 (Wheaton et al., 2010; Eamer and Walker, 2013). Because variation in microtopography in particular fine scale topographic features such as intertidal creeks, depressions, platforms, levees and variable vegetation cover and seasonality will affect DEMs comparison (Montané and Torres, 2006; Chassereau et al., 2011; McClure et al., 2016), the geomorphological analysis in this study had to be carefully limited to designated areas of the saltmarsh such as the saltmarsh edge and to quantify the lateral movement of the saltmarsh or the pioneer/mudflat zones where the vegetation have little impact as possible on the DEM elevation comparisons.

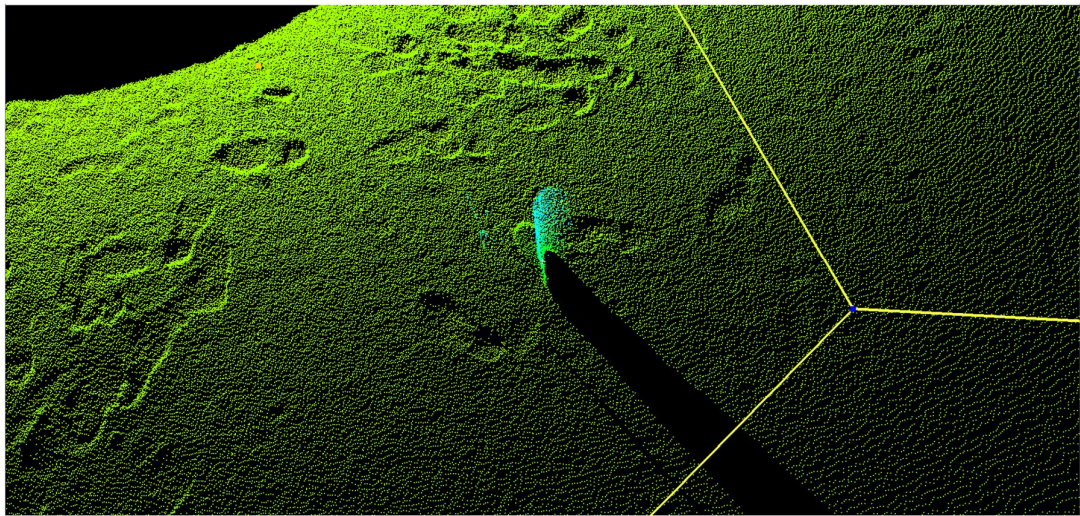


Figure B - 2: Using remote sensing (TLS) to a millimetre precision is a challenge. Extract of TLS point cloud data showing noise on soft sandy surface: light blue hues data points representing difference in height from reference target and ground surface have been removed, however footprints depression have not and become part of the ground surface.

Survey dataset was post-processed (to assess uniformity and extent, noise removal, etc.) was executed in CloudCompare (3D point cloud processing software from [www.danielgm.net/cc/](http://www.danielgm.net/cc/)) and time series DEM changes was generated in ArcGIS using the GCD toolbox package.

### **Dataset precision and selection**

Although all data captured during this project provided a RMSE (x, y and z) ranging from 0.007m to 0.054m (Table B- 1 and section 3.4.1.4), the analysis still produces large differences depending on the dataset or methods used. A two-step demonstration highlights the challenges in quantifying time-series topographical changes in saltmarsh systems which can be attributed to . First, the percentage difference between two methods to quantify accretion and erosion on the saltmarsh is presented and these lead on to

a statistical assessment of the differences in order to select the best dataset for use for small -scale mapping. As for large-scale mapping, to reduce vertical error contained within saltmarsh's DEMs and following McClure et al., 2016, TLS and RTK GPS data were used when possible (e.g. detailed topographical analysis such as saltmarsh edge movement, sedimentation plates elevation change).

**Table B- 1: Summary of the dataset used to analyse topographical changes on the saltmarsh sites**

	$\pm$ RMSE (m)	MR	FM	ANK
2011 Lidar	0.054	✓	✓	✓
TLS 2014	0.032	✓	(west breach only)	
TLS 2015	0.007	✓		
TLS 2016	0.009		✓	✓
TLS 2017	0.007		✓	✓
Orthophotography 2017	0.023	✓	✓	✓

Two methods may be used to quantify volumetric and areal changes on the sites:

- Method A- non-cumulative method to obtain percentage changes by subtracting 2017 orthophotography from 2011 LiDAR;
- Method B- cumulative method to obtain percentage changes by averaging the volumetric and areal changes between 2011 and 2017 using Lidar, TLS and orthophotography data.

A small volumetric difference (<15%) was observed between methods A and B for the three sites, however areal differences per sites especially between MR and ANK were greater ranging from 26.79% to 80.79% (Table B- 2). A selective approach analysing only the pioneer and low marsh zones (to reduce the influence of vegetation on generation of the elevation models) is possible, but the differences were considered still too large (Table B- 3).

**Table B- 2: Percentage differences between the volumetric and areal changes results using non-cumulative method A (2011 Lidar & 2017 Orthophotography DEMS).**

	% differences between methods (ANK)	% differences between methods (FM)	% differences between methods (MR)
<b>Volumetric</b>	11.18 $\pm$ 2.3	13.57 $\pm$ 2.8	8.56 $\pm$ 0.6
<b>Areal</b>	34.11 $\pm$ 8.4	80.79 $\pm$ 17.3	26.79 $\pm$ 4.2

**Table B- 3: Percentage differences on pioneer and low marsh zones exclusively between the volumetric and areal changes results using cumulative method B (changes from 2011 to 2017).**

	% differences between methods (ANK)	% differences between methods (FM)	% differences between methods (MR)
<b>Volumetric</b>	47.13 $\pm$ 9.9	13.57 $\pm$ 2.8	3.17 $\pm$ 0.2
<b>Areal</b>	67.96 $\pm$ 16.2	80.79 $\pm$ 17.3	1.27 $\pm$ 0.2

The type of data source may be the reason of these differences but when using long time series it is not always possible to keep equipment standardised, thus excluding method proposed by Wheaton et al., 2010 to account for uncertainty in repeat topographic surveys. Although, the volumetric differences were small, the large areal differences between the two methods suggest also that the use of only two datasets (i.e.

2017-2011) may amplify differences which are only temporary and may not reflect the longer dynamics of the environment especially in saltmarsh system which are known to respond quickly to environmental forcing (i.e. tides). The use of precise ground surveys may then be preferred than systematic survey such as LIDAR or orthophotography which covers large scale without taking into account varied type of topographical landscape (waterlogged, highly or poorly vegetated zones on a very shallow gradient) and requires further post-processing to adjust results to errors generated by the terrain. DGPS may be a solution, but the coverage is limited as some areas are physically difficult to access, and the reported of  $\pm 7$  cm vertical accuracy (Montané and Torres, 2006) is seen as too inaccurate and imprecise to quantify saltmarsh sedimentation rates at this multi-annual time scale. In Nigg Bay, DGPS monitoring of the three sites was carried out on sixty targeted locations which was revisited height times during the project (see sampling design in 3.3.2.2). Measurements carried out in March 2017 provided ground control points to evaluate if the variability in error was spatially correlated to the site and/or saltmarsh zone and further deduct if vegetation may be a factor in height changes. Subtracting the vertical data of 2017 DGPS from Lidar 2011 provided an average difference of  $0.02 \pm 0.01$  m (ranging from -0.15 to 0.17 m - Figure B - 3 ) which is well within the centimetre-level accuracy of Leica DGPS equipment used for field survey and may reflect the sedimentation rate that took place during this period. Similarly, subtraction of March 2017 DGPS to 2017 orthophotography provided an average difference of  $-0.03 \pm 0.01$  m (ranging from -0.19 to 0.25 - Figure B - 4 ). The statistical results presented on Figure B - 5a and Figure B - 6a shows strong positive relationship between the surveys which is further confirmed for the surveys height difference variability (Figure B - 5b and Figure B - 6b) on all saltmarsh sites except for orthophotography carried out on ANK (Figure B - 5a and b). For this reason, this dataset was removed from the time series. It is possible that the camera model which differed from the one used for MR and FM survey had not enough field of depth or poorer sensor to deal with landscape variation present on saltmarshes (dark vegetation, terrain, etc.).

Furthermore, as ground surveys are preferred options, TLS data in 2017 was favoured over 2017 orthophotography to quantify erosion and accretion on the fronting marsh. 2017 orthophotography was kept for the MR and FM site timeseries.

**As a recap,**

able B- 4 below summarised the selection of the dataset used to quantify accretion and erosion for our three sites between 2011 to 2017 (results in Chapter 5).



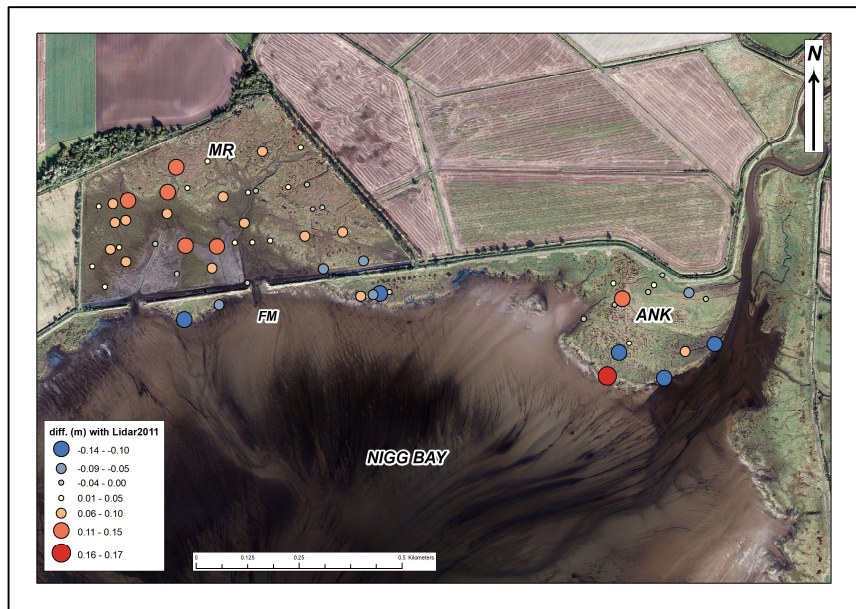


Figure B - 3 : Map of the vertical height difference (m) between 2017 DGPS control data and Lidar 2011 (using size and colour symbology values of height differences). Height differences were not found statistically significant between the sites' saltmarsh zone which is confirmed by the height differences' random spatial distribution. The distribution further suggests little correlation between spatial variability and the presence of vegetation where we would have expected larger error where higher vegetation density (e.g. on HM zone). Furthermore, these differences could be attributed to real gain in height as the mean height difference of  $0.01 \pm 0.01\text{m}$  (within both survey method accuracy see table B-1).

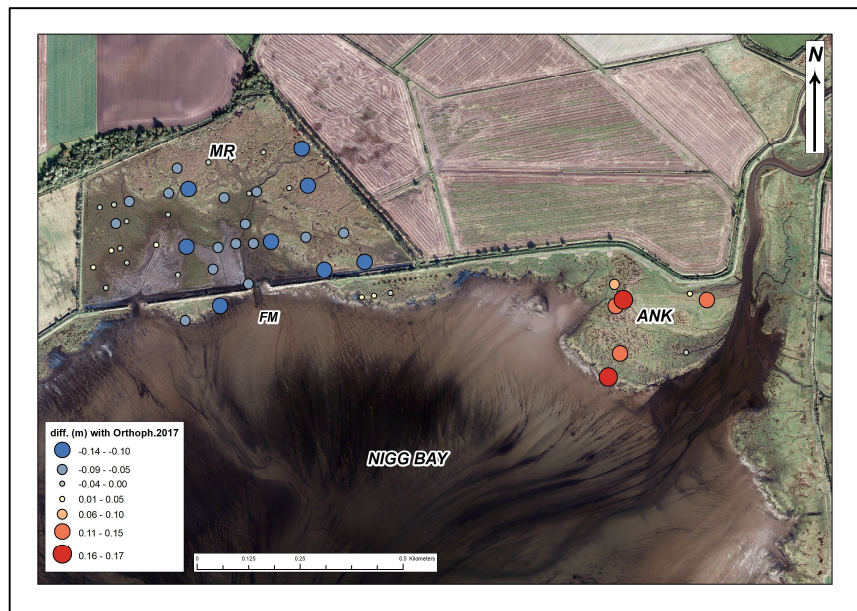


Figure B - 4 : Map of the vertical height difference (m) between 2017 DGPS control data and 2017 Orthophotography (using size and colour symbology values of height differences) were not found statistically significant between the sites' saltmarsh zone which is confirmed by the height differences' random spatial distribution leading to similar conclusion than Figure B-3. Height differences between DGPS 2017 and Orthophoto 2017 shows that mean height differences is  $0.05 \pm 0.02\text{ m}$  (within both survey method accuracy see table B-1).

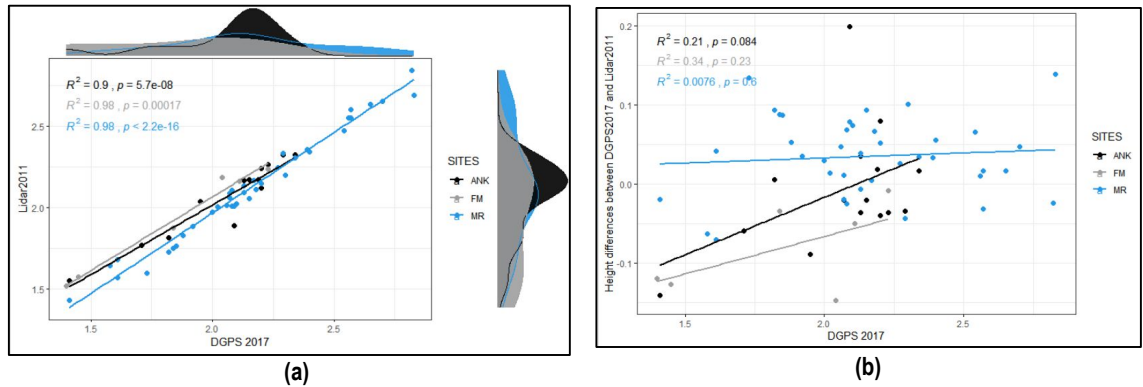


Figure B - 5: Overall ground controls elevation heights (DGPS 2017) and Lidar 2011 have a strong positive and statistically significant relationship ( $t= 1.03, p < 0.001$ ) where 95.8 % of the variation in height differences can be explained by the LIDAR survey.

- a) The scatter plot (a) confirms this strong positive relationship between surface heights in 2011 and 2017 for each saltmarsh site with  $R^2$  is  $0.9^{***}$ ,  $0.98^{***}$  and  $0.98^{***}$  for ANK, FM and MR respectively.
- b) Furthermore , the scatter plot b suggests that on each marsh, the variation in the surveys' height differences for each site are not likely be attributed to the DGPS 2017 survey (by the low  $R^2$  and non-significant p-value).

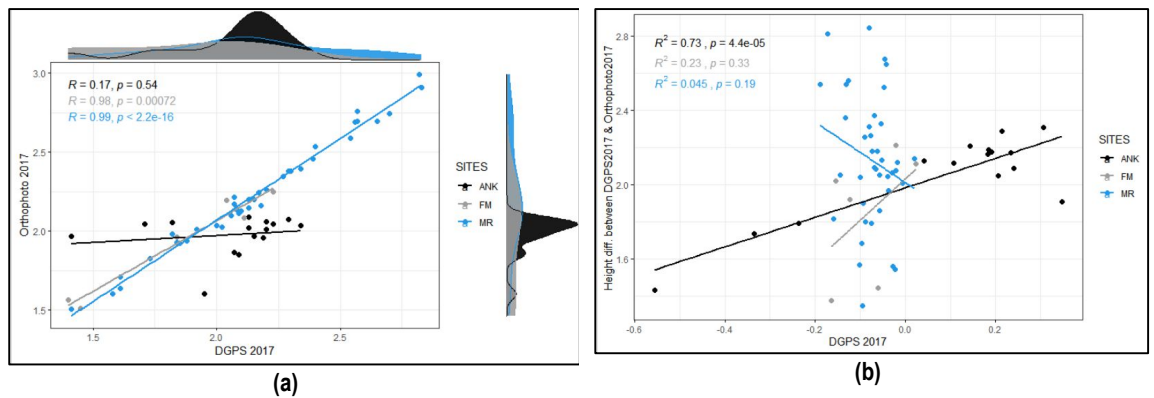


Figure B - 6: Overall ground controls elevation heights (DGPS 2017) and Orthophotography have a strong positive and statistically significant relationship ( $t= 0.89, p < 0.001$ ) where 80.7 % of the variation in height differences can be explained by the Orthophotography survey.

- a) Although the scatter plot (a) confirms this strong positive relationship between surface heights in DGPS and Orthophotography on FM and MR ( $R^2$  is  $0.98^{***}$  and  $0.98^{***}$  respectively), there is no relationship that can be established between heights surveyed using DGPS and Orthophotography on ANK.
- b) The scatter plot (b) confirms that the surveys' height difference variation between the two surveys on FM and MR are not significantly explained by the control survey points, whereas  $73\%^{***}$  of this variation can be explained by the ground controls elevation heights (DGPS 2017). This finding lead to exclude 2017 ANK's orthophotography from the elevation change analysis.

able B- 4: Summary of the dataset used to analyse topographical changes (small-scale mapping) on the saltmarsh sites.

	MR	FM	ANK
2011 Lidar	✓	✓	✓
TLS 2014	✓		
TLS 2015	✓		
TLS 2016		✓	✓
TLS 2017		✓	✓
Orthophotography 2017	✓	✓	



## APPENDIX.C Supplementary references for Chapter 4

### C.1. Sediment

#### Filter Discs sediment deposition rates

**Table C- 1:** Linear regression model between Filter Discs Sediment Deposition between saltmarsh sites and zones. Using a Box-Cox power transformation to determine whether the data could be transformed suggested that a best lambda value of 0.3 for transformation. Results below are transformed following this formula. Note: that the table also reports a test of the factor (i.e. category = zones and sites) as a whole instead of a test against the reference level (with Sum of Sq. from ANOVA- type II of the model).

Linear Regression between Filter discs deposition rates and saltmarsh sites and Zones	
Dependent variable:	
(DISCS_average.g.per.day_gm2^0.3)	
HM_FM	-0.29 (±0.36)
HM_MR	0.48 (±0.4)
<b>LM_ANK</b>	<b>-0.84** (±0.37)</b>
LM_MR	0.47 (±0.32)
<b>MM_ANK</b>	<b>0.76** (±0.34)</b>
MM_FM	-0.09 (±0.38)
MM_MR	0.02 (±0.36)
<b>PM_ANK</b>	<b>0.72* (±0.39)</b>
PM_FM	0.73 (±0.51)
PM_MR	0.15 (±0.34)
Constant	1.54*** (±0.28)
Observations	304
R2	0.13
Adjusted R2	0.1
Residual Std. Error	1.21 (df = 293)
F Statistic	4.27*** (df = 10; 293)
Site&Zones Sum Sq.	<b>62.81 (df = 10)***</b>
Residual Sum Sq.	431.06 (df = 293)
Note: **p<0.1; *p<0.01; ***p<0.001	

**Table C- 2:** The table presents Welch's Anova and Games-Howell post hoc (adjusted with Bonferroni correction) statistical analysis results to test differences filter discs sediment deposition ( $\text{g m}^{-2} \text{day}^{-1}$ ) and collection dates. Using a Box-Cox power transformation to determine whether the data could be transformed suggested that a best lambda value of 0.3 for transformation. Results below are transformed following this formula.

ANOVA – Welch's Anova test (formula = (DISCS_average.gm2.per.day ^ 0.3) ~ Collection_Date)						
Source	DFNum	DF Den	F-Value	p. value & significance		
Months	10	96.2	11.1	<0.001***		
Games-Howell post hoc adjusted with Bonferroni correction						
group1- collection date	group2 - collection date	estimate	conf.low	conf.high	p.adj.	p. significance
09/03/2016	17/10/2016	1.60	0.21	2.99	0.01	*
09/03/2016	14/11/2016	1.83	0.47	3.19	0.00	**
09/03/2016	14/12/2016	1.27	0.01	2.53	0.05	*
21/04/2016	17/10/2016	1.21	0.02	2.40	0.04	*
21/04/2016	14/11/2016	1.44	0.30	2.59	0.01	**
06/06/2016	14/11/2016	1.02	0.02	2.02	0.04	*
06/06/2016	31/01/2017	-0.95	-1.87	0.03	0.04	*
04/07/2016	14/11/2016	1.07	0.12	2.02	0.02	*
04/07/2016	31/01/2017	-0.90	-1.76	0.04	0.03	*
03/08/2016	17/10/2016	1.51	0.50	2.52	0.00	***
03/08/2016	14/11/2016	1.74	0.79	2.70	3.80E-06	****
03/08/2016	14/12/2016	1.18	0.41	1.95	0.00	***
18/09/2016	31/01/2017	-1.21	-2.16	0.27	0.00	**
17/10/2016	31/01/2017	-1.73	-2.69	0.77	5.53E-06	****
14/11/2016	31/01/2017	-1.97	-2.86	-1.07	4.15E-08	****
14/12/2016	31/01/2017	-1.40	-2.10	0.71	3.89E-07	****

**Table C- 3: Linear regression model results to test relationships between filter discs sediment deposition rates (g m<sup>-2</sup> day<sup>-1</sup>), collection dates, sites and sites and saltmarsh Zones. Using a Box-Cox power transformation to determine whether the data could be transformed suggested that a best lambda value of 0.3 for transformation for model (1) and (2) and lambda value of 0.15 for model (3). Results below are transformed following these formulae. The table presents linear model results and reports a test of the factor (with Sum of Sq. from ANOVA- type II of the model).**

Linear Regression between Filter discs deposition rates and collection dates, sites and zones			
Dependent variable:			
	(DISCS_average.g.per.day_gm2^0.3) (1)	(DISCS_average.g.per.day_gm2^0.3) (2)	(DISCS_average.g.per.day_gm2^0.15) (3)
Apr-16	0.39 (±0.37)	0.39 (±0.37)	0.35. (±0.20)
May-16	<b>0.83* (±0.40)</b>	<b>0.81* (±0.40)</b>	<b>0.62** (±0.21)</b>
Jun-16	<b>0.81* (±0.35)</b>	<b>0.81* (±0.35)</b>	<b>0.59** (±0.18)</b>
Jul-16	<b>0.76* (±0.34)</b>	<b>0.76* (±0.34)</b>	<b>0.55** (±0.18)</b>
Aug-16	0.09 (±0.33)	0.07 (±0.33)	0.15 (±0.17)
Sep-16	<b>1.08** (±0.33)</b>	<b>1.06** (±0.33)</b>	<b>0.66*** (±0.17)</b>
Oct-16	<b>1.60*** (±0.33)</b>	<b>1.58*** (±0.33)</b>	<b>0.87*** (±0.17)</b>
Nov-16	<b>1.83*** (±0.33)</b>	<b>1.82*** (±0.33)</b>	<b>1.01*** (±0.18)</b>
Dec-16	<b>1.27*** (±0.33)</b>	<b>1.25*** (±0.33)</b>	<b>0.85*** (±0.17)</b>
Jan-17	-0.13 (±0.33)	-0.15 (±0.33)	0.05 (±0.17)
SITEFM		-0.31. (±0.18)	
SITEMR		0.04 (±0.14)	
HM_FM			-0.17 (±0.18)
HM_MR			0.28 (±0.20)
LM_ANK			<b>-0.44* (±0.18)</b>
LM_MR			<b>0.32* (±0.16)</b>
MM_ANK			<b>0.41* (±0.17)</b>
MM_FM			0.07 (±0.19)
MM_MR			0.15 (±0.18)
PM_ANK			<b>0.56** (±0.19)</b>
PM_FM			0.28 (±0.25)
PM_MR			0.08 (±0.17)
Intercept/Constant	<b>1.08*** (±0.26)</b>	<b>1.13*** (±0.28)</b>	<b>0.49* (±0.20)</b>
Observations	304	304	304
R2	0.26	0.27	0.35
Adjusted R2	<b>0.25</b>	<b>0.24</b>	<b>0.31</b>
Residual Std. Error	1.12 (df = 293)	1.12 (df = 291)	0.6 (df = 283)
F Statistic	<b>10.05*** (df = 10; 293)</b>	<b>8.78*** (df = 12; 291)</b>	<b>7.55*** (df = 20; 283)</b>
CollectDates Sum Sq.	<b>126.15 (df = 10)***</b>	<b>125.52 (df = 10)***</b>	<b>33.6 (df = 10)***</b>
Sites Sum Sq.		5.04 (df = 2)	
Sites&Zones Sum Sq.			<b>20.4 (df = 10)***</b>
Residual Sum Sq.	301.59 (df = 273)	362.68 (df = 291)	100.4 (df = 283)

Note: \*\*p<0.1; \*p<0.01; \*\*\*p<0.001

**Table C- 4: Linear regression model results to test relationships between filter discs sediment deposition rates (g m<sup>-2</sup> day<sup>-1</sup>) and collection dates for each saltmarsh sites. Note1: Box-Cox power transformation has been used for sediment deposition rates using a lambda value of 0.3. The table presents linear model results and reports a test of the factor (with Sum of Sq. from ANOVA- type II of the model). Note2: Model (- FM -) constant is not significant, thus suggesting that there isn't sufficient statistical evidence to use the model to make a prediction for a point that is outside the range of this dataset because the relationship between the variables might change. The value of the constant is a prediction for the response value when all predictors equal zero. However, the model allows to get a sense of the variation between the sediment deposition rates and collection dates.**

Linear Regression between Filter discs deposition rates pern sites and collection dates			
Dependent variable:			
	(DISCS_average.g.per.day_gm2^0.3) (ANK_)	(DISCS_average.g.per.day_gm2^0.3) (FM_)	(DISCS_average.g.per.day_gm2^0.3) (MR_)
Apr-16	-1.20. (±0.65)	<b>2.08* (±0.81)</b>	<b>1.04* (±0.51)</b>
May-16	0.05 (±0.69)	0.92 (±0.99)	<b>1.26* (±0.51)</b>
Jun-16	0.78 (±0.63)	-0.31 (±0.76)	<b>1.27** (±0.44)</b>
Jul-16	-0.30 (±0.63)	1.34. (±0.74)	<b>1.25** (±0.43)</b>
Aug-16	-0.59 (±0.61)	0.59 (±0.74)	0.32 (±0.41)
Sep-16	0.67 (±0.61)	<b>1.64* (±0.74)</b>	<b>1.11** (±0.41)</b>
Oct-16	0.72 (±0.61)	<b>1.57* (±0.74)</b>	<b>2.15*** (±0.41)</b>
Nov-16	0.69 (±0.63)	<b>3.16*** (±0.74)</b>	<b>2.03*** (±0.41)</b>
Dec-16	0.64 (±0.61)	<b>2.01** (±0.74)</b>	<b>1.38*** (±0.41)</b>
Jan-17	-1.09. (±0.61)	0.31 (±0.57)	0.16 (±0.41)
Constant	<b>1.87*** (±0.49)</b>	0.313 (±0.571)	<b>0.87* (±0.34)</b>
Observations	102	57	145
R2	0.29	0.469	0.364

Adjusted R2	0.212	0.354	0.317
Residual Std. Error	1.202 (df = 91)	1.139 (df = 46)	0.951 (df = 134)
F Statistic	3.716*** (df = 10; 91)	4.064*** (df = 10; 46)	7.674*** (df = 10; 134)
CollectDates Sum Sq. (df = 10)	53.647***	52.7***	69.5***
Residual Sum Sq.	131.4 (df = 91)	59.7(df = 46)	121.3 (df = 134)
Note: **p<0.1; ***p<0.01; ****p<0.001			

Sediment Deposition rates from AstroTurf mats

**Table C- 5: Statistical analysis results to test differences between AstroTurf mats sediment deposition (g m<sup>-2</sup> day<sup>-1</sup>) and collection dates. Using a Box-Cox power transformation to determine whether the data could be transformed suggested that a best lambda value of 0.2 for transformation. Results below are transformed following this formula. The table presents Welch's Anova and Games-Howell post hoc (adjusted with Bonferroni correction).**

ANOVA – Welch's Anova test (formula = (DISCS_average.gm2.per.day ^ 0.3) ~ Collection_Date						
Source	DFNum	DF Den	F-Value	p. value & significance		
Months	11	68.98	8.65	<0.001***		
Games-Howell post hoc adjusted with Bonferroni correction						
group1- collection date	group2 - collection date	estimate	conf.low	conf.high	p.adj.	p. significance
09/03/2016	18/09/2016	1.3650419	0.0156497	2.7144342	0.004	**
09/03/2016	17/10/2016	1.7647561	0.4021942	3.127318	0.000256	***
09/03/2016	14/11/2016	1.830752	0.4746724	3.1868316	0.000254	***
09/03/2016	14/12/2016	1.4157401	0.185835	2.6456451	0.001	***
21/04/2016	17/10/2016	1.3786479	0.2267288	2.530567	0.000562	***
21/04/2016	14/11/2016	1.4446438	0.3009199	2.5883677	0.0000783	****
21/04/2016	14/12/2016	1.0296319	0.0520457	2.0072181	2.48E-07	****
06/06/2016	14/11/2016	1.0176101	0.016304	2.0189161	2.24E-07	****
04/07/2016	17/10/2016	1.0018752	0.0438753	1.9598751	3.84E-07	****
04/07/2016	14/11/2016	1.0678711	0.1206401	2.0151022	0.000454	****
03/08/2016	17/10/2016	1.3190176	0.3155141	2.322521	0.000149	***
03/08/2016	14/11/2016	1.3850135	0.3916445	2.3783825	0.004	**
03/08/2016	14/12/2016	0.9700016	0.2031159	1.7368872	0.003	**
18/09/2016	31/01/2017	-1.373809	-2.285805	-0.461813	0.004	**
17/10/2016	31/01/2017	-1.773523	-2.708272	-0.838774	0.004	**
14/11/2016	31/01/2017	-1.839519	-2.763148	-0.91589	0.004	**
14/12/2016	31/01/2017	-1.424507	-2.0859	-0.763114	0.004	**

**Table C- 6: Linear regression model results to test relationships between AstroTurf mats sediment deposition rates (g m<sup>-2</sup> day<sup>-1</sup>), collection dates (model 1 to 3), sites (model 2) and sites and saltmarsh Zones (model 3). Note 1: Using a Box-Cox power transformation to determine whether the data could be transformed suggested that a best lambda value of 0.2 for transformation for the three models. Results below are transformed following this formula. Note 2: The table presents linear model results and reports a test of the factor (with Sum of Sq. from ANOVA- type II of the model). Note3: Model 1 & 2 constant is not significant, thus suggesting that there isn't sufficient statistical evidence to use the model to make a prediction for a point that is outside the range of this dataset because the relationship between the variables might change. The value of the constant is a prediction for the response value when all predictors equal zero. However, the model allows to get a sense of the variation between the sediment deposition rates and collection dates.**

Linear Regression between Filter discs deposition rates and collection dates, sites and zones			
Dependent variable:			
	(1)	(2)	(3)
	(MATS_average.g.per.day_gm2^0.2)		
Apr-16	1.00*** (±0.22)	0.99*** (±0.22)	0.96*** (±0.2)
May-16	1.10*** (±0.21)	1.09*** (±0.2)	1.05*** (±0.18)
Jun-16	1.04*** (±0.2)	1.06*** (±0.2)	1.05*** (±0.18)
Jul-16	0.91*** (±0.2)	0.92*** (±0.2)	0.89*** (±0.17)
Aug-16	0.95*** (±0.2)	0.97*** (±0.2)	0.95*** (±0.18)
Sep-16	1.29*** (±0.2)	1.31*** (±0.2)	1.29*** (±0.18)
Oct-16	1.59*** (±0.2)	1.61*** (±0.2)	1.59*** (±0.18)
Nov-16	1.73*** (±0.2)	1.73*** (±0.19)	1.73*** (±0.17)
Dec-16	1.52*** (±0.2)	1.54*** (±0.2)	1.50*** (±0.17)
Jan-17	1.15*** (±0.2)	1.16*** (±0.2)	1.12*** (±0.17)
Feb-March 17	1.26*** (±0.2)	1.28*** (±0.2)	1.24*** (±0.18)
SITEFM		-0.07 (±0.12)	
SITEMR		-0.22** (±0.09)	
HM_FM			-0.15 (±0.21)
HM_MR			-0.13 (±0.21)
LM_ANK			-0.62*** (±0.2)
LM_MR			-0.14 (±0.17)
MM_ANK			0.47*** (±0.17)
MM_FM			0.11 (±0.18)
MM_MR			-0.31* (±0.18)

	PM_ANK	PM_MR	Constant
	0.23 (±0.15)	0.34** (±0.16)	0.02 (±0.2)
			0.09 (±0.18)
			0.27 (±0.19)
Observations	196	196	196
R2	0.37	0.39	0.54
Adjusted R2	0.33	0.35	0.48
Residual Std. Error	0.56 (df = 184)	0.55 (df = 182)	0.49 (df = 175)
F Statistic	9.76*** (df = 11; 184)	8.94*** (df = 13; 182)	10.12*** (df = 20; 175)
CollectDates Sum Sq.	33.34 (df = 11)***	33.754 (df = 11)***	33.46 (df = 11)***
Sites Sum Sq.		1.933 (df = 2)*	
Sites&Zones Sum Sq.			15.201 (df = 9)***
Residual Sum Sq.	57.158 (df = 184)	55.225(df = 182)	41.957 (df = 175)

Note: \*\*p<0.1; \*p<0.01; \*\*\*p<0.001

**Table C- 7: Linear regression model results to test relationships between AstroTurf mats sediment deposition rates (g m<sup>-2</sup> day<sup>-1</sup>) and collection dates for each saltmarsh sites. Note1: Box-Cox power transformation has been used for sediment deposition rates using a lambda value of 0.2. The table presents linear model results and reports a test of the factor (with Sum of Sq. from ANOVA- type II of the model). Note2: Model FM and MR constants are not significant, thus suggesting that there isn't sufficient statistical evidence to use the model to make a prediction for a point that is outside the range of these particular datasets because the relationships between the variables might change. The value of the constant is a prediction for the response value when all predictors equal zero. However, the model allows to get a sense of the variation (as a percentage) between the sediment deposition rates and collection dates as all collections are found to be statistically significant.**

Linear Regression between AstroTurf mats deposition rates per sites and collection dates

	(MATS_average.g.per.day_gm2^0.2) (ANK)	(MATS_average.g.per.day_gm2^0.2) (FM)	(MATS_average.g.per.day_gm2^0.2) (MR)
Apr-16	0.403 (±0.436)	1.888*** (±0.345)	1.137*** (±0.314)
May-16	0.501 (±0.418)	1.684*** (±0.308)	1.343*** (±0.281)
Jun-16	1.058** (±0.436)	1.210*** (±0.345)	1.042*** (±0.256)
Jul-16	0.484 (±0.418)	1.155*** (±0.308)	1.148*** (±0.256)
Aug-16	0.68 (±0.436)	1.188*** (±0.308)	1.093*** (±0.256)
Sep-16	1.291*** (±0.436)	1.296*** (±0.308)	1.354*** (±0.263)
Oct-16	1.510*** (±0.436)	1.691*** (±0.308)	1.674*** (±0.256)
Nov-16	1.307*** (±0.404)	2.244*** (±0.308)	1.864*** (±0.256)
Dec-16	1.340*** (±0.418)	1.426*** (±0.308)	1.711*** (±0.256)
Jan-17	0.780* (±0.418)	1.288*** (±0.308)	1.373*** (±0.256)
Feb-March 17	0.790* (±0.436)	1.975*** (±0.308)	1.366*** (±0.256)
Constant	0.640** (±0.309)	0 (±0.218)	0 (±0.199)
Observations	66	34	96
R2	0.329	0.769	0.464
Adjusted R2	0.193	0.653	0.393
Residual Std. Error	0.690 (df = 54)	0.378 (df = 22)	0.487 (df = 84)
F Statistic	2.409** (df = 11; 54)	6.653*** (df = 11; 22)	6.603*** (df = 11; 84)
CollectDates Sum Sq. (df = 11)	12.612*	10.434***	17.2***
Residual Sum Sq.	25.701 (df = 54)	3.137 (df = 22)	19.89 (df = 84)

Note: \*\*p<0.1; \*p<0.01; \*\*\*p<0.001

### Accretion rates

**Table C- 8: Dunn's pairwise multi-comparison controlled using the Benjamini-Hochberg (BH) adjustment testing for Accretion Rates (cm.yr-1) calculated for deposition from filter discs and AstroTurf mats between saltmarsh sites**

Dunn's pairwise multi-comparison controlled using the Benjamini-Hochberg (BH) adjustment							
group1	group2	n1	n2	statistic	p	p.adj	p.adj.signif
DISCS_ANK	DISCS_FM	98	56	-2.017	0.044	0.082	*
DISCS_ANK	DISCS_MR	98	130	2.637	0.008	0.025	**
DISCS_FM	DISCS_MR	56	130	4.320	0.000	0.000	***
MATS_ANK	MATS_FM	66	34	-1.090	0.276	0.414	ns
MATS_ANK	MATS_MR	66	96	-0.716	0.474	0.642	ns
MATS_FM	MATS_MR	34	96	0.579	0.563	0.649	ns

**Table C- 9: Dunn's pairwise multi-comparison controlled using the Benjamini-Hochberg (BH) adjustment testing for Accretion Rates (cm.yr-1) calculated for deposition from filter discs between saltmarsh sites and zones**

Dunn's pairwise multi-comparison controlled using the Benjamini-Hochberg (BH) adjustment							
group1	group2	n1	n2	statistic	p	p.adj	p.adj.signif
DISCS_ANK_HM	DISCS_ANK_MM	19	39	3.402	0.001	0.005	***
DISCS_ANK_LM	DISCS_ANK_MM	21	39	4.585	0.000	0.000	***
DISCS_ANK_LM	DISCS_MR_LM	21	57	3.618	0.000	0.003	***

DISCS_ANK_MM	DISCS_ANK_PM	39	19	-2.530	0.011	0.037	*
DISCS_ANK_MM	DISCS_FM_MM	39	21	-4.732	0.000	0.000	***
DISCS_ANK_PM	DISCS_MR_PM	19	28	2.443	0.015	0.045	*
DISCS_FM_HM	DISCS_FM_PM	28	7	2.102	0.036	0.089	*
DISCS_FM_MM	DISCS_FM_PM	21	7	2.987	0.003	0.013	**
DISCS_FM_MM	DISCS_MR_MM	21	28	3.057	0.002	0.011	**

**Table C- 10: Dunn's pairwise multi-comparison controlled using the Benjamini-Hochberg (BH) adjustment testing for Accretion Rates (cm.yr<sup>-1</sup>) calculated for deposition from AstroTurf Mats between saltmarsh sites and zones**

Dunn's pairwise multi-comparison controlled using the Benjamini-Hochberg (BH) adjustment							
group1	group2	n1	n2	statistic	p	p.adj	p.adj.signif
MATS_ANK_HM	MATS_ANK_MM	17	24	2.728	0.006	0.036	**
MATS_ANK_LM	MATS_ANK_MM	13	24	4.478	0.000	0.000	***
MATS_ANK_MM	MATS_ANK_PM	24	12	-2.824	0.005	0.030	**
MATS_ANK_MM	MATS_FM_MM	24	23	-3.332	0.001	0.013	***
MATS_ANK_MM	MATS_MR_MM	24	23	-3.114	0.002	0.017	**
MATS_ANK_HM	MATS_ANK_MM	17	24	2.728	0.006	0.036	**

**Table C- 11: Linear regression model results to test relationships between AstroTurf mats and filter discs accretion rates (cm.year<sup>-1</sup>) between sites and saltmarsh zones' sites. Box-Cox power transformation has been used for accretion rates using a lambda value of 0.3 for model 1 to 3, 0.15 for model 4 and 0.1 for model 5. The table presents linear model results and reports a test of the factor (with Sum of Sq. from ANOVA- type II of the model).**

Dependent variables:					
	Filter Discs Accretion Rates (cm.yr <sup>-1</sup> ^0.3)		AstroTurf Mats Accretion Rates (cm.yr <sup>-1</sup> ^0.3)	Filter Discs Accretion Rates (cm.yr <sup>-1</sup> ^0.15)	AstroTurf Mats Accretion Rates (cm.yr <sup>-1</sup> ^0.1)
	1	2	3	4	5
FM	-0.17** (±0.08)				
MR	0.12* (±0.07)				
ANK_LM		-0.21 (±0.15)	-0.28* (±0.15)	-0.19* (±0.11)	-0.30*** (±0.09)
ANK_MM		0.41*** (±0.13)	0.59*** (±0.13)	0.32*** (±0.1)	0.21*** (±0.08)
ANK_PM		0.22 (±0.15)	-0.04 (±0.16)	0.32*** (±0.11)	-0.01 (±0.09)
FM_HM		-0.05 (±0.14)	-0.04 (±0.16)	-0.08 (±0.1)	-0.03 (±0.09)
FM_MM		-0.09 (±0.15)	0.01 (±0.13)	0.02 (±0.11)	0.002 (±0.08)
FM_PM		0.41* (±0.21)		0.26* (±0.15)	(±)
MR_HM		0.24 (±0.16)	-0.03 (±0.16)	0.20* (±0.12)	-0.07 (±0.09)
MR_LM		0.29** (±0.13)	-0.02 (±0.12)	0.26*** (±0.09)	-0.08 (±0.07)
MR_MM		0.21 (±0.14)	-0.06 (±0.13)	0.22** (±0.1)	-0.1 (±0.08)
MR_PM		0.38*** (±0.14)	0.14 (±0.14)	0.32*** (±0.1)	0.05 (±0.08)
09.03.2016				-0.25** (±0.11)	-0.69*** (±0.09)
21.04.2016				-0.05 (±0.11)	-0.12 (±0.09)
06.05.2016				0.15 (±0.11)	-0.01 (±0.09)
06.06.2016				0.13 (±0.1)	-0.02 (±0.08)
04.07.2016				0.1 (±0.09)	-0.11 (±0.08)
03.08.2016				(±)	-0.07 (±0.08)
18.09.2016				0.27*** (±0.09)	0.09 (±0.08)
17.10.2016				0.34*** (±0.09)	0.17** (±0.08)
14.11.2016				0.39*** (±0.09)	0.19** (±0.08)
14.12.2016				0.34*** (±0.09)	0.16* (±0.08)
31.01.2017				-0.18** (±0.09)	0.05 (±0.08)
Constant	0.82*** (±0.05)	0.65*** (±0.11)	0.68*** (±0.1)	0.51*** (±0.1)	0.84*** (±0.08)
Observations	284	284	196	284	196
R2	0.05	0.16	0.22	0.39	0.53
Adjusted R2	0.04	0.12	0.19	0.34	0.47
Residual Std. Error	0.50 (df = 281)	0.47 (df = 273)	0.42 (df = 186)	0.35 (df = 263)	0.24 (df = 175)
F Statistic	6.99*** (df = 2; 281)	5.04*** (df = 10; 273)	5.98*** (df = 9; 186)	8.36*** (df = 20; 263)	9.81*** (df = 20; 175)
SITE Sum Sq.	3.45 (df = 2)**				
Sites & Zones Sum Sq.		11.321(df = 10)***	9.41(df = 9)***	11.8988(df=10)***	8.7953(df=11)***
CollectionDate Sum Sq.				7.8999(df=10)***	2.6854(df=9)***
Residual Sum Sq.	69.21(df = 281)	61.33 (df = 273)	32.52 (df = 186)	31.4491(df=263)	10.128(df=175)

Note: \*\*p<0.1; \*p<0.01; \*\*\*p<0.001

## C.2. Vegetation

**Table C- 12: Summary statistics of above ground biomass (g m<sup>-2</sup>) per sites per saltmarsh zones.**

Above ground biomass (g m <sup>-2</sup> ) per sites per saltmarsh zones.		
ANK	FM	MR

	Mean	SD	Median	Sampling	Mean	SD	Median	Sampling	Mean	SD	Median	Sampling
overall	430	154	461	11	348	80	385	6	446	135	446	17
HM	264	67	264	2	364	45.9	390	3	554	60.1	554	2
MM	461	100	461	4	310	152	310	2	521	186	593	3
LM	482	150	542	3					467	129	540	7
PM	456	299	456	2	380	NA	380	1	332	46.9	316	5

Above ground organic content (OC<sub>g,m2</sub>) per sites per saltmarsh zones.

	ANK				FM				MR			
	Mean	SD	Median	Sampling	Mean	SD	Median	Sampling	Mean	SD	Median	Sampling
overall	193	69.4	207	11	157	36	173	6	201	60.7	201	17
HM	119	30.2	119	2	164	20.7	176	3	249	27	249	2
MM	207	45.1	207	4	139	68.3	139	2	235	83.8	267	3
LM	217	67.7	244	3					210	57.8	243	7
PM	205	135	205	2	171	NA	171	1	149	21.1	142	5

**Table C- 13: Regression Analysis between vegetation characteristics (height, density, cover) , processes (above ground organic content- OC g.m<sup>2</sup>) and NVC vegetation assemblages. . In Linear Model - LM 1, log10 was used to transform both OC and vegetation height to meet linear assumption; in Linear Model - LM - 6, Box-Cox power transformation has been used for vegetation density using a lambda value of 0.2. The table presents linear model results and reports a test of the factor (with Sum of Sq. from ANOVA- type II of the model).**

	Dependent variables:						
	Above ground Organic Carbon (OC <sub>g,m2</sub> )		Vegetation Height (cm)			Vegetation Density ^0.2	Vegetation Cover (%)
	LM 1 (log10(OC_g_m2))	LM2	LM3	LM4	LM5	LM6	LM7
Vegetation Height (cm)		3.54***(±1.1)					
Log10 Veg. Height (cm)	0.51***(±0.11)						
Veg.Density (per m2)				-0.0004*** (±0.0001)	-0.0003* (±0.0002)		
SM13b		-6.46(±27.48)	5.51(±4.78)		8.65*(±4.86)	0.58(±0.41)	4.39(±13.23)
SM13d		-47.64(±28.95)	1.83(±5.15)		1.46(±4.92)	-0.12(±0.44)	-0.97(±14.29)
SM16a			-5.78(±5.72)		-1.96(±5.83)	0.90*(±0.49)	-1.68(±15.9)
SM16c		66.21*(±32.67)	4.05(±6.7)		5.37(±6.44)	0.43(±0.58)	-22.71(±18.71)
SM16d		-51.13(±37.83)	16.27**(±6.7)		13.37*(±6.58)	-1.02*(±0.58)	8.01(±18.71)
SM8		-20.65(±41.61)					
SM8		-22.18(±24.52)	-6.8(±4.17)		-3.35(±4.38)	0.76**(±0.36)	45.25***(±11.46)
Constant	1.58***(±0.15)	133.60***(±29.22)	22.23***(±2.86)	1.67***(±3.56)	27.66***(±3.98)	7.01***(±0.25)	89.34***(±7.64)
Observations	33	33	33	33	33	33	34
R2	0.38	0.51	0.39	0.21	0.46	0.37	0.46
Adjusted R2	0.36	0.38	0.24	0.19	0.31	0.22	0.34
Residual Std. Error	48.62 (df = 31)	48.06 (df = 25)	8.58 (df = 26)	8.88 (df = 31)	8.19 (df = 25)	0.74 (df = 26)	24.15 (df = 27)
F Statistic	19.09*** (df = 1; 31)	3.75*** (df = 7; 25)	2.71** (df = 6; 26)	8.43*** (df = 1; 31)	3.05** (df = 7; 25)	2.49** (df = 6; 26)	3.84*** (df = 6; 27)
veg. Height Sum Sq.	45117***(df =1)	24008**(df =1)					
veg. Density Sum Sq.				664.79**(df =1)	235.83.(df =1)		
NVC Sum Sq.		15528(df =6)	1197.2*(df =6)		768.2(df =6)	8.1852*(df =6)	13438**(df =6)
Residual Sum Sq.	73276(df =31)	57747(df =25)	1911.8(df =26)	2444.16(df =31)	1675.97(df =25)	14.2299(df =26)	15747(df =27)

Note: \*\*p<0.1; \*\*\*p<0.01; \*\*\*\*p<0.001

Water Levels

**Table C- 14: Linear Regression Model between hydroperiod parameters (flood depth, flood frequency, hydroperiod) and saltmarsh sites. Note that the table also reports a test of the factor (i.e. category = sites- NVC) as a whole instead of a test against the reference level (with Sum of Sq. from ANOVA- type II of the model).**

SITE - FM	Dependent variable:		
	sqrt(Flood depth -m) (1)	sqrt(Flood frequency -%) (2)	sqrt(Hydroperiod -m) (3)
	0.05*** ±(0.001)	1.04*** ±(0.01)	0.06*** ±(0.001)



SITE - MR	<b>0.04*** ±(0.0005)</b>	<b>0.64*** ±(0.01)</b>	<b>0.05*** ±(0.001)</b>
Constant	<b>0.33*** ±(0.0004)</b>	<b>2.56*** ±(0.01)</b>	<b>0.32*** ±(0.0005)</b>
Observations	285285	285285	285285
R2	0.026	0.033	0.026
Adjusted R2	<b>0.026</b>	<b>0.033</b>	<b>0.026</b>
Residual Std. Error (df = 285282)	0.12	0.212	0.140
F Statistic (df = 2; 285282)	<b>3737.64***</b>	<b>4805.60***</b>	<b>3,876.842***</b>
Sites Sum Sq. (df =2)	<b>103.77***</b>	<b>35919.11***</b>	<b>152.76***</b>
Residual Sum Sq. (df =285282)	3960.08	1066160	5620.46

Note: \*p<0.1; \*\*p<0.01; \*\*\*p<0.001

**Table C- 15: Linear Regression Model between hydroperiod parameters and saltmarsh sites and zones. Note that the table also reports a test of the factor (i.e. category = sites and zones) as a whole instead of a test against the reference level (with Sum of Sq. from ANOVA- type II of the model).**

Linear Regression between hydroperiod parameters and saltmarsh sites and zones

	Dependent variable:		
	sqrt(Flood depth - m) (1)	sqrt(Flood frequency - %) (2)	sqrt(Hydroperiod - m) (3)
ANK_LM	<b>0.034*** ±(0.001)</b>	<b>0.15***±(0.01)</b>	<b>0.02***±(0.001)</b>
ANK_MM	<b>0.041*** ±(0.001)</b>	<b>0.24***±(0.01)</b>	<b>0.03***±(0.001)</b>
ANK_PM	<b>0.266*** ±(0.001)</b>	<b>4.87***±(0.01)</b>	<b>0.34***±(0.001)</b>
FM_HM	<b>0.028*** ±(0.001)</b>	<b>0.31***±(0.01)</b>	<b>0.02***±(0.001)</b>
FM_LM	<b>0.193*** ±(0.003)</b>	<b>3.15***±(0.04)</b>	<b>0.22***±(0.003)</b>
FM_PM	<b>0.254*** ±(0.001)</b>	<b>4.66***±(0.01)</b>	<b>0.32***±(0.001)</b>
MR_HM	<b>-0.048*** ±(0.001)</b>	<b>-0.69***±(0.01)</b>	<b>-0.06***±(0.001)</b>
MR_LM	<b>0.135*** ±(0.001)</b>	<b>1.49***±(0.01)</b>	<b>0.14***±(0.001)</b>
MR_MM	<b>0.021*** ±(0.001)</b>	<b>-0.03***±(0.01)</b>	<b>0.01***±(0.001)</b>
MR_PM	<b>0.205*** ±(0.001)</b>	<b>3.50***±(0.01)</b>	<b>0.24***±(0.001)</b>
Constant	<b>0.284*** ±(0.0004)</b>	<b>1.98***±(0.01)</b>	<b>0.27***±(0.001)</b>
Observations	285285	285285	285285
R2	0.60	0.68	0.64
Adjusted R2	<b>0.60</b>	<b>0.68</b>	<b>0.64</b>
Residual Std. Error (df = 285274)	0.08	1.12	0.09
F Statistic (df = 10; 285274)	<b>43650***</b>	<b>59780***</b>	<b>51790***</b>
Sites_Zones Sum Sq. (df =10)	<b>2497.86***</b>	<b>746050***</b>	<b>3669.47***</b>
Residual Sum Sq. (df = 285274)	1606.2	356029	2103.75

\*p<0.1; \*\*p<0.01; \*\*\*p<0.001

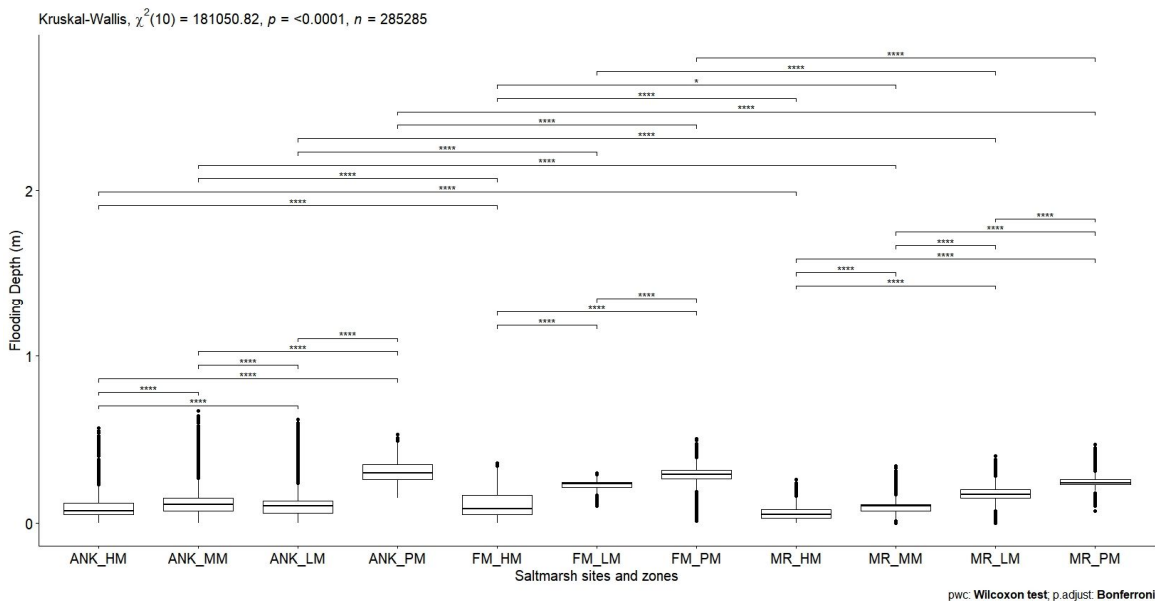


**Figure C - 1: Boxplot of the average flood depth (m) for the sediment deposition campaign showing significant differences between saltmarsh sites and zones (Kruskal-Wallis H test and Mann-Whitney-Wilcoxon tests results symbolised by the**

p-value significance - ns, \*\*,\*\*\* - for each pairwise tests). Boxplots represent median (middle line) interquartile range (box), 1.5 times interquartile range (bar) and outliers (black dots).

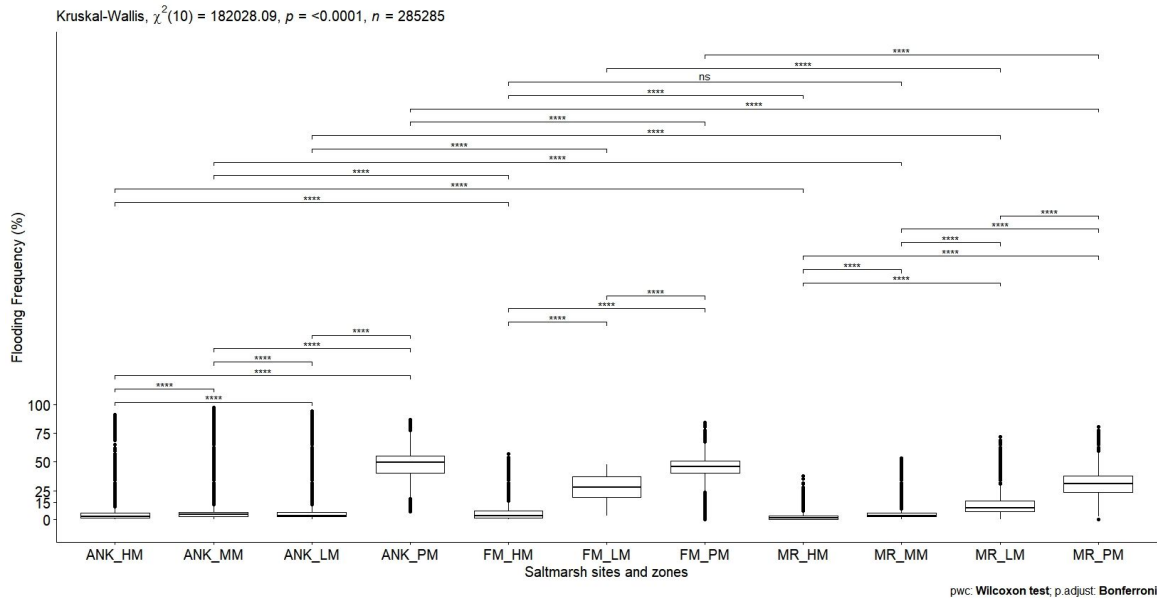


Figure C - 2: Boxplot of the average Flood frequency (%) for the sediment deposition campaign showing significant differences between saltmarsh sites and zones (Kruskal-Wallis H test and Mann-Whitney-Wilcoxon tests results symbolised by the p-value significance - ns, \*\*,\*\*\* - for each pairwise tests). Boxplots represent median (middle line) interquartile range (box), 1.5 times interquartile range (bar) and outliers (black dots).

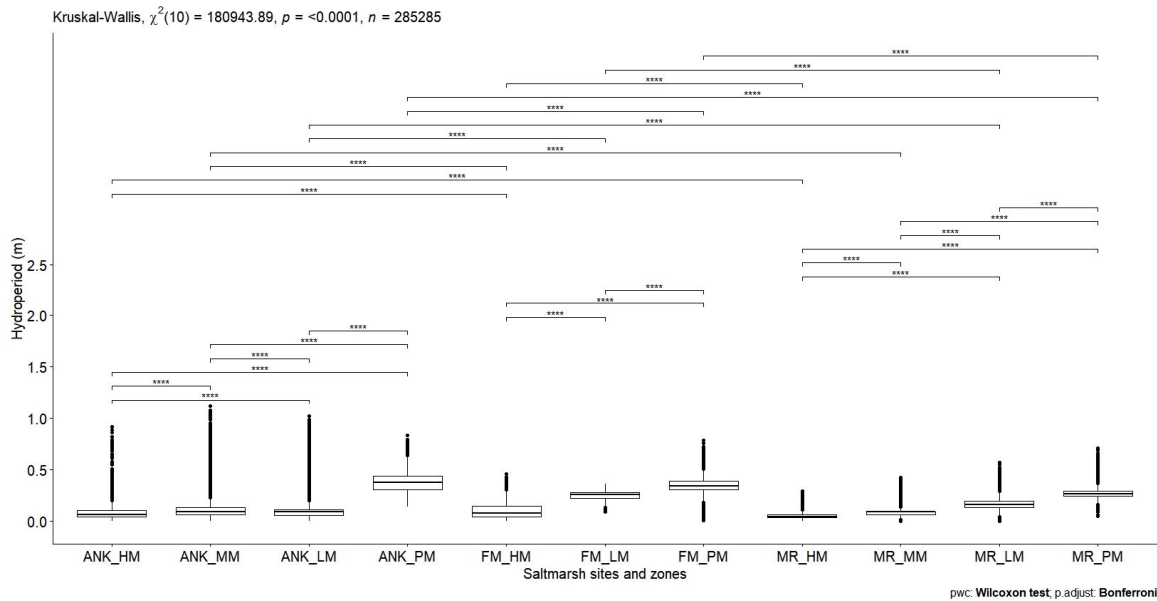


Figure C - 3: Boxplot of the average hydroperiod (m) for the sediment deposition campaign showing significant differences between saltmarsh sites and zones (Kruskal-Wallis H test and Mann-Whitney-Wilcoxon tests results symbolised by the p-value significance - ns, \*\*,\*\*\* - for each pairwise tests). Boxplots represent median (middle line) interquartile range (box), 1.5 times interquartile range (bar) and outliers (black dots).

Table C- 16: Games-Howell post hoc results determining which flood depth's and hydroperiod's dates differs significantly.

group 1- collection date	group 2- collection date	Variable	estimate	conf.low	conf.high	p.adj. and significance	Variable	estimate	conf.low	conf.high	p.adj. and significance
90316	210416	FloodDepth	-0.05	-0.05	-0.05	<0.001 ****	Hydroperiod	0.14	0.14	0.14	<0.001 ****
90316	60516	FloodDepth	0.01	0.01	0.02	<0.001 ****	Hydroperiod	0.05	0.05	0.05	<0.001 ****
90316	60616	FloodDepth	0.02	0.02	0.02	<0.001 ****	Hydroperiod	0.09	0.09	0.09	<0.001 ****

90316	40716	FloodDepth	-0.02	-0.03	-0.02	<0.001	****	Hydroperiod	0.04	0.04	0.04	<0.001	****
90316	30816	FloodDepth	-0.14	-0.15	-0.14	<0.001	****	Hydroperiod	-0.10	-0.10	-0.10	<0.001	****
90316	180916	FloodDepth	0.06	0.05	0.06	<0.001	****	Hydroperiod	0.05	0.04	0.05	<0.001	****
90316	171016	FloodDepth	0.02	0.02	0.03	<0.001	****	Hydroperiod	0.01	0.00	0.01	5.06E-14	****
90316	141116	FloodDepth	0.06	0.06	0.06	<0.001	****	Hydroperiod	0.03	0.03	0.03	<0.001	****
90316	141216	FloodDepth	0.03	0.03	0.03	<0.001	****	Hydroperiod	0.01	0.01	0.01	<0.001	****
90316	310117	FloodDepth	-0.14	-0.15	-0.14	<0.001	****	Hydroperiod	-0.08	-0.08	-0.08	<0.001	****
90316	10317	FloodDepth	-0.10	-0.10	-0.10	<0.001	****	Hydroperiod	-0.08	-0.08	-0.08	<0.001	****
210416	60516	FloodDepth	0.07	0.06	0.07	<0.001	****	Hydroperiod	-0.09	-0.10	-0.09	<0.001	****
210416	60616	FloodDepth	0.07	0.07	0.07	<0.001	****	Hydroperiod	-0.05	-0.06	-0.05	<0.001	****
210416	40716	FloodDepth	0.03	0.02	0.03	<0.001	****	Hydroperiod	-0.10	-0.10	-0.10	<0.001	****
210416	30816	FloodDepth	-0.09	-0.10	-0.09	<0.001	****	Hydroperiod	-0.24	-0.25	-0.24	<0.001	****
210416	180916	FloodDepth	0.11	0.11	0.11	<0.001	****	Hydroperiod	-0.09	-0.10	-0.09	<0.001	****
210416	171016	FloodDepth	0.08	0.07	0.08	<0.001	****	Hydroperiod	-0.13	-0.14	-0.13	<0.001	****
210416	141116	FloodDepth	0.11	0.11	0.11	<0.001	****	Hydroperiod	-0.11	-0.11	-0.11	<0.001	****
210416	141216	FloodDepth	0.08	0.08	0.08	<0.001	****	Hydroperiod	-0.13	-0.13	-0.13	<0.001	****
210416	310117	FloodDepth	-0.09	-0.09	-0.09	<0.001	****	Hydroperiod	-0.22	-0.22	-0.22	<0.001	****
210416	10317	FloodDepth	-0.05	-0.05	-0.04	<0.001	****	Hydroperiod	-0.22	-0.22	-0.22	<0.001	****
60516	60616	FloodDepth	0.00	0.00	0.01	2.26E-07	****	Hydroperiod	0.04	0.04	0.04	<0.001	****
60516	40716	FloodDepth	-0.04	-0.04	-0.04	<0.001	****	Hydroperiod	-0.01	-0.01	0.00	8.62E-14	****
60516	30816	FloodDepth	-0.16	-0.16	-0.16	<0.001	****	Hydroperiod	-0.15	-0.15	-0.15	<0.001	****
60516	180916	FloodDepth	0.04	0.04	0.04	<0.001	****	Hydroperiod	<b>0.00</b>	<b>0.00</b>	<b>0.00</b>	<b>0.814</b>	ns
60516	171016	FloodDepth	0.01	0.01	0.01	<0.001	****	Hydroperiod	-0.04	-0.04	-0.04	<0.001	****
60516	141116	FloodDepth	0.04	0.04	0.05	<0.001	****	Hydroperiod	-0.02	-0.02	-0.01	<0.001	****
60516	141216	FloodDepth	0.02	0.01	0.02	<0.001	****	Hydroperiod	-0.04	-0.04	-0.03	<0.001	****
60516	310117	FloodDepth	-0.16	-0.16	-0.16	<0.001	****	Hydroperiod	-0.13	-0.13	-0.13	<0.001	****
60516	10317	FloodDepth	-0.11	-0.11	-0.11	<0.001	****	Hydroperiod	-0.13	-0.13	-0.13	<0.001	****
60616	40716	FloodDepth	-0.04	-0.05	-0.04	<0.001	****	Hydroperiod	-0.05	-0.05	-0.04	<0.001	****
60616	30816	FloodDepth	-0.16	-0.17	-0.16	<0.001	****	Hydroperiod	-0.19	-0.19	-0.19	<0.001	****
60616	180916	FloodDepth	0.04	0.03	0.04	<0.001	****	Hydroperiod	-0.04	-0.04	-0.04	<0.001	****
60616	171016	FloodDepth	0.00	0.00	0.01	8.66E-08	****	Hydroperiod	-0.08	-0.08	-0.08	<0.001	****
60616	141116	FloodDepth	0.04	0.04	0.04	<0.001	****	Hydroperiod	-0.06	-0.06	-0.05	<0.001	****
60616	141216	FloodDepth	0.01	0.01	0.01	<0.001	****	Hydroperiod	-0.08	-0.08	-0.07	<0.001	****
60616	310117	FloodDepth	-0.16	-0.16	-0.16	<0.001	****	Hydroperiod	-0.17	-0.17	-0.17	<0.001	****
60616	10317	FloodDepth	-0.12	-0.12	-0.11	<0.001	****	Hydroperiod	-0.17	-0.17	-0.17	<0.001	****
40716	30816	FloodDepth	-0.12	-0.12	-0.12	<0.001	****	Hydroperiod	-0.14	-0.15	-0.14	<0.001	****
40716	180916	FloodDepth	0.08	0.08	0.08	<0.001	****	Hydroperiod	0.01	0.00	0.01	3.02E-13	****
40716	171016	FloodDepth	0.05	0.05	0.05	<0.001	****	Hydroperiod	-0.04	-0.04	-0.03	<0.001	****
40716	141116	FloodDepth	0.08	0.08	0.09	<0.001	****	Hydroperiod	-0.01	-0.01	-0.01	<0.001	****
40716	141216	FloodDepth	0.05	0.05	0.06	<0.001	****	Hydroperiod	-0.03	-0.03	-0.03	<0.001	****
40716	310117	FloodDepth	-0.12	-0.12	-0.12	<0.001	****	Hydroperiod	-0.12	-0.12	-0.12	<0.001	****
40716	10317	FloodDepth	-0.07	-0.08	-0.07	<0.001	****	Hydroperiod	-0.12	-0.12	-0.12	<0.001	****
30816	180916	FloodDepth	0.20	0.20	0.20	<0.001	****	Hydroperiod	0.15	0.15	0.15	<0.001	****
30816	171016	FloodDepth	0.17	0.17	0.17	<0.001	****	Hydroperiod	0.11	0.11	0.11	<0.001	****
30816	141116	FloodDepth	0.20	0.20	0.21	<0.001	****	Hydroperiod	0.13	0.13	0.14	<0.001	****
30816	141216	FloodDepth	0.17	0.17	0.18	<0.001	****	Hydroperiod	0.11	0.11	0.12	<0.001	****
30816	310117	FloodDepth	<b>0.00</b>	<b>0.00</b>	<b>0.00</b>	<b>0.983</b>	ns	Hydroperiod	0.02	0.02	0.02	<0.001	****
30816	10317	FloodDepth	0.05	0.04	0.05	<0.001	****	Hydroperiod	0.02	0.02	0.02	<0.001	****
180916	171016	FloodDepth	-0.03	-0.03	-0.03	<0.001	****	Hydroperiod	-0.04	-0.04	-0.04	<0.001	****
180916	141116	FloodDepth	0.00	0.00	0.00	0.026	*	Hydroperiod	-0.01	-0.02	-0.01	<0.001	****
180916	141216	FloodDepth	-0.03	-0.03	-0.02	<0.001	****	Hydroperiod	-0.03	-0.04	-0.03	<0.001	****
180916	310117	FloodDepth	-0.20	-0.20	-0.20	<0.001	****	Hydroperiod	-0.13	-0.13	-0.12	<0.001	****
180916	10317	FloodDepth	-0.15	-0.16	-0.15	<0.001	****	Hydroperiod	-0.13	-0.13	-0.13	<0.001	****
171016	141116	FloodDepth	0.03	0.03	0.04	<0.001	****	Hydroperiod	0.03	0.02	0.03	<0.001	****
171016	141216	FloodDepth	0.01	0.00	0.01	1.77E-13	****	Hydroperiod	0.01	0.00	0.01	1.35E-13	****
171016	310117	FloodDepth	-0.17	-0.17	-0.17	<0.001	****	Hydroperiod	-0.09	-0.09	-0.08	<0.001	****
171016	10317	FloodDepth	-0.12	-0.12	-0.12	<0.001	****	Hydroperiod	-0.09	-0.09	-0.09	<0.001	****
141116	141216	FloodDepth	-0.03	-0.03	-0.03	<0.001	****	Hydroperiod	-0.02	-0.02	-0.02	<0.001	****
141116	310117	FloodDepth	-0.20	-0.20	-0.20	<0.001	****	Hydroperiod	-0.11	-0.11	-0.11	<0.001	****
141116	10317	FloodDepth	-0.16	-0.16	-0.15	<0.001	****	Hydroperiod	-0.11	-0.12	-0.11	<0.001	****
141216	310117	FloodDepth	-0.17	-0.18	-0.17	<0.001	****	Hydroperiod	-0.09	-0.09	-0.09	<0.001	****
141216	10317	FloodDepth	-0.13	-0.13	-0.13	<0.001	****	Hydroperiod	-0.09	-0.09	-0.09	<0.001	****
310117	10317	FloodDepth	0.05	0.04	0.05	<0.001	****	Hydroperiod	<b>0.00</b>	<b>0.00</b>	<b>0.00</b>	<b>0.561</b>	ns

### C.3. Relationships between sediment, vegetation and physical processes

#### Physical controls on short-term (annual) deposition and accretion rates

Table C- 17: Linear Regression Models between sediment deposition rates ( $g.m^{-2}.day^{-1}$  filter discs) and elevation (m) for the months of April, November 2016 and January 2017, between December's sediment deposition and distance to HWM (m) and between July's sediment deposition and elevation, BDD ( $g.cm^{-3}$ ) and distance to saltmarsh edge (m). Note: Data transformation required to meet normality assumptions are annotated in the table

Linear Regression between filter discs sediment deposition rates and hydroperiod parameters

=====

	Dependent variable:				
	sqrt(April 2016 Sediment Deposition) (1)	sqrt(July 2016 Sediment Deposition) (2)	sqrt(November 2016 Sediment Deposition) (3)	December 2016 Sediment Deposition (4)	January 2017 Sediment Deposition (5)
sqrt(Elevation)	-14.77*** (±3.25)	-8.37*** (±3.2)	-19.89*** (±6.47)		
Elevation					-2.91*** (±0.84)
sqrt(BDD)		8.59** (±3.13)			
sqrt(Distance to SM Edge)		0.16* (±0.08)			
Sqrt (Dist_to HWM)				2.69** (±0.98)	
Constant	22.79*** (±4.47)	6.26* (±5.2)	34.33*** (±9.10)	10.62*** (±4.5)	7.15*** (±1.66)
Observations	18	28	31	34	34
R2	0.56	0.38	0.25	0.19	0.27
Adjusted R2	0.54	0.31	0.22	0.16	0.25
Residual Std. Error	1.38 (df = 16)	1.59 (df = 24)	3.64 (df = 29)	11.86 (df = 32)	1.43 (df = 32)
F Statistic	20.66*** (df = 1; 16)	4.95*** (df = 3; 24)	9.45*** (df = 1; 29)	7.45** (df = 1; 32)	12.03*** (df = 1; 32)

Note: \*p<0.1; \*\*p<0.01; \*\*\*p<0.001

**Table C- 18: Linear Regression Models between June and December's sediment deposition (g.m-2day<sup>-1</sup>- filter discs) and Vegetation Assemblages - NVC.** Note1: Data transformation required to meet normality assumptions are annotated in the table; Note2: that the table also reports a test of the factor (i.e. category = Vegetation assemblage- NVC) as a whole instead of a test against the reference level (with Sum of Sq. from ANOVA- type II of the model).

Linear Regression for filter discs sediment deposition rates over the sediment collection period		
	Dependent variable:	
	sqrt(June 2016 Sediment Deposition )	sqrt(December 2016 Sediment Deposition )
SM13b	3.25*** (±0.98)	13.37** (±6.06)
SM13d	-1.75* (±0.98)	-6.11 (±6.55)
SM16a	-0.37 (±1.08)	-5.93 (±7.29)
SM16c	-3.39** (±1.25)	-0.84 (±8.58)
SM16d	-0.68 (±1.67)	4.42 (±8.58)
SM8	0.91 (±0.98)	14.55*** (±5.25)
Constant	3.39*** (±0.59)	17.16*** (±3.5)
Observations	25	34
R2	0.65	0.40
Adjusted R2	0.53	0.27
Residual Std. Error	1.56 (df = 18)	11.07 (df = 27)
F Statistic	5.59*** (df = 6; 18)	3.04** (df = 6; 27)
Veg.-NVC Sum Sq.	8163 (df = 6)**	2236 (df = 6)*
Residual Sum Sq.	43.779 (df = 18)	3310.41 (df = 18)

Note: \*p<0.1; \*\*p<0.01; \*\*\*p<0.001

**Table C- 19: Linear Regression Models between filter discs sediment deposition rates (in g per m<sup>2</sup> per year) and flood depth (model 1), hydroperiod (model 2), flood depth and NVC-vegetation assemblages (model 3), hydroperiod and vegetation assemblages (model 4). Box-Cox power transformation has been used for sediment deposition rates using a lambda value of 0.3. The table presents linear model results and reports a test of the factor (with Sum of Sq. from ANOVA- type II of the model).**

Linear Regression between average deposition accretion rates and physical controls to saltmarsh development				
	Dependent variable (Box Cox transformed) (Deposition rates in g.m2.yr <sup>-1</sup> ) <sup>0.3</sup>			
	(model 1)	(model 2)	(model 3)	(model 4)
Flood depth (m)	0.54*** (±0.07)		0.87*** (±0.09)	
Hydroperiod (m)		0.61*** (±0.08)		0.97*** (±0.1)
SM13b			0.25*** (±0.07)	0.25*** (±0.07)
SM13d			0.02 (±0.08)	0.02 (±0.08)

SM16a			-0.1 (±0.09)	-0.07 (±0.09)
SM16c			-0.05 (±0.1)	-0.07 (±0.1)
SM16d			<b>0.66*** (±0.12)</b>	<b>0.66*** (±0.12)</b>
SM8			<b>-0.19** (±0.07)</b>	<b>-0.19** (±0.07)</b>
Constant	<b>0.68*** (±0.03)</b>	<b>0.70*** (±0.02)</b>	<b>0.65*** (±0.04)</b>	<b>0.66*** (±0.04)</b>
Observations	304	304	304	304
R2	<b>0.15</b>	<b>0.16</b>	0.28	0.29
Adjusted R2	0.15	0.16	<b>0.26</b>	<b>0.28</b>
Residual Std. Error	0.44 (df = 302)	0.43	0.41 (df = 296)	0.4 (df = 296)
F Statistic	<b>53.71*** (df = 1; 302)</b>	<b>57.81***</b>	<b>16.49*** (df = 7; 296)</b>	<b>17.49*** (df = 7; 296)</b>
Flood depth Sum Sq. (df = 1)			<b>15.21***</b>	<b>16.02***</b>
Hydroperiod Sum Sq. (df = 1)			<b>8.78***</b>	<b>8.94***</b>
Vegetation Sum Sq. (df = 6)				47.93
Residual Sum Sq. (df = 296)			48.75	
Note:			*p<0.1; **p<0.01; ***p<0.001	

**Table C- 20: Linear Regression Models between filter discs accretion rates (in cm per year) and hydroperiod, distance to saltmarsh edge, flood depth and NVC-vegetation assemblages. Box-Cox power transformation has been used for accretion rates using a lambda value of 0.3. The table presents linear model results and reports a test of the factor (with Sum of Sq. from ANOVA- type II of the model).**

	Dependent variable (Box-Cox transformed)					
	<b>(Accretion rates cm.yr<sup>-1</sup>)<sup>0.2</sup></b>					
	(1)	(2)	(3)	(4)	(5)	(6)
Hydroperiod (m)	<b>0.65*** (±0.09)</b>	<b>0.72*** (±0.09)</b>			<b>1.09*** (±0.11)</b>	
Distance to SM edge (m)		<b>0.001*** (±0.0003)</b>		<b>0.001*** (±0.0003)</b>		
Flood depth (m)			<b>0.58*** (±0.08)</b>	<b>0.63*** (±0.08)</b>		<b>0.99*** (±0.1)</b>
SM13b					<b>0.35*** (±0.08)</b>	<b>0.35*** (±0.08)</b>
SM13d					0.04 (±0.09)	0.04 (±0.09)
SM16a					-0.09 (±0.1)	-0.13 (±0.1)
SM16c					-0.06 (±0.12)	-0.03 (±0.12)
SM16d					<b>0.74*** (±0.13)</b>	<b>0.74*** (±0.13)</b>
SM8					<b>-0.25*** (±0.08)</b>	<b>-0.25*** (±0.08)</b>
Constant	<b>0.77*** (±0.03)</b>	<b>0.66*** (±0.05)</b>	<b>0.76*** (±0.03)</b>	<b>0.66*** (±0.05)</b>	<b>0.73*** (±0.05)</b>	<b>0.71*** (±0.05)</b>
Observations	304	304	304	304	304	304
R2	<b>0.14</b>	0.17	<b>0.14</b>	0.16	0.3	0.29
Adjusted R2	0.14	<b>0.16</b>	0.13	<b>0.15</b>	<b>0.29</b>	<b>0.28</b>
Residual Std. Error	0.49 (df = 302)	0.49 (df = 301)	0.50 (df = 302)	0.49 (df = 301)	0.45	0.45
F Statistic	<b>50.56*** (df = 1; 302)</b>	<b>30.46*** (df = 2; 301)</b>	<b>47.24*** (df = 1; 302)</b>	<b>28.10*** (df = 2; 301)</b>	<b>18.44*** (df = 7; 296)</b>	<b>17.61*** (df = 7; 296)</b>
Hydroperiod Sum Sq. (df = 1)		<b>14.05***</b>		<b>13.1***</b>	<b>20.41***</b>	
Distance to SM edge SumSq. (df = 1)		<b>2.14**</b>		<b>1.89**</b>		
Flood depth Sum Sq. (df = 1)						<b>19.59***</b>
Vegetation Sum Sq. (df = 6)					<b>13.74***</b>	<b>13.62***</b>
Residual Sum Sq.		71.33 (df = 301)		72.27 (df = 301)	59.72 (df = 296)	60.54 (df = 296)
Note:			*p<0.1; **p<0.01; ***p<0.0001			

### Physical controls on biological processes

**Table C- 21: Linear Regression Models between vegetation cover (in % box-cox transformed using  $[y^{5.1}-1/5.1]$  to meet linearity assumptions) and elevation ((1) in m), hydroperiod ((2) in  $\sqrt{m}$ ), flood frequency ((3) in %) and flood depth ((4) in  $\sqrt{m}$ ).**

Linear regression between Vegetation Cover and physical controls to saltmarsh development	
Dependent variable:	

	(1)	Vegetation cover (% <sup>5.1</sup> -1/5.1)		(4)
		(2)	(3)	
Elevation	1.717e+09*** (±4.3e+08)			
sqrt(Hydroperiod)		-3.184e+09*** (±9.8e+07)		
sqrt(flood frequency)			-2.542e+09*** (±7.3e+07)	
sqrt(FD)				-3.379e+09*** (±1.1e+09)
Constant	-1.748E+09** (±8.4e+08)	2.786E+09*** (±3.9e+08)	2.444E+09*** (±2.7e+08)	2.881E+09*** (±4.4e+08)
Observations	34	34	34	34
R2	<b>0.34</b>	<b>0.25</b>	<b>0.28</b>	<b>0.23</b>
Adjusted R2	0.32	0.23	0.25	0.2
Residual Std. Error (df=32)	7.25E+08	7.71E+08	7.58E+08	7.83E+08
F Statistic (df=1;32)	16.24***	10.66***	12.18***	9.31***
Note:	*p<0.1; **p<0.01; ***p<0.001			

**Table C- 22: Linear Regression Models between vegetation height (in cm log transformed to meet linearity assumptions) and elevation ((1) in m log), BDD ((2) in g.cm<sup>3</sup>), distance to saltmarsh edge ((3) in √m) hydroperiod ((4) in √m), flood frequency ((5) in √%) and flood depth ((6) in √m).**

Linear regression between Vegetation height and physical controls to saltmarsh development

	Dependent variable:					
	Vegetation Height (in m log10)					
	(1)	(2)	(3)	(4)	(5)	(6)
log10(Elevation)	1.66*** (±0.36)					
BDD		0.02** (±0.01)				
sqrt(dist to Sm Edge)			-0.35** (±0.14)			
sqrt(Hydroperiod)				-0.06*** (±0.01)		
sqrt(flood frequency)					-0.91*** (±0.2)	
sqrt(FD)						-0.85*** (±0.17)
Constant	0.84*** (±0.11)	1.15*** (±0.07)	1.56*** (±0.1)	1.52*** (±0.05)	1.66*** (±0.08)	1.63*** (±0.07)
Observations	33.0	33.0	33.0	33.0	33.0	33.0
R2	<b>0.40</b>	<b>0.17</b>	<b>0.17</b>	<b>0.42</b>	<b>0.40</b>	<b>0.44</b>
Adjusted R2	0.38	0.15	0.14	0.40	0.38	0.42
Residual Std. Error (df=31)	0.14	0.17	0.17	0.14	0.14	0.14
F Statistic (df=1;31)	20.98***	6.48**	6.34**	22.28***	20.92***	24.01***
Note:	*p<0.1; **p<0.01; ***p<0.001					

**Table C- 23: Linear Regression Models between vegetation density (n per m<sup>2</sup>) and (1) elevation (in m); (2) hydroperiod (in m); and (3) distance to saltmarsh edge (in √m).**

Linear regression between Vegetation Density and physical controls to saltmarsh development

	Dependent variable:		
	Vegetation density (n per m2)		
	(1)	(2)	(3)
Elevation	-13935.45** (±6426.33)		
Hydroperiod		43079.23** (±20930.49)	
sqrt(dist. To SM edge)			-1372.13*** (±403.34)
Constant	50609.25*** (±12646.47)	16720.12** (±3802.8)	36234.40*** (±4126.58)
Observations	33	33	33
R2	<b>0.13</b>	<b>0.12</b>	<b>0.27</b>
Adjusted R2	0.11	0.09	0.25
Residual Std. Error (df=31)	10871.34	10943.01	9955.55



Note: \*\*p<0.1; \*p<0.01; \*\*\*p<0.001

**Table C- 24: Models between biomass (g.m<sup>2</sup> log) and distance to saltmarsh edge (in √m (model1)) and BDD (in g.cm<sup>3</sup> (model2)) and aboveground organic content (in g.m<sup>2</sup>) distance to saltmarsh edge (in √m (model3)) and BDD (in g.cm<sup>3</sup> (model4)).**

Linear regression between Biomass and Aboveground Organic Content (OC) and Physical Controls to Saltmarsh Development

	Dependent variable:			
	log10(Biomass g.m <sup>2</sup> )		Above ground OC (g.m <sup>2</sup> )	
	(1)	(2)	(3)	(4)
sqrt(Dist_SM_Edge)	0.01**(±0.01)		5.43**(±2.31)	
BDD	-0.30**(±0.12)		-119.07**(±52.96)	
Constant	2.48*** (±0.06)	2.87*** (±0.11)	139.89*** (±23.59)	293.46*** (±49.96)
Observations	33	33	33	33
R2	<b>0.16</b>	<b>0.16</b>	<b>0.15</b>	<b>0.14</b>
Adjusted R2	0.14	0.14	0.12	0.11
Residual Std. Error (df=31)	0.13	0.13	56.92	57.3
F Statistic (df=1;31)	6.02*	6.05*	5.54*	5.05*

Note: \*\*p<0.1; \*p<0.01; \*\*\*p<0.001

**Water Levels and biological processes**

**Table C- 25: Calculated average flood depth (m) between vegetation assemblages for the sediment deposition campaign (filters and AstroTurf mats) from 09<sup>th</sup> March 2016 to 01<sup>st</sup> March 2017. Note that n correspond to a 1\*1 m cell size.**

NVC - Vegetation assemblages	Variable	n	Mean	SD	median	IQR	Kruskal-Wallis chi-squared	p-value
SM8	Flood depth	59574	0.26	0.0497	0.24	0.0598	H = 179804, df = 10	<2e-16 ***
SM13a	Flood depth	66926	0.165	0.0588	0.17	0.07		
SM13a + SM16a	Flood depth	292	0.22	0.0307	0.234	0.0281		
SM13b	Flood depth	40769	0.113	0.0573	0.11	0.08		
SM13b + SM13d	Flood depth	31819	0.0836	0.0541	0.1	0.06		
SM16a	Flood depth	34382	0.0879	0.0754	0.07	0.09		
SM16a + SM13d	Flood depth	6092	0.19	0.0588	0.197	0.0714		
SM16c	Flood depth	4289	0.0903	0.0581	0.0736	0.0709		
SM16c + SM13d	Flood depth	15942	0.0635	0.0424	0.0572	0.0631		
SM16d	Flood depth	119135	0.0193	0.0353	0	0.03		
SM28	Flood depth	1263	0.0215	0.0379	0	0.0338		

**Table C- 26: Calculated average flood frequency (%) between vegetation assemblages for the sediment deposition campaign (filters and AstroTurf mats) from 09<sup>th</sup> March 2016 to 01<sup>st</sup> March 2017. Note that n correspond to a 1\*1 m cell size.**

NVC - Vegetation assemblages	Variable	n	Mean	SD	median	IQR	Kruskal-Wallis chi-squared	p-value
SM8	Flood frequency	35.9	13.3	36	17	35.9	H = 181133, df = 10	<2e-16 ***
SM13a	Flood frequency	12.3	10.8	8.48	7.97	12.3		
SM13a + SM16a	Flood frequency	24.8	9.78	25.4	14.1	24.8		
SM13b	Flood frequency	5.97	8.07	4.37	3.6	5.97		
SM13b + SM13d	Flood frequency	4.45	4.48	3.34	2.57	4.45		
SM16a	Flood frequency	6.93	10.7	3.08	5.14	6.93		
SM16a + SM13d	Flood frequency	18.4	12.8	15.2	20.8	18.4		

SM16c	Flood frequency	4.97	6.11	2.83	4.37	4.97
SM16c + SM13d	Flood frequency	2.66	2.32	2.31	2.06	2.66
SM16d	Flood frequency	2.1	2.09	1.54	2.82	2.1
SM28	Flood frequency	1.99	2.16	1.54	2.57	1.99

**Table C- 27: Calculated average Hydroperiod (m) between vegetation assemblages for the sediment deposition campaign (filters and AstroTurf mats) from 09<sup>th</sup> March 2016 to 01<sup>st</sup> March 2017. Note that n correspond to a 1\*1 m cell size.**

NVC - Vegetation assemblages	Variable	n	Mean	SD	median	IQR	Kruskal-Wallis chi-squared	p-value
SM8	Hydroperiod	59552	0.297	0.0826	0.274	0.0909	H = 180485, df = 10	<2e-16 ***
SM13a	Hydroperiod	66070	0.16	0.07	0.15	0.08		
SM13a + SM16a	Hydroperiod	292	0.23	0.05	0.25	0.05		
SM13b	Hydroperiod	40664	0.10	0.07	0.09	0.07		
SM13b + SM13d	Hydroperiod	26953	0.08	0.04	0.09	0.04		
SM16a	Hydroperiod	29652	0.09	0.08	0.06	0.07		
SM16a + SM13d	Hydroperiod	6081	0.19	0.08	0.19	0.11		
SM16c	Hydroperiod	4076	0.08	0.06	0.06	0.07		
SM16c + SM13d	Hydroperiod	14171	0.06	0.04	0.05	0.05		
SM16d	Hydroperiod	37322	0.0502	0.0331	0.0411	0.038		
SM28	Hydroperiod	452	0.0486	0.0372	0.0408	0.0306		

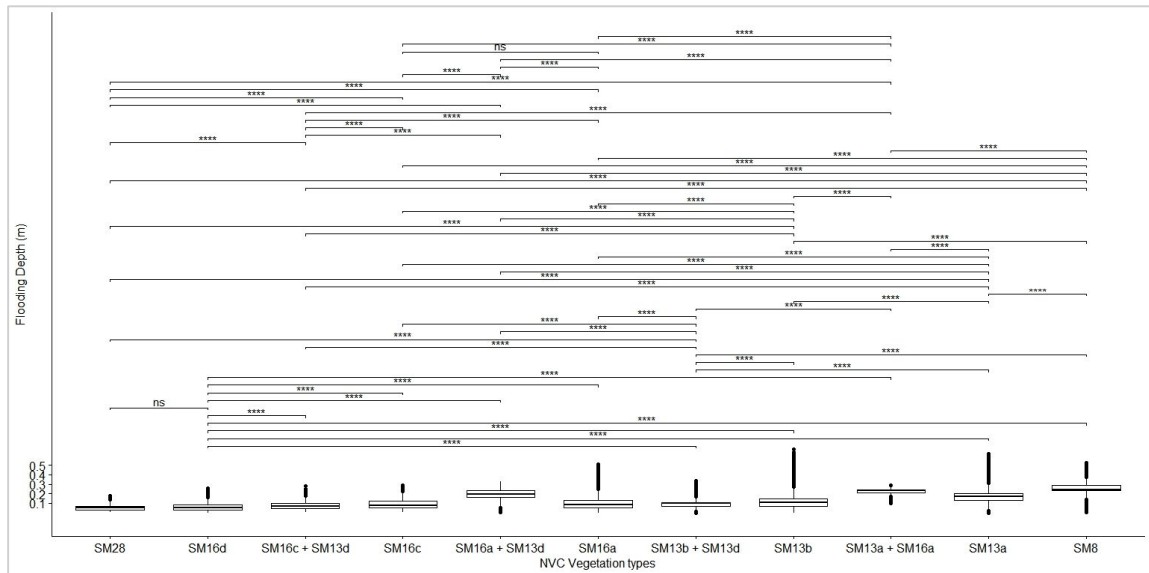


**Figure C - 4: Boxplot of the flood depth (m) for the sediment deposition campaign showing significant differences between vegetation assemblages (Mann-Whitney-Wilcoxon tests results symbolised by the p-value significance - ns, \*, \*\*, \*\*\* - for each pairwise tests). Boxplots represent median (middle line) interquartile range (box), 1.5 times interquartile range (bar) and outliers (black dots).**

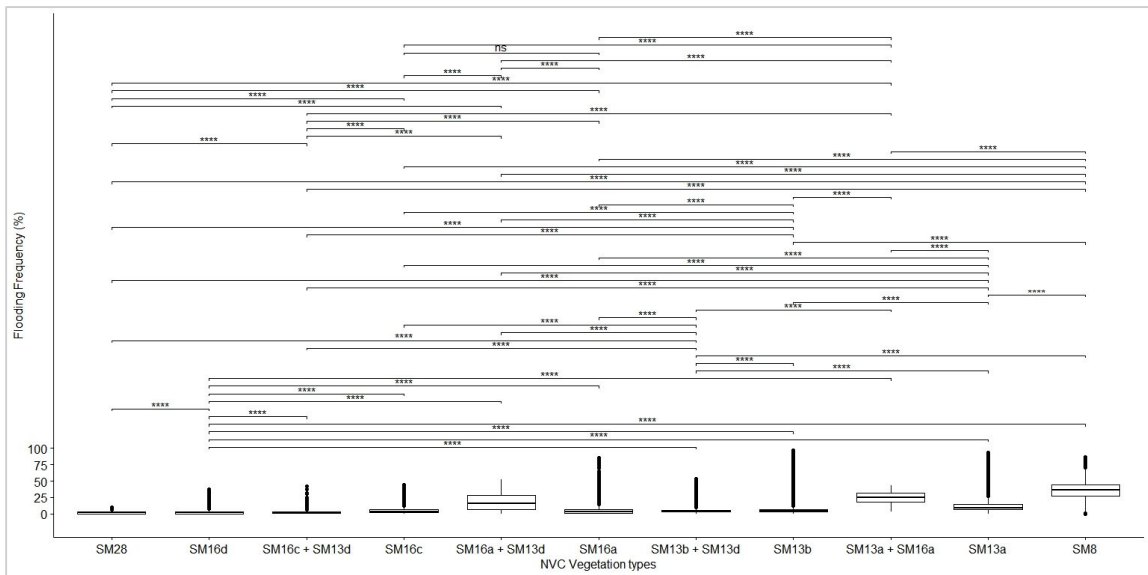


Figure C - 5: Boxplot of the flood frequency (%) for the sediment deposition campaign showing significant differences between vegetation assemblages (Mann-Whitney-Wilcoxon tests results symbolised by the p-value significance - *ns*, \*, \*\*, \*\*\* - for each pairwise tests). Boxplots represent median (middle line) interquartile range (box), 1.5 times interquartile range (bar) and outliers (black dots).

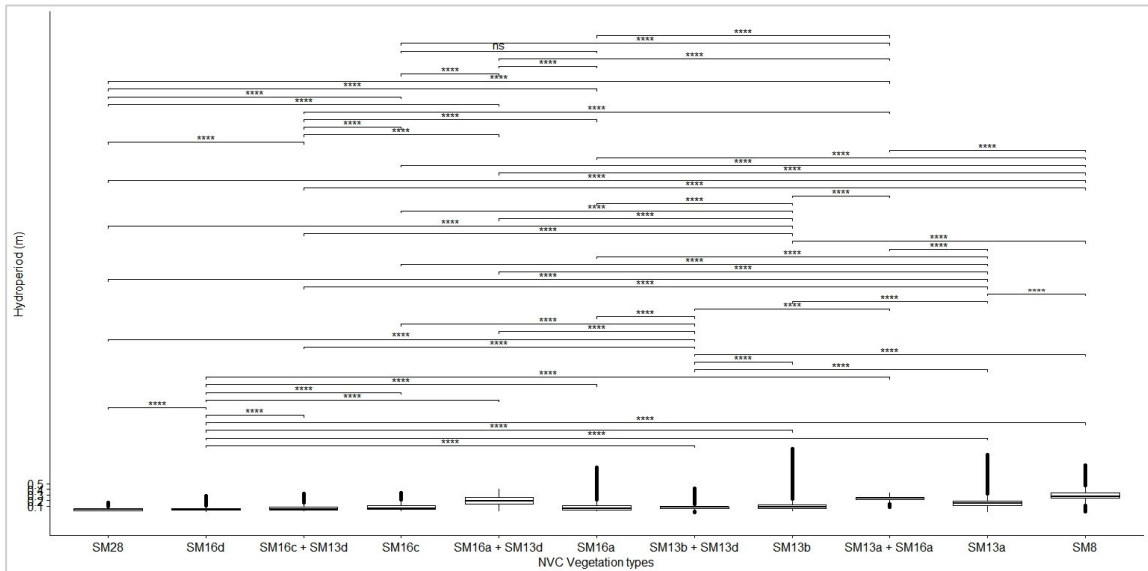


Figure C - 6: Boxplot of the hydroperiod (m) for the sediment deposition campaign showing significant differences between vegetation assemblages (Mann-Whitney-Wilcoxon tests results symbolised by the p-value significance - *ns*, \*, \*\*, \*\*\* - for each pairwise tests). Boxplots represent median (middle line) interquartile range (box), 1.5 times interquartile range (bar) and outliers (black dots).

Table C- 28: Linear Regression Model between Hydroperiod parameters and Vegetation Assemblages - NVC. Note that the table also reports a test of the factor (i.e. category = Vegetation assemblage- NVC) as a whole instead of a test against the reference level (with Sum of Sq. from ANOVA- type II of the model).

Linear Regression between Water Levels parameters and Vegetation Assemblages -NVC			
	Dependent variable:		
	sqrt(Flood depth) (1)	sqrt(Flood frequency) (2)	sqrt(Hydroperiod) (3)
SM13a + SM16a	0.05*** ± (0.003)	12.52*** (0.56)	0.09*** (0.01)
SM13b	-0.05*** ± (0.0003)	-6.31*** (0.06)	-0.09*** (0.001)
SM13b + SM13d	-0.07*** ± (0.0004)	-7.84*** (0.07)	-0.11*** (0.001)

SM16a	-0.07***±(0.0004)	-5.35***±(0.07)	-0.11***±(0.001)
SM16a + SM13d	0.02***±(0.001)	6.09***±(0.13)	0.04***±(0.001)
SM16c	-0.07***±(0.001)	-7.32***±(0.15)	-0.12***±(0.001)
SM16c + SM13d	-0.10***±(0.0005)	-9.63***±(0.09)	-0.16***±(0.001)
SM16d	-0.11***±(0.0003)	-10.19***±(0.06)	-0.18***±(0.001)
SM28	-0.11***±(0.002)	-10.30***±(0.45)	-0.18***±(0.004)
SM8	0.09***±(0.0003)	23.65***±(0.05)	0.15***±(0.0005)
Constant	0.17***±(0.0002)	12.29***±(0.04)	0.39***±(0.0003)
-----			
Observations	285285	285285	285285
R2	0.63	0.62	0.62
Adjusted R2	<b>0.63</b>	<b>0.62</b>	<b>0.62</b>
ResidualStd.Error (df=285274)	0.05	9.58	0.09
Fstatistic (df=10;285274)	<b>47952.52***</b>	<b>46767.02***</b>	<b>47190.63***</b>
Veg.-NVC Sum Sq. (df = 10)	<b>1334.66***</b>	<b>42895940***</b>	<b>3598.11***</b>
Residual Sum Sq. (df=285274)	794.6	26166082	2175.11
=====			
Note:	*p<0.1; **p<0.01; ***p<0.001		

### Influences of vegetation on sediment deposition and accretion rates

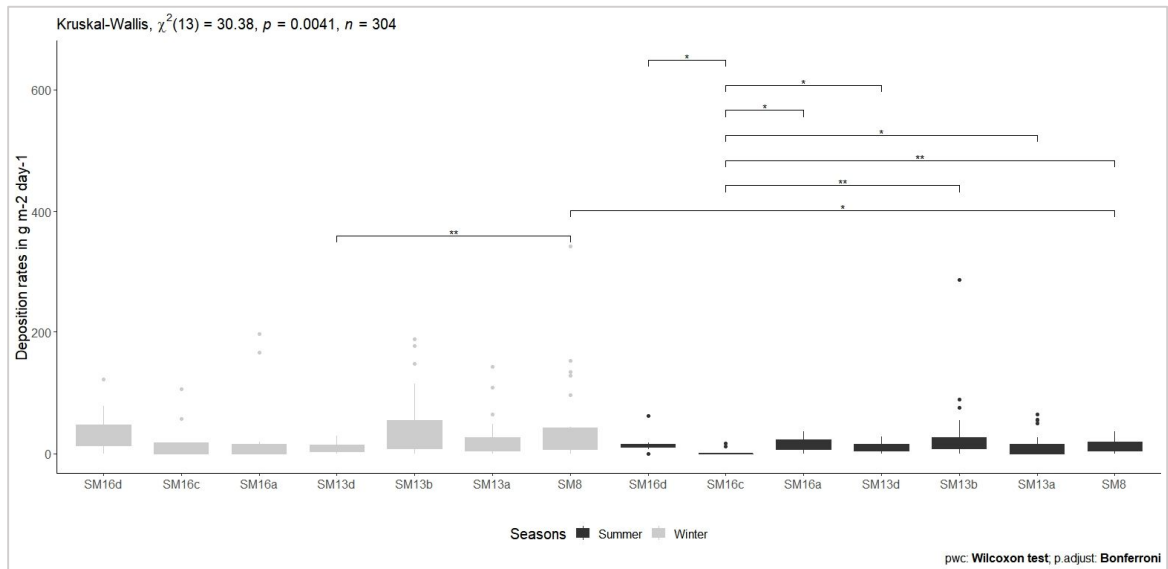


Figure C - 7: Boxplot of deposition rates ( $\text{g}\cdot\text{m}^{-2}\cdot\text{day}^{-1}$ ) per season (summer/winter) showing significant differences between vegetation assemblages (Mann-Whitney-Wilcoxon tests results symbolised by the p-value significance - ns, \*, \*\*, \*\*\* - for each pairwise tests). Boxplots represent median (middle line) interquartile range (box), 1.5 times interquartile range (bar) and outliers (black dots).

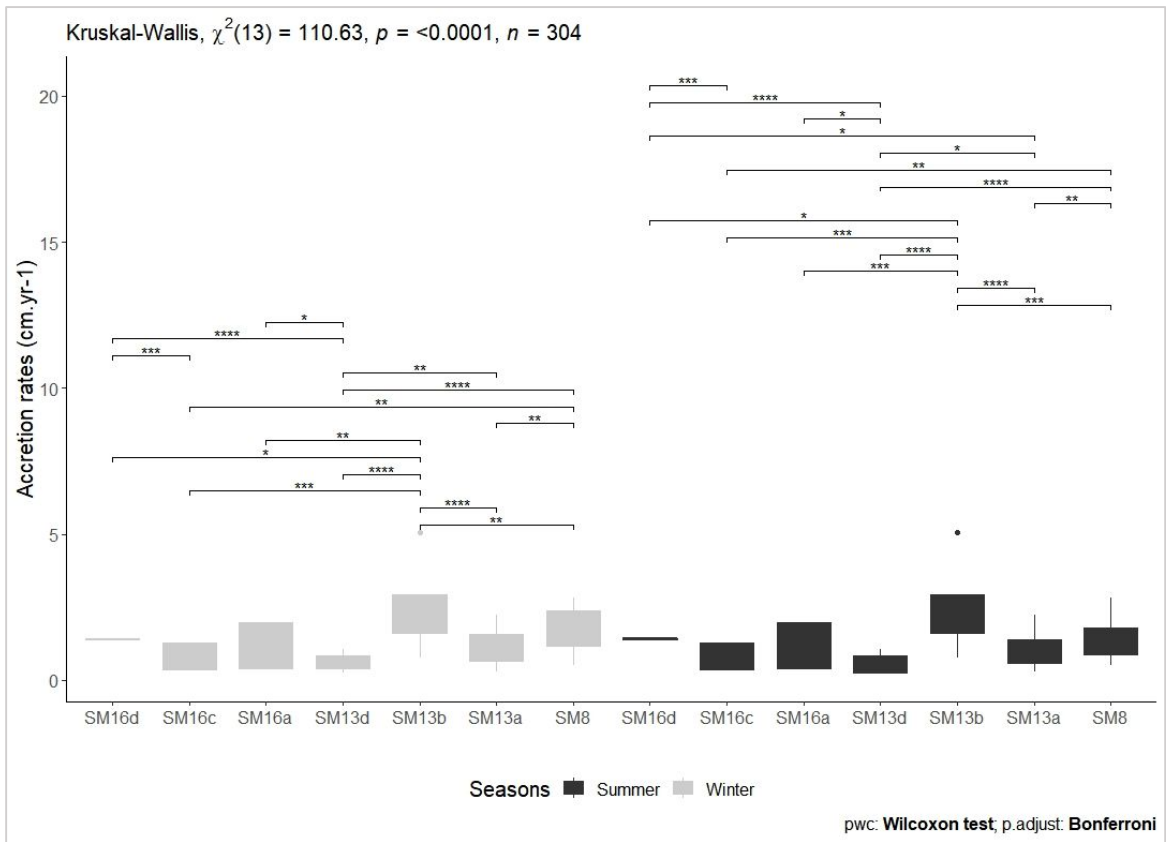


Figure C - 8: Boxplot of accretion rates (cm yr<sup>-1</sup>) per season (summer/winter) showing significant differences between vegetation assemblages (Mann-Whitney-Wilcoxon tests results symbolised by the p-value significance - ns, \*, \*\*, \*\*\* - for each pairwise tests). Boxplots represent median (middle line) interquartile range (box), 1.5 times interquartile range (bar) and outliers (black dots).

Table C- 29: Linear Regression Models between monthly filter discs sediment deposition rates (in g per m<sup>2</sup> per year) and NVC-vegetation assemblages, overall (model 1), on ANK (model 2), on FM (model 3) and finally on MR (model 4). Box-Cox power transformation has been used for sediment deposition rates using a lambda value of 0.3 except on Fm which uses a lambda value 0.2. The table presents linear model results and reports a test of the factor (with Sum of Sq. from ANOVA-type II of the model for the collection dates and vegetation assemblages).

Linear Regression between average deposition accretion rates and physical controls to saltmarsh development

=====

Categorical variables	Dependent variable (Box Cox transformed)			
	(Discs_Deposition rates in g.m2.yr-1) <sup>0.3</sup> (model 1)	ANK (Discs_Deposition rates in g.m2.yr-1) <sup>0.3</sup> (model 2)	FM (Discs_Deposition rates in g.m2.yr-1) <sup>0.2</sup> (model 3)	MR (Discs_Deposition rates in g.m2.yr-1) <sup>0.3</sup> (model 4)
21.04.2016.	0.29 (±0.36)	-0.97* (±0.53)	1.66** (±0.82)	1.08** (±0.52)
06.05.2016.	0.80** (±0.39)	0.33 (±0.57)	0.92 (±0.97)	1.19** (±0.52)
06.06.2016.	0.83** (±0.34)	1.05** (±0.52)	-0.42 (±0.76)	1.24*** (±0.44)
04.07.2016.	0.77** (±0.33)	-0.02 (±0.52)	1.14 (±0.73)	1.20*** (±0.43)
03.08.2016.	0.07 (±0.32)	-0.28 (±0.5)	0.39 (±0.73)	0.3 (±0.41)
18.09.2016.	1.06*** (±0.32)	0.98* (±0.5)	1.44* (±0.73)	1.09*** (±0.41)
17.10.2016.	1.58*** (±0.32)	1.04** (±0.5)	1.37* (±0.73)	2.12*** (±0.41)
14.11.2016.	1.82*** (±0.32)	0.96* (±0.52)	2.96*** (±0.73)	1.99*** (±0.41)
14.12.2016.	1.25*** (±0.32)	0.96* (±0.5)	1.81** (±0.73)	1.36*** (±0.41)
31.01.2017.	-0.16 (±0.32)	-0.77 (±0.5)	0.49 (±0.73)	0.13 (±0.41)
SM13b	0.58*** (±0.2)	1.64*** (±0.25)		-0.37 (±0.32)
SM13d	-0.08 (±0.21)			-0.4 (±0.25)
SM16a	-0.01 (±0.24)	0.77** (±0.3)	0.3 (±0.45)	
SM16c	-0.65** (±0.28)		-0.43 (±0.36)	
SM16d	0.37 (±0.29)			0.03 (±0.26)
SM8	0.33* (±0.18)	1.56*** (±0.3)	0.49 (±0.47)	-0.31 (±0.2)
Constant	0.96*** (±0.28)	0.53 (±0.45)	0.53 (±0.59)	1.05*** (±0.35)
Observations	304	102	57	145
R2	0.31	0.54	0.52	0.39
Adjusted R2	0.27	0.48	0.37	0.32

=====

Residual Std. Error	1.09 (df = 287)	0.98 (df = 88)	1.12 (df = 43)	0.95 (df = 130)
F Statistic	<b>8.18*** (df = 16; 287)</b>	<b>8.04*** (df = 13; 88)</b>	<b>3.58*** (df = 13; 43)</b>	<b>5.88*** (df = 14; 130)</b>
CollectionDate Sum Sq. (df = 10)	<b>126.92***</b>	<b>55.174***</b>	<b>46.855**</b>	<b>68.509***</b>
Vegetation Sum Sq.	<b>28.52(df=6)***</b>	<b>46.798(df=3)***</b>	5.727(df=3)	4.487(df=4)
Residual Sum Sq.	339.21(df=287)	84.586(df=88)	53.957(df=43)	116.807(df=130)
=====				
Note:	*p<0.1; **p<0.01; ***p<0.001			

**Table C- 30: Linear Regression Models between monthly filter discs accretion rates (in cm per year) and NVC-vegetation assemblages, overall (model 1), on ANK (model 2), on FM (model 3) and finally on MR (model 4). Box-Cox power transformation has been used for sediment deposition rates using a lambda value of 0.3 except on Fm which uses a lambda value 0.2. The table presents linear model results and reports a test of the factor (with Sum of Sq. from ANOVA- type II of the model for the collection dates and vegetaion assemblages)**

	Dependent variables:			
	Filter Discs Accretion Rates (cm.yr-1 ^ 0.15)	ANK Filter Discs Accretion Rates (cm.yr-1 ^ 0.15)	FM Filter Discs Accretion Rates (cm.yr-1 ^ 0.15)	MR Filter Discs Accretion Rates (cm.yr-1 ^ 0.15)
	1	2	3	4
SM8	<b>0.17*** (±0.06)</b>	<b>0.47*** (±0.11)</b>	0.08 (±0.18)	0.04 (±0.06)
SM13b	0.1 (±0.06)	<b>0.55*** (±0.1)</b>		-0.16 (±0.09)
SM13d	0.01 (±0.07)			0.01 (±0.07)
SM16a	-0.09 (±0.08)	0.19 (±0.11)	0.09 (±0.16)	
SM16c	<b>0.34*** (±0.09)</b>		-0.19 (±0.13)	
SM16d	0.04 (±0.1)			-0.07 (±0.07)
09.03.2016	<b>-0.25** (±0.11)</b>	0.05 (±0.18)	-0.18 (±0.26)	<b>-0.50*** (±0.12)</b>
21.04.2016	-0.08 (±0.11)	-0.28 (±0.17)	<b>0.46* (±0.27)</b>	-0.09 (±0.14)
06.05.2016	0.15 (±0.12)	0.24 (±0.18)	0.11 (±0.33)	0.1 (±0.14)
06.06.2016	0.12 (±0.1)	<b>0.49** (±0.16)</b>	-0.41 (±0.25)	0.09 (±0.11)
04.07.2016	0.09 (±0.1)	0.09 (±0.16)	0.22 (±0.24)	0.04 (±0.11)
18.09.2016	<b>0.25** (±0.1)</b>	<b>0.47** (±0.16)</b>	0.39 (±0.24)	0.08 (±0.11)
17.10.2016	<b>0.29*** (±0.09)</b>	<b>0.48** (±0.16)</b>	0.25 (±0.24)	0.22 (±0.1)
14.11.2016	<b>0.34*** (±0.09)</b>	<b>0.43** (±0.16)</b>	<b>0.66*** (±0.24)</b>	<b>0.18* (±0.1)</b>
14.12.2016	<b>0.32*** (±0.09)</b>	<b>0.47** (±0.16)</b>	<b>0.54* (±0.24)</b>	0.14 (±0.11)
31.01.2017	<b>-0.17* (±0.1)</b>	-0.18 (±0.16)	0.03 (±0.24)	-0.28 (±0.11)
Constant	<b>0.66*** (±0.08)</b>	<b>0.22* (±0.13)</b>	<b>0.47* (±0.19)</b>	<b>0.89*** (±0.08)</b>
=====				
Observations	284	98	56	130
R2	0.3	0.53	0.51	0.39
Adjusted R2	<b>0.26</b>	<b>0.46</b>	<b>0.35</b>	<b>0.32</b>
Residual Std. Error	0.35 (df = 267)	0.36 (df = 84)	0.39 (df = 42)	0.27 (df = 115)
F Statistic	<b>7.23*** (df = 16; 267)</b>	<b>7.23*** (df = 13; 84)</b>	<b>3.32*** (df = 13; 42)</b>	<b>5.30*** (df = 14; 115)</b>
CollectionDate Sum Sq.	<b>10.281(df=10)***</b>	<b>7.4892(df=10)***</b>	<b>5.0545(df=10)**</b>	<b>4.8114(df=10)***</b>
Vegetation Sum Sq.	<b>4.307(df=6)***</b>	<b>4.8341(df=3)***</b>	0.6869(df=3)	0.3583(df=4)
Residual Sum Sq.	33.604(df=267)	10.6378(df=84)	6.4034(df=42)	8.1755(df=115)
=====				
Note:	**p<0.1; **p<0.01; ***p<0.001			



## APPENDIX.D Supplementary references for Chapter 5

### D.1. Areal historical changes

Table D- 1: Summary of areal changes (in ha and %) providing cumulative (from 1878 to 2012) and non-cumulative rate of change (between 1878 & 2012) for Nigg Bay for the area extent as depicted in red box from Figure 5.11 to Figure 5.13.

	1878-1977				1977-2012				1872-2012			
	ha	error	%	error	ha	error	%	error	ha	error	%	error
Loss	38.1	0.7	32.0	0.6	10.2	0.2	9.0	0.2	19.8	0.4	16.2	0.3
Gain	24.4	0.4	20.5	0.4	32.2	0.6	28.5	0.5	27.5	0.5	22.5	0.4
No Change	56.6	1.0	47.5	0.9	70.8	1.3	62.6	1.1	75.2	1.3	61.3	1.1
Average change	-13.7	-0.2	-11.5	-0.2	22.0	0.4	19.5	0.3	7.7	0.1	6.3	0.1
Rate (ha. yr <sup>-1</sup> )	-0.13	-0.002	-11.5	-0.2	0.7	0.001	19.5	0.3	0.06	0.001	6.3	0.1
Cumulative rate (ha. yr <sup>-1</sup> )									0.03	0.001	4.0	0.1

### D.2. Sedimentation rates derived from sedimentation plates supplementary tables and statistics

Table D- 2: Analysis of Variance on Ranks for the overall sedimentation rates (cm.yr<sup>-1</sup>) using sedimentation plates between saltmarsh sites.

<b>Normality Test (Shapiro-Wilk):</b>		Failed (P < 0.050)			
Test execution ended by user request, ANOVA on Ranks begun					
<b>Kruskal-Wallis One Way Analysis of Variance on Ranks</b>					
Dependent Variable: SR_monitoring_cm_yr					
<b>Group</b>	<b>N</b>	<b>Missing</b>	<b>Median</b>	<b>25%</b>	<b>75%</b>
ANK	105	17	0.0950	-0.702	0.978
FM	42	7	-0.200	-1.070	0.970
MR	273	15	0.675	-0.307	2.250
H = 18.141 with 2 degrees of freedom. (P = <0.001)					
The differences in the median values among the treatment groups are greater than would be expected by chance; there is a statistically significant difference (P = <0.001)					
To isolate the group or groups that differ from the others use a multiple comparison procedure.					
All Pairwise Multiple Comparison Procedures (Dunn's Method) :					
<b>Comparison</b>	<b>Diff of Ranks</b>	<b>Q</b>	<b>P</b>	<b>P&lt;0.050</b>	
MR vs FM	63.367	3.194	0.004	Yes	
MR vs ANK	45.287	3.331	0.003	Yes	
ANK vs FM	18.080	0.822	1.000	No	

**Table D- 3 Analysis of Variance on Ranks for the overall sedimentation rates (cm.yr<sup>-1</sup>) using sedimentation plates between saltmarsh sites' zones.**

<b>One Way Analysis of Variance</b>					
Dependent Variable: SR_monitoring_cm_yr					
<b>Normality Test (Shapiro-Wilk):</b> Failed (P < 0.050)					
Test execution ended by user request, ANOVA on Ranks begun					
<b>Kruskal-Wallis One Way Analysis of Variance on Ranks</b>					
Dependent Variable: SR_monitoring_cm_yr					
Group	N	Missing	Median	25%	75%
ANK_LM	28	4	0.135	-0.480	0.595
ANK_MM	35	5	-0.105	-0.655	1.565
ANK_PM	14	2	-0.575	-2.540	0.290
ANK_HM	28	6	0.425	-0.410	2.290
FM_HM	21	3	-0.260	-1.707	1.025
FM_MM	14	3	-0.730	-1.750	0.0800
FM_PM	7	1	1.405	0.450	2.580
MR_HM	91	5	0.275	-0.643	1.458
MR_MM	49	2	0.0900	-0.630	1.400
MR_LM	84	2	1.265	0.495	3.753
MR_PM	49	6	0.610	-0.510	2.730
H = 53.458 with 10 degrees of freedom. (P = <0.001)					
The differences in the median values among the treatment groups are greater than would be expected by chance; there is a statistically significant difference (P = <0.001)					
To isolate the group or groups that differ from the others use a multiple comparison procedure.					
All Pairwise Multiple Comparison Procedures (Dunn's Method) :					
Comparison	Diff of Ranks	Q	P	P<0.050	
MR_LM vs ANK_LM	95.382	3.732	0.010	Yes	
MR_LM vs MR_MM	77.246	3.834	0.007	Yes	
MR_LM vs MR_HM	67.363	3.963	0.004	Yes	
Note: The multiple comparisons on ranks do not include an adjustment for ties.					

**Table D- 4: Analysis of Variance on Ranks for the overall sedimentation rates (cm.yr<sup>-1</sup>) using sedimentation plates between monitoring period.**

<b>One Way Analysis of Variance</b>					
Dependent Variable: SR_monitoring_cm_yr					
<b>Normality Test (Shapiro-Wilk):</b> Failed (P < 0.050)					
Test execution ended by user request, ANOVA on Ranks begun					
<b>Kruskal-Wallis One Way Analysis of Variance on Ranks</b>					
<b>Data source:</b> Data 1 in Notebook1					
Dependent Variable: SR_monitoring_cm_yr					
Group	N	Missing	Median	25%	75%
SR_to_nov_cm	60	36	4.025	0.0750	5.310
SR_to_feb_cm	60	2	0.655	-1.113	3.603
SR_to_april_cm	60	1	2.020	0.350	4.100
SR_to_jul_cm	60	0	0.385	-0.623	1.708
SR_to_oct_cm	60	0	0.0800	-0.985	1.090
SR_to_march_cm	60	0	0.0300	-0.575	0.715
SR_to_sept_cm	60	0	0.160	-0.362	0.688
H = 45.782 with 6 degrees of freedom. (P = <0.001)					

The differences in the median values among the treatment groups are greater than would be expected by chance; there is a statistically significant difference (P = <0.001)

To isolate the group or groups that differ from the others use a multiple comparison procedure.  
All Pairwise Multiple Comparison Procedures (Dunn's Method) :

Comparison	Diff of Ranks	Q	P	P<0.050
SR_to_nov_cm vs SR_to_oct_cm	111.846	4.205	<0.001	Yes
SR_to_nov_cm vs SR_to_march_cm	111.029	4.174	<0.001	Yes
SR_to_nov_cm vs SR_to_sept_cm	102.079	3.838	0.003	Yes
SR_to_nov_cm vs SR_to_jul_cm	81.221	3.054	0.047	Yes
SR_to_april_cm vs SR_to_oct_cm	97.293	4.818	<0.001	Yes
SR_to_april_c vs SR_to_march_c	96.476	4.778	<0.001	Yes
SR_to_april_c vs SR_to_sept_cm	87.526	4.335	<0.001	Yes
SR_to_april_cm vs SR_to_jul_cm	66.668	3.302	0.020	Yes

Note: The multiple comparisons on ranks do not include an adjustment for ties.

**Table D- 5: Analysis of Variance on Ranks for the overall sedimentation rates (cm.yr<sup>-1</sup>) using sedimentation plates between saltmarsh vegetation assemblages (NVC).**

**Kruskal-Wallis One Way Analysis of Variance on Ranks**

Dependent Variable: SR\_monitoring\_cm\_yr

Normality Test (Shapiro-Wilk): Failed (P < 0.050)

Group	N	Missing	Median	25%	75%
SM13a	112	6	0.985	0.138	2.598
SM13b	56	5	0.430	-0.640	1.550
SM8	70	9	0.420	-0.630	2.360
SM16a	35	7	0.545	-0.285	1.705
SM16c	14	2	-0.665	-2.465	-0.0650
SM13d	42	5	-0.0800	-0.825	0.525
SM16d	91	5	0.275	-0.643	1.458

H = 27.835 with 6 degrees of freedom. (P = <0.001)

The differences in the median values among the treatment groups are greater than would be expected by chance; there is a statistically significant difference (P = <0.001)

To isolate the group or groups that differ from the others use a multiple comparison procedure.  
All Pairwise Multiple Comparison Procedures (Dunn's Method) :

Comparison	Diff of Ranks	Q	P	P<0.050
SM13a vs SM16c	118.369	3.529	0.009	Yes
SM13a vs SM13d	83.865	3.988	0.001	Yes
SM13a vs SM13b	59.085	3.148	0.034	Yes

Note: The multiple comparisons on ranks do not include an adjustment for ties.

**Table D- 6: Regression Analysis for sedimentation rates and sites, saltmarsh zones, Vegetation type (NVC assemblage – see Table 3-1 in Chapter 3 and Table A-2) and monitoring period (timelag between surveys)**

Linear Regression between Sedimentation rates and sites, zones, collection dates and vegetation assemblages

=====

Dependent variable:

---

	(1)	(2)	(3)	(4)
		<b>Sedimentation in cm .yr<sup>-1</sup></b>		
FM		-0.25 (±0.46)		
MR		<b>1.08*** (±0.28)</b>		
ANK		0.06 (±0.24)		

---

ANK_LM	-0.92 (±0.65)			
ANK_MM	-1 (±0.62)			
ANK_PM	<b>-2.63*** (±0.79)</b>			
FM_HM	<b>-1.32* (±0.7)</b>			
FM_MM	<b>-1.99** (±0.82)</b>			
FM_PM	0.58 (±1.02)			
MR_HM	-0.37 (±0.53)			
MR_LM	<b>0.99* (±0.53)</b>			
MR_MM	-0.59 (±0.57)			
MR_PM	0.26 (±0.58)			
SM13b			-1.38*** (±0.39)	
SM13d			-1.59*** (±0.44)	
SM16a			-0.69 (±0.49)	
SM16c			-2.25*** (±0.7)	
SM16d			-0.94*** (±0.33)	
SM8			-0.84** (±0.37)	
SR_to_feb_cm (0.5yrs)				-1.83*** (±0.54)
SR_to_april_cm (0.7yrs)				-0.77 (±0.54)
SR_to_jul_cm (1yrs)				-2.22*** (±0.54)
SR_to_oct_cm (1.2yrs)				-2.71*** (±0.54)
SR_to_march_cm (1.6yrs)				-2.66*** (±0.54)
SR_to_sept_cm (2.1yrs)				-2.57*** (±0.54)
Constant	<b>1.01** (±0.47)</b>	0.06 (±0.24)	1.57*** (±0.22)	2.77*** (±0.45)
Observations	381	381	381	381
R2	0.14	0.05	0.06	0.13
Adjusted R2	<b>0.12</b>	<b>0.05</b>	<b>0.05</b>	<b>0.11</b>
Residual Std. Error	2.21 (df = 370)	2.30 (df = 378)	2.29 (df = 374)	2.22 (df = 374)
F Statistic	<b>6.15*** (df = 10; 370)</b>	<b>10.6*** (df = 2; 378)</b>	<b>4.27*** (df = 6; 374)</b>	<b>9.02*** (df = 6; 374)</b>
Timelag Sum Sq.				<b>265.98 (df = 6)***</b>
Sites Sum Sq.		<b>111.71 (df = 2)***</b>		
Veget Sum Sq.			<b>265.98 (df = 6)***</b>	
Sites&Zones Sum Sq.	<b>299.81 (df = 10)***</b>			
Residual Sum Sq.	<b>1804.01(df = 370)</b>	<b>1992.1(df = 3780)</b>	<b>1837.84 (df = 374)</b>	<b>1837.84(df = 374)</b>
=====				
Note:		**p<0.1; **p<0.01; ***p<0.001		

**Table D- 7: Multiple Regression Analysis for sedimentation rates and physical and biological variables**

<b>Multiple Linear Regression</b>					
SR_monitoring_cm_yr = 1.622 - (0.0546 * Veg_Height_est.) - (0.0000474 * Veg_Pop.m2_est.) + (0.0254 * Vegetated_cover) - (0.270 * Slope_percent) + (0.0807 * curv_pl)					
N = 381 Missing Observations = 39					
R = 0.404		Rsqr = 0.163		Adj Rsqr = 0.152	
Standard Error of Estimate = 2.167					
<b>Coefficient</b>	<b>Std. Error</b>	<b>t</b>	<b>P</b>	<b>VIF</b>	

Constant	1.622	0.653	2.486	0.013	
Veg_Height_est.	-0.0546	0.0140	-3.908	<0.001	1.237
Veg_Pop.m2_est.	-0.0000474	0.0000130	-3.641	<0.001	1.258
Vegetated_cover	0.0254	0.00537	4.734	<0.001	1.210
Slope_percent	-0.270	0.0534	-5.061	<0.001	1.117
curv_pl	0.0807	0.0306	2.635	0.009	1.054

Analysis of Variance:

	DF	SS	MS	F	P
Regression	5	342.661	68.532	14.592	<0.001
Residual	375	1761.159	4.696		
Total	380	2103.820	5.536		

Column	SSIncr	SSMarg
Veg_Height_est.	3.062	71.734
Veg_Pop.m2_est.	136.603	62.272
Vegetated_cover	68.036	105.254
Slope_percent	102.342	120.281
curv_pl	32.618	32.618

The dependent variable SR\_monitoring\_cm\_yr can be predicted from a linear combination of the independent variables:

	P
Veg_Height_est.	<0.001
Veg_Pop.m2_est.	<0.001
Vegetated_cover	<0.001
Slope_percent	<0.001
curv_pl	0.009

All independent variables appear to contribute to predicting SR\_monitoring\_cm\_yr (P < 0.05).

Normality Test (Shapiro-Wilk) Failed (P = <0.001)

Constant Variance Test (Spearman Rank Correlation): Failed (P = <0.001)

Power of performed test with alpha = 0.050: 1.000

**Table D- 8: Multiple Regression Analysis for ANK sedimentation rates and physical and biological variables**

Multiple Linear Regression					
ANK SR_monitoring_cm_yr = -7.382 + (0.0601 * Veg_Cover) + (3.078 * BDD)					
N = 88					
R = 0.545 Rsqr = 0.297 Adj Rsqr = 0.281					
Standard Error of Estimate = 1.760					
	Coefficient	Std. Error	t	P	VIF
Constant	-7.382	1.634	-4.518	<0.001	
Veg_Cover	0.0601	0.0102	5.868	<0.001	1.502
BDD	3.078	1.286	2.394	0.019	1.502

Analysis of Variance:

	DF	SS	MS	F	P
Regression	2	111.367	55.683	17.970	<0.001
Residual	85	263.386	3.099		
Total	87	374.753	4.308		

Column	SSIncr	SSMarg
Veg_Cover	93.614	106.711
BDD	17.753	17.753

The dependent variable ANK SR\_monitoring\_cm\_yr can be predicted from a linear combination of the independent variables:

	P
Veg_Cover	<0.001
BDD	0.019

All independent variables appear to contribute to predicting SR\_monitoring\_cm\_yr (P < 0.05).

Normality Test (Shapiro-Wilk) Failed (P = 0.001)

Constant Variance Test (Spearman Rank Correlation): Passed (P = 0.052)

Power of performed test with alpha = 0.050: 1.000

**Table D- 9: Multiple Regression Analyses for FM sedimentation rates and physical and biological variables**

**Linear Regression**

**Data source:** Data 3 in Notebook1

FM SR\_monitoring\_cm\_yr = -1.807 + (8.649 \* Hydroperiod)

N = 35

R = 0.383 **Rsqr = 0.147** Adj Rsqr = 0.121

Standard Error of Estimate = 1.927

	<b>Coefficient</b>	<b>Std. Error</b>	<b>t</b>	<b>P</b>
Constant	-1.807	0.753	-2.401	0.022
Hydroperiod	8.649	3.632	2.382	0.023

Analysis of Variance:

	<b>DF</b>	<b>SS</b>	<b>MS</b>	<b>F</b>	<b>P</b>
Regression	1	21.051	21.051	5.672	0.023
Residual	33	122.477	3.711		
Total	34	143.528	4.221		

Normality Test (Shapiro-Wilk) Failed (P = 0.021)

Constant Variance Test (Spearman Rank Correlation): Passed (P = 0.593)

Power of performed test with alpha = 0.050: 0.627

**Table D- 10: Multiple Regression Analysis for MR sedimentation rates and physical and biological variables**

**Multiple Linear Regression**

MR SR\_monitoring\_cm\_yr = -2.087 + (0.0245 \* Veg\_Cover) - (0.323 \* Slope\_percent) + (2.893 \* BDD)

N = 258

R = 0.324 **Rsqr = 0.105** Adj Rsqr = 0.0946

Standard Error of Estimate = 2.279

	<b>Coefficient</b>	<b>Std. Error</b>	<b>t</b>	<b>P</b>	<b>VIF</b>
Constant	-2.087	1.009	-2.069	0.040	
Veg_Cover	0.0245	0.00727	3.373	<0.001	1.024
Slope_percent	-0.323	0.0856	-3.774	<0.001	1.030
BDD	2.893	1.145	2.526	0.012	1.007

Analysis of Variance:

	<b>DF</b>	<b>SS</b>	<b>MS</b>	<b>F</b>	<b>P</b>
Regression	3	154.947	51.649	9.947	<0.001
Residual	254	1318.887	5.192		
Total	257	1473.834	5.735		

<b>Column</b>	<b>SSIncr</b>	<b>SSMarg</b>
Veg_Cover	39.424	59.068
Slope_percent	82.394	73.963
BDD	33.129	33.129

The dependent variable MR SR\_monitoring\_cm\_yr can be predicted from a linear combination of the independent variables:

	<b>P</b>
Veg_Cover	<0.001
Slope_percent	<0.001
BDD	0.012

All independent variables appear to contribute to predicting SR\_monitoring\_cm\_yr (P < 0.05).

Normality Test (Shapiro-Wilk) Failed (P = <0.001)

Constant Variance Test (Spearman Rank Correlation): Failed (P = <0.001)

Power of performed test with alpha = 0.050: 1.000



**D.3. Water levels (Flood depth, Flood frequency and Hydroperiod) over 2.14 years sedimentation plates monitoring period**

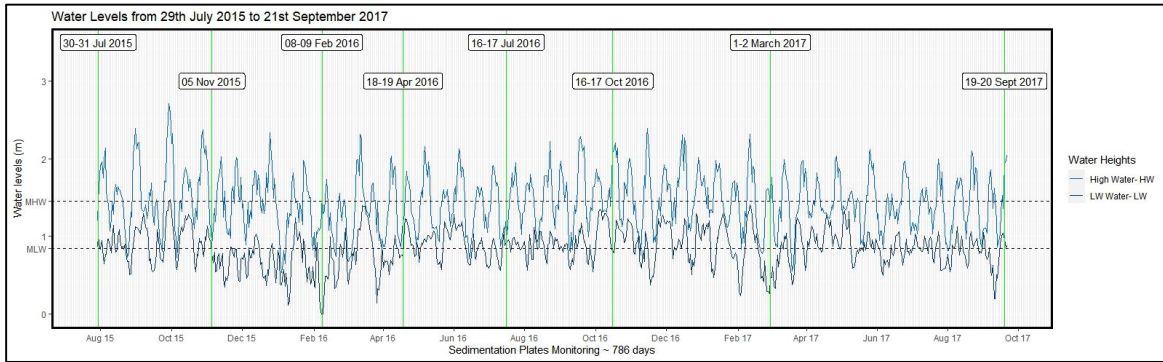


**Figure D- 1: High Water (HW) and Low Water (LW) levels from the 30th July 2015 to 20th September 2017 where the dates and green lines correspond to sedimentation plates monitoring dates. The overall time series statistics are as follows:**

	<i>mean</i>	<i>sd</i>	<i>median</i>	<i>trimmed</i>	<i>mad</i>	<i>min</i>	<i>max</i>	<i>range</i>	<i>skew</i>	<i>kurtosis</i>	<i>se</i>
<b>all</b>	1.03	0.34	0.99	1.01	0.28	-0.02	2.71	2.72	0.74	1.35	0
<b>LW</b>	0.84	0.25	0.85	0.85	0.24	-0.02	1.47	1.49	-0.31	0.14	0.01
<b>HW</b>	1.45	0.37	1.44	1.44	0.38	0.54	2.71	2.17	0.23	-0.28	0.01

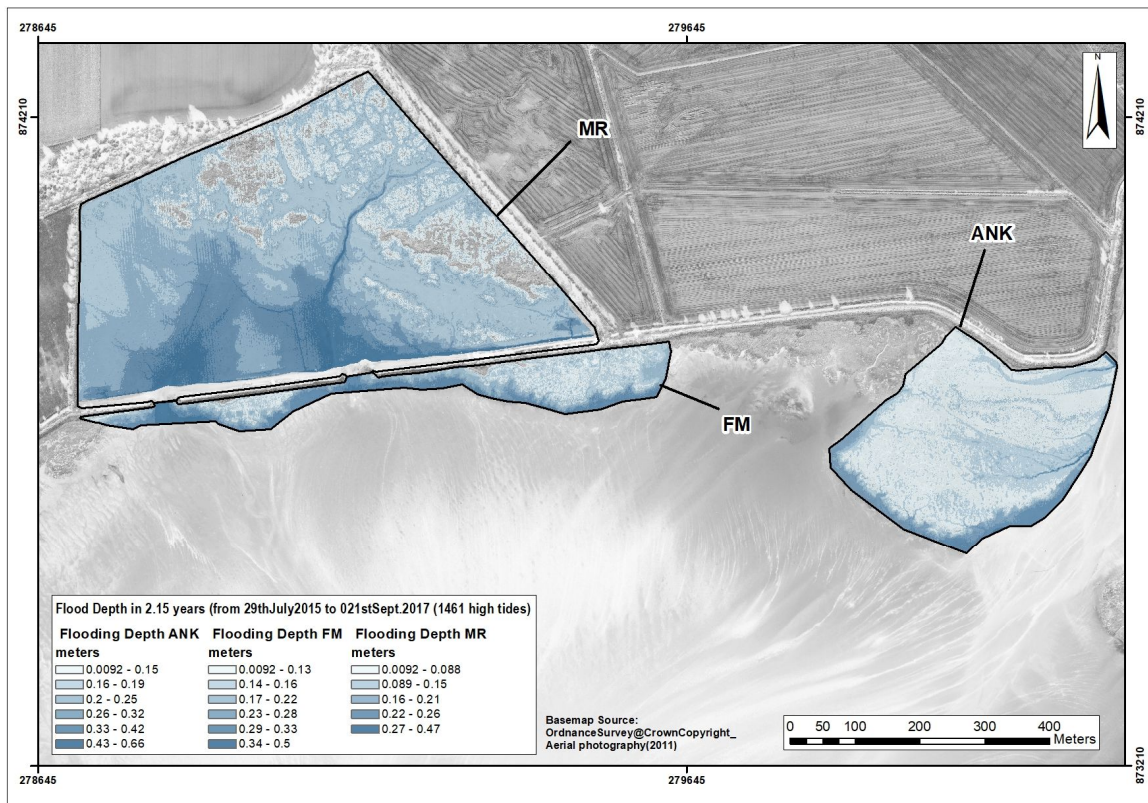


**Figure D- 2 Average flood depth (m) calculated at a 1m<sup>2</sup> cell scale size for the three saltmarsh sites over 785.5 days.**

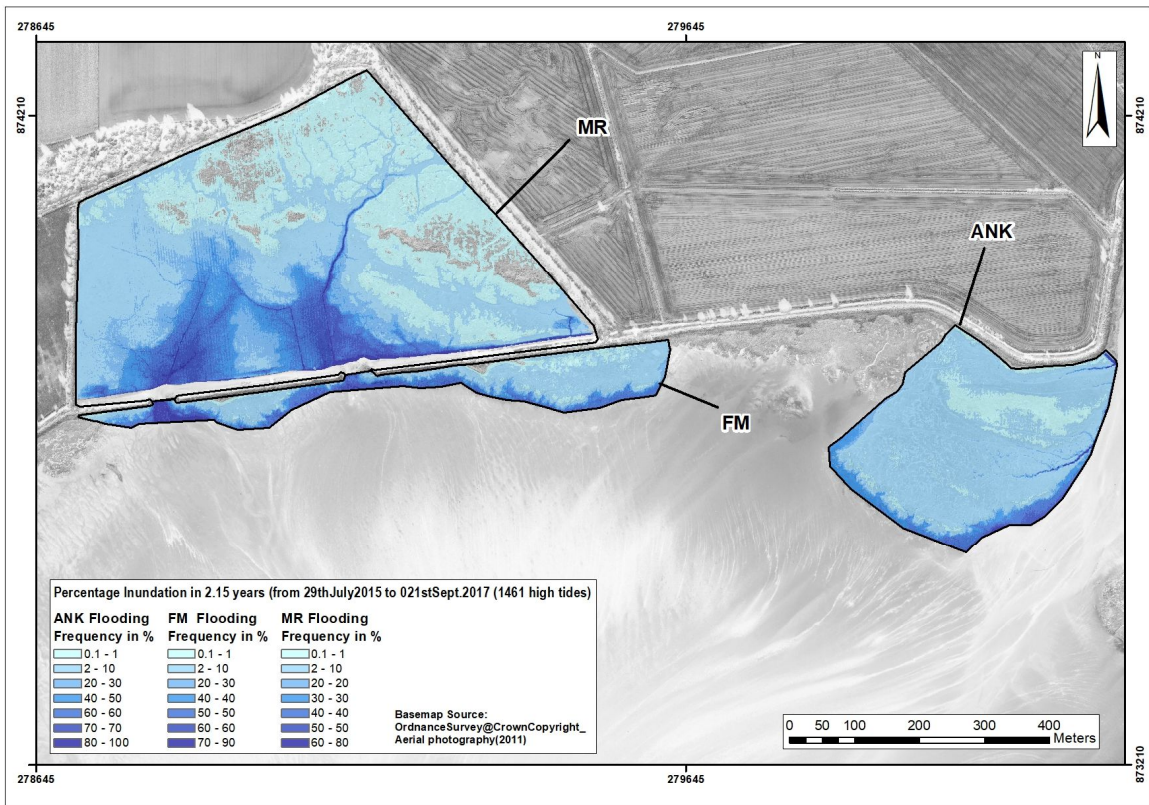


Figure D- 3: Average flood frequency (%) calculated at a 1m<sup>2</sup> cell scale size for the three saltmarsh sites over 785.5 days.

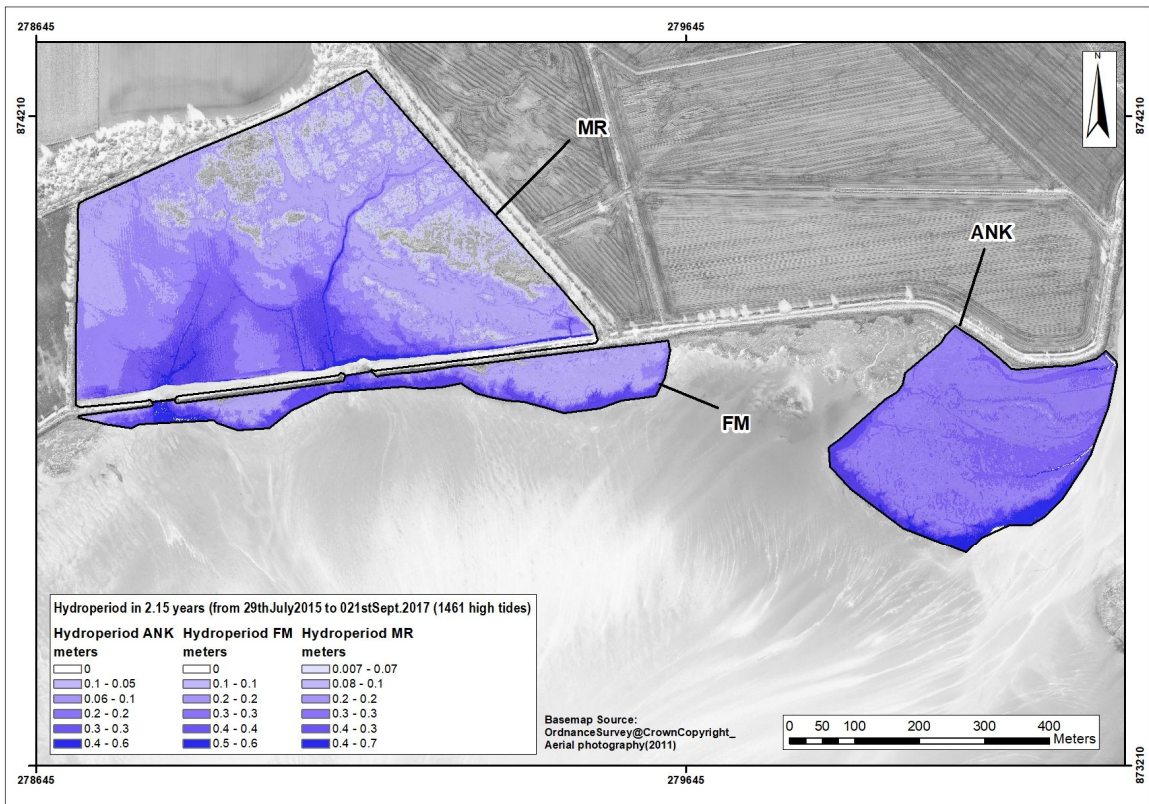


Figure D- 4: Average hydroperiod (m) calculated at a 1m<sup>2</sup> cell scale size for the three saltmarsh sites over 785.5 days.



## APPENDIX.E Supplementary reference for Chapter 6

### E.1. Below ground organic and inorganic saltmarsh evolution: shallow coring programme

Photographs of 17 (out of 23) cores collected on MR, FM and ANK saltmarshes

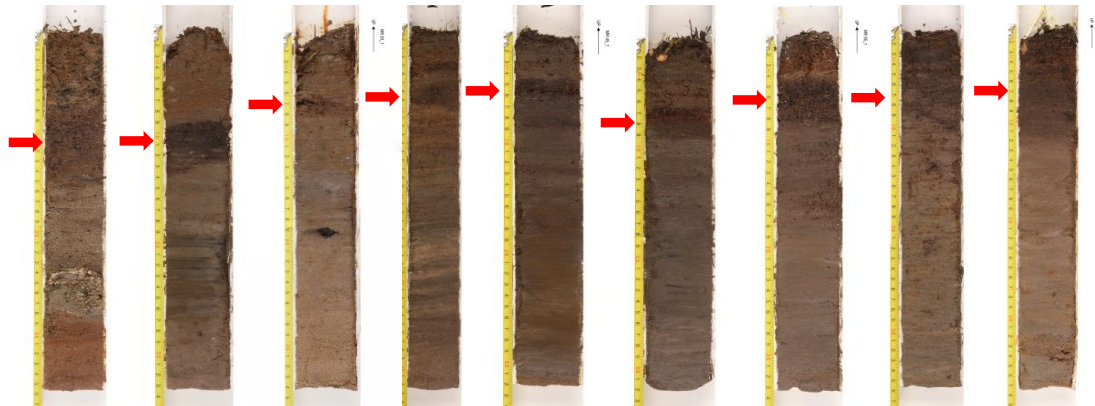


Figure E- 1 a) Cores from Nigg Managed Realignment (MR) from PM to HM in ascending elevation height order: MR24 (PM-1.57mOD), MR47(PM-1.82mOD), MR53(LM-1.86mOD), MR26(LM-2.04mOD), MR45 (LM-2.05mOD), MR38 (LM-2.06OD), MR55 (MM-2.08mOD), MR19 (HM-2.37mOD), and MR60 (HM-2.54mOD). Red arrow  $\rightarrow$  represents clear stratigraphic break associated with change in soil colour present in 7 out of 9 cores photographed and interpreted as reclamation years.



Figure E- 1b) Cores from Nigg natural saltmarsh ANK (ANK – left cluster) from left to right: A1, A2, A6, A5 and A9 and Fronting marsh (FM – right cluster) showing FM, FM3 and FM4.

### E.2. Bulk Dry Density – BDD and Water content

Table E- 1: Analysis of Variance on Ranks for BDD ( $\text{g cm}^{-3}$ ) sites' saltmarsh zones.

Group	N	Missing	Median	25%	75%
MR_HM	96	0	1.040	0.375	1.290
MR_PM	61	1	1.010	0.443	1.377
ANK_MM	94	0	0.595	0.460	0.793
ANK_PM	72	1	1.130	0.840	1.360
FM_MM	39	0	1.260	1.090	1.510
ANK_LM	36	0	0.490	0.400	1.067
MR_MM	17	0	0.550	0.195	0.745
FM_HM	64	0	0.875	0.522	0.977
MR_LM	74	0	0.925	0.597	1.255
ANK_HM	55	0	1.000	0.810	1.160

H = 112.995 with 9 degrees of freedom. (P = <0.001)

The differences in the median values among the treatment groups are greater than would be expected by chance; there is a statistically significant difference (P = <0.001)

To isolate the group or groups that differ from the others use a multiple comparison procedure.

All Pairwise Multiple Comparison Procedures (Dunn's Method) :

Comparison	Diff of Ranks	Q	P	P<0.050
FM_MM vs MR_MM	296.891	5.835	<0.001	Yes
FM_MM vs ANK_MM	262.916	7.884	<0.001	Yes
FM_MM vs FM_HM	212.538	5.976	<0.001	Yes
ANK_HM vs ANK_MM	142.314	4.788	<0.001	Yes
ANK_HM vs ANK_LM	135.520	3.611	0.014	Yes
MR_PM vs MR_MM	168.570	3.504	0.021	Yes
MR_PM vs ANK_MM	134.594	4.652	<0.001	Yes
MR_PM vs ANK_LM	127.800	3.462	0.024	Yes

Note: The multiple comparisons on ranks do not include an adjustment for ties.

**Table E- 2: Analysis of Variance on Ranks for soil moisture (%) between sites, saltmarsh zones and sites' saltmarsh zones.**

**One Way Analysis of Variance**

Dependent Variable: 60 WATER loss

Normality Test (Shapiro-Wilk): Failed (P < 0.050)

Equal Variance Test (Brown-Forsythe): Failed (P < 0.050)

Test execution ended by user request, ANOVA on Ranks begun

**Kruskal-Wallis One Way Analysis of Variance on Ranks**

Data source: Data 1 in cores.JNB

Dependent Variable: 60 WATER loss

Group	N	Missing	Median	25%	75%
MR	248	1	27.990	19.030	57.680
ANK	257	2	37.810	26.680	56.080
FM	103	0	31.460	24.180	44.810

H = 13.488 with 2 degrees of freedom. (P = 0.001)

The differences in the median values among the treatment groups are greater than would be expected by chance; there is a statistically significant difference (P = 0.001)

To isolate the group or groups that differ from the others use a multiple comparison procedure.

All Pairwise Multiple Comparison Procedures (Dunn's Method) :

Comparison	Diff of Ranks	Q	P	P<0.050
ANK vs MR	55.469	3.555	0.001	Yes
ANK vs FM	44.750	2.193	0.085	No
FM vs MR	10.719	0.523	1.000	No

Note: The multiple comparisons on ranks do not include an adjustment for ties.

**One Way Analysis of Variance** Dependent Variable: 60 WATER loss

Normality Test (Shapiro-Wilk): Failed (P < 0.050)

Test execution ended by user request, ANOVA on Ranks begun

**Kruskal-Wallis One Way Analysis of Variance on Ranks**

Dependent Variable: 60 WATER loss

Group	N	Missing	Median	25%	75%
HM	215	1	30.475	23.183	51.665
PM	133	2	28.980	18.520	40.440
MM	150	0	45.550	27.372	56.830
LM	110	0	39.125	18.690	61.815

H = 28.366 with 3 degrees of freedom. (P = <0.001)

The differences in the median values among the treatment groups are greater than would be expected by chance; there is a statistically significant difference (P = <0.001)

To isolate the group or groups that differ from the others use a multiple comparison procedure.

All Pairwise Multiple Comparison Procedures (Dunn's Method) :

Comparison	Diff of Ranks	Q	P	P<0.050
MM vs PM	109.868	5.256	<0.001	Yes
MM vs HM	62.067	3.335	0.005	Yes
LM vs PM	63.526	2.810	0.030	Yes

**One Way Analysis of Variance**

Dependent Variable: 60 WATER loss

Normality Test (Shapiro-Wilk): Failed (P < 0.050)  
 Test execution ended by user request, ANOVA on Ranks begun

**Kruskal-Wallis One Way Analysis of Variance on Ranks** Dependent Variable: 60 WATER loss

Group	N	Missing	Median	25%	75%
MR_HM	96	1	24.340	19.750	60.120
MR_PM	61	0	23.390	16.985	56.150
ANK_MM	94	0	49.705	44.838	58.405
ANK_PM	72	2	30.555	20.175	37.043
FM_MM	39	0	22.090	19.910	26.120
ANK_LM	36	0	60.310	20.910	65.210
MR_MM	17	0	59.930	39.820	77.365
FM_HM	64	0	39.975	31.362	55.525
MR_LM	74	0	37.670	18.578	48.045
ANK_HM	55	0	29.050	24.330	33.850

H = 117.890 with 9 degrees of freedom. (P = <0.001)

The differences in the median values among the treatment groups are greater than would be expected by chance; there is a statistically significant difference (P = <0.001)

To isolate the group or groups that differ from the others use a multiple comparison procedure.

All Pairwise Multiple Comparison Procedures (Dunn's Method) :

Comparison	Diff of Ranks	Q	P	P<0.050
MR_MM vs FM_MM	281.555	5.542	<0.001	Yes
MR_MM vs MR_PM	194.038	4.048	0.002	Yes
MR_MM vs MR_HM	175.856	3.820	0.006	Yes
MR_MM vs MR_LM	164.144	3.492	0.022	Yes
ANK_MM vs FM_MM	262.159	7.874	<0.001	Yes
ANK_LM vs ANK_PM	131.250	3.661	0.011	Yes
FM_HM vs FM_MM	205.260	5.781	<0.001	Yes

Note: The multiple comparisons on ranks do not include an adjustment for ties.

### E.3. Below ground Organic matter - SOM

#### SOM results and dataset adjustments

Selection As discussed in Chapter 3 – 3.4.3.2, the appropriate choice of ignition temperatures is closely linked to sediment characteristics and reproducibility is not always reached (Craft et al., 1991; Plater et al., 2015). This hypothesis may not answer this thesis aims, it impacts on its results and quantification carbon content. This hypothesis is quickly tested here by presenting differences between LOI at 375 °C and 450 °C results leading to small adjustments to dataset.

SOM results between LOI at 375°C and LOI at 450°C were overall highly correlated ( $\rho=0.91$  \*\*\*) but not perfect (1) due to one core (A5) as displayed scatterplot in Figure E- 1. Core A5 located on the ANK's easternmost PM alongside Ankerville's river display c. 28% loss between the two procedures ( $\rho=0.86$  \*\*\*). This extremely large differences compared to all other cores ( $0.085\pm 0.025$  %) may indicate the presence of minerals or carbonates losing carbon dioxide at higher temperature (Sutherland and Walton, 1990; Santisteban et al., 2004; Wang et al., 2011). Given the low variability between the two ignition temperatures results for all other cores, it seemed appropriate to use the results from the combustion at 450°C. However, removing core A5 from the dataset leads to exclude it from the sampling design aiming to characterise

SOM as a function of space (all saltmarsh sites and zones zones) and depth/time. A comprehensive assessment of the values was then made by comparing this core to other at same elevation and geomorphic settings (zonal and distances to saltmarsh edge, etc.), and it was decided to estimate Core A5 values at 450 °C from results of regression analysis ( $r^2_{adj}$  99.58%,  $p < 0.001^{***}$ ) using equation  $LOI_{450 (loge)} = 0.09478 + (0.98092 * LOI_{375 (loge)})$  as described in Table E-3.

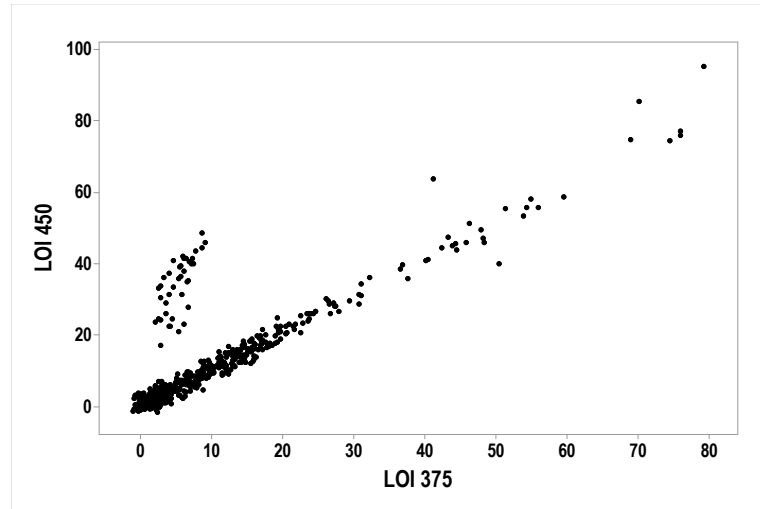


Figure E- 1: relationships between LOI at 375°C versus 450°C ( $\rho=0.91$ ;  $p$ -value $<0.001^{***}$ ) following a trend of  $LOI_{375(\%Loge)}$  =  $0.01323 + 0.8753 * LOI_{450(\%Loge)}$ . The scatterplot highlights core A5 overestimation at a combustion of 450 °C.

Table E- 3: Regression Analysis of overall LOI 450 (Loge) versus LOI 375 (Loge)

Analysis of variance					
Source	DF	Adj SS	Adj MS	F-Value	P-Value
Regression	1	720.560	720.560	114170.94	<0.001***
LOI 375 (Loge)	1	720.560	720.560	114170.94	<0.001***
Error	482	3.042	0.006		
Total	483	723.602			
Model Summary					
S	R-sq	R-sq(adj)	R-sq(pred)		
0.0794433	99.58%	99.58%	99.58%		
Coefficients					
Term	Coef	SE Coef	T-Value	P-Value	VIF
Constant	0.09478	0.00601	15.77	<0.001***	
LOI 375 (Loge)	0.98092	0.00290	337.89	<0.001***	1.00
Regression Equation					
$LOI_{450 (loge)} = 0.09478 + (0.98092 * LOI_{375 (loge)})$					

Table E- 4 Analysis of Variance on Ranks for SOM (%) between saltmarsh sites and between saltmarsh zones.

<b>One Way Analysis of Variance</b> Dependent Variable: LOI450(from 60)_adapted2 for Core A5					
Normality Test (Shapiro-Wilk):    Failed    (P < 0.050)					
Test execution ended by user request, ANOVA on Ranks begun					
<b>Kruskal-Wallis One Way Analysis of Variance on Ranks</b> Dependent Variable: LOI450(from 60)_adapted2 for Core A5					
Group	N	Missing	Median	25%	75%
MR	248	0	4.640	1.418	15.692



ANK	257	2	7.038	2.920	14.140
FM	103	0	4.380	2.190	8.740

H = 8.195 with 2 degrees of freedom. (P = 0.017)

The differences in the median values among the treatment groups are greater than would be expected by chance; there is a statistically significant difference (P = 0.017)

To isolate the group or groups that differ from the others use a multiple comparison procedure.

All Pairwise Multiple Comparison Procedures (Dunn's Method) :

Comparison	Diff of Ranks	Q	P	P<0.050
ANK vs FM	53.396	2.612	0.027	Yes
ANK vs MR	32.300	2.069	0.116	No
MR vs FM	21.096	1.028	0.912	No

Note: The multiple comparisons on ranks do not include an adjustment for ties.

---

**One Way Analysis of Variance**      Dependent Variable: LOI450(from 60)\_adapted for core A5  
**Normality Test (Shapiro-Wilk):**      Failed      (P < 0.050)

Test execution ended by user request, ANOVA on Ranks begun

**Kruskal-Wallis One Way Analysis of Variance on Ranks**  
Dependent Variable: LOI450(from 60)\_adapted for core A5

Group	N	Missing	Median	25%	75%
HM	215	0	4.170	2.360	13.110
PM	133	2	4.318	1.000	8.280
MM	150	0	11.350	2.905	14.520
LM	110	0	8.435	1.982	19.267

H = 29.186 with 3 degrees of freedom. (P = <0.001)

The differences in the median values among the treatment groups are greater than would be expected by chance; there is a statistically significant difference (P = <0.001)

To isolate the group or groups that differ from the others use a multiple comparison procedure.

All Pairwise Multiple Comparison Procedures (Dunn's Method) :

Comparison	Diff of Ranks	Q	P	P<0.050
MM vs PM	107.540	5.136	<0.001	Yes
MM vs HM	53.063	2.849	0.026	Yes
LM vs PM	86.842	3.835	<0.001	Yes
HM vs PM	54.477	2.807	0.030	Yes

Note: The multiple comparisons on ranks do not include an adjustment for ties.

**Table E- 5: Analysis of Variance on Ranks for SOM (%) between saltmarsh sites, saltmarsh zones and sites' saltmarsh zones.**

<b>One Way Analysis of Variance</b>	Data source: Data 1 in cores.JNB				
Dependent Variable: LOI450(from 60)_adapted for Core A5					
<b>Normality Test (Shapiro-Wilk):</b>	Failed      (P < 0.050)				
Test execution ended by user request, ANOVA on Ranks begun					
<b>Kruskal-Wallis One Way Analysis of Variance on Ranks</b>	Dependent Variable: LOI450(from 60)_adapted for Core A5				
<b>Group</b>	<b>N</b>	<b>Missing</b>	<b>Median</b>	<b>25%</b>	<b>75%</b>
MR_HM	96	0	3.373	1.957	32.474
MR_PM	61	0	2.010	0.958	14.239
ANK_MM	94	0	12.729	10.579	14.825
ANK_PM	72	2	4.592	2.622	6.566
FM_MM	39	0	1.790	1.220	2.930
ANK_LM	36	0	20.320	2.525	26.315
MR_MM	17	0	31.050	11.095	47.740
FM_HM	64	0	6.475	3.832	14.563
MR_LM	74	0	6.660	1.390	11.617
ANK_HM	55	0	2.800	1.920	4.370

H = 129.266 with 9 degrees of freedom. (P = <0.001)

The differences in the median values among the treatment groups are greater than would be expected by chance; there is a statistically significant difference ( $P = <0.001$ )

To isolate the group or groups that differ from the others use a multiple comparison procedure.

All Pairwise Multiple Comparison Procedures (Dunn's Method) :

Comparison	Diff of Ranks	Q	P	P<0.050
MR_MM vs FM_MM	344.087	6.762	<0.001	Yes
MR_MM vs MR_PM	252.135	5.251	<0.001	Yes
MR_MM vs MR_LM	201.197	4.273	<0.001	Yes
MR_MM vs MR_HM	191.505	4.157	0.001	Yes
ANK_LM vs ANK_HM	180.367	4.805	<0.001	Yes
ANK_LM vs ANK_PM	165.674	4.614	<0.001	Yes
ANK_LM vs MR_LM	122.687	3.448	0.025	Yes
ANK_MM vs FM_MM	262.889	7.883	<0.001	Yes
ANK_MM vs ANK_HM	177.679	5.978	<0.001	Yes
ANK_MM vs ANK_PM	162.986	5.897	<0.001	Yes
FM_HM vs FM_MM	204.082	5.738	<0.001	Yes
FM_HM vs ANK_HM	118.872	3.693	0.010	Yes

Note: The multiple comparisons on ranks do not include an adjustment for ties.

#### E.4. Water content, BDD and Organic matter for cores collected along the fronting marsh (FM) and Managed realignment (MR) transects.

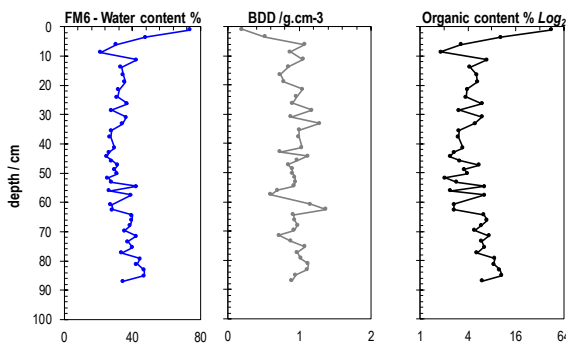


Figure E- 2: FM6 (FM mid marsh) Water content (%), BDD (g/cm-3) and OM (Log2 %)

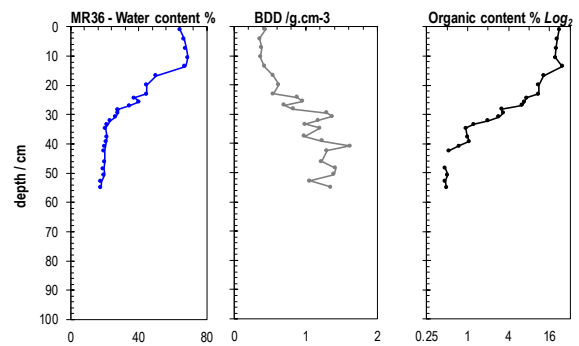


Figure E- 3: MR36 (MR pioneer marsh) Water content (%), BDD (g/cm-3) and OM (Log2 %)

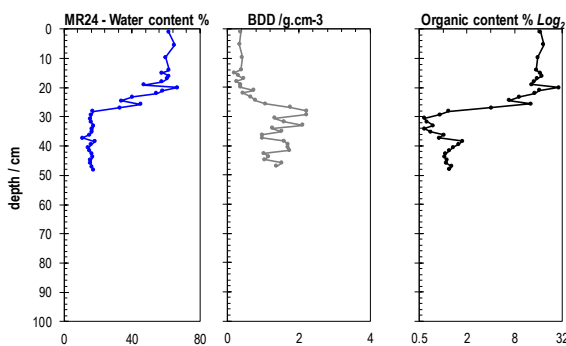


Figure E- 4: MR24 (MR pioneer marsh) Water content (%), BDD (g/cm-3) and OM (Log2 % & organic content combusted at 375°C instead of 450°C)

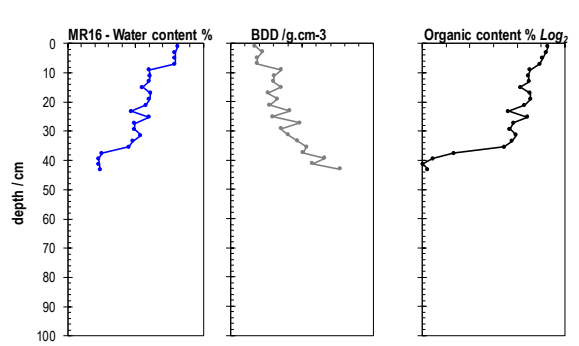


Figure E- 5 : MR16 (MR low marsh) Water content (%), BDD (g/cm-3) and OM (Log2 %)

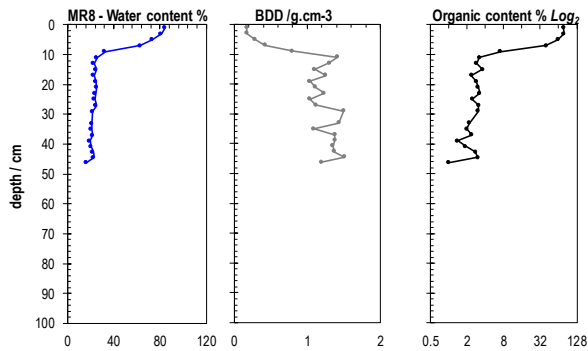


Figure E- 6: MR8 (MR high marsh) Water content (%), BDD (g/cm-3) and OM (Log2 %)

E.5. Water content, BDD and Organic matter for cores collected along the natural saltmarsh (ANK) Transect.

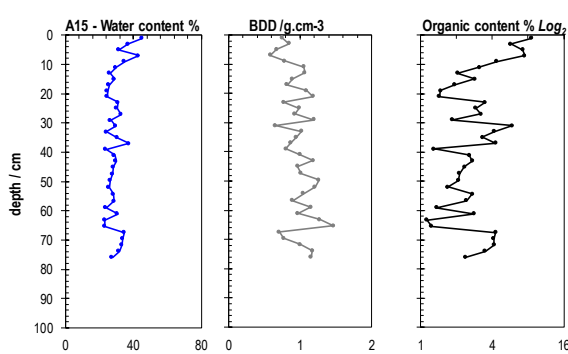


Figure E- 7: A15 (natural high marsh – cliff edge) Water content (%), BDD (g/cm-3) and OM (Loge %)

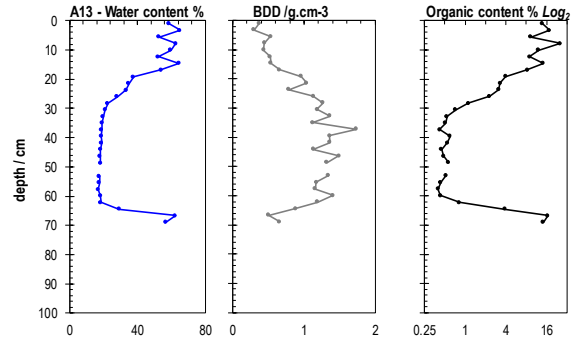


Figure E- 8: A13 (natural pioneer marsh) Water content (%), BDD (g/cm-3) and OM (Loge %)

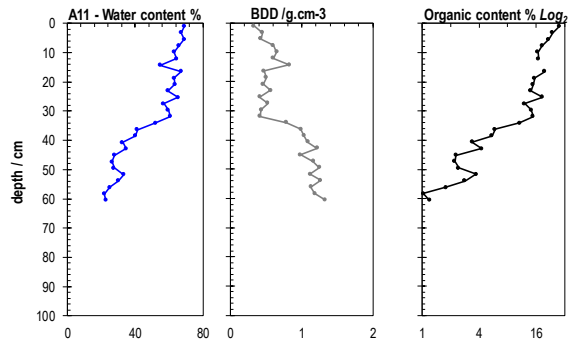


Figure E- 9: A11 (natural mid-marsh) Water content (%), BDD (g/cm-3) and OM (Loge %)

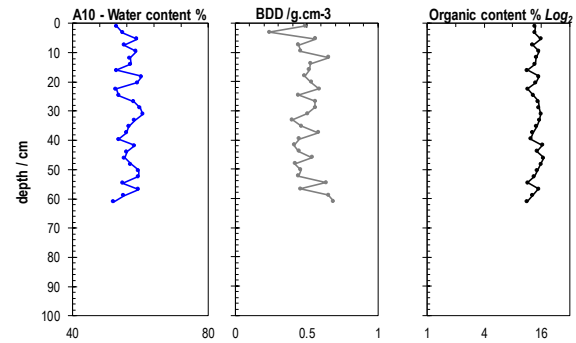


Figure E- 10: A10 (natural low marsh) Water content (%), BDD (g/cm-3) and OM (Loge %)

Table E- 6: Overall SOM (%) per sites per saltmarsh zones at depth of 10cm interval to 50 and 50 to 87 cm (corrected for compaction).

	ANK					FM					MR				
	Min	Max	Mean	SD	n	Min	Max	Mean	SD	n	Min	Max	Mean	SD	n
Core depth [1-10 cm]															
	ANK					FM					MR				
Overall						55.3	15.0				2.88	97.2	38.4		5
I	2.726	58.47	17.7	12.7	49	1.29	7	7	17.87	17	2.88	7	8	23.55	1
HM	4.37	58.47	25.97	18.60	13	17.8	55.3	33.1		5	7.04	97.2	54.2		2
						0	7	7	17.36	5	7.04	7	1	21.62	4

MM	9.20	27.95	15.71	5.33	15	1.29	44.7 7	7.53	11.99	12	43.00	73.7 2	53.0 5	14.03	4
LM	12.98	32.08	21.35	8.52	9						2.88	45.9 1	19.7 0	9.13	1 7
PM	2.73	25.32	8.50	6.96	13						15.79	22.2 2	19.1 0	2.40	6
<b>Core depth [10-20 cm]</b>															
	<b>ANK</b>					<b>FM</b>					<b>MR</b>				
Overall I	1.321	25.23	10.17	6.126	48	0.98	18.1 9	6.55	6.161	18	1.55	85.9 2	15.7 9	16.93 4	5 1
HM	1.47	20.82	7.64	6.22	13	14.5 4	18.1 9	15.8 3	1.47	5	1.68	53.4 9	12.6 6	15.68	2 1
MM	6.98	19.59	11.87	3.52	14	0.98	6.98	2.98	1.85	13	34.87	85.9 2	54.2 5	23.23	4
LM	11.38	25.23	17.81	4.94	8						1.55	29.3 8	8.82	6.75	1 5
PM	1.32	14.21	6.18	3.76	13						11.06	28.9 6	17.2 7	5.39	1 1
<b>Core depth [20-30 cm]</b>															
	<b>ANK</b>					<b>FM</b>					<b>MR</b>				
Overall I	1.11	27.37	9.224	6.591	50	0.74	14.5 7	5.95 7	5.443	17	0.6	31.0 5	6.05 2	5.543	5 9
HM	1.44	3.50	2.52	0.66	13	13.1 1	14.5 7	13.8 0	0.70	5	1.25	6.10	2.85	1.20	2 5
MM	10.36	18.65	13.13	2.24	15	0.74	6.01	2.69	1.81	11	9.45	31.0 5	19.2 2	9.25	4
LM	11.46	27.37	17.72	4.92	10						0.60	11.1 0	6.55	3.69	1 6
PM	1.11	6.56	4.52	1.75	12						0.92	16.4 8	7.44	4.85	1 4
<b>Core depth [30-40 cm]</b>															
	<b>ANK</b>					<b>FM</b>					<b>MR</b>				
Overall I	0.42	26.57	7.242	6.425	45	0.69	18.1 2	6.24 1	6.746	17	0.529 3	13.7 4	2.75 4	3.124	5 7
HM	1.13	5.89	2.46	1.58	12	14.5 3	18.1 2	16.0 5	1.73	5	0.53	6.98	1.94	1.59	1
MM	3.36	14.88	9.58	3.35	11	0.69	6.00	2.15	1.77	12	2.77	12.5 0	8.42	4.43	5
LM	12.39	26.57	17.73	5.25	8						0.68	13.7 4	3.55	3.55	1 6
PM	0.42	6.57	3.51	2.38	14						0.58	2.91	1.15	0.62	1 5
<b>Core depth [40-50 cm]</b>															
	<b>ANK</b>					<b>FM</b>					<b>MR</b>				
Overall I	0.45	25.55	5.936	6.326 5	32	1.74	15.0 8	4.14 6	3.446 3	13	0.47	4.31	1.26 6	0.958 2	2 7
HM	1.47	2.72	2.04	0.43	10	15.0 8	15.0 8	15.0 8		1	0.99	4.31	2.58	1.25	5
MM	2.22	4.26	2.91	0.89	5	1.74	5.59	3.24	1.09	12					
LM	14.4 6	25.5 5	17.6 5	3.97	6						0.50	2.57	1.02	0.81	1 0
PM	0.45	9.04	4.46	3.35	11						0.47	1.29	0.93	0.30	1 2
<b>Core depth [50-87 cm]</b>															
	<b>ANK</b>					<b>FM</b>					<b>MR</b>				
Overall I	0.4	16.53	5.108	5.337	31	2.06	10.6 5	5.83 7	2.451	21	0.47	0.51	0.49	0.02	3
HM	1.13	4.27	2.65	1.16	12										
MM	1.03	3.71	2.11	1.14	5	2.06	10.6 5	5.84	2.45	21					
LM	11.37	14.97	13.14	1.49	6										
PM	0.40	16.53	4.64	6.73	8						0.47	0.51	0.49	0.02	3

## E.6. Carbon density SOC

**Table E- 7: Regression Analysis LOI450 or SOM (*Loge*) versus BDD in g.Ccm<sup>3</sup> *Loge***

Analysis of variance					
Source	DF	Adj SS	Adj MS	F-Value	P-Value
Regression	1	646.110	646.110	1478.22	<0.001***
Vegetation Type	1	646.110	646.110	1478.22	<0.001***
Error	603	263.563	0.437		
Total	604	909.674			

Model Summary			
S	R-sq	R-sq(adj)	R-sq(pred.)
0.661125	71.03%	70.98%	70.84%

Coefficients					
Term	Coef	SE Coef	T-Value	P-Value	VIF
Constant	1.2252	0.0295	41.52	<0.001***	
BDD <i>Loge</i>	-1.8162	0.0472	-38.45	<0.001***	1.00

Regression Equation	Fits and Diagnostics for Unusual Observations Plots
$\%SOM_{log_e} = 1.2252 - (1.8162 * BDD \text{ } Loge)$	

**Table E- 8: Analysis of Variance on Ranks for SOC in g.Ccm<sup>3</sup> between saltmarsh zones.**

One Way Analysis of Variance					
Dependent Variable: SOC gCcm3					
Normality Test (Shapiro-Wilk): Failed (P < 0.050)					
Test execution ended by user request, ANOVA on Ranks begun					
Kruskal-Wallis One Way Analysis of Variance on Ranks					
Dependent Variable: SOC gCcm3					
Group	N	Missing	Median	25%	75%
HM	215	1	0.0142	0.00845	0.0313
PM	133	6	0.0189	0.00349	0.0270
MM	150	1	0.0258	0.0127	0.0332
LM	110	0	0.0242	0.00847	0.0357
H = 26.404 with 3 degrees of freedom. (P = <0.001)					
The differences in the median values among the treatment groups are greater than would be expected by chance; there is a statistically significant difference (P = <0.001)					
To isolate the group or groups that differ from the others use a multiple comparison procedure.					
All Pairwise Multiple Comparison Procedures (Dunn's Method) :					
Comparison	Diff of Ranks	Q	P	P<0.050	
MM vs PM	98.850	4.722	<0.001	Yes	
MM vs HM	65.479	3.540	0.002	Yes	
LM vs PM	73.586	3.259	0.007	Yes	
Note: The multiple comparisons on ranks do not include an adjustment for ties.					

**Table E- 9: Analysis of Variance on Ranks for SOC in g.Ccm<sup>3</sup> between sites' saltmarsh zones.**

One Way Analysis of Variance

Dependent Variable: SOC gCcm3

**Normality Test (Shapiro-Wilk):** Failed (P < 0.050)

Test execution ended by user request, ANOVA on Ranks begun

**Kruskal-Wallis One Way Analysis of Variance on Ranks**  
Dependent Variable: SOC gCcm3

Group	N	Missing	Median	25%	75%
MR_HM	96	1	0.0132	0.00600	0.0398
MR_PM	61	4	0.0137	0.00302	0.0259
ANK_MM	94	1	0.0281	0.0238	0.0342
ANK_PM	72	2	0.0207	0.00840	0.0287
FM_MM	39	0	0.00972	0.00559	0.0148
ANK_LM	36	0	0.0346	0.0119	0.0501
MR_MM	17	0	0.0437	0.0324	0.0657
FM_HM	64	0	0.0222	0.0136	0.0321
MR_LM	74	0	0.0205	0.00608	0.0291
ANK_HM	55	0	0.00971	0.00694	0.0157

H = 110.001 with 9 degrees of freedom. (P = <0.001)

The differences in the median values among the treatment groups are greater than would be expected by chance; there is a statistically significant difference (P = <0.001)

To isolate the group or groups that differ from the others use a multiple comparison procedure.

All Pairwise Multiple Comparison Procedures (Dunn's Method) :

Comparison	Diff of Ranks	Q	P	P<0.050
MR_MM vs FM_MM	309.187	6.137	<0.001	Yes
MR_MM vs MR_PM	271.638	5.670	<0.001	Yes
MR_MM vs MR_LM	210.437	4.514	<0.001	Yes
MR_MM vs MR_HM	208.933	4.577	<0.001	Yes
ANK_LM vs ANK_HM	191.445	5.152	<0.001	Yes
ANK_LM vs ANK_PM	135.214	3.803	0.006	Yes
ANK_LM vs MR_LM	126.878	3.602	0.014	Yes
ANK_MM vs ANK_PM	118.284	4.312	<0.001	Yes
FM_HM vs FM_MM	156.378	4.441	<0.001	Yes
FM_HM vs ANK_HM	122.195	3.834	0.006	Yes

Note: The multiple comparisons on ranks do not include an adjustment for ties.

**Table E- 10: Analysis of Variance on Ranks for SOC in g.Ccm<sup>3</sup> between Vegetation type and Regression Analysis of SOC (g.Ccm<sup>3</sup>) and Vegetation type (Assemblage in A.2. – in Chapt. 3 -Table 3-4)**

Dependent Variable: SOC gCcm3

**Normality Test (Shapiro-Wilk):** Failed (P < 0.050)

Test execution ended by user request, ANOVA on Ranks begun

**Kruskal-Wallis One Way Analysis of Variance on Ranks**  
Dependent Variable: SOC gCcm3

Group	N	Missing	Median	25%	75%
SM16d	96	1	0.0132	0.00600	0.0398
SM8	133	6	0.0189	0.00349	0.0270
SM13b	111	1	0.0297	0.0239	0.0371
SM13d	39	0	0.00972	0.00559	0.0148
SM13a	110	0	0.0242	0.00847	0.0357
SM16a	98	0	0.0129	0.00858	0.0199
SM16c	21	0	0.0322	0.0298	0.0359

H = 100.988 with 6 degrees of freedom. (P = <0.001)

The differences in the median values among the treatment groups are greater than would be expected by chance; there is a statistically significant difference (P = <0.001)

To isolate the group or groups that differ from the others use a multiple comparison procedure.

All Pairwise Multiple Comparison Procedures (Dunn's Method) :

Comparison	Diff of Ranks	Q	P	P<0.050
------------	---------------	---	---	---------



SM16c vs SM13d	276.319	5.889	<0.001	Yes
SM16c vs SM16a	214.221	5.139	<0.001	Yes
SM16c vs SM8	209.631	5.134	<0.001	Yes
SM16c vs SM16d	176.064	4.212	<0.001	Yes
SM16c vs SM13a	136.045	3.296	0.021	Yes
SM13b vs SM13d	224.228	6.941	<0.001	Yes
SM13b vs SM16a	162.131	6.733	<0.001	Yes
SM13b vs SM8	157.541	6.977	<0.001	Yes
SM13b vs SM16d	123.974	5.106	<0.001	Yes
SM13b vs SM13a	83.955	3.592	0.007	Yes
SM13a vs SM13d	140.274	4.342	<0.001	Yes
SM13a vs SM16a	78.176	3.247	0.025	Yes
SM13a vs SM8	73.586	3.259	0.023	Yes
SM16d vs SM13d	100.255	3.041	0.050	Yes

Note: The multiple comparisons on ranks do not include an adjustment for ties.

Call:  
lm(formula = SOC.gCcm3 ~ NVC\_Veg, data = AllCore\_depth)

Residuals:  
Min 1Q Median 3Q Max  
-0.029736 -0.012318 -0.003500 0.007026 0.229885

Coefficients:  
Estimate Std. Error t value Pr(>|t|)  
(Intercept) 0.0252376 0.0019349 13.043 < 2e-16 \*\*\*  
NVC\_Veg\_Oct2021SM13b 0.0076280 0.0027364 2.788 0.005479 \*\*  
NVC\_Veg\_Oct2021SM13d -0.0137799 0.0037820 -3.644 0.000292 \*\*\*  
NVC\_Veg\_Oct2021SM16a -0.0070724 0.0028189 -2.509 0.012375 \*  
NVC\_Veg\_Oct2021SM16c 0.0097700 0.0048326 2.022 0.043659 \*  
NVC\_Veg\_Oct2021SM16d 0.0002706 0.0028423 0.095 0.924198  
NVC\_Veg\_Oct2021SM8 -0.0075172 0.0026432 -2.844 0.004609 \*\*  
---  
Signif. codes: 0 '\*\*\*' 0.001 '\*\*' 0.01 '\*' 0.05 '.' 0.1 ' ' 1

Residual standard error: 0.02029 on 593 degrees of freedom  
(8 observations deleted due to missingness)  
Multiple R-squared: 0.09563, Adjusted R-squared: 0.08648  
F-statistic: 10.45 on 6 and 593 DF, p-value: 4.93e-11

Anova Table (Type II tests)

Response: SOC.gCcm3  
Sum Sq Df F value Pr(>F)  
NVC\_Veg\_Oct2021 0.025823 6 10.451 4.93e-11 \*\*\*  
Residuals 0.244209 593  
---  
Signif. codes: 0 '\*\*\*' 0.001 '\*\*' 0.01 '\*' 0.05 '.' 0.1 ' ' 1

## APPENDIX.F Supplementary references for Chapter 7

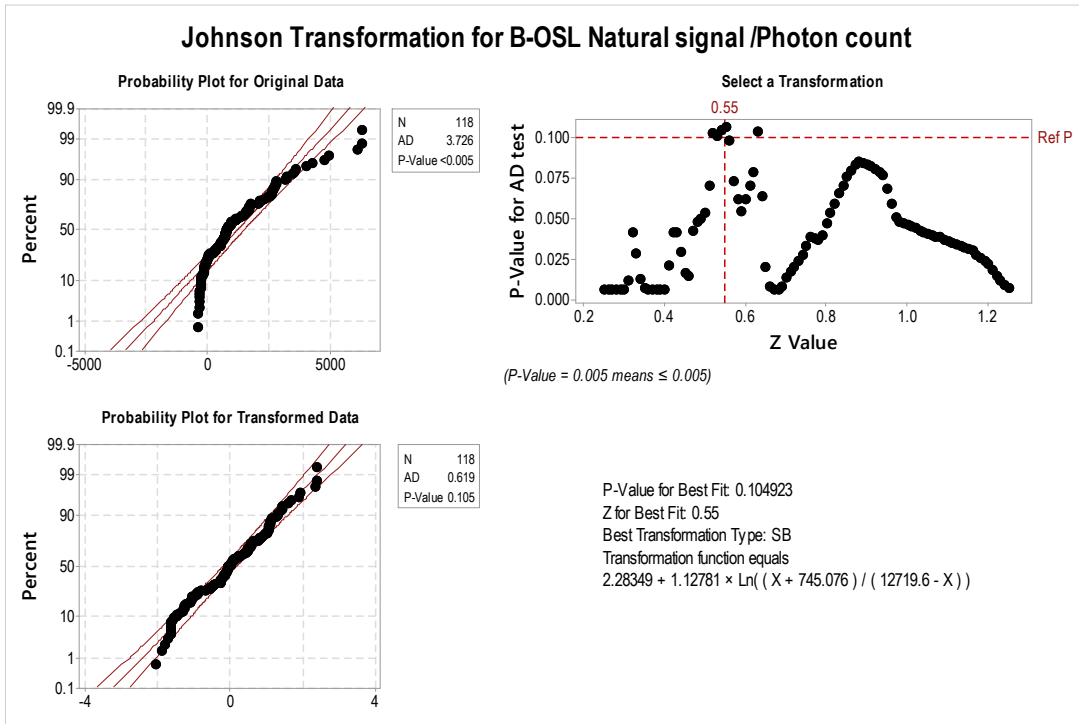


Figure F- 1: results of Johnson transformation used to normalise Natural B-OSL (in Photon count).

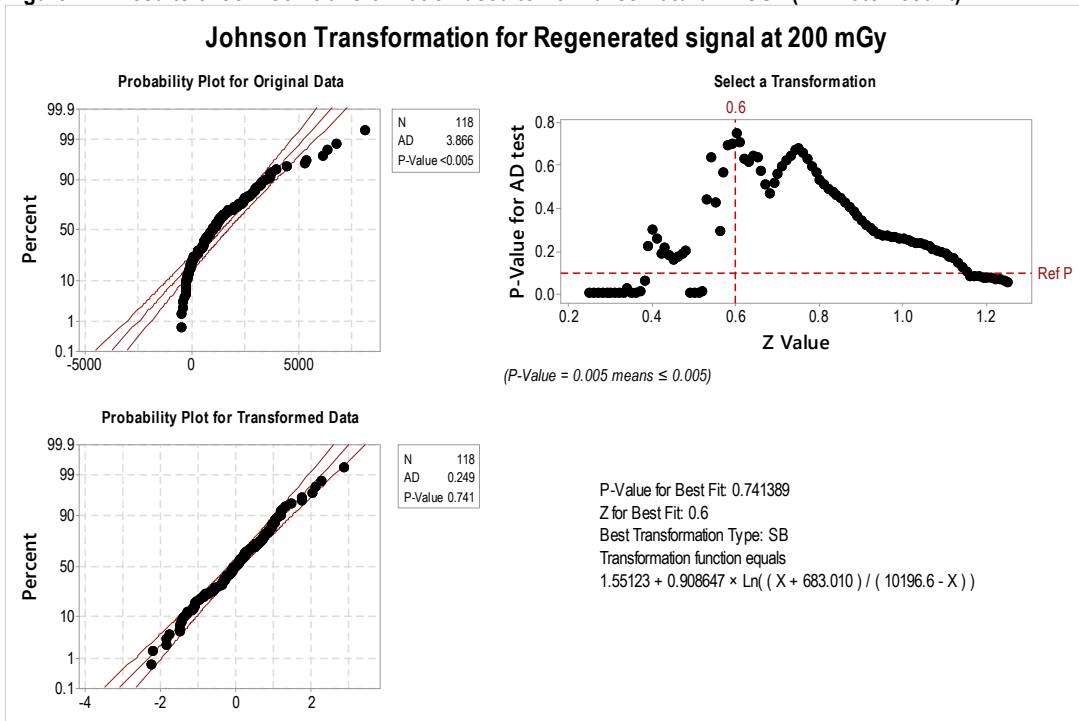


Figure F- 2: results of Johnson transformation used to normalise regenerated B-OSL signal (in Photon count) at a laboratory dose of 200 mGy.

Table F- 1: Correlations between luminescence signal and weight ( Spearman's Rho coefficient and  $p$ -values:  $p < 0.001^{***}$ ,  $p < 0.01^{**}$ ,  $p < 0.05^*$ ) following procedure applied to each sample. Note the moderate influence of sample weight on irradiation.

	250-150	150-90	90-30	<30

Natural signal vs sample weight	0.45 **	0.36 *	-0.03	0.33
Bleached signal ~1hr vs sample weight	0.13	0.00	0.40 *	
Bleached signal >21hrs signal vs sample weight		0.25	0.45 *	0.20
Regenerated at 200mGy signal vs sample weight	0.51 ***	0.42 **	0.37 *	0.43 *

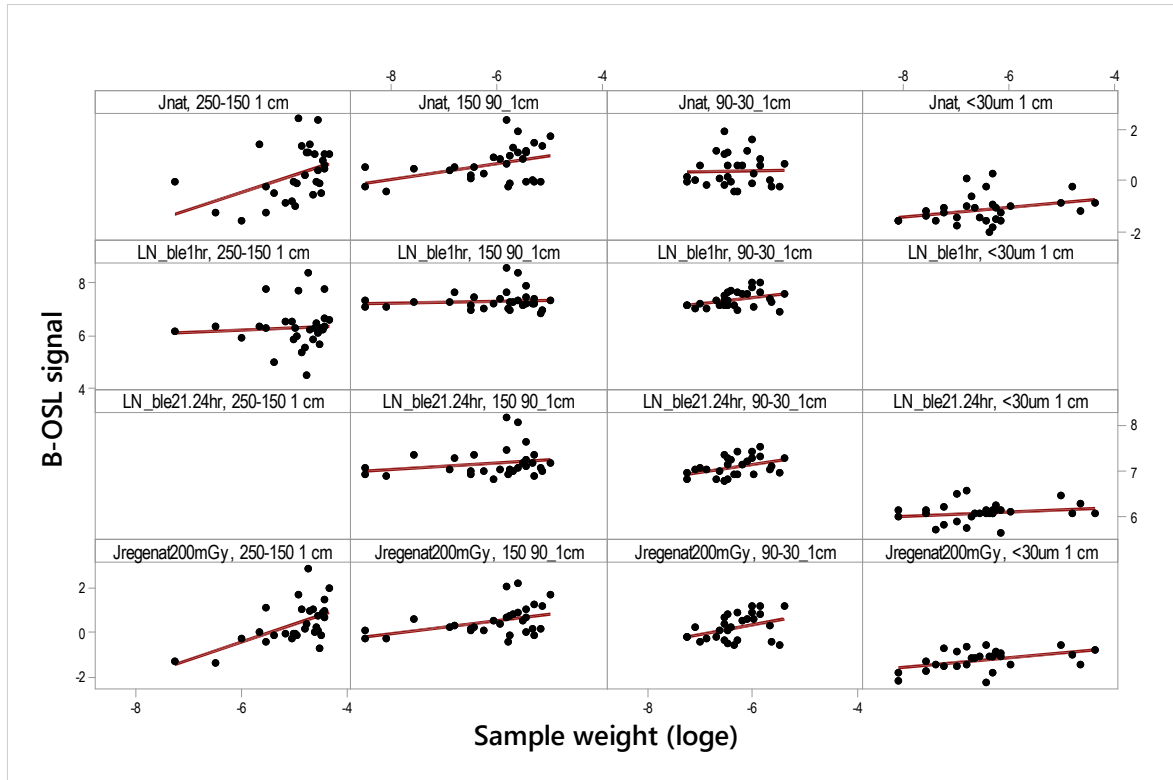


Figure F- 3: Matrix plot highlighting the B-OSL signal (y-axis) versus sample weight (x-axis) for each investigated fractions (column from left to right: 250-150; 150-90; 90-30 and <30  $\mu\text{m}$ ) using portable unit. Units for signal are photon counts transformed using Johnson transformation for natural (top row) and regenerated at 200mGy (bottom row) signals and *Loge* for bleached signals photon count (middle rows).

Table F- 2: Overall net B-OSL natural signal per aliquots (A & B) with results of two sample t-test performed on normalised data by Johnson transformation.

Grain size ( $\mu\text{m}$ )	Natural signal	$\pm$	SE	T-value	<i>p-value</i>
250-150	1514	$\pm$	463.21	-0.27	0.79
	1585	$\pm$	444.62		
150-90	1965	$\pm$	403.82	-0.08	0.94
	1935	$\pm$	317.84		
90-30	1439	$\pm$	332.74	-0.35	0.73
	1540	$\pm$	274.48		
<30	-63.33	$\pm$	89.13	0.77	0.415
	-119.1	$\pm$	107.28		

Table F- 3: Regression Analysis of the overall regenerated signal (photon count *Loge*) at a Dose of 200 mGy

Analysis of variance					
Source	DF	Adj SS	Adj MS	F-Value	P-Value
Regression	1	109.769	109.769	369.87	<0.001***
B_OSL Natural <sub>Loge</sub>	1	109.769	109.769	369.87	<0.001***
Error	146	43.330	0.297		
Lack-of-Fit	142	39.912	0.281	0.33	0.981

Pure Error	4	3.418	0.854		
Total	147	153.099			
<b>Model Summary</b>					
<b>S</b>	<b>R-sq</b>	<b>R-sq(adj)</b>	<b>R-sq(pred)</b>		
0.544775	71.70%	71.50%	70.77%		
<b>Coefficients</b>					
<b>Term</b>	<b>Coef</b>	<b>SE Coef</b>	<b>T-Value</b>	<b>P-Value</b>	<b>VIF</b>
Constant	1.336	0.313	4.27	<0.001***	
B_OSL Natural <sub>Loge</sub>	0.8190	0.0426	19.23	<0.001***	1.00
<b>Regression Equation</b>					
$Regenerated\ B\ OSL_{Loge} = 1.336 + 0.8190\ Regenerated\ B\ OSL_{Loge}$					
<b>Fits and Diagnostics for Unusual Observations Plots:</b>					

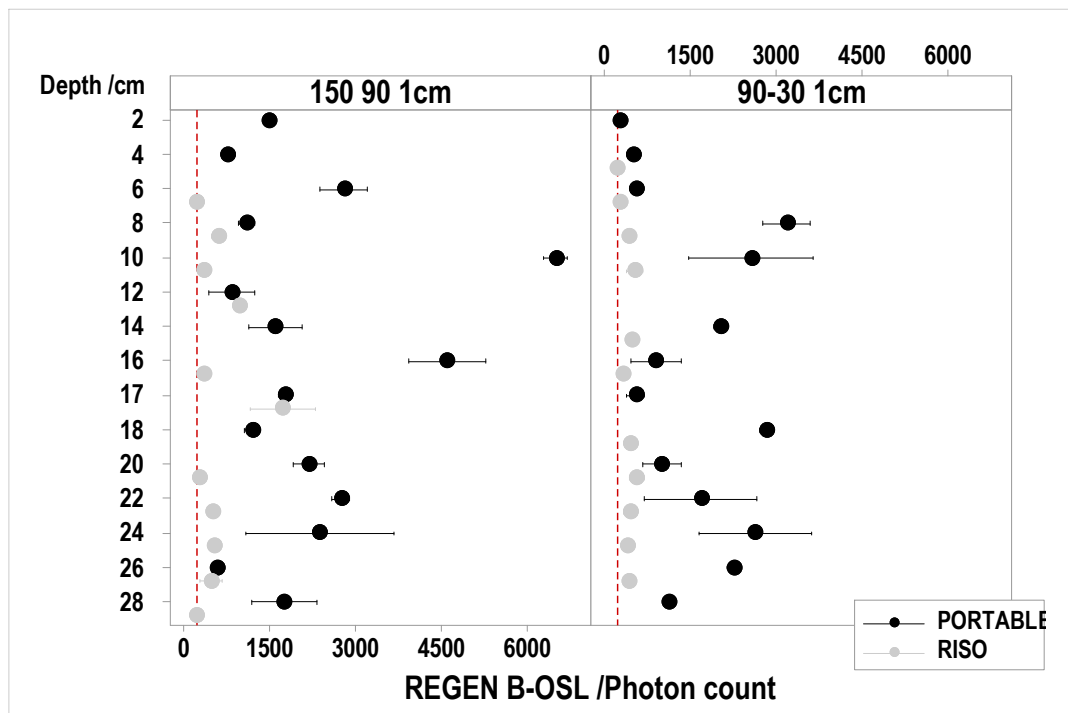


Figure F- 4: 200 mGy regenerated B-OSL signal (in photon count) measured with the portable reader (black) and automated Risø (grey) for fractions 150-90  $\mu\text{m}$  and 90-30  $\mu\text{m}$  on 1cm disc samples. Error bars using individual SD and red dashed line represents the overall dark count limit.

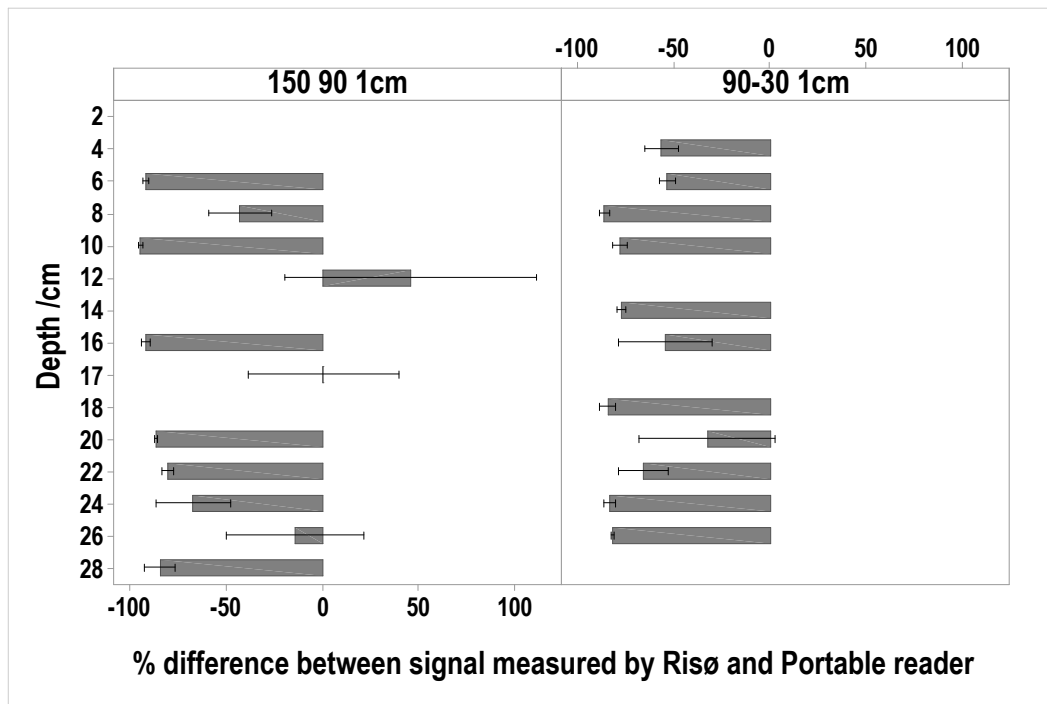


Figure F- 5: Percentage (% and error bar using SD) between 200 mGy regenerated B-OSL signal measured with the portable reader and automated Risø for fractions 150-90 μm and 90-30 μm on 1cm disc samples. Error bars using individual SD and red dashed line represents the overall dark count limit.

Table F- 4: Calibration results for the Fontainebleau quartz providing ratio  $0.965 \pm 0.009$  Gy between Manual Source and Automated Source Risø 1 and  $1.016 \pm 0.009$  between two samples in Risø 1.

Net signal		error			
<b>OSL1</b>		<b>OSL2</b>		<b>OSL1/OSL2</b>	
<b>210s Manual Beta</b>		<b>10 s Risoe 1</b>			
161635	430.9257	169961	452.6135	0.95101229	0.003584
192096	469.6552	195921	491.1568	0.98047682	0.003433
226515	516.793	235278	541.0213	0.9627547	0.003119
				<b>Mean</b>	<b>0.96474794</b>
				<b>SE</b>	<b>0.00872532</b>
<b>10 Second Risoe 1</b>		<b>10 Second Risoe 1</b>			
83566	313.1581	81338	315.8291	1.02739187	0.005544
37560	212.5982	36339	216.7787	1.03360026	0.0085
144600	408.4654	144719	420.4295	0.99917772	0.004049
70452	287.0331	70331	295.951	1.00172044	0.005867
				<b>Mean</b>	<b>1.01547257</b>
				<b>SE</b>	<b>0.00878126</b>
<b>Blank discs</b>		<b>10 Second Risoe 1</b>			
384	36.90528	109650	358.1983	0.00350205	0.000337
192	33.82307	76455	300.7906	0.00251128	0.000443
155	34.19064	100012	347.1772	0.00154981	0.000342

127	33.8969	105163	353.3709	0.00120765	0.000322
				Mean	0.0021927
				SE	0.00051636

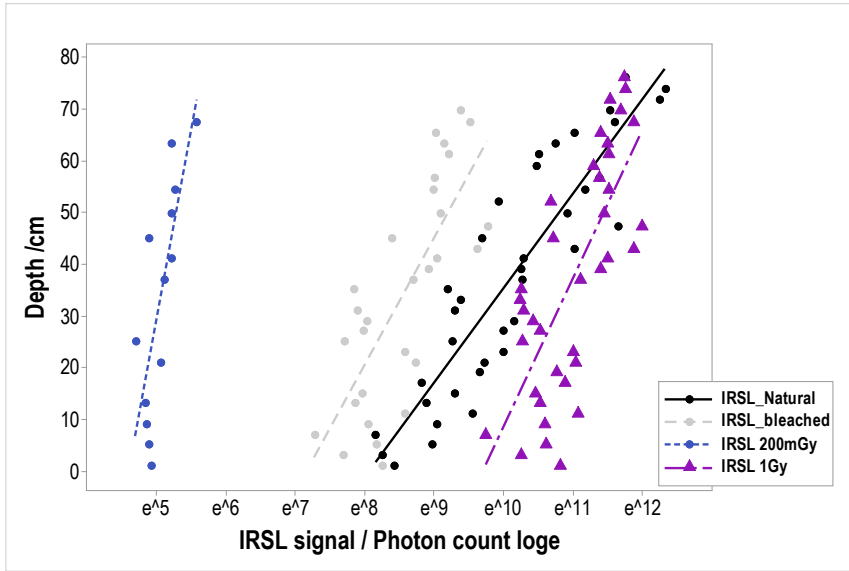


Figure F- 6: IRSL signals (in photon count  $\text{Log}_e$ ) for core A15 sediment samples All sediments ( $< 30 \mu\text{m}$ ) dispensed on 3 cm discs at each measurements step with natural signal (black), artificially bleached in grey, 200 mGy (blue) and 1 Gy (purple).

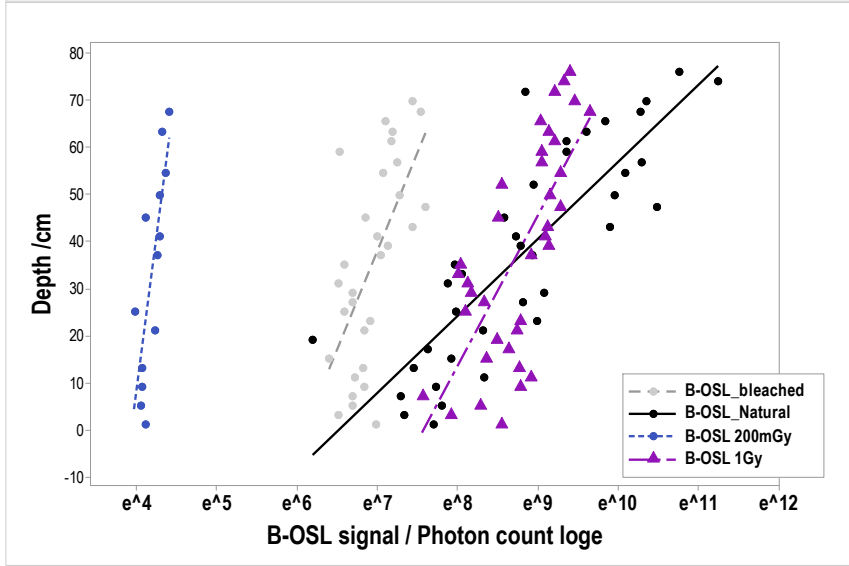


Figure F- 7: B-OSL signals (in photon count  $\text{Log}_e$ ) for core A15 sediment ( $< 30 \mu\text{m}$ ) samples dispensed on 3 cm discs at each measurements step with natural signal (black), artificially bleached in grey, 200 mGy (blue) and 1 Gy (purple).



## APPENDIX.G Supplementary references for Chapter 8

Table G- 1: Sedimentation Rates from SEDIMENTATION rates Versus FILTER DISCS Accretion Rates & Deposition rates per sites and season. In bold italic are statistically significant correlations and Spearman's rho coefficient in yellow shade are weak correlation and red moderate to strong correlations; *p-values*:  $p < 0.001^{***}$ ,  $p < 0.01^{**}$ ,  $p < 0.05^*$ .

		AR Discs	DR Discs
Overall		<b>0.4<sup>***</sup></b>	<b>0.3<sup>***</sup></b>
ANK		<b>0.7<sup>***</sup></b>	<b>0.6<sup>***</sup></b>
FM	SR	-0.2	-0.1
MR	Plates	-0.1	0.1
MR		-0.1	0.1

